0830-H-10
D312

NAS1.55:3098

NASA Conference Publication 3098

JAN 12 1991

Paired and Interacting Galaxies

International Astronomical Union Colloquium No. 124

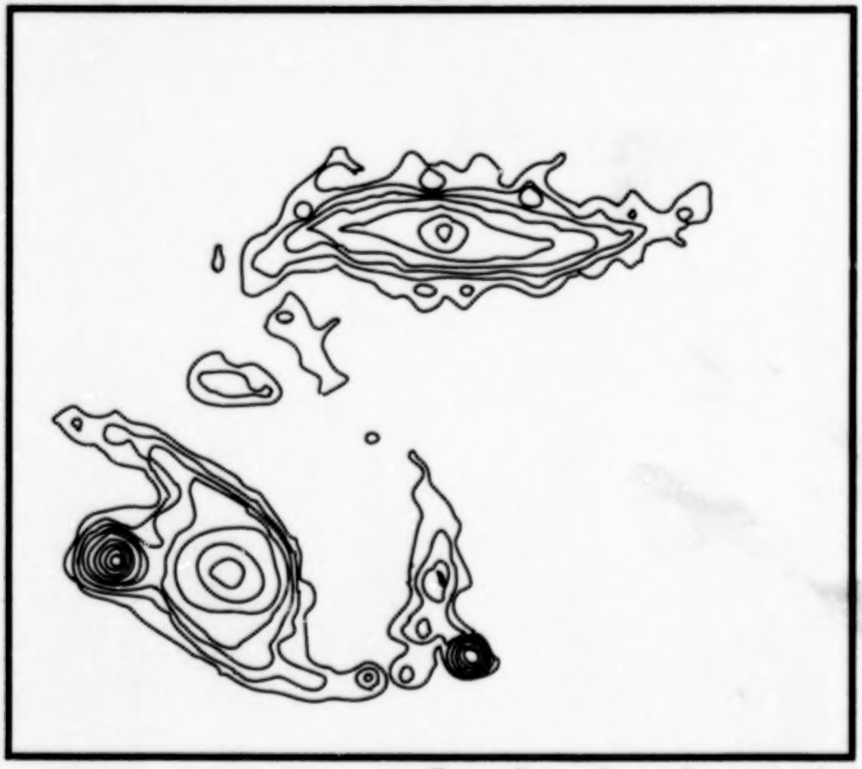

Proceedings of a conference held at
the University of Alabama at Tuscaloosa
Tuscaloosa, Alabama
December 4–7, 1989

NASA Conference Publication 3098

Paired and Interacting Galaxies

International Astronomical Union Colloquium No. 124

Edited by
J. W. Sulentic and W. C. Keel
University of Alabama at Tuscaloosa
Tuscaloosa, Alabama

C. M. Telesco
George C. Marshall Space Flight Center
Marshall Space Flight Center, Alabama

Proceedings of a conference sponsored by the
International Astronomical Union,
the University of Alabama at Tuscaloosa, and the
National Aeronautics and Space Administration and held at
the University of Alabama at Tuscaloosa
Tuscaloosa, Alabama
December 4–7, 1989

NASA
National Aeronautics and
Space Administration
Office of Management
Scientific and Technical
Information Division
1990

PREFACE

The subject labeled "interacting galaxies" is an unusual research area in the sense that many people work in it but rather few focus all of their effort in that area. The study of galaxies in pairs and groups is undeniably attractive. They represent some of the most beautiful and flamboyant examples of classical physics in action. Few can forget their first view of the "Cartwheel system" on the negatives of the ESO Sky Survey. The pairs and groups command our attention at other wavelengths, as well, because their enhanced emission frequently places an abundance of them in flux-limited samples. Ultimately, however, we study interacting systems because we hope that investigations of galaxies in nonequilibrium states will provide fundamental insights into their physical properties. As Chip Arp pointed out in the introduction to the Atlas of Peculiar Galaxies (1966) "if we could analyze a galaxy in the laboratory, we would deform it, shock it, probe it in order to discover its properties".

The motivation for IAU Colloquium #124 was to bring together theorists and observers, from a diverse array of specializations and wavebands, to summarize the current state of our knowledge of galaxies in pairs. The hope was to stimulate a confrontation between theorists and observers so that each group could fully understand the needs of the other. The conference attempted to cover both classical problems associated with the study of pairs such as sample selection, classification and dynamical modeling. Much time was also devoted to problems connected with understanding the effects of interaction upon individual galaxies in such systems. This topic embraces most of extragalactic astronomy, from ideas about star formation to the origin of the AGN phenomenon. We decided to include studies of compact groups of galaxies in the program since many of the observational and theoretical ideas about them relate to pairs as well. Much recent work has been done on these $n \geq 4$ systems and they represent a special challenge to dynamical theory.

The Astronomy group in the Department of Physics and Astronomy at the University of Alabama was pleased to host this conference. Astronomical activity began very early at this University (1844), cut short by political upheaval, but only within the last ten years has a significant research program emerged. A considerable fraction of this activity involves studies of pairs and groups, hence the decision to organize a conference on that topic at this place and time.

We thank the many individuals who assisted with the organization and success of this conference. We especially thank the scientists who attended the conference and who contributed such an impressive array of ideas and observations.

Jack W. Sulentic
William C. Keel

SCIENTIFIC ORGANIZING COMMITTEE

G. Burbidge (USA)
A. Cavaliere (Italy)
G. Contopoulos (Greece)
P. Hickson (Canada)
R. Joseph (UK)
I. Karachentsev (USSR)
C. Lonsdale (USA)
R. Miller (USA)
M. Noguchi (Japan)
J. Sulentic (USA– Chairman)

LOCAL ORGANIZING COMMITTEE

R. Buta
G. Byrd
D. Crocker
W. Keel (Chairman)
J. Sulentic
C. Telesco
W. Zheng

SPONSORS

International Astronomical Union

University of Alabama

NASA Marshall Space Flight Center

National Science Foundation

State of Alabama EPSCoR Program

Oak Ridge Associated Universities

COLLOQUIUM PARTICIPANTS

V. L. Afanasjev, Special Astrophysical Observatory, U.S.S.R.
P. Amram, Observatoire de Marseille, FRANCE
J. P. Anosova, Leningrad State University, U.S.S.R.
P. Appleton, Iowa State University, U.S.A.
L. Armus, University of Maryland, U.S.A.
E. Athanassoula, Observatoire de Marseille, FRANCE
D. S. Balsara, University of Illinois, U.S.A.
J. Bartlett, University of Alabama, U.S.A.
S. F. Beaulieu, Space Telescope Science Institute, U.S.A.
K. Bernlohr, Max Planck Institut für Astronomie, F.R.G.
B. Bhattacharya, Space Telescope Science Institute, U.S.A.
J. Bland, Rice University, U.S.A.
K. D. Borne, Space Telescope Science Institute, U.S.A.
W. van Breugel, UC Berkeley/Radio Astronomy Laboratory, U.S.A.
G. Burbidge, UC San Diego, U.S.A.
H. Bushouse, Northwestern University, U.S.A.
R. Buta, University of Alabama, U.S.A.
G. Byrd, University of Alabama, U.S.A.
M. Calvani, SISSA/ISAS, ITALY
C. Carignan, Université de Montréal, CANADA
C. Carilli, National Radio Astronomy Observatory/VLA, U.S.A.
F. Casoli, Radioastronomie ENS, FRANCE
T. Chang, University of Alabama at Huntsville, U.S.A.
J. C. Charlton, Steward Observatory, U.S.A.
T. K. Chatterjee, Facultad de Ciencias/FM, MEXICO
A. D. Chengalur, U.S.A.
J. Cocke, Steward Observatory, U.S.A.
F. Combes, Radioastronomie Millimetrique/Demirm, FRANCE
D. A. Crocker, University of Alabama, U.S.A.
R. M. Cutri, Steward Observatory, U.S.A.
A. Dey, UC Berkeley, U.S.A.
M. Dietrich, Universitats Sternwarte Gottingen, F.R.G.
K. Dow, Steward Observatory, U.S.A.
J. T. Foley, Mississippi State University, U.S.A.
D. Forbes, Institute of Astronomy, U.K.
K. J. Fricke, Universitats Sternwarte Gottingen, F.R.G.
A. M. Fridman, Academy of Sciences, U.S.S.R.
G. Galletta, Università di Padova, ITALY
J. Gallimore, University of Alabama, U.S.A.
R. A. Gerber, University of Illinois, U.S.A.
F. D. Ghigo, National Radio Astronomy Observatory/Greenbank, U.S.A.
P. GoudFrouij, Astronomical Institute/University of Amsterdam, THE NETHERLANDS
T. Hara, Kyoto Sangyo University, JAPAN
P. Hardee, University of Alabama, U.S.A.
J. J. E. Hayes, Space Telescope Space Institute, U.S.A.
T. Heckman, Johns Hopkins University, U.S.A.
C. A. Heisler, Yale University, U.S.A.
P. Hickson, University of British Columbia, CANADA
P. Hintzen, NASA/Goddard Space Flight Center, U.S.A.
S. Howard, Los Alamos National Laboratory, U.S.A.

J. B. Hutchings, Dominion Astrophysical Observatory, CANADA
D. James, University of Rochester, U.S.A.
M. Kalinkov, Bulgarian Academy of Sciences, BULGARIA
E. van Kampen, Sterrewacht Leiden, THE NETHERLANDS
I. D. Karachentsev, Special Astrophysical Observatory, U.S.S.R.
W. C. Keel, University of Alabama, U.S.A.
A. Kembhavi, Inter University Centre for Astron./Astrophys., INDIA
R. C. Kennicutt, Steward Observatory, U.S.A.
E. Y. Khachikian, Byurakan Observatory, U.S.S.R.
M. Klaric, University of Alabama, U.S.A.
R. K. Kochhar, Indian Institute of Astrophysics, INDIA
W. Kollatschny, Universitats Sternwarte Gottingen, F.R.G.
T. Koupelis, University of Alabama, U.S.A.
I. Kuneva, Bulgarian Academy of Sciences, BULGARIA
S. A. Lamb, University of Illinois, U.S.A.
H. F. Levison, US Naval Obsevatory, U.S.A.
F. Macchetto, Space Telescope Space Institute, U.S.A.
J. MacKenty, Space Telescope Space Institute, U.S.A.
R. Madejsky, Landessternwarte Heidelberg, F.R.G.
M. E. Mahon, University of Florida, U.S.A.
G. Mamon, Observatoire De Paris/Astrophysics, FRANCE
M. Marcelin, Observatoire de Marseille, FRANCE
P. Marziani, Università di Padova, ITALY
R. H. Miller, University of Chicago, U.S.A.
G. A. van Moorsel, ST ECF/European Southern Observatory, F.R.G.
R. Muradian, Byurakan Observatory, U.S.S.R.
P. M. S. Namboodiri, Indian Institute of Astrophysics, INDIA
J. Navarro, Harvard-Smithsonian Center for Astrophysics, U.S.A.
S. G. Neff, NASA/Goddard Space Flight Center, U.S.A.
M. Noguchi, Nobeyama Radio Observatory, JAPAN
L. Noreau, University of Toronto, CANADA
C. Norman, Space Telescope Space Institute, U.S.A.
R. Norris, CSIRO/Division of Radiophysics, AUSTRALIA
T. Oosterloo, European Southern Observatory, F.R.G.
D. E. Osterbrock, Institute for Advanced Study/Lick Observatory, U.S.A.
G. G. C. Palumbo, Università di Bologna, ITALY
C. J. Peterson, University of Missouri, U.S.A.
A. Petrosian, Byurakan Astrophysical Observatory, U.S.S.R.
V. Polyachenko, Academy of Sciences, U.S.S.R.
I. Pronik, Crimean Astrophysical Observatory, U.S.S.R.
P. Prugniel, European Southern Observatory, F.R.G.
H. Quintana, Universidad Católica de Chile, CHILE
F. M. Rabaca, Universidade de Sao Paulo/IAG, BRAZIL
R. Rampazzo, Osservatorio Astronomico di Brera, Milano, ITALY
V. P. Reshetnikov, Leningrad State University, U.S.S.R.
M. Roberts, National Radio Astronomy Observatory/Charlottesville, U.S.A.
N. Roos, Sterrewacht Leiden, THE NETHERLANDS
H. Salo, University of Helsinki, FINLAND
S. E. Schneider, University of Massachusetts, U.S.A.
N. A. Sharp, National Optical Astronomy Observatories, U.S.A.
I. Shlosman, Caltech, U.S.A.
S. Simkin, Michigan State University, U.S.A.
C. E. Simpson, University of Florida, U.S.A.
E. P. Smith, NASA/Goddard Space Flight Center, U.S.A.

N. Ya Sotnikova, Leningrad University, U.S.S.R.
W. B. Sparks, Space Telescope Science Institute, U.S.A.
A. Stanford, University of Wisconsin, U.S.A.
C. Struck-Marcell, Iowa State University, U.S.A.
J. W. Sulentic, University of Alabama, U.S.A.
B. Sundelius, Chalmers University of Technology, SWEDEN
Y. Taniguchi, Kiso Observatory, JAPAN
M. Thomasson, Onsala Space Observatory, SWEDEN
R. C. Thomson, Institute of Astronomy, UK
W. G. Tifft, Steward Observatory, U.S.A.
K. Turner, National Science Foundation, U.S.A.
M. Valtonen, Turku University Observatory, FINLAND
G. Vettolani, Istituto di Radioastronomia, ITALY
J. F. Wallin, Naval Research Laboratory, U.S.A.
R. H. Warmels, European Southern Observatory, F.R.G.
K. Weaver, University of Maryland, U.S.A.
P. A. Wehinger, Arizona State University, U.S.A.
R. E. White, III, University of Alabama, U.S.A.
B. Whitmore, Space Telescope Science Institute, U.S.A.
B. A. Williams, University of Delaware, U.S.A.
E. Wolf, University of Rochester, U.S.A.
G. S. Wright, Joint Astronomy Center, U.S.A.
E. Xanthopoulos, York University, CANADA
C. Xu, International Centre for Theoretical Physics, ITALY
T. Yamagata, National Astronomical Observatory, JAPAN
G. J. Yates, Nuffield Radio Astronomy Laboratory, U.K.
A. V. Zasov, Sternberg Astronomical Institute, U.S.S.R.
S. E. Zepf, Johns Hopkins University./STScI, U.S.A.
W. Zheng, University of Alabama, U.S.A.

TABLE OF CONTENTS

I. CLASSICAL OBSERVATIONS OF PAIRS 1

HOMOGENEOUS SAMPLE OF BINARY GALAXIES: BASIC OBSERVATIONAL PROPERTIES 3
I. D. Karachentsev

PAIRS OF GALAXIES IN LOW DENSITY REGIONS OF A COMBINED REDSHIFT CATALOG 19
J. C. Charlton and E. E. Salpeter

MORPHOLOGICAL TYPE CORRELATION BETWEEN NEAREST NEIGHBOR PAIRS OF GALAXIES 25
T. Yamagata

STELLAR KINEMATICS OF ELLIPTICAL GALAXIES IN PAIRS 33
R. Madejsky and R. Bender

DYNAMICS OF GROUPS AROUND INTERACTING DOUBLE ELLIPTICALS: MEASURING DARK MATTER HALOES 37
H. Quintana

THE INTERACTING PAIR MKN 305/306 43
M. Dietrich

GEOMETRICAL PARAMETERS OF E+S PAIRS 47
R. Rampazzo and J. W. Sulentic

AN ATLAS OF MIXED MORPHOLOGY PAIRS 53
N. A. Sharp

MULTI-COLOR IMAGING OF SELECTED SOUTHERN INTERACTING GALAXIES 55
E. P. Smith and P. Hintzen

MULTI-WAVEBAND OBSERVATIONS OF COLLIDING GALAXIES 59
P. N. Appleton, E. I. Robson and J. N. Schombert

TIDAL DISTORTIONS IN PAIRS OF EARLY-TYPE GALAXIES 65
P. Prugniel and E. Davoust

A MULTI-FREQUENCY STUDY OF THE PECULIAR INTERACTING SYSTEM ARP206 69
L. Noreau and P. P. Kronberg

II. CLASSICAL OBSERVATIONS OF MULTIPLETS 75

OBSERVATIONAL PROPERTIES OF COMPACT GROUPS OF GALAXIES 77
P. Hickson

VLA NEUTRAL HYDROGEN IMAGING OF COMPACT GROUPS 93
B. A. Williams, P. M. McMahon and J. H. van Gorkom

BLUE ELLIPTICALS IN COMPACT GROUPS 99
S. E. Zepf and B. C. Whitmore

WHAT IS THE NUMBER OF SPIRAL GALAXIES IN COMPACT GROUPS? 105
A. N. Tikhonov

TRIPLE GALAXIES AND A HIDDEN MASS PROBLEM 115
I. D. Karachentsev, V. E. Karachentseva and V. S. Lebedev

HI STUDIES OF THE SCULPTOR GROUP GALAXIES 129
C. Carignan and D. Puche

A STUDY OF THE COMPACT GROUP OF GALAXIES SHAHBAZIAN 4 133
C. R. Lynds, E. Ye. Khachikian and A. S. Amirkhanian

ISOLATED GALAXIES: PAIRS AND GROUPS OF GALAXIES 143
I. Kuneva and M. Kalinkov

CORRELATION FUNCTIONS FOR PAIRS AND GROUPS OF GALAXIES 149
M. Kalinkov and I. Kuneva

III. OBSERVATIONS OF RELATED OBJECTS 157

HIDDEN INTERACTION IN SBO GALAXIES 159
G. Galletta, D. Bettoni, G. Fasano and T. Oosterloo

THE ENVIRONMENTS OF MARKARIAN GALAXIES 165
J. W. MacKenty, B. McLean and C. Simpson

THE COMPLEX NATURE OF THE SEYFERT GALAXY NGC 7592 169
P. Rafanelli and P. Marziani

THE HI CONTENT OF NON-ISOLATED GALAXIES 175
A. V. Zasov

HI AND MASS DISTRIBUTION OF GR8 183
S. Beaulieu and C. Carignan

THE RINGED X-GALAXY NGC 7020 189
R. Buta

THE CD GALAXY IN ABELL CLUSTER 1775 195
J. J. E. Hayes and B. Bhattacharya

NEW DATA ON THE PECULIAR GALAXY MRK 273 201
A. S. Asatrian, A. R. Petrosian and F. Börngen

HI OBSERVATIONS OF THE PECULIAR GALAXY NGC 660 209
S. T. Gottesman and M. E. Mahon

A SPIRAL-LIKE DISK OF IONIZED GAS IN IC 1459: SIGNATURE OF A MERGING COLLISION? 215
P. Goudfrooij, H. U. Nørgaard-Nielsen, H. E. Jørgensen, L. Hansen and T. de Jong

OBSERVATIONS OF MULTIPLE NUCLEUS GALAXIES 221
W. Kollatschny

THE DOUBLE NUCLEUS GALAXIES MKN 423 AND MKN 739 225
P. Rafanelli and P. Marziani

THE POLAR-RING GALAXIES NGC 2685 AND NGC 3808B (VV300) 231
V. P. Reshetnikov and V. A. Yakovleva

THE MORPHOLOGY OF SÉRSIC-PASTORIZA GALAXIES 245
G. J. Yates, A. Pedlar, D. J. Saikia, S. W. Unger and D. J. Axon

INTERACTING NUCLEI IN DISTANT GALAXIES 251
W. Zheng and S. Grandi

ALIGNMENT OF CD-GALAXIES WITH THEIR SURROUNDINGS 255
E. van Kampen and G. Rhee

DUMB-BELL GALAXIES IN SOUTHERN CLUSTERS: CATALOG AND PRELIMINARY STATISTICAL RESULTS 261
G. Vettolani, L. Gregorini, P. Parma and H. R. de Ruiter

PANEL DISCUSSION: DEFINITIONS OF THE TIDAL INTERACTION AND MERGER PHENOMENA 265
Summary by W. Keel

IV: OBSERVATIONS OF GLOBAL ACTIVITY DUE TO INTERACTION 267

GLOBAL EFFECTS OF INTERACTIONS ON GALAXY EVOLUTION 269
R. C. Kennicutt Jr.

A MULTIWAVELENGTH SURVEY OF INTERACTING GALAXIES 285
H. Bushouse, S. Lamb, K. Y. Lo, S. Lord and M. Werner

FIR STATISTICS OF PAIRED GALAXIES 291
J. W. Sulentic

QUANTIFYING THE FIR INTERACTION ENHANCEMENT IN PAIRED GALAXIES 297
C. Xu and J. W. Sulentic

STAR FORMATION IN INFRARED BRIGHT AND INFRARED FAINT STARBURST INTERACTING GALAXIES 303
S. A. Lamb, H. A. Bushouse and J. W. Townes

RADIO LOUD FAR-INFRARED GALAXIES 309
A. Dey, W. van Breugel and J. C. Shields

ON A CONNECTION BETWEEN SUPERNOVA OCCURRENCE AND TIDAL INTERACTION IN EARLY-TYPE GALAXIES 315
R. K. Kochhar

INFRARED IMAGES OF MERGING GALAXIES 321
G. S. Wright, P. A. James, R. D. Joseph, I. S. McLean and R. Doyon

GALAXY INTERACTIONS AND STAR FORMATION: RESULTS OF A SURVEY OF GLOBAL $H\alpha$ EMISSION IN SPIRAL GALAXIES IN 8 CLUSTERS 327
C. Moss

OBSERVATIONAL EFFECTS OF INTERACTION IN THE SEYFERT GALAXY NGC 7469 331
I. Pronik and L. Metik

RADIO EMISSION IN PECULIAR GALAXIES 343
D. F. de Mello Rabaça and Zulema Abraham

THE KINEMATICS AND MORPHOLOGY OF NGC 520: ONE, TWO, OR THREE GALAXIES? 347
S. A. Stanford and M. Balcells

STATISTICS OF ASSOCIATIONS AMONG IR GALAXIES 353
J. Gallimore and W. Keel

V: OBSERVATIONS OF NUCLEAR AND NEAR-NUCLEAR ACTIVITY 357

GALAXY INTERACTIONS AND THE STIMULATION OF NUCLEAR ACTIVITY 359
T. M. Heckman

TIDAL EVENTS AND GALACTIC ACTIVITY 383
J. B. Hutchings and S. G. Neff

ARE EXTREMELY LUMINOUS FAR-INFRARED GALAXIES THE RESULT OF MERGING QUASAR CORES? 387
R. P. Norris

CENTRAL ACTIVITY IN 60 MICRON PEAKERS 393
C. A. Heisler, J. P. Vader and J. A. Frogel

GALAXY INTERACTIONS AND STRENGTH OF NUCLEAR ACTIVITY 399
S. M. Simkin

COOL INFALLING GAS AND ITS INTERACTION WITH THE HOT ISM OF ELLIPTICAL GALAXIES 403
W. B. Sparks and F. D. Macchetto

THE NATURE OF THE EMISSION-LINE NEBULAE IN POWERFUL FAR-INFRARED GALAXIES 409
L. Armus, T. M. Heckman and G. K. Miley

NUCLEAR AND EXTENDED INFRARED EMISSION IN PAIRED AND ISOLATED GALAXIES 415
R. M. Cutri

SIGNS OF INTERACTION OF THE NGC 1275 NUCLEUS WITH THE HIGH VELOCITY SYSTEM ACCORDING TO 0.7 ARCSEC SEEING OBSERVATIONS 421
V. N. Dudinov, V. S. Tsvetkova, S. B. Novikov and I. I. Pronik

DUST AND IONIZED GAS IN ACTIVE RADIO ELLIPTICAL GALAXIES 431
D. A. Forbes, W. B. Sparks and F. D. Macchetto

CORRELATIONS BETWEEN ENVIRONMENTAL PARAMETERS AND NUCLEAR ACTIVITY 437
W. Kollatschny and K. J. Fricke

THE ROLE OF SHOCKS IN NGC 6240 441
W. C. Keel

DEEP FABRY-PEROT IMAGING OF NGC 6240: KINEMATIC EVIDENCE FOR MERGING GALAXIES 445
J. Bland Hawthorn, A. S. Wilson and R. B. Tully

IC 5063: A MERGER WITH A HIDDEN LUMINOUS ACTIVE NUCLEUS 451
L. Colina, W. Sparks and F. Macchetto

VI: REDSHIFT RELATED PROBLEMS 457

PANEL DISCUSSION REDSHIFT RELATED PROBLEMS 459
G. Burbidge, M. Roberts (Chairman), S. Schneider, N. Sharp, W. Tifft

RADIO STRUCTURES IN QSO-GALAXY PAIRS 467
C. E. Akujor

RADIO LINE AND CONTINUUM OBSERVATIONS OF QUASAR-GALAXY PAIRS AND THE ORIGIN OF LOW REDSHIFT QUASAR ABSORPTION LINE SYSTEMS 473
C. L. Carilli, J. H. van Gorkom, E. M. Hauxthausen, J. T. Stocke and J. Salzer

PROPERTIES OF THE REDSHIFT 479
W. G. Tifft and W. J. Cocke

SELECTION EFFECTS IN BINARY GALAXY SAMPLES: UNDERSTANDING TIFFT'S PHENOMENON 485
S. E. Schneider and E. E. Salpeter

A TENTATIVE EXPLANATION OF COSMOLOGICAL REDSHIFT 491
T. Chang and D. G. Torr

MERGING GALAXIES AND BLACK HOLE EJECTIONS 497
M. J. Valtonen

VII: CLASSICAL THEORY OF PAIRS **503**

DYNAMICAL INTERACTIONS OF GALAXY PAIRS 505
E. Athanassoula

A STATISTICAL STUDY OF MERGING GALAXIES– THEORY AND OBSERVATIONS 519
T. K. Chatterjee

PROBING THE TIDES IN INTERACTING GALAXY PAIRS 537
K. D. Borne

DYNAMICAL FRICTION IN PAIRS OF ELLIPTICAL GALAXIES 543
P. Prugniel and F. Combes

AN EXPERIMENTAL STUDY OF COUNTER–ROTATING CORES IN ELLIPTICAL GALAXIES 549
R. H. Miller, G. R. Roelofs and B. F. Smith

ON LEADING SPIRAL ARMS IN CLOSE PAIRS OF GALAXIES 555
A. M. Fridman

A SIMULATION SURVEY OF GALAXY INTERACTIONS 565
G. Byrd, W. Keel and S. Howard

A DYNAMICAL PROXIMITY ANALYSIS OF INTERACTING GALAXY PAIRS 569
T. K. Chatterjee

M51'S SPIRAL STRUCTURE 577
S. Howard and G. G. Byrd

THE SPIRAL–COMPACT GALAXY PAIR AM 2208-251: COMPUTER SIMULATIONS VERSUS OBSERVATIONS 583
M. Klarić and G. G. Byrd

ENERGY AND ANGULAR MOMENTUM TRANSFER IN BINARY GALAXIES 589
P. M. S. Namboodiri and R. K. Kochhar

SIMULATIONS OF DISK–DISK ENCOUNTERS WITH CO–MOVING POLAR GRIDS 595
H. Salo

WHAT DETERMINES THE BULGE–TO–DISK RATIO OF GALAXIES 601
N. Roos

VIII: CLASSICAL THEORY OF MULTIPLETS **607**

DYNAMICAL THEORY OF DENSE GROUPS OF GALAXIES 609
G. A. Mamon

EXPLAINING COMPACT GROUPS AS CHANCE ALIGNMENTS 619
G. A. Mamon

TYPICAL MOTIONS IN MULTIPLE SYSTEMS 629
J. P. Anosova

DYNAMICS AND CONFIGURATIONS OF GALAXY TRIPLETS 633
J. P. Anosova, V. V. Orlov, A. D. Chernin, A. V. Ivanov and L. G. Kiseleva

DRAGGING FORCE ON GALAXIES DUE TO STREAMING DARK MATTER 645
T. Hara and S. Miyoshi

TRIPLETS OF GALAXIES: THEIR DYNAMICS, EVOLUTION AND THE ORIGIN OF CHAOS IN THEM 651
A. D. Chernin and A. V. Ivanov

A CLASSIFICATION OF THE GALAXY GROUPS 659
J. P. Anosova

VIRIAL COEFFICIENT AND HIDDEN MASS IN THE GALAXY GROUPS 667
J. P. Anosova, V. V. Orlov and L. G. Kiseleva

ON THE LARGE-SCALE STRUCTURES FORMED BY WAKES OF OPEN COSMIC STRINGS 677
T. Hara, S. Morioka and S. Miyoshi

COLLISIONAL REMOVAL OF HI FROM THE INNER DISKS OF VIRGO CLUSTER GALAXIES 683
M. Valluri and C. J. Jog

IX: THEORY OF INTERACTION STIMULATED EFFECTS 687

INDUCED STARBURST AND NUCLEAR ACTIVITY: FAITH, FACTS AND THEORY 689
I. Shlosman

STATIONARY ORBITS OF THE SATELLITES OF GALAXIES 705
V. L. Polyachenko

NUMERICAL SIMULATIONS OF INTERACTING DISC GALAXIES 711
M. Noguchi

GAS FLOW IN S-E BINARY SYSTEMS OF GALAXIES 717
N. Sotnikova

OBSERVATIONS AND MODELS OF STAR FORMATION IN THE TIDAL FEATURES OF INTERACTING GALAXIES 727
J. F. Wallin, J. M. Schombert and C. Struck-Marcell

STARBURSTS IN INTERACTING GALAXIES: OBSERVATIONS AND MODELS 731
K. Bernlöhr

DYNAMICAL EXPERIMENTS ON MODELS OF COLLIDING DISK GALAXIES 737
R. A. Gerber, D. S. Balsara and S. A. Lamb

CAUSTIC WAVES IN GALAXY DISKS PRODUCED IN COLLISIONS WITH LOW MASS COMPANIONS 743
C. Struck-Marcell

SIMULATIONS OF GAS CLOUDS IN INTERACTING GALAXIES 749
M. Thomasson

DO ELLIPTICAL GALAXIES HAVE THICK DISKS? 755
R. C. Thomson and A. E. Wright

WING GALAXIES: A FORMATION MECHANISM OF THE CLUMPY IRREGULAR GALAXY MARKARIAN 297 759
Y. Taniguchi and M. Noguchi

PAIRED AND INTERACTING GALAXIES: CONFERENCE SUMMARY 765
C. Norman

I. CLASSICAL OBSERVATIONS

OF

PAIRS

A HOMOGENEOUS SAMPLE OF BINARY GALAXIES: BASIC OBSERVATIONAL PROPERTIES

I. D. Karachentsev
Special Astrophysical Observatory, USSR Academy of Sciences
st. Zelenchukskaya, Stavropol Territory, 357147, USSR

ABSTRACT

A survey of optical characteristics for 585 binary systems, satisfying a condition of apparent isolation on the sky, is presented. Influences of various selection effects distorting the average parameters of the sample are noted. The pair components display mutual similarity over all the global properties: luminosity, diameter, morphological type, mass-to-luminosity ratio, angular momentum etc., which is not due only to selection effects. The observed correlations must be caused by common origin of pair members. Some features (nuclear activity, color index) could acquire similarity during synchronous evolution of double galaxies.

Despite the observed isolation, the sample of double systems is seriously contaminated by accidental pairs, and also by members of groups and clusters. After removing false pairs estimates of orbital mass-to-luminosity ratio range from 0 to 30 $f_\odot$, with the mean value (7.8 ± 0.7) $f_\odot$. Binary galaxies possess nearly circular orbits with a typical eccentrity $e = 0.25$, probably resulting from evolutionary selection driven by component mergers under dynamical friction. The double-galaxy population with space abundance 0.12 ± 0.02 and characteristic merger timescale $0.2\ H^{-1}$ may significantly influence the rate of dynamical evolution of galaxies.

1. INTRODUCTION

Every year interest increases in investigating the structure and dynamics of systems of galaxies. The main stimulus here is the search for "missing" virial mass in these systems, which gives this problem somewhat of a detective nature. In the wide range of hidden mass searches pairs occupy an important place, as the simplest of galactic systems. Investigation of pairs allows us to approach the hidden mass problem at an elementary, "cellular", level. Binary galaxies are also especially interesting because of the accelerated rates of evolution as compared to solitary ones. Because of galaxies' mutually proximity in pairs, gravitational tides play a major part in their fate, star-formation bursts and dynamical friction effects. There are grounds to think that pairs significantly influence the dynamical evolution of galactic systems in general.

The first systematic studies of double galaxies were carried out by the Swedish astronomers Lundmark (1927) and Holmberg (1937, 1954), who suggested quantitative definitions of binary systems. Further progress in this study was achieved by Page. He made the first systematic measurements of radial velocities in binaries and worked out mass calculation methods with different assumptions on the kind of orbital motions in pairs (Page 1952, 1960, 1967).

Zwicky *et al.* (1961-1968) and Vorontsov-Velyaminov *et al.* (1962-1968) compiled extensive galaxy catalogs, in which among others numerous examples of close binary systems are marked. Impressive collections of peculiar and interacting pairs are represented in the atlases by Arp (1966) and Vorontsov-Velyaminov (1959,1977). But in these catalogs, the binary galaxies do not form homogeneous samples because quantitative criteria had not been used in their selection. The pairs were selected according to strong signs of interaction as by-products of the main program. In time, the necessity of having a new double-galaxy catalog became apparent. It should be characterized by homogeneous observational data and be based on strict selection criteria of isolated pairs. Such a task was set by the author and realized in the form of the "Catalogue of isolated pairs of galaxies in the northern hemisphere" (Karachentsev, 1972). When preparing the catalogue, including 603 pairs, we kept a rule to inspect in detail the neighborhoods of all galaxies brighter than a fixed photometric limit, using the POSS prints. The search and selection of isolated binary systems was based on quantitative criteria for measuring mutual distances and angular diameters of the galaxies. A similar approach was used later by Turner (1976), Peterson (1979) and Schweizer (1987). According to our criterion, two galaxies with apparent magnitudes

$$m_1, m_2 < 15.7,$$

angular diameters a_1, a_2, and angular separation X are isolated relative to neighboring (in projection) galaxies, when the conditions

$$\mathrm{X}_{1i}/\mathrm{X}_{12} > 5a_i/a_1,$$

$$\mathrm{X}_{2i}/\mathrm{X}_{12} > 5a_i/a_2,$$

are satisfied ; i denotes any "significant" neighbouring galaxy, whose angular diameter a_i lies in the interval

$$4a_1 > a_i > a_1/2,$$

$$4a_2 > a_i > a_2/2,$$

Without going into detail, we may say that this criterion selects double systems with local density contrast on the sky more than 25.

Mass radial velocity measurements in isolated pairs aiming to study the kinematics and dynamics of double galaxies were undertaken (Karachentsev, 1980, Tifft, 1982). As a result of the combined efforts of several observers the program of radial velocity determination had been completed by 1983. Compared to previous episodic observations of galaxies in pairs, higher accuracy of radial velocity measurements was achieved, which allowed determination of masses of double systems with greater reliability.

After reduction of apparent magnitudes and angular diameters of galaxies to a standard system, specifying morphological and spectral types (and also excluding 18 single objects) the final version of the catalog was published in the book "Binary galaxies" (Karachentsev, 1987).

The present report contains the main conclusions drawn when analysing the above-mentioned sample of 585 isolated pairs. In the interest of brevity, we must omit arguments for most of the statements.

2. OBSERVATIONAL PROPERTIES OF THE SAMPLE AND SELECTIVITY

Using the objective isolation criterion allowed us to account for various selection effects, badly affecting binary system sample characteristics. We investigated the efficiency and selectivity of the pair criterion with the help of Monte Carlo numerical experiments. Simulation of the apparent distribution of galaxies was carried out, accounting for their spatial clustering in systems of various scale and population. Approaching this simulated galaxy distribution by the same double system selection criterion as that used in the real catalogue, we obtained the following result. Among the catalogue objects 11% are optical pairs, caused by accidental projection in the line of sight of galaxies that are not in spatial proximity. About 32% the of catalog pairs are false double systems, formed by projection of two members of one group or cluster on the line of sight. Earlier the role of false pairs (system members) was much underestimated, which gave anomalously high values of average orbital mass for binary galaxies. The low efficiency of any pair criterion is associated with the large luminosity dispersion of galaxies, because of which apparent magnitude or angular diameter of a galaxy are unreliable indicators of its distance.

The simulation results were used to recover true (space) characteristics of double system using their catalogued characteristics, distorted both by projection effects and by presence of non-isolated pairs in the catalog. If we exclude 98 pairs with orbital mass-to-luminosity ratio $f > 100\, f_\odot$ as being false, then for the remaining 487 systems the distribution according to radial velocity difference is shown by a histogram in Figure 1. After correction for velocity measurement errors the distribution has a form close to the exponential one with the average $< y >= 120$ km/s.

Unlike radial velocities, angular separations between galaxies are directly included in the isolation criterion. As a result of this, double galaxies' distribution in projected linear separation, X, is subjected to strong selection. Thus, when $X > 100$ Kpc, about 90% of pairs are omitted by the isolation criterion. This circumstance together with the increasing contribution of false pairs with increasing X does not let us determine the true number of wide double systems in a unit volume of space. The distribution of 487 isolated pairs according to their linear separations is shown in Figure 2. It is well represented by a gamma function, $n\ (X) \sim X^{1/2}\exp(-X/C)$, with mean value 33.2 kpc,the Hubble constant being taken as $H_0=75$ km/s Mpc. About 70% of the catalog objects are rather tight systems where the mutual distance of components does not exceed their combined diameters. After correction for the selection criterion the mean spatial separation for galaxies in isolated pairs is $< r_{12} > = 83$ kpc.

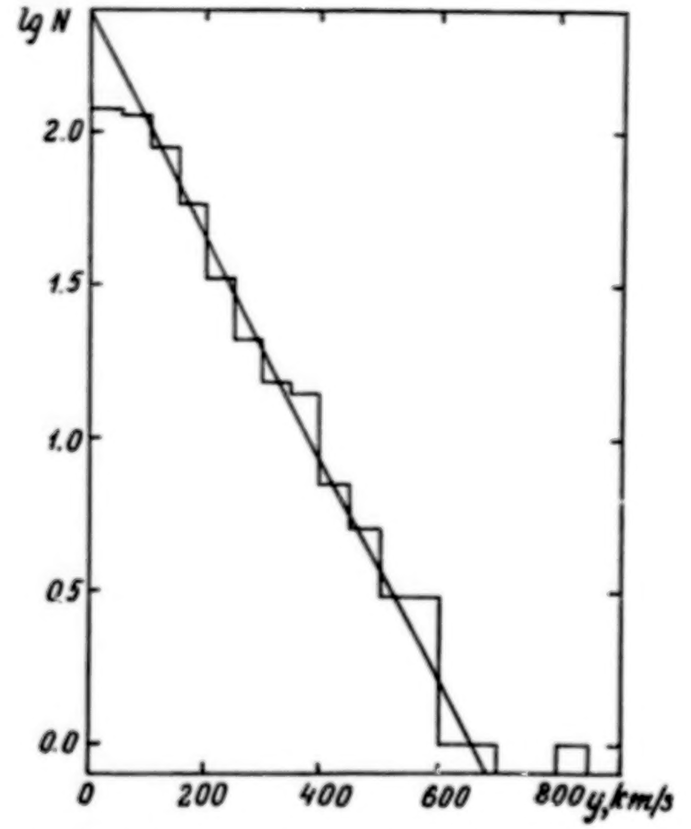

Fig. 1. Distribution of radial velocity difference (km/s) for components of 487 pairs.

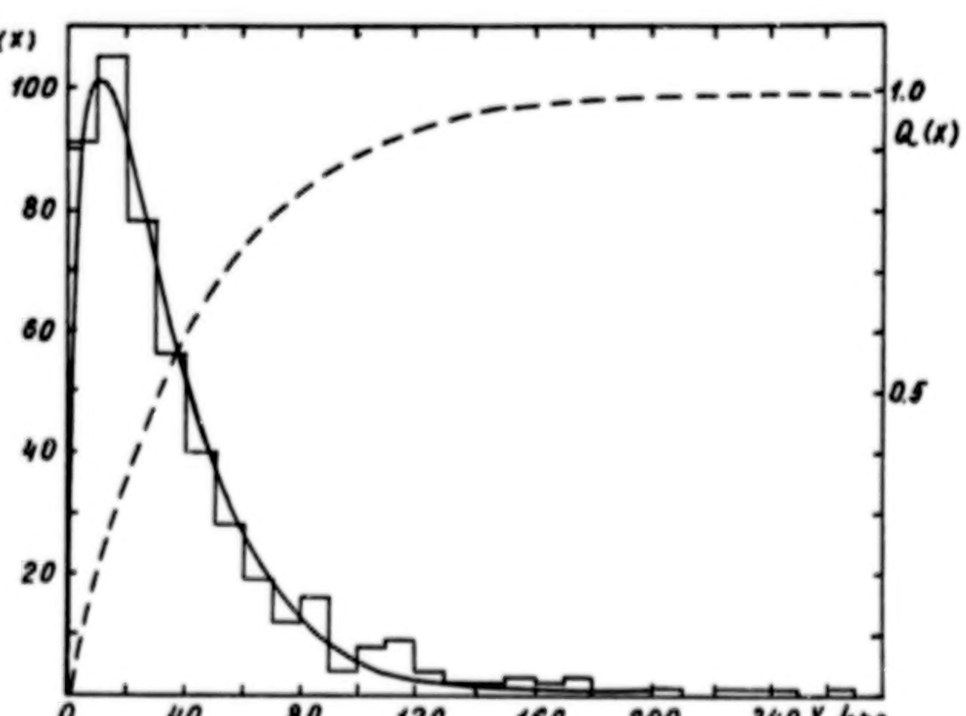

Fig. 2. Distribution of 487 isolated binary systems according to projected separation of their components. Dashed curve shows selectivity function for the criterion (right scale).

The variety of selection factors for binary galaxies makes determining their spatial luminosity function $\Phi(M_1,M_2)$ rather complicated. As compared to field galaxies, pair components show a luminosity excess by 1.7 times on average. The observed positive correlation for absolute magnitudes of double galaxies is not only due to selection effects in the sample, but is caused by real physical similarity of objects inside one system. As with the luminosity correlation, so its excess, evidently, reflects the special conditions under which common formation of double galaxies took place.

3. ORBITAL MASSES

The hidden mass problem certainly should be placed first in the study of double systems. It had been repeatedly supposed that pairs of galaxies are surrounded by invisible massive coronae, and therefore Keplerian description of their dynamics is not appropriate. To motivate such a statement some indirect arguments are drawn 'from below' (flat rotation curves for individual galaxies) and 'from above' (a virial mass excess for X-ray clusters). Besides such indirect considerations, direct evidence of mass excess in double systems has been inferred from their high mean orbital mass-to-luminosity ratio ($\approx 60\ f_\odot$), obtained by Page (1952), Turner (1976) and Peterson (1979). The "anatomy" of this excess was discussed at length in the book "Binary Galaxies" (Karachentsev, 1987). Those data allow us to affirm that the paramount reason for high estimates of orbital mass is that a large number of false pairs is present in the catalog samples. The histogram in Figure 3 shows the distribution of 585 binary systems according to their orbital mass-to-luminosity ratio,

$$f = \frac{32 X_{12}\, y^2_{12}}{3\pi G(L_1 + L_2)},$$

where G is the gravitational constant and $(32/3\pi)$ the average projection factor for circular motions. Regions occupied by true pairs, optical pairs and non-isolated pseudo-pairs, i.e. group and cluster members, are indicated. After a correct accounting for fictitious double systems, and also radial velocity measurement errors, the average orbital mass-to-luminosity ratio corresponds well with individual values obtained from galaxy rotation curves. We will stress here, that we are dealing with more than a coincidence of average values. Corrected for projection effects, pair members' orbital mass-to-total luminosity ratio appears distributed in a narrow range of values [0, 30] $f_\odot$with average (7.8 ± 0.7) $f_\odot$and standard deviation 6.5 $f_\odot$. Nearly this distribution law is characteristic for field galaxies' individual mass-to-luminosity ratios. An important circumstance here is also the good correspondence of orbital and individual f-values for various types of galaxies along the Hubble sequence (Figure 4). Comparison of binary galaxies' orbital mass with their sum of individual masses determined from internal motions shows that the main part of their mass is concentrated inside the standard optical radius R_{25} . Though the most of the catalog objects are close (contact) systems, broad pairs with $X >$ 100 Kpc also possess a low average ratio of orbital mass-to-luminosity which would not agree with the hypothesis of massive invisible coronae.

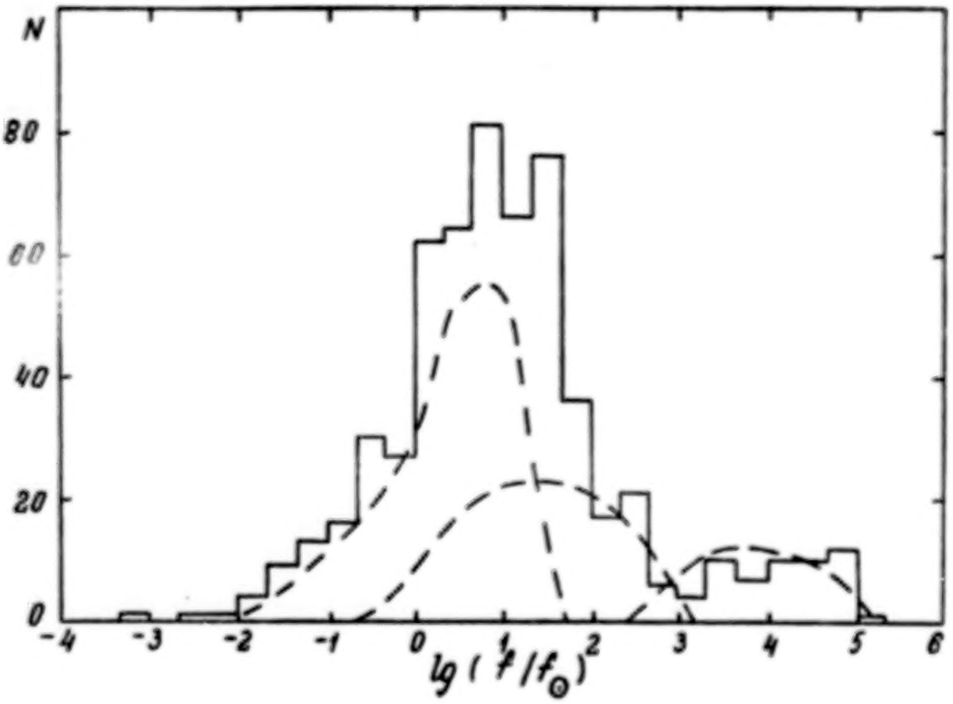

Fig. 3. Distribution of 585 catalogued pairs according to their orbital mass-to-luminosity ratio in solar units (histogram). The dashed curves show the simulated distributions for true binaries (left), members of groups (middle), and optical pairs (right).

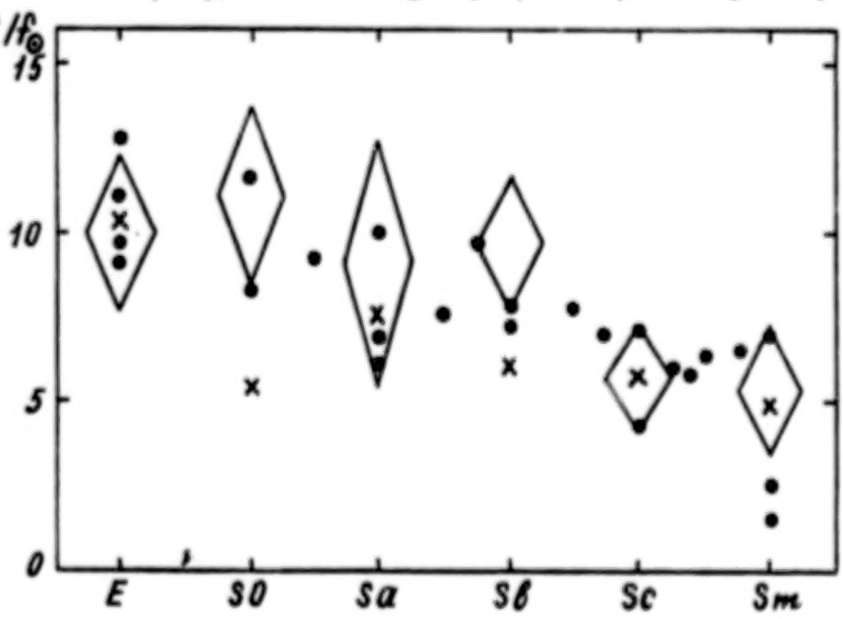

Fig. 4. Average mass-to-luminosity ratio for various structural type galaxies from different sources (points). Oblique crosses are used to distinguish mean values for components of pairs. Rhombs mark mean values of orbital mass-to-luminosity ratio for pairs with similar types of galaxies.

Thus, pairs of galaxies seem a missing link in the chain of various scales of systems in a hierarchy, others of which show virial mass excess. The strange character of this situation should be specially stressed.

Observational data place limits on the possible kinds of orbital motions of galaxies in pairs. Using different methods, we came to the conclusion that binary galaxy orbits are close to circular. The best agreement with observational data is obtained with orbital eccentrity $e = 0.25$.

4. MORPHOLOGY AND ACTIVITY.

Rich opportunities for testing scenarios of origin and evolution of galaxies are given by analysis of the population of binary galaxies according to their morphological and spectral types, signs of interaction, color indices etc. In this problem only "the upper cultural layer" has been taken up.

Binary systems, as compared to single ones, contain a higher percentage of earlier structural type objects. Besides, the relative number of elliptical galaxies is falling with increasing separation of pair components. It is necessary to note here, that the observed frequency of binary systems with similar Hubble type components is considerably higher than that expected for accidental combinations of these features. The correlation function of pairs according to their morphological types is presented in Figure 5.

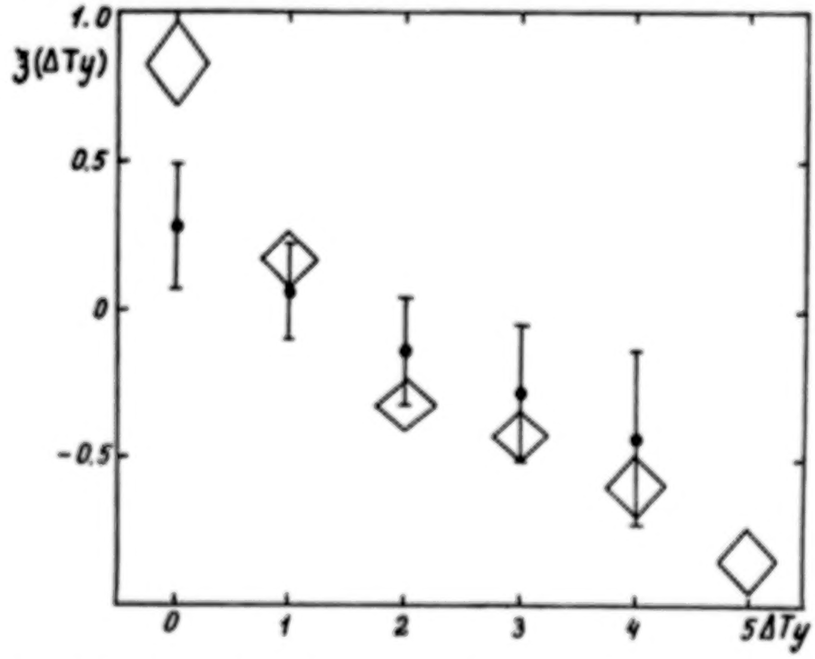

Fig. 5. Correlation function of binary systems according to a structural type of their components. Rhomboids are data for the whole 487 pair sample, points - for 118 wide pairs with $X > 50$ Kpc.

About 60% of the catalogued pairs show traces of tidal interaction. As analysis shows, all structural types of galaxies are present among the interacting ones in equal proportion. But their distribution according to interaction types is highly inhomogeneous.

Such linear structures as tails and bridges (see Figure 6) are characteristic of objects with dominant stellar populations of the disk with almost circular velocities. In elliptical binary galaxies, with significantly elongated stellar orbits, amorphous symmetric atmospheres are usually observed. The relation between interaction signs and character of stellar motions in pairs members usually agrees with results of numerical experiment (Clutton-Brock , 1972).

Considering spectral and morphological types of binary galaxies together with their interaction types shows that tidal interaction is favourable for galaxies to have strong emission features. Activity of galactic nuclei is apparently intensified by the flow of gas to it as a result of collision and loss of momentum of gas clouds caused by tidal perturbation. Another mechanism - gas exchange between pair components - does not take any significant part, judging by the absence of emission in spectra of elliptical galaxies in contact with a spiral partner.

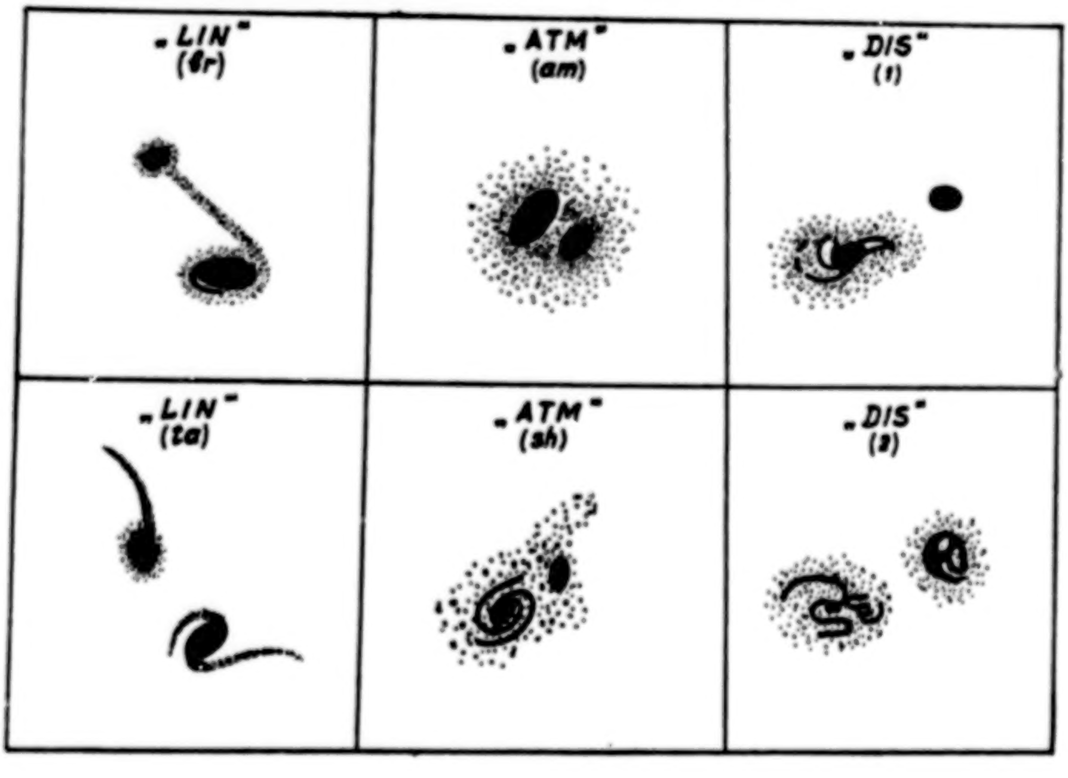

Fig. 6. Scheme of interaction signs for the pair members. "LIN" - linear structures of bridge type (br) or the tail, one (ta)."ATM" - amorphous (am) or shredded (sh) atmosphere. "DIS" - structure distortion in one (1) or both (2) components.

Recently much evidence has been gathered in favor of the fact that star-formation processes in binary systems go more actively, than in field galaxies or members of rich clusters. This is indicated by: the observed infrared and radio emission excess in binary galaxies (Stocke, 1978, Lonsdale *et al.* , 1984; Sulentic, 1989), increased frequency of supernova outbursts (Smirnov, Tsvetkov, 1981), and a high percentage of double systems among Seyfert objects and quasars (Heckman *et al.* , 1984; Dahari, 1984). In pairs with small radial-velocity difference and small separation of their components, i.e. where tidal interaction is most effective, blue Markarian galaxies are met especially often.

According to photoelectric data (Demin *et al.* , 1984), binary system components show a relationship in color indices (Holmberg effect). For spiral galaxies in pairs their bluish color and correlation of color indexes may, probably, be explained by simultaneous star-formation bursts, periodically repeated because of mutual tidal perturbation. In pairs with elliptical components, where gas resources for such bursts are not large, the observed color correlation might result from similar chemical abundances of components at the epoch of their mutual origin.

5. PAIRS AS A POPULATION

Considering binary galaxies as a metagalactic population, we may note the following properties of their distribution.

a) The relative number of galaxies in the sample brighter than $m = 15.7$ is 0.042, and their abundance per unit volume is rather higher : 0.12 ± 0.02.

b) The spatial distribution of pairs obeys a common law of hierarchical clustering. About 90 per cent of nearby pairs are members of known nearby galaxy groups. Not less than half of binary systems with radial velocities $V_0 < 2400$ km/s form part of the Local Supercluster.

c) The two-point correlation function for pair centers has a shallower slope in the interval 1-10 Mpc, than the standard Peebles function (1980). This means that binary galaxies usually avoid dense supercluster regions. Such a tendency is seen in Figure 7, where the overall distribution of pair centers in the sky is shown in equatorial coordinates.

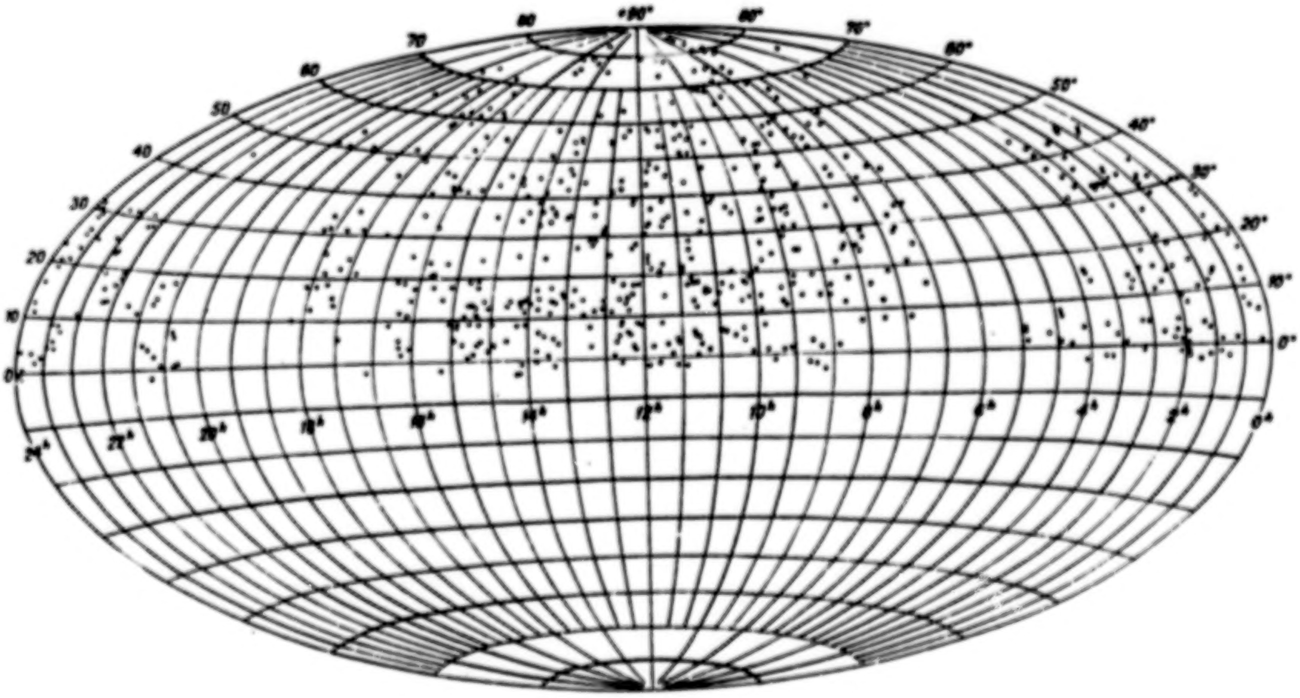

Fig. 7. Distribution of pairs on the sky in equatorial coordinates.

d) Pairs of galaxies in groups and clusters are distinguished by small values of mutual distance between their components. Pairs, compared to single members of a system, reveal a distinct tendency to be located mainly in the less dense peripheral regions of groups and clusters. The hypothesis of tidal destruction of wide pairs in systems gives us an estimate of the system mass, which satisfactorily agrees with the virial mass.

e) The RMS difference of radial velocities for catalogued binary galaxies is 170 km/s. Nearly the same value (194 km/s) was obtained by Davis and Peebles (1983) from the CfA survey data. Using a relation between distance modulus and average velocity for nearby pairs we estimated the value of peculiar motions of their centers: $\sigma(v_p) < 80$ km/s. In the picture of galaxian gravitational clustering (Turner *et al.* , 1979), this estimate corresponds to an open cosmological model with density parameter $\Omega_0 < 0.1$.

6. ANGULAR MOMENTA

To understand the conditions of formation and dynamical evolution of binary systems, data on the magnitudes and mutual orientations of angular momenta of galaxies in pairs have principle significance. Until recently, this question did not attract proper attention. Because of the almost circular character of their motions, double galaxies possess large orbital momentum. In 75% of catalogued pairs the orbital momentum exceeds the value of total rotational momentum for our Galaxy.

The relation $\mu_{12} = |\mathrm{K}_{12}|/[|\mathrm{K}_1| + |\mathrm{K}_2|]$ between a pair's orbital momentum value and the sum of spins of pair components essentially depends on galaxy structural type (see Figure 8). Double systems of spiral galaxies possess relative momentum $\mu_{12} \approx 1.3 - 2.5$, pairs with galaxies of Sm type occupy the region $\mu_{12} \approx 1$, and for double elliptical galaxies the main part of angular momentum is caused by orbital motions ($\mu_{12} \approx 10$).

In almost all scenarios of galaxy formation some preferred orientation of orbital and spin momenta is predicted for binary galaxies. Attempts to find such tendencies were not successful. The distribution of pair components in position angle of major axes and inclination angle testifies to a chaotic orientation of rotation vectors. Some authors' indications of excess numbers of pairs with antiparallel spins (Helou, 1984) should be further tested in observations. An initial ordering of spins in binary galaxies might be destroyed due to loss of mass and angular momentum during a stage of violent dynamic evolution. A notable part might be played by precession and nutation processes. Thus, for spiral galaxies in contact pairs a typical precession period is only 2×10^9 years.

7. ON THE RATE OF DYNAMICAL EVOLUTION

Galaxies in double systems reveal mutual correlation in almost all their integral properties : luminosity, linear diameter, structural type, mass-to-luminosity ratio, angular momentum etc.. Relationship of components according to these parameters is not due only to observational selection, but has a physical basis. As the above-mentioned features characterize the global structure of a galaxy, it seems improbable that such resemblance might appear in pair components during the process of their common evolution. Without risk of serious error, we may suppose that the structural similarity of binary galaxies is caused by similar conditions in which the system components were being formed.

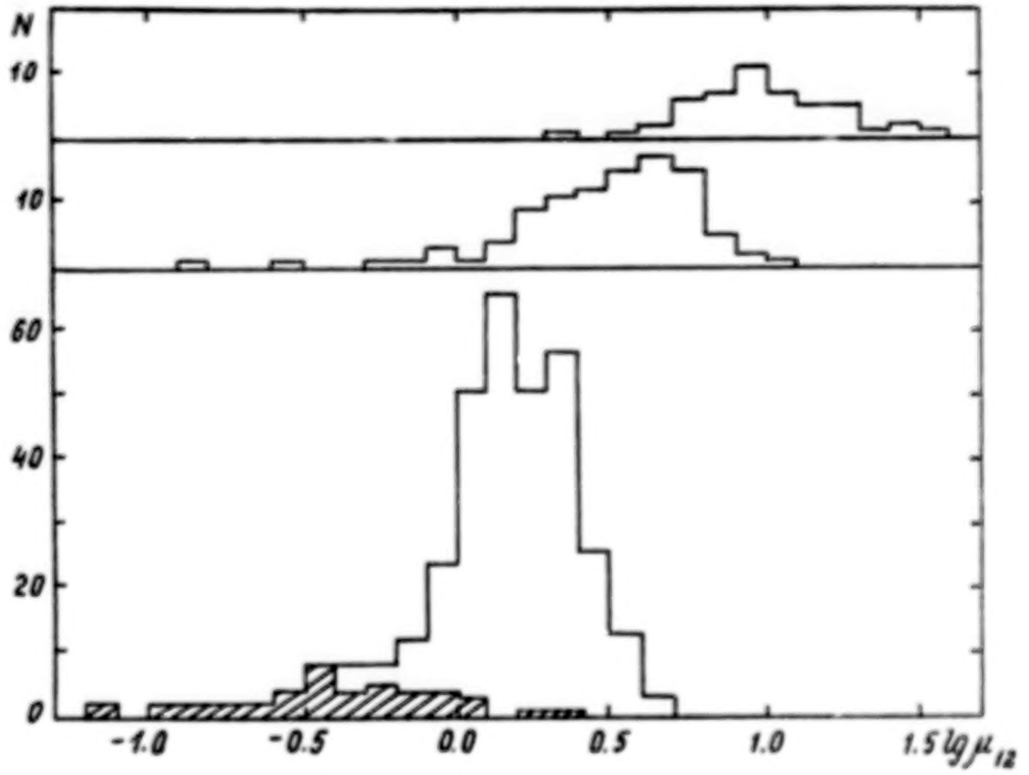

Fig. 8. Distribution of binary systems according to the ratio of their orbital momentum to sum of spins . From bottom to top, pairs with SS, SE and EE components, relatively, are shown. Pairs consisting of one or two Sm galaxies are hatched.

Along with signs of "genetic", relic relationship, binary galaxies show positive correlations of spectral types (emission features) and color indexes. An approach to common values of these properties should apparently take place under active coevolution subject to mutual tidal perturbation (the gaseous component of a galaxy is dynamically more active than the stellar one).

Numerical experiments conducted by Toomre and Toomre (1972), White (1978), and other authors, pointed out the important role of dynamical friction in double galaxies' evolution. After approaching to a distance equal to the sum of their diameters, pair members manage to perform only 2-3 damping revolutions and merge into a single system.

Ostriker and Turner (1979) drew attention to the fact that pairs with large massive components merge fastest. For reason, a lack of giant galaxies among tight binary systems should be observed. As is seen from Figure 9 such an effect for the catalogued pairs is really present, but is hard to distinguish from a result of the selection criterion.

The process of dynamical friction may lead to a specific evolutionaary selection of pairs acording to their orbital eccentrity. If an elongated orbit and small perigalaxian distance favour a merging, then only binary systems with mainly circular orbits survive to the present epoch.

According to the data of Figure 10, the median orbital period for the pair members is $\tau_m = 0.06$ in units of cosmological age H^{-1} . As the merging time exceeds the orbital

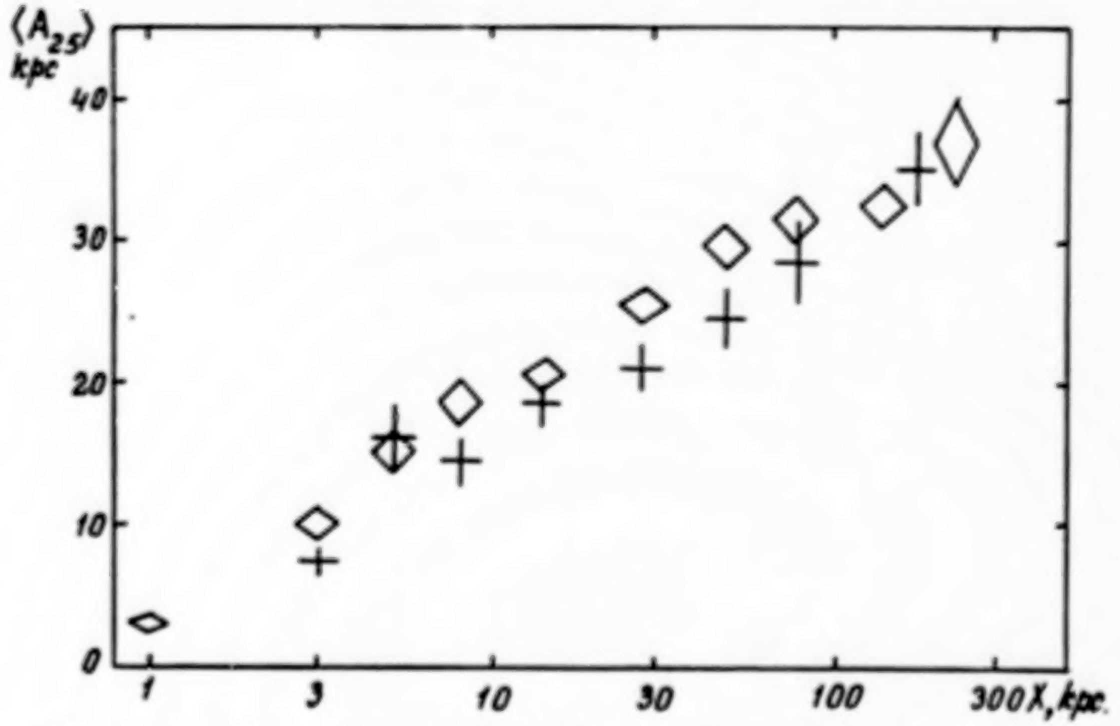

Fig. 9. Dependence of average linear diameter of pair components on their projected separation. Rhomboids show catalogued pairs, crosses simulated pairs. For the simulated pairs the "diameter versus separation" correlation is caused exclusively by selection effects.

period by only 2-3 times, during $\tau_m = 0.1 - 0.3$ most of the catalogued pairs should become single objects. Such a short scale for merging of double galaxies is argued thus: during $\tau = 1$ the merging process would lead to an irreversible accumulation of single galaxies in numbers significantly exceeding the observed relative number $\delta_1 < 0.05$ of isolated galaxies. However, this is only an apparent contradiction, as binary systems' distribution is subject to a general law of hierarchical clustering. Having experienced merging, pairs in groups and clusters do not become isolated objects of a metagalactic field.

With the relative abundance of binary galaxies $\delta_2 = 0.12$ and characteristic merging scale $\tau_m = 0.2$ the expected number of merging acts per galaxy is $< m > \approx 0.6$ during the cosmological time $\tau = 1$. If in earlier epochs the pair merging rate was higher, by the present time many galaxies should be considered to have experienced several mergers. Indirect affirmation may be provided by the increased number of blue objects among faint remote galaxies (Zepf and Koo, 1989). During their merging, double galaxies experienced bursts of star formation, becoming bluer and thereby more notable at large distances.

If many galaxies possess extended massive coronae, their presence should accelerate a merging process. As a result, a peculiar evolutionary selection might appear: we observe binary systems without coronae now, because their merging rate is not so high as in the rest of galaxies.

These discussions give us a picture of rather violent dynamical evolution of galaxies and their systems, where the most active role belongs to double galaxies. To understand to what extent this scenario is justified, further observational efforts are needed.

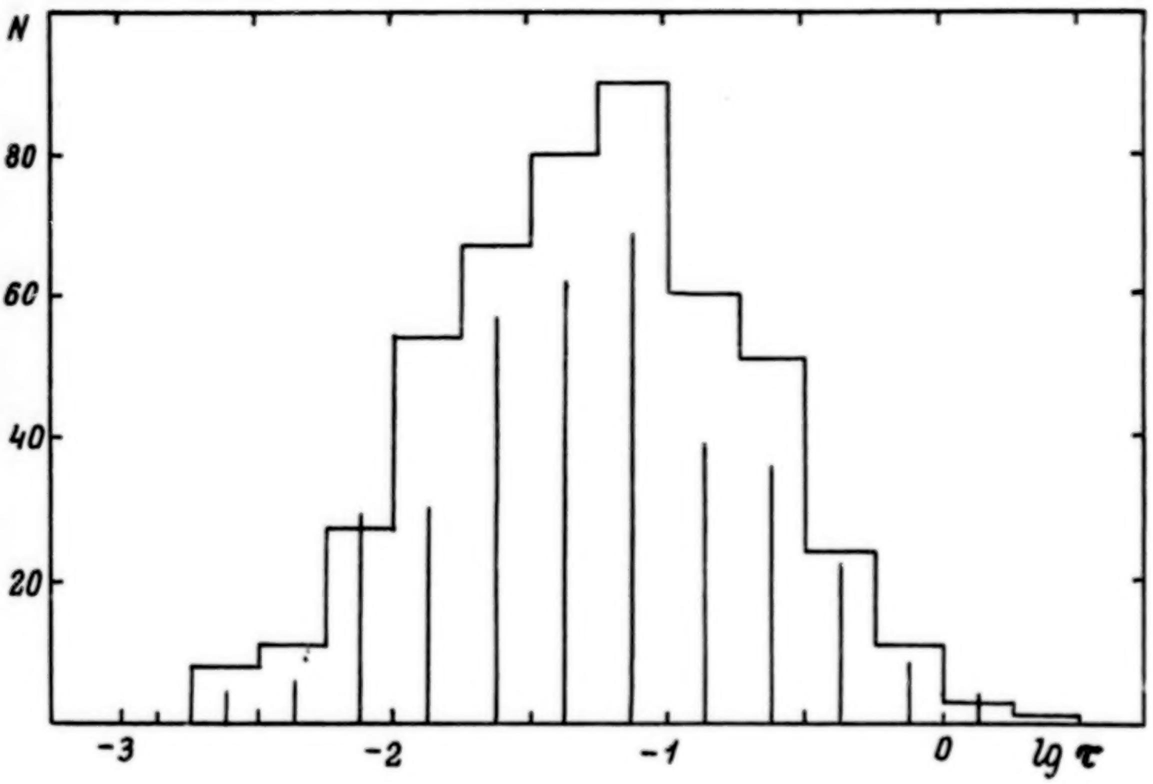

Fig.10. Distribution of isolated pairs according to their dimensionless orbital period, expressed in the units of inverse value of the Hubble constant. Histogram - period estimations based on separations and luminosities of binary galaxies, vertical segments - estimates using separations and radial velocity differences.

8. CONCLUDING REMARKS

Until recently, simulations of dynamical phenomena in pairs of galaxies were limited by rather primitive schemes: single encounter event, a single-component structure of galaxies and ignoring the role of collective processes. There is a pressing need to perform numerical experiments accounting for the kinematic properties of flat and spheroidal components of double galaxies, and also the presence of gas in their disks. Many double galaxies have inner rotation periods close to their orbital period. The characteristic time of a burst of star formation is of the same order, when triggered in galactic disks because of mutual tides. Coincidence of three characteristic times may lead to the intensifying and interweaving of various resonance effects. Therefore, active synchronous evolution of binary galaxies may proceed far from the evolution tracks of single galaxies.

REFERENCES

Arp, H.,1966, Atlas of peculiar galaxies. Astrophys. J. Suppl.Ser.,14, 3.
Clutton-Brock M., 1972, Astrophys. Space Sci., 17, 292.

Dahari O., 1984, Astron. J., 89, 966.

Davis M., Peebles P.J.E., 1983, Astrophys. J., 267, 465.

Demin V.V., Zasov A.V., Dibaj E.A., Tomov A.N., 1984, Astron. Zh., 61, 625.

Heckman T.M., Bothun G.D., Balick E., Smith E.P., 1984,Astron. J., 289, 1958.

Helou G.,1984, Astrophys. J., 284, 471.

Holmberg E. 1937, A Study of Double and Multiple Galaxies - Annals of the Observ. of Lund, 6, 5.

Holmberg E., 1954, Medd. Lunds. Astron. Obs., Ser.1, No 186, 1.

Karachentsev I.D., 1972, Catalogue of isolated pairs of galaxies in northern hemisphere. Soobshch. Spets. Astrofiz. Obs., 7, 3.

Karachentsev I.D., 1980, Astrophys. J. Suppl.Ser., 44, 137.

Karachentsev I.D., 1987, Binary galaxies, Moscow, Nauka.

Londsdale C.J., Persson S.E., Mathews K., 1984, Astrophys. J.,287,95.

Lundmark K., 1927, Uppsala obs. medd., 30, 3.

Ostriker J.P., Turner E.L.,1979, Astrophys. J.,234, 785.

Page T., 1952, Astrophys. J., 116, 63.

Page T., 1960, Astrophys. J., 132, 910.

Page T., 1967, In: Proc. of 5 Berkeley Sympos. Math. Statist. and Probability - Berkeley-Los Angeles, 31.

Peterson S.D., 1979, Astrophys. J. Suppl. Ser., 40, 527.

Schweizer L.Y., 1987, Astrophys. J. Suppl. Ser., 64, 411.

Smirnov M.A., Tsvetkov D.Yu., 1981, Astron. Zh. Let., 7, 154.

Stocke J.T., 1978, Astron. J., 83, 348.

Sulentic J., 1989, Preprint.

Turner E.L., 1976, Astrophys. J., 208, 20.

Turner E.L., Aarseth S.J., Gott J.R., Mathieu R.D., 1979, Astrophys. J., 228, 684.

Tifft W.G., 1982, Astrophys. J. Suppl. Ser., 50, 319.

Toomre A., Toomre J., 1972, Astrophys. J., 178, 623.

White S.D.M., 1978, Mon. Not. R. Astron. Soc., 184, 185.

Vorontsov-Velyaminov B.A., Krasnogorskaya A.A., Arkhipova V.P. 1962, Morphological Catalog of Galaxies, I-IV, Moscow, MGU.

Vorontsov-Velyaminov B.A., 1959, Atlas and catalog of interacting galaxies, Moscow, MGU.

Vorontsov-Velyaminov B.A., 1977, Atlas of interacting galaxies, Astron. Astrophys. Suppl. Ser., 28, 1.

Zepf S.E., Koo D.C., 1989, Astrophys. J. 337, 34.

Zwicky F., Herzog E., Wild P., Karpowicz M., Kowal C., 1961-1968, Catalogue of Galaxies and of Clusters of Galaxies, I-VI, California Institute of Technology, Pasadena.

DISCUSSION

Miller: There are many spiral-spiral pairs in your catalog. A simple observational feature is the number of pairs in which both members have the same sense of spiral pattern as contrasted with the number in which they have the opposite sense of pattern. This relates to the question of whether galaxy rotation might result from gravitational torques.

Karachentsev: Among 54 physical (ΔV_{12} < 500 km/s) SS-pairs with distinct spiral patterns for both components, there are 17 cases with the same sense (9 SS and 8 ZZ) and 37 ones with the opposite senses (17 SZ and 20 ZS).

Xu: While the entire CPG catalog is homogeneous, we found that the E + E subsample is highly inhomogeneous. There is a strong concentration of E + E pairs around $V_r \sim 7000$ km/sec. Could you explain the reason for this effect?

Hickson: Your binaries seem to be very uniformly distributed on the sky, and you mentioned that they avoid clusters. Could this be a result of your isolation criterion?

Karachentsev: Yes, this is one of probable reasons of the effect. Another one may be related to a tidal disruption of wide pairs inside dense regions of clusters. As a matter of fact, tidal mass estimations for the Coma and Virgo clusters are in good agreement with their virial masses.

Roos: Several of your conclusions depend on the orbital angular momentum of the pairs in your catalogue. You found a mean value of the orbital eccentricity of only ~0.25. Could you give us an estimate of the width of the distribution of ellipticities?

Karachentsev: According to my data, for the observed sample of 487 binaries their mean value of orbital eccentricity lies in the interval 0 to 0.55.

Chatterjee: What is the observational value of the frequency of merging galaxies in the present and past epoch?
A comment: most of the mergers take place in 2 to 3 orbital periods. The first orbit affects the circularization.

Karachentsev: Two observational quantities, the relative number of binary galaxies ($\delta_2 = 0.12$) and the typical merger time scale ($t_m \approx 0.2\ H^{-1}$) , give us a characteristic number of mergers, $\langle m \rangle \approx \delta_2/\tau_m \approx 0.6$, per galaxy during the H^{-1} time. Taking into account the possibility of more favorable conditions for a merger in the past (small mutual separations, much more orbits with high eccentricity), the true cumulative frequency of mergers may be as high as $\langle m \rangle > 1$.

PAIRS OF GALAXIES IN LOW DENSITY REGIONS OF A COMBINED REDSHIFT CATALOG

Jane C. Charlton (University of Arizona)

Edwin E. Salpeter (Cornell University)

Abstract

The distributions of projected separations and radial velocity differences of pairs of galaxies in the CfA and SSRS redshift catalogs are examined. We focus on pairs that fall in low density environments rather than in clusters or large groups. The projected separation distribution is nearly flat, while uncorrelated galaxies would have given one linearly rising with r_p. There is no break in this curve even below 50 kpc, the minimum halo size consistent with measured galaxy rotation curves. The significant number of pairs at small separations is inconsistent with the N-body result that galaxies with overlapping halos will rapidly merge, unless there are significant amounts of matter distributed out to a few hundred kpc of the galaxies. This dark matter may either be in distinct halos or more loosely distributed. Large halos would allow pairs at initially large separations to head toward merger, replenishing the distribution at small separations. In the context of this model, we estimate that roughly $10 - 25\%$ of these low density galaxies are the product of a merger, compared with the elliptical / S0 fraction of 18%, observed in low density regions of the sample.

Introduction

The classical samples of binary galaxies (e.g., those of Turner (1976) and Kharachentsev (1974)) included pairs on the basis of their projected separation, but the availability of redshift catalogs now allows the incorporation of radial velocities in a pair selection criterion. We examine the distributions of radial velocity difference Δv and projected separation r_p of pairs in the Northern CfA 14.5 magnitude limited, and the comparable Southern Sky Redshift Survey diameter limited, redshift catalogs. This study is similar in style to those of Rivolo and Yahil (1981) and of Davis and Peebles (1983). In order to reduce the degree of contamination by pairs that are members of triplets or larger groups, it is common to apply an isolation criterion (e.g., Turner 1979; Rivolo and Yahil 1981). We do not apply an isolation criterion, so as to avoid any subtle selection biases it might introduce, but instead use an overall density criterion to separately consider pairs in low and high density regions. In this paper, we focus on pairs residing in low density regions which may include members of small groups, as well as isolated binaries. The Δv and r_p histograms in conjunction with previous N-body results will allow us to draw conclusions about the sizes of galactic halos. Finally, a revival of the replenishment picture of galaxy mergers (Ostriker and Turner 1979) will allow a rough estimate of the galaxy merger rate.

The Redshift Samples

We consider a combined pair sample extracted from the Northern CfA and the Southern Sky Redshift Survey catalogs (SSRS). The Northern region ($\delta \geq 0$, $b \geq 40\,\mathrm{deg}$) of the CfA redshift survey (Huchra and Geller 1982), complete to magnitude 14.5, contains ~ 1900 galaxies. Many now have 21 cm redshift measurements so that the median error in the radial velocity, v, is 23 km/s. The SSRS region ($\delta \leq -17.5\,\mathrm{deg}$, $b \leq -30\,\mathrm{deg}$) (da Costa, *et. al.* 1988) is roughly comparable in area (~ 1.75 steradians) and contains roughly the same number of galaxies since its diameter limit (≤ 1.26 ') is comparable to the Northern magnitude limit. We compute the selection function (which decreases by a factor of ~ 10 over the range $1100 < v < 4500$ km/s in these catalogs), and use it to compensate the observed density at different v. (Fortunately this does not bias the r_p distribution, since pairs with larger r_p are equally likely to be excluded.)

We classify each galaxy as being in a high or low density environment by counting the number of neighbors within $r_p < 5$ Mpc (using $h = 0.75$) and $\Delta v < 375$ km/s of each galaxy and, using the selection function, scaling this count to the number that would be expected if the primary galaxy were at $v = 1100$ km/s. (This volume, although it is much larger than small groups and cluster cores, is smaller than a supercluster.) This procedure yields a median body-centered density of ~ 0.06 galaxies / Mpc^3 brighter than absolute magnitude $M = -15.7 + 5\log h$. Galaxies with densities lower than the median are considered to be in a low density region, and are very seldom members of known clusters such as Virgo, Eridanus, or Fornax. The low density galaxies have a median density of ~ 0.03 galaxies / Mpc^3, while the corresponding number for high density is 0.1 galaxies / Mpc^3.

Radial Velocity Difference and Projected Separation Distributions

Radial velocity difference histograms for pairs with r_p in various ranges are given in Figures 1a-d. Only pairs with the primary member in a low density environment are included in the histograms. A primary galaxy must be at least as far from the catalog edges as the maximum Δv or r_p of pairs displayed in the histogram so that catalog edges do not lead to bias in the distribution. The full sample (solid line) includes "isolated pairs" as well as "group pairs", and "deceptive velocity difference pairs" (DVDP). In some cases the isolated pairs are the brightest two members of a distant group, but most of the group pairs do not contain both of the two brightest members. In "deceptive velocity difference pairs" the peculiar velocities of pair members (relative to smooth Hubble flow) are oriented so as to yield small values of Δv, although the true physical separation in the z direction is quite large. These are to be distinguished from "optical pairs" that have small r_p, but large Δv. In Figure 1 we see that the level of the histogram at large Δv increases with r_p, as would be expected due to the increased area of the bin. At all r_p there is an excess, over the background, of pairs with small Δv (< 150 km/s); so we focus on these pairs and examine their r_p distribution. Figure 2a gives the distribution of r_p out to 3 Mpc, and Figure 2b is a "blow-up" of the region at small r_p (< 0.4 Mpc) that is of particular interest. The distribution is remarkably flat, with equal numbers in equal r_p bins, even down to r_p values as low as 20 kpc. No significant kinks or breaks in the curve are apparent. (For larger Δv pairs the slope of the r_p distribution increases, with fewer pairs at small r_p.) We see that the phase space density of pairs is largest when both r_p and Δv are small.

"Halo" Sizes

First, we should note that observed galaxy rotation curves demonstrate that a $\rho \sim r^{-2}$ halo is present, in many instances, out to 50 kpc. Thus we know that pairs with separations ≤ 100 kpc are likely to have overlapping halos. This is important because N-body simulations (White 1978; Carlberg 1982) demonstrate that once halos overlap mergers occur readily (within $\sim$ one orbital period) due to dynamical friction. The observed flat, smooth, r_p distribution is inconsistent with a picture in which halos truncate at small r_p, since rapid depletion of $r_p < 2R_{halo}$ pairs would occur while the r_p distribution at larger

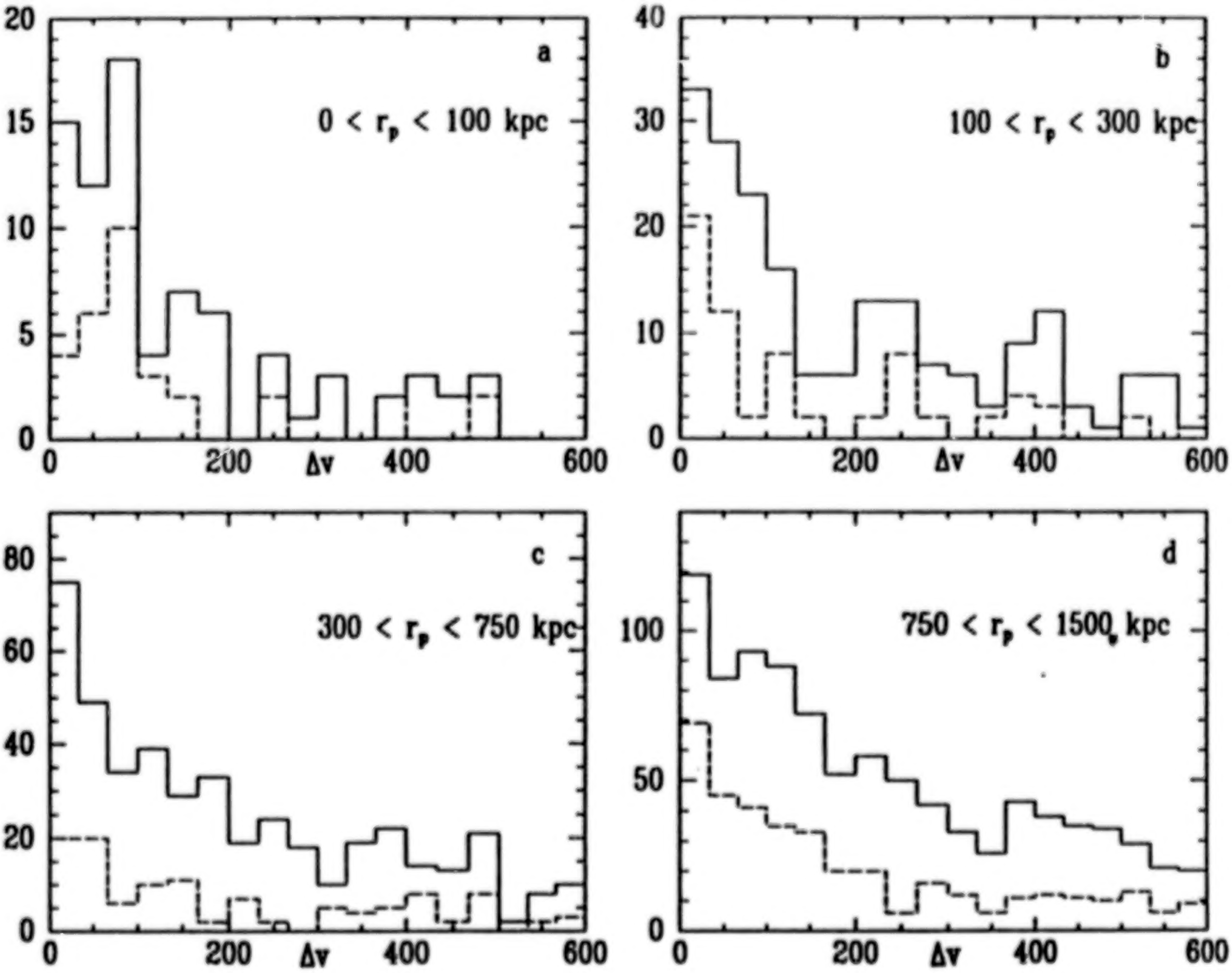

Figure 1: Histograms of the radial velocity differences Δv of pairs of galaxies in low density environments, for four different ranges of pair projected separation r_p, are given. The units of Δv on the horizontal axis are km/s. The solid curve represents all low density pairs, while the dotted curve is only those that are isolated within 300 km/s in Δv and 0.75 Mpc in r_p.

values would remain intact. Larger halos could preserve a flat r_p distribution because the small r_p region, depleted by rapid mergers, would be replenished by originally larger r_p pairs headed toward merger (see Ostriker and Turner 1979). In a realistic model, halos would have a range of sizes, and orbits, a range of eccentricities, thus it is difficult to give a specific lower limit on halo sizes. For $r_p >$ several hundred kpc many pairs are likely to have orbital periods exceeding a Hubble time, thus complete depletion of smaller r_p would not be expected. It is clear, however, that halos smaller than a few hundred kpc are inconsistent with the observed flat r_p distribution.

We want to emphasize that we are using the term "halo" quite loosely. The above arguments cannot distinguish between a $\rho \sim r^{-2}$ halo cutting off abruptly at a few hundred kpc, and one that has relatively less mass beyond ~ 50 kpc, (e.g., $\rho \sim r^{-3}$). Alternatively, the dark matter could be evenly distributed on larger scales and loosely concentrated about pairs and groups of galaxies, rather than attached in the form of individual halos.

The above picture can be described by the parameter $\dot{R}$, the orbit averaged rate of change of a pairs' three dimensional separation. The shape of the r_p distribution allows us to place loose constraints on the dependence of $\dot{R}$ on the separation R of a pair. Roughly speaking, $\dot{R} \sim R^{\beta}$ where $-1/2 \leq \beta \leq 0$ would be consistent, since for $\beta = -1/2$ the increase in speed as the galaxies approach could be compensated in the r_p distribution by projection effects. The simple picture in which the approach is at a constant rate, $\beta = 0$, (shifting the r_p distribution to the left with time) is also certainly allowed, and we shall estimate the galaxy merger rate in this context.

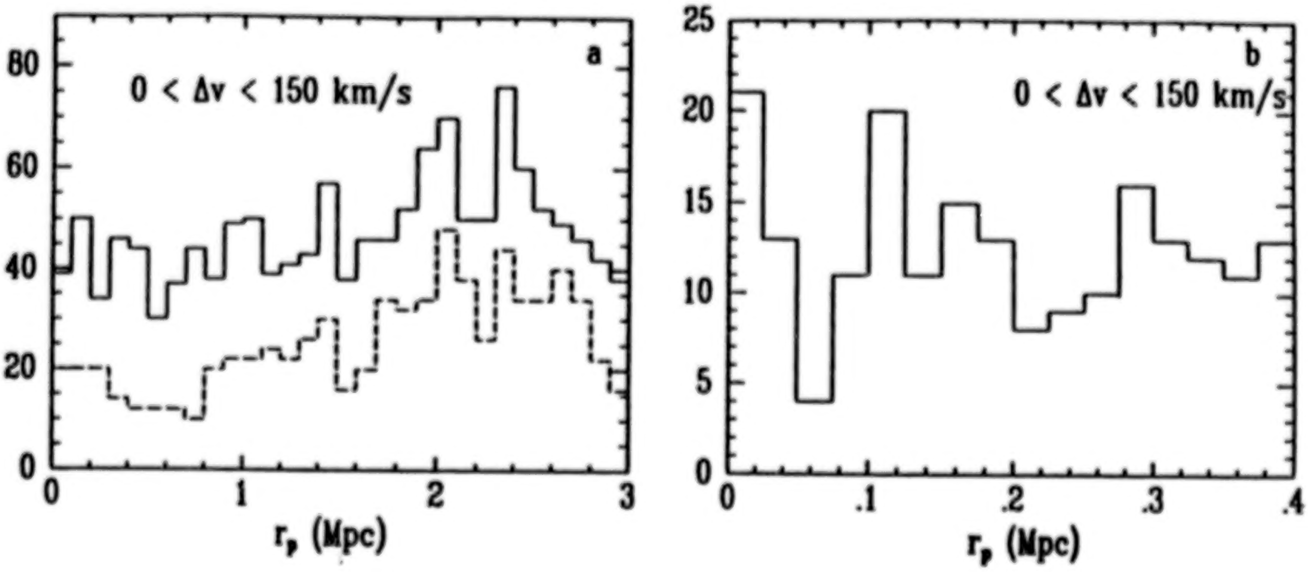

Figure 2: The projected separation r_p distribution is given for low density pairs with small Δv ($0 < \Delta v < 150$ km/s). The solid and dotted curves are the full sample and isolated pairs respectively, as in Figure 1. In a, the range of r_p from 0 to 3 Mpc is examined, while b is a more detailed representation of small values of r_p for the same distribution.

Galaxy Merger Rate

The present galaxy merger rate can be estimated, using $\dot{R}$ and the present distribution of r_p. For example, if $\dot{R}$ is constant ($\beta = 0$) the initial r_p distribution is simply shifted toward smaller values, retaining its shape. (Results will be quantitatively different for non-zero values of β.) The number of pairs to merge within a Hubble time t_H is then the number of pairs in the present r_p distribution with $r_p < \dot{R} \times t_H \times \sqrt{3}/2$, where $\sqrt{3}/2$ is a geometric factor due to projection. This is equal to the total number of low density pairs to merge by the present, assuming that the now hidden portion of the initial distribution of r_p, that has been shifted to merger, was also flat. The merger rate is conveniently expressed in terms of the dimensionless ratio $\xi = \dot{R}/\Delta v_{3D}$ where Δv_{3D} is the median three dimensional velocity difference between pairs. We estimate that $\Delta v_{3D} \sim 150$ km/s for "real pairs" from Figure 1, and ξ can be computed from N-body results for particular orbits. Thus pairs with $r_p < 1.9\xi$ Mpc have merged by the present, resulting in $\sim 49\xi\%$ of low density primaries as merger products. From simulations of the merger of two $N = 250$ galaxies on orbits with eccentricities ranging from circular to radial, we extract typical values of ξ of $0.2 - 0.5$, yielding roughly $10 - 25\%$ of low density galaxies as merger products. In this sample 18% of low density primaries are observed to be elliptical or S0 galaxies.

Further Work

In this paper we have chosen to focus on pairs in low density regions, specifically their implications for galactic halo sizes and the galactic merger rate. This work is part of a larger study (Charlton and Salpeter 1990, in preparation) that will include a more detailed study of the above issues as well as a presentation of r_p and Δv distributions for pairs in high density regions. In addition, we have analyzed scatter diagrams of r_p, Δv, and the geometric mean pair luminosity L_{gm}, and find none of the correlations that would have been expected for Kepler orbits (e.g., $\Delta v \sim r_p^{-1}$). In fact, we see a puzzling tendency for larger luminosity pairs to have smaller Δv. We would like to acknowledge support from NSF grant AST 87-14475 at Cornell and NSF grant AST 88-22297 at Steward Observatory.

References

Carlberg, R. G. 1987, *M. N. R. A. S.*, **199**, 1159.

da Costa, L. N., Pellegrini, P. S., Sargent, W. L., Tonry, J., Davis, M., Meiksin, A., Latham, D. W., Menzies, J. W., and Coulson, I. A. 1988, *Ap. J.*, **257**, 423.

Davis, M., and Peebles, P. J. E. 1983, *Ap. J.*, **267**, 465.

Huchra, J., and Geller, M. 1982, *Ap. J.*, **257**, 423.

Kharachentsev, I. D. 1990, in *Paired and Interacting Galaxies: I.A.U. Colloquium 124*, ed. J. W. Sulentic, W. Keel, and C. Telesco (N.A.S.A.), in press, p. 3

Ostriker, J. P., and Turner, E. L. 1979, *Ap. J.*, **234**, 785.

Rivolo, A. R., and Yahil, A. 1981, *Ap. J.*, **251**, 477.

Turner, E. L. 1976, *Ap. J.*, **208**, 20.

White, S. D. M. 1978, *M. N. R. A. S.*, **184**, 185.

MORPHOLOGICAL TYPE CORRELATION
BETWEEN
NEAREST NEIGHBOR PAIRS OF GALAXIES

Tomohiko Yamagata
National Astronomical Observatory, Mitaka, Tokyo 181, Japan

I. INTRODUCTION

Although the morphological type of galaxies is one of the most fundamental properties of galaxies, its origin and evolutionary processes, if any, are not yet fully understood. It has been established that the galaxy morphology strongly depends on the environment in which the galaxy resides (e.g. Dressler 1980).

Galaxy pairs correspond to the smallest scales of galaxy clustering and may provide important clues to how the environment influences the formation and evolution of galaxies. Several investigators pointed out that there is a tendency for pair galaxies to have similar morphological types (Karachentsev and Karachentseva 1974, Page 1975, Noerdlinger 1979).

We analyzed morphological type correlation for 18,364 nearest neighbor pairs of galaxies identified in the magnetic tape version of the Center for Astrophysics Redshift Catalogue (Huchra 1987, hereafter CfA Catalog).

II. SAMPLE DEFINITION AND CORRELATION ANALYSIS

a) CfA Catalog

The CfA catalog contains 18,364 galaxies for which radial velocity data are available. This catalog is based on much of the latest velocity data from many sources. There are some galaxies which happen to be registered twice or more. We have adjusted these galaxies as much as we could find, consequently resulting in 18,323 galaxies to be used as sample galaxies in this study.

b) Definition of Nearest Neighbor Pairs

Simply applying the Hubble law, we assigned the distances to the galaxies from us as $r = v/H_0$, where H_0 is the Hubble constant. Thus the distance between a certain galaxy and another is defined by,

$$d^2 = r_1^2 + r_2^2 - 2r_1r_2\cos\theta \tag{1}$$

where θ is the angular separation between the two galaxies. The distances between galaxies of all the possible pairs were calculated using equation (1). Then, the nearest neighboring partners were derived for all the sample galaxies except for one galaxy having two nearest partners at the same distance. We excluded this galaxy in our analysis.

In the CfA catalog, morphology indices are presented, which are mainly based on the Second Reference Catalogue of Bright Galaxies (de Vaucouleurs *et al.* 1976). Galaxies with $-6 \leq T \leq -4$ are ellipticals, $-3 \leq T \leq 0$ are S0's, and spirals are $1 \leq T \leq 9$. Galaxies lacking detailed classification are assigned type indices $T = -7, 15, 16$, and 20 in the CfA Catalog.

We note that our nearest pairs are not always the galaxy pairs in the ordinary sense, for example, when the nearest galaxy to A is B, the nearest to B is not necessarily A but may be a third galaxy C. Other than those exceptional pairs, the same pairs are used twice in the analysis.

c) Morphological Type Correlation

In order to represent the morphological type correlation, we defined the type correlation spectrum $C(\Delta T)$ by

$$C(\Delta T) \equiv \left(\sum_{i-j=\Delta T} n_i^j \right) \Big/ \left(\sum_{i-j=\Delta T} n_i \cdot n_j N \right) \tag{2}$$

where n_i^j gives the number of pairs having the type $T = i$ for the sample galaxy and $T = j$ for its nearest neighbor, and n_i, n_j are the total number of galaxies of $T = i, T = j$ respectively. The total number of nearest pairs is given by N.

We excluded pairs including one or two galaxies having type indices $T \leq -7$ or $T \geq 15$, which means peculiar and/or unclassified morphology. But those pairs are, of course, included in N.

Figure 1 shows the presence of the type correlation at $\Delta T = 0$ for the nearest neighboring pairs of galaxies. If there is no morphological type correlation, then $C(\Delta T) = 1$ for all ΔT (dotted line in Figure). Error bars represent $\pm 1\sigma$ statistical errors due to Poisson distribution.

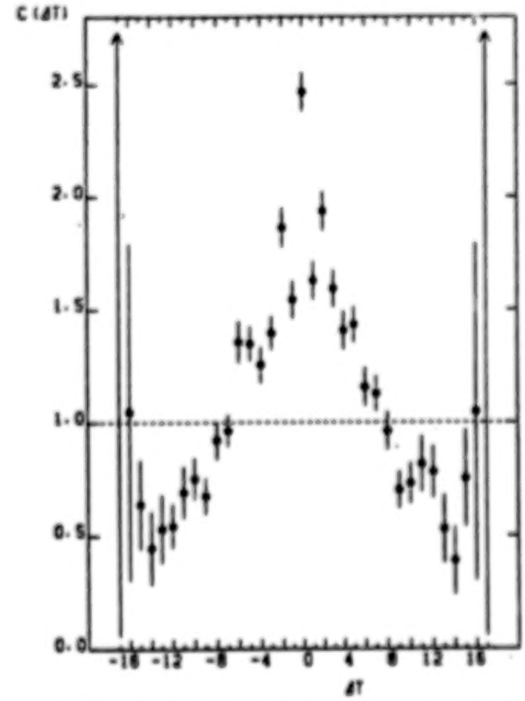

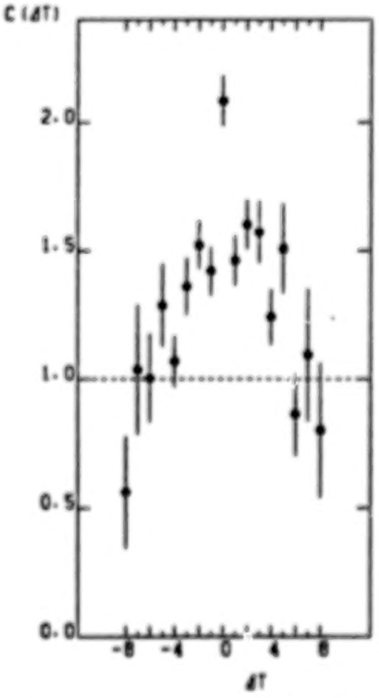

Fig 1 (left). The morphological type correlation spectrum $C(\Delta T)$ for the total sample. The abscissa is the difference of the type indices between nearest-neighbor pairs.

Fig 2 (right). Same as Fig. 1, but the data are limited to spiral-spiral pairs of galaxies.

It is well known that there exists the morphology segregation between spirals and non-spirals (Dressler 1980, Postman and Geller 1984). Moreover the morphological type of galaxies was classified in much more detail for spirals than for ellipticals in our sample. These facts naturally leads to enhancement of $C(\Delta T)$ around $\Delta T = 0$. In order to check these effects, a similar analysis was carried out for a sample limited to spiral-spiral pairs $(1 \leq T_1, T_2 \leq 9)$. By removing elliptical galaxies from sample pairs, it is expected to see the type correlation free of morphological segregation between spirals and non-spirals. The derived type correlation spectrum for spiral-spiral pairs is shown in Figure 2. This figure also assures the presence of an excess of spectrum at $\Delta T = 0$.

d) IRAS catalog

Our sample galaxies were identified with objects in the IRAS catalog to classify them into two categories: an *IRAS galaxy* which has a counterpart in the IRAS catalog within the following error box, and a *non-IRAS galaxy* with no IRAS counterpart. The error box is defined as follows:

$$\begin{cases} |\alpha - \alpha_0| & < 180" \\ |\delta - \delta_0| & < 180" \end{cases} \tag{3}$$

where (α_0, δ_0) is the coordinate of the galaxy. The identification yields 5,262 IRAS and 13,061 non-IRAS galaxies. We divided 18,322 nearest neighbor pairs into three classes; the pairs in the first class consist of both non-IRAS galaxies, the pairs consisting of both IRAS galaxies for the second class, and those of an IRAS and a non-IRAS galaxy for the third. The number in each class is 10,201, 2,425, and 5,696 pairs, respectively.

The type correlation spectrum is re-calculated for each of three classes. The total number of pairs with classified types is given by $(N_p \equiv \sum_{i,j=-6}^{11} n_i^j$, and amounts to 3,004, 1,315, and 2,608 for each of three classes respectively.

The results are shown in Figures 3a, b, and c. The strong type correlation peaked around $\Delta T = 0$ can only be seen for pairs of both non-IRAS galaxies (Figure 3a) while no correlation for pairs of both IRAS galaxies showing only statistical fluctuation at the level of $C(\Delta T) = 1$ except for $\Delta T = 0$ (Figure 3b). For the third class, there can be seen only statistical fluctuation around $C(\Delta T) = 1$ (Figure 3c). We note that there are spikes at $\Delta T = 0$ both in figures 3a and 3b but not in figure 3c.

III. DISCUSSION

a) Completeness in the catalogs

The CfA Catalog contains velocity data from many sources, which are distributed over the whole sky. Galaxies in the CfA Catalog do not form a complete sample, in the sense that each source has different limiting magnitude. We neglected the incompleteness of the catalog in this study. A Complete sample of galaxies can be obtained from the CfA Catalog, if the restricted area of the sky is adopted. One of such examples is called "North Zwicky Forty" (Huchra *et al.* 1983). The type correlation spectra were calculated with the sample limited to the "North Zwicky Forty" region. The results are essentially similar to those of Figures 1 and 2, except for the increase of the statistical fluctuation due to the smaller number of sample galaxies, thus confirming that the incompleteness of the CfA catalog does not affect our conclusion.

As for figures 3, the bias effect is introduced by the difference of the surveyed depth between CfA galaxies and IRAS galaxies. In order to check this effect, the morphological type correlation is calculated for the sample limited to the galaxies having radial velocity less than $5000 kms^{-1}$. Comparing with figures 3, the results are essentially similar except for the increase in statistical uncertainties due to the smaller number of the sample pairs.

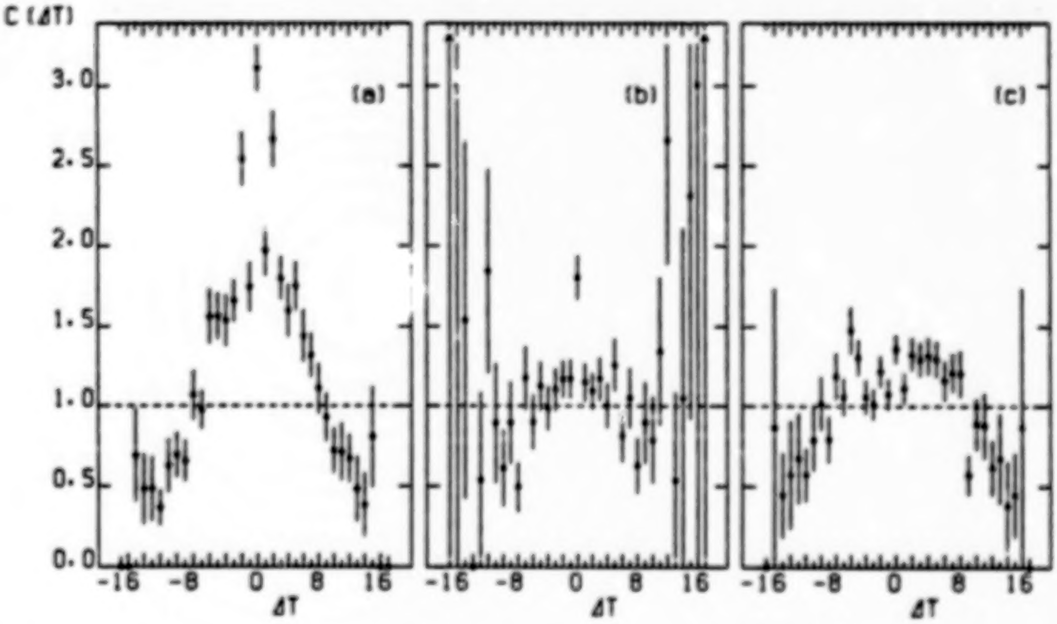

Fig 3. The morphological type correlation spectrum $C(\Delta T)$ for various sub-samples. (a)For the pairs of both non-IRAS galaxies. (b)For the pairs of both IRAS galaxies. (c)For the pairs of IRAS galaxy and non-IRAS galaxy.

In order to clarify that our results are not due to the selection effect, we carried out the morphological correlation analysis upon the sample in which galaxies are distributed randomly in the space of $0 < x, y, z < 30000$. The number of each morphological type is taken as the same as the real sample. As the consequence, there is no correlation seen for this random sample.

b) Morphology Density Relation

It is natural to consider that IRAS galaxies are gas-rich galaxies (e.g., Sanders and Mirabel 1985) which agrees with the fact that IRAS galaxies are mostly spirals (de Jong *et al.* 1984). The gaseous content of field galaxies are richer than that of cluster galaxies (Giovanelli and Haynes 1985, Haynes *et al.* 1984). This is also true for IRAS galaxies, since luminous IRAS galaxies are found in field galaxies and not in cluster galaxies (Bicay and Giovanelli 1987).

According to Postman and Geller (1984), the fraction of spirals or ellipticals is constant in the region of the galaxy density less than 5 galaxies Mpc^{-3}, that is, no morphology density relation is shown, while a clear relation is present for galaxy density greater than 5 galaxies Mpc^{-3}. These facts suggest the possibility that most of IRAS galaxies reside in the region of the galaxy density less than 5 galaxies Mpc^{-3}, while non-IRAS galaxies are considered to be in the region of the density greater than 5 galaxies Mpc^{-3}, if we assume that the origin of the strong correlation in non-IRAS galaxy pairs and no correlation for other pairs is the same as that of the morphology density relation. The morphology segregation is existent even within spiral galaxies (Giovanelli *et al.* 1986). Thus, the same tendency of the morphological type correlation seen in the spiral-spiral pairs (Figure 2) is naturally understood.

c) Twin Galaxies

As seen in Figure 3a, the spiky enhancement of $C(\Delta T)$ at $\Delta T = 0$ is exceptionally high. Moreover, there can also be seen the enhancements of $C(\Delta T)$ at $\Delta T = 0$ for both-IRAS pairs (figures 3b). It is not clear whether these are completely ascribed to the morphology density relation. One explanation is that mechanisms in the early phase of galaxy formation should be responsible to these enhancements. This fact leads us to point out the existence of twin galaxies which are the extreme case of morphological type correlation (Yamagata *et al.* 1989). Twin galaxies are defined as pairs of galaxies which have not only the same morphological type but also similar internal structures. Our nearest neighboring pairs with $\Delta T = 0$ are possible candidates for twin galaxies. It is interesting that the spiky enhancement is seen only in the galaxy pairs with similar IR characteristics (i.e. both-IRAS-galaxy pairs and both-non-IRAS-galaxy pairs). This may suggest that the infrared properties are also similar in twin galaxies as well as other characteristics. All the candidates of twin galaxies were examined by Palomar Sky Survey or ESO prints confirming that both-IRAS pair candidates are mostly spirals. Many of both-IRAS pair candidates have no disturbed shapes expected from galaxy-galaxy collision, thus implying that far-infrared emission in both-IRAS pair candidates is not always due to galaxy interaction.

We are grateful to the Astronomical Data Center at the NASA Goddard Space Flight Center for providing the magnetic tape version of the CfA Redshift Catalogue. T.Y. is indebted to the Japan Society for the Promotion of Science and the Inoue Foundation for Science. This work was supported by the Grant-in-Aid for Encouragement of Young Scientists from the Ministry of Education, Science and Culture, Japan (63790140).

REFERENCES

Bicay, M. D., and Giovanelli, G. L. 1987, *Ap. J.* **321**, 645.

de Jong, T., Clegg, P. E., Soifer, B. T., Rowan-Robinson, M., Habing, H. J., Houck, J. R., Aumann, H. H., and Raimond, E. 1984, *Ap. J.*, **278**, L67

de Vaucouleurs, G., de Vaucouleurs, A., and Corwin, H. G. 1976, *Second Reference Catalogue of Bright Galaxies* (Austin: University of Texas Press)

Dressler, A. G. 1980, *Ap. J.*, **236**, 351.

Giovanelli, R., Haynes, M. P., and Chincarini, G. L. 1986, *Ap. J.* **300**, 77.

Giovanelli, G. L., and Haynes, M. P., 1985, *Ap. J.* **292**, 404.

Haynes, M. P., Giovanelli, R., and Chincarini, G., L. 1984, *Ann. Rev. Astr. Ap.*, **22**, 445.

Huchra, J. P. 1987 *Center for Astrophysics Redshift Catalogue* (CfA Catalog)

Huchra, J. P., Davis, M., Latham, D. W. and Tonry, J. 1983, *Ap. J. Suppl.*, **52**, 89

Huchra, J. P., Geller, M. J., Lapparent, V. and Corwin, H. 1988, in preparation

IRAS Point Source Catalog, 1985, Joint IRAS Science Working Group (Washington, D. C. : NASA) (IRAS Catalog)

Karachentsev, I. D., and Karachentseva, V. E. 1974, *Astr. Zh.*, **51**, 724. (English translated in *Soviet Astr.*, **18**, 428.)

Noerdlinger, P. D. 1979 *Ap. J.*, **229**, 877.

Page, T., 1975 in *Stars and Stellar Systems, Vol.9, Galaxies and Universe* ed. A. Sandage,

M. Sandage, and J. Kristian (Chicago: The University of Chicago Press) P541.
Postman, M., and Geller, M. J. 1984 *Ap. J.*, **281**, 95.
Sanders, D. B., and Mirabel, I. F. 1985, *Ap. J.*, **298**, L31.
Yamagata, T., Noguchi, M., and Iye, M. 1989 *Ap. J.*, **338** 707 (Paper I).

DISCUSSION

Zasov: Could it be that a correlation between morphological types of nearby galaxies is just another manifestation of the so-called Holmberg effect, that is, a colour-index correlation of galaxies in pairs and probably in groups?

Yamagata: The main difference is that our sample doesn't always consist of binary galaxies but nearest-neighbor pairs. The number of pairs in our sample is larger than in any other previous work. A similar analysis was done by Page (1975) for only 427 pairs found by Zonn and Cook (1963). Therefore, the Holmberg effect is one interpretation of our morphological-type correlation.

Mamon: (answer to Zasov's comment) - Hickson's compact groups show morphological correlations as shown by Sulentic (1987) and Hickson, Kindl, and Huchra (1988). I've looked for the same effect for the quartets and quintets in the CFA group catalog of Geller and Huchra (1983) and found no correlation: the fraction of groups with concordant general type (E + L versus S) is consistent with the expected fraction. If morphological correlations are caused by initial conditions at galaxy formation, then one needs to explain why this effect is more pronounced for Hickson's groups than for Geller and Huchra's looser quartets and quintets.

Sulentic: While morphologically concordant pairs certainly exist in great numbers, I would point out that one out of four "physical" pairs in the CPG of Karachentsev (1972) are of mixed (E + S) morphology. They are a striking challenge for galaxy formation theories that correlate galaxy morphology with environmental conditions.

Yamagata: I think it very interesting to investigate whether there is difference between the spatial distribution of the pairs of mixed morphology and that of concordant pairs. Because if there's a difference, we may then know the spatial distribution of the primordial proto-galaxy cloud.

Dey: You showed that there is an effect for spiral-spiral pairs to be of the same morphological type, but that there is very little effect for "IRAS active" pairs. Could you comment on this?

Yamagata: The detection limit of IRAS galaxies is brighter than that of CFA galaxies. We checked the correlation for distance-limited data (V < 5000, V < 6000, V < 7000), the results are essentially the same....no correlation, but enhancement at $\Delta T = 0$. Several possibilities for this phenomena are considered. For example, morphology segregation in spirals existed only in "IRAS-quiet" galaxies, but, frankly speaking, an exact interpretation is not available.

Keel: How much of your type-correlation signal is due to nearest neighbors that are too far apart to be considered physical pairs of galaxies?

Yamagata: As to the separation distance of the pairs, there is essentially no effect on the conclusion. (We checked by the separation-distance-limited data. The correlation is stronger.)

STELLAR KINEMATICS OF ELLIPTICAL GALAXIES IN PAIRS[1]

Rainer Madejsky[2] and Ralf Bender
Landessternwarte Königstuhl
D-6900 Heidelberg, F.R.Germany

1. Introduction: General properties of Arp 166 and 3C 278

Observations of elliptical galaxy pairs allow the study of different states of tidal interaction between galaxies. The comparison with normal elliptical galaxies directly reveals the disturbed morphological and kinematical properties. Numerical simulations have shown that with the known initial luminosity profile, the time elapsed since closest approach between two galaxies can be estimated from the radial position of the disturbances (Aguilar and White, 1986).

The two galaxy pairs Arp 166 (NGC 750/1) and 3C 278 (NGC 4782/3) considered here exhibit distorted and nonconcentric isophotes (cf. Madejsky, 1989). In Arp 166 the major relative shift of the centers of the isophotes occurs in the outer parts while in 3C 278 the nonconcentric isophotes are more pronounced in the inner parts of the galaxies, suggesting that more time has elapsed since the moment of closest approach in Arp 166 than in 3C 278. Furthermore, in Arp 166, both galaxies have the same radial velocity, implying that their orbital plane is perpendicular to the line of sight. In turn, the galaxies NGC 4782 and NGC 4783 are moving with a very high radial velocity difference of 680kms^{-1}. Taking into account the location of both galaxies, which are the dominant members of a small group of about 25 galaxies (De Souza and Quintana, 1990), the true velocity difference probably is not much higher than the observed radial velocity difference. Therefore it is very likely that we are viewing at high inclination onto (i.e. nearly parallel to) the orbital plane of the galaxies NGC 4782 and 4783.

CCD photometry for both galaxy pairs was obtained at the 1.23m telescope of the German-Spanish Astronomical Center on Calar Alto, Spain. The morphology of both galaxy pairs is displayed and briefly discussed in Madejsky (1989).

2.Spectroscopy of Arp166 and 3C278

The long-slit spectroscopic data for NGC 4782 and 4783 were obtained at the ESO 3.6m telescope (for details see Madejsky et al, 1990). The result for the southern galaxy NGC 4782 for position angle 70° is displayed in Fig. 1. The velocity dispersion increases from the center towards the east by a large amount and also slightly towards the west. The region of maximum velocity dispersion is nearly coincident with the centers of the outer isophotes.

---

[1] Based on observations collected at the European Southern Observatory, La Silla, Chile

[2] Visiting Astronomer, German-Spanish Astronomical Center, Calar Alto, operated by the Max-Planck-Institut für Astronomie Heidelberg jointly with the Spanish National Commission for Astronomy

The spectroscopic data for Arp 166 were obtained at the 3.5m telescope on Calar Alto, Spain. For each galaxy, NGC 750 and NGC 751, we obtained longslit spectra for two slit positions, at position angle 60° and 90°, respectively. All slit positions are nearly perpendicular to the line connecting both galaxies and always the slit was centered on the galaxy center. The results for position angle 60° are displayed in Fig. 2 (the kinematical data for slit position 90° are comparable to those displayed here). The central radial velocity of the northern galaxy NGC 750 is 5200(±10)kms^{-1} and there are only slight variations of the radial velocity with radius. No rotation seems to be present in this direction. The central velocity dispersion increases from the central value of 220(±10)kms^{-1} radially outwards. The increase towards the east is very small. Towards the west, however, there is a substantial increase over a large region of more than 10 arcsec (or 5 kpc). The velocity dispersion does not decrease for larger radii within the observational radial limit. The southern galaxy NGC 751 perhaps was rotating rapidly before the tidal interaction. A strong gradient of the radial velocity indicates rotation, but the central part (innermost 6 arcsec or 3kpc) seems to be kinematically separted from the motion of the surrounding envelope. Also in the east part the radial velocity exhibits irregularities. The central radial velocity is 5225(±10)kms^{-1}. The velocity dispersion increases from the central value of

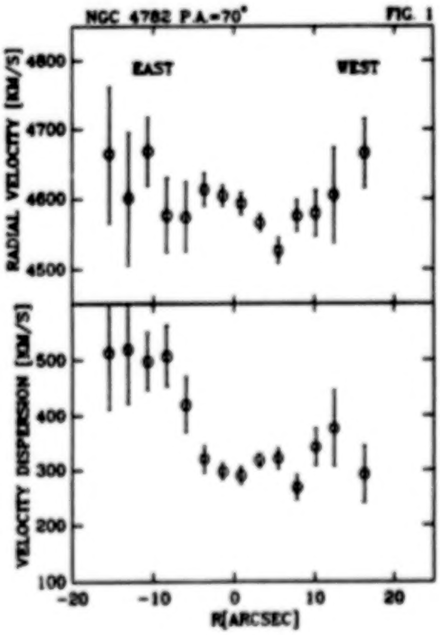

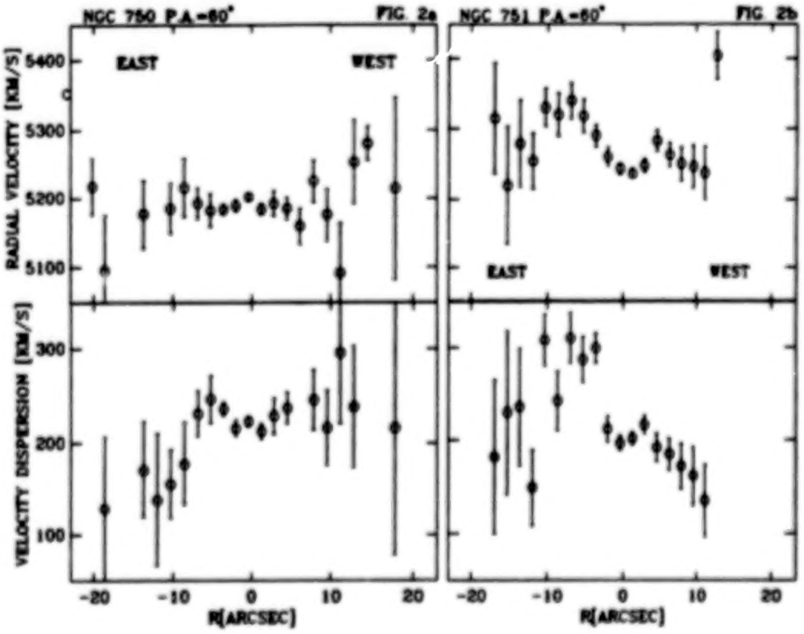

Fig. 1.(left) Radial velocity (upper panel) and velocity dispersion of NGC 4782 along slit position 70°. The velocity dispersion increases radially from the center towards the east by a large amount. Note the slight increase towards the west. The region of maximum velocity dispersion is located near the center of the outer isophotes

Fig. 2a and b.(right) The kinematical results for a) NGC 750 and b) NGC 751 for slit position 60°. In the upper panels are displayed the radial velocities, the lower panels give the velocity dispersions of the stars. Note that the velocity dispersions in both galaxies reach their maximum values outside the centers (see text).

200(±10)kms^{-1} radially towards the east and reaches a maximum value of 300(±25)kms^{-1} in the region 4...10 arcsec (or 2...5 kpc) east of the center of the galaxy. Like in the galaxies NGC 4782 and NGC 4783 we find radially increasing velocity dispersion in both galaxies NGC 750 and NGC 751. In all galaxies the regions of maximum velocity dispersion are found near the centers of the **outer** isophotes, and in both pairs, the galaxy with a steeper luminosity profile exhibits the more pronounced increase of the velocity dispersion.

3. Conclusions

In both galaxy pairs Arp 166 and 3C 278 we find radially increasing velocity dispersions indicating a perturbed, non-equilibrium state of the galaxies after the tidal interaction. In all galaxies, the increase is most pronounced in the regions which correspond to the centers of the outer isophotes. We suggest a scenario in which the galaxies are strongly decelerated on their orbits during the encounter. The deceleration depends on the radial position in the perturbed galaxy and vanishes in the center of the perturbed galaxy (Spitzer, 1958). In addition, the crossing time of the stars near the center is very short, implying that the tidal perturbations can be averaged over several orbital periods (e.g. Binney and Tremaine, 1987). In consequence, the central parts are not affected by the tidal interaction while the outer parts are strongly decelerated. This leads to a displacement of the central parts of the galaxies with respect to their envelopes in an antisymmetrical way for the two components of each galaxy pair. The motions of the central parts subsequently are opposed by dynamical friction with the surrounding envelopes. Due to dynamical friction, the density of the stars increases in the wakes of the moving central parts (Mulder, 1983). The overdensity of stars in the wakes of the moving central parts efficiently decelerates the motions of the central parts. The reaction of the stars in the overdensity regions leads to an increase of the velocity dispersion mainly along the orbits of the moving central parts. The presented observations, especially the asymmetrical luminosity profiles and the radially increasing velocity dispersions support consistently the above scenario of tidal interaction between galaxies. Further spectroscopic observations are necessary in order to investigate the degree of anisotropy in the kinematically perturbed regions.

References

Binney, J., Tremaine, S.: 1987, Galactic Dynamics, ed. J.P. Ostriker, Princeton University Press

Madejsky, R.: 1989, Astrophys. Space Sci. **156**, 223

Madejsky, R., Bender, R., Möllenhoff, C.: 1990, submitted to Astron. Astrophys.

Mulder, W.A.: 1983, Astron. Astrophys. **117**, 9

Spitzer, L., Jr.: 1958, Astrophys. J. **127**, 17

DISCUSSION

Roos: The impulsive approximation gives you only an order of magnitude estimate for the cases you discussed. Did you compare your observational results with the numerical M-body models that have been done for this interacting pair?

Madejsky: In this case of a high-velocity encounter of two galaxies the impulsive approximation probably gives a very good estimate for the energy exchange of most stars. However, detailed numerical simulations are necessary to verify whether the proposed scenario is true. Our observational results are very new and we have not yet combined with numerical simulations, but we will do so.

Navarro: You're a little surprised that galaxies undergoing such a violet encounter are still well-fitted by a deVaucouleurs law. Could you comment on this?

Madejsky: From the morphological and kinematical properties we estimate a time of $\sim 2 \cdot 10^7$ yrs elapsed since the moment of closest approach. In the inner parts of the galaxies where the crossing times of the stars are comparatively short, the dynamical response to the violent encounter can directly be seen in the azimuthal variations of the luminosity profiles (inside 15"). The outer parts are highly disturbed; however, due to the recent tidal interaction, damage on these outer parts is not yet visible.

Chatterjee: What is the ratio of the distance between the nuclei of the two galaxies, compared to their total extent (from luminosity profiles)?

Madejsky: The galaxy centers are separated by 40 arcsec. This corresponds to $\sim$15 kpc. The luminosity profiles I have shown extend out to 130 arcsec corresponding to $\sim$50 kpc. The real extent of both galaxies is not known. The luminosity profiles most probably are limited by the S/N-ratio of the CCD images. We are doing further very deep CCD photometry to study the distribution of globular clusters, then I can tell you whether both galaxies extend beyond 50 kpc or not.

Khachikian: Have you data about distribution of radial velocities along these galaxies?

Madejsky: Yes, we have detailed kinematical information along the line connecting both galaxy centers. The high radial velocity difference of 680 km s^{-1} is indicated by the radial velocity curves; however, no internal rotation can be seen. The range between both galaxies cannot be considered since both luminosity profiles are superposed there and do not give correct kinematical information.

Fridman: What may you say about percent of interacting elliptical galaxies with relative spin direction of components?

Madejsky: In our sample of interacting galaxy pairs, we have observed spectroscopically only double elliptical galaxies, where most galaxies appear very round; i.e., at present we do not expect to detect considerable rotation. Only five galaxy pairs exhibit considerable rotation in both components. Therefore, no statistical conclusion can be drawn on relative spin.

DYNAMICS OF GROUPS AROUND INTERACTING DOUBLE ELLIPTICALS: MEASURING DARK MATTER HALOES

H. Quintana
Astrophysics Group, P. Universidad Católica de Chile

INTRODUCTION

Binary galaxies, as binary stars, are important to measure masses, as suggested by Page (1952). Because three orbit parameters are measurable for galaxies at one instant of time, severe uncertainties remain in the orbit and mass determinations. These uncertainties can partly be overcome by statistical studies of selected samples and/or n-body simulations. Close double galaxies (and isolated galaxies) could also be useful to estimate dynamical masses if we can find test particles around them.

Interacting elliptical pairs or dumb-bell galaxies are found with a large range, between 0-1200 km s^{-1}, of relative radial velocities. Standard 2-body orbit calculations, highly uncertain due to projection factors, suggest for the largest velocity differences very large galaxy masses, if the systems are bound and stationary. However, recent n-body simulations model these binaries as galaxies captured from hyperbolic orbits, requiring masses of order a few times $10^{11} M_{\odot}$ (Borne *et al.* 1988), but producing systems that are short lived.

A different picture appears when we study observationally the dynamical mass of interacting double ellipticals using faint satellite galaxies. These satellites contribute little luminosity and, presumably, little mass to the system. We present results of two such groups, basically forming systems of test particles, around the dumb-bells NGC 4782/3 and IC5049. We also briefly discuss the satellite group around the central dumb-bell in the cluster Sersic 40/6. Apparently we detect large quantities of dark matter in the vicinity of these dumb-bell galaxies, because the system masses of $\sim 4.5 \times 10^{13} M_{\odot}$ and $8 \times 10^{13} M_{\odot}$ for NGC 4782/3 and IC 5049, respectively, are quite high. Likewise, the mass of the Sersic 40/6 inner core is $7 \times 10^{13} M_{\odot}$. The possibility that a common massive dark matter halo increases the merging times of these types of galaxies is suggested. In this paper we assume $H_0 = 100$ km s $^{-1}$ Mpc^{-1}.

RESULTS AND DISCUSSION

We briefly discuss below the three cases mentioned.

a)] IC 5049 ≡ ESO 341-IG15.

Lauberts (1982) classifies it as a $m_B = 14.69$ E+E system with a common envelope, apparently belonging to the NGC 6958 galaxy group (v=2,757 km s^{-1}). However, spectra taken at the 100" Du Pont telescope at Las Campanas Observatory with the 2D-Frutti detector, showed that the mean E+E velocity is 11,700 km s^{-1}, with relative velocity between the E components of 890 km s^{-1}. Inspection of the field reveals a concentration of very faint galaxies in the area. The spectra of 15 galaxies showed that 11 faint satellite galaxies form a group centered at 11,871 km s^{-1}, with 31% chance of a gaussian distribution centered at the mean db velocity. Velocity dispersion of this group is an outstanding 580 (±160, -90) km s^{-1} and its velocity histogram is consistent with a gaussian distribution.

No faint galaxies were found in front of the group and 2 were background galaxies at v$\simeq$ 27,000 km s^{-1}. Literature velocities in the neighbourhood list NGC 6958 at 2,757 km s^{-1}, 341-IG6 at 6,969 km s^{-1} and 341-IG16 at v = 12,689 km s^{-1}. A number density map of 260 galaxies in a 2° × 2° area down to m = 18, approximately, shows a sharp symmetrical enhancement that peaks at the position of IC 5049, due mostly to faint galaxies. This density distribution strongly suggests the group effectively cluster around IC 5049, with a scale of order 300 kpc. From inspection of the plates the combined luminosity of the faint galaxies can be estimated to be of order 20-25% of the group luminosity.

Application of a mass estimator for test particles around a single massive object (Bahcall and Tremaine 1981) gives $M_s = 4.3\times10^{13}M_\odot$. Likewise, use of the virial theorem, median mass, average mass and projected mass estimators following Heisler *et al.* (1985) discussion for equal mass self-gravitating systems, gives masses of similar order, as shown in Table 1.

If mass is concentrated following luminous matter, then each db component has an associated mass roughly 40% of these values. Even if the masses of the db galaxies themselves correspond to traditional M/L ~ 30 for E galaxies, then they, or the group, have a large amount of dark matter concentrated in a small volume beyond the optical galaxies and with a scale out to about 300 kpc.

These measurements should be confirmed by a wider dynamical analysis of the neighbourhood of IC 5049, to ascertain we are not measuring the effects of superposed groups unrelated to IC 5049 or the projection of a galaxy filament or wall around IC 5049. Anyway, the density maps do not suggest outlying structures.

b)] The group around NGC 4782/3.

This system has been studied by de Souza and Quintana (1990), who give observational details. Summarizing, this system formed by a $m_B = 12.1$ EO+EO pair of interacting elliptical galaxies is at v = 4,544 km s^{-1} with 650 km s^{-1} velocity difference between components. Borne *et al.* (1988) proposed a model in which these galaxies are located at the closest point of an hyperbolic encounter with small impact parameter, producing a bound system as orbital momentum is transferred to internal stellar motions. In fact, internal dispersions are rather high, ~400 km s^{-1} and ~300 km s^{-1}, for each member. The resulting timescale of the merger is of order 10^8 years. Using OPTOPUS at the ESO 3.6m telescope, de Souza and Quintana observed the surrounding group of fainter galaxies. They found 13 members (plus 17 galaxies at v = 17,000 km s^{-1} or higher) with a group velocity dispersion of 450 km s^{-1}. Assuming a single point mass surrounded by test particles a mass of $3.6\times10^{13}M_\odot$ is obtained as indicated in Table 1. A similar discussion as in the previous system leads us to assign corresponding masses of $1-2\times10^{13}M_\odot$ to each of the db components, either associated to the outskirts of the luminous mass or to the group, which has typical dimensions of order 300 kpc. In any case, most of this large amount of mass is in dark form as again the resulting global M/L is of the order ~1000 $(M/L)_\odot$, while the M/L of the luminous galaxies is typically ~10-30, as assumed by Borne *et al.* (1988).

c)] The E+E interacting system at the center of the Sersic 40/6 cluster.

This system has been studied by Quintana and Ramírez (1990), where details are presented. The db components have a velocity difference of ~ 300 km s^{-1}, with internal dispersions of 250 km s^{-1} at the nuclei and ~650 km s^{-1} at the outer optical halo (Carter *et al.* , 1985). This value is close to the 710 km s^{-1} dispersion of the faint group of closest 10 galaxies to the db, thus significantly lower than the cluster global dispersion of 1440 km s^{-1}, obtained from 80 galaxies. A mass of $\sim 7 \times 10^{13} M\odot$ is derived for this inner core, if assumed bound. This mass is basically associated to the central db. If we take typical values for the ellipticals M/L ratio, then this large amount of mass must be in the form of dark matter. We note that similar methods applied to the central core of the cluster A 496 give a mass $\sim 2.5 \times 10^{12} M_{\odot}$ associated to the cD galaxy in that cluster, in fair agreement with usual dominant E galaxy masses.

From the evidence of these three db systems, we can tentatively conclude the following:

The motion of faint galaxies (approximately test particles) around some pairs of interacting E galaxies seems to measure very large system masses, which for the most part must consist of dark matter. If dark matter follows luminous matter, most of this dark matter is associated to the bright E galaxies themselves as dark haloes, with values of the order of 10^{13} $M_{\odot}$ per galaxy. Otherwise, a large common halo of dark matter is present around some systems of galaxies. This could be a characteristic of some dumb-bell systems. In both hypotheses it seems that the ratio of luminous to dark matter can vary widely in different galaxy systems.

The tidal distortions shown by db galaxies could be interpreted as due to short, transient collisions, with estimated lifetimes of ~1.5 dynamical times, as recently done in the literature. In this case, these systems should be rather rare. However, we see many examples of db's, isolated, in groups or in clusters (some classified as multiple nuclei cD's). The large amounts of dark matter associated to the db galaxies in these examples (to individual or to common extended haloes) could alter the conditions of those encounters in such a way that merging times become extended. The possibility of seeing massive dark halo effects in other systems remain open and the results of Dressler *et al.* (1986) for NGC 720 are a hint in this direction.

References

Bahcall, J. and Tremaine, S.: 1981, *Ap.J.* **244**, 805.

Borne, K.O., Balcells, M. and Hoessel, J.G.: 1988, *Ap.J.* **333**, 567.

Carter, D., Inglis, I., Ellis, R.S., Efstathiou, G. and Godwin, J.G.: 1985, *M.N.R.A.S.* **212**, 471.

de Souza, R. and Quintana, H.: 1990, *A.J.* **99**, 1065.

Dressler, A., Schechter, P.L. and Rose, J.: 1986, *A.J.* **91**, 5.

Heisler, J., Tremaine, S. and Bahcall, J.: 1985, *Ap.J.* **298**, 8.

Lauberts, A.: 1982 "The ESO/Uppsala Survey of the ESO (B) Atlas". Garching, F.R.G.

Page, T.: 1952, *Ap.J.* **116**, 63.

Quintana, H. and Ramírez, A.: 1990, submitted to *A.J.*

Table 1: Masses of Group Systems Centered on db Galaxies

($H_0 = 100$ km s^{-1} Mpc^{-1})

System	M$_V$ $10^{13}M_\odot$	M$_M$ $10^{13}M_\odot$	M$_A$ $10^{13}M_\odot$	M$_P$ $10^{13}M_\odot$		MS$_V$ $10^{13}M_\odot$	MS$_P$ $10^{13}M_\odot$
IC 5049	8.2	6.8	7.8	10.2	*	4.3	6.9
				20.4	**		13.8
N4782/3	4.5	4.9	4.2	5.3	*	3.6	5.7
				10.6	**		11.4
Sersic 40/6	7.1	8.2	7.5	11.4	*	3.6	6.2
(db inner core)				22.8	**		12.4

Notes:

a) * : isotropic orbits; ** : radial orbits.

b) M denotes total mass of equal-mass self-gravitating system; MS denotes total mass of system of test particles around a massive particle. M$_V$ and MS$_V$ = Virial Mass; M$_M$ = Median Mass; M$_A$ = Average Mass; M$_P$ and MS$_P$ = Projected Mass.

DISCUSSION

Schneider: Could you comment on the degree of bimodality in the velocity distribution within the groups and whether it might be indicative of an unbound collision between two groups?

Quintana: The histogram for the velocities for both groups shows no evidence for bimodality. However, one has 13 members in each and more data could perhaps show such an effect. So far, we have just one group in each case.

Miller: Most of your galaxies in the field of these double systems seem to be dwarfs. Is that typical of most galaxies, or is it an unusual feature of the dumbbells? Is this telling you something about the dynamics of these systems?

Quintana: It is believed that most groups are deficient at the faint end of the luminosity function. In this sense these two groups are atypical. However, with just two examples it is hard to ascertain special properties of the faint galaxies found. In fact, many dumbbells are in groups, and velocity data is needed to decide on membership of individual faint galaxies.

Borne: The simulations only indicate the mass on the scale of the luminous matter, and cannot tell anything about the mass of possible dark matter on larger scales. Even so, the observed distortions are not consistent with a circular orbit for the dumbbell in NGC 7482/83, but with an unbound trajectory. The high velocity dispersion of the surrounding group may simply result from the superposition of two groups following each of the galaxies. This unbound group would not be virialized, and your mass estimates would be invalid.

Quintana: Certainly the mass estimators measure the mass on the scale size of the group, which is of order 200-300 kpc in radius in these examples. The velocity histograms show no sign of being two distributions. If the E galaxies are followed by accompanying groups, the resulting group should be highly anisotropic as the satellite galaxies will not have the same type of collision as the central pair. In fact, it is unlikely that the resulting system will remain bound, given the initial conditions for velocity and mass assumed in the hyperbolic orbit simulations. This should be borne out by analysis of additional groups. It is surprising that the examples observed turned out so similar. If E galaxies have groups of faint galaxies normally associated with them, then the hypothesis of group superposition could be tenable. As far as I know the simulations have not considered dark matter halos. These factors should be investigated with models before we can reject other alternatives.

THE INTERACTING PAIR MKN 305/306

Matthias Dietrich
Universitätssternwarte Göttingen
Geismarlandstraße 11
D-3400 Göttingen, FRG

Direct images and spectra at different slit positions of the interacting system Mkn 305/306 are discussed. Both galaxies show starburst properties due to tidal interaction. The morphology and velocity structure of Mkn 306 reveals the strongest warp of a stellar disk so far known.

The galaxies Mkn 305 and Mkn 306 form a double system with 30 arcsec separation and having a common envelope at $m_B \geq 24.5$. Furthermore a small tidal tail west of Mkn 306A, an isophote twist of Mkn 305 and the near identical redshifts of the two galaxies prove that this is a physical pair. Mkn 306 itself was classified as a double nucleus galaxy (Petrosyan et al., 1978). The optical morphology of Mkn 306 has the form of an integral sign which is similar to the radio morphology of strongly warped galaxies (Bottema et al., 1987). But in the optical the warp of the stellar component is normally far weaker than in the radio for the HI-gas. Therefore we investigated whether the double nucleus structure of Mkn 306 is real

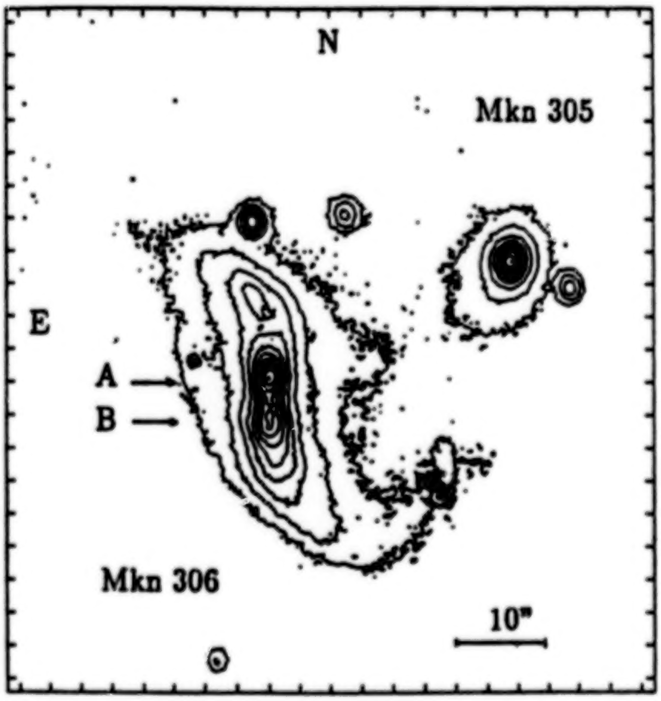

Fig. 1 — Contourplot of the interacting galaxy system in the B-band

or an artefact due to an extreme warp in the optical. The origin for the warp phenomenon is not clear yet: merging, tidal interaction or accretion of intergalactic matter (IGM).

Direct images of the galaxy system were taken with the Calar Alto 2.2m telescope in the B-band (Fig. 1) and at La Silla in the r-band using the 2.2m telescope; low dispersion spectra (240 Å/mm) as well as high dispersion spectra (56 Å/mm) for studying the velocity field were taken with the Calar Alto 3.5m telescope at different position angles. Also a spectrum of Mkn 305 was taken at Calar Alto with the 3.5m telescope covering the whole spectral range (240 Å/mm) .

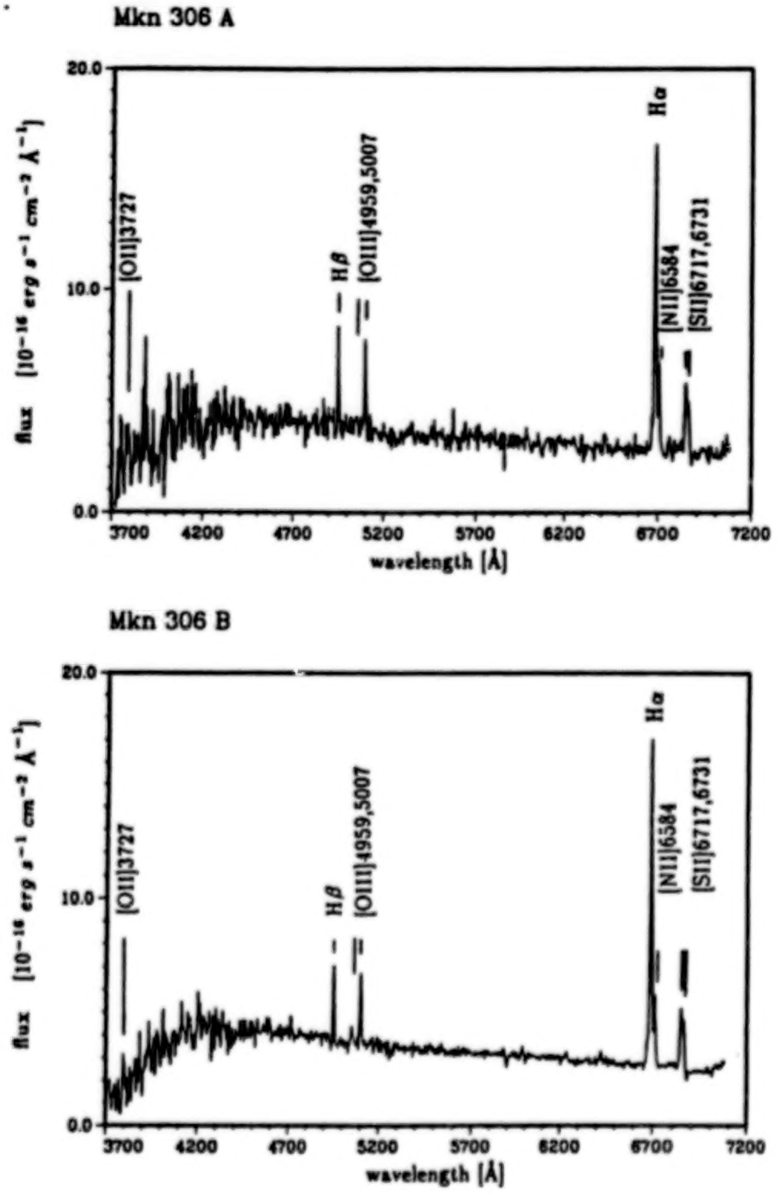

Fig. 2 — Optical spectra Mkn 306 A, B

Redshifts of z=0.0195 for Mkn 306 (m_B=14.6) and z=0.0194 for Mkn 305 (m_B=16.8) were determined from the emission and absorption lines, leading to a distance of D=77.7 Mpc for the system (H_o=75 km s^{-1} Mpc^{-1}). The two central emission regions of Mkn 306 are

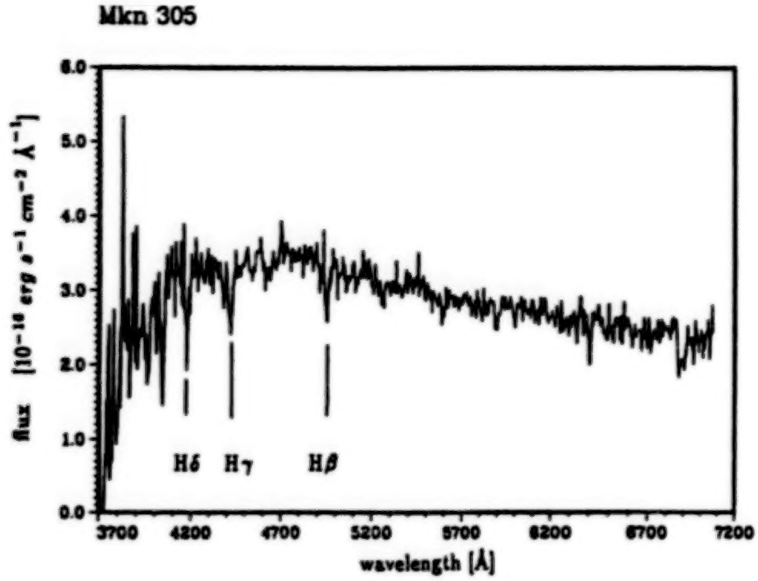

Fig. 3 — Post starburst spectrum of Mkn 305

separated by 5.6 arcsec corresponding to 2.1 kpc. The projected separation of Mkn 305 and Mkn 306A amounts to 12.4 kpc.

The spectra of Mkn 306A and B (Fig. 2) are typical for starburst activity with respect to their line intensity ratios of I([OIII]5007)/I(Hβ) vs. I([NII]6584)/I(Hα) or I([OI]6300)/I(Hα) (Veilleux and Osterbrock, 1987). The overall spectrum from the radio to the optical range shows a FIR-excess typical for dust re-emission of a strong starburst. The observed spectrum of Mkn 305 can be characterized as a post-starburst spectrum (Fig. 3); this is very unusual considering the elliptical morphology of this galaxy.

The velocity field of Mkn 306 was determined parallel (Fig. 4) and perpendicular to the major axis. A comparsion of these velocity measurements correspond very good with the observations and theoretical model calculations of Brinks (1985) for the warped radio velocity field of NGC 224. The warp leads to an additional linear velocity structure with a smaller gradient in the central region of the galaxy in comparison to 'normal' velocity gradients. The superposition of both velocity curves results in a stepwise velocity structure. Model calculations show the existence of a warp and the projection effect simulating the double nuclear structure of Mkn 306. In addition the velocity curves perpendicular to the major axis of Mkn 306A and B which are anti-symmetrical prove this result.

Furthermore the optical morphology of Mkn 306 is very similar to the radio morphology of NGC 4013 (Bottema et al., 1987). Both galaxies are shaped like an integral sign and show double nucleus structure due to the strong warp. In the case of Mkn 306 the warp was induced by means of tidal interaction with Mkn 305.

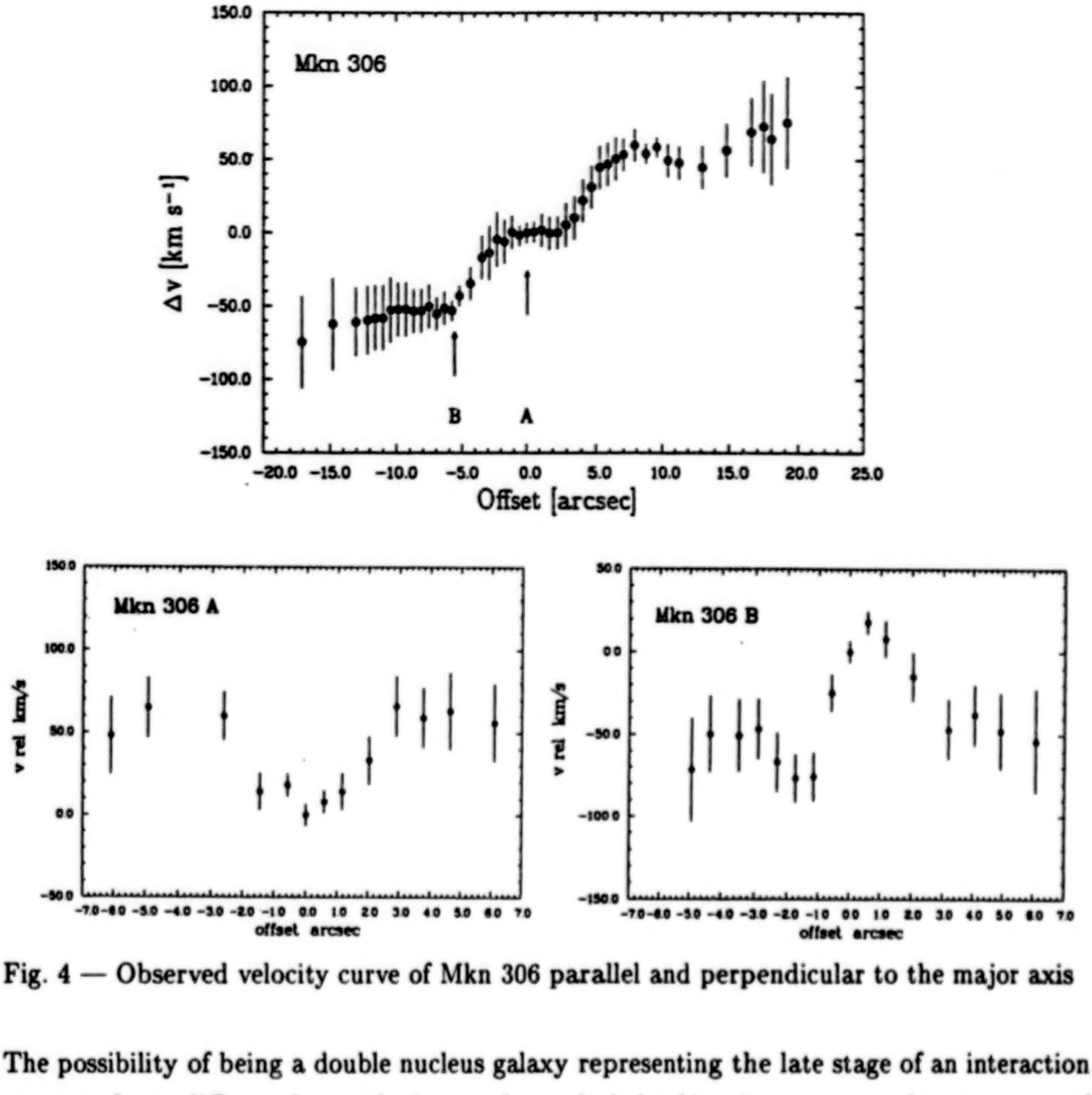

Fig. 4 — Observed velocity curve of Mkn 306 parallel and perpendicular to the major axis

The possibility of being a double nucleus galaxy representing the late stage of an interaction process of two different host galaxies can be excluded taking into account the symmetry of the velocity field and the physical similarities of the two nuclei: their emission line ratios, the relative abundances, the dust content and even the Hα-luminosity and the deduced number of OB-stars (Kollatschny and Dietrich, 1990).

References

Bottema, R., Shostak, G.S., van der Kruit, P.C.: Nature,**328**, 401 (1987)
Brinks, E.: PhD, Leiden, 1984
Kollatschny, W., Dietrich, M.,: Astron.Astrophy. in press, (1990)
Petrosyan, A.R., Saakyan, K.A., Khachikyan, E.E.: Astrophysics, **14**, 36 (1978)
Veilleux, S., Osterbrock, D.E.: Ap.J.Suppl.**63**, 295 (1987)

GEOMETRICAL PARAMETERS OF E+S PAIRS

Roberto Rampazzo[1] and Jack W. Sulentic[2]
[1] Osservatorio Astronomico di Brera, Milano - Italy
[2] University of Alabama, Tuscaloosa - USA

INTRODUCTION

• **Clues Concerning Galaxy Formation.** Local environmental conditions (i.e. density and angular momentum properties of protogalactic clouds) are thought to be factors affecting the ultimate morphology of a galaxy. The existence of significant numbers of mixed morphology (E/S0 + S) pairs of galaxies would represent a direct challenge to this idea unless all early-type components are formed by mergers. We wish to isolate candidate E+S pairs for detailed study with several questions in mind:

a) Are most of the pairs true E+S systems **OR**, as the theory would suggest more morphologically concordant pairs involving primarily late–type or disky galaxies alone (i.e. misclassified lenticulars)?

b) Assuming that many of the pairs are E+S, do their properties differ in any way from E and S galaxies in the field?

c) Is their evidence that E galaxies in mixed pairs are preferentially merger products?

• **Interaction Induced Activity.** Evidence has accumulated at optical, IR and radio wavelengths for the inducement of enhanced disk and nuclear activity in galaxies due to environment. Boxy isophotes are supposed to be the result of cylindrical rotation of a stellar component induced by strong interactions such as the merging of dwarf galaxies with a giant disk object or collision of equal size members of a pair under special inpact condition (Binney and Petrou 1985). S+E pairs offer a unique vantage point from which to study these effects because we have a single gas rich galaxy and a relatively "clean" perturber.

a) Do the early type components of the pairs show systematic evidence for geometrical distortion (i.e. isophotal twisting, boxy isophotes)?

b) If such evidence is observed, does it correlate with any possible measure of interaction (i.e. optical morphology, IRAS emission, apparent separation)?

c) Is it possible that some of the S components in mixed pairs have spiral structure that was induced by the interaction?

OBSERVATIONS and REDUCTION

We have observed 22 pairs of mixed morphology galaxies (containing at least one early-type component) selected from a catalog of Sulentic (1988: unpublished) based upon the ESO sky survey. A large fraction of the objects are found in the catalogue of Arp & Madore (1987). Table 1 summarizes the observed sample and relevant morphological and interaction characteristics.

Our observational material consists of 385×574–22μm square pixel CCD images in two colors (some also in U) obtained at the Cassegrain focus of the 2.2m MPI/ESO telescope. The scale is 0.257 arcsec pixel^{-1}. The filters match the Johnson UBV bands.

TABLE 1
MIXED PAIR MORPHOLOGY

PAIR #	SEP (arcmin)	IRAS 60μm	HUBBLE TYPE	COMMENTS (*=STRONG I/A)	INTERACTION TYPE
5	0.9		E+S	* I/A ARMS	LIN(br+ta)
8	0.6	0.79	SO+S	DISKY PAIR	DIS(1)
9	0.9	0.69	E+S		DIS(1)
11	0.6		E+S		DIS(1)
12	1.2		E+SBO	EARLY PAIR	JUS
13	0.5		E/SO+SO	DISKY PAIR	JUS
18	1.3		E+S	I/A ARMS	LIN(br+ta)
31	1.6		E+S	*	DIS(1)
53	2.1		E+SBO	EARLY PAIR	JUS
54	0.5	2.68	E+S	*	DIS(1) CONTACT
64	1.4	0.53	E+S		JUS
69	0.4		E+S	*	DIS(1)
70	0.4		E+S	*	DIS(1) CONTACT
86	1.2		E+S		JUS
87	0.4		E+S	*	LIN(br)
90	1.0	1.01	SBO+S	DISKY PAIR	JUS
96	0.5		E/SO+S	*DISKY PAIR	ATM(am) CONTACT
97	0.8		E+S	*I/A ARMS	LIN(br+ta)
104	1.0		E+S		DIS(1) SHELL
108	0.6		E/SO+SO	EARLY PAIR	DIS(1) SHELL?
109	0.4		MULTI/MERGER?	*E+S?	ATM(sh) CONTACT
115	0.3		E/SO+SO	*DISKY PAIR	DIS(1) CONTACT

During the observing run we had variable seeing conditions (0.8≤ σ ≤2.0 arcsec). All frames were pre–processed (bias removal, flat–fielding, and cleaning. Galaxy isophotes were interpolated with ellipses using the NMP package (cf. Fasano & Bonoli 1989) in use at the Observatory of Brera. We operated on the original images with an adaptive filter (cf. Caon et al. 1989) in order to reach the faintest possible level in the outskirts of the galaxies. Fig. 1 shows an example of the geometrical profiles obtained in U (circles), B (stars) and V (squares). θ is the position angle of the major axis, (r = a =semi–major axis), measured NE; $\epsilon = 1 - b/a$ is the ellipticity of the isophotes; a(4)/a is the fourth cosine coefficient of the Fourier series expansion of the deviation from a pure ellipse divided by the actual semi-major axis. This latter is an isophote shape parameter the sign of which indicates boxy (a(4)< 0) or *disky* (a(4)> 0) even if its absolute value depends upon projection effects.

In Table 2 we report the relevant geometrical properties of the galaxies. We list the maximum values measured for the ellipticity and the a(4)/a shape parameter together with the total measured twisting along the profile beyond the seeing disk (we set an inner limit of 3 arcsec). An asterisk indicates objects in which a(4)/a is neither predominantly boxy nor disky.

TABLE 2
GEOMETRICAL PARAMETERS

CODE	B_T	cz	ϵ_{max}			Δ P.A.			$a(4)/a_{max}$ × 100		
		(km s^{-1})	U	B	V	U	B	V	U	B	V
5				0.28	0.32		22.2	8.9		-1.81	-1.98
5				0.39	0.35		16.3	19.7		2.99	2.58
8			0.17	0.18	0.19	60.4	52.3	43.5	-3.32	-1.55	-3.01
9			0.10	0.13	0.14	35.4	16.8	62.1	1.15	-1.19	-1.85
11	16.3			0.33	0.34		9.1	9.9		-4.18	-2.91
11	15.1			0.72	0.68		14.6	4.8		-3.50	-2.46
12	13.5			0.11	0.12		24.7	11.1		1.46*	-0.82*
12				0.31	0.36		31.4	31.5		2.99	4.42
13	15.2			0.16	0.17		35.0	20.6		2.45	5.46
13	17.0			0.38	0.42		24.9	18.2		3.45	1.49
18	14.6			0.17	0.12		45.2	19.9		-2.15*	2.11*
18	14.9										
31	15.8			0.38	0.37		14.2	8.0		-2.77	-1.67
31	15.1										
53	13.2	4925	0.37	0.37	0.38	14.2	16.8	17.3	-2.31	-3.44	-1.72
53	14.8	4700	0.40	0.42	0.45	20.4	70.7	73.6	-9.19	-6.00	-7.25
54	13.4	2437	0.23	0.24	0.29	10.6	33.4	29.2	2.84	2.08	1.35
54	12.6	2512									
64				0.12	0.18		50.0	41.2		2.18*	1.26*
64	14.8			0.76	0.76		3.8	5.6		6.64*	9.14*
69	15.0	5970	0.23	0.22	0.22	11.8	14.6	11.1	4.26	-2.03	-1.93
69	15.4		0.75	0.68	0.71	10.3	8.9	7.3	6.62	2.82	0.79
70	14.4		0.23	0.29	0.29	19.3	7.1	14.7	1.52	-1.86*	-1.02*
70											
86				0.26	0.26		16.6	11.8		2.15	2.24
86											
87	16.6		0.27	0.31	0.38	32.3	9.6	4.2	5.47	-0.86*	-1.35*
87	16.4										
90			0.28	0.35	0.34	69.1	64.9	77.7	5.72	4.80	4.06
96				0.34	0.32		9.9	7.5		-4.18	-2.45
97			0.18	0.30	0.30	16.4	22.7	23.4	2.23	4.60	3.22
104			0.29	0.30	0.27	12.4	12.5	7.4	2.32	3.26	0.92
104											
108				0.11	0.11		56.6	56.9		-1.37*	1.14*
108				0.38	0.34		31.8	35.3		3.71*	3.10*
109	14.4			0.22	0.22		9.7	14.4		-1.42	-5.95
115	15.2			0.17	0.21		52.1	61.3		-1.28	-1.69
115	14.7			0.55	0.56		30.3	31.3		-3.01	-2.76

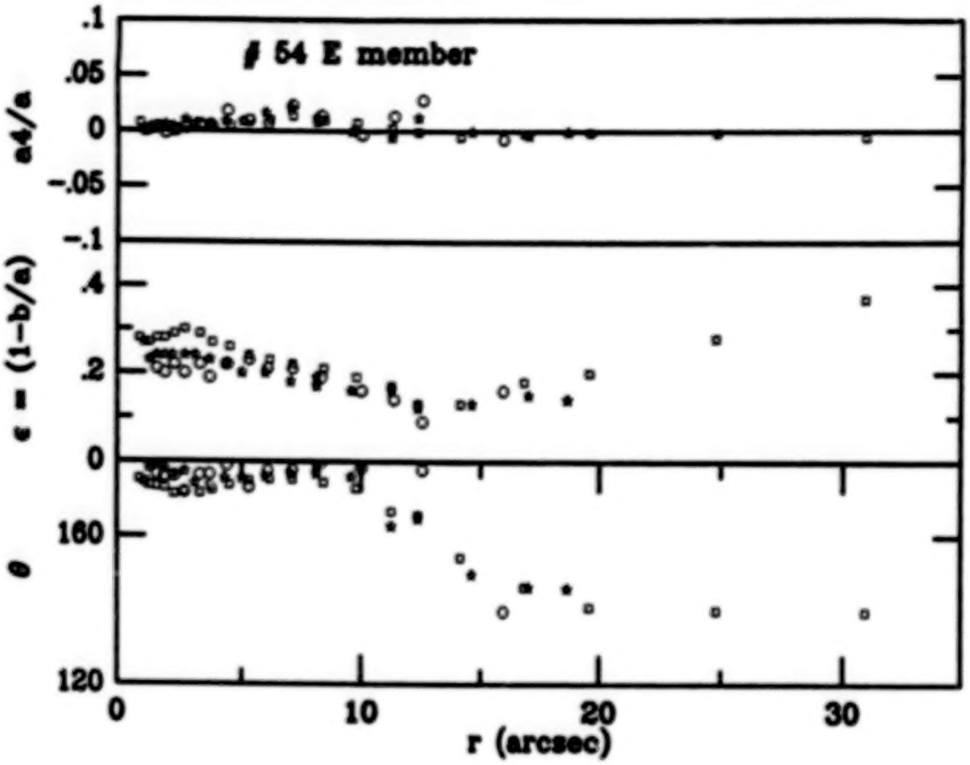

FIG. 1 Pair 54 (E = NGC 6483). Twisting (lower), ellipticity (middle) and shape (upper) profiles as function of the isophotal semi-major axis (for detailed explanations cf. text).

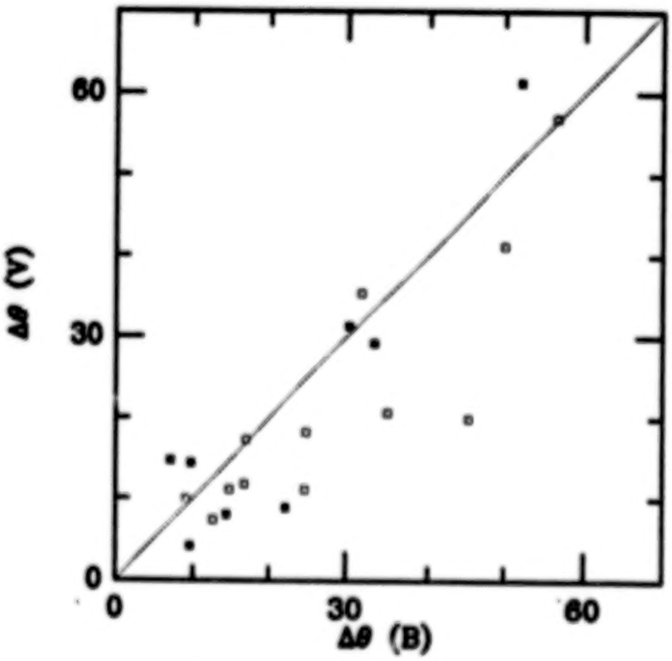

FIG. 2 Comparison between the total measured twisting, θ, in the B and V bands for early-type objects in pairs. Strongly visibly interacting objects are marked as solid squares.

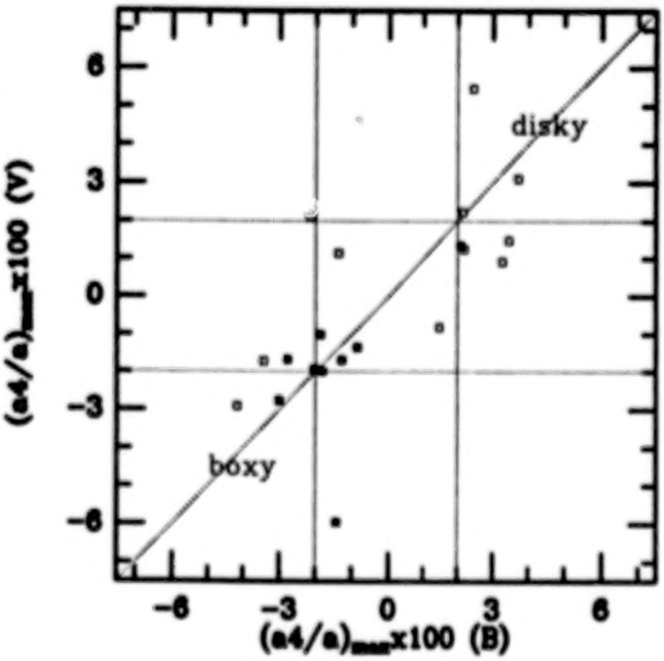

FIG. 3 Comparison between the shape parameter a4/a in the B and V bands for early-type objects in pairs. Strongly visibly interacting galaxies are marked as solid squares.

RESULTS

• Clues Concerning Galaxy Formation.

a) We find a large number of true mixed pairs with 13/22 E+S pairs in the present sample. The remaining objects include 5 disk pairs (composed of S0 and S members) and 3 "early-type" pairs comprising E and S0 members. We estimate that between 25 and 50% of the pairs in any complete sample will be of the E+S type. This suggests that 100–200 such pairs exist on the sky brighter than m_{pg}=16.0.

b) We find no global evidence for a difference between E members of this sample and those in more general samples (e.g. Bender et al. 1989). In particular, we find that about 30% of the early-type galaxies cannot be classified either predominantly boxy or disky because the a(4)/a profile shows 1) both of these features at a comparable level or 2) does not show any significant trend.

Isophotal twisting (Fig. 2) is observed with a range and distribution consistent with general samples (ΔPA between 0–70°). Two spirals show significant twisting in their bulge components.

c) We observe two early-type components with shell structure and at least 6 objects with twisting values greater than about 30°. Countering any attempt to ascribe all or most of these features to merger events is the low detection rate in the IRAS catalog especially for a sample of pairs with V_o generally less than 10^4 km s^{-1}.

• Interaction Induced Activity.

a) About 40% of early-type components show predominantly boxy isophotes while 30% show disky ones at or near the 2% level (measured by the a(4)/a parameter). As mentioned above, both E and S components show significant isophotal twisting.

b) The presence of disky isophotes or isophotal twisting does not appear to correlate with strength of interaction. We divided the sample into "strong" and moderate-weak interactors based upon optical morphology. Early-type systems in the strong interaction class show a distinct preference for boxy isophotes (Fig. 3: solid squares) and a weaker avoidance for disky ones. Figure 3 shows this tendency in both B and V bands. Amplitude of isophotal twisting does not appear to correlate with our measure of interaction strength (Figure 2: solid squares).

Three of the S components of our E+S pair sample show spiral structure comprising very open spiral arms not associated with a disk component. If these objects were not originally spirals then some E+S pairs may be "created" by the interaction process.

References

Arp, H.C. and Madore, B. 1987: *A Catalogue of Southern Peculiar Galaxies and Associations*, Cambridge Univ. Press.

Bender, R., Surma, P., Döberainer, S. Möllenhoff, C. and Madejsky, R. 1989: *Astron. & Astrophys.*, **217**, 35.

Binney, J.J and Petrou, M. 1985: *M.N.R.A.S.*, **214**, 449.

Caon, N., Capaccioli, M. and Rampazzo, R. 1989: *Astron. & Astrophys. Sup. Ser.*, submitted.

Fasano, G. and Bonoli, C. 1989:*Astron. & Astrophys. Sup. Ser.*, **79**, 291.

AN ATLAS OF MIXED-MORPHOLOGY PAIRS

N. A. Sharp
National Optical Astronomy Observatories
P.O.Box 26732, Tucson AZ 85726–6732

Current theories of galaxy formation imply that environment is the most important factor in deciding whether a collapsing region becomes a spiral galaxy or an elliptical galaxy. If this is the case, then isolated pairs comprising a galaxy of each morphology provide an especially interesting test, since, strictly speaking, they should not exist.

The first phase of studying E–S pairs is to define a sample which is genuinely isolated and genuinely E–S. The catalog compiled by Karachentsev is the most useful northern hemisphere starting point, containing 603 pairs which obeyed certain well-defined angular isolation criteria. All of these pairs now have velocities, enabling further removal of at least some of the non-physical binaries. The conventional cutoff at 500 km s^{-1} was used for this purpose.

However, the morphological types were estimated from Palomar Sky Survey prints, and are consequently not very accurate. It was therefore decided to obtain good CCD images in the B-band of all pairs from the Karachentsev sample which were classified as either E–S (73 pairs) or E–S0 (91 pairs), for a total of 164 pairs. This includes the 24 pairs with known redshift differences greater than 500 km s^{-1} (9 E–S and 15 E–S0), which were also imaged in this survey, not only for completeness but also in case the criteria were later changed, or the redshifts were found to be in error.

A total of 198 CCD frames were obtained between February 1986 and the present, with most of the observations being completed by the summer of 1987. A number of missing 'stragglers' and replacements for poor quality images were taken more recently. Most observations used the #1–0.9m telescope at Kitt Peak, with a few frames from the 2.1m. Some pairs required more than one image due to their separation. The morphological study did not require photometric conditions, but calibrations were made for almost all images anyway, and the weather was probably photometric at least half of the time, at least to an accuracy of around 0.1 magnitudes.

The results of this first phase will be published in the form of an Atlas, from which any interested readers will be able to select their own sub-sample using their preferred morphological criteria. Preliminary classifications suggest that less than half of the 140 physical pairs are actually genuine E–S systems, with about 35 certain pairs, and about the same number of less certain systems (Irregular rather than S, possibly S0 rather than E). Some of these uncertainties will be settled with further analysis of the existing data (e.g., using calibrated radial profiles), but some will require further observations.

Once the sample has been refined to genuine E–S pairs, further photometric data will be obtained, in at least the B and V pass-bands. Kinematical data may also be useful. The properties of the refined sample will then be compared to those of 'regular' field galaxies.

Fig. 1: Example of planned atlas page

In each picture, the lower scale bar is one arc minute in length when solid, and 0.5 arc minutes in length when dashed. The upper scale bar is 10 kpc in length, based on the mean redshift and a Hubble constant of 100 km s^{-1} Mpc^{-1} (dashed bars would be 5 kpc, if the image scale was such that 10kpc did not fit). Pairs with a redshift difference in excess of 500 km s^{-1} do not have the physical scale bar included. All binaries are identified by their number in the Karachentsev catalog. All pictures have North up and East to the left.

BLANK

PAGE

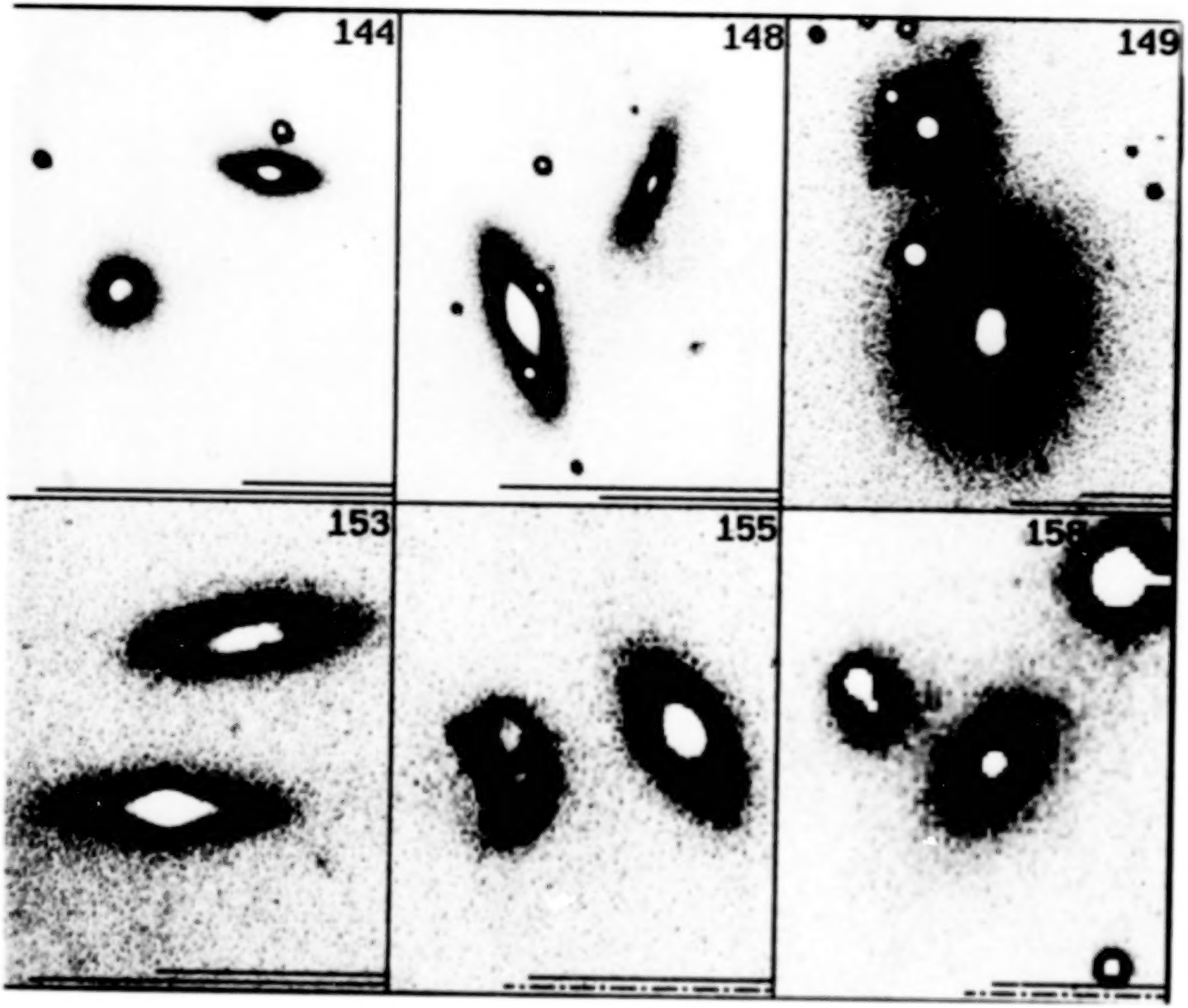
144
148
149
153
155
158

MULTI-COLOR IMAGING OF SELECTED SOUTHERN INTERACTING GALAXIES

Eric P. Smith and Paul Hintzen
Laboratory for Astronomy and Solar Physics
Goddard Space Flight Center
Greenbelt, MD 20771 USA

Introduction

We present preliminary results from a study of selected Arp-Madore Southern Hemisphere peculiar galaxies. Broadband CCD images (*BVRI*) of a subset of these galaxies allow us to study each galaxy's optical morphology, color, and (in a crude manner) degree of nuclear activity, and to compare them with similar data we possess on other active galaxies. Many of these galaxies have optical morphologies closely resembling those of powerful radio galaxies (Smith and Heckman 1989), yet their radio emission is unremarkable. Accurate positions for subsequent spectroscopic studies have been determined along with broad band photometry and morphology studies. Detailed observations of these comparatively bright, low-redshift, well-resolved interacting systems should aid our understanding of the role interactions play in triggering galaxy activity. This work is the initial effort in a long term project to study the role played by the dynamics of the interaction in the production and manifestations of activity in galaxies, and the frequency of galaxy mergers.

Preliminary Results

Galaxies were selected from the *Catalogue of Southern Peculiar Galaxies and Associations* (Arp and Madore 1987) based upon their morphology. We specifically chose galaxies from category 15 -"Loops, Tails, and Debris" (many of which are also listed in category 2,"Interacting Doubles") - because we were looking for those systems which contained evidence for, or suggestions of interacting spiral galaxies. A total of 31 systems were imaged on 14-17 March 1989 with the CTIO 4-meter using a TI CCD and the standard *B, V, R, I* filter set. The data were bias-subtracted and flat fielded using standard procedures, and *R* and *I* frames subsequently corrected for fringing using images of blank sky fields. Before performing our photometry we carefully edited each frame to remove stellar images which overlay or were close to the galaxy images. The details of this method may be found in Smith and Heckman (1989). We performed synthetic aperture photometry, and found the agreement between our measurements and previous photometry to be very good (better than 0.1 mag). Magnitudes have been corrected for Galactic reddening using the HI maps of Burstein and Heiles (1982).

We are in the midst of our data analysis and therefore the results we discuss are preliminary. In figure 1 we present two representative galaxies from our sample. The obvious damage these galaxies have sustained penetrates deep within their isophotal structure, not being restricted to low surface brightness distortions. This suggests that these are recent mergers or interactions which have not had time to virialize even their densest regions. For the system 0642-801 we find that the small galaxy to the west have colors and a surface brightness profile like those of a normal elliptical. The morphologically peculiar galaxy has colors which are blue by about 0.1 mag (in $(B\text{-}V)$ relative to a normal elliptical. This system was detected by IRAS in the point source survey at $60\mu m$ ($f_{60\mu m}$ = 0.68Jy). The second system, 1255-430 is extremely peculiar, and may possess multiple nuclei though spectroscopy is needed for confirmation. This galaxy was not detected by IRAS in the point source survey and has colors typical of an Sb galaxy ($(B\text{-}V)$ = 0.77).

Morphologically, the sample is (not surprisingly!) dominated by galaxies which display one or more tails (extended features whose length/width $\geq$ 3) with 19 out of 31 systems having these types of features. More importantly, 17 of the systems clearly display multiple intensity peaks within the main luminous body (some of which may be caused by dust lanes) or are clearly two galaxies embedded in a common envelope. Spectra of these objects will be studied to investigate the detailed kinematics of the interactions. The galaxies in our sample display a wide range of color index values (figure 2) and color index gradients. These colors and gradients are strongly influenced by dust present in these galaxies (35% of the sample objects are listed in the IRAS Point Source Catalog), and the likely presence of nonstellar emission-lines and bursts of star formation. Until spectra (or narrow band images) are obtained we cannot separate nonstellar emission from the underlying stellar continuum emission. We have, along with N. Kassim (NRL), observed six of the objects from our full sample ($\sim$80 systems) with the VLA. Three objects were detected ($\sim$10 mJy level) while the three others were not. Two of the systems detected do not show any radio structure while the third does appear to be resolved.

References

Arp, H. C., and Madore, B. F. 1987, *A Catalogue of Southern Peculiar Galaxies and Associations* (Cambridge University Press).

Burstein, D. A., and Heiles, C. 1982, *A. J.*, **87**, 1165.

Smith, E. P., and Heckman, T. M. 1989, *Ap. J. Suppl.*, **69**, 365.

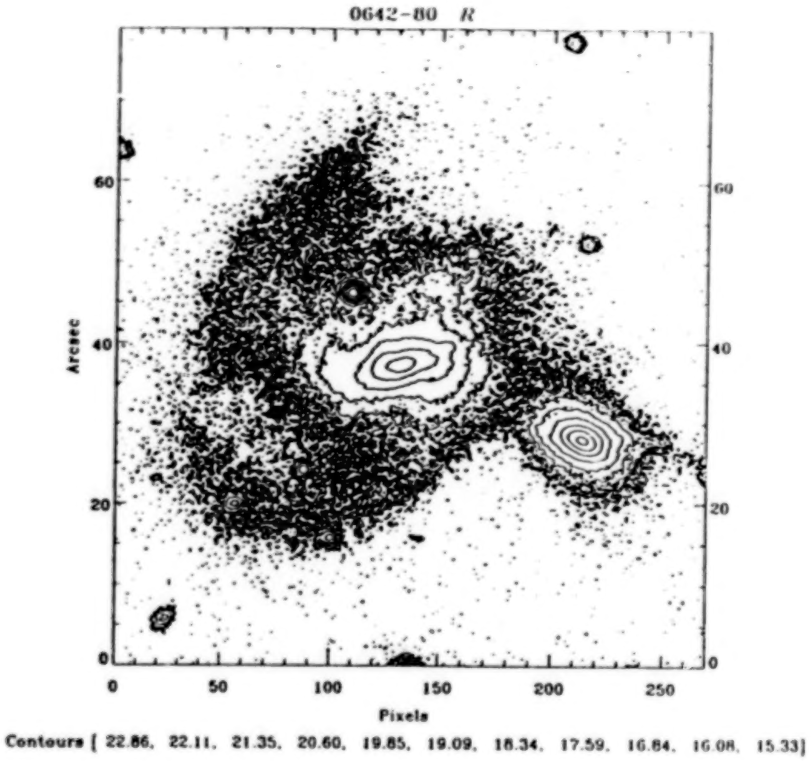

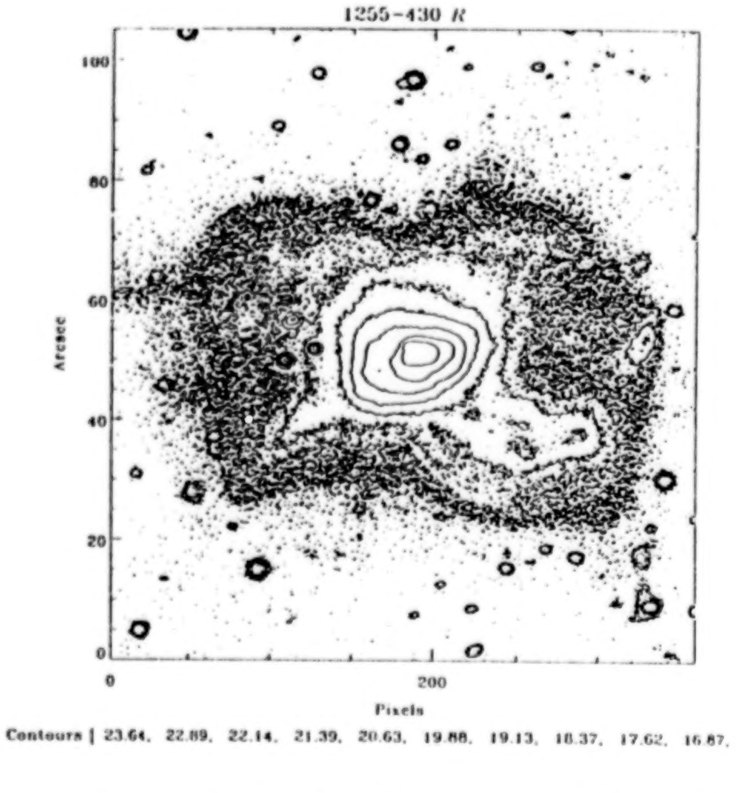

Figure 1: Contour images (in *R* with North on top, East to the or two of the galaxies in the sample 0642-801 and 1255-430. Contour levels in *R* itudes/arcsec^2 are listed below each plot. Images were edited to remove stars prior t hetic aperture photometry.

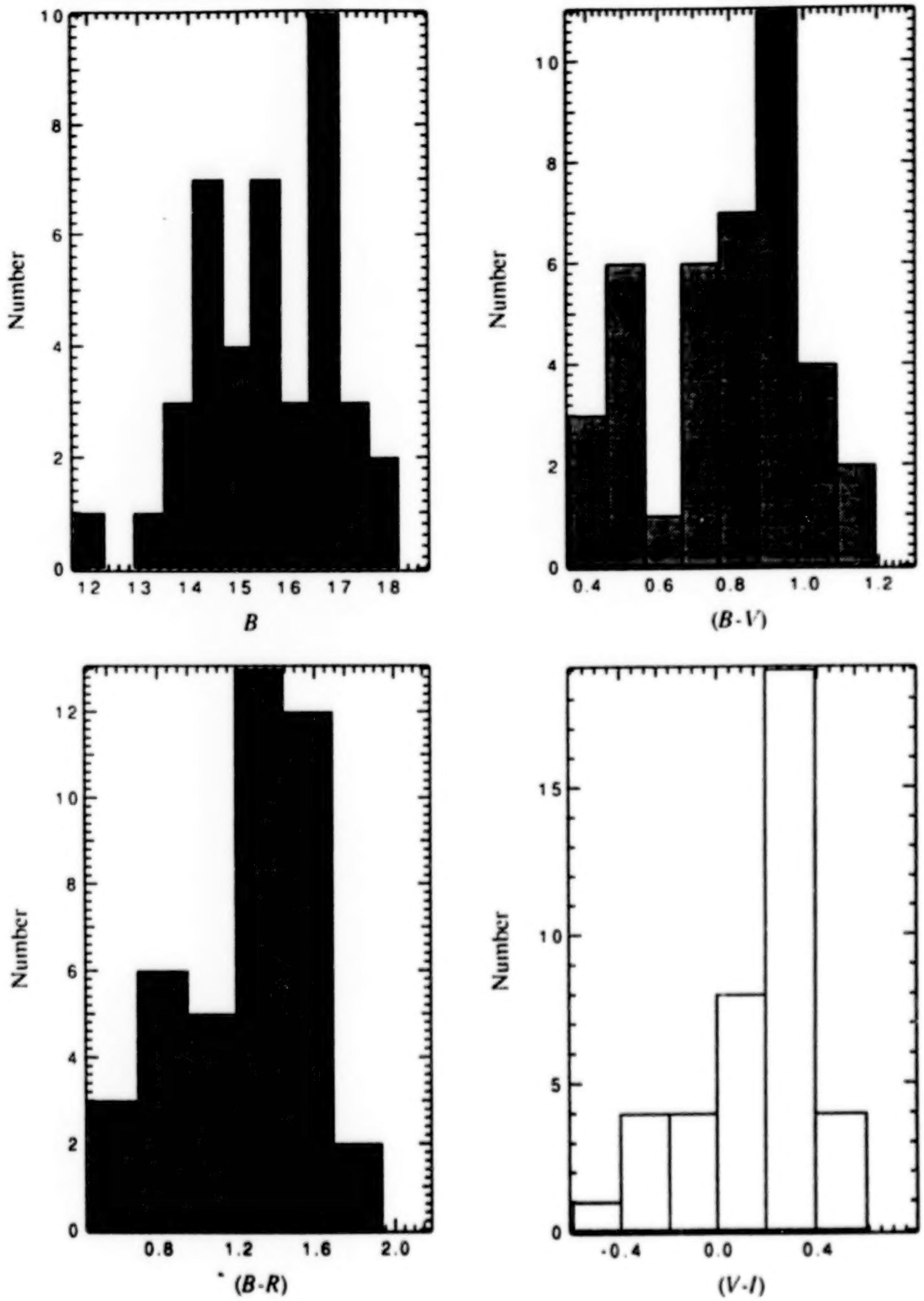

Figure 2: Distribution of *B* magnitudes and color indices for the sample galaxies. Apparent magnitudes and colors for closely overlapping galaxies taken from apertures with radii smaller than the galaxy separation.

MULTI-WAVEBAND OBSERVATIONS OF COLLIDING GALAXIES

P.N.Appleton
Iowa State University
Ames, Iowa 50011, U.S.A.

E.I.Robson,
Lancashire Polytechnic,
Preston, U.K.

and

J.M.Schombert,
University of Michigan,
Ann Arbor, Michigan 48109, U.S.A.

1. Introduction

Colliding galaxies represent a major challenge to both theorists and observers because of the large variety of phenomina which are expected to come into play during the interaction. Strong gravitational fluctuations may drive non-linear waves and instabilities throughout the stars and gas leading to enhanced star formation, nuclear activity and ultimately a mixing of the morphological components of the original galaxies. One relatively uncomplicated class of colliding galaxy where stellar waves play an important role in star formation are "ring" galaxies. Ring galaxies are probably formed when a companion galaxy passes through the centre of a disk system driving circular waves through the disk (Lynds and Toomre 1976,Toomre 1978, Struck-Marcell 1990). Off-centre collisions can generate non-circular waves and can be loosely described as banana-shaped although they may exhibit more complex forms as the waves expand into the disk (See also Struck-Marcell; this volume). The propagation of such stellar and gaseous waves through the disk leads to enhanced star formation (e.g. Appleton and Struck-Marcell 1987a; Jeske 1986) and provides a unique probe of the response of the ISM to a propagating wave (See Appleton and Struck-Marcell 1987b).

2. The Observations

We report here results for 3 systems; the irregular ring Arp143 (=VV117); Wakamatsu's Seyfert ring (A0959-755;see Wakamatsu and Nishida 1987; hereafter HN) and the brighter member of the pair of ring galaxies comprising of AM1358-221. The most complete multi-wavelength data is for Arp143. We will describe optical CCD observations made with the 60" Palomar telescope at BV and r band, near-IR images at J (1.25 microns),H (1.65 microns) and K (2.2 microns) bands from the IRCAM InSb array camera on the 3.8m UKIRT telescope and VLA observations at at 20cm in both the neutral hydrogen line and radio continuum. The observations of Wakamatsu's ring and AM1358 where made only in the near-IR, and a comparison is made with available optical plate material.

3. The Results

Figs. 1a and b show the optical IIIaJ image of Wakamastu's ring (taken from WN) and the K-band near-IR image of the same object.

Fig.1a Wakamatsu's Ring: Optical

Fig.1b Wakamatsu's Ring: K-Band

In the optical, the galaxy is composed of an irregular ring of bright knots, brighter to the south, which surround the off-centre Seyfert-1 nucleus. To the western-edge a jet-like filament extends out of the ring to the north. This filament is almost certainly the highly distorted companion galaxy which created the ring and is itself now suffering the consequences of dynamical heating. The most prominent K-band emission comes from the ring nucleus and the peculiar companion. However what is remarkable about the near-IR images is the lack of a well-defined ring when compared with sharpness of the optical ring. A diffuse underlying disk is detected clearly with only a hint of an enhancement near the bright optical knots. We will show later that in the regions of the optical knots the near-IR colors are abnormal and are strongly suggestive of thermally heated dust.

The AM1358-221 system is a pair of southern rings which are separated by 5 arcminutes. Figure 2a and b show the optical and K-band images of AM1358-221 respectively. The brighter of the pair (boxed) was imaged through J and K filters at UKIRT. As with Wakamatsu's ring, it is striking that the bright optical ring is very weak when seen in the IR.

The detection of only a weak enhancement of the ring component in the near-IR is perhaps not totally unexpected since the optical light ought to be dominated by young stars. A similar result has been reported by M.Joy (personal communication) in an ongoing study of the Cartwheel ring galaxy. The low surface-density contrast in the light of the old stellar population provides support for the idea that the star-formation is triggered by cloud-cloud collisions due to crowding in the gas wave (See Struck-Marcell and Appleton 1987b) rather than the star formation being a result of gas responding to the weak stellar potential in the wave. Evidently a rather

Fig.2a AM1358-221: Optical

Fig.1b AM1358-221: K-Band

low over-density threshold in the gas wave is suffiecient to drive a strong and vigourous starburst seen in the optical ring.

A consideration of the J-H, H-K colors of Wakamatsu's ring show that all the points measured in the disk, nucleus and companion occupy a region intermediate between the colors of starburst galaxies and QSO's. The nuclei of both galaxies in the Wakamatsu system have IR colors similar to the FIRG (or ELF!) galaxy Arp220. Even the disk component of Wakamatsu's ring has a large H-K color suggesting considerable dust distribution a result perhaps not unexpected given the high total far-IR emission ($L(80)= 1.1\times 10^{11} L_\odot$) from the ring noted by WN. One knot in Wakamatsu's ring (marked W1 in Figure 1a) has an extreme H-K color like that of a QSO's and yet is clearly non-nuclear.

In the ramaining part of this paper I will turn my attention to Arp143. This galaxy (shown in Fig. 3a), classified as an irregular ring by de Vaucouleurs de Vaucoulears and Corwin (1976), is obviously not a classical ring but rather a collection of luminous blue knots surrounding the nucleus. The object was first described as a "Nest" (of galaxies) by Verontsov-Velyaminov(1959). HI observations confirm that the blue knots are part of a rotating disk system (NGC2445), and are probably not dynamically separate entities (Appleton et al 1987). The system was also the subject of an early study by Burbidge and Burbidge (1959). The Burbidge's concluded their paper by suggesting that NGC2445 (the more disk-like component of the system) was probably either a galaxy forming in the wake of the elliptical companion NGC2444 or was a galaxy strongly disturbed by a head-on collision with its companion.
The latter view is supported by Appelton et al. who also discovered a huge plume of HI extending away from the system to a distance of 150kpc. A faint optical plume is also detected. We interpret the plume as further evidence that a galaxy has plowed through NGC2445.

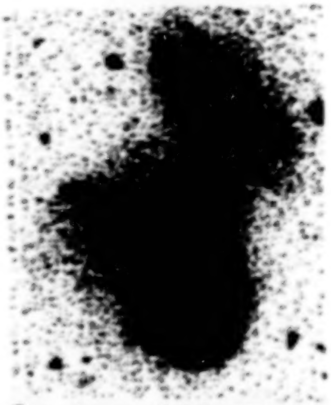

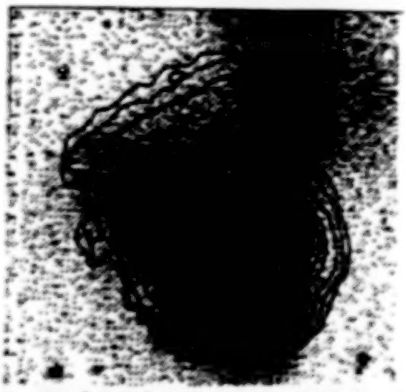

Fig.3a Arp 143=VV117 (V-Band) Fig.3b HI Emission and Optical Knots

The same HI observations also show that the HI disk of NGC2445 has approximately circular outer contours with a strong banana-shaped wave superimposed on its western edge (See Fig.3b). The bright optical knots (shown in Figure 3b) lie on the OUTER-EDGE of the banana-like wave. The morphology of the HI wave is precisely what would be expected from an off-centre collision between a galaxy and a gas-rich disk (See Appleton and Struck-Marcell 1987b). Hence Arp143 would appear to be a ring-galaxy in the process of "turning-on" optically, the optical knots being giant HII regions forming on the leading-edge of the density wave generated in the gas. The optical knots are very blue (B-V ~ 0.4 to 0.6) and show H(alpha) emission (Burbidge and Burbide 1959). If the banana-shaped HI wave is indeed a density wave driven through the gas disk of NGC2445, then a faint stellar wave should also be present in the underlying old stellar disk.

Such a wave might be seen in the K-band light and should be spatially coincident with the HI wave. Figure 3c and d show the

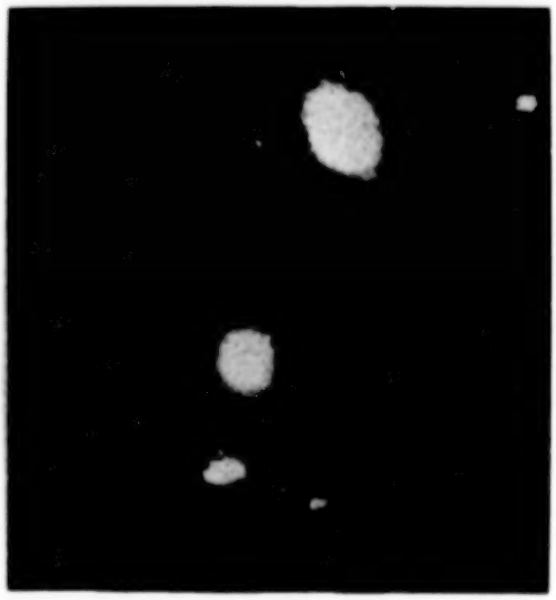

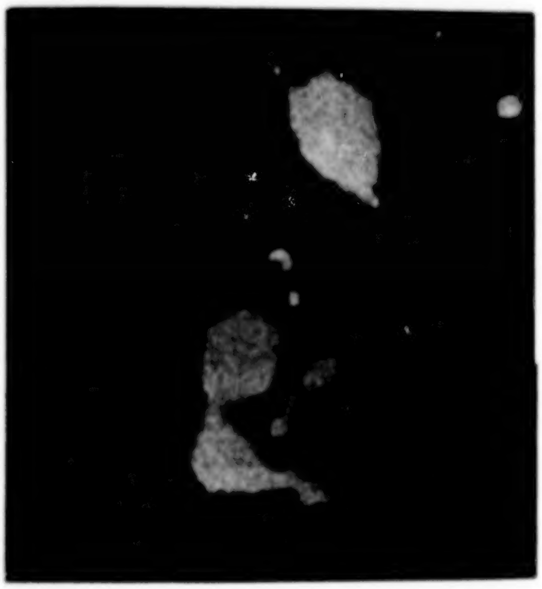

Fig.3c Arp143 (K-Band) Fig.3d Arp143 Smoothed K-band Image

K-band image of Arp143 both before (1.2 arcsec/pix) and after convolving with a 3x3 pix box function. Although very faint optically, a near-IR structure is found which co-incides with the HI wave. This feature is indicated in Fig. 3d and may be part of a large half-ring which encircles the inner disk. The same structure is present much less obvious in the optical images. In contrast, the bright optical knots which lie on the outer edge of the HI wave are very luminous in the K-band image. (One of the knots is probably a late G-type foreground star which was noted by the Burbidges). We note that with the exception of two of the brighter knots, most of the IR emission is consistant with the colors of late-type stars. Power spectra of some selected features obtained by combining the data from the Palomar CCD and the IRCAM photometry clearly show that the emission from the bright knots splits into two separate components, a hot component corresponding to young massive stars and a cooler component. The cooler "bump" in the IR spectrum may either be generated by young supergiants or old disk giants and dwarfs.

This latter ambiguity between old and young stellar populations leads to some problems in the full interpretation of the "knots". If the JH and K emission in the knots is dominated by supergiants (a resonable assumption given the identical spatial position of the IR knots wrt the optical) then the knots are bright "beads" of young stars. On the other hand, the models of Struck-Marcell (1990) predict that caustic "hotspots" can also be produced as stellar disk stars stream through each other. In this case the IR enhancements would be in the old stellar disk, although some star formation would occur as gas piled up at those points. A radio-continuum image of the system (not shown here) shows extended emission associated with the knots lending support to the view that the "chics" in the "Nest" of Arp143 are indeed transient young starforming regions and may well soon be replaced with a fully-fledged ring structure in a few million years from now.

References

Appleton,P.N. & Struck-Marcell,C. 1987a, Ap.J., 312,566.
Appleton,P.N. & Struck-Marcell,C. 1987b, Ap.J., 318,103.
Appleton,P.N., Ghigo,F.D.,van Gorkom,J.H.,Schombert,J.M. & Struck-Marcell,C., 1987,Nature,330,140,(and 330,300).
Burbidge,E.M. & Burbidge,G.R. 1959, Ap.J, 130,12.
de Vaucouleurs,G.,de Vaucouleurs,A. & Corwin,H. 1976. Second Ref. Catalogue of Bright Galaxies, (TUP,Austin).
Jeske,N. 1986. Ph.D.Thesis, University of California,Berkeley.
Lynds,R. & Toomre,A. 1976, Ap.J.,209,382.
Struck-Marcell,C.1990. A.J.,99,71.
Toomre,A. 1978, in IAU. Symposium Number 79.,ed. M.S. Longair & J.Einasto (D.Reidel),p109.
Verontsov-Velyaminov,B.A.,1959, Atlas and Catalogue of Interacting Galaxies,(Sternberg Institute, Moscow).
Wakamatsu,K. & Nishida,M.T. 1987, Ap.J.(Letts),315,L23. (WN)

DISCUSSION

Chatterjee: Is Wakamatsu's ring in the final stage of evolution (like the simulations of Spiegel and Theys)?

Appleton: I do not believe so. Rather I believe it is a young ring. I do not believe that the optical "beads" are a result of the Theys and Spiegel mechanism. Indeed, the "beads" probably do not form from the self-gravity ot the ring. The stars propagate through the ring on a timescale which is very short compared with the gravitational free-fall time for the formation of clumps. This is supported by N-body simulations of James and Appleton (1989).

Cutri: I would suggest imaging the galaxies in the 2 μm photospheric CO band. This feature is quite strong in supergiants, but is much weaker in MS stars. Shocked gas, of course, should not exhibit the absorption. Such a measurement might help differentiate between the two cases.

Appleton: I hope you are right! Thank you.

Tidal distortions in pairs of early-type galaxies

Ph. Prugniel
European Southern Observatory
Karl-Schwarzschild Str. 2
D-8046, Garching, Fed. Rep. of Germany

and

E. Davoust
Observatoire Midi Pyrénées
14, Av. E. Belin
F-31400, Toulouse, France

We are conducting an imaging survey of pairs of elliptical galaxies which has already produced interesting results. Some pairs present a common pattern of distortion interpreted in terms of tidal effects (Davoust and Prugniel, 1988; Prugniel et al., 1989). Other examples drawn from the literature (Borne and Hoessel, 1988; Colina and Pérez-Fournon, 1990) share the same morphology. This *Poster* presents new cases and lists the characteristics of 24 such systems.

Our pairs are drawn from a sample of binary and multiple galaxies which has in turn been extracted from the CGCG, UGC (Nilson, 1973) and VV (Vorontsov-Velyaminov, 1959) catalogues. This sample includes that of Karachentsev (1972). It contains 1800 pairs, among which 700 are S – S or mixed morphology pairs. We are working on the remainder to produce a sample of close *physical* pairs of elliptical galaxies (we also include bulge dominated S0's since the morphological discrimination from ellipticals is often ambiguous, in particular for interacting galaxies).

One of the interests of this work is to provide a sample selected on purely optical criteria, at variance with other works (e.g. Valentijn and Casertano, 1988). This will allow statistical studies of non-optical properties of these pairs (in particular radio emission).

We have so far obtained CCD-images of 125 pairs with the 2 m telescope of Pic du Midi in V and/or R. Velocities and velocity differences of 78 pairs have been obtained using the 1.93 meter telescope of Observatoire de Haute Provence and from the literature. One is an optical pair (VV 190). Eighteen of our pairs present the morphological effect described in Davoust and Prugniel (1988): the external parts of each member are stretched in opposite senses in a direction roughly perpendicular to the pair axis. The proportion of 15±4% distorted pairs confirms previous estimates.

Except for a few cases involving flattened galaxies with nearly aligned major axes which deserve careful detailed analysis (Prugniel, 1989), the apparent distortions do correspond to physical distortions. We have searched the literature for isophote maps showing this effect. In the survey of radio galaxies by Colina and Pérez-Fournon (1990), 7 out of 20 pairs show this characteristic distortion. Such a high rate (35%) suggests a relation between the strength of the interaction and radio activity (if we consider that the magnitude of the distortion is related to the strength of the interaction).

On the other hand, among the optically selected distorted pairs, 42% are radio galaxies while only 5% of all E–E Karachensev pairs are detected in radio (Stocke, 1978; this proportion rises to 7% if we only consider pairs with a separation of less than 10 kpc). This is not a rigorous statistical analysis since thresholds for radio detection and also for distortion detection are not homogeneously defined. However, the contrast is strong and we consider this as an indication for a possible relation between distortion and radio emission.

The comparison of the distributions of projected separations for distorted and undistorted pairs gives only marginal results. For 17 distorted pairs with measured radial velocities, the average separation is 9.4 kpc with a variance of 5.0 kpc, and for 74 non-distorted pairs, these values are respectively 11.0 and 10.0. The F-test allows us to reject the hypothesis of the equality of the two variances at a confidence level of 99.5%. However, the difference between the two distributions almost disappears when we reject the pairs with a velocity larger than 10000 km/s. This effect is certainly due to the cutoff in angular separation present in our sample: the average projected separation is about 30 arcsec, and only a few pairs are separated by more than 1 arcmin. Thus, the pairs within 50 Mpc and separated by more than 15 kpc are basically absent from our sample. To avoid this selection effect, Table 1 shows the proportion of distorted pairs in three bins of projected separation (assuming $H_o = 100 km/s/Mpc$).

Table 1

Distance range (kpc)	Proportion of distorted pairs
0 – 10	22% (12/54)
10 – 15	17% (3/18)
>15	10% (2/19)

This analysis suffers from the too small statistical sample, but it strengthens the result of Stocke (1978) suggesting that both radio emission and morphological distortion are stronger in close than in loose pairs.

The isophote maps of 4 new pairs are presented in Fig. 1 and the characteristics of all known pairs are listed in Table 2.

In conclusion, we would like to stress the usefulness of distortions of this kind for establishing that binary galaxies are actually interacting, and thus good candidates for investigating other effects of interaction, such as radio emission, star formation, number of globular clusters, and possibly merging.

Figure 1:

Figures 1a to 1d give the isophote maps of 4 distorted pairs: UGC 367, MRK 1435, NGC 7148 and 7774. These V-band images were taken with the 2 m telescope of Pic-du-Midi observatory. The step between each level is one magnitude. The orientation is such that the pair-axis is vertical, the large galaxy stretched toward the left and the small toward the right.

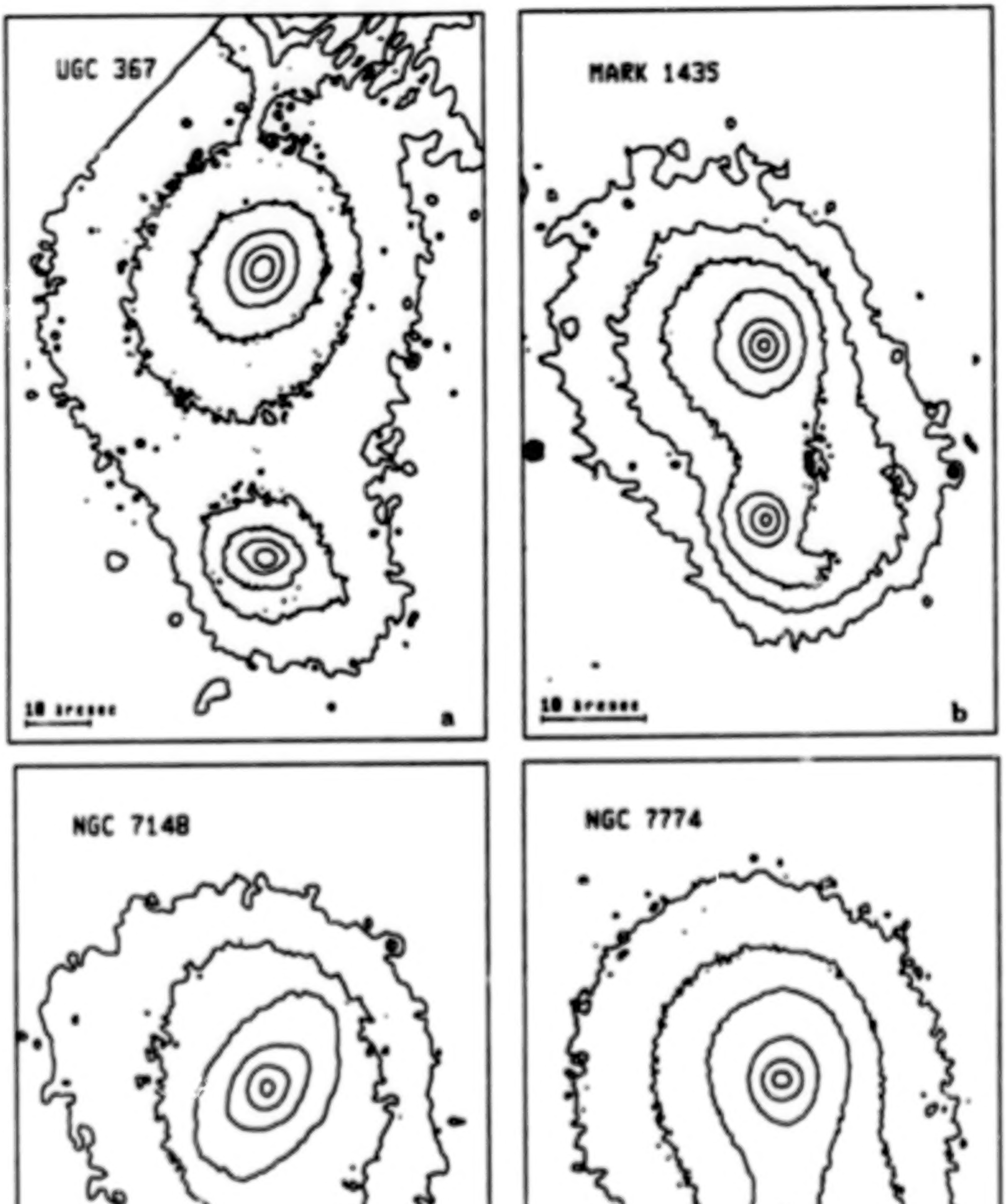
UGC 367
10 arcsec
a
MARK 1435
10 arcsec
b
NGC 7148
5 arcsec
c
NGC 7774
10 arcsec
d

Table 2
distorted pairs

Identification	Coordinates		Velocity	Separation		Effective radii		Lumin.	Radio	Source
	α_{50}	δ_{50}	km s^{-1}	arcsec	kpc	(1)	(2)	Ratio	Iden.	
UGC 367	00 34.4	25 25	9620	42	19.6	13.3	6.6	4.8	B2	1
UGC 1093	01 29.1	17 19	8650	51.0	21.0	11.6	6.6	3.0		1
NGC 741/2	01 53.8	05 23	5490	50	11	31.1	4.6	11.6	4C	2
UGC 1841	02 20.0	42 46	6450	23.7	7.4			7.0	3C66B	1
NGC 1044	02 38.4	08 31	6420	18.6	5.8			(7)	4C	4
NGC 1129	02 51.3	41 23	5150	25.9	6.5	(85)	3.5	22.		1
VV7.08.14	03 26.0	39 37	7290	23.2	8.2			(5)	B2	4
NGC1409/10	03 38.7	-01 27	7400	7.0	2.5	14.6	4.7	4.7		1
UGC 2992	04 11.1	01 38	5030	18.0	4.4			2.2		1
NGC 1587/8	04 28.1	00 33	3800	59.4	12	14.0	4.6	3.8	Radio	2
UGC 3710	07 06.4	28 45	7350	7.4	2.6	7.2	4.5	1.3		1
NGC 2672/3	08 46.5	19 16	4300	33.0	7	29.4	4.7	11.5		2
MRK 1435	10 33.6	55 02	3360	17.2	2.8	6.2	3.6	4.0		1
NGC 4782/3	12 51.9	-12 17	4140	42	8	20.0	16.0	1.6	3C278	2
NGC 4893	12 57.7	37 27	10400	19.2	9.7	22.0	7.9	3.9		1
NGC 5718	14 38.1	03 40	8260	60	24.0			(1.5)	Radio	3
B2 inA1984	14 50.4	28 10	38000	9.8	18.0			(1)	B2	4
In A2172	16 15.0	42 34	39300	6.5	12.4			(7)	B2	4
UGC 11804/5	21 42.3	46 02	5600	33.0	9			1.4		1
NGC 7148	21 49.8	03 12		13.0		6.2	3.0	3.9		1
NGC 7236/7	22 12.3	13 35	7810	34.0	13	47.0	4.6	3.3	3C442	1
UGC 12064	22 29.1	39 06	5130	36.0	12	8.7	4.6	3.9	3C449	2
NGC 7578	23 14.8	18 26	12020	33.8	19.5			(2)	Radio	3
NGC 7774	23 49.6	11 12	6700	15.5	5.0	10.8	5.0	4.0		1

Notes: Effective radii are given for the two galaxies of each pair in arcsec, values in parentheses are uncertain. The luminosity ratio is in linear flux computed from the asymptotic magnitude. Sources of images: (1) This *poster*, (2) Davoust and Prugniel (1988), (3) Arp (1966), (4) Colina and Pérez-Fournon (1990).

References

Borne, K.D., Hoessel, J.G.: 1988, *Astrophys. J.* **330**, 51

Colina, L., Pérez-Fournon, I.: 1990, *Astrophys. J. Suppl.* **000**, 000

Davoust, E., Prugniel, Ph.: 1988, *Astron. Astrophys. Letters* **201**, L30

Karachensev, I.D.: 1972, *Commun. Special Astrophys. Obs. USSR* **7**,1

Nilson, P.: 1973, *Uppsala Astron. Annals* **6**

Prugniel, Ph., Davoust, E., Nieto, J.-L.: 1989, *Astron. Astrophys.* **222**, 5

Prugniel, Ph.: 1989, in *1st ESO/ST-ECF Data Analysis Workshop*, ed. Grosbol, P.J. *et al.*, p. 161

Stocke, J.T.: 1978, *Astron. J.* **83**, 348

Valentijn, E.A., Casertano, S.: 1988, *Astron. Astrophys.* **206**, 27

Vorontsov-Velyaminov, V.A.: 1959, *Atlas and Catalogue of Interacting Galaxies* (Sternberg State Astron. Inst., Moscow)

A MULTI-FREQUENCY STUDY OF THE PECULIAR INTERACTING SYSTEM ARP 206

Louis Noreau
Department of Astronomy, University of Toronto and
Département de Physique & Observatoire Astronomique du Mont Mégantic, Université Laval
and
Philipp P. Kronberg
Department of Astronomy, University of Toronto

I. INTRODUCTION

Arp 206 is a nearby (7.8 Mpc), relatively large (7.′5 × 2.′0), and bright ($B_T^{b,i} = 11.07$) interacting system comprising unequal members: NGC 3432 and UGC 5983. A third anonymous galaxy, "Arp 206c", is visible in the field. (see Figure 1a) Vorontsov-Velyaminov (1959) included the NGC 3432-UGC 5983 pair in his ***Atlas and Catalogue of Interacting Galaxies*** (VV-11). On the other hand Arp (1966) interpreted the system as a galaxy with material ejected from the nucleus (Arp 206).

Bertola (1966, 1968, and priv. comm.) obtained long-slit spectra of the largest galaxy of the pair, NGC 3432. This showed strong non-circular motions that could be interpreted as an explosion in its nucleus. This work is in line with a similar study of another system, Arp 205 (Bertola *et al.* 1983, Noreau and Kronberg 1986, 1987). In this first case it was found that the non-circular radial velocities were caused by the 're-entry' of galactic material torn away by the interacting system.

In their seminal paper, Toomre and Toomre (1972) mentioned two striking consequences of interaction: *(1)* the spectacular distortion in the usually symmetric outer isophotes of a galaxy, and *(2)* the infall on the central part of the galaxy of material is no longer held in balance by the symmetric gravitational potential. These effects are present in a large number of system (Kennicutt 1990, this conference) However, detail case studies of individual galaxies are rare because for maximal usefulness they must involve an extensive array of observations at different wavelengths and using very different observational techniques.

We present here one such study and a preliminary discussion of the results. We used the VLA to perform a full synthesis map in the λ 21 cm line. In addition to these observations, we obtained VLA maps of the radio continuum at $\lambda\lambda$ 22, 18 and 6 cm. The radio maps are complemented with CCD images through B, V, and R broad-band filters and Hα, [S II], and [N II] interference filters obtained at the 1.6 meter telescope of the Mont Mégantic Observatory.

II. OBSERVATIONS AND DATA PROCESSING

A) Radio Observations

All radio data were taken with the NRAO Very Large Array in the 3 kilometre ("C") configuration. For all observations 3C286 and 1128+385 were used as primary and secondary calibrators, respectively. Details of the line and continuum observations are given in Table I.

The visibilities at 1385 and 1470 MHz were combined together to produce a naturally weighted map. (Figure 1c) A uniform-weight map at 1635 MHz was also produced but is not displayed here. No polarisation was detected from the galaxy down to the noise level. The 4885 MHz map was also produced with natural weighting of the (u, v) data. (See Figure 1d.)

The $\lambda 21$ cm data for Arp 206 were obtained with full (u, v) track observations. We made a bandpass calibration based on 3C286 observations. Maps with both natural and uniform weightings of the (u, v) data were produced and the former was found more satisfactory. Line signals were found in 19 maps ranging from 446.2 to 756.7 $\mathrm{km\,s^{-1}}$. We found it necessary to clean the line maps after subtracting a continuum map made of 12 channels in which no emission was found. The map noise was 0.54 millijansky beam^{-1}; and the resolution was $22\overset{''}{.}19 \times 17\overset{''}{.}65$ at $P.A. = 87\overset{\circ}{.}8$.

TABLE I: Summary of Observations

ν_{eff} or λ_{eff}	$\Delta\nu$ or $\Delta\lambda$	T_{int}	date (y/m/d)	description
1.385 GHz	25 GHz	15.0 min.	83/03/06	21.6 cm continuum
1.385 GHz	25 GHz	50.0 min.	83/05/11	21.6 cm continuum
1.470 GHz	25 GHz	62.3 min.	83/05/11	20.4 cm continuum
1.635 GHz	25 GHz	16.7 min.	83/03/06	18.3 cm continuum
1.635 GHz	25 GHz	49.4 min.	83/05/11	18.3 cm continuum
4.885 GHz	50 GHz	10.3 min.	83/05/11	6.14 cm continuum
1.417 GHz	32×97.7 kHz	5.88 hrs	84/04/09	$\lambda 21$ cm line
4400 Å	~ 980 Å	1000 sec.	86/03/31	Johnson B
5500 Å	~ 890 Å	800 sec.	86/03/31	Johnson V
6400 Å	~ 800 Å	600 sec.	86/03/31	Kron-Cousins R
6577 Å	10 Å	2 × 2000 sec.	86/03/24	Hα $\lambda 6563$Å
6727 Å	50 Å	2000 sec.	86/03/31	[S II] $\lambda\lambda 6716, 6731$Å
6002 Å	10 Å	2000 sec.	86/03/31	[N II] $\lambda 6583$Å

B) Optical Observations

For the optical observations of Arp 206, the Cassegrain focus of the Mont Mégantic 1.6 meter telescope was equipped with a focal reducer, an inclinable filter holder and a CCD camera. Details of the observations are given in Table I. The usual processing step (debiasing, dark count removal, and flatfielding) were done using the IRAF CCDRED package. The latter steps of the processing were done using the AIPS software. Four stars from the HST Guide Star Catalog were used to orient the images relative to 1950.0 sky coordinates. A crude B, and V calibration was made in the natural system of the CCD using published B and V magnitudes. In addition, $(B-V)$, $(V-R)$ and $(B-R)$ images were also produced. We subtracted the R image from the narrow bandwidth images to produce continuum-free Hα, [S II], and [N II] line images. The Hα image is displayed in Figure 1b. The calibration of the the Hα, [S II], and [N II] images was made by using published spectrophotometric data of Staufer (1982).

III. DISCUSSION

A) Arp 206 as a Pair of Galaxies

The CCD images show a well-developed bridge between NGC 3432 and UGC 5983. On the other hand, the complex H I tails are not visible in the optical. In the total H I map, the bridge is lost in a general envelope encompassing both galaxies. The "bridge" also appears to have some radio emission.

On the total H I map the system is rather edge-on, far more than it would appear in optical wavelengths. UGC 5983 falls exactly in line with NGC 3432. The velocity of the centres of mass of NGC 3432 and UGC 5983 are 530 $\mathrm{km\,s^{-1}}$ and 630 $\mathrm{km\,s^{-1}}$, respectively. In view of the considerable "damage" sustained by NGC 3432 and the apparent low mass of UGC 5983, it appears that the passage must have been at near parabolic speed, with a small pericentric distance and a very low inclination with respect to the disk of NGC 3432. The apparent distribution of H I along the z axis of the galaxy could be accounted for by projection effects.

The tidal appendage found at higher velocities, which rises at a $P.A. \simeq 25°$ west of the main body of the galaxy is probably the "tail", the part of the tidal "damage" away from the perturbing companion. (see Figures 1a and b) The "bridge" may be rising north-east from the galaxy and then continue "under" to the south of the galaxy. The relative sizes of the appendages would indicate that the pericentre was crossed *recently*. Any further inferences about the collision parameters will need to await the results of detailed computational modelling of the interaction.

We now summarize the observational characteristics of the individual galaxies:

B) NGC 3432

The brightest isophotes of the galaxy show a wiggly line of "knots". In the R image, the central region dominates the emission. The northeast part of the galaxy dominates in the Hα, [S II], and [N II] line maps and the 4885 MHz continuum map. (see Figure 1) The bluest ones are visible in the north-eastern part of the knot ridge. The peak of radio emission does not correspond with the nucleus but rather with the regions where the bluest knots are found. This region also corresponds with the local maxima of the Hα, and [S II] maps. The radio emission observed is most probably due to star formation and supernova activity.

It is interesting to note that the main body of NGC 3432 was not disturbed by the interaction. The H I is concentrated into two maxima on either side of the optical "nucleus" itself does not appear to be prominent in the radio continuum at either "C" or "L" band.

It is interesting to note that the non-radial motions reported by Bertola (1966, 1968, and priv. comm.) were not reproduced in the H I line maps. (Noreau *et al.* 1990)

C) UGC 5983

Detailed examination of the H I line maps indicates that the location of the NE secondary maximum in the channel maps from 487.6 to 570.3 km s^{-1} shifts with increasing velocity along a line at $P.A. \simeq 44^\circ$. This could be the rotation axis of UGC 5983. Some of the tidal material, especially in the NE, could perhaps have been part of UGC 5983 at some point.

The fact that both galaxies are found in a common H I envelope also suggests that material from NGC 3432 might have fallen toward its smaller companion. We suggest that actually, gas fell on the companion and triggered star formation. This scenario is supported by the discovery of continuum radio emission at 21.6 cm which is coincident with the Hα emission seen in UGC 5983. (see Figures 1b and 1c.)

D) Arp 206c

Arp 206c was not detected in any of the radio continuum or optical interference filter images. Some H I emission appears in projection with Arp 206c, but they undoubtly are extensions of of the tidal features of NGC 3432. Arp 206c is most probably an unrelated background object.

Acknowledgements

We would like to thank the following individuals for help, insight, suggestions related to this project: Rick Perley, and Jacqueline van Gorkom of the VLA; Jean-René Roy of Université Laval for the use of his focal reducer and his interference filters; and René Racine, Bernard Malenfant and Ghislain Turcotte at the Mont Mégantic Observatory. This work was started during the tenure of a Québec-Ontario Graduate Scholarship by LN at the University of Toronto from the *Fonds FCAC* of the Government of Québec; he later was supported as a Post-doc at Université Laval by a *Fonds FCAR* grant to the *Observatoire Astronomique du Mont Mégantic*. PPK and LN both acknowledge the support of the National Science and Engineering Research Council of Canada (NSERC) for Research Grants and a double Québec-Ontario and Ontario-Québec grants.

References

Arp, H. C. 1966 *Atlas of Peculiar Galaxies* (Caltech: Pasadena).

Bertola, F. 1966, *Mem. Soc. Astr. It.* **37**, 433.

Bertola, F. 1968 *IAU Symposium no. 29.* **29**, 97)

Bertola, F., Casini, C., Bettoni, D., Galetta, G., Noreau, L., and Kronberg, P. P. 1984 *A. J.*, **89**, 350.

Noreau L., and Kronberg P. P. 1986 *A. J.*, **92**, 1048.

Noreau L., and Kronberg P. P. 1987 *A. J.*, **93**, 1045.

Noreau L., Kronberg P. P., Bertola F., Galletta, G., and Casini, C. 1990, in prep.

Stauffer, J R. 1982 *Ap. J. Supp.*, **50**, 517.

Toomre, A., and Toomre, R., 1971 *Ap. J.*, **178**, 623.

Vorontsov-Velyaminov, Ya. (1959) *Atlas and Catalogue of Interacting Galaxies.* (Moscow)

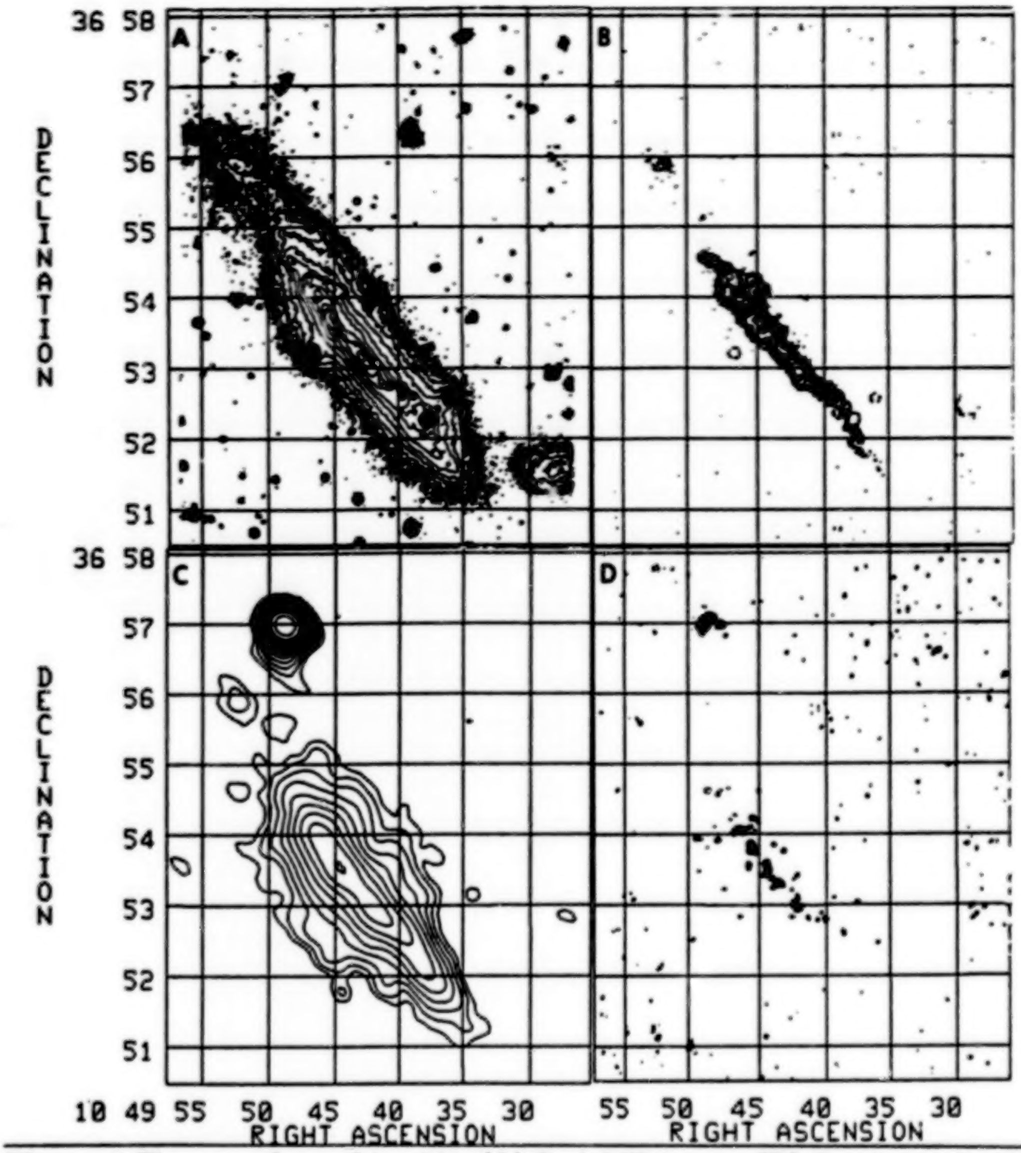
36 58
57
56
55
54
53
52
51
DECLINATION
A
B
C
D
10 49 55 50 45 40 35 30
RIGHT ASCENSION
55 50 45 40 35 30
RIGHT ASCENSION

Figure 1 The many faces of Arp 206: **(A)** Red CCD image; **(B)** Continuum-free Hα CCD image; **(C)** VLA map of the continuum emission at 21.6 cm. **(D)** VLA map of the radio continuum emission at 6.1 cm.

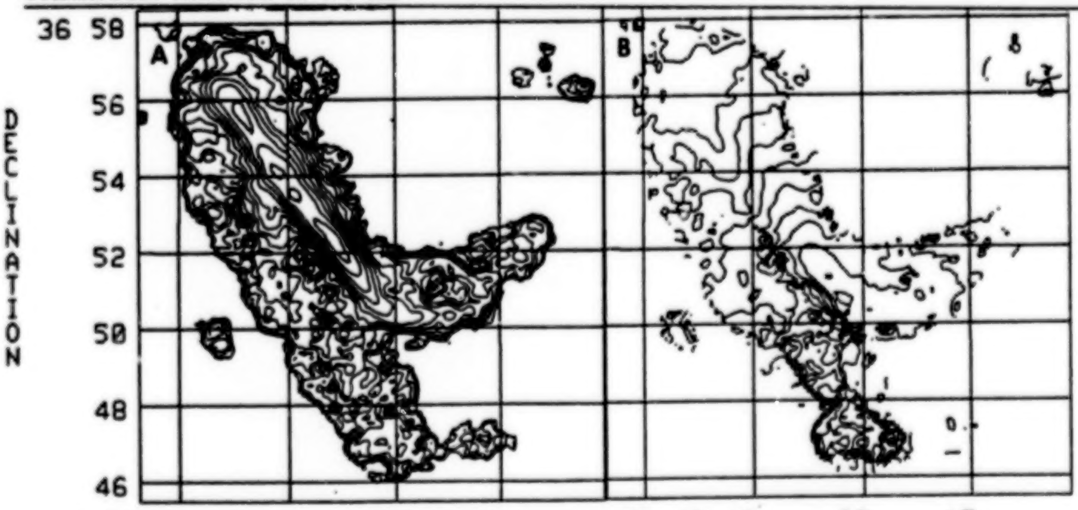
36 58
56
54
52
50
48
46
DECLINATION
A
B
10 50 00 49 45 30 15
RIGHT ASCENSION
00 49 45 30 15
RIGHT ASCENSION

Figure 2 Arp 206 in the λ21 cm line: **(A)** Total H I map; **(B)** Velocity map.

II. CLASSICAL OBSERVATIONS
OF
MULTIPLETS

OBSERVATIONAL PROPERTIES OF COMPACT GROUPS OF GALAXIES

Paul Hickson
Department of Geophysics and Astronomy
University of British Columbia

1. Introduction

Compact groups are small, relatively isolated, systems of galaxies with projected separations comparable to the diameters of the galaxies themselves. Two well-known examples are Stephan's Quintet (Stephan, 1877) and Seyfert's Sextet (Seyfert 1948a,b). In groups such as these, the apparent space density of galaxies approaches 10^6 Mpc^{-3}, denser even than the cores of rich clusters. The apparent unlikeliness of the chance occurance of such tight groupings lead Ambartsumyan (1958, 1975) to conclude that compact groups must be physically dense systems. This view is supported by clear signs of galaxy interactions that are seen in many groups. Spectroscopic observations reveal that typical relative velocities of galaxies in the groups are comparable to their internal stellar velocities. This should be conducive to strong gravitational interactions – more so than in rich clusters, where galaxy velocities are typically much higher. This suggests that compact groups could be excellent "laboratories" in which to study galaxy interactions and their effects.

Because of their small sizes, compact groups have relatively short dynamical times. The orbital times of galaxies in such groups is of order a tenth of the Hubble time. It seems unlikely that the densest groups could avoid destruction by galaxy mergers for the age of the universe. They must therefore be young systems. We are thus faced with the related questions of how they form, and what becomes of them. If, as suggested by numerical simulations, the merger products resemble elliptical galaxies, what fraction of present day ellipticals were made in compact groups?

A complication to this picture is the amount and extent of dark matter in compact groups. It has been known since the work of Burbidge and Sargent (1971) that the velocity dispersions of many compact groups are larger than expected if the only mass in the groups is that associated with the galaxies. Mass to light ratios inferred from the virial theorem are often larger than those of individual galaxies by as much as an order of magnitude. Either the groups are not in equilibrium, or the majority of mass in the group is in an unseen form, possibly as a smooth envelope through which the galaxies move.

Compact groups often contain one or more galaxies whose redshift differs greatly from those of the other group members. If these galaxies are at the same distance as the other members, either entire galaxies are being ejected at high velocities from these groups, or some new physical phenomena must be occurring. If their redshifts are cosmological, we must explain why so many discordant galaxies are found in compact groups.

In recent years much progress has been made in addressing these questions. In this review I discuss the current observational data on compact groups and their implications. The dynamical theory of dense groups of galaxies has been reviewed by Barnes (1990), and by Mamon in these proceedings. The reader is also referred to the review by White (1990) of apparent paradoxes posed by compact groups. Effects of the environment on galaxies in clusters and compact groups have recently been reviewed by Whitmore (1990).

2. Catalogs

The Palomar Observatory Sky Survey (POSS), completed almost forty years ago, provided a unique database for studies of compact groups of galaxies. The first catalog containing compact groups, the 'Atlas of Interacting Galaxies" (Vorontsov-Vel'yaminov 1959, 1977 hereafter VV) contains galaxies and small groups selected on the basis of visible signs of interaction on the POSS prints. Although group membership was not a selection criterion, this catalog contains Stephan's Quintet and Seyfert's Sextet and similar groups such as the famous galaxy chain VV172. The catalog also contains about 200 objects referred to as "nests" by Vorontsov-Vel'yaminov (eg. VV644, VV645) which look like small groups of very blue galaxies in physical contact. Subsequent studies of several VV nests (Barbieri *et al* 1979, Arkhipova 1982, Arkhipova *et al* 1987, Vorontsov-Vel'yaminov, Dostal', and Metlov 1980) have shown that many of these nests are in fact single irregular galaxies. The Arp "Atlas of Peculiar Galaxies" (Arp 1966), contains galaxies selected on the basis of peculiar appearance on the POSS prints. It contains a number of small groups, many of which are compact, including many of the Vorontsov-Vel'yaminov compact groups as well as several new systems. The high-resolution photographs in this atlas clearly illustrate the kinds of interaction seen in many compact groups.

In 1957, Shakhbazyan discovered a remarkable group of 12 faint galaxies which appear so compact that they were originally mistaken for stars (Shakhbazyan 1957). Subsequent investigations of Shakhbazyan 1 (Robinson and Wampler 1973, Arp, Burbidge and Jones 1973, Beekman 1974, Klimek 1974,Thompson 1976, Massey 1977, Shakhbazyan 1978, Kirshner and Malumuth 1980) revealed it to be a small cluster of luminous red compact elliptical galaxies with a recession velocity of 33000 km s^{-1} and a velocity dispersion of only 62 km s^{-1}. Over a period of several years, Shakhbazyan and collaborators surveyed over 200 POSS prints, covering about 18% of the sky, in search of similar groups. They used three selection criteria:

There must be at least 5 members, but large clusters are excluded.
Most members must appear compact on either the red or blue print.
The group itself must be sufficiently isolated or compact.

The results were published in 10 lists containing a total of 377 "compact groups of compact galaxies" (Shakhbazyan 1973, Shakhbazyan and Petrosyan 1974, Baier *et al* 1974, Petrosyan 1974, 1978, Baier and Tiersch 1975, 1976a,b, 1978, 1979, hereafter CGCG). Some general properties of 305 CGCG were reviewed by Tiersch (1976). Most of these appear to be groups of red compact galaxies. They have a wide range of densities and velocity dispersions. This sample of groups contains many interesting objects which have been the subject of detailed studies (Börngen and Kalloglyan 1974, Mirzoyan, Miller and Osterbrock 1975, Shakhbazyan and Amirkhanyan 1978, Amirkhanyan and Egikyan 1987, Kodaira, Iye Okamura and Stockton 1988).

The first large statistical study of compact groups was published by Rose (1977) who examined 69 blue POSS plates and also 23 plates from the Yale-Columbia survey (Wesselink 1974) covering a total area of about 7.5% of the sky. Rose used two quantitative selection criteria,

$$n \geq 3 \text{ with } m \leq 17.5$$
$$\sigma_f A_G \leq 0.0035$$

where n is the number of members, m the estimated galaxy magnitude, σ_f the average surface density of field galaxies, and A_G the area of sky covered by the group. The second criterion corresponds to requiring the group to have a surface density enhancement of about a factor of 1000 over the field. Rose found 170 galaxy triplets, 33 quartets and 2 quintets obeying these criteria. The typical magnitude spread between galaxies in a group is small, less than about 1.5. The typical area of a group is less than one square arcmin. Rose also obtained photographic photometry for 2 groups, in order to look for diffuse background light from stars stripped from the galaxies by gravitational interactions (Rose 1979).

The most recent, and largest, survey of compact groups is that of Hickson (1982) who visually inspected all the red POSS prints, covering about 67% of the sky. Three selection criteria were used

$$n \geq 4 \text{ with } m \leq m_B + 3$$
$$R_N \geq 3R_G$$
$$\bar{\mu}_G < 26$$

where m_B is the estimated red magnitude of the brightest group member, R_G is the radius of the smallest circle containing the centers of the group members, $\bar{\mu}_G$ is the mean surface brightness contained by this circle and R_N is the distance from the center of the circle to the nearest nonmember galaxy satisfying the same magnitude criterion. Exactly 100 groups were found which satisfied all three criteria. Some minor changes to the membership of the original catalog were made by Hickson, Kindl and Auman (1989), to ensure compliance with the selection criteria using photometric magnitudes derived from CCD images. The catalog contains 60 quartets, 25 quintets, 8 sextets, 6 septets and one octet. These include the classical compact groups, several VV, Arp, CGCG and Rose groups plus a number of new groups. These groups have apparent space densities spanning a range of over four orders of magnitude, including the highest density systems known. The faintest galaxies in the sample have blue magnitudes of 19 to 20.

This sample has received extensive observational study. Optical spectra and redshifts have now been obtained for nearly all galaxies (Hickson *et al* 1984, Tikhonov 1986, Hickson, Kindl and Huchra 1988b, Hickson and Huchra, 1990, and work in progress). 6-m photographic plates have been obtained for all groups (Tikhonov 1987a,b, 1989), and broad-band (B and R) CCD images have been obtained for all galaxies (Hickson, Kindl and Auman 1989) magnitudes and Hubble types have been derived from both these data sets. Radio studies include HI line observations (Williams and Rood 1987, Williams and van Gorkum 1988) and continuum observations (Menon and Hickson 1985). Infrared (Hickson *et al*) studies based on the IRAS data base have now been published, and X-ray observations exist for several groups (Bahcall, Harris, and Rood 1984). In addition, there have been several detailed studies of the neighborhoods of these compact groups (Sulentic 1987, Rood and Williams 1989, Kindl 1990).

Hickson's catalog is now perhaps the best studied sample of compact groups, and much of the discussion that follows in this review will be based on it.

3. Spatial Distribution and Environment

The environment of compact groups provides important clues to their nature. Are they truly isolated, or are they associated with large clusters, or with looser groups of galaxies? A cursory examination reveals that Hickson's compact groups (hereafter HCGs) are quite uniformly distributed on the sky (away from the galactic plane). They do not concentrate toward the supergalactic equator, nor do they show any clear preference for identifiable clusters or clouds of galaxies with comparable redshifts. In a careful study of the environment of compact groups, Sulentic (1987) finds that only 8 HCGs are in or near rich clusters or groups.

A more difficult question is whether the groups are associated with poor groups, or with other galaxies in their vicinity. Rose (1977) concluded that most of his groups appear to be surrounded by a "halo" of one or more galaxies with a typical radius of 5 to 10 group radii. Sulentic (1987) examined all galaxies within 1° of all HCGs and concluded that the average surface density of galaxies increases slightly within 0°.5 of a group, where it is comparable to that of the lowest density loose groups. He found that typical HCGs have density enhancements of a factor of 100 or more, and about a third have density enhancements of over 500. Rood and Williams (1989) examined galaxies within 10 group radii of the HCGs, and found no significant excess of galaxies in the neighborhoods of two thirds of them. They estimated that on the average there is one physical neighbor for every 3.3 group members, which seems to be in accord with the findings of Rose. Kindl (1990) examined all galaxies within $1.125h^{-1}$ Mpc. of 97 HCGs with known redshifts, and estimated their magnitudes and Hubble types. (h is the Hubble constant in units of 100 km s^{-1} Mpc^{-1}.) This is the largest environment survey, comprising almost 4000 galaxies. He finds that 78% of the groups show no significant excess of galaxies within $0.5h^{-1}$ Mpc. Kindl confirms the conclusion by Rood and Williams that the HCGs have a lower spiral fraction than their neighborhoods, and that this difference is *more* pronounced for groups with a significant excess of nearby galaxies. This result is of particular significance in indicating that compact groups are physically distinct from their environments.

These three studies agree that most HCGs are truly isolated, showing no significant excess of galaxies in their vicinity. However, about one in five groups do appear to be associated with larger systems, typically poor groups. There is evidence that the fraction of spirals in the groups is smaller than in their environments, particularly for the groups associated with larger systems.

4. Morphology

Since the HCGs form a relatively large, homogeneous sample, it is possible to draw general conclusions about their average properties. At this stage it will be useful to summarize the principal observational results:

a) *optical*

Many galaxies in compact groups are interacting. It is estimated that roughly one third of the galaxies in HCGs show clear signs of interaction, such as tidal distortion or truncation in the imaging data alone (Palumbo *et al* 1990). When spectroscopic data are included, the number may be even higher. Fully two thirds of the 33 spiral galaxies observed by Rubin, Hunter and Ford (1990) have peculiar rotation curves. Galaxies that are not now interacting may have suffered past interactions or mergers. Zepf and Whitmore (these proceedings) have confirmed that several of the elliptical galaxies in the HCGs have unusually blue colors that may have resulted from a recent burst of star formation.

The morphological types of galaxies in the HCGs show several interesting trends. The fraction of spirals in the groups averages about 50%. This fraction correlates weakly with group density (see the discussion in Whitmore 1990), more strongly with group luminosity, and most strongly with group velocity dispersion (Hickson, Kindl and Huchra 1988b). Groups with high velocity dispersion contain few spirals. This seems to be opposite to what would be expected if elliptical galaxies are being produced by dynamical evolution. Gravitational interactions and mergers should proceed more rapidly in groups with low velocity dispersions as slow encounters are more effective in disrupting galaxies. Hickson, Kindl and Auman (1989) conclude that the morphology – velocity dispersion correlation is most likely due to environmental effects at the time of galaxy formation.

A related correlation first noted by Sulentic (1987) is that of morphology concordance. Galaxies within a group are more likely to have the same morphological type (spiral or nonspiral) than a random sample. White (1990) has pointed out that such a correlation is expected as a consequence of the morphology-velocity dispersion relation. It should be possible, by numerical calculations, to determine whether this effect is strong enough to explain the observed degree of concordance.

It is generally agreed that mergers should produce elliptical galaxies, and so it was expected that the first ranked galaxies in groups should have a lower spiral fraction than the other galaxies. It was therefore a surprise when Hickson (1982) (also Hickson, Kindl and Huchra 1988b) found no significant difference between the morphological type of the first ranked galaxy and the others. Whitmore (1990), however has argued that this can be explained by the binning used in these studies. If S0 galaxies are grouped with spirals rather than ellipticals, on the grounds that they are not expected to be produced by mergers, a significant correlation does emerge. This suggests that some merging has already occurred in many groups.

Preliminary studies of the optical luminosity function of galaxies in compact groups indicate that it is similar to that of field galaxies (Hickson *et al* 1984). Using the completeness corrections of Hickson, Kindl and Auman (1988), Hickson (1989, unpublished) estimates the luminosity density of all galaxies in compact groups to be of order 2×10^6h $L_\odot$ Mpc^{-3}. Using the estimate 3×10^8h $L_\odot$ Mpc^{-3} for the luminosity density of all galaxies (Bingelli, Sandage and Tamman 1988), he concludes that compact groups contain almost 1% of the light of the total galaxy population. Compact groups contain a significant fraction of the total light of galaxies in the universe. Although the overall luminosity function may be normal, within individual groups, their are deviations. Heiligman and Turner (1980), Hickson (1982) both report evidence for a deficiency of fainter galaxies, compared to a normal luminosity function. For the HCGs this may be due, at least in part, to the selection criteria, which encourages luminosity concordance. It remains to be seen whether this can account for the observed anomalies. If the effect is real, it would indicate that mass segregation is an important aspect in the formation or evolution of compact groups.

The shapes of compact groups have been investigated by Turner and Sargent (1974), Rose (1977), Hickson *et al* (1984), Malyck and Orlov (1986). The first two studies concluded that the observed elongations of compact groups were consistent with a random distribution of galaxies. The latter studies examined the HCGs and concluded that the groups are more elongated than a random distribution, and cannot therefore be explained by chance superpositions of galaxies. The data indicate that the groups are best represented by intrinsically prolate spheroids. Of course the shape of any small dense group will change significantly in a crossing time (the time taken for a typical galaxy to move a distance equal to the radius of the group). Prolate average shapes could arise from radial galaxy orbits, or outlying members in circular orbits.

b) *radio*

Hydrogen line radio observations have been made of spiral galaxies in 51 HCGs by Williams and Rood (1987). They find that these spirals have generally only about half as much neutral hydrogen as a comparable sample of isolated galaxies. They also find that about a third of these galaxies have distorted line profiles. Higher-resolution studies (Williams and van Gorkom, 1988, Williams, McMahon and, van Gorkom, these proceedings) show the HI emission encompassing the whole group in three of the four groups studied.

Menon and Hickson (1985), have observed 88 HGC with the VLA at a wavelength of 20 cm. Many of these have subsequently been observed at 6 cm. 41 sources were found above a flux limit of 1.5 mJy. In the spiral radio galaxies, emission is seen predominantly from the circumnuclear regions, but in elliptical galaxies, only nuclear emission is seen. These radio ellipticals are almost always first-ranked optically, but surprisingly, the optical luminosity of the galaxy is not strongly correlated with the radio emission. The relative rank of a galaxy seems to be more important than its luminosity in determining the frequency of radio emission. This result suggests that the radio emission is related to the galaxy's location or prominence in a group. Precisely the same effect has been independently found by Tovmasyan and Shakhbazyan (1981) in loose groups and double galaxies.

Another interesting feature of the radio observations is the almost total absence of extended radio emission. The observed flux is contained mostly within the visible galaxy. No extended sources such as the large double-lobed or head-tail sources that are seen in clusters are present. Either the physical processes in these galaxies are different or the activity has started only recently and extended components have not had time to develop.

c) *infrared*

In a recent study based on the IRAS data base, Hickson *et al* (1989) conclude that the far infrared emission of galaxies in HCGs is enhanced by about a factor of two compared to a sample of isolated galaxies. The infrared luminosity function they derive is comparable to that of the IRAS bright galaxy sample (Soifer *et al* 1987). From this they conclude that about 1% of all IRAS bright galaxies are in compact groups. This agrees with the observation that 3 of the 324 galaxies in the Soifer *et al* sample are in fact in Hickson's compact group catalog.

d) *X-ray*

Very little X-ray data is available for compact groups. Bahcall, Harris and Rood (1984) observed five HCGs with the Einstein observatory. Three of these were detected and two showed diffuse soft X-ray emission typical of hot intracluster gas. Hickson *et al* (1989) searched data from the HEAO 1 A-2 experiment (Rothschild *et al* 1979) for counts in the fields of the HCGs. However, it was possible only to place an upper limit on the 2-10 keV luminosity, which is consistent with the Einstein results.

5. Discordant Redshifts

The problem of discordant redshifts in compact groups remains unresolved after many years. The key question is whether discordant redshifts in compact groups can be explained by chance superpositions of unrelated galaxies near the line of sight. Arguments against this hypothesis have been advanced by Burbidge and Burbidge (1961), Arp (1973), Arp and Lorre (1976), Sulentic (1983), Sulentic and Arp (1983), Sulentic and Lorre (1983) among others. Studies supporting the superposition hypothesis have been published by Rose (1977) and Hickson, Kindl and Huchra (1988a). Two basic arguments have been raised against the hypothesis: 1) that there is evidence of physical association between discordant and accordant redshift galaxies and 2) that the required chance superpositions are unlikely. The first argument remains controversial, neither side having convinced the other. The second argument can be examined by statistical analysis.

The most recent work is that of Hickson, Kindl and Huchra (1988a) who use the homogeneity of the HCG sample to estimate the number of discordant redshift quintets expected by chance superposition. They predict that about 35% of all compact quintets should contain one galaxy with a discordant (more than 1000 km s^{-1} from the mean) redshift. Although the redshift measurements for this sample are not yet complete, this figure is in agreement with the observation that 4 of the 10 quintets with complete redshifts have one discordant redshift. From this it would appear that there is no compelling reason to believe that the number of groups with discordant redshifts is significantly greater than the number expected from chance superpositions. However, the case is not yet closed. It will be interesting to see if this prediction still holds when complete redshifts are obtained for the full sample of 25 quintets. In addition, the observed discordant-redshift galaxies show a strong preference for central location, which would not be expected from chance superpositions. A possible explanation for this effect could come from gravitational lensing (Hammar and Notale 1986). Amplification of the light from background passing through the gravitational potential of the group would increase the probability of finding a superposed background galaxy near the center of the mass distribution of the group. It should be possible to test this hypothesis statistically with the HCG sample when the redshift survey is complete. If gravitational lensing is a significant factor, it may even be possible to obtain mass estimates for the groups independent of the virial theorem.

6. Physical Nature

Also controversial is the nature of the groups themselves. A non-detection of background light in two groups led Rose (1979) to conclude that "the most plausible explanation for compact groups is that they are temporary unbound configurations forming within loose groups". This explanation was rejected by Mamon (1986) who concluded that most HCGs are "chance alignments of galaxies within loose groups", and therefore are not physically dense.

Hickson and Rood (1988) summarized the observational evidence for high group density, and concluded, from a Monte-Carlo computation of alignment probabilities, that the probability of forming the HCGs by chance alignment is very small. Walke and Mamon (1989, see also Mamon's paper in these proceedings) obtained similar probability estimates, but argued that the richest loose groups have a significant chance of having compact subgroups from chance alignments. They concluded that "roughly half of Hickson's compact groups are chance alignments of galaxies within intermediate density groups and small clusters". This explanation, however, requires that almost all compact groups should occur in clusters. Walke and Mamon predict that 6 times as many compact configurations will occur in the Virgo cluster than in the entire Tully (1987) loose group catalog. This seems to be inconsistent with the observation that hardly any of the HCGs are found in clusters.

One should not conclude that there is no contamination of compact groups with unrelated galaxies. Indeed, the contamination is likely to be significant. From the environment studies describe above, Hickson (1990, unpublished) estimates that about 13% of galaxies in HCGs are superposed members of a loose group, and another 17% are superposed field galaxies with a discordant redshift. Thus perhaps 30% of the galaxies in the HCGs are superpositions.

7. Dynamics

The redshift survey of Hickson and Huchra (1990) reveals a wide range of radial velocity dispersions in the HCGs, with a median of about 200 km $\sec^{-1}$. The median projected separation between galaxies is about $40h^{-1}$ kpc, and the median mass-to-light ratio, estimated from the virial theorem is about 40h $M_\odot/L_\odot$. This is larger than typical mass-to-light ratio of typical galaxies by almost an order of magnitude. Either the groups are unbound (Ambartsumyan 1958) or they contain a substantial amount of dark matter. The conventional picture (eg. Barnes 1985, 1989, 1990) is that compact groups evolve from looser groups and will be destroyed by mergers on a relatively short timescale. Estimates of the typical lifetime of compact groups vary, but a reasonable estimate is of order a tenth of the age of the universe (White 1990). Assuming that the present epoch is in no way special, one expects as many as ten merger products of compact groups for every compact group seen today. Many studies suggest that these relics would resemble elliptical galaxies. Thus as much as 10% of the light of the total galaxy population may result from relics of compact groups. This figure is probably an upper limit as several effects can reduce it. The presence of substantial dark matter in the groups increases the dynamical friction timescale, increasing the lifetimes. Also, the luminosity density of compact groups may be overestimated because of brightening of the galaxies due to star formation triggered by interactions (this would increase both the number of detected groups and the mean luminosity per group). Certainly, this number is not inconsistent with Schechter and Dressler's(1987) estimate that at least 15% of the luminosity density comes from elliptical galaxies. Of course it remains to be demonstrated that the relics would have the required properties. Further observations, many of which are now in progress, combined with increasingly more sophisticated dynamical studies, should elucidate the role of compact groups in the formation and evolution of galaxies.

Acknowledgements

I thank Kochu Menon and Claudia Mendes de Oliveira for helpful discussions and comments on the manuscript. This work was supported by a grant from the Natural Sciences and Engineering Research Council of Canada.

References

Ambartsumyan, V. A. 1958, *Izv. Acad. Nauk. Arm. SSR, Fiz.-Mat.*, **11**, 9.

Ambartsumyan, V. A. 1975, *Astrofiz.*, **10**, 471.

Amirkhanyan, A. S., and Egikyan, A. G 1987, *Astrofiz.***27**, .

Arkhipova, V. P. 1982 *Astron. Zh.*, **59**, 202.

Arkhipova, V. P., Zasov, A. V., Noskova, R. I., and Sil'chenko, O. K. 1987 *Astron. Zh.*, **64**, 1161.

Arp, H. C. 1966, *Ap. J. Suppl.*, **14**, 1.

Arp, H. C. 1973, *Ap. J.*, **183**, 411.

Arp, H. C., and Lorre J. J. 1976, *Ap. J.*, **210**, 58.

Arp, H. C., Burbidge, G. R., and Jones, T. W. 1973, *P. A. S. P.*, **85**, 423.

Bahcall, N. A., Harris, D. E., and Rood, H. J. 1984, *Ap. J. (Letters)*, **284**, L29.

Baier, F. W., Petrosyan, M. B., Tiersch, H., and Shakhbazyan, R. K. 1974, *Astrofiz.*, **10**, 327.

Baier, F. W., Tiersch, H. 1975, *Astrofiz.*, **11**, 221.

Baier, F. W., Tiersch, H. 1976a, *Astrofiz.*, **12**, 7.

Baier, F. W., Tiersch, H. 1976b, *Astrofiz.*, **12**, 409.

Baier, F. W., Tiersch, H. 1978, *Astrofiz.*, **14**, 279.

Baier, F. W., Tiersch, H. 1979, *Astrofiz.*, **15**, 33.

Barbieri, C. , Casini, C. , Jeidmann, J., di Serego, S., and Zambon, M. 1979, *Astr. Ap. Suppl.*, **37**, 559.

Barnes, J. 1985, *M. N. R. A. S.*, **215**, 517.

Barnes, J. 1989, *Nature*, **338**, 123.

Barnes, J. 1990, to appear in *Dynamics and Interactions of Galaxies*, ed. R. Wielen (Heidelberg: Springer-Verlag).

Beekman, G. W. 1974, *Zenit*, **1**, 24.

Bingelli, B., Sandage, A., and Tamman, G. A. 1988, *Ann. Rev. Astr. Ap.*, **26**, 509.

Börngen, F., and Kalloglyan, A. T. 1974, *Astrofiz.*, **10**, 21.

Burbidge, E. M. and Burbidge, G. R. 1961, *Ap. J.*, **134**, 244.

Burbidge, E. M. and Sargent, W. L. W. 1971, *Ap. J.*, in *Nuclei of Galaxies*, ed. D. J. K. O'Connell (Amsterdam: North-Holland).

Hammar, F. and Nottale, L. 1986, *Astr. Ap.*, **155**, 420.

Heiligman, G. M., and Turner, E. L 1980, *Ap. J.*, **236**, 745.

Hickson, P. 1982, *Ap. J.*, **255**, 382.

Hickson, P., and Huchra, J. P. 1990, in preparation.

Hickson, P., Kindl, E., Auman, J. R. 1989, *Ap. J. Suppl.*, **70**, 687.

Hickson, P., Menon, T. K., Palumbo, G. G. C., and Persic, M. 1988, *Ap. J.*, **341**, 679.

Hickson, P., Ninkov, Z., Huchra, J., and Mamon G. 1984, in *Clusters and Groups of Galaxies*, ed F. Mardirossian, G. Giuricin, and M. Mezzetti (Dordrecht: Reidel), p. 367.

Hickson. P., Richstone, D. O., and Turner, E. L. 1977, *Ap. J.*, **213**, 323.

Hickson, P., Kindl, E., and Auman, J. R. 1989, *Ap. J. Suppl.*, **70**, 687.

Hickson, P., Kindl, E., and Huchra, J. P. 1988a, *Ap. J. (Letters)*, **329**, L65.

Hickson, P., Kindl, E., and Huchra, J. P. 1988b, *Ap. J.*, **331**, 64.

Hickson, P., and Rood, H. J. 1988, *Ap. J.*, **331**, L69.

Kindl, E. 1990, Ph. D. Thesis, University of British Columbia.

Kirshner, R. P., and Malumuth, E. M. 1980, *Ap. J.*,**236**, 366.

Klimek 1974, *Urania Kraków*, **45**, 34.

Kodaira, Iye, Okamura, and Stockton 1988, *Pub. Astr. Soc. Japan*, **40**, 533.

Massey, P. 1977, *P. A. S. P.*, **89**, 13.

Malykh, S. A., and Orlov, V. V. 1986. *Astrofiz.*. **24**, 445.

Mamon, G. A. 1987, *Ap. J.*, **321**, 622.

Menon, T. K., and Hickson, P. 1985, *Ap. J.*, **296**, 60.

Mirzoyan, L. V., Miller, J. S., and Osterbrock, D. E. 1975, *Ap. J.*, **196**, 687.

Palumbo, G. G. C., Tornatore, V., Baiesi-Pillastrini, G., Hickson, P., and Mendes de Oliveira, C. 1990, in preparation.

Petrosyan, M. B. 1974, *Astrofiz.*, **10**, 471.

Petrosyan, M. B. 1978, *Astrofiz.*, **14**, 631.

Robinson, L. B., and Wampler, E. J. 1973, *Ap. J. (Letters)*, **179**, L135.

Rood, H. J., and Williams, B. A.. 1989, *Ap. J.*, **339**, 772.

Rose J. A. 1977, *Ap. J.*, **211**, 311.

Rose J. A. 1979, *Ap. J.*, **231**, 10.

Rothschild, R., *et al* 1979, *Space Sci. Instrum.*, **4**, 269.

Rubin, V. C., Hunter, D., and Ford. W. K., Jr. 1990, in preparation.

Seyfert, C. K. 1948a, Phys. Rev., **74**, 129.

Seyfert, C. K. 1948b, *A. J.*, **53**, 203.

Schechter, P. L., and Dressler, A. 1987, *A. J.*, **94**, 563.

Shakhbazyan, R. K. 1957, *Astron. Tsirk.*, **177**, 11.

Shakhbazyan, R. K. 1973, *Astrofiz.*, **9**, 495.

Shakhbazyan, R. K. 1978, *Astrofiz.*, **14**, 273.

Shakhbazyan, R. K., and Amirkhanyan 1978, *Astrofiz.*, **14**, 455.

Shakhbazyan, R. K. and Petrosyan 1974, *Astrofiz.*, **10**, 13.

Soifer, B. T., Sanders, D. B., Madore, B. F., Neugebauer, G., Danielson, G. E., Elias, J. H., Lonsdale, C. J., and Rice, W. L., 1987, *Ap. J.*, **320**, 238.

Stephan, M. E. 1877, *M. N. R. A. S.*, **37**, 334.

Sulentic, J. W. 1983, *Ap. J.*, **270**, 417.

Sulentic, J. W. 1987, *Ap. J.*, **322**, 605.

Sulentic, J. W., and Arp, H. C. 1983, *A. J.*, **88**, 267.

Sulentic, J. W., and Lorre, J. J. 1983, *Astr. Ap.*, **120**, 36.

Thompson, L. A. 1976, *P. A. S. P.*, **88**, 662.

Tiersch, H. 1976, *Astron. Nachr.*, **297**, 301.

Tikhonov, N. A. 1986, *Soobshch. Spets. Astrofiz. Obs.*, **49**, 69.

Tikhonov, N. A. 1987a, *Soobshch. Spets. Astrofiz. Obs.*, **52**, 51.

Tikhonov, N. A. 1987b, *Astrofiz.*, **27**, 253.

Tikhonov, N. A. 1989, private communication.

Tovmasyan, G. M., and Shakhbazyan, É. Ts. 1981, *Astrofiz.*, **17**, 265.

Tully, R. B. 1987, *Ap. J.*, **321**, 280.

Turner, E. L., and Sargent W. L. W. 1975, private communication.

Vorontsov-Vel'yaminov, B. A., Dostal', V. A., and Metlov, V. G. 1980, Pis'ma Astron. Zh., **6**, 394.

Walke, D. G., and Mamon, G. A. 1989 *Astr. Ap.*, **295**, 291.

Wesselink, A. J. 1974, in *New Problems in Astrometry, IAU Symposium No. 61*, ed. W. Gliese, C. A. Murray, and R. H. Tucker (Dordrecht: Reidel), p. 201.

White, S. D. M. 1990, to appear in *Dynamics and Interactions of Galaxies*, ed. R. Wielen (Heidelberg: Springer-Verlag).

Whitmore, B. C. 1990, to appear in the Proceedings of the 1989 STScI Workshop, *Clusters of Galaxies*, (Cambridge: Cambridge University Press).

Williams, B. A., and Rood, H. J. 1987, *Ap. J. Suppl.*, **63**, 265.

Williams, B. A., and van Gorkom, J. H. 1988, *Ap. J.*, 287, 66.

Vorontsov-Vel'yaminov, B. A. 1959, *Atlas and Catalog of Interacting Galaxies*, Vol **1** (Sternberg Institute, Moscow State University, Moscow).

Vorontsov-Vel'yaminov, B. A., *Atlas of Interacting Galaxies, Part II*, *Astr. Ap. Suppl.*, **28**, 1.

DISCUSSION

Petrosian: Did you look at the relationship of AGN's and emission-line galaxies to HCGs?

Hickson: It is a question for the future. We must have more homogeneous high-resolution spectral observations for all members of HCGs to get the correct answer to this question.

Burbidge: Surely your last point is the most important one. Until you can place limits on the behavior of the IMF in these systems, all of the conclusions concerning star formation and evolution are meaningless.

Kennicutt: The situation is not quite that bad! The agreement in the star formation rates derived from Hα, UV, and UBV data, all which trace different parts of the IMF, tells us that the rates cannot be in error by more than factors of a few, and hence the orders-of-magnitude bursts which are observed in many interacting systems cannot be simply artifacts of an unusual IMF. However I wholly agree that our ignorance about the IMF in these galaxies is the main impediment to understanding their detailed evolutionary properties.

DISCUSSION

Roberts: The M/L value of 40 that you quoted was for the entire sample. Have you computed M/L's using only those galaxies within groups that show signs of interaction?

Hickson: The value of 40 is the median of all groups with three or more measured velocities. As you know M/L estimators are rather unstable when such small numbers of galaxies are involved. I am hesitant to consider subdivision of the sample until we have finished measuring redshifts for all of the galaxies.

Zasov: A small comment about nests. We have observed spectroscopically at least a dozen nests and related objects. In most cases a nest is in reality a single object with clumpy structure without any hint to be a merger. I wonder if the nests also follow dependencies that you obtained for the other compact systems.

Hickson: I think that the Vorontsov-Vel'yaminov nests are rather different from the compact groups that I described. The components of nests are not clearly recognizable as spiral or elliptical galaxies. As you say, these objects may be single galaxies, in general. It is possible that a few of the groups in my catalog (No. 18, for example) may be single irregular galaxies, but this would be a very small minority.

Appleton: Your plot of spiral fraction versus velocity dispersion is interesting. As the velocity dispersion goes up, the spiral fraction goes down. Are the spirals replaced with giant ellipticals, dwarf ellipticals, or irregulars.?

Hickson: In calculating spiral fraction, I group blue irregular galaxies with spiral galaxies. In the higher velocity dispersion groups, the spiral galaxies are replaced by elliptical galaxies in general. These are not dwarf ellipticals, but have typical absolute blue magnitudes of order -20.

Hutchings: Can you make a statistical test on discordant velocities on the basis of whether they are foreground or background?

Hickson: In most cases, the discordant galaxies have higher redshifts that the other group members, smaller sizes, and fainter magnitudes. Those with lower redshifts tend to be larger and brighter, as you would expect if their redshifts are cosmological. I haven't tried to quantify this, but it might lead to interesting results.

Navarro: Could you comment on J. Barnes simulations of the dynamical evolution of a compact group, especially on his suggestion that compact groups might be the final product of the dynamical evolution of loose groups.

Hickson: I think that the general picture of loose groups being progenitors of compact groups is probably correct, although one has to look carefully at the lifetimes and relative numbers. It would seem likely that compact groups could form from bound subcondensations in loose groups, by dynamical friction. Barnes' simulations beautifully illustrate the evolution of such systems, once they are already quite dense, but many questions remain to be answered. The dark matter, for example, is very important. At what point does it detach from individual galaxy halos and become distributed throughout the group?

Muradian: What can you say about the possible rotation of the dense groups? Is there direct or indirect evidence for the rotation of such groups as a whole?

Hickson: I do not find any systematic trends in the galaxy velocities that could be attributed to rotation of the groups. However, the HI observations of Williams and van Gorkom do show systematic rotation of the large HI clouds enveloping the groups that they studied.

Forbes: What do the X-ray observations of the Hickson groups show?

Hickson: The only positive detection of X-ray emission from compact groups is reported by Bahcall, Harris and Rood (1984). They detected three of five groups (not all HCGs) with the Einstein observatory. In two of these groups, Stephan's quintet and Arp 330, extended soft X-ray emission was found which is likely caused by hot intracluster gas. They conclude that the X-ray luminosities and temperatures are consistent and extrapolation from richer groups and clusters. In the third detected group (Arp 318) the X-ray emission may originate in the member galaxies.

Mamon: You mentioned that 30% of the galaxies in your compact groups are morphologically disturbed. What is the fraction of groups that contain at least 3 morphologically disturbed galaxies (thus showing groups with more than just one interacting binary)?

Hickson: About one third of all groups.

Khachikian: What do you mean when you say that there are not enough faint galaxies in the groups?

Hickson: Individual groups have typically four or five bright galaxies, but relatively few faint ones. Whereas, in a random sample of field galaxies there are more faint galaxies than bright ones. Since the overall luminosity of the compact group galaxies appears to be similar to that of the field, this observation implies that there is luminosity concordance in the groups. In other words, there are groups of bright galaxies, and groups of faint galaxies. This may be a result of the selection criteria, or it may be due to physical processes.

VLA Neutral Hydrogen Imaging of Compact Groups

B. A. Williams
University of Delaware
P. M. McMahon
Columbia University
J. H. van Gorkom
Columbia University/NRAO

We present images of the neutral hydrogen (H I) in the direction of the compact groups of galaxies, HCG 31, HCG 44, and HCG 79. We find in HCG 31 and HCG 79, emission contained within a cloud much larger than the galaxies as well as the entire group. The H I emission associated with HCG 44 is located within the individual galaxies but shows definite signs of tidal interactions. We have imaged the distribution and kinematics of neutral hydrogen at the two extremes of group sizes represented in Hickson's sample. HCG 44 is at the upper limit while HCG 18, HCG 31, and HCG 79 are at the lower end. Although the number of groups that have been imaged is still very small, there may be a pattern emerging which describes the H I morphology of compact groups. The true nature of compact groups has been the subject of considerable debate and controversy. The most recent observational and theoretical evidence strongly suggest that compact groups are physically dense, dynamical systems that are in the process of merging into a single object (Williams and Rood 1987, Hickson and Rood 1988, Barnes 1989). The neutral hydrogen deficiency observed by Williams and Rood (1987) is consistent with a model in which frequent galactic collisions and interactions have heated some of the gas during the short lifetime of the group. The H I disks which are normally more extended than the luminous ones are expected to be more sensitive to collisions and to trace the galaxy's response to recent interactions. Very Large Array observations can provide in most cases the spatial resolution needed to confirm the dynamical interactions in these systems.

Spectral-line observations of HCG 31 and HCG 79 were made with the VLA in the C-array and of HCG 44 in the D-array. In the C-array, the angular resolution is 20 arcsec and the velocity resolution is 21 km s^{-1}. The rms noise in the channel maps of HCG 31 and HCG 79 is 0.6 and 0.9 mJy per beam, respectively. The limiting column density (3σ) is $\approx 10^{20}$ H cm^{-2}. In the D-array, the angular resolution is 60 arcsec and the velocity resolution is 40 km s^{-1}. The rms noise in the channel maps is 0.4 mJy per beam which gives a limiting column density (3σ) of 2×10^{19} H cm^{-2}.

The H I emission detected in the smaller groups, HCG 31 and HCG 79 is shown overlaid on POSS photographs in figure 1. As is the case with HCG 18 (Williams and van Gorkom 1988), the integrated H I emission from HCG 31 and HCG 79 is far more extended than the optical group, and peaks at the position of the galaxies or at bright luminous clumps associated with the group. The total amount of hydrogen detected is 2.1×10^{10} M_o and 2.3×10^9 M_o for HCG 31 and HCG 79, respectively.

The H I emission from HCG 79 is strongly peaked in an elliptical-shaped cloud centered on the only late-type galaxy (Sbc) in the group. At this position, the column density is 5×10^{21} H cm^{-2}. Extended emission is also distributed in a relatively narrow tail which curves as far as 2' from the center of the cloud where the column density drops to $2 X 10^{20}$ H cm^{-2}. Approximately 18% of the total hydrogen detected is associated with the emission from the tail structure.

Figure 1b shows the systematic variation in the radial velocity across the main portion of the cloud centered on the edge-on galaxy. The radial velocity gradient runs along the same direction as the disk of galaxy d. If we interpret the systematic motions as due to rotation, at least 2.5×10^{10} M_o is needed to stabilize the inner regions of the cloud. The optical plume of galaxy b and the curved gas feature are good reasons to suspect tidal interactions between the galaxies.

The H I emission in the direction of HCG 31 is contained within two cloud structures: a) the 3' linear feature superposed on the brighter members and b) the diffuse feature located 2' northwest of the group. The peak emission has a column density of 4×10^{21} H cm^{-2} and is coincident with the two interacting galaxies a and c. In the southern part of the ridge structure, both emission peaks with column densities greater than 3×10^{21} H cm^{-2} are located at the newly identified H-alpha emission-line objects (Rubin et al. 1988). The diffuse cloud to the north also contains several condensations (10^{21} H cm^{-2}) that upon close inspection of the POSS print are coincident with very faint extended optical emission.

At the positions of the brighter galaxies with measured optical velocities (figure 1d), the agreement between the motions of the gas and that of the galaxies is remarkable. Systematic motions are observed along two directions within the ridge-like feature. Between 4120 and 4150 km s^{-1}, systematic motions are aligned with the disks of the brightest members. For radial motions below 4100 km s^{-1}, systematic motions occur along a position angle of 120°. This configuration suggest that the major cloud structure can be resolved into two kinematical systems 2-6 times larger than the individual galaxies within the group. The relative position of the two gas systems may indicate a recent collision which probably initiated the current episode of star formation (Rubin et al. 1989) along their interface.

In contrast, the neutral hydrogen gas in HCG 44 is located within the individual galaxies as shown in figure 2a. Although the location of the gas is normal, its asymmetric distribution suggest that the galaxies have experienced tidal interactions. The warping clearly visible in the luminous disk of galaxy d is also followed by the distribution of the gas which flares above and below the principal plane. An even better case is shown in figure 2c where a bridge of very weak (at the 2 sigma level) H I emission can be seen connecting galaxies a and c.

Although our sample is still very small, there may be a pattern emerging which describes the most compact systems. The morphology of the neutral hydrogen in compact groups may be correlated with their stage of evolution, i.e., more evolved groups have a single cloud of emission while the least evolved groups have their gas still asssociated with the individual galaxies. This correlation would be similar to that proposed by Forman and Jones for the X-ray morphology of early and 'evolved' clusters of galaxies. By observing more groups, eventually all of the Hickson compact groups, it should be possible to determine if such a correlation exist.

References

Barnes, J. E. (1989). Nature **338**, 123.

Rubin, Ford, and Hunter, 1989, STScI Workshop, May 1989.

Hickson, P. and Rood, H. J. (1988). Astrophy. J. **331**, L69.

Williams, B. A. and Rood, H. J. (1987). Astrophy. J. Suppl., **63**, 265.

Williams, B. A. and van Gorkom, J. H. (1988). Astron. J. **95**, 352.

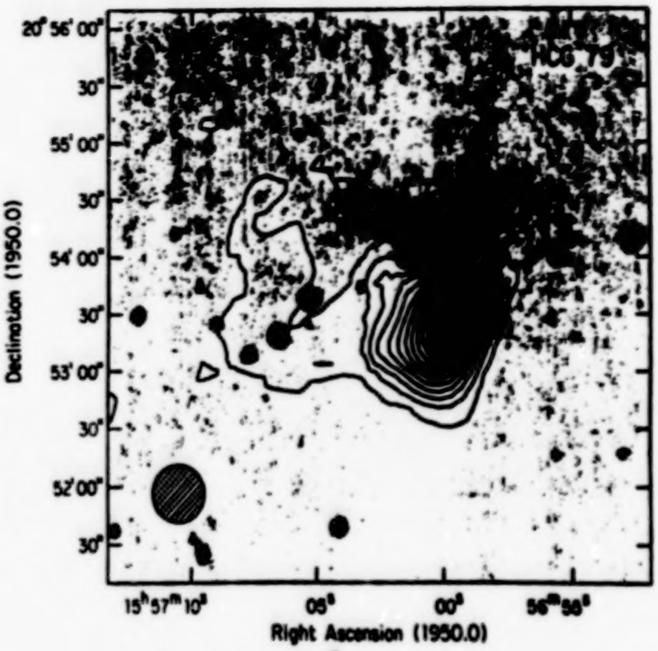
HCG 79
Declination (1950.0)
20° 56' 00"
55' 00"
54' 00"
53' 00"
52' 00"
15h 57m 10s
05s
00s
56m 55s
Right Ascension (1950.0)

a

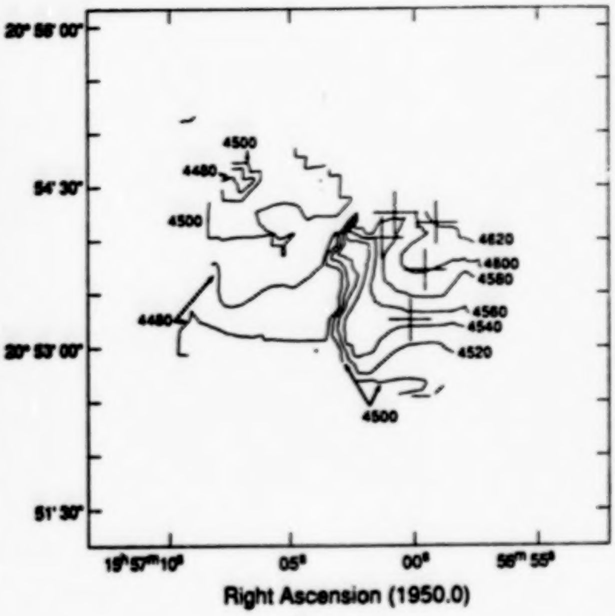
20° 55' 00"
54' 30"
20° 53' 00"
51' 30"
4500
4480
4500
4480
4620
4600
4580
4560
4540
4520
4500
15h 57m 10s
05s
00s
56m 55s
Right Ascension (1950.0)

b

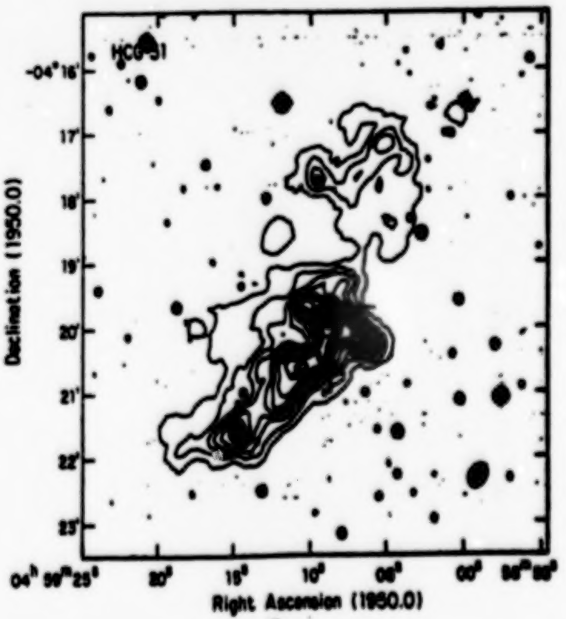
HCG 31
Declination (1950.0)
-04° 16'
17'
18'
19'
20'
21'
22'
23'
04h 59m 25s
20s
15s
10s
05s
00s
58m 55s
Right Ascension (1950.0)

c

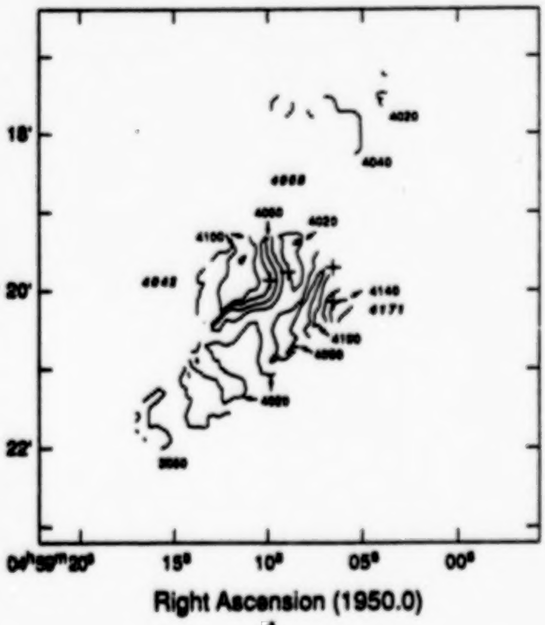
18'
-04° 20'
22'
4020
4040
4060
4080
4020
4100
4140
4171
4100
4080
4060
4060
4060
04h 59m 20s
15s
10s
05s
00s
Right Ascension (1950.0)

d

Figure 1a. VLA integrated map of the H I emission in HCG 79. The lowest contour is 0.04 Jy km s^{-1} per beam and the contour interval is 0.11 Jy km s^{-1} per beam.

Figure 1b. Map of the H I velocity field (km s^{-1}) of the inner third of the cloud in HCG 79.

Figure 1c. VLA integrated intensity map of the H I emission in HCG 31. The lowest contour is 0.05 Jy km s^{-1} per beam and the contour interval is 0.11 Jy km s^{-1} per beam.

Figure 1d. Map of the H I velocity field (km s^{-1}) of the gas in HCG 31.

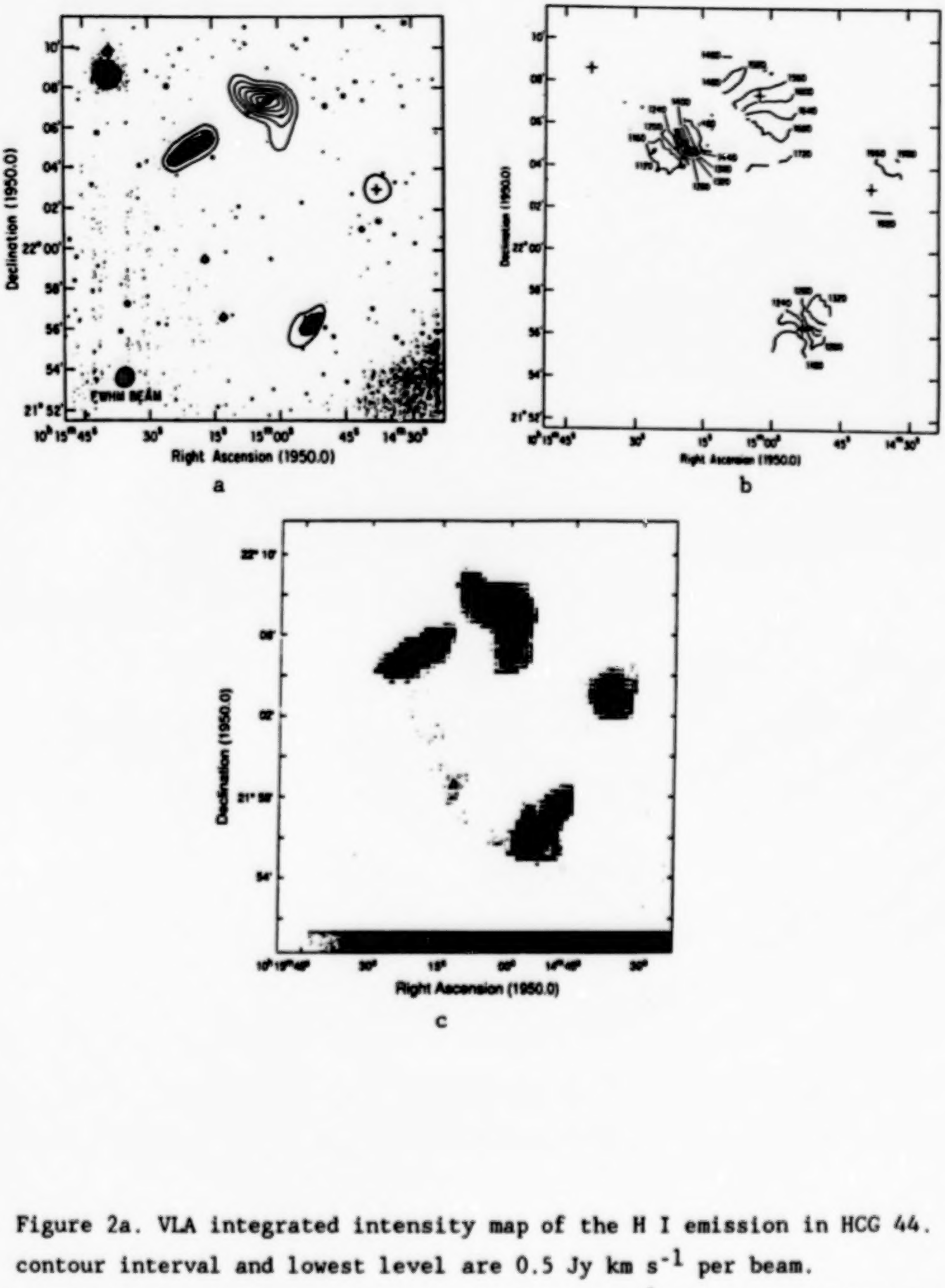
Declination (1950.0)
Right Ascension (1950.0)
FWHM BEAM
a
b
c

Figure 2a. VLA integrated intensity map of the H I emission in HCG 44. The contour interval and lowest level are 0.5 Jy km s^{-1} per beam.
Figure 2b. Map of the H I velocity fields (km s^{-1}) of the galaxies in HCG 44.
Figure 2c. VLA integrated intensity map of the H I emission in HCG 44 which reveals the weak bridge between galaxy a and c. The lowest grey scale is 0.12 Jy km s^{-1} per beam.

DISCUSSION

Carilli: Do you find any difference between total HI observed with Arecibo versus that observed with the VLA?

Williams: No, except in Hickson 31.

Heckman: Paul Hickson showed an example of a compact group with hot diffuse inter-galactic material (X-ray emitting). You showed an example where the diffuse inter-galactic material was cold (HI). If these groups are produced by collision/interactions of gas-rich (spiral) galaxies, what determines whether the intra-group gas is virialized by shocks (collisions) to $\sim 10^7$ K or remains as cold HI?

Williams: The velocity dispersion of the galaxies would determine whether the gas is heated to temperatures of $\sim 10^7$ K after a collision. The energy for heating comes from the relative motion of the galaxies involved in the interaction. Hickson showed Stephan's Quintet which has a velocity dispersion of ~500 km/s. This is much larger than the velocity dispersion of the galaxies in the groups that I have shown.

Hutchings: Is the HI deficiency consistent with ionization or stripping due to interactions?

Williams: All of the groups discussed here except for HCG 79 are significantly deficient in neutral hydrogen relative to the amount of blue light in the groups. Assuming these galaxies initially had normal neutral hydrogen gas contents, the observed deficiency is consistent with some form of heating of the gas either through tidal encounters or galactic collisions.

Shlosman: It seems you have shown that as a result of galaxy interactions in compact groups, the ISM is actually expelled from the galaxy. Is this a wrong impression?

Williams: We can only argue that the amount of mass needed to stablize each cloud can be provided by the luminous mass associated with the galaxies. One obvious interpretation, and not the only one, is that the gas was originally bound to one of the galaxies in the group and has been stipped from the galaxies via collisions or tidal interactions. The interstellar medium has been removed from the galaxies rather than expelled by the galaxies.

BLUE ELLIPTICALS IN COMPACT GROUPS

Stephen E. Zepf
Space Telescope Science Institute and the Johns Hopkins University
and
Bradley C. Whitmore
Space Telescope Science Institute

Abstract

We examine the hypothesis that mergers of spiral galaxies make elliptical galaxies by studying galaxies in compact groups. We combine dynamical models of the merger-rich compact group environment with stellar evolution models and predict that roughly 15% of compact group ellipticals should be 0.15 mag bluer in $B - R$ color than normal ellipticals. The published colors of these galaxies suggest the existence of this predicted blue population, but a normal distribution with large random errors can not be ruled out based on these data alone. However, we have new *UBVRI* data which confirm the blue color of the two ellipticals with blue $B - R$ colors for which we have our own colors. This confirmation of a population of blue ellipticals indicates that interactions are occurring in compact groups, but a blue color in one index alone does not require that these ellipticals are recent products of the merger of two spirals. We demonstrate how optical spectroscopy in the blue may distinguish between a true spiral + spiral merger and the swallowing of a gas-rich system by an already formed elliptical. We also show that the sum of the luminosity of the galaxies in each group is consistent with the hypothesis that the final stage in the evolution of a compact group is an elliptical galaxy.

I. Introduction

Toomre and Toomre's (1972) hypothesis that mergers play a fundamental role in determining the morphology of a galaxy has continued to gain support both from observations of nearby merging systems and from N-body simulations. However, as first noted by Ivan King (1977), the evolutionary sequence from ongoing merger to normal elliptical suffers from a lack of transitional cases. Most studies addressing the "merger hypothesis" have concentrated on systems in which tails and other morphological features indicative of a spiral + spiral merger are still present, but unfortunately the final state of these systems is not conclusively an elliptical galaxy.

We are testing the "merger hypothesis" in a direct way by studying elliptical galaxies in the Hickson compact groups (Hickson 1982). These groups are regions of high spatial density and low relative velocity dispersion where recent interactions and mergers should be most common. The rapid merging of galaxies in such environments is graphically demonstrated by the N-body simulations of compact groups of galaxies by Barnes (1989). These simulations indicate that the time scale for two spirals to collapse into an elliptical looking system is shorter than the time scale for the stellar population of two spirals to evolve to the red color of elliptical galaxies. Therefore, the merger hypothesis predicts that recently merged spirals should have the morphology of an elliptical, but with significantly bluer color than normal ellipticals, both because of the younger population of the merged spirals and because of the burst of star formation associated with the merger.

II. Models

In order to make more detailed predictions about the fraction of compact group ellipticals expected to be blue, we have combined dynamical models of compact group evolution (Barnes 1989) with models of the optical colors of stellar populations (Larson and Tinsley 1978), and the simple assumption that mergers of spiral form ellipticals. Based on these models, we predict that about 15% of the ellipticals should be bluer than $(B-V)_T^0 < 0.80$, compared to $(B-V)_T^0 = 0.90$ typical of normal ellipticals (details of the models are discussed in Zepf and Whitmore 1990).

III. Optical Colors

Our first step in this project was to test the prediction of the existence of a population of unusually blue ellipticals in compact groups by comparing the distribution of $B-R$ colors (Hickson et al. 1989) to those in a general sample of early-type galaxies (Sandage and Visvanathan 1978). We find (Zepf and Whitmore 1989, and Figure 1) that a substantial population of blue ellipticals exists in the compact groups, but several suspicious effects present in these $B-R$ colors suggest caution in interpreting these data. For example, the stars in Figure 1b represent ellipticals in Hickson groups in which all of the early-type galaxies in that group are abnormally blue, suggesting the possibility of problems with the calibration of the frames of these groups. Even after removing these cases, seven ellipticals are abnormally blue and reside in groups in which at least one galaxy has a color normal for its type (these seven are encircled in Figure 1b).

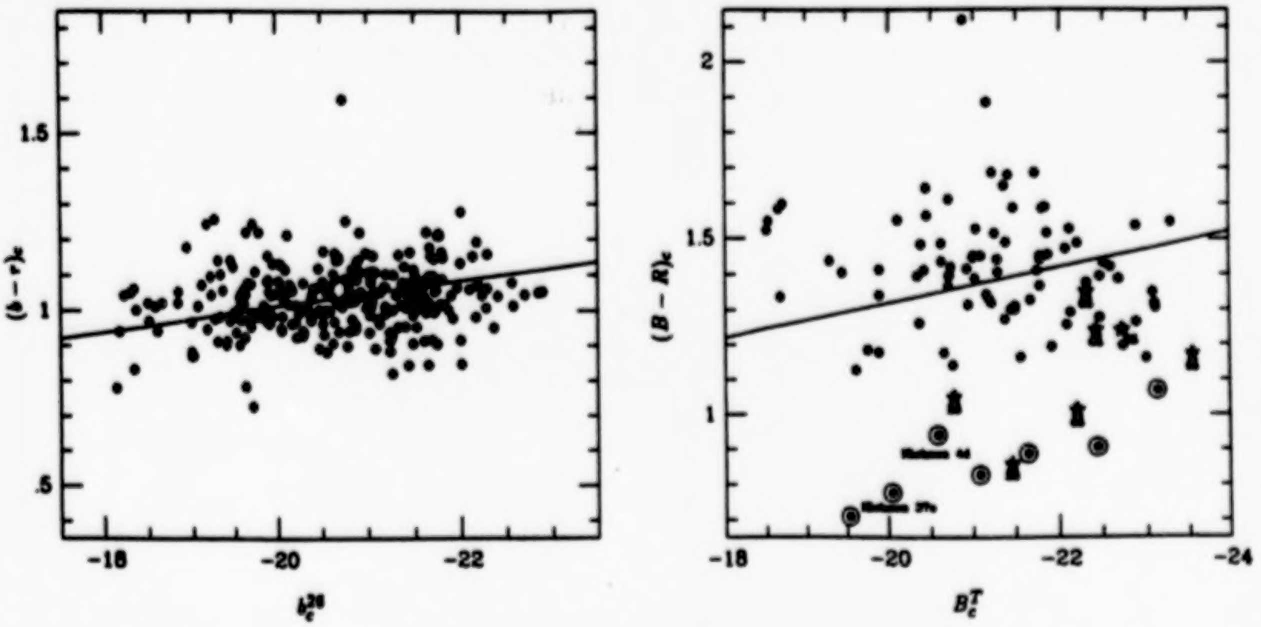

Figure 1. (a) The color-magnitude plot for all of the early-type galaxies in Sandage and Visvanathan (1978). (b) The color-magnitude plot for all of the elliptical galaxies in the Hickson compact groups (Hickson et al. 1989). The seven candidate blue ellipticals are encircled.

Although the $B-R$ colors are suggestive of a population of blue ellipticals in compact groups, a normal distribution of colors with large random errors can not be ruled out based on these data alone. In order to test the reality of the suspected population of blue ellipticals, we undertook an extensive observational program to obtain CCD surface photometry in good photometric conditions for a large sample of early-type galaxies in compact groups. We now have obtained *UBVRI* images for approximately 60 ellipticals in compact groups, completing this aspect of the project. The data reduction is still in progress, but a preliminary result is that for the two cases in which we have reduced our own colors of an elliptical with blue colors in the Hickson et al. data, we confirm their blue color (Hickson 37e $(B-V)^0_T = 0.75$ and Hickson 4d $(B-V)^0_T = 0.52$). We also find that the 15 other ellipticals in compact groups which we have reduced have normal colors ($(B-V)^0_T = 0.91 \pm 0.02$). The discovery that about 15% of the ellipticals in compact groups are unusually blue, in general agreement with the predictions of our models, represents the major result of this paper.

IV. Spectroscopy

Even with multicolor data, several different origins are possible for any given blue elliptical. With broad-band colors alone it is difficult to distinguish between an already formed elliptical swallowing a gas rich galaxy and the merger of two spirals creating a new elliptical. As the second step in this project we are undertaking a spectroscopic study of the stellar absorption lines. This spectroscopy directly probes the stellar populations and offers a way to determine the progenitors of the blue ellipticals.

Our spectroscopy centers on the Balmer lines $H\gamma$, $H\delta$, and $H\epsilon$, and the corresponding nearby metal lines. The young stellar populations of a recent merger of two spiral galaxies will be evident in strong Balmer lines in absorption. Ongoing mergers such as NGC 7252 and NGC 3921 invariably show this signature, which is also observed in about 20% of the shell galaxies observed by Carter et al. (1989). However, only when one of the progenitors was an already formed elliptical will the blue elliptical have strong metal lines in addition to the strong Balmer lines. Strong Balmer lines and weak metal lines are clearly evident in the spectrum of NGC 7252, a prototypical spiral + spiral merger. Much of our future effort will be devoted to developing more detailed and quantitative tools with which to analyse the spectroscopy (Zepf and Whitmore 1990).

V. Luminosities of Final Products of Compact Groups

All of the available data are consistent with the hypothesis that galaxies are merging and forming ellipticals in compact groups. Within the context of the merger hypothesis, each compact group we observe today is destined to become a single elliptical galaxy. Therefore, the sum of the luminosities of the galaxies in the group should be consistent with luminosities of normal ellipticals in equivalently selected samples. Because of the complex selection criteria applied by Hickson to define his compact group sample (Hickson 1982, and this volume), it is difficult to define an exact comparison sample. However, to first-order the compact group sample is equivalent to a magnitude or diameter limited catalog. For the sample of Sadler and Gerhard (1985), which is both magnitude and diameter limited, we find that the mean $M_{B_T^0} = -21.2$ and the median $M_{B_T^0} = -21.7$, and the magnitude limited RSA (Sandage and Tamman 1987) sample gives approximately the same value (mean $M_{B_T^0} = -21.3$).

The simplest way to calculate the expected luminosity of the product of the merging of compact group galaxies into a single elliptical is to sum the luminosities of all of the galaxies in each of the groups. This summation gives a mean $M_{B_T^0} = -21.9$ and a median of $M_{B_T^0} = -22.6$. A more realistic approach is to model the aging of the stellar populations after the galaxies have merged. Presumably, once the group has coalesced into a single system, star formation will cease, and the resulting galaxy will grow redder in time. We model this evolution by first assuming that each galaxy will redden to the color of a elliptical and then use the models of Larson, Tinsley, and Caldwell (1980) to find the resulting fading in B. Summing these total, corrected blue luminosities as in the no-evolution case, we find that the mean $M_{B_0^T} = -21.4$, and the median $M_{B_0^T} = -21.6$. The similarity of the distribution of the absolute magnitudes in this case with the observed distribution of ellipticals in similarly selected samples is further evidence that the properties of compact groups are consistent with our current understanding of merging and evolution in compact groups.

VI. Conclusions

1. A population of blue ellipticals exists in compact groups.
2. This population of blue ellipticals as well as the total magnitudes of compact group galaxies are consistent with the hypothesis that galaxies in compact groups are merging and forming new ellipticals.
3. Optical spectroscopy may be able to distinguish a blue elliptical which is the result of the merger of two spirals from an already formed elliptical swallowing a gas rich system.

References

Barnes, J. 1989, *Nature*, **338**, 123.

Carter, D., Prieur, J.-L., Wilkinson, A., Sparks, W.B., and Malin, D.F. 1988, *M. N. R. A. S.*, **235**, 813.

Hickson, P. 1982, *Ap. J.*, **255**, 382.

Hickson, P., Kindl, E., and Aumann, J. 1989, *Ap. J. Suppl.*, **70**, 687.

King, I.R. 1977, in *The Evolution of Galaxies and Stellar Populations*, ed. R.B. Larson and B.M. Tinsley (New Haven: Yale University Observatory), p. 418.

Larson, R.B., and Tinsley, B.M. 1978, *Ap. J.*, **219**, 46.

Larson, R.B., Tinsley, B.M., and Caldwell, C.N. 1980, *Ap. J.*, **237**, 692.

Sadler, E.M., and Gerhard, O.E. 1985, *M. N. R. A. S.*, **214**, 177.

Sandage, A., and Visvanathan, V. 1978, *Ap. J.*, **225**, 742.

Toomre, A., and Toomre, J. 1972, *Ap. J.*, **178**, 623.

Zepf, S.E., and Whitmore, B.C. 1989, in *The Interactions and Dynamics of Galaxies*, ed. Roland Wielen, in press.

Zepf, S.E., and Whitmore, B.C. 1990, *Ap. J.*, in preparation.

DISCUSSION

Struck-Marcell: Could you tell me what burst strengths you used in your models, and whether you think that a SF burst using gas dumped onto a pre-existing elliptical could account for the blue colors?

Zepf: A blue color in a single color index (e.g., B-V) can be explained either by a pre-existing elliptical swallowing a gas-rich, star-bursting system or by two spirals merging to form a new elliptical. This degeneracy when using a single color index is precisely the reason we use UBVRI colors and optical spectroscopy.

Hutchings: Do you have a comment on the old E galaxies in the Hickson sample? Could it be dust?

Zepf: The red elliptical galaxies might be explained by dust (as an example, NGC 5128 would appear at the top of this plot). However, the elliptical with the reddest colors in the Hickson et al. data appears to actually have normal colors, with the very red color being due to photometric error. I think we will be able to answer this question better when our photometric survey is complete.

Mamon: The blue ellipticals in your luminosity-color plot of Hickson compact groups tend to be faint, and are often, from the examples you have shown, among the fainter members of their groups. Comment: The statistics on the bright end of the luminosity functions of Hickson's compact groups (based on a test devised by Tremaine and Richstone 1977) show no signs of mergers in these groups. Perhaps the bright-end luminosities are not the ones to study when searching for mergers?!

Zepf: It is certainly true observationally that the blue ellipticals do not seem to be biased to the higher luminosities.

WHAT IS THE NUMBER OF SPIRAL GALAXIES IN COMPACT GROUPS?

N. A. Tikhonov
Special Astrophysical Observatory
USSR Academy of Sciences
st. Zelenchukskaya, Stavropol Territory
357147, USSR

ABSTRACT. The distribution of morphological types of galaxies in compact groups is studied on plates from the 6 m telescope. In compact groups there are 57% galaxies of late morphological types (S + Irr), 23% lenticulars (SO) and 20% ellipical galaxies. The morphological content of compact groups is very nearly the same as in loose groups. There is no dependence of galaxy morphology on density in all compact groups (and possibly in loose groups). Genuine compact groups form only 60% if Hickson's list.

INTRODUCTION

As numerical calculations show (Ishisawa et al., 1983; Mamon, 1987; Barnes, 1988) the dynamical evolution of small close systems of galaxies must lead to formation of elliptical galaxies after successive merging of all its neighbors to the central galaxy. To test the results of such calculations in observations, the most suitable objects are compact groups of galaxies, a homogeneous list of which is presented by Hickson (1982). There were also earlier lists of compact groups of galaxies compiled by Shakhbasian and her colleagues (1973) and also the list of Roe (1977), but these results could not be used for statistical conclusions, because of the sample being incomplete or group selection criteria being applied incorrectly.

In Hickson's list (1982) the space density of galaxies in the group reaches 10^6 gal/Mpc and interaction effects may be expected to appear must strongly maximally in such groups. If the numerical calculations are correct, and the compact groups are physically related systems with sufficient lifetimes for evolutionary change, the morphological content must systematically differ between compact groups and looser groups of galaxies.

As galaxy classification using plates obtained with a wide-angle telescope leads to significant losses of spiral galaxies (Wirth and Gallagher, 1980) morphology of galaxies in compact groups was determined based on large-scale plates obtained by the author at the 6 m telescope. The first results were obtained studying 40 groups. Addition of twenty more plates did not change the main conclusions of the work (Tikhonov, 1986) but at the same time allowed further specification of the results.

OSBSERVATIONS

Photographic observations were carried out by the author in 1984-85 with the 6 m telescope of the Special Astrophysical Observatory, USSR Academy of Sciences, plates were obtained at the prime 24 m focus of the telescope. The large scale of the plates (8.19"/mm) allowed determination of the galaxy type confidently, using the Hubble classification. Almost all the plates were obtained using IIaO and 103aO emulsions in the "B" system.

When obtaining the plates the emphasis was on close groups where morphology is impossible to study using the POSS, on groups possessing a small number of spiral galaxies and groups showing traces of interaction between galaxies. Plates of 60 compact groups with the numbers: 1, 2, 3, 5, 6, 7, 8, 10, 12, 13, 14, 15, 17, 20, 25, 34, 35, 38, 39, 41, 43, 45, 46, 49, 50, 51, 54, 56, 57, 58, 61, 66, 68, 70, 71, 72, 73, 74, 75, 76, 77, 78, 80, 81, 82, 84, 85, 88, 89, 92, 93, 94, 95, 96, 97, 98, 99, and 100 were obtained.

These plates were later used for photometry of galaxies in groups.

Besides photographic observations, at the 6 m telescope spectral observations of about 60 galaxies in various groups and group neighborhoods were carried out. This allowed estimation of dynamic mass of groups, the ratio M_{VT}/L and comparison of compact and loose groups of galaxies more completely. However, this article deals only with morphology of galaxies in groups, considering the results of spectral observations, as well.

CRITICAL REMARKS

The list of compact groups by Hickson (1982) is the most complete and homogeneous of all the existing ones. Unfortunately it also contains errors, mainly associated with the isolation criterion.

Precise position measurement of galaxies on the 6 meter telescope plates has shown that the isolation criterion is broken rather often, i.e., that inside the $3R_G$ circle galaxies brighter than $(m_a - 3)$ are present. Including such galaxies into the group breaks the other group selection criteria, and we cannot thereafter consider such groups compact and isolated. I can give some examples of such groups: 1, 12, 20, 45, 46, 57, 70, 71, 72, 76, 83, 94.

Radial velocity measurements of galaxies in some compact groups and study of other authors' results led us to a new revision of the compact groups list. Some quartets turned into triplets and we should not consider them groups according to Hickson's criteria ($N \geq 4$). They are groups 38, 61, 77, and probably some others. Groups 18 and 54 are single galaxies with HII regions (Williams and van Gorkom, 1988; Arkhipova et al., 1981) and they must also be excluded from the list.

Radial velocities obtained on the 6 meter telescope and also comparison of Hickson's list (1982) with the group lists of other authors showed that some compact groups are central condensations in loose groups and we must not consider them isolated. They are the groups: 8, 10, 35, 44, 58, 60, 61, 68, 79, and 95. Absence of complete data on radial velocities of compact groups of galaxies and neighboring galaxies does not allow me to enlarge the list.

So the initial list of Hickson contains several types of objects: nuclei of loose groups of galaxies, compact groups, double or triple galaxies with background galaxy superposition, single galaxies with HII regions. This should be borne in mind when discussing the morphological composition of compact groups from Hickson's list (1982).

RESULTS AND DISCUSSION

In the 59 groups of galaxies for which direct plates were obtained (excluding group 54) 278 galaxies were classified. The results are presented in Table 1.

TABLE 1

GALAXY CLASSIFICATION IN COMPACT AND LOOSE GROUPS OF GALAXIES

Groups	S	SO	E	The Authors
loose	65	18	10	Bhavsar, 1981
loose	62	20	17	de Souza et al., 1982
loose	64	20	15	de Souza et al., 1982
compact	38	28	34	Hickson (from Williams and Rood, 1987)
compact	46	--	--	Hickson and Kindl, 1988, 60 groups
compact	61	26	13	Williams and Rood, 1987, 60 groups
compact	57	23	20	6 m telescope, 60 groups
compact	61	22	17	the first-ranked galaxies, 6 m telescope, 60 groups

The results of Table 1 show great scatter of the results when the same groups of galaxies are used. This is largely caused by the small apparent size of the galaxies, and in this case the number of galaxies classified as spirals must reduce when passing from near to distant groups. In Figure 1 the relation between spiral-galaxy fraction in the group and the distance to the group, according to Hickson and Kindl (1989) is shown. The decrease in number from ~60% in nearby groups to 20% in distant ones is clearly seen. The decrease begins with Z = 0.04; this is the very limit of distance up to which we can classify galaxies correctly with good imaging.

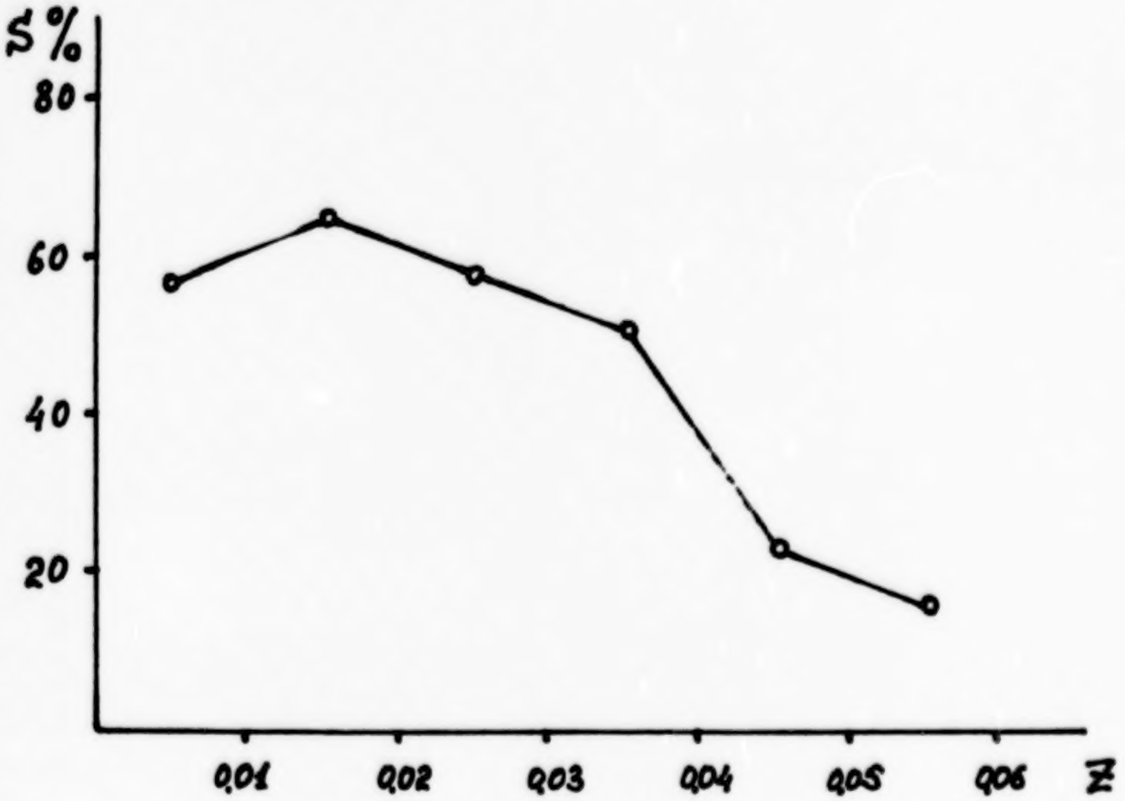

Figure 1. Changing of the number of spiral galaxies in compact groups through distances (from the data of Hickson and Kindl, 1988).

Since loose groups of galaxies are as a rule at close distances, misclassifications are less possible for them. So, the morphological composition of compact groups is only slightly different from the composition of loose groups. Among the brightest galaxies in the compact groups spiral galaxies constitute 61%, which indicates that morphological type is preserved during merging or that merging is rare.

Interacting galaxies are observed in 31 of 59 groups, but these are interactions of pairs of galaxies. In seven groups interaction of three or more galaxies is observed. They are the groups 2, 38, 49, 70B, 80, 92, 95. In only two cases all four galaxies are interacting (groups 49 and 80). As for galaxy merging, it is observed only in Group 8. The processes of galaxy merging are very rare which leads to preservation of morphological composition in the groups.

The similarity between compact and loose groups is seen also from comparing the "Morphology-density" relation. From Dressler (1980) this relation is known for clusters of galaxies. Later it was obtained for smaller groups of galaxies, too (Bhavsar, 1981; de Souza et al., 1982; Postman and Geller, 1984). After radial velocity measurements and determination of space density of the galaxies with the 6 meter telescope it became clear that compact groups do not follow Dressler's "morphology-density" relation. As for compact and loose groups of galaxies the identical morhphological composition and spatial density of compact and loose groups suggest that a continuous "morphology-density" relation must be observed for small groups of any compactness.

In Figure 2 the results after combining the data by several authors are presented. It is seen, that with space densities ~10^2 gal/Mpc^3 a shift from Dressler's relation is outlined, and this shift is present for both compact and loose groups of galaxies. The most probable reason for such a shift is the presence of a relation not only with space density of galaxies, but also with the number of galaxies in the group.

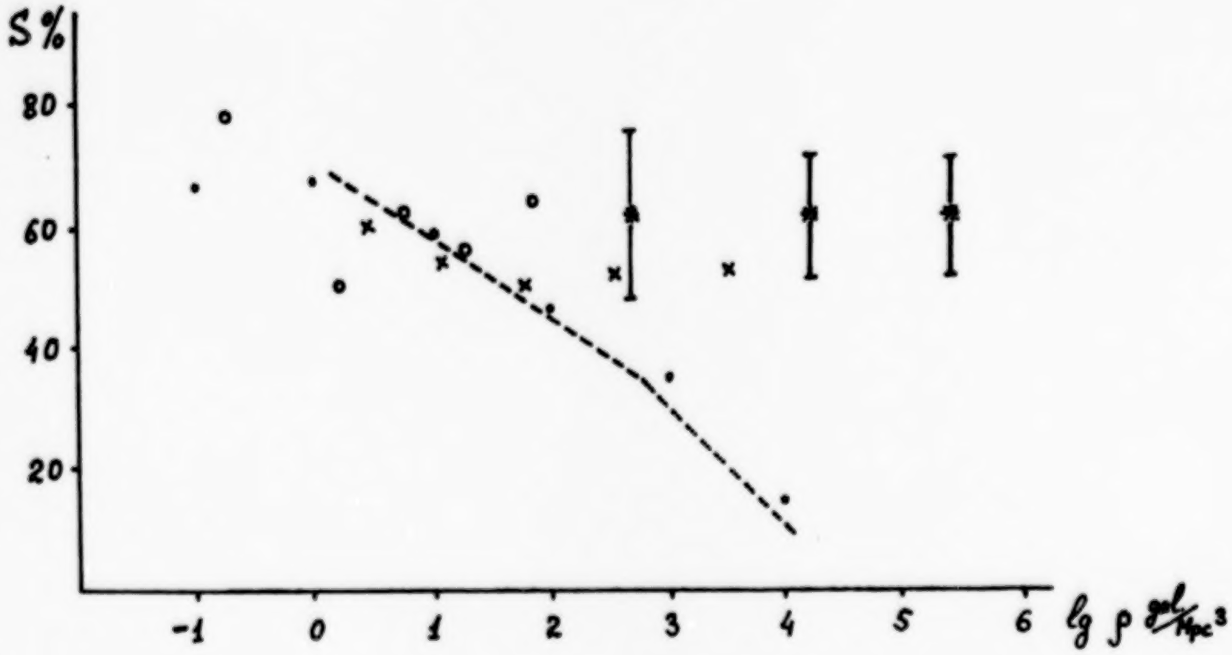

Figure 2. Morphology-density relation for compact and loose groups of galaxies.

x x x - Bhavsar (1981),

o o o - de Souza et al. (1982),

. . . - Postman and Geller (1984),

----- - Dressler (1980),

* * * - Tikhonov, this paper.

CONCLUSIONS

In the list by Hickson (1982) genuine compact groups constitute about 60%.

Compact and loose groups of galaxies possess identical morphological compositions.

Compact (and loose) group do not follow Dressler's "morphology-density" relation.

In compact groups galaxy merging or absorption processes are rather small in number.

REFERENCES

Arkhipova, W. P., et. al. 1981, Astron. Zh., **58**, 490.

Barnes, J. E. 1988, Princeton JASOL, preprint 73.

Bhavsar, S. P. 1981, Astrophys. J. Lett., **246**, L5.

Dressler, A. 1980, Astrophys. J., **236**, 351.

Hickson, P. 1982, Astrophys. J., **255**, 382.

Hickson, P., Kindl, E. 1988, Astrophys. J., **331**, 64.

Ishisawa, T., Matsumoto, R., Tajita, T., Kageyama, H., and Sakai, H. 1983, Publ. Astr. Soc. Japan, **35**, 61.

Mamon, G. A. 1987, Astrophys. J., **321**, 622.

Postman, M., and Geller, M. J. 1984, Astrophys. J., **281**, 95.

Rose, J. A. 1977, Astrophys. J., **211**, 311.

Shakhbasian, R. K. 1973, Astrofizika, **9**, 495.

de Souza, R. E., Capelato, H. V., Arakaki, L., and Logullo, C. 1982, Astrophys. J., **263**, 557.

Tikhonov, N. A. 1986, Soobshch. Spets. Astrofiz. Obs., **52**, 51.

Williams, B. A., and van Gorkom, J. H. 1988, Astron. J., **95**, 352.

Willaims, B. A., and Rood, H. J. 1987, Astrophys. J. Suppl. Ser., **63**, 265.

Wirth, A., and Gallacher, J. S. 1980, Astrophys. J., **242**, 469.

TRIPLE GALAXIES AND A HIDDEN MASS PROBLEM

I.D.Karachentsev, V.E.Karachentseva, V.S.Lebedev
Special Astrophysical Observatory, USSR Academy of Sciences
st. Zelenchukskaya, Stavropol Territory, 357147, USSR

ABSTRACT

We consider a homogeneous sample of 84 triple systems of galaxies with components brighter than $m = 15.7$, located in the northern sky and satisfying an isolation criterion with respect to neighboring galaxies in projection. The distributions of basic dynamical parameters for triplets have median values as follows: radial velocity dispersion 133 km/s, mean harmonic radius 63 kpc, absolute magnitude of galaxies $M_B = -20.38$, crossing time $\tau = 0.04\ H^{-1}$. For different ways of estimation the median mass-to-luminosity ratio is (20 - 30)$f_{\odot}$.

A comparison of the last value with the ones for single and binary galaxies shows the presence of a virial mass excess for triplets by a factor 4. The mass-to-luminosity ratio is practically uncorrelated with linear size of triplets or with morphological types of their components.

We note that a significant part of the virial excess may be explained by the presence of nonisolated triple configurations in the sample, which are produced by debris of more populous groups of galaxies.

1. INTRODUCTION

On comparing a recent survey on dark matter in the Universe (Trimble, 1987) with the preceding one covering the topic (Faber, Gallagher, 1979), the following tendencies are apparent.

The idea, that at rather large scales ($L > 50$ kpc) hidden mass in the Universe dominates over visible matter, is becoming more and more popular. Inflationary cosmological theories have played a significant part here. Concerning observational arguments, their quantity and quality are higher, as the scale or population of the system of galaxies considreed is larger. But information on the nature and distribution of the hidden mass is still rather primitive. The least reliable evidence seems to be that for galaxian systems of low multiplicity. According to Karachentsev (1987), the overall observational data on the most numerous ($n \approx 600$) and homogeneous binary-galaxy sample can be explained without requiring hidden mass there, on scales $20 - 1200$ kpc.

Therefore the need to investigate low-multiplicity systems of galaxies, including triple systems, is clear. The first, and as far as we are concerned, still unique attempt to study triple galaxies systematically was made by Karachentseva *et al.* (1979). A criterion of local isolation was applied to the observed distribution of galaxies brighter than $m = 15.7$.

Three galaxies were considered as forming an isolated system if 'significant' neighbors were standing at least three times as far from them, as the triplet galaxies were from one another. Significant neighbors were taken as surrounding galaxies with angular diameters not more than a factor two different from the triplet members' diameters. Such a condition selects systems with 10× and higher excess of galaxy surface density over the average background.

If we compare the criterion for isolated triplets with an analogous double-system criterion (Karachentsev, 1972), it is actually less restrictive for triple galaxies (the avoidance zone around a pair exceeded 5 component separations). Nevertheless, among 27,841 galaxies in the northern sky brighter than $m = 15.7$ only 84 triplets satisfy this isolation criterion, which is 7 times smaller than the number of isolated pairs.

It is important to note that galaxy membership in a triple system was determined without recourse to radial velocity. Therefore a system might be isolated only in projection on the sky, but not three-dimensional space.

The program of radial velocity measurements for triple galaxies was performed mainly at the 6-m telescope. The results so obtained together with data from other sources were compiled in a previous article (Karachentseva *et al.* 1988). There a complete radial velocity summary for triple galaxies, their angular diameters and apparent magnitudes reduced to the standard isophotal diameter (R_{25}) and Holmberg magnitude (m^c_{Ho}) system, and also more detailed determinations of morphological types of the galaxies were presented. We will consider below how triple systems are distributed according to linear dimensions, velocity dispersion, total luminosity and other characteristics bearing on the dynamical conditions of triple galaxies.

2. MAIN PARAMETERS

In describing triple galaxies we will use two mutually complementary approaches.

a) Triplet as a unit dynamical system. It is characterized by the following values: centroid mean radial velocity

$$< v >= \sum_{k=1}^{3} v_k/3 \tag{1}$$

where v_k is the component radial velocity, corrected for the solar motion using the standard formula (de Vaucouleurs *et al.* 1976);

rms velocity of galaxies relative to the centre,

$$S_v = [\sum_{k=1}^{3}(V - < V >)^2]^{1/2} \tag{2}$$

projected linear separation between components,

$$r_{ik} =< V > H^{-1}X_{ik} \tag{3}$$

where X_{ik} is the angular separation, and H the Hubble constant, taken as 75 km/s Mpc;

average projected harmonic separation,

$$r_H = [\sum_{i,k} r_{ik}{}^{-1}]^{-1} \tag{4}$$

galaxy luminosity in solar units,

$$L_k = \mathrm{dex}[0.4(5.40 - M_k)], \tag{5}$$

where the absolute magnitude M_k is calculated using the average radial velocity $< V >$, and apparent magnitude m_{H_o} in the Holmberg system with corrections for obscuration in our Galaxy, cosmological K-effect, and internal absorption in the considered galaxy;

virial mass to total luminosity-ratio for a triplet,

$$f = \frac{3\pi n(n-1)S^2{}_v r_H}{G\sum_k L_k} \tag{6}$$

where G is the gravitational constant, $n = 3$, and 3π is the mean projection factor according to Limber and Mathews (1960);

a statistically unbiased estimator of the virial mass-to-luminosity ratio,

$$f^c = f\frac{1 - 2\sigma^2{}_v}{3S^2{}_v} \tag{7}$$

where σ_v is the rms error of radial velocity measurement for triple galaxies;

dimensionless "crossing time" of a system,

$$\tau = 2Hr_H/S_v \tag{8}$$

expressed in units of the Hubble time, H^{-1}.

Integral characteristics of each triple system are presented in the summary (Karachentsev *et al.* 1989). The reduced data from the reference list (Karachentseva *et al.* 1988), were used for their calculations.

Similar calculations were repeated for triple systems with each galaxy given a weight proportional to its luminosity. In most cases differences between weighted and unweighted parameters turned out negligible.

b) Triple system as a set of pairs. Previous estimates of triple-system masses were based on the supposition that the ratio of system kinetic to potential energy $k = 2T/\ |U|$, does not change with time and equals unity. Simulating triple-system evolution, Anosova and Orlov (1985) showed that the virial coefficient k undergoes considerable fluctuations $< \Delta k^2/k^2 > \approx 1$. Additional uncertainty in virial mass estimation would be introduced by projection factors. As Bahcall and Tremaine noted (1981), the estimation of f from expression (6) is not statistically robust. Thus they suggested that f be determined not according to the average harmonic radius $< r_{ik}{}^{-1} >$, but according to an average value $< (V_i - V_k)r_{ik}{}^2 >$. This approach corresponds to interpretation of a triple system as an ensemble of galaxy-satellite systems, revolving around the main (most massive) component.

Formally dividing a triple system into three pairs of galaxies and for definiteness positing circular motions in the pairs, we obtain an estimate of orbital mass-to-luminosity ratio,

$$\mathrm{f}_{ik} = \frac{32r_{ik}(\mathrm{V}_i - \mathrm{V}_k)^2}{3\pi \mathrm{G}(L_i + L_k)} \tag{9}$$

and also the unbiased estimate with correction for radial velocity measurement errors:

$$\mathrm{f}^c{}_{ik} = \mathrm{f}_{ik}[1 - (\sigma_i{}^2 + \sigma_k{}^2)/(\mathrm{V}_i - \mathrm{V}_k)^2] \tag{10}$$

Here the projected linear separation between galaxies is expressed through the pair's average radial velocity,

$$r_{ik} = X_{ik}\mathrm{H}^{-1}(\mathrm{V}_i + \mathrm{V}_k)/2 \tag{11}$$

and the galaxy luminosity through its individual radial velocity.

As mentioned above, the isolation criterion for a triple system of galaxies was chosen softer than the pair criterion. According to the data of Karachentsev (1987) only 57% of binary systems are true isolated pairs, so we may expect that in the list of triple galaxies a considerable number are false ones. To verify this suggestion we used numerical simulations of the apparent galaxian distribution (Karachentsev, Shcherbanovskij, 1979). The main results of the simulation concerning the triple systems have already been discussed by Karachentseva and Karachentsev (1982).

In 127 fields, imitating the POSS prints, among 9433 galaxies brighter than $m = 15.7$ 71 isolated triple systems were selected, applying the above-mentioned criterion. We used them as a reference sample when analyzing properties of catalogued triplets. Without going into details, we shall note only two important results of the simulation: A) The isolation criterion removes about 2/3 of triple systems, all of whose components are brighter than the sample limit of $m = 15.7$; the criterion is strongly selective, favoring "survival" of the tightest systems. B) The isolation condition is satisfied by a large number of false triple systems. Among 71 simulated triplets only 5 (or 7%) are true physical triple systems; 31 triplets (44%) are formed by galaxies which are members of a group or a cluster , and the remaining part of the sample (49%) constitute optical triplets. Among the last category are 5 completely spurious triplets and 30 "semi-optical" triplets - i.e. a pair or two system members plus a background galaxy.

Let us consider the distribution of triple galaxies according to their relative radial velocities. The data are presented in Figure 1. The left histogram shows the number of catalogued triplets versus radial velocity difference for the components. The distribution of relative radial velocities for 585 isolated pairs (Karachentsev, 1972) is dashed for comparison. The right side gives analogous data for the simulated triple systems. True physical triplets are marked with double hatching, non-isolated triple galaxies, consisting of group or cluster members with single hatching, and optical systems are not hatched.

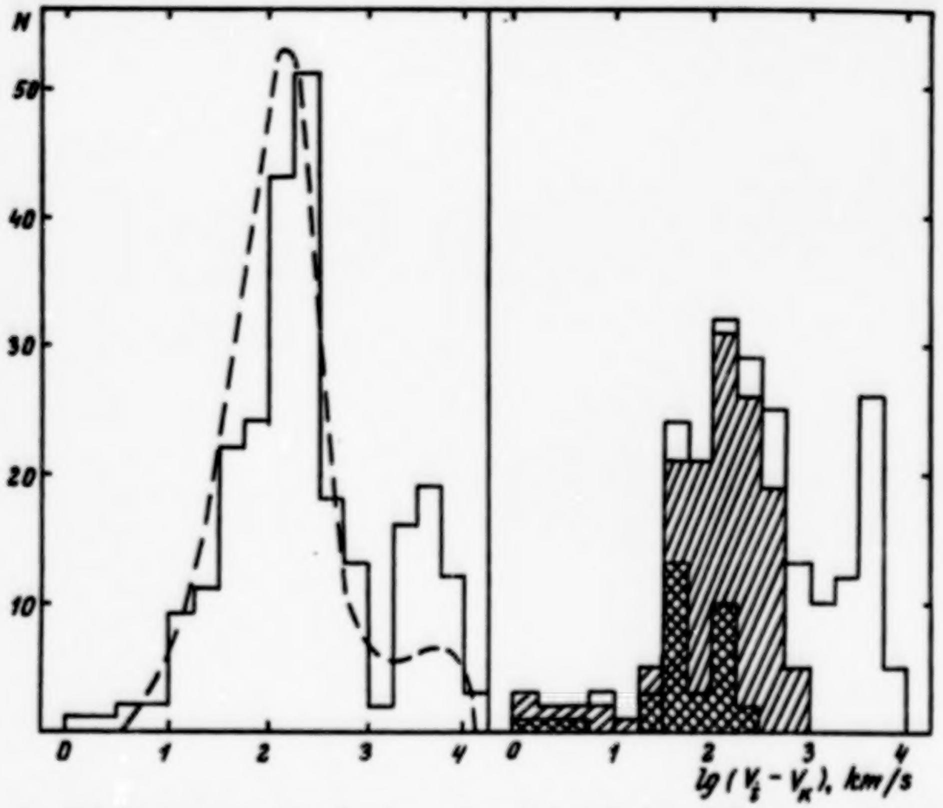

Fig. 1. Triple galaxy distribution of radial velocity difference. Catalogue triplets are to the left, simulated ones to the right. Double-hatched regions are physical systems, single-hatched are non-isolated members of groups and clusters. The dashed curve reflects the distribution for 585 isolated pairs.

As we can see, the distribution has an asymmetric shape. Besides the main maximum at 100 km/s a secondary rise in the region $(10^3 - 10^4)$ km/s is observed. An obvious reason for the secondary peak is the contribution of optical triple systems. Pairs of galaxies from the catalogue of Karachentsev (1972), selected according to a stricter isolation criterion, also show an excess of cases in this region.

Turning to the right side of Figure 1, we may claim satisfactory correspondence between the distributions of simulated and catalogued triplets. Though optical and physical triplets overlap slightly, there is no difficulty in distinguishing between them. According to the results of numerical simulations, optical triplets dominate in the region $S_v > 300$ km/s or $(V_i - V_k) > 600$ km/s. It is different with triple systems whose members belong to some group or cluster. They overlap so completely with true isolated triplets that we don't see any simple method to separate them.

In distributions of a random variable with a large asymmetry coefficient, the sample mean depends strongly on one or two maximum values at the tail of a sample. Because of this, many authors prefer to use a distribution median instead of the average, as a more robust estimator. We also follow this approach. The distributions of radial-velocity difference for members of catalogued and simulated triplets are characterized by medians 198 km/s and 217 km/s, respectively. For comparison we note that for 585 isolated pairs the median is considerably smaller, 130 km/s.

In Figure 2 the distributions of catalogued (left) and simulated triplets are presented according to projected linear separation r_{ik}. Various types of the simulated triplets are distinguished as in Figure 1. The dashed curve shows a smoothed distribution for 585 isolated pairs. Median values are 77 Kpc for the catalogued triplets and 90 Kpc for the simulated ones. Isolated pairs (dashes) are tighter systems on average; their median separation is only 30 Kpc.

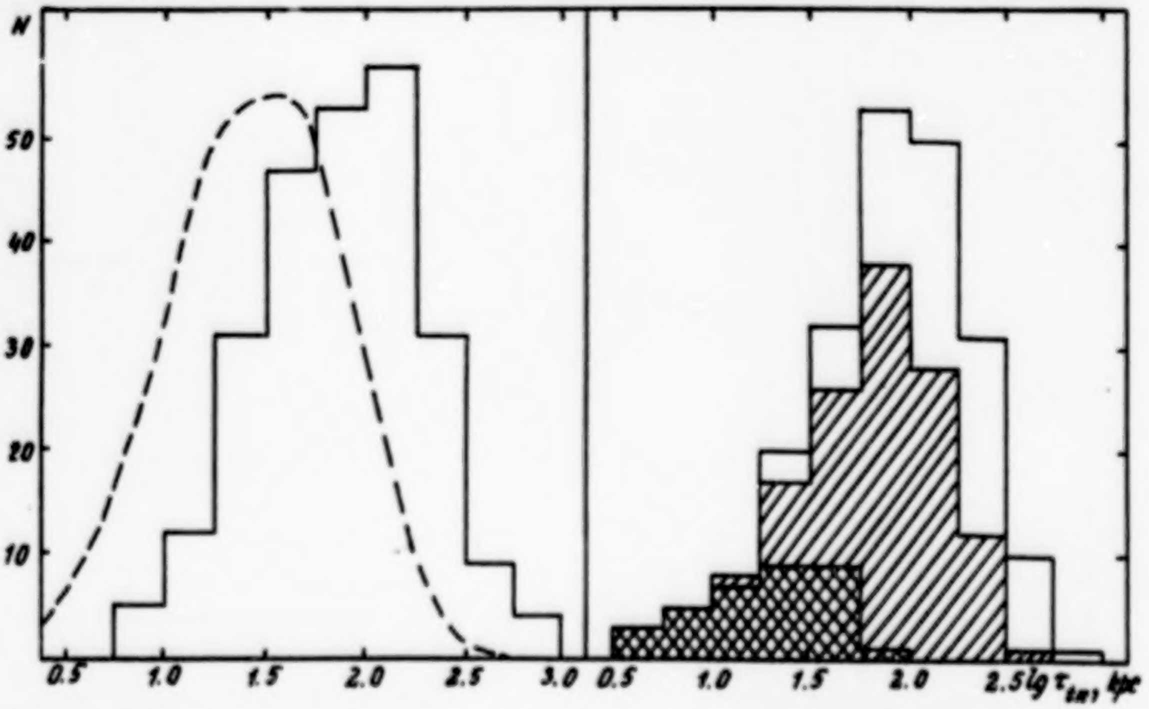

Fig. 2. Triple-system distribution in projected linear separation between the components. Hatching shows the same categories of objects as in Figure 1.

The distribution of catalogued triplets in S_v, r_H - coordinates is shown in Figure 3. Triple systems in this diagram are concentrated in distinct groups, which may indicate dynamical or structural inhomogeneity of the sample. On the whole a tendency is evident for velocity dispersion to decrease for triple systems on passing from tight systems to wide ones. Such a feature is characteristic also of the $(V_i - V_k)$, r_{ik} distribution. The presence of a weak negative correlation between mutual velocities and separations of galaxies should be expected, if their motions in triple systems are close to Keplerian.

As the results of numerical simulations show, selection effects in triple systems are quite strong and various. Practically all the catalogued parameters of triple galaxies are distorted both by selection conditions and the presence of false triplets. Several examples of these will be given below.

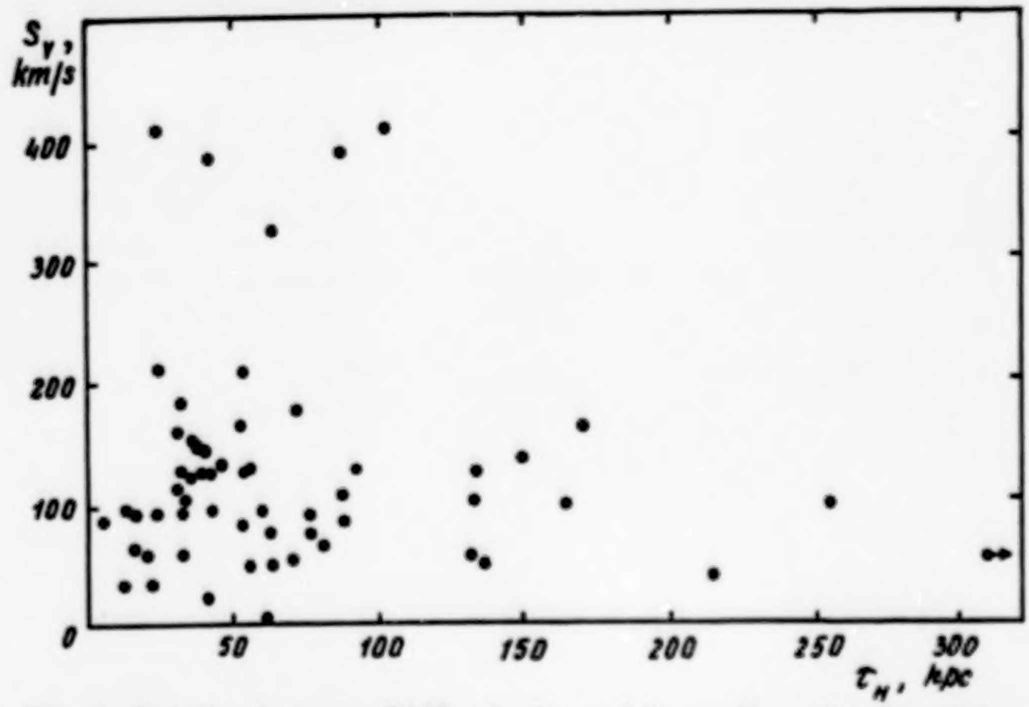

Fig. 3. Relation between RMS velocity and linear dimension for triplets.

3. VIRIAL MASS-TO-LUMINOSITY RATIOS

Mass-to-luminosity ratios in triplets were determined in several ways. The results are presented in Figure 4. The upper histogram (A) shows the distribution of the number of systems according to log f obtained from eq. (6). The middle histogram (W) reflects the distribution of f weighting each galaxy proportionally to its luminosity. The lower diagram (P) shows the distribution of f_{ik}, i.e. orbital mass-to-luminosity ratio for each pair of triplet members according to eq. (9). The dashed curve shows an analogous dependence for 585 catalogued pairs. In all three histograms common features may be noted : a broad interval of the argument covering 6-7 orders of magnitude; the location of a primary maximum near $f \approx 30f_{\odot}$, and the existence of a secondary rise in the region $(10^3 - 10^5)$ $f_{\odot}$.

Using the data on mutual velocities, separations and luminosities for components of the simulated triplets, we determined virial ratios f, f_w , and f_{ik} for them, using the same formulae as for real systems. Though such an approach is particularly formal, it has practical sense, as it allows us to estimate the role of projection factors and the presence of background objects. The distribution medians for physical triplets (T), group and cluster members (G) and optical systems (O) are shown with arrows in each of the diagrams A, W, P of Figure 4. According to the results of numerical experiments we may assert, that using all the methods of f-estimation the region of a secondary maximum, $(10^3 - 10^5)$ $f_{\odot}$, appears to be occupied mainly by optical triplets. Spatially isolated triplets and false triple systems (of members of one group or cluster) have similar medians and are difficult to distinguish inside the common main maximum. In the W- and P-histograms one could suspect such a distinction, but it is washed out by random projection factors.

Table 1 presents median estimates of the virial mass-to-luminosity ratio, obtained by different methods. Together with biased f-values we give also median f^c -values, reduced for radial velocity measurement errors according to eqs. (7) and (10). To account for the effects of optical triple systems, we give also data for truncated samples. In one case 25 triplets with $f > 10^3\ f_\odot$ were excluded, in the other - 30 systems, where the radial velocity difference exceeds 500 km/s for at least one pair of components. The last line of the table shows medians for 585 pairs; the conditions $f < 10^3\ f_\odot$ and $(V_i\text{-}V_k) < 500$ km/s preserve 531 and 497 binary systems in this sample, respectively. Analysis of the data allows us to draw the following conclusions.

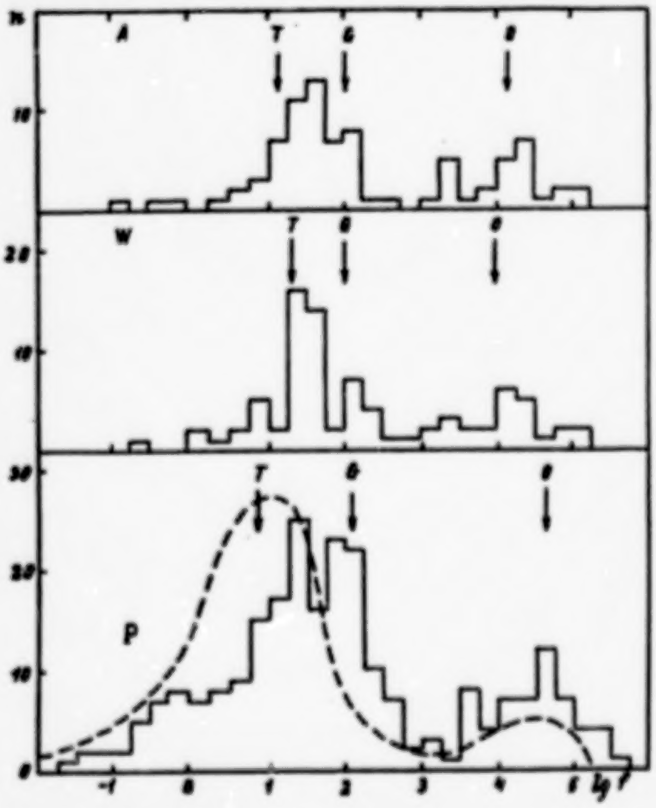

Fig. 4. Distribution of the triplets in virial mass-to-luminosity ratio in solar units. At the top, mean arithmetic estimates (A), in the middle, average weighted over luminosity (W), and at the bottom, pair orbital mass estimations. Arrows show median values for true triplets (T), group members (G) and optical systems (O) according to the results of numerical simulation.

a) Accounting or not-accounting for radial velocity measurement errors weakly influences median estimate of virial mass-to-luminosity ratio. A typical difference between them is only 0.07 dex.

b) The median weakly depends on how we estimate mass-to-luminosity ratio. There is an average difference of 0.04 dex between a simple arithmetic estimate (A) and the value weighted according to luminosity (W), i.e. equipartition is practically absent for giant and dwarf galaxies. Description as a sum of pairs with circular motions of galaxies gives the median close to other methods. We note that for the best agreement of all the median values in different lines of Table 1 it is sufficient to suggest elliptical orbital motions with the eccentrity, $e = 0.40 - 0.55$.

c) From the last line one can see that triplets have a systematic excess of virial mass-to-luminosity ratio in comparison with isolated pairs. As for the whole sample of triple systems, so for the truncated samples the value of such excess is nearly the same and constitutes a factor of $\approx$ 5. This feature is clearly seen in the lower part of Figure 4.

d) For different ways of excluding optical systems (the condition $f < 10^3 f_\odot$ or $\Delta V_{ik} <$ 500 km/s) and various ways to estimate virial mass (A, W, P) medians $[f^c]_{0.5}$ are concentrated in a narrow interval [20 -29] $f_\odot$. Comparing them to the median of individual mass-to-luminosity ratios $[f_{ind}]_{0.5} = 5.9 f_\odot$, determined from 227 galaxies (Karachentsev, 1985), we obtain the value of virial mass excess for triplets, (3.4-4.9), i.e. similar to the previous one.

e) In the initial list all triple systems were divided into types : T - triangle, more or less close to an equilateral one, L - components are linar, D - two close galaxies with a distant satellite. The latter configuration is often called hierarchical. It is the most stable during dynamical evolution (Anosova, Orlov, 1985). Having arranged triplets according to their virial mass-to-luminosity ratio we didn't find any significant differences between hierarchical configurations and the rest.

f) One of the main tests for the presence of hidden mass in galaxian systems is the character of the "virial mass - system size" relation. Such data for triplets are given in Figure 5 and 6. The first reflects the distribution of triplets according to unbiased virial mass-to-luminosity ratio and average harmonic separation. The expected increase (in the presence of hidden mass) of $f^c(r_H)$ is shown very weakly and has low statistical reliability.

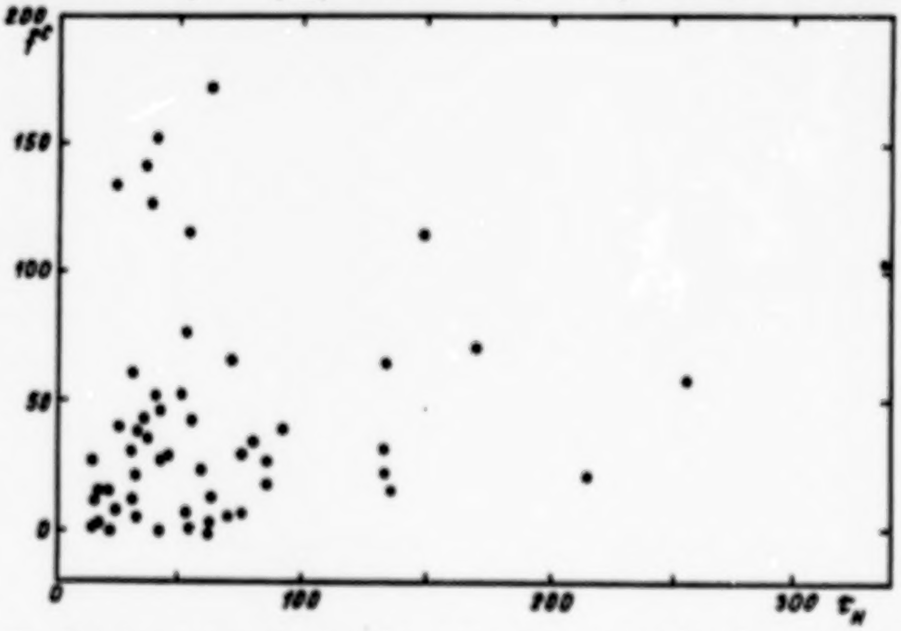

Fig. 5. Triple-system distribution according to unbiased mass-to-luminosity ratio and linear harmonic separation (kpc).

In Figure 6 the orbital mass-to-luminosity ratio is presented versus projected linear separation for triple system components. Negative $f^c]_{ik}$ values correspond to cases when velocity measurement errors exceed the radial velocity difference. Judging by the relative number of such cases and the amplitudes of negative values, velocity measurement errors do not vastly influence dynamical parameters of the sample in general. As in the previous Figure, the increase of orbital mass-to-luminosity ratio with the growth of distance between galaxies reveals only a weak trend. Among wide pairs with $r_{ik} > 100$ kpc two subsystems can be seen : for the first the $f^c{}_{ik}$ values are located in a horizontal band [+25, -10] $f_\odot$, for the second - at the rising branch. This subdivision of objects into two subsystems is not accompanied by any significant distinction of galaxies according to their morphological types, luminosities or other integral parameters.

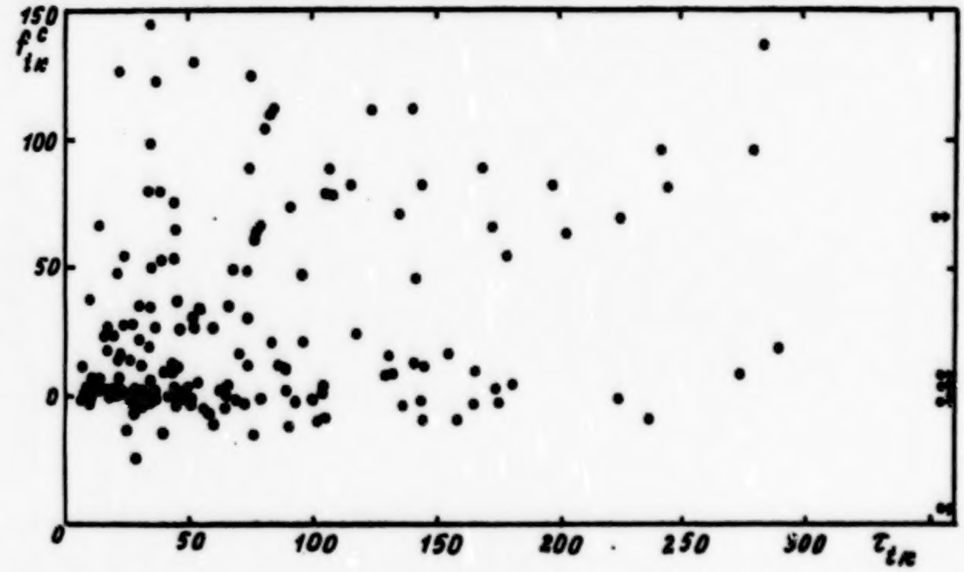

Fig. 6. Relation between orbital mass-to-luminosity ratio and linear projected separation for galaxies in the triplets. Arrows show the pairs with separation greater than 350 kpc.

4. CROSSING TIME

When calculating virial masses it is necessary to make certain, that triplets of galaxies had enough time for dynamical relaxation. Using the average projected harmonic radius of a triplet r_H and rms velocity along the line of sight S_v , we determined from eq. (8) the dimensionless crossing time of the system τ. The distribution of triple galaxies in log τ is shown in the upper part of Figure 7. It has quite a symmetric shape with median $\tau_{0.5}$= dex -1.40.

Another estimate of τ was obtained by considering pairwise combinations of galaxies in the triplet. If the motion of two galaxies is circular, the rotation period around their common gravitation center can be expressed as

$$\tau_{ik} = 4Hr_{ik}/(V_i - V_k)$$

where the numerical value of the coefficient was obtained by assuming chaotic orientation of orbits relative to the line of sight. The distribution of dimensionless rotation periods is shown on a logarithmic scale in the lower histogram of Figure 7. Some of the pairs formed from triplet members have rotation periods exceeding the Hubble time . In this region ($\tau > 1$) the cases prevail for which when projected velocity difference for two galaxies is less than its measurement error (hatched). The median orbital period is dex -1.05.

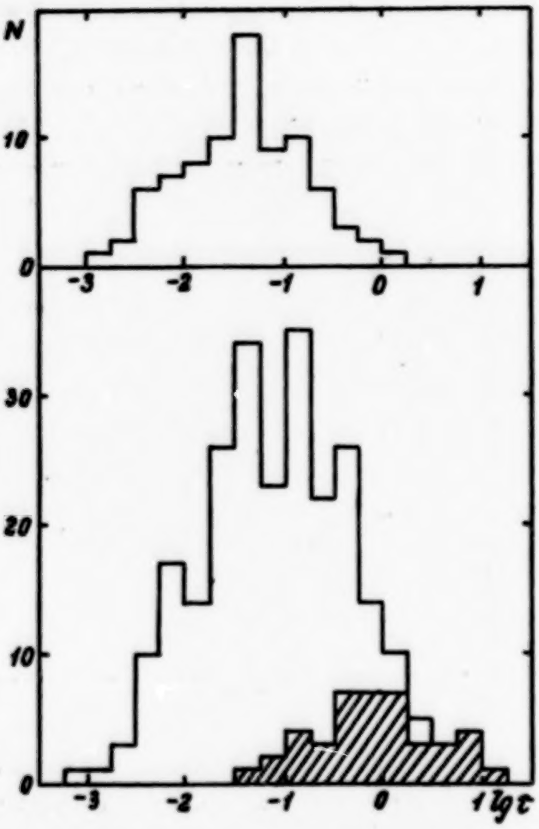

Fig. 7. Triple-system distribution according to crossing time (top) and orbital period (below) in units of the Hubble time, H^{-1}. Hatching shows the pairs in which the radial velocity difference is less than its measurement error.

It should be noted that crossing time might be determined by using the observed values in different ways. Thus, Gott *et al.* (1973) used a “virial” crossing time, which is less than the one calculated according to eq. (8) by $(20\sqrt{5}/3\pi) \approx 4.7$ times. Jackson (1975) suggested expressing the estimate of τ through the RMS system radius and S_v (“inertial” crossing time). Gott and Turner (1974) prefer a “linear” time $\tau_L = (2H/\pi) < r_{ik}/(< V_i - V_k >)$, which is less sensitive to the presence of closely projected pairs and background objects. According to numerical simulation of the collapse and relaxation of a group of galaxies (Gott and Turner, 1977), a triple system reaches virial equilibrium when its crossing time $\tau = 2Hr_H/S_v \lesssim 0.4$. As is seen from Figure 7, about 95% of triplets satisfy this condition; in other words, almost all the triple systems have already passed the initial period of their dynamical evolution.

5. CONCLUSION

Using various ways to estimate virial mass and various methods of excluding optical systems we found that the median mass-to-luminosity ratio for the sample of 84 triplets ranges from 20 to 30 $f_\odot$. This value is 3-4 times less than the one obtained for triple systems from the lists of groups by Geller, Huchra (1983) and Vennik (1986). But it is 4 times as large as the median mass-to-luminosity ratio ($\approx 6f_\odot$) which follows from rotation curves of separate galaxies or analysis of orbital motions in pairs.

To explain this excess it is sufficient to suppose that about 80% of triplets' total mass is hidden matter. But there are serious grounds for believing that the sample considered is strongly contaminated by false non-isolated "triplets", which are fragments of systems with higher multiplicity. Therefore all this virial excess may be an "artifact", originating from the extreme rareness of true autonomous triple systems.

REFERENCES

Anosova J.P., Orlov V.V. 1985, Uchenye Zapiski LGU (Leningrad State University), mathematics, 82, No 416, 66-144.

Bahcall J.N., Tremaine S. 1981, Astrophys. J. 224, 805-820.

Faber S.M., Gallagher J.S. 1979, Ann. Rev. Astron. Astrophys. 17, 135-187.

Gott J.R., Turner E.L. 1977, 213, 309-322.

Gott J.R., Wrixon G.T., Wannier P. 1973, Astrophys J. 186, 777-785.

Jackson J.C. 1975, Mon. Not. R. Astron. Soc. 173, 41.

Karachentsev I.D. 1972, Catalog of isolated pairs of galaxies in the northern hemisphere, Soobshch. Spets. Astrofiz. Obs. Akad. Nauk USSR, 7, 1-91.

Karachentsev I.D., Shcherbanovskij A.L. 1978, Soobshch. Spets. Astrofiz. Obs. 24, 5-46.

Karachentsev I.D. 1985, Astron. Zh. 62, 417-431.

Karachentsev I.D. 1987, Binary galaxies (*Dvoinye Galaktiki*), Moscow, Nauka.

Karachentsev I.D., Karachentseva V.E., Lebedev V.S. 1989, Izv. Spets. Astrofiz. Obs. Akad. Nauk USSR, 27, 67.

Karachentseva V.E., Karachentsev I.D., Shcherbanovskij A.L. 1979, Izv. Spets. Astrofiz. Obs. Akad. Nauk USSR, 11, 51.

Karachentseva V.E., Karachentsev I.D. 1982, Astrofizika, 18, 5-16.

Karachentseva V.E., Karachentsev I.D., Lebedev V.S. 1988, Izv. Spets. Astrofiz. Obs. Akad. Nauk USSR, 26, 42.

Limber D.N., Mathews W.G. 1960, Astrophys. J. 132, 286.

Trimble V. 1987, Ann. Rev. Astron. Astrophys. 25, 425-472.

Vaucouleurs G. de, Vaucouleurs A. de, Corwin H.C. 1976, Second Reference Catalogue of Bright Galaxies, Univ. of, Texas Press, Austin.

Vennik, J.A. 1986, Astron. Nachr. 307, 157.

TABLE 1

MEDIAN VIRIAL MASS-TO-LUMINOSITY RATIO FOR 84 TRIPLETS

Estimator	Whole Sample		Objects with f< 10^3		Objects with $\Delta V_{ik} < 500$ km/s	
	log $f_{0.5}$	log $f^c{}_{0.5}$	log $f_{0.5}$	log $f^c{}_{0.5}$	log $f_{0.5}$	log $f^c{}_{0.5}$
A	1.83	1.76	1.53	1.46	1.49	1.43
W	1.70	1.66	1.49	1.46	1.49	1.43
P	1.73	1.69	1.44	1.38	1.35	1.30
Pairs ($n = 585$)	0.93	0.86	0.83	0.70	0.75	0.60

Plate 1. Two examples of triple systems having a moderate virial mass-to-luminosity ratio ($\approx$ 100 $f_\odot$). *a*) T 50 = Hickson 68 with radial velocities +2410, +2115, and +3096 km/s for A, B, C -components, respectively.
b) T 83 = Hickson 99 with radial velocities +9084 (A), +9066 (B), and +8259 (C) km/s. Both photographs in blue light were obtained by N. Tikhonov, with the 6-meter telescope.

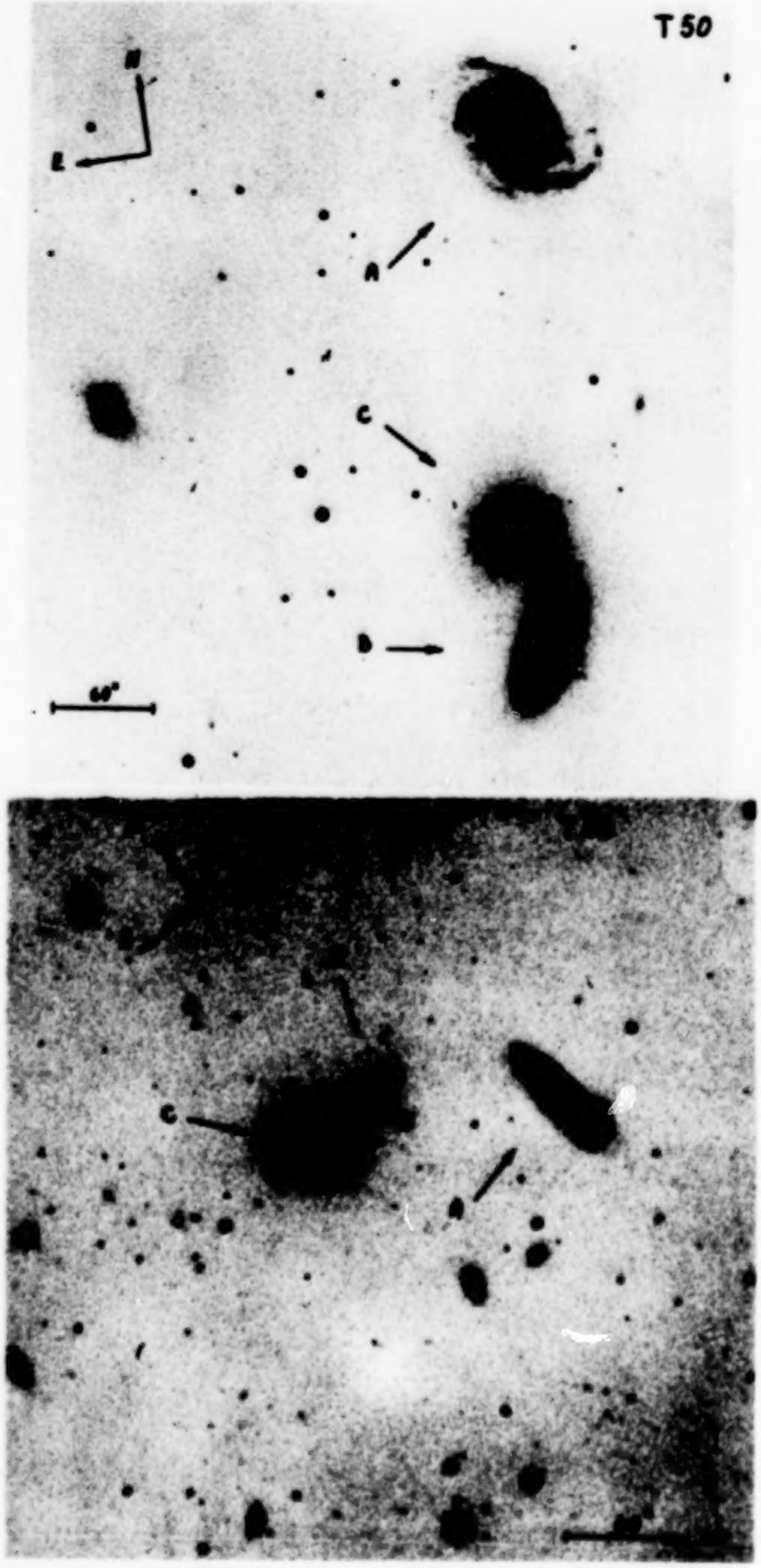

HI STUDIES OF THE SCULPTOR GROUP GALAXIES

Claude Carignan, Université de Montréal

and

Daniel Puche, Very Large Array, NRAO

ABSTRACT

Results from large-scale mapping of the HI gas in the Sculptor group are presented. From our kinematic analysis, a mean global $(M/L_B) \simeq 9$ $M_\odot/L_\odot$ (at the last observed velocity point) is found for the individual galaxies. This is only a factor ~ 10 smaller than the $(M/L_B)_{dyn} \simeq 90$ $M_\odot/L_\odot$ derived from a dynamical study of the whole group. The parameters derived from the mass models suggest that most of the unseen matter has to be concentrated around the luminous galaxies. Under the assumption that the Sculptor group is a virialized system and that all the mass is associated with the galaxies, an upper limit of ~ 40 kpc is derived for the size of the dark halos present in the five late–type spirals of the group.

1. Introduction

Dynamical studies of individual galaxies, groups of galaxies, and clusters of galaxies have led to a large variety of sometimes contradictory values of dynamical mass–to–light ratios (M/L_B). The present situation can be summarized as follows. According to the scale considered, determinations of M/L_B range from 1 to 500 $M_\odot/L_\odot$. In this interval, the most cited numbers are $\simeq 2$–10 for individual galaxies (from rotation curves of spirals), $\simeq 30$–100 for binaries and small groups, and $\simeq 200$ for rich clusters (Faber and Gallagher 1979). The obvious conclusion is that there is a large quantity of dark matter (DM) present in these systems. However, *the question of whether this unseen matter is associated with the individual galaxies, is more uniformly distributed, or both, still remains to be settled.*

The closest group of galaxies outside the Local Group for which we can study the kinematics and the distribution of DM is the Sculptor group. It covers an area of 20° in diameter centered at $\alpha = 0^h30^m$ and $\delta = -30°$. Prior to this study, the kinematical data on the Sculptor group galaxies were of unequal quality, sensitivity and resolution (optical Fabry–Pérot, single dish HI, Owens Valley interferometry ...). We now present a homogeneous data set from new HI line observations obtained at the Very Large Array (VLA). Because Sculptor is a nearby group (~ 2.5 Mpc), the resolution of $30''$ to $60''$ ($\sim$ 500 pc), obtained with the C/D configuration, is ideal to allow detailed modeling of the mass distribution.

2. Dynamical Study of the Sculptor Group

The first step of the analysis is to determine the membership of the group. For this, we use the dynamical mass estimators derived by Heisler, Tremaine, and Bahcall (1985) for a system of self-gravitating objects of comparable masses. This approach is justified since all the galaxies have equivalent absolute magnitudes ($\langle M_B \rangle \simeq -18.2 \pm 0.6$). This shows the group to be mainly composed of five members: NGC 7793, NGC 55, NGC 247, NGC 253, and NGC 300 (Puche and Carignan 1988). Two other galaxies, NGC 45 and NGC 24, which are observed in the general direction of the Sculptor group are found to be more distant objects. As for the dwarfs known to belong to Sculptor (e.g. SDig: Lausten *et al.* 1977), they need not be considered because of their small contribution to the dynamics of the group.

Assuming that the Sculptor group is a virialized system, a total dynamical mass of 2.0×10^{12} M$_\odot$ is derived. This is an upper limit since the virialized state of the group can be questioned (de Vaucouleurs 1959). This gives a total $(M/L_B)_{dyn} \simeq 90$ M$_\odot$/L$_\odot$.

3. Kinematic Studies of the Sculptor members

All the galaxies were observed in HI at the VLA. NGC 7793, being on the far side of the group could be studied with only one field (HPBW $\simeq 32'$). However, for NGC 55 and NGC 300, which are on the near side of the group, a 'mosaicing' technique had to be used to get sufficient sensitivity in the outer parts. For NGC 55, which is nearly edge-on, two fields were sufficient while five fields had to be combined for NGC 300. The two other galaxies, NGC 247 and NGC 253, which are at the mean distance of the group, were observed with only one field. Since the detected HI extends to $\sim 30'$, they clearly need to be reobserved in two fields.

The velocity fields of the five galaxies were analysed using a full tilted ring model. Important warps of the HI plane are clearly seen for NGC 7793, NGC 253 and NGC 300. Using the derived rotation curves, the mass distribution was analysed for each galaxy using multi-component models (Carignan and Freeman 1985). The contribution from the stellar disk is calculated by a straight inversion of the luminosity profile (Kalnajs 1983) where the $(M/L_B)_*$, assumed constant throughout the disk, is the only free parameter. The surface density profile of the HI gas is obtained by elliptically averaging the total HI maps ($\times 4/3$ to account for primordial He). The DM halo is modeled by an isothermal sphere potential (Carignan 1985). This component has two free parameters: a radial scaling r_c (core radius) and a velocity scaling σ (one dimensional velocity dispersion). The central density is then given by $\rho_0 = 9\sigma^2/4\pi G r_c^2$.

Using the results of the mass models, a mean $(M/L_B)_{global} = 9.2 \pm 4.6$ is found for the five members of Sculptor at the last measured velocity point of the rotation curve. The $(M/L_B)_{global}$ range from 5 for NGC 7793 to 15 for NGC 253. It is important to notice that the mean $(M/L_B)_{global}$ is only a factor 10 smaller than the $(M/L_B)_{dyn}$ obtained for the group as a whole.

4. Discussion

Combining the results from the dynamical analysis of the Sculptor group with the results obtained from the kinematics of its individual members, two main conclusions can be reached. The mass models give us a measure of the mean density of DM in the five galaxies. At the last measured velocity point of the rotation curves, we find $\langle \rho_{DM} \rangle \simeq 5.0 \times 10^{-3}$ $M_\odot$ pc^{-3}. If the DM was uniformly distributed in the group, its mean density would only be $\simeq 5.0 \times 10^{-6}$ $M_\odot$ pc^{-3}. This gives a density enhancement for the DM in the halos of $\sim 10^3$ which suggests that *a large fraction of the unseen matter has to be concentrated in the neighborhood of the luminous galaxies.*

Following this result, if one assumes that all the DM is associated with the optical galaxies and that the Sculptor group is a virialized system, the *dark halos only need to extend to* $\sim$ 40 *kpc* so that each galaxy has a $(M/L_B)_{global} \simeq 90$, which is the $(M/L_B)_{dyn}$ derived for the whole group. Because Sculptor may not be virialized, this value of 40 kpc is an upper limit.

Finally, the results from this study cannot easily be used to make inferences on the possible nature of DM. The uncertainties on the modeling of the mass distribution are still too large to derive severe constraints (see e.g. Lake 1989). Suffice to say that the mean density of DM in the halos of the Sculptor galaxies $\rho_{DM} \simeq 0.005$ $M_\odot$ pc^{-3} corresponds to only $\simeq 5$ pc^{-3} Jupiter size bodies. This is very low considering, for example, that brown dwarfs, which are serious baryonic DM contenders, could have masses an order of magnitude greater than Jupiter; hence, the density of such objets would only need to be ≤ 1 pc^{-3}.

References

Carignan, C. 1985. *Ap. J.*, **299**, 59.
Carignan, C., and Freeman, K.C. 1985. *Ap. J.*, **294**, 494.
Faber, S.M., and Gallagher, J.S. 1979. *Ann. Rev. Astron. Astrophys.*, **17**, 135.
Heisler, J., Tremaine, S., and Bahcall, J.N. 1985. *Ap. J.*, **298**, 8.
Kalnajs, A. 1983. In *IAU Symp. 100, Internal Kinematics and Dynamics of Galaxies*, ed. E. Athanassoula (Dordrecht: Reidel), p. 87.
Lake, G. 1989. *A. J.*, **98**, 1253.
Laustsen, S., Richter, N., van der Lans, J., West, R.M., and Wilson, R .N. 1977. *Astron. Astrophys.*, **54**, 639.
Puche, D., and Carignan, C. 1988. *A. J.*, **95**, 1025.

A STUDY OF THE COMPACT GROUP OF GALAXIES SHAHBAZIAN 4

C. R. Lynds[1], E. Ye. Khachikian[2], and A. S. Amirkhanian[2]

ABSTRACT. For the members of the compact group of galaxies Shahbazian 4 the radial velocities are defined. The velocity dispersion is 440 km s^{-1}. Moreover the appparent and absolute magnitudes of galaxies in the V band as well as the mass-to-luminosity ratio are obtained. The latter is approximately 220 $M_{\odot}/L_{\odot}$. The "crossing time" for the group Shahbazian 4 is equal to 4.7×10^7 years. It is one of the densest group of galaxies with $n \sim 10^4$ galaxies Mpc^{-3}.

---

[1] Kitt Peak National Observatory, operated by AURA, Inc., under contract with the National Science Foundation

[2] Byurakan Astrophysical Observatory

Considerable attention has been given recently to the so-called Shahbazian's compact groups of the compact galaxies (Shahbazian 1973; Ambartsumian et al., 1975). This is one of the interesting classes of groups of galaxies. At present a large number of these groups are known and moreover some of them have been studied morphologically (Shahbazian and Amirkhanian, 1978) and photometrically (Shahbazian, 1978; Amirkhanian and Egikian, 1987; Amirkhanian, 1988; Amirkhanian et al., 1990). Because of the considerable distance of the majority of the compact groups and the faintness of their members spectral studies of these objects are not numerous. We should like to note pioneering work by Robinson and Wampler (1973) concerned with the spectral study of the group Shahbazian 1.

At this time interest in compact groups of galaxies has been stimulated for two principal reasons:

1. These are the most compact objects among the known groups of galaxies; the space density of galaxies in these groups is very high.

2. The first determination of the mass-to-luminosity (M/L) ratio for the group Shahbazian 1 (Robinson and Wampler, 1973; see also Shahbazian, 1978) has given a value one order of magnitude less than M/L for double galaxies and close to that of globular clusters.

However, later, a small value of the M/L ratio for the group Shahbazian 1 has not been confirmed (Kirshner and Malumuth, 1980). For other groups the mass-to-luminosity ratio has been found greater as well, from 30 to 260 $M_\odot/L_\odot$ (see Amirkhanian and Egikian, 1987; Amirkhanian, 1989; Amirkhanian, et al., 1990). A detailed study of the compact groups of galaxies in the lists of Shahbazian et al. is of great interest from the point of view of the evolution of galaxy groups, too.

In this work results of spectral and photometric study of one of the most remarkable groups in Shahbazian's lists (No. 4) are presented. The late publication of the spectral observations is due both to objective and subjective reasons.

In June 1973 spectral observations of five galaxies from the compact group Shahbazian 4 were carried out with the 84-inch telescope at Kitt Peak National Observatory (USA) in order to obtain their radial velocities. The spectra were acquired with the grating spectrograph at the Cassegrain focus of the telescope. The six-camera secondary electron image intensifier of type P829D supplied with a "Lynds mask" (with the photoemulsion extension in the direction perpendicular to the dispersion during the exposure) was used as the photodetector. The image intensification was great enough to detect individual photoelectrons in the spectrum image.

The wavelength range 3500 - 7500 A with a dispersion of 240 A/mm and a spectral resolution of about 10 A was covered during one exposure. In Shahbazian 4 the radial velocities of five galaxies (out of seven) are defined by a correlation analysis method. The root-mean-square error in determination of radial velocities is about 100 km s^{-1}. The radial velocities of group member galaxies V_o are given in Table 1. These velocities were corrected for solar motion by the formula:

$$\Delta V_o \text{ (km s}^{-1}) = 300 \sin \ell^{II} \cdot \cos \beta^{II}$$

TABLE 1

Galaxy	Corrected Radial Velocity V_o (km s^{-1})
C. G. 4(1)	29 520
(2)	29 110
(3)	30 220
(4)	30 100
(5)	29 220

From the data in Table 1 the mean velocity $\langle V_o \rangle = 29\,630$ km s^{-1}, that corresponds to a group distance of 395 Mpc (here and throughout $H_o = 75$ km s^{-1} Mpc^{-1}). The mean harmonic distance between the galaxies is $\langle R^{-1} \rangle^{-1} = 37$ kpc. The radial velocity dispersion $\langle \Delta V^2 \rangle^{1/2}$ corrected for observational errors is 440 km s^{-1}.

Taking for the virial mass definition an expression according to Karachentsev and Karachentseva (1975) we have:

$$M = 3\pi G^{-1} \frac{n}{n-1} \langle \Delta V^2 \rangle \langle R^{-1} \rangle^{-1} = 1.8 \cdot 10^{13} M_\odot ,$$

where n - the number of galaxies in group.

A picture of this group obtained by one of the authors (E. Ye. Khachikian) on hypersensitized emulsion Kodak IIIaJ emulsion (GG385 filter with 45 minutes exposure at the prime focus of the 4 meter telescope at Kitt Peak Observatory) is given in Figure 1. The plate limiting magnitude is about $23^m.5$.

The apparent magnitudes of the galaxies in V have been determined by detailed surface photometry of plates obtained at the prime focus of the 2.6 meter telescope of the Byurakan Astrophysical Observatory using extrafocal images of stars for calibration. The plate scale is about 21 "/mm. The plates have been measured with the Shnell microphotometer. The size of the scanning aperture corresponds to 100 μm x 100 μm. The total apparent and corresponding absolute magnitudes (corrected for absorption in our Galaxy and for redshift according to Peterson (1970) and Whitford (1971)) are given in Table 2.

TABLE 2

Galaxy	Apparent Magnitude m_V	Absolute Magnitude M_V
C.G. 4(1)	17.04	- 21.34
(2)	17.72	- 20.66
(3)	18.19	- 20.19
(4)	17.87	- 20.51
(5)	18.46	- 19.92
(6)	19.5	- 18.88
(7)	19.73	- 18.65

The total luminosity of the seven galaxies $8.1 \times 10^{10}\ L_\odot$ and the mass-to-luminosity ratio is about 220 $M_\odot/L_\odot$.

The estimate of the "crossing time" for this group is of interest as well. According to Gott, Wrixon and Wanner (1973) we get an expression for the crossing time

$$\Delta t = (3/5)^{3/2} \langle R \rangle \langle \Delta V \rangle^{-1/2} = 4.7 \times 10^7 \quad \text{years}$$

(the quantity $\langle R \rangle$ is equal to 0.045 Mpc for the compact group Shahbazian 4).

Such a small crossing time corresponding to approximately 1/300 of the age of the Universe age. may be interpreted in two ways:

a. The group has a very small age (of order 10^8 years) and, possibly, it is not stable;

b. If the group has an age of order $H^{-1} = 13 \times 10^9$ years it is undoubtedly gravitationally connected.

In the second case one can suppose that the observable group was a considerably richer cluster in the past which lost most of its "lighter" (i.e., fainter) members in the process of dynamical evolution. In the favor of this view the fact speaks that five galaxies from seven ones have the higher luminosities from -20^m up to $-21^m.3$.

It is important to call attention to a high space density of galaxies in the group of order 10^4 galaxies Mpc^{-3} which is considerably higher than that of the central regions of the regular clusters of galaxies. According to Bahcall (1975) the space density of the galaxies amounts from 60 to 300 galaxies Mpc^{-3} for 15 clusters with the richness classes 0, 1, and 2 from the Abell's list (1958). The group consists exclusively of E and SO/a galaxies. According to Postman and Geller (1984) the overwhelming majority of the galaxies in the densest regions of the groups and clusters ($n \gtrsim 600$ galaxies Mpc^{-3}) belong to E and SO types. This fact is interpreted by them as a result of effects in the outer regions of galaxies of stripping mechanisms effective at such high space densities. Quite possibly the same mechanism acts in the case of compact group Shahbazian 4.

REFERENCES

Abell, G. O. 1958, Ap. J. Suppl., 3, 211.

Ambartsumian, V. A., Arp, H. C., Hoag, A. A., and Mirzoyan, L. V. 1975, Astrofizika, **11**, 193.

Amirkhanian, A. S., and Egikian, A. G. 1987, Astrofizika, **27**, 395.

Amirkhanian, A. S. 1989, Soobsch. Byurakan. Observ., 61, 25.

Amirkhanian, A. S., Egikian, A. G., Tikhonov, N. A., and Shahbazian, R. K. 1990, Soobsch. Byurakan. Observ. (in press).

Bahcall, N. A. 1975, Ap. J., **198**, 249.

Gott, III, J. R., Wrixon, G. T., and Wanner, P. 1973, Ap. J., **186**, 777.

Karachentsev, I. D., and Karachentseva, V. E. 1975, Pis'ma v Astron. J., 1, No. 5, 3.

Kirshner, R. P., and Malumuth, E. M. 1980, Ap. J., **236**, 366.

Peterson, B. A. 1970, Ap. J., **75**, 695.

Postman, M., and Geller, M .J. 1984, Ap. J., **281**, 95.

Robinson, L. B., and Wampler, E. J. 1973, Ap. J. (Letters), **179**, L135.

Shahbazian, R. K. 1973, Astrofizika, 9, 495.

Shahbazian, R. K. 1978, Astrofizika, **14**, 273.

Shahbazian, R. K., and Amirkhanian, A. .S. 1978, Astrofizika, **14**, 455.

Whitford, A. E. 1971, Ap. J., **169**, 215.

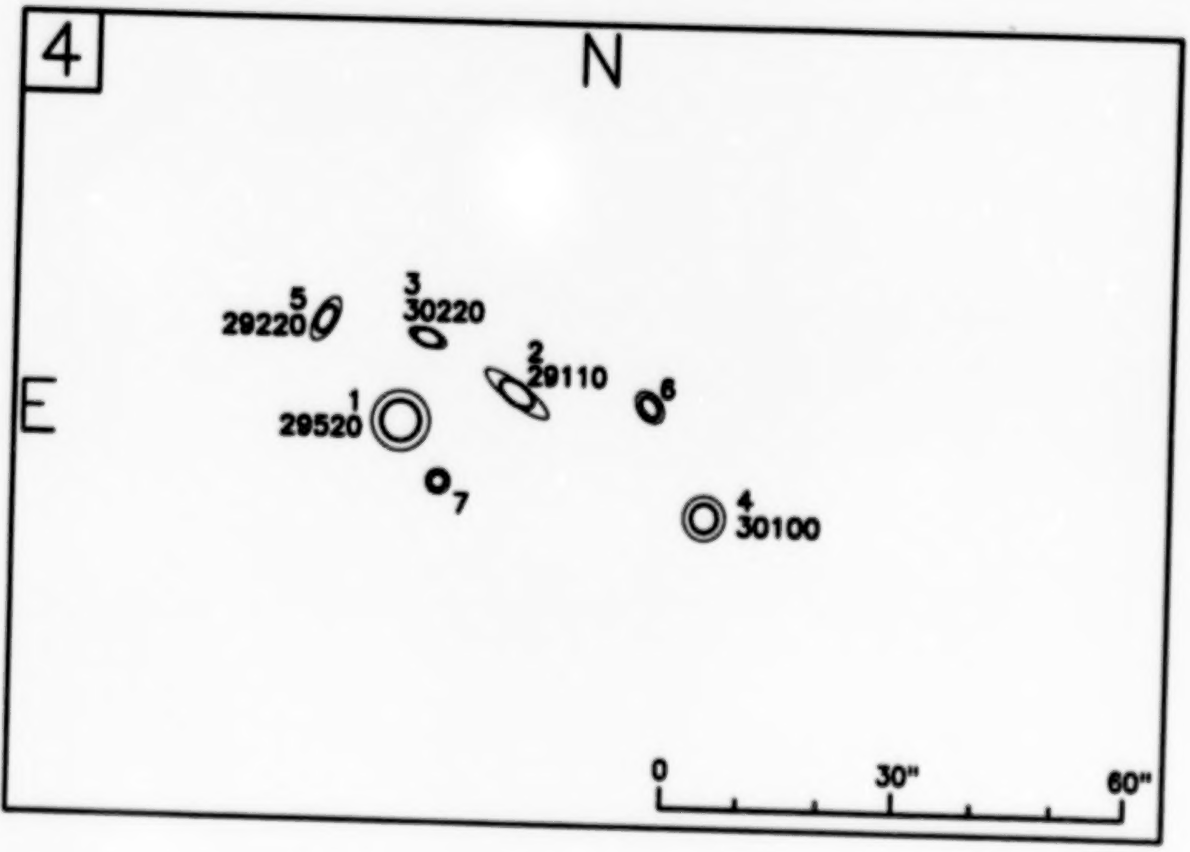
4
N
E
5
29220
3
30220
2
29110
1
29520
6
7
4
30100
0
30"
60"

ISOLATED GALAXIES, PAIRS AND GROUPS OF GALAXIES

I. Kuneva and M. Kalinkov
Department of Astronomy, Bulgarian Academy of Sciences
72 Lenin blvd, 1184 Sofia, Bulgaria

We searched for isolated galaxies, pairs and groups of galaxies in the CfA survey (Huchra *et al.* 1983). It was assumed that the distances to galaxies are given by $R = V/H_0$, where $H_0 = 100$ km s^{-1} Mpc^{-1} and $R > 6$ Mpc.

The searching procedure is close to those, applied to find superclusters of galaxies (Kalinkov and Kuneva 1985,1986). A sphere with fixed radius r^* is described around each galaxy. The mean spatial density in the sphere is m. Let G^1 be any galaxy and G^2 be its nearest neighbor at a distance R_2. If R_2 exceeds the 95% quintile in the distribution of the distances of the second neighbors, then G^1 is an isolated galaxy. Let the midpoint of G^1 and G^2 be O_2 and $r_2 = R_2/2$. For the volume V_2, defined with the radius r_2, the density $D_2 = 2/V_2$ is calculated. Here 2 stands for the number of galaxies in the volume V_2. We use inequalities to establish regions with density enhancements higher than k um. Thus, if $D_2 < k\mu$, the galaxy G^2 is a single one and the procedure for searching for pairs and groups, beginning with this object is over and we have to pass to another object. If $D_2 > k\mu$, the searching procedure goes on. Let then G^3 be the third neighbor of O_2 and let O_3 be the center of G^1, , G^2 and G^3 ; $r_3 = \max(O_3G^1, O_3G^2, O_3G^3)$ is calculated and around O_3 we describe a sphere with radius r_3 of volume V_3 and density $D_3 = 3/V_3$. If $D_3 < k\mu$, it might be concluded that the galaxies G^1 and G^2 form a pair for the specific choice of k and r . The pair is isolated, if the distance O_2G^3 exceeds the 95% quintile in the distribution of the distances of the third neighbors. Then the procedure for the galaxy G^1 ends. For $D_3 > k\mu$, the procedure continues. Generally, the procedure for searching for multiplets continues for $D_i > k\mu$. If $D < k\mu$, the procedure stops with the finding of a multiplet consisting of i-1 members (i = 2,3,...) and the test for isolation with the 95% quintile in the distribution of the distances to the i-th neighbors.

The algorithm is objective, but it is not always commutative because of the local character of the spatial density. The main difference however between our and some other procedures is the local density. In many cases our groups are closed - it means that the multiplets are independent of the choice of galaxy with which the search has started. But there are some groups which are open - their membership is slightly different, depending on the galaxy with which the procedure has started.

Here the authors present the groups - isolated and nonisolated - with $n > 3$, found in the CfA survey in the Northern galactic hemisphere. The parameters used are $k = 10$ and $r^* = 5$ Mpc. Table 1 contains: (1) the group number, (2) the galaxy, nearest to the multiplet center, (3) multiplicity n, (4) the brightest galaxy if it is not listed in (2); (5) and (6) are R.A. and Dec. (1950), (7) - mean distance D in Mpc. Further there are the mean density ρ (8) of the multiplet (galaxies Mpc^{-3}), (9) the density ρ^* for $r^* = 5$ Mpc and (10) the density ρ_g for the group with its nearest neighbor. The parenthesized digits for densities in the last three columns are powers of ten.

TABLE 1

	Center	n	Brightest	α	δ	D	ρ	ρ^*	ρ_g
1	N2769	4	N2693	9 02.0	51 09	48.5	5.8(−1)	1.3(−2)	6.8(−2)
2	U04906	3	N2701	9 05.8	52 53	22.8	6.7(−1)	1.7(−2)	4.0(−2)
3	N2780	3	N2770	9 08.4	34 33	19.7	6.1	2.9(−2)	5.4(−2)
4	N2799	4	N2712	9 11.2	42 29	18.2	4.7(−1)	4.4(−2)	5.4(−2)
5	U04870	3		9 14.4	46 41	42.7	3.2(−1)	9.6(-3)	2.4(−2)
6	N2856	4	N2776	9 17.5	47 12	26.7	4.8(−1)	1.1(−2)	4.6(−2)
7	N2814	4	N2805	9 19.2	64 00	16.4	9.5(−1)	8.8(−2)	9.9(−2)
8	N2914	4	U05189	9 33.5	10 02	31.7	8.2(−1)	1.1(−2)	2.2(−2)
9	N3024	3	N3020	9 49.1	11 51	14.8	2.6	8.6(−2)	3.0(−1)
10	N3011	7	N3003	9 49.3	32 02	14.9	1.7	1.2(−1)	5.6(−1)
11	U05520	3	N2909	10 02.9	65 40	33.1	2.7(−1)	1.3(−2)	4.3(−2)
12	U05459	5	N3079	10 04.9	54 53	11.1	2.9	2.2(−1)	6.0(−1)
13	I 591	3	N3107	10 05.6	13 06	27.5	1.1	2.1(−2)	2.8(−2)
14	N3104	4	N3184	10 09.3	43 56	6.1	4.2	3.7(−1)	7.6(−1)
15	N3169	5	N3166	10 11.1	4 20	13.0	1.5	1.4(−1)	4.9(−1)
16	N3189	10	N3227	10 19.6	22 03	13.0	1.8	1.7(−1)	1.2
17	N3245	5		10 25.5	28 24	13.9	1.9	1.6(−1)	6.5(−1)
18	N3353	3	N3310	10 35.7	55 26	9.6	1.0(+1)	2.9(−1)	3.3(−1)
19	U05760	7	N3367	10 39.0	14 00	29.9	3.4(−1)	2.7(−2)	7.4(−2)
20	N3346	5	N3338	10 42.2	14 38	12.6	2.2	1.8(−1)	6.7(−1)
21	N3381	6	N3294	10 42.4	34 38	15.9	1.4	1.1(−1)	4.1(−1)
22	U05955	3	N3403	10 43.0	73 20	11.9	3.5	1.6(−1)	1.2(−1)
23	N3368	3		10 45.9	12 52	9.0	2.0(+1)	3.5(−1)	6.0(−1)
24	N3433	3		10 50.1	10 22	26.9	5.1(−1)	2.5(−2)	3.7(−2)
25	N3414	3		10 52.6	28 26	14.2	5.7	1.6(−1)	6.0(−1)
26	N3454	5	N3457	10 53.2	18 16	11.3	1.5(+1)	2.9(−1)	1.3
27	N3486	3	N3344	10 53.2	27 52	7.0	6.5	4.6(−1)	1.0
28	U06106	3	U06135	10 59.5	45 55	64.9	3.2(−1)	1.2(−2)	1.8(−2)
29	N3489	5	N3627	10 59.6	13 32	7.1	6.1	4.3(−1)	1.7
30	N3625	9	N3613	11 09.2	57 57	19.7	1.4	5.3(−2)	3.8(−1)
31	U06296	3	N3507	11 09.8	18 16	9.7	1.1(+1)	4.7(−1)	1.6
32	N3549	4		11 10.2	52 41	28.6	2.1(−1)	2.1(−2)	7.4(−2)
33	N3628	3		11 15.6	15 12	8.3	5.4	4.4(−1)	8.5(−1)
34	U06345	3	N3630	11 16.8	3 37	15.8	2.3	7.3(−2)	1.7(−1)
35	N3686	5	N3596	11 20.1	17 05	11.9	7.6	4.1(−1)	1.7
36	N3665	4		11 20.8	39 01	20.8	8.6	3.2(−2)	1.3(−1)
37	N3556	3		11 29.1	55 14	6.8	5.7	3.4-(1)	1.2
38	N3788	4	N3687	11 32.6	31 46	26.2	2.3(−1)	2.1(−2)	6.6(−2)
39	N3755	3	N3813	11 35.3	36 22	15.4	1.3	7.4(−2)	4.8(−2)

TABLE 1 (continued)

	Center	n	Brightest	α	δ	D	ρ	ρ^*	ρ_g
40	N3735	3		11 35.4	70 53	27.4	1.0	3.8(−2)	1.1(−1)
41	N3853	6	N3800	11 38.2	17 13	33.0	3.5	3.2(−2)	1.8(−1)
42	N3770	10	N3963	11 38.7	59 47	32.0	5.1(−1)	3.6(−2)	1.9(−1)
43	N3817	4	N3839	11 39.2	10 36	61.0	2.0(−1)	1.9(−2)	9.4(−2)
44	N3816	3		11 40.6	20 20	55.1	9.2(−1)	1.1(−2)	4.6(−2)
45	U06575	16	N3898	11 41.0	58 57	12.3	2.6	2.2(−1)	1.7
46	N3837	3	N3842	11 41.7	20 10	62.8	3.3(−1)	2.9(−2)	1.5(−1)
47	N3900	3		11 44.0	27 35	18.0	3.7	6.1(−2)	4.5(−2)
48	N3902	6	N3812	11 45.0	25 46	36.7	9.4(−1)	4.0(−2)	2.2(−1)
49	N3929	3	N3883	11 48.1	21 08	70.5	4.6(−1)	2.1(−2)	6.6(−2)
50	N3906	13	N3726	11 48.2	49 45	9.5	1.3(+1)	3.4(−1)	2.6
51	U06923	9	N3992	11 54.2	53 23	10.8	4.4	2.8(−1)	1.9
52	U06925	10	N3995	11 54.3	32 28	31.5	3.3(−1)	3.1(−2)	1.9(−1)
53	N4005	4		11 55.7	25 26	44.2	5.5(−1)	9.6(−3)	4.4(−2)
54	N4004	3	N4017	11 55.7	28 07	34.6	9.2(−1)	5.0(−2)	1.8(−1)
55	N4026	3		11 56.5	52 10	8.7	2.6(+1)	3.4(−1)	3.7
56	N3949	18	N3938	11 59.1	46 49	7.6	6.6	4.6(−1)	2.6
57	N4061	4	N4070	12 02.0	20 41	73.2	1.0	1.0(−3)	1.5(−2)
58	N4128	3		12 03.7	69 30	23.2	7.8(−1)	4.0(−2)	1.7(−1)
59	N4117	6	N4151	12 04.2	41 56	9.8	6.6	3.8(−1)	1.6
60	N4116	3	N4123	12 07.0	2 34	13.0	3.0	2.9(−1)	6.1(−1)
61	N4205	4	N4036	12 09.2	63 59	14.3	1.8	1.8(−1)	8.0(−1)
62	N4189	3		12 09.8	14 08	21.6	1.3	1.2(−1)	2.8(−1)
63	N4185	8	N4169	12 10.1	29 22	38.8	4.7(−1)	2.9(−2)	3.4(−2)
64	N4081	3	N4125	12 10.2	65 08	13.3	5.7	1.7(−1)	1.2
65	N4197	4	N4215	12 12.6	6 01	20.9	2.4	1.4(−1)	6.7(−1)
66	U07395	3	N4229	12 12.9	32 23	67.6	1.2(−1)	1.0(−2)	2.2(−2)
67	N4256	5		12 13.8	66 19	25.4	7.3(−1)	5.5(−2)	2.0(−1)
68	N4200	3	N4168	12 14.5	12 48	23.2	2.2	1.0(−1)	3.3(−1)
69	N4235	8	N4378	12 16.4	6 44	25.9	1.4	7.8(−2)	5.2(−1)
70	I3115	9	N4261	12 16.8	6 09	22.8	1.6	1.2(−1)	6.4(−1)
71	N4254	3		12 16.9	13 42	24.8	1.3	8.6(−2)	2.6(−1)
72	N4251	3	N4314	12 17.8	29 24	10.1	1.1(+1)	5.1(−1)	9.6(−1)
73	N4303	3		12 18.5	4 33	15.8	1.2(+2)	2.1(−1)	7.8(−1)
74	N4290	3		12 18.5	58 24	30.8	6.0(−1)	3.8(−2)	1.0(−1)
75	N4306	3	N4313	12 20.1	12 16	15.1	3.3	2.5(−1)	2.5(−1)
76	N4274	4		12 20.7	30 24	9.0	1.5(+1)	5.5(−1)	2.3
77	N4510	5	N4545	12 22.1	64 56	27.8	8.5(−1)	5.3(−2)	2.7(−1)
78	N4335	4		12 22.4	57 50	46.4	2.4(−1)	1.3(−2)	3.9(−2)

TABLE 1(continued)

	Center	n	Brightest	α	δ	D	ρ	ρ^*	ρ_g
79	N4472	7		12 23.4	8 07	10.2	7.7	4.2(−1)	4.8
80	N4340	14	N4293	12 24.0	15 03	9.4	6.1	5.0(−1)	3.1
81	U07428	3	N4525	12 24.2	31 35	12.1	5.7	3.7(−1)	5.5(−1)
82	N4412	6	N4527	12 24.4	4 08	17.1	4.8	1.6(−1)	8.8(−1)
83	N4414	3		12 24.4	29 25	7.2	1.1(+1)	5.4(−1)	2.8
84	N4461	4		12 24.6	13 02	19.2	4.4	1.6(−1)	5.7(−1)
85	N4308	5	N4631	12 25.0	31 04	6.2	1.9(+1)	5.1(−1)	3.3
86	N4519	12	N4486	12 25.3	9 25	12.4	4.2	3.4(−1)	2.6
87	N4421	6	N4321	12 25.6	15 09	16.1	2.8	2.0(−1)	1.0
88	N4477	6		12 26.0	13 18	13.7	4.0	3.2(−1)	1.6
89	N4458	4	N4206	12 26.6	14 01	6.8	7.6	4.8(−1)	2.5
90	I3521	9	N4526	12 26.7	10 07	5.6	6.8	4.2(−1)	1.3
91	N4350	4		12 26.7	17 16	12.7	4.4	3.7(−1)	1.7
92	N4291	8		12 27.8	74 40	17.0	5.1(−1)	5.0(−2)	3.0(−1)
93	N4435	4	N4382	12 29.2	15 35	7.9	7.6	4.7(−1)	1.4
94	N4501	3		12 29.4	14 41	22.8	1.4	1.1(−1)	4.7(−1)
95	1226+43	14	N5055	12 30.0	44 11	5.3	5.4	4.8(−1)	5.1
96	N4568	4		12 33.6	10 35	22.5	1.9	1.2(−1)	4.1(−1)
97	N4623	3	N4570	12 34.1	7 56	17.7	3.5	1.5(−1)	5.4(−1)
98	N4587	3	N4636	12 34.2	3 15	9.1	1.7(+1)	3.6(−1)	1.2
99	N4596	3		12 34.6	10 39	18.5	2.1	1.7(−1)	9.0(−1)
100	N4564	8	N4649	12 34.9	11 24	11.	1.1(+1)	4.0(−1)	2.8
101	N4598	4	N4535	12 35.1	7 58	19.	2.0	1.6(−1)	5.8(−1)
102	N4600	10	N4665	12 37.2	5 03	7.	5.4	3.7(−1)	2.3
103	I3651	3	N4615	12 38.8	26 33	47.	3.3	9.6(−3)	2.7(−2)
104	N4687	3	U07812	12 42.6	34 32	42.	6.7(−2)	5.7(−3)	5.2(−3)
105	N4725	3		12 43.7	26 02	12.	5.7	3.3(−1)	7.2(−1)
106	N4695	4	N4686	12 45.0	54 39	49.4	9.0(−1)	1.7(−2)	2.7(−2)
107	N4762	3	N4654	12 45.9	11 13	10.2	1.1(+1)	4.0(−1)	2.1
108	N4795	3		12 52.1	8 53	28.0	2.6	2.3(−2)	4.3(−2)
109	N4816	4	N4819	12 54.0	27 57	68.2	2.8(−1)	2.5(−2)	6.8(−2)
110	N4904	3	N4845	12 54.9	1 13	11.8	4.3	2.5(−1)	4.1(−1)
111	N4853	3	N4839	12 55.2	27 42	75.5	5.4(−1)	1.7(−2)	6.9(−2)
112	I4189	5	N4914	13 01.5	36 28	47.4	4.4(−1)	1.2(−2)	1.0(−2)
113	N4966	3	N4944	13 04.7	29 14	69.9	2.6(−1)	1.9(−2)	3.5(−2)
114	N5056	3		13 12.1	30 34	56.0	1.5(−1)	1.2(−2)	2.0(−2)
115	N5112	3		13 15.8	38 22	9.8	6.5	3.3(−1)	7.6(−1)
116	N5218	3		13 22.6	62 51	28.9	8.6(−1)	3.8(−2)	6.4(−2)
117	N5142	3	N5149	13 23.1	36 30	53.6	9.0(−2)	5.7(−3)	5.8(−3)

TABLE 1(continued)

	Center	n	Brightest	α	δ	D	ρ	ρ^*	ρ_g
118	N5208	3	I 900	13 30.8	8 12	68.0	1.5(−1)	1.3(−2)	1.8(−2)
119	U08561	3		13 32.0	34 11	72.9	4.2(−1)	1.2(−2)	3.2(−2)
120	N5221	3	N5230	13 32.7	14 00	69.8	7.6(−1)	1.7(−2)	3.6(−2)
121	N5320	7	N5371	13 47.3	40 54	25.9	1.1	5.7(−2)	3.5(−1)
122	N5379	5	N5322	13 47.5	60 25	17.8	1.0	7.8(−2)	2.0(−1)
123	N5300	3	N5364	13 51.0	4 59	11.9	2.3	2.1(−1)	4.7(−1)
124	I 948	3		13 51.1	14 09	68.8	1.2	9.6(−3)	1.6(−2)
125	N5383	7		13 51.8	41 15	22.6	9.9(−1)	8.0(−2)	4.6(−1)
126	N5341	4	N5395	13 53.6	37 54	35.6	2.8(−1)	2.3(−2)	4.8(−2)
127	U08883	3	U08827	13 54.2	15 30	56.1	5.7(−1)	1.5(−2)	3.2(−2)
128	N5382	3	N5374	13 55.5	6 29	43.0	9.0(+1)	1.5(−2)	4.1(−2)
129	N5416	3		14 00.0	9 42	61.7	2.4(−1)	1.2(−2)	3.2(−2)
130	N5434	3	N5417	14 00.1	8 38	46.6	2.0(−1)	1.5(−2)	1.5(−2)
131	N5445	4	N5444	14 01.2	35 24	38.6	5.5(−1)	2.9(−2)	9.5(−2)
132	U09081	3	N5406	14 02.1	39.28	52.9	1.8(−1)	1.2(−2)	1.6(−2)
133	U09056	7	N5448	14 05.1	49 49	20.0	9.9(−1)	8.8(−2)	7.9(−1)
134	U08980	3	U08975	14 05.7	39 16	58.0	1.2(−1)	1.2(−2)	1.9(−2)
135	U09062	3	N5490	14 08.7	19 01	50.4	1.8(−1)	1.2(−2)	2.3(−2)
136	N5631	8	N5678	14 13.1	56 48	19.7	9.3(−1)	8.0(−2)	4.9(−1)
137	I1000	3		14 20.2	18 07	56.6	2.2(−1)	1.2(−2)	2.2(−2)
138	N5590	5	N5557	14 20.8	36 06	32.5	3.7(−1)	3.2(−2)	1.4(−1)
139	U09356	6	N5665	14 25.4	12 32	22.7	2.7(−1)	1.7(−2)	8.6(−2)
140	N5641	3		14 26.8	28 59	43.5	6.4(−1)	1.3(−2)	5.1(−2)
141	N5649	3		14 27.7	14 10	51.9	1.2	1.2(−2)	4.8(−2)
142	N5653	3		14 27.8	32 16	35.1	1.1	2.7(−2)	6.1(−2)
143	N5669	3		14 28.1	10 32	13.5	8.9(−1)	8.6(−2)	1.1(−1)
144	N5689	7	N5676	14 31.6	49 34	21.8	1.0	8.4(−2)	4.4(−1)
145	N5675	3	N5695	14 33.2	36 41	41.7	5.7(−1)	1.9(−2)	2.8(−2)
146	N5735	3		14 35.1	29 40	37.8	1.8(−1)	1.3(−2)	3.2(−2)
147	N5692	19	N5566	14 36.1	3 35	15.9	1.0	8.0(−2)	6.0(−1)
148	U09519	4	N5798	14 44.0	32 06	17.5	2.7(−1)	2.3(−2)	3.1(−2)
149	N5804	4	N5797	14 55.8	49 58	40.9	9.3(−1)	1.2(−2)	3.3(−1)
150	N5838	3		15 01.3	2 04	13.9	4.8	7.8(−2)	3.3(−1)
151	N5820	6	N5905	15 03.9	54 46	32.3	2.0(−1)	1.9(−2)	5.1(−2)
152	N5906	3	N5866	15 17.3	56 24	6.6	4.1(+1)	2.0(−1)	6.1(−1)
153	N5930	4	N5899	15 21.7	41 40	25.8	1.7	1.3(−2)	4.6(−2)
154	N5985	3		15 28.7	59 41	25.4	4.7-1	1.9(−2)	2.3(−2)
155	I4564	6	I4567	15 32.3	43 27	56.7	1.8(−1)	1.5(−2)	1.7(−2)
156	N5974	3	N5958	15 34.3	30 35	19.5	3.6(−1)	1.5(−2)	3.0(−2)

TABLE 1(continued)

	Center	n	Brightest	α	δ	D	ρ	ρ^*	ρ_g
157	N5956	8	N5962	15 35.5	14 14	419.1	5.2(−1)	2.8(−2)	8.1(−2)
158	N5982	3		15 39.0	59 13	29.3	1.6	1.9(−2)	4.2(−2)
159	I1151	3		15 50.7	18 21	21.5	3.8(−1)	2.3(−2)	6.8(−2)
160	U10127	3	N6052	15 57.3	20 59	48.0	2.1(−1)	1.9(−2)	4.2(−2)
161	I1174	3	N6021	16 02.1	16 02	47.3	3.0(−1)	1.5(−2)	4.0(−2)

There are many coincidences between groups from Table 1 and groups from other catalogs (Turner and Gott 1976, Huchra and Geller 1982, Vennik 1984, Tully 1987). Some groups from the Geller and Huchra (1983) catalog are merged in Table 1 and vice versa, some groups from Table 1 are merged in the GH catalog.

We thank D. Stefanova who helped in the preparation of the catalog. This work is supported in part by the Bulgarian Committee for Science (contract 943).

REFERENCES

Geller, M. J., and Huchra, J. P. 1983, Ap.J.Suppl., 52, 61.
Huchra, J., Davis, M., Latham, D., and Tonry, J. 1983, Ap.J.Suppl., 52, 89.
Huchra, J. P., and Geller, M. J. 1982, Ap.J., 257, 423.
Kalinkov, M., and Kuneva, I. 1985, Astr.Nach., 306, 283.
——. 1986, M.N.R.A.S., 218, 49p.
Tully, R. B. 1987, Ap.J., 321, 280.
Turner, E. L., and Gott, J. R. 1976, Ap.J.Suppl., 32, 409.
Vennik, J. 1984, Tartu Astr.Obs. Teated, No. 73, p. 3.

CORRELATION FUNCTIONS FOR PAIRS AND GROUPS OF GALAXIES

M. Kalinkov and I. Kuneva

Department of Astronomy, Bulgarian Academy of Sciences
72 Lenin blvd, 1784 Sofia, Bulgaria

1. INTRODUCTION

There are many studies on the correlation functions of galaxies, of clusters of galaxies, even of superclusters (e.g. Groth and Peebles 1977; Davies and Peebles 1983; Kalinkov and Kuneva 1985, 1986; Bahcall 1988 and references therein) but not so many on pairs and groups of galaxies.

Results of the calculations of two-point correlation functions for some catalogs of pairs and groups of galaxies are given in this paper. It is assumed that the distances to pairs and groups of galaxies are given by their mean redshifts according to $R = \sum_{i=1}^{n} V_i / nH_0$, where n is the number of galaxies in the system and $H_0 = 100$ km s^{-1} Mpc^{-1}.

2. METHOD

The spatial correlation functions for the systems centers is determined from the relation,

$$\xi_{pp,grgr} = n_0/(n_r(r) - 1)$$

Here $n_0(r)$ is the number of systems, the centers of which are located in the interval $(r - \Delta r/2, r + \Delta r/2)$; n is the corresponding number for the objects from the random catalogs; ξ_{pp} and ξ_{grgr} stand for pair-pair and group-group correlation functions.

For random catalog generation it is necessary to reproduce all selections applied to the observed sample. The method used here is as follows. The apparent distribution of the system centers in the Northern and Southern galactic hemispheres, more often in elementary cells $\Delta l \times \Delta b = 10^\circ \times 5^\circ$, were investigated. In each strip along l, for a given b there is a test for which cells the counts of the systems centers may be regarded as uniformly distributed. The whole strip is broken up in parts and in each part there are generated as many random centers as there are uniformly distributed counts. In the case, when the count in one cell is significantly higher/lower than in the neighboring cells, the randomly generated number of centers is equal to the observed count. For a given interval Δl the galactic longitudes are purely randomly distributed, but the latitudes are generated according to

$$b = \begin{cases} \pi/2 - \cos^{-1}(1 - \xi_k), & b > 0^\circ, \\ \cos^{-1}(1 - \xi_k) - \pi/2, & b < 0^\circ \end{cases}$$

where ξ_k are uniformly distributed random numbers in the interval [0,1). It is thus taken into account that the longitude circles approach the poles.

Afterwards a *distance function N(R)*, which is the number of centers up to a given R, is introduced. This function is approximated with several (5 to 15) linear regressions, and random distances according to the regressions are generated. For example for Karachentsev's sample of isolated pairs ($b > 0^\circ$) from R = 54.5 to 60.3 Mpc (for N=143 to 159), the distance function is

$$N(R) = -20.06 + 2.97R.$$

Therefore for this regression line 17 distances are generated according to $R = 54.5 + 5.72\xi_k$.

Thus the random catalogs (usually 100) are generated separately for the Northern and Southern galactic hemispheres.

There are many ways to determine the two-point spatial correlation functions (e.g. Davis and Peebles 1983; Blanchard and Alimi 1988, Borner *et al.* 1989). The described method for calculating the correlation functions for the galaxies from the CfA survey, and CfA slice survey, for clusters of galaxies, for superclusters and for quasars were tested by the authors. The results do not differ substantually from other calculations (Davis *et al.* 1988; Borner and Mo 1990; de Lapparent *et al.* 1988; Kalinkov and Kuneva 1985, 1986; Bahcall 1988). The results for quasars especially are very close to those obtained with the so called scrambling method (Osmer 1981), but without the weakness of this technique, as demonstrated by Anderson *et al.* (1988).

3. RESULTS

(i) The Karachentsev Sample

Karachentsev's catalog (1972,1987) of isolated pairs of galaxies contains 603 objects. We excluded the 18 non-pairs and all pairs having $\Delta V > 1000$ km/s, and $|b| < 20°$. Thus in the NGH and SGH there are 363 and 127 isolated pairs respectively. The correlation function is given in Table 1, where the statistical uncertainty is $\Delta\xi = [(1+\xi)/n_r]^{1/2}$ and ${\xi_{pp}}^W$ is the function weighted for the NGH and SGH. This two-point pair-pair correlation function is in no way related to the function shown in Fig. 44 of Karachentsev (1987), which is approximated by $\xi = 36/r$, $0.7 < r < 8$ Mpc (for $H_0 = 75$ km s^{-1} Mpc^{-1}). For the first 4 points from Table 1 one gets $\xi_{pp}^W = 1.78 - 0.24r$, $r < 7$ Mpc ($H_0 = 100$ km s^{-1} Mpc^{-1}).

TABLE 1

r (Mpc)	ξ_{pp}^N	$\Delta\xi$	ξ_{pp}^N	$\Delta\xi$	ξ_{pp}^W
1	1.52	0.38	1.73	1.57	1.57
3	1.00	0.16	1.10	0.53	1.03
5	0.48	0.09	0.84	0.32	0.57
7	0.18	0.07	-0.02	0.18	0.13
9	0.06	0.06	0.07	0.16	0.06
11	-0.09	0.05	0.01	0.13	-0.06
13	-0.16	0.04	-0.11	0.11	-0.15

It is important to note that some centers of pairs in Karachentsev's sample are located very closely. The distance between K302 and K310 is only 0.2 Mpc; for K255 and K263 it is 0.5; for K133 and K218 - 0.6 Mpc and so on. Altogether 75 mutual distances are smaller than 2.5 Mpc.

(ii) The Hickson Sample

There are 100 compact groups of galaxies in this catalog (Hickson 1982). The redshifts of 96 groups are given by Hickson *et al.* (1988). We have calibrated the redshifts, using the magnitudes from Hickson *et al.* (1989). The linear regressions are

$$\log z = \begin{cases} -4.2399 + 0.1747\ \mathrm{B}_{TC} \\ -4.3463 + 0.1730\ \mathrm{B}_{I} \end{cases}$$

where B_{TC} is the asymptotic magnitude corrected for internal and external extinction and B_I is the magnitude within the $m_B = 24.5$ mag arcsec^{-2} isophote. For Hickson groups 27, 36, 41 and 50 we obtained redshifts 0.0554, 0.0373, 0.0291 and 0.1172 respectively. After rejection of the groups with $|b| < 25°$ and of the most distant group (H50), there remain 50 and 45 groups in the NGH and SGH respectively. There is insufficient statistics for scales smaller than 10 Mpc. From the two-point group-group correlation function (Table 2) we might conclude that the amplitude for the NGH is very small and for the SGH it is zero. Since $\Delta\xi$ is not a standard deviation but a simple statistical uncertainty, it might turn out the $\xi^{N}_{grgr} > 0$ for $r < 30$ Mpc.

TABLE 2

r, Mpc	ξ^{N}_{grgr}	$\Delta\xi$	ξ^{S}_{grgr}	$\Delta\xi$
5	0.48	0.74	-0.05	0.48
15	0.22	0.31	-0.08	0.20
25	0.28	0.21	0.06	0.15
35	-0.06	0.14	-0.10	0.11

(iii) The Huchra-Geller Sample

This catalog (Huchra and Geller 1982) contains 92 groups, found in the whole-sky catalog of galaxies brighter than $M_B = 13.2$, using a general search algorithm. There are 58 and 30 groups in the NGH and SGH after excluding 4 groups with $|b| < 20°$. It may be seen (Table 3) that $\xi^N > 0$ for $r < 12$ Mpc and $\xi^S > 0$ for $r < 4$ Mpc.

TABLE 3

r, Mpc	ξ^{N}_{grgr}	$\Delta\xi$	ξ^{S}_{grgr}	$\Delta\xi$	ξ^{W}_{grgr}
2	1.33	0.62	0.46	0.40	1.03
5	0.40	0.19	-0.22	0.14	0.19
8	0.16	0.12	0.01	0.13	0.11
11	0.17	0.09	-0.06	0.13	0.09
14	0.07	0.08	0.18	0.16	0.11
17	-0.11	0.06	-0.05	0.16	-0.09
20	0.02	0.07	-0.17	0.16	-0.04

(iv) The Geller-Huchra Sample

There are 176 groups in this catalog (Geller and Huchra 1983) - 123 and 53 in the NGH and SGH, respectively. They are found with the general searching, algorithm of Huchra-Geller among the galaxies in the CfA survey (Huchra *et al.* 1983). Table 4 shows that $\xi^{N}_{grgr} > 0$ for $r < 8$ Mpc; it may well be that a small amplitude of 0.05 is preserved as far as 40 Mpc. Possibly $\xi^{S}_{grgr} > 0$ up to 8 Mpc.

TABLE 4

r, Mpc	ξ^{N}_{grgr}	$\Delta\xi$	r, Mpc	ξ^{S}_{grgr}	$\Delta\xi$	r, Mpc	ξ^{N}_{grgr}	$\Delta\xi$	ξ^{S}_{grgr}	$\Delta\xi$
1	1.39	0.72	2	0.35	0.60	5	0.08	0.05	0.17	0.14
3	0.53	0.22	5	0.01	0.27	15	-0.05	0.03	-0.01	0.06
5	0.18	0.13	8	0.08	0.20	25	0.08	0.03	0.11	0.06
7	0.08	0.10	11	0.43	0.18	35	0.05	0.03	-0.05	0.05
9	-0.06	0.08	14	-0.07	0.13	45	-0.06	0.03	-0.16	0.06
11	-0.12	0.07				55	0.02	0.03		
						65	-0.03	0.03		

(v) The Vennik Sample

There are 126 groups and subgroups in this catalog (Vennik 1984) with a depth of 3500 km/s. We excluded 4 objects - 3 for having $|b| < 20°$ and the first object V1A (the Milky Way group). The amplitude of ξ^{S}_{grgr} is not significantly different from zero and $\xi^{N} > 0$ for $r < 6 - 7$ Mpc (Table 5).

TABLE 5

r, Mpc	ξ^{N}_{grgr}	$\Delta\xi$	r, Mpc	ξ^{N}_{grgr}	$\Delta\xi$
1	1.77	0.77	6	0.22	0.08
2	1.77	0.35	7	0.06	0.07
3	0.58	0.17	8	-0.02	0.06
4	0.38	0.12	9	-0.06	0.06
5	0.06	0.08	10	-0.25	0.05

(vi) The Ramella-Geller-Huchra Sample

The statistical sample of 95 groups (Ramella *et al.* 1989), found with the general searching algorithm of HG in the deeper CfA survey - the slice is used. It is evident (Table 6) that $\xi > 0$ up to $r = 20$ Mpc.

TABLE 6

r, Mpc	ξ_{grgr}	$\Delta\xi$
2.51	2.26	0.50
7.51	1.17	0.19
12.51	0.12	0.10
17.51	0.17	0.08
22.51	0.10	0.08
27.51	-0.19	0.06
32.51	-0.22	0.05

(vii) The Maia-da Costa-Latham Sample

This catalog (Maia *et al.* 1989) contains 92 groups of galaxies identified in the Southern galactic gap (da Costa *et al.* 1988). The group finding algorithm of HG was used. The amplitude of the correlation function (Table 7) is positive up to 13 Mpc.

(viii) The New CfA Group Sample

There are 161 groups of galaxies found in the CfA survey in the NGH for V> 600 km/s using an algorithm developed by Kuneva and Kalinkov (1990). The amplitude of the correlation function is positive up to 6 Mpc. The statistical properties of this catalog do not differ from the previous seven catalogs.

TABLE 7

r, Mpc	ξ_{grgr}	$\Delta\xi$
1	2.49	0.90
3	1.32	0.32
5	0.39	0.17
7	0.02	0.12
9	0.17	0.11
11	0.09	0.10
13	0.02	0.10
15	-0.10	0.09
17	-0.25	0.08

TABLE 8

r, Mpc	ξ_{grgr}	$\Delta\xi$
1-2	0.38	0.17
3	0.34	0.12
4	0.41	0.10
5	0.14	0.08
6	0.07	0.07
7	-0.05	0.06
8	-0.07	0.05
9	-0.16	0.05

4. DISCUSSION

From general considerations it might be expected that ξ_{grgr} will have amplitudes higher than ξ_{pp}. Since the amplitudes of the cluster-cluster correlation function are higher than those of the galaxy-galaxy correlation function (Bahcall 1988), it could be concluded that

$$\xi_{gg} < \xi_{pp} < \xi_{grgr} < \xi_{cc}.$$

Hamilton and Gott (1988) pointed out that existing measurements of three-point and four-point correlation amplitudes imply that pairs and triples are more clustered than galaxies.

According to Groth and Peebles (1977) and Davis and Peebles (1983)

$$\xi_{grgr}(r) = 20r^{-1.8} = (r/5)^{-1.8}, r < 20\ h^{-1}\ \mathrm{Mpc}.$$

and neither amplitude of ξ_{pp} and ξ_{grgr} in Tables 1-8 exceeds ξ_{gg}.

It seems that an explanation for this unexpected result might be found in two directions: (a) The estimates of ξ_{pp} and ξ_{grgr} are biased and other methods of measurements have to be applied. (b) The existing samples of pairs and groups of galaxies are not fair samples (Peebles 1973).

Acknowledgement is due to D. Stefanova and H. Macrelov for their help. This work is supported in part by the Bulgarian Committee for Science (Contract 943).

REFERENCES

Anderson, N., Kunth, D., and Sargent, W. L. W. 1988, A.J., 95, 644.

Bahcall, N. A. 1988, Ann.Rev.Astr.Ap., 26, 631.

Blanchard, A., and Alimi, J.-M. 1988, Astr.Ap., 203, L1.

Borner, G., and Mo, H. J. 1990, Astr. Ap., 227, 324.

Borner, G., Mo, H., and Zhou, Y. 1989, Astr.Ap., 221, 191.

da Costa, L. N., Pellegrini, P. S., Sargent, W. L., Tonry, J., Davis, M., Meiksin, A., Latham, D. W., Menzies, J. W., and Coulson, I. A. 1988, Ap.J., 327, 544.

Davis, M., Meiksin, A., Strauss, M. A., da Costa, L. N., and Yahil, A. 1988, Ap.J.Letters, 333, L9.

Davis, M., and Peebles, P. J. E. 1983, Ap.J., 267, 465.

Geller, M. J., and Huchra, J. P. 1983, Ap.J.Suppl., 52, 61.

Groth, E., and Peebles, P. J. E. 1977, Ap.J., 217, 385.

Hamilton, A. J. S., and Gott, J. R. 1988, Ap.J., 331, 641.

Hickson, P. 1982, Ap.J., 255, 382.

Hickson, P., Kindl, E., and Auman, J. R. 1989, Ap.J.Suppl., 70, 687.

Hickson, P., Kindl, E., and Huchra, J. P. 1988, Ap.J., 331, 64.

Huchra, J., Davis, M., Latham, D., and Tonry, J. 1983, Ap.J.Suppl., 52, 89.

Huchra, J.P., and Geller, M. J. 1982, Ap.J., 257, 423.

Kalinkov, M., and Kuneva, I. 1985, Astr.Nach., 306, 283.

——. 1986, M.N.R.A.S., 218, 49p.

Karachentsev, I. D. 1972, Comm. Spets. Ap. Obs. USSR, 7, 3.

——. 1987, *Dvoinye Galaktiki* (Moscow: Nauka).

Kuneva, I. and Kalinkov, M. 1990, this volume.

de Lapparent, V., Geller, M. J., and Huchra, J. P. 1988, Ap.J., 332, 44.

Maia, M. A. G., da Costa, L. N., and Latham, D. W. 1989,Ap.J.Suppl., 69, 809.

Osmer, P. S. 1981, Ap.J., 247, 762.

Peebles, P. J. E. 1973, Ap.J., 185, 413.

Ramella, M., Geller, M.J., and Huchra, J.P. 1989, Ap.J., 344, 57.

Vennik, J. 1984, Tartu Astr. Obs. Teated, No.73, p.3.

DISCUSSION

Hickson: Very few of the groups that I found occur in rich clusters of galaxies, presumably because of the isolation criterion that I used. The correlation function of these groups may also be strongly affected by the selection criteria.

Kalinkov: You are quite right. I agree with you.

III. OBSERVATIONS

OF

RELATED OBJECTS

Hidden Interaction in SB0 galaxies

G.Galletta[1], D.Bettoni[2], G.Fasano[2], T.Oosterloo[3]
1: Dipartimento di Astronomia, Università di Padova, Italy
2: Osservatorio Astronomico di Padova, Italy
3: European Southern Observatory, Germany F.R.

Botany of Interactions

Galaxies, like plants, show a large variety of grafts: an individual of some type connects physically with a neighborhood of same or different type. The effects of these interactions between galaxies have a broad range of morphologies depending, among other quantities, on the distance of the closest approach between systems and the relative size of the two galaxies. A sketch of the possible situations is shown in Table 1. This 'botanical' classification is just indicative, because the effects of interactions can be notable also at relatively large separations, when additional conditions are met: as for example low density of the interacting systems or the presence of intra-cluster gas. In spite of the large variety of encounters and effects, in the literature the same terms are often used to refer to different types of interactions.

Table 1: Indicative classification of different types of interaction between galaxies as a function of their closeness and of their relative mass. The phenomenon implied is indicated in the table, with the possible results of the interaction suggested in parenthesis. Three cases of mass ratio are considered: *i*) galaxies with same mass, *ii*) comparable masses between the *primary* galaxy and its *satellite*, *iii*) mass of the companion negligible (*point-mass*).

$\frac{M_{companion}}{M_{primary}}$	Closeness		
	In contact	**Close to very close**	**Bound**
$\simeq 1$	merging (*E galaxy*)	tides (*bridges, tails distortions*)	clustering (*double or multiple systems*)
<0.1	accretion (*gas rings, kinematical decoupling, counterrotation*)	perturbation (*warps, bridges, tails, shells*)	capture (*satellite*)
$\ll 1$	evaporation (*increase of bulge or halo size*)	capture (*halo star cluster*)	capture (*intergalactic star cluster*)

As can be seen from Table 1, only few of the situations show evident signs of interaction. They appear to be most relevant when the size of the two galaxies is comparable. Bridges and tails, like the well known case of NGC 4038/39, *the Antennae*, are only observed for a very low percentage of all galaxies (~0.38%, Arp & Madore 1977). In most cases of gravitational bond between two galaxies, the effects of interactions are not relevant or evident. For instance, the detection of stellar shells (Malin & Carter 1983), which have been attributed to the accretion of gas stripped from another galaxy or to the capture and disruption of a small stellar system (Quinn 1984), requires particular observing and reduction techniques. Besides these difficulties of detection, time plays an important role in erasing, within a massive galaxy, the effects of interactions with smaller objects. This can happen on a timescale shorter than the Hubble time, so the number of systems now showing signs of interaction suggests a lower limits to the *true* frequency of interactions in the life-time of a stellar system.

Hidden interactions

In this paper we want to discuss one type of interaction whose effects are not manifest, but hidden within the main body of the galaxy. In Table 1, the last two items of the first column describe this type of interaction. Differently from merging, which implies the complete absorption of the components of the galaxies into one another, accretion of a small quantity of matter (gas or a whole stellar system) does not alter the structure of the original galaxy. The evidence for this kind of interaction should be easier to detect than a complete merging, since the residuals of the acquired galaxy do not lose their identity within the host galaxy for a long time. In addition, we must expect that a destructive merging, like that of two equal-sized galaxies, should yield configurations trending toward dynamical and structural entropy, like elliptical galaxies. On the contrary, the above mentioned accretion process could be sought within both ellipticals and S0 galaxies, increasing the number of candidates. We shall discuss later what morphology the phenomenon could assume when accretion involves spiral galaxies.

Keeping in mind these differences, a more or less recent accretion of gas (and possibly stars) could produce irregularities in the galaxy kinematics or in the gas distribution. For example, the existence of elliptical galaxies with dust and gas rings along the apparent minor axis (Bertola & Galletta 1978) could be a clue of accretion, especially if this gas exhibit a kinematics independent from that of the stars (Sharpless *et al.* 1983, Caldwell 1984, Bertola *et al.* 1985, Wilkinson *et al.* 1986). A similar kinematical decoupling has been also observed in some S0's, where a gas ring extending far out the stellar body rotates perpendicularly to the stellar disk (polar ring galaxies, see Schweizer *et al.* 1983). Such kinematical decoupling is not a prerogative of dust-lane ellipticals or polar-ring S0's, but is also present in normal elliptical galaxies with emission lines (see Bettoni 1984 for a collection of cases). In the context, the observations of some galaxies where gas and stars rotate in opposite directions (Bettoni 1984, Caldwell *et al.* 1986, Galletta 1987, Rubin 1988, Bertola *et al.* 1988, Bertola & Bettoni 1988, Schweizer *et al.* 1989) is another tessera completing the mosaic of galaxy interactions.

This kinematical feature, *gas counterrotation*, is particularly interesting when observed in S0 galaxies. The complex structure of such stellar systems supports, as stated before, the hypothesis of acquisition of a small quantity of gas that is unable to perturb the global structure of the host galaxy. The two SB0s studied by us, NGC 4546 and NGC 2217, do indeed not reveal any particular anomaly in the distribution or in the kinematics *of the stars.* Their main peculiarity is only apparent in long-slit spectra, that show emission and absorption lines inclined in opposite directions.

In the cases of NGC 4546 (Galletta 1987, Bettoni *et al.* 1990b) and of another S0 galaxy, NGC 1216 (Rubin 1988), both galaxies are seen relatively edge-on and simple geometrical considerations imply that the opposite inclination of the emission- and absorption lines in the spectra arise from two almost coplanar disks of gas and stars rotating in opposite sense. An Hα knot, possibly the residual of the accreted object, has been detected near the bright Hα nucleus of NGC 4546 (Bettoni *et al.* 1990b). When the gas entered the galaxy, it settled in the plane of the galaxy following the global potential. An estimate of the time needed by the gas to completely settle in the equatorial plane is of order of hundred million years (Galletta 1987), while possible interactions with stars by dynamical friction would take $\sim 10^{10}$ years to become effective. This would not be the case if some appreciable amount of gas pre-existed in the galaxy (as in the case of spiral galaxies). Since the velocity differences between gas and stars are, for NGC 4546, $\sim$400 km s^{-1}, it is possible to imagine that a collision between existing clouds and newly entering gas would have enough energy to create high-energy radiation. The shock-heated gas could diffuse within and around the galaxy, eventually *evaporating* in a low density halo. On the contrary, also the H I observed in NGC 4546 has the same sense of rotation as the ionized gas, and none of the galaxies with counterrotating gas are known to be luminous at X-ray wavelengths.

In other words, we think that it is unlikely that a relatively stationary disk of counterrotating gas can occur in spiral galaxies, and that galaxies showing gas counterrotation, Ellipticals and S0s, were gas free at the epoch of last accretion. To support this statement, we note that neither counterrotating gas nor polar rings have been observed in (gas-rich) Spirals. The unstable structures resulting from such accretions should probably be searched among the many irregular objects existing in the Universe or in something similar to the H I clouds with anomalous velocities detected in M101 or in other spirals (van der Hulst & Sancisi 1988).

To complicate the picture, not all cases where in long-slit spectra the lines of gas and

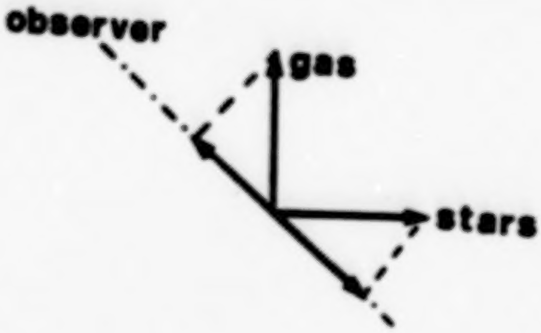

Figure 1: Two motions reciprocally perpendicular could be observed as opposite, generating an *apparent* counterrotation

stars exhibit an opposite tilts are examples of gas counterrotation. In fact, the opposite tilt of emission and absorption lines only imply that along the line-of-sight the rotational velocities are opposite, not necessarily that the gas and star disks have antiparallel spins. An example of this is the barred S0 galaxy NGC 2217 (Bettoni *et al.* 1990a): Contrary to the previous edge-on cases, this galaxy is seen almost face-on, but the stellar rotation is still clearly observable. Near the nucleus of the galaxy, a gas disk, perpendicular to the (stellar) equatorial plane, is projected on the sky almost edge-on. So we observe two disks rotating almost perpendicularly, as in polar-ring galaxies. It is possible to show that the motions of two such disks, rotating perpendicularly in space, have opposite velocity components along the line-of-sight when seen from particular viewing angles (see Fig.1). In NGC 2217 we are observing a case of perpendicular spins and not a true case of counterrotation. In fact, in the outer regions, where, driven by the bar, the inclination of the gas-disk changes and it coincides with the galactic plane, gas and stars show the same direction of motion. This pretty peculiarity is important when one is dealing with elliptical galaxies, where the orientation with respect to the line-of-sight is unknown. The existence of a projection effect similar to that observed in NGC 2217, as also discussed by Bertola & Bettoni (1988), would reduce the *true* frequency of occurrence of the counterrotating gas in elliptical galaxies. But no statistics could be done with the small number of cases known until now.

As a final consideration, we note that over 15 SB0 studied by us in a long-term project on the dynamics of this type of galaxies, 4 of them show emission lines. Among these four cases, for three there is clear evidence that this gas has been accreted: NGC 4546, with counterrotation, NGC 2217, with perpendicular and unstable disk, and NGC 4684, with filaments and irregular gas kinematics. This high occurrence of peculiarities poses the question, appearing sometimes in the literature, if all the gas in early-type galaxies has been accreted.

REFERENCES

Arp,H., & Madore, B.F., (1977). *Q. Jl. R. Astr. Soc.* **18**, 234.
Bertola,F., and Bettoni,D. (1988). Astrophys.J., **329**, 102.

Bertola,F., Buson, L., and Zeilinger, W.W. (1988). Nature, **335**, 705.

Bettoni,D. (1984). The Messenger, **37**, 17.

Bettoni,D., Fasano,G., Galletta,G. (1990). preprint.

Bettoni,D., Galletta,G., Oosterloo,T. (1990). preprint.

Caldwell, N., Kirshner, R.P., and Richstone, D. (1986). Astrophys.J., **305**, 136.

Galletta,G. (1987). Astrophys. J., **318**, 531.

Malin,D.F., & Carter,D. (1983). Astrophys.J., **274**, 534.

Quinn,P.J. (1984). Astrophys.J., **279**, 596.

Rubin,V.C. (1988). In *Large scale motions in the Universe: a Vatican study week* V.C. Rubin and C.V.Cohen (Princeton Univ., Princeton) p.541.

Schweizer,F., Whitmore, B.C., & Rubin, V.C. (1983). Astron.J., **88**, 909.

Schweizer, F., van Gorkon, J., and Seitzer, P. 1989, Astrophys. J., **338**, 770.

van der Hulst, J.M. & Sancisi, R. 1988, Astron. J., **95**, 1354.

DISCUSSION

R.Kennicut: Do you know anything about the ionization properties of the counterrotating gas?

G.Galletta: Our spectra were taken at intermediate resolution, to investigate in detail the velocity field, and the emission lines present are only [O III] and Hβ. Our requests to ESO for observing time in order to study the chemical composition of the counterrotating gas were never accepted until now. If done, they could reveal if this gas really comes from the accretion of a late-type system or if we are dealing with primordial material falling on the galaxy from the environment.

R.Kennicut: Do your galaxies show any other evidence of recent mergers, such as tidal tails, etc.?

G.Galletta: No tidal tails are visible from our images. Features more difficult to detect, like shells, need a technique that we have not applied to our frames. A warped and twisted gas layer is present in NGC 2217.

A.Zasov: What do you think about the fate of the counterrotating gas in the galaxies considered?

G.Galletta: Following the current theories, the fate of the gas accreted by the SB0 galaxy strongly depends on the impact angle. If this is close to the plane of the disk, the gas forms before a warped plane, than settles on the same plane of the stars in a short time. If the impact direction is very inclined with respect to the disk plane, the external part slowly settles on it, while the inner part, perpendicular to the bar, could precess differentially and finish later to collapse toward the center. Only almost perpendicular orbits could form a polar ring in equilibrium configuration.

A.Zasov: It is possible to obtain some restriction on the density of "native" gas in galaxies which should actively interact with the counterrotating gas?

G.Galletta: Since the velocity differences between gas and stars are very high, but no X-ray emission caused by collisions between native and accreted gas has been detected, I can estimate the native gas density to be very low. But I cannot quantify this estimate.

A.Fridman: Did you try to estimate the damping-time of gas component because of interaction with stellar component in NGC 4546?

G.Galletta: In the literature, there are some estimates of the time the gas settles in the plane of the disk. In a case like NGC 4546, it is expected this phenomenon takes place in a time of few 10^9 years.

A.Fridmann: What do you think about the possibility of a gas disk with two counterrotating parts?

G.Galletta: Contrary to the stars, the gas strongly interacts with pre-existing gas. I am expecting two counterrotating disks of gas cannot co-exist in the same galaxy. Two masses of gas could eventually survive as two concentric rings, if dissipation or differential precession do not destroy this peculiar configuration. But we have no indications that a galaxy with such configuration exists.

Khachikian: What is the distance between the two nuclei of NGC 4546?

G.Galletta: The projected separation between the two nuclei is ~350 kpc.

The Environments of Markarian Galaxies

John W. MacKenty, Brian McLean
Space Telescope Science Institute, Baltimore
and
Caroline Simpson
U. Florida, Gainesville

The extensively studied Markarian sample of 1500 ultraviolet excess galaxies contains many Seyfert, starburst, and peculiar galaxies. Using the 20 minute V plates obtained for the construction of the Hubble Space Telescope Guide Star Catalog, we have investigated the morphologies of the Markarian galaxies and the environments in which they are located. This paper reports on the relationship between the types of nuclear activity and the morphologies and environments of the Markarian galaxies.

Previous studies of the environments of Seyfert galaxies establish a connection between the nature of the activity in the nuclear regions of the galaxy and its external environment. Petrosian (1982) finds that type II Seyfert galaxies are located in regions of higher density than type I Seyfert galaxies. Dahari (1985) finds an excess of close companions to Seyfert galaxies compared to field galaxies. MacKenty (1989) confirms these results. However, MacKenty (1989) finds that non-Seyfert Markarian galaxies have the same frequency of companion galaxies as Seyfert Markarian galaxies. He uses their IRAS colors to argue that the companion galaxies tend to enhance star formation rather than directly influence the nuclear activity. The influence of companion galaxies has also been demonstrated on emission line galaxies (Kennicutt and Keel 1984; Keel et al. 1985; Cutri and McAlary 1985) and on IRAS infrared luminous galaxies (Lonsdale, Persson, and Matthews 1984).

Sample Selection and Data

The sample is drawn from Markarian Lists I - XV (Markarian 1967, Markarian, Lipovetskii, and Stepanian 1979) and is based on the data in Mazzarella and Balzano (1986). Joe Mazzarella kindly provided a digital copy of their tables. The sample contains 970 Markarian galaxies (including 116 Seyferts) after the exclustion of:

: 280 galaxies without redshifts
: galaxies with redshifts < 2000 or > 15000 km/s
: 12 special galaxies (i.e. BL Lac, NELG)
: about 20 galaxies with confused positions or identifications

Regions 7 by 7 arcminutes in size (with a pixel size of 1.7 arcsec) were extracted from the 20 min V band Schmidt plates obtained for the Hubble Space Telescope Guide Star Catalog (see Lasker et al. 1990 for a description of the GSC). A COSMOS type algorithm was used to locate and classify all objects on the extracted images. Objects were classified as stellar, non-stellar, or galactic. All but the stellar objects will be taken to be galaxies in this analysis. All galaxies detected within 50 kpc projected radius of each Markarian galaxy were counted. These counts were analyzed first using all of the galaxies and then were re-analyzed excluding those galaxies with whose total intensity (on the Schmidt plates) differed from the Markarian galaxy's by more than a factor of 5 and by more than a factor of 2.

Morphological Classification

The central 80 by 80 pixel regions of the extracted images were mosaiced into 100 object composites and examined visually on an image display device. Each Markarian galaxy was assigned a simple morphological classification based on the following scheme:

: Stellar or Nearly Stellar
: Extended but No Evident Structure
: Spiral Structure Evident (but no Bar)
: Spiral with Bar or Ring
: Peculiar or Significant Asymmetry
: Multiply Nuclei or Probable Interacting Pair
: Highly Peculiar (Jets or Strong Interaction)
(In the present analysis the last three classes are combined.)

Results

From the table below, it is evident that Seyfert galaxies do NOT have a higher frequency of close (within 50 kpc) neighbors than Star Burst galaxies or the Unclassified Markarian galaxies. There may be a slight trend for Seyfert galaxies to have fewer neighbors than other Markarian galaxies but this is not conclusive. This result is independent of our efforts to reduce contamination by foreground and background galaxies (although excluding potential neighbors based on the ratio of their total intensity to the Markarian galaxy's removes the bias to find an excess of neighbors in the vicinity of lower redshift galaxies).

Local Density versus Type of Nuclear Activity

	Seyfert	Star Burst	Unclassified
(No Limit on Neighbors)			
Neighbors	64.7% (75)	81.3% (78)	75.2% (568)
Average Number	2.26	4.62	3.16
(Neighbors within a Factor of 5 in Total Intensity)			
Neighbors	15.5% (18)	18.7% (18)	28.7% (217)
Average Number	0.19	0.28	0.43
(Neighbors within a Factor of 2 in Total Intensity)			
Neighbors	6.0% (7)	6.2% (6)	13.8% (104)
Average Number	0.06	0.09	0.17
Number of Galaxies	116	96	755

Furthermore, as seen in the following table, there is no strong correlation between the type of nuclear activity and the morphology of the host galaxy. That Bars and Rings seem to be more common in both the Seyfert and Star Burst populations compared to the Unclassified population may be the result of greater study of these relatively closer galaxies.

Morphology versus Type of Nuclear Activity

Morphology	Seyfert	Star Burst	Unclassified
Stellar	4.3% (5)	6.2% (6)	10.8% (82)
Extended	38.8% (45)	27.8% (27)	46.5% (352)
Spiral	21.6% (25)	17.5% (17)	15.3% (116)
Bar or Ring	14.7% (17)	13.4% (13)	4.0% (30)
Peculiar or Interacting	20.7% (24)	35.1% (34)	23.4% (177)

Conclusions

From this study, we conclude that the ***type of nuclear activity*** present in the galaxies of the Markarian sample is ***not dependent on either the morphology or the local environment*** of the galaxy. This is not to imply that nuclear activity per se is not influenced by the environment in which the nucleus is located. Rather the ***type*** of nuclear activity (at least in the Markarian population) does not appear to be determined by the environment.

References

Cutri, R.M. and McAlary, C.W. 1985, *Astrophys.J.*,**296**,90.

Dahari, O. 1985, *Astrophys.J. Suppl.*, **57**,643.

Keel et al. 1985, *Astron.J.*,**90**,708.

Kennicutt, R.C. Jr. and Keel, W.C. 1984, *Astrophys.J.(Letters)*, **279**,L5.

Lonsdale, C.J., Persson, S.E. , and Matthews, K. 1984, *Astrophys.J.*, **287**,95.

MacKenty, J.W. 1989, *Astrophys.J.*, **343**,125.

Markarian, B.E. 1967, *Astrofizika*,**3**, 55.

Markarian, B.E., Lipovetskii, V.A., and Stepanian, D.A. 1979, *Astrofizika*,**15**, 549.

Mazzarella and Balzano 1986 *Astrophys.J. Suppl.*, **62**,751.

Petrosian, A.R. 1982, *Astrofizika*, **18**, 548.

Lasker, B.M., Sturch, C.R., McLean, B.J., Russell, J.L., Jenkner, H. Shara, M.M. 1990, STScI Preprint No. 363.

THE COMPLEX NATURE OF THE SEYFERT GALAXY NGC 7592

Piero Rafanelli
Department of Astronomy, University of Padova, Italy
Paolo Marziani
International School for Advanced Studies, Trieste, Italy

1. *Morphology*

NGC 7592 ≡ VV 731 ≡ MCG–01–59–017 is a system of close interacting galaxies. Two main galactic bodies are present in the CCD R-band image taken at the 1.8m, F/9 telescope of the Asiago Observatory and shown in Figure 1:

- a north-western (NW) component (≡VV 731B), whose starlike nucleus (A) shows a Seyfert-type spectrum (Archipova *et al.*, 1981). A is surrounded by a nearly spheroidal envelope, with an extension in the west at *P.A.* = 290° detected up to a distance from A of ≈ 9 *arcsec*, which corresponds to $\approx 2.5h^{-1}kpc$ of projected linear distance (1 *arcsec* $\approx .35\ h^{-1}kpc$ at the redshift $z = 0.0244$; $H_0 = 100\ h\ km\ s^{-1}Mpc^{-1}$). This extension seems to bend in the northern direction and to join a bright wing, detected up to ≈ 22 *arcsec* from A, which turns to east and resembles a spiral arm or a tidal tail.
- The envelope around A is connected (over ~ 20 *arcsec* $\approx 7h^{-1}kpc$) to a second galactic body (SE) located in the south-east of it. Its nucleus (B), identified by Markarian and Lipovetskii (1976) as the nucleus of Mkn 928, is located at $d_{AB} \sim 11$ *arcsec*($\sim 4h^{-1}kpc$) from A at *P.A.* = 100°. The morphology of this component is highly peculiar. In the central region, B is linked to two fainter knots which extend up to $d'' \sim 4$ *arcsec* at *P.A.* = 90°. This structure gives to the region surrounding B an elongated and distorted shape. Moreover, a bar-like structure is detected on either sides of B. The north-eastern side of the bar (*P.A.* = 40°) joins a slightly distorted loop of condensations, which can be traced from *P.A.* = 335° (at a distance from B ≈ 6 *arcsec* $\approx 2.1\ h^{-1}kpc$) to *P.A.* = 100° and from *P.A.* = 200° to *P.A.* = 240°, but not in corrispondence of the contact region between the two galaxies. This structure seems to be drained and distorted in the direction of a third condensation C at $d_{BC} \approx 11.7$ *arcsec* ($\approx 4.1\ h^{-1}kpc$) from B at *P.A.* = 212°. A faint plume bent in a direction opposite to that expected for spiral arms of the SE galaxy appears to extend from the west side of C.

2. *Spectroscopy*

Long slit spectra of NGC 7592 were taken on Sep. 26–30, 1989 at the 1.52 cm ESO telescope, equipped with a Boller and Chivens spectrograph and an RCA High Resolution CCD camera. The covered spectral ranges are 3700–7300 Å with resolution ≈ 3.7 Å, and 4500–5500 Å and 6300–7300 Å with resolution ≈ 1.8 Å. NGC 7592 was observed at two position angles: *P.A.* = 212° (along B and C), and *P.A.* = 100° (along B and A), with a slit width of ≈ 2 *arcsec* $\approx 700\ h^{-1}pc$.

2.1 *Physical conditions*

The Hα, Hβ, [OIII]$\lambda\lambda$4959,5007, [NII]$\lambda\lambda$6548,6583, [SII]$\lambda\lambda$6717,6731, and [OII] λ3727 emission lines have been found to be spatially extended. The strongest ones, Hα and [OII]λ3727, are detected over ≈ 30 *arcsec* $\approx 10.5\ h^{-1}kpc$ at *P.A.* = 100° and ≈ 28 *arcsec* $\approx 9.8\ h^{-1}kpc$. The size of the emitting regions is comparable with the size of the galaxies belonging to the system NGC 7592 measured on its broad band image. A more refined analysis of the cross dispersion profile of Hα permits to isolate 6 different emitting regions

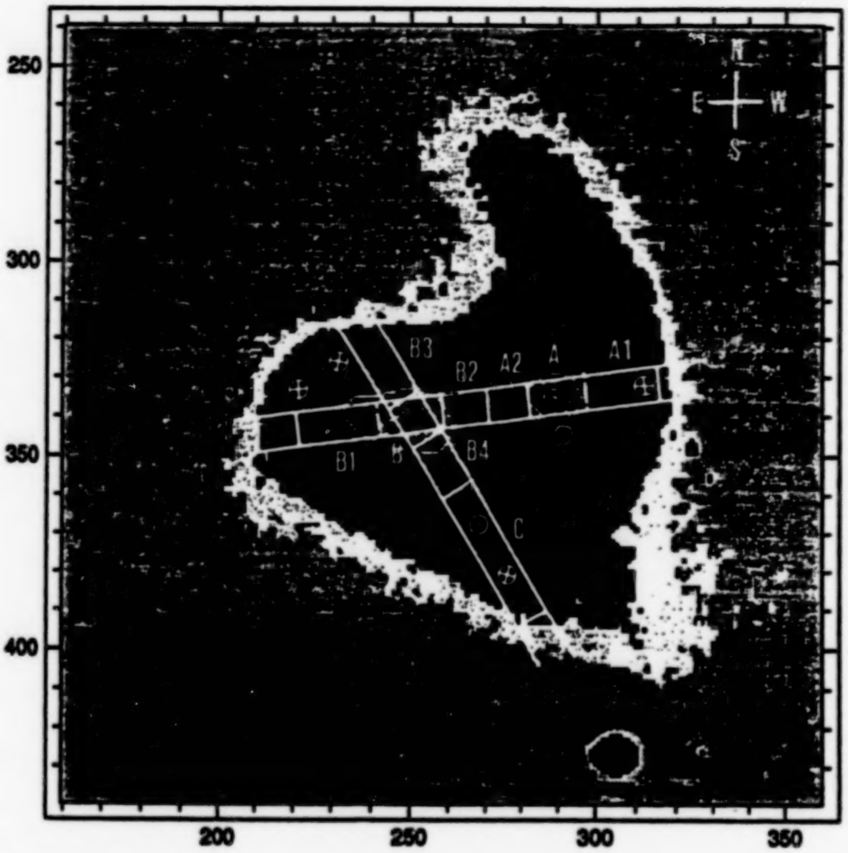

FIG. 1

(A1,A,A2,B2,B,B1) along $P.A. = 100^\circ$ and 4 regions (C,B4,B,B3) along $P.A. = 212^\circ$. The slit positions and the regions analyzed are marked in Figure 1.

The diagnostic diagrams proposed by Veilleux and Osterbrock (1987) were used to analyze whether the ionization of the line emitting gas is produced by a thermal (HII regions) or by a non-thermal continuum (AGN), Figures 2a,2b,2c. The Seyfert nucleus A of the NW component and A2, a region very close to A on its eastern side, are photoionized by a non-thermal source. All the other emitting regions are in the area typical of HII regions. This finding has been also tested using the diagnostic diagram based on the line ratios [OII]λ3727/[OIII]λ5007 and [OIII]λ5007/Hβ (Baldwin *et al.*, 1981), which further allows to distinguish between gas photoionized by thermal sources and shock-heated gas. We found that A and A2 are the only regions not located in the HII area.

The spectrum of the Seyfert nucleus A shows a faint broad component of Hα, already suspected by Archipova *et al.* (1981), whose $FWZI$ measured in the high resolution spectra is 3200 km/s (Figure 3a). An upper limit to its flux is $5 \times 10^{-14} erg\ cm^{-2} s^{-1}$, being $H\alpha_{BC}/H\alpha_{NC} \approx 0.7$. Since no broad component is present in Hβ, A can be classified as a Seyfert 1.9 nucleus. The FWZI of the [OIII]$\lambda\lambda$4959,5007 lines is $\sim 1500 km\ s^{-1}$, namely about twice the FWZI of Hβ, $\sim 800\ km\ s^{-1}$. This is due to the presence of a semi-broad component of the [OIII]$\lambda\lambda$4959,5007 lines displaced toward the red (Figure 3b). The semi-broad component indicates that there is a region whose density is larger than the density of the Narrow Line Region of A, $n_{e,A} \geq 2 \times 10^2 cm^{-3}$ (estimated employing the [SII]λ6731/λ6716 ratio, after correcting for the B-band absorption) and smaller than the density typical of the Broad Line Region $n_e > 10^9 cm^{-3}$. The active nucleus ionizes the interstellar gas between A and B (see also the results on the kinematics), and provides the main ionization source up to a distance of 5.1 $arcsec \approx 1.8\ h^{-1} kpc$ (region A2). It is noteworthy that outside of A and

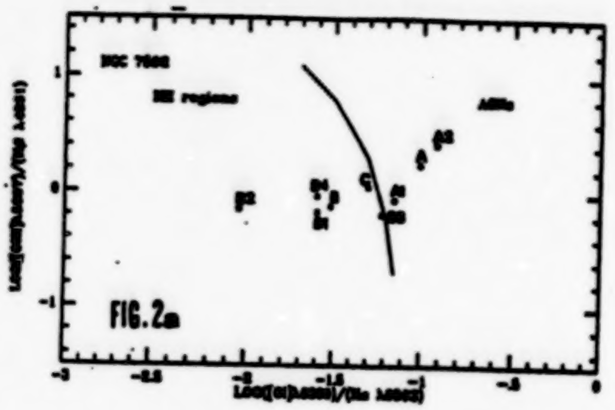

FIG.2a

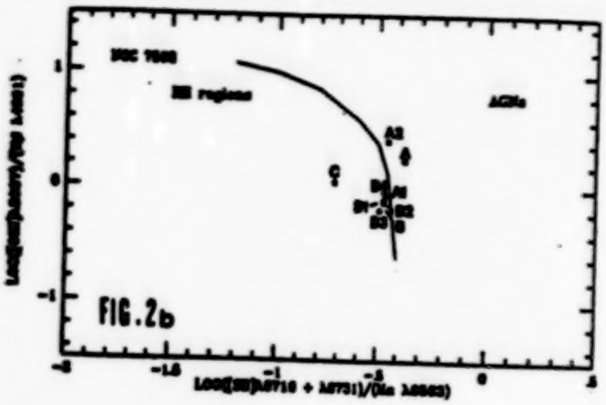

FIG.2b

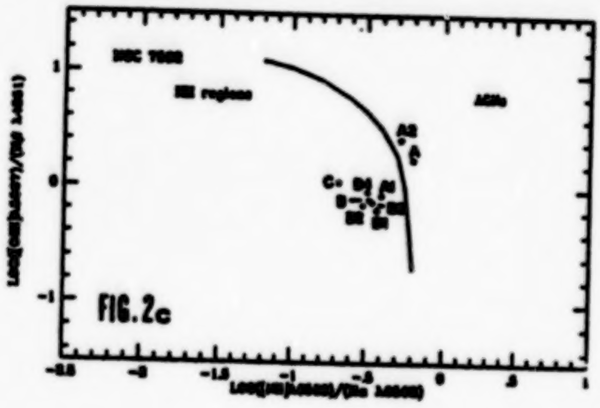

FIG.2c

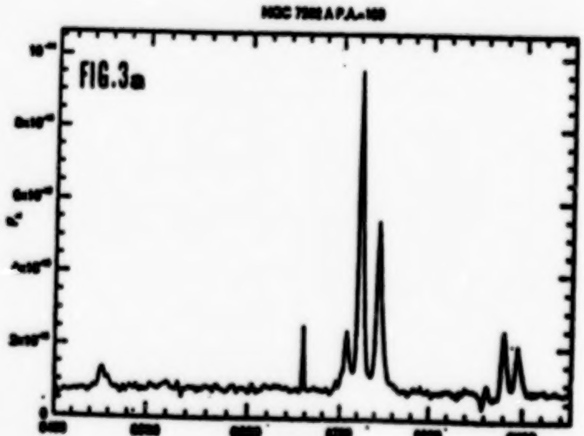

FIG.3a

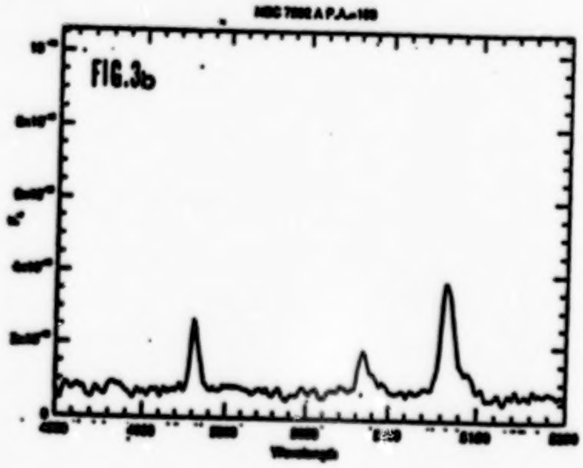

FIG.3b

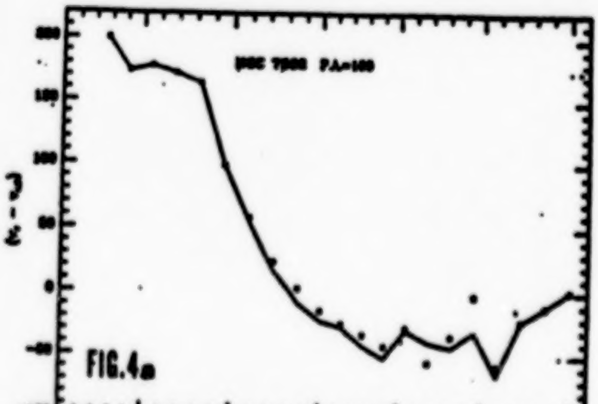

FIG.4a

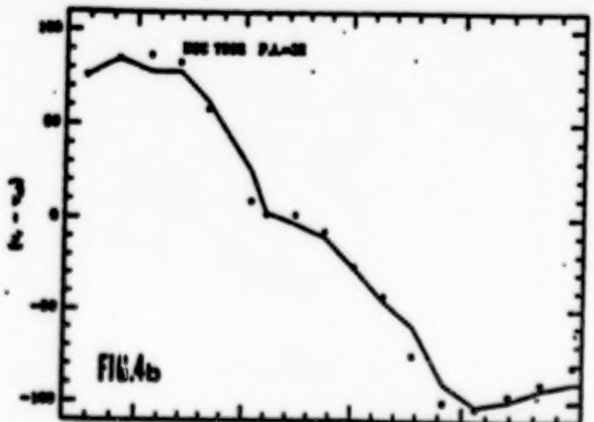

FIG.4b

A2 the line emission is due to photoionization by a thermal continuum provided by O and B stars, and that the Hα luminosity of A, $L(H\alpha)_A \approx 4.8 \times 10^{40}\ h^{-1} erg\ s^{-1}$ is less than that of B and C, being $L(H\alpha)_B \approx 6.1 \times 10^{40}\ h^{-1} erg\ s^{-1}$ and $L(H\alpha)_C \approx 5.4 \times 10^{40}\ h^{-1} erg\ s^{-1}$. A comparison with the Hα luminosity function for starburst galactic nuclei published by Kennicutt *et al.* (1989) shows that the Hα luminosities of B and C are typical of this class of objects and that they are too high for disk HII regions. The Hα luminosities of the regions A1, B1, B2, B3, B4 range from $\approx 2 \times 10^{40} erg\ s^{-1}$ to $\approx 3 \times 10^{40} erg\ s^{-1}$ and are located on the high luminosity tail of the luminosity function of disk HII regions of Kennicutt *et al.*(1989).

2.2 *Kinematics*

The velocity curves at $P.A. = 100°$ and at $P.A. = 212°$ are shown in Figure 4a and 4b respectively. The heliocentric radial velocity ($V_{r,B} = 7320 \pm 10\ km\ s^{-1}$) and the position of B have been taken as zero points of the coordinates. The velocity curve at $P.A. = 212°$ is described by a straight line from ≈ -7 *arcsec* to $\approx +3$ *arcsec*. This region corresponds to the bar-like structure revealed by the R image. The velocity curve considerably flattens beyond both edges of the linear part, and a shallow decrease begins in corrispondence of C ($d'' \sim 12$ *arcsec*), which has an heliocentric radial velocity $V_{r,C} = 7230 \pm 10\ km\ s^{-1}$. At $P.A. = 100°$, on the eastern side of B a steep velocity gradient is present up to ≈ 7 *arcsec*, and it is followed by a flatter part, which can be traced up to ≈ 12 *arcsec*. As a whole, the velocity curve resembles that of a normal spiral galaxy.

On the western side of B, the gas motions are peculiar. A contour plot of the spectral region around Hβ and Hα (Figures 5a and 5b) shows that the gas turns to higher radial velocities (v_r increases from $\approx 7300\ km\ s^{-1}$ to $\approx 7490\ km\ s^{-1}$) up to the position of A. In correspondence of A the profiles of the lines Hα, Hβ and the [NII]λλ6548,6583 are double and show:

1. a strong *blue* component, at heliocentric radial velocity $v_{r,A} = 7280\ km\ s^{-1}$, which is due to the Narrow Line Region of the Seyfert nucleus. $v_{r,A}$ has been assumed as the systemic velocity of the Seyfert nucleus;

2. a fainter *red* component, related to the extended emitting regions connecting B with A. Its peak velocity is $v_r \approx 7445\ km\ s^{-1}$. This component may give a contribution up to ≈ 30 % to the total Hα flux (the value given above may therefore be overestimated by the same fraction).

On the western side of A (A1) the velocity curve turns swiftly toward higher radial velocities.

3. *Discussion*

The problem of the nature of C is addressed at first. C shows an heliocentric radial velocity very similar to that of A and B. Moreover, the arm departing from C is most probably a tidal tail, because its extension is large and its orientation is peculiar. The high Hα luminosity of C is typical of a starburst nucleus. These facts argue in favour of C being the nucleus of a third galactic component (southern component S) physically interacting with the SE component of NGC 7592. The directions of the velocity vectors in various regions of NGC 7592 are marked in Figure 1. It is noteworthy that the SE component rotates clockwise, if the radial velocity difference Δv_r from its nucleus B is due to rotation. Under the same assumption for the $\Delta v_r = v_r - v_{r,A}$, the NW component seems to rotate counterclockwise. Thus, the gas in the regions where the two galactic bodies are in contact moves in the same way, suggesting that a prograde encounter is occurring. It is known (*e.g.* Toomre and Toomre, 1972) that prograde encounters have the most disruptive effects on the interacting galaxies, leading to the formation of tidal tails. The interpretation of the wing of the NW component in terms of a tidal tail thus appears very likely. Figure 1 shows that a similar situation holds for the interaction between SE and S too, where S rotates counterclockwise. The interpretation of the arm departing from C as a tidal tail is supported also in this case. The difference in radial

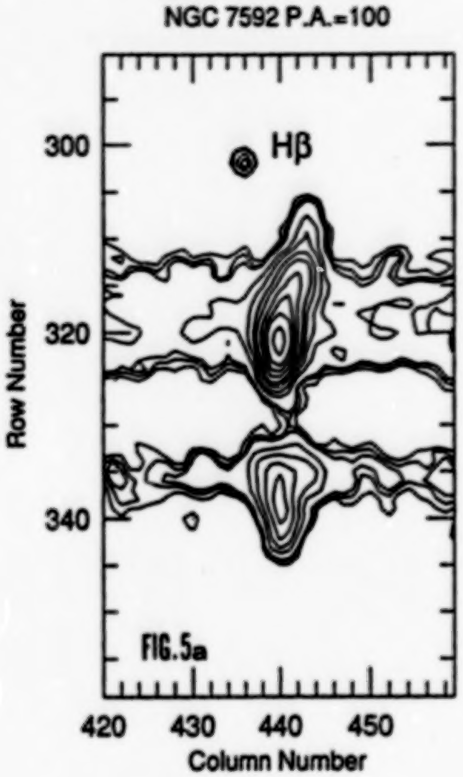

FIG.5a

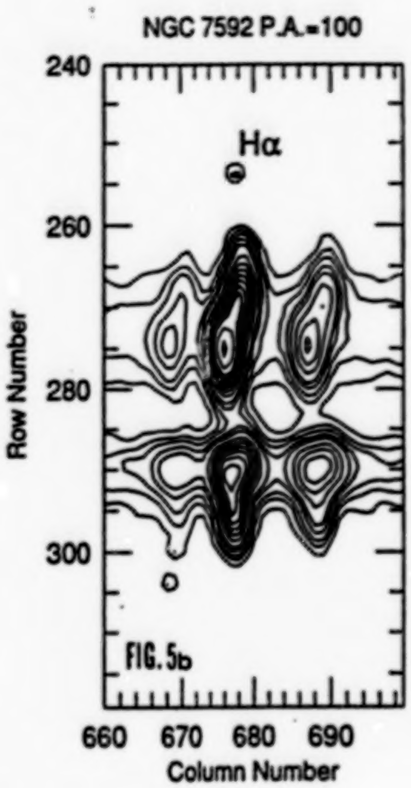

FIG.5b

velocity between A and B ($\Delta v_r \approx -40\ km\ s^{-1}$) and the morphology of NGC 7592 suggest that the NW component is beyond the SE one and is approaching it. The most heavily reddened regions ($E(B-V) \approx 0.7$, derived from the $H\alpha/H\beta$ ratio) are B2 and B4, namely the regions between A and B. Moreover, the small difference in radial velocity between A,B,C suggests that the three galaxies form a bound system, and their kinematics hints that they are most probably in the early stage of a merging phenomenon. In addition, the emitting gas connected to the *red* component of Hα on A appears to regress from the observer. An appealing hypothesis would be to consider the line emitting gas as infalling toward A, perhaps ultimately accreting onto the central core of the active nucleus.

References

Archipova V.P. *et al.*: 1981, *Soviet Astron.* **25**, 277
Baldwin J.A., Phillips M.M., Terlevich R.: 1981, *P.A.S.P.* **93**,5
Kennicutt R.C., Keel W.C., Blaha C.A.: 1989, *Astron. J.* **97**, 1022
Markarian B.E, Lipovetskii V.A., Stefanian D.A. :1977, *Astrofisica* **13** , 225
Veilleux S., Osterbrock D.E.: 1987, *Astroph. J. Suppl.* **63**, 295
Toomre A., Toomre J.: 1972, *Astroph. J.*, **178**, 623

THE HI CONTENT OF NON-ISOLATED GALAXIES

Anatoli V. Zasov
Sternberg Astronomical Institute
Moscow, USSR

It seems obvious that the evolution of star formation rate and hence of gas content in galaxies strongly depends on their environment. It reveals itself in particular in enhanced star formation or even in a strong burst of activity of massive stars often observed in an interacting galaxies. Nevertheless it should be noted that the time scale for the gas to be exhausted in these galaxies is unknown even approximately. To clarify a role of surroundings in the evolution of disk galaxies we should compare the HI content of isolated and non-isolated galaxies otherwise similar by their properties.

It was claimed elsewhere (see e.g., L. Bottinelli et al., 1982), that the isolated galaxies are probably richer in gas than others of the same morphological type (all references here and below are found in [1,2]). The main problem is to choose the right way to compare galaxies each with other. What should be taken as a "normal" amount of interstellar gas for a galaxy of a given type, mass or diameter?

Usually a mass of gas (or HI) is compared with a galaxy's total luminosity or with the square of its diameter. Mean values of hydrogen mass to luminosity (M_H/L) or to D^2 ratios for a given morphological type are used as reference points. But both of these ratios are characterized by large dispersion (especially

M_H/L) and may in turn depend on other parameters of galaxies, such as velocity of rotation or total luminosity, even within the same morphological type. On the other hand, galaxy morphology is subject to effects of interaction with neighbors which may be a source of systematic error in classification.

The idea we propose is to tie hydrogen mass M_H with kinematical parameters of galaxies, which are practically not subjected to evolution, namely with the specific angular momentum V_mD_O. Here V_m is maximal or asymptotic velocity of rotation, measured as half-width of the 21 cm HI line, corrected for inclination; D_O - corrected optical diameter (according to RC 2-catalogue by G.de Vaucouleurs et al., 1976). The existence of an M_H-D_O relation was noted by M. Abramian, D. Sedrakian (1985) and earlier--in a slightly different form--by A. Zasov (1974).

Fig. 1 plots the M_H data of a sample of isolated galaxies versus V_mD_O. All radio data were taken from M. Haynes and R. Giovanelli (1984). Galaxies of Sbc and later types which have a cosmological redshift cz >400 km/s and a large angle of inclination $i>45°$ were considered; the Hubble constant was taken to be H_O = 75 km/s/Mpc. A linear dependence stretches for at least two orders of magnitudes. In reality it goes even further. As preliminary results show, the inclusion of clumpy irregulars and blue dwarf galaxies, some of which have very low luminosity, prolongs this line without changing its slope up to four orders of M_H altogether.

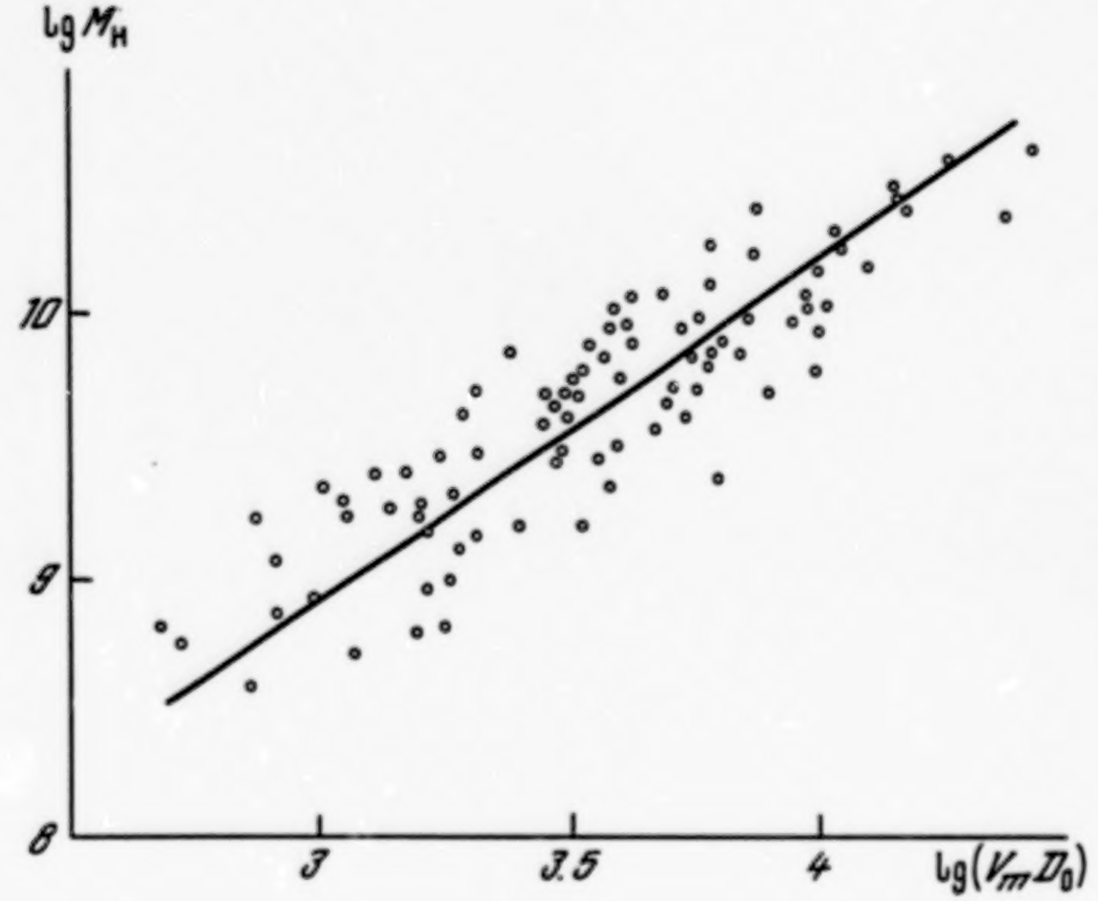

An advantage of the relationship we speak about is that it has a theoretical justification. There is an old idea proposed by W. Quirk (1972) that the local surface density of gas in disk galaxies is determined by a marginal gravitational stability condition of the gaseous layer. In the case of marginal stability a critical value of the surface density of gas is

$$(Q_g)_c = c_s\kappa/\pi G \times f(c_s,\Omega,\Omega') .$$

Here c_s is the sound velocity (or velocity dispersion of gas) which is usually about 10 km/s, κ is the ipicyclic frequency,

$f(v,\Omega,\Omega')$ is a function of local kinematical parameters equal to unity for radial perturbations (Goldreich-Lynden-Bell criterion) and is a little less than unity for the more general case, when non-radial perturbation are taken into account (Morozov's criterion).

A qualitative comparison of $(\sigma_g)_c$ with the observed gas density distribution $\sigma_g(r)$ in spiral galaxies have been undertaken by A. Zasov and A. Morozov (1985), A. Zasov and S. Simakov (1988), and R. Kennicutt (preprint, 1989). In all of these papers good agreement is found between these quantities for gas-rich late-type spirals over a large range of radius. The surface density of gas in early-type galaxies is in most cases well below its critical value, so they are not considered.

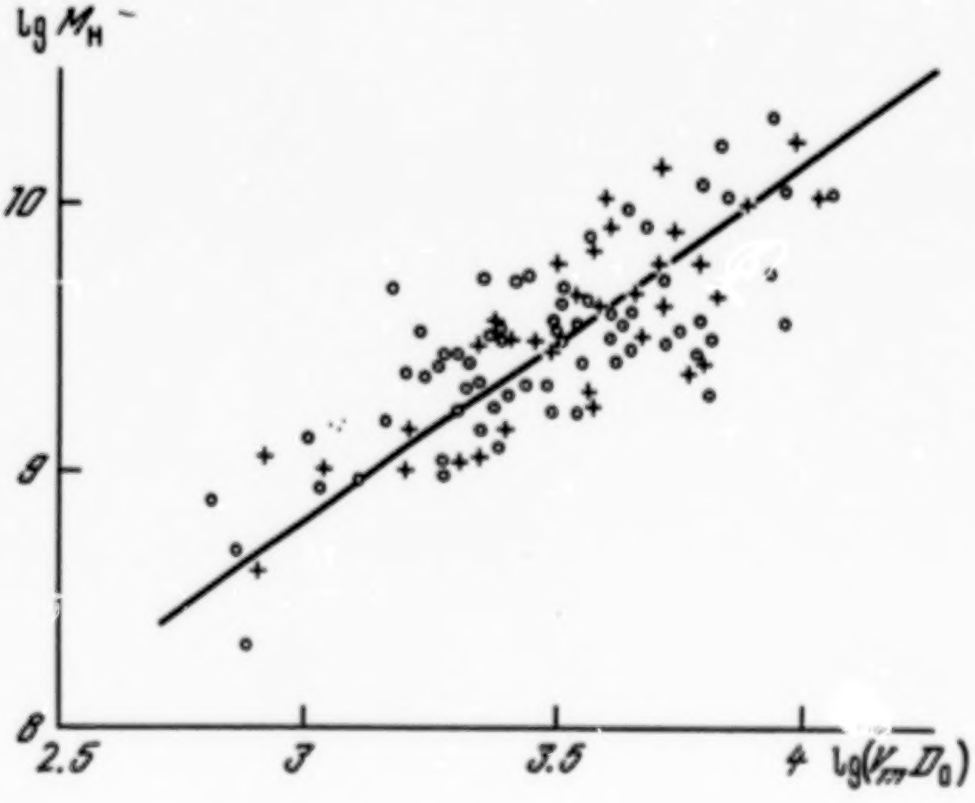

Here we don't care much about the precise value of $f(v,\Omega,\Omega')$. What is essential for us is that for the fixed c_g the critical gas density should be proportional to $\kappa(r)$, and hence to $\Omega(r)$, or to V_m/r (the shapes of V(r)-curves in galaxies are taken to be flat or at least similar). Then the mass of gas within the optical diameter D_O, which includes most of the gas in a galaxy, should be equal to

$$M_g \sim 2\pi \int_o^{D_o/2} \kappa(r)\, dr \sim V_m D_O,$$

which is the very relation we observe for M_H.

Now we can compare isolated and non-isolated galaxies putting them on the $M_H - V_m D_O$ diagram. Figure 2 plots the data for the sample of the so-called "best observed galaxies" from Bottinelli et al. (1982). This sample includes galaxies with the most accurately determined parameters. Only late-type spirals Sbc-Sd are taken. The regression line in Figure 2 is transferred from a similar diagram for isolated galaxies (see Figure 1). There is no noticeable difference between these galaxies.

The sample of the "best observed galaxies" is not homogeneous by itself: it includes single galaxies as well as galaxies in groups or pairs. Those galaxies which are members of systems or have close companions are marked by crosses. The difference between these two subsamples appears to be negligible: for the same angular momentum the mean $\overline{\Delta\ \lg M_H} = 0.01 \pm 0.05$.

To compare interacting and non-interacting galaxies in another way we have used HI measurements obtained by Davis and

Seaquist (1983). They have observed interacting galaxies along with the galaxies of Catalogue of Isolated Galaxies by V. Karachentseva. Again we restricted ourselves to late types of galaxies with i>45°. Nearby systems with cz<1000 km/s were excluded. Only those interacting galaxies were considered for which an individual estimates of fluxes and widths of HI line were available. A diagram M_H - $V_m D_O$ for these galaxies is shown in Figure 3 (crosses refer to interacting galaxies).

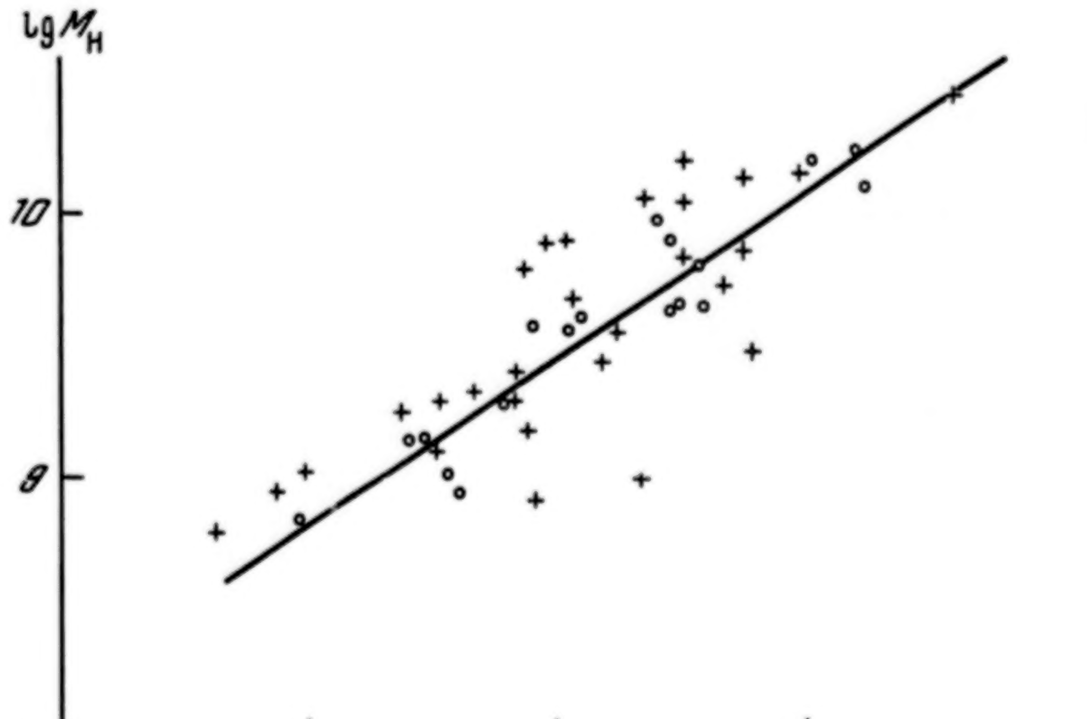

The mean difference between M_H of interacting and non-interacting galaxies with the same angular momentum appears to be small again: $\overline{\Delta \lg M_H} = 0.05 \pm 0.06$, although the dispersion is probably larger for interacting galaxies.

Thus we come to the conclusion that there are no systematic differences between HI content in isolated and non-isolated late-type galaxies: in spite of the differences of star formation rates their hydrogen mass is determined by slowly evolving kinematic parameters of the disk. Enhanced star formation in interacting galaxies, if it lasts long enough, must have an initial mass function enriched in massive stars in order not to significantly reduce the supply of gas.

Certainly these conclusions are not valid for galaxies which are members of rich clusters such as Virgo or Coma, where HI-deficiency really exists, possibly due to the interaction of interstellar HI with hot intergalactic gas.

The main results of this work were published in the following papers:

(1) A. V. Zasov, T. V. Rubtsova. Letters in Astron. J. (Russian), 1989, v. 15, p. 118.

(2) A V. Zasov, S. G. Simakov. Astrofizika (in Russian), 1988, v. 29, p. 190.

DISCUSSION

Roberts: Your HI mass versus angular momentum is closely related to the two Tully-Fisher relations, luminosity versus rotational velocity and luminosity versus size (radius). Since HI mass is closely related to luminosity the question arises as to what or which is fundamental among these interrelations. What is your view?

Zasov: I think that the fundamental relation concerning the total mass of gas is the dependence $M_{gas} \sim V_m D_o$. It has nothing to do with luminosity, so you can't get it from Tully-Fisher relations, but if you take into account the existence of the nearly linear dependence between velocity of rotation V_m and diameter D_o of galaxies, it is easy to show that a well known approximate constancy of surface gas density stems from this fundamental dependence. So kinematic properties of late-type galaxies appear to be of the greatest importance.

HI and Mass Distribution of GR8

Sylvie Beaulieu, Space Telescope Science Institute

and

Claude Carignan, Université de Montréal

ABSTRACT

The dwarf irregular galaxy GR8, which is at the extreme faint end of the luminosity and mass functions, is studied using optical photometry and 21cm HI line observations. It is shown that rotation is only important to the gravitational support of the system in the inner parts ($r < 250$ pc). GR8 is one of the very few non–elliptical systems known (with M81dwA) where the random motions provide essentially all the support in the outer parts ($r \geq 500$ pc). The Gaussian nature of the HI distribution and the isothermal distribution of the HI velocity dispersion implies $M \propto R^3$ in the outer regions of GR8 (ie the stellar disk and the HI lie in the approximately uniform density core of the dark halo).

1. Introduction

A few years ago, a program was undertaken to extend the mass and luminosity range of galaxies with well studied and understood mass distribution. The technique consists essentially in getting the kinematics to large galactocentric distances using high sensitivity HI observations and to complement this with optical surface photometry studies. The HI kinematics allows us to derive the total mass distribution (out to the last measured velocity point) in the system while the surface photometry tells us about the mass contribution of the luminous stellar disk. The data is usually analyzed in terms of a two-component model: a maximum luminous stellar disk and a minimum dark halo represented by an isothermal sphere potential or some other similar forms.

We have already reported the results on three late-type spirals in the Sculptor Group with $M_B \approx -18$, and on the Magellanic-type spiral NGC 3109 at $M_B \approx -17$ (Carignan and Freeman 1985). More recently, the luminosity range was extended toward still fainter systems with the study of the dwarf "regular" galaxy UGC 2259 at $M_B \approx -16.5$ (Carignan *et al.* 1988), and the dwarf irregular galaxy DDO 154 at $M_B \approx -14$ (Carignan and Beaulieu 1989; Carignan and Freeman 1988). It is with the goal of extending this kind of study to the extreme faint end of the luminosity and mass functions of normal galaxies, that we undertook the present study of GR8 ($M_B \approx -11$)

2. Optical observations

→ Well defined luminosity profiles were derived in B, V, and R, which show very regular exponential decline for $r \geq 30''$. An exponential fit to the B profile yields an extrapolated central surface brightness $B(0)_c = 22.6 \pm 0.2$ mag arcsec^{-2} and a scale length of 76 ± 7 pc ($\Delta = 1.1$ Mpc).

→ The colors are not as blue as previously suggested ($(B - V) \simeq 0.06$; Hodge 1967) but are more typical of the expected colors for Im galaxies, with $(B - V) = 0.38$.

3. HI line observations

→ The velocity width $\Delta V_{20} = 37$ km s^{-1} indicates that rotation is present in this system: the velocity field shows random motions with a fairly constant velocity dispersion $\sigma \approx 9.8 \pm 2.2$ km s^{-1}.

→ By integrating the global profile, a total HI mass of $2.0 \pm 0.2 \times 10^6$ $M_\odot$ is derived, for a $M_H/L_B = 0.8$.

→ The HI distribution is clumpy, with the clumps located just outside the optical structure. Its radial distribution is well approximated by a Gaussian having a scale length of 268 pc along the kinematical major axis.

→ The most striking result from the kinematical analysis is that the gas is rotating with its rotation axis roughly parallel and not perpendicular to the common major axis of the optical and HI distributions.

4. Mass distribution

→ For the stellar disk, the colors suggest a $M_*/L_B \simeq 0.5$ which, when combined with the observed total luminosity, yield a stellar mass of $M_* \simeq 1.2 \times 10^6$ $M_\odot$. Combining the mass in stars with our derived HI mass gives a total luminous mass of $M_{lum} = 3.2 \times 10^6$ $M_\odot$.

→ From Table I, it can be seen that rotation is only important in the inner parts (R < 250 pc) and that, in the outer parts (R ≈ 500 pc), random motions are really what provide the gravitational support to the system. Contrary to a common misconception, GR8 and M81dwA (Sargent, Sancisi, and Lo 1983) are the *only* two non-elliptical systems where this is observed.

→ The total dynamical mass within R=500 pc is 3.9×10^7 $M_\odot$, which strongly indicates that the luminous component of GR8 is immersed in the usual dark halo. The integrated M_{global}/L_B ratio within 0.5 kpc is 16.

5. Conclusion

The mean density of the dark halo of GR8 ($\langle\rho_{dark}\rangle \simeq 0.07$ $M_\odot$ pc^{-3}) appears to be unusually high compared to the densities of halos seen in spirals. However, it is comparable to what is seen in dwarf spheroidals (Kormendy 1987). The limited extent of the HI distribution means that little more can be said about its other parameters, such as its core radius and total mass. However, the Gaussian nature of the HI distribution and the isothermal distribution of the HI velocity dispersion implies that $M \propto R^3$ in the outer regions of GR8 (Carignan, Beaulieu, and Freeman 1990).

This suggests that the luminous matter (stars & HI) lies within the approximately uniform density region of the core of the dark halo. This feature is not peculiar to extreme dwarfs such as GR8. For example, an analysis of the rotation curve of the dwarf spiral UGC 2259 (Carignan *et al.* 1988) shows again that most of the luminous matter lies within the nearly constant density core region of its dark halo.

Our results reinforce the view that even the faintest dwarfs have dark halos (Carignan and Beaulieu 1989; Skillman *et al.* 1987; Sargent, Sancisi, and Lo 1983). They also support earlier suggestions (Kormendy 1987; Carignan and Freeman 1988) that the halos of the faintest dwarfs are densest.

REFERENCES

Carignan, C., and Freeman, K.C. (1985). Astrophys.J. **299**, 59.

Carignan, C., and Freeman, K.C. (1988). Astrophys.J.Lett. **332**, L33.

Carignan, C., Sancisi, R., and Albada, T.S. van (1988). Astron.J. **95**, 37.

Carignan, C., and Beaulieu, S. (1989). Astrophys.J. **347**, in press.

Carignan, C., Beaulieu, S., and Freeman, K.C. (1990). Astron.J., in press.

Hodge, P.W. (1967). Astrophys.J. **148**, 719.

Kormendy, J. (1987). In *Dark Matter in the Universe*, ed. J. Kormendy and G.R. Knapp (Dordrecht, Reidel), p. 139.

Sargent, W.L.W., Sancisi, R., and Lo, K.-Y. (1983). Astrophys.J. **265**, 711.

Skillman, E.D., Bothun, G.D., Murray, M.A., and Warmels, R.H. (1987). Astron. Astrophys. **185**, 61.

TABLE I. MASS ESTIMATES FOR GR8

R (pc) (1)	$M(R)$ ($M_\odot$) (2)	$f_{rot}^{\dagger}$ (3)
125	2.2×10^6	0.73
250	6.9×10^6	0.32
500	3.9×10^7	0.03

$^{\dagger}f_{rot}$ is the fractional contribution of rotation to the support of GR8.

THE RINGED X-GALAXY NGC 7020

Ronald Buta
Department of Physics and Astronomy, University of Alabama, U.S.A.

I. Introduction

The southern S0$^+$ galaxy NGC 7020 presents an unusual morphology: it includes a very regular outer ring which is completely detached and which envelops an inner ring/lens zone with a *hexagon* surrounding an X shape (Figures 1a and 1b). The outer ring has a high contrast compared to those usually observed in barred galaxies, yet NGC 7020 is not obviously barred. The morphology of this galaxy poses an interesting puzzle in that the hexagonal/X zone is not a typical type of feature to find in the interior of such a regular ring. Instead, the zone bears a striking resemblance to the edge-on galaxy IC 4767, recently studied by Whitmore and Bell (1988 = WB88) and dubbed by them as the "X-galaxy" because its inner regions appear to be crossed by two distinct enhancements lined at ±22° with respect to the major axis. The observation of a similar phenomenon in NGC 7020 is interesting because of the suggestion by WB88 that "X" structures could be related to accretion of matter associated with a merger or tidal encounter between an S0 and a small satellite galaxy. If this interpretation is correct for NGC 7020, then it has important implications for the nature of the outer ring. An alternative interpretation is that the inner hexagonal/X zone is a region where resonant periodic orbits in a weak bi-symmetric potential perturbation are influencing the morphology more strongly than might be expected. In this paper, I give a brief summary of a more extensive paper (Buta 1990c = B90c) and a few other details concerning this interesting galaxy.

II. Structure

Details of the hexagonal/X zone are highlighted in Figure 1b. This image has had a bulge model (B90c) removed in order to enhance the features. A very regular pattern is evident. The inner zone appears crossed by two distinct enhancements that look like an X (see arrows). The arms of the X make angles of ±25° with respect to the major axis. At the major axis points of the inner zone there are two bright knots (indicated by the letters "k"). These are interesting because they resemble the "ansae" often seen in edge-on S0 galaxies, features which are usually interpreted as due to an inner ring (de Vaucouleurs 1959). However, in a non-edge-on galaxy, such knots must be distinct objects, not artifacts of tilt. A definite boxy character is evident in the region within 10″ of the core. The combination of this region, the X, and the short sides of the hexagon gives a diamond-shaped character to the dips in surface brightness at $\pm 23''$ from the nucleus along the major axis.

The X character does not show well on isophote maps, and one could argue that it is not real. In such maps one sees instead a distinctive sequence of isophote shapes, ranging from nearly circular in the core, to elliptical, to rectangular, to hexagonal, to pointed oval (Figure 1d). The map also highlights how two of the shorter sides of the hexagon are brighter than the other two, which gives the impression of a two-armed spiral pattern connecting to the boxy zone.

III. **Properties**

Is there anything unusual about other characteristics of NGC 7020? The absolute blue magnitude is about −20.0 and the outer ring is about 20 kpc in diameter ($H_o = 100$ scale), neither of which is very extreme. The galaxy is a member of a sparse group having $< V_\odot > = 3{,}000$ km s^{-1}, but is not obviously interacting with any other member of that group. After allowance for the more spherical shape of the bulge, Fourier intensity analysis reveals significant $m = 2$ amplitude only in the region of the knots, and negligible odd amplitudes. The galaxy is remarkably symmetric. The outer ring appears as a distinct blue enhancement in a color index map (Figure 1c, which is U−B), suggesting that it is a region with a somewhat more active star formation history than its surroundings (B90c). This is a typical property of most galaxy rings (Buta 1988 and references therein; Buta 1990a,b).

Color index maps like Figure 1c also reveal little color differentiation in the inner hexagonal zone, except for a color gradient in the inner few arcseconds. The knots are found to have colors (integrated over a $4''$ aperture) of B−V = 0.99 and U−B = 0.55, compared to 1.04 and 0.63, respectively, for a $6''$ diameter region centered on the nucleus. The knots are therefore made mostly of old stars.

The outer ring contributes only a small fraction of the total luminosity. The enhanced region between $63''$ and $91''$ radius contributes about 17% of the total V-band luminosity. A useful parameter for comparing with other galaxies is the luminosity (L_R^B) of the ring plus outer disk compared to the luminosity (L_c^B) of the inner regions (B-band). These luminosities are obtained by dividing the galaxy at the minimum of the gap region (Wakamatsu 1990). The ratio obtained, $L_R^B/L_c^B = 0.50$, is comparable to what has been found for normal barred outer-ringed galaxies by Wakamatsu (1990).

IV. The Nature of the Hexagonal/X Zone

The most promising interpretation of this zone is that it is related to an unusual type of bar and inner ring. The ratio of the diameter of the outer ring to the separation of the knots is 2.3, very similar to the mean ratio of outer ring to bar diameters in SB galaxies (Kormendy 1979) and the mean ratio of outer to inner ring diameters in double-ringed SB galaxies (Athanassoula et al. 1982). This ratio is also close to expected resonance radius ratios for a velocity = constant rotation curve: r(OLR)/r(CR) = 1.7, where OLR = outer Lindblad resonance and CR = corotation; r(OLR)/r(4:1) = 2.6, where r(4:1) is the radius of the inner 4:1 resonance; and r(OLR)/r(6:1) = 2.2, where r(6:1) is the radius of the inner 6:1 resonance. The observed ratio suggests that the inner zone is possibly associated with the 4:1 and 6:1 ultraharmonic resonances, which could explain the rectangular and hexagonal shapes so evident in that region. However, the sharpness of these features is difficult to understand in a galaxy where no conventional bar is apparent. Either the knots contain enough mass to define an $m = 2$ perturbation, or the inner zone is a bar in its own right which is cold enough so that random motions have not washed out some of the finer details of the stellar orbits. An interpretation in terms of planar bar orbits in an integrable galactic model has been discussed by Contopoulos (1988). Vertical resonant orbits may also be important, because these are known to be capable of causing a bar to appear boxy if viewed nearly edge-on (Combes and Sanders 1981; Pfenniger 1984, 1985).

It is more difficult to make a case for the external dynamics interpretation of the inner zone. In this interpretation, a small gas-rich companion is disrupted into an oblique orbit around an S0 galaxy. Before differential precession causes the material to settle into the plane of the S0 disk, the oblique disk spreads into a cone-shaped distribution, which, when viewed edge-on, appears as an X. This could cause the appearance of a "peanut-bulge" as in IC 4767 (WB88). For NGC 7020, the model would require that the outer ring and inner hexagonal zone are not in the same plane, the inner zone being viewed more edge-on. Arguments in favor of the interpretation are the striking resemblance of IC 4767 to the inner zone, both in general appearance and isophote shapes, the group membership of NGC 7020, the similar relative angles of the X-arms of IC 4767 and NGC 7020 with respect to the major axis, and the resemblance of the outer ring to that in Hoag's Object (believed to be of the accretion type by Schweizer et al. 1987). However, arguments against the model are the non-edge-on orientation ($i = 69°$) and obvious outer disk, the similar projected shapes of the inner hexagonal zone and the outer ring, and the lack of evidence for any merger remnant in the core (see WB88).

V. CONCLUSIONS

An unambiguous interpretation of the structure of NGC 7020 will require kinematic and HI observations. If the hexagonal/X zone has been affected by a merger, then the outer ring could itself be an accretion feature, for example, like that in Hoag's Object. *This very interesting possibility would imply that the ringed galaxy class does not consist entirely of internally derived structures.* Until kinematic and HI observations are obtained, the present observations tentatively favor the internal dynamics interpretation of the galaxy's structure, that is, that the inner zone is related to a weak bar and inner ring, most likely inside CR, and that the outer ring is related to OLR. The resemblance to IC 4767 may only mean that different mechanisms can lead to a similar observed morphology. However, the problem of how a weak bi-symmetric distortion could have generated orbits with the sharp corners observed needs to be investigated. It is also essential to measure velocity dispersions in the inner zone, since the significant structure would not be expected if this ring/lens zone is as hot as the lenses observed by Kormendy (1984a,b).

References

Athanassoula, E., Bosma, A., Creze, M., and Schwarz, M. P. 1982, **Astr. Ap. 107**, 101.
Buta, R. 1988, **Ap. J. Suppl. 66**, 233.
...... 1990a, **Ap. J. 351**, 62.
...... 1990b, **Ap. J. 354**, in press.
...... 1990c, **Ap. J. 356**, in press (B90c).
Combes, F. and Sanders, R. H. 1981, **Astr. Ap. 96**, 164.
Contopoulos, G. 1988 in *Integrability in Dynamical Systems, Annals of the New York Academy of Sciences, Vol. 536*, eds. J. R. Buchler, J. R. Ipser, and C. A. Williams (New York: New York Academy of Sciences), p. 1.
de Vaucouleurs, G. 1959, **Handbuch der Physik 53**, 275.
Kormendy, J. 1979, **Ap. J. 227**, 714.
...... 1984a, **Ap. J. 286**, 116.
...... 1984b, **Ap. J. 286**, 132.
Pfenniger, D. 1984, **Astr. Ap. 134**, 373.
...... 1985, **Astr. Ap. 150**, 112.
Schweizer, F., Ford, W. K., Jedrzejewski, R., and Giovanelli, R. 1987, **Ap. J. 320**, 454.
Wakamatsu, K. 1990, **Ap. J. 348**, 448.
Whitmore, B. C. and Bell, M. B. 1988, **Ap. J. 324**, 741 (WB88).

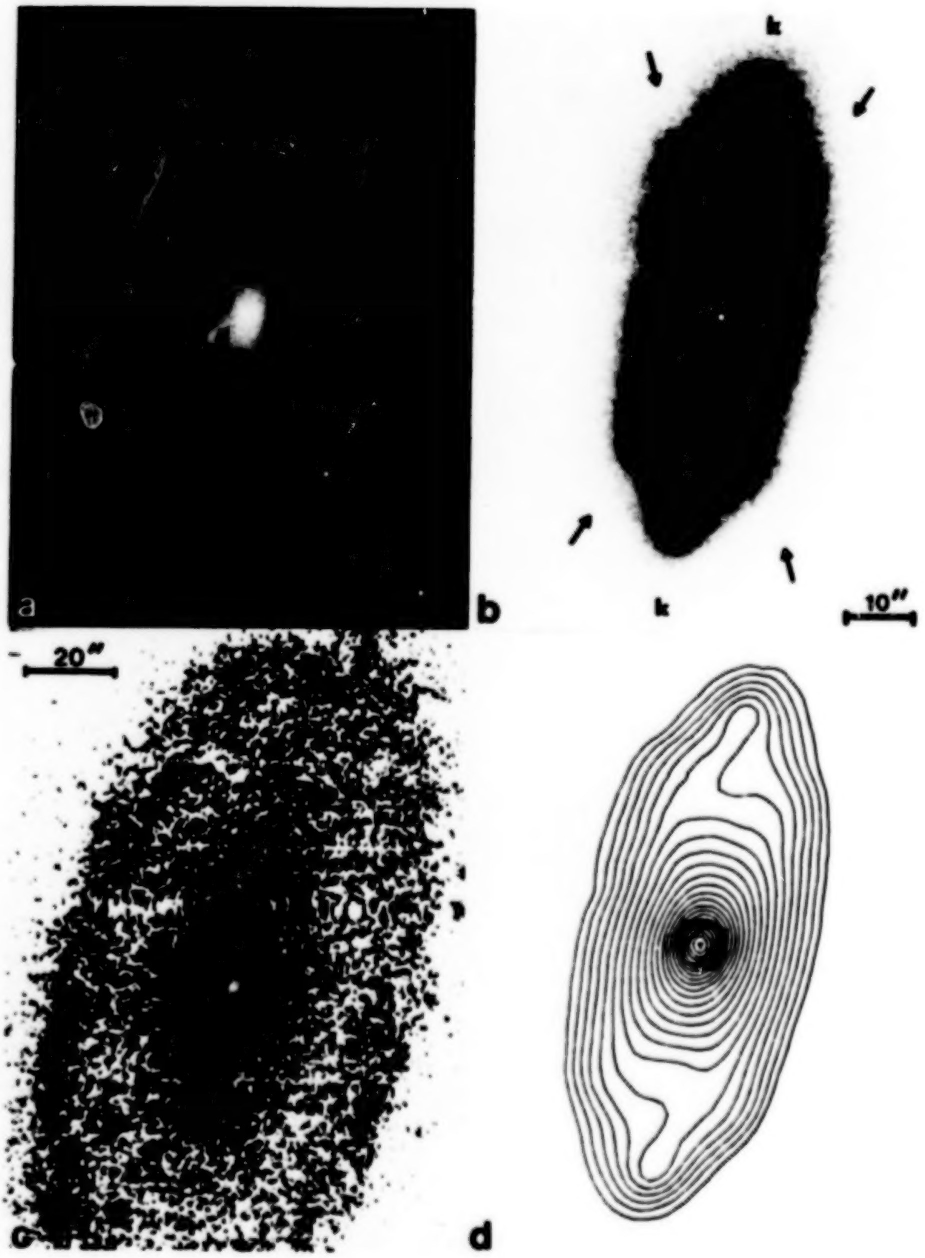

Fig. 1 - Images of NGC 7020: (a) V-band CCD mosaic image (units of mag arcsec^{-2}); (b) enlargement of inner hexagonal zone (V-band), with arrows indicating the "X" and the letters "k" indicating the knots discussed in text; (c) U−B color index map, coded such that "blue" features are dark while "red" features are light; (d) V-band isophote map showing distinctive sequence of shapes. Largest isophote corresponds to $\mu_V = 22.37$ mag arcsec^{-2}, and each successive isophote is -0.20 mag arcsec^{-2} brighter than the previous larger one. Panels (b) and (d) have nearly the same image scale.

The cD Galaxy in Abell Cluster 1775

J. J. E. Hayes and B. Bhattacharya
Space Telescope Science Institute
3700 San Martin Drive
Baltimore, MD 21218

ABSTRACT: Over the last 20 years, a number of workers have studied the multiple nuclei cD galaxy in the rich Abell cluster 1775, trying to discover its nature. In all the cases though, very little has been published concerning its morphology. The majority of arguments about the nature of the this object have been based on the relative radial velocities of the 2 components with each other and with the other galaxies in the cluster, or its radio morphology. Very little work has been done on the optical morphology. To rectify that lack of data, we have obtained BVRI CCD images of the cD. We find from our CCD data that the cD is unlikely to be a bound object and that there is strong evidence for an collision.

1 Introduction

The cD system in Abell cluster 1775 has been studied by a number of workers in the past. Chincarini *et al.* (1971), using Palomar Schmidt plates and image-tube spectra, argued that this object was a gravitationally bound pair, forming a stable system having a mass of a few times 10^{13} solar masses. They noted that the pair was in a sparse region of the cluster and that the colours of both components were "normal" for ellipticals. The conclusion was that such an isolated system which appeared to be undisturbed would be a stable, bound system. However, Hintzen (1979) using his original spectroscopy confirmed that the relative velocities of the two galaxies were $\approx$ 1700 km s^{-1} and noted the discovery by Miley and Harris (1977) of a 300 kpc long *straight* radio-tail emerging from the SE galaxy (assuming $H_o = 75\,\mathrm{km\,s^{-1}\,Mpc^{-1}}$). From these data Hintzen concluded that the A1775 system could not be a stable bound system, but either a superposition of two galaxies in two different clusters, or some sort of interaction. The latter conclusion seems to be supported by the discovery of O'Dea and Owen (1985) that the NW component is a wide-angle-tail source. Hayes (1982), using Palomar Schmidt plates modeled the cD system using the "standard" King (1966) models and found that both the stable bound model and the superposition ideas were both unlikely, leaving the collision model. We have now obtained broadband BVRI CCD images of the cD, and it is this data that we present here.

2 Observations

The BVRI CCD images of the A1775 cD were obtained 10 June 1986 under the KPNO Request Observing Program. The #1-0.9 m telescope was used in conjunction with the TI2 CCD. The f-ratio used was f/7.5, giving an image scale of 0.43" pixel^{-1}. The seeing was mostly near 2". Initial flattening, etc., was done on the mountain while the actual reductions were done at STScI using the UNIX-based version of the "Vista" reduction package. The filters used are the KPNO standard broadband set.

3 Discussion

The most remarkable feature of the A1775 cD is the unusual shape of the common envelope which surrounds the two nuclei. In all of our images it shows up as having a very square or boxy appearance — indeed, *truncated*. In Figure 1 we plot the R isophotes.

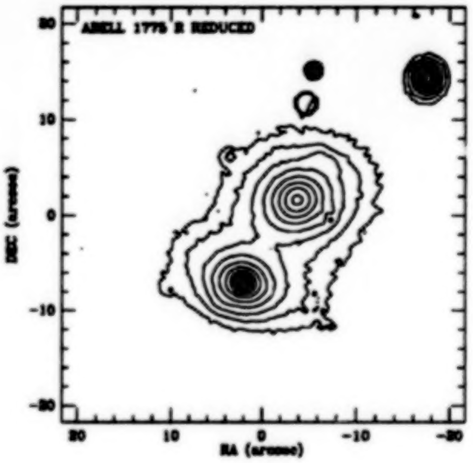

Figure 1: Half-magnitude R isophotes of the A1775 cD. North is at the top, East to the left

Indeed, there is a very steep fall off of light in the outer regions of the SE component which shows up in the brightness profiles of the system. Figure 2 is the V brightness profile at position angle = 125.3°. The profile shows that there is 30% more light between the two than one would expect for a simple superposition of two ellipticals, thus confirming one of Hayes' (1982) conclusions that the system is not a superpostion of two ellipticals.

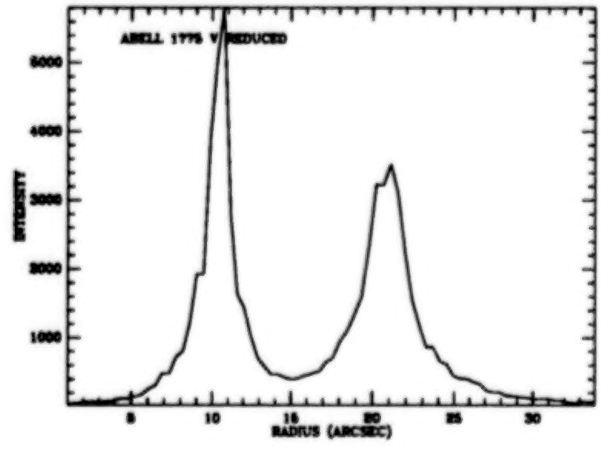

Figure 2: V band brightness profile of A1775. SE is to the left. Position angle of the cut is 125.3°.

In addition, the fainter (NW) component shows very strong isophotal twists and radial variations in ellipticity. This would seem to indicate that this component at least is suffering from some sort of perturbation. The brighter (SE) component also shows isophotal twists and ellipticity changes, but not to the same extent. We plot the isophotal twists and the variations in ellipticity in Figures 3 and 4 below.

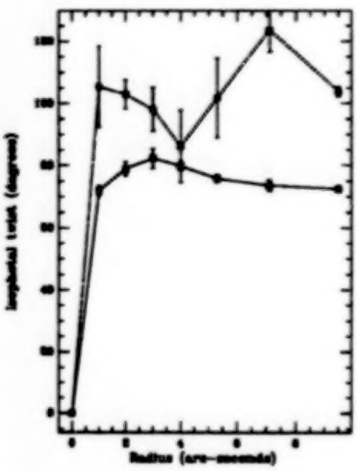

Figure 3: Average isophotal twists. The open symbols and solid line are for the SE (brighter) component, while the solid symbols and dotted line refer to the NW component.

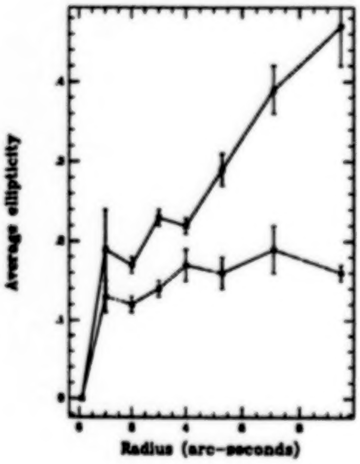

Figure 4: Average ellipticity of the cD system. The symbols have the same meaning as in Figure 3.

We have also looked at the (B-V) colours of the two components. We find that for both components, (B-V) decreases (as expected for ellipticals) from 1.06 to about 0.80. However, the gradient of the index is sharp; the colour drops ≈ 0.2 magnitudes in only a few arc-seconds, supporting our notion that the profiles are being truncated by a collision. We see no evidence for star formation.

Other data come from looking at the brightness profiles and comparing them to the deVaucouleurs (1948) $r^{1/4}$ law. In Figure 5 we plot the surface brightness profiles for the two components in each of BVRI (in relative magnitudes) and a scaled deVaucouleurs law in each of the frames. One notices immediately that none of the profiles are well-fit by the deVaucouleurs model. In the outskirts of most of the profiles, the model is too faint by a factor of 0.2 magnitudes.

Our last data comes from looking at the residuals of models constructed using our photometric fits subtracted from theobserved data. We see that the SE component is fairly well modeled (except for the core, which is expected as we have not deconvolved the seeing from the images), but there is a great deal of low luminosity diffuse brightness left over from the NW component, indicating that this component is not being well-modeled after all.

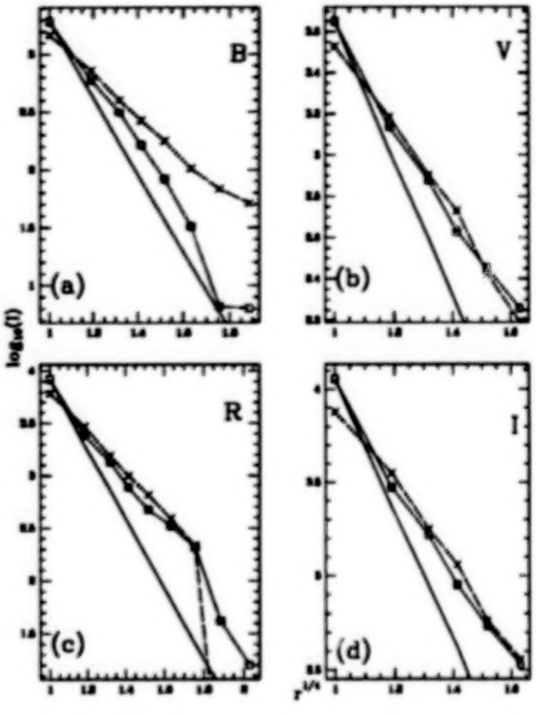

Figure 5: Brightness profiles of A1775. The dotted line is the SE component; the dashed line the NW component, and the solid line is the $r^{1/4}$ law. We see that in virtually all cases, the observed profiles are brighter than the model. Subfigure (a) is the B data; (b) the V data; (c) is the R data, and (d) is the I data. Overall the data fits the model quite poorly, something expected for a collision.

We believe that this is caused by the effects of a collision, which is being seen in the NW component more because it is about half the mass of the SE component (see Conclusions below). In Figure 6 we plot the residual contours for the I filter data.

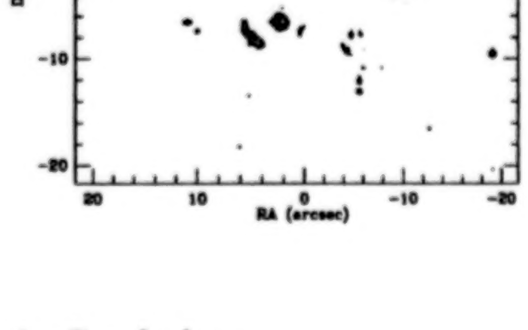

Figure 6: Residual contours of I filter data. Note the large, diffuse area near the position of the NW component, showing that the model is not adequate, and we believe is indicative of a collision. Both cores are not well-modeled as we have not deconvolved the seeing from the data.

4 Conclusions

From the isophotal structure, previous measures of the relative velocities of the two components (Chincarini *et al.* (1971), Jenner (1974) and Huchra (1982)), and the radio morphology mentioned above, we believe that the bound stable model proposed by Chincarini *et al.* is not tenable. Also, looking at the the (B-V) colour index we see that the colour gradient is steep, but that the range in (B-V) (from about 1.06 to about 0.8) is typical for normal elliptical galaxies. The brightness profile of the two galaxies is also diagnostic, in that the amount of light coming from between them is more than one would expect if the cD was a simple superposition of two galaxies that followed the "standard" King model in brightness (see also Hayes (1982)). On the basis of this data, we believe that the idea that the cD is a simple superposition can also be ruled out.

This leaves us with a collision as the best model left for A1775. The steepness of the colour gradients for both components, the boxy-shaped halo, the very poor fits by the deVaucouleurs $r^{1/4}$ law to the brightness profiles, and the residual brightness from the model fitting are all evidence for an unusual interaction. It appears that both components are strongly affected by each other, and that there has been some severe modification of the normal brightness profile (assuming the $r^{1/4}$ law *is* universal in all enviroments). Also of interest are the isophotal twists because while the outer isophotes of the NW component do point towards the SE component, the SE component's isophotes do not seem to point to the NW (see Figure 1). In this case we believe we may be seeing the effects of the difference in mass between the two components. The SE component's core is about twice as bright as the NW component's core in all colours. If we assume a constant M/L ratio for both galaxies, then the SE component is about twice the mass of the NW component. Therefore, the NW component of the pair would manifest the effects of the collision first and to a greater degree that the more massive SE partner. One is inclined to point out that the high relative velocities between the two components (about 1700 km s^{-1}) is an argument against the galaxies being in the same cluster. However, both A98 and A2152 have cluster velocity dispersions which are roughly the same as difference in velocities of the two components in A1775 (Noonan 1981), so it seems reasonable to assume that the two components are in the same cluster. Therefore, we are probably seeing a high speed collision of two unequal mass ellipticals.

Finally, we would like to thank George Jacoby at NOAO who took the CCD images.

REFERENCES

Chincarini, G., Rood, H.J., Sastry, G.N., Welch, G.A.; (1971) *Ap. J.*, **168**, 11
deVaucouleurs, G.; (1948) *Ann. d'Ap.*, **11**, 247
Hayes, J.J.E.; (1982) unpublished M.Sc. thesis, Saint Mary's University, Halifax
Hintzen, P.; (1979) *Pub. A.S.P.*, **91**, 426
Huchra, J.P.; (1982) — *private communication*
Jenner, D.C.; (1974) *Ap. J.*, **191**, 55
King, I.R.; (1966) *Astron. J.*, **71**, 64
Miley, G. and Harris D.; (1977) *Astr. Ap (Letters).*, **61**, L23
Noonan, T.W.; (1981) *Ap. J. Supp. Ser.*, **45**, 613
O'Dea, C.P. and Owen, F.N.; (1985) *Astron. J.*, **90**, 927

NEW DATA ON THE PECULIAR GALAXY MRK 273

A. S. Asatrian and A. R. Petrosian
Byurakan Astrophysical Observatory, ARMENIA

F. Börngen
Tautenburg Observatory, DDR

ABSTRACT. On the basis of direct UBV and spectral observations at Tautenburg (DDR) 2m and Special Observatory (USSR) 6m telescopes respectively the colorimetric and spectral investigations of the megamaser galaxy MRK 273 are carried out. It is seen that: MRK 273 is in a physical group of galaxies, which contains at least five members. Two bright central condensations of MRK 273 are Seyfert nuclei. The area of the main body of MRK 273 which contains both Seyfert nuclei and from which comes out a straight tail, is redder than the remaining part of the galaxy. The tail has a pronounced blue color and most probably radiates in [OIII] λ5007 line. Observed radio continuum, OH and HI absorption features are related to bright "a" nucleus of galaxy. We come to the conclusion that MRK 273 which is the member of the group of the galaxies is itself a close system of two objects with AGNs. The tail, with radiation being of thermal origin, probably is the result of the interaction of these galaxies.

INTRODUCTION - OBSERVATIONS AND PROCESSING

MRK 273 is one of the most interesting galaxies in the Markarian lists. It is a megamaser (Baan et al. 1985) and ultraluminous infrared galaxy (Sanders et al. 1988) with peculiar morphological structure (Korovyakovskij et al. 1981) and with an AGN (Kachikian and Weedman 1974). In the present work detailed spectral and colorimetric investigations of the MRK 273 are carried out on the basis of high resolution spectra and direct UBV observations.

Direct UBV observations at the Schmidt focus of the Tautenburg observatory 2 m telescope are carried out. A selected combination of the plates and the UBV filters ensures system very close to the international. Plates were processed on the complex PDS1010A+SM4 of Byurakan Observatory with the scanning diagram 0.5 x 0.5 arcsec. The mean accuracy of the surface photometry was estimated as $0^{m}.07 \pm 0^{m}.06$.

Spectra for MRK 273 and its neighbors at the prime focus of the Special Observatory 6 m telescope, with spectral resolution about 6A and for seeing 1.5-2 arcsec (spatial scale is about 17 arcsec per mm) are carried out. The stars BD 25°3941 and Feige 92 (Stone 1977) were used for comparison.

A copy of the field around MRK 273 from the B plate of the 2 m telescope is presented in Figure 1a. Observed neighbors of MRK 273 are identified in it. Two positions of the spectrograph slit and three condensations in main body of the galaxy are indicated in Figure 1b on an isodensitometric picture of MRK 273 (Korovyakovskij et al. 1981).

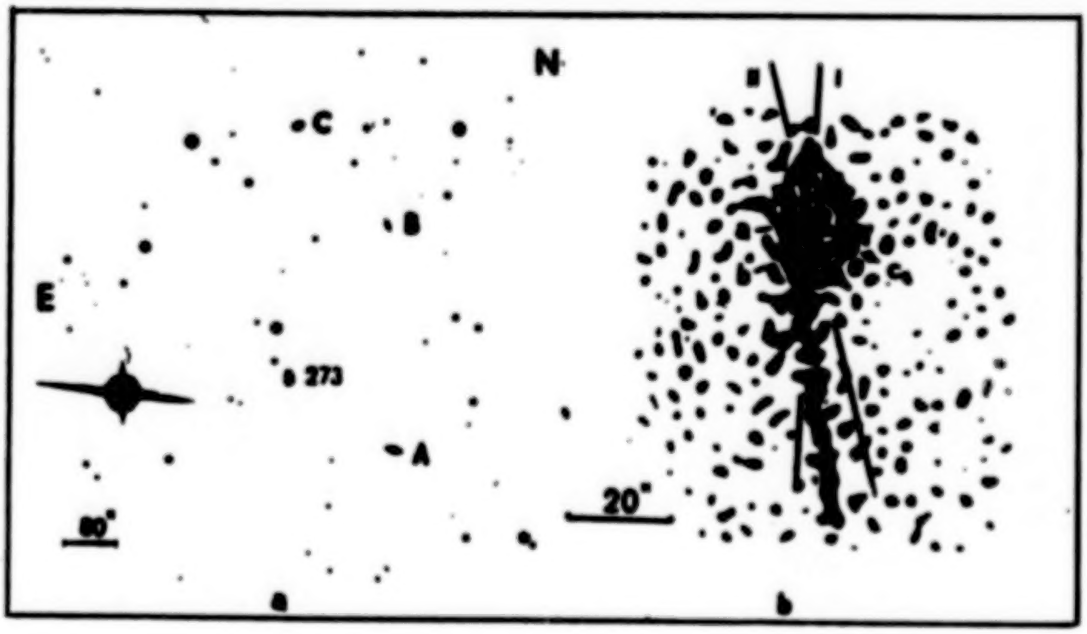

Figure 1.

RESULTS

In the spectra of all three neighbors of MRK 273 absorption lines of Ca+ H and C and G band are identifed. In Table 1 are presented radial velocities of MRK 273 and its three neighbors corrected for the solar motion, their total B magnitudes and colors as well as morphological classes.

Table 1.

Galaxy	Other name	V ($km\cdot s^{-1}$)	B	U-B	B-V	Morph.
MRK 273	MCG 9-23-4	11730	14.90	0.05	0.75	Pec.
A neighb.	MCG 9-23-2	11700	15.41	0.44	0.90	SO
B neighb.		12150	16.95	0.32	0.96	Sa
C neighb.	MCG 9-23-2	11480	15.93	0.05	0.82	Sbc

With the first position of the spectrograph slit we had spectral information about the tail and the main body of MRK 273. In Figure 2 an isodensitometric picture of the spectral region [OIII] λ5007 - H_β for MRK 273 for the first position of the slit is presented. Continuum radiation of the main body of MRK 273 is strong. Emission lines with composite structure are broadened. The tail obviously does not radiate in continuum but its radiation exists in [OIII]λ5007 line after subtraction of the night sky [NI]λ5200 line intensity.

For the second position of the spectrograph slit the spectra of the "a" and "b" condensations of MRK 273 are clearly separated. Both condensations show broad emission lines with corrected FWHM as 780±90 $km\cdot s^{-1}$ respectively. To characterize the dominant energy source producing the line emissions in both condensations we have followed the work of Veilleiux and Osterbrock (1987) using line ratios - ([OIII]λ5007)/Hβ, ([SII]λ6716+6731)/Hα, (NII]λ6583)/Hα and ([OI] λ6300)/Hα. Both condensations of MRK 273 fall clearly within the line ratio characteristics of Sy2 type AGNs.

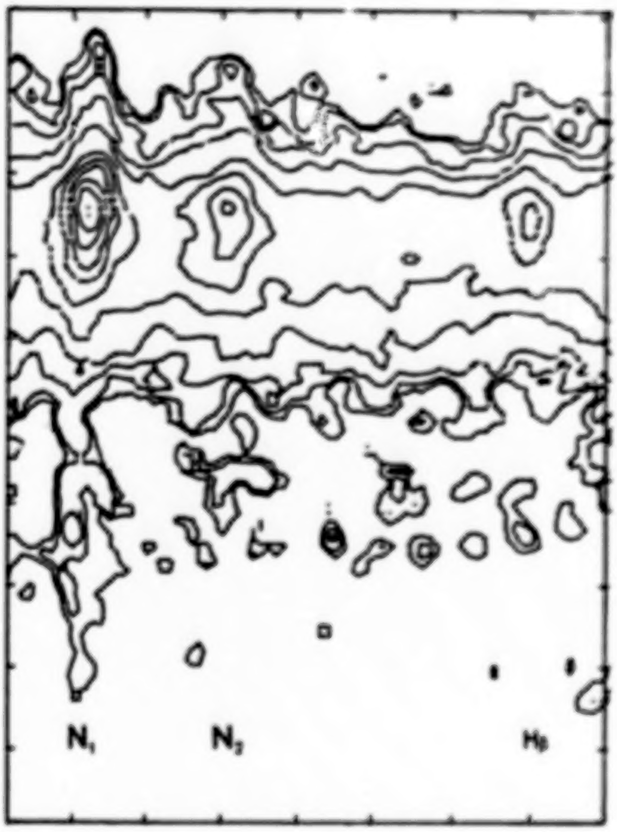

Figure 2.

In Figure 3 a contour map of MRK 273 in (U-B) color is presented. On the map by solid lines the (U-B) <0 and by dotted lines the (U-B) > 0 values are marked. As is seen in Figure 3 the area of the main body of MRK 273 which contains both Seyfert nuclei and from which the straight tail comes out is redder than the remaining part of the galaxy. The tail has a pronounced blue color with two or three comparatively red condensations.

DISCUSSION

The data of Table 1 show that MRK 273 and its three neighbors are physically related. As mentioned by Sanders et al. (1988) there is another starlike blue galaxy approximately 40" north of the main body on a direct line with the tail of MRK 273,

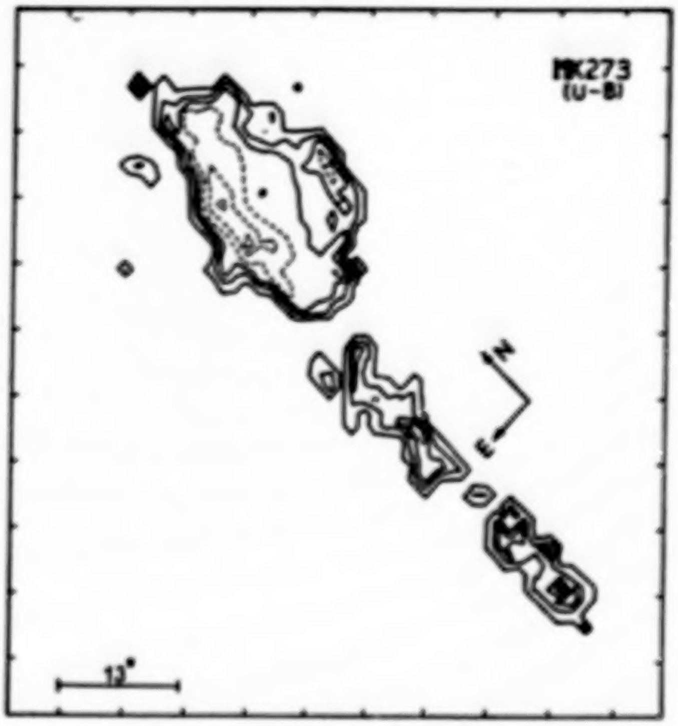

Figure 3.

whose redshift is only 50 km·s^{-1} different from that of MRK 273. We identified this object on the direct plates from the Tautenburg Observatory 2 m and Byurakan Observatory 2.6 m telescopes with a starlike object not at 40" but about 80" north from the main body of MRK 273. So MRK 273 with at least four other galaxies forms a physical group of galaxies. This can be an additional proof that all megamasers are members of the groups or clusters of galaxies (Henkel et al. 1987).

It is well determined that all ultraluminous infrared galaxies, including megamasers, are interacting or merging systems (e.g. Henkel et al. 1987; Sanders et al. 1988). Our data allow to suppose that MRK 273 is a close system of two probably disk type objects with AGNs, in which it resembles ARP 220 (Diamond et al. 1989). By color the third-"c" condensation probably is a giant HII region and the straight tail is the result of the interaction of these galaxies.

Because of blue color and the probable presence of [OIII] 5007 line in its spectra the latter looks by nature like a spiral arm containing young stars and ionized gas in abundance.

On plates of 2 m telescope with accuracy $\pm 0\overset{s}{.}666$ and $\pm 0\overset{''}{.}21$ by right ascension and declination the positions of three condensations in MRK 273 are measured. The comparison of the measured optical positions of the condensations with high resolution radio, OH and HI data show that the bright radio component in 6 cm map of VLA-A (Ulvestad and Wilson 1984), megamaser emission (Schmelz et al. 1987) and HI absorption features (Schmelz et al. 1988) are related to the "a" nucleus of MRK 273. The second compact radio source (Ulvestad and Wilson 1984) is not identified with any optical detail in MRK 273. As in the case of the double nuclei of MRK 463 it may be related to some other, strongly reddened, invisible condensation (Neff and Ulvestad 1988) or, as in the case of MRK 266, it might be conditioned by interaction between galaxies (Mazzarella et al. 1988).

REFERENCES

Baan, W. A., Haschick, A. D., and Schmelz, J. T. 1985, Astrophys. J. Letters, **298**, L51.

Diamond, P. G., Norris, R. P., Bean, W. A., and Booth, R. S. 1989, Astrophys. J. Letters, **340**, L49.

Henkel, C., Gusten, R., Baan, W. A. 1987, Astron. and Astrophys, **185**, 14.

Khachikian, E. E. and Weedman, D. W. 1974, Astrophys. J., **192**, 581.

Korovyakovskij, Y. P., Petrosyan, A. R., Saakyan, K. A., and Khachikian, E. E. 1981, Astrophysics, **17**, 121.

Mazzarella, J. M., Gaume, R. A., Aller, H. D., and Hughes, P. A. 1988, Astrophys. J., **333**, 168.

Neff, S. G., and Ulvestad, J. S. 1988, Astron, J., **96**, 841.

Neugebauer, G., and Scoville, N. Z. 1988, Astrophys. J., **325**, 74.

Sanders, D. B., Soifer, B. T., Elias, J. H., Madore, B. F., Matthews, K., Neugebauer, G., Scoville, N. Z. 1988, Astrophys. J., **325**, 74.

Schmelz, J. T., Baan, W. A., and Haschick, A. D. 1987, Astrophys. J., **321**, 225.

Schmelz, J. T., Baan, W. A., Haschick, A. D. 1988, Astrophys. J., **329**, 142.

Stone, R. P. S. 1977, Astrophys. J., **218**, 767.

Ulvestad, J. S. and Wison, A. S. 1984, Astrophys. J., **278**, 544.

Veilleux, S. and Osterbrock, D. E. 1987, Astrophys. J. Suppl. Ser., **63**, 295.

HI OBSERVATIONS OF THE PECULIAR GALAXY NGC 660

Stephen T. Gottesman and Mary Elaine Mahon
Department of Astronomy
University of Florida
Gainesville, Florida

We present observations of HI emission from the peculiar galaxy NGC 660. HI was detected in the companion galaxy UGC 01195 as well. Sixteen hours of observations were obtained with the VLA telescope of the National Radio Astronomy Observatory during December 1986 and March 1987.

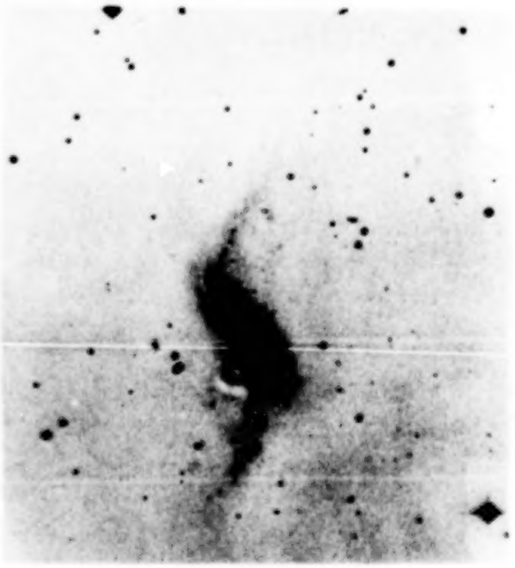

Figure 1

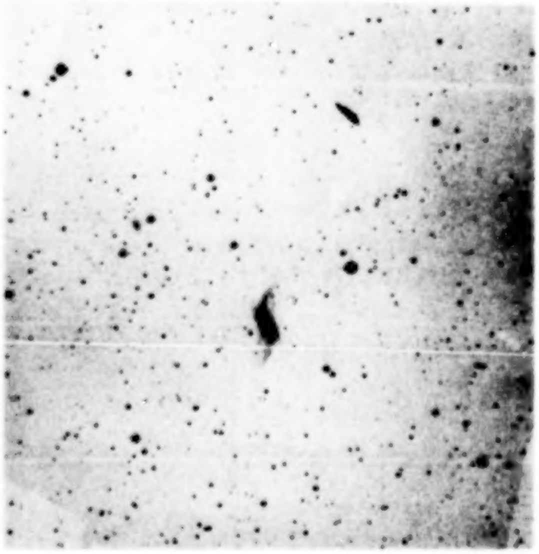

Figure 2

Photographs of NGC 660 show a central bar-like structure crossed by two systems of absorption, as well as an outer ring or disk inclined about 50 degrees with respect to the major axis of the central body (see figure 1). Figure 2 shows UGC 01195, an irregular, distorted galaxy located 22 arcminutes or 72 kpc N.W. of NGC 660. In table 1 we list the systemic parameters of interest.

The Continuum Emission

The high resolution (2") maps of Condon, Condon, and Puschell (1982) at 20-cm show two peaks in the extended central continuum source of more than 5" in extent. The smeared peak (589°K) of these continuum features, seen in our maps with 14" resolution (figure 3), agrees with the IR and optical position of the galaxy to better than 6". At a lower intensity, the emission extends for more than 2 arcminutes along position angle 46 degrees in the general direction of the narrow dust lane.

Table 1

Observational and Related Parameters

	NGC 660	UGC 01195
Right Ascension	$01^h40^m.36$	$01^h39^m.7$
Declination	13°23'.64	13°43'
Type	SBa pec	irregular
[a]Dimensions on PSS plate	10'.0 X 4'.5	3'.5 x 1'.1
[a]Photographic magnitude	12.8	13.9
[b]$\log(L_{TOT}/L_\odot)$	10.9	
Systemic Velocity of HI ($V_\odot$)	842 km/s	[c]772 km/s
Distance (H=75 km/s/Mpc)	11.2 Mpc	
Angular Resolution	14".89 X 13".50	14".89 X 13".50
Linear Resolution (kpc)	0.81 X 0.73	0.81 X 0.73
RMS Sensitivity	0.76 mJy/Beam	0.76 mJy/Beam
....	2.2°K	2.2°K
Total Integrated Flux	164 Jy*km/s	
Detected HI Mass	$4.9 \times 10^9\ M_\odot$	
Velocity Resolution	21 km/s	21 km/s
[d]Keplerian mass of NGC 660	$1.2 \times 10^{11} M_\odot$	

a. UGC Catalogue of Galaxies
b. $L_{TOT} = L_{FIR} + L_B$ from Young, J.S., Kleinman, S.G., Allen, L.E. 1988, Ap. J. 334: L63-67.
c. Calculated as the average velocity over the channels in which it appeared.
d. $M=R^*(V_{RAD}(R)^*\csc I)^2/G$, where R=17 kpc, $V_{RAD}(R)$=150 km/s, and I(HI ring)=60°.

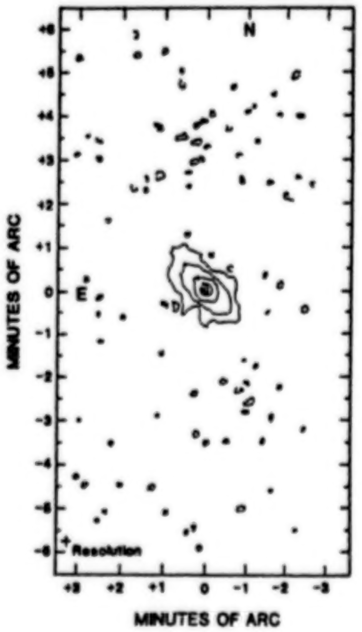

Figure 3: The continuum structure of NGC 660 at 20-cm. The peak brightness temperature in the map is 589°K and the contour levels are 2.95, 11.78, 58.90, 294.50, and 589.00°K.

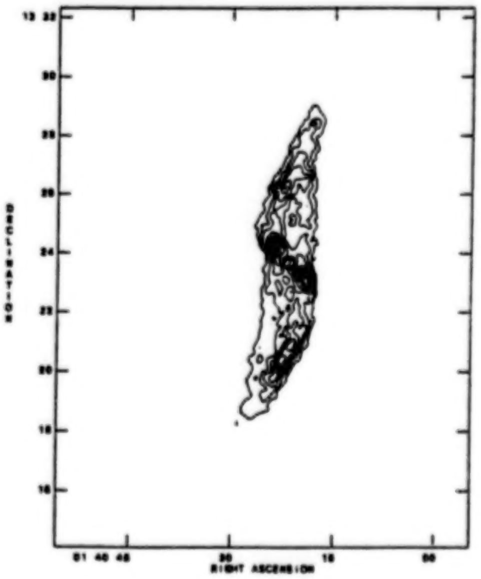

Figure 4: The integrated HI flux of NGC 660. The peak flux observed is 1.6167×10^3 Jy/Beam*m/s and the contour levels are at $1.8615 \times 10^2 \times (1, 2, 3, 4, 5, 6, 7, 8)$ Jy/Beam*m/s. Owing to absorption at the center of the galaxy, there is a hole in the map.

HI Emission

NGC 660 appears to be a disturbed galaxy for which there is strong evidence that two HI kinematical systems exist: one along the principal axis of the ellipsoidal optical system and one inclined to it by about 53°. A kinematic fit to the line of nodes for the extended HI component gives a major axis position angle of -7°, inclination I = 60.5° , and a systemic velocity V = 842 km/s. The position angle for the continuum major axis and narrow dust lane is 46°. A contour map of the integrated flux (figure 4) reveals that the short, intense diagonal feature is associated with the narrow equatorial dust lane, while the extended gas is associated with the tilted asymmetric ring.

Even though rotation dominates the velocity pattern of the gas, gross deviations from circular motion are apparent (see figure 5). A comparison of the corrected H-alpha maps of Young, Kleinman, and Allen (1988), to our HI velocity field shows that there may be a connection between the disturbed velocity contours in HI (see figures 5 and 6) and an arc of HII regions, seen in the H-alpha maps, extending towards the southwest.

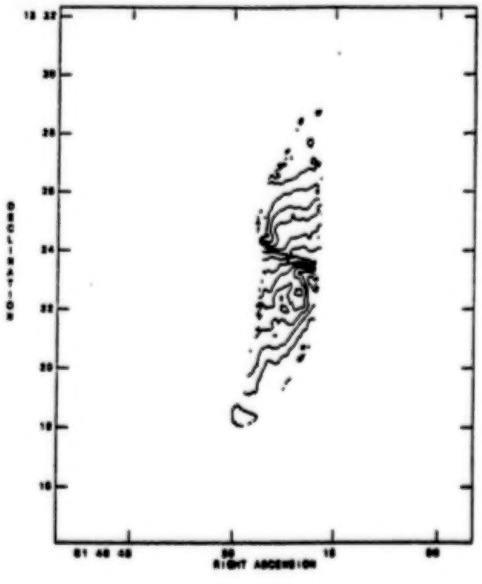

Figure 5: Integrated Mean Velocity field of NGC 660. The contour levels are at 700, 720, 740, 760, 780, 800, 820, 840, 860, 880, 900, 920, 940, 960, and 980 km/s.

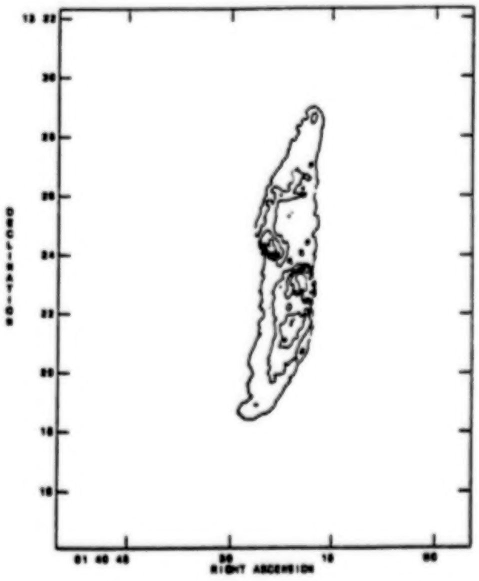

Figure 6: Integrated Mean Velocity Dispersion. The peak contour level observed is 61.5 km/sec. Contour levels are drawn at 10, 20, 30, 40 50, and 60 km/s.

The axis velocity diagram, drawn along P.A. 46° (figure 7) shows clearly the multi-peaked HI spectra in emission and complex, broad, deep absorption at the galactic center. Where the two systems intersect along the line of sight the observed HI brightness temperature is 60°K. The axis velocity diagram for P.A. -7° is given in figure 8.

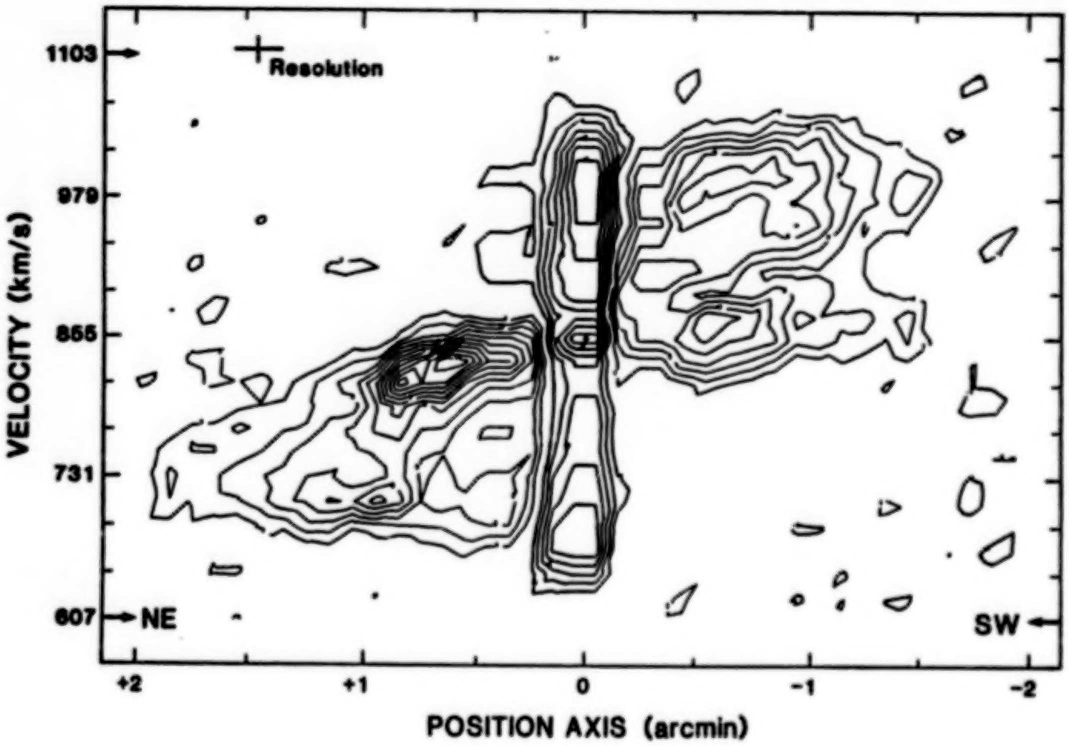

Figure 7: Axis Velocity Profile through the center at P.A. 46°. Contours are plotted at intervals of 4.5°K. The dark contours are negative and represent absorption. The deepest feature is less than -31°K and the brightest feature is greater than 49°K. Note the multiple peaks in the spectra.

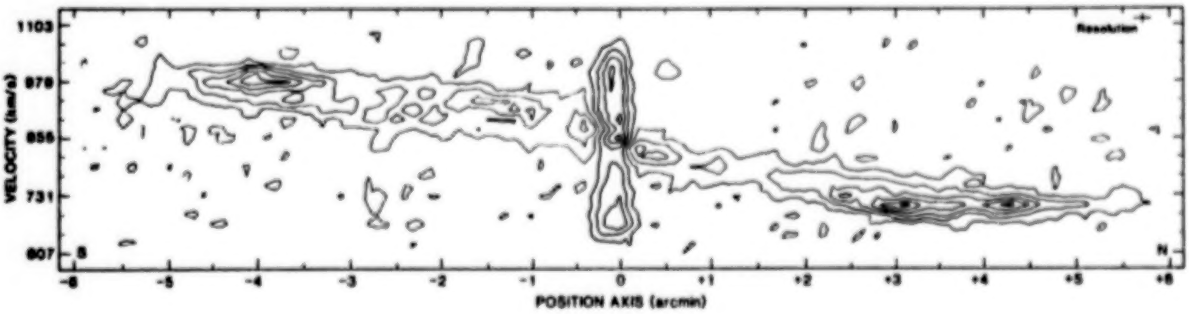

Figure 8: Axis Velocity Profile through the center at P.A. -7°. Contour intervals are at -31.36, -22.40, -13.44, -4.48, 4.48, 13.44, 22.40, 31.36, 40.32, and 49.28°K.

Absorption of the strong central continuum source by HI can be seen in both axis velocity profiles. The mean velocity of the absorbing gas appears to vary systematically across the weakly resolved source, with the width of both components exceeding the half power width of the beam by about 30 percent. The absorbing gas could be associated with a rotating nuclear ring or disk, or it may be distributed along the line of sight and associated with the two inclined kinematical systems. Higher resolution observations of the absorption are required in order to distinguish between these two possibilities. In addition, we note a velocity difference of 20-40 km/s between the absorption and emission peaks at the low velocity end of the profile taken along P.A. 46°. This velocity difference may be indicative of outflow.

The apparently disturbed nature of this galaxy, its nuclear structure, and its starburst characteristics provide strong support for the hypothesis that this is a merged or merging system in which interaction between the systems triggered an intense burst of star formation.

The Companion Galaxy, UGC 01195

The companion galaxy to NGC 660, UGC 01195 is described in the UGC Catalogue of Galaxies as an irregular, distorted, slightly arc-shaped galaxy that exhibits no spiral structure. The rotation of the hydrogen in UGC 01195 is shown schematically in figure 9, by superposition of every other channel in which it was detected. Our channel maps give a total velocity width of 124 km/s and a mean systemic velocity of 772 km/s, corresponding to an observed radial velocity difference between NGC 660 and UGC 01195 of 70 km/s. Ignoring unknown projection effects, the mass required to bind UGC 01195 is 4.1 X $10^{10} M_{\odot}$. This is significantly less than the Keplerian estimate of the mass of NGC 660; thus, it is not improbable that UGC 01195 is a bound satellite.

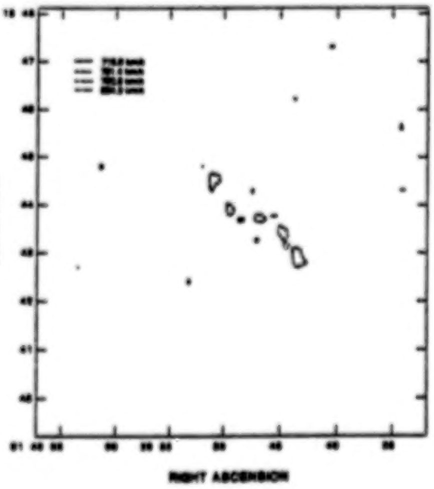

Figure 9: The rotation of UGC 01195 is shown by superposition of every other channel in which HI was detected.

References

Condon, J.J., Condon, M.A., Gisler, G., and Puschell, J.J. 1982, Ap. J., 252, 102.

Young, J.S., Kleinman, S.G., and Allen, L.E. 1988, Ap. J. 334, L63.

A SPIRAL-LIKE DISK OF IONIZED GAS IN IC 1459: SIGNATURE OF A MERGING COLLISION?

Paul Goudfrooij[1], H.U. Nørgaard-Nielsen[2], H.E. Jørgensen[3], L. Hansen[3]
and T. de Jong[1]

[1]Astronomical Institute "Anton Pannekoek", University of Amsterdam,
Roetersstraat 15, 1018 WB Amsterdam, The Netherlands
[2]Danish Space Research Institute, Gl. Lundtoftevej 15, 2800 Lyngby, Denmark
[3]Copenhagen University Observatory, Øster Voldgade 3, 1350 København K, Denmark

Abstract. We report the discovery of a large (15 kpc diameter) Hα+[NII] emission-line disk in the elliptical galaxy IC 1459, showing weak spiral structure. The line flux peaks strongly at the nucleus and is more concentrated than the stellar continuum. The major axis of the disk of ionized gas coincides with that of the stellar body of the galaxy. The mass of the ionized gas is estimated to be $\sim 1\ 10^5$ M$_\odot$, less than 1% of the total mass of gas present in IC 1459. The total gas mass of 4 10^7 M$_\odot$ has been estimated from the dust mass derived from a broad-band colour index image and the IRAS data. We speculate that the presence of dust and gas in IC 1459 is a signature of a merger event.

1. Introduction

Contrary to the traditional view of elliptical galaxies as being essentially free of interstellar matter, advances in instrumental sensitivity have caused a recent renaissance of interest in dust and gas in elliptical galaxies. Many elliptical galaxies are now known to contain dust (*e.g.*, Véron-Cetty and Véron [1988] and references therein), HI gas (Knapp *et al.*, 1985), hot ($\sim 10^7$ K) X-ray gas (Canizares *et al.*, 1987) and ionized gas (Phillips *et al.*, 1986). Moreover, Jura *et al.* (1987) have shown that the *Infrared Astronomical Satellite* (IRAS) detected more than 50% of the elliptical galaxies with $B_T^0 < 11$ mag. in the *Revised Shapley-Ames Catalog* (RSA, Sandage and Tammann, 1981), indicating the presence of $10^7 - 10^8$ M$_\odot$ of cold interstellar matter. Thus dust and gas in ellipticals seems to be quite common.

The origin and evolution of the dust and gas are still not fully understood. To study the origin and evolution of interstellar matter in elliptical galaxies systematically we are currently undertaking a survey of all ellipticals with $B_T^0 < 12$ mag. in the RSA catalog. This survey aims at obtaining deep CCD colour index images and narrow-band (Hα+[NII]) images as well as spectroscopic data.

The CCD images of IC 1459, one of the galaxies in our sample, turned out to be so striking and unusual that we decided to present the results here.

The giant elliptical IC 1459 is a member of a group of galaxies (group no. 15 of Huchra and Geller (1982)), containing 10 galaxies. As already noticed by Sparks *et al.* (1985), there is some dust absorption near its centre. The colour index image presented here confirms this result. It is one of the few ellipticals which are detected by IRAS in all four passbands (Jura *et al.*, 1987). It is also a compact, powerful radio source with a brightness of 1.0 Jy at 6 cm (Sadler *et al.*, 1989). Finally, it has been detected by the EINSTEIN satellite (Forman *et al.*, 1985). Franx and Illingworth (1988) discovered a fast (170±20 km s^{-1}) counter-rotating core, which is suggestive of a recent merging collision.

2. Observations and Results

Deep CCD imaging of IC 1459 has been performed using the ESO/MPI 2.2m and Danish 1.5m telescopes on La Silla, Chile. The galaxy was observed through Johnson B and V filters as well as through two narrow-band filters: one centered on the redshifted Hα line and one on the nearby continuum.

The final B−V colour index image of IC 1459 was obtained by dividing the (processed) V image by the B image. With the present high-quality data this technique reliably reveals features redder than about 0.005 in B−V over their surroundings.

To produce the final emission-line maps, we scaled the continuum image to the on-line image by comparing the counts in the two frames not too close to the dusty features as determined from the colour index image. After scaling the continuum image it was subtracted from the on-line image, yielding an image containing emission only.

A detailed account of the reduction and analysis method is given elsewhere (Goudfrooij *et al.*, 1990). Here we only present results on the dust and ionized gas in IC 1459.

2.1. Mass of neutral gas

In the B−V image (Fig. 1a) a red, diffuse nuclear region shows up. The mean colour excess of the dusty feature equals $E_{B-V} = 0.03$ over an area of 1083 $('')^2$. Assuming $H_0 = 50$ km s^{-1} Mpc^{-1} and $N_H/E_{B-V} = 5.8\ 10^{21}$ cm^{-2} mag^{-1} (Bohlin *et al.*, 1978) we find $M_{gas,B-V} = 3.6\ 10^7 M_\odot$. This mass estimate may be compared with an estimate based on the *IRAS* 60 and 100 μm data, using $M_{dust} = F_\lambda R^2 / [\kappa_\lambda B_\lambda(T)]$ where F_λ is the observed fluxdensity at distance R, κ_λ is the dust opacity and $B_\lambda(T)$ is the Planck function. Adopting $\kappa_\lambda \propto \lambda^{-1}$, a uniform temperature of 35 K as derived from the *IRAS* S_{100}/S_{60} ratio (Jura *et al.*, 1987) and $M_{gas}/M_{dust} = 100$, we find $M_{gas,IRAS} = 3.9\ 10^7 M_\odot$. This agrees very well with $M_{gas,B-V}$. The gas masses mentioned above are in agreement with the upper limit $M_{HI} < 2\ 10^8$ $M_\odot$ as derived by Welsh *et al.* (1990) from radio observations.

2.2. *Mass of ionized gas*

In Fig. 1b the Hα+[NII] emission-line map is shown. The ionized gas is distributed in an extended disk, showing weak spiral structure.

Using the emission-line ratio [NII]λ6583/Hα = 1.44 as determined by Phillips *et al.* (1986) from a long-slit spectrum of IC 1459 taken in P.A. 144°, *i.e.* refering to the nuclear region only, we derive L(Hα) = 5.3 10^{40} erg s^{-1} from our Hα+[NII] map. Adopting an electron density of $\sim 10^3$ cm^{-3} as implied by the [SII]$\lambda\lambda$6717,6731 doublet ratio in the spectrum of Phillips *et al.* and standard (case B) recombination theory we derive a mass of ionized gas $M_{HII} = 1.2\ 10^5 M_\odot$.

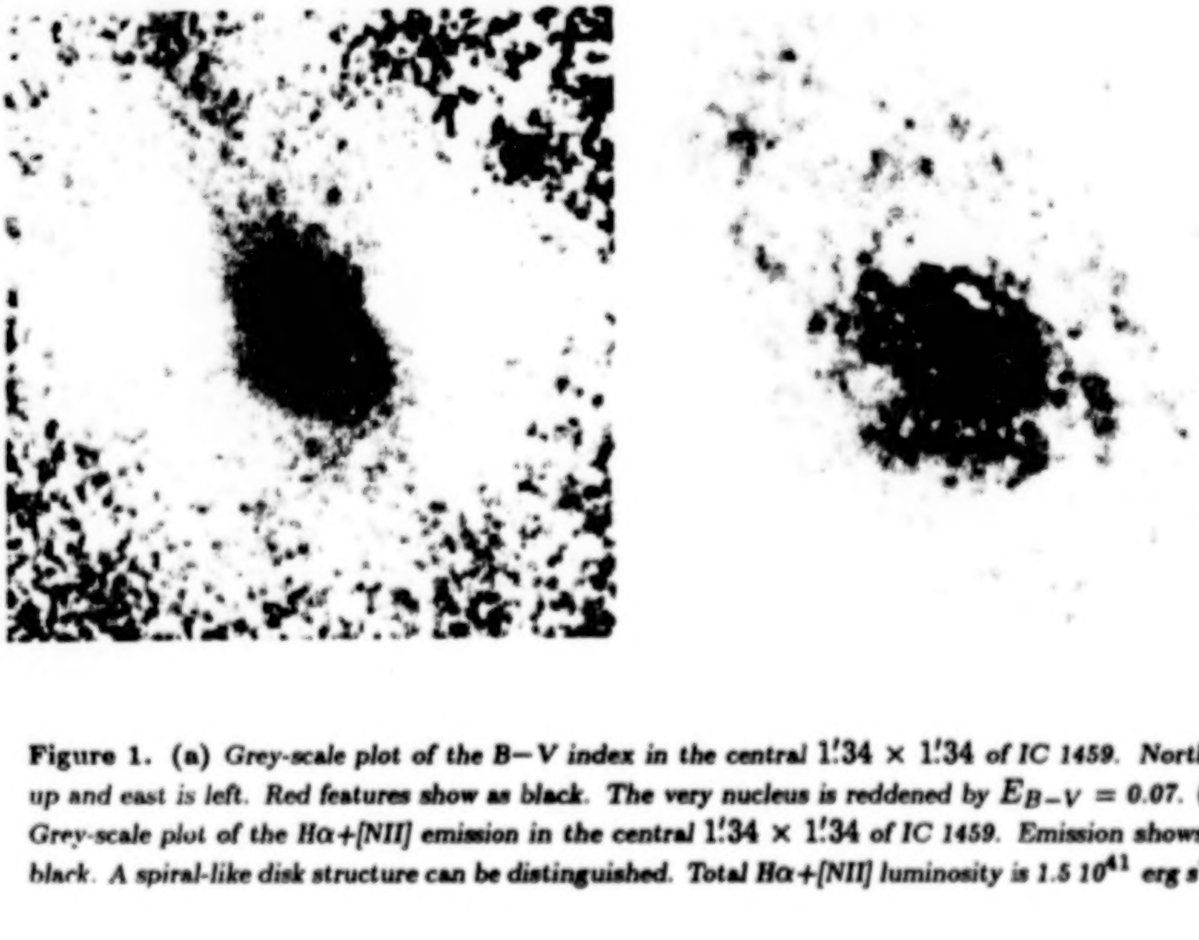

Figure 1. **(a)** *Grey-scale plot of the B−V index in the central 1.'34 × 1.'34 of IC 1459. North is up and east is left. Red features show as black. The very nucleus is reddened by E_{B-V} = 0.07.* **(b)** *Grey-scale plot of the Hα+[NII] emission in the central 1.'34 × 1.'34 of IC 1459. Emission shows as black. A spiral-like disk structure can be distinguished. Total Hα+[NII] luminosity is 1.5 10^{41} erg s^{-1}.*

3. Discussion

3.1. *On the morphology of the ISM in IC 1459*

The colour index map and the Hα+[NII] map show some interesting differences. First, the colour index map shows a smooth, diffuse colour gradient in the central region, whereas the Hα+[NII] intensity peaks very strongly at the centre. Secondly, the diffuse "dust patches" as seen in Fig. 1a extend into the outer parts of the galaxy along a position angle which deviates from that of the major axis of the disk of ionized gas. Thus the neutral and ionized gas in IC 1459 are probably distributed in a different way.

The morphology of the interstellar medium in IC 1459 suggests that the presence of dust and gas in this galaxy is due to a merger event. Since the disk of ionized gas coincides with the photometric major axis throughout its measurable size of 15 kpc, the study by Tohline *et al.* (1982) suggests that the merging collision has taken place ~3 10^9 yrs ago. This estimate depends on the original alignment of the smaller galaxy with the giant elliptical. The innermost part of the emission-line region is not ellipsoidal but rather irregular, indicating a young phenomenon. As to the weak spiral structure of the extended disk, this is probably not a remnant of the intrinsic shape of the smaller gas-rich galaxy. Tidal forces during the merging collision will have removed any pre-existing structure. The spiral-like structure might reflect the response of the gas in the gravitational potential of the elliptical galaxy.

3.2. Possible ionization mechanisms for the gas

Heat conduction from hot X-ray gas: This possibility has recently been put forward by Sparks *et al.* (1989) and de Jong *et al.* (1990) for the dominant cluster elliptical NGC 4696 in which the dust and ionized gas are distributed similarly. However, this mechanism does not seem to be able to account for the Hα emission of IC 1459. Although IC 1459 has been detected by the EINSTEIN satellite, the data by Canizares *et al.* (1987) show that its X-ray luminosity is probably dominated by the contribution of discrete sources (*e.g.*, binary X-ray sources and globular clusters). Thus the amount of hot gas in IC 1459 is presumably small.

Ionization by shock-heating in cloud-cloud collisions: This is to be expected while the gas captured by the giant elliptical is settling down to a rotating disk.

Photoionization by a central non-thermal source: Many features in the nucleus point at this possibility. The spectrum of the nucleus of IC 1459 by Phillips *et al.* (1986) is typical of a LINER and broad [NII]λ6583 line (426 km s^{-1} FWHM). Moreover, IC 1459 is identified with the radio source PKS 2254−367 which is a compact active radio galaxy with a spectral index ~0.0 (Disney and Wall, 1977) and it has a large far-infrared S_{25}/S_{60} ratio, characteristic of an active nucleus (de Grijp *et al.*, 1985; de Grijp and Goudfrooij, 1990).

Burst(s) of star formation, triggered by the merging collision: It seems that we may not discard this possibility, at least for the outer parts of the disk. From the observed Hα flux we derive a total Hydrogen recombination rate which can be maintained by ~3 10^4 B0 stars. Adopting M_V = −4.0 and B−V = −0.29 for a B0 star (Kurucz, 1979) we obtain B ~ 16.6 due to early-type stars. The observed B magnitude in the corresponding area equals B = 12.7 so that the observed amount of Hα emission could be due to recently formed early-type stars, which are unobservable in the broad-band photometry.

More severe constraints on the source of ionization and the kinematics of the extended emission-line regions in IC 1459 cannot be put until high signal-to-noise spectroscopic data are available.

Acknowledgements. This work is based on observations collected at the European Southern Observatory, La Silla, Chile. P.G. acknowledges ***Leids Kerkhoven Bosscha Fonds*** and IAU travel grants, and thanks Bill Sparks for useful discussions.

References

Bohlin, R.C., Savage, B.D., Drake, J.F.: 1978, *Ap. J.* **224**, 132

Canizares, C.R., Fabbiano, G., Trinchieri, G.: 1987, *Ap. J.* **312**, 503

Disney, M.J. and Wall, J.V.: 1977, *Mon. Not. R. Astron. Soc.* **179**, 235

Forman, W., Jones, C., Tucker, W.: 1985, *Ap. J.* **293**, 102

Franx, M. and Illingworth, G.D.: 1988, *Ap. J. Lett.* **327**, L55

Goudfrooij, P., Nørgaard-Nielsen, H.U., Hansen, L., Jørgensen, H.E., de Jong, T.: 1990, *Astron. Ap. (Lett.)*, in press

de Grijp, M.H.K., Miley, G.K., Lub, J., de Jong, T.: 1985, *Nature* **314**, 240.

de Grijp, M.H.K. and Goudfrooij, P.: 1990, in preparation.

Huchra, J. and Geller, M.: 1982, *Ap. J.* **257**, 432

de Jong, T., Nørgaard-Nielsen, H.U., Hansen, L., Jørgensen, H.E.: 1990, *Astron. Ap.*, in press

Jura, M., Kim, D.W., Knapp, G.R., Guthathakurta, P.: 1987, *Ap. J. Lett.* **312**, L11

Knapp, G.R., Turner, E.L., Cunniffe, P.E.: 1985, *A. J.* **90**, 454

Kurucz, R.L.: 1979, *Ap. J. Suppl.* **40**, 1

Phillips, M.M., Jenkins, C.R., Dopita, M.A., Sadler, E.M., Binette, L.: 1986, *A. J.* **91**, 1062

Sadler, E.M., Jenkins, C.R., Kotanyi, C.G.: 1989, *Mon. Not. R. Astron. Soc.*, in press

Sandage, A. and Tammann, G.A.: 1981, *A Revised Shapley-Ames Catalog of Bright Galaxies*, Carnegie Institution of Washington. (RSA)

Sparks, W.B., Wall, J.V., Thorne, D.J., Jorden, P.R., van Breda, I.G., Rudd, P.J., Jørgensen, H.E.: 1985, *Mon. Not. R. Astron. Soc.* **217**, 87

Sparks, W.B., Macchetto, F., Golombek, D.: 1989, *Ap. J.* **345**, 153

Tohline, J.E., Simonson, G.F., Caldwell, N.: 1982, *Ap. J.* **252**, 92

Véron-Cetty, M.P. and Véron, P.: 1988, *Astron. Ap.* **204**, 28

OBSERVATIONS OF MULTIPLE NUCLEUS GALAXIES

W. Kollatschny
Universitäts-Sternwarte
D-3400 Göttingen, F.R.G.

Disturbed Galaxies with two nuclei display the final state of the interaction process of two galaxies (Kollatschny et al., 1986; Fricke and Kollatschny, 1989). A few of these double nucleus galaxies contain Seyfert nuclei.

Seyfert galaxies with multiple nuclei

The "Catalogue of Quasars and AGN's" of Veron & Veron (1989) contains 243 galaxies of Seyfert-type 1, 2 or 3 with $m_V \leq 15$ and $v_{rad} \leq 20{,}000$ km s $^{-1}$. Seven of these Seyfert galaxies have two optical nuclei; the nuclei have typical separations of 3 to 10 arcsec corresponding to 2 - 6 kpc.

For all these morphological disturbed multiple Seyfert galaxies, it is necessary to determine the internal velocity field to be sure that they are two galaxies in the late stages of merging. Direct images and the velocity fields along the line joining the two nuclei are shown in Figs 1 and 2 for the Seyfertgalaxies Mkn 266 and Mkn 739 (Kollatschny and Fricke, 1984; Netzer et al., 1987).

Table 1: Luminosities of multiple nucleus and 'undisturbed' Seyfert galaxies

	mult. nucl.	undist.	
$\log L_V[w]$	37.40	36.99	Sey 1
	37.14	36.66	Sey 2
$\log L_B[w]$	37.05	36.64	Sey 1
	37.09	36.22	Sey 2
$\log L_{FIR}[w]$	37.63	36.70	Sey 1
	37.88	36.76	Sey 2
$\log L_{radio(6cm)}[w]$	32.12	31.39	Sey 1
	32.81	31.71	Sey 2
$\log H\alpha[w]$	35.96	35.21	Sey 1
	34.85	34.21	Sey 2

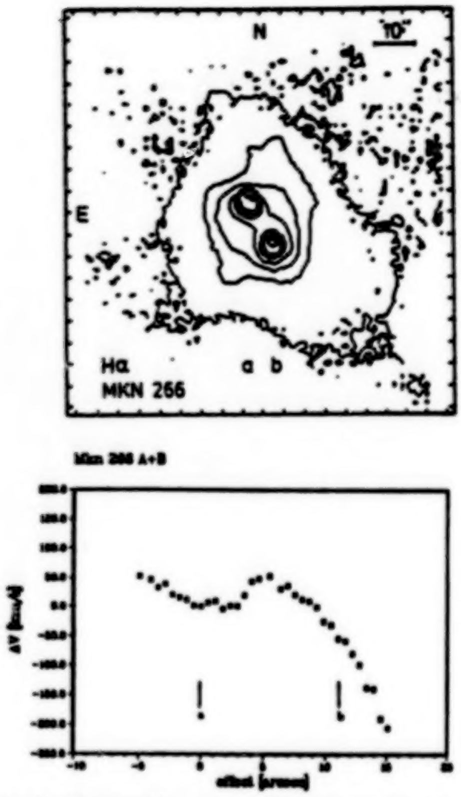

Fig. 1a,b: Optical image and relative velocity of the gas parallel to the nuclei of Mkn 266

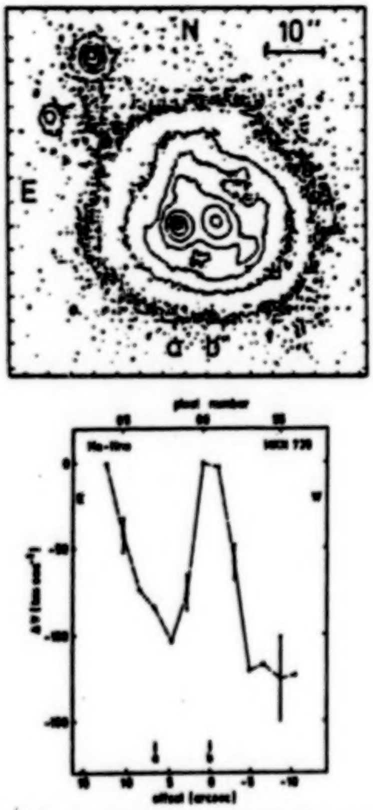

Fig. 2a,b: Optical image and relative velocity of the gas parallel to the nuclei of Mkn 739

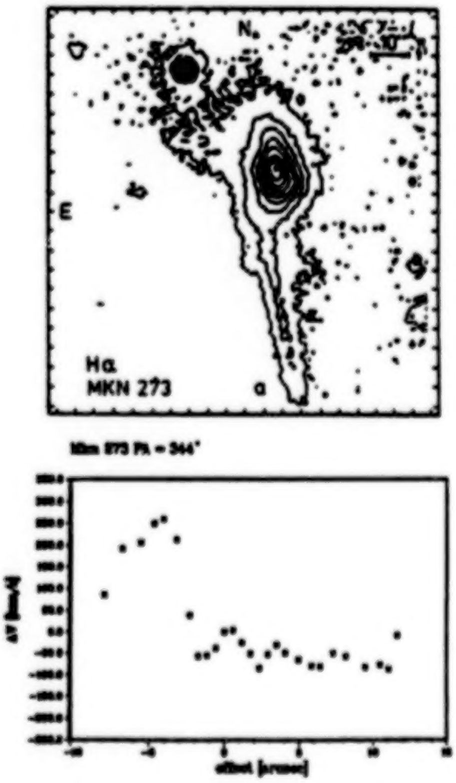

Fig. 3a,b: Optical image and relative velocity (P.A.:344°) of the gas of Mkn 273

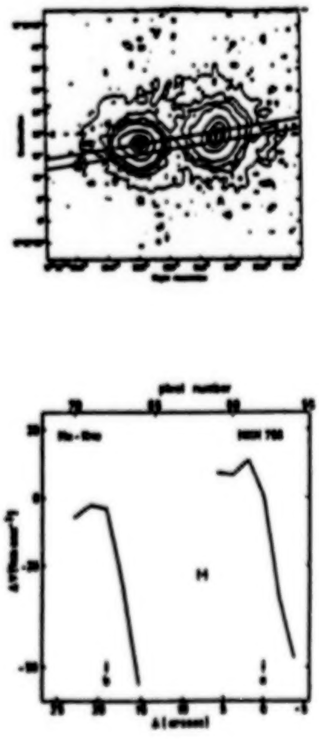

Fig. 4a,b: Optical image and relative velocity of the gas parallel to the two nuclei of Mkn 788

Making the assumption that the Seyfert galaxies Mkn 231 and Mkn 273 (Fig. 3) (Yorke and Kollatschny, 1985) are galaxies in the final state of merging, having strong tidal arms but unresolved nuclei, one can estimate that 4 percent of all Seyfert galaxies are in the merging process.
The luminosities of multiple nucleus Seyfert galaxies are extremely high in comparison to morphologically undisturbed Seyfert galaxies. In Table 1, mean values of the visual and blue luminosities and of the far-infrared and radio (6 cm) luminosities as well as the Hα fluxes are listed for both classes. In addition we have separated Seyfert 1 and Seyfert 2 galaxies.

In all cases the luminosities of double nucleus Seyfert galaxies are higher by a factor of more than two with respect to 'undisturbed' Seyfert galaxies. This result might be explained by higher luminosities in the early phases of a Seyfert's life - under the assumption that the nonthermal activity is triggered by tidal interaction - and/or additional strong starburst phenomena.
Due to strong nuclear absorption, the UV spectra of these Seyfert nuclei are unusually weak.

Non-Seyfert nuclei in double nucleus galaxies

Corresponding to the Seyfert survey, we have obtained the Hα and FIR luminosities as well as the [OIII]5007/Hβ line ratios of a small sample of non-Seyfert nuclei in double nucleus galaxies. Figs. 4a,b show the direct image and the velocity field of the double starburst galaxy Mkn 788 (Kollatschny et al., 1986). We have compared our measurements with those of 'normal' interacting galaxies of Keel et al. (1985) and Bushouse (1987). The mean FIR luminosity per nucleus in multiple systems is the same as that of interacting galaxies. But the mean Hα luminosities as well as the [OIII]/Hβ line ratios (see Fig. 5) are higher by a factor of 1.5 - 2 than those of 'normal' interacting galaxies.

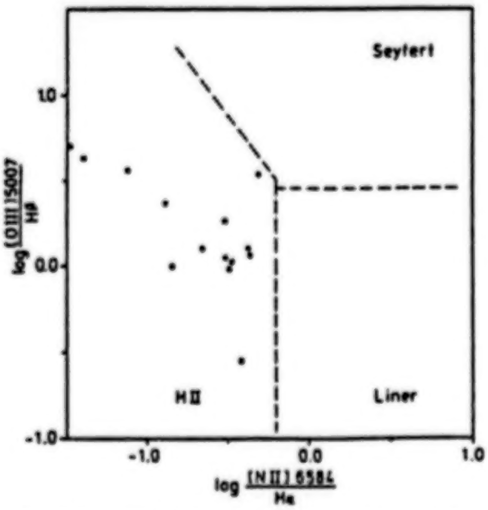

Fig. 5a: Line ratios for the individual non-Seyfert nuclei of the double nucleus galaxies Mkn 296, 463, 480, 739, 788, 789, 930, 1027

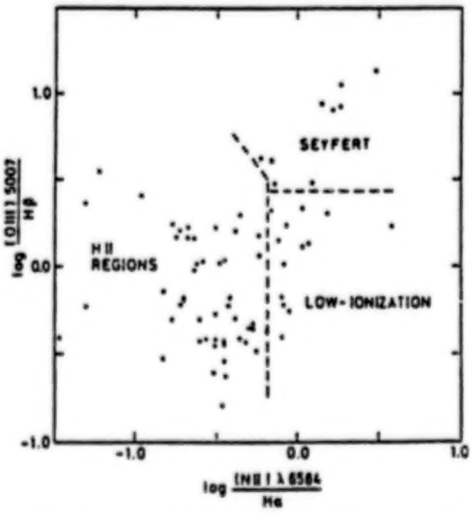

Fig. 5b: Observed line ratios in the spectra of interacting galaxies (Keel, 1985)

Partly based on observations at the German-Spanish Astronomical Center, Calar Alto, operated by the Max-Planck-Institut für Astronomie in Heidelberg, jointly with the Spanish National Commission for Astronomy.

References

- Bushouse, H.A., 1987: *Astrophys. J.* **320**, 49
- Fricke, K.J., Kollatschny, W., 1989: *IAU-Symp. 134 on "Active Galactic Nuclei"* (D. Osterbrock ed.), p. 425
- Keel, W.C. et al., 1985: *Astron. J.* **90**, 708
- Kollatschny, W., Fricke, K.J., 1984: *Astron. Astrophys.* **135**, 171
- Kollatschny, W., Fricke, K.J., Hellwig, J., 1986: *Proc. on "Structure and Evolution of Active Galactic Nuclei"* (G. Giuriccin ed.), p. 605
- Kollatschny, W., Netzer, H., Fricke, K.J., 1986: *Astron. Astrophys.* **163**, 31
- Netzer, H., Kollatschny, W., Fricke, K.J., 1987: *Astron. Astrophys.* **171**, 41
- Veron-Cetty, M.-P., Veron, P., 1989: A Catalogue of Quasars and Active Galactic Nuclei (4th Edition), *ESO Scientific Report No. 7*
- Yorke, H.W., Kollatschny, W., 1985: Proc. on *"Extragalactic Infrared Astronomy"* (P.M. Goudhalekar ed.), p. 1

THE DOUBLE NUCLEUS GALAXIES MKN 423 AND MKN 739

Piero Rafanelli
Department of Astronomy, University of Padova, Italy
Paolo Marziani
International School for Advanced Studies, Trieste, Italy

1. *Mkn 423*

1a. *Introduction*

Long slit spectroscopy and imaging of Mkn 423 and Mkn 739 have been performed at the 2.2 m and 3.5 m telescopes of the Calar Alto Observatory using both CCD and photographic detectors. Low and medium resolution spectra (1.8Å, 3.5Å, 6.0Å) together with V images have permitted to demonstrate the merging nature of Mkn 423 and the double structure of the NLR of its Seyfert component. This last feature has been found also in the NLR of the Seyfert component of Mkn 739, a double system the two components of which are counterrotating.

1b. *Morphology*

Mkn 423 is a Seyfert galaxy located in the Abell cluster No. 1257 at an angular distance of 10 arcmin from its center, which at the redshift of the galaxy z=0.0325 corresponds to a linear distance of 0.28/*h Mpc* (scale=0.47/*h kpc/arcsec*). The complex nature of this galaxy was firstly recognized by Markarian and Lipovetskii (1974), who described Mkn 423 as a spherical galaxy with a jet. More recently Dahari (1985) classified this object as *a double nucleus galaxy with distorted morphology* in his survey of Seyfert galaxies with companions. The contour map of a deep image, Figure 1, shows the presence of a resolved structure of elliptical shape B, located at a distance d=9 *arcsec* (P.A.=169°) from the bright Seyfert nucleus A. The major and minor axis of B have angular size a=4.5 *arcsec*, b=3 *arcsec* respectively and the P.A. of a is 188°. The Seyfert nucleus A has spherical symmetry and its radius is 5 *arcsec*. A and B are connected by a bridge of matter and are both surrounded by a pear-shaped structure of size 30×19 *arcsec*.

1c. *Emission-line regions*

Long slit spectra obtained setting the slit in the N-S direction along the Seyfert nucleus A and the region B show strong emission lines of [SII], [NII], Hα and Hβ, which extend on the southern side of the spectrum of A. Hα peaks in correspondence of B and lengthens over the southern part of the galaxy indicated with C in Figure 2. Conversely the [OIII] nebular lines are not extended, but confined to the spectrum of A. The contour map of the [OIII]λ5007 nebular line, Figure 3, shows that the core of the line is formed by two knots A1 and A2 of different heliocentric radial velocity, v_{A1}=9580 *km/s*, v_{A2}=9760 *km/s*, from which two components stream out each up to a distance of 5 *arcsec* from the nucleus: one from A1 towards southern,the other one from A2 towards northern. We take v_{A2} as the systemic velocity. The centers of A1 and A2 are not aligned along the direction of the dispersion, Figure 3, A2 being located ≤ 1.0 *arcsec* to the northern of A1. However the spatial separation along the slit of the two nuclear blobs is not large enough to extract their spectra.

The three regions A, B and C, indicated in Figures 1, 2, have been then used for the diagnostics of the emitting gas. The spectrum of the nucleus A is characterized by the presence beneath Hα of a broad component, not present in the Hβ profile, as it is common in Seyfert 1.9 galaxies.

The [OIII]λ5007/Hβ versus [SII]$\lambda\lambda$(6716+6731)/Hα and [OIII]λ5007/Hβ versus [NII]λ 6583/Hα diagnostic diagrams, Figures 4a,b, (Veilleux and Osterbrock, 1987) indicate that the Narrow Line Region of A is produced by gas photoionized by a non thermal source, while B and C are both low excitation HII regions. The FWHMs of the narrow lines are significant for the Seyfert nucleus A only (FWHM=400±64 *km/s*) since they are typical of the instrumental profile for the B and C regions.

The narrow component of Hα in the spectrum of A has luminosity $L(H\alpha)_A = 3.34\times10^{40}/h^2$ *erg/s* (Osterbrock, 1981). It follows that $L(H\alpha)_B = 2.25\times10^{40}/h^2$ *erg/s*, $L(H\alpha)_C = 0.40\times10^{40}/h^2$ *erg/s* which correspond to a number of ionizing photons $Q(H)_B = 4.75\times10^{52}/h^2/s$, $Q(H)_C = 8.44\times10^{51}/h^2/s$. A comparison of the H$\alpha$ luminosities of B and C with those typical of Hot Spots, Disk HII Regions, Starburst Nuclei and HII Nuclei (Kennicut *et al.*, 1989) shows that C can be classified as a Disk HII Region, while B can be either one of the most luminous known Disk HII Regions or a Starburst Nucleus.

1d. *Kinematics*

The velocity curve of Mkn 423 is shown in Figure 5 where we have indicated the position and the size of the emitting regions A, B and C. It is evident that A and B are two counterrotating systems since their rotation curves have an opposite inclination. In addition the systemic velocity of B is 100 *km/s* smaller than the systemic velocity of A suggesting that A and B could be two independent, very close systems. The velocity curve of C is the continuation of the southern branch of the velocity curve of B and keeps its inclination. The same behavior is shown by the velocity curve between A and B. This suggests that C and the region between A and B belong to B itself as it is further supported by their comparable size and by their symmetric position relative to the center of B.

1e. *Discussion*

The data collected in this work lead to some interesting conclusion on the complex nature of Mkn 423. The presence of two emitting blobs A1 and A2 in the Seyfert nucleus A reminds the results obtained by Whittle *et al.* (1988) in their study of 'Radio lobes and [OIII] profile sub-structure in Seyfert galaxies' where they found that emission line gas is closely associated with individual radio lobes. This strongly suggests that high resolution radio mapping of the nucleus of Mkn 423 should reveal the presence of at least two radio lobes in the position of A1 and A2 respectively. Many of our results hint the idea that the B region is a galaxy which is merging with the Seyfert nucleus. The morphology and the size of B, its Hα luminosity, typical of a Starburst nucleus, and finally its kinematical independency from the Seyfert nucleus are all evidences that support the classification of B as a galaxy and then the merging nature of Mkn423.

2. *Mkn 739*

2a. *Morphology*

Mkn 739 was firstly recognized as a double nucleus galaxy by Petrosian *et al.* (1979). Its two stellar components, a Seyfert nucleus A and a compact emission line region B, Figure 6, are aligned along the east–west direction and their angular separation is ~ 6 *arcsec*, which at the redshift of the galaxy z=0.0300 corresponds to ~ 2.64 $h^{-1}kpc$ (Scale = 0.44 $h^{-1}kpc$). The two nuclei are located close to the center of a nearly spherical envelope of radius ~ 20 *arcsec* which shows a slight deformation towards northern on its upper side.

2b. *Emission line regions*

Long slit spectra, obtained setting the slit in the east–west direction along the two nuclei A and B, permit to isolate 4 emitting line regions: the two nuclei A and B and two regions C and D located on the western side of B and on the eastern side of A respectively, Figure 6. The contour map of the spectral region Hβ–[OIII]λ5007, Figure 7, gives the size and the location of the regions A, B, C and D. It is worth noting that the spectrum of D, Figure 7, is characterized by the lack of any trace of Hβ and by a strong [OIII]λ5007 line, conversely the spectra of B and C show either lines. Since the [OIII]λ5007/Hβ ratio is an indicator of the ionization degree, it is evident that this is higher in D than in B and C. Another interesting feature is the presence of two blobs A1 and A2 of different radial velocity v_{A1}=8870 *km/s*

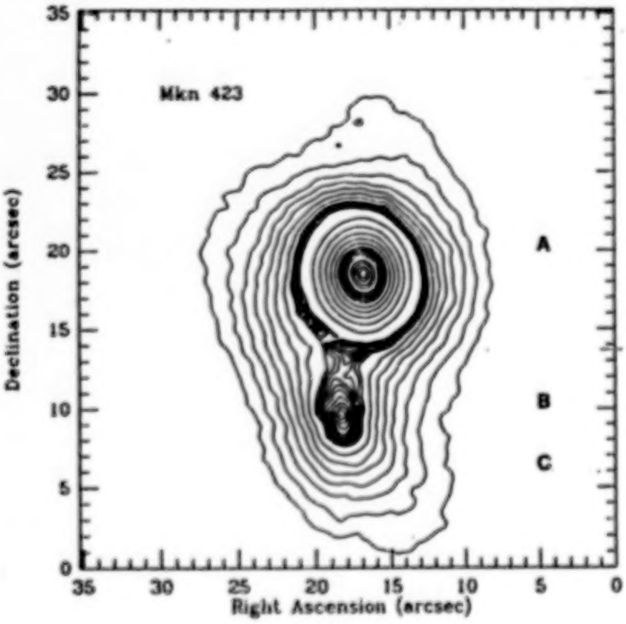

FIG. 1

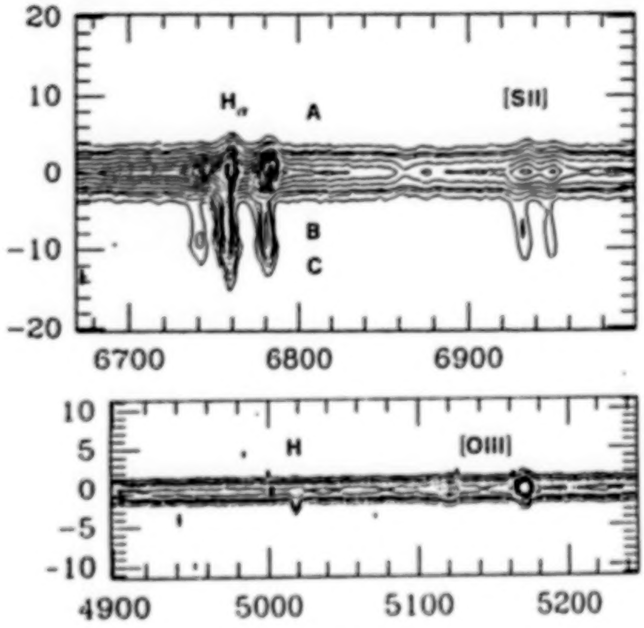

FIG. 2

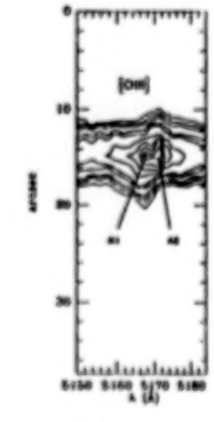

FIG. 3

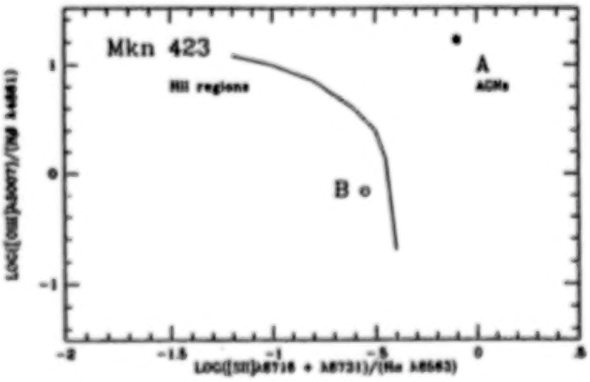

FIG. 4a

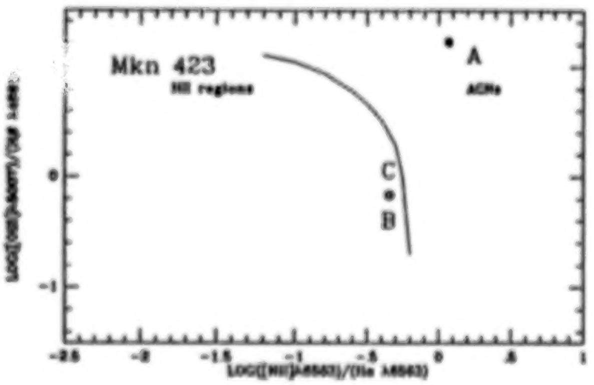

FIG. 4b

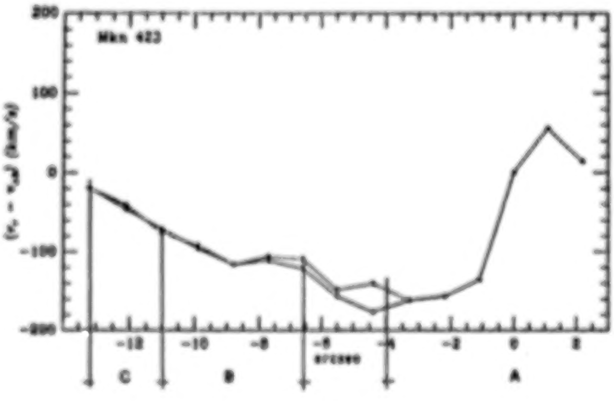

FIG. 5

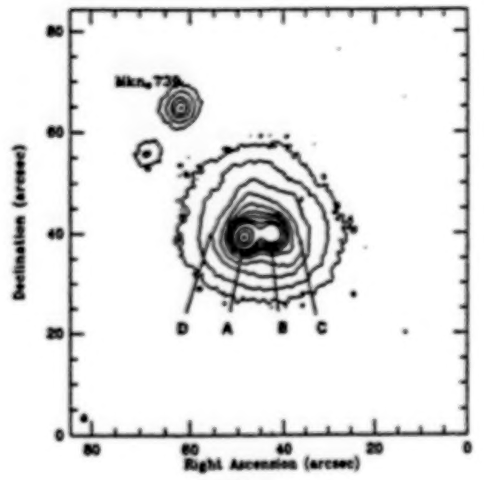

FIG.6

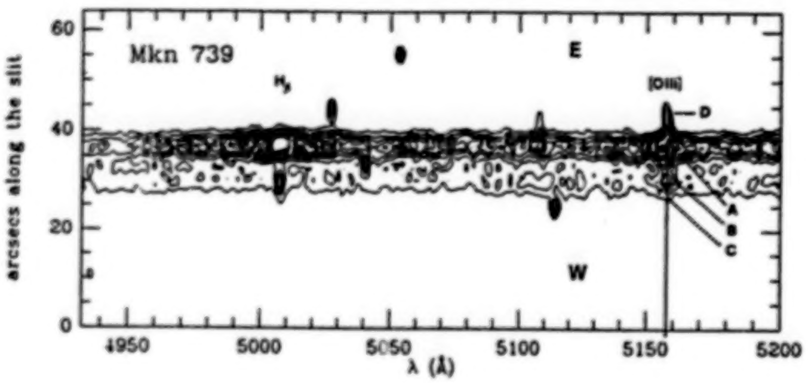

FIG.7

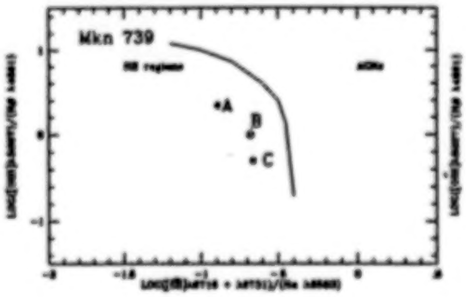

FIG.8a

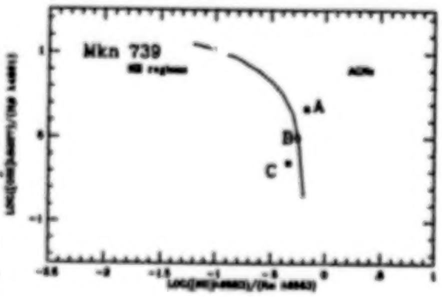

FIG.8b

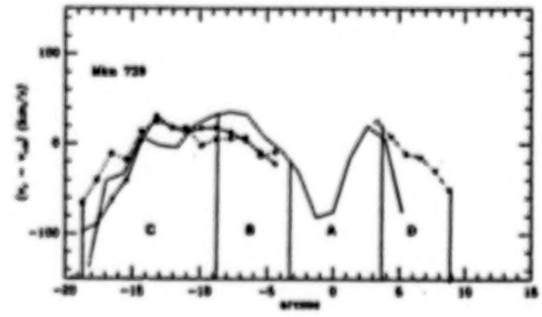

FIG.9

v_{A2}=9020 *km/s* in the core of the line [OIII]λ5007, Figure 7, emitted by the Seyfert nucleus A. The two blobs are located along the direction of the dispersion (east–west) and are not spatially separated along north–south. It is evident from Figure 7 that the systemic velocity of B, C and D corresponds to that of A2 as it is confirmed by the position of their Hα and [NII] lines. We take v_{A2} as the systemic velocity of Mkn 739.

The two blobs A1 and A2 can be considered as the optical counterpart of the two radio lobes observed at 6 cm and 20 cm by Netzer *et al.* (1981) in the nucleus A of Mkn 739. Their position along the north–south direction and their small separation ≤0.3 *arcsec* in the radio maps are consistent with their lack of separation in the optical. The FWHM of the narrow lines in the spectrum of the Seyfert nucleus A is ~290 *km/s*, conversely all spectral lines of B, C and D have an instrumental profile. However the profile of [OIII]λ5007 in the spectrum of the Seyfert nucleus is composite. It shows two peaks which correspond to the two blobs observed in the contour map of the line and an underlying semibroad component with FWZI~2900 *km/s*.

The diagnostic diagrammes of of Veilleux and Osterbrock (1987) applied to the line ratios of B, C, D and to those of the narrow component of A show, Figures 8 a, b, that B and C are typical low excitation HII regions, that D is ionized by a nonthermal source ([OIII]λ5007/Hβ $\geq$1.1) and that the NLR of A can be classified either as a HII region or as a region ionized by a nonthermal source. This ubiquity in the classification of A can be explained in terms of an underestimate of the intensity of the [SII] lines. Since the [SII] doublet is partially plunged in the atmospheric absorption band, the [SII]/Hα ratio is reduced and the point representing A in Fig. 8a is moved towards the area typical of the HII regions. The luminosity of the narrow component of the Hα line emitted by the Seyfert nucleus A is $L(H\alpha)_A=7.14\times10^{40}/h^2\ erg/s$ (Shuder and Osterbrock 1981). It follows that $L(H\alpha)_B=2.93\times 10^{40}/h^2 erg/s$, $L(H\alpha)_C=2.57\times 10^{40}/h^2 erg/s$, which correspond to a number of ionizing photons $Q(H)_B=6.18\times 10^{52}/h^2 photons/s$, $Q(H)_C=5.42\times 10^{52}/h^2 photons/s$.

The Hα luminosities of B and C, the two regions which are ionized by thermal sources, have been compared, as in the case of Mkn 423, with the typical Hα luminosities of Hot Spots, Disk HII Regions, Starburst Nuclei, HII Nuclei. It results that B can be classified as a Starburst Nucleus connected to a giant HII Region C.

2c. *Kinematics*

The velocity curve along the line joining the two nuclei is shown in Figure 9. The velocity of the nucleus B has been arbitrarily put equal to zero while the zero of the angular distances has been put in correspondence of the Seyfert nucleus A. The strange shape of the velocity curve within the nuclear region A arises from the double structure of the core of the narrow lines like [OIII]λ5007. In fact the different intensity and extension along the slit of the two components the line produces a typical U displacement of the center of their blend along the normal to the dispersion. The extranuclear region C connected to the nucleus B and the region D connected to the nucleus A are characterized by a velocity distribution of opposite inclination which suggests counterrotation of the two nuclei and of their connected gas.

2d. *Discussion*

The results of this investigation can be summarized as follows:

1. The NLR of the Seyfert component A is formed by two blobs of different radial velocity, likely due to rotation around their center of mass.

2. The eastern extranuclear region D is ionized by the nonthermal nucleus A.

3. The two main components the system are counterrotating.

References

Dahari O.: 1985, Astron. J. **90**, 1772
Kennicut R.C., *et al.* : 1989 Astron. J. **97**, 1022)
Markarian B.E., Lipovetskii V.A.: 1974, Astrophysics **8**, 89
Netzer H., *et al.* :1981 Astron. Ap.,**171**,41
Osterbrock D.E.: 1981, Ap. J. **249**, 462
Petrosian A.S., *et al.* :1979, Astrophysics **15**, 250)
Shuder J.M., Osterbrock D.E.: 1981, Ap. J. **250**, 55
Veilleux S., Osterbrock D.E.: 1987, Ap.J. Suppl. **63**, 295
Whittle M., *et al.* : 1988, Ap.J. **326**,125

THE POLAR-RING GALAXIES NGC 2685 AND NGC 3808B (VV 300)

V. P. Reshetnikov and V. A. Yakovleva
Astronomical Observatory
Leningrad State University
USSR

INTRODUCTION

Polar-ring galaxies (PRG) are among the most interesting examples of interaction between galaxies. A PRG is a galaxy with an elongated main body surrounded by a ring (or a disk) of stars, gas, and dust rotating in a near-polar plane (Schweizer, Whitmore, and Rubin, 1983). Accretion of matter by a massive lenticular galaxy from either intergalactic medium or a companion galaxy is usually considered as an explanation of the observed structure of PRG. In the latter case there are two possibilities: (1) capture and merging of a neighbor galaxy, and (2) accretion of mass from a companion galaxy during a close encounter. Two PRG formation scenarios just mentioned are illustrated here by the results of our observations of the peculiar galaxies NGC 2685 and NGC 3808B.

NGC 2685

NGC 2685 is one of the best known PRG's (Figure 1). The photographic observations of this galaxy were made in March 1978 using 2.6 m telescope of Byurakan Astrophysical Observatory (USSR). The prime focus plates (scale 21"/mm) were obtained in the UBV standard system (3 exposures in each band). For the details of the reduction procedure see Makarov, Reshetnikov, and Yakovleva (1989).

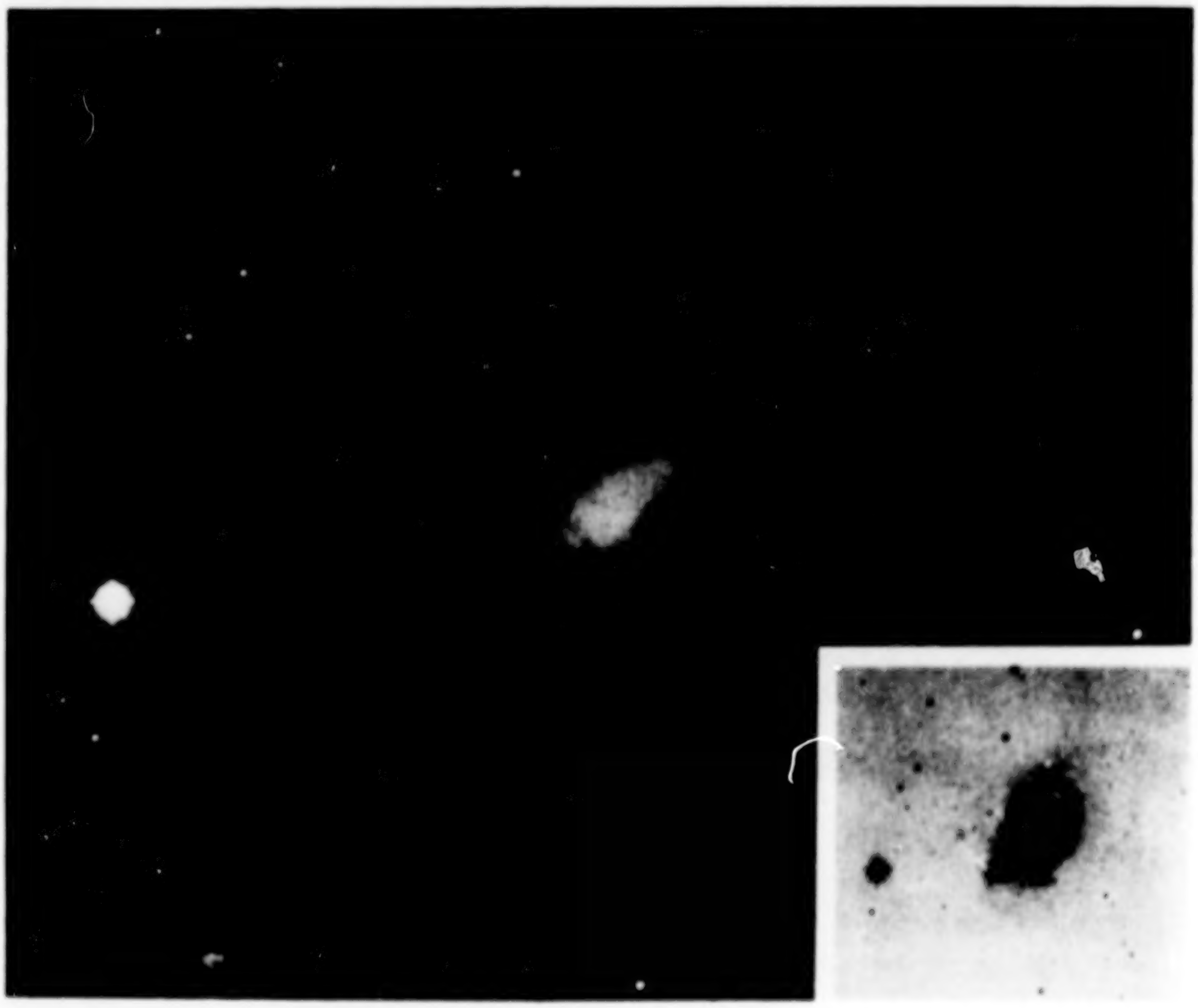

Figure 1. Reproduction of NGC 2685 from THE HUBBLE ATLAS OF GALAXIES (scale 1 mm = 2".2).

Main Body

Figure 2 shows the B-band isophotes of NGC 2685. One can see that in the SW part of the galaxy undistorted by absorption the isophotes are nearly elliptical. Figure 3 is a plot of the orientation of these ellipses and their apparent axial ratios as a function of radial distance. The shapes of the curves are typical for two-component SO galaxies.

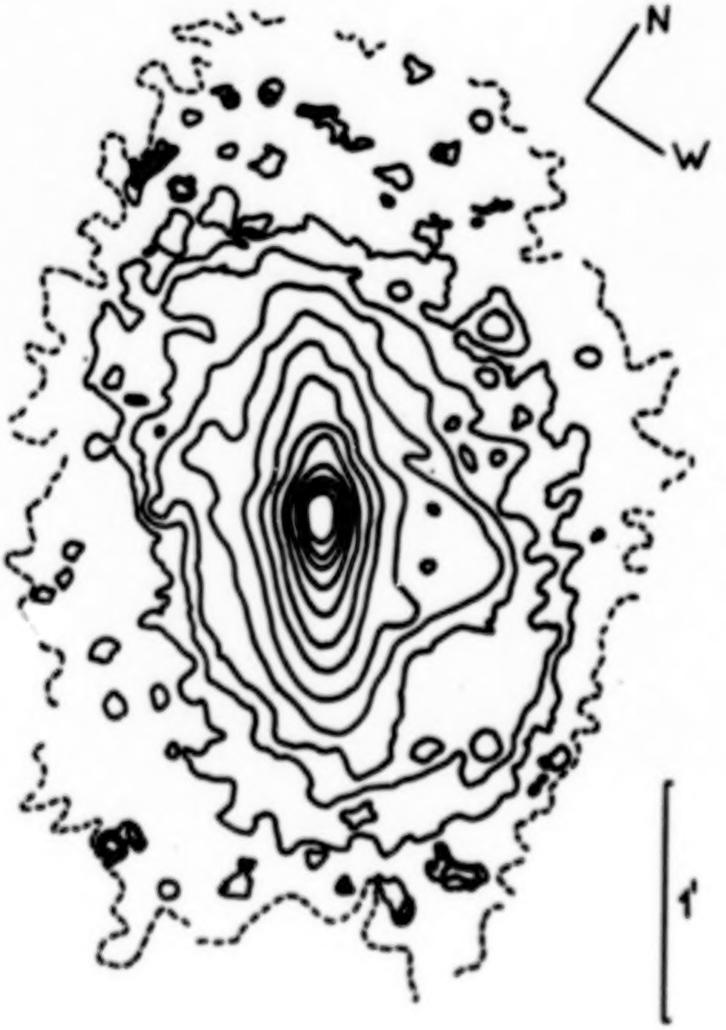

Figure 2. Low-resolution B-band isophotes of NGC 2685. Solid contour levels are drawn with the brightest level of 19.0 mag arcsec^{-2} and a step of 0.5 mag arcsec^{-2}, external dashed contours - 25.5 mag arcsec^{-2}.

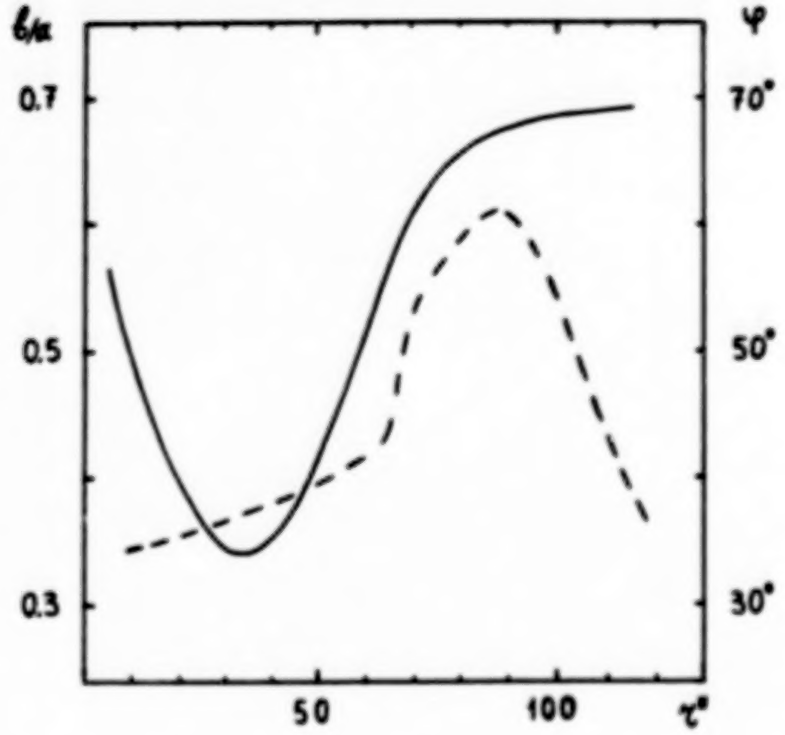

Figure 3. Orientation (dashed line) and apparent axial ratio (solid line) of the isophotes in the SW-part of NGC 2685.

Figure 4 shows the B-brightness profile measured along the major axis in the SW-side of the galaxy (circles). Solid lines show the best-fit profiles for the two-component model ($r^{1/4}$ spheroid + exponential disk). The parameters of the bulge and the disk corresponding to this fit are given in Table 1.

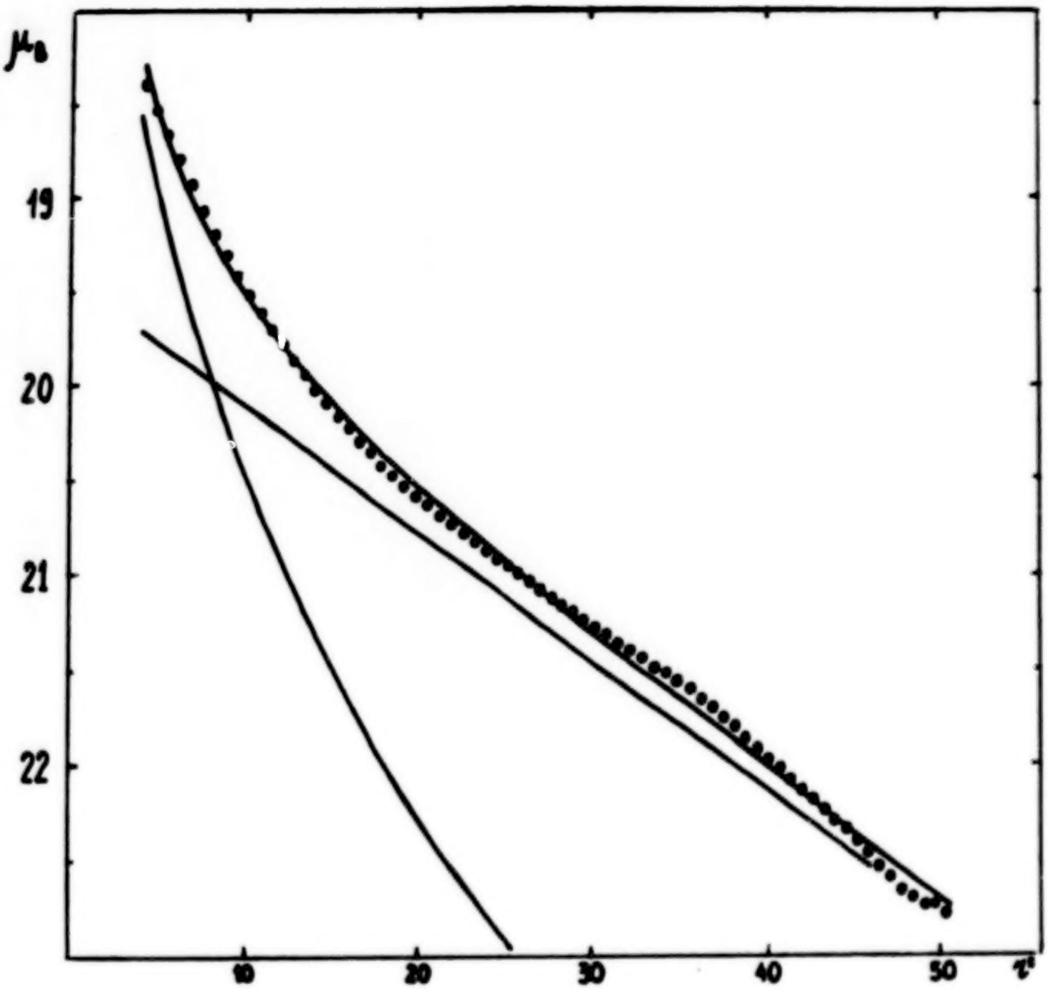

Figure 4. Two-component model of the light distribution as compared with major axis profile (SW-side of NGC 2685).

System of Polar Rings

The main body of NGC 2685 is intersected by a system of dark arcs transforming into light rings off the main body (Figure 1). The major axis of the brightest ring is about 80" (6.6 kpc), P. A. = 100°.

All the features between the main body of the galaxy and the isophote $\mu_u = 23.0$ mag arcsec^{-2} were taken into account in estimating photometric parameters of the polar rings. These parameters are shown in Table 1. The integrated colors of the rings are typical for Sbc - Sc spirals.

The system of rings contains numerous condensations, with characteristics ($B - V = +0.45$, $U - B = -0.3$, $M_B = -12$ to -14) typical for giant HII-regions in the arms of spiral galaxies.

The estimate of the mass of HI associated with the rings ($M(HI) = 5 \times 10^8 M_o$) has been given by Shand (1980). Hence the ratio of HI mass to B-luminosity of rings is $M(HI)/L_B = 1.3$. The luminosity of the ring system given in Table 1 is a lower limit to the total luminosity. However, the absolute magnitude of the rings must be increased by $\sim 1^m$ because of projection effects. The resulting $M(HI)/L_{Bo}$ ratio is then ~0.5. This value is typical for late type spirals.

Origin of Polar Rings

The body of available data, i.e., the size of the rings, their luminosity, mean colors, value of $M(HI)/L_{Bo}$, and presence of large-scale magntic fields (Hagen-Thorn, Popov, and Yakovleva, 1979) lead to the conclusion that the system of rings is a spiral galaxy. This conclusion is supported by the fact that luminous rings and dust lines crossing the NE-side of the main body have systematic shifts, which is usual for the arms of spiral galaxies. Therefore the apparent structure of NGC 2685 may be explained as a result of collision of normal SO and Sbc - Sc galaxies.

NGC 3808B

The Sc galaxy NGC 3808B is a component of an interacting pair with NGC 3808A (VV 300, Arp 87). It is located on the end of the spiral arm of NGC 3808A. On plates (Figure 5) one can see that the spiral arm appears to wrap around NGC 3808B.

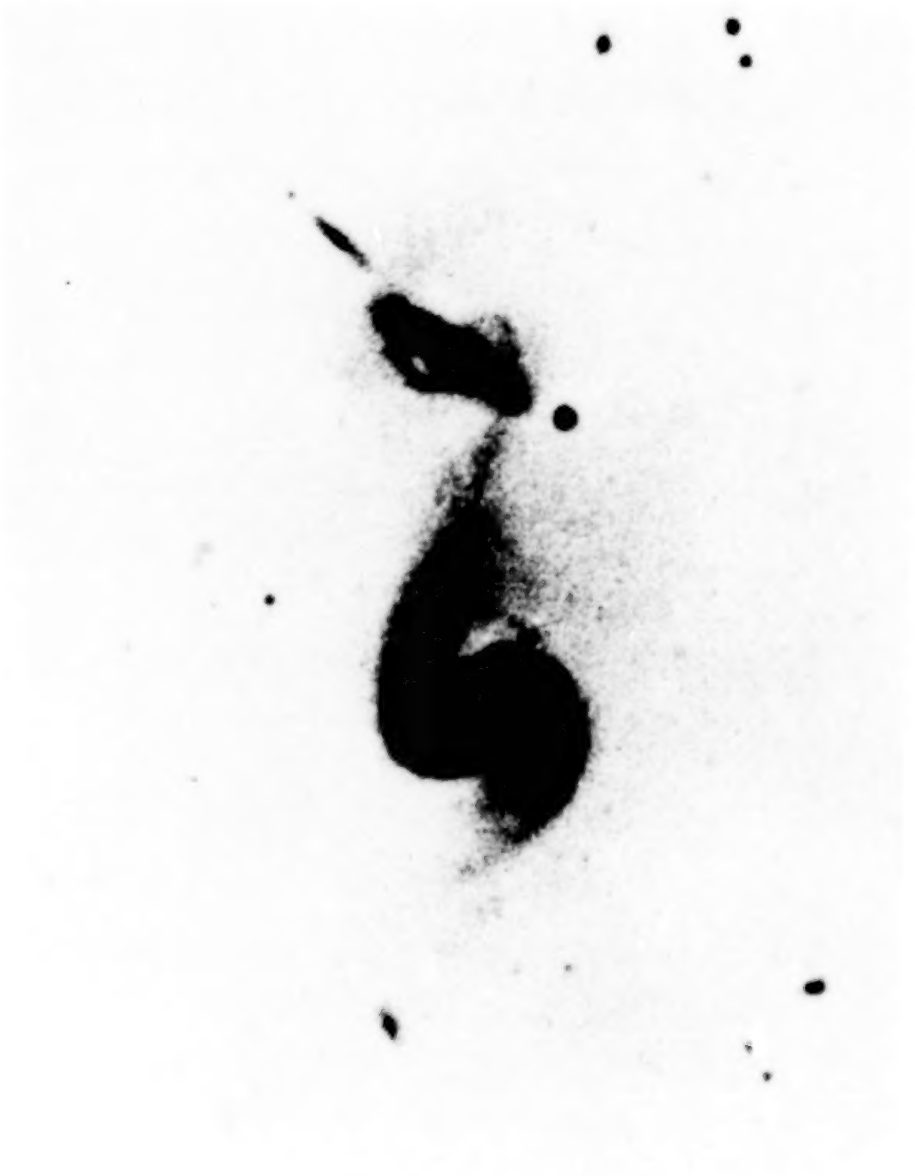

87

Figure 5. Reproduction of VV 300 (Arp 87) from the ATLAS OF PECULIAR GALAXIES (scale 1 mm = 1″.5).

Spectral observations of NGC 3808B were made in February 1989 with the 6 m telescope of the Special Astrophysical Observatory (USSR) using the two-dimensional photon counting system "Kvant" in "long-slit" mode (Aliavdin et al., 1988).

Two spectrograms of this galaxy were obtained, with the slit positional angles P. A. = 56° (major axis) and P. A. = 145° (minor axis). On both spectra the Hα and [NII] emission lines are tilted (Figures 6 and 7). The natural interpretation of this fact is rotation of ionized gas both around minor and major axes of the galaxy.

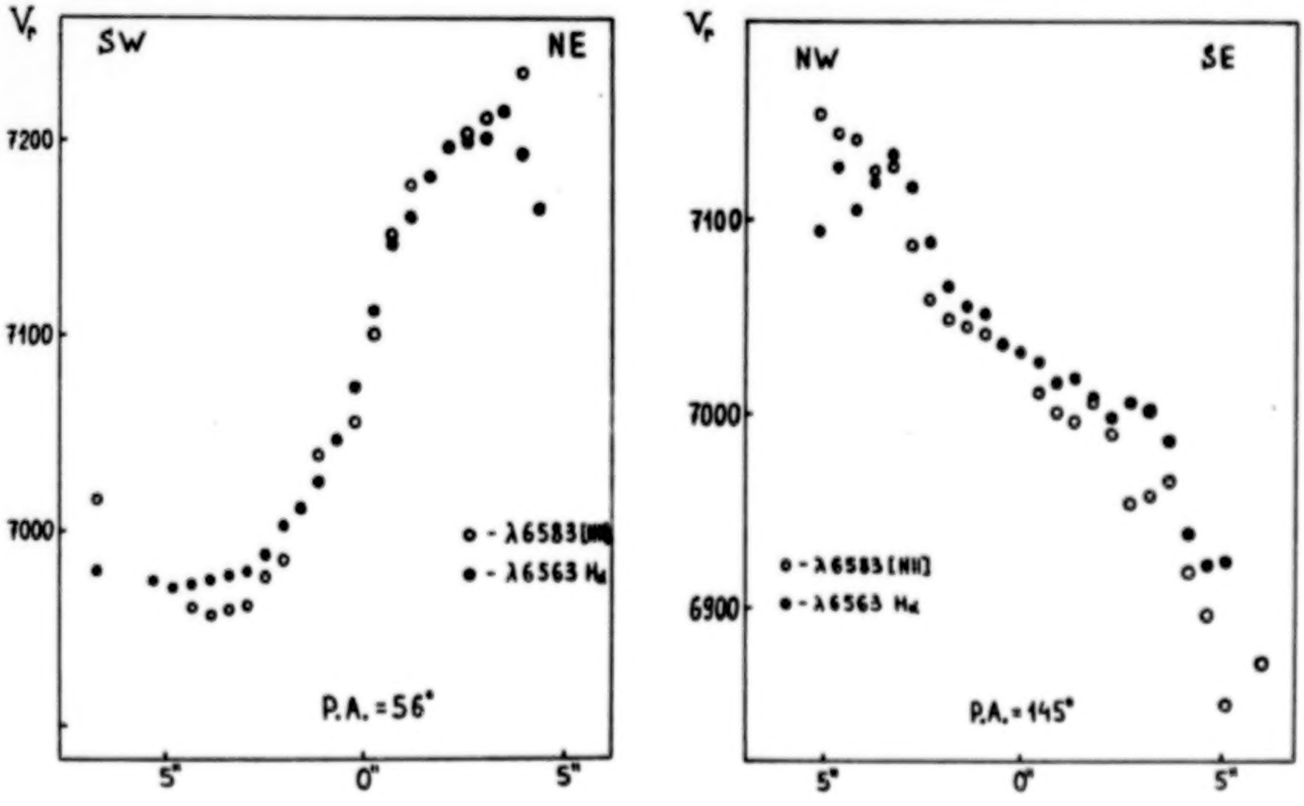

Figures 6 and 7. The observed rotation curves of NGC 3808B at different position angles.

The averaged rotation curves of NGC 3808B are shown in Figure 8 (heliocentric velocity of the nucleus is V_r = 7086 ± 10 km/s). The observed rotation velocities in the plane of the galaxy and perpendicular to it are practically equal at r = 5". But since the main body of NGC 3808B is seen nearly edge-one the observed velocities measured along its major axis are luminosity-weighted averages over all the gas along the line of sight. A crude estimate shows that the value of the correction for this effect may be as large as (20 - 30)%. Hence the real velocity of rotation at r = 5" may be larger (30 - 40) km/s as compared to the observed value. Then, with a small extrapolation, the estimate of distance where the polar and equatorial velocities are equal increases to r = 7". The optical radius of NGC 3808B is 20" (R_{25}) (de Vaucouleurs, de Vaucouleurs, and Corwin, 1976). Therefore, Vpol ≈ Veqv at r ≈ (1/3)R_{25}. It means that probably nearly spherical dark halo may be an important mass component even within the inner part of this galaxy.

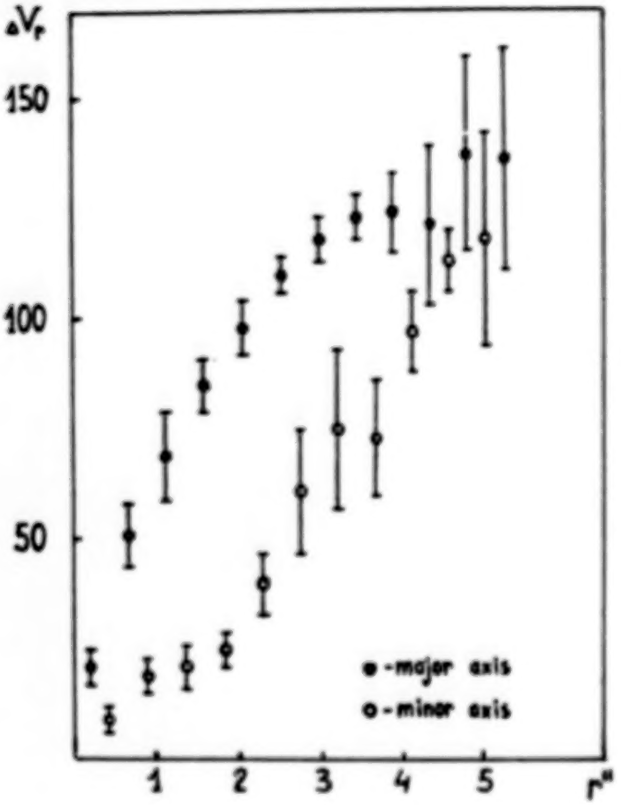

Figure 8. Rotation curves of NGC 3808B folded about the center.

Recent observations of three SO PRG's (Whitemore, McElroy, and Schweizer, 1987) have shown that dark spherical halo must be the dominant mass contributor even within the inner parts of these galaxies (at $r \approx 0.6R_{25}$). We have obtained similar result for Sc galaxy. This is in agreement with the conclusion made by Rubin (1987), according to which in spirals of all morphological types within the optical image of galaxy the dark matter contributes about 1/2 of its total mass.

NGC 3808B is probably an illustration of the scenario of polar ring formation as a result accretion of matter from a nearby galaxy.

However, since NGC 3808B is a late type galaxy with large extended disk, if the accretion is stopped, the lifetime of the ring will be relatively small (<< 10^9 years).

REFERENCES

Aliavdin, M. S., Afanasyev, V. L., Berline, A. B., Burenkov, A. N., and Savadskaja, O. O. 1988, Soobsch. Special Astrophys. Obs., 59, 68.

Burstein, D., and Heiles, C. 1984, Astrophys. J. Suppl. Ser., 54, 33

Hagen-Thorn, V. A., Popov, I. I., and Yakovleva, V. A. 1979, Pis'ma Astron. Zh., 5, 8.

Makarov, V. V., Reshetnikov, V. P., and Yakovleva, V. A. 1989, Astrofizika, 30, 15.

Schweizer, F., Whitmore, B. C., and Rubin, V. C. 1983, Astrophys. J., 88, 909.

Shane, W. W. 1980, Astron. Astrophys., 82, 314.

Rubin, V. C. 1987, in Dark Matter in the Universe, J. Kormendy and G. R. Knapp, eds., IAU Symposium No. 117, p. 51.

de Vaucouleurs, G., deVaucouleurs, A., and Corwin H. G. 1976, Second Reference Catalogue of Bright Galaxies, Austin, University of Texas Press.

Whitmore, B. C., McElroy, D. B., and Schweizer, G. 1987,
Astrophys. J., **314**, 1987.

TABLE 1

Parameters of NGC 2685

I.	General Properties:				
	Distance (Mpc)(1)	17			
	Galactic absorption(2)	0.15			
	Absolute B mag, M_{Bo}	-19.6			
	$(B - V)_T$(3)	+ 0.85			
II.	SO Component:				
	M_{Bo}	-19.45			
	$(B - V)_o$	+ 0.95			
	$(U - B)_o$	+ 0.3			
Bulge:	μ_e^B	19.32	Disk:	μ_o^B	19.43
	r_e	5.″9 (0.49 kpc)		α^{-1}	16.″1 (1.32 kpc)
	b/a	0.6:		b/a	0.35
	Bulge-to-disk ratio, B/D	0.94			
III.	Polar Ring Component:				
	M_{Bo}	<-16.0			
	$(B - V)_o$	+ 0.50			
	$(U - B)_o$	- 0.05			
	$M(HI)/L_{Bo}$	0.5:			

(1) Shane (1980)

(2) Burstein and Heiles (1984)

(3) de Vaucouleurs, de Vaucouleurs, and Corwin (1976)

THE MORPHOLOGY OF SÉRSIC-PASTORIZA GALAXIES

G.J. Yates[1], A. Pedlar[1], D.J. Saikia[1,2],
S.W. Unger[3], D.J. Axon[1],

[1]University of Manchester, Nuffield Radio Astronomy Laboratories,
Jodrell Bank, Macclesfield, Cheshire SK11 9DL, England

[2]GMRT project, Tata Institute of Fundamental Research,
Poona University Campus, Ganeshkhind, Pune 411007, India

[3]Royal Greenwich Observatory, Herstmonceux Castle,
Hailsham, East Sussex, BN27 1RP, England

Abstract

In this paper we present the preliminary results of our radio-continuum and neutral hydrogen observations of Sérsic-Pastoriza (S-P) galaxies. We show that the central regions contain a population of compact features thought to be young supernova remnants (SNRs) and discuss the overall morphology of the nuclei.

1. Introduction

The definition of a galaxy with a morphologically peculiar nucleus as one which exhibits a change in the slope of the luminosity profile and evidence of some structure (Sérsic & Pastoriza 1965, 1967; Sérsic 1973), includes galaxies with diffuse and amorphous nuclei in addition to the well-known hot-spot systems. Morgan (1958) first noticed that the nuclear regions of some spiral galaxies consist of bright spots, which he termed nuclear 'hot-spots'. We refer to this broad spectrum of galaxies with morphologically peculiar nuclei as Sérsic-Pastoriza or S-P galaxies (*c.f.* Osmer, Smith & Weedman 1974). The nuclei of S-P galaxies with hot-spots appear as clusters of bright spots in the optical, although their visual appearance could be as much due to extinction as to variations in stellar population and density (*e.g.* Wynn-Williams & Becklin 1985).

Although spectroscopic observations have shown these hot-spots are mostly luminous H II regions, there have also been evidence in some cases for the presence of weak Seyfert nuclei (*e.g.* Edmunds & Pagel 1982; Véron-Cetty & Véron 1985; Hummel, van der Hulst & Keel 1987). The existence of both starburst and Seyfert activity makes them particularly interesting for studying their kinematics, evolution and possible relationships between the two forms of activity. With these objectives in mind and also to understand any relationships between the different types of galaxies with peculiar nuclei (*c.f.* Prabhu 1980), we have begun a systematic study of a sample of Sérsic-Pastoriza or S-P galaxies at different wavebands.

2. Observations: radio-continuum and neutral hydrogen

High angular resolution radio-continuum observations were made with the VLA at $\lambda20$ and 6cm in order to study the central morphology of Sérsic-Pastoriza galaxies (Saikia *et al.* 1988, 1989; Yates *et al.* 1989). The maps made at $\lambda6$ and 20cm, like the optical contour plots of Prabhu (1980) show a number of different forms, although there appears to be no one-to-one correspondence between the optical and radio components in the same galaxy. Some of the S-P galaxies appear as single unresolved components (such as NGC 2196); others have a number of components in an extended region of emission (NGC 1365), some of which exhibit a ring-like (NGC 3310) or spiral form (NGC 6951).

In particular, the λ6cm map of one galaxy, NGC 1808, has yielded the most striking discovery (Saikia *et al.* 1989, 1990). This observation revealed a population of compact ($\lesssim 1$ arcsec) radio sources, reminiscent of those found in the archetypal starburst galaxies M 82 and NGC 253. Except for the brightest radio component (likely to be the nucleus of the galaxy), these compact features are not coincident with the optical hot-spots and are likely to be individual or unresolved groups of SNRs. The number of such sources is possibly a lower limit since each component could be composed of two or more sources, also confusion from the diffuse extended emission may be hiding much weaker, compact radio sources.

These components are more luminous than Cas A and overlap with some of the brighter ones in M 82. For comparison, we note that Cas A, the Galactic supernova remnant which is the most luminous in the radio, would have a flux density of 0.02 mJy at the distance of NGC 1808, and would be almost impossible to distinguish from the diffuse emission. For the minimum energy calculations, we assumed the total flux density of the compact source to be equal to its peak brightness, its size equal to the restoring beam, ratio of proton to electron energy to be unity and also a filling factor of unity. The equations used in the minimum-energy calculations are from Moffet (1975). The total minimum energy for the compact components in NGC 1808 ranges from ~2 to 9×10^{51} ergs. Excluding the nuclear component, the median values of the equipartition energy density and magnetic field are 1.8×10^{-10} ergs cm^{-3} and 43 μG respectively. It should, however, be noted that we need to observe this source with higher resolution to get more reliable flux densities of the individual compact features. These equipartition values for the minimum magnetic field, energy density, and total energy are comparable to the values calculated by Sanqvist, Jörsäter and Lindblad (1982) for another S-P galaxy, NGC 1365.

In the case of NGC 1808, severe confusion caused by the diffuse emission and the relatively coarse resolution (~90 pc at the distance of NGC 1808) of our observations compared to the sizes of SNRs which are at best a few pc, makes it difficult to estimate any reasonable lower limit to the SN rate. We can, however, set an upper limit (Saikia *et al.* 1990 and references therein) by assuming that the entire FIR energy is reprocessed SN energy. The FIR flux density of NGC 1808 is $\sim 5\times10^{-12}$ W m^{-2}. At a distance of 16.4 Mpc this corresponds to a luminosity of 1.6×10^{44} ergs s^{-1} or 4.0×10^{10} $L_{\odot}$. Using the canonical value of 10^{51} ergs of light and kinetic energy per SN yields a maximum of 5 SN per year. To get a better estimate of the SN rate, a higher resolution radio map with better sensitivity would be useful.

In order to establish the large-scale dynamics of NGC 1808, H I observations were made with the VLA while the array was in the B/C configuration. Hopefully these observations will help us to understand the supply of fuel to the central starburst/Seyfert activity and to investigate the possibility of ejection of high velocity gas from the nucleus. The neutral hydrogen is largely concentrated in a central bar, with weak emission from the spiral arms. An absorption profile against the radio emission from the nuclear region shows two features straddling the systemic velocity. The velocity field of the galaxy is largely consistent with rotation in an inclined galaxy, although there is evidence of significant non-circular motions in the bar. The possible relationship between these non-circular motions and the central region of NGC 1808 are of importance in understanding the formation of starburst nuclei and active galactic nuclei (STB/AGN) in these galaxies.

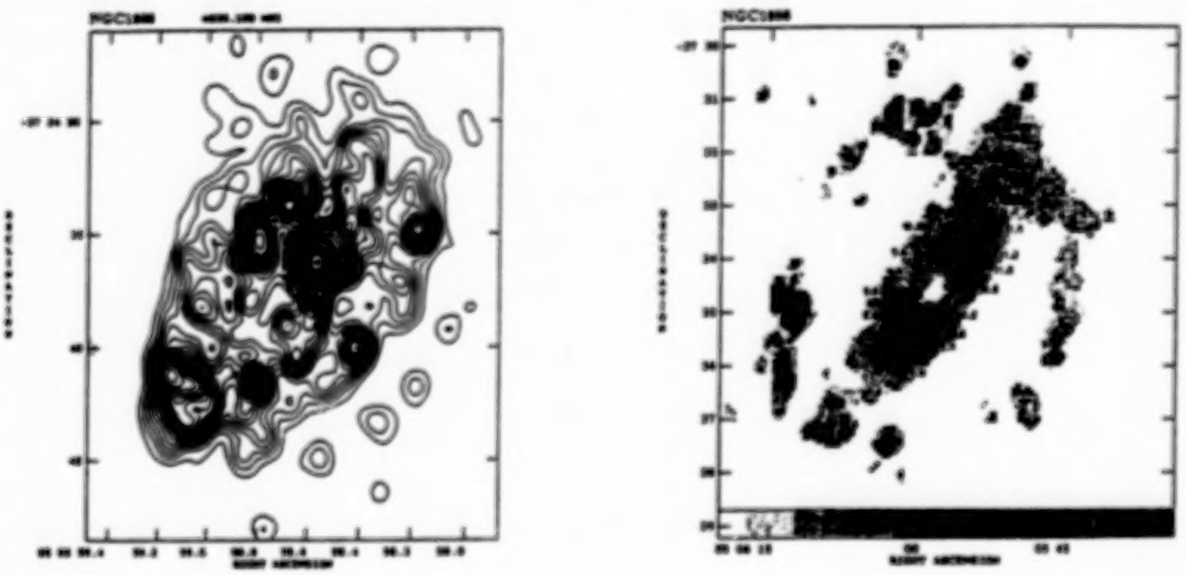

Figure 1. On the left, the brightness distribution of the central region of NGC 1808 at λ6 cm with an angular resolution of 1.23×1.05 arcsec^2 along PA 9.6°; peak brightness 16.6 mJy/beam. On the right, the distribution of the integrated neutral hydrogen and the velocity field on NGC 1808, with velocities marked in hundreds of km sec^{-1}.

Our neutral hydrogen observations of NGC 1808 show that the H I emission is dominated by the H I bar which has a 'hole' at the position of the nucleus, and a weaker emission which forms a ring-like structure. There is a close association of the H I distribution with the optical features. The bar is elongated along the major axis of the bright central part of the optical galaxy (Laustsen, Madsen & West 1987) while the weak ring-like structure is associated with the spiral arms where both features are visible. The spiral arms are extremely faint in the optical images of this galaxy as well, but appear to be marginally brighter in the north-western end of the galaxy compared to the south-east. Some evidence for such an asymmetry can also be seen in the H I distribution. The brightest regions are, however, closer to the nucleus with several total-intensity peaks, particularly to the north-west, suggesting that the emission along the bar is clumpy.

Even so, the absorption profile appears biased towards higher velocities, implying that on either interpretation there could be a component of neutral hydrogen gas infalling towards the nuclear region. This infalling gas could perhaps be the source of fuel and be responsible for triggering the activity in the nuclear region. Most hydrodynamic models show that the gas in the bar goes either into the nucleus or the cusp regions at the end of the bar (Roberts, Huntley & van Albada 1979; Sanders & Tubbs 1980; Tubbs 1982). The present observations of NGC 1808 are consistent with such a scenario. A more detailed study of the dynamics of the galaxy using the present data and Taurus Hα images is in progress.

3. Morphology of components

The shape of the star forming regions in starburst nuclei and active galactic nuclei had been thought to be a random distribution. Arsenault (1989) has commented on the preponderance of bar and ring features in starburst galaxies and lists S-P galaxies with circumnuclear Hα rings such as NGC 4321, NGC 1097 and NGC 3310. Combes (1986) has pointed out that nuclear H II regions in galaxies are often distributed on a circle or an ellipse centred on the nucleus.

Prabhu (1980) made a systematic, photographic study of a large sample of S-P galaxies showing that all S-P galaxies have several interesting features and broadly exhibit two distinct components: a nucleus (300–900 pc radius) and a perinuclear formation (1.3–2.4 kpc radius). This could be in the form of a pseudo ring formed by two spiral arms. Prabhu has suggested a possible classification scheme based on the relative brightness of the nuclear and perinuclear formations. This divides them into various categories: the κ (compact), ϵ (elliptical), σ (spiral), and ι (irregular); additionally, there are two intermediate forms, $\epsilon\sigma$ and $\sigma\iota$. The progression from κ to ι reflects the decrease in the ratio of the brightness of the nucleus to the perinuclear region: type κ having a very bright nucleus and a very faint or absent perinuclear region, while type ι has no clear nucleus and an extended, often bar-like, perinuclear region. We have used IRAS flux estimates for these galaxies and the luminosity trend is for the types $\epsilon\sigma$ and σ to have the highest luminosities and ι, $\sigma\iota$ the lowest. The radio fluxes give a similar luminosity relationship.

Pişmiş and Moreno (1987) have argued that the tightly wound spiral structure in the nuclei of some σ type S-P galaxies provides evidence of nuclear activity and that such spirals may be the loci of plasma ejected in a bi-polar fashion from the equator of a rotating nucleus and funneled by a magnetic field. García-Barreto and Pişmiş (1985, 1987) have made 6 and 20-cm continuum observations of the SBb galaxy NGC 4314, in which a tight spiral is observed. They have found that the radiation is essentially non-thermal and that polarization vectors (at 20-cm) are consistent with the existence of magnetic lines of force along the tight spiral.

It is also suggested (Arsenault *et al.* 1988 and references therein) that the nuclear rings are associated with the Inner Linblad Resonance (ILR) and thus the star formation activity in the annulus can be explained by the perturbation of orbits enhancing the collision rate between the molecular clouds which stimulates the star formation.

In general (Puxley, Hawarden & Mountain, 1988) galaxies of type Sab have compact core sources, flat or inverted radio spectra and high brightness temperature; the emission from an active nucleus is responsible for compact core sources. Type Sb and later have complex sources and steep non-thermal spectra; thus supernovae and H II regions in a vigorous burst of star formation are the most likely power source for systems with this extended complex structure. Prabhu (1979) finds that the mean Hubble type changes from Sab to Sc in the parent S-P galaxy as one moves from type ϵ to ι in the nucleus. It therefore seems possible that we are seeing an evolutionary sequence where type σ (Sbc) with its complex spiral structure of sources produced by a vigorous starburst and its associated H II regions and SNRs (possibly a few young hidden Seyferts) evolves as the star formation consumes the gas and it changes into the (Sab) type with its compact elliptical core, less dust and no Hα. Also the types ϵ, $\epsilon\sigma$, and σ are more luminous and contain a greater proportion of barred or intermediate spirals than the types $\sigma\iota$ and ι. The types $\sigma\iota$ and ι are less luminous because they occur in galaxies with less gas in the bar-disk region; therefore the activity is on a smaller scale. Once the gas condenses to the centre it is ruled by the bar potential and hence the nucleus is more prolate.

Finally, we note that the sort of compact features located in the central regions of NGC 1808 also occur in a number of other S-P galaxies, and are likely to be found in many STB or AGN when observed with adequate sensitivity and resolution.

References

Arsenault, R., Boulestreix, J., Georgelin, Y., Roy, J.-R., 1988. *Astr. Astrophys.*, **200**, 29.

Arsenault, R., 1989. *Astr. Astrophys.*, **217**, 66.

Combes, F., 1986. In: *Galactic and Extragalactic Star Formation*, NATO Advanced Study Institute proceeding, p. 475, eds Pudritz, R.E. & Fich, M.

Edmunds, M.G. & Pagel, B.E.J., 1982. *Mon. Not. R. astr. Soc.*, **198**, 1089.

García-Barreto, J.A., and Pişmiş, P., 1985. *Bull. Am. astr. Soc.*, **17**, 893.

García-Barreto, J.A., and Pişmiş, P., 1987. In: *Proceedings of IAU Symposium No. 115*, 626.

Hummel, E., van der Hulst, J.M. & Keel, W.C., 1987. *Astr. Astrophys.*, **172**, 32.

Laustsen, S., Madsen, C. & West, R.M., 1987. In: *Exploring the Southern Sky: A Pictorial Atlas from the European Southern Observatory*, Springer-Verlag.

Moffet, A.T., 1975. In: *Stars and Stellar Systems*, **9**, 211, eds Sandage, A., Sandage, M. & Kristian, J., University of Chicago Press, Chicago.

Morgan, W.W., 1958. *Publ. astr. Soc. Pacific*, **70**, 364.

Osmer, P.S., Smith, M.G. & Weedman, D.W., 1974. *Astrophys. J.*, **192**, 279.

Prabhu, T.P., 1979. *Ph.D. Thesis.*

Prabhu, T.P., 1980. *J. Astrophys. Astr.*, **1**, 129.

Pişmiş, P., Moreno, E., 1987. In: *Proceedings of IAU Symposium No. 121*, p. 477.

Puxley, P.J., Hawarden, T.G., Mountain, C.M., 1988. *Mon. Not. R. astr. Soc.*, **231**, 465.

Roberts, W.W.Jr., Huntley, J.M. & van Albada, G.D., 1979. *Astrophys. J.*, **233**, 67.

Saikia, D.J., Yates, G.J., Pedlar, A., Axon, D.J., van Gorkom, J., Wolstencroft, R.D., Unger, S.W., 1988. In: *Active Galactic Nuclei*, p. 140, eds Miller, H.R. & Wiita, P.J., Springer-Verlag.

Saikia, D.J., Unger, S.W., Pedlar, A., Yates, G.J., Axon, D.J., Wolstencroft, R.D., Taylor, K. and Gyldenkerne, K., 1989. In: *ESO Workshop on Extranuclear Activity in Galaxies, Garching, 16-18 May 1989*, p.95, eds Meurs, E.J.A. & Fosbury, R.A.E.

Saikia, D.J., Unger, S.W., Pedlar, A., Yates, G.J., Axon, D.J., Wolstencroft, R.D., Taylor, K. and Gyldenkerne, K., 1990. *Mon. Not. R. astr. Soc.*, Accepted.

Sanders, R.H. & Tubbs, A.D., 1980. *Astrophys. J.*, **235**, 803.

Sanqvist, A., Jörsäter, S., and Lindblad, P.O., 1982. *Astr. Astrophys.*, **110**, 336.

Sérsic, J.L., 1973. *Publ. astr. Soc. Pacific*, **85**, 103.

Sérsic, J.L. and Pastoriza, M.G., 1965. *Publ. astr. Soc. Pacific*, **77**, 287.

Sérsic, J.L. and Pastoriza, M.G., 1967. *Publ. astr. Soc. Pacific*, **79**, 152.

Tubbs, A.D., 1982. *Astrophys. J.*, **255**, 458.

Véron-Cetty, M.-P. & Véron, P., 1985. *Astr. Astrophys.*, **145**, 425.

Wynn-Williams, C.G. & Becklin, E.E., 1985. *Astrophys. J.* **290**, 108.

Yates, G.J., Saikia, D.J., Pedlar, A., Axon, D.J., 1989. *Astrophys. Space Sci.*, **157**, 271.

INTERACTING NUCLEI IN DISTANT GALAXIES

Wei Zheng, University of Alabama, U.S.A.
and
Steven A. Grandi, National Optical Astronomy Observatories, U. S. A.

The interaction of galaxies not only occurs in galactic scales, but also may be linked to the binary cores in active galactic galaxies. The presence of a binary in the center of galaxies was suggested by Begelman, Blandford and Rees (1980). Gaskell (1983) suggests that supermassive binaries may account for the observed structure of emission line profiles such as double peaks displaced by a significant velocity difference. Collin-Souffrin, *et al.* (1986) argue that line emission may be formed in the outer part of an accretion disk. The resultant profile, as expected from rotational motion, would be very broad and often possess a double-horn shape. However, the emission line profiles in most active galactic nuclei do not share such a resemblance, and there are only two reported cases, 3C390.3 (Pérez *et al.* 1987) and Arp102B (Chen, Halpern and Filippenko 1989), in which the broad Balmer line profile may be of such a shape. Therefore, the assumption for accretion disk is to be verified with care.

The N-galaxy 3C 390.3 has been monitored spectroscopically since 1974 (Osterbrock, Koski and Phillips 1975; Oke 1988). From various archives and literature, it is found that the Balmer lines change their intensities and profiles in a dramatic manner. The $H\alpha$ profile is very broad (FWHM $\approx$ 15000 km s^{-1}) and peculiar, and the relative intensities of its two humps (see figure 1) changes consistently with time, possibly periodically. Before 1980, the blue hump was significantly stronger than the one in the red. From 1980 to 1983 the blue hump became stronger (see Oke 1988). After 1983 the $H\alpha$ profile has returned to its early shape and seems to have pleted a full circle. Unlike the rapid (on the order of a month or even less) and aperio riation in the continuum and integrated line intensities, the change in broad profile s low and consistent.

Taking the analogy c lysmic variables: the double-horn profiles have been observed in cases of interacting st or example, the emission lines, both in He II and hydrogen Balmer lines in GD 552 (r 1985) show double-horn profiles and periodical changes in their line profiles, includin he change in ratios of two humps. It is understood that the that the D-wave components (Smak 1976) are the signature of an emitting disk and the S-wave component is from the emission at a hot spot which rotates and results in a moving component in the velocity space. the mass flow from the nearby interacting star provides the stream toward the core of a neutron star or white dwarf. Therefore, it is proposed that the variation of broad line profiles observed in 3C 390.3 may be the result of a pair of interacting massive cores. The rotational velocity dominates and produces a variable double-horn profile. However, the line widths observed in broad line radio galaxies are one order larger than that in interacting stars. The Balmer decrements imply a much smaller density (10^{10-12} cm^{-3}) than that in the cataclysmic variables. The much larger velocity and much thinner density make it unlikely that the broad line emission is simply formed in an accretion disk. We postulate that a significant rotational motion is involved.

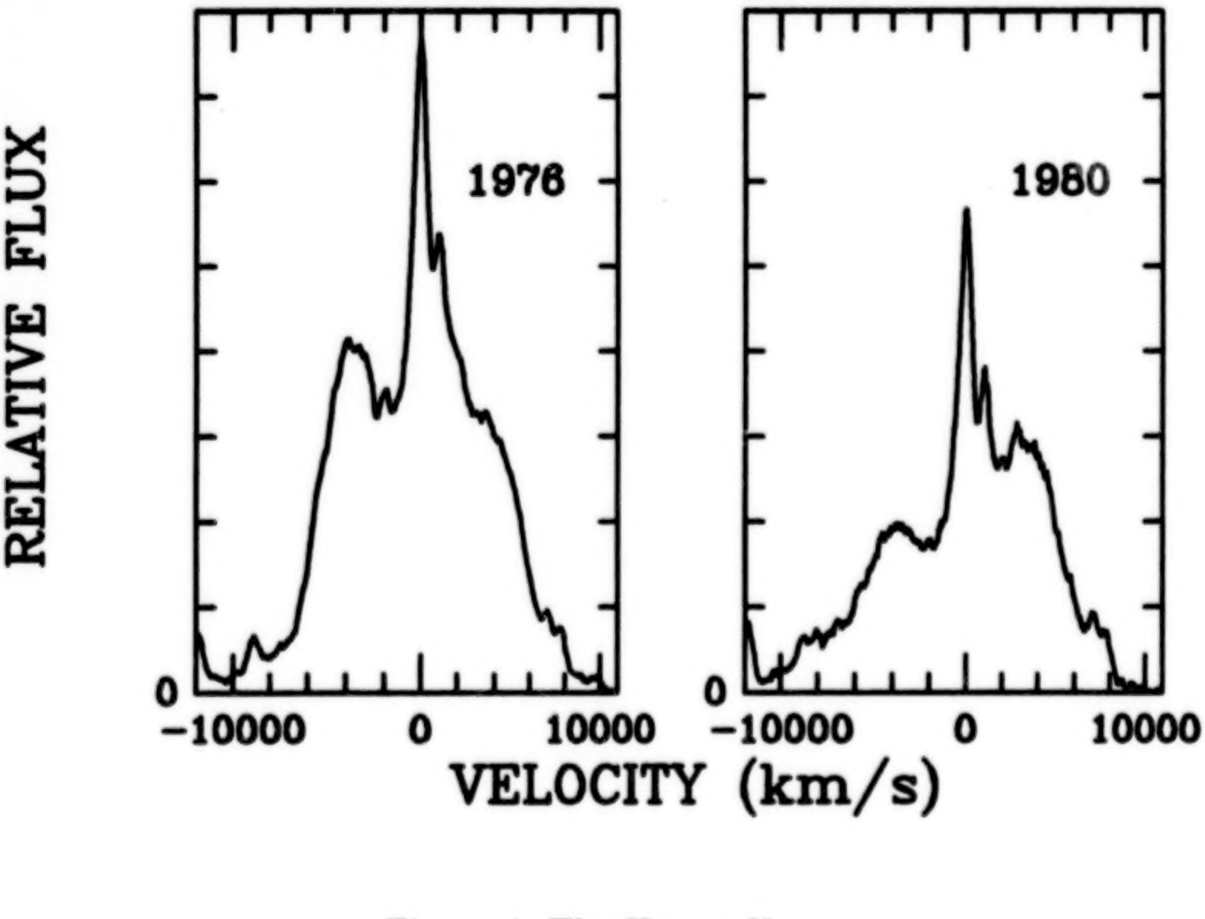

Figure 1, The Hα profile

If the observed "squared" profiles are indeed due to the rotational velocity field, one can naturally explain their rare occurrence: only in the cases of double cores, the gas around the central engine has low enough velocity to be confined within the Roche lobe and engaged in a rotational motion which dominates. In other cases where only a single core is present, either the radiative or gravitational fields are radial and make it difficult to form a rotating line-emitting region. Thus, the profiles most commonly observed in extragalactic objects are logarithmic. Furthermore, it is possible to deduce the central mass from the rotational period and the distance to the central engine. Previous estimates can be made only by the order of magnitude. Preliminary result indicates that for 3C 390.3 the value is $7 \times 10^7\ M_\odot$.

REFERENCES

Begelman, M. C., Blandford, R. D., and Rees, M. J. 1980, *Nature*, **287**, 307.

Chen, K., Halpern, J. P., and Filippenko, A. V. 1989, *Ap. J.*, **339**, 742.

Collin-Souffrin, S., Dumont, S., Joly, M., and Péquignot, D. 1986, *Astr. Ap.*, **166**, 27.

Gaskell, C. M. 1983, in *Quasars and Gravitational Lenses*, Proc. 24th Liège Int. Ap. Coll. (Liège: Institut d'Astrophysique, Université de Liège), p. 473.

Oke, J. B. 1987, in *Superluminal Radio Sources*, eds. J. A. Zensus, and T. J. Pearson, (Cambridge: Cambridge University Press), p. 267.

Osterbrock, D. E., Koski, A. T., and Phillips, M. M. 1975, *Ap. J. (Letters)*, **197**, L41.

____________. 1976, *Ap. J.*, **206**, 898.

Pérez, E., Penston, M. V., Tadhunter, C., Mediavilla, E., and Moles, M. 1988, *M.N.R.A.S.*, **230**, 353.

Smak, J. 1976, *Acta Astr.*, **26**, 277.

Stover, R. J. 1985, in *Cataclysmic Variables and Low-Mass X-ray Binaries*, ed. D. Q. Lamb and J. Patterson (Dordrecht: Reidel), p. 379.

ALIGNMENT OF cD-GALAXIES WITH THEIR SURROUNDINGS

Eelco van Kampen and George Rhee
Sterrewacht Leiden
Leiden, the Netherlands

Abstract

For a sample of 122 rich Abell clusters we find a strong correlation of the position angle (orientation) of the first-ranked galaxy and its parent cluster. This alignment effect is strongest for cD-galaxies. Formation scenarios for cD galaxies, like the merging scenario, must produce such a strong alignment effect. We show some N-body simulations done for this purpose.

Introduction

Orientation effects like alignments might constrain initial conditions for the formation of clusters and their member galaxies. Cluster collapse models by Doroshkevich (1973) and Icke (1973) predict - if galaxies are formed during this collapse of shortly afterwards - an isotropic galaxy position angle distribution when the collapse process is symmetrical, but if this collapse is asymmetrical the galaxies are expected to be aligned with their cluster. It can be argued that the angular momenta of galaxies have changed little since this formation epoch, so observing the present distribution of the angular momenta teaches us something about this formation process. The angular momentum of a galaxy is aligned with the visual polar axis, i.e. the axis perpendicular to the disk for spirals and the short axis for ellipticals (Franx, Illingworth and Heckman 1989). On the sky we can only observe the 2-dimensional projection of galaxies, which gives us a position angle and an ellipticity, but gives us two possible polar axes. Still one hopes to be able to use position angle distributions with appropriate statistics to constrain formation models and initial conditions. As a first step we obtained position angles for the 10-20 brightest galaxies in a sample of rich Abell clusters, and did some preliminary N-body simulations on simple cluster collapse models in order to explain found alignment effects and other phenomena in clusters of galaxies.

Observed alignment effects

For a complete sample of 122 rich Abell clusters we obtained cluster position angles by scanning POSS-plates on the Leiden Astroscan machine. From the resulting digitized images galaxies were recognized semi-automatically. The cluster position angle is then obtained by Fourier-analysis of the azimuthal galaxy distribution (Rhee *et al.* 1990). The position angle of the member galaxies are calculated from the digitized galaxy images subtracted from the cluster images, by means of intensity weighted moments.

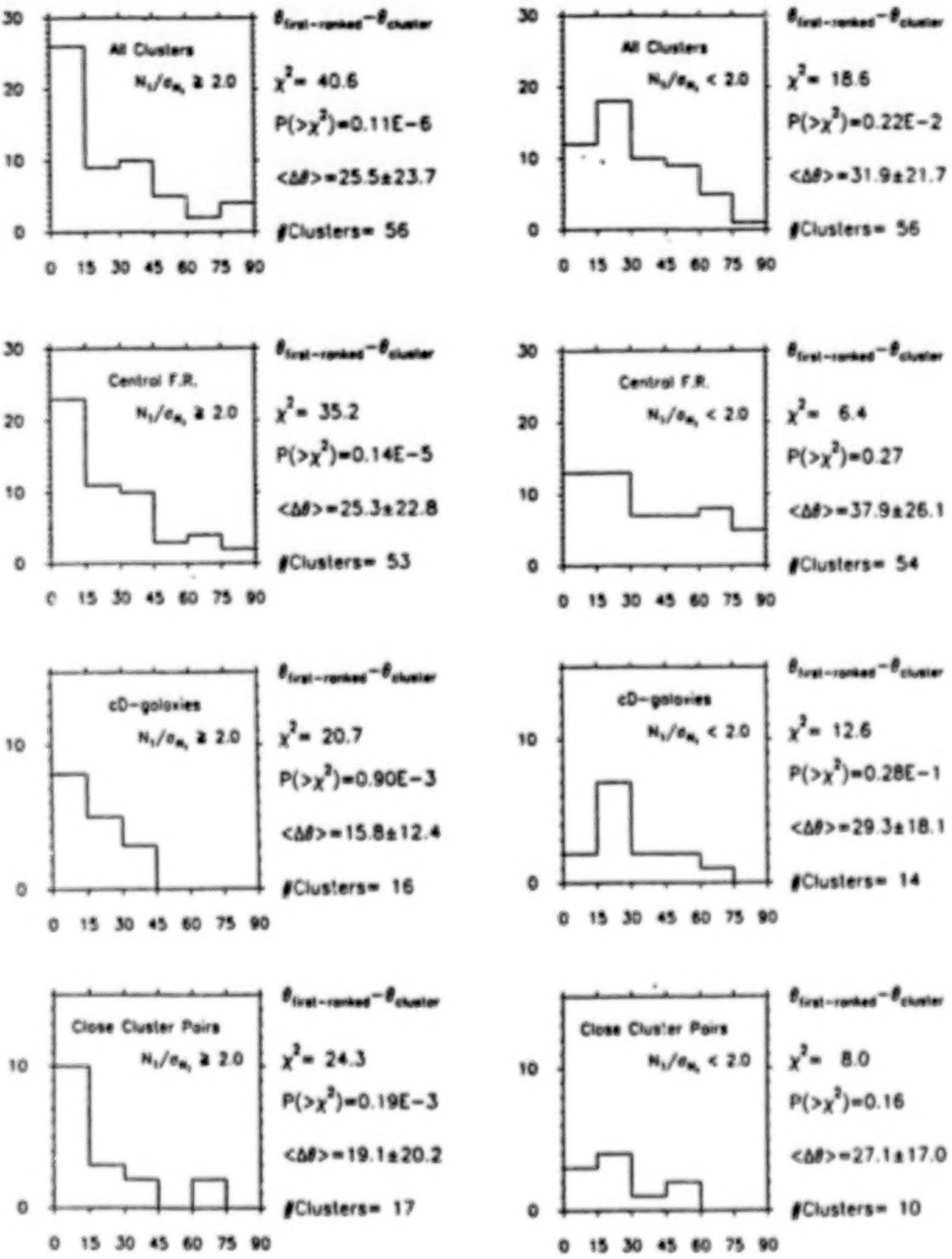

Figure 1

First-ranked galaxy alignment histograms showing the binned number distributions of the relative angle of the orientations of clusters and their first-ranked (brightest) galaxies. The left hand column shows elongated clusters (elongation strength $\frac{N_1}{\sigma_{N_1}} \geq 2.0$*), the right hand column shows more spherical clusters (*$\frac{N_1}{\sigma_{N_1}} < 2.0$*). Each column consists of histograms for: a) all clusters, b) clusters with the first-ranked galaxy selected within 0.5 Mpc of the centre (central-first-ranked), c) clusters with a cD-galaxy as the first-ranked, and d) clusters in the 27 closest cluster pairs.*

We find no preferred orientations or an alignment with the parent cluster for the 10-20 brightest galaxies except for the *first-ranked* galaxy (van Kampen and Rhee 1990). The observed first-ranked alignment effect is shown in figure 1 for several types of first-ranked galaxies. We devided our sample of clusters in two subsamples, 'elongated' and 'round' clusters, using an elongation strength parameter derived from the azimuthal galaxy distribution, as defined and obtained by Rhee *et al.* (1990).

The effect is much stronger for elongated clusters than for more spherical clusters. Without splitting up the sample part of the effect would be hidden. The scatter in alignment histograms is therefore partially due to the error in the cluster position angle (which is larger for more spherical clusters), but could also be caused by projection of intrinsic alignment effects. Further information on this - and other - alignment effect can be found in van Kampen and Rhee (1990).

First-ranked galaxies

The alignment found is an exclusive effect for the first-ranked galaxies, especially for cD-galaxies and other giant Brightest Cluster Ellipticals (BCE's). So these galaxies seem to play a special role in clusters of galaxies. Other evidence for an intimate connection of BCE's with their parent clusters is found in the fact that they are mostly sitting in the centre of the potential well, and show their ellipticity to increase strongly as a function of radius (Porter 1988). All this has to be produced by some formation scenario for giant first-ranked galaxies, like cluster collapse models or merging scenarios. One can imagine the formation of a giant galaxy at the centre of a collapsing aspherical protocloud. This asphericity continues down to the scale of the forming giant galaxy, thereby producing the alignment effect. During and after the formation, merging and cannibalism will have an effect on the evolution of the galaxy, and the question is what remains of the alignment effect. In order to find out, N-body simulations are a proper way of exploring this.

N-body simulations

As a start, Rhee and Roos (1989) studied the dissipationless collapse of a moderately aspherical initial system, using 4096 particles, evolved with the hierarchical tree-code written by Barnes and Hut (1986). The initial system is a homogeneous prolate ellipsoid (1:1:2) or a homogeneous oblate ellipsoid (1:2:2). The prolate simulation was also performed including substructure. They found in their simulations that the central part of the collapsed and virialized system does show the same orientation as the initial system if this initial system is *prolate*. This is shown in figure 2, where the prolate and oblate case can be compared. In figure 2 it is also shown how the effect of the increasing ellipticity as a function of radius found by Porter (1988) (see above) is produced by this simulations. Furthermore, the results does not differ if one starts with or without substructure.

The central part of the system could become the aligned first-ranked galaxy, thereby explaining the alignment effect. This first-ranked galaxy forming in the centre can grow further by merging, where dynamical friction causes victim galaxies to spiral in. In an elongated cluster, these inward orbits are preferentially elongated and aligned with the cluster.

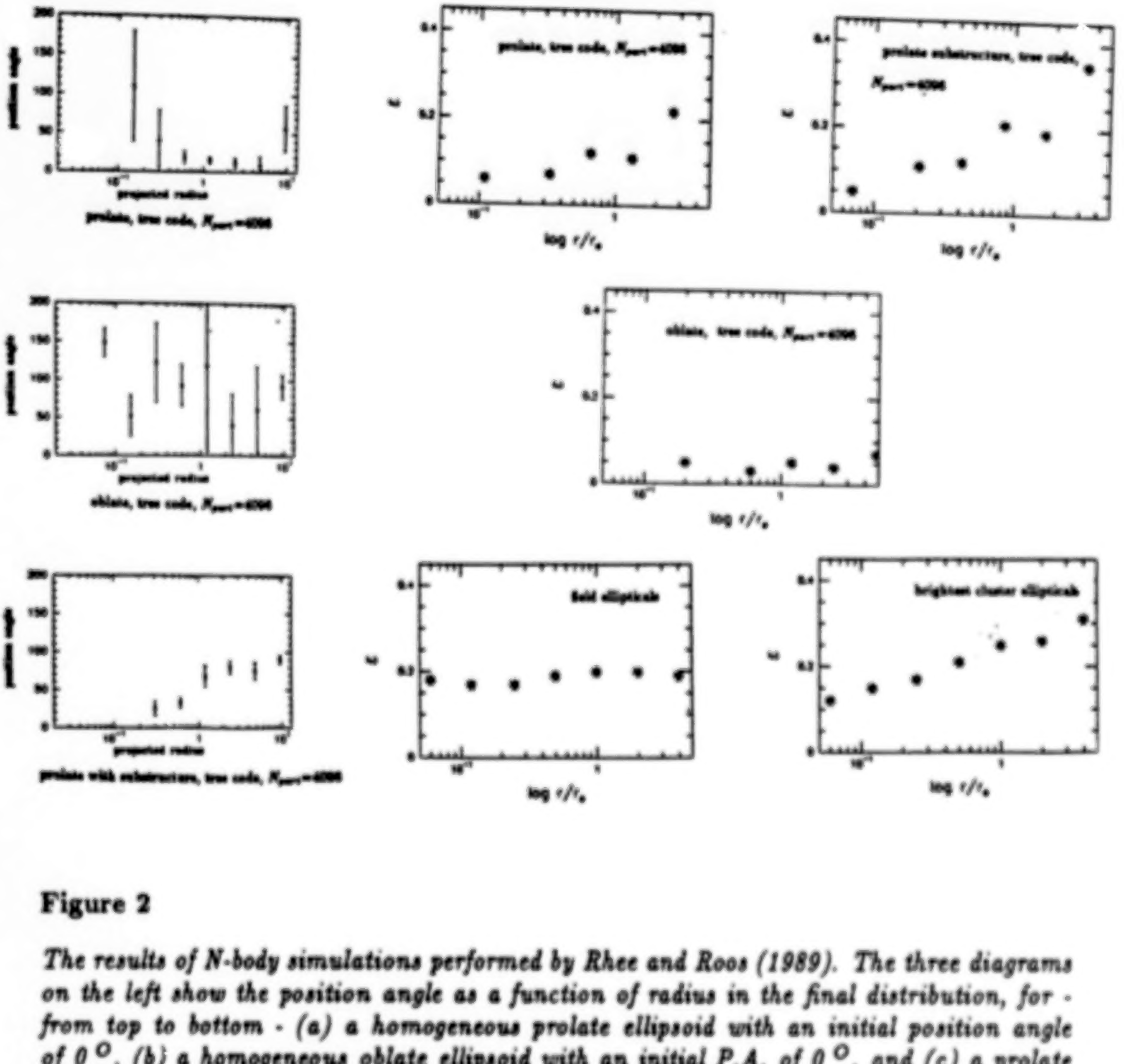

Figure 2

The results of N-body simulations performed by Rhee and Roos (1989). The three diagrams on the left show the position angle as a function of radius in the final distribution, for - from top to bottom - (a) a homogeneous prolate ellipsoid with an initial position angle of 0 °, (b) a homogeneous oblate ellipsoid with an initial P.A. of 0 °, and (c) a prolate ellipsoid containing substructure (homogeneous clumps) with an initial P.A. of 90 °. For the cases (a) and (c) the P.A. is aligned with the initial P.A. over a range of 30 in radius. The other 5 diagrams show the comparison of simulations and observations with respect to the ellipticity as a function of radius. On top cases (a) and (c) as above, in the middle case (b), down left a sample of field ellipticals (Djorkovski 1985), and down on the right a sample of brightest cluster ellipticals (Porter 1988). As can be seen, cases (a) and (c), the prolate ellipsoids, generate what is observed. Of course this is not unique.

During this infall, the victims are stripped and contribute to the central giant (or cD) galaxy and its envelope, conserving or possibly increasing the found alignment effect with the surrounding galaxy distribution (the cluster). These predictions will be tested by us using more particles and a N-body code containing more physics. We will also start with more realistic initial conditions, like originating from a Cold Dark Matter spectrum.

Conclusions

We found the first-ranked galaxy of a cluster to be aligned with its parent cluster, especially cD-galaxies. This effect is strongest for elongated clusters, and exclusive for the first-ranked galaxy, which seems to play a special role in clusters. Resulting from N-body simulations, it was found that during the dissipationless collapse of an initially homogeneous ellipsoid, the information on the orientation is transferred to the centre if the initial mass distribution is prolate.

References

Barnes, J. and Hut, P. 1986, *Nature* **324**, 446
Djorkovski, S. 1985, Ph.D. Thesis, University of California at Berkeley
Doroshkevich, A.G. 1973, *Soviet Astr. - AJ* **16**, 986
Franx, M., Illingworth, G.D. and Heckman, T.M. 1989, submitted to *Astrophys. J.*
Icke, V. 1973, *Astron. Astrophys.* **27**, 1
van Kampen, E., and Rhee, G.F.R.N. 1990, submitted to *Astron. Astrophys.*
Porter, A.C. 1988, Ph.D. Thesis, California Institute of Technology
Rhee, G.F.R.N., van Haarlem, M.P., and Katgert, P. 1990, submittcd to *Astron. Astrophys. Suppl.*
Rhee, G.F.R.N., and Roos, N. 1989, *Preprint*

DISCUSSION

Bland: To what extent are cD galaxies simply the density cusps at the cores of your collapsing ellipsoids? This is potentially important, since then we would have direct evidence that merged systems form something which in many respects looks like an elliptical galaxy.

Van Kampen: We don't pretend to simulate cD-formation, we just show that you can transfer orientational information over quite a large range (~30). My quess is that cD galaxies are mostly primordial, as single density cusps at the centers of collapsing ellipsoidal distributions, (if that is the way clusters form). But they certainly might grow by merging/ cannibalism to become as giant as they are now. The observed alignment effect has to be maintained, of course, during this evolution.

Osterbrock: Your paper, like many others before it, shows the physical significance of cD galaxies, a classification type originally defined on completely empirical, morphological grounds by W. W. Morgan. In another paper, at this Colloquium, R. K. Kochhar mentioned that "nearly every SO galaxy seems to be peculiar." This is a point also previously made by Morgan; on morphological grounds he classified the so-called SO galaxies into several other different types, including D, E, and peculiar. I would suggest that researchers in the field of paired and interacting galaxies try analyzing their results in terms of Morgan's entire classification system, as well as the standard one, and see which one works best.

Van Kampen: I agree. With some communication between observers, collecting morphological data could be used to test morphology classifications, or even find a new one, which you would like to be as continuous as possible.

Smith: What was the mean isophotal magnitude at which your position angle determination for the first-ranked systems was made? Have you looked for the isophotal major-axis position-angle twists ($\Delta\theta/\Delta R$) seen in many ellipticals and cDs, and how sensitive is your conclusion to this effect?

Van Kampen: We determined galaxy position angles using intensity-weighted moments, with maximum weighting mostly between the 20th and the 22nd magnitude isophotes.

DUMB-BELL GALAXIES IN SOUTHERN CLUSTERS: CATALOG AND PRELIMINARY STATISTICAL RESULTS

G. Vettolani [1],L. Gregorini[1,2], P. Parma[1],H.R. de Ruiter [3]

[1] *Istituto di Radioastronomia del CNR, Bologna, Italy*

[2] *Dipartimento di Astronomia, Università di Bologna, Italy*

[3] *Osservatorio Astronomico, Bologna, Italy*

1. Introduction

The dominant galaxy of a rich cluster is often an object whose formation and evolution is closely connected to the dynamics of the cluster itself. Hoessel (1980) and Schneider *et al.* (1983) estimate that 50 % of the dominant galaxies are either of the dumb-bell type or have companions at projected distances less than 20 kpc, which is far in excess of the number expected from chance projection (see also Rood and Leir 1979).

Presently there is no complete sample of these objects, with the exception of the listing of dumb-bell galaxies in BM type I and I-II clusters in the Abell statistical sample of Rood and Leir (1979).

Recent dynamical studies of dumb-bell galaxies in clusters (Valentijn and Casertano, 1988) still suffer from inhomogeneity of the sample. The fact that it is a mixture of optically and radio selected objects may have introduced an unknown biases, for instance if the probability of radio emission is enhanced by the presence of close companions (Stocke, 1978, Heckman *et al.* 1985 , Vettolani and Gregorini 1988) a bias could be present in their velocity distribution. However this situation is bound to improve: a new sample of Abell clusters in the Southern Hemisphere has been constructed (Abell et *al.*, 1988 hereafter ACO), which has several advantages over the original northern catalog. The plate material (IIIaJ plates) is of better quality and reaches fainter magnitudes. This makes it possible to classify the cluster types with a higher degree of accuracy, as well as to fainter magnitudes. We have therefore decided to reconsider the whole problem constructing an new sample of dumb-bell galaxies homogeneously selected from the ACO survey.

2. Selection rules and samples

We have extracted from the ACO catalog two samples of clusters which were independently inspected on the ESO-SRC J plates by two of us (with subsamples inspected more than once at different times); the brightest member was classified according to the rules described below.

The first sample has been prepared in order to obtain a complete homogeneous volume limited sample of dumb-bell galaxies for further study of their dynamics, radio emission etc. It has been constructed examining all the BM type I an I-II clusters, independently of any other cluster parameter.

The second sample contains all clusters, regardless of their BM type, with distance either measured or estimated (Scaramella *et al.* 1989), less than $z = 0.07$. This sample has been prepared in order to study the properties of dumb-bell galaxies in relation to the cluster environment (dominant/non-dominant cluster galaxy) and their space density, formation probability etc.

We classified the brightest member according to a five mark classification in which 4 denotes a dumb-bell galaxy, essentially according to the original definition given by Matthews *et al.* (1964): two objects with a difference in magnitude of at most 2 magnitudes, embedded in a common halo. In class 3 clusters there are two galaxies inside the halo, but with a large difference in luminosity (visually estimated as ≥ 2 magnitudes). In classes 2 and 1 there is a companion galaxy outside the envelope either with a large luminosity difference (2) or with similar luminosity but at a distance from the brightest cluster galaxy which is more than twice the radius of the latter (1). These two classes could contain a few real dumb-bells , but are mainly composed of optical pairs. Many objects will simply be satellite galaxies. Only spectroscopy and surface photometry will help to disentangle these cases. In class 0 clusters the brightest member is fairly isolated from other cluster galaxies.

A catalog of clusters of type 3 and 4 for the volume limited sample is given in Table I.

3. Selection effects

These selection criteria are clearly subjective and rather strongly depend on one, or a combination, of the following parameters: distance, galactic latitude, cluster richness.

Distance The effect of distance is to increase the number of galaxies per unit area, thus increasing the number of apparently close ellipticals. Moreover common halos are no longer clearly discernable because of their limited angular extent.

Galactic latitude The effect of galactic latitude is twofold: on the one hand the increasing number of stars per unit area contaminates the sample of Galaxy/Star pairs misclassified as dumb-bells beyond the magnitude at which stars and galaxies can be easily separated visually (around 17-18 mags), on the other hand increasing absorption dims the halo to the point at which a true dumb-bell is misclassified as a pair of E galaxies because of the lack of a common halo.

Cluster Richness The probability of chance superposition of two E galaxies is clearly dependent on the cluster richness. Especially at large distances, when the envelope is not clearly visible, this effect increases the number of interlopers.

Evidently also the plate scale and the color have important effects, but all clusters were inspected on the same plate material (ESO SERC J Sky Atlas film copies) so in this respect the present search is homogeneous.

Table I Dumb-bell galaxies in southern clusters ($z < 0.07$)

Name	RA (1950)	DEC (1950)	M 10	R	Class	BM type
419	3 06 00	-23 53	16.0	0	3	I-II
533	4 59 12	-22 42	15.5	0	3	III
548	5 44 54	-25 39	14.6	2	4	I-II
2401	21 55 36	-20 21	15.6	1	3	I
2412	22 01 18	-21 41	16.1	0	4	I-II
2799	0 35 06	-39 24	16.0	1	3	I-II
2800	0 35 30	-25 22	15.6	1	4	III
2819	0 43 42	-63 52	15.8	2	3	I-II
2824	0 46 06	-21 37	15.3	0	4	III
2854	0 58 36	-50 48	15.6	1	3	I-II
2860	1 01 48	-40 03	16.0	0	4	I
2911	1 23 48	-38 14	16.1	1	4	I-II
3009	2 20 18	-48 48	16.1	1	3	I
3089	3 06 12	-36 54	15.6	0	3	I-II
3093	3 09 12	-47 35	16.2	2	3	I
3094	3 09 18	-27 07	16.1	2	3	I-II
3095	3 10 18	-27 20	16.1	0	3	I-II
3104	3 12 36	-45 36	16.0	0	3	I
3111	3 16 06	-45 55	16.1	1	3	I-II
3112	3 16 12	-44 25	15.9	2	3	I
3151	3 38 24	-28 52	15.9	1	4	I-II
3158	3 41 42	-53 48	15.6	2	4	I-II
3164	3 44 42	-57 12	15.5	0	3	I-II
3225	4 08 24	-59 44	15.6	0	3	II
3266	4 30 30	-61 35	15.3	2	4	I-II
3323	5 09 24	-29 03	16.1	0	3	I
3368	5 48 24	-22 33	16.1	0	4	I-II
3390	6 23 18	-37 19	14.7	1	3	II
3391	6 25 12	-53 39	16.1	0	4	I
3395	6 26 30	-54 22	15.9	1	3	II
3497	11 57 30	-31 07	16.0	0	3	I-II
3505	12 06 06	-34 10	16.0	1	3	I-II
3528	12 51 36	-28 45	15.9	1	4	II
3530	12 52 54	-30 05	15.6	0	4	I-II
3532	12 54 36	-30 06	15.8	0	4	II-III
3556	13 21 18	-31 24	16.0	0	3	I
3559	13 27 06	-29 16	15.3	3	4	I
3560	13 29 00	-32 58	14.7	3	3	I
3570	13 43 54	-37 40	15.5	0	4	I-II
3581	14 04 36	-26 47	15.2	0	3	I
3695	20 31 36	-36 00	16.1	2	4	I
3716	20 47 54	-52 54	14.9	1	4	I-II
3744	21 04 18	-25 41	14.5	1	4	II-III
3771	21 26 06	-51 02	16.1	0	4	III
3822	21 50 36	-58 05	16.2	2	4	II-III
3880	22 25 00	-30 50	15.6	0	3	II

4. Dumb-bells as brightest cluster members

Bautz-Morgan (Bautz and Morgan 1970,hereafter BM) I and I-II clusters of galaxies are dominated by an outstandingly large, luminous galaxy, almost invariably a cD, as defined by Mattews *et al.* (1964), while at the opposite extreme in BM class III clusters no member stands out against the other galaxies. Rood and Leir (1979), examining the Abell (1958) statistical sample (which is confined to clusters of richness 1 or greater) showed that 23 per cent (28 out of 112) of the dominant galaxies in BM I and I-II clusters are binary supergiant galaxies. On the contrary BM III type clusters contain only 3 per cent of multiple galaxies. This implies that the cD dominated clusters are physically different from the BM III clusters as to the multiple nature of the dominant galaxies.

The simple statistics in Table II on the present complete volume limited sample confirms the Rood and Leir (1979) results on the northern clusters sample, namely that in the clusters dominated by an outstanding bright galaxy (cD) the probability of having a dumb-bell (or a multiple component supergiant galaxy) is 2.5 times higher than in other BM type clusters.

References

Abell,G.O. 1958 ***Astrophys. J. Suppl.*** **3**, 211
Abell,G.O., Corwin,H., Olowin,R. 1989 ***Astrophys. J. Suppl.*** **70**, 1
Bautz,L.P., Morgan,W.W. 1970 ***Astrophys. J. Lett.*** **162**, L149
Heckman,,T.M. *et al.* 1985 ***Astrophys. J.*** **288**, 122
Hoessel *et al.* 1980, ***Astrophys. J.*** **241**, 486
Matthews,T.A., Morgan,W.W., Schmidt,M. 1964 ***Astrophys. J.*** **140**, 35
Rood,H.J., Leir,A.W. 1979 ***Astrophys. J. Lett.*** **231**, L3
Schneider *et al.* 1983, ***Astrophys. J.*** **264**, 337
Stocke 1978, ***Astron. J.*** **83**, 348
Valentijn and Casertano 1988, ***Astron. Astrophys.*** **206**, 27
Vettolani,G., Gregorini, L. 1988 ***Astron. Astrophys.*** **189**, 39

Table II Clusters with $z < 0.07$

Multiplicity	I and I-II	Fm II to III
all	81	76
0 - 2	47 (58%)	64 (84%)
3 and 4	34 (42%)	12 (16%)

PANEL DISCUSSION:
DEFINITIONS OF THE TIDAL INTERACTION AND MERGER PHENOMENA

A panel on these issues was held with G. Burbidge as moderator and contributions from T. Chatterjee, T. Heckman, J. Hutchings, M. Noguchi, S. Simkin, and W. Keel (who prepared this summary).

Tidal interactions:

Several panelists stressed the need for care in defining observational criteria for considering a system interacting, beyond some kind of morphological peculiarity. Inevitably, some theoretical guidance is needed in this kind of interpretation. For example, narrow bridges and tails are well understood as results of certain kinds of interactions involving disk systems. Heckman stressed that such features should be seen in the old stellar population (the " Crimson Tide" approach) to avoid confusion with line emission or modest amounts of recent star formation that might have been influenced by hydrodynamical processes. Systems of these kinds will generally have an identifiable companion, perhaps tidally stripped or with its own tidal distortions, allowing further consistency checks on an interaction.

For ellipticals, there has been considerable success in modelling the broad tidal distortions characteristic of the high stellar velocity dispersions found in these galaxies. Further evidence of interaction with disk systems, or gas-rich companions, is made possible by this large velocity dispersion and the almost total lack of cool interstellar matter in ellipticals – stars from a cannibalized disk will form shells or rings, and substantial amounts of H I or dust are often associated with other indicators of interaction, such as environment or morphology. Note that these indicators require the (rare?) occurrence of significant mass transfer between two interacting systems.

The situation for AGNs and QSOs is less clear. As noted in Heckman's review, it is not clear what population we should compare QSO host galaxies with. Simkin proposed that in some kinds of apparent double systems, the mere fact of the presence of an active nucleus raises the probability that we are observing a physically interacting double.

Mergers:

The degree of certainty about defining a galaxy merger depends strongly on when we observe it. Early on, two nuclei may still be distinct; note that some care may be needed to avoid confusion of a region of rapid star formation, but dynamically insignificant mass, with a genuine galactic nucleus. When the nuclei can no longer be distinguished, more circumstantial tracers such as shells or H I in ellipticals must be used. The discovery of counter-rotating systems of stars or gas in several E and S0 systems in recent years is very interesting in this connection. In disk systems, early-type spirals sometimes seem capable of exhibiting shells after accretion of a dynamically cold companion, and disturbance of the disk velocity field (or global H I profile) may be observable when there is little morphological trace of the merger. When AGNs are involved, one can seek to measure an externally imposed tidal torque via precession of radio jets.

The frequent associations of starbursts and mergers of various kinds leads to the possibility of associating disturbed galaxies with strong bursts uniquely with mergers, though there is a serious risk of presupposing the effect to be measured. A potentially promising technique for tracing the fraction of E/S0 systems that are products of disk mergers is through globular-cluster counts, since the specific frequency of globulars depends on morphological type of the original host system.

Theoretical Issues:

Noguchi discussed the possibility that star formation may occur in different regimes in interacting and merging galaxies, driven by changes in the dominant kinds of cloud collisions. Collision velocities in a tidally perturbed disk will be relatively modest (of order 10 km s^{-1}, brought on by crossing of nearby orbits ("intra-galactic collisions"). In mergers, some "inter-galactic" collisions should have much higher velocities, as material originally part of different galaxies comes into contact as fast as several hundred km s^{-1}. Since cloud disruption is likely for most such fast collisions, differences in the resulting star formation might be detectable.

Chatterjee addressed the expected relative frequencies of tidal encounters and mergers, pointing out that most mergers must take place within 2-3 times the orbital period shortly before mergers. If mergers take much longer, the statistics of pairs and apparent merger remnants would be violated. This may require the common presence of massive halos in systems merging at the present epoch.

Unresolved Questions:

How large a tidal event should we regard as "significant"?
How many early-type galaxies are merger products?
What is the evolution of interaction and merger rates with cosmic time?

IV. OBSERVATIONS

OF

GLOBAL ACTIVITY

DUE TO INTERACTION

GLOBAL EFFECTS OF INTERACTIONS ON GALAXY EVOLUTION

Robert C. Kennicutt, Jr.
Steward Observatory, University of Arizona
Tucson, Arizona, USA

ABSTRACT

Recent observations of the evolutionary properties of paired and interacting galaxies are reviewed, with special emphasis on their global emission properties and star formation rates. Data at several wavelengths provide strong confirmation of the hypothesis, proposed originally by Larson and Tinsley, that interactions trigger global bursts of star formation in galaxies. The nature and properties of the starbursts, and their overall role in galactic evolution will also be discussed.

I. INTRODUCTION

The preponderance of tidally disturbed pairs of galaxies among samples of starbursting objects such as Markarian galaxies (Karachentsev and Karachentseva 1974), emission-line galaxies (Wasilewski 1983), and the ultraluminous IRAS galaxies (Soifer *et al.* 1984) shows that interactions can be a significant, if not dominant factor in galaxy evolution. The quantitative foundation for our understanding of the relationship between interactions and global star formation in galaxies was laid out in an influential paper by Larson and Tinsley (1978). "LT" demonstrated that interacting galaxies possess an unusually large dispersion in UBV colors, which they attributed to global bursts of star formation, and by fitting simple color evolution models to these observations they were able to derive the first quantitative estimates of the amplitudes and lifetimes of the starbursts. In retrospect it is fair to say that this paper had as stimulating an effect on the observers' community that the famous Toomre and Toomre (1972) paper had for theoretical work in the field.

The main goal of this review is to summarize what we have learned since 1978 about the evolution of interacting galaxies, with special emphasis on their global star formation properties, an area where much progress has been made. Several surveys of the integrated emission properties of interacting galaxies at visible, infrared, and radio wavelengths are now available, and these provide a self-consistent picture of how interactions affect the stellar birthrate in galaxies. I will also briefly discuss what can be learned about the starbursts from modelling the observations; these analyses not only provide us with information on the temporal properties of the bursts, but they also allow us to address such fundamental questions as whether the star formation in the bursts differs differs in any fundamental way (e.g., efficiency, IMF) from the steady state star formation in galaxies, or whether interactions trigger a significant fraction of the star formation in the universe, either now or at earlier cosmological epochs.

Throughout this paper I will emphasize the *global* effects of interactions on galaxy evolution; a companion review by Heckman discusses the effects of interactions on nuclear activity and star formation. Other topics which I will only address briefly, since they are reviewed elsewhere, include the morphologies, kinematics, and gas distributions in interacting galaxies (see papers by Karachentsev and Hickson), and the role of interactions and mergers in the formation of elliptical galaxies and spiral bulges. The latter subject deserves a review of its own, and for that I refer the reader to a lively and provocative paper by Schweizer (1990).

II. INTEGRATED PROPERTIES OF PAIRED AND INTERACTING GALAXIES

Recent observations provide a compelling case for a link between close tidal interactions and large star formation bursts. Since the original LT analysis two key improvements have been made, the development of optical, infrared, and radio tracers of the young star forming populations, and the observation of complete samples of paired and isolated galaxies, which allows us to derive unbiased statistics on the global role of interactions for galactic evolution.

UBV Colors and Surface Photometry

Since the LT study integrated multicolor photometry has been obtained for a considerably larger number of interacting galaxies. Observations of northern galaxies have been compiled by Demin, Dibai, and Tomov (1981) and Arkhipova (1982). The Demin *et al.* paper includes a recalibration of the previously published photometry of Tomov, and supercedes those earlier studies. A longstanding program of photometry of southern pairs has been conducted by the ESO/Uppsala group, as part of their large southern galaxy survey (e.g., Ardeberg and Bergvall 1977, Bergvall *et al.* 1978, Johansson 1988). These data confirm the large color dispersion which characterizes close pairs, and the extremely blue colors of the most active starbursting systems.

The advent of wide-field CCD cameras has recently led to a considerable body of data on the luminosity and color distributions of interacting systems (e.g., Armus, Heckman, and Miley 1987, Friedman *et al.* 1987, Fried and Lutz 1988, Bothun *et al.* 1989, Schombert, Wallin, and Struck-Marcell 1990). The Schombert *et al.* study is of particular interest, because it provides the first comprehensive data on the photometric properties of the faint tidal bridges, tails, and envelopes in close pairs. A focal reducer camera on the Palomar 1.5m telescope was used to obtain deep *BVri* surface photometry to study the structure and colors of the tidal features in 25 pairs selected from the Arp (1966) atlas. Several interesting new results emerge from this study. The tidal features contain a large fraction of the total luminosity of the systems, 25% on average, and up to 60% in extreme cases. The tidal bridges, tails, and plumes are systematically bluer than the parent galaxies, with colors that indicate that excess star formation, rather than low metallicity, is responsible for most of the difference. This would suggest that active star formation has persisted over very long ($\sim 10^8 yr$) timescales in many of the pairs. The Schombert et al. analysis illustrates the rich variety of problems in this area which can now be attacked with CCD imagers on modest aperture telescopes, especially when the data are combined with color evolution models and kinematic observations.

Hα Emission and Massive Star Formation Rates

The colors of interacting galaxies provide strong evidence for abnormal star formation rates (SFRs), but the quantitative interpretation of such data is limited. Integrated colors are only weakly dependent on the current SFR (e.g., Searle, Sargent, and Bagnuolo 1973), and they are subject to large systematic errors due to variations in reddening and metallicity. On the other hand the luminosity of a hydrogen recombination line such as Hα provides a direct, quantitative tracer of the SFR for massive stars ($> 10 M_\odot$), and when combined with the UBV data can provide quantitative estimates of the SFR integrated over all stellar masses (Kennicutt 1983, Gallagher *et al.* 1984).

Hα surveys of paired and interacting galaxies have been made by Dostal' (1982), Bushouse (1987) and Kennicutt *et al.* (1987). Although the techniques used in these surveys were similar, the sample selection criteria were quite different. Dostal' and Bushouse studied unusually perturbed pairs, using the morphological descriptions in the V–V and UGC catalogs for the initial selection. This provides an uncontaminated sample of pairs which probe the maximum effects of interactions on the SFR. Kennicutt et al. observed a similar sample of disturbed systems drawn from the Arp atlas, but they also formed a complete magnitude-limited sample of close spiral and irregular pairs, using a statistically generated catalog of van Albada (private communication), combined with redshift information to eliminate visual pairs. The complete sample provides a reliable assessment of the overall influence of interactions on paired galaxies.

All of these samples show evidence of abnormally high SFRs. As an example, Figure 1 shows the Hα-derived SFRs from Bushouse (1987), compared to a set of isolated spirals taken from Kennicutt and Kent (1983). The median Hα fluxes, normalized to the disk area or to the red continuum luminosity of the galaxies, show enhancements ranging from 30% in the complete pairs sample of Kennicutt et al. to factors of 2.2–2.5 for the morphologically selected samples. Note that the use of normalized luminosities minimizes any Malmquist bias or other observational selection effects in the comparisons.

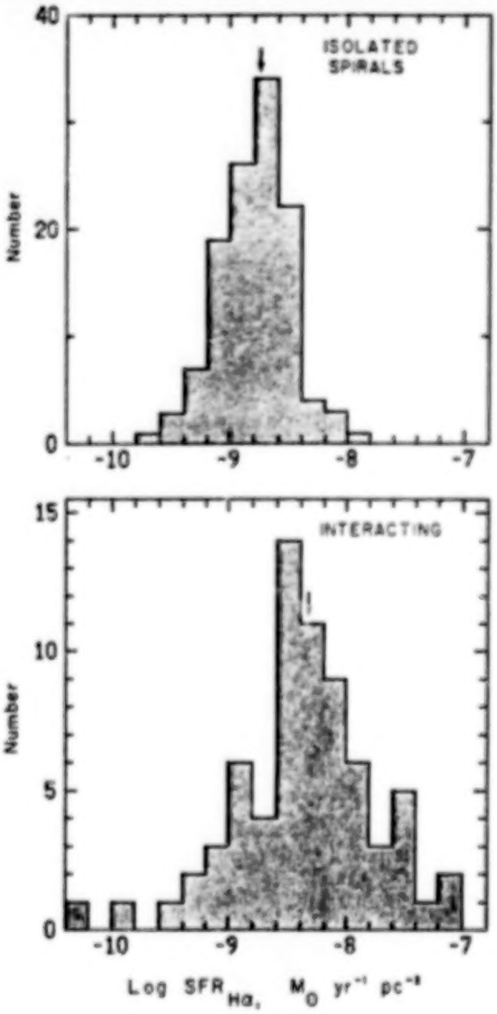

Fig. 1. Comparison of SFRs (normalized to disk area) for a sample of highly perturbed interacting galaxies, and a comparison sample of isolated galaxies, from Bushouse (1987).

It is evident from Figure 1 that the response of individual galaxies varies enormously. Several factors contribute to this dispersion, including the wide range of morphological types and gas content, the range of evolutionary stages (relative to the peak star formation episode), and a real variation in peak response to the interactions (see Sec. IV). Of special interest are the most active, starbursting systems. Inspection of Figure 1 reveals that there is a subpopulation of extreme emission-line galaxies which is almost uniquely associated with interactions. For example, galaxies with Hα equivalent widths above 50 Å comprise a quarter of the Kennicutt *et al.* (1987) sample, as opposed to only 4% among isolated galaxies. This is far more than can be accounted for by a mere shifting of the emission distribution of normal galaxies to a higher median level, and it suggests a highly nonlinear response of the SFR to the dynamical stimulation in many systems. On the other hand, it is important to remember that such starbursting systems are extremely rare; the average SFR enhancement in these samples, even in the most disturbed systems, is never much more than a factor of two.

Most of the Hα data were obtained with imaging detectors, so they also provide information on the spatial distribution and luminosity functions of the star forming regions. Perhaps the most interesting result is a strong tendency for the star formation in interacting spirals to be concentrated toward the nucleus (Bushouse 1987, Kennicutt *et al.* 1987). There is also a significant correlation between the level of activity in the nuclei and disks, above what is normally observed along the Hubble sequence (see Heckman's review for more details). Less is known about the azimuthal variation of the SFR in interacting galaxies. Hodge (1975) analyzed the H II region distributions in 14 systems and found severe distortions in several. In the Kennicutt *et al.* sample there is a qualitative trend of unusually strong spiral patterns in the close pairs, consistent with tidal triggering or 'swing amplification' of spiral density waves.

The trends observed in the total SFRs of interacting galaxies are also manifested in the properties of their largest H II region complexes. Petrosian, Saakian, and Khachikian (1985) have shown that the frequency of giant H II complexes or "superassociations" is twice as high in close pairs as in isolated galaxies. A detailed follow-up to this study is being pursued by Keel and collaborators.

Far-Infrared Properties

Currently the most active area of interest in this field is the far-infrared (FIR) emission of interacting galaxies, especially the extraordinary IR-luminous interacting/merging systems. Several recent reviews of this subject are available (e.g., Joseph 1987, 1988, Telesco 1988), and I will limit my discussion to the evidence for extranuclear star formation.

As with the Hα studies described above, the FIR surveys can be loosely divided into two groups according to the selection criteria applied, either interacting galaxies chosen by morphological criteria (e.g., Joseph *et al.* 1984, Lonsdale, Persson, and Mathews 1984; Bushouse, Lamb, and Werner 1988; Telesco, Wolstencroft, and Done 1988; Sulentic 1989), or comparisons of paired and isolated galaxies selected without regard any direct evidence of interactions (e.g., Kennicutt *et al.* 1987, Haynes and Herter 1988).

Again several common patterns emerge from these studies. The unbiased samples of galaxy pairs show modest (20-60%) enhancements in average FIR luminosity, and they contain few if any examples of ultraluminous systems. The latter result is consistent with the low space density of the ultraluminous galaxies, and the association of such objects with mergers, rather than discrete pairs. The percentage of excess FIR emission on average is similar the that observed at Hα, suggesting that increased star formation is the principle source of the IR excess. The strongly perturbed systems show considerably larger FIR enhancements, by factors of 2–3, and a significant fraction of ultraluminous systems. Only the most strongly interacting systems (or mergers) show extreme values of FIR excess. In parallel with the increase in FIR luminosity, there is a trend toward hotter color temperatures for the emitting dust (e.g., Bushouse *et al.* 1988, Telesco *et al.* 1988).

Unfortunately the interpretation of these data is more complicated than for the optical results discussed above. Usually the IRAS beam size at 60 and 100 μm is much larger than the galaxies in question (often the entire pair is unresolved), so it is not known *a priori* whether the excess FIR emission originates in the nuclei or the main bodies of the galaxies. The heating source of the dust is also unclear; massive young stars, the general interstellar radiation field, and nonthermal radiation from the nucleus may all contribute (e.g., Lonsdale and Helou 1987, Walterbos and Schwering 1987). Groundbased 10–20 μm measurements of selected galaxies indicate that a considerable fraction of the FIR emission in the most luminous objects is emitted by the nucleus (e.g., Lonsdale, Persson, and Mathews 1984, Cutri and McAlary 1985). On the other hand high-resolution IR images of systems such as Arp 299 (Telesco, Decher, and Gatley 1985) and Arp 118 (Joy and Ghigo 1988) reveal extensive regions of extranuclear emission associated with massive star formation.

Although it is premature to draw firm conclusions from the currently available data, the observations are consistent with enhanced extranuclear SFRs in the interacting galaxies. In contrast to the optical studies, however, which revealed a relatively homogeneous class of star forming (mainly disk) systems, there is evidence from the FIR surveys for a second population of ultraluminous merging galaxies, distinct in terms of not only the FIR luminosity but also their morphologies, kinematics, and spectroscopic properties. The nature and source of the FIR emission in these systems may be quite different from that which characterizes the steady-state emission of normal galaxies.

Radio Continuum Emission and Supernova Rates

Radio continuum studies of interacting and paired galaxies by Sulentic (1976) and Stocke (1978) provided some the earliest evidence for the abnormal emission properties of these objects. These results have since been confirmed by other workers (e.g., Hummel 1981, Condon *et al.* 1982). The mean enhancements are similar to those seen at Hα and the FIR, typically a factor of two.

The physical origin of the excess radio emission is less certain. At centimeter wavelengths the overwhelming fraction of the radio emission is nonthermal, and possible causes for the enhanced emission include nuclear emission, magnetic field compression in the disks, not unexpected in strong tidal encounters, or a burst of energetic charged particles from supernovae formed in a starburst. Hummel (1981) obtained spatially resolved maps for complete samples of paired and isolated spirals, and found that most of the excess radio emission in pairs originates in the nuclear regions. Subsequent studies at higher resolution by Condon *et al.* (1982) and Hummel *et al.* (1987, 1990) confirm the excess nuclear activity in interacting systems, but the question of whether the disk emission is enhanced remains open. A modest excess (30–50%) in disk emission, consistent with what is seen in Hα and the FIR, is not ruled out by the available data.

Detailed aperture synthesis mapping of nearby systems is beginning to reveal more about the nature of the radio emission. A survey of radio-bright galaxies by Condon (1983) revealed several examples of interacting galaxies with bright radio disks, though Condon has emphasized that an interaction is not a necessary condition for such disks. Hummel and van der Hulst (1986) have published a detailed multi-frequency study of 'The Antennae' (NGC 4038/39), and demonstrate that the strongly enhanced nonthermal disk emission in this pair is produced by increases in both the magnetic field strength and the charged particle densities. The latter is consistent with an elevated supernova rate, which in turn is consistent with the blue colors and bright Hα emission in the system. High-resolution radio maps of some nearby starburst and (supposedly) interacting galaxies show direct evidence of high supernova rates. Maps of M82 and NGC 3448 by Kronberg, Biermann, and Schwab (1985) and Noreau and Kronberg (1987) show large numbers of compact, unresolved sources which are almost certainly supernova remnants.

These conclusions are borne out by the statistics of the supernovae themselves in interacting galaxies. Smirnov and Tsvetkov (1981) have compared the supernova rates in isolated, paired, and interacting galaxies, and found that supernovae occur twice as frequently in the interacting systems. These authors are also able to exclude the possibility that the difference in rates arises from observational selection effects.

III. PECULIAR GALAXIES ASSOCIATED WITH INTERACTIONS

Many of the studies summarized above were limited to pairs in which two distinct galaxies can be recognized, and where the morphological types of the components can be classified on a normal system. However there are several types of peculiar objects, such as ring galaxies, amorphous galaxies, or multiple-nucleus galaxies, which appear to form predominantly or exclusively from interactions. Since these systems represent some of the most extreme forms of interactions, it is useful to summarize their properties.

Ring Galaxies

Ring galaxies probably form as the result of the direct impact of an intruding mass through the center of a disk (Lynds and Toomre 1976, Theys and Spiegel 1976). Few and Madore (1986) examined the morphologies and environments of 69 southern ring systems, and found that those showing evidence of recent star formation also possess a higher than normal frequency of close companions. Appleton and Struck-Marcell (1987) used the IRAS database to determine L_{FIR}/L_B ratios and 60/100 μm color temperatures for 26 rings, and found that they exhibit the FIR excesses and high temperatures which are characteristic of active star forming galaxies. Detailed optical and near-infrared imaging of selected systems by Bonoli (1987) and Joy *et al.* (1988) show similar evidence of recent star formation.

Amorphous (I0) Galaxies

Hubble and Lundmark both recognized the existence of a subpopulation of irregular galaxies, typified by M82, which could not be placed in the normal morphological sequence, and galaxies of this type are referred to variously as Irregular II, I0, or Amorphous galaxies. While it is likely that this collection of outcasts from the Hubble sequence may have several formation mechanisms (Krienke and Hodge 1974), the presence of tidal bridges and tails around several systems has led to the suggestion that most may be formed in interactions or mergers (e.g., Cottrell 1978). Keel *et al.* (1985) noted that the frequency of amorphous galaxies in a complete sample of close pairs is 5 times higher than in the field, lending additional support to this idea. Not all such galaxies can be readily identified with interactions, however. Gallagher and Hunter (1987) found evidence of recent interactions in only 20–60% of a sample of 16 nearby amorphous galaxies. This is very high fraction compared to what would be expected if amorphous galaxies were a normal population, but it does suggest that other formation mechanisms may be necessary.

Several recent observations indicate that amorphous galaxies are often the sites of large global star formation bursts. Gallagher and Hunter (1987) found that the mean SFRs in their sample, as derived from both UBV colors and Hα fluxes, are essentially the same as in a comparison sample of active star forming Magellanic irregulars. The detection of compact radio sources, probably supernova remnants, in M82 and NGC 3448 by Kronberg *et al.* (1985) and Noreau and Kronberg (1987) adds support to this conclusion. In many of these galaxies the intense star formation activity is confined to the near-nuclear regions (Gallagher and Hunter 1987), a result which is reminiscent of Bushouse's (1987) result for interacting spirals.

Mergers and Multiple Nucleus Galaxies

The identification of the most luminous IRAS galaxies with mergers, combined with the suggestion that elliptical galaxies may form via mergers (e.g., Toomre 1977), has led to a widespread interest in these objects. As discussed earlier the nature of the enormous infrared luminosities of the IRAS galaxies is very controversial, but there is mounting evidence for *global* star formation bursts in many of these objects. The most direct evidence comes from near-infrared imaging (e.g., Stanford and Balcells 1990), which can penetrate the dust with shrouds the cores of many mergers, but unfortunately such data are only available for a few objects. The observation of strong, spatially extended Balmer absorption lines in the composite spectra of several mergers provides indirect evidence for enormous fossil ($\tau \sim 10^6 yr$) starbursts (Schweizer 1978, 1990; Hamilton and Keel 1987).

It has long been recognized that multiple-nucleus galaxies are unusually common in the Markarian sample (Petrosian, Saakyan, and Khachikian 1978). Systematic studies of the structure and spectroscopic properties of these galaxies have been conducted by Petrosian et al. (1980a, b) and Mazzarella (1990). The mere existence of these galaxies in such large numbers suggests a causal connection between close encounters/mergers and nuclear and/or disk activity. Perhaps the most notable property of the class is an unusually high fraction of Seyfert nuclei (Mazzarella 1989), though this may partly be a selection effect in the Markarian survey itself.

Schweizer (1990) summarizes a long series of observations in support of the hypothesis that mergers were the primary formation mechanism for elliptical galaxies and spiral bulges. The evidence, in addition to the observations summarized above, includes the $r^{1/4}$ luminosity distributions in many mergers, and the presence of counter-rotating cores in both mergers and some E/S0 galaxies (discussed extensively elsewhere in this volume). Although the role of mergers in galaxy formation is still unclear, especially from an observational perspective, I do believe that the data point to a very different mode of starburst activity in these objects, relative to what is seen in normal disks. The presence of enormous ($L \sim 10^{11-13} L_{\odot}$) infrared luminosities, dense and massive central molecular disks, large amounts of interstellar dust, spheroidal morphologies, and Balmer-dominated spectra all represent more than a simple extrapolation of the star formation properties on normal disks; these are phenomena which appear to be almost uniquely identified with mergers. It is very tempting to associate these activities with the formation of stars in galactic spheroids and/or nuclei, regardless of their association with proto-elliptical galaxies and bulges.

IV. DEPENDENCE OF ACTIVITY ON INTERACTION PARAMETERS

Considerable effort has been directed at understanding the parameters and processes which regulate the starbursts in interacting systems. The traditional approach to this question has been to correlate the emission levels with various interaction parameters, such as pair separation or velocity difference. Another approach is to start with what we know (or think we know!) about the star formation properties of normal galaxies, and examine these same trends in the interacting systems. The latter approach provides some interesting physical perspectives, so I begin there.

The SFR in isolated galaxies is most strongly correlated with Hubble type and gas content, as illustrated in Figures 2 and 3, respectively. In each case the SFR tracer plotted is the integrated equivalent width of the Hα emission line, which provides a measure of the total SFR in the galaxies, normalized to total (continuum) luminosity. Among isolated galaxies (labelled the "control sample" in each plot), there are strong correlations between this SFR and both galaxy type and gas density, albeit with considerable scatter about the mean.

When the same comparisons are made for interacting galaxies, however, these correlations largely disappear. The SFR in an interacting galaxy is virtually independent of its morphological type or gas content, and hence is effectively decoupled from its star formation properties prior to the encounter. Apparently interactions do not merely amplify a pre-existing level of star formation, they induce bursts which are regulated by mechanisms which are quite distinct from those which control the steady-state star formation in disks.

The Holmberg Effect

One of the best demonstrations of the dominating influence interactions can have on the global SFR is the "Holmberg effect," the tendency for the individual members of a pair to exhibit similar integrated colors (Holmberg 1958, Ardeberg and Bergvall 1977, Metik and Pronik 1978, Demin *et al.* 1984, Madore 1986). Part of the correlation is due to morphological segregation, the tendency for pairs to contain galaxies of similar morphological type (see the paper by Yamagata in this volume), but in many pairs the dominant cause is simultaneous star formation bursts in the two galaxies (Demin *et al.* 1984, Madore 1986). This is particularly true of the bluest pairs ($B - V < 0.5$), because such blue colors can only be produced in short-lived star formation bursts (e.g., Searle *et al.* 1973).

Similar correlations are also seen in the Hα equivalent widths (Kennicutt *et al.* 1987) and FIR properties (Cutri, private communication) of close pairs.

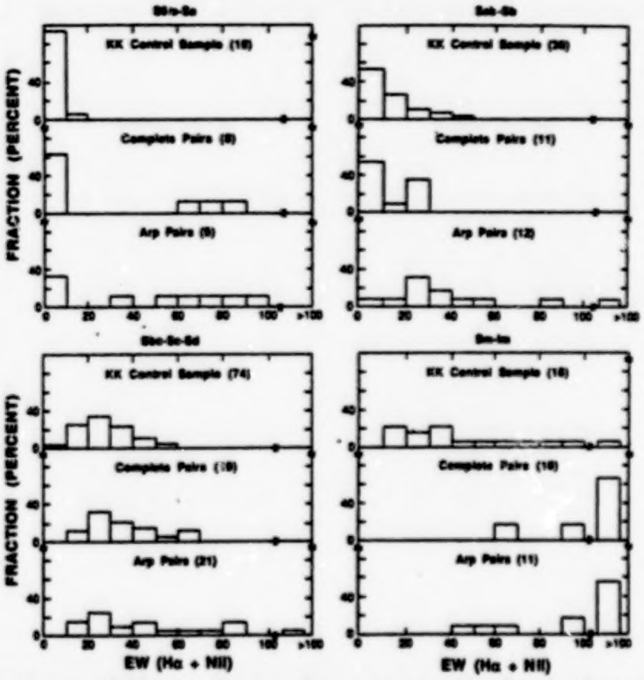

Fig. 2. Distributions of Hα emission line strengths for isolated (control) and interacting (complete, Arp) galaxies, subdivided by Hubble type.

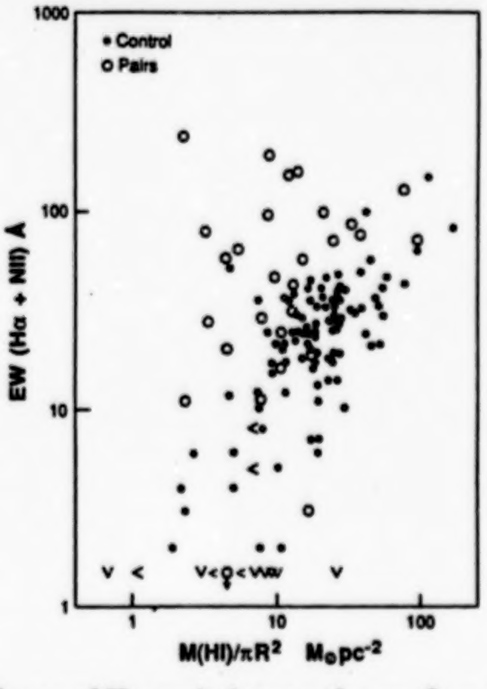

Fig. 3. Dependence of Hα emission on the surface density of atomic hydrogen, for isolated (solid points) and interacting galaxies (open circles).

Dependence on Pair Separation and Velocity Difference

The tidal perturbations in an interaction are the strongest for close, slow encounters, so if dynamical parameters regulate the SFR one would expect the emission levels to be inversely correlated with the projected separations and velocity differences of the pairs. Both trends are observed. Closer pairs show an excess of Markarian galaxies (Casini and

Heidmann 1975, Karachentsev 1981), bluer colors (Madore 1986), higher average levels of Hα emission (Tifft 1985, Kennicutt *et al.* 1987) stronger FIR emission (e.g., Bushouse *et al.* 1988, Jones and Stein 1989), and hotter FIR color temperatures (Telesco *et al.* 1988).

Figure 4, taken from Jones and Stein (1989), illustrates the dependence of the FIR/B ratio on separation, and provides a case study in some of the ambiguities inherent in this sort of analysis. The unmarked points are pairs taken from the Bushouse *et al.* (1988) optically-selected sample, while the labeled points are ultraluminous IRAS galaxies taken from Sanders *et al.* (1988). The mean level of FIR emission shows a weak separation dependence at best, but the upper envelope of the distribution rises rapidly with decreasing separation, especially when the ultraluminous galaxies are included. This is an excellent illustration of the nearly unique association of the ultraluminous FIR galaxies with close violent mergers, but these objects are so rare and so distinct in their properties that their separation distribution should probably be considered separately from that of the Bushouse sample.

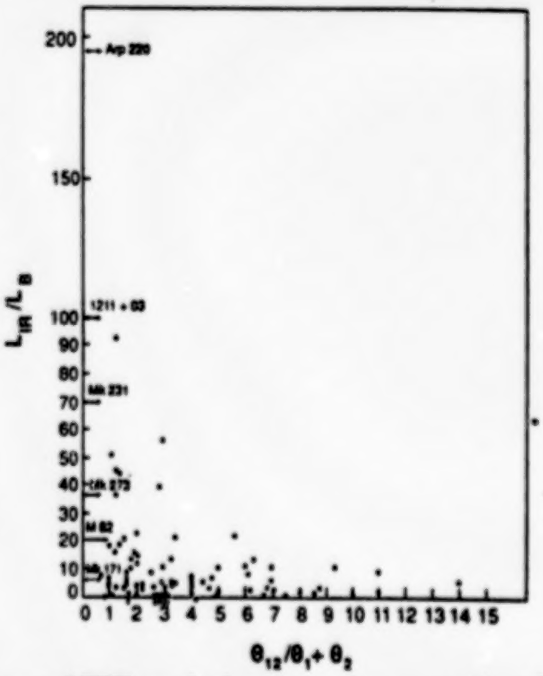

Fig. 4. Dependence of FIR emission on pair separation for a sample of interacting galaxies studied by Jones and Stein. Ultraluminous FIR galaxies are labeled individually.

Less is known about the dependence of emission properties on the radial velocity separations of the components. Karachentsev (1981) demonstated that pairs containing Markarian galaxies show significantly smaller differences in velocity than normal pairs. Tifft (1985) examined the redshift differences in a sample of 250 close pairs, and found a pronounced increase in the frequency of emission line detections with decreasing velocity difference. Tifft also investigated the dependence of emission properties on the product of velocity separation and projected linear separation, and finds a correlation there as well. Unfortunately his (photographic) spectra are uncalibrated, so a more quantitative analysis would be very useful.

While these sorts of statistical studies provide convincing qualitative confirmation of the expected dependences of the SFRs on orbital properties, the trends are so noisy that a detailed physical interpretation is not yet possible. The large dispersion in emission properties is not unexpected if one considers the wide range in projection angles, orbital velocities, orientations of rotation and orbital axes, and evolutionary stages. While these problems may be redressed somewhat by observing larger samples, the most productive observations in the future may be those which match detailed kinematic observations of individual pairs with dynamical simulations (e.g., Jenkins 1984, Borne 1988a, b; Borne and Hoessel 1988, Hernquist 1990).

V. INTERPRETATION AND MODELLING

In contrast to the extensive observational work described above, relatively little effort has been devoted to the modelling of these data in order to to derive the evolutionary properties of the systems. Fortunately the original Larson and Tinsley (1978) model has stood up very well against the new observations, and it provides an excellent starting point for this discussion.

Properties of Star Formation Bursts

Figure 5, taken from the LT paper, shows the observed *UBV* colors of normal (left) and peculiar galaxies from the Arp atlas (right), together with curves which depict the expected colors of model stellar populations. The normal galaxies are well fitted by a sequence of fixed-IMF, fixed-age models with variable star formation histories (cf. Searle *et al.* 1973). On the other hand the blue colors of many of the interacting galaxies require strong star formation bursts superimposed on the underlying populations. The upper envelope to the observed color distribution requires relatively short-lived bursts, 20 Myr in the case of the upper curve in Fig 5b. The lower envelope of the color distribution imposes a limit on the strength of the burst (i.e., the fraction of the total mass of stars in the galaxy formed in the bursts), and for the Arp sample the inferred burst strengths are all below 5%. Hence the blue colors of the interacting galaxies can be reproduced with very modest starbursts, in terms of the total mass of stars formed, but the models do require that the star formation take place over a time interval which is short compared to the dynamical time scales of most encounters.

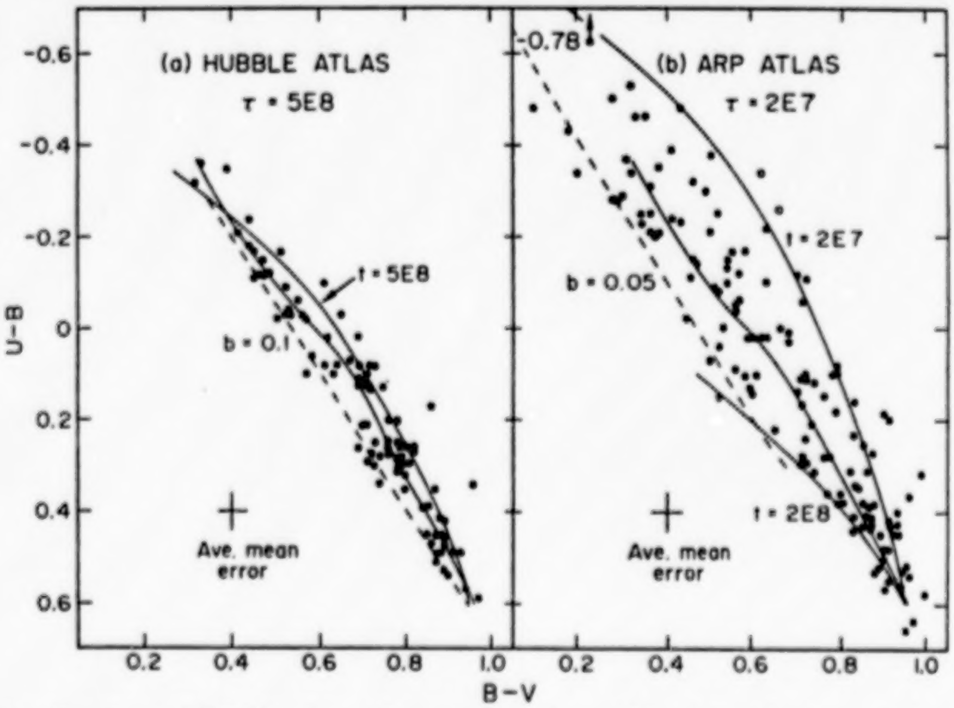

Fig. 5. Distribution of UBV colors of normal and peculiar (mostly interacting) galaxies, along with evolutionary models fitted to the data, from Larson and Tinsley (1978). See text for a description of the models.

Kennicutt *et al.* (1987) extended this approach by calculating the evolution of the Hα emission line fluxes and equivalent widths as well as the colors. The Hα fluxes provide a direct measurement of the SFR during the interaction, as well as independent constraints on the time scales and initial mass function (IMF) of the bursts. We found that the Hα equivalent widths and colors for most interacting galaxies could be fitted with burst properties falling within the LT parameter space, namely durations of less than 20 Myr, a normal (Salpeter) IMF, and a total mass in new stars of a few percent or less of the total disk mass. Over the entire sample, the colors can be fitted with bursts of duration 3–50 Myr, amplitudes of order 0.1–100 times the pre-existing SFR, and absolute SFRs of order 0.1–100 $M_{\odot}yr^{-1}$. These imply total masses of up to $10^9 - 10^{10}$ $M_{\odot}$ in stars formed over the duration of the burst.

An independent upper limit on the lifetime of the star formation bursts can be imposed by comparing the peak SFR to the total mass of interstellar gas available in the star forming region. In strong starburst galaxies these yield total consumption times of order 0.1–1 Gyr if the total gas mass is used (i.e., 100% star formation efficiency), and proportionally less if a smaller total efficiency is assumed. The latter are consistent with the photometrically inferred time scales.

These models barely manage to reproduce the very high Hα fluxes and equivalent widths of the most active starburst galaxies, those lying in the upper envelope of Fig. 5. In the standard LT model these extreme photometric properties require very young ($\tau \ll 10 Myr$) starbursts, but such short-lived bursts appear to be inconsistent with the fraction of interacting galaxies observed in this stage. The only alternative is to question the assumptions underlying the models, and of those the most likely culprit is the assumed IMF.

Initial Mass Function and Star Formation Efficiency

Although most models for the evolution of interacting galaxies presume for simplicity's sake a universal IMF, there is accumulating evidence for abnormal IMFs in the most active star forming systems. Unfortunately, constraining even the rough form of the IMF in these galaxies is itself a highly model-dependent exercise, and in some cases the various determinations are mutually inconsistent. For example, the blue colors and high Balmer emission-line equivalent widths in the most active galaxies are best understood if the IMF is heavily enriched in massive stars (M = 10–100 $M_{\odot}$) relative to the solar neighborhood (Huchra 1977, Kennicutt *et al.* 1987). On the other hand, the high fraction of nonthermal radio emission in these objects (as compared to ordinary giant H II regions) has led Gehrz, Sramek and Weedman (1983) and Nakagawa *et al.* (1989) to suggest a *deficiency* of stars more massive than 30 $M_{\odot}$.

The most detailed model of the IMF in a starburst region has been constructed for M82 by Rieke *et al.* (1980). In addition to using the ionizing properties to constrain the upper IMF, they used the dynamical mass and IR luminosity of the region to investigate the IMF at low stellar masses. Their best fitting models require both upper and lower mass cutoffs to the IMF, with a typical range of 5–30 $M_{\odot}$. Although more recent models by Bernlohr (this conference) relax the lower mass limits considerably, the observed properties of the starbursts are still difficult to reconcile with a normal IMF.

Careful examination of these various models reveals a complex interplay between the IMF parameters and the temporal properties of the starbursts, and I suspect that the constraints on the IMF are considerably weaker than the authors (this one included) would hope. Another fundamental issue which has yet to be addressed conclusively is whether the unusual IMFs attributed to these regions are unique to interacting (or luminous starburst) galaxies, or whether they merely reflect a general difference or bimodality in the IMF between active star forming regions and the integrated population of an entire galaxy.

Some of these models also suggest unusually high efficiencies of star formation in the starbursts. In the M82 core, for example, the observed luminosities and gas contents require efficiencies of order 10–100%, regardless of the IMF (Rieke *et al.* 1980). This dilemma can be relaxed if much of the gas involved in the star formation has been driven away, but it is difficult to see how this could explain the entire difference in efficiencies. Again it is important to note that this problem may not be unique to interacting or IR-luminous galaxies (cf. Kennicutt and Chu 1988). The unusually high ratios of FIR to CO molecular line luminosity in many interacting galaxies has been used to argue for abnormally high global star formation efficiencies (e.g., Young *et al.* 1986, Solomon and Sage 1988). This result verifies that the SFRs in these galaxies are not the result of abnormally high gas contents.

Global Role of Interactions in Star Formation and Galactic Evolution

An interesting quantity which can be derived from the evolution models is the fraction of star formation in the universe which is triggered by interactions. Kennicutt *et al.* (1987) combined their SFR study of a complete sample of pairs with the fraction of such pairs in the Shapley-Ames catalog, and estimated that interactions are responsible for 6±3% of the current star formation in nearby spiral galaxies. The main uncertainties in this result are the definition of an interacting galaxy, Malmquist bias in the pairs catalog, and the assumption that the IMF in the interacting systems is the same as in normal spirals.

This fraction was probably much higher at earlier cosmological epochs, and it is becoming possible to test this hypothesis observationally. Lavery and Henry (1988) show that most of the blue galaxies in a rich cluster at $z = 0.2$ possess companions or other visible evidence of recent interactions, and they propose that interactions may be the primary cause of the Butcher-Oemler effect in more distant clusters. Along similar lines Zepf and Koo (1989) have used a deep survey of distant field galaxies to compare the frequency of close pairs at faint magnitudes ($B \leq 22$) with the fraction among bright, nearby galaxies. They find a statistically significant excess of faint pairs, which is consistent with an increase in the frequency of interactions $f \propto (1 + z)^{4.0 \pm 2.5}$. This implicitly assumes that the detection of the faint pairs has not been biased by luminosity evolution effects, so the conclusion remains tentative until better data can be obtained.

As an amusing, albeit speculative exercise, one can combine the Kennicutt *et al.* fraction of current star formation from interactions with the Zepf and Koo redshift dependence for the interaction frequency, in order to estimate the redshift at which interactions dominate the global star formation in galaxies. Using the numbers above, including all of the uncertainties, yields a range of 'formation' redshifts $z = 0.5 - 3$. Systematic errors tend to bias this result in the direction of lower z, but this back of the envelope calculation does emphasize the likely importance of interactions at early epochs, even if their global role is quite minor at the current time.

VI. CONCLUDING REMARKS

The main accomplishment in this field over the past decade has been the quantitative verification, sometimes in spectacular fashion, of the Larson and Tinsley (1978) hypothesis that interactions are an important trigger of star formation bursts in galaxies. The second-order questions, such as the dependence of the star formation on the physical and kinematic properties of the pairs, the relative roles of nuclear and extranuclear emission, etc., are less well understood, but considerable progress in these areas can be expected over the next few years.

Now that the easy work has been done, further interpretation of the statistics of optical, IR, and radio emission properties of these galaxies is becoming increasingly limited by fundamental uncertainties in our physical understanding of the nature of the stellar populations and the dynamical properties of the interactions themselves. Among the most important questions:

1. What is the physical nature of the "starbursts" in interacting galaxies, and how many starburst phenomena are we observing? Most current surveys implicitly assume that we observing a single generic type of star formation activity, but the recent observations, particularly those at infrared wavelengths, suggest the presence of at least two distinct modes of activity, with very different dependences on interaction properties. The simplest consideration of galactic structure and evolution suggests that we should see at least three distinct types of starbursts, one associated with an enhanced level of disk star formation, another associated with the formation of galactic spheroids, and perhaps another associated

with the formation of the dense mass concentrations in the centers of galaxies. Before we can fully understand the nature of the "starburst phenomenon" we need to establish how many processes we are actually observing.

2. What are the physical mechanisms which trigger and regulate the starbursts? Both observations and theory suggest that gas dynamics, possibly coupled to a strong star formation threshold (e.g., Quirk 1972, Kennicutt 1989) are central elements of the triggering mechanism, but to date relatively little observational effort has been devoted toward measuring the dynamical properties of the stars and gas in interacting galaxies. The recent discoveries of U-shaped rotation curves and counter-rotating cores in isolated E galaxies and mergers are impressive illustrations of how important such observations can be.

3. What is the nature of the star formation in the starbursts, especially the IMF, relative to that in normal star forming galaxies? This question is of more than pure theoretical interest. The interpretation of virtually all photometric tracers of star formation rates in galaxies, regardless of wavelength, rests heavily on the assumed form of the IMF. Until the IMF is understood both our observational and theoretical understanding of the evolution of these objects will be severely handicapped.

Significant future progress in our understanding of the evolution of interacting (and normal!) galaxies will require more than a mere extention of current surveys to larger samples. Observations which will be especially crucial for disentangling the questions cited above include detailed kinematic studies of individual systems, preferably coordinated with simulations of the dynamics of the encounters, high-resolution maps of the atomic and molecular gas distributions and kinematics, and multi-wavelength observations of the stellar populations in a range of systems. Such observations may lead not only to a better understanding of tidal interactions, but also to important insights into the mechanisms regulating galactic evolution in general.

I am grateful to my collaborators W. Keel, E. Hummel, and J. M. van der Hulst, as well as H. Bushouse, R. Cutri, T. Heckman, A. Petrosian, S. White, and A. Zasov for very useful discussions about this subject. I also thank H. Bushouse, R. Larson, and W. Stein for permission to reproduce their figures in this paper. This work was supported in part by NSF Grant AST89-96123.

REFERENCES

Appleton, P. N., and Struck-Marcell, C. 1987, *Ap. J.*, **312**, 566.
Ardeberg, A., and Bergvall, N. 1977, *Astr. Ap.*, **61**, 493.
Arkhipova, V. P. 1982, *Astr. Zh.*, **59**, 209.
Armus, L., Heckman, T., and Miley, G. 1987, *A. J.*, **94**, 831.
Bergvall, N. Å. S. *et al.* 1978, *Astr. Ap. Suppl.*, **33**, 243.
Bonoli, C. 1987, *Astr. Ap.*, **174**, 57.
Borne, K. D. 1988a, *Ap. J.*, **330**, 38.
Borne, K. D. 1988b, *Ap. J.*, **330**, 61.
Borne, K. D., and Hoessel, J. G. 1988, *Ap. J.*, **330**, 51.
Bothun, G. D., Halpern, J. P., Lonsdale, C. J., Impey, C., and Schmitz, M. 1989, *Ap. J. Suppl.*, **70**, 271.
Bushouse, H. A. 1987, *Ap. J.*, **320**, 49.
Bushouse, H. A., Lamb, S. A., and Werner, M. W. 1988, *Ap. J.*, **335**, 74.
Casini, C., and Heidmann, J. 1975, *Astr. Ap.*, **39**, 127.
Condon, J. J. 1983, *Ap. J. Suppl.*, **53**, 459.
Condon, J. J., Condon, M. A., Gisler, G., and Puschell, J. J. 1982, *Ap. J.*, **252**, 102.
Cottrell, G. A. 1978, *M.N.R.A.S.*, **184**, 259.

Cutri, R. M., and McAlary, C. W. 1985, *Ap. J.*, **296**, 90.
Demin, V. V., Dibai, E. A., and Tomov, A. N. 1981, *Astr. Zh.*, **58**, 925.
Demin, V. V., Zasov, A. V., Dibai, E. A., and Tomov, A. N. 1984, *Astr. Zh.*, **61**, 625.
Dostal', V. A. 1982, *Armenian Astrofisica*, **18**, 201.
Few, J. M. A., and Madore, B. F. 1986, *M.N.R.A.S.*, **222**, 673.
Fried, J. W., and Lutz, D. 1988, *Astr. Ap.*, **197**, 52.
Friedman, S. D., Cohen, R. D., Jones, B., Smith, H. E., and Stein, W. A. 1987, *A. J.*, **94**, 1480.
Gallagher, J. S., Hunter, D. A., and Tutukov, A. V. 1984, *Ap. J.*, **284**, 544.
Gallagher, J. S., and Hunter, D. A. 1987, *A. J.*, **94**, 43.
Gehrz, R. D., Sramek, R. A., and Weedman, D. W. 1983, *Ap. J.*, **267**, 551.
Hamilton, D., and Keel, W. C. 1987, *Ap. J.*, **321**, 211.
Haynes, M. P., and Herter, T. 1988, *A. J.*, **96**, 504.
Hernquist, L. 1990, in *Dynamics and Interactions of Galaxies*, ed. R. Wielen (Dordrecht: Kluwer), in press.
Hodge, P. W. 1975, *Ap. J.*, **202**, 619.
Holmberg, E. 1958, *Medd. Lunds Astr. Obs.*, **2**, No. 136.
Huchra, J. P. 1977, *Ap. J.*, **217**, 928.
Hummel, E. 1981, *Astr. Ap.*, **96**, 111.
Hummel, E., and van der Hulst, J. M. 1986, *Astr. Ap.*, **155**, 151.
Hummel, E., van der Hulst, J. M., Keel, W. C., and Kennicutt, R. C. 1987, *Astr. Ap. Suppl.*, **70**, 517.
Hummel, E., van der Hulst, J. M., Kennicutt, R. C., and Keel, W. C. 1990, *Astr. Ap.*, submitted.
Jenkins, C. R. 1984, *Ap. J.*, **277**, 501.
Johansson, L. 1988, *Astr. Ap. Suppl.*, **73**, 335.
Jones, B., and Stein, W. A. 1989, *A. J.*, **98**, 1557.
Joseph, R. D. 1987, in *Starbursts and Galaxy Evolution*, ed. T. X. Thuan, T. Montmerle, J. Tran Thanh Van (Paris: Editions Frontieres), p. 293.
Joseph, R. D. 1988, in *Comets to Cosmology*, ed. A. Lawrence (Berlin: Springer), p. 234.
Joseph, R. D., Meikle, W. P. S., Robertson, N. A., and Wright, G. S. 1984, *M.N.R.A.S.*, **209**, 111.
Joy, M., Ellis, H. B., Tollestrup, E. V., Brock, D., Higdon, J. L., and Harvey, P. M. 1988, *Ap. J. (Letters)*, **330**, L29.
Joy, M., and Ghigo, F. D. 1988, *Ap. J.*, **332**, 179.
Karachentsev, I. D., and Karachentseva, V. E. 1974, *Astr. Zh.*, **51**, 724.
Karachentsev, I. D. 1981, *Pis'ma Astr. Zh.*, **7**, 3.
Keel, W. C., Kennicutt, R. C., Hummel, E., and van der Hulst, J. M. 1985, *A. J.*, **90**, 708.
Kennicutt, R. C. 1983, *Ap. J.*, **272**, 54.
Kennicutt, R. C. 1989, *Ap. J.*, **344**, 685.
Kennicutt, R. C., and Chu, Y.-H. 1988, *A. J.*, **95**, 720.
Kennicutt, R. C., and Kent, S. M. 1983, *A. J.*, **88**, 1094.
Kennicutt, R. C., Keel, W. C., van der Hulst, J. M., Hummel, E., and Roettiger, K. A. 1987, *A. J.*, **93**, 1011.
Krienke, O. K., and Hodge, P. W. 1974, *A. J.*, **79**, 1242.
Kronberg, P. P., Biermann, P., and Schwab, F. R. 1985, *Ap. J.*, **291**, 693.
Larson, R. B., and Tinsley, B. M. 1978, *Ap. J.*, **219**, 46.
Lavery, R. J., and Henry, J. P. 1988, *Ap. J.*, **330**, 596.
Lonsdale, C. J., and Helou, G. 1987, *Ap. J.*, **314**, 513.
Lonsdale, C. J., Persson, S. E., and Mathews, K. 1984, *Ap. J.*, **287**, 95.
Lynds, C. R., and Toomre, A. 1976, *Ap. J.*, **209**, 382.
Madore, B. F. 1986, in *Spectral Evolution of Galaxies*, ed. C. Chiosi and A. Renzini (Dordrecht: Reidel), p. 97.
Mazzarella, J. 1989, Ph.D. thesis, University of Michigan.

Metic, L. P., and Pronik, I. I. 1978, *Astr. Zh.*, **55**, 249.
Nakagawa, T., Nagata, T., Geballe, T. R., Okuda, H., Shibai, H., and Matsuhara, H. 1989, *Ap. J.*, **340**, 729.
Noreau, L., and Kronberg, P. P. 1987, *A. J.*, **93**, 1045.
Petrosian, A. R., Saakian, K. A., and Khachikian, E. E. 1978, *Astrofisica*, **14**, 69.
Petrosian, A. R., Saakian, K. A., and Khachikian, E. E. 1980a, *Pis'ma Astr. Zh.*, **6**, 262.
Petrosian, A. R., Saakian, K. A., and Khachikian, E. E. 1980b, *Pis'ma Astr. Zh.*, **6**, 552.
Petrosian, A. R., Saakian, K. A., and Khachikian, E. E. 1985, *Astrofisica*, **21**, 57.
Quirk, W. J. 1972, *Ap. J. (Letters)*, **176**, L9.
Rieke, G. H., Lebofsky, M. J., Thompson, R. I., Low, F. J., and Tokunaga, A. T. 1980, *Ap. J.*, **238**, 24.
Sanders, D. B., Soifer, B. T., Elias, J. H., Madore, B. F., Matthews, K., Neugebauer, G., and Scoville, N. Z. 1988, *Ap. J.*, **325**, 74.
Scalo, J. M. 1986, *Fund. Cos. Phys.*, **11**, 1.
Schombert, J. M., Wallin, J. F., and Struck-Marcell, C. 1990, *A. J.*, **99**, 497.
Schweizer, F. 1978, in *Structure and Properties of Nearby Galaxies*, ed. E. M. Berkhuijsen and R. Wielebinski (Dordrecht: Reidel), p. 279.
Schweizer, F. 1990, in *Dynamics and Interactions of Galaxies*, ed. R. Wielen (Dordrecht: Kluwer), in press.
Searle, L., Sargent, W. L. W., and Bagnuolo, W. G. 1973, *Ap. J.*, **179**, 427.
Smirnov, M. A., and Tsvetkov, D. Yu. 1981, *Pis'ma Astr. Zh.*, **7**, 154.
Soifer, B. T., *et al.* 1984, *Ap. J. (Letters)*, **278**, L71.
Solomon, P. M., and Sage, L. J. 1988, *Ap. J.*, **334**, 613.
Stanford, S. A., and Balcells, M. 1990, *A. J.*, in press.
Stocke, J. T. 1978, *A. J.*, **83**, 348.
Sulentic, J. W. 1976, *Ap. J. Suppl.*, **32**, 171.
Sulentic, J. W. 1989 *A. J.*, **98**, 2066.
Telesco, C. M. 1988, *Ann. Rev. Astr. Ap.*, **26**, 343.
Telesco, C. M., Decher, R., and Gatley, I. 1985, *Ap. J.*, **299**, 896.
Telesco, C. M., Wolstencroft, R. D., and Done, C. 1988, *Ap. J.*, **329**, 174.
Theys, J. C., and Spiegel, E. A. 1977, *Ap. J.*, **212**, 616.
Tifft, W. G. 1985, *Ap. J.*, **288**, 65.
Tinsley, B. M., and Danly, L. 1980, *Ap. J.*, **242**, 435.
Toomre, A. 1977, in *The Evolution of Galaxies and Stellar Populations*, ed. B. M. Tinsley and R. B. Larson (New Haven: Yale Univ.), p. 401.
Toomre, A., and Toomre, J. 1972, *Ap. J.*, **178**, 623.
Walterbos, R. A. M., and Schwering, P. B. W. 1987, *Astr. Ap.*, **180**, 27.
Wasilewski, A. J. 1983, *Ap. J.*, **272**, 68.
Young, J. S., Schloerb, F. P., Kenney, J. D., and Lord, S. D. 1986, *Ap. J.*, **304**, 443.
Zepf, S. E., and Koo, D. C. 1989, *Ap. J.*, **337**, 34.

DISCUSSION

Bland:

For NGC 4647, where an extended population of HII regions cut off suddenly and the HI is observed to extend much further, if there is no evidence for bars or external dynamics, you probably have direct evidence of the importance of disk self-gravity. Have you measured the gas stability in this object, say, with Toomre's criterion?

Kennicutt: Yes! In a recent study of the star formation law in disks (Kennicutt 1989), I compared to locations of the observed star formation thresholds with the predicted gravitational stability threshold according to the Toomre criterion. There is a remarkable agreement between the predicted and observed thresholds, which suggests that gravitational stability may be the main regulator of the large scale star formation in late-type galaxies (including NGC 4647). This confirms a long-standing prediction by Quirk (1972).

Burbidge: Surely your last point is the most important one. Until you can place limits on the behavior of the IMF in these systems, all of the conclusions concerning star formation and evolution are meaningless.

Kennicutt: The situation is not quite that bad! The agreement in the star formation rates derived from Hα, UV, and UBV data, all which trace different parts of the IMF, tells us that the rates cannot be in error by more than factors of a few, and hence the orders-of-magnitude bursts which are observed in many interacting systems cannot be simply artifacts of an unusual IMF. However, I wholly agree that our ignorance about the IMF in these galaxies is the main impediment to understanding their detailed evolutionary properties.

A MULTIWAVELENGTH SURVEY OF INTERACTING GALAXIES

H. Bushouse[1], S. Lamb[2], K.-Y. Lo[2], S. Lord[3], and M. Werner[3]
[1]Dept. of Physics and Astronomy, Northwestern Univ., Evanston, IL
[2]Dept. of Astronomy, University of Illinois, Urbana, IL
[3]Space Sciences Division, NASA-Ames Res. Ctr., Moffett Field, CA

I. Introduction

Galaxy-galaxy collisions are known to produce drastic changes in morphology and, in many cases, enhance the level of star formation activity in galaxies. In order to better quantify the effects that interactions have on the star formation characteristics of galaxies we have undertaken a multiwavelength survey of a large sample of interacting disk-type galaxies. The sample is optically-selected, the inclusion of systems having been based upon the presence of unusual morphological features—such as tidal tails, plumes, rings, warped disks—suggestive of tidal interaction. The sample is composed of about 115 systems, most of which are spiral-spiral pairs, with a few spiral-elliptical pairs and a few merging systems (see Bushouse 1986 for more details of the sample selection). This sample has now been studied in the optical, infrared, and radio regimes, including optical spectra and Hα images, near-infrared photometry and imaging, far-infrared photometry, H I 21cm emission-line measurements, VLA 20cm maps, and CO emission-line measurements. This paper presents an overview and comparison of the results of the optical, infrared and CO surveys. With these data we can compare the far-infrared and CO properties of the galaxies with the classic optical and radio indicators of star formation activity and thereby determine what, if any, relationships exist between star formation activity and the far-infrared and CO properties of the galaxies.

II. Optical Properties

Global star-formation rates (SFRs) derived from Hα emission-line luminosities span a wide range with a large fraction of the interacting galaxies having SFRs indistinguishable from that of isolated spirals (Bushouse 1987). On average, however, the global SFRs of the interacting galaxies are a factor of 2.5 higher than that of isolated spiral galaxies of similar luminosity. The level of enhanced activity does not depend strongly on either galaxy size or the proximity of companions, although high levels of star formation activity are seen more often in close pairs. All possible combinations of activity, i.e. pairs in which both galaxies are active or inactive and pairs in which only one galaxy is active, appear to occur in roughly equal numbers.

Quantitative analysis of the spatial distribution of Hα emission in the interacting galaxies indicates that the majority of interaction-induced star formation activity occurs preferentially in the near-nuclear regions. Modest enhancements in the level of disk star formation are also seen to occur in a few systems. Given the fact that the radial distribution of star-forming regions in isolated spirals approximately follows the integrated light of the stellar disk (Hodge and Kennicutt 1983), we conclude that interaction-induced star formation usually does not follow the same pattern as preinteraction star-formation activity.

Emission-line ratios of most nuclear region spectra are consistent with photoionization by H II regions, with only a few showing LINER and Seyfert characteristics. Thus it appears that in the vast majority of systems in this sample interactions are triggering "normal" modes of star formation activity, while the creation or activation of nuclear "monsters" occurs infrequently.

III. Far-Infrared Properties

Far-infrared (42-122μm) luminosities derived from IRAS data for the interacting systems again cover a wide range, showing considerable overlap with the luminosities of isolated spirals (Bushouse, Lamb and Werner 1988). However, the median far-infrared luminosity of the interacting galaxies is about a factor of four greater than that of a sample of isolated spiral galaxies. Some of this increase is most certainly due to the fact that the sample of interacting galaxies is somewhat biased towards intrinsically more luminous galaxies, therefore the ratio of infrared-to-optical luminosity is a more appropriate property for comparison. We find that the median $L_{\rm IR}/L_B$ value for the interacting galaxies is about a factor of two greater than that of isolated spirals. Thus, by this measure, interactions are producing an approximate doubling of infrared luminosity. Assuming that this increase is tied to increased heating of interstellar dust due to enhanced star formation, this result is entirely consistent with the factor of two or so increase in optically-derived star formation rates which was found previously.

The median 12μm/25μm and 60μm/100μm colors of the interacting galaxies are also different from those of isolated spirals, with the interacting galaxies having larger 60μm/100μm and smaller 12μm/25μm flux ratios. The higher 60μm/100μm flux ratios, which imply higher dust temperatures, are consistent with the assumption that the increase in far-infrared emission is due to an increase in the population of young stars.

Two curious phenomena are revealed when comparing the relationship between $L_{\rm IR}/L_B$ and L_B for the interacting and isolated galaxy samples. First, there are no isolated galaxies, of any optical luminosity, with $L_{\rm IR}/L_B$ much greater than 10, whereas fully one-third of the interacting systems have $L_{\rm IR}/L_B$ ratios above this level and several have $L_{\rm IR}/L_B > 30$ (see figure 6 in Bushouse, Lamb and Werner 1988). Therefore it is likely that galaxy-galaxy interactions are a necessary requirement for significant enhancements in infrared luminosity. Second, there appears to be a cutoff at $L_B \sim 10^9\ L_\odot$, below which no systems—neither interacting nor isolated—show a significant enhancement in infrared luminosity. This result is consistent with Smith *et al.* (1987) who find that galaxies of low blue luminosity are not strong infrared emitters.

We have searched for correlations between classic optical indicators of star-formation activity and far-infrared properties in order to determine to what extent the far-IR emission is driven by star formation. We have found that on an individual galaxy-by-galaxy basis there is only a modest correlation between the star-formation rate per unit area of a galaxy (as derived from Hα emission-line luminosities) and the far-infrared "excess" ($L_{\rm IR}/L_B$) and infrared colors. There is a much stronger correlation, however, between star-formation activity and both $L_{\rm IR}/L_B$ and far-infrared colors when the sample of galaxies is broken into groups based on their optical spectral characteristics. Those galaxies having spectra characteristic of an old "dormant" stellar population have an average $L_{\rm IR}/L_B$~2.5 and very low 60μm/100μm and 25μm/12μm flux ratios, while galaxies showing strong H II region-type emission features have an average $L_{\rm IR}/L_B$~14 and 60μm/100μm and 25μm/12μm flux ratios a factor of 2–3 higher than galaxies with low SFRs. Systems that appear to be in the process of merging into a single body have the highest values of all, with $L_{\rm IR}/L_B$~55 and colors a factor of 3–4 higher than low SFR systems.

While the majority of interacting pairs are too closely spaced to be resolved by IRAS, detailed analysis of the IRAS data has allowed us to measure the levels of 25μm and 60μm emission from the individual galaxies in approximately 20 pairs. Contrary to the results of Telesco, Wolstencroft, and Done (1988), we find that in most spiral-spiral pairs both galaxies are far-infrared emitters. It is usually the case, however, that one of the galaxies is brighter at 60μm than its companion by a factor of 2–4, although in a few pairs both galaxies are equally bright.

IV. Molecular Gas Properties

CO (J=1–0) emission-line observations have been obtained for 24 of the interacting systems with the NRAO 12-m telescope (Bushouse *et al.* 1990). CO observations for another 11 systems in the present sample are available in the literature. In agreement with previous studies, we find a strong correlation between far-infrared luminosity and molecular gas content for the interacting systems that have been observed. We also find strong correlations between the FIR luminosity-to-molecular gas ratio and both the 60μm/100μm flux ratio and $L_{\rm IR}/L_B$. The molecular gas contents of the interacting galaxies span a large range but are, on average, a factor of 3–4 higher than that of isolated spiral galaxies. These systems also have an average $L_{\rm IR}/M({\rm H_2})$ ratio about a factor of 2 higher than isolated spirals, which others have interpreted as a higher SFR per unit gas mass for interacting galaxies (*e. g.* Young *et al.* 1986; Solomon and Sage 1988). Systems suspected to be in the process of merging—*e. g.* Arp 193, Arp 243, and Arp 299—have the largest $L_{\rm IR}/M({\rm H_2})$ values in the sample. The molecular-to-atomic gas ratio, $M({\rm H_2})/M({\rm H\,I})$, has a relatively constant value of ~1.5 among the systems that have been observed and does not depend strongly on $L_{\rm IR}/L_B$, which has been found to correlate with star-formation activity (§III). Only those systems with very low $L_{\rm IR}/L_B$ also have unusually low $M({\rm H_2})/M({\rm H\,I})$ ratios $\lesssim 0.4$. Therefore systems with higher SFRs are not necessarily overabundant in terms of molecular gas relative to atomic gas.

A comparison of optically-determined SFRs with the molecular gas content of the interacting galaxies shows that there is a modest correlation between the ratio of SFRs for the two galaxies in an individual pair and the ratio of molecular gas content for that pair of galaxies. In other words, it appears that the relative molecular gas content of the two galaxies in a pair is at least partially responsible for the relative level of interaction-induced star-formation activity. There are exceptions to this, however, as there are some pairs composed of two galaxies with nearly equal molecular gas content and yet one galaxy has a SFR as much as 9 times higher than its companion. Therefore, orbital and other internal properties of the galaxies must also play a role in determining the level of interaction-induced star-formation activity.

V. Unusual Interacting Systems

In spite of the correlations between various observable properties as discussed in the previous sections there are, of course, some systems that do not fit the general trends. As is often the case, these exceptions can reveal many interesting properties. First, while many of the interacting galaxies have very high SFRs, there are also many systems that have very low optically-determined SFRs and low far-infrared luminosities. Furthermore, many of these low SFR galaxies occur in pairs with a companion that has a very high SFR. These low SFR galaxies have optical luminosities that are typical for normal isolated spirals and also have normal atomic H I gas contents, while their molecular gas contents span a large range. Therefore these are not intrinsically small or "anemic" galaxies and so the low levels of star formation activity are not simply due to a lack of fuel. Orbital and other internal properties must again play a role here.

Second, while we found that galaxies with optical indications of high SFRs usually have significantly higher than average L_{IR}/L_B and "warm" far-infrared colors, there are several systems with strong H II region-type spectra that have very low far-infrared luminosities and cool colors. Further analysis has shown that these systems have low optical luminosities ($L_B \sim 5 \times 10^8\ L_\odot$), but relatively normal atomic gas content ($M(\mathrm{H\,I}) \sim 4 \times 10^9\ M_\odot$). Optical emission-line ratios indicate that these galaxies are metal-poor, having O/H ratios 3–4 times lower than the high SFR systems that have high far-infrared luminosities. CO observations of these systems have yielded null detections, indicating very low molecular gas contents of $M(\mathrm{H_2}) < 10^9\ M_\odot$. Therefore, the lack of far-infrared emission from these galaxies may be due to the absence of a sufficiently massive ISM necessary to convert UV/optical radiation into the far-infrared. Futhermore, if these galaxies maintain their current SFRs, they will exhaust their molecular gas supplies in a few × 10^8 years.

VI. Near-Infrared Imaging

We have obtained J (1.25μm) and K (2.2μm) images of about 20 of the interacting galaxies using the Kitt Peak National Observatory 58 x 62 element infrared camera (Bushouse and Werner 1990). In most systems the large-scale infrared morphology is similar to that seen in optical continuum images. However, in many systems there are small-scale features that are strikingly different from their optical counterparts, which we believe to be due mainly to the obscuring effect of dust at optical wavelengths. In some galaxies the infrared images have revealed the locations of previously invisible nuclei. In NGC 520, for example, the infrared images show the primary nucleus to be located at the very center of the massive dust lane that dominates optical images of the system. They also suggest that the fainter concentration to the northwest may be the nuclear remnant of a second galaxy. In general there is little correlation between the near-infrared and Hα morphologies of the galaxies. Only the very brightest H II complexes stand out from the background stellar population in the infrared images.

An analysis of the spatial distribution of infrared colors has shown that virtually all of the galaxies become redder towards their nuclei. On average, the nuclei are 0.4 and 0.9 mag redder in $J-K$ and $R-K$, respectively, than the disk regions. The majority of this effect appears to be due to an increase in the amount of dust in the nuclei of the galaxies. The ratio of color changes in $R-K$ and $J-K$ is, however, somewhat less than the value for reddening by dust alone, suggesting that metallicity and population gradients are also present. The "excess" reddening in $J-K$ relative to $R-K$ might also arise if the dust is well mixed with the stars, in which case the infrared colors would have a larger contribution from stars with large amounts of extinction. It appears that little, if any, of the red nuclear colors is due to thermal emission from dust since of the two galaxies in the sample that are experiencing the largest nuclear starbursts—NGC 1614 and NGC 7714—neither show unusually red nuclear colors relative to lower SFR systems.

References

Bushouse, H. A. 1986, Ph.D. thesis, University of Illinois.
————. 1987, *Ap.J.*, **320**, 49.
Bushouse, H. A. and Werner, M. W. 1990, *Ap.J.*, in press.
Bushouse, H. A., Lamb, S. A. and Werner, M. W. 1988, *Ap.J.*, **335**, 74.
Bushouse, H. A., Lamb, S. A., Lo, K.-Y., Lord, S. D. and Werner, M. W. 1990, in preparation.
Hodge, P. W. and Kennicutt, R. C. 1983, *Ap.J.*, **267**, 563.
Smith, B. J., Kleinmann, S. G., Huchra, J. P. and Low, F. J. 1987, *Ap.J.*, **318**, 161.
Solomon, P. M. and Sage, L. J. 1988, *Ap.J.*, **334**, 613.
Telesco, C. M, Wolstencroft, R. D., and Done, C. 1988, *Ap.J.*, **329**, 174.
Young, J. S. *et al.* 1986, *Ap.J.(Letters)*, **311**, L17.

DISCUSSION

Osterbrock: I believe the relatively small number of AGNs or Seyfert galaxies which you mentioned can be understood as resulting from the fact that your sample is selected as strongly interacting, violently disturbed systems. Dahari and others have shown observationally that mild interactions tend to enhance Seyfert activity, but violent interactions do not. Presumably the explanation is connected with the situations in which gas can be delivered near the nucleus with nearly zero angular momentum.

Bushouse: Yes, this result may be consistent with the study by Dahari, although it's interesting to note that the few liner's in my sample seem to occur preferentially in the on-going merger systems which are obviously the most strongly interacting systems. I think the sample of ultraluminous IRAS galaxies studied by Sanders et al. also shows evidence for larger than normal contributions from AGN-type activity.

Zasov: Can you compare briefly the behavior of late- and early-type interacting galaxies? For example, is there any noticable difference between fractions of galaxies which have experienced enhanced SF among different morphological types?

Bushouse: Unfortunately the disturbed morphologies of many of these galaxies do not allow us to accurately classify them by Hubble sub-types. However, I believe that in their sample, Keel and Kennicutt did determine Hubble sub-types and essentially found no correlation between star formation activity and morphological type across the spiral sequence.

Kennicutt: (Comment in reply to a question from Zasov to Bushouse - dependence of star formation on morphological type.) In our study the distributions of H-alpha emission are nearly independent of Hubble type. However there may be some differences in the spatial distributions of the emission. In those early-type spirals (Sa-Sb) which have high levels of emission the activity is often confined to the nuclear regions.

FIR STATISTICS OF PAIRED GALAXIES

Jack W. Sulentic

University of Alabama, Tuscaloosa 35487 USA

Introduction

Much progress has been made in understanding the effects of interaction on galaxies (see reviews in this volume by Heckman and Kennicutt). Evidence for enhanced emission from galaxies in pairs first emerged in the radio (Sulentic 1976) and optical (Larson and Tinsley 1978) domains. Results in the FIR lagged behind until the advent of the IRAS satellite. The last five years have seen numerous FIR studies of optical and IR selected samples of interacting galaxies (e.g., Cutri and McAlary 1985; Joseph and Wright 1985; Kennicutt et al. 1987; Haynes and Herter 1988). Despite all of this work, there are still contradictory ideas about the level and, even, the reality of an FIR enhancement in interacting galaxies. Much of the confusion originates in differences between the galaxy samples that were studied (i.e., optical morphology and redshift coverage). We report on a study of the FIR detection properties for a large sample of interacting galaxies and a matching control sample. We focus on the distance independent detection fraction (DF) statistics of the sample. The results prove useful in interpreting the previously published work. A clarification of the phenomenology provides valuable clues about the physics of the FIR enhancement in galaxies.

Data Samples

The Catalog of Galaxy Pairs (CPG) (Karachentsev 1972 and review in this volume) was used for this study. The CPG has numerous advantages.

1) **Large Sample:** There are 509 pairs after allowance is made for discordant redshifts, misclassified single galaxies, and pairs not surveyed by IRAS.

2) **Physical Pairs:** Pairs were selected using an isolation criterion expressed in terms of component size and separation. This increases the likelihood that they are physical systems. The existence of complete redshift data permitted us to refine the sample even further in this direction.

3) **Morphological Diversity:** Selection criteria accepted all isolated pairs irrespective of type. The large and unbiased sample means that we are able to discriminate DF as a function of both component Hubble and pair interaction morphology.

4) **Control Sample:** A final advantage is that the CPG can be compared to a catalog of isolated galaxies (CIG) (Karachentseva 1973) that was assembled using many of the same selection criteria . Its advantages are the same ones as listed for the CPG except that there is less morphological data available for most CIG galaxies (see Sulentic 1989 for details).

The FIR data for the optically selected pairs was taken from version II of the IRAS Point

Source Catalog (PSC). The PSC provides data on unresolved sources over 96% of the sky. It is complete to about 0.6Jy at 60μ which is the wavelength of most sensitivity and least confusion for galaxies. The resolution at this wavelength is 1.0 arcmin (FWZI; in–scan direction) which means that the vast majority of our pairs will be unresolved. We accepted all hour–confirmed detections from the PSC.

DF Enhancement For A Spiral Galaxy

Table 1 lists the detection fractions for the principal morphological classes in the CPG and CIG. Initially we distinguish only between spiral–spiral (SS), spiral–E/S0 (ES), and E/S0–E/S0 (EE) pairs. Not surprisingly, we see large differences in DF between these three groups with very few early type galaxies detected in the PSC. After allowance for spiral galaxies misidentified as E/S0, we get a DF = 0.06±0.04 for EE pairs. Comparison of these results with those for the CIG control sample indicates a significant DF enhancement for both SS and ES pairs.

TABLE 1
DETECTION FRACTIONS

TYPE	NUMBER IN CAT.	DETECTION FRACTION	TYPE	NUMBER IN CAT.	DETECTION FRACTION
All Pairs	509	0.63±0.02	All Isolated	1029	0.32±0.01
SS Pairs	297	0.78±0.02	LIN Pairs	92	0.77±0.04
ES Pairs	148	0.54±0.04	ATM Pairs	78	0.40±0.05
EE Pairs	63	0.11±0.04	DIS Pairs	118	0.79±0.04
S Isolated	864	0.35±0.02	JUS Pairs	224	0.57±0.03
E/S0 Isolated	165	0.17±0.03			

We can use the results for ES pairs to estimate the enhancement in DF for a spiral galaxy in a pair. The "normal" detection level for isolated spirals is DF=0.35 which implies DF=0.58 for two spirals in an optical pair. This is the probability that one or both components are detected and ignores any contribution to the DF from two (individually undetected) spirals whose combined weak emission raises them above the detection threshold. We note, however, that DF=0.54 for ES pairs which we can use to estimate the threshold effect. We assume this value to represent the detection probability for an interaction enhanced spiral assuming the E/S0 component contribution to the FIR emission in pairs is negligible. Two such enhanced spirals in a pair would yield DF=0.79 as the probability of detection. We observe DF=0.78 from the CPG sample of SS pairs. This agreement between prediction and observation suggests that the contribution to DF from threshold crossing pairs is negligible. The difference between the DF for isolated S and for SE pairs will then give us P=0.19 for the average enhancement in DF for a spiral galaxy due to membership in a pair. This result applies to pairs brighter than $m_{pg} \approx 15.0$ and within $V_0 \approx 11\times10^3$ km/s. The enhancement increases from 0.10±0.05 nearby to 0.30±0.05

at 11×10^3 km/s. At a distance corresponding to 16×10^3 km/s we expect interacting pairs to be the dominant contributor to FIR selected samples. These results suggest that studies restricted to low redshift (i.e. $m_{pg} \leq 13.5$) samples or those containing many early-type galaxies will lead to underestimates of the enhancement.

At first glance, the above result might suggest that, on average, both components of an SS pair are enhanced at the same level. Of course, the resolution of IRAS does not allow us to say anything about the flux ratio in SS pair components. We have used the ES pairs to overcome, as much as is possible, the resolution problem. If certain assumptions are valid, we are able to estimate the average component enhancement in pairs containing spiral members. It is possible that the flux ratio is sensitive to the details of the encounter geometry. The evidence that threshold crossing pairs contribute little to the DF is one argument that a single component dominates the FIR emission in most pairs. A similar conclusion was reached by Telesco et al. (1988).

DF and Optical Morphology

Figure 1 presents the correlation of DF with: **(UL)**–Hubble component morphology; **(UR)**–pair interaction morphology; **(LL)**–diameter ratio of the pair components; **(LR)**–component separation. The DF for an unenhanced (i.e., optical) spiral pair is indicated by a dotted line in the latter three panels. We will discuss the four panels of Figure 1 in the following paragraphs.

(UL). The principal handicap to a study of the DF–galaxy morphology correlation involves the uncertain (Palomar Sky Survey based) types assigned to CPG and CIG galaxies. Improved Hubble types are now available from 6m (Zelenchuk) plates and from other sources (see Karachentsev 1987). This heterogeneous, but improved, data permits us to study the correlation for the principal spiral types using both SS pairs with two components of like morphology and the ES pairs. A comparison of the DF for early and late type spirals shows that the enhancement in DF is not in close proportion to the average fraction of non-stellar material (as estimated from 21cm studies). Even the relatively gas/dust poor Sa spirals show a significant enhancement. This indicates that the *efficiency* of the enhancement process (encounter geometry, mass ratio, ratio of disk to nuclear emission, etc.) is an important consideration.

(UR). The CPG also assigned interaction types to pairs. We display the principal interaction types for SS and ES pairs in this panel. The LIN class represents pairs with the clearest signs of interaction involving bridges or tails. The ATM class represents pairs with components imbedded in a common envelope. The DIS class involves pairs where one or both components show signs of distortion. This is a more subjective criterion but, still, one assigned independently of the IRAS survey. The JUS class represents pairs with no obvious signs of disturbance. The importance of an efficiency measure is again emphasized by the small difference in DF between pairs with and without optical signs of interaction. Apparently obvious optical signs of interaction do not always accompany the enhancement process. The picture is yet incomplete, since we do not consider here the intrinsic properties of the detected pairs (see Xu and Sulentic this volume).

(LL). We have used uneven binning in this display in order to keep the 1σ rms at about

0.07. The leftmost SS point represents ratios between 1.0 and 1.1. A search for a correlation of DF with the ratio of component major axis diameters offers an opportunity to study the efficiency mechanism in a different way. This is the simplest approach to searching for a possible correlation with the component mass ratio. We are restricted in this test to relatively equal size pairs because the selection criteria for the CPG are biased against the inclusion of hierarchical pairs. Over the range of ratios represented, there is no evidence for equal size pairs to be more frequently detected. This suggests that a companion can still be an effective perturber even if it is as much as a factor of four smaller in mass than the primary (again, we are not considering average FIR luminosities here). This result offers additional support for the idea that a single component of most pairs contributes most of the flux (see also Telesco et al. 1988). This interpretation is clouded because we do not yet know how efficiently gas rich "dwarf" companions are stimulated by their larger neighbors.

FIGURE 1

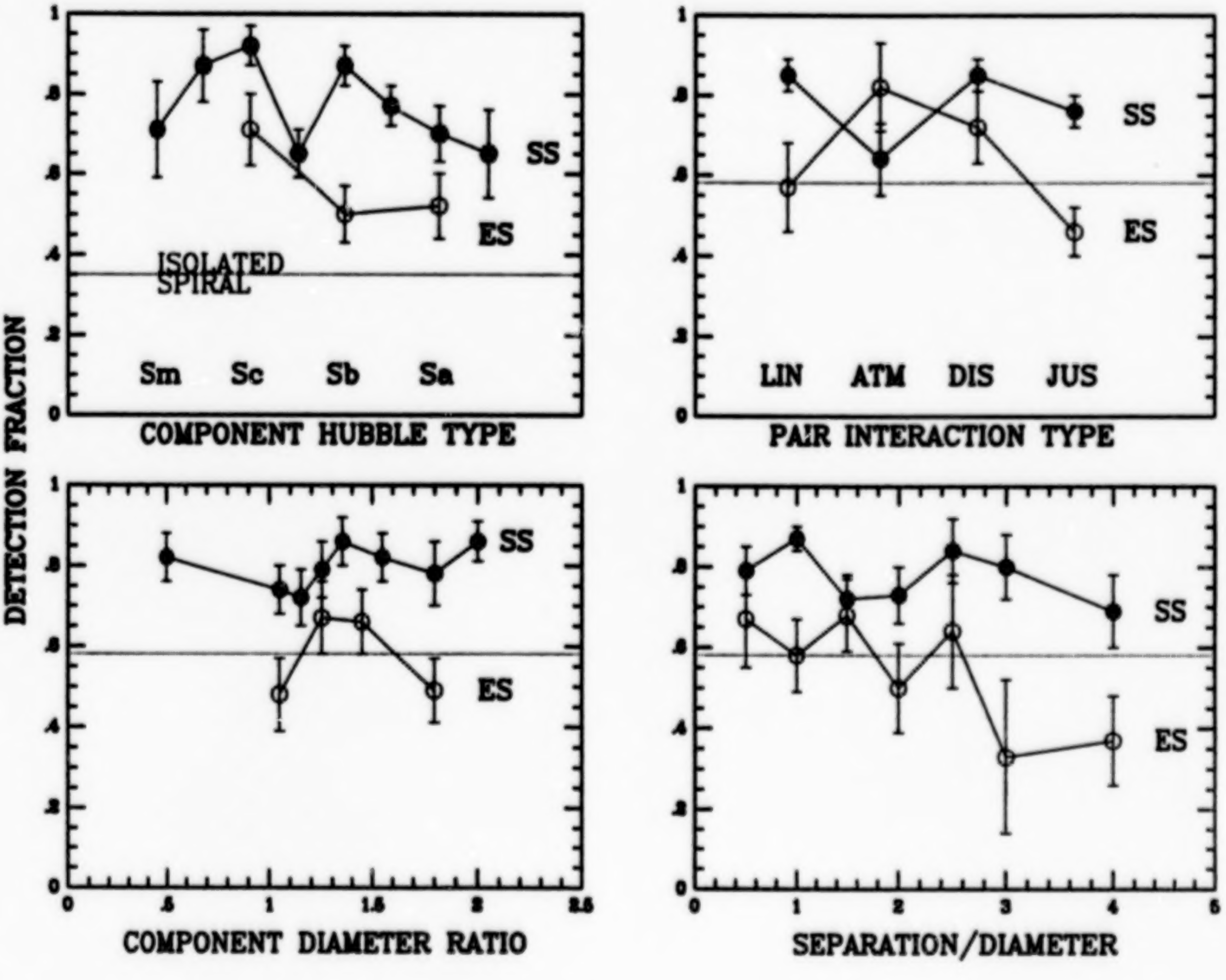

(LR). A study of DF vs. the primary diameter/separation ratio offers the chance to detect the critical separation at which FIR enhancement sets in. We see only weak evidence for enhanced DF in closer pairs. especially among the SS pairs. This may indicate that most spirals in pairs are stimulated to emit in the FIR but that the luminosity of close pairs is higher. Another possibility is that the enhancement persists long after the initial stimulation either through slow nuclear fuelling or amplification of a stochastic star formation process. Only at separations of three or four times the primary diameter do the DF levels fall towards "isolated" levels.

Summary

1) In determining existence and level of an FIR enhancement in pairs one must consider both **morphology** and **redshift coverage**.

2) An enhancement exists in both SS and ES pairs. It is strongest in SS pairs but it is significant in ES pairs.

3) The strongest enhancement occurs for pairs with LIN(br) and DIS interaction morphologies but an enhancement also exists in JUS (plain) pairs.

4) The weak correlation of component Hubble type with DF suggests that DF is not a simple function of gas/dust content but that **efficiency** of encounter stimulation plays an important role. This is also supported by the lack of correlation between DF and component size ratio.

5) There is little correlation between DF and component separation.

6) We are probably missing the most dramatic examples of FIR enhancement when considering samples of binary galaxies with an isolation criterion. It is not the primordial pairs but the random encounters that are likely to exhibit the strongest effects.

References

Cutri, R. and McAlary, C. 1985, *Astrophys. J.*, **296**, 90.
Haynes, M. and Herter, T. 1988, *Astron. J.*, **96**, 504.
Joseph, R. and Wright, G. 1985, *M.N.R.A.S.*, **214**, 87.
Karachentsev, I. D. 1972, *Comm. Spec. Astrophys. Obs.*, **7**, 1.
Karachentsev, I. D. 1987, *Double Galaxies*, (Nauka, Moscow).
Kennicutt, R., Keel, W., van der Hulst, J., Hummel, E. and Roettiger, K. 1987, *Astron. J.*, **93**, 1011.
Larson, R. and Tinsley, B. 1978, *Astrophys. J.*, **219**, 46.
IRAS Point Source Catalog, Version 2. 1988, Joint IRAS Science Working Group (Washington, DC: GPO).
Sulentic, J. W. 1976, *Astrophys J. Suppl. Ser.*, **32**, 171.
Sulentic, J. W. 1989, *Astron. J.*, **98**, 2066.
Telesco, C., Wolstencroft, R. and Done, C. 1988, *Astrophys. J. Letters*, **329**, L74.

DISCUSSION

S. Schneider: Did you see any far-infrared enhancement in the discordant redshift pairs?

J. Sulentic: There is no sign of enhanced DF for the discordant pairs, although 14 were classified as LIN, ATM, or DIS in the CPG.

QUANTIFYING THE FIR INTERACTION ENHANCEMENT IN PAIRED GALAXIES

Cong Xu
International Center for Theoretical Physics, P.O. Box 586, I-34100 Trieste, Italy

Jack W. Sulentic
University of Alabama, Tuscaloosa 35487 USA

I. Introduction

We study the "Catalogue of Isolated Pairs of Galaxies in the Northern Hemisphere" (CPG hereafter) by Karachentsev (1972), and a well matched comparison sample taken from the "Catalog of Isolated Galaxies" (Karachentseva 1973, CIG hereafter), in order to quantify the enhanced FIR emission properties of interacting galaxies (see Sulentic 1989 for details of the samples). The isolation criterion used in compiling the CPG and the CIG means that both the pairs and single galaxies have been little influenced by their environment for a long time ($t \gtrsim 10^9$ yrs: Stocke et al 1978).

Some relevent issues addressed in the study are:

1. How populous are isolated pairs? What is the contribution of the paired galaxies to the optical luminsity function of field galaxies?
2. What is the contribution of CPG pairs to the Far-Infrared (IRAS) luminosity function?
3. Does the FIR enhancement of a pair depend on (1) the existance of particular signs of interaction (tails, bridges, etc.) or (2) the separation between the two components?

II. Optical luminosity functions (OLF's)

We use the classical estimator of the luminosity function (Felten 1976). The $< V/V_m >$ tests demonstrate that neither the pair sample nor the comparison sample is complete at any magnitude level. However, the redshift distributions of the two samples are fairly homogeneous. The incompleteness is corrected using the method suggested by Huchra and Sargent (1973). For CPG samples the correction is about a factor 2. For the comparison sample, it is about a factor of 5, which also takes into account the incompleteness of the redshift data.

Figure 1 plots the OLF's for individual galaxies in the CIG and in the CPG pairs. CPG pairs are dominant by SS pairs in general. There is a deficiency of early type dwarf galaxies (fainter than -18 magnitude) in EE pairs. The shape of OLF of galaxies in SE pairs is middle way between the OLF's of galaxies in SS pairs and of galaxies in EE pairs. The parameters of the best fitting Schechter function for the OLF of CPG galaxies are $\alpha = -1.2$ and $M_* = -20.0$. For CIG galaxies, $\alpha = -1.3$ and $M_* = -19.4$. Galaxies in pairs are about 0.6 magnitude brighter than CIG galaxies. Comparing with the OLF of CFA field galaxies (Davis and Huchra 1982), we find that paired galaxies represent about 10% of field galaxies over the entire luminosity range.

III. FIR luminosity functions (FIRLF's)

The FIR data of both the CPG and the CIG is generally taken from the second version of IRAS Point Source Catalog (PSC). The only exceptions are some galaxies larger than $D = 5$ arcmin, for which coadded data are taken from the literature.

Since most pairs in the CPG sample are unresolved by IRAS, we can not derive the FIR luminosity functions for individual CPG galaxies. The FIRLF's for SS pairs and for SE pairs are calculated separately. The FIR luminosity of SE pairs is attributed exclusively to the S component (Paper I). We did not calculate the FIRLF for EE pairs, because the IRAS detection rate is very low (<11%). The FIRLF of S/Irr galaxies is derived for the comparison sample.

Because both the pair sample and the comparison sample are optically selected, the FIR luminosity functions are derived from the corresponding optical luminosity functions and the fractional bivariate functions between the FIR and optical luminosities. The correction for incompleteness of the samples affects the FIR luminosity function through the optical luminosity function. In order to take into account the information content of upper limits, the Kaplan-Meier estimator (Schmitt 1985; Feigelson and Nelson 1985), has been used in computing the bivariate functions and the associated errors.

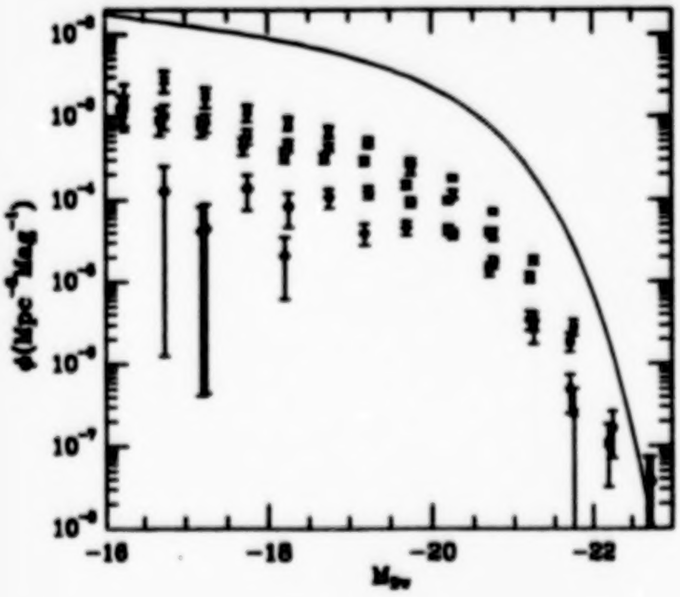

Fig.1 The OLF of CPG galaxies (solid squares), which is decomposed to 3 components: of galaxies in SS pairs (open squares), of galaxies in SE pairs (open diamonds), and of galaxies in EE pairs (solid diamonds). The crosses stand for the OLF of CIG galaxies. The solid curve illustrates the OLF of CFA field galaxies (Davis and Huchra 1982).

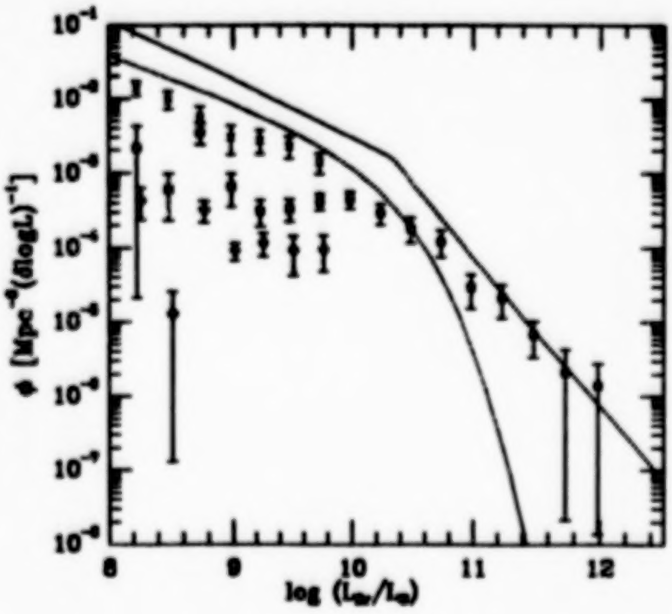

Fig.2 The FIRLF's of of SS pairs (open squares), of CIG S/Irr galaxies (crosses), and of SE pairs (open diamonds). The dotted curve represents the FIRLF of the synthetic pairs. The solid curve illustrates the FIRLF of bright IRAS galaxies (Soifer et al. 1987).

FIRLF's are plotted in Fig.2. We divide them into two parts (i.e. above and below $10^{10}L_{\odot}$). In the faint part, the contribution from SS pairs to the IRAS luminosity function is generally less than 10%. In the bright part, the contribution from SS pairs increases with luminosity, becoming dominant beyond $2 \times 10^{11} L_{\odot}$. For isolated S/Irr galaxies the contribution is about 20—30% in the faint part, and decreases rapidly in the bright part. SE pairs never give a significant contribution to the IRAS luminosity function. The mean $\log(L_{fir}/L_\odot)$ of SS pairs is 9.88 ± 0.05. For isolated S/Irr galaxies, it is 9.10 ± 0.05. Therefore, SS pairs are about a factor of 6 brighter ($\sim 10\sigma$ level) in FIR than isolated S/Irr galaxies on average. The mean $\log(L_{fir}/L_\odot)$ of SE pairs is 9.52 ± 0.09.

For comparison, we have also calculated the FIR luminosity function for a sample of synthetic pairs, which are constructed from isolated S/Irr galaxies. We take into account the fact that CPG pairs are biased to have members of similar optical brightness. The result is represented by the dotted curve. Comparing with it, we find that SS pairs are under-represented in the faint part, and over-represented in the bright part.

VI. The FIR to optical luminosity ratio and the FIR color

The FIR to optical luminosity ratio and the FIR color (the ratio between the fluxes at 60 microns and at 100 microns) are two important FIR emission indicators. In the folllowing we will concentrate on the SS subsample of CPG and CIG S/Irr galaxies. The FIR properties of SE pairs will be discussed in a separate paper (Sulentic, in preparation).

Upperlimits in FIR data are taken into account in the analyses of the FIR to optical luminosity ratio, and the Kaplan-Meier estimator is used. The cumulative $R = \log L_{fir}/L_B$ distributions of SS pairs and of CIG S/Irr galaxies are different at 10^{-3} significance level. The differential R distribution of SS pairs (Fig.3) tiltes reletive to that of isolated S/IR galaxies, in the sense that SS pairs show high R more frequently, and low R less frequently. No evidence of bimodality in the distribution is found. The mean R of SS pair is -0.16 ± 0.03, more than 3σ higher than that of isolated spirals, which is -0.30 ± 0.03. The indicated enhancement in the FIR to optical luminoisty ratio is a factor of 1.4.

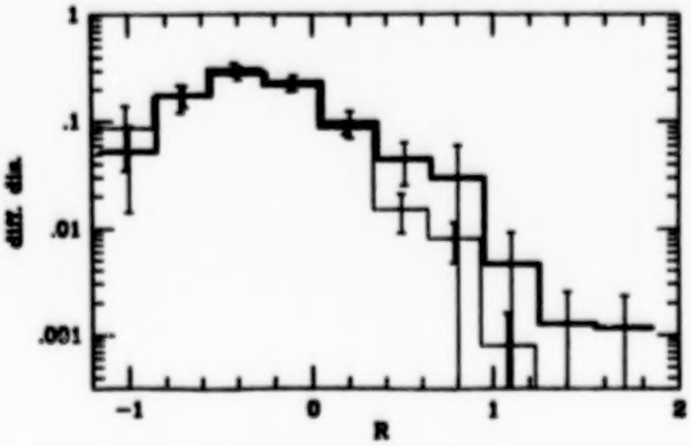

Fig.3 The differential distribution of $R = \log L_{fir}/L_B$. The thick line is the distribution of SS pairs. The thin line is the distribution of isolated S/Irr galaxies.

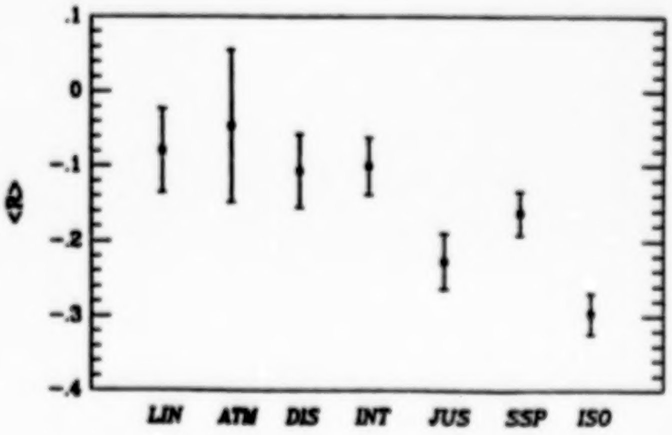

Fig.4 The < R > versus interaction morphology plot (see the text for definitions).

Figure 4 plots the dependence of mean R on the interaction morphology. LIN represents pairs with bridges and/or tails. ATM are pairs in a common luminous envelope. DIS are pairs with one or both of the components showing signs of distortion. INT represents interacting pairs on the whole, which is the summary of the above three subclasses. JUS represents pairs without obvious signs of interaction. SSP is the entire sample of SS pairs, which is the combination of INT pairs and JUS pairs. ISO stands for the isolated S/Irr galaxy sample. The $< R >$ of INT pairs is significantly higher than isolated S/Irr galaxies (at 4.2σ level) and than JUS pairs (at 2.4σ level). There is a slight enhancement of $< R >$ of JUS pairs comparing to isolated S/Irr galaxies (at 1.5σ level). There is no significant difference in $< R >$ among the three subclasses of interacting pairs.

We define a redshift-independent separation parameter SEP as the ratio between the separation of two components and the size of the primary:

$$SEP = \frac{\text{component separation (arcmin)}}{\text{size of primary (arcmin)}}$$

INT pairs with $SEP \leq 1$ demonstrate significantly higher $< R >$ (at 3.2σ level) than JUS pairs with $SEP \leq 1$. On the other hand, no difference in $< R >$ is found between INT and JUS pairs of $SET > 1$. Moreover, $< R >$ of INT pairs with SEP≤ 1 is systematically larger than that of INT pairs with SEP> 1 (at 2.3σ level).

Only detected FIR data are included in the analysis of the FIR color. The cumulative $C = \log F_{60\mu}/F_{100\mu}$ distributions of SS pairs and of CIG S/Irr galaxies are different at $< 10^{-3}$ significance level. The differential C distribution of SS pairs (Fig.5) shows a systimatical shift toward the bright end comparing to isolated S/IR galaxies. Again no evidence of bimodality in the distribution is found. The mean C of SS pairs is -0.36 ± 0.01, more than 5σ higher than that of isolated spirals, which is -0.42 ± 0.01.

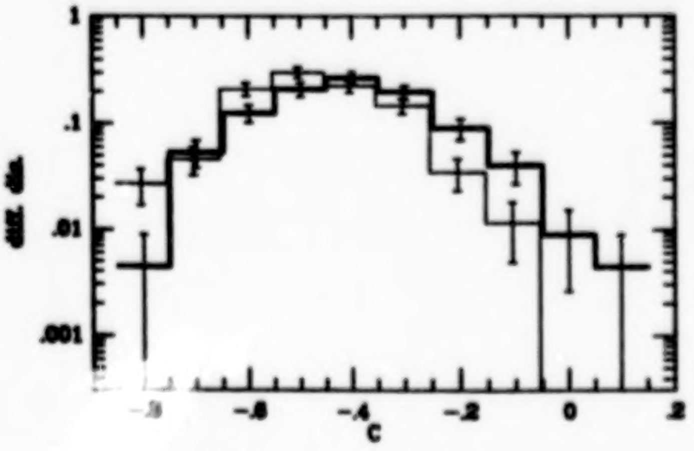

Fig.5 The differential distribution of $C = \log F_{60\mu}/F_{100\mu}$. The thick line is the distribution of SS pairs. The thin line is the distribution of isolated S/Irr galaxies.

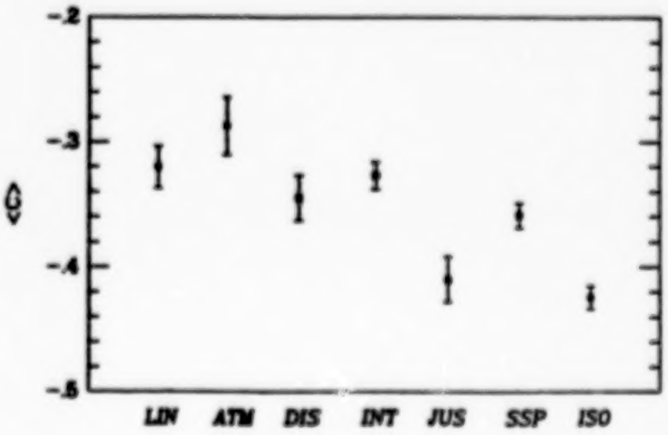

Fig.6 The $< C >$ versus interaction morphology plot.

Figure 6 plots the dependence of mean C on the interaction morphology. We find no significant difference between JUS pairs and isolated galaxies, nor among the three subclasses of interacting pairs. The difference between INT pairs and JUS pairs is obvious (at 3.9σ level).

The dependence of $< C >$ on SEP is essentially the same with that of $< R >$. INT pairs with $SEP \leq 1$ show significantly higher $< C >$ than JUS pairs (at 4.6σ level) and than INT pairs with SEP> 1 (at 2.6σ level).

In summary, it appears that the SS pairs which show signs of interaction, and whose component galaxies are close to each other ($SEP \leq 1$) demonstrate the most significant enhacement in their mean R and mean C relative to isolated S/Irr galaxies, while other SS pairs show only weak FIR enhancement. We will refer the former as close interacting pairs. In the SS sample, 120 pairs belong to this class, representing 40% of all (299) SS pairs.

Our results support a bimodal star-formation scenario. The self propagating-regulating mode controls the star-formation in isolated galaxies, while an interaction-stimulated mode should be added to paired galaxies. The amplitude of the later depends on the strength of interaction. For those pairs other than close interacting ones, the effect of the interaction induced star-formation is so weak that it is almost buried by the normal starformation. For close interacting pairs in the SS pair sample, the interaction provides a significant but not ultraluminous effect.

Summary

(1) About 10% field galaxies are in isolated pairs.

(2) SS pairs dominate the bright end of the IRAS FIRLF ($L_{fir} > 2 \times 10^{11}\ L_{\odot}$), while their contribution to the faint part of the IRAS luminosity function ($L_{fir} < 10^{10} L_{\odot}$) is low (<10%).

(3) SS pairs on the whole show statistically significant enhancements in their mean FIR to optical luminosity ratio ($\sim 3\sigma$) and in their FIR color ($\sim 5\sigma$), comparing to isolated S/Irr galaxies.

(4) Detailed study shows that the amplitude of FIR enhancement depends on the intensity of interaction. For the SS pairs which show signs of interaction (tails, bridges, common envelops, distortions, etc.), and whose component galaxies are close to each other ($SEP \leq 1$) the enhancement is significant. These "close interacting pairs" represent ~ 40% of all SS pairs. For other SS pairs, the enhancement is weak.

References

Davis, M. and Huchra, J. (1982), *Ap.J.*, **254**, 437.

Felten, J. E. (1976), *Ap.J.*, **207**, 700.

Feigelson, E. D. and Nelson, P. I. (1985), *Ap.J.*, **293**, 192.

Huchra, J. and Sargent, W. L. W. (1973) *Ap.J.*, **186**, 433.

Schmitt, J. H. M. M. (1985), *Ap.J.*, **293**, 178.

Soifer, B. T., Sanders, D. B., Madore, B. F., Neugebauer, G., Danielson, G. E., Elias, J. H., Lonsdale, C. J. and Rice, W. L. (1987), *Ap.J.*, **320**, 238.

Stocke, J., Tifft, W. and Kaftan-Kassim, M. (1978), *A.J.*, **83**, 322.

Sulentic, J. (1989), *A.J.*, **98**, 2066 (Paper I).

BLANK PAGE

Star Formation in Infrared Bright and Infrared Faint Starburst Interacting Galaxies.

Susan A. Lamb,[*†] *Howard A. Bushouse,*[§] *and John W. Towns*[*]

Abstract.

Short wavelength IUE spectra of Arp 248b and UGC 8315N are combined with optical spectra and interpreted using a combination of spectrum synthesis and spectral diagnostics to place constraints on the massive star populations of the central regions of these galaxies and to deduce information about the star formation histories in the last 10^8 years. We find that both galaxies have substantial fractions of their optical light coming from massive stars and that Arp 248b may be dominated in the UV by WR stars. The UV spectra are dominated by radiation from evolved massive stars and we place an age on the burst in Arp 248b of a few tens of millions of years.

I. Introduction.

The stellar content and star formation histories of interacting and merging galaxies are of particular interest because they are of relevance to many aspects of the evolution of these systems. For example, the number of and distribution with mass of massive stars produced will effect the eventual supernova rate and return of energy and material to the interstellar media.We need to know the stellar population produced if we wish to have an understanding of the processes that occur when two galaxies collide, for example, the amount of mass going into massive versus low mass stars will influence the total infrared flux of the galaxies. Ultraviolet radiation from galaxies comes predominantly from the massive star population ($M > 10M_{\odot}$) and thus provides a useful probe of this end of the mass spectrum, although dust obscuration in the UV is very high and has to be taken into account when interpreting observations. Because of the complications introduced by the pesence of dust, the general method of interpreting UV spectra relies on the use of spectral diagnostics, such as the shape and depth of the Si IV and C IV lines, rather than detailed spectrum synthesis and is most useful when the UV data is complimented by spectrum synthesis of optical spectra of the same region of the object. Here we report on a preliminary investigation, using this method, of the massive star content of two galaxies for which we already had optical data. We obtained UV (IUE) spectra of UGC 8315N and Arp 248b, which are both high star formation rate galaxies as observed from their optical spectra, and members of strongly interacting binary systems. They were chosen from the Bushouse (1986) sample of closely interacting galaxies and as such were selected to show optical morphological evidence of prior interaction in the combined system, *i.e.*, optical photographs show evidence of bridges and tails.

II. Interacting Galaxies: Data and Subsamples.

The study of the UV properties of interacting galaxies is part of a larger project to investigate the star formation histories and stellar content of these systems using observations in various wavelength regions as well as theoretical modelling (see Gerber, Balsara, and Lamb, this volume). The Bushouse sample, from which our two galaxies were chosen, has been the focus of these investigations. Nuclear region optical spectra (Bushouse, 1986b) and global Hα fluxes (Bushouse, 1987) together with IRAS observations (Bushouse, Lamb, and Werner, 1988) have shown a large span of stellar population mixes among the sample members, ranging from strong stellar burst like to elliptical galaxy like populations.This indicates a wide range in star formation activity over the last billion years.

One important result found by Bushouse, Lamb, and Werner (1988) for the strongly interacting systems is that they can be subdivided into at least five groups based upon their optical and far infrared (IRAS) properties. Some of these properties are listed in Table 1 for the five groups and for the Ultraluminous IRAS galaxies studies by Sanders et al. (1988), as a comparison. We note that the value of L_{IR}/L_B increases from a value of 2.5 for the low star formation rate galaxies to one of 162 for the ultraluninous systems. Also at the low end is a group of high star formation, low infrared flux systems. These consist of low mass, dwarf galaxies and presumably contain little dust, however optical observations indicate high rates of star formation. In this paper we concentrate on sample members of two of these groups; UGC 8315N is a member of the 'High SFR-Low IR' group, and Arp 248b is a member of the 'High SFR' group.

Table 1
MEAN PROPERTIES OF SUBSAMPLES

SAMPLE	$L_{IR}(10^9 L_O)$	$L_B(10^9 L_O)$	L_{IR}/L_B	$\log(f_{60}/f_{100})$
Low SFR	12.	3.8	2.5	-0.55
High SFR- Low IR*	1.	0.4	2.5	-0.32
Disk SF	36.	3.9	9.3	-0.35
High SFR*	34.	1.4	14.2	-0.21
High LIR/LB	118.	2.4	54.0	-0.15
Ultraluminous IRAS galaxies†	766.	8.5	162.0	+0.02

*We here study galaxies from these two subsamples.
†From Sanders et al. (1988)

III. IUE and Optical Spectra.

The two galaxies studied here show strong evidence from their optical spectra of high levels of current star formation and hence are classified as starburst galaxies, but they differ in that Arp 248b has a large far infrared luminosity of 2.225 x 10^{10} L_O and a $L_{IR}/L_{H\alpha}$ of 333, whereas UGC 8315N is barely detected by IRAS. The two galaxies are thus representative of different classes of starburst galaxies (as discussed above). UGC 8315N is in a system of two dwarf galaxies in contact and with tails, whereas Arp 248b is one of a pair of spirals connected by a bridge and also having tails. Some properties of the two galaxies are given in Table 2.

Table 2

GALAXY PROPERTIES

Galaxy	UCG 8315N	Arp 248b
Distance	16 Mpc	68 Mpc
Ang. size	15" x 10"	40" x 30"
L_B	2.7 x 10^7 L_O	1.61 x 10^9 L_O
L_{IR}	<8 x 10^7 L_O	22.25 x 10^9 L_O
L_B/L_{IR}	<1.8	13.8
H_α(EW)	190 A	62.8 A
E(B-V)	0.10	0.47
A_V	0.32	1.4
O/H	2. x 10^{-4}	6.5 x 10^{-4} (~ solar)

The IUE ultraviolet observations were obtained on DATE. They are short wavelength (1150 - 1950 A) and of low dispersion (~6 A/mm.). The large aperture (10" x 20") was used for both observations and covers the whole of UGC 8315N but only the nucleus of Arp 248b. The exposure times for the two galaxies respectively were 10.4 and 14.28 hours. The exposure on UGC 8315N was shortened by observational constraints and was marred by a high dispersion residual from a previous overexposure of the camera. The resulting spectra is thus of low signal to noise. However, enough information is available to provide a rough comparison with the spectrum of Arp 248b which has a signal to noise of 175/105. The ultraviolet spectra of the two galaxies is shown in Figure 1. and is superimposed on a model fit which is discussed below.

The optical observations of UGC 8315N were obtained in April, 1984 at Steward Observatory on the 90" telescope with the reticon spectrograph: the aperture was 5" in diameter. Those of Arp 248b were obtained in the same month at Kitt Peak using the IRS (intensified reticon spectrograph): the aperture was 22" in diameter. Both observations covered the galactic nuclei on

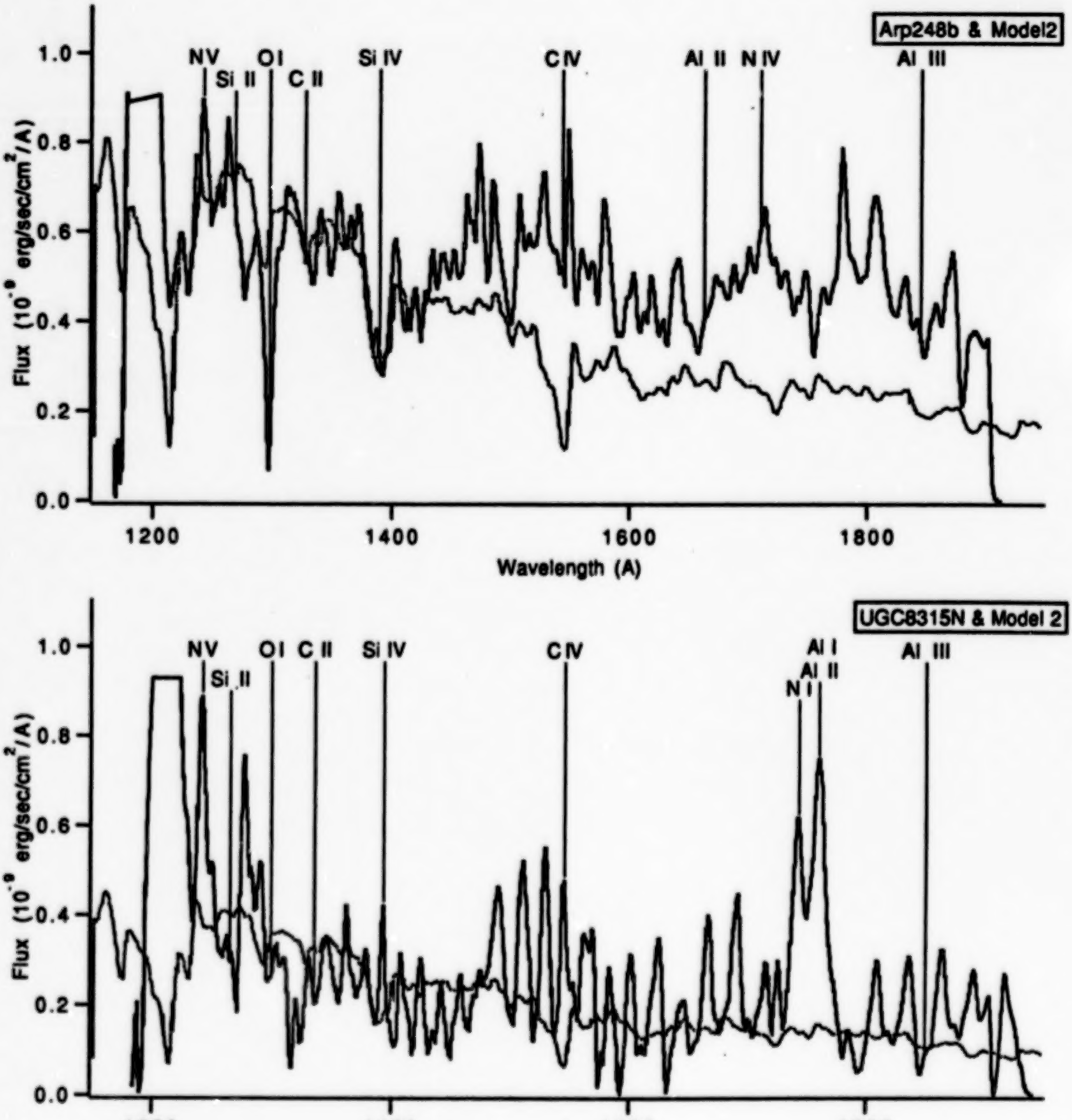

Figure 1. The IUE spectra of Arp 248b and UGC 8315N (dark lines) and a model fit (dotted lines). Arp 248b appears to have a large component of WR stars giving rise to the emission humps between 1450 and 1900 A.

IV. Population Synthesis and Interpretation.

The spectrum of Arp 248b is of sufficiently good signal to noise that absorption lines of O I (λ 1302 A), Si IV (λ 1394, 1403 A), C IV (λ 1548, 1551 A), and Al III (λ 1855 A) are well observed. However in UGC 8315N only emission lines of N V (λ 1239, 1243 A), N I (λ 1743, 1745 A), and Al I/II (λ 1766 - 1776 A) are easily identified. Comparison between the UV spectrum of Arp 248b and the best model fit (discussed below) indicates the presence of emission humps between 1450 and 1900 A similar to those found in WN8 UV spectra (see Nussbaumer et al. 1982).

Concentrating on the spectrum of Arp 248b, we note that the lack of significant C IV absorption implies the absence of any large component of massive main sequence stars, and C IV emission (if present) implies very hot massive stars. The Si IV absorption is moderately strong and there is a hint of a P Cygni profile. This implies the presence of evolved massive stars, ie. supergiants. The very strong O I absorption line can indicate the presence of main sequence B stars. This line is found to be strongest for the B5 V class. Lastly, the emission humps strongly suggest the presence of a substantial number of WR stars.

Spectrum synthesis of the optical spectra of UGC 8315N and Arp 248b indicate that OB stars contribute ~ 50% and ~ 30% of the optical radiation, respectively. However, the UV spectra are not fit by any normal models based on the Wu et al.(1983) IUE spectral atlas of stars. (This atlas does not include WR stellar spectra). We compared the observed spectra with models covering a range of parameters, including age of population, high mass cutoff of the initial mass function, and spread in creation times of the individual stars in the population (for a discussion of the set of models see Lamb, Hunter, and Gallagher, 1990). The best fit for Arp 248b was model 2 (displayed in figure 1) which is for a single stellar burst of age 3 million years. The fit is not sensitive to the upper mass cutoff of the initial mass function. Model 2 is also used to compare with the spectrum of UGC 8315N, although most of the models can be fit to this spectrum as it has poor signal to noise. This comparison helps provide the evidence for a large population of WR stars in Arp 248b but not in UGC 8315N. The flat UV spectra found in both cases is similar to those often observed for 'starburst' nuclei and is interpreted as due to massive hot stars. The UV spectrum of Arp 248b is not unique and has similarities to that of DDO 50, a dwarf galaxy dominated by WR stars (see Lamb, Hunter and Gallagher, 1990). WR stars have also been detected in other powerful far-infrared, starburst galaxies (see Armus, Heckman, and Miley, 1988).

A direct interpretation of the optical and UV data for Arp 248b would give a picture of the galaxy as having experienced a 'starburst' at least a few million years ago. Evidence of continuing star formation is not present in the UV spectrum. The maximum age of the burst if just one, of short duration, occurred, is a few tens of millions of years. However, there are complications involving the dust. The extinction in the UV is sufficiently large that we may be viewing only those massive stars that have 'broken out' of their natal gas and dust. This would preclude observation in the UV of the youngest massive stars and could hide current and recent star formation. It would complicate comparisons between observations of galaxies in which dust is clumped differently, or in which the amount of dust is very different. We do not anticipate that dust would obscure most WR stars, however, and we thus conclude that the difference between our two program galaxies in this respect is real.

V. Conclusions.

We conclude that short wavelength IUE spectra of colliding galaxies supports the idea that large numbers of massive stars ($M>20\ M_{\odot}$) are produced in bursts. The massive stellar populations may be somewhat different in the two galaxies studied here. That in UGC 8315N may be hotter than in Arp 248b. The optical spectra support this. (However metallicity differences may confuse the issue). We also find evidence that Arp 248b contains many WR stars, unlike UGC 8315N. We are observing evolved massive stars in the UV. This may simply reflect ageing single bursts of star formation, or it may be due to preferential obscuration of young stars by dust.

References.

Armus, L., Heckman, T. M., and Miley, G. K. (1988) Ap.J., **326**, L45.
Bushouse, H. A. (1986) **Ph.D. thesis**, University of Illinois.
Bushouse, H. A. (1986) A.J., **91**, 255; 1987.
Bushouse, H. A. (1987) Ap.J., **320**, 49.
Bushouse, H. A., Lamb, S. A., and Werner, M. W. (1988) Ap.J., **335**, 74.
Lamb, S. A., Hunter, D. A., and Gallagher, J. S. (1990) submitted to Ap. J.
Nussbaumer, H., Schmutz, W., Smith, L. J., and Willis, A. J. (1982) Astron. Astrophs. Suppl., **47**, 257.
Sanders, D. B., Soifer, B. T., Elias, J. H., Madore, B. F., Matthews, K., Neugebauer, G., and Scoville, N. Z. (1988) Ap.J., **325**, 74.
Wu, C. -C. et al. (1983) **IUE Ultraviolet Spectral Atlas**, IUE NASA Newsletter No. 22.

* *Department of Physics, University of Illinois, Urbana, Illinois 61801.*
† *Department of Astronomy, University of Illinois, Urbana, Illinois 61801.*
§ *Department of Physics, Northwestern University, Evanston, Illinois 60201*

RADIO LOUD FAR-INFRARED GALAXIES

Arjun Dey
Astronomy Department, University of California at Berkeley
Wil van Breugel
Institute of Geophysics and Planetary Physics, LLNL, Livermore
Joseph C. Shields
Astronomy Department, University of California at Berkeley

Abstract

We present the first results of a multiwavelength study of *IRAS* galaxies with excess radio emission. The sample was selected by cross-correlating the *IRAS* Faint Source Survey (for $|b| \geq 50°$) and the Point Source Catalogue (for $10° < |b| < 50°$) with the Texas radio survey. Recent optical (imaging and spectroscopic) and radio (VLA) observations are discussed. These observations will be used to investigate possible connections between radio galaxy activity, star formation and galaxy interactions.

Introduction

Increasing evidence exists for a possible evolutionary connection between galaxy interactions, central starbursts and activity of galaxy nuclei (e.g. Heckman 1987; Norman and Scoville 1988). A popular scenario is that tidal interactions between galaxies trigger a central starburst in one of them. This starburst then evolves into a black hole and/or increases its fuelling rate, resulting in enhanced activity of the galaxy nucleus. To a large extent such models have been motivated by studies of galaxies discovered by the IRAS survey.

Optical imaging of ultraluminous far-infrared (FIR) galaxies has shown that many are interacting with nearby companions. Interacting systems are also frequently found associated with Seyferts, powerful radio galaxies and quasars. These galaxies are often FIR emitters and can be selected from IRAS catalogs by their "warm" colors. Large populations of relatively young stars, inferred from stellar absorption lines, exist in many ultraluminous FIR galaxies (e.g. Armus *et al.* 1990). Similar evidence for the other classes of galaxies is more difficult to obtain, but some good examples are known such as the radio galaxy 3C 459 (Miller 1981), and the quasar 3C 48 (Boroson and Oke 1982; Neugebauer *et al.* 1982). The interpretation of emission-line data is more ambiguous and different sources of ionisation (H II regions, LINERs and AGNs) might contribute (Armus *et al.* 1990). Bulk outflow, either in the form of hot winds or collimated jets, occurs in all above mentioned classes of objects. Taken together one may think that there is some observational support for a "grand unified theory of active galaxies", but better evidence is needed. In order to study various FIR/radio/optical relationships we have defined a sample of sources from the *IRAS* Point Source Catalog (PSC) and Faint Source Survey (FSS). We have not used any additional IR color, luminosity or optical selection criteria.

Sample Selection and Observations

Our radio sources were taken from the Texas catalogue at 365 MHz (Douglas *et al.* 1980). This catalogue is $\sim 90\%$ complete to a flux density limit of 250 mJy for sources of angular sizes $\lesssim 1$ arcminute , and the version that we used covered the region $-35° < \delta < 40°$, $|b| > 10°$. Sources from this catalogue were compared with the *IRAS* FSS (for $|b| > 50°$; an overlap of ~ 1.9 steradians) and the *IRAS* PSC (for $|b| < 50°$; an overlap of ~ 4.7 steradians) for 60μ sources with positional

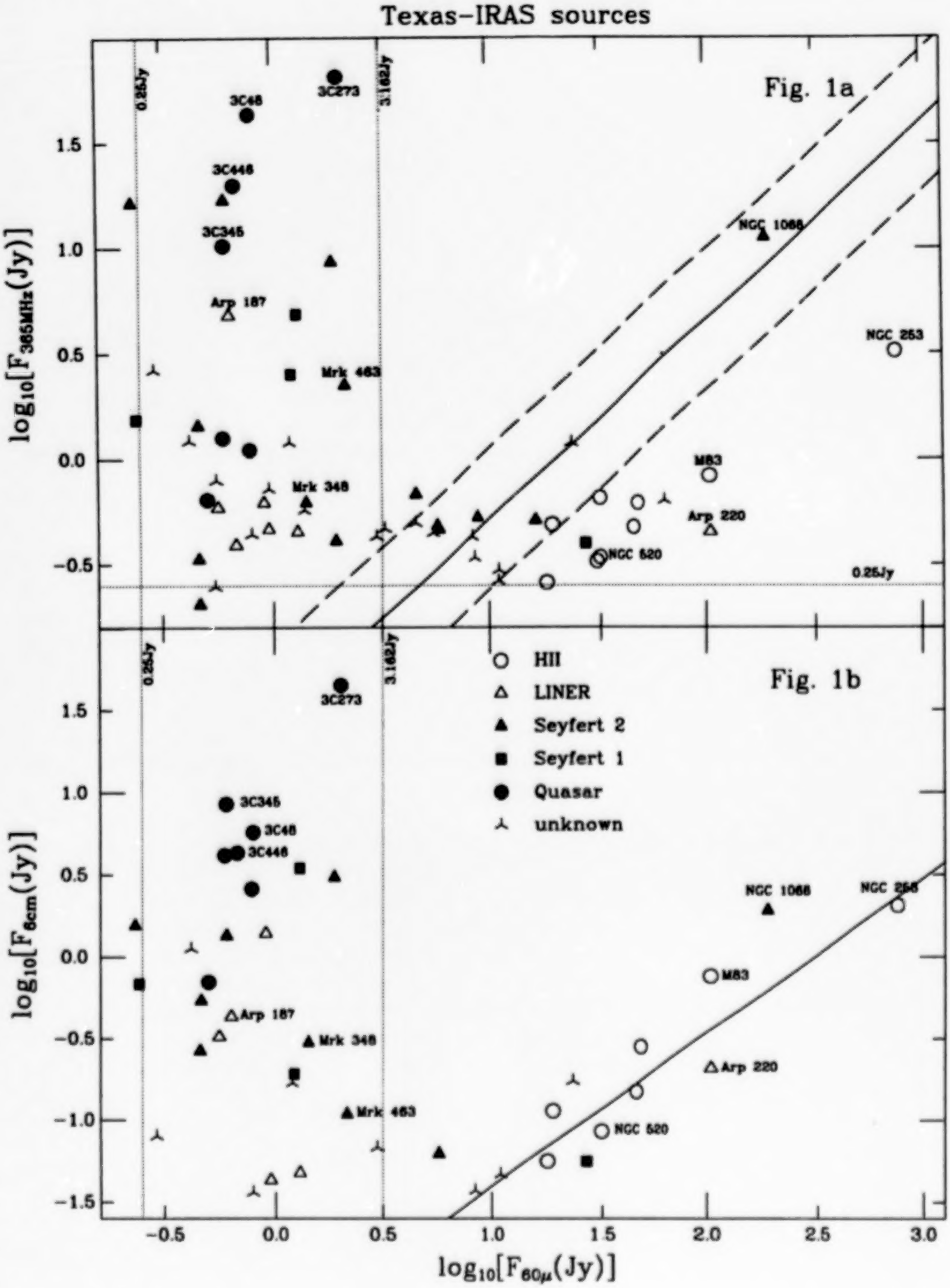
Texas-IRAS sources
Fig. 1a
Fig. 1b
log10[F365MHz(Jy)]
log10[F6cm(Jy)]
log10[F60μ(Jy)]
0.25Jy
3.162Jy
3C273
3C48
3C446
3C345
Arp 187
Mrk 463
Mrk 348
NGC 1068
NGC 253
M83
Arp 220
NGC 520
HII
LINER
Seyfert 2
Seyfert 1
Quasar
unknown
1.5
1.0
0.5
0.0
−0.5
−1.0
−1.5
2.0
2.5
3.0

coincidence within 60″. This resulted in 67 sources from the PSC and 32 sources from the FSS. The Texas radio source positions are accurate to about 1″, allowing optical identifications to be found on Palomar Sky Survey prints. A total of 60 IRAS/radio/optical identifications were found, of which 34 had $\log[F_{60\mu}(\mathrm{Jy})] < 0.5$. The remaining 26 objects are mostly well studied nearby bright galaxies.

All sources with $\log[F_{60\mu}(\mathrm{Jy})] < 0.5$ were mapped at 21 cm using the VLA in the A-array configuration. We obtained optical images of these sources at Lick Observatory using the 1-metre Nickel and 3-metre Shane telescopes. Optical spectra were also obtained at a resolution of ~ 15Å.

Preliminary Results

Figure 1*a* shows the 365 MHz flux density (from the Texas catalogue) plotted against the 60μ flux density (from *IRAS*) for the sources in our sample. Figure 1*b* shows the same plot, but using the 6 cm flux densities for the sources as listed in the catalogue constructed by Becker *et al.* 1990 from the Condon *et al.* (1989) 6 cm Green Bank survey, and the Parkes catalogue. The diagonal lines in Figure 1*a* indicate where the 6 cm - 60μ correlation for spiral galaxies from de Jong *et al.* (1985) would fall when shifted to 365 MHz using a spectral index of 0.7 (lower dashed line), 1.0 or 1.3 ($S_\nu \propto \nu^{-\alpha}$). All the objects with $\log_{10}[S_{60\mu}(\mathrm{Jy})] < 0.5$ lie above this correlation; we refer to these as "radio loud".

We also note that the actual 365 MHz flux densities for $\log_{10}[S_{60\mu}(\mathrm{Jy})] > 0.5$ galaxies are considerably *below* their predicted values using a typical (high frequency) spectral index of 0.7 or larger. This effect is clearly demonstrated by comparing Figure 1*a* with Figure 1*b*. The diagonal line in Figure 1*b* shows the de Jong *et al.* 6 cm - 60μ correlation which, as expected, agrees with the IR-bright galaxies sources in our sample. Many of these sources are well studied galaxies (Arp 220, NGC 253, NGC 1052, NGC 1068, *etc.*). In the case of Arp 220 a possible explanation for the flattening of the radio spectrum at lower frequencies is free-free absorption by dense gas (Sopp and Alexander 1989). This may also be the case for the other IR-bright galaxies. Further radio spectral information of the sources in our sample will be needed to investigate the generality of this phenomenon.

Figure 2 shows an *IRAS* color-color plot for the sources in our sample. The dashed lines outline the regions enclosing the *mean* (± one standard deviation) spectral indices for normal spirals, starbursts, and Seyfert 2 galaxies (Sekiguchi 1987). Vertical and horizontal arrows indicate that only upper limits to the 25μ and 100μ flux densities were available. Although our sample was not selected on the basis of IR colors, most of our sources exhibit IR colors typical of active galaxies.

We have also examined the radio - IR (60μ) luminosity distribution of our sample (not shown). Our sample has a high median IR luminosity ($L_{60\mu} \sim 4 \times 10^{11} L_\odot, H_o = 50\mathrm{km/s/Mpc}$), quite different from the $L_{60\mu}$ distribution of the Bright Galaxy Sample (Soifer *et al.* 1989), but more similar to that of Seyferts and quasars (Neugebauer *et al.* 1986). Sanders *et al.* (1988) have suggested that IR-ultraluminous galaxies like Arp 220 might be powered by quasar-like nuclei. We find very little overlap between our radio-loud sample and that of Sanders *et al.* Only Arp 220 is a strong enough radio emitter to be common to both samples over the appropriate area of sky. A more detailed analysis of the IR colors and optical spectra of our radio-loud FIR galaxies is needed to see whether there are other differing properties.

Of the radio loud FIR galaxies, 40% have flat radio spectra ($\alpha \lesssim 0.5$) and very compact radio cores. Of the remaining 60% with relatively steep spectra, 80% have their dominant radio emission on small angular scales ($\lesssim 5''$). These sources are entirely embedded within their parent galaxies and are ideal sources in which to study the interaction between radio sources and their surrounding interstellar medium. One example, Arp 187, is shown in Figure 3 which includes an R-band image (3*a*), 21 cm VLA map (3*b*) and optical spectrum (3*c*). Note that Hβ appears in absorption, indicating the possible presence of a large young stellar population in the galaxy.

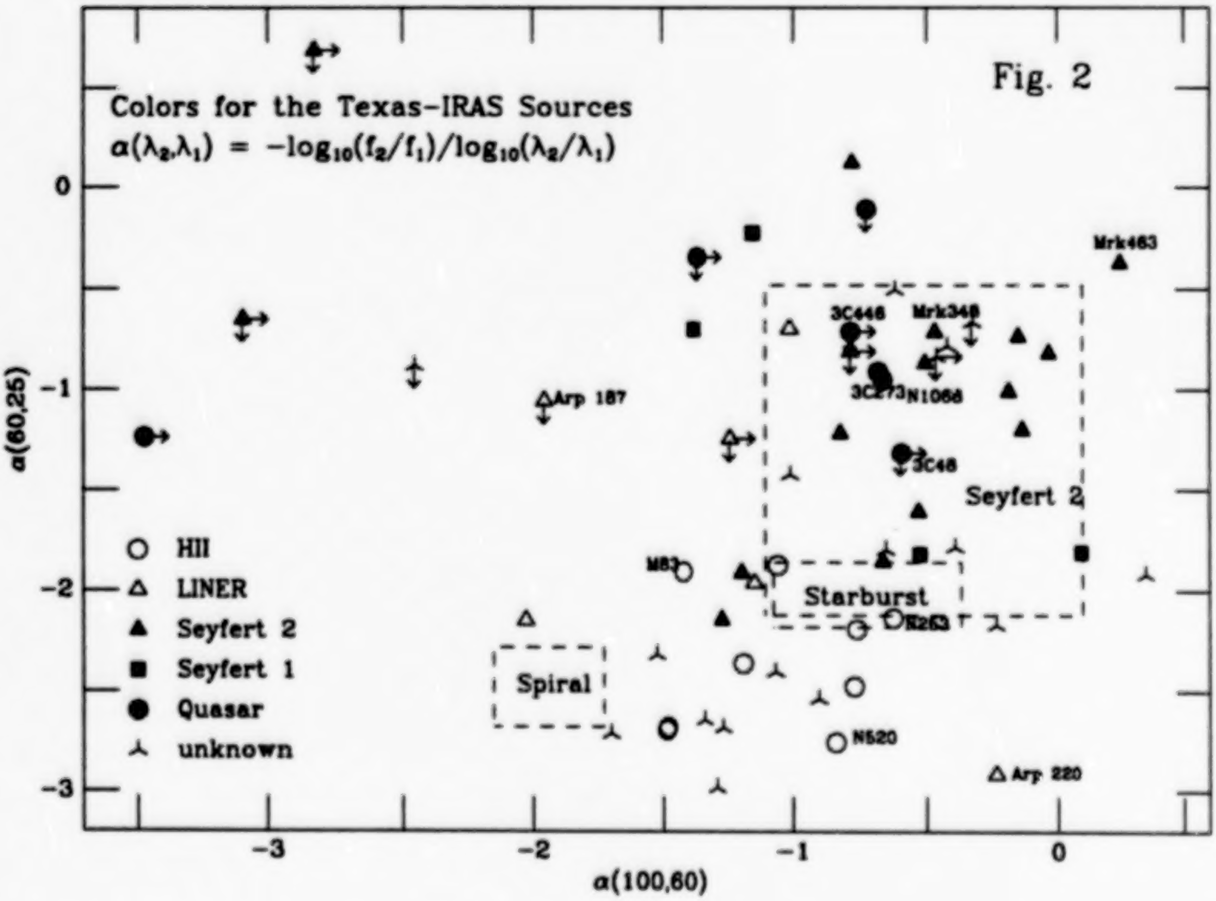

Of the galaxies in our radio-loud sample, 7 are LINERs, 3 are Seyfert 1 galaxies, 10 are Seyfert 2 or radio galaxies, and 7 are quasars. Thus our sample encompasses a large variety of galaxy activity. More detailed studies, and increasing the sample size, may help us better understand possible links between these classes of objects and starburst activity.

References

Armus, L. Heckman, T. M. and Miley, G. K., 1990, preprint

Becker, R. H., White, R. L. and Edwards, A. L., 1990, preprint

Boroson, T. A., and Oke, J. B., 1982, *Nature*, **296**,397.

Condon, J. J., Broderick, J. J. and Seielstad, G. A., 1989,*Astron. J.*, **97**,1064.

de Jong, T., Klein, U., Wielebinski, R., and Wunderlich, E., 1985,*Astron. Astrophys.*, **147**,L6

Douglas, J. N., Bash, F. N., Torrence, G. W., and Wolfe, C., 1980,Univ. Texas Publ. Astron. no.17

Heckman, T. M. , 1987,in *Starbursts and Galaxy Evolution*, T. X. Thuan, T. Montmerle, J. T. T. Van, Eds. (Gif sur Yvette: Editions Frontieres)

Miller, J. S. 1981,*Pub.A.S.P*, **93**, 681.

Neugebauer, G., Soifer, B. T., and Miley, G. K., 1982,*Astrophys. J. Lett.*, **295**,L27.

Neugebauer, G., Miley, G. K., Soifer, B. T. and Clegg, P. E., 1986,*Astrophys. J.*, **308**,815

Norman, C. and Scoville, N. Z., 1988, *Astrophys. J.*, **332**, 124.

Sanders, D. B., Soifer, B. T., Elias, J. H., Madore, B. F., Matthews, K., Neugebauer, G., and Scoville, N. Z., 1988, *Astrophys. J.*, **325**,74

Sekiguchi, K., 1987, *Astrophys. J.*, **316**,145

Soifer, B. T., Boehmer, L., Neugebauer, G., and Sanders, D. B., 1989,*Astron. J.*, **98**,766

Sopp, H. M. and Alexander, P., 1989, *Astrophys. Space Sc.*, **157**,287

BLANK

PAGE

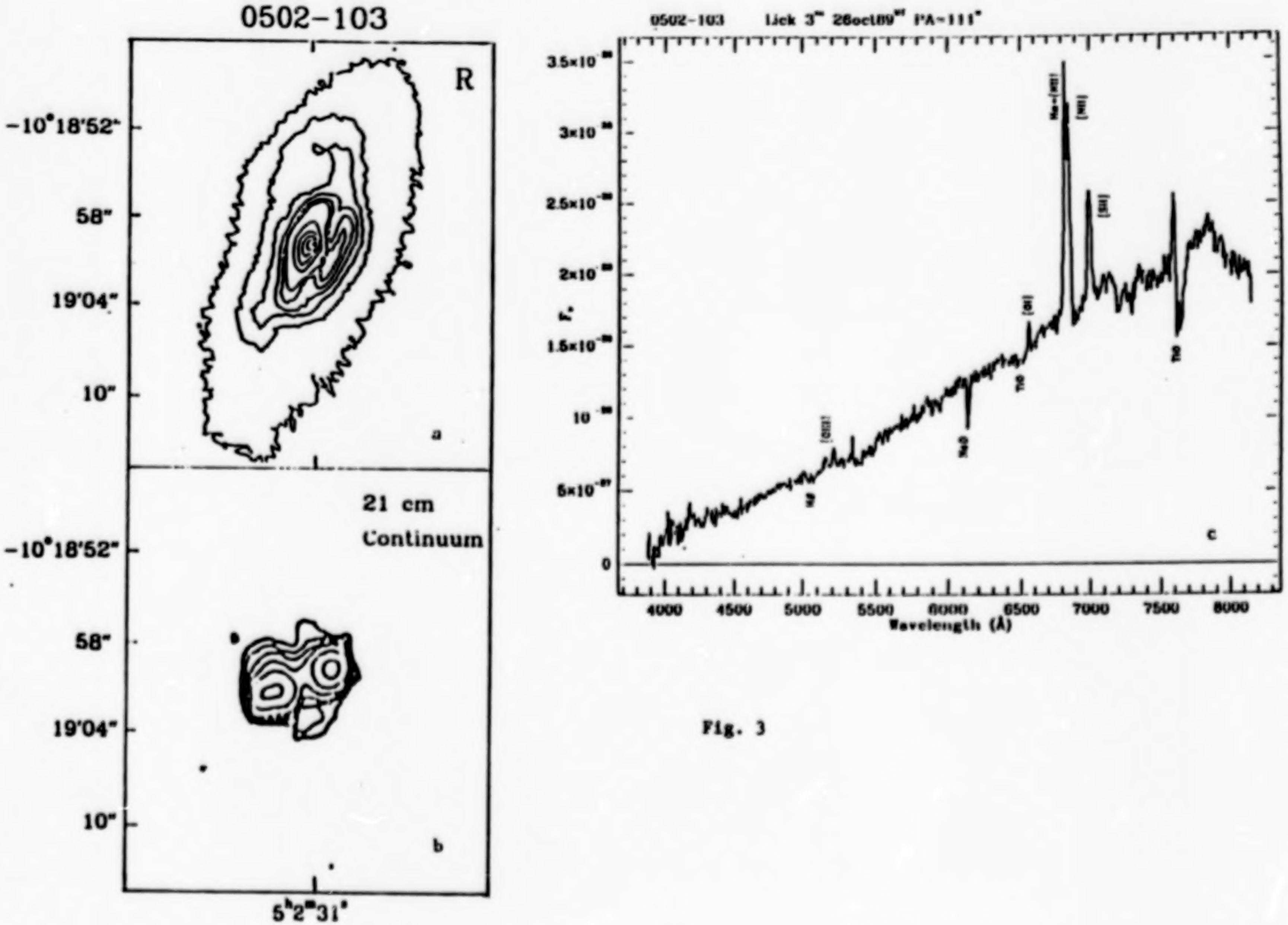
0502-103
R
-10°18'52"
58"
19'04"
10"
a
21 cm
Continuum
b
5h2m31s
0502-103 Lick 3" 26oct89 PA=111°
3.5×10
3×10
2.5×10
2×10
1.5×10
10
5×10
0
Fν
Mg
[OIII]
NaD
TiO
[OI]
Hα+[NII]
[NII]
[SII]
O2
c
4000
4500
5000
5500
6000
6500
7000
7500
8000
Wavelength (Å)

Fig. 3

DISCUSSION

Norris: What is the distribution of far-IR color in your radio-loud sample? It would be very interesting to see if your sample consists only of warm (Seyfert-like) objects, or whether cooler, starburst galaxies could also be radio-loud.

Dey: So far 6 out of 39 galaxies have HII-region type spectra. The colors of our sample scatter over a large range, but on average are warmer than any flux-limited IRAS sample. There are some objects whose IRAS colors are similar to those of starbursts.

ON A CONNECTION BETWEEN SUPERNOVA OCCURRENCE AND TIDAL INTERACTION IN EARLY TYPE GALAXIES

R.K.KOCHHAR
Indian Institute of Astrophysics
Koramangala Bangalore 560034 India

There are three types of supernovae: two subtypes SNIa and Ib; and SNII. Late type galaxies produce all types of SN, whereas early types (E,SO, and non-Magellanic irregulars IO) have hosted only SNIa. The recently identified SNIb, like SNII, have massive stars as their progenitors.

Reviving Oemler & Tinsley's (1979) suggestion that SNIa also come from short-lived stars, we have asserted that they need not occur in all early-type galaxies. SNIa occur only in those galaxies that have access to gas and can form stars in their main body. (SN in nuclear regions are a different matter altogether). In this model, SNIa are not associated with typical stellar population of E/SOs but with regions of localized star formation. Note that data on SNIa from spirals is already consistent with this model (see Kochhar 1989 for references and details).

The fact that E, SO, and IO galaxies have so far produced only SNI implies that stars $> 6-7M_{\odot}$ do not form in them. It needs to be emphasized that the question before us is: what are the immediate precursors of SNIa? Their ultimate progenitors in any case are $4-7M_{\odot}$ stars which leave behind a CO degenerate core, whose deflagration produces a model SNIa. If SNIa are to be associated with the typical population of E/SOs, then delayed deflagration is achieved by placing these cores in low-accretion binaries. In our model there is no delay in their deflagration so that SNIa are associated with events of recent star formation (see Kochhar 1989). The required gas in the early-type galaxies can come from a variety of sources: mergers (Fornax A, Persius A); past tidal interactions (N 5253); neighbours (N 3226). Alternatively a galaxy may accrete from its own halo (M 86) or from the intracluster medium (M 87, Coma A).

Environmental factors

If SNIa came from low-mass long-lived stars, typical of E/SOs, then the occurrence of SN would be an intrinsic property of the host galaxy, independent of galactic ecology. That this is not the case becomes immediately obvious when we consider Coma cluster. It is compact, dynamically evolved, spiral poor,.and fairly uniform in galaxy type. It shows a central maximum density and a symmetrical decrease towards the boundaries. If all galaxies were equally likely to produce SN, we would expect the supernovic E/SOs to have the same spatial distribution as the galaxies in general. This, however, is not the case. All supernovic galaxies in Coma are confined to a plane (Figure 1). The reason must be that the hot intracluster gas has settled in a central disc, and been accreted by the galaxies there. There are 8 SN in the disc, and two of the host galaxies are IO type, clearly a result of accretion.

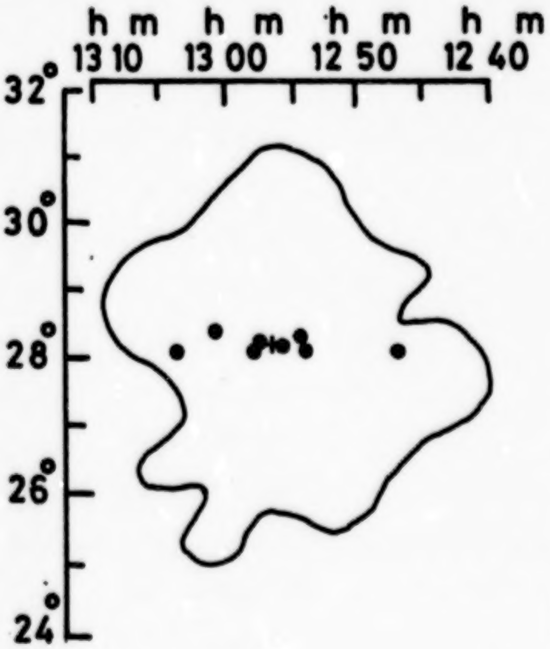

Figure 1. The supernovic galaxies in the Coma cluster (Barbon 1978).

In contrast to Coma is the Virgo cluster, in which galaxies carry their own reservoirs of gas in the form of hot halos. Although it contains only 11 % of all NGC early-type galaxies it accounts for 30 % of the supernovic E/SOs. Thus Virgo galaxies are thrice as SN prone as a general sample is. According to Tammann (1974) the effect is real and not an artifact of higher search intensity.

X-ray luminosity

The X-ray luminosity of early-type galaxies in Virgo and elsewhere can be explained by gravitational heating only if SN heating is not important. A specific model for N 4472 (Thomas 1986) requires a SN rate of 0.01 SNU, much lower than the estimates of 0.22 (Tammann 1974) or 0.07 (Evans et al. 1989). The problem is more serious than realized because if any thing Virgo SN rate is higher than the average. In our model, SN occur in regions of recent star formation. The SN energy is used in dispersing the dense gas clouds and thus does not contribute towards X-ray luminosity.

Supernovic E/SOs

IO galaxies are essentially E,SO galaxies that have been excessively contaminated by gas and dust. They all show signs of star formation and are prolific producers of SN, significantly only SNIa. Five of them have produced 8 SN: N 2968, 3656, 4753^2, 5195^2, 5253^2; superscript 2 denotes the occurrence of 2 SN. Of special interest is NGC 5253, which along with N 5102, 5128(Cen A) and 5236 constitutes Centaurus chain. Accretion of gas from a common envelope has resulted in star formation in N 5253; enhanced star formation rate in N 5236 (5 SN); fuelled the radio source in N 5128; and produced a burst of star formation 10^8 yr ago in N 5102. Three other galaxies with 2 SN underline the role of supply of gas. N 1316 (For A) has certainly swallowed one possibly many gas rich companion galaxies. N 4874 lies at the centre of Coma cluster with access to intracluster gas (see above). The non-descript MCG 5-27-53 is an SO galaxy in the Zwicky cluster 156-14. Both the SN lie on a faint ring around it. This galaxy forms a pair (Ho 244) with the barred spiral MCG 5-27-52, 2 arcmin away, which is presumably the source of gas for the supernovic galaxy.

There are 12 SO galaxies that have produced SN (N 1332, 1411, 3570, 4340, 4382, 4410, 4451, 4526, 4887, 5485, 6835, and 7634). Six of these are paired galaxies, eight carry the tag peculiar, doubtful, or uncertain in RC2 — again suggesting a connection between SN occurrence and external factors. There are 17 ellipticals that have produced SN : N 1275 (Per A), 1316 (For A), 2672, 3226, 3574, 3904, 4335, 4374 (M 84), 4406 (M 86), 4486 (M 87), 4564, 4621, 4636, 4782, 4874 (Com A), 5128 (Cen A), 7619.

M 86's SN is within its hot halo and on intergalactic bridge to M84. Four of the remaining 16 galaxies form pairs with other galaxies which can supply gas. An additional seven show hot gas which can cool to form stars. 12 out of 16 show one activity or other. Two of the remaining four (N 4564 and 4621) are in Virgo cluster. They are only two galaxies whose only claim to fame has been the SN. These four and their SN certainly deserve a second look.

One is confronted with a north-south divide while trying to correlate SN occurrence with other properties. Most supernovic galaxies are in the northern skies whereas most recent studies are of the southern. Since only complete radio samples are available, we compare in Figure 2 radio and SN activities. It can be seen that the fraction of radio emitters in a subsample of supernovic ellipticals is much higher than in the general sample. The numbers involved are small, but the trend is unmistakable. In view of the well attested correction of the radio property with the others, we conclude that SN activity is indeed related to the others.

Since SN occurrence in E/SOs requires localized star formation, integrated fixed-aperture photometry is not expected to show these galaxies to be significantly bluer than a general sample. We have started an observational program using La Palma 1 m telescope to see if regions around SN show signs of recent star formation (I.Perez Fournon & R.K.Kochhar in preparation).

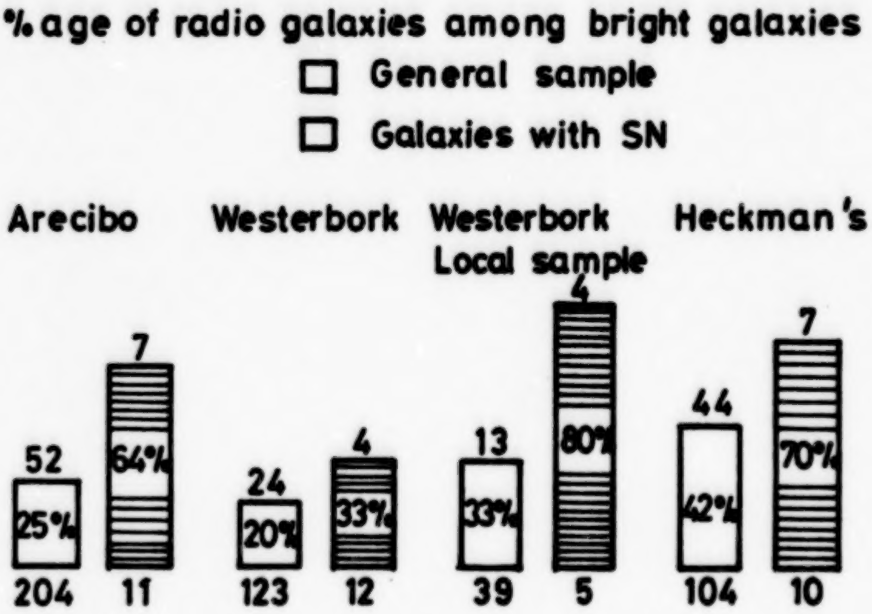

Figure 2. The percentages of radio galaxies in samples of bright galaxies and in subsamples of bright supernovic galaxies (Kochhar 1989).

References

Barbon,R. (1978) Astr. J. 83, 13

Evans,R., van den Bergh,S & McClure,R.D. (1989) Ap. J. 345,752.

Kochhar,R.K. (1989) Ap. Sp. Sci. 157, 305.

Oemler,A. & Tinsley,B.M. (1979) Astr. J. 84, 985.

Tammann,G.A. (1974) in Supernovae and Supernova Remnants (Ed.: C.B. Cosmovici), Reidel.

Thomas,P.A. (1986) M.N.R.A.S. 220, 949.

DISCUSSION

Hutchings: Can SN be detected spectroscopically in the bright inner regions of star-forming galaxies? (What is the expected SN rate for a starburst?)

Kochhar: R. Terlevich (1989, RGO preprint 100) has identified the rapid flare in spectral variability in Sy 1 galaxies N 5548, 1275, 4151, and 3516 with the SN flash. The longer term variability has been attributed to the evolution of the SN remnants. (The expected SN rate is about one per year.)

INFRARED IMAGES OF MERGING GALAXIES

G. S. Wright[1], P. A. James[2], R. D. Joseph[3], I. S. McLean[3], and R. Doyon[4]

1) Joint Astronomy Centre, 665 Komohana Street, Hilo, HI96720.

2) Institute for Astronomy, 2680 Woodlawn Drive, Honolulu, HI96822.

3) Dept. of Astronomy and Physics, UCLA, 405 Hilgard Ave., Los Angeles, CA90024.

4) Blackett Laboratory, Imperial College, London, SW7 2BZ.

1. INTRODUCTION

Infrared imaging of interacting galaxies is especially interesting because their optical appearance is often so chaotic due to extinction by dust and emission from star formation regions, that it is impossible to locate the nuclei or determine the true stellar distribution. However, at near-infrared wavelengths extinction is considerably reduced, and most of the flux from galaxies originates from red giant stars that comprise the dominant stellar component by mass. Thus near infrared images offer the opportunity to study directly components of galactic structure which are otherwise inaccessible. Such images may ultimately provide the framework in which to understand the activity taking place in many of the mergers with high IRAS luminosities.

2. MULTIPLE NUCLEI

Infrared imaging is a powerful tool for the identification of galactic nuclei, since the nuclear regions of many galaxies are often too heavily enshrouded by dust for optical images to show the underlying structure. A well known example of this is Arp220, where the two optical maxima are due to a dust lane which bisects the galaxy and neither of them are associated with galaxy nuclei. We have obtained K (2.2 μm) images of two galaxies, Mkn788 and IRAS0857+3912 which have previously been described as the result of galaxy mergers on the basis of two equally bright optical peaks. Our image of Mkn788 (Joseph et al. 1988) shows that the western source is much more sharply peaked and has twice the integrated luminosity of the other. The brightest infrared source is coincident with the VLA source (Kollatschny et al. 1986), suggesting that it is the true nucleus of Mkn788. The broader, lower intensity K source which corresponds to the other "optical nucleus" could be interpreted as a giant extra-nuclear HII region similar to the jumbo HII region in NGC3310 (cf. Telesco & Gatley 1984). In IRAS0857+3912 we find a similar result. The optical image presented by Sanders et al. (1988) shows two almost equally bright optical lobes, whereas in our K image the north-western source has almost an order of magnitude higher peak surface brightness than its neighbour. This extremely red source is quite possibly the nucleus of the IRAS galaxy. However, a third very red source, which is barely apparent even at J (1.25 μm) is also clearly detected in the K image of this very disturbed galaxy.

Infrared images have also been useful in identifying double structures in the nuclei of interacting galaxies which have not even been hinted at by optical observations. A striking example of this is given by the K images of Arp220. Graham et al. (1990) have used high resolution imaging to show that it has a double nucleus coincident with the radio sources in the middle of the dust lane.

The results discussed above suggest that caution should be applied in the identification of optical bright spots as multiple nuclei in the absence of other evidence. They also illustrate the advantages of using infrared imaging to study the underlying structure in merging galaxies.

3. SURFACE PHOTOMETRY

We have begun a programme to take near infrared images of galaxies which are believed to be mergers of disk galaxies because they have tidal tails and filaments. In many of these the merger is thought to have induced exceptionally luminous infrared emission (cf. Joseph and Wright 1985, Sanders et al. 1988). Although the optical images of the galaxies show spectacular dust lanes and filaments, the K images all have a very smooth distribution of light with an apparently single nucleus. Several authors (e.g. White 1979, Farouki & Shapiro 1982, Barnes 1989) have predicted that over a period of ~ 10^9 yrs mergers should produce a mass distribution indistinguishable from that of an elliptical galaxy, based on n-body simulations of merging disk galaxies. Observational evidence in support of this idea is presented by Schweizer (1982), who showed that the V-light profile of NGC7252 is indeed well fitted by the $r^{1/4}$ de Vaucouleurs law. We have used the K images to test the hypothesis that other mergers are also developing elliptical-like light profiles.

Figure 1a shows profiles for Arp 220 and NGC 2623, in which K surface brightness within elliptical annuli is plotted against radius$^{1/4}$. The characteristic de Vaucouleurs law for elliptical galaxies is a straight line on this plot. The lines shown were obtained by a least-squares fit to all points except for the inner two, which are artificially reduced due to seeing and decentering effects. The lines are clearly a good fit to the data over a range of about 4 magnitudes and linear scales of about 5 kpc in radius, using $H_0 = 50$ km s^{-1} Mpc^{-1}. This similarity with ellipticals is strengthened by the half-light scale lengths for the two mergers. The effective radius containing half the K light is 1.6 kpc for NGC2623, and 3.4 kpc for Arp220, consistent with published values for ellipticals (Kormendy 1982). Unfortunately the limited area covered by these data makes it impossible to rule out absolutely the existence of a more extended disk. We nevertheless conclude, on the basis of our present data, that Arp220 and NGC2623 have stellar light profiles which closely resemble those of elliptical galaxies.

K images for the remaining four galaxies show light profiles which are not those of spiral or elliptical galaxies. Figure 1b shows examples of the kinds of deviation from simple light profiles which we have found. IC883 (shown) and NGC4194 are well fitted by an $r^{1/4}$ law beyond approximately 1 kpc, but the profile is significantly flattened within this radius. NGC6240 and NGC6052 (shown) differ from ellipticals or spirals over the entire surface brightness range. It is probably significant that these four galaxies all have nuclei substantially offset from the centre of the outer isophotes. The fact that the light profiles of Arp220 and NGC2623 are a much better fit to an $r^{1/4}$ law than the other galaxies we have imaged so far suggests that Arp220 and NGC2623 may be the most dynamically evolved of the merger remnants associated with IRAS sources. In the case of Arp220 it is tempting to speculate that its stage of dynamical evolution is related to other suggestions that Arp220 is one of the "oldest" of the IR luminous mergers, based on scenarios for the evolution of the luminosity source.

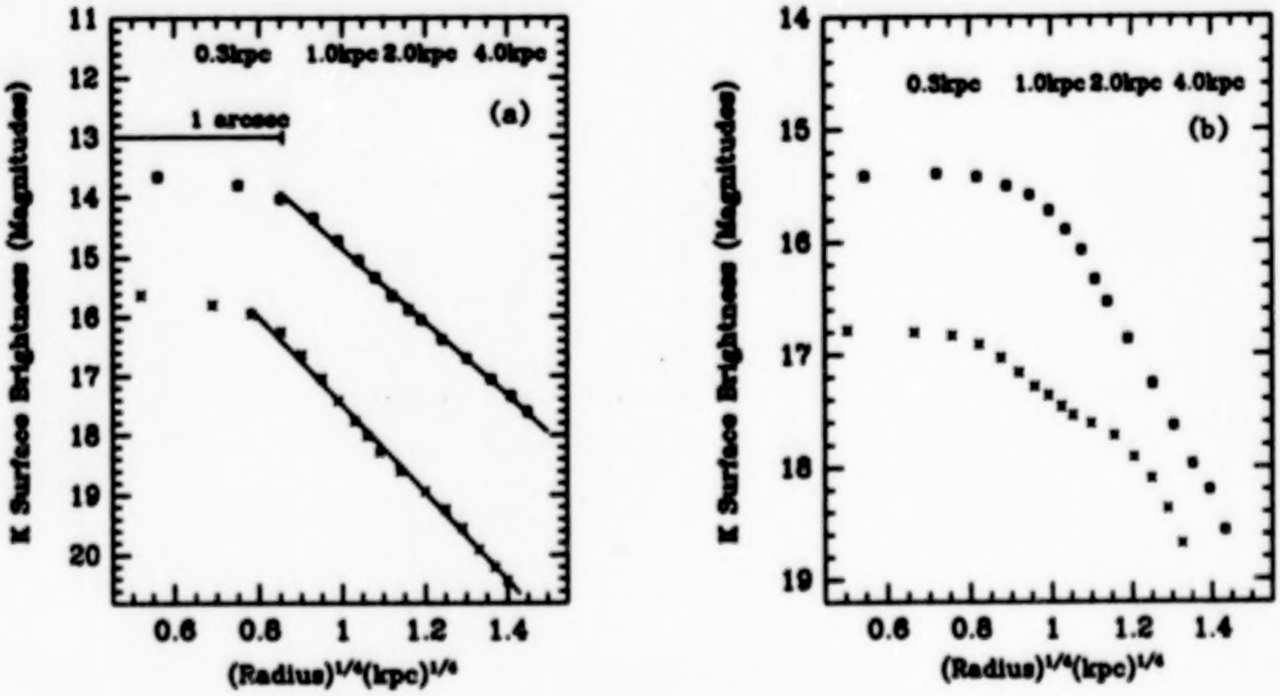

Figure 1 K surface brightness (mag/arcsec^2) plotted vs. the fourth root of the radius for a) Arp220 (□) and NGC2623 (×) and b) IC883 (□) and NGC6052 (×). The plot for NGC2623 has been offset by +2 magnitudes for clarity. The scale along the top of both plots is radius in kpc, assuming $H_0 = 50$ km s $^{-1}$ Mpc^{-1}.

While Arp220 and NGC2623 may have developed the mass distribution of an elliptical galaxy, they still have much more gas and dust. If merger remnants are actually to evolve into elliptical galaxies there must be some mechanism which removes the interstellar material. The activity which powers the luminous IR emission of these galaxies may play a key role in this process. For example, Graham et al. (1984) argue that a consequence of starbursts is a sufficiently high supernova rate to severely deplete the gas.

Similarly it has been suggested (eg. Carlberg 1989, Efstathiou & Rees 1988) that a quasar-like active nucleus could consume the gas in less than a Hubble time. We suggest therefore that the high IRAS luminosities of merging galaxies provide a clue to the means by which they could become as gas free as ellipticals.

4. CONCLUSIONS

Near infrared images are a much better way to investigate the existence of multiple nuclei than optical images because extinction and the emission from hot young stars are much reduced at 2.2 μm . Our images of Mkn 788 and IRAS 0857+3912 are strikingly different from optical images in that only one nucleus clearly dominates in the near-IR. This suggests that in the absence of other evidence for interaction care should be taken in classifying potential mergers on the basis of nuclear structure in optical images alone.

2.2 μm surface photometry of several high luminosity mergers of disk galaxies has been used to test the idea that they may be evolving into ellipticals. Arp220 and NGC2623 obey the characteristic de Vaucouleurs law of ellipticals at 2.2 μm over several kpc, contrary to the impression given by optical images. We suggest that this provides support for the idea that mergers will evolve into elliptical-like objects. It is clear that the relation between degree of relaxation and other evolutionary processes in mergers is a very important question. By obtaining infrared images of a larger sample of mergers going to fainter isophotes we plan a more definitive study of the evolution of merger remnants with high IRAS luminosities.

REFERENCES

Barnes, J. E. 1989 *Nature* **338**, 123.

Carlberg, R. G. 1989 *Astrophys. J. preprint*

Efstathiou, G. & Rees, M.J. 1988 *Mon. Not. R. astr. Soc.* **230**, 5p.

Farouki, R. T. & Shapiro, S. L. 1982 *Astrophys. J.* **259**, 103.

Graham, J. R., Wright, G. S., Meikle, W. P. S., Joseph, R. D., & Bode, M. F. 1984 *Nature* **310**, 213.

Graham, J. R., Carico, D. P., Matthews, K., Neugebauer, G., Soifer, B. T. & T. D. Wilson 1990 *Astrophys. J. Lett. preprint*

Joseph, R. D. & Wright, G. S. 1985 *Mon. Not. R. astr. Soc.* **214**, 87.

Joseph, R. D., Wright, G. S., James, P. A., & McLean, I. S. 1988 *Mon. Not. R. astr. Soc.* **232**, 7p.

Kollatschny, W., Netzer, H. & Fricke, K. J., 1986 *Astr. Astrophys.*, **163**, 31.

Kormendy, J. 1982 *Morphology and Dynamics of Galaxies* ed. Martinet, L. *SAAS-FEE* 115.

Sanders, D. B., Soifer, B. T., Elias, J. H., Madore, B. F., Matthews, K., Neugebauer, G. & Scoville, N. Z. 1988 *Astrophys. J.* **325**, 74.

Schweizer, F. 1982 *Astrophys. J.* **252**, 455.

Telesco, C. M., Decher, R. & Gatley, I., 1985. *Astrophys. J.* **299**, 896.

Telesco, C. M. & Gatley, I., 1984 *Astrophys. J.* **284**, 557.

White, S. D. M. 1979 *Mon. Not. R. astr. Soc.* **189**, 831.

DISCUSSION

Lamb: I suggest a mechanism for the production of a large HII region away from the nucleus of an interacting galaxy. If two disk galaxies with gas collide and overlap for awhile, it is possible under some circumstances for the angular momentum to cancel in regions away from the nuclei. If this region contains gas, the collision may leave behind a region which is a prime candidate for star formation. Is it possible that there is another galaxy close to the one you are investigating which might have produced such an HII region?

Wright: Yes, this emphasizes why a single optical photograph does not necessarily show two nuclei, if it has two bright sources. Other information, (which may be a K image) is needed to establish a merger. In fact, for one of the images I showed, notice that there is a third source which may be a companion galaxy on the K image.

Moreau: What kind of dynamical evidence do we have that Arp 220 is actually merging? I mean spectra from which we can derive Doppler-shift information.

Wright: Dr. Norris drew attention to spectra showing line widths in excess of 1500 km/s and to the large velocities seen in molecular gas.

Khachikian: Do you think that superassociations can be the nuclei of galaxies?

Wright: Yes, an HII region can be at the nucleus of a galaxy, where by nucleus I mean the peak of the stellar density. But optical images showing two bright knots in a galaxy are not sufficient on their own to show that the galaxy has two nuclei and therefore must be a merger. Other data must also be used.

Heckman: What is the evidence that either the "nuclear" or "extra-nuclear" K-band light originates from an old stellar population? If the near-IR is produced by young stars, its $r^{1/4}$ surface brightness law is not readily explained by standard merger simulation. The two-color diagrams you showed suggested that the near-IR continuum was not from a normal old stellar population.

Wright: In general, the K band light off the nucleus does trace the old stellar population, and JHK colors are consistent with this. This need not be so on the nucleus (central 1-2 kpc). Near-IR colors can show a contribution to the K-light due to hot dust, non-thermal emission, young stars, etc. The figure I showed for IRAS 08572 + 3912, showed nuclear colors indicating components that are not necessarily stars.

GALAXY INTERACTIONS AND STAR FORMATION: RESULTS OF A SURVEY OF GLOBAL Hα EMISSION IN SPIRAL GALAXIES IN 8 CLUSTERS

C. Moss
Institute of Astronomy, Cambridge, U.K.

Kennicutt & Kent (1983) have shown that the global Hα emission from a spiral galaxy is an indicator of the formation rate of massive stars. Moss, Whittle & Irwin (1988) have surveyed two clusters (Abell 347 and 1367) for galaxies with Hα emission using a high dispersion objective prism technique. The purpose of the survey is to investigate environmental effects on star formation in spiral galaxies, and in particular to ascertain whether star formation is enhanced in cluster spirals. Approximately 20 % of CGCG galaxies were detected in emission. Two plates of excellent quality were obtained for each of the two clusters, and galaxies were only identified to have emission if this was detected on both plates of a plate pair. In this way, plate flaws and other spurious identifications of emission could be rejected, and weak emission confirmed.

The results of this survey have been discussed by Moss (1987). The detected galaxies are of types S0–a and later. The frequency with which galaxies are detected in emission increases towards later morphological type as expected (cf. Kennicutt & Kent 1983). There is no evidence of any dependence of the frequency of detected emission on the absolute magnitude of the galaxy (cf. Moss & Whittle 1990), but there is a strong correlation between a disturbed morphological appearance of the galaxy and the detection of emission. Furthermore it is found that the emission is more centrally concentrated in those galaxies which show a disturbed morphology. It may be noted that the objective prism plate gives a spectrum of a 400 Å region around rest wavelength Hα, but superposed on this is the Hα emission from the galaxy which, because the light is essentially monochromatic, results in a true two-dimensional image of the Hα distribution. The visual appearance of the emission on the prism plates was classified according to its diffuseness on a 5 point scale ('very diffuse', 'diffuse', 'intermediate', 'compact' and 'very compact'). In Table 1 the relation is shown between this classification and a morphologically disturbed appearance for the galaxy. Galaxies have been divided into ones with *compact* emission (classification of 'intermediate', 'compact' and 'very compact' on the scale discussed above), and ones with *diffuse* emission (classification of 'diffuse' and 'very diffuse'). There is a noticeable tendency for morphologically disturbed galaxies to have

TABLE 1

Relation of tidally disturbed galaxy morphology and the compactness of global Hα emission for CGCG galaxies in Abell 347 and 1367

	Emission-line galaxies	
	Tidally disturbed	Other
Compact emission	14	6
Diffuse emission	4	12

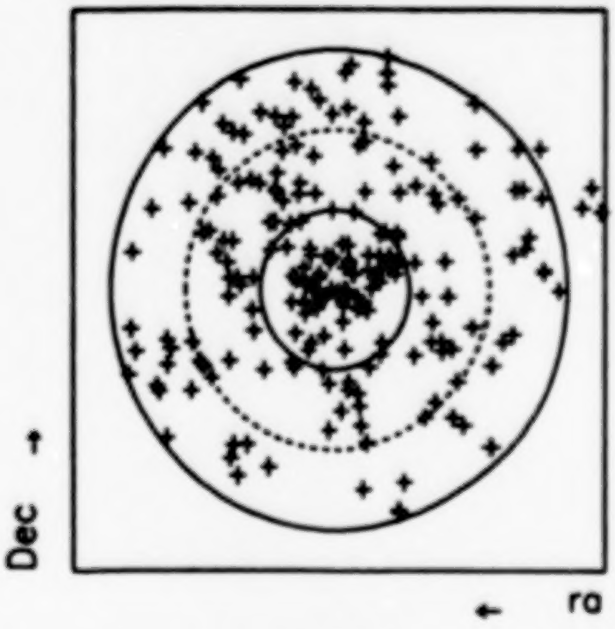

FIGURE 1

The distribution of the sample of galaxies, types Sa and later, surveyed for Hα emission. The sample comprises UGC galaxies in 8 clusters (Abell 262, 347, 400, 426, 569, 779, 1367 and 1656) and additional CGCG galaxies in Abell 347 and 1367. The distributions for the individual clusters have been scaled according to the value of the Abell radius for each cluster and then superposed. The three circles are of radii 0.5, 1.0 and 1.5 Abell radii respectively.

more compact emission. This correlation has been demonstrated independently in the case of radio emission from spirals by Hummel (1980, 1981), Condon *et al.* (1982) and Urbanik, Grave & Klein (1985), and in the case of Hα emission from tidally interacting galaxies by Bushouse (1987) and by Kennicutt *et al.* (1987).

The objective prism Hα survey has been extended to include UGC galaxies in eight clusters (Abell 262, 347, 400, 426, 569, 779, 1367 and 1656). The galaxies surveyed were of types Sa and later and are within 1.5 Abell radii of the cluster centres. The combined distribution of these galaxies together with the other CGCG spirals of types Sa and later surveyed in Abell 347 and 1367, is shown in Figure 1. As is seen there is a noticeable, but not very strong, density increase towards the cluster centre. As expected this effect is strongest for the earliest spiral types.

In Figures 2 and 3 are shown the distribution of detected emission-line galaxies. In Figure 2 is shown the distribution of galaxies with *compact* emission and in Figure 3 is shown the distribution of galaxies with *diffuse* emission. A Mann-Whitney U test was used to compare the radial distributions of the various galaxy samples. Galaxies with compact emission have a radial distribution which is more strongly concentrated towards the cluster centre than the radial distribution of other galaxies in the total sample. This effect is significant at the 3.0 sigma level, and is the more striking since the proportion of

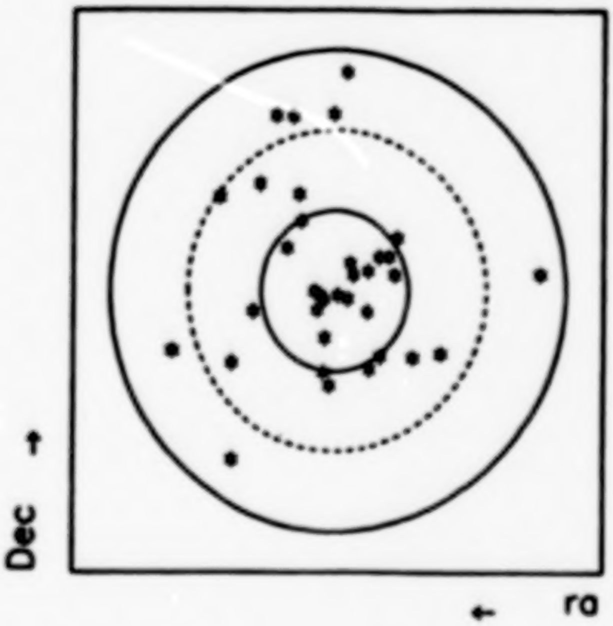

FIGURE 2

As Figure 1, showing the distribution of galaxies with *compact* emission.

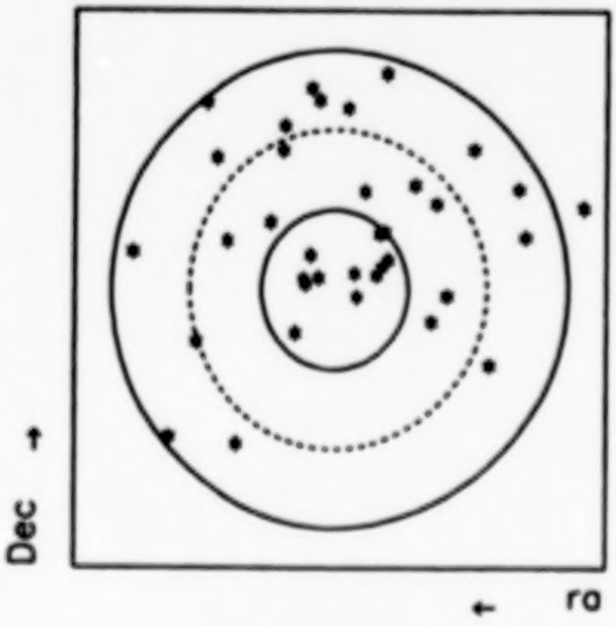

FIGURE 3

As Figure 3, showing the distribution of galaxies with *diffuse* emission.

early type spirals increases towards the cluster centre, and these galaxies are *less* likely to have emission. By contrast, the radial distribution of galaxies with diffuse emission is less concentrated towards the cluster centre than the radial distribution of other galaxies in the total sample, although the difference in these distributions is hardly statistically significant.

There is a simple explanation for the above data. Since compact emission is known to correlate with disturbed morphology, we can explain the centrally concentrated distribution of galaxies with compact emission as due to induced star formation in galaxies undergoing tidal interactions within approximately 0.5 Abell radii of the cluster centres. It would seem likely that these are galaxy–galaxy interactions. A potential difficulty is the high velocity dispersion in clusters which would not allow such tidal interaction to become significant. However Moss (1987) has shown that for two clusters studied in detail, disturbed, peculiar and interacting galaxies can be easily separated into pairs or small groups with low velocity dispersion, although the velocity dispersion of the whole sample is very high. By contrast the galaxies with diffuse emission are likely to be spirals with more normal star formation. The tendency for the percentage of these detected in emission to be less towards the cluster centre can be explained as the combination of two possible effects: the increasing proportion of early type galaxies towards the cluster centre which are less likely to be detected in emission, and possible HI deficiency in cluster spirals close to the cluster centre which is also likely to reduce star formation.

Finally it may be noted that the enhancement of star formation in spirals towards the cluster centre is due to galaxies with compact emission. This emission is strongly correlated with a disturbed morphology of the galaxy. This is an argument against the attribution of enhanced star formation in cluster spirals to ram-pressure effects of the intracluster gas as suggested by Gavazzi & Jaffe (1985) since this would affect the outer halo of the HI gas of the galaxy, but not the morphological appearance of the stellar component.

REFERENCES

Bushouse, H.A. 1987. *Astrophys. J.*, **320**, 49.
Condon, J.J., Condon, M.A., Gisler, G. & Puschell, J.J. 1982. *Astrophys. J.*, **252**, 102.
Hummel, E. 1980. *Astr. Astrophys.*, **89**, L1.
Hummel, E. 1981. *Astr. Astrophys.*, **96**, 111.
Cavazzi, G. & Jaffe, W. 1985. *Astrophys. J.*, **294**, L89.
Kennicutt, R.C., Keel, W.C., Van der Hulst, J.M., Hummel, E. & Roettiger, K.A. 1987. *Astr. J.*, **93**, 1011.
Kennicutt, R.C. & Kent, S.M. 1983. *Astr. J.*, **88**, 1094.
Moss, C. 1987. In: *Starbursts and Galaxy Evolution, Proc. 22nd Rencontre de Moriond*, eds. Thuan, T.X., Montmerle, T. & Tran Thanh Van, J., Editions Frontières, France.
Moss, C., Whittle, M. & Irwin, M.J. 1988. *Mon. Not. R. astr. Soc.*, **232**, 381.
Moss, C. & Whittle, M. 1990. In preparation.
Urbanik, M., Grave, R. & Klein, U. 1985. *Astr. Astrophys.*, **152**, 291.

OBSERVATIONAL EFFECTS OF INTERACTION IN THE SEYFERT GALAXY NGC 7469

I. Pronik and L. Metik
Crimean Astrophysical Observatory
USSR

ABSTRACT. Some pecularities of the circummucleus of the Seyfert galaxy NGC 7469 were revealed, plausibly caused by interaction with the satellite IC 5283 and a starlike detail, situated on the edge of the west spiral branch 14" from the nucleus. Shock excited HII regions were noted in the part of NGC 7469 turned toward the satellite IC 5283. The galaxy's central radio structure ($\lambda \sim 6$ cm) stretches in the direction toward the satellite IC 5283 and the starlike detail. The spectum and color index of the starlike detail suggest that it is a cluster of early type stars ($M_V = -19^m$) and dust clouds ($A_V = 3^m$), in NGC 7469.

NGC 7469 = MGC I-58-25 = Arp 298 is the main member of the pair Holmberg 803, having as a satellite the irregular galaxy IC 5283 (see Figure 1). Its morphological type is Sa (Humason et al., 1956), z = 0,0170 (Burbidge et al., 1963), $M_V = -21^m$ (DeRoberts and Pogge, 1986). We take 1" at the distance of NGC 7469 to be 325 pc. Interstellar absorption in our Galaxy in the NGC 7469 region is not high - $A_V = 0{,}25^m$ (Weedman, 1973). NGC 7469 has two spiral structures - the inner bright and outer faint, dimensions of which are 33" or 11 kpc and 100" or 33 kpc correspondingly. Position angle of the line of nodes is equal to 121° (Burbidge et al., 1963) and 1350 (DeRobertis and Pogge, 1986).

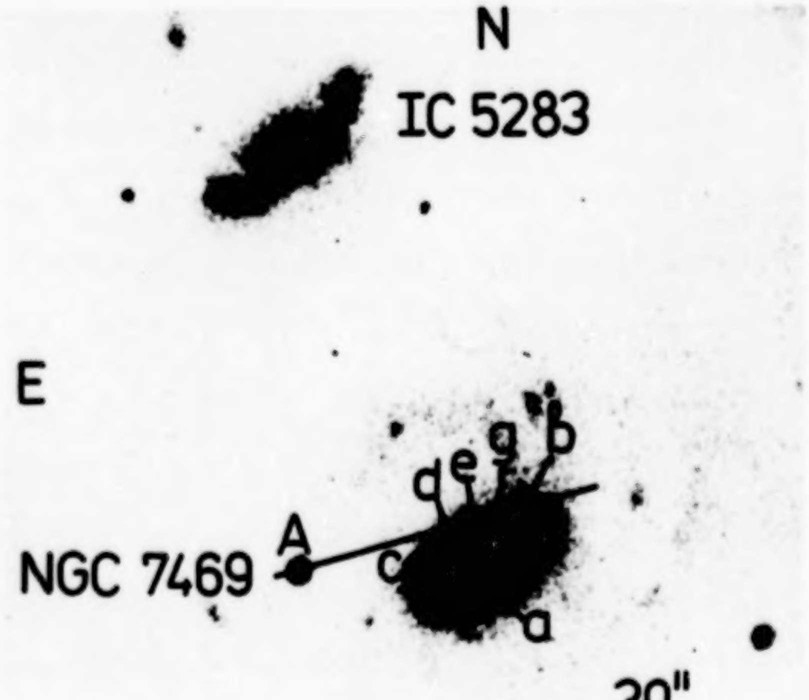

Figure 1. Holm.803 pair photo according to Burbidge et al. (1963). a - nuclear region, b, c, d, e, - details of NGC 7469. Ab - shows direction of spectrograph slit (see text).

Figure 1 shows that both galaxies of the pair are oriented in such a way, that a large part of each galaxy surface turns toward its neighbor. The projected distance between the members of the pair is 1,2 or 23,5 kpc. This distance is less than the dimension of the outer spiral structure of NGC 7469. The difference in radial velocities of the pair members is 68 km/s (de Vaucouleurs and de Vaucouleurs, 1964). So it is very possible that effects of tidal action will be noticeable. Published and our data confirm this supposition as applied to the inner spiral structure.

The inner spiral structure of NGC 7469 surrounds its central region containing a typical Sy I nucleus (Khachikian and Weedman, 1974), widths of permitted lines being 10 - 15 000 km/s (Pronik, 1975). This nucleus has large UV excess (Lyutyi, 1972), bright X-ray emission (Marshall et al., 1981; Petre et al., 1984). Figure 1 shows that inner spiral structure is more regular in the southern part of the galaxy opposite the satellite IC 5283. Its amorphous structure is turned toward the satellite. Spiral arms come to an end on starlike details "b" and "c", between which amorphous details "d" and "e" are seen. One can suppose that tidal forces do not permit the formation of regular spiral structure toward IC 5283 side. DeRobertis and Pogge (1986) supposed that detail "b" is a star of our Galaxy. While analyzing published data we have noticed that detail "b" is connected with the circumnuclear structure of NGC 7469. Figure 1 shows that the western spiral arm makes an abrupt turn to the "b" detail and a jet-like filament "g" is directed from the nucleus to this detail. One can see that NGC 7469 interacts not only with the satellite IC 5283, but also with the detail "b".

Let us consider Figure 2, which illustrates that in the 6-cm radio on 6 cm of NGC 7469 there are three directions of extension: (1) along the line of nodes, (2) toward object "b", and (3) toward IC 5283. Thus the radio sources are located along the direction of the greatest stellar space density in the galaxy and in two directions, fixed by the satellite and the starlike object "b".

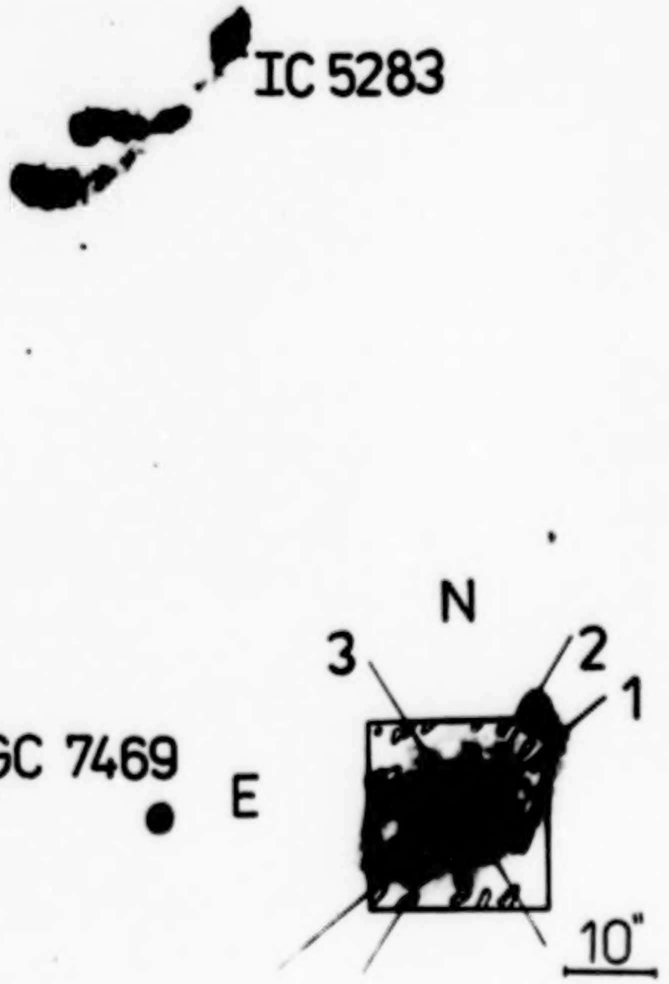

Figure 2. Radio isophotes of central region of NGC 7469 at 6 cm according to Ulvestadt et al. (1981) projected on the photo of the galaxy. 1,2,3 - directions of radio isophotes stretching.

The Seyfert nucleus of NGC 7469 is surrounded by large numbers of young stars and HII regions, as shown by spectral, photometrical, IR, and radio investigations. Humason et al. (1956) estimated the spectral type of the central region of NGC 7469 as F5, Cutri et al. (1984) observed the galaxy in CO band, 3,2 μ and calculated, that the heating of observed dust to $T = 300$ K can be made by centers of star formation. Active star formation here is confirmed by radio observations at 6 cm within a 10" region (Ulvestad et al., 1981). Wilson et al. (1986) estimated the lower limit of bolometric luminosity of central group of young stars as $10^9 - 6.10^{10}\ L_\odot$. Together with the young blue stars in the central part of NGC 7469 there are extensive gaseous nebulae with various mechanisms of excitation. According to Burbidge et al. (1963), H_α + [NII] emission is observed to 10" from the center. Now together with H_α + [NII] and λ 5007 A [0111] emission of H_α, 2,12 μ, and CO 2,6 mm is observed in the $7''.5$ diameter. HII regions are partly divided by mechanisms of excitation if they are located on the satellite side or on the opposite side. In Figure 3 one can see boundaries of HII regions according to DeRobertis and Pogge (1986) data. Gaseous fields, having high and low $I_\beta/I_{[o111]}$ relations are shown by thick and dotted lines correspondingly. The first are the regions where hot stars are responsible for hydrogen excitation. They are concentrated in the central and south part of the galaxy. The second regions can be excited by collision. They prefer the satellite side of the galaxy. It is interesting that both types of HII regions avoid the surroundings of detail "b".

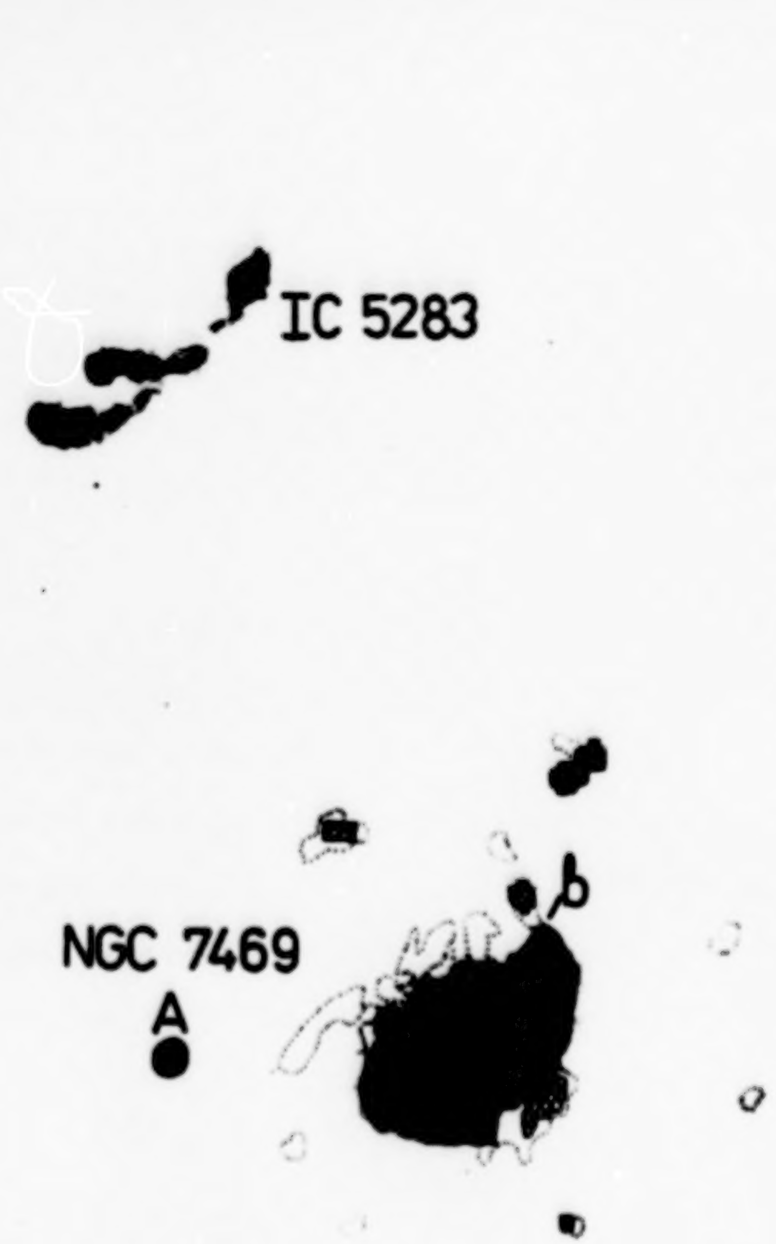

Figure 3. Boundaries of HII regions of different relations $I_\beta/I[OIII]$ according to De Robertis and Pogge (1986) projected on the photo of the galaxy: solid lines and shaded regions - $I_\beta/I_{[OIII]}$ being high, dotted lines - $I_\beta/I_{[OIII]}$ being low.

In order to investigate this phenomenon, we obtain spectra at 6-m telescope with dispersion 95 Å/mm and scale 17″.5 per mm, and direct images with the glass filters at the TV MTM-500 telescope of the Crimean Observatory. Unwidened spectra were obtained with slit width 0″.8 and 10 min exposures. Seeing was 1"5. The slit crossed details "b", "c", "d", and "e" simultaneously. Figure 4 shows two spectral regions for the details. In the spectrum of detail "b" there are no bright emission, or absorption, lines. According to the spectrum of detail "c" it is a typical HII region excited by hot stars: H_β line is brighter than [OIII], H_α is brighter than [NII]. Quite different relations of forbidden and permitted line intensities show in the spectra of details "d" and "e": here the forbidden lines are almost equal in intensity to the neighboring permitted lines. The relative intensities of these lines are shown in the Table. Errors obtained from doublet members' intensities are equal to ±8%. So the spectral data confirm the supposition that HII regions on the satellite side may be excited by collisions.

TABLE

Relative Intensities of Emission Lines in the "d" Detail Spectrum

$I_{\lambda 1}/I_{\lambda 2}$	Theory	Observations
5007/4959	2,96	2,94
4959+5007/H_β		1,45
6583/6548	3,00	2,54
6583+48/H_α		1,08

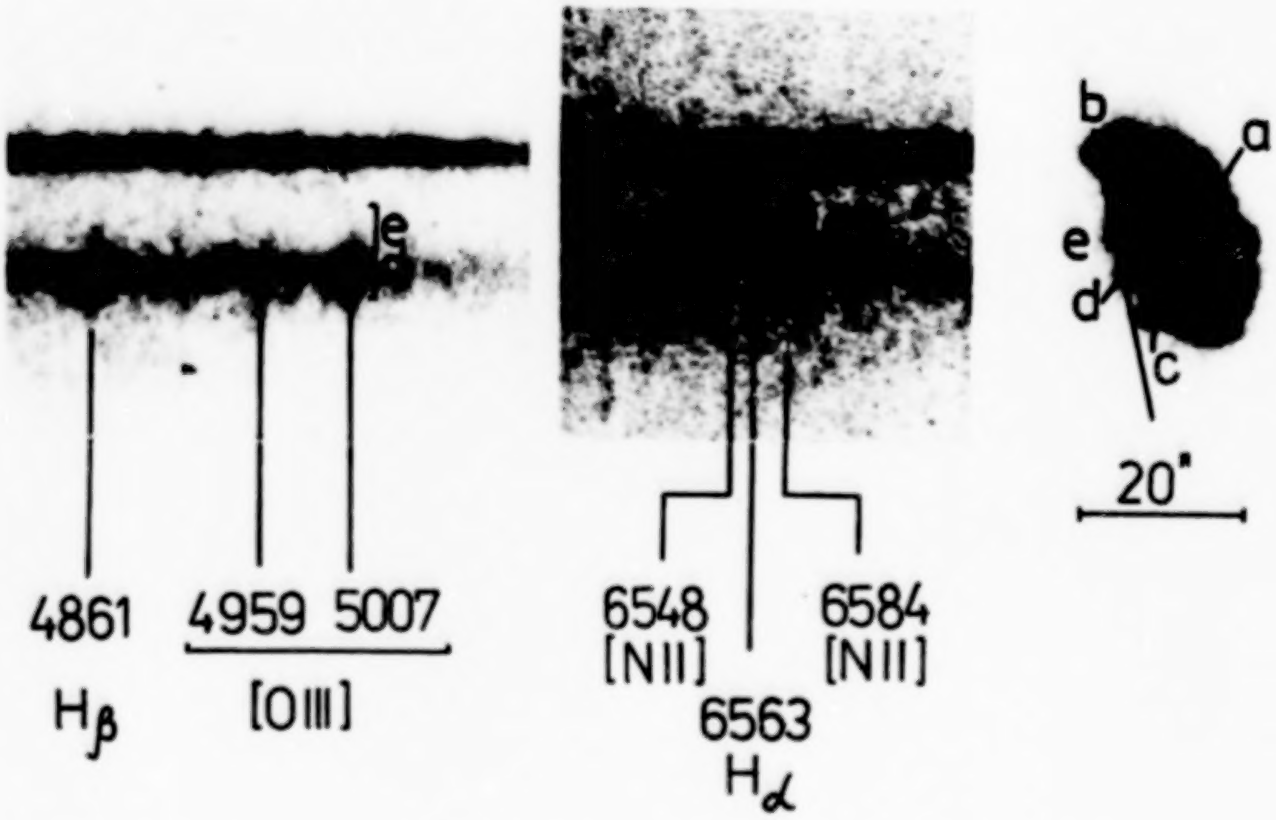

Figure 4. Right - photo of NGC 7469 with the details as on Figure 1. Left - spectrum of the regions obtained with the slit position Ab.

What is the nature of object "b" according to its spectrum? In the spectral region 4000-7000 A there are but three prominant emission lines, which in the scale of laboratory wavelengths coincide with λ 5050 A, 5100 A, and 6800 A. There exist also some weak absorption and emission details. We tried to identify these spectral details and were forced to assume that they belong to the gas systems of different radial velocities (see Figure 5). If our assumption is correct, then the galaxy NGC 7469 contains three gas systems with different radial velocities: 5075, 6300, and 10,800 km/s. It is well known that here exist two gas systems of different radial velocities in NGC 1275: 5000 and 8000 km/s (Minkowski, 1957). It is worth noting that the gas systems of NGC 7469 are markedly weaker and smaller than those of NGC 1275. It is interesting to note that the gas of the lowest velocities in both galaxies contains more or less extensive regions of shock excitation. On Figure 6 one can see relative intensities of emission lines of several know low velocity gas spectra; they correspond more to the status of gas in the Cygnus Loop (a known supernova remnant, the mechanism of excitation being of shock origin), than to regular gaseous nebulae in spiral arms of galaxies.

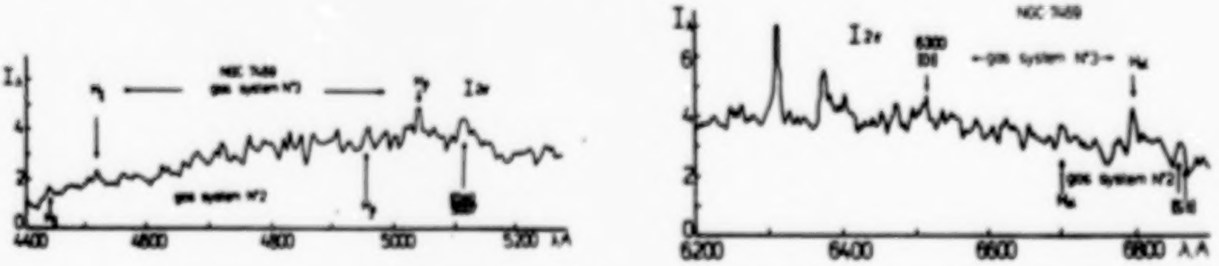

Figure 5. Spectrum tracing of object "b" in the blue (a) and red (b) with the proposed identification of emission lines (see text).

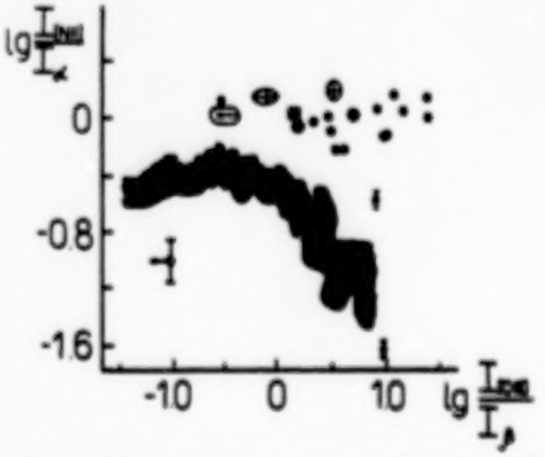

Figure 6. Relative intensities of emission lines for HII regions of spiral galaxies (shaded arc and circles), gas of low velocity in NGC 1275 (ovals) and in NGC 7469 (square) and Cygnus Loop (points) (Metik and Pronik, 1990).

Results of BVR photometry of object "b" are shown on Figure 7. Its position on two-color diagram shows that if it is a star of our Galaxy, then it belongs to K2-K5 spectral class. But the spectrum of the object does not show the typical blend in the region 5000 - 5200 A - MgI + MgH band. Therefore we assume that this object is a group of early stars and dust where the absorption is not less than $A_V = 3^m$ (see Figure 7).

If the object "b" really belongs to NGC 7469, it must be a huge compact group of stars with absolute magnitude $M_V = -19^m$. It contains a lot of early stars and dust but is almost free from gas. Such huge star cluster must be responsible for perturbation, leading to gravitational instability of the galaxy disc, thus causing a reason of matter to fall toward the center of the galaxy (Sotnikova, 1988). Gas accumulation in the center of galaxy creates there the conditions for recent star formation and generation of Seyfert nuclei.

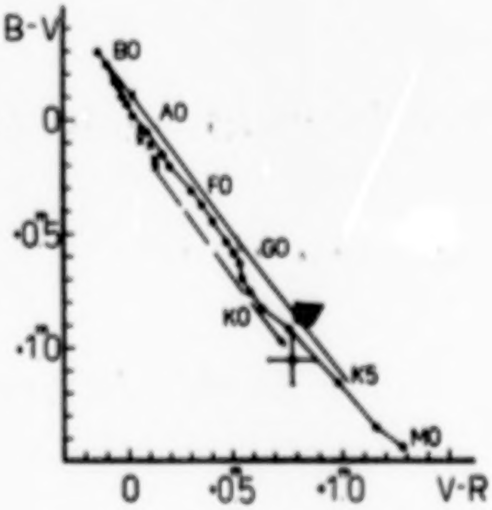

Figure 7. Two-color diagram for MS stars (Straizys, 1977), NGC 7469 object "b" (cross) and details of NGC 1433 SBab galaxy (shaded quadrangle - Buta, 1986). The arrow shows the line of reddening.

REFERENCES

Burbidge E. M., Burbidge, G. R., and Prendergast K. H. 1963, *Astrophys. J.*, 137, 1022.

Buta, R. 1986, *Astrophys. J. Suppl. Ser.*, 61, 631.

Cutri, R. M., Rudy, R. J., Rieke, G. H., Tokunaga, A. T., and Willner, S. P. 1984, *Astrophys. J.*, 280, 521.

DeRobertis, M. M., and Pogge, R. W. 1986, *Astron. J.*, 91, 1026.

deVaucouleurs, G., and deVaucouleurs, A. 1964, Reference Catalogue of Bright Galaxies, The University of Texas Press, Austin.

Humason, M. L., Mayall, N. U., and Sandage, A. R. 1956, *Astron. J.*, 61, 97.

Khachikian, E., and Weedman, D. 1974, *Astrophys. J.*, 192, 581.

Lyutyi, V. M. 1972, *Russian Astron. J.*, 49, 930.

Marshall, N., Warwick, R., and Pounds, K. 1981, *Monthly Not. Roy. Astron. Soc.*, 194, 983.

Metik, L. P., and Pronik, I. I. 1990, *Izv. Krimsk. Astrofiz. Obs.*, 82, in press.

Minkowski, R. 1957, "Radio Astronomy," Proc. IAU Sum. No. 4, ed. H. C. Van der Hulst, Cambridge, Cambridge University Press, p. 107.

Petre, R., Mushotzky, R. F., Krolik, J. H., and Holt, S. S. 1984, Astrophys. J., **280**, 499.

Pronik, I. I. 1975, "Variable Stars and Stellar Evolution," Proc. IAU Sym No. 67, 605.

Sotnikova, N. Y. 1988, Avtoreferat Kandidat. Dissertation, Leningrad.

Straizys, V. L. 1977, "Multicolor Photometry of the Stars," Mokslas, Vilnius, p. 105.

Ulvestadt, J. S., Wilson, A. S., and Sramek, R. A. 1981, Astrophys. J., **247**, 419.

Weedman, D. 1973, Astrophys. J., **183**, 29.

Wilson, A. S., Baldwin, J. A., Sun Sze-Dung, and Wright, A. E. 1986, Astrophys. J., **310**, 121.

RADIO EMISSION IN PECULIAR GALAXIES

Dulia F. de Mello Rabaça and Zulema Abraham
Instituto Astronomico e Geofisico - USP
C.P. 30627, 01051, Sao Paulo, Brazil

During the last decades a number of surveys of peculiar galaxies have been carried out and accurate positions become available. Since peculiarities are a possible evidence of radio emission (Wright, 1974; Sulentic, 1976; Stocke et al.,1978), we have selected a sample of 24 peculiar galaxies with optical jet-like features or extensions in different optical catalogues, mainly the Catalogue of Southern Peculiar Galaxies and Associations (Arp and Madore, 1987) and the ESO/Uppsala Survey of the ESO(B) Atlas (Lauberts, 1982) for observation at the radiocontinuum frequency of 22 GHz. The sample is listed in the Table.

Sol (1987) studied this sample and concluded that the majority of the jet-like features seem to admit an explanation in terms of interactive galaxies with bridges and/or tails due to tidal effects. Only in few cases the "jets" seem to be possibly linked to some nuclear activity of the host galaxy.

The observations were made with the 13.7m-radome enclosed Itapetinga Radiotelescope (HPBW of 4.3 arcmin), in Brazil. The receiver was a 1 GHz d.s.b. super-heterodine mixer operated in total-power mode, with a system temperature of aproximately 800K. The observational technique consisted in scans in right ascention, centralized in the optical position of the galaxy. The amplitude of one scan was 43 arcmin, and its duration time was 20 seconds. The integration time was at least 2 hours (12 ten-minute observations) and the sensibility limit adopted was an antenna temperature greater than 3 times the r.m.s. error of the baseline determination. Virgo A was used as the calibrator source.

Three galaxies were detected for the first time as radio sources and four other known galaxies at low frequencies had their flux densities measured at 22 GHz. The results for these sources are presented in the figures (a) to (f).

Sample of Peculiar Galaxies

SOURCE	DESIG	R.A. (1950)	DEC. (1950)	PECULIARITY	
		h m s	o ' "		
0113-52		01 13 06	-52 55 00	jet	(S)
0145-48		01 45 06	-48 39 00	tail	(S)
0147-27	414IG4	01 47 13	-27 56 54	tail	(L)
0149-48		01 49 30	-48 51 00	jet	(AM)
0207-49	197IG25	02 06 59	-49 31 18	jet	(AM)
0214-26	478G19	02 14 03	-26 10 54	streamer	(L)
0229-58	115G15 (*)	02 29 41	-58 08 18	S0 in cl	(L)
0256-36	356IG24	02 56 56	-36 48 48	jet	(L)
0339-54	156IG7	03 39 56	-54 09 57	streamer	(L)
0349-27	(*)	03 49 32	-27 53 32	jet	(C)
0404-52	156G38	04 04 52	-52 47 48	b dwarf	(S)
0422-51	202G14	04 22 30	-51 42 48	jet	(AM)
0426-55	157G32	04 26 44	-55 09 40	interact	(S)
0430+05	3C120 (*)	04 30 30	+05 15 00	jet	(AM)
0521-36	(*)	05 21 13	-36 30 16	jet	(S)
0606-29	425G9	06 06 37	-29 32 00	jet	(L)
0646-64	87IG41	06 46 37	-64 54 12	pair	(L)
2030-66		20 30 18	-66 26 00	jet	(AM)
2110-61	144G20	21 09 55	-61 29 48	jet	(AM)
2155-69	75G45	21 55 06	-69 43 30	jet	(AM)
2207-67	108IG17	22 07 00	-67 06 54	jet	(AM)
2300+16		23 00 30	+16 20 00	Mkr	(S)
2329-41		23 29 24	-41 00 00	jet	(AM)
2331-38	347G22	23 30 49	-38 52 54	jet	(AM)

Columns are: (1) galaxy name; (2) ESO/Uppsala designation, an asterisk indicates radio emission in low frequencies; (3)-(4) equatorial coordinate s; (5) peculiarities; and (6) references: (S) Sol (1987), (L) Lauberts (1982) , (AM) Arp and Madore (1987), and (C) Christiansen (1977)

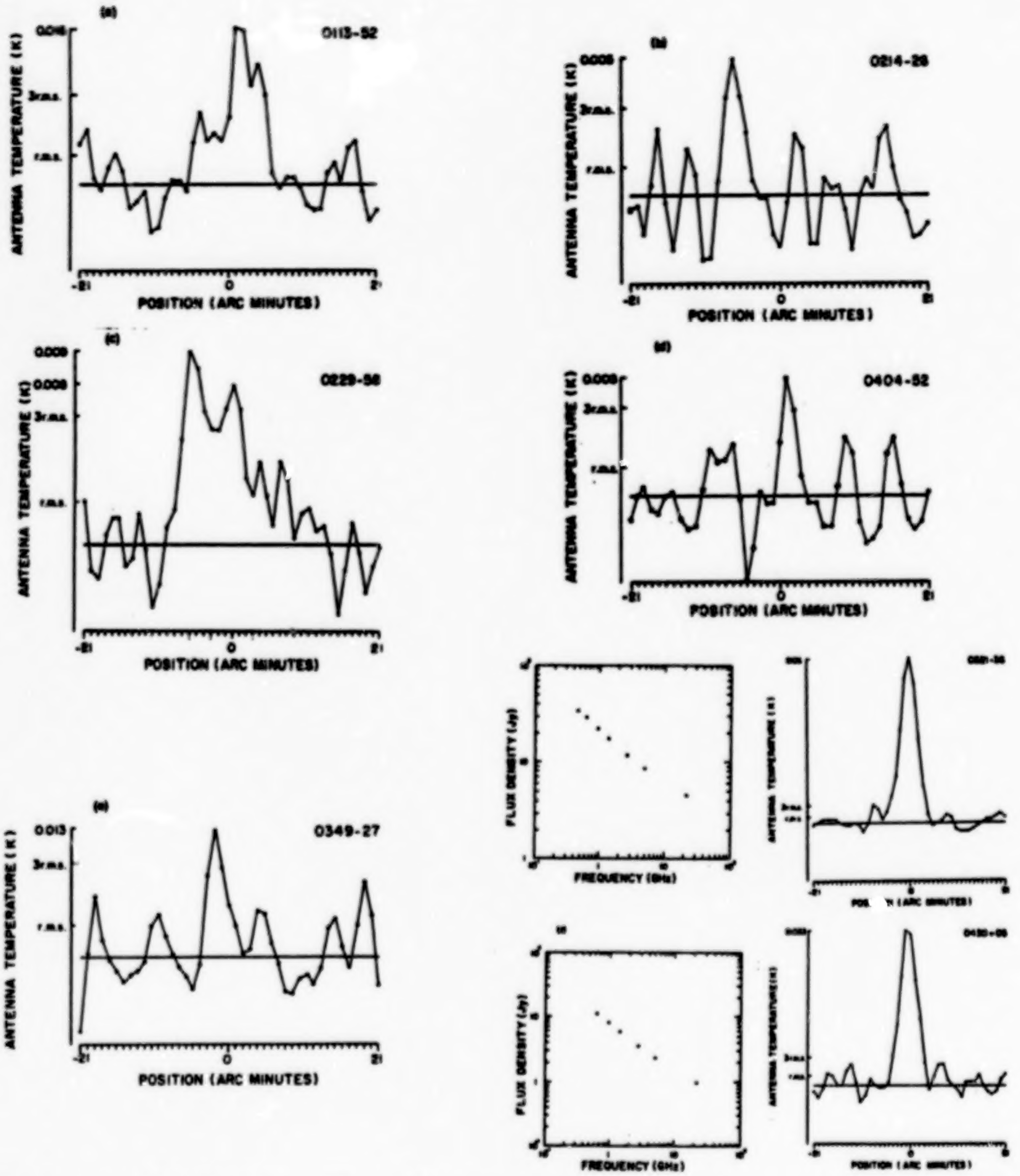

Figures are: (a) 0113-52 - The radio source position coincides with the optical galaxy. The flux density is (1.2 ± 0.2)Jy. (b) 0214-26 - The radio source is shifted 7 arcmin from the optical galaxy. Since the redshift of this object is not known, it is not possible to calculate the actual distance between the radio and optical sources. If we suppose a common redshift for galaxies like 0.02, the distance will be 200 Kpc, a typical value between the radio source and the optical counterpart. The flux density is (0.4 ± 0.1)Jy.

(c) 0229-58 - The radio source is about 6 arcmin shifted from the galaxy. Using a radial velocity of 9590 Km/s (Lauberts, 1982) for calculation, the distance between the optical position and the maximum of the radio emission is 335 Kpc. The maximum flux density is (0.7 ± 0.2)Jy. (d) 0349-27 - The radio source position coincides with the optical galaxy. The flux density is (1.0 ± 0.2)Jy. This source has fluxes measured at low radio frequencies (Wills, 1975) and a typical non-thermal steep-spectrum. (e) 0404-52 - The radio source coincides with the optical galaxy. The flux density is (0.6 ± 0.2)Jy. (f) 0430+05 and 0521-36 - Both galaxies are well known radio sources at low radio frequencies. The flux densities at 22 GHz are (2.5 ± 0.2)Jy and (4.5 ± 0.2)Jy, respectively. The spectrum is non-thermal in both cases, and their radio emission coincides with the optical position.

ACKNOWLEDGEMENTS

We would like to thank Helene Sol for the sample and suggestions and Carlos R. Rabaca for many comments. This work was partially supported by the Brazilian agencies CNPq and FAPESP.

REFERENCES

Arp, H.; Madore, B.F. (1987) *A Catalogue of southern peculiar galaxies and associations.* University of Toronto.

Christiansen, W.N.; Frater, R.H.; Watkinson, A.; O'Sullivan, J.D.; Lockhart, I.A.; Goss, W.M. (1977) M.N.R.A.S., 181, 183.

Lauberts, A. (1982) *The ESO/Uppsala Survey of the ESO(B) Atlas.*

Sol, H. (1987) *Jets et sources radio extragalactiques.* These de Doctorat D'Etat, Universite de Paris VII.

Stocke, J.T.; Tiftt, W.G.; Kaftan-Kassim, M.A. (1978) Astron. J., **83**, 322.

Sulentic, J.W. (1976) Astrophys. J. Suppl. Series, **32**, 171.

Wright, A.E. (1972) M.N.R.A.S., **167**, 251.

THE KINEMATICS AND MORPHOLOGY of NGC 520: ONE, TWO, or THREE GALAXIES?

S.A. Stanford and M. Balcells
University of Wisconsin

ABSTRACT

The peculiar galaxy NGC 520 (Arp 157) is often interpreted as an interacting pair of galaxies. The identification of the two bulges and overall morphology of the two galaxies has long been a puzzle which we attempt to solve in this paper. New longslit optical spectroscopy and near-infrared images of NGC 520 are presented. These data suggest that the northwest peak is the bulge of one of two galaxies in the system. The other larger bulge is clearly evident in the K band image in the middle of the dust lane. The stellar radial velocity profile in the central 10" of the larger bulge is consistent with counterrotation seen in the molecular gas component. This kinematic subsystem could be the remains of a merged gas-rich irregular.

I. INTRODUCTION

Understanding the peculiar system NGC 520 (Arp 157) has been the goal of several workers using observations from many wavelength regions. One of the most basic questions about the system has been if the system is one disturbed galaxy or two interacting galaxies. From single dish H I mapping, Thuan and Wadiak (1983; hereafter TW) concluded that only one galaxy is present in the system. Stockton and Bertola (1980; hereafter SB) studied the optical emission line kinematics and concluded that there was evidence for two colliding galaxies in NGC 520.

An optical image of the system may be interpreted as a collision of two disk galaxies seen crossed and nearly edge-on. For ease of discussion, these disk-like structures shall be refered to as the east-west and southeast-northwest galaxies. The deep (~4.5 hours) photograph of NGC 520 in SB shows a long tidal tail apparently pulled from the southeast-northwest galaxy. This tail stretches south from the northwestern end of NGC 520, curving to the east and then north around the main body up to a distance of ~32 kpc (H_0=75 km s^{-1} Mpc^{-1}). Here we present new optical longslit spectroscopy and infrared imaging of NGC 520. These data suggest the location of two bulges within NGC 520. The presence of a counterrotating core in the larger bulge suggested by CO observations is consistent with the observed stellar kinematics in the central 10".

II. OBSERVATIONS

Longslit optical spectra were obtained with the GoldCam spectrograph on the 2.1 m telescope at KPNO in December 1988 with spectral coverage from 3880 to 4872 Å and a dispersion of 1.24 Å $pixel^{-1}$. The slit measured 2" by 4' with a spatial resolution of 0.78" $pixel^{-1}$. Two slit positions were observed at PA=87° and at PA=125°. Each night F, G and K type standard stars were observed to be used as velocity templates in the fourier quotient and cross-correlation analyses (hereafter FQ and XC, respectively; Sargent *et al.* 1977). Reductions were performed with IRAF[1] using standard procedures. Each aperture extracted from the two slit positions was the sum of three columns, which corresponds to a width of 2.34". Near-infrared JHK broadband images were obtained using IRIM on the 1.3 m telescope at KPNO on 11 December 1988 UT. The spatial resolution was 1.35" pixel^{-1} and the seeing was estimated to be 1.5-2" at the time of the observations. Exposures of the blank sky in each band at several positions near NGC 520 before and after the object images were used for sky-subtraction at each wavelength, which accounted for the subtraction of the dark count in the process. Flatfield images were obtained by median summing all the sky images obtained in the course of one night at each wavelength at each integration time. Observations were obtained of standard stars taken from Elias *et al.* (1982) to calibrate the photometry.

III. RESULTS

Radial velocity profiles of both optical spectroscopy slit positions were first obtained with the XC routine and then velocity dispersions were obtained with the FQ routine. The XC-determined velocities were used as input to the FQ program. Because of the low signal to noise ratio at most points along the slit, pairs of apertures were added in order to obtain more accurate velocity dispersions. Thus, the points in the plotted dispersion profiles represent 4.7" apertures. The XC radial velocities for slits 1 and 2 are shown in Figure 1, along with the velocity dispersions obtained from the FQ routine. All radial velocities shown in this paper are heliocentric. The zeropoint on the abscissa corresponds to the nucleus position of the east-west galaxy (henceforth called the primary nucleus), as determined from a K band image (see below).

A contour plot of the single frame K band image is presented in Figure 2 which covers the central 78" x 84" of NGC 520. Using the APPHOT package in IRAF, magnitudes were obtained of selected areas of the JHK images using 2.7" apertures as shown in Figure 2. The K band image shows one bulge in the middle of the east-west dust lane, and another peak which coincides with the optical northwest emission peak. The colors obtained at the larger bulge indicate that although there is a significant amount of obscuration and hot dust emission, the elongated shape in the central 10" is primarily due to stellar light.

IV. DISCUSSION

As stated in the introduction, the first question to be answered is whether NGC 520 is a single disturbed galaxy, or two interacting galaxies. Perhaps the most interesting and important

---

[1] Image Reduction and Analysis Facility is distributed by the NOAO, which is operated by the Association of Universities for Research in Astronomy, Inc., under contract to the National Science Foundation.

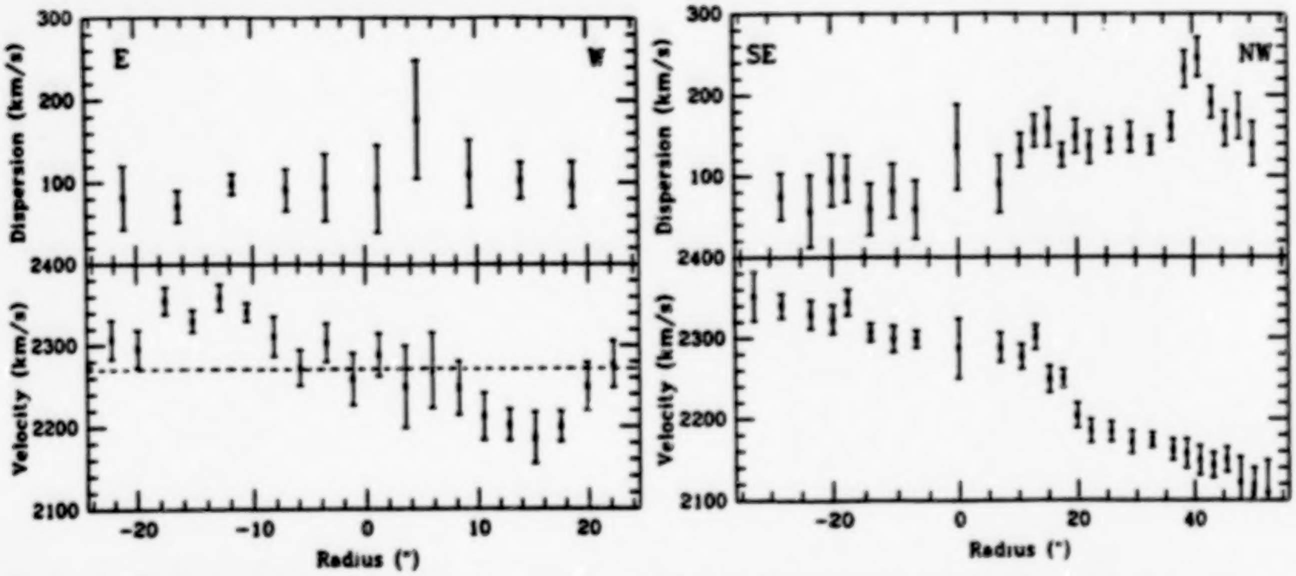

Figure 1. Radial velocity and dispersion profiles of slits 1 (left) and 2 (right). The velocities were obtained from the average of all slit 1 exposures, using the XC routine to find the radial velocties and the FQ routine to find the velocity dispersions. Except as noted in the text, each point represents a three column wide aperture ~2.3". The errorbars represent one σ errors. The zeropoint in radius is at the position of the primary nucleus. The horizontal dashed line in the slit 1 profile represents the systemic velocity of the nucleus.

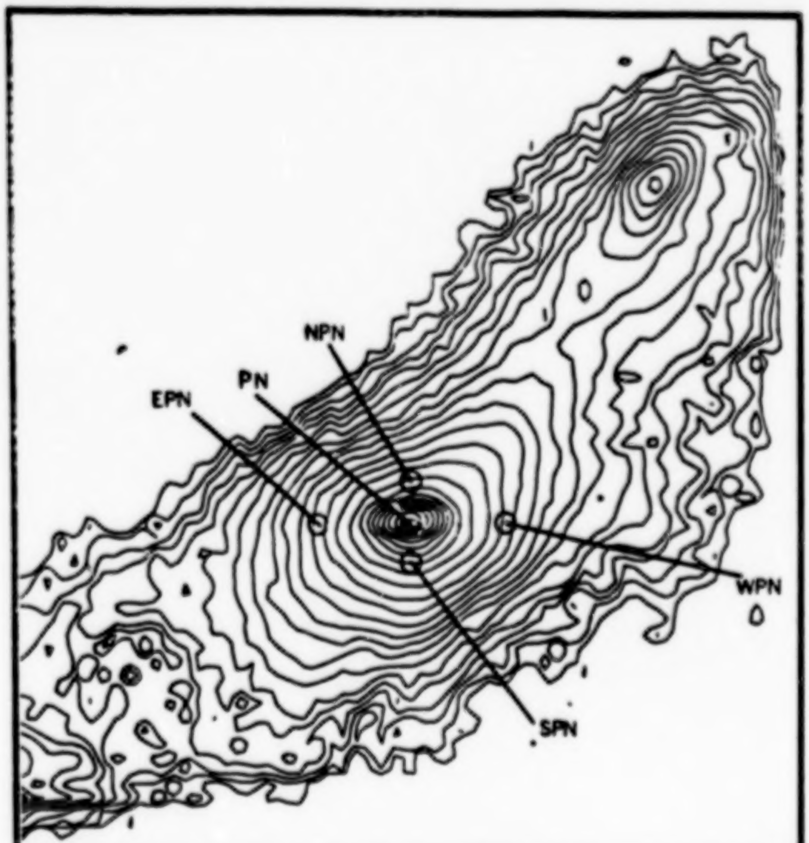

Figure 2. Contour map of the K band image. The lowest contour represents 19.0 magnitudes arcsec^{-2} and the contour interval is 0.2 magnitudes. The scale is 1.35 arcsec pixel^{-1} and the axes are in units of pixels. The positions of the small aperture photometry are shown by the circles whose diameter equals the aperture size.

result bearing on this question is seen in the velocity dispersion profile from slit 2. At the position of the northwest emission peak there is a sharp rise of 100 km s^{-1} to a peak value of 240 km s^{-1} which quickly drops back to ~140 km s^{-1} to the northwest. We believe that this dispersion peak is real because it is seen in the profiles determined separately from the night 3 and night 4 spectra. That the dispersion peak is due to the presence of a bulge is a natural explanation because galactic bulges have high dispersions. The calculated dynamical mass at the dispersion peak of ~1.5 x 10^{10} $M_{\odot}$ is reasonable for a 1.5 kpc diameter region centered at a galactic bulge. We suggest that the northwest peak is one of the bulges of the galaxies in NGC 520.

Next, we discuss the slit 1 velocity profiles obtained for the east-west galaxy. The velocity at the nucleus position r=0 is taken to be the systemic velocity. The velocity profile has an overall S shape. Over the central 30"=4.5 kpc, the radial velocity points can be fitted fairly well by a straight line, indicative of solid body rotation. In the central 15" of the slit 1 velocity profile, there is a hint of a series of velocity reversals. The error bars are too large for us to be confident in the reality of the reversals. However, they trace a pattern which is highly symmetric about the nucleus position and velocity. Moreover, this pattern is seen in the profiles obtained from the separate spectra of night 1 and night 3, lending credence to the reality of the reversals. Complicating the interpretation of the apparent bumps is that slit 1 may lie at an angle to the major axis of the east-west galaxy, and that the stellar light from the central 15" contains contributions from both bulge and disk stars.

The kinematics of the primary nucleus has also been investigated in the CO line (Sanders *et al.* 1988). The CO linecenter V_0(CO)=2261 km s^{-1} agrees with the systemic V_0(stellar)=2275 km s^{-1} found in the slit 1 velocity profile at the position of the primary nucleus. More interesting is that the CO profile over the central 6" is in counterrotation with respect to the overall decline in velocity in the east to west direction seen by SB and by us. The elongated morphology and the velocity profile of the CO emission shows that the molecular gas probably lies in a rapidly-rotating disk. The counterrotating molecular disk gives support to believing the reversals seen in our stellar radial velocity profile. Such velocity reversals have been observed in other galaxies (Kormendy 1984; Jedrzejewski and Schechter 1988; Balcells and Stanford 1989). The reversals have been described as counterrotation due to a cannibalized dwarf elliptical galaxy (Balcells and Quinn 1989) or to a young stellar disk formed out of an ingested irregular galaxy. There is one important problem with the counterrotation interpretation. SB found a monotonic decline in the optical emission line velocities over the central 6" at the primary nucleus, indicating the ionized gas does not also show counterrotation. No firm conclusion can be drawn on the possible velocity reversals until better longslit spectra can be obtained along the east-west galaxy.

At the primary bulge, Young, Kleinmann and Allen (1988) find apparently strong Hα emission veiled by dust. The Hα data argue in favor of current star formation within the central 20" of the primary bulge. The morphology of this region suggests an explanation of the star formation. At the primary nucleus, the K band image shows the same elongated structure seen in the CO source. The ratio of the axes at r=8" is about 2:1 in the K band light. We speculate that massive stars recently formed out of the CO disk, and have become red supergiants which dominate the K band light in the central 6". Hence, instead of the spherical shape seen in the K band contours at radii outside of the 12" diameter CO source, an elongated shape is seen in the central 6" because the dominant stars formed out of a nuclear disk. Furthermore, if we firmly believed that the primary contained a merged, counterrotating system, then we could further speculate that the kinematics of a counterrotating gas disk would be likely to cause a burst of star formation by producing a higher than normal cloud-cloud collision rate.

We thank the IAU for providing a travel grant to enable SAS to attend IAU Colloquium 124. SAS acknowledges support from NASA grant NAS5-25451, and MB from a subcontract to NASA contract NAS7-918.

REFERENCES

Balcells, M.C., and Quinn, P. 1989, *ApJ.*, submitted.

Balcells, M.C., and Stanford, S.A. 1989, *ApJ.*, submitted.

Elias, J.H., Frogel, J.H., Matthews, K., and Neugebauer, G. 1982, *AJ.*, **87**, 1029.

Jedrezejewski, R., and Schechter, P.L. 1988, *ApJ. Lett.*, **327**, L55.

Kennicutt, R. 1983, *ApJ.*, **272**, 45.

Kormendy, J. 1984, *ApJ.*, **287**, 577.

Sanders, D.B., Scoville, N.Z., Sargent, A.I., and Soifer, B.T. 1983, *ApJ. Lett.*, **324**, L55.

Sargent, W.L.W, Schechter, P.L., Boksenberg, A., and Shortridge, K. 1977, *ApJ.*, 212, 326.

Stanford, S.A. and Balcells, M. 1990, *ApJ.*, in press.

Stanford, S.A. 1989, *ApJ.*, submitted.

Stockton, A., and Bertola, F. 1980, *ApJ.*, **235**, 37.

Young, J.S, Kleinmann, S.G., and Allen, L.E. 1988, *ApJ. Lett.*, **334**, L63.

Thuan, T.X. and Wadiak, E.J 1983, *ApJ.*, **252**, 125.

STATISTICS OF ASSOCIATIONS AMONG IR GALAXIES

Jack F. Gallimore
and
William C. Keel
Dept. of Physics and Astronomy, University of Alabama

I. Introduction

In the course of expanding the search of Kleinmann *et al.* (1988) for distant, infrared-luminous objects, we noticed (as is often remarked) that a large number of infrared-selected galaxies have close neighbors or show merger characteristics (e.g. tidal tails, distorted disks). Because the sample size is large (567 infrared galaxies and 2182 field galaxies), this sample is ideal for statistically examining the importance of interactions among infrared galaxies. In particular, we compare the nearest-neighbor distribution and the two-point correlation function of our sample with that of a control sample of field galaxies.

II. — The Sample

a) Selection Criteria

The IR galaxies in this sample are chosen from the IRAS Point-Source Catalog (PSC) (1985) such that they are detected at 60 μm ($F(60) > 0.5$ Jy), have non-stellar colors ($F(25)/F(60) < 4$), are southern sky objects with declination $-40° < \delta \leq -30°$ (to make use of the ESO/SRC J films), and have galactic latitude $|b| > 30°$. Close-ups of these objects were made from ESO/SRC J sky survey films onto 35 mm film, with scale information preserved on each frame. If J films were unavailable (approx. 20% of the sample), R films were used in place. The resulting individual fields covered on the average $24' \times 18'$ rectangles centered on each IR galaxy. In the event that more than one galaxy was found at the IRAS location, the optically brightest galaxy was (arbitrarily) chosen to be the IR galaxy. Because our analysis resolves angular separations no finer than $1'$, spuriously identifying an IR galaxy with a field galaxy at a separation of less than $1'$ will have an insignificant or no effect on the final results. The field sample consists of all non-IR galaxies on each frame.

b) The Data

The angular dimensions of the bright core (a_1, a_2) and the visible extent (b_1, b_2, to the sky background) were measured for all sample galaxies. A weighted area, $A = (10(a_1a_2) + 3(b_1b_2))/13$, was then calculated for each galaxy, and we computed a linear least-squares fit between $\log A$ and blue magnitudes (B) obtained for 306 IR galaxies from Lauberts and Valentijn (1989). The resulting fit is good with an estimated standard deviation of 0.68 magnitude. Field galaxies fainter than 17th magnitude are undersampled, but IR galaxies appear to be undersampled fainter than 15th magnitude. This is likely a result of the optical selection procedure; therefore, we maintain that the limiting magnitude of the entire sample is 17.

III. — Analysis

The field and IR samples were divided into three magnitude-selected sub-samples: $15 \leq B < 16$, $16 \leq B < 17$, and $15 \leq B < 17$. Brighter galaxies were not considered because the maximum angular extent of the frames is smaller than the expected nearest-neighbor distance for $B < 15$. To remove the effects of the IR sample, statistics for the field sample were only calculated from those frames where the IR galaxy did not belong to the corresponding sub-sample.

We calculated the angular correlation function $w(\theta)$ for each sub-sample by comparing the counts of galaxy pairs at a given angular separation to corresponding counts of pairs of points which were uniformly distributed over an identical geometry (Peebles, 1980, Peebles and Hauser, 1974). This technique has the advantage of removing edge effects due to the limited geometry. The standard deviation for each bin is estimated by $\sigma = (1 + w(\theta))/n_p$, where n_p is the number of sample pairs with separation θ. As shown by Sharp (1979), this is actually an over-estimate of σ. The estimates for w are shown in figure 1.

The nearest neighbor distribution F_{nn} was calculated for each sub-sample using survival analysis techniques (Feigelson and Nelson, 1985). Whenever the distance from a galaxy to the field edge was smaller than the angular separation to that galaxy's nearest neighbor on a given frame, the distance to the field edge was taken as a lower limit to the true nearest-neighbor separation. With our data censored in this manner, we were able to estimate F_{nn} using the Kaplan-Meier product-limit estimate and compare F_{nn} for the field and IR samples using the logrank and Peto tests, which are relatively insensitive to the censoring distributions. To optimize the results for the field galaxies and eliminate double-counting of pairs, only the field galaxy closest to the center of a given field frame is used for these computations. The estimates for F_{nn} are shown in figure 2, and the results of the logrank and Peto tests are given in table 1.

Table 1

Results of the Peto and Logrank Tests

Group	N_{IR}	$\%_C$	N_F	$\%_C$	Peto	p	logrank	p
$15 \leq B < 16$	191	72	376	89	3.113	0.0019	3.174	0.0015
$16 \leq B < 17$	88	42	479	71	2.811	0.0049	3.110	0.0019
$15 \leq B < 17$	279	25	288	59	4.984	< 0.0001	5.473	< 0.0001

N_{IR} and N_F are the counts within each sub-sample of IR and field galaxies, respectively. $\%_C$ is the percentage of lower limits detected for for each preceding group. p is the probability that both samples have the same parent distribution according to the preceding test.

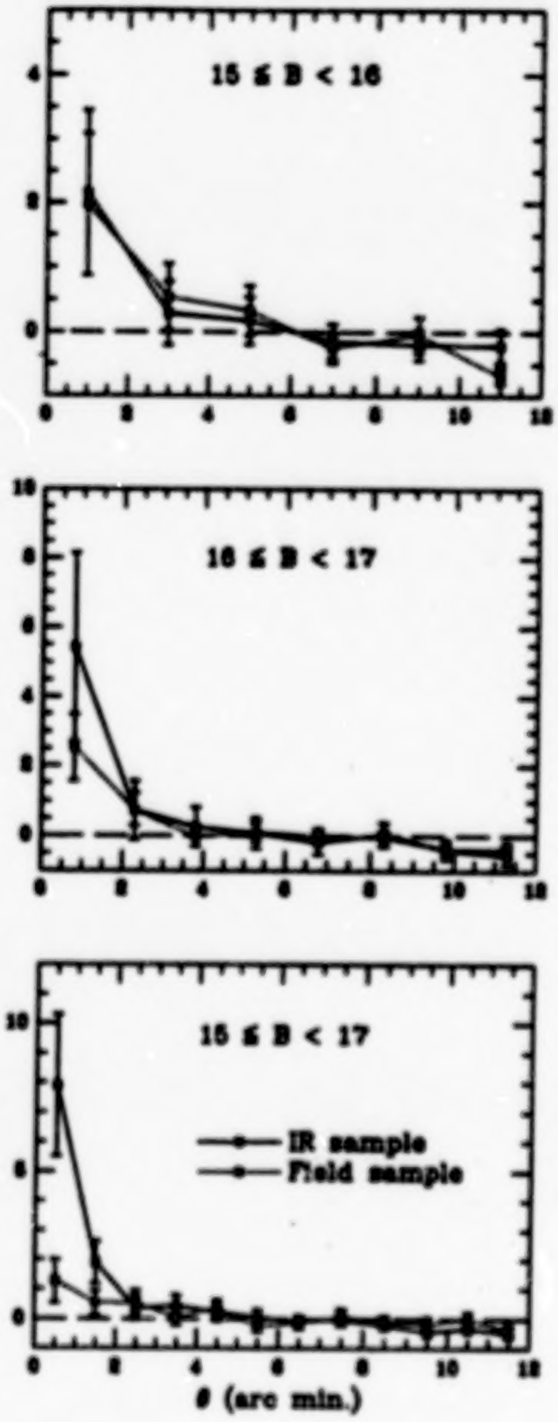

Figure 1

The estimated two-point angular correlation function for IR and field galaxies in each magnitude-selected group. Errorbars shown are 2σ.

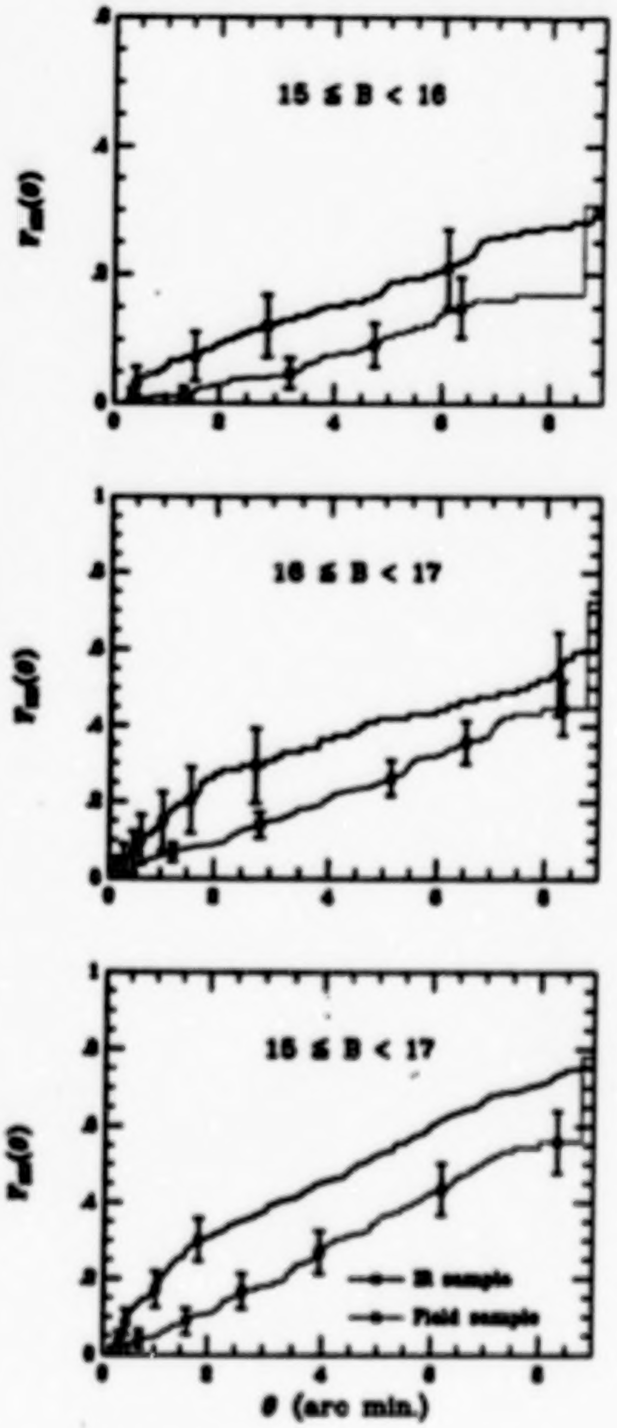

Figure 2

The estimate of the cumulative nearest neighbor distribution function for IR and field galaxies in each magnitude-selected group. 2σ errorbars are shown.

IV. — Results

IR galaxies show the greatest enhancement in correlation for the $15 \leq B < 17$ sample, where the restriction in pairing by magnitude is weaker, and the IR galaxies are better removed from the field statistics. Also, the IR galaxies in all three subsamples display an enhanced probability of pairing relative to the field sample as shown by the nearest-neighbor statistics.

A final consideration is whether the enhanced IR flux for these galaxies is actually related to physical interactions with neighboring galaxies or is simply the combined flux of several proximate galaxies of comparable brightness. In our survey, 4% of the IR galaxies with $15 \leq B < 17$ had 3 or more neighbors within 2.5 arc minutes whose brightness differed with the IR galaxy by no more than 1 magnitude, so the percentage of galaxies spuriously identified as infrared bright is probably small. Therefore, we now have quantitative evidence that confirms the conventional (qualitative) wisdom: there is a strong tendency for galaxies with enhanced infrared luminosity to be found in physical associations.

References

Feigelson, E.D., and Nelson, P.I. 1985, *Ap J.*, **293**, 192.

IRAS Point Source Catalog 1985, Joint IRAS Science Working Group (Washington, D.C.: U.S. Government Printing Office).

Kleinmann, S.G., Hamilton, D., Keel, W.C., Wynn-Williams, C.G., Eales, S.A., Becklin, E.E., and Kuntz, K.D. 1988, *Ap J.*,**328**, 161.

Lauberts, A., and Valentijn, E.A. 1989, *The Surface Photometry Catalogue of the ESO-Uppsala Galaxies* (Garching bei München: European Southern Observatory)

Peebles, P.J.E. 1980, *The Large Scale Structure of the Universe* (Princeton: Princeton University Press.

Peebles, P.J.E., and Hauser, M.G. 1974, *Ap J Suppl.*,**28**, 19.

Sharp, N.A. 1979, *Astr. Ap.*, **74**, 308.

V. OBSERVATIONS OF NUCLEAR AND NEAR–NUCLEAR ACTIVITY

GALAXY INTERACTIONS AND THE STIMULATION OF NUCLEAR ACTIVITY

Timothy M. Heckman
Department of Physics & Astronomy
The Johns Hopkins University
and
The Space Telescope Science Institute

I. INTRODUCTION AND DEFINITIONS

The idea that interactions between galaxies can lead to enhanced galactic activity has a long and noble lineage. Since the early days of Baade and Minkowski (1954), through the seminal paper of Toomre and Toomre (1977) with its "stoking the furnace" imagery, to the similarly colorful and influential "feeding the monster" paper of Gunn (1979), and the landmark work by Larson and Tinsley (1978), this idea was elaborated upon and generalized. The pace of development of this hypothesis has accelerated greatly on both the observational and theoretical fronts during the 1980's, due in part to a growing perception that the AGN phenomenon could only be understood when the role of the environment in triggering or nurturing the activity was understood (cf. Balick and Heckman 1982). In recent years, the impact of the extragalactic IRAS database (on the observational side) and of the new generation of supercomputers and innovative software (on the numerical side) have led to an almost explosive growth in the number of papers written about this subject.

In the present review, I can not hope to discuss all the interesting papers (or even all the interesting ideas) that are germane. The reader is encouraged to consult four other recent reviews whose scopes overlap significantly with that of the present paper. Stockton (1990) has reviewed the connection between galaxy interactions and nuclear activity with an emphasis on the QSO phenomenon. Fricke and Kollatschny (1989) summarized the more general topic of the role of the environment in the AGN phenomenon. Kennicutt (this volume) reviews the effects of galaxy interactions on the stimulation of global star-formation in galaxies and Schlosman (also this volume) discusses current theoretical ideas about how galaxy interaction might lead to the fueling of nuclear activity.

I would now like to loosely define some of the terms that I will be using throughout this review:

Nuclear - I will consider the "nucleus" to be the central kpc of a galaxy. This is largely a matter of observational convenience, in that most of the data available on nuclear activity in galaxies has been obtained with an effective aperture size of a kpc or so. Moreover, such phenomena as nuclear starbursts, the Narrow-Line- Region in classical AGN's, radio sources in Seyfert galaxies, and the thermal far-IR sources in many active galaxies have characteristic sizes of about a kpc (cf. Wilson and Heckman 1985; Telesco 1988).

Activity - By "activity" I mean luminosities that are significantly larger and/or high energy phenomena that are significantly stronger than could be sustained over a Hubble time by a normal population of stars. This definition explicitly includes "classical" AGN's (Seyfert galaxies, radio galaxies, QSO's) whose properties probably require the presence of a supermassive black hole (e.g. Rees 1984), optically-selected starburst nuclei (e.g. Balzano

1893), and the IR-bright galaxies whose ultimate energy source is still controversial (e.g. Sanders *et al.* 1988a; Rieke 1988).

Interaction - I will include the full range of phenomena from mild "grazing" encounters to highly dissipative collisions (mergers). The nature (and limitations) of the evidence from which it is inferred that a given galaxy is "interacting" will be discussed in some detail in §III below.

II. MOTIVATION

In this section I would like to briefly discuss whether, quite apart from the observational evidence, there is a strong theoretical or heuristic motivation for investigating galaxy interactions as stimulators of nuclear activity in galaxies. As noted previously, detailed theoretical arguments concerning the mechanisms by which nuclear activity might be "fueled" are given elsewhere in this volume by Isaac Schlosman.

A. Nuclear Starburst/IR Galaxies

Nuclear starburst galaxies (a class in which I include the majority of IR-bright galaxies) require the presence of substantial interstellar matter within their central kpc. The relatively low efficiency of stellar thermonuclear processes ($10^{-3}c^2$), coupled with the severe energetic demands (ranging from 10^{59} ergs for an M82-class starburst up to 10^{61} ergs for "ultraluminous" starbursts) mean that interstellar masses of at least 10^8 to 10^{10} $M_\odot$ are needed to fuel a nuclear starburst, even assuming 100% efficiency for the conversion of gas into high mass stars. In a growing number of cases, mm-wave interferometric maps of the molecular gas provide direct observational evidence for such material (cf. Sanders *et al.* 1988b and references therein).

As Larson (1987) and others have argued, the surface mass density of the cold interstellar matter in starburst nuclei is so high (typically 1000 $M_\odot$ pc^{-2}), that the growth time for gravitational instabilities is extremely short (a million years). Moreover, the timescales for gas depletion via star-formation and/or supernova-driven outflows are also short compared to typical galaxian dynamical timescales (10^7 to 10^8 years vs. 10^8 to 10^9 years respectively). Larson therefore argues that since the gas that fuels the starburst must be assembled faster than it is consumed, and since the gas has a mass comparable to the entire mass of the ISM in a normal galaxy, powerful nuclear starbursts can only occur when some process allows a substantial fraction of the ISM of a galaxy to flow inward by an order-of-magnitude in radius at velocities $\gg$ than the typical non-circular velocities in ordinary disk galaxies ($v_{infall} \gg 10$ km/sec). By way of illustration, Larson emphasizes that the collapse of a self-gravitating system implies a maximum infall rate 25 $(v_{infall}/50 \text{ km/sec})^3$ $M_\odot$/year. This can be compared to typical estimated star-formation rates of 10 to 100 $M_\odot$/year in starburst nuclei. To summarize, the fueling of a starburst nucleus requires a mechanism that can induce non- circular motions that are both large in amplitude and involve a substantial fraction of the ISM of the galaxy.

Thus, galaxy interactions are a very attractive mechanism for triggering nuclear starbursts for two primary reasons: 1) nuclear starbursts involve interstellar masses $\approx$ the mass of the galaxian ISM (meaning that they probably require transporting material in from large radii where tidal forces should be most important), and 2) nuclear starbursts require that the material be moved inward by a modest radial factor ("only" an order-of-magnitude!), an effect that has been observed in several recent N-body simulations by

Noguchi (1988) and Hernquist (1989) of interactions between galaxies with dissipative particles (an "ISM").

B. Classical AGN's

The motivation for investigating galaxy interactions as stimulators of low-luminosity AGN's is less clear than in the case of the starburst nuclei (at least within the standard "supermassive-black-hole-plus-accretion" paradigm for AGN's):

First, the high efficiency of accretion into a relativistic potential (20% c^2) implies that only modest accretion rates are needed to power even a bright Seyfert nucleus (e.g. 0.01 $M_\odot$/year for the nucleus of NGC 1068, or a total accreted mass of 10^6 $M_\odot$ for a nominal AGN lifetime of 10^8 years). Moreover, there is as yet little direct observational evidence that low-luminosity AGN's are characteristically accompanied by large nuclear masses of interstellar gas. For example, the mass of H II in the kpc-scale Narrow-Line-Region is only 10^3 to 10^6 $M_\odot$ in typical Seyferts. Of course, the total interstellar mass in this region may be much larger than this. Meixner *et al.* (1990) have recently observed three Seyfert galaxies with strong mm-wave CO emission and find bright nuclear CO sources in two of them. In these two cases (NGC 3227 and NGC 7469 - both interacting galaxies), the implied molecular masses within the central few hundred pc are $\approx 10^8$ $M_\odot$. It is clearly important to determine whether such structures are commonly present in typical Seyfert nuclei.

Second, the region of energy extraction in the standard model of an AGN is many orders-of-magnitude smaller than the characteristic dimensions of the region susceptible to tidal forces during a galaxy encounter. That is, to explain the transport of material inward to the accretion disk, one must appeal to processes in addition to those directly resulting from a galaxy interaction.

Thus, galaxy interactions may be neither necessary nor sufficient for triggering low-luminosity AGN's because: 1) the fueling of low-luminosity AGN's probably involves masses $\ll$ the mass of the galaxian ISM (meaning that they would not require transporting material in from the large radii where tidal forces should be most important), and 2) AGN's require that the material be moved inward to radii that are many orders-of-magnitude smaller than the region that is directly effected by tidal forces during a galaxy interaction.

The situation may be quite different for the very powerful AGN's (particularly the most powerful QSO's and radio galaxies that exist almost exclusively at large redshifts). Again, within the standard AGN paradigm (Eddington-limited accretion), the most powerful QSO's require black hole masses of $10^9 - 10^{10}$ $M_\odot$ (the mass of powerful starburst nuclei and a substantial fraction of the mass of the ISM). The formation of such a black hole surely involves spectacular dynamical processes, but the need to invoke (proto?)galaxy interactions is not clear.

III. TYPES OF EVIDENCE AND SOME CAVEATS

A. Galaxy Morphology

One of most frequently employed criteria for classifying a galaxy as "interacting" is morphological peculiarity. The greatest advantage of this criterion (apart from the relative ease of obtaining optical images) is that morphological peculiarities can provide evidence that a severe interaction has occurred within the last Gigayear even when there is no presently obvious candidate for the perturbing galaxy (i.e. after the perturber has merged with the galaxy in question or moved several hundred kpc away from it). However, using morphological peculiarities to link galaxy interactions to the fueling of nuclear activity does have some potential pitfalls, as I now describe in the form of four propositions.

1. The most convincing evidence that morphological peculiarities in active galaxies have arisen via tidal forces is to show that the peculiarities are present in the old (¿ Gigayear) stellar population (i.e. detect what we might call "Crimson Tides" in honor of our Alabama hosts). The least convincing evidence is when such structures are present only in the gas.

My point here is that when one is dealing with a galaxy having a highly active nucleus, the possibility of morphological peculiarities that have arisen through hydrodyamical processes driven by the nuclear activity must be considered. That is, the nuclear activity may be able to could propel gas outward and possibly even induce star-formation in this compressed, accelerated material (cf. Williams and Christiensen 1985).

One place where such processes are probably operating is in the high-redshift radio galaxies. Their distorted "multi-modal" optical morphology and high-velocity non-circular gas motions were initially cited as strong evidence that they were collisions or mergers of gas-rich galaxies (e.g. Djorgovski 1987). However, these peculiar structures were subsequently shown to be preferentially aligned with the radio source axis (McCarthy *et al.* 1987; Chambers, Miley, and van Breugel 1987), and they are therefore more likely to be the result of the interaction between the radio plasma and the inter-stellar/circum-galactic medium ("jet-induced starbursts", cf. Chambers 1989; Begelman and Cioffi 1989).

Closer to home, there is a mounting body of evidence that the kinetic energy supplied by massive stars and supernovae in the nuclei of starburst galaxies can drive galaxy-scale outflows (see Heckman, Armus, and Miley 1990 and references therein). In extreme cases (the "ultraluminous" IR galaxies) these "superwinds" can produce galaxy-scale regions in which the local gas pressures ($P/k > 10^6$ K cm^{-3}) are orders-of-magnitude larger than normal interstellar pressures. The superwinds are clearly shaping the morphology and kinematics of the ionized gas, and might conceivably be responsible (via induced star-formation) for at least some of the structural peculiarities commonly visible in optical continuum images of IR-luminous galaxies.

2. It is important to have a good control sample to determine what fraction of non-active galaxies would be classified as morphologicallly peculiar. At the very least, the criteria used to classify a galaxy as "peculiar" need to be as quantitative and reproducable as possible.

This is a tired and trite truism that is not always adhered to in investigations of the link between morphological peculiarities and nuclear activity (including some of the author's own efforts in this regard!). Part of the problem is that it is not always clear that an appropriate comparison sample can be defined (e.g. what is the proper comparison sample for high-redshift QSO's?).

3. Not all peculiar structures have morphologies that can be readily explained as tidal features.

While numerical simulations of galaxy interactions have been remarkably successful in reproducing the kinds of peculiar structures that populate the Arp Atlas, there are some counter-examples that are very difficult to ascribe to tidal forces (see the recent review by

Keel 1987). The most spectacular and well- known example is probably NGC 1097 with its multiple radial "jets", some of which show remarkable right angle bends.

4. Some apparent morphological peculiarities are simply the result of the overlap of the images of two or more structurally normal galaxies.

Some very nice illustrations of this can be found in a recent paper by Lauer (1989). His "deconvolutions" of images of multiple-nucleus galaxies at the centers of galaxy clusters showed that in only about half of the cases were the individual galaxian sub- components actually distorted.

B. Proximity

This type of evidence for an interaction ("guilt by association") is typically provided by counting the number of galaxies within several galaxy diameters of the active galaxy (with the neighboring galaxies often weighted by their size and/or proximity to the active galaxy). This scheme is designed to quantify the likely importance of tidal stresses suffered by a galaxy within the last Gigayear (i.e. within the last few galaxy dynamical timescales). Some rather obvious caveats:

1. It is important that the explicit and implicit selection criteria used in generating the sample of active galaxies be fully understood and that this understanding then be used to create a suitable comparison sample of non-active galaxies.
2. The galactic background should be well-determined so that the counts of neighbors can be statistically corrected for contamination by foreground/background galaxies, or the background should clearly be shown to be negligible. This is particularly important when the active galaxies under investigation are at high redshifts and when the lower end of the companion galaxy luminosity function is being probed (cf. Smith and Heckman 1990a).

C. Kinematic Evidence

Kinematic evidence for an interaction or past merger includes the detection of non-circular motions at v≫10 km/sec and the discovery of kinematically-distinct subsystems in a galaxy. Again, some of the potential pitfalls in linking kinematic peculiarities to galaxy interactions are:

1. Peculiar kinematic structures in the gas may arise through gravitational forces or through hydrodynamical ones associated with the nuclear activity. This is essentially the same argument as given above for morphological peculiarities. Stellar-dynamical investigations of active galaxies are less ambiguous in this regard, but far more difficult observationally.
2. Investigations of the kinematics of gas based on emission- lines are subject to ambiguity in the sign of any radial motions that are detected. While infalling gas could be linked to the cause of nuclear activity, outflowing gas is more plausibly ascribed to the effect. Absorption-line studies of gas seen in front of active nuclei are clearly superior in this regard, even though they probe only a single line-of-sight.
3. Kinematic sub-structures in galaxies may be very long-lived, and so provide no evidence that an interaction or merger has occurred recently enough to plausibly link it to the triggering of nuclear activity. For example, the counter-rotating stellar cores found in some nearby elliptical galaxies could have formed a Hubble time ago (cf. Franx and Illingworth 1989). Similarly, if elliptical galaxies are triaxial, it is possible for a stable (long-lived) gaseous disk to exist that is strongly warped and/or misaligned with the principal

photometric axes of the galaxy (see van Albada, Schwarzschild, and Kotanyi 1982).

IV. EVIDENCE LINKING INTERACTIONS TO NUCLEAR ACTIVITY

A. Infrared/Starburst Galaxies

My emphasis here will primarily be on galaxies with high rates of star formation in their nuclei and/or galaxies whose IR luminosities are large compared to typical galaxies ($L_{IR} > 10^{44}$ erg/sec). The detailed consideration of whether relatively mild enhancements in the global rate of star-formation are induced by galaxy interactions can be found in the review by Rob Kennicutt elsewhere in this volume. It is beyond the scope of this paper to review the evidence that the majority of IR-luminous galaxies are indeed powered by star-formation occurring within their central- most kpc (see recent reviews by Soifer, Houck, and Neugebauer 1987 and Telesco 1988).

Investigations of the link between high rates of nuclear star formation and galaxy interactions can be divided into two principal categories: 1) determination of the nuclear star-formation rates in samples of known interacting galaxies (e.g. pairs of galaxies or galaxies in the Arp Atlas) and 2) determination of the optical morphology and/or local environment of galaxies selected to have abnormally high star-formation rates (e.g. strong IRAS sources). The former studies usually provide the best statistics about low- level activity, while the latter type provide information about the relatively rare, powerful nuclear starbursts.

i) Star-Formation Rates in "Known" Interacting Galaxies

The star-formation rates in pairs of galaxies have been compared to those in isolated galaxies using Hα luminosities and equivalent-widths, mid- and far-IR luminosities, and nonthermal radio powers (Bushouse 1986,1987; Bushouse, Lamb, and Werner 1987; Cutri and McAlary 1985; Hummel 1981; Keel *et al.* 1985; Kennicutt *et al.* 1987; Sulentic 1976,1990; Stocke 1978). Taken together, these many studies lead to the following conclusions (see Kennicutt's review for more details): 1. The enhancement in the global star-formation rate in the pairs is modest (increased by an average of 50-100% relative to the isolated galaxies), but statistically significant. 2. The enhancement in the nuclear star-formation rate is stronger (by an average factor of at least three compared to isolated galaxies). 3. There is no strong dependence of the amount of enhanced star- formation on the pair separation.

Samples of "strongly interacting" galaxies (usually selected from the Arp Atlas on the basis of morpholgical evidence that they are undergoing an interaction) have been investigated in the IR, optical, and radio by Bushouse (1986,1987), Bushouse, Lamb, and Werner (1988), Carter *et al.* (1988), Heckman (1983), Hickson *et al.* (1989), Joseph and Wright (1985), Joseph *et al.* (1984), Keel *et al.* (1985), Kennicutt *et al.* (1987), Larson and Tinsley (1978), Lonsdale, Persson, and Mathews (1984), and Sulentic (1976). These represent a more heterogeneous set of galaxies than those in the "pairs" sample (and present a greater challenge in properly constructing a comparison sample). However, they are important to investigate because they are undergoing stronger and more damaging tidal encounters than the typical galaxy in the "pairs" samples. The principal results of the papers cited above can be summarized as follows: 1. The data imply that the global star-formation rates in these galaxies are enhanced relative to "normal" disk galaxies by average factors of at least two. 2. The enhancement in star-formation is most pronounced in the nuclei of the galaxies (at least as evidenced by the distribution and brightness of the Hα line emission). 3. The "Toomre-type" candidates for on-going mergers of two major disk galaxies (e.g. Toomre 1977) are exeptionally luminous in the IR and radio. I will shortly discuss this result and its implications. 4. Elliptical galaxies with shells are unusually likely to have strong Balmer absorption-lines compared to normal ellipticals (Carter *et al.* 1988). The Balmer lines are considerably stronger than those in spirals with the same broad-band colors, so these galaxies can not be simply interpreted as merged spirals with normal stellar populations. Rather, they represent evidence for fossil starbursts (10^8 to 10^9 years ago), possibly triggered by the capture event that produced the shells. Schweizer and Seitzer (1990) have reached similar conclusions for ellipticals with very subtle fine-scale substructure.

While the case for the stimulation of star-formation by galaxy interactions seems clearly established, there are several points I would like to emphasize concerning the reliability or meaning of the "enhancement factors" summarized above.

First, the projected aperture sizes (in square parsecs) used to measure the Hα and the near/mid-IR properties for the paired or interacting galaxies are typically larger (sometimes by substantial factors) than for the "control" galaxies. This is usually because the latter data were gathered from the literature and had been obtained for the nearest, brightest "normal" galaxies (i.e. galaxies significantly nearer than typical Arp Atlas galaxies). In many cases, honest efforts to estimate, correct for, or otherwise mitigate against the potential biases introduced by these aperture mismatches have been made. For example, the Hα equivalent width (which is far less aperture dependent than the Hα luminosity) is frequently employed in the comparisons of the galaxy samples. Nevertheless, the aperture effect sometimes makes it difficult to compare the interacting and "normal" galaxies in a detailed and rigorously quantitative sense.

Second, in most cases, the star-formation rates in the interacting (or paired) samples and "control" samples are compared after being normalized to the blue luminosity of the galaxy. This is designed to cancel out (statistically) any effect as trivial as big and optically-bright galaxies being bright at other wavelengths as well. However, the origin of the blue light in an interacting galaxy is a little unclear - such galaxies could have their blue luminosities boosted by enhanced star-formation or depressed by increased internal extinction. A better normalization would be to the mass of the galaxy (difficult to obtain) or possibly to the luminosity at J or H where the effects of dust and young stars should be greatly diminished. A related difficulty (particularly for the often badly-distorted galaxies in the Arp Atlas) is in selecting the proper mix of Hubble types in the comparison sample. This problem is acute because of the well-known correlation between Hubble type and star-formation. One really wants to know the Hubble type of the interacting/peculiar galaxy before it interacted!

Third, it is important to note that there is certainly no one-to-one match between interactions and enhanced star-formation. There is a substantial overlap in the estimated star-formation rates between the samples of interacting and normal galaxies. Indeed, Bushouse (1986) emphasized that the nuclei of about 30% of his strongly interacting galaxies showed no optical evidence for recent star-formation (see also Joseph *et al.* 1984).

Finally, the translation of IR luminosities, nonthermal radio powers, recombination-line luminosities, etc. into estimates of the star-formation rate are fraught with many uncertainties (e.g. the importance of dust, the nature of the IMF and the time-history of the star-formation, the potential roles of the old stars or an AGN, the uncertain physics of the origin of the radio synchrotron emission, etc.). These problems are particularly vexing in the nuclei of galaxies. Multi-wavelength investigations are essential to attack these problems.

Before concluding this subsection, I want to just briefly explore some of the implications of the strongly enhanced radio and IR luminosities of the galaxies that Toomre (1977) selected as the best local examples of two major disk galaxies in the process of merging to form an elliptical galaxy. The radio properties of this kind of galaxy were explored by Heckman (1983) and the mid-IR properties by Joseph and Wright (1985). I have listed in Table 1 the optical and far-IR properties of the 10 Toomre disk-disk merger candidates with redshifts known to me. As a class, these galaxies are characterized by large far-IR

TABLE 1

IR and Optical Properties of Toomre's Disk-Disk Merger Candidates

(1) Galaxy	(2) *cz*	(3) log L_{FIR}	(4) L_{FIR}/L_B	(5) F_{100}/F_{60}
NGC 4038/9	1650	10.5	1.8	1.2
NGC 4676	6600	10.5	1.7	1.1
NGC 7592	7300	11.1	3-5	0.8
NGC 6621/2	6250	10.9	2.0	1.1
NGC 3509	7650	10.4	0.6	1.8
NGC 520	2150	10.6	1.7	0.9
NGC 2623	5450	11.3	11	0.7
NGC 3256	2900	11.3	4.6	0.8
NGC 3921	6000	10.0	0.2	1.2
NGC 7252	4750	10.5	0.6	1.0

NOTES

Col. 3 - The log of the far-IR (40 to 120μ) luminosity (in $L_\odot$) calculated from the "FIR" flux given in ***Cataloged Galaxies and Quasars Observed with IRAS*** assuming $H_0 = 75$ km sec^{-1} Mpc^{-1}.

Col. 4 - L_B is calculated using $M_{B,\odot} = 5.48$ and apparent B magnitudes (B_T scale) for the galaxies taken from the Revised Shapley Ames Catalog, the Uppsala General Catalog of Galaxies, and the Second Reference Catalog of Bright Galaxies. They have been corrected for foreground Galactic extinction, but not for extinction internal to the galaxies. These references give no B magnitude for NGC7592, so I used a rough estimate based on L_B for the other galaxies.

Col. 5 - The ratio of the IRAS fluxes (P) at 100μ and 60μ. Note that Bothun, Lonsdale, and Rice (1989) argue that the far-IR luminosity can be used to estimate the star-formation rate for $F_{100}/F_{60} < 1.5$ in my units.

luminosities (average $L_{FIR} = 8 \times 10^{10}\ L_{\odot}$), large ratios of IR to optical luminosity (average $L_{FIR}/L_B \approx 3$), and "warm" far-IR colors (average ratio of S at 60 μ and 100 $\mu \approx 1.0$). This suite of characteristics suggests that they are forming massive stars at rates well in excess of those in typical bright spiral galaxies (cf. Bothun, Lonsdale, and Rice 1989). Toomre has argued that his set of galaxies represent various evolutionary stages in the merging process, from the NGC 4038/39 system (two well-separated galaxies) to NGC 7252 (a candidate "proto-elliptical" with a single main body plus two well-defined tidal tails). The enhanced IR emission is seen throughout the sample, with no obvious trend along Toomre's suggested evolutionary sequence. This suggests that the duration of the enhanced star-formation induced by the merger process is at least as long as the timescale for a merger (> a few $\times 10^8$ years).

The average far-IR luminosity of the disk-disk merger candidates implies a star-formation rate of 50 $M_{\odot}$ per year, assuming a Salpeter IMF and a constant star-formation rate (cf. Hunter *et al.* 1986). If this lasts for 300 Megayears, the implied total mass of stars formed as a result of the merger is $1.5 \times 10^{10}\ M_{\odot}$. In most well-studied IR-luminous galaxies, much/most of the star-formation is occurring within a radius of a kpc of the nucleus in a massive disk of molecular gas (cf. Sanders *et al.* 1988b and references therein). If this is the case in the merger candidates, and if Toomre's hypothesis concerning the formation of elliptical galaxies is correct, then the aftermath of the merger will be a galaxy whose global structure and dynamics is that of a bright elliptical, but whose core contains a rapidly rotating "post-starburst" disk with a mass of $10^{10}\ M_{\odot}$ and a size of about a kpc. Even after several Gigayears, when this disk might no longer be photometrically obvious, it could be recognized through its kinematic signature. If a substantial fraction of elliptical galaxies formed this way, might not such dynamically-distinct cores be common? The recent discovery of kinematically-distinct cores in bright elliptical galaxies is extremely interesting in this regard (Franx and Illingworth 1988; Jedrzejewski and Schecter 1988). The large fraction of "shelled" ellipticals with post-starburst nuclear spectra may also be relevant (Carter *et al.* 1988).

ii) The Morphology and Environment of IR and Starburst Galaxies

The bulk of the data concerning either the optical morphology or the local environment of galaxies with known/suspected nuclear starbursts concerns galaxies selected on the basis of strong far- IR emission (cf. Armus, Heckman, and Miley 1987,1990; Fairclough 1986; Lawrence *et al.* 1989; Sanders *et al.* 1988a). Such samples are easily generated, but suffer from some ambiguity of interpretation (as noted above, there is still some controversy about what fraction of far-IR-luminous galaxies are indeed powered by nuclear starbursts vs. a "buried QSO" or even vs. an unusually heavily obscured "normal" stellar population). The imaging surveys listed above document a trend towards an increased fraction of morphologically peculiar galaxies in systems of higher IR luminosity:

> About 10% of the galaxies with IR luminosities ranging from 10^{10} to $10^{11}\ L_{\odot}$ are morphologically peculiar. This is not significantly different from the fraction of morphologically peculiar galaxies in randomly-selected samples of field galaxies (cf. Lawrence *et al.* 1989; Armus, Heckman, and Miley 1987). It is important to realize that this luminosity range brackets the "knee" in the IR luminosity function of galaxies: thus, the galaxies that dominate IR-flux- limited samples do not have a strongly abnormal incidence rate of peculiar

optical morphologies.

> About 50% of the galaxies with IR luminosities in the range 10^{11} to 10^{12} $L_\odot$ are classified as morphologically peculiar, and the fraction reaches essentially 100% for the rare "ultraluminous" galaxies with $L_{IR} > 10^{12}$ $L_\odot$.

> It is a peculiar morphology (presumably indicative of severe tidal damage - but see §IIIA above) rather than the mere presence of companion galaxies that seems to be the key characteristic that sets apart the powerful IR galaxies ($L_{IR} > 10^{11}$ $L_\odot$) from more normal galaxies. About half of the powerful IR galaxies studied by Armus, Heckman, and Miley (1987;1990) are peculiar in optical morphology, but are not observed to be obviously interacting with any other galaxy. In more detail, Lawrence *et al.* have classified their IR-selected and control (field galaxy) samples into six interaction classes ranging from 0 (no companions, normal morphology), 1-4 (normal morphology, but progressively brighter and closer companions), through 5 and 6 (galaxy pair with peculiar morphology and "merger" = single galaxy with peculiar morphology). Interestingly the ratio of powerful IR galaxies in classes 1-4 to those in Class 0 is similar to the same ratio for the field galaxies. The powerful IR galaxies are distinguished from the field galaxies by the relatively large fraction in Classes 5 and 6 (morphologically peculiar).

> The incidence rate of multiple nuclei (visible in high resolution near-IR images) is at least 50% in the "ultraluminous" IR galaxies (Carico *et al.* 1990; Graham *et al.* 1990; Illingworth *et al.* in preparation). The typical inter-nuclear separation is only a few kpc, and the timescale for the final coalesence of the nuclei via dynamical friction is then only 10^8 years. This suggests that the ultraluminous phase corresponds to the final 10^8 years of a merger. This age estimate is consistent with other estimates of the duration of nuclear starbursts.

There has been less analysis of the possible role of galaxy interactions in the optically-selected samples of nuclear starburst and Blue Compact Dwarf ("BCD" or "HII") galaxies (cf. Balzano, 1983; Melnick 1987; Salzer 1987). Both Campos-Aguilar and Moles (1990) and Melnick (1987) find that only a minority (20-30%) of the BCD's are members of interacting systems. Brinks (1990) has suggested (based on 21cm HI maps of two BCD's) that they may be triggered by collisions of HI clouds rather than collisions of galaxies. Campos-Aguilar and Moles (1990) find that all the nuclear starburst and irregular blue galaxies in their sample have massive companion galaxies. Finally, Condon *et al.* (1982) have emphasized the role of galaxy interactions in triggering starbursts in a radio-selected sample of spiral galaxies (a sample which was subsequently discovered to contain an abundance of now-famous IRAS galaxies).

B. Seyfert Galaxies

As in the case of starburst/IR galaxies, studies of the link between galaxy interactions and the Seyfert phenomenon fall into two primary categories: comparisons of the optical morphology and local environments of known Seyfert galaxies to those of non- Seyferts and comparisons of the strength and incidence rate of Seyfert nuclei in samples of interacting and non-interacting galaxies.

i) The Morphology and Environment of Known Seyfert Galaxies

There have been several recent observational investigations of the local environments of large samples of Seyfert galaxies. The studies have reached somewhat different conclusions, and therefore I will describe them in some detail.

Dahari (1984) determined the fraction of Seyferts with close (¡three galaxy diameters) companion galaxies. His sample included 103 Seyfert galaxies, with Seyferts in rich clusters being specifically excluded. His control sample consisted of randomly- selected galaxies in the same general fields as the Seyfert galaxies whose diameters were 75-150% those of the Seyferts. After correcting for the background using estimates based on the Shane-Wirtanen Catalog, he found that 15% of the Seyferts had close companions vs. 3% of the control sample (a significant difference). He subsequently (Dahari 1985) obtained redshifts for 33 of the Seyfert companions, and found no correlation between either radio continuum power or Hα luminosity and any measure of the importance of tidal interaction (e.g. pair separation, relative size of companion, redshift differences). The Seyferts with close companions did not differ in either radio power or Hα luminosity from isolated Seyferts at a statistically significant level.

Dahari and DeRobertis (1988) investigated a sample of 194 Seyfert galaxies, searching for relationships between tidal interactions and the properties of the nuclei. They found no statistically significant differences between the Seyferts with and without companions, except that the type 2 Seyferts with companions had excess infrared and radio-continuum emission (by an average factor of 5) compared to those without. Dahari and DeRobertis suggest that this excess IR and radio emission may be due to enhanced star-formation rather than exceptionally powerful nuclear activity.

MacKenty (1989) compared the environments of 51 Seyfert galaxies to those of 51 "control" galaxies (chosen in a similar manner to those of Dahari). He found that 71% of the Seyferts had an apparent companion galaxy within 10 galaxy diameters vs. only 26% of the control sample. Since he did not explicitly correct for background galaxies, the true fraction of companions will be lower in both samples (presumably by similar amounts). He also found that a higher fraction of type 2 Seyferts had close companions than did type 1 Seyferts (however, the statistical significance level of this result is marginal). Finally, he showed that IR "colors" indicative of star-formation were preferentially associated with the Seyferts having close companions, and concluded that galaxy interactions may trigger excess star-formation in Seyferts (in accord with Dahari and DeRobertis).

Fuentes-Williams and Stocke (1988) measured the density of galaxies within 1 Mpc of a sample of 53 Seyfert and 30 control galaxies. The galaxy density was quantitatively parameterized in several different ways, some of which were weighted strongly towards the nearest, brightest companions. Only galaxies with implied linear diameters between 15-50 kpc (corresponding to galaxies with absolute magnitudes near the fiducial Schecter L^* and comparable to those of the Seyferts themselves) were initially included as physical companions. No correction for the background was made. Unlike both Dahari and MacKenty, Fuentes-Williams and Stocke selected their control sample to match the Seyferts in Hubble type as well as absolute magnitude. They found no statistically-significant difference between the Seyfert and control samples in any of the quantities measuring local galaxy density. However, when apparent companion galaxies with diameters < 15 kpc were included, the Seyferts did show statistically significant excesses of companions (though less dramatic than the excesses found by Dahari and by MacKenty).

Finally, Kollatschny and Fricke (1989) obtained spectra of 113 galaxies in 15 loose groups containing a Seyfert and 9 loose groups without. They found an excess of galaxies with strong emission-lines ($L(H\alpha > 10^{41}$ erg/sec) in the former compared to the latter groups (excluding the Seyfert galaxy itself). This is a fascinating result, but its connection to the triggering of Seyfert nuclei via galaxy interactions is not clear.

Can the results of Fuentes-Williams and Stocke be reconciled with those of the Dahari and MacKenty? There are several possibilities, some of which were discussed by Fuentes-Williams and Stocke:

> "Bad Luck" at the 2-3σ level.

> There is a true excess of companions to Seyferts, but only for intrinsically faint companions.

> The stronger excesses found by Dahari and MacKenty are (in part) artifacts of the way they defined a control sample. A random sample of field galaxies will tend to be more strongly weighted toward late-type galaxies than a sample of Seyferts (which are known to be primarily early-type spiral galaxies - cf. Simkin, Su, and Schwarz 1980). Since there is a well-known morphology-density relation such that galaxies of earlier Hubble type live preferentially in regions of higher galaxy density (Dressler 1980; Postman and Geller 1984), the Dahari/MacKenty control samples may be biased towards lower galaxy densities than their Seyfert samples.

> The effect (excess of close companions) may be stronger for type 2 Seyferts than type 1's (MacKenty 1989; Petrosian 1982; Dahari and DeRobertis 1988). If we include the type 1.5 Seyferts as type 1's and types 1.8 and 1.9 as type 2's, then the relative fraction of type 2 Seyferts in the samples of Fuentes-Williams and Stocke, MacKenty, and Dahari are 21%, 28%, and 57% respectively.

Since the pioneering work of Adams (1977), there have been several investigations of the morphology of Seyfert galaxies, most of which have noted the "surprisingly large" fraction of Seyferts with peculiar morphologies. This fraction ranges from 16% (Adams 1977) to 30% (MacKenty 1990) to 40% (Wehinger and Wyckoff 1977). The fraction of morphologically peculiar Seyferts seems to rise as the mean redshift of the sample under investigation rises. This may mean that the connection between galaxy interactions and the Seyfert phenomenon is strongest for the most luminous Seyfert nuclei. MacKenty also emphasized the significant fraction of Seyferts with amorphous morphologies, but colors too blue for E or S0 galaxies. He speculates that they may be post-merger/post- interaction galaxies (see also Hernquist 1989).

Simkin, Su, and Schwarz (1980) discussed images of the nearest Seyfert galaxies ($cz < 5000$ km/sec). They do not address the incidence of peculiar or interacting galaxies in this sample. Rather, they show that Seyferts can be comfortably accomodated within the standard Hubble/deVaucouleurs classification scheme, but that (compared to galaxies as a whole) the Seyferts are preferentially early-type spirals with inner and/or outer rings. They interpret these rings as signs of oval distortions in the disks, and speculate that such distortions lead to radial inflow of disk gas at a rate sufficient to fuel the nucleus. While they therefore favor an internal dynamical process for fueling the nucleus, galaxy interactions seem proficient at inducing bars/oval distortions in galactic disks (as reviewed elsewhere in this volume by Athanassoula).

ii) Seyfert Nuclei in Samples of Interacting Galaxies

As in the types of investigations summarized above, there have been several well-conceived and carefully-executed spectroscopic surveys of the nuclei of interacting galaxies that have come to somewhat different conclusions concerning the incidence of Seyfert nuclei.

Keel *et al.* (1985) have compared the incidence rate of Seyfert nuclei in three samples: 1. a control sample consisting of 87 spiral galaxies in the Keel (1983) and Stauffer (1982) surveys of the nuclei of typical (non-interacting) galaxies 2. a complete sample of physical pairs of galaxies (61 galaxies) 3. 99 galaxies selected from the Arp Atlas to represent strongly interacting galaxies. The incidence rate of Seyferts was 5.6% in the control sample, 10.6% in the "pairs" sample, and 8.2% in the "Arp" sample. The excess of Seyferts in the "pairs" sample vs. the "control" sample is only marginally significant (2σ). If only the closest (separation < a galaxy radius) pairs are considered, the incidence rate of Seyfert nuclei rises to 25% (a 3σ excess compared to the control sample). Because the galaxies in the "Arp" sample are more luminous (in the optical) than the galaxies in the control sample, and because the incidence rate of Seyfert nuclei increases with the optical luminosity of the host galaxy, Keel *et al.* argue that there is actually a deficiency of about a factor of two in the fraction of Seyfert nuclei in the "Arp" sample relative to a "luminosity- adjusted" control sample. Keel *et al.* also find that the Seyfert nuclei and LINER's in interacting galaxies may be slightly more luminous (on-average) than those in the control sample. Note that this does not agree with the results of Dahari and DeRobertis (1988).

Dahari (1985) obtained spectra of 167 galaxies selected from the Vorontsov-Vel'yaminov Atlas and Catalogue of Interacting Galaxies ("VV Catalogue"). He found that the fraction of Seyfert nuclei among the strongly interacting galaxies in the VV Catalogue (Interaction Class - "IAC" = 4,5 or 6) was 13.2% vs. 5.6% for the weakly interacting (IAC = 2 or 3) VV galaxies vs. 4.6% for his control sample (the Keel + Stauffer noninteracting spirals). The excess of Seyferts in the strongly interacting VV sample compared to the control sample is significant at the 98% confidence level (2.5σ). While Dahari emphasizes a possible deficiency of Seyfert nuclei among the most strongly interacting VV galaxies (IAC = 6 has no Seyferts among 14 galaxies), this is not a statistically significant result (only 88% confidence level). Note that Dahari has made not made a correction (analogous to the one applied by Keel *et al.*) to account for possible differences in the absolute magnitudes of the galaxies in the control and VV samples.

Finally, Bushouse (1986) has obtained spectra of 94 disk galaxies selected from the Uppsala Galaxy Catalog (UGC) on the basis of morpholgical evidence for an interaction. He reports a deficiency of Seyfert nuclei in the interacting galaxies: 1% incidence rate vs. 5% in field spirals. However, I find that the statistical significance of the "deficiency" is only about 85% (when tested against the Keel+Stauffer control sample used by Dahari). Nevertheless his survey provides no evidence that interactions foster Seyfert nuclei.

Can all these results be made consistent? The simplest explanation is that (insofar as the neither the positive nor negative results are of overwhelming statistical significance) we are again being bedeviled by "bad luck" at the $2\text{-}3\sigma$ level. It is also possible that the probability of detecting a Seyfert nucleus in an interacting galaxy is a complex function of the detailed properties of the interaction and of its constituent galaxies (as discussed by Byrd, Sundelius, and Valtonen 1987). In any case, it is difficult to ascribe the difference between Dahari and Keel *et al.* on the one hand and Bushouse on the other to any fundamental differences in either sample selection or observational approach. It therefore appears that samples of order 100 galaxies are not large enough to sort this out in a thoroughly convincing fashion (a depressing thought indeed).

C. Radio Galaxies

There have been myriad empirical investigations into the connection between radio emission from galaxies and their environments. I will limit the scope of the brief review to follow in two ways. First, I use the term "radio galaxy" only for cases in which the radio power at 1.4 GHz is greater than about 10^{23} Watts/Hz. My intent here is to exclude both galaxies in which the radio emission may be powered by a starburst (e.g. Condon etal. 1982) and typical Seyfert galaxies (e.g. Wilson and Heckman 1985) - both of which classes have been discussed above. Second, I will focus on environmental parameters that are the most likely to be related to galaxy interactions, namely the galaxy morphology and the local environment (within 100-200 kpc or so of the radio galaxy). In particular, I will not review the fascinating data concerning the membership of radio galaxies in rich clusters as a function of redshift (see, for example Prestage and Peacock 1988 and Yates, Miller, and Peacock 1990). Note that a somewhat expanded version of the following can be found in a recent review by Smith and Heckman (1990a).

Broadly speaking, there are two classes of radio galaxies (cf. Hine and Longair 1979 and Stocke and Perrenod 1981). The first class has weak optical emission-lines (usually LINER-type when classifiable) and the radio emission is dominated by emission from the jets with the brightness generally declining with distance from the nucleus (the so-called "FR I" radio morphology - after Fanaroff and Riley 1974). This class dominates the radio galaxy population for moderate radio powers ($P_{1.4} = 10^{23} - 10^{25}$ Watts/Hz). The second class of radio galaxy has strong (generally Seyfert-like) optical emission-lines and the radio emission is dominated by the outer lobes/hotspots (a "classical double" or "FR II" radio morphology). This class dominates the radio galaxy population at high radio powers ($P_{1.4} > 10^{25}$ Watts/Hz). I will henceforth use the terms "low-power" and "high-power" as a shorthand notation for the two respective classes.

i) Low-Power Radio Galaxies

There are many studies that have shown that the low-power radio galaxies are generically giant ellipticals (or related objects like cD galaxies) - see Smith and Heckman (1989a,b) for a recent quantitative investigation of a large sample of such galaxies. That being the case, it is instructive to compare the local environments of low-power radio galaxies and optically similar, radio-quiet giant elliptical galaxies. Heckman, Carty, and Bothun (1985) conducted such an investigation using both the Palomar Sky Survey and CCD frames to measure the local galaxy density (within a projected radius of 100 h^{-1} kpc) for samples of 47 radio-loud and 46 radio-quiet galaxies. They found that the low-power radio galaxies inhabit regions with average galaxy densities 2 to 3 times larger than the control sample (different at 4σ level). Using a complementary approach that was less subject to subtle selection effects, Gavazzi and Jaffe (1986) searched for radio emission from nearly 300 E and S0 galaxies in the Coma/A1367 supercluster. They found that the isolated E and S0 galaxies (no neighbors within 300 kpc) were low by a factor of 5 in radio power compared to the E's and S0's in denser environments. The Heckman, Carty, and Bothun and the Gavazzi and Jaffe papers together confirmed and extended the results in several important earlier papers - for example Dressel (1981) and Adams, Jensen, and Stocke (1980).

Smith and Heckman (1989) and Heckman *et al.* (1986) found that low-power radio galaxies seldom show the type of structural peculiarities associated with galaxy interactions that involve one or more dynamically-cold systems (disk galaxies). That is, fewer than 10% exhibit "tails", "bridges", or "shells" having V-band surface brightnesses higher than 25 magnitudes per arcsec^2. It is possible however that a greater fraction of such radio galaxies are strongly interacting with a neighbor (cf. Colina and Perez- Fournon 1990). This is because the radio galaxies themselves and their near neighbors tend to be early-type galaxies (E's and S0's), and the morphological signatures of interactions between two such dynamically-hot systems can be quite subtle. Careful analysis may be required to distinguish tidal deformations from effects caused merely by overlapping the images of structurally normal galaxies (cf. Borne 1988; Lauer 1989). Moreover, since a large fraction of radio-quiet ellipticals show isophotal twists and nonconcentric isophotes (see the recent review by Kormendy and Djorgovski 1989), their mere presence in many low-power radio galaxies is not necessarily evidence that galaxy interactions are linked to the radio galaxy phenomenon. A rigorous comparison of the amplitude of such effects between radio-loud and radio-quiet ellipticals is needed, but has yet to be done. A possibly related effect is the claim by Bender and Möllenhoff (1987) that radio-loud ellipticals (what I would call low-power radio galaxies) tend to have "boxy" optical isophotes while radio-quiet ones tend to have "disky" isophotes. Neither the connection of boxy isophotes to past galaxy interactions nor the longevity of such structures is yet clear however (see Binney and Petrou 1985).

ii) High-Power Radio Galaxies

The relationship between galaxy interactions and high-power radio galaxies has only recently been addressed. This is largely because their low space density (and strong cosmological evolution) means that significant numbers of such objects are encountered only for $cz > 10^4$ km/sec. The nearest high-power radio galaxy with strong optical emission-lines is the pathological object NGC1275. Other relatively local "famous" examples are 3C 120 and Cygnus A. The large distances to these galaxies make them rather difficult to investigate optically. To give several examples of some of the more subtle difficulties: 1) The effects of the general background of faint galaxies need to be carefully and explicitly calculated before the galactic clustering environments of the radio galaxies can be determined 2) It is difficult to devise a suitable comparison or control sample (for better or worse, the morphologies and environments of the radio galaxies are usually compared to those of luminous elliptical galaxies in our local universe) 3) The radio galaxies often have large, bright, and morphologically complex emission-line nebulae (cf. Baum and Heckman 1989a,b; McCarthy 1989). Such a nebula can affect broad-band measurements of the properties of the stellar component of a radio galaxy (absolute magnitude, morphology, color), and so must be corrected for in some way. More rarely, a strong nonthermal (optical) nuclear source may be present and its effects accounted for.

Heckman *et al.* (1986) published the results of an imaging survey of 43 (mostly high-power) radio galaxies. This sample was later enlarged to 72 galaxies with a median redshift of 0.06 by Smith and Heckman (1989a,b). The latter paper also presented color data (in the form of (B-V) global colors and color maps) for 56 of the radio galaxies. Hutchings (1987) and Yates, Miller, and Peacock (1990) have each discussed images of 25 more powerful and more distant (median z 0.22 and 0.31 respectively) radio galaxies. Smith and Heckman (1990b) have determined the local environment (within 100 h^{-1} kpc) of high-power radio galaxies, and have calculated the luminosity function of the associated galaxies (see also Fuentes-Williams and Stocke 1988). Finally, Smith, Heckman, and Illingworth (1990) have compared the stellar dynamical properties of high-power radio galaxies and normal giant elliptical galaxies. The principal results of these surveys are as follows:

> Estimates of the fraction of high-power (strong-emission-line) radio galaxies that are morphologically distorted range from about 32% (Yates, Miller, and Prestage 1990) to nearly 100% (Hutchings 1987). Heckman *et al.* (1986) and Smith and Heckman (1989b) find that about half of this type of radio galaxy is morphologically- distorted at moderately high levels of surface brightness (brighter than 25 V magnitudes per arcsec^2 in the radio galaxy rest-frame). The distortions they discuss take the form of tails, bridges to apparent companion galaxies, shells or fans, and strong dust lanes. In the great majority of their cases these are continuum-emitting structures (presumably starlight) and not merely emission-line gas. This is far greater than the incidence rate of such structures they found in the lower-powered radio galaxies with weak optical emission-lines (10%), even though such features should have been more readily detectable in these latter galaxies because of their lower redshifts.

> The high-power radio galaxies have (on-average) two bright companion galaxies ($L > 0.2 L^*$) within 100 kpc. While this may imply that interactions are occurring, this local density is no higher than that around typical radio-quiet ellipticals. However, the shape of the luminosity function of the companions differs from that of the standard Schecter function, having an enhanced relative number of bright galaxies. This might imply that interactions between massive galaxies can lead to strong radio emission.

> The optical colors of the high-power radio galaxies are (on- average) several tenths of a magnitude bluer than those of either low-power radio galaxies or radio-quiet ellipticals of similar absolute magnitude. The two-dimensional color maps and radial color profiles show strong spatial variations, evidently reflecting the competing effects of dust and "young" ($\ll$10 Gigayear) stars.

> The stellar dynamics of the radio galaxies with peculiar optical morphologies are also peculiar. The velocity dispersions are lower (by 0.1 dex on-average) and rotational support is more important (average v_{rot}/σ greater by a factor of 2 to 3) than in radio-quiet ellipticals and morphologically-normal radio galaxies with similar absolute magnitudes.

The picture that emerges from these investigations is somewhat ambiguous. Strictly on the basis of morphology, the majority of powerful radio galaxies with strong emission-lines could be interpreted as mildly-damaged giant elliptical galaxies. That is, the structural peculiarities are transient and dynamically insignificant events that have not/will not change the Hubble type of the galaxy. This is the interpretation implicitly favored by Yates, Miller, and Peacock. The fact that many of these radio galaxies also have global colors that are significantly bluer than normal giant ellipticals could be explained by interaction-induced starbursts involving only a few percent mass of the "underlying" old (elliptical) galaxy (cf. Larson and Tinsley 1978). The excess blue light from a (post?) starburst population could explain the fact that the morphologically peculiar radio galaxies are about 1 magnitude brighter (at V) than normal ellipticals with the same velocity dispersion (Smith, Heckman, and Illingworth 1990).

On the other hand, the rapid rotation that characterizes many of the morphologically peculiar galaxies is less easy to explain if these are just mildly damaged giant ellipticals. If the rapid rotators are the products of galaxy interactions or mergers, these must have been severe enough to affect the internal dynamics in a substantial way. Moreover, about one-third of the morphologically peculiar radio galaxies in Heckman *et al.* and Smith and Heckman appear likely (on morphological grounds) to be mergers or interactions involving two disk galaxies, because they exhibit two tail-like structures (cf. Toomre 1977). The clearest example of this is 3C 305, and other possibly related radio galaxies are 3C 120, 3C 171, 3C 223, 3C 285, 3C 382, 3C 459, PKS 1345+125, and PKS 2300-189.

At redshifts $z > 0.5$ or so, the optical properties of high- power radio galaxies become even stranger. I have briefly described these galaxies in §IIIA above, and have argued there that the strong alignment between their optical and radio axes makes me skeptical that they can be simply interpreted as tidal interactions between galaxies (to paraphrase George Miley (1990) in his recent review of high-redshift radio galaxies, these galaxies are clearly "interacting", but probably not with another galaxy!). I will not discuss these fascinating objects further.

iii) Gas Kinematics in Radio Galaxies

The presence of appreciable interstellar gas in radio galaxies is often taken as evidence for an accretion event. This is particularly suggestive because the specific angular momentum of the gas is often much larger than (and sometimes misaligned with) the specific angular momentum of the stellar body of the galaxy (cf. Heckman *et al.* 1985 and references therein). The kinematics of the H I is the most illuminating, as van Gorkom *et al.* (1989) discuss. They have detected H I in absorption toward the nuclei of about 25% of a sample of low-redshift radio galaxies, and find the gas to be infalling. Since the detection of gas in absorption against a compact nuclear radio source requires a favorable viewing geometry, they suggest that most radio galaxies may have infalling HI. It is possible that the infalling H I is material that has condensed out of a cooling flow, rather than tidally captured material. Maps of the H I in emission are important in this regard, but will be very difficult to obtain.

D. QSO's

The observational and interpretational difficulties I described regarding the investigation of galaxy interactions involving high-power radio galaxies are even more severe in the case of QSO's. I will concentrate on low-redshift QSO's (at $z < 0.5$), since our information concerning the host galaxies and environments of QSO's at higher redshifts is less complete.

i) Environments of QSO's

Radio-loud QSO's have more near-neighbors (within 100 h^{-1} kpc) than do typical galaxies by a factor of 4-5 (see Yee and Green 1984 and Smith and Heckman 1990b).

In fact, the latter authors find an average of 2 physically-associated near-neighbors with L> 0.2 L^*. These results are intriguing, but their significance is clouded by the well-known morphology-density relation for galaxies. That is, while radio-loud QSO's have more near-neighbors than do galaxies as a whole, they do not differ significantly in this regard from radio-quiet giant elliptical galaxies. Thus, whether or not the radio-loud QSO's have an unusual number of near-neighbors depends on the nature of the appropriate comparison sample, which in turn depends on the (uncertain) nature of the QSO host galaxy.

> Radio-quiet QSO's have fewer average near-neighbors than the radio-loud QSO's by a factor of 2 (Yee and Green 1984; Smith and Heckman 1990b). This means that they have about a factor of two more near-neighbors than average galaxies, but this result is only significant at the 2σ level. Again, the nature of the appropriate comparison sample of normal galaxies is not entirely clear.

> As in the case of the high-power radio galaxies (see above), the luminosity function of the near-neighbors of the radio-loud QSO's is unusually flat at the high luminosity end compared to a standard Schecter function (see Smith and Heckman 1990b). The redshifts of the QSO's under consideration are too low (typically 0.1 to 0.3) for this to have arisen due to the general evolution of typical galaxies. Moreover, Smith and Heckman find that the luminosity function of the near-neighbors of the radio-quiet QSO's is normal. The interpretation of this result is unclear, but one possibility is that it is a selection effect: if radio-loud QSO's and high- power radio galaxies are often triggered by the close encounter of two (or more) luminous galaxies, then the luminosity function of the near-neighbors will be biased towards the presence of such luminous galaxies.

> While the environments of low-z QSO's are locally dense, they are rarely located inside rich clusters of galaxies. Yee and Green (1984) suggest that QSO's are preferentially found in dense groups, and this suggestion is corraborated by the relatively small typical velocity differences between the QSO's and those near-neighbors with measured redshifts (cf. Heckman *et al.* 1984). This situation changes at $z > 0.5$, where QSO's are often located in rich clusters (Yee and Green 1987).

> The great majority (90%) of the apparent near-neighbors to low- z QSO's (galaxies projected to lie within 100 h^{-1} kpc of the QSO) are in fact physically associated with the QSO because they have the same redshift (Heckman *et al.* 1984, and see also Stockton 1978).

ii) Morphology of QSO Host Galaxies

There have been several broad-band imaging surveys of low-z QSO's that have emphasized the large fraction of QSO host galaxies that appear to be "disturbed" or "interacting": e.g. 35-55% (Smith *et al.* 1986) and 30-40% (Hutchings, Crampton, and Campbell,1984). The fraction of "disturbed/interacting" host galaxies may be particularly high for the radio-loud QSO's: 70% (Hutchings 1987), 77% (Smith *et al.* 1986), 50% (Hutchings, Crampton, and Campbell 1984),> 68% (Hutchings, Janson, and Neff 1989).

While these results are tantalizing, they do not yet constitute a water-tight case linking galaxy interactions to the QSO phenomenon. Some of the morphologically peculiar structures visible in the broad-band images of the radio-loud QSO's are likely to be produced by emission-line gas rather than starlight (for which there is considerable ambiguity in interpretation - see below). No one has yet made a rigorous effort to compare the fraction of "disturbed/interacting" QSO hosts to any realistic comparison sample of non-active galaxies (recall that the number of near-neighbors around low-z QSO's may or may not be unusually large, depending on the Hubble type of the QSO host). For example, Lawrence *et al.* (1989) found that about 18% of optically-selected "field" galaxies with redshifts comparable to those of low-z QSO's were classified by them as morphologically peculiar. While this fraction is significantly smaller than the fractions of "peculiar" QSO hosts quoted above, it is slightly worrying that the morphological classifications of the QSO and field galaxies were not made by the same people using the same data. At least we do have spectroscopic confirmation that many of the near- neighbors/interaction-partners are indeed galaxies at the same redshift of the QSO (see Stockton 1978 and Heckman *et al.* 1984).

Complimentary data have been published by Stockton and MacKenty (1987), who imaged 47 low redshift QSO's through narrow- band filters centered on the redshifted [O III] λ5007 emission-line. They found that about 25% of these QSO's had luminous and highly structured emission-line nebulae with sizes of several tens of kpc. They noted that these nebulae were preferentially associated with the QSO's having strong, spatially-extended radio emission. They also emphasized that many of the QSO's with such nebulae were likely to be situated in interacting galaxies, and speculated that the nebulae might be gaseous tidal debris photoionized by the QSO.

An alternative interpretation of the QSO nebulae has been championed by Fabian and collaborators in a recent series of papers (cf. Crawford, Fabian, and Johnstone 1988 and references therein). They argue that the high densities inferred for the clouds in the nebulae require a high-pressure confining medium to be present. They therefore postulate that the visible nebulae are dense clouds photoionized by the QSO and imbedded in a hot X-ray-emitting medium akin to the "cooling flows" associated with many cluster-dominant giant ellipticals. In their view the nebulae do not represent evidence for a tidal interaction. Moreover, Baum and Heckman (1988b) concluded that the nebulae were morphologically aligned with the axis of the radio source (as is the case for radio galaxies with similar radio properties). This raises the possibility that the morphology of the nebulae might be influenced by hydrodynamical processes associated with the outflowing radio plasma. Investigations of the dynamics of the gas might be able to discriminate between these various hypotheses, but most spectroscopy to date has been low-dispersion data with relatively poor velocity resolution (cf. Boroson, Persson, and Oke 1985; Crawford, Fabian, and Johnstone 1988).

V. CONCLUSIONS

If nothing else, I hope this review has conveyed to the reader an impression of the amount of data, the number of different papers, and the multiplicity of approaches that deal with the question of the relationship between galaxy interactions and activity in galactic nuclei. To my mind there is little doubt that such a relationship exists. The more difficult question is whether galaxy interactions are the dominant mechanism by which nuclear activity is triggered. Somewhat surprisingly, the evidence seems to me to be in reasonable agreement with the theoretical/heuristic arguments summarized in §II above.

I think the case is strongest for the luminous IR galaxies ($L_{IR} > 10^{11}$ $L_{\odot}$). Over half of such galaxies have strongly peculiar optical morphologies. The redshifts of these galaxies are low enough that these morphological peculiarities can be compared to the results of simulated galaxy interactions, and the qualitative agreement is generally satisfactory. The high incidence rate of multiple nuclei in the most luminous such galaxies is very striking, because these are the very cases where the circumnuclear region is being subjected to maximal tidal stress. My only residual worry is that in some cases the peculiar structures visible in IR-luminous galaxies might have a hydrodynamical origin.

The QSO's and powerful radio galaxies with strong emission- lines (at $z < 0.5$ where the optical/radio alignment effect is unimportant) are the next most convincing cases in my view. HST observations that more clearly delineate the optical morphology will be important (especially for the QSO's, where the amount of morphological information available in the present images is rather limited).

There is also suggestive evidence linking galaxy interactions to both the Seyfert and low-power radio galaxy phenomena. However (despite valiant efforts by several different groups working on large samples) this evidence remains at about the 2 to 4σ level. This suggests to me that galaxy interactions are a significant, but probably not dominant, mechanism by which low-power nuclear activity is fuelled.

REFERENCES

Adams, T.F. 1977, Ap.J.Suppl., 33, 19.

Adams, M.T., Jensen, E.B., and Stocke, J.T. 1980, Astr.J., 85, 1010.

Armus, L., Heckman, T.M, and Miley, G. 1987, Astr.J., 94, 831.

Armus, L., Heckman, T.M., and Miley, G.K. 1990, Ap.J., in press.

Baade, W., and Minkowski, R. 1954, Ap.J., 119, 206.

Balick, B. and Heckman, T.M. 1982, Ann.Rev.Astr.Ap., 20, 431.

Balzano, V.A. 1983, Ap.J., 268, 602.

Baum, S.A., and Heckman, T.M. 1989a, Ap.J., 336, 681.

Baum, S.A., and Heckman, T.M. 1989b, Ap.J., 336, 702.

Begelman, M., and Cioffi, D. 1989, Ap.J.Lett., 345, L21.

Bender, R., and Mollenhoff, C. 1987, Astr.Ap., 177, 71.

Binney, J., and Petrou, M. 1985, MNRAS, 214, 449.

Borne, K. 1988, Ap.J., 330, 38.

Boroson, T.A., Persson, S.E., and Oke, J.B. 1985, Ap.J., 293, 120.

Bothun, G., Lonsdale, C., and Rice, W. 1989, Ap.J., 341, 129.

Brinks, E. 1990, in Galaxy Dynamics and Interactions, ed. A. Toomre and R.Wielen, in press.

Bushouse, H. 1986, Astr.J., 91, 255.

Bushouse, H. 1987, Ap.J., 320, 49.

Bushouse, H., Lamb, S., and Werner, M. 1988, Ap.J., 335, 74.

Byrd, G., Sundelius, B., and Valtonen, M. 1987, Astr.Ap., 171, 16.

Campos-Aguilar, A., and Moles, M. 1990, preprint.

Carico, D., Graham, J., Matthews, K., Wilson, T., Soifer, B.T., Neugebauer, G., and Sanders, D. 1990, preprint.

Carter, D., Prieur, J., Wilkinson, A., Sparks, W.B., and Malin, D.M. 1988, MNRAS, 235, 813.

Chambers, K. 1989, Ph.D. thesis, The Johns Hopkins University.

Chambers, K., Miley, G., and van Breugel, W. 1987, Nature, 329, 604.
Colina, L., and Perez-Fournon, I. 1990, Ap.J., 349, 45.
Condon, J, Condon, M., Gisler, G., and Puschell, J. 1382, Ap.J., 252, 102.
Crawford, C.S., Fabian, A., and Johnstone, R. 1988, MNRAS, 235, 183.
Cutri, R., and McAlary, C. 1985, Ap.J., 296, 90.
Dahari, O. 1984, Astr.J., 89, 966.
Dahari, O. 1985a, Astr.J., 90, 1772.
Dahari, O. 1985b, Ap.J.Suppl., 57, 643.
Dahari, O., and DeRobertis, M. 1988, Ap.J., 331, 727.
Djorgovski, S. 1987, in Starbursts and Galaxy Evolution, ed. T. Thuan, T. Montmerle, and J. Tran Thanh Van (Editions Frontieres: Paris), p. 401.
Dressel, L.L. 1981, Ap.J., 245, 25.
Dressler, A. 1980, Ap.J., 236, 351.
Fairclough, J. 1986, MNRAS, 219, 1P.
Fanaroff,B., and Riley, J. 1974, MNRAS, 167, 31P.
Franx, M., and Illingworth, G.D. 1988, Ap.J.Lett., 327, L55.
Fricke, K.J., and Kollatschny, W. 1989, in Proc. IAU Symp. 134, ed. D. Osterbrock and J.S Miller (Kluwer: Dordrecht), p. 425.
Fuentes-Williams, T., and Stocke, J. 1988, Astr.J., 96, 1235.
Gavazzi, G., and Jaffe, W. 1986, Ap.J., 310, 53.
Graham, J., Carico, D., Matthews, K., Neugebauer, G., and Soifer, B.T. 1990, preprint.
Gunn, J. 1979, In Active Galatio Nuclei, ed. C. Hazard, S. Mitton, p.213 (Cambridge University Press).
Heckman, T.M. 1983, Ap.J., 268, 628.
Heckman, T.M., Bothun, G.D., Balick, B., and Smith, E. 1984, Astr.J., 89, 958.
Heckman, T.M., Illingworth, G.D., Miley, G.K., and van Breugel, W. 1985, Ap.J., 299, 41.
Heckman, T.M., Armus, L., and Miley, G.K. 1990, Ap.J., in press.
Heckman, T.M., Carty, T., and Bothun, G. 1985, Ap.J., 288, 122.
Heckman, T.M., Smith, E., Baum, S., van Breugel, W., Miley, G., Illingworth, G., Bothun, G., and Balick, B. 1986, Ap.J., 311, 526.
Hernquist, L. 1989, Nature, 340, 687.
Hickson, P., Menon, T., Palumbo, G., and Persic, M. 1989, Ap.J., 341, 679.
Hine, R., and Longair, M. 1979, MNRAS, 188, 111.
Hummel, E. 1981, Astr.Ap., 96, 111.
Hunter, D., Gillet, F., Gallagher, J., Rice, W., and Low, F. 1986, Ap.J., 303, 171.
Hutchings, J. 1987, Ap.J., 320, 522.
Hutchings, J., Crampton, D., and Campbell, B. 1984, Ap.J., 280, 41.
Hutchings, J., Janson, T.,and Neff, S. 1989, Ap.J., 342, 660.
Hutchings, J., and Neff, S. 1988, Astr.J., 96, 1575.
Jedrzejewski, R., and Schecter, P. 1988, Ap.J.Lett., 330, L87.
Joseph, R., and Wright, G. 1985, MNRAS, 214, 87.
Joseph, R., Meikle, W., Robertson, N., and Wright, G. 1984, MNRAS, 209,111.
Keel, W.C. 1983, Ap.J.Suppl., 52, 229.
Keel, W.C. 1987, in Proc. IAU Symp. 121, ed. K.J. Fricke, E. Khachikian, and J. Melnick.

Keel, W., Kennicutt, R., Hummel, E., and van der Hulst, J. 1985, Astr.J., 90, 708.

Kennicutt, R., Keel, W., van der Hulst, J., Hummel, E., and Roettiger 1987, Astr.J., 93, 1011.

Kollatschny, W., and Fricke, K. 1989, Astr.Ap., 219, 34.

Kormendy, J., and Djorgovski, S. 1989, Ann.Rev.Astr.Ap., 27, 235.

Larson, R. 1987, in Starbursts and Galaxy Evolution, ed. T. Thuan, T. Montmerle, and J. Tran Thahn Van (Editions Frontieres: Paris), p. 467.

Larson, R., and Tinsley, B. 1978, Ap.J., 219, 46.

Lauer, T. 1988, Ap.J., 325, 49.

Lawrence, A., Rowan-Robinson, M., Leech, K., Jones, D., and Wall, J. 1989, MNRAS, 240, 329.

Lonsdale, C., Persson, S.E., and Matthews, K. 1984, Ap.J., 287, 95.

MacKenty, J. 1989, Ap.J., 343, 125.

MacKenty, J. 1990, preprint.

McCarthy, P. 1988, Ph.D. thesis, University of California, Berkeley.

McCarthy, P., van Breugel, W., Spinrad, H., and Djorgovski, S. 1987, Ap.J.Lett., 321, L29.

Meixner, M., Blitz, L., Puchalsky, R., Wright, M., and Heckman, T. 1990, Ap.J., in press.

Melnick, J. 1987 in Starbursts and Galaxy Evolution, ed. T. Thuan, T. Montmerle, and J. Tran Thanh Van (Editions Frontieres:Paris), p. 215.

Miley, G.K. 1990, in Galaxy Dynamics and Interactions, ed. A. Toomre and R.Wielen (in press).

Noguchi, M. 1988, Astr.Ap., 203, 259.

Petrosian, A.R. 1982, Astrofizika, 18, 548.

Postman, M., and Geller, M. 1984, Ap.J.. 281, 95.

Prestage, R., and Peacock, J. 1988, MNRAS, 230, 131.

Rees, M. 1984, Ann.Rev.Astr.Ap., 22, 471.

Rieke, G.H. 1988, Ap.J.Lett., 331, L5.

Salzer,J. 1987, Ph.D. thesis, University of Michigan.

Sanders, D., Soifer, B.T., Elias, J., Madore, B., Matthews, K., Neugebauer, G., and Scoville, N. 1988a, Ap.J., 325, 74.

Sanders, D., Scoville, N., Sargent, A., and Soifer, B.T. 1988b, Ap.J., 324, L55.

Schweizer, F., and Seitzer, P. 1990, preprint.

Simkin, S.M., Su, H.J., and Schwarz, M.P. 1980, Ap.J., 237, 404.

Smith, E., Heckman, T., Bothun, G., Romanishin, W., and Balick, B. 1986, Ap.J., 306, 64.

Smith, E., and Heckman, T. 1989a, Ap.J.Suppl., 69, 365.

Smith, E., and Heckman, T. 1989b, Ap.J., 641, 358.

Smith, E., and Heckman, T. 1990a, Ap.J., in press.

Smith, E., and Heckman, T. 1990b, in Galaxy Dynamics and Interactions, ed A. Toomre and R. Wielen (in press).

Smith, E., Heckman, T., and Illingworth, G. 1990, Ap.J., in press.

Soifer, B.T., Houck, J.R., and Neugebauer, G. 1987, Ann.Rev.Astr.Ap., 25, 187.

Stauffer, J. 1982, Ap.J.Suppl., 50, 517.

Stocke, J.T. 1978, Astr.J., 83, 348.

Stocke, J.T., and Perrenod, S. 1981, Ap.J., 245, 375.

Stockton, A. 1978, Ap.J., 223, 747.

Stockton, A. 1990, in Galaxy Dynamics and Interactions, ed. A. Toomre and R. Wielen (in press).

Stockton, A., and MacKenty, J. 1987, Ap.J., 316, 584.

Sulentic, J.W. 1976, Ap.J.Suppl., 32, 171.

Sulentic, J.W. 1990, preprint.

Telesco, C. 1988, Ann.Rev.Astr.Ap., 26, 343.

Toomre, A. 1977, in Evolution of Galaxies and Stellar Populations, ed. B.M. Tinsley and R.B. Larson, p.401 (Yale University Observatory).

Toomre, A., and Toomre, J. 1972, Ap.J., 178, 623.

van Albada, T., Kotanyi, C., and Schwarzchild, M. 1982, MNRAS, 198, 303.

van Gorkom, J., Knapp, G., Ekers, R., Ekers, D., Laing, R., and Polk, K. 1989, Astr.J., 97, 708.

Wehinger, P., and Wyckoff, S. 1978, MNRAS, 184, 335.

Williams, R.E., and Christiensen, W. 1985, Ap.J., 291, 80.

Wilson, A.S., and Heckman, T.M. 1985, in Astrophysics of Active Galaxies and QSO's, ed. J. Miller (University Science Books:Mill Valley, CA).

Yates, M.G., Miller, L., and Peacock, J.A. 1990, MNRAS, in press.

Yee, H., and Green, R. 1984, Ap.J., 280, 79.

Yee, H., and Green, R. 1987, Ap.J., 319, 28.

G. Burbidge: I believe that your point that Seyfert galaxies are found in regions of higher galaxy density than average is very important. The same result is found for low-z QSOs, as you said. It is also found in the situation where the QSOs and galaxies have very different red shifts, based on a very large sample of QSO-galaxy pairs studied in Burbidge, Hewitt, Narlikar, and Das Gupta. There are also reports that the same result is being found by Hammer and his colleagues for high redshift radio galaxies. Thus a general rule is emerging. Whereever we see a non-thermal source it is most likely with it has been generated in a region of high galaxy density. Since gravitational microlensing will not account for the QSO-galaxy pairs where $z_G < z_Q$, we are then forced to the conclusion that the non-thermal source is ejected from "normal" galaxies.

Kochhar: You said that tidal interactions do not seem to be very important in determining Seyfert activity. What role do internal dynamics play? (After all, spirals already have gas, and all they need is a way of channelling it to the center, unlike ellipticals which need gas.)

T. Heckman: The interesting paper by Simkin, Su, and Schwarz suggested (on the basis of the optical morphology) that internal dynamical processes were very important in fueling Seyfert nuclei. There is still not enough *dynamical* data to corroborate this idea.

Neff: Comment: Many Seyferts show signs of *previous* interactions when studied carefully.

Osterbrock: To me the statistical evidence that a surplus of galaxies undergoing interactions are Seyferts, and that a surplus of Seyferts (compared with other galaxies) are undergoing interactions is quite persuasive. Doubtless there are additional cases of interactions not directly counted as galaxies with nearby "neighbors" or "companions"---cases in which the perturbing galaxy is below the magnitude limit, cases in which the perturber is not seen because of projection effects, and cases in which the perturber has already merged with the galaxy it perturbed. That a large fraction of the perturbers are dwarf galaxies can be understood from the fact that a large fraction of galaxies are dwarfs.

Heckman: I agree that the existing investigations may well underestimate both the fraction of Seyferts undergoing interactions and the fraction of interacting galaxies that have Seyfert nuclei. Nevertheless, careful studies by independent authors have reached conflicting results. This suggests (to me) that the Seyfert/interaction connection is subtle, complex, and (possibly) rather weak.

TIDAL EVENTS AND GALACTIC ACTIVITY

J.B.Hutchings
Dominion Astrophysical Observatory, Victoria, B.C., Canada
S.G.Neff
NASA Goddard Space Flight Center, Greenbelt, MD, USA

Summary. We report some results from recent and ongoing work which relate to the connection between nuclear activity and tidal interactions. We suggest that tidal events are in general a necessary but not sufficient condition for nuclear activation. We also suggest that nuclear activity generally develops at a 'late stage' of a tidal encounter, following star-formation and dust evaporation, and when the most obvious morphological disturbances may have disappeared.

Table 1 summarizes the quantitative results from four programs which relate to the present topic. The full details are found in the references given. Our summary comments follow:

1. QSO imaging. In an investigation of matched samples of radio-loud and radio-quiet QSOs and radio galaxies, the results (Table 1) indicate disturbances of the host galaxy (indicating tidal encounters) in essentially *all* radio-luminous objects. (In the QSOs it is harder to see the closest companions and disturbances because of the bright nuclear light source.) The fraction (or strength) of interaction is lower in the radio-quiet QSOs. There is a range of M_V and colour for the host galaxies that makes them significantly different by K-S significance tests. The sense of these differences is consistent with different amounts of star-formation in the three types of object, widespread throughout galaxies with initially similar luminosities.

2. Radio evolution. In the references given, we have argued for a general time sequence of radio source evolution from unresolved (C) to one-sided (CL) to triple (T) structures. We have looked at optical morphology of redshift-matched samples of each radio type to see if a similar time sequence is indicated. The results (Table 1) are ambiguous, indicating possible complication by the merging/passing-interaction dichotomy, by hidden close companions, or by beaming of the core radiation. However, the companion separations among T sources (increasing with radio size), and the luminosity sequence in the host galaxies (star-formation in the youngest sources) do support the scenario. The high fraction of interactions among all radio types suggest that the radio evolution of a source is more rapid than the optical.

3. H I observations. In samples of AGN, and of IR-detected galaxies, the H I profile is frequently disturbed, but more so in the clearly interacting systems. There is a correlation between the H I and IR luminosity which presumably links gas and dust. Note also that there is a higher fraction of AGN in the IR-selected sample's 'non-interacting' systems.

This may indicate that (weaker?) AGN form after the initial interaction has died away. This needs to be reconciled with the radio source evolution timescales.

4. IRAS source survey. We find that optical object types are fairly well separated in the $L_{60\mu}/L_{(25/60\mu)}$ plane (Fig 1). We have obtained optical and radio continuum images of ~80 objects covering the range of these IR parameters. In detailed studies of several of the objects, we find that the IR luminosity is approximately equal to the hidden optical luminosity of hot stars/AGN reddened by dust.

So far, the optical imaging data indicate a progression of optical interaction and dust symptoms from left to right across the diagram. This may indicate either a time sequence or a dependence on the overall initial strength or type of an interaction (or both). Table 1 indicates the quantities we are investigating in this survey, with some preliminary qualitative findings. We hope that this work may clarify the evolution of AGN and tidal events, and the role of dust and star-formation.

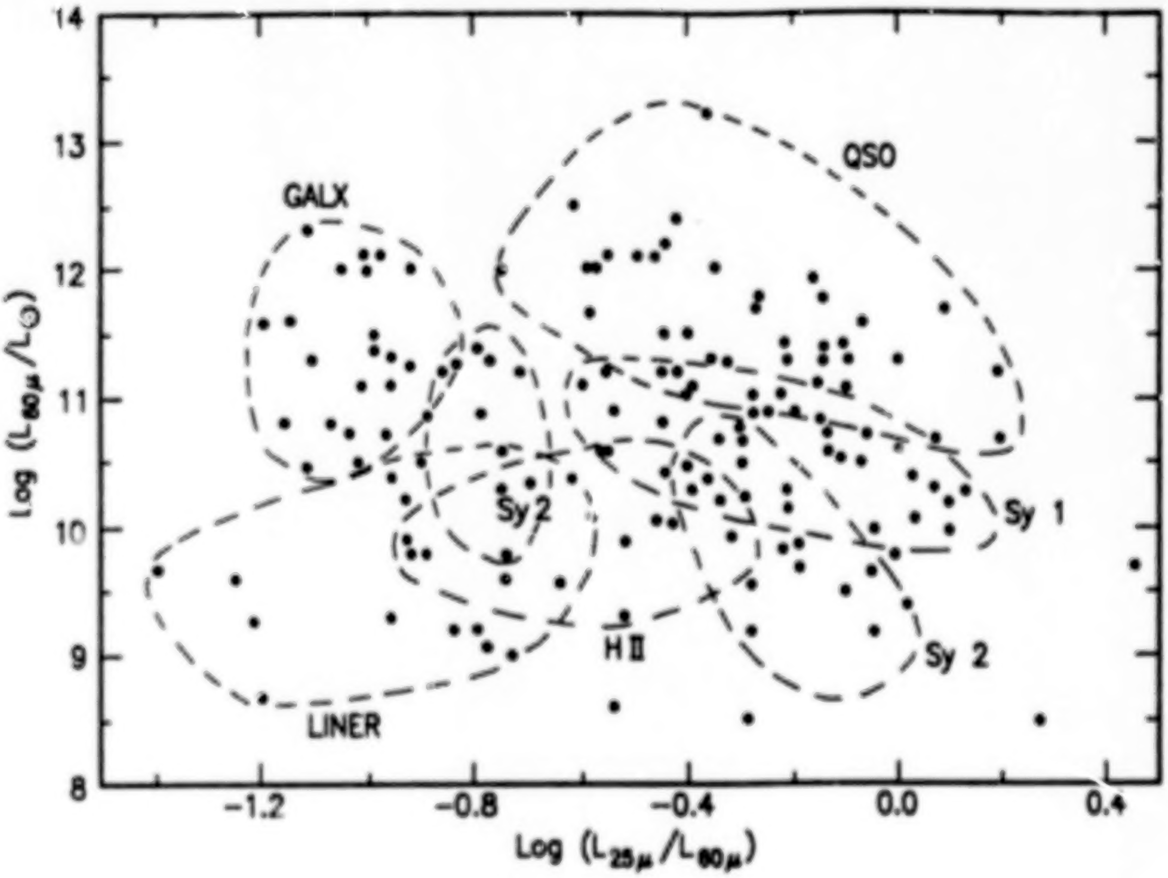

Fig 1. Objects in IR-selected survey in IR colour-luminosity plane. Outlines show where populations of optically different objects lie. We are investigating optical and radio continuum morphologies of these, as well as emission-line gas and H I dynamics, to discover the connections between the groups.

Table 1: summary of results

1. QSO optical imaging (matched samples of >100)

	Radio QSO	R-Q QSO	R-galaxy
Interacting	>68%	57%	84%
$-M_{galx}{}^*$	22.0	20.7	21.1
$(B-R)_0$	.29	.94	.68

* *distributions significantly different*

Refs: Hutchings 1987, Hutchings, Neff, and Janson 1989

2. Evolution of radio quasars (250 radio, 50 optical)

	C	CL	T
Interacting	75%	62%	70%
$-M_{galx}$	23.1	21.9	22.2
companion (kpc)	27	17	32
# companions	3.6	8.8	7.5

Refs: Hutchings, Price and Gower 1988; Neff, Hutchings, Gower 1989; Hutchings and Neff 1990

3. H I observations of IRAS sources (50)

	Int	Non-int
H I normal	50%	69%
H I asymm	50%	31%
$\log(L_{HI})$	2.2	1.7
AGN?	30%	85%

Refs: Hutchings, Price and Gower 1986; Hutchings 1989

4. IRAS source survey (80: radio, opt)

- Almost all are interacting or merging -

	Galaxies	NL AGN	BL AGN
Interactions	high	?	lower
Dust	high	?	lower
L_{IR}	high	range	high
α_{IR}	steep	range	flat
L_{radio}	?	?	?
population dens	?	?	?

Refs: Hutchings and Neff 1988, and ongoing

References

Hutchings J.B. 1987 *Ap.J.* **320**, 122.
Hutchings J.B. 1989 *A.J.* **98**, 524.
Hutchings J.B., Neff S.G., Janson T. 1989 *Ap.J.* **342**, 660.
Hutchings J.B., Neff S.G. 1988 *A.J.* **96**, 1575.
Hutchings J.B., Neff S.G. 1990 A.J. (preprint)
Hutchings J.B., Price R., Gower A.C. 1988 *Ap.J.* **329**, 122.
Neff S.G. Hutchings J.B., Gower A.C. 1989 *A.J.* **97**, 1291.

ARE EXTREMELY LUMINOUS FAR-INFRARED GALAXIES THE RESULT OF MERGING QUASAR CORES?

R.P.Norris, Australia Telescope National Facility

Extremely Luminous far-infrared galaxies (ELFs) are a class of galaxy discovered independently by several groups. The class is characterised by a quasar-like total luminosity ($10^{11} - 10^{13}$ $L_\odot$) which is radiated almost entirely in the far-infrared, and it has been suggested that obscured quasar cores may be responsible for generating this luminosity. Here I demonstrate that ELFs appear in several guises which can be characterised by the number of quasar cores they contain (zero, one or two), and develop a unified model to account for these differences.

ARP 220: EVIDENCE FOR MERGING QUASAR CORES

Arp 220 (IC 4553) has become regarded by many as the archetypal ELF. Evidence for intense starburst activity in it is provided by the optical spectra and high molecular density (e.g. Solomon *et al.* 1990). In addition, the disturbed morphology, extended tidal plumes and shock- excited infrared spectrum (Joseph *et al.* 1984) all strongly suggest that Arp 220 is the result of a recent merger.

However, the 40 or so magnitudes of extinction to the core of Arp 220 prevent us from using optical techniques to probe its innermost secrets. Radio observations, on the other hand, are not affected in this way, and have demonstrated the presence of a quasar-like core. The evidence for this is principally the existence of a compact radio nucleus with a high brightness temperature (Norris, 1985, 1988), but is supported by the broad lines seen in Brackett-alpha emission (DePoy *et al.* 1987) and in Hβ absorption (Heckman *et al.* 1983).

Radio observations at sub-arcsec resolution (Norris, 1988) have produced the surprising result that the nucleus of Arp 220 contains not one but two compact radio cores. These probably represent two separate quasar nuclei for the following reasons: (i) the appearance, surface brightness, and scale of these differ sufficiently from the classical 'radio doubles' to indicate that they cannot be easily explained in terms of lobes from a common nucleus; (ii) VLBI observations (Diamond *et al.* 1989) indicate that both have pc-sized central components; (iii) high-resolution near-infrared images (Carico *et al.* 1990; Graham *et al.* 1990) show two condensations, which are presumably galactic nuclei, coincident with the radio cores.

Each of these cores therefore bears the hallmarks of a compact quasar nucleus, indicating that the pair represents either a gravitationally lensed core or else a pair of merging nuclei. Because of the strong evidence for a merger, and in the absence of any other evidence for a gravitational lens, I consider here only the hypothesis that Arp 220 contains a pair of merging nuclei.

The two nuclei of Arp 220 have a projected separation of about 350 pc, compared to the kpc separations normally observed in interacting active galaxies. Modelling and numerical calculations (e.g. Begelman *et al.* 1980; Roos, 1985) have shown that two merging nuclei would spend only a short period at such a small separation before spiralling in towards their common potential well. Thus such a configuration is so rare that it can account for only a small fraction of ELFs.

I conclude that Arp 220 no longer appears archetypal, but instead appears to be an extremely peculiar ELF. It has been noticeable in this conference how many graphs have been shown with their axes extended to accommodate Arp 220! It has many superlative claims: it has the highest far-IR excess of any UGC galaxy; it was the first OH megamaser (and still the brightest) to be discovered; and it refuses to obey the well- established radio-FIR correlation. Its optical spectrum appears at first to be that of a starburst, but closer examination (and infrared spectra) show broad quasar-like wings. Of the tens of ELFs now studied in detail, Arp 220 remains unique. Thus there is no conflict with the inferred brief lifetime and rarity of its closely separated cores.

Arp 220 is in many senses the most extreme ELF, and yet typifies many of the properties of other ELFs, and so we must consider its position in the hierarchy of ELFs.

ARE QUASAR CORES PRESENT IN ALL ELFS?

The evidence that Arp 220 is powered by an obscured quasar core has led to the suggestion (Sanders *et al.* 1988) that all such objects are powered by quasar cores, and that ELFs represent nascent quasars. However, the competing hypotheses that at least some of these objects are powered by 'super-starburst' activity or by inter-galactic collisions have also gained currency. The plot is thickened further by the common occurrence of tidal tails, interacting companions, and other evidence of disruption.

A long-baseline radio interferometer provides a keen tool for discriminating between these mechanisms, since such an observation is sensitive only to fine structure with high brightness temperature. The 275-km Parkes-Tidbinbilla Interferometer (PTI) has therefore been used to survey a sample of Seyferts, starbursts, and ELFs. The PTI can detect pc-sized quasar cores, with brightness temperatures $\approx 10^8$ K, but is blind to the extended kpc-sized starburst regions which have typical brightness temperatures of 10^4 K.

In our sample of normal starbursts and Seyferts, we found (Norris *et al.* 1988, 1990) that radio cores are common in optically selected Seyferts, but rare in optically selected starburst galaxies, confirming that the Seyferts are intrinsically different from starbursts, and verifying the validity of the technique.

When we turned our attention to a sample of ELFs previously classified by their optical spectral line ratios into Seyfert-like and starburst-like, we found that radio cores are common in ELFs with Seyfert-like spectra, but rare otherwise. These results demonstrate that there are two separate populations of objects masquerading as ELFs. In one of these populations, the ELFs do contain quasar cores and betray them by a Seyfert-like spectrum. However, those in the other population, which includes some of the most luminous ELFs, do not, and therefore require some other mechanism to explain their activity.

TOWARDS A UNIFIED MODEL FOR ELFS

We are forced into the unsatisfactory situation of requiring two different types of ELFs: those with Seyfert-like spectra which often contain a radio core, and those with starburst-like spectra which rarely contain a radio core. Our observations so far place tens of members in each class. Arp 220 appears to occupy a third class: a starburst galaxy concealing two quasar cores. Obviously, a model to explain ELFs must explain these results, and must also embody the strong evidence for interactions in ELFs of all classes.

Here I speculate on one such model, although clearly variations on this theme are also possible. I assume that some, but not all, galaxies contain quiescent massive black holes (MBH) at their centres, legacies of their quasar youths, and consider the later stages of the merging of two galaxies. The models and timescales used here are derived from calculations and simulations such as those of Begelman *et al.* (1980), Roos (1981, 1989), and Hernquist (1989).

(i) Two spiral galaxies, which may or may not contain a quiescent MBH, start the merging process by entering a decaying binary orbit with a separation of a few kpc. During this process, shock waves in the disks of the galaxies cause bursts of star formation and the consequent heating of large masses of dust. In this stage the object appears as a starburst-like ELF. If a MBH is present, then the kinematic disruption within the body of the galaxy may start re-fuelling of the MBH, resulting in a mildly Seyfert-like ELF. The Seyfert or quasar core may not appear optically at this stage because of the high extinction to the galactic centre. This phase lasts for perhaps 10^9 years.

(ii) Dynamical friction eventually causes the two galactic nuclei to approach each other to within a few hundred parsecs, with the luminosity of both starburst and Seyfert activity increasing. If two MBH are present, both are fuelled, giving the appearance of two independent quasar cores, as in Arp 220. Note that if there are no MBH then no quasar cores will be present, so presumably the object will appear as a particularly luminous starburst-like ELF. This phase lasts for perhaps $10^7 - 10^8$ years.

(iii) Eventually, the binary orbit decays and the nuclei merge. The starburst activity and MBH refuelling (if present) will continue, but gradually the dust will be blown away (or converted into stars) exposing the nucleus. The galaxy will then appear as a normal Seyfert or starburst galaxy, depending on whether a MBH is present. This activity may continue for about $10^7 - 10^8$ years until the starburst cycle ends, the MBH loss-cone orbits are depleted, and the galaxy returns once more to its inactive state.

Other embellishments to this model are also possible. For example, we may consider whether we should, instead of simply classifying objects as Seyfert or starburst, place them on a starburst-Liner-Seyfert scale. Their position on this scale would then be determined by the ratio of MBH to starburst activity, which in turn may depend simply on the masses of MBH within the galaxies. We can also speculate whether the eventual product of several such mergers might be an elliptical galaxy.

Finally, I note that the model above is not a unique solution to the observational data. It is obvious that there is a diversity of significant relationships between the different classes of active galaxy, and consequently the time is ripe for an 'HR diagram' or 'periodic table' of active galaxies in general. Further observations, particularly at radio and infrared wavelengths, will be required before we can determine whether the model presented here, or some other model, may play a central role in the construction of this diagram.

ACKNOWLEDGEMENTS

I thank James Graham and Dave Carico for permission to cite material prior to publication, and Dave Allen, Jim Caswell, and Alan Roy for comments on this paper.

REFERENCES

Begelman, M. C., Blandford, R. D., & Rees, M. J., 1980, Nature, 287,307.

Carico, D. P., Graham, J. R., Matthews, K., Wilson, T. D., Soifer, B. T., Neugebauer, G., & Sanders, D. B., 1990, Astrophys. J., 349, L39.

DePoy, D. L., Becklin, E. E., & Geballe, T. R., 1987, Astrophys. J. Lett., 316, L63.

Diamond, P. J., Norris, R. P., Baan, W. A., & Booth, R. S., 1989, Astrophys. J., 340, L49.

Graham, J. R., Carico, D. P., Matthews, K., Neugebauer, G., & Soifer, B. T., 1990. in preparation.

Heckman, T. M., van Breugel, W., Miley, G. K., & Butcher, H. R., 1983, Astron. J., 88, 1077.

Hernquist, L., 1989, Nature, 340, 687.

Joseph, R. D., Wright, G. S., & Wade, R., 1984, Nature, 311, 132.

Norris, R. P., 1985, Mon. Not. R. astr. Soc., 216, 701.

Norris, R. P., 1988, Mon. Not. R. astr. Soc., 230, 345.

Norris, R. P., Kesteven, M. J., Allen, D. A., & Troup, E. R., 1988, Mon. Not. R. astr. Soc., 234, 51p.

Norris, R. P., Allen, D. A., Sramek, R. A., Kesteven, M. J., & Troup, E. R., 1990, Astrophys. J., in press.

Roos, N., 1981. Astron. Astrophys., 104, 218.

Roos, N., 1985, Astrophys. J., 294, 479.

Roos, N., 1989, in *Active Galactic Nuclei*, ed. D. E. Osterbrock & J. S. Miller, (Kluwer, Dordrecht).

Sanders, D. B., Soifer, B. T., Elias, J. H., Neugebauer, G., and Matthews, K. 1988, Astrophys. J., 328, L35.

Solomon, P. M., Radford, S. J. E, & Downes, D., 1990, Astrophys. J., 348, L53.

Kembhavi: Could Sey-Elfs be relativistically beamed Sb-Elfs?

Norris: This is a very interesting question that we are actively pursuing. My quess is that a beaming model (as suggested by Barthel (1989 and others may be a factor, but it cannot explain everything. For example, Barthel's model would suggest that we should detect SyIs more often than SyIIs, whereas, if anything, we detect more SyIIs than SyIs.

Heckman: It is very interesting that you find that many FIRG's/ELF's (like Arp 220) probably have "buried" AGN's. However, it is not clear that these AGN's make important contributions to the overall energy budget. Rieke showed that "ultra-luminous" far-IR galaxies are strongly deficient in hard X-ray emission compared to the hypothesis that all of the IR emission is powered by a standard QSO. He concluded that AGN's could contribute only a small fraction of the IR luminosity, unless they were very peculiar AGN's that were abnormally weak at 10 keV.

Norris: Yes. It's interesting that, although we've shown that some, like Arp 220, do contain a buried quasar, many ELF's don't contain one, and so we are now forced to search for an alternative mechanism. Given the existence of this mechanism, we must then ask how important it is in things like Arp 220. I don't have an answer, but my quess is that, as you suggest, the quasar core may not at present be the dominant energy source. The existence of a quasar core, however, may still be important as we try to place ELF's into the "periodic table" of galaxies, and the core may evolve with time into a dominant position.

van Breugel: What are the spectral indices of the two radio components in Arp 220? If both components (one is even resolved) have a steep spectral index and indeed are AGN's, then what is the physical nature of the radio emission (AGN's at radio wavelengths normally have flat radio spectra and are extremely compact; i.e., synchrotron self-absorbed.

Simkin: Comment on discussion by Norris and Van Breugel--"Why is the core of Arp 220 not a flat spectrum radio source?" (by Van Breugel). Seyferts are not radio loud.

Norris: I agree. It's dangerous to assume that Seyferts should have flat-spectrum cores like the radio-loud quasars do. Observationally, most Seyferts do not seem to have flat-spectrum cores, and their radio luminosities would classify most of them as radio-quiet quasars.

Norris: They both have steep ($\alpha \sim -0.7$) indices, but then observationally I would say that most Seyferts have steep-spectrum cores, too. As for the physical origin of this spectral index, I'm not sure what it's telling us. Perhaps an appreciable amount of the core emission is actually from a nuclear starburst. In the case of Arp 220 I presume that, in addition to quasar cores, starburst activity contributes a substantial fraction of the energy.

CENTRAL ACTIVITY IN 60 MICRON PEAKERS

Charlene A. Heisler[1] and J.P. Vader[2]
Yale University, Dept. of Astronomy
Box 6666, New Haven, CT , 06511
and
Jay A. Frogel[1]
Ohio State University, Dept. of Astronomy
174 W. 18th Avenue, Columbus, OH, 43210

Abstract

We present CCD imaging results of our sample of IRAS galaxies with spectral energy distributions peaking at 60μm (Vader et al 1988). The results support our suggestion that the activity in 60μm peaking galaxies is centrally concentrated, and represents an early stage of dust-embedded nuclear activity. This activity is probably triggered by a recent interaction/merger event as indicated by their peculiar optical morphologies. We propose that 60μm peakers are the precursors of S0's in the case of amorphous systems, and ellipticals in the case of interacting galaxies.

Data Analysis and Results

The Far-Infrared luminosity of 60μm Peakers spans a range of four orders of magnitude, with a median value of $3 \times 10^{10}\, L_{\odot}$. This median value is a factor of 2 greater than the Bushouse (1986) interacting sample and 10 greater than the control sample of isolated spirals. (Fig.1) The lowest luminosity objects - IIZw40 and NGC5253- are well studied, nearby prototypes of amorphous galaxies. The highest luminosity sources are ultraluminous galaxies ($L_{FIR} > 4 \times 10^{11}\, L_{\odot}$), which are dust-enshrouded quasars (Frogel et al. 1989), and presumably are the result of a recent merger/interaction event.

All of the 60μm Peakers are emission line galaxies that are HII region-like (36%), Seyfert type 2 (54%), and Seyfert type 1 (10%). A catalog of the spectra is in preparation (Vader et al 1990).

---

[1] Guest Investigator Cerro Tololo Inter-American Observatories, N.O.A.O., operated by AURA Inc., under contract with the National Science Foundation

[2] Guest Investigator Very Large Array, N.R.A.O., operated by AURA Inc., under contract with National Science Foundation

Figure One

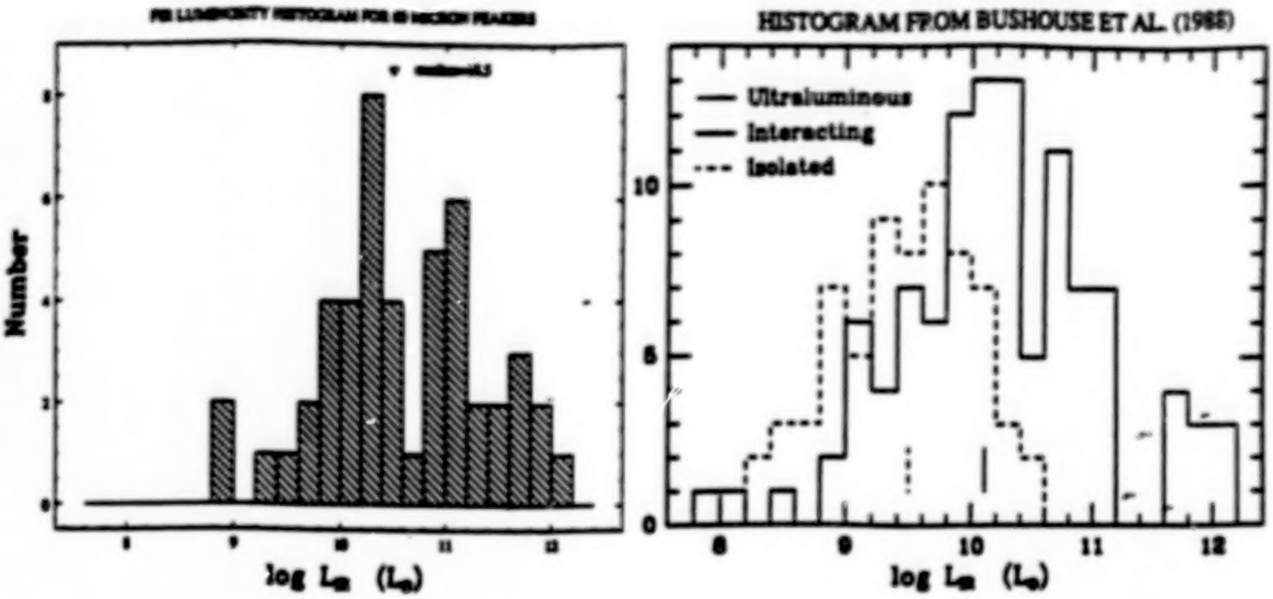

Centrally concentrated activity was shown for all galaxies in our sample for which Hα imaging was obtained. The galaxies observed thus far have 80% of the total measured Hα flux contained within a region which is ~0.8 kpc to 3 kpc. On the other hand we find that in the B broadband filters the galaxies are more diffuse - 80% of the blue flux is contained in a region 1.5 to 4 times the size of the Hα emission line region (Table I). We compare the Hα flux measured from our CCD images to those determined from our nuclear spectra, and find agreement to within a factor of 2. In Fig. 2 we plot the Hα flux (corrected for galactic and internal reddening) versus the far-infrared flux. For the 60μm Peakers, the ratio of the FIR to the Hα luminosities is fairly constant, and is intermediate between that of optically selected spirals (Persson and Helou 1987), and interacting galaxies (Bushouse 1987). The lower values of $L_{FIR}/L_{H\alpha}$ for optically selected spirals is due to the absence of a dust obscured central source, while the higher values for the strongly interacting sample may be understood in terms of a cirrus component which is insignificant in the 60μm Peakers.

We can now use the far-infrared and Hα luminosities to calculate the covering factor of the central active source. The expected ratios of the Lyman continuum luminosity, L_{UV}, to Hα luminosity depends on the UV spectral energy distribution. Values of order 30 are obtained for both OB-star clusters (Mezger et al. 1974), and non-thermal sources (cf. Heisler et al. 1989). Taking into account that about 60% of the total UV luminosity is directly absorbed by the dust one expects $L_{60\mu} \simeq 45 L_{H\alpha}$ for optically thin dust, as is observed for normal HII regions. The UV luminosity inferred from $L_{H\alpha}$ represents a fraction 1-f of the total UV luminosity and, given that in the optically thick case $L_{60\mu}/L_{H\alpha} = 45f/(1-f)$, we find a typical covering factor of about 80%.

Table I

IRAS NAME	$R(H\alpha)_{80\%}$ (kpc)	$R(B)_{80\%}$ (kpc)
05570-8123	0.87	1.54
06488+2731	3.27	6.94
08014+0515	0.98	3.06
09497+0122	0.85	1.67
10567-3323	3.51	5.12
13329-3402	0.35	1.51
14082+1347	3.24	6.52
14167-7236	1.54	4.97
16380-8120	1.25	2.38
183343-6528	1.31	3.62
20253-8152	1.24	3.77
20481-5715	3.39	6.14

An estimate of the location of the dust can be obtained by assuming that the dust is concentrated in a spherical shell of radius r centered on the nuclear source, in which case

$$r = 440\left(\frac{50K}{T}\right)^{5/2}\left(\frac{L_{60\mu}}{10^{10}L_{\odot}}\right)^{1/2} \text{pc.}$$

For a dust temperature of 50K (inferred from the 60 and 100μm fluxes for dust with emissivity proportional to frequency, and $L_{60\mu} = 10^{10}$ to 10^{12} $L_{\odot}$) this yields radii in the range 0.1 to 1kpc, which is comparable to the size of the narrow line region in Seyfert galaxies, and suggests that the obscuring dust is close to the nucleus. The close proximity of obscuring dust to the central source points towards the relative youth of central activity in these objects. The 60μm Peakers are generally kiloparsec-scale radio sources, and some of them show dust obscured Seyfert 1 nuclei in polarized light (Miller and Goodrich 1987; Kay and Miller 1989), which further attests to the youth of the central activity.

Figure Two

FIR Versus H-alpha Fluxes

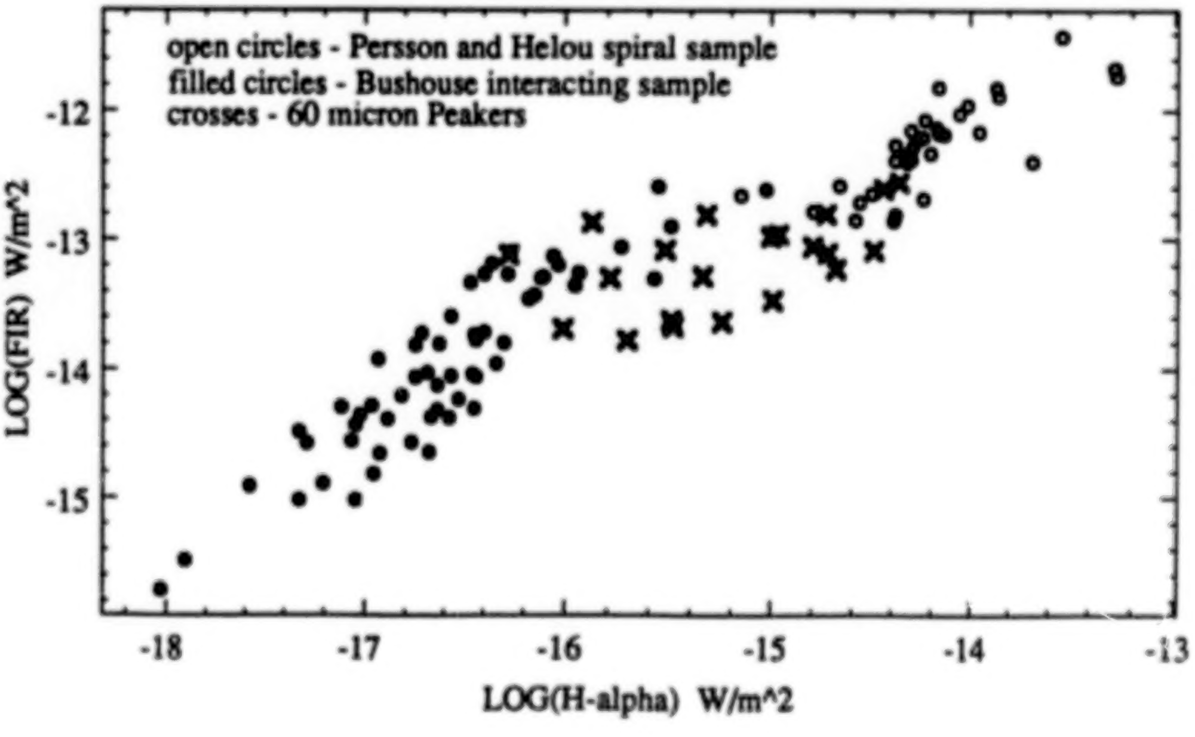

Figure Three

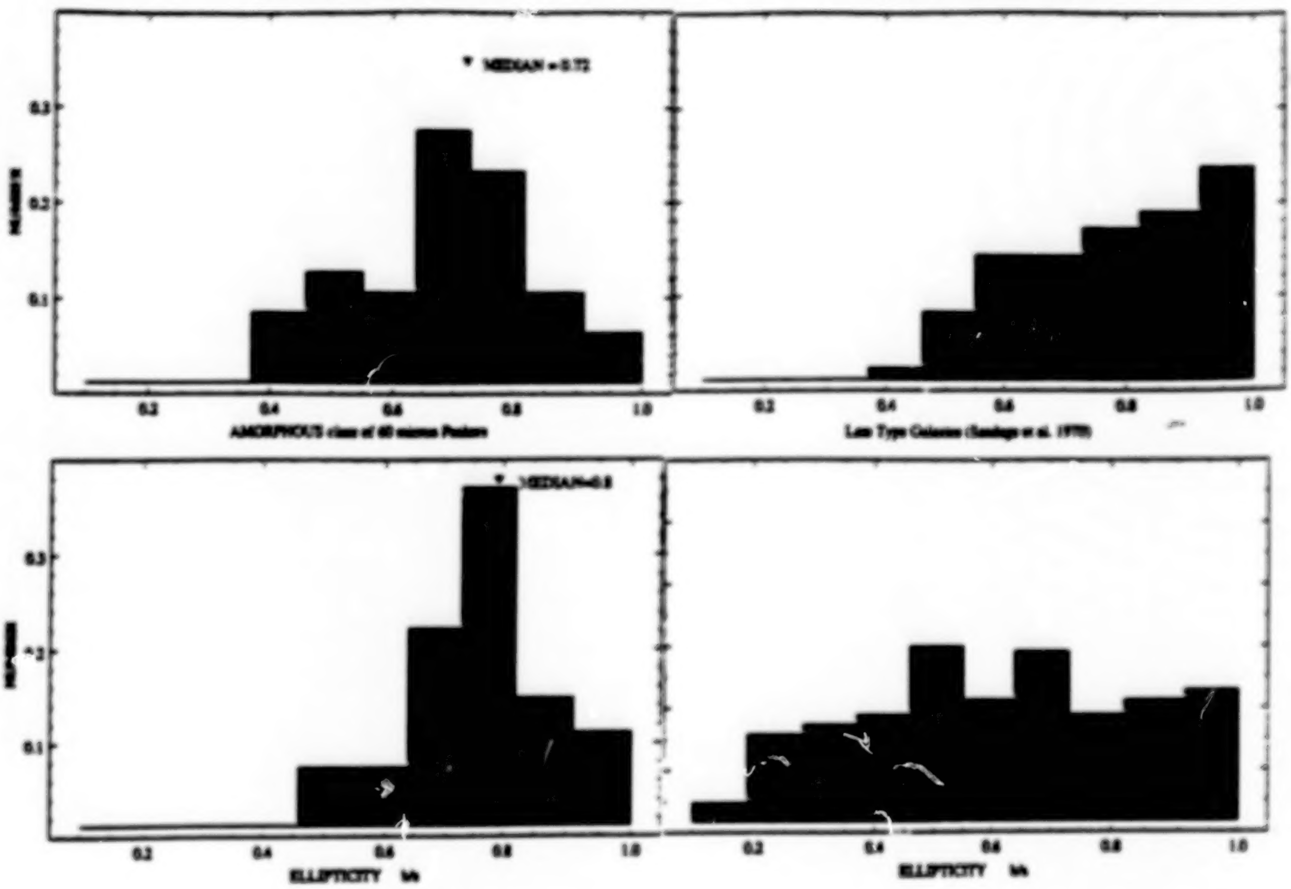

The optical morphologies of the 60μm Peakers can be classified as having a disturbed appearance (25%), or as having a smooth light distribution (70%). The remaining 5% of the 60μm Peakers are normal spirals. The amorphous, S0's, and early type galaxies have all been combined into a class of objects possesing a smooth light distribution, because the above distinctions are not clear cut. For example NGC5253 is a prototype amorphous galaxy, but has also been classified as E and S0 by others. Nearly half of the amorphous galaxies show evidence for a recent interaction/merger event (shells,rings, dust patches). This classification issue can be further addressed by examining the ellipticities of the galaxies.

We have measured the apparent ellipticity of the 60μm Peakers at an isophotal blue magnitude of approximately 22 mag/arcsec^2. Ellipticity distributions are shown in Fig. 3. A chi-squared test tells us that to a confidence level better than 99%, the whole sample of the 60μm Peakers does not have the same ellipticity distribution as either early or late type galaxies (Sandage et al 1970), and similarly when one considers only the amorphous sytems. Preliminary results indicate that the amorphous galaxies have surface brightness profiles consistent with S0's. We suggest that the amorphous galaxies in our sample are the precursors of S0 galaxies, and, as has been proposed by others (eg. Toomre and Toomre 1972), the strongly interacting galaxies are precursors of ellipticals, some of which may develop into strong radio sources.

Conclusion

We have presented evidence that the activity in 60μm Peakers is centrally concentrated and heavily obscured at optical wavelengths. We propose that nuclear activity in these galaxies is a recent phenomenon, and our data supports numerical simulations that show that an interaction/merger event can drive gas to the center of a galaxy in a short time scale (~10^8 yrs), and provide fuel for an active nucleus and/or intense centrally concentrated starburst (eg. Hernquist private comm., Noguchi 1988). Our results suggest that 60μm Peakers may be the precursosrs of S0's in the case of amorphous galaxies, and ellipticals in the case of strongly interacting systems.

References

Bushouse H. (1986), Ph.D. thesis, University of Illinois

Bushouse H. (1987), Astrophys. J., **320**,49

Bushouse H.A., Lamb S.A., and Werner M.W., (1988), Astrophys. J.,**335**,79

Frogel J.A., Gillett F.C., Terndrup D.M. and Vader J.P., (1989), Astrophys J.,**343**,672

Heisler C.A., Vader J.P., and Frogel J.A., (1989), Astron. J.,**97**,986

Kay L.E. and Miller J.S., (1989), B.A.A.S.,**21**,1099

Mezger P.G., Smith L.F., Churchwell E., (1974), Astron. and Astrophys.,**32**,269

Miller J.S. and Goodrich R.W., (1987), B.A.A.S.,**19**,695

Noguchi, (1988), Astron. and Astrophys.,**201**,37

Persson Lonsdale C.J. and Helou G., (1987), Astrophys. J.,**314**,1

Sandage A., Freeman K.C. and Stokes N.R., (1970) Astrophys. J., **160**,831

Toomre A. and Toomre J., (1972), Astrophys. J., **178**,623

Vader J.P., Frogel J.A. and Gillett F.C., (1988), in *Active Galactic Nuclei*, conference proceedings held at Georgia State University, (Springer-Verlag), eds. H.R. Miller and P.J. Wiita., p 134

DISCUSSION

Kennicutt:
1. Have you compared the properties of your 60 μ selected sample to other surveys of hot IRAS galaxies based on 25 μ emission?

2. Is there any confirming evidence from the morphologies or kinematics of these galaxies for the idea that they are in early stages of activity?

Heisler:
1. The fractions of Seyfert and starburst galaxies in 60 μm peakers are fairly typical for IRAS galaxies with warm 60 μm/25 μm colours.

2. We do not have kinematical data. The morphology of the objects indicate a recent interaction. The evidence for an early stage of activity is the centrally concentrated activity, compact central radio source (~ kpc scale), and a dust-enshrouded central source which is still close to the nucleus and thus fairly warm and producing the warm FIR colours.

Sulentic: One group of 60 μm peakers is the amorphous class of galaxies. We have obtained spectra of another member of this class NGC 2777, and find it to have a remarkably early (A type) absorption spectrum. Other galaxies in this class also show such a population. Has anyone observed an old stellar component in any of this class?

Goudfrooij: You showed from your two-colour plot that the galaxies in your sample are reddened by an amount of E(B-V) = 0.4. Do you also find this value when determining the Hα/Hβ ratios in your optical spectra? Does the difference of the two E(B-V) values (if present) vary with the type of emission-line activity of the galaxy?

Heisler: The Hα/Hβ ratios indicate an average internal reddening of E(B-V) ~ 0.5. The emission-line activity type of the galaxy does not seem to affect the E(B-V) value.

Galaxy Interactions and Strength of Nuclear Activity

S. M. Simkin
Michigan State University
East Lansing, MI 48824

INTRODUCTION

Almost a decade ago, the morphological similarities between patterns seen in Seyfert galaxies and those produced by gravitational forcing led to the suggestion that Seyfert activity might be fueled by material inflow induced by either a central bar or a perturbing companion (Simkin, Su, and Schwarz, 1980). More recent theoretical calculations suggest that such a feeding mechanism may involve a central bar-like, structure even if initially induced by the tidal effects of a companion galaxy (Noguchi, 1988a,b).

The recent literature on the prevalence of Seyfert galaxy companions, however, is somewhat confusing and, at initial glance, contradictory (Byrd, et al., 1987, Dahari, 1984, 1985, Fuentes-Williams, and Stocke, 1988, Keel, et al., 1985, Kennicutt, and Keel, 1984, Kollatschny and Fricke, 1989, Petrosian, 1982, and Petrosian and Turatto, 1986). Most studies find either a weak correlation between excess companions or none at all. All of these different studies are subject to different selection criteria, and most authors have attributed their disparate conclusion to selection effects (op. cit.).

An independent analysis of the material in these papers by the present author seems to suggest an excess of nearby companions for Seyfert 2 galaxies, but not for Seyfert 1 galaxies (with the term *nearby* subject to different defining criteria for different studies). On the other hand, two of the cited studies show no significant difference in excess companion density between the two Seyfert classes (Byrd, et al., 1987, and Kollatschny and Fricke, 1989). Both of these latter studies, however, deal with small numbers of objects.

DIFFERENCES BETWEEN TYPE 1 and TYPE 2 SEYFERTS

When all of the data in the papers cited above are combined, an interesting trend emerges. There are 34 pairs for the Seyferts with companions and $z \leq 4000$ km s^{-1}. This comprises roughly 40% of the known Seyferts with z in this redshift range. Given the very different selection criteria of the different studies which have been included, it is difficult to evaluate just how representative these data are. However, twelve of these pairs contain Seyfert 1 galaxies and twenty two contain Seyfert 2's. Thus the ratio of Sey 1's to Sey 2's (approximately 1:2) is similar to that found for nearby, volume limited samples of Seyfert galaxies irrespective of their status as companions (Simkin, Su, and Schwarz, 1980). Although this does not prove the sample is unbiased, it does support its credibility.

Converting angular separation to projected physical separation using a Hubble distance based on $H_o = 100$ and ploting this against radial velocity difference for each pair gives the results shown in Figure 1. The plot demonstrates a fairly clear distinction between Seyfert 1 and Seyfert 2 galaxies. For the objects in this sample, 10 (90 %) of the Seyfert 1 galaxies are separated from their "companions" by projected distances of *more* than 75 kpc while 18 (90%) of the Seyfert 2's are separated by *less* than 75kpc.

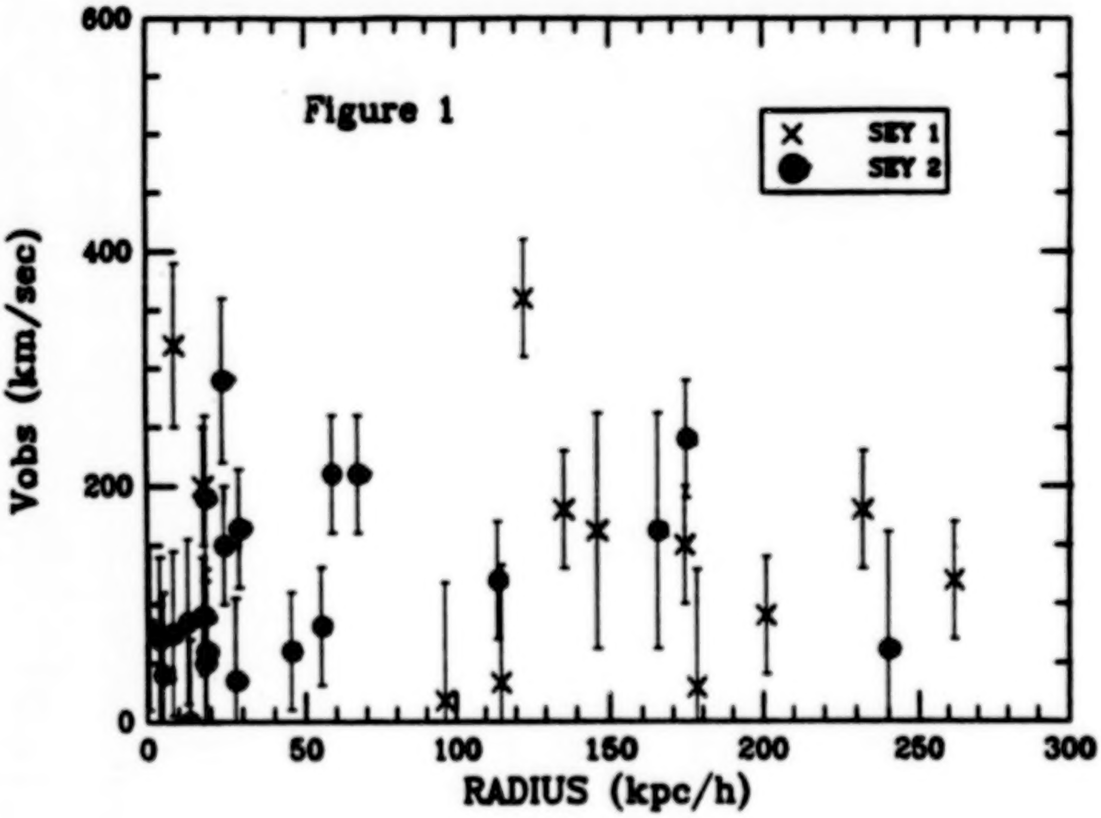

DISCUSSION

There are two straightforward interpretations of the difference between Seyfert 1 and Seyfert 2 galaxies shown in Figure 1: i) either most Seyfert 1 galaxies do not have companions (the plotted points represent chance projection) while Seyfert 2 galaxies do, or ii) there is a true physical distinction between the two types of galaxies and this distinction is related to the nature of the tidal pertubation they have experienced. The first possibility seems somewhat unlikely since, as noted above, the *fraction* of Sey1 and Sey2, galaxies with respect to those in a volume limited sample, is the same for those with "companions" as for those without. In addition, the selection criteria used in the studies from which these data were taken included a limit on velocity, thus sharply reducing the number of expected pairs attributable to projection effects.

The second possibility is supported by the fact that there is other, independent evidence for morphological differences between type 1 and type 2 Seyferts which may also be attributed to differences in the histories of their gravitational disturbances. Seyfert 1 galaxies have narrower spiral arm (or ring) widths than Seyfert 2 galaxies of similar physical size (Simkin et al., 1989, 1990). Again, there are two possiblities which immediately come to mind: i) the arm-ring features in the Seyfert 1 galaxies may be produced by gravitational disturbances leading to pattern speeds which generate more narrow features (sharper shocks) than those for the Seyfert 2's, or ii) the Seyfert 2 galaxies may have evolved from Seyfert 1's with their arm-ring features spreading out in width with age.

This "aging" interpretation of arm width difference is unlikely, however, because the UVB colors for the disks of nearby Seyfert galaxies show no distinctions between type 1 and type 2, and the colors of stars produced in spiral arm shocks should redden with age (Simkin et al., 1990). Thus it is most likely that the much larger average projected separation found between Sey 1's and their companions than between Sey 2's and theirs, represents a real physical distinction.

One other interesting result can be obtained from the sample of Seyfert galaxies discussed here. If one assumes that all of the objects are true physical companions (in effect, using nuclear activity as a diagnostic of gravitational interaction), then a crude analysis gives the following mean physical parameters for the sample: mean mass $\sim 10^{12} M_\odot$, mean size $\sim$ 30 - 40 kpc, mean $M/L \sim$ 8 - 10 solar units. These are quite comparable to the values reported in this conference for the binary galaxy sample of Karechentsev, either an amusing coincidence or additional support for the interaction hypothesis.

CONCLUSIONS

Analysis of data in the literature for differential velocities and projected separations of nearby Seyfert galaxies with possible companions shows a clear difference in projected separations between type 1's and type 2's. This kinematic difference between the two activity classes reinforces other independent evidence that their different nuclear characteristics are related to a non-nuclear physical distinction between the two classes. The differential velocities and projected separations of the galaxy pairs in this sample yield mean galaxy masses, sizes, and mass to light ratios which are consistent with those found by the statistical methods of Karachentsev. Although the galaxy sample discussed here is too small and too poorly defined to provide robust support for these conclusions, the results strongly suggest that nuclear activity in Seyfert galaxies is associated with gravitational perturbations from companion galaxies, and that there are physical distinctions between the host companions of Seyfert 1 and Seyfert 2 nuclei which may depend both on the envronment and the structure of the host galaxy itself.

REFERENCES

Byrd, G., Sundelius, B., and Valtonen, 1987, Astron. and Ap., **171**, 16.

Dahari, O., 1984, A.J., **89**, 966.

Dahari, O., 1985, A.J., **90**, 1772.

Fuentes-Williams, T. and Stocke, J. T., 1988, A.J., **96**, 1235.

Keel, W.C., et al., 1985, A.J., **90**, 708.

Kennicutt, R.C., and Keel, W.C., 1984, Ap. J. Lett., **279**, L5.

Kollatschny W., and Fricke K.J., 1989, Astr. and Ap., **219**, 34.

Noguchi, M., 1988a, M.N.R.A.S. **288**, 635.

Noguchi, M., 1988b, *IAU Collquium No. 96.*

Petrosian, A.R., 1982, Astrofizika, **18**, 548.

Petrosian, A.R., and Turatto, M., 1986, Astr. and Ap., **163**, 26.

Simkin, S.M., Su, H-J., and Schwarz, M.P., 1980, Ap.J., **237**, 404.

Simkin, S.M., Mehlberg, L., 1989, B.A.A.S., **21**, 776.

Simkin, S.M., Geimer, S. and Mehlberg, L., 1990 *in preparation*

DISCUSSION

Kochhar: In your picture what separates Seyferts from non-Seyferts?

Simkin: All I was addressing was a mechanism for redistributing angular momentum to permit disk material to flow towards the nucleus. We need to study many systems (get rotation curves, simulate encounters with companions, etc.) to see if the difference between Seyferts and other galaxies with significant redistribution of disk angular momentum is global or if both Seyferts and non-Seyferts have the same global properties but non-Seyferts form "starbursts" while Seyferts also have a "monster" at the center.

COOL INFALLING GAS AND ITS INTERACTION WITH THE HOT ISM OF ELLIPTICAL GALAXIES

W.B. Sparks[1] **and F.D. Macchetto**[1,2]
[1]Space Telescope Science Institute, 3700 San Martin Drive, Baltimore MD 21218*

ABSTRACT

We describe work leading to the suggestion that interaction between infalling cool gas and ambient hot, coronal plasma in elliptical galaxies is responsible for emission filaments, and might remove the need for large mass depositions in cooling flows. A test of the hypothesis is undertaken — the run of surface brightness with radius for the emission lines — and the prediction agrees well with the data.

INTRODUCTION

Observations indicate that infall events are common in elliptical galaxies – high specific angular momentum gas discs, counter-rotating cores, normal dust properties, misaligned and warped dust lanes and Malin-Carter shells. This provides an obvious and likely origin for the extended low excitation emission nebulae and dust lanes often seen in active elliptical galaxies. For example, Sparks, Macchetto and Golombek (1989), Forbes *et al.* this conference, show in all four cases studied extended low excitation optical line emission associated with an infall or merger event.

There is however good evidence indicating that optical line emission is related to the X-ray properties and in particular it preferentially occurs in those galaxies with short cooling time, Hu (1988). This has lead to the proposition that optical emission filaments arise in a cooling flow. Phillips *et al.* (1986) from spectroscopy of nuclei, and Trinchieri & di Serego Alighieri (1989) from imaging found a similar correlation for normal elliptical galaxies, with higher $H\alpha$ line fluxes in galaxies showing X-ray excesses.

This is a clear contradiction. On the one hand there is every reason to think that emission filaments arise from infall events, while on the other there is very good evidence that they are associated with the X-ray properties. Our observations of nearby radio ellipticals indicate that thermal conduction may provide the solution to these two apparently contradictory observational results ***by allowing the infall event to influence the X-ray properties.*** Cool infalling gas in the presence of effective thermal conduction can drain significant energy from a hot X-ray emitting halo thereby mimicing symptoms of the cooling flow. The energy transfer is adequate to power the optical line emission and infra-red radiation.

PREVIOUS OBSERVATIONAL WORK

Sparks *et al.* (1989) describe observations of NGC 4696, the dominant cD galaxy at the center of the Centaurus cluster. The emission-line filament system and dust lane in the central regions of this classical 'cooling-flow' galaxy are more plausibly explained by an external origin for the cooler material than by condensations in a cooling flow — the dust is spatially coincident with the ionised gas, its extinction variation with wavelength is normal, there is kinematic substructure in the galaxy, Danziger & Focardi (1988), and there is a large low surface brightness linear feature which is reasonably explained as a tidal tail, Malin (1985).

Given that an external origin for the cooler gas is favoured, the question of how infalling gas would interact with the ambient hot medium arises, and particularly with regard to energy transfer from the hot plasma to the cool gas. Our observations of the dust lane place good constraints on the dust-lane covering factor which together with the published X–ray gas properties, Matilsky, Jones and Forman (1985), allow us to deduce an available energy input rate of 3×10^{43}erg s^{-1} from saturated electron heat conduction. This compares well to a radiated flux of 1×10^{43}erg s^{-1} in the far-infra-red, Jura *et al.* (1987), and to 0.9×10^{43}erg s^{-1} from line emission, Sparks *et al.* (1989). Energetically, in other words, heat conduction could provide ample power for all the line emission and infra-red radiation we observe. However, if this occcurs, it represents a severe drain of energy from the hot gas — greater than the X–ray losses over a much larger region.

COOL PROPOSITION

Given the fundamental nature of an energy transport process such as electron conduction, i.e. if electron conduction is an effective transport mechanism in one hot plasma it is likely to be so in essentially all, we propose that the *general* explanation for low excitation optical filaments in X–ray luminous elliptical galaxies is *infall*. The short X–ray 'cooling-times' then arise simply as a local depression of temperature caused by heat lost to the dust-lane/filament system.

Infall events are transient, and we propose that in the absence of infalling gas when the cloud has evaporated, formed into stars or been lost to the nucleus, that the hot gas will return to a stable configuration with the rather modest losses due to X–ray emission being balanced by an ample heat supply from elsewhere in the cluster. D'Ercole *et al.* (1989) show that using nominal supernova rates alone there is greater energy input per unit time at the present than there is energy lost from X–ray emission in all elliptical galaxies, and since our original proposition was that heat conduction is effective, then such energy input *is* available to the hot medium as a whole. Kochhar (1989) in fact shows enhanced supernova rates in active ellipticals, which may arise from star formation associated with the infall event and can assist the hot gas in returning to its equilibrium configuration. The criticism that for heat conduction models to be viable requires 'fine tuning' is not valid since we are considering a dynamic transient state in which the cool phase is forced only temporarily on the hot, stable long lived phase.

The heated nature of the debate and July weather in Baltimore lead us to suggest 'coolers' as a concise description of the process advocated.

OBSERVATIONAL TESTS

Having arrived at a very different interpretation of existing observations, we clearly need to investigate predictions and possible tests. For the present work, one particular test is described, namely the run of emission-line surface brightness with radius.

If the conduction model is correct, then the $H\alpha$ line flux should be directly related to the X–ray halo properties, and without any recourse whatsoever to the optical data, it is possible to make a simple prediction of the emission-line surface brightness as a function of radius given the halo properties. Consistent surface brightness distributions have proven a severe problem area for the cooling-flow model, Heckman *et al.* (1989).

Two galaxies have been investigated. M87 is probably the best studied from the X-ray point of view although the emission filament system is somewhat fragmentary. In the innermost regions though, it covers a wider area of the galaxy and the test may be carried out. Heckman *et al.* (1988 preprint) present a surface brightness profile for $H\alpha$ line emission which we calibrated using the information in that paper and the fluxes of Ford & Butcher (1979). Schreier *et al.* (1982) give a simple description of the X-ray gas temperature and density. Using this and setting predicted surface brightness equal to 1% of the available saturated heat flux, $Q_{\rm sat} \propto n_e T^{3/2}$, we obtain the line shown in Figure 1. Outside of regions where seeing and the non-thermal nucleus are likely to confuse, the agreement is extremely good. There is no *a priori* reason why the two curves need be even remotely similar since the prediction was made entirely on the basis of the X-ray atmosphere, yet they lie within a factor of two over two orders of magnitude in surface brightness.

The second galaxy investigated is NGC 1052 the well-know active southern radio elliptical. Here the X-ray data are not so good, but the optical data are more extensive, Sparks *et al.* 1990 in preparation, Forbes *et al.* this conference. Forbes *et al.* summarise the good reasons for believing the gas in NGC 1052 is external in origin. In order to estimate a 'predicted surface brightness', we assumed a galaxy mass distribution given by the light, and solved for an isothermal hot atmosphere. There are more free parameters in this model: the temperature translating into a scale length and density related to the total X-ray flux, and an overall normalization corresponding to the efficiency of energy transfer. We can get a good description of the surface brightness profile for values of these parameters which are all reasonable, again at least to within factors of two or so — $T \approx 5 \times 10^6$K, central density $n_0 \approx 5\text{cm}^{-3}$ but falling quite rapidly, see Figure 2. In this case, other possibilities are also viable and in particular photoionization by the active nucleus is a strong contender.

We conclude, nevertheless, that even though this analysis does not *prove* the validity of the conduction hypothesis, the results *are consistent* with the model and that from the point of view of the test as initially set, the theory passes, and passes well.

CONCLUSIONS

- Observations suggest cool gas comes from infall.
- Observations, statistics and theory imply effective conduction would be energetically important *for all of the X-ray gas, emission-line radiation and infra-red flux.*
- *If conduction does operate, infall events will profoundly affect the hot gas and the cool gas, and may dominate the physical state adopted by both phases.*

Figure 1 $H\alpha$ emission line surface brightness profile of M87 compared to 1% × $Q_{\rm sat}$, the straight line. Log $r = 2$ is ≈ 1.4 arcsec.

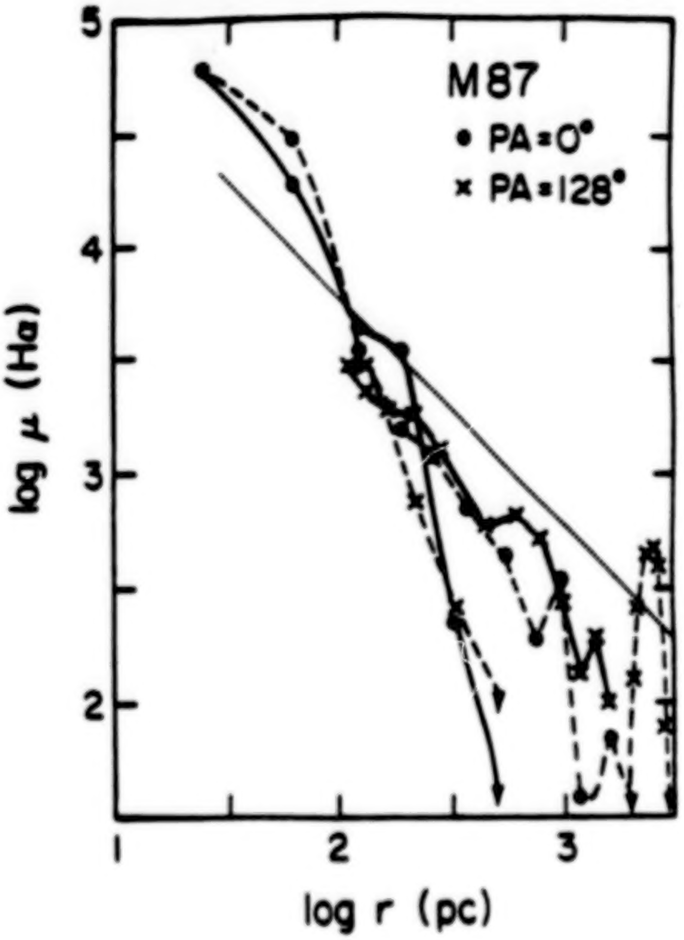

Figure 2 $H\alpha + [NII]$ emission line surface brightness profile for NGC 1052 compared to a thermal conduction heating model. The upper and lower curves are estimates of the uncertainty and the data are cut off at ≈ 40 arcsec.

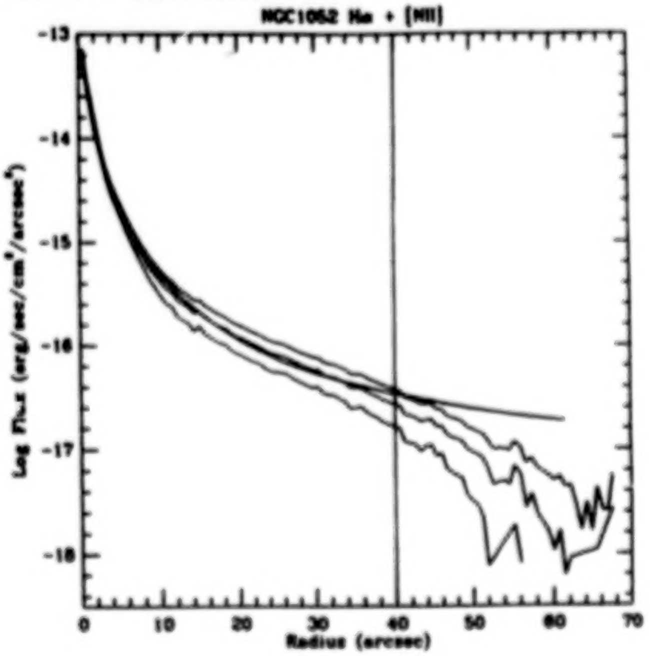

References

Danziger, J., Focardi, P. 1988, in *Cooling Flows in Clusters and Galaxies*, ed. A.C. Fabian (Dordrecht:Kluwer)

D'Ercole, A., Renzini, A., Ciotti, L., Pellegrini, S., 1989, *Ap. J. (Lett)*,**341**,L9.

Ford, H.C., Butcher, H., 1979, *Ap. J. Supp.*,**41**, 147.

Heckman, T.M, Baum, S.A., van Breugel, W.J.M., McCarthy, P., 1989, *Ap. J.*, **338**, 48.

Hu, E. 1988, in *Cooling Flows in Clusters and Galaxies*, ed. A.C. Fabian (Dordrecht:Kluwer)

Jura, M., *et al.* 1987, *Ap J. (Lett)*, **312**,L11

Kochhar, R.K., 1989, *Astrophys. and Space Sci.*, **157**, 305.

Malin, D.F., 1985, in *New Aspects of Galaxy Photometry* ed. J.-L. Nieto,(NY:Springer)

Matilsky, T., Jones, C., Forman, W., 1985, *Ap. J.*,**291**, 621.

Phillips, M.M., Jenkins, C.R., Dopita, M.A., Sadler, E.M., Binette, L., 1986, *A.J.*,**91**, 1062.

Schreier, E.J., Gorenstein, P., Feigelson, E.D., 1982, *Ap.J.*, **261**, 45.

Sparks, W.B., Macchetto, F., and Golombek, D. , 1989, *Ap.J.*, **345**, 153.

---

[1] *Affiliated with the Astrophysics Division, Space Science Department, European Space Agency (ESA).*

[*] *Operated by the Association of Universities for Research in Astronomy. Inc., under contract with the National Aeronautics and Space Administration.*

DISCUSSION

Carilli: What about magnetic fields?

Sparks: Laing & Bridle (1987 MNRAS **228**, 557) resolved out rotation-measure structure elsewhere in the Virgo cluster, suggesting ordered fields on scales $\lesssim$ 2 kpc. Ordered fields don't make much difference to conduction. Rosner & Tucker (1989 Ap. J. **338**, 761) argued that even if fields are tangled, conduction can still be important.

The Nature of the Emission-line Nebulae in Powerful Far-infrared Galaxies

Lee Armus and Timothy M. Heckman
The Johns Hopkins University

George K. Miley
Sterrewacht Leiden

Abstract

We discuss our program of narrow-band (Hα + [NII]) imaging of a sample of 30 powerful far-infrared galaxies (FIRG's) chosen to have far-infrared spectral energy distributions similar to the prototype FIRG's Arp 220, NGC 3690, NGC 6240, and M82. The emission-line nebulae of these IR color-selected sample (ICSS) galaxies as a class are both impressively large (mean half light radius, r ~1.3 Kpc, and mean diameter, D ~16 Kpc) and luminous ($L_{TOT} \sim 10^8 L_\odot$; uncorrected for internal extinction). The mean total Hα + [NII] luminosity of the FIRG's is comparable to that found for pairs of optically selected interacting galaxies (Bushouse, Lamb, and Werner 1988), but is a factor of ~5 greater than that of isolated spirals (Kennicutt and Kent 1983). Only ~25% of the nearby ($z \leq 0.10$) FIRG's have morphologies suggesting that large HII-regions contribut significantly to their emission-line appearance. The broad-band morphologies of our IR color-selected galaxies fall into three major categories. Nearly 75% are single galaxy systems, with the remaining FIRG's being either multiple nuclei systems, or members of interacting pairs. Since we see few (10%) currently interacting FIRG's, yet many (80%) with highly distorted continuum morphologies, our IR color criteria may be preferentially selecting galaxies that have undergone highly inelastic, rapidly merging interactions.

As a class, FIRG's have far-infrared luminosities, $L_{FIR} = 10^{10} - 10^{12} L_\odot$, and far-infrared to blue luminosity ratios $L_{FIR} / L_B = 10 - 100$. The far-infrared radiation from these galaxies is believed to be primarily generated by warm (T ~50 K) dust. The optical spectra of the FIRG's are almost always dominated by emission-lines. The most prominent of these lines are Hα, [NII] λλ6548,6583Å, [SII] λλ6717,6731Å, [OI] λ6300Å, Hβ, and [OIII] λλ4959,5007Å. The sizes, morphologies, and overall luminosities of the FIRG emission-line nebulae are an important probe of their interstellar media. As such, they shed valuable light on the nature of the energy source behind the enhanced activity that readily manifests itself in the far-infrared.

Prior to the present investigation, continuum subtracted narrow band images existed for only a handful of these powerful far-infrared galaxies. Nonetheless it was clear that their emission-line morphologies were nothing like the HII-region dominated disks of normal spiral galaxies. Studies of Arp 220 and NGC 6240 have revealed large scale (tens of Kpc) intricate emission-line nebulosities (Heckman, Armus, and Miley 1987). Narrow-band imaging of the closest FIRG, M82, has uncovered a complex filamentary nebula (McCarthy, Heckman, and van Breugel 1987).

In an attempt to determine whether such spectacular morphology is common among the FIRG's as a class, we have undertaken a narrow-band (Hα + [NII]) survey of 30 galaxies having spectral indices, $\alpha \leq -1.5$ betwee 25μ and 60μ, and $\alpha \geq -0.5$ between 60μ and 100μ (where $S_\nu \propto \nu^\alpha$). The 30 galaxies that make up this study span a large range in redshift ($z = 0.001$-0.169) and far-infrared luminosity ($L_{FIR} = 10^{10}$ - 10^{12} $L_\odot$).

The results of our narrow-band imaging study can be summarized as follows:

(1) - The ICSS FIRG's posess nebular morphologies that range from smooth and structureless to highly complex and chaotic (see Fig. 1), with some showing evidence for ordered structure on scales of a few Kpc to tens of Kpc. Of the 7 ICSS FIRG's that are apparently highly flattened in R ($a/b \geq 2.0$), 6 have Hα + [NII] isophotes that are either more circular than, or perpendicular to their continuum isophotes. This structure may represent emission-line gas that is extended out of the plane of the galaxy.

(2) - Overall the ICSS FIRG emission-line nebulae are quite large, having a mean diameter (maximum extent), D ~16 Kpc, and a mean half-light radius, r_e ~1.3 Kpc. Typically 2/3 of the total Hα + [NII] emission originates from beyond a radius of 1 Kpc.

(3) - The mean total Hα + [NII] luminosity of the nebulae is $\sim 5 \times 10^{41}$ erg s^{-1} (uncorrected for internal extinction). This is comparable to that found for systems (pairs) of optically selected interacting galaxies (Bushouse, Lamb, and Werner 1988), but is a factor of ~5 greater than that found for isolated spirals (Kennicutt and Kent 1983; see Fig. 2). Typical ICSS FIRG's however, may have *intrinsic* Hα + [NII] luminosities that are up to 30 times greater than average non-interacting spiral galaxies, and up to 6 times greater than the most luminous known non-interacting spiral galaxies (Kennicutt 1983). Only ~25% of the nearby ($z \leq 0.10$) ICSS FIRG's have morphologies suggesting that large HII-regions contribute significantly to their emission-line appearance. While previous studies indicate that young stars dominate the optical spectra of the ICSS FIRG's (Armus, Heckman, and Miley 1989), a majority of the nebulae are evidently not powered by hot, young stars distributed in the same manner as they are in normal spiral galaxies (within giant OB associations).

(4) - The Hα + [NII] and the far-infrared luminosities are correlated with the R-band luminosity, with both $\propto L_R^{1.5\text{-}1.7}$ (see Fig. 3).

Nearly 75% of the ICSS FIRG's are single galaxy systems, with the remaining galaxies being either multiple nuclei systems, or members of interacting pairs. Since only ~10% are currently interacting, yet nearly 80% have distorted continuum morphologies, our IR color criteria may be preferentially selecting galaxies undergoing highly inelastic, rapidly merging interactions. A small, but non-neglegible fraction (~20%) of all the ICSS FIRG's appear completely undisturbed morphologically. These morphologically quiescent ICSS FIRG's have far-infrared luminosities that are comparable to those found for the sample as a whole.

Conclusions

The morphologies of the ICSS FIRG nebulae are very different from those of normal star-forming disk galaxies, yet young stars apparently dominate the optical continua (Armus, Heckman, and Miley 1989). We therefore propose that a FIRG be visualized as a galaxy-scale "super-giant" HII-region: a galaxy whose large-scale ISM is being ionized by UV radiation and possibly mass outflows produced by an intense circumnuclear burst of star formation. In the vast majority of FIRG's this enhanced star formation has apparently been triggered by a galactic interaction. The fact that we see few *currently* interacting sample galaxies suggests that FIRG's may be the victims of rapidly merging encounters.

References

Armus, L., Heckman, T.M., and Miley, G.K. 1989, *ApJ.*, **347**, 747.
Bushouse, H.A., Lamb, S.A., and Werner, M.W. 1988, *ApJ.*, **335**, 74.
Heckman, T.M., Armus, L., and Miley, G.K., 1987, *AJ.*, **93**, 276.
Kennicutt, R.C. 1983, *ApJ.*, **272**, 54.
Kennicutt, R.C., and Kent, S.M. 1983, *AJ.*, **88**, 1094.
McCarthy, P.J., Heckman, T.M., and vanBruegel, W. 1987, *AJ.*, **93**, 264.

Figure Captions

Fig. 1 - Emission-line (Hα + [NII]) and continuum (R-band) contour plots of select FIRG's. The lowest level is 10^{-16} erg cm^{-2} s^{-1} arcsec^{-2} (in the galaxy rest frame) in the Hα + [NII] contours, and 4 x rms in the sky for the R-band contours. All levels are a factor of 2 higher in flux above the previous level. For each galaxy the Hα + [NII] contour is on the left and the R-band contour is on the right. In all cases North is towards the top, East is towards the left, and a projected angular size of 10 arcseconds is indicated by a bar.

Fig. 2 - Plot of the far-infrared luminosity (L_{FIR}) against the total Hα + [NII] luminosity (L_{TOT}) for the sample FIRG's. Also plotted are the loci of interacting spiral galaxies taken from Bushouse, Lamb, and Werner (1988), and the loci of isolated spiral galaxies taken from Kennicutt and Kent (1983). The solid diagonal lines represent select ratios of Hα + [NII] to far-infared luminosity. Note that the L_{TOT} and L_{FIR} for the interacting galaxies of Bushouse, Lamb, and Werner (1988) represent 1/2 of the total system Hα + [NII] and far-infrared luminosities, respectively.

Fig. 3 - Plot of (a) the total Hα + [NII] luminosity against the total absolute R-band magnitude, and (b) the far-infrared luminosity against the total absolute R-band magnitude for the sample FIRG's. The linear least-squares fit to the data is drawn as a dotted line in Figs. 3a and 3b.

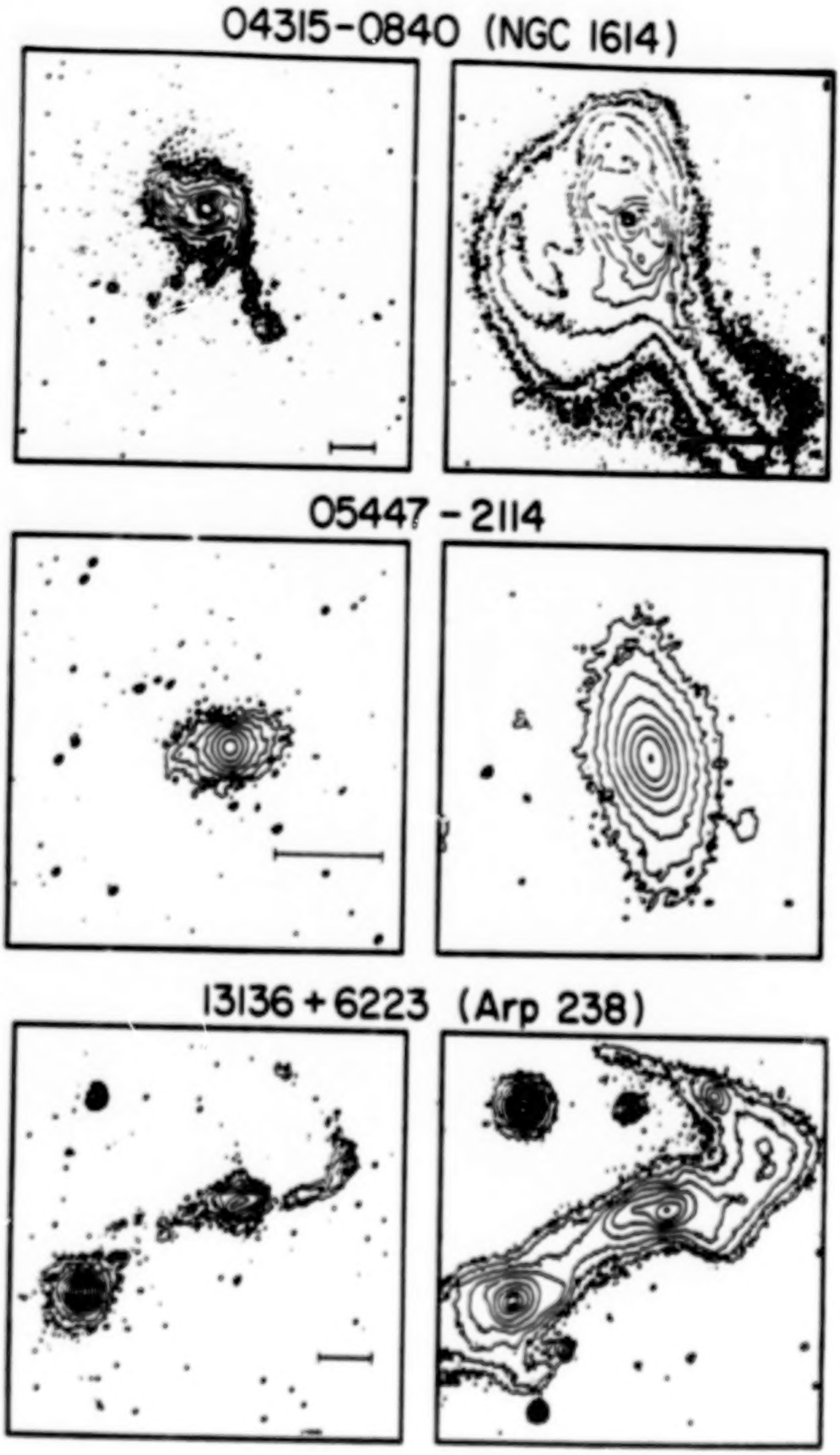

Fig. 1

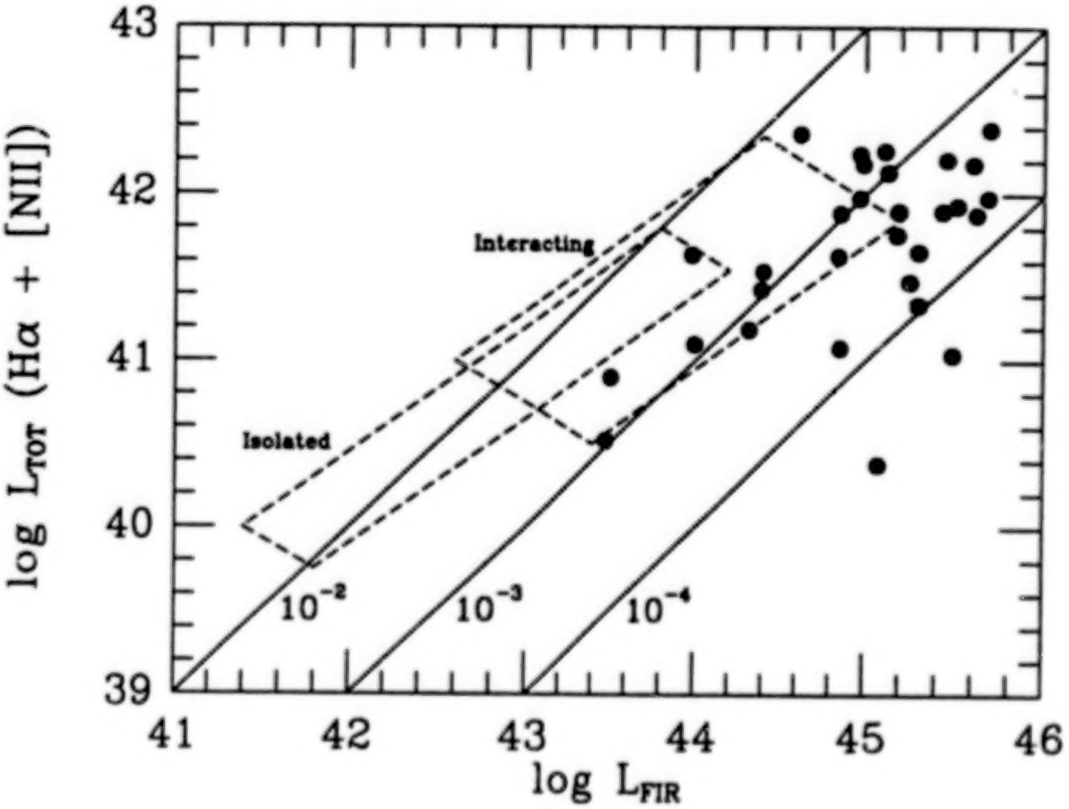
43
42
41
40
39
log L_TOT (Hα + [NII])
Interacting
Isolated
10^-2
10^-3
10^-4
41
42
43
44
45
46
log L_FIR

Fig. 2

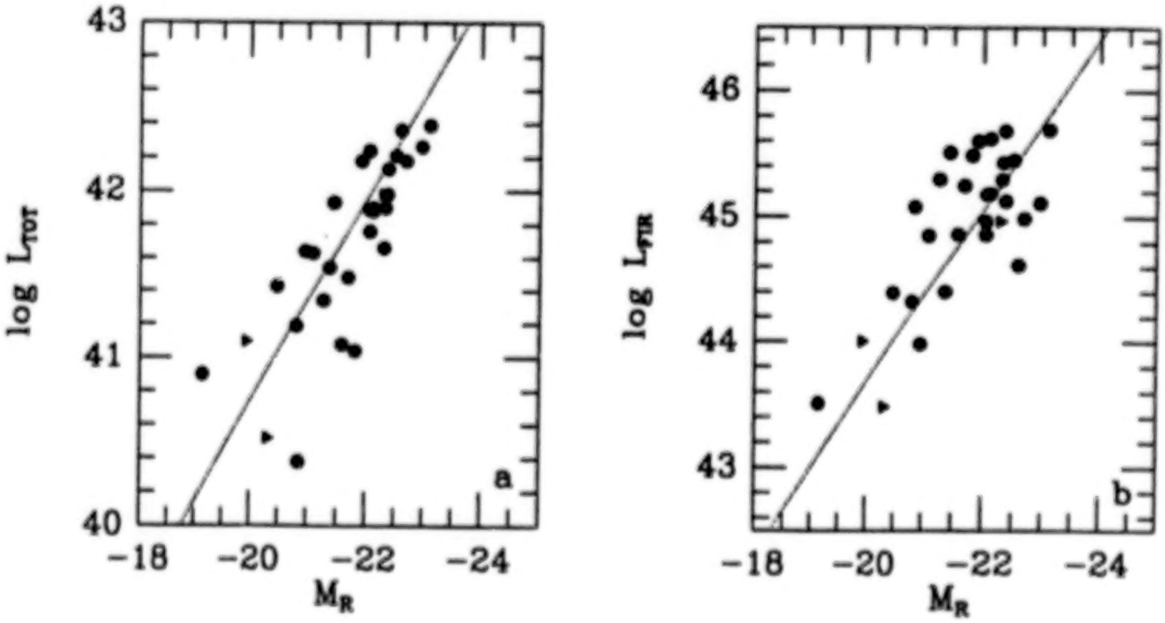
43
42
41
40
log L_TOT
a
−18
−20
−22
−24
M_R
46
45
44
43
log L_FIR
b
−18
−20
−22
−24
M_R

Fig. 3

BLANK PAGE

NUCLEAR AND EXTENDED INFRARED EMISSION IN PAIRED AND ISOLATED GALAXIES

Roc M. Cutri
Steward Observatory
University of Arizona

I. INTRODUCTION

The empirical connection between gravitational and collisional interactions among galaxies and enhanced activity has been well-documented. However, the physical mechanisms which are responsible for triggering the various forms of activity have not been determined. We present the preliminary results of a study of the nuclear and integrated infrared properties of galaxies chosen from the *Catalog of Isolated Pairs of Galaxies in the Northern Hemisphere* (Karachentsev 1972; hereafter CPG) and the *Catalog of Isolated Galaxies* (Karachentseva 1973; hereafter KI). Observations of these large, unbiased samples of paired and isolated galaxies are analyzed with the hope of identifying which aspects of galaxy encounters are most closely coupled to the presence of activity.

II. NUCLEAR PROPERTIES

Cutri and McAlary (1985) reported that the 10 μm luminosity distribution of a sample of CPG galaxies exhibited a high luminosity tail not present in the distribution of a control sample of bright spiral galaxies and Virgo spirals. Although the CPG and control samples had very similar absolute B magnitude distributions, the CPG sample spanned a larger range in redshift space than the non-interacting samples, and it was felt that the result could suffer from a Malmquist bias. Therefore, we have begun to re-examine this relationship by using the excellent performance of the new Multiple Mirror Telescope Bolometer system to obtain sensitive broadband 10.4 μm measurements of a sample of KI galaxies which better match the redshift range of the CPG sample.

The subsets of the CPG and KI for this study were chosen to have $m_{pg} \leq 14.0$ or $m_{tot} \leq 13.3$ for close pairs, and $0° \leq \delta \leq 37°$. For the CPG sample, Cutri and McAlary obtained data for pairs with LIN, DIS or ATM classifications (i.e. showing some sign of disturbed morphology). We have begun to carry out new photometry of the non-disturbed (SEP) pairs, as well. To date, approximately 2/3 of the new KI sample has been observed, and the 10 μm luminosity distributions of the CPG and KI samples are shown in Figure 1. As before, the CPG sample exhibits a distribution essentially similar to the non-interacting KI sample, except for a population of sources with $L_{10} > 10^9 L_\odot$. The KI distribution shows several galaxies with higher luminosities than the earlier control samples, but still $< 10^9 L_\odot$. It should be noted that although they satisfy the isolation criteria of the KI, the two most luminous galaxies in the sample, KI 359 (=NGC 2960) and KI 1004 (=NGC 7479), both appear disturbed on POSS plates. The statistical significance of the difference between the two distributions is difficult to assess since the CPG galaxies exhibit a base population similar to that of the KI sample. However, a Gehan two-sample test does reject the hypothesis that the two are drawn from the same parent population at better than the 98% level.

Figure 2 shows the ratio of the IRAS 12 μm flux density to the small aperture 10 μm flux density for the CPG and KI galaxies, giving a measure of the extent of the mid-infrared emission. Bearing in mind that the IRAS beam sampled roughly 100 times the area of our small aperture measurements, these data show that wherever nuclear 10 μm emission is detected it is strongly concentrated within a diameter of 1 kpc. This compactness is consistent with the characteristic sizes of galactic nuclei at 10 μm measured by Rieke (1976).

The nuclei of the high luminosity sources from the CPG sample all show HII region or Liner optical spectra, indicating that the elevated luminosities are due to enhanced star formation in and around the nuclear regions. The presence of enhanced nuclear 10 μm emission in the interacting systems suggests that mass transfer between galaxies is probably not the mechanism which triggers the activity, because of the difficulty of transporting infalling material directly to the nuclei. Such a conclusion was also reached by Keel *et al.* (1985), whose proposed that tidally enhanced fueling of the nuclei might lead to the nuclear activity. Finally, we find no obvious dependence in the 10 μm luminosity distribution on pair separation, angular size, velocity difference or interaction morphology.

III. EXTENDED PROPERTIES

We have examined IRAS ADDSCAN data for a large subset of both the CPG and KI to investigate galaxy-wide emission in interacting and isolated systems. Because the ADDSCAN processing co-adds all IRAS survey scans covering a source, these data provide the most sensitive survey measurements from the IRAS mission, typically 2-3 times better than the Point Source Catalog. This enables better assessment to be made of the mid-infrared (12 and 25 μm) emission, which can contribute significantly to the total infrared luminosity. Furthermore, ADDSCAN source profiles of the CPG galaxies can be examined to determine more accurately whether close pairs of galaxies have been resolved. The magnitude limit of the samples was $m_{pg} \leq 15.0$ or $m_{tot} \leq 14.3$ for close pairs.

The distributions of the integrated 12-100 μm luminosities of the KI and CPG sample galaxies are shown in Figure 3. The CPG pairs have been divided into two sets: the first being pairs with projected separations smaller than the IRAS beam size (unresolved pairs) and those separated widely enough to have been resolved by the satellite. Unlike the nuclear 10 μm luminosities, there is no significant difference in the distributions of the CPG and KI integrated luminosities. Haynes and Herter (1988) found a similar null result when examining the 60 and 100 μm emission from widely separated CPG pairs.

The presence of a nearby companion does have some influence on the integrated infrared properties of a galaxy, however, as shown in Figure 4. The distribution of the ratio of infrared-to-optical luminosities of CPG systems ranges extends nearly an order of magnitude higher than for KI galaxies. If the ratio L_{ir}/L_{opt} can be taken in part as a measure of the star formation rate in a galaxy, then on average, close pairs exhibit only a slight enhancement in galaxy-wide star forming activity. This concurs with the findings of Kennicutt *et al.* (1987) who found only a mild enhancement in disk star formation in their sample of interacting pairs. Interestingly, the CPG galaxies with the highest values of L_{ir}/L_{opt} are not the most luminous cases.

CPG and KI galaxies span a similar range in mid- and far infrared colors, as is shown in Figure 5. The CPG source do exhibit a slightly larger scatter in each color, reminiscent of the larger scatter in optical colors found in interacting galaxies by Larson and Tinsley (1978). We do not find evidence for systematically higher color temperatures among close pairs, as was reported by Telesco, Wolstencroft and Done (1988) for pairs drawn from the Arp Atlas. In addition, we have been unable to find any correlation between the infrared luminosity, L_{ir}/L_{opt}, or infrared color of the CPG pairs and pair separation, relative size or relative velocities. If outright collisions or mergers lead to extremely luminous infrared emission (e.g. Sanders *et al.* 1988), our analysis may be expected to miss such sources since the CPG is biased against very close pairs and mergers.

There does appear to be a weak dependence of L_{ir} on interaction morphology, as is shown in Figure 6, which is also present in L_{ir}/L_{opt} (not shown). If the interaction morphology can be interpreted as an approximate age indicator of the encounter through comparison with numerical simulations, the SEP systems should be the youngest (no sign of disturbance) or possibly the oldest, followed by the disturbed pairs (DIS), the LIN pairs - those showing linear bridges or tails, and finally the pairs enshrouded by common envelopes (ATM). The median luminosities and colors then show when the induced star formation in each class must reach its peak. Considerable dispersion is introduced due to the different morphological types involved in the interactions, uncertain viewing geometries, and coarse morphological classifications. One means of clarifying this relationship may be to correlate the ages of interactions deduced from numerical simulations to ages from starburst models.

REFERENCES

Cutri, R.M. and McAlary, C.W. 1985, *Ap.J.*, **296**, 90.

Haynes, M.P. and Herter, T. 1988, *A.J.*, **96**, 504.

Karachentsev, I.D. 1972, *Comm.Spec.Astrofiz.Obs.*, **7**, 1.

Karachentseva, V.E. 1973, *Comm.Spec.Astrofiz.Obs.*, **8**, 1.

Keel, W.C., Kennicutt, R.C., Hummel, E. and van der Hulst, J.M. 1985, *A.J.*, **90**,708.

Kennicutt, R.C., Keel, W.C., van der Hulst, J.M., Hummel, E. and Roettiger, K.A. 1987, *A.J.*, **93**, 1011.

Larson, R.B. and Tinsley, B.M. 1978, *Ap.J.*, **219**, 46.

Rieke, G.H. 1976, *Ap.J.(Letters)*, **206**, L15.

Sanders, D.B., Soifer, B.T., Elias, J.H., Madore, B.F., Neugebauer, G. and Scoville, N.Z. 1988, *Ap.J.*, **325**, 74.

Telesco, C.M., Wolstencroft, R.D. and Done, C. 1988, *Ap.J.*, **329**, 174.

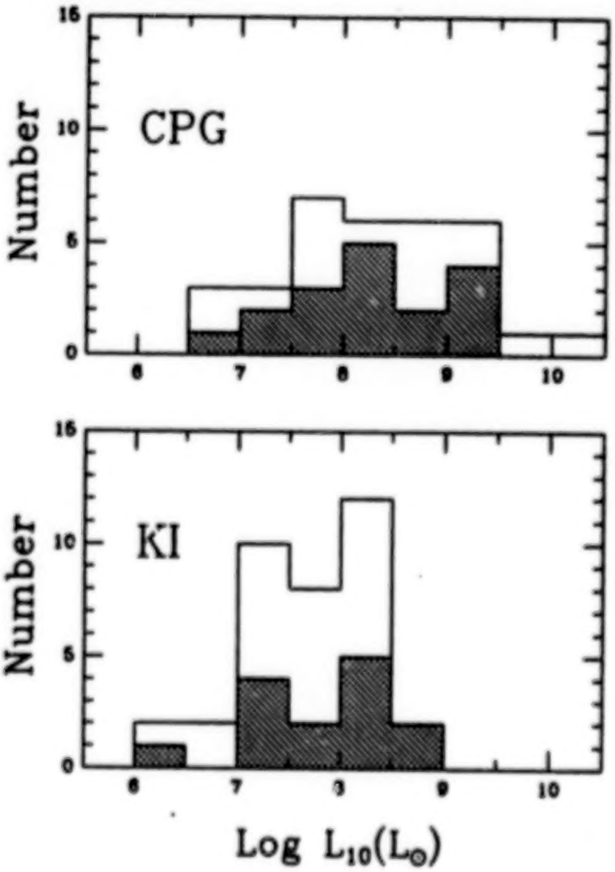

Figure 1 – The 10 µm luminosity distribution of CPG galaxies (top) and KI galaxies (bottom). Open boxes represent 3σ upper limits to luminosities.

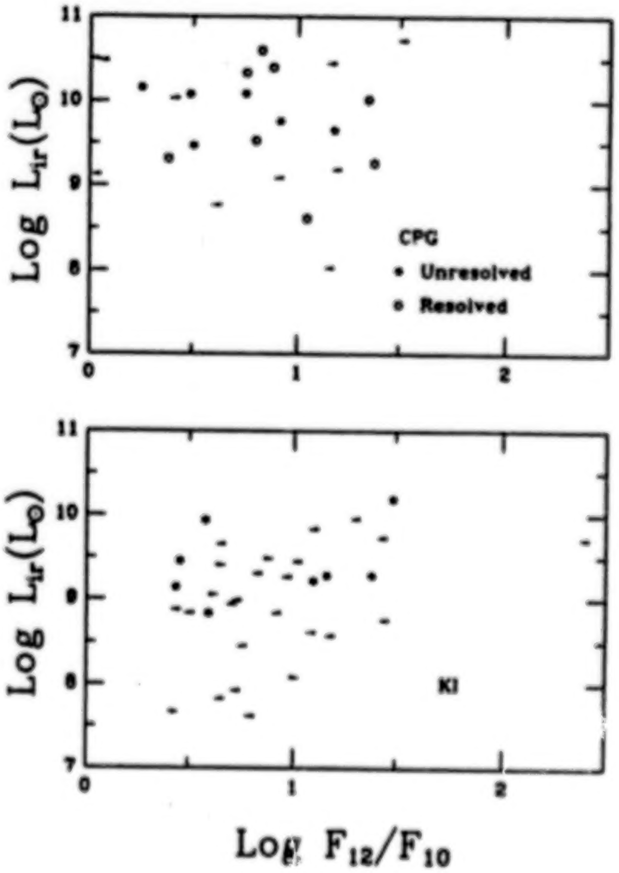

Figure 2 – The ratio of large beam IRAS 12 µm flux densities to small aperture ground based 10.4 µm flux densities. Upper and lower limits are denoted by arrows.

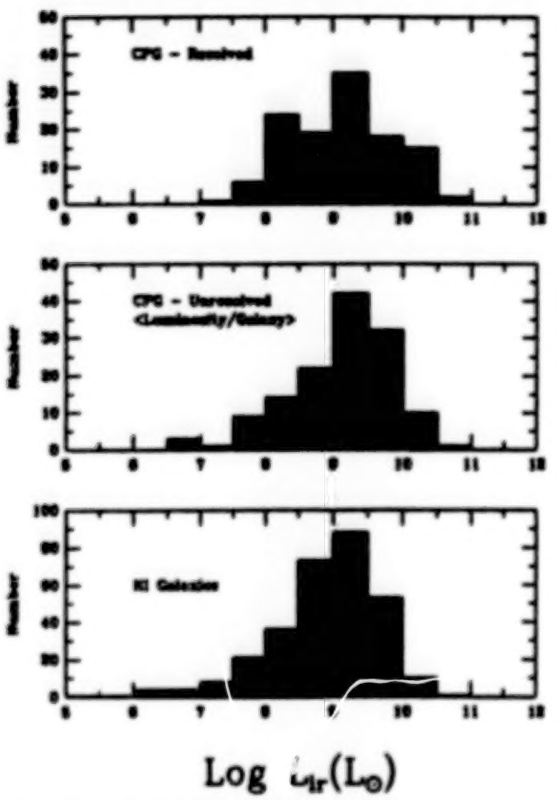

Figure 3 – The integrated 12-100 µm luminosities for CPG and KI galaxies calculated using IRAS ADDSCAN data. For unresolved CPG pairs (center) the average luminosity per galaxy is displayed.

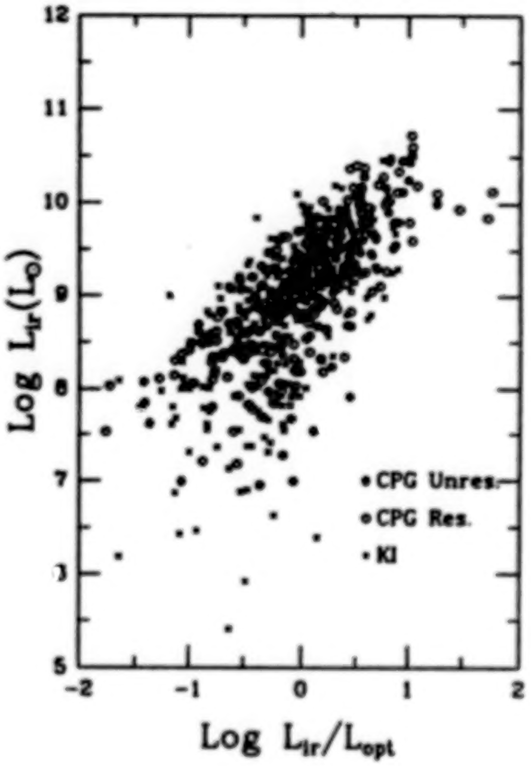

Figure 4 – The integrated infrared luminosity of CPG and KI galaxies as a function of infrared-to-optical luminosity ratio.

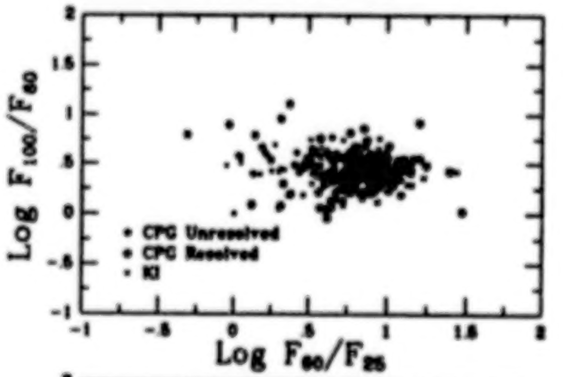

Figure 5 – The mid- and far-infrared colors of CPG and KI galaxies taken from IRAS ADDSCAN data.

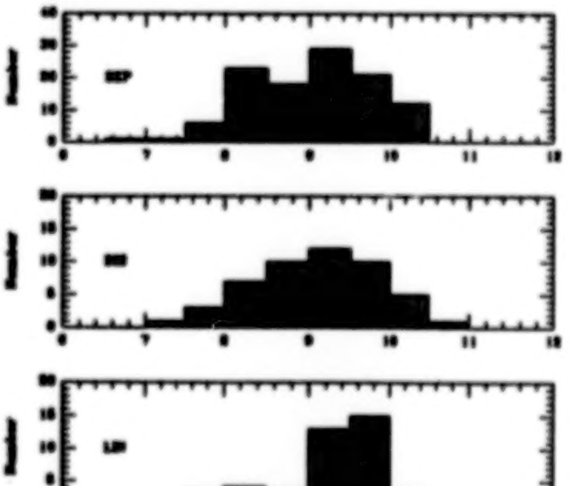

Figure 6 – The integrated infrared luminosity distribution for each class of CPG interaction morphology. Luminosities for resolved pairs are shaded with ////, and unresolved pairs with \\\\.

BLANK PAGE

420

SIGNS OF INTERACTION OF THE NGC 1275 NUCLEUS WITH THE HIGH-VELOCITY SYSTEM ACCORDING TO $0\overset{''}{,}7$ SEEING OBSERVATIONS

V. N. Dudinov and V. S. Tsvetkova
Astronomical Observatory of Kharkov University, USSR

S. B. Novikov
Sternberg State Astronomical Institute, USSR

I. I. Pronik
Crimean Astrophysical Observatory, USSR

ABSTRACT. The nucleus of the Seyfert galaxy NGC 1275 was observed in the B system on 12-1-1989 with seeing $0\overset{''}{,}7$ using the Zeiss-1000 telescope on Mount Majdanak in Central Asia. Special methods of processing reveal low-contrast details. The nucleus and circumnucleus are stretched in NW-SE direction. There are two narrow filaments near the nucleus in position angles roughly 340° and 320°. The first is directed near the radio jet of the nucleus, the second has broken details curved to the NW or toward the high-velocity system of NGC 1275.

The NGC 1275 system consists of a main gE galaxy, having a radial velocity 5200 km/s (Burbidge, Burbidge 1965) and of an irregular galaxy (L-galaxy - late type spiral) with radial velocity 8200 km/s, located to the NW of the main one (Minkowski, 1957). Both galaxies are rich in gas. The gas of the main galaxy looks like a giant Crab, or burst, of dimensions equal to those of the gE galaxy (Burbidge, Burbidge 1965; Lynds 1970). The nature of the L-galaxy is widely discussed. The first discoverer of this galaxy, Minkowski, supposed that it is colliding with the gE one. The Burbidges (1965) discussed the ejection of L from gE galaxy, Shields and Oke (1975) and van den Bergh (1977) supposed that L-galaxy is projected to the gE galaxy. The colliding hypothesis is favored from HI observations of L-galaxy in the 21 cm Hl line found in absorption against the radio continuum emission of the NGC 1275 bright nucleus (de Young et al., 1973). In all hypotheses there are intrinsic difficulties. The important problem up to now is how the two galaxies interact and whether the interaction exists or not. One supposition about the site of interaction was made by Metik and Pronik (1979): near the starlike object located 7" NE from the NGC 1275 nucleus (later object "b"). Meaburn et al. (1989) supposed that interaction produces a fine filament of optical continuum emission with ionized knots along its length presented in PA = 295°. For further discussion of this problem it is important to reveal the details of the nucleus and circumnucleus of NGC 1275.

The Burbidges were the first to discover irregularity in the structure of the NGC 1275 nucleus (1965): they pointed out a knot 3" to the NW of it (later detail "c"). Metik and Pronik (1979, 1984, 1987, 1988, ab,b) showed that the circumnuclues is stretched in the direction of this arched detail "c" in UV continuum and in 14 emission lines. This stretched structure consists of blue stars and gas. Its direction is very near to the radio jet one (Pedlar et al., 1983). It was supposed that active nucleus of NGC 1275 interacts with the circumnucleus through this stretched structure. Now new details of circumnuclear region of NGC 1275 are obtained using photonegatives with resolution $0\overset{''}{,}7$.

Observations were made 12-1-89 on mountain Majdanak in Central Asia with $0\overset{''}{,}7$ seeing using the Zeiss-1000 telescope. Six negatives with 15 min exposure were obtained in the B photometric system. Figure 1 shows a print of one of the negatives. One can see the nucleus "a", starlike object "b" and stars - photometric standards: C, Cl, C2, C3, 1, 2 - from Lyutyi's list (1972), D, Dl, D2, D3, D4 - secondary standards, obtained by extrapolation. All measurements were made with an iris photometer. The results are shown in Table 1.

Table 1. B magnitudes of nucleus "a" and object "b" and secondary standards near the nucleus of NGC 1275

detail, star	B	star	B
a	15,75±0,08	D2	15,56±0,05
b	16,33±0,01	D3	16,16±0,10
D	14,05±0,05	D4	16,41±0,10
DI	15,83±0,08		

The magnitude of object "b" is in accordance with Selove's estimate $B = 16\overset{m}{,}3$ (1969). The magnitude of nucleus "a" obtained from its photometric profile in a circle of 2" diameter is $15\overset{m}{,}63$ very near to Table 1's value. According to Lyutyi (1991)

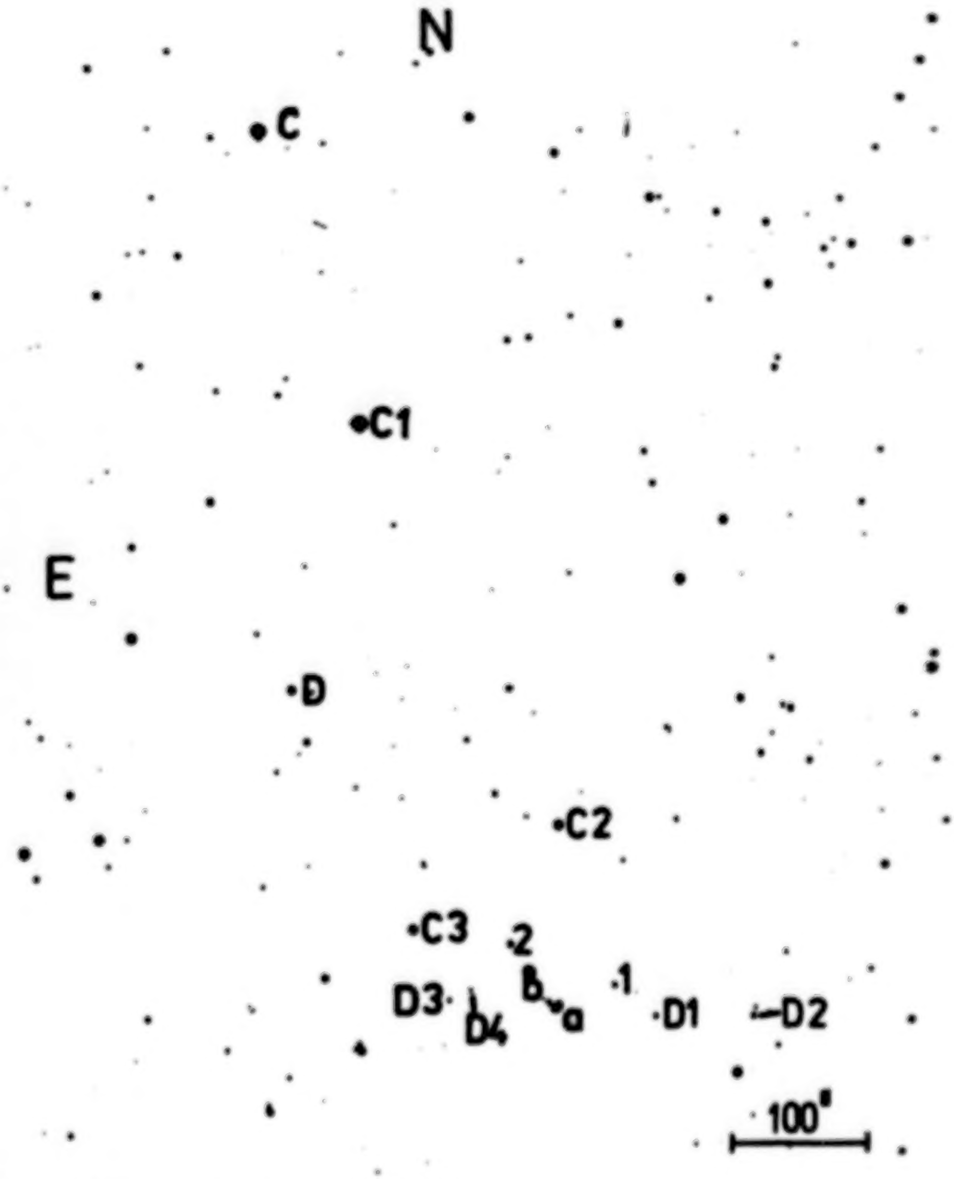

Figure 1. Photo of the NGC 1275 region in the B photometric system, obtained with the Zeiss-1000 telescope on Mount Majdanak 12-1-89. The photometric standards are pointed. a - circumnucleus, b - starlike object (see text).

the active nucleus of NGC 1275 galaxy has been in a deep minimum from 1980 up to now. Observations made by Zasov and Lyutyi (1973) in 1967-1970 give $B(5'') = 14\overset{m}{,}61$. Now on February 1988 and October 1989 Lyutyi's data give $B(5'') = 15\overset{m}{,}74$: - $1\overset{m}{,}13$ weaker than in years of the nucleus' high activity. The dimension of the nucleus also decreases. Obtained in 1977 it was $\sim 1\overset{''}{,}5$ (Metik, Pronik, 1984). Nowadays the dimension of the nucleus was calculated using $0\overset{''}{,}7$ resolution observation on 12-1-89. Taking into account that the brightness distributions in the images of objects "a" and "b" are near to Gaussian the dimensions of the objects can be calculated using the relation:

$$\sigma_0^2 = \sigma_t^2 + \sigma_s^2$$

here σ_0^2, σ_t^2, σ_s^2 are dispersions of observed, true and stellar photometric profiles respectively. Object "b", to the limits of the errors, is not distinct from the star. The true FWHM of the nucleus is $0\overset{''}{,}5$. Thus with the decreased level of nuclear activity its dimension decreased too.

The best negatives available (for stellar FWHM = $0\overset{''}{,}7$) were taken for special processing. All negatives selected were added with the help of optical combining equipment. The combined positive was put for linear filtration using the optical coherence arrangement of Kharkov University (Dudinov et al., 1979, 1989; Tsvetkova et al., 1984).

Figure 2 shows the photo of the circumnucleus of NGC 1275 obtained after summed image filtration. Weakening of the nucleus, high spatial resolution and special processing methods permit us to reveal new details in the circumnucleus of NGC 1275. In addition to arch "c" there are structures connecting it with the nucleus and structures in opposite SE side. Figure 3 shows isophotes of this region obtained with scanning step $0\overset{''}{,}25$.

Figures 2 and 3 show that nucleus of NGC 1275 is stretched in the NW-SW direction at all intensity levels from 0.9 to 0.2.

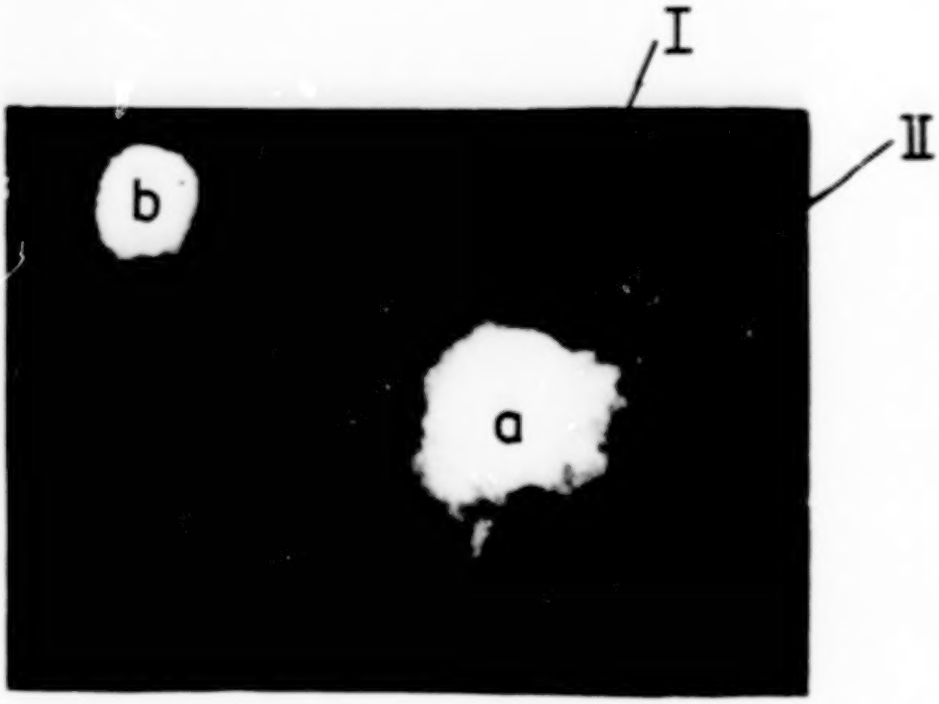

Figure 2. Photo of the circumnucleus of NGC 1275 and object "b" after spatial processing. I, II - filaments of low intensity emission.

I_{max} and this stretching is observed to the distances ±5" or ±1800 pc from the nucleus. The stretched circumnucleus measuring $3\overset{"}{.}5$ or 1200 pc is divided into two streams in its NW part: I - in PA ~340°; II - in PA ~320°. The first has an extension to the SE side of the nucleus. Its PA is very near the PA of the nuclear radio jet observed at 73 cm (Pedlar et al. 1983). The second filament (II) has no continuation on the SE side of the nucleus. It envelops the nucleus from the W side by many little curved streams, the longest of them near the PA 300 of gas knots observed by Meaburn et al. (1989) and the direction of the L-galaxy. Arch "c" connects filaments I and II in the NW part. Its brightness is not homogeneous. The extended weakest

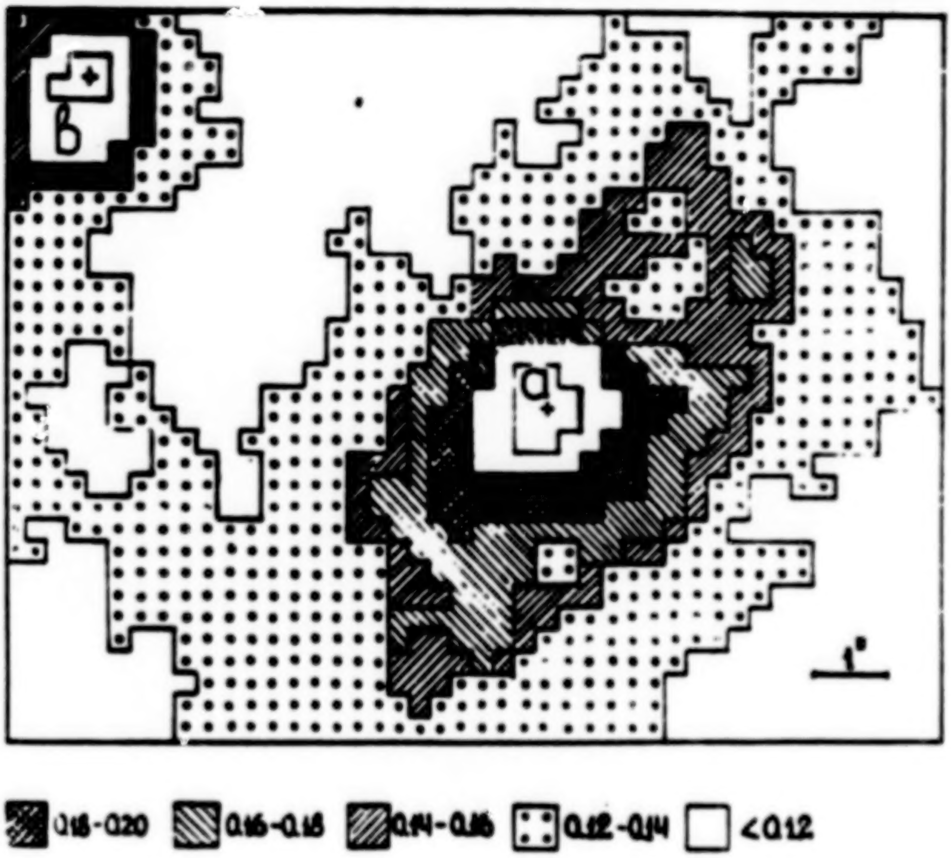

Figure 3. Isophotes of circumnucleus of NGC 1275. Step of scanning is 0.25. Intensities are in units of I_{max} of the nucleus.

emission of the level < 0.2 I_{max} (of the nucleus) on SE side has a curved jut directed to object "b" which, at low intensity levels, has emission directed to this feature.

What may be the nature of filaments I and II of Figure 2 and 3? In the B photometric system the lines [OII] and [OIII] of the low and high velocity gas are passed. So it is not necessary to suppose, that filaments I and II consist but of stars, but they may contain gas of low and high velocity. Spectral investigation (Metik, Pronik, 1979) shows that arch "c" is a superassociation of early-type stars of dimension ~1000 pc. It is rich in gas and belongs to the low-velocity system. The spectra of the SE stretched part of the NGC 1275 circumnucleus also show gas of low and partly high velocity. For the interpretation of filaments I and II it is important to observe their spectra with high spectral and position resolutions.

In conclusion one can say that photo of NGC 1275 circumnucleus obtained with spatial resolution $0\overset{''}{.}7$ in B shows signs of interaction with: I - the radio jet, 2 - knots of gas observed by Meaburn et al. (1989) on the NW side of the nucleus and 3 - object "b". The most prominent interaction is with the radio jet. Interactions 2 and 3 are at lower levels.

REFERENCES

van den Bergh, S. 1977, Lick Obs. Bull. No. 765.

Burbidge, E. M., and Burbidge, G. R. 1965, Astrophys. J., **142**, 1351.

de Young, D. S., Roberts, M. S., and Saslaw, W. C. 1973, Astrophys. J., **185**, 809.

Dudinov, V. N., Tsvetkova, V. S., and Krishtal, B. A. 1979, New Technique in Astronomy, **6**, 60.

Dudinov, V. N., Novikov, S. B., Tsvetkova, V. S., and Shulga, V. V. 1989, Russian Astron. J., **66**, 631.

Lynds, R. 1970, Astrophys. J., **159**, L 151.

Lyutyi, V. M. 1972, Russian Astron. J., **49**, 930.

Lyutyi, V. M. 1991, Russian Astron. J., in press.

Meaburn, J., Allen, P. M., Claiton, C. A., Marston, A. Pl., Whitehead, M. J., and Metik, P. 1989, *Astron. Astrophys.*, **208**, 17.

Metik, P. 1979, *Astrofizika*, **15**, 37.

Metik, P. 1984, *Astrofizika*, **21**, 233.

Metik, P. 1987, *Izv. Krimsk. Astrofiz. Obs.*, **76**, 80.

Metik, P. 1988,a, *Izv. Krimsk. Astrofiz. Obs.*, **78**, 74.

Metik, P. 1988,b, *Izv. Krimsk. Astrofiz. Obs.*, **80**, 76.

Minkowski, R. 1957, "Radio Astronomy", IAU Symp. No. 4., ed. H. C. van der Hulst, Cambridge, Cambridge University Press, p. 107.

Pedlar, A., Booler, R. V., Davies, R. D. 1983, *Monthly Not. Roy. Astron. Soc.*, **203**, 667.

Selove, D. M. 1969, *Astrophys. J.*, **158**, L 19.

Shields, G. A., Oke, J. B. 1975, *Publ. Astron. Soc. Pacific*, **87**, 879.

Tsvetkova, V. S., Chernyi, V. G. 1984, *Pisma v. Astron. J.*, **10**, 469.

Zasov, A. V., and Lyutyi, V. M. 1973, *Russian Astron. J.*, **50**, 253.

BLANK PAGE

DUST AND IONIZED GAS IN ACTIVE RADIO ELLIPTICAL GALAXIES

D.A. Forbes[1,2], W.B. Sparks[1] and F.D. Macchetto[1,3]
[1]Space Telescope Science Institute, 3700 San Martin Drive, Baltimore MD 21218*
[2]Institute of Astronomy, Madingley Road, Cambridge CB3 0HA, U.K.

ABSTRACT

We present broad and narrow bandwidth imaging of three southern elliptical galaxies which have flat–spectrum active radio cores (NGC 1052, IC 1459 and NGC 6958). All three contain dust and extended low excitation optical line emission, particularly extensive in the case of NGC 1052 which has a large H_α + [NII] luminosity. Both NGC 1052 and IC 1459 have a spiral morphology in emission-line images. All three display independent strong evidence that a merger or infall event has recently occurred, i.e., extensive and infalling HI gas in NGC 1052, a counter-rotating core in IC 1459 and Malin-Carter shells in NGC 6958. This infall event is the most likely origin for the emission-line gas and dust, and we a currently investigating possible excitation mechanisms (Sparks *et al.* 1990).

INTRODUCTION

Optical line emission, radio emission, nuclear activity and the presence of X–ray emitting coronal halos often occur together in elliptical galaxies (e.g., Baum *et al.* 1988). There is good evidence to link optical line emission with mergers, or infall events, when in the presence of counter-rotating cores, dust lanes, discrete stellar components and Malin-Carter shells for example. Sparks *et al.* (1989) proposed that the cooler infalling gas can significantly modify the properties of the ambient hot medium via thermal conduction, and that the large mass deposition rates inferred from X–ray observations are not present (see also Sparks 1989, this meeting).

Here we present CCD continuum and emission-line imaging obtained using EFOSC on the ESO 3.6-m telescope at La Silla, Chile. We investigate three nearby active elliptical galaxies which show independent evidence that infall has recently occurred; namely NGC 1052, IC 1459 and NGC 6958. All three objects were known to have flat-spectrum radio-core emission (Sparks *et al.* 1984) and dust features (Sparks *et al.* 1985). Thomas *et al.* (1986) present and interpret X–ray observations of two of these galaxies in terms of a 'standard' cooling-flow model. Our observations taken together with data already available lead us to conclude that the most likely origin for the extensive emission-line filament systems and dust patches which we find, is an external one.

The observations consist of short (~ 3 sec), medium and long (~ 1200 sec) exposures with typical seeing of 1.5 arcsec. Images in the same band were merged, with $1/\sigma^2$ weighting to maximise signal-to-noise, to give a master image free of saturated regions. Ellipses were fitted to the master images and models of the underlying light distribution were thereby constructed. Finally the data was calibrated using aperture photometry and absolute flux determinations made. A value of $H_o = 50$ km s^{-1} Mpc^{-1} is used throughout.

NGC 1052

Properties:

- Distance = 29.31 Mpc.
- Contains a $\approx$ 1 Jy flat-spectrum variable radio core, a VLBI jet, and relatively compact double radio source (Fosbury *et al.* 1978; Wrobel 1984; Davies and Illingworth 1986).
- HI mass = 11.5×10^{8} $M_{\odot}$ (van Gorkom *et al.* 1986).
- $L_X = 5.46 \times 10^{40}$ erg s^{-1} (Fabbiano *et al.* 1989); a typical value for an elliptical with a large non-stellar contribution from a hot gaseous halo.
- *IRAS* measurements suggest a long wavelength infrared excess consistent with thermal radiation from $\sim 10^{7}$ $M_{\odot}$ of dust (Knapp *et al.* 1989).
- Exhibits extended LINER emission (Fosbury *et al.* 1978; Davies and Illingworth 1986).

Evidence for a Merger:

- The large misalignment of the rotation axis of the stars compared to the HI and ionized gas, and its high angular momentum strongly suggests that it has been accreted rather than arising from mass loss from the stars (Davies and Illingworth 1986).
- The HI gas shows a 'tidal tail', indicative of a recent merger (van Gorkom *et al.* 1986).
- HI is seen in absorption at both the galaxy systemic velocity and redshifted, implying the presence of infalling gas (van Gorkom *et al.* 1986).
- CCD images revealed the presence of a prominent minor axis dust-lanes (see Sparks *et al.* 1985 and Fig. 1). confirming that the gas is not of primordial origin.
- A gas-to-dust ratio of $\sim$ 100, normal for spiral galaxies, also suggests an accretion origin rather than primordial or internal stellar mass loss processes (van Gorkom *et al.* 1986).

Results:

The image of dust optical depth (Fig. 1) shows far more extensive absorption than previously seen (Sparks *et al.* 1985) i.e., additional dust covers essentially the whole Western half of the galaxy, with structure primarily in the minor axis direction. The emission-line image (Fig. 2) displays an irregular spiral morphology. These together suggest an obvious model for the system, whereby we are observing an inclined disc of cool gas passing through the galaxy and intersecting the nucleus. The sense of the spiral pattern is correct for a trailing spiral if the inclination is as suggested by the dust i.e., 'in front' to the West (kinematics from Davies and Illingworth 1986). We therefore favor a situation whereby the HI gas lies in a disc and is ionised in its inner regions either by the active nucleus or by interaction with the hot X-ray gas associated with the galaxy. It is seen in absorption where it crosses in front of the galaxy (as proposed by Sparks *et al.* 1985), while the optical emission-line gas is seen on both sides. Note that this implies (i) the gas cannot be primordial (ii) a spherical distribution for the filament system is unlikely.

We find the H_{α} + [NII] emission extends about 40 arcsec from the center of the galaxy with a total luminosity of 1.4×10^{41} erg s^{-1}.

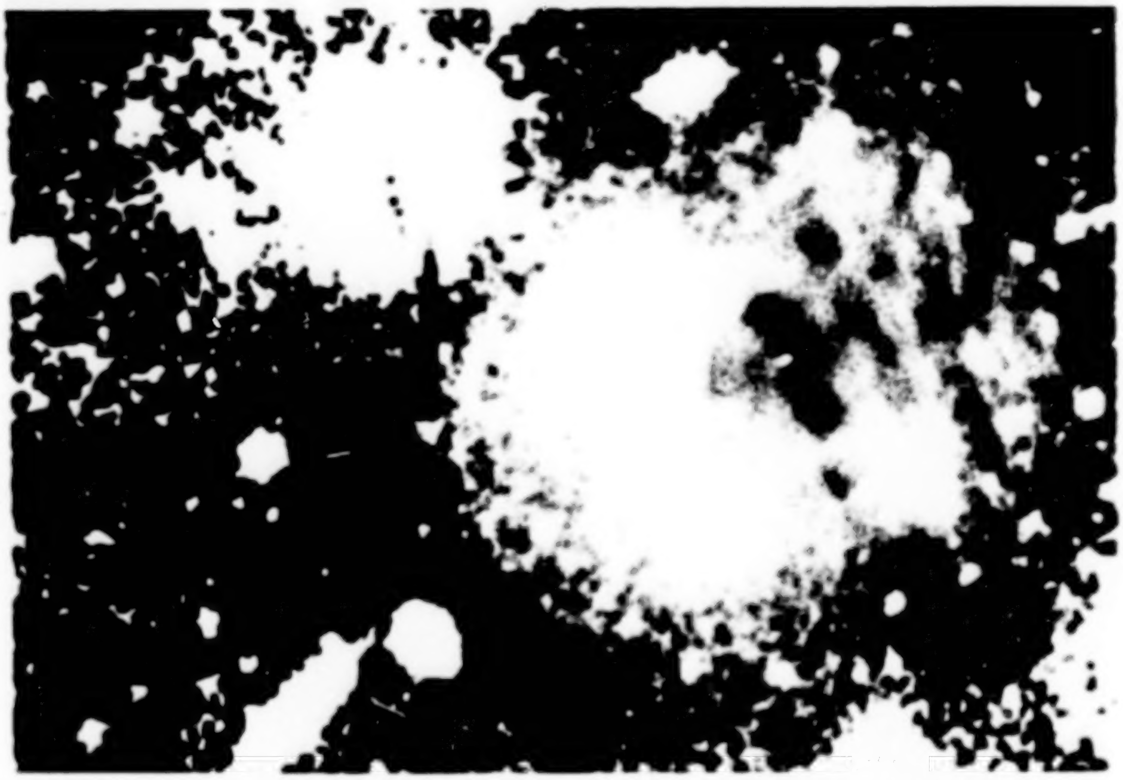

Figure 1 B–R dust map for NGC 1052. Note extensive dust lanes parallel to the minor axis on the West side of the galaxy. North is up and East is left in all figures, which have a width ≈ 3.7 arcmin.

Figure 2 H_α + [NII] image for NGC 1052 after continuum subtraction.

IC 1459

Properties:

- Distance = 32.77 Mpc.
- Has a dominant ≈ 1Jy non–variable flat–spectrum radio core (Sparks *et al.* 1984).
- HI mass $< 7.5\times10^{8}$ $M_\odot$ (Walsh *et al.* 1989).
- $L_X = 4.30 \times 10^{40}$ erg s^{-1} (Fabbiano *et al.* 1989); we find the X–ray emission is extended probably due to a hot gaseous halo (some contribution from discrete stellar sources is possible).
- *IRAS* measurements suggest $\sim 10^7$ $M_\odot$ of dust (Knapp *et al.* 1989).

Evidence for a merger:

- Exhibits a counter-rotating core (Franx and Illingworth 1988), in which the stars and gas are rotating in opposite directions, strongly suggesting that a 'cold' stellar system has merged and settled at the core (Balcells and Quinn 1989).
- Photographic enhancement reveals a faint one-arm extended spiral structure (Malin 1985), although some form of interaction with the companion galaxies may well be responsible.
- It has strongly 'twisted isophotes' (Evans 1951; Williams and Schwarzchild 1979). This may be indicative of a recent merger or interaction (see Bender *et al.* 1989).

Results:

We find a long single 'spiral arm' emission feature, with a suggestion of fainter irregular structure. The direction and sense of the arm is consistent with an extrapolation of the feature found by Malin (1985). To maintain this coherent filamentary structure over length scales larger than the optical image of the galaxy again implies an external infall origin.

NGC 6958

Properties:

- Distance = 53.41 Mpc.
- Exhibits a weak flat–spectrum radio core and is peculiarly blue for a radio elliptical (Sparks *et al.* 1984), although it has a very red nucleus (Sparks *et al.* 1986).
- HI mass $< 15.3\times10^{8}$ $M_\odot$ (Walsh *et al.* 1989).
- The *IRAS* data suggests a cool ISM is present (Walsh *et al.* 1989). Wilkinson *et al.* (1987) find $\mathrm{Log}(F_{IR}/F_B) = 0.89$, indicating a very high star formation rate for an elliptical.

Evidence for a Merger:

- The presence of Malin-Carter shells strongly suggests the recent infall of a small galaxy about 10^9 years ago (Quinn 1984).

Results:

We find dust patches ~ 30 arcsec to the East of the nucleus much more clearly than in Sparks *et al.* (1985), and in addition that the dust extends over the whole of the Northern half of the image. A long slit spectrum shows extended low excitation line emission with a considerable velocity gradient indicative of rapid rotation.

SUMMARY

We find NGC 1052 and NGC 6958 have much more extensive dust than previously realised. All three galaxies contain highly extended regions of optical line emission, with a spiral morphology in the cases of NGC 1052 and IC 1459. An external origin for these cooler gaseous components is favoured. Our goal in these investigations is to understand the excitation mechanism of optical line emission in elliptical galaxies and to understand the relationships between the different phases of the ISM. We wish to know if the infall process can affect the X–ray halo properties of elliptical galaxies, perhaps removing the requirement for the relatively large mass depositions of the conventional cooling-flow picture.

Two very different models for NGC 1052 are currently being considered (Sparks *et al.* 1990). One is photoionization by an active nucleus, the other thermal electron conduction in which the emission flux is assumed to be proportional to the energy available by conduction. There are few free parameters in our thermal conduction model, yet with plausible values a remarkably good fit is obtained to the surface brightness profile. In conclusion, we deduce that mergers can, from an optical perspective, appear quite similar to cooling flows. To establish how fundamental these similarities are further work is required.

References

Balcells, M., and Quinn, P. J. 1989, *Astrophys. and Space Sci.*, **156**, 133.

Baum, S. A., *et al.* 1988, *Ap. J. (Suppl*, **68**, 833.

Bender, R., *et al.* 1989, *Astron. and Astr.*, **217**, 35.

Davies, R. L., and Illingworth, G. 1986, *Ap. J.*, **302**, 234.

Evans, D. S. 1951, *M. N. R. A. S.*, **111**, 526.

Fabbiano, G., Gioia, I. M., and Trinchieri, G. 1989, *Ap. J.*, **347**, 127.

Fosbury, R. A. E., *et al.* 1978, *M. N. R. A. S.*, **183**, 549.

Franx, M., and Illingworth, G. 1988, *Ap. J. (Letters)*, **327**, L55.

Malin, D. F. 1985, in *New Aspects of Galaxy Photometry*, ed. J. L. Nieto (Berlin: Springer–Verlag) p27.

Quinn, P. J. 1984, *Ap. J.*, **279**, 596.

Knapp, G. R., Kerr, F. J., and Williams, B. A. 1978, *Ap. J.*, **222**, 800.

Knapp, G. R., Beis, W. E., and van Gorkom, J. H. 1989, preprint.

Sparks, W. B., *et al.* 1984, *M. N. R. A. S.*, **207**, 445.

Sparks, W. B., *et al.* 1985, *M. N. R. A. S.*, **217**, 87.

Sparks, W. B., Hough, J. H., Axon, D. J., and Bailey, J. 1986, *M. N. R. A. S.*, **218**, 429.

Sparks, W. B., Macchetto, F. D., and Golombek, D. 1989, *Ap. J.*, **345**, 153.

Sparks, W. B., Forbes, D. A., Macchetto, F. D. and Golombek, D. 1990, in preparation.

Thomas, P. A., *et al.* 1986, *M. N. R. A. S.*, **222**, 655.

van Gorkom, J. H., *et al.* 1986, *A. J.*, **91**, 791.

Walsh, D. E. P., *et al.* 1989, submitted to Ap. J.

Williams, T. B., and Schwarzschild, M. 1979, *Ap. J.*, **227**, 56.

Wilkinson, A., Browne, I. W. A., and Wolstencroft, R. D. 1987, *M. N. R. A. S.*, **228**, 933.

Wrobel, J. M. 1984, *Ap. J.*, **284**, 531.

---

[3] *Affiliated with the Astrophysics Division, Space Science Department, European Space Agency (ESA).*

[*] *Operated by the Association of Universities for Research in Astronomy. Inc., under contract with the National Aeronautics and Space Administration.*

BLANK PAGE

CORRELATIONS BETWEEN ENVIRONMENTAL PARAMETERS AND NUCLEAR ACTIVITY

W. Kollatschny, K.J. Fricke
Universitäts-Sternwarte
D-3400 Göttingen, F.R.G.

The occurrence and quantitative properties of Seyfert 1 and Seyfert 2 galaxies as a function of the galaxy environment have been studied in a systematic way. For this investigation we have selected from the Catalogue of Quasars and Active Nuclei (Veron & Veron,1989) all Seyfert galaxies with the following properties:

(i) $m_V \leq 15$,
(ii) listed classification as Sey 1, Sey 2, or Sey 3,
(iii) $v_{rad} \leq 20000$ km s^{-1}.

This results in a sample size of 242 Seyfert galaxies. For all these objects their galaxy environment has been inspected on POSS and ESO/SRC plates.

The vicinity of each sample Seyfert galaxy was searched for companion galaxies out to at least 0.5 Mpc. Lacking redshift information we adopted as a companion galaxy any galaxy in this area having a size between 20 and 200 percent of the Seyfert galaxy size.

As an important environmental parameter for Seyfert activity we consider here the galaxy density within an environment of 500 kpc radius. We distinguish four density classes:

D1: no companion (isolated Seyfert)
D2: 1 companion
D3: 2-5 companions (group)
D4: ≥ 6 companions (dense group)

Table 1: The distribution of the various Seyfert classes among the density classes

	density class D			
	1	2	3	4
Sey 1	13 (11)	27 (22)	61 (50)	21 (17)
Sey 2	3 (3)	21 (20)	62 (60)	18 (17)
Sey 3	0 (0)	3 (19)	9 (56)	4 (25)

D = 1 for isolated Seyfert, D = 4 for Seyfert in dense group

In brackets are given the relative percentages.

The distribution of the various Seyfert classes among these density classes is listed in Table 1, both in absolute numbers and in percentages (given in brackets). From this statistics the environments of Sey 1, Sey 2, and Sey 3 galaxies do not differ in general with the exception that among the isolated galaxies the Seyfert 1 galaxies dominate conspicuously. No significant dependence of morphological type (de Vaucouleurs T-type) on density class is observed both for Sey 1 and Sey 2 galaxies (cf. Fig. 1g).

On the basis of an extensive search of the Seyfert literature we also investigated the dependence of the intrinsic parameters of the sample Seyfert galaxies on density class. In Figs. 1a - f we plot the absolute visual and blue luminosity L_V and L_B; the FIR luminosity L_{FIR}; radio luminosity L_{6cm}; the dereddened Hα luminosity $L_{H\alpha}$, and the dereddened [OIII] 5007 luminosity $L_{[OIII]}$ as functions of density class. Numerically, these functions (including the error bars) are presented in Table 2.

The following trends can be derived from Table 2:

The Seyfert galaxies which are located in the densest environments show the lowest absolute luminosities in the continuum and in the emission lines. The luminosities decrease by more than a factor of 2 with increasing environment density, both for Seyfert 1 and Seyfert 2 galaxies.

This trend is weaker in the far-infrared; probably due to starbursts triggered in denser environments.

The results for the isolated Seyfert 2 galaxies (D1 class) have no high significance; only 3 galaxies of this type exist. The decreasing of the luminosity of isolated Seyfert 1 galaxies might be explained with the late state of the Seyfert activity triggered a long time ago by a distant neighbour.

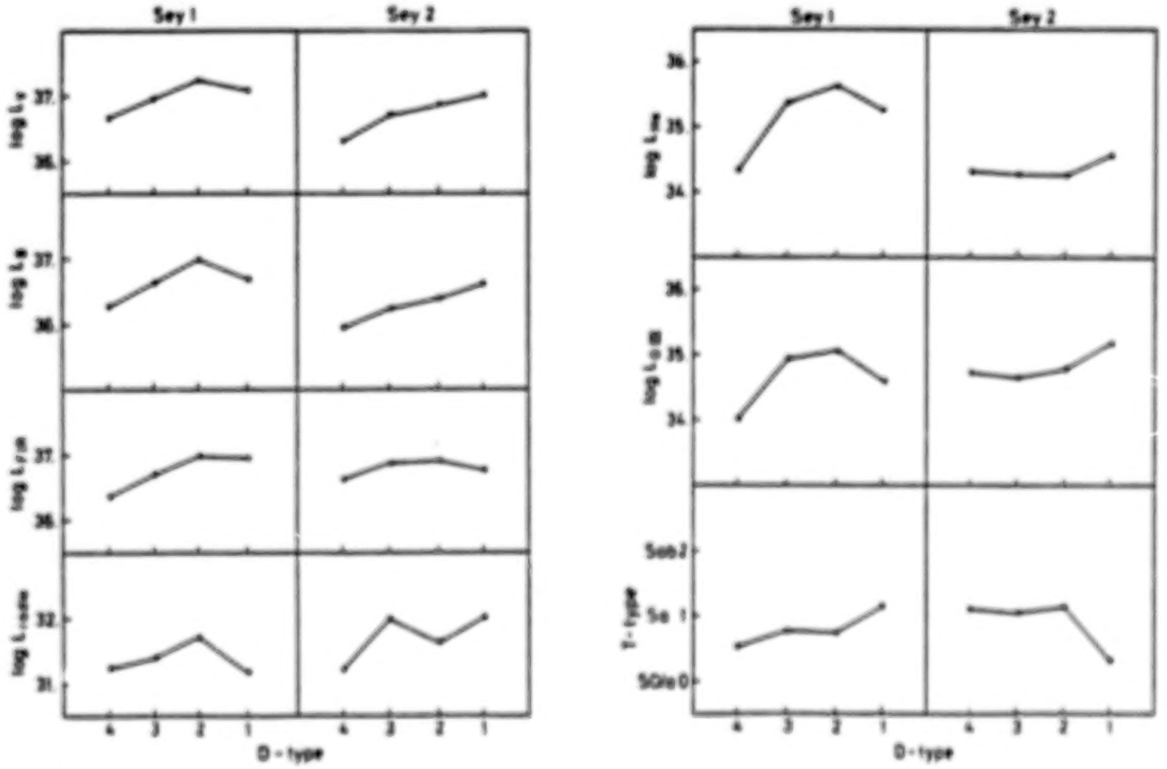

Figs. 1a-g: Dependence of various properties of Seyfert galaxies (type 1 left-hand frames, type 2 right-hand frames) as functions of density class D: a) log L_V, b) log L_B, c) log L_{FIR}, d) log L_{6cm}, e) log $L_{H\alpha}$, f) log L_{OIII}, g) de Vaucouleurs morphological type 1. Luminosities are given in Watts.

Table 2: Intrinsic mean properties and morphological type of Sey 1 and Sey 2 galaxies as functions of density class (log of luminosities given in Watts)

Sey 1

D-type	4	3	2	1
L_V	36.67±.14	36.98±.06	37.25±.07	37.07±.14
L_B	36.28±.15	36.64±.08	37.01±.10	36.70±.22
L_{FIR}	33.37±.24	36.72±.81	36.98±.16	36.96±.16
L_{radio}	31.23±.23	31.38±.13	31.71±.16	31.19±.52
$L_{H\alpha}$	34.32±.31	35.38±.10	35.64±.20	35.26±.32
L_{OIII}	34.02±.25	34.94±.10	35.07±.14	34.60±.37
T-type	.52±.60	.77±.24	.74±.41	1.14±.69

Sey 2

D-type	4	3	2	1
L_V	36.32±.56	36.73±.07	36.88±.09	37.03±.39
L_B	35.96±.16	36.26±.09	36.40±.12	36.64±.39
L_{FIR}	36.64±.15	36.88±.10	36.91±.15	36.78±.55
L_{radio}	31.21±.40	31.99±.19	31.64±.16	32.01±.16
$L_{H\alpha}$	34.32±.29	34.27±.16	34.25±.24	34.56±1.03
L_{OIII}	34.72±.29	34.63±.18	34.78±.24	35.1[illegible]±.98
T-type	1.11±.57	1.03±.25	1.14±.50	.33±.88

As demonstrated in a previous paper (Kollatschny and Fricke 1989) it is crucial to analyse in detail the properties of all the companions concerning their redshift and activity state in order to assess the impact of the environment on Seyfert activity. In the quoted paper a smaller sample had been analysed in such detail. As a result it was possible to identify the group member which was involved in the interaction and triggering process via a hyperbolical encounter, as well as to determine the activity patterns of the surounding groups. In Fig. 2 the Hα fluxes of the companions as a function of their separation from the Seyfert galaxies are reproduced from the paper quoted above. The nearby companions develop on average pronounced higher fluxes than the more distant ones.

The existence of similar groups as those investigated here, which are not hosting a Seyfert galaxy, indicates that a suitable group environment provides only a necessary condition for the development of Seyfert activity which in addition requires favourable conditions within the host galaxy itself.

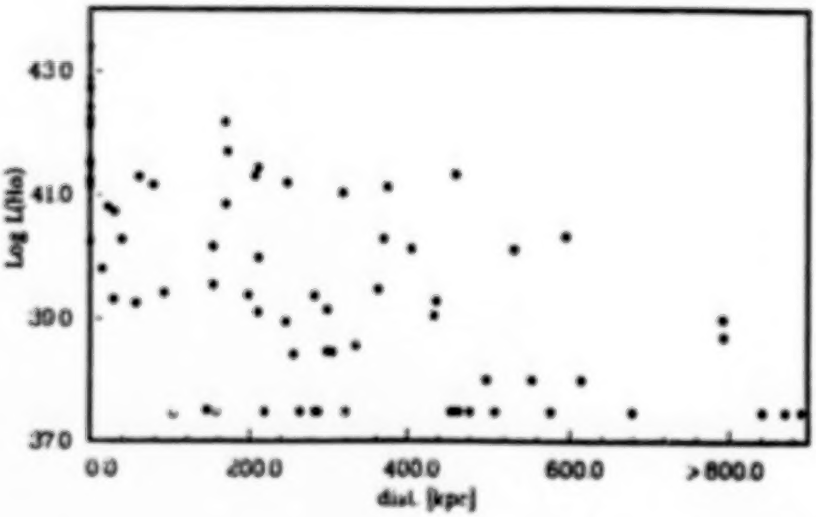

Fig. 2: The Hα luminosity as a function of projected distance from the Seyfert galaxy for all Seyfert group members

References

Kollatschny, W., Fricke, K.J., 1989: *Astron. Astrophys.* **219**, 34

Veron-Cetty, M.-P., Veron, P., 1989: A Catalogue of Quasars and Active Galactic Nuclei (4th Edition), *ESO Scientific Report* No. 7

THE ROLE OF SHOCKS IN NGC 6240

William C. Keel
University of Alabama

One of the most notable results of the IRAS mission was the recognition of a class of galaxies with large bolometric luminosities, most of whose radiation emerges in the far-infrared (typically 50-100μ). The space density of these "IRAS galaxies" approaches that of QSOs for comparable luminosities, so that these are a significant component of the population of galaxies. The frequent occurrence of interacting and merging galaxies among these infrared-bright systems has underscored the importance of understanding how various energetic processes (active nuclei, starbursts) are related to the disturbances produced during galaxy encounters. The same material directly responsible for the signature infrared excess of these systems degrades many of the diagnostics normally useful for probing the nature of he observed activity, so that in many systems it remains unclear just what kinds of phenomena are being observed.

The case of the infrared-bright system NGC 6240 encapsulates in many ways the major issues in understanding processes in infrared-bright systems in general. Its morphology strongly suggests that this is a merger in progress, with energetic phenomena being triggered as evidenced by strong radio emission and optical emission lines as well as the strong far-infrared output.

Evidence has been produced supporting various schemes for producing the energy being radiated by this object. Early work on the optical spectrum suggested a Seyfert 2 classification, but the ionization level and spatial extent of the emission implied a more distributed source of energy. IR line studies found evidence for young supergiants, and for immense amounts of H_2 excited by low-velocity shocks, which might contribute to a large enhancement in star-formation rate. Finally, the radio-continuum morphology shows compact sources possibly associated with active nuclei in both remnants of the merger.

This is one of the nearest IR-bright galaxies objects at high luminosity ($cz = 7500$ km s^{-1}), so that spatially resolved studies can yield further insight into which of these processes are most important - star formation, nuclear activity, or shock excitation.

NEW OBSERVATIONS: SPECTROSCOPY

The velocity field, linewidth distribution, and ionization structure of the gas in NGC 6240 has been mapped with the Dense-Pak fiber-optic array on the Kitt Peak 4-m telescope. In all, 135 spectra were obtained through an array of 2" apertures, with considerable overlap between many of the adjacent apertures produced by offsetting the telescope between the exposures. As the strongest features with $\lambda < 1.1\mu$, Hα and the adjacent [N II] lines were observed, along with the neighboring [O I] and [S II] features. Maps of velocity and line width were constructed by interpolating measurements from these spectra onto a regular grid, and show irregular patterns with large velocity gradients and, particularly, an extended region of large local (shear?) velocity width.

The character of the emission is also revealing. Only in a few locations do the emission lines show ratios and widths indicating normal H II regions photionized by young stars (Fig. 1). Most of the emission is of a LINER-like character, and has FWHM for the lines of order 500 km s^{-1}. Such emission might in principle reflect shock

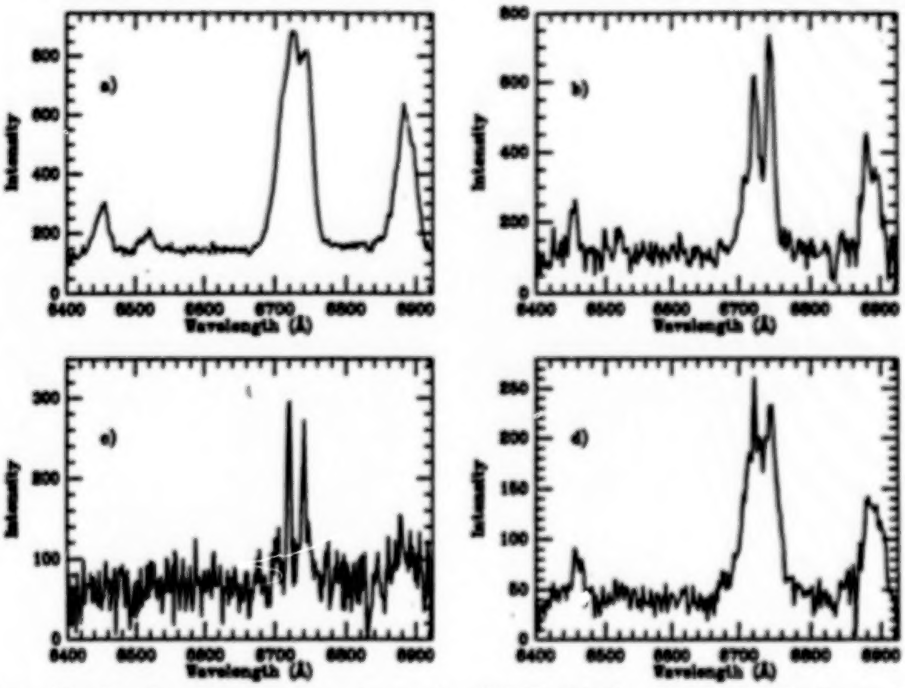

Fig. 1: Four kinds of emission spectrum in NGC 6240. a) relatively broad lines on the brighter nucleus, b) very extended LINER-line emission with linewidths ≈ 500 km s^{-1} FWHM, c) H II regions near the edge of the mapped region, d) very broad wings on Hα+[N II] suggesting reflected light from a broad-line nucleus.

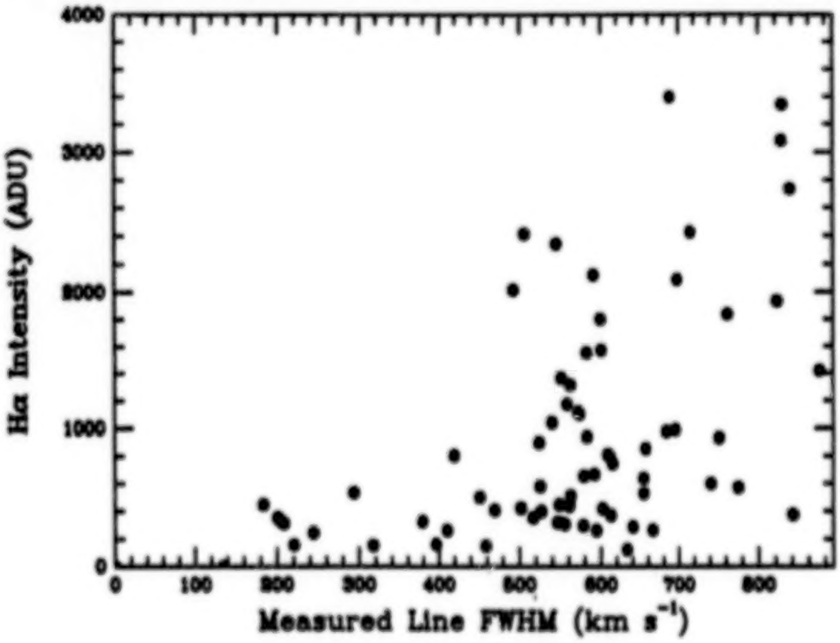

Fig. 2. Emission-line intensity versus local line width (FWHM) for NGC 6240, excluding areas within 2 arcseconds of the brighter nucleus.

excitation (at velocities of order 100 km s^{-1} or photoionization by a weak flat-spectrum source (such as an active nucleus). The structure of the gas provides a clue for discriminating between these possibilities - the line intensity and inferred ionization parameter do not show symmetry about the nucleus, but the line intensity is coupled to the local line width, as if the processes driving the local velocity structure are also responsible for the ionization of the gas. The relation between line intensity and emission-line FWHM is shown in Fig. 2 for all positions except the two nuclei and their immediate vicinity.

The relation between line width (dominated by local velocity structure) and maximum line intensity is a strong argument that shocks are dominant in ionizing the interstellar medium throughout the inner 5 kpc of NGC 6240.

NEW OBSERVATIONS: IMAGING

New images, from B to K bands, have also been obtained, including a set taken with the ESO/MPI 2.2-m telescope in subarcsecond seeing. Seeing deconvolution (via a modified CLEAN algorithm) has been used to examine the two apparent nuclei and their surroundings. The two optical objects appear to be genuine stellar concentrations, with symmetric (and very compact) structures and quite similar, heavily reddened, continuum energy distributions. The latter implies that both are deeply imbedded in the extensive dust distribution of the system, and thus are close together in space as well as in projection.

Analysis of the imaging data also allows a new assessment of the contribution of reradiated starlight to the overall far-IR luminosity of the system. Considering both the strong dust lanes and the widespread diffuse dust responsible for most of the extinction, a lower limit of about 15% may be set for the contribution of a component analogous to galactic cirrus emission, in which the grains are heated by ambient visible-wavelength starlight as opposed to the UV continuum of a starburst population. As a lower limit, this calls into question the need for a strong burst of star formation on strictly energetic grounds, as has been done by Thronson *et al.* (1990) as well.

EMISSION-LINE ENERGETICS

The ionization of the observed gas appears to be dominated by shock heating, but closer examination is needed to assess the roles of star formation and possibly nuclear activity as well in contributing to the overall luminosity of the system. Since the emission-line luminosity is only a small fraction of the bolometric luminosity, it is not obvious that the kinetic energy of the system of gas clouds being released via collisions is sufficient to power the far-infrared excess for a significant time.

The kinetic-energy content of the gas may be expressed as

$$E = \frac{3m_{\rm H}D^2(v-\bar{v})^2}{2\pi f_i n_e \alpha h\nu \mathrm{I}_{line}}$$

where integration over the whole emission region is assumed. Here m_H is the mass of the hydrogen atom, D is the system's distance, v the radial velocity at each point and $\bar{v}$ the mean (the factor 3 assumes isotropic motions), f_i is the ionized fraction of the gas by mass, n_e the electron density, and I_{line} the intensity of a recombination line at frequency ν with recombination coefficient α. The energy content of the gas in NGC 6240 may be estimated using n_e from the [S II] λλ 6717,6731 doublet ratio and direct integration of the intensity and velocity maps. Local gas motions (reflected in the line widths) dominate over large-scale motions (those that are spatially resolved) by about a factor 10. For a value $f_i = 0.01$, $E = 2 \times 10^{56}$ erg s^{-1}, scaling inversely as the ionized fraction. Only for $f_i < 10^{-4}$ could cloud collisions power the total energy output of NGC 6240 in the far-infrared for the 10^7 years needed for a nontrivial chance of seeing the system in such a phase. The large CO luminosity of NGC 6240 does suggest a large value of f_i, but the relation between CO emission and H_2 mass needs to be better understood in such systems for reliable conclusions.

Particularly if most of the gas in NGC 6240 is neutral or molecular, the situation is remniscent of the proposal by Harwit *et al.* (1987) that collisional heating could be dominant in IR-bright galaxies. If the optical and near-IR line emission from such systems is dominated by shocked gas (as proposed here), searches for such systems via, for example, $2 - 4\mu$ slitless or multiobject spectroscopy from space to search for strong H_2 emission, could yield a direct tracer of the rate of disk galaxy mergers and its evolution with cosmic time.

A full presentation of the data, and details of the analysis, have been submitted to the *Astronomical Journal.*

This study was made possible by allocations of observing time at Kitt Peak National Observatory, the European Southern Observatory, and the Observatorio del Roque de los Muchachos, and supported in part by EPSCoR grant RII-8610699.

REFERENCES

Harwit, M., Houck, J.R., Soifer, B.T., and Palumbo, G.G.C. 1987, Astrophys. J. 315, 28.

Thronson, H. A., Jr., Majewski, S., Descartes, L., and Hereld, M. 1990, Astrophys. J. (submitted).

DEEP FABRY-PEROT IMAGING OF NGC 6240:
KINEMATIC EVIDENCE FOR MERGING GALAXIES

J. Bland Hawthorn
Dept. of Space Physics and Astronomy, Rice University, Houston, TX 77251-1892

A. S. Wilson
Astronomy Program, University of Maryland, College Park, MD 20742

R. B. Tully
Institute for Astronomy, Honolulu, Hawaii 96822

ABSTRACT. We have observed the superluminous, infrared galaxy NGC 6240 ($z = 0.025$) at Hα with the Hawaii Imaging Fabry-Perot Interferometer (HIFI - Bland and Tully 1989). During the past decade, observational evidence from all wavebands indicates that the unusual appearance of NGC 6240 has resulted from a collision between two gas-rich systems, a view which is supported by our spectrophotometric data. However, the origin of the enormous infrared luminosity (4×10^{11} $L_\odot$) detected by IRAS remains highly controversial, where opinions differ on the relative roles of large-scale shocks, massive star formation or a buried "active" nucleus. These mechanisms are discussed in the light of our Fabry-Perot observations.

OBSERVATIONS

The HIFI system was mounted at the Cassegrain focus of the University of Hawaii 2.2m telescope. We observed 12 frames for a total of six hours at 68 km s^{-1} increments across the Hα line, which is comparable to the spectral resolution of the high finesse (60) etalon, providing a velocity coverage of 820 km s^{-1}. A low read-noise (~$4e^{-}$), 385 × 576 format GEC CCD was placed at the image plane. The f/2 input beam yielded an angular resolution of 0.85" per pixel providing an overall field-of-view of 8' by 5'. These observations have been supplemented with Hα, [OIII]λ5007 and Hβ narrowband imagery using the Prime Focus CCD at the CTIO 4m telescope. The RCA 512 × 320 CCD has an angular resolution of 0.60" per pixel providing an overall field-of-view of 5' × 3'. The total integration time for each on-band and off-band image is 1200s. The thinned chip has fringing problems that are largely divided out using flatfields except for the Hα observation where a dome flat was not taken. Charge transfer "bleeding" about bright stars has been removed using row-oriented, sinc interpolation. The normal stages of photometric calibration (bias and sky subtraction, relative scaling with field stars, etc.) have been applied to all images, the results of which are shown in Figs. 1 and 2.

RESULTS

Fosbury and Wall (1979) first drew attention to the unusual appearance of NGC 6240: their photographic plates taken at the ESO 3.6m telescope showed clearly a number of plumes extending in all directions from a bright, central region. Fig. 1(a) shows an optical continuum image that exhibits all of these features. Fosbury and Wall suggested that most of the flux arising from the central region is line emission, a supposition that is confirmed by the Hα and [OIII]λ5007 images in Figs. 2(a) and 2(b) respectively. Even with the limited velocity coverage of the Fabry-Perot spectra, a comparison of the integrated line emission shown in Fig. 3(a) with Fig. 2(a) and the imagery of Heckman, Armus and Miley (1987) demonstrates that we detect most of the Hα flux to the limits of these CCD images (~6×10^{-17} erg cm^{-2} s^{-1} $arcsec^{-2}$). However, in a few specific locations, there is some confusion between line and continuum in that these are indistinguishable in the HIFI data for lines broader than 600 km s^{-1} FWHM. Indeed, the HIFI data show that the bright inner region is dominated by emission with line

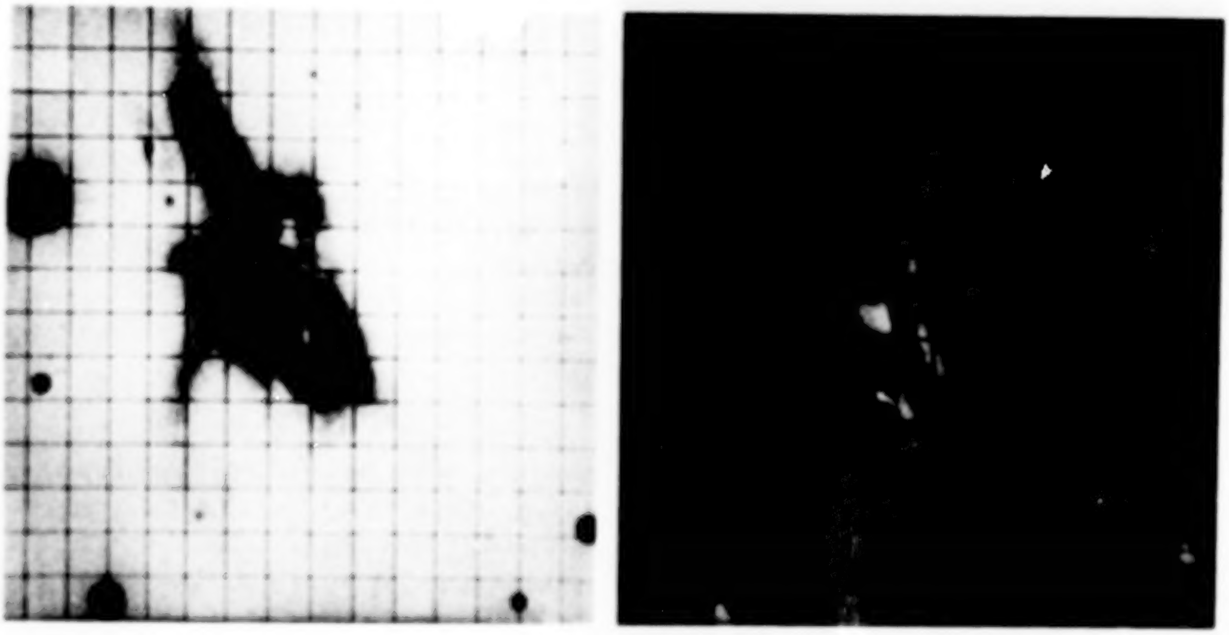

Figure 1(a). An optical continuum image of NGC 6240 formed from the sum of two images taken through 100Å filters, centered at λ5400 and λ7080, using the Prime Focus CCD at the CTIO 4m telescope. For all plates, the field-of-view shown is 90" × 90" where north is upwards and east is to the left. The grid lines are spaced at 6" intervals along both axes to aid comparisons between the figures. (b). An image formed from the ratio of the two continuum images used in (a). Light and dark areas show regions of relatively high and low extinction. The double nucleus, seen at the center of the image, occurs along one of the low extinction bands.

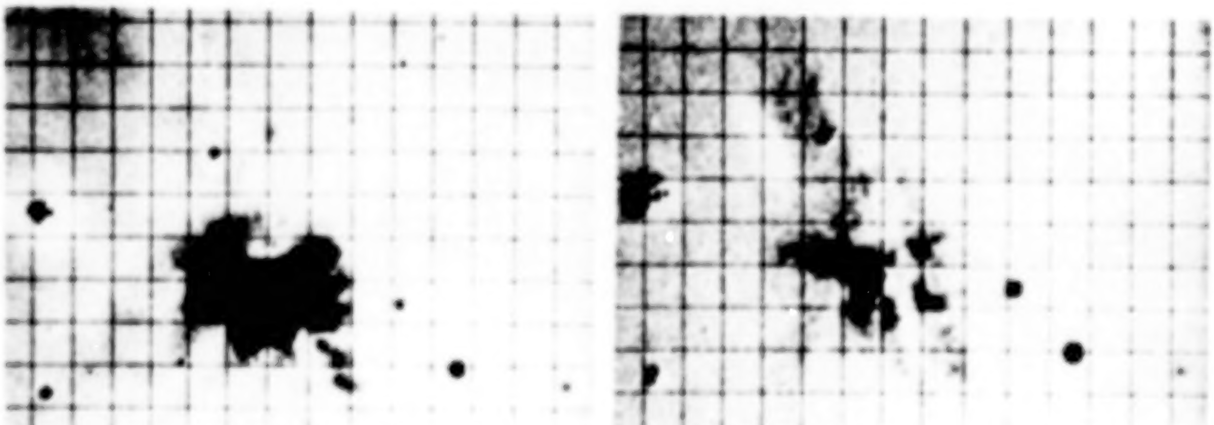

Figure 2(a). The Hα line flux distribution in the central regions of NGC 6240 obtained from on-band/off-band imaging with the CTIO Prime Focus CCD. The fringes arise from night-sky lines within the filter bandpass. (b). The [OIII]λ5007 line flux distribution in the central regions of NGC 6240. Notice the residuals from the double nuclei resemble the residuals from the field stars. The two HII regions to the west are roughly a magnitude brighter in [OIII]λ5007 than in Hα.

widths ~1000 km s^{-1} FWHM. Long-slit spectra covering the wavelength range λ4200-λ5300 taken at the CTIO 4m telescope confirm this same behavior in the [OIII]λ5007 line emission. Moreover, both the Hα and the [OIII]λ5007 line profiles are observed to broaden as the flux within the line increases (see also Keel, this conference).

Figure 1(b) shows the ratio of the off-band continuum images centered at λ5400 and λ7080 and serves to illustrate regions of relatively low (dark) and high (light) dust extinction. Parallel strands of low and high extinction are observed to run from NE to SW with the SE plume exhibiting a similar behavior. The resolved double nucleus, first identified at radio (Condon et al. 1982) and optical wavelengths (Fried and Schulz 1983) is easily seen in the center of the image and lies along a strand of relatively low extinction. The ratio of the Hβ to Hα line flux images confirms our interpretation of Fig. 1(b). While the [OIII]λ5007/Hα ratio tracks the Hβ/Hα ratio rather closely, the imagery was not considered to be good enough to correct the [OIII]λ5007 flux for extinction effects. Over the bright inner region, the Hβ/Hα ratio implies a magnitude of extinction between these wavelengths favoring a visual extinction, $A_V \approx 3$-4 mag and a total Hα luminosity, $L_{H\alpha} \sim 5 \times 10^{42}$ erg s^{-1}.

The Fabry-Perot data and Fig. 2(a) demonstrate that the line emission separates into at least three distinct components: (i) several filamentary "arms" that extend across the entire field-of-view, (ii) a diffuse envelope with dimensions 80" × 50" whose long axis is aligned with the long axis of the galaxy, which encompasses (iii) a luminous "spur" ($L_{H\alpha} \sim 2 \times 10^{41}$ ergs^{-1}) that extends 20" SW from the double nucleus. There is marginal evidence for a limb-brightened "bubble" 35" due north of the nucleus as only in this region are narrow spectral lines observed to split with a maximum separation of ~350 km s^{-1}. The bow-shock morphology is similar to the bipolar bubbles in M82 (Bland and Tully 1988) although the distance to NGC 6240 (98 Mpc) makes this feature much larger (~17 kpc).

The HIFI spectra show that while the Hα line profiles are both broad and display complex structure over the inner region, all profiles exhibit a bright component that dominates the line emission. These have been fitted with gaussians and the resultant velocity field is presented in Fig. 3(b). While the velocity field appears complicated, large-scale patterns do emerge. The gross distribution of the line flux in Fig. 3(a) can be described in terms of two axes, one that runs from SW to NE through the double radio source (Axis 1), and another that crosses the top of the latter from SE to NW (Axis 2). Both of these directions define the steepest gradients through the velocity field. Along Axis 1, the gradient is ~300 km s^{-1} over about 15" centered on the double nucleus, turning over in both directions outside of this range. The gradient along Axis 2 is much steeper at ~500 km s^{-1} over about 5" centered on a point 10" NE of the compact radio source. If the latter defines the systemic velocity, the second system is redshifted by only 70 km s^{-1} with respect to the nucleus. A preliminary interpretation (Bland, Wilson and Tully, in prep.) suggests that the velocity field may be explained in terms of two rotating discs that are only 5 kpc apart in projection, as illustrated by the two ellipses in Fig. 3(b).

PRELIMINARY INTERPRETATION

Evidence for an "active" nucleus. The idea of a buried AGN was originally proposed to explain the non-thermal spectrum of the compact, double radio source (Condon et al. 1982). The extended LINER spectrum of the diffuse, ionized gas (Heckman, Armus and Miley 1987) might even seem to support this view (however, see below). The non-thermal nature of these compact sources has been confirmed by more recent optical, infrared and radio observations (Keel, this conference; Eales et al. 1988; Neff 1990, personal communication). Interestingly, the luminous "spur" has some of the characteristics of a Seyfert-like, narrow line region. It is aligned roughly with the axis of the double radio source and displays broad lines (~300 km s^{-1} FWHM) with blue wings up to 10 kpc from the galactic nucleus. If the extinction towards the nucleus is indicated by the strength of the Bγ line (Depoy et al. 1986), the SW spur has a corrected luminosity of $L_{H\alpha} \sim 2 \times 10^{42}$ erg s^{-1} which is comparable to that observed in luminous Seyfert 1 galaxies.

Evidence for transience. The kinematic data indicate the presence of two dynamical systems, closely spaced in velocity and position, that are almost perpendicular to each other. A more detailed study suggests that Axis 2 is

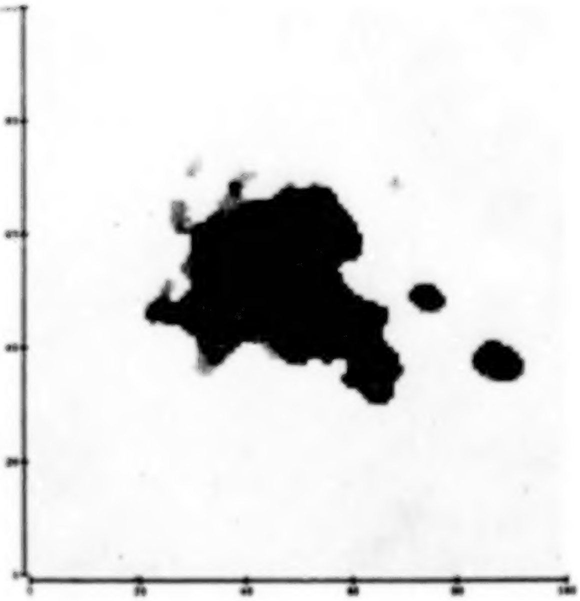

Figure 3(a). The Hα line flux over the inner 43" × 43" of NGC 6240 obtained from integrating over the HIFI line profiles. Only values that exceed a surface brightness of 2.5×10^{-16} erg cm^{-2} s^{-1} $arcsec^{-2}$ are shown. The darkest regions correspond to a surface brightness that is 5 magnitudes larger than the adopted cut-off. The brighter of the double nuclei occurs at pixel position (52,50); two bright HII regions are seen west of the nucleus at pixel positions (74,51) and (85,62).

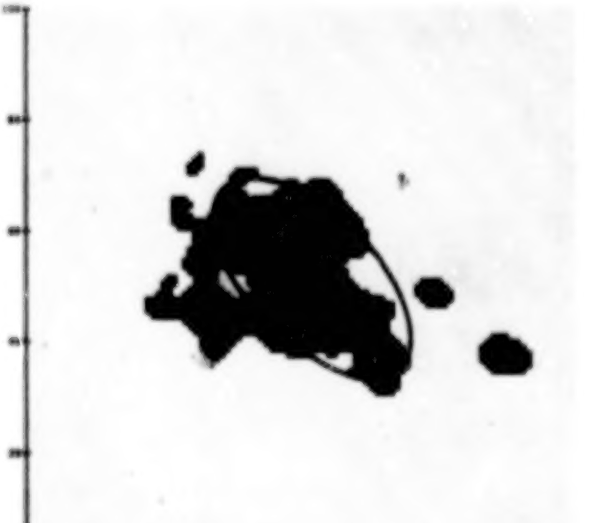

Figure 3(b). The Hα velocity field obtained from gaussian fits to the brightest component in the Hα line profiles. The velocities are shown only for those line profiles whose integrated surface brightness exceeds the cut-off used in Fig. 3(a). The lightest and darkest regions correspond to maximum velocities of -300 kms and 300 kms with respect to the velocity of the double nucleus. The two HII regions to the west are highly redshifted with respect to the nuclear velocity.

the dense core of a disc that has been disrupted, while Axis 1 defines the major axis of a system that is undergoing coalescence with the second system. Dynamical simulations (Hernquist 1990, personal communication) show that these systems will be merged completely on a dynamical timescale ($< 10^8$ years).

Evidence for large-scale shocks. Harwit and collaborators (Harwit et al. 1986; Harwit and Fuller 1988) have shown how the kinetic energy release from two colliding galaxies can give rise to large-scale shocks which subsequently heat the dust grains. The line flux arising from the ram pressure in the shocks is proportional to $V_S{}^n$, where V_S is the relative velocity of impact, and n ($\sim$3) and depends on many factors. Both optical (Fosbury and Wall 1979; Fried and Schulz 1983) and molecular spectroscopy (Lester, Harvey and Carr 1988) seem to indicate that shocked gas is present. It is tempting to suggest that the line flux – line width relation and the structure of the dust bands are somehow connected to the existence of large-scale shocks. In this event, we would expect to observe a line width – line excitation dependence in this region.

Evidence for a massive starburst. Of the suggested mechanisms, we favor a model in which the merger has triggered an episode of vigorous star formation. When two gas sheets are compressed at speeds of ~500 km s^{-1}, the onset of instabilities will generate large dense clumps which supersede star formation. The evidence for a wind-blown bubble supports the view of Heckman, Armus and Miley (1987) who suggest that the LINER spectrum of the ionized gas arises in shocks powered by starburst-driven winds. These authors find from a few long-slit positions that the ionized gas is overpressured with respect to the gravitational potential. The tenfold increase in the size of the putative nebula compared with M82 may reflect a similar increase in the supernova rate (Draine and Woods 1989). The main objection to the starburst picture has been the paucity of ionizing photons (Depoy et al. 1986) and the strength of the CO bands (Lester, Harvey and Carr 1988) which require a peculiar initial mass function. However, an evolved dense starburst produces many supernova remnants which, in our own galaxy, are strong sources of molecular hydrogen (Oliva and Moorwood 1988). In this case, a post-starburst phase could have only a few hot stars and radiate large amounts of H_2 and [Fe II] line emission.

Acknowledgments

JBH and RBT acknowledge the support of NSF grant AST 88-18900 and discussions with Martin Harwit, Lars Hernquist and Jon Weisheit.

References

Bland, J. and Tully, R. B. 1988, *Nature* **334**, 43.
Bland, J. and Tully, R. B. 1989, *Astron. J.* **98**, 723.
Condon, J. J. et al. 1982, *Ap. J.* **252**, 102.
Depoy, D., Becklin, E. E. and Wynn-Williams, C. G. 1986, *Ap. J.* **307**, 116.
Draine, B. T. and Woods, D. T. 1989, *Ap. J.*, preprint.
Eales, S. A. et al. 1988, *Infrared Arrays*, p. 345, eds. C. G. Wynn-Williams and E. E. Becklin.
Fosbury, R. A. E. and Wall, J. V. 1979, *MNRAS* **189**, 79.
Fried, J. W. and Schulz, H. 1983, *Astr. Ap.* **118**, 166.
Harwit, M. et al. 1986, *Ap. J.* **315**, 28.
Harwit, M. and Fuller, C. E. 198, *Ap. J.* **328**, 111.
Heckman, T. M., Armus, L. and Miley, G. K. 1987, *Astron. J.* **92**, 276.
Joseph, R. D., Wright, G. S. and Wade, R. 1984, *Nature* **311**, 132.
Lester, D. F., Harvey, P. M. and Carr, J. 1988, *Ap. J.* **329**, 641.
Oliva and Moorwood 1988, *Astr. Ap.*, preprint.
Rieke, G. H. et al. 1985, *Ap. J.* **290**, 116.

BLANK PAGE

IC5063: A MERGER WITH A HIDDEN LUMINOUS ACTIVE NUCLEUS

L. Colina*, W. Sparks, F. Macchetto*

Space Telescope Science Institute, Baltimore, U.S.A.
* Affiliated to the Astrophysics Division, ESTEC, Noordwijk, The Netherlands.

1. INTRODUCTION

Despite intense theoretical and observational effort during the past few years, two important questions in the field of active galaxies remain open and are the subject of vigorous debate.

The first concerns the connection between the interaction/merger of galaxies and the generation of starburst and/or active nuclei. A large fraction of high luminosity radio galaxies (Baum et al. 1988), quasars (Hutchings, 1987) and IRAS galaxies (Sanders et al. 1988), show the presence of a large companion or have a peculiar optical morphology which is offen interpreted as evidence of a recent merger or interaction. In Seyferts, there are also several examples of individual galaxies with clear evidence of interaction/merger (Colina et al. 1987; Fricke and Kollatschny, 1989; Macchetto et al. 1990). Also a significant fraction of low luminosity radio galaxies are associated with a system of two elliptical galaxies in interaction (Colina and Péres-Fournon, 1990a,b).

The second question concerns the anisotropy of the non-thermal nuclear source. A large body of evidence has been collected during the past five years showing that all types of active galaxies could radiate anisotropically (obscuration/beaming/accretion disc/ionisation cones) and suggesting therefore that the diversity of AGNs can simply be explained by a different viewing angle (see Browne, 1989 for a review).

IC5063 is a nearby galaxy classified as an SO and containing a system of dust lanes parallel to its major optical axis (Danziger, Goss and Wellington, 1981; Bergeron, Durret and Boksenberg, 1983). Extended emission line regions with high excitation properties have been detected over distances of up to 19 kpc from the nucleus. This galaxy has been classified as Seyfert 2 on the basis of its emission line spectrum. These characteristics make IC5063 one of the best candidates for a merger remnant and an excellent candidate for a hidden luminous active nucleus. Based on new broad and narrow band images and long-slit spectroscopy obtained at the ESO 3.6m telescope using EFOSC, we present some preliminary results supporting this hypothesis.

2. RESULTS AND DISCUSSION

(a) Origin of the gas/dust: merger remnant

Fig.1a shows the image of IC5063 in the B broad-band filter while Fig.1b presents an extinction map derived by ratioing the B image to an elliptical model of the R image (Sparks et al. 1985). This shows a complex system of dust lanes mostly in the northern half of IC5063. The morphology represents a zig-zagging distribution running roughly parallel to the major axis of IC5063 extending from very large radii all the way into the nucleus. This supports the idea that the dust has an external origin since such structures are unlikely to survive for long due to differential rotation effect. We are witnessing gas in the process of relaxing into the principal plane of the galaxy.

The distribution of the ionized gas is presented in Figure 1c & d. We see a main body with three radial filaments in position angles 285°–290°, 310°–315° and 325°–330°. The size of these emission regions is ≈ 69" by 20" (i.e. 22 by 6.4 kpc for H_0= 50 km s^{-1} Mpc^{-1}) along the major and minor axis respectively. Also an extension of the PA285° filament is detected in [OIII] bending toward west at PA270° and at distances of up to 90" from the nucleus (i.e. 29 kpc).

The morphological characteristics, together with the kinematic properties and heavy element abundances of the gas suggest an external origin (Colina et al. 1990, in preparation).

(b) Hidden Luminous Active Nucleus

The high S/N of our spectrum enables us to find evidence for the presence of a very powerful non-thermal source hidden in the nucleus of IC5063. First, we detect high excitation emission lines of [FeVII]λ 5721, 6087 (ionisation potential Fe^{6+}= 100 eV) and less clearly, [CaV]λ5309 and [FeX]λ6375. These lines are only detected within 1.5–2" around the nucleus (see Figure 2), indicating therefore the presence of a local and hard extreme ultraviolet ionizing source. We do not have any temperature indicator for the regions emitting these lines but in other Seyfert galaxies where these high excitation lines have been detected (i.e. Tol0109–383: Fosbury and Sansom 1983), the temperatures were consistent with photoionisation.

Second, we detect a faint broad Hα emission line. This component is also only observed within 1" of the nucleus (see Figures 3a,b). Its FWZI corresponds to a velocity of 6000 km s^{-1}, which confirms the claim by Bergeron, Durret and Boksenberg (1983) based on deblending techniques. This faint broad emission component may arise in an obscured broad line region.

3. SUMMARY

The results obtained using new deep optical images and long-slit spectroscopy of IC5063 and its associated extended emission line regions, can be summarised as follows:

(a) We detect a system of zig-zagging dust lanes over the whole galaxy, concentrated in the northern regions, and running approximely parallel to the major optical axis. We also detect high excitation extended emission line regions concentrated along the major axis of the galaxy and with a total size of 22 x 6.4 kpc. This system of gas and dust with its peculiar morphology most likely has an external origin and can be considered as the likely remnant of a recent merger.

(b) The spectra of the nucleus of IC5063 shows high excitation lines like [FeVII]λ6087 and a faint broad Hα emission line component (FWZI$\approx$ 6000 km$\cdot$ s^{-1}) This is evidence for the presence of a hidden Seyfert 1 type nucleus located at the center of IC5063.

REFERENCES

Baum, S.A., Heckman, T.M., Bridle, A., van Breugel, W., and Miley, G., 1988, *Ap. J. Suppl.*, **68**, 526.

Bergeron, J., Durret, F., and Boksenberg, A., 1983, *Astr. Ap.*, **127**, **322**.

Browne, I.W.A., 1989, *ESO Workshop on Extranuclear Activity in Galaxies*, Ed: E.J.A. Meurs and R.A.E. Bosbury, p. 379.

Colina, L., Fricke, K.J., Kollatschny, W., and Perryman, M.A.C. 1987, *Astr. Ap.*, **178**, 51.

Colina, L., and Péres-Fournon, I., 1990a, *Ap. J. Suppl.*, **72**, 000.

Colina, L., and Péres-Fournon, I., 1990b, *Ap. J.*, **348**, 000.

Danziger, I.J., Goss, W.M., and Wellington, K.J., 1981, *M.N.R.A.S.*, **196**, **845**.

Fosbury, R.A.E., Sansom, A.E., 1983, *M.N.R.A.S.*, **204**, 1231.

Fricke, K.J., and Kollatschny, W., 1989, I.A.U. Symposium 134, *Proc. Conf. Active Galactic Nuclei*, ed: D.E. Osterbrock and J.S. Miller, (Dordrecht: Reidel), p.425.

Hutchings, J.B., 1987, *Ap. J.*, **320**, 122.

Macchetto, F.D., Colina, L., Golombek, D., Perryman, M.A.C., and di Serego Alighieri, 1990, *Ap. J.*, , in press.

Sanders, D.B., Soifer, B.T., Elias, J.H., Madore, B.F., Matthews, K., Neugebauer, G., and Scoville, N.Z., 1988, *Ap. J.*, **325**, 74.

Sparks, W.B., Wall, J.V., Thorne, D., Jordan, P., van Breda, I.G., Rudd, P., Jorgensen, H.E., 1985, *M.N.R.A.S.*, **217**, 87.

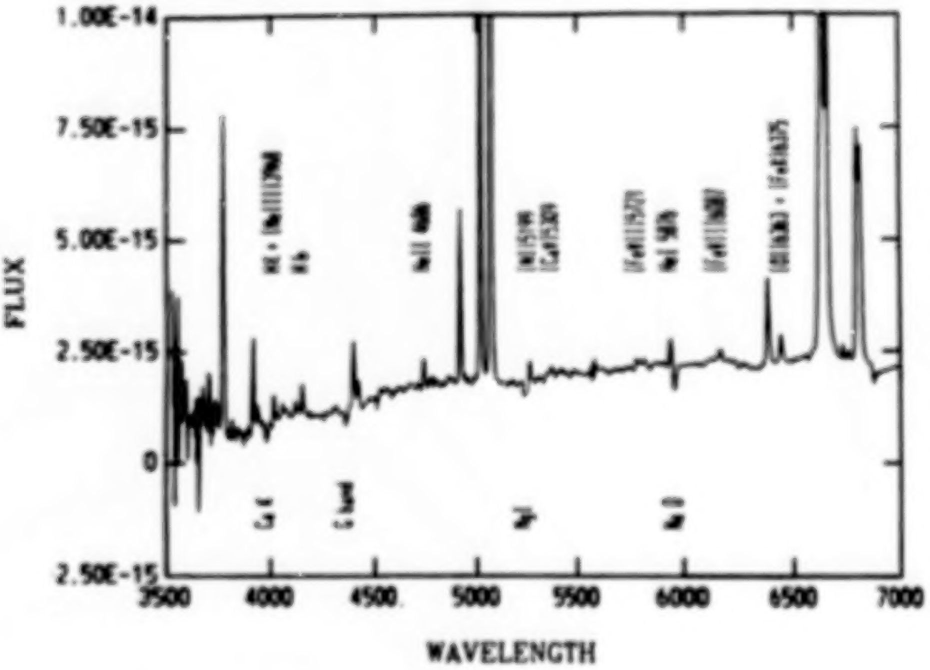

Figure 2: Spectrum of IC5063 nucleus showing all the strong emission lines and the faint high excitation lines.

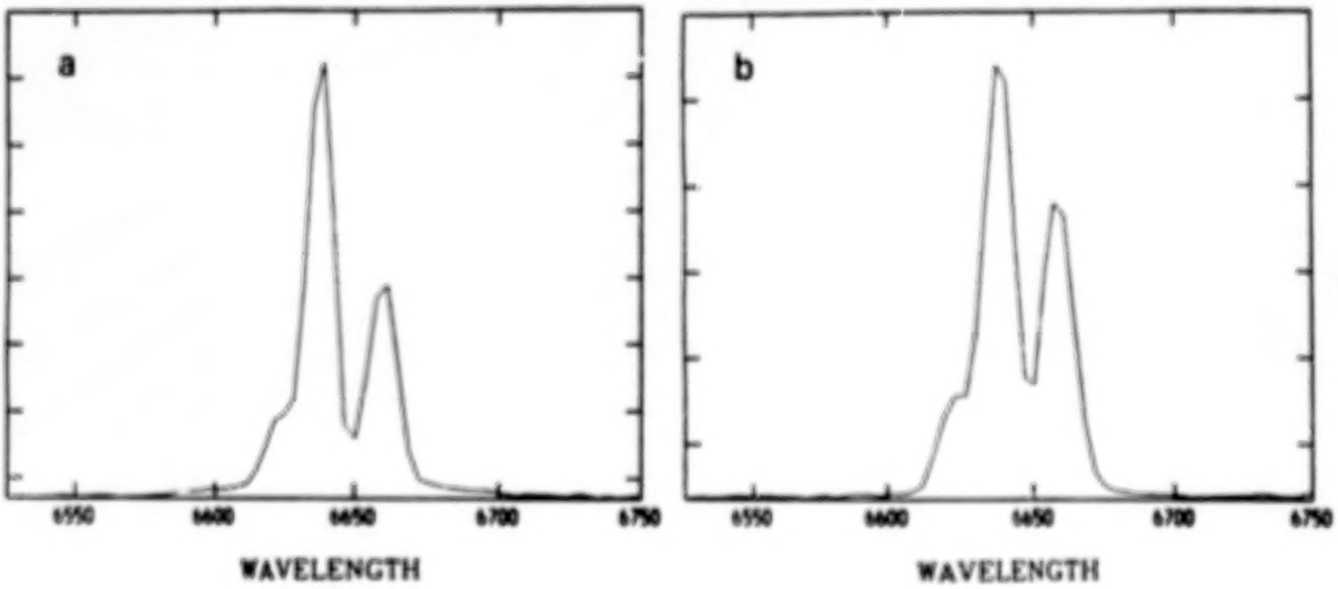

Figure 3: (a) Profile of the Hα line centered on the nucleus. The faint broad emission line component with FWZI≈ 6000 km· s^{-1} is clearly visible. (b) The same emission line profile but centered at 1.4″SE of the nucleus along PA289°. Note that the broad component is no longer present.

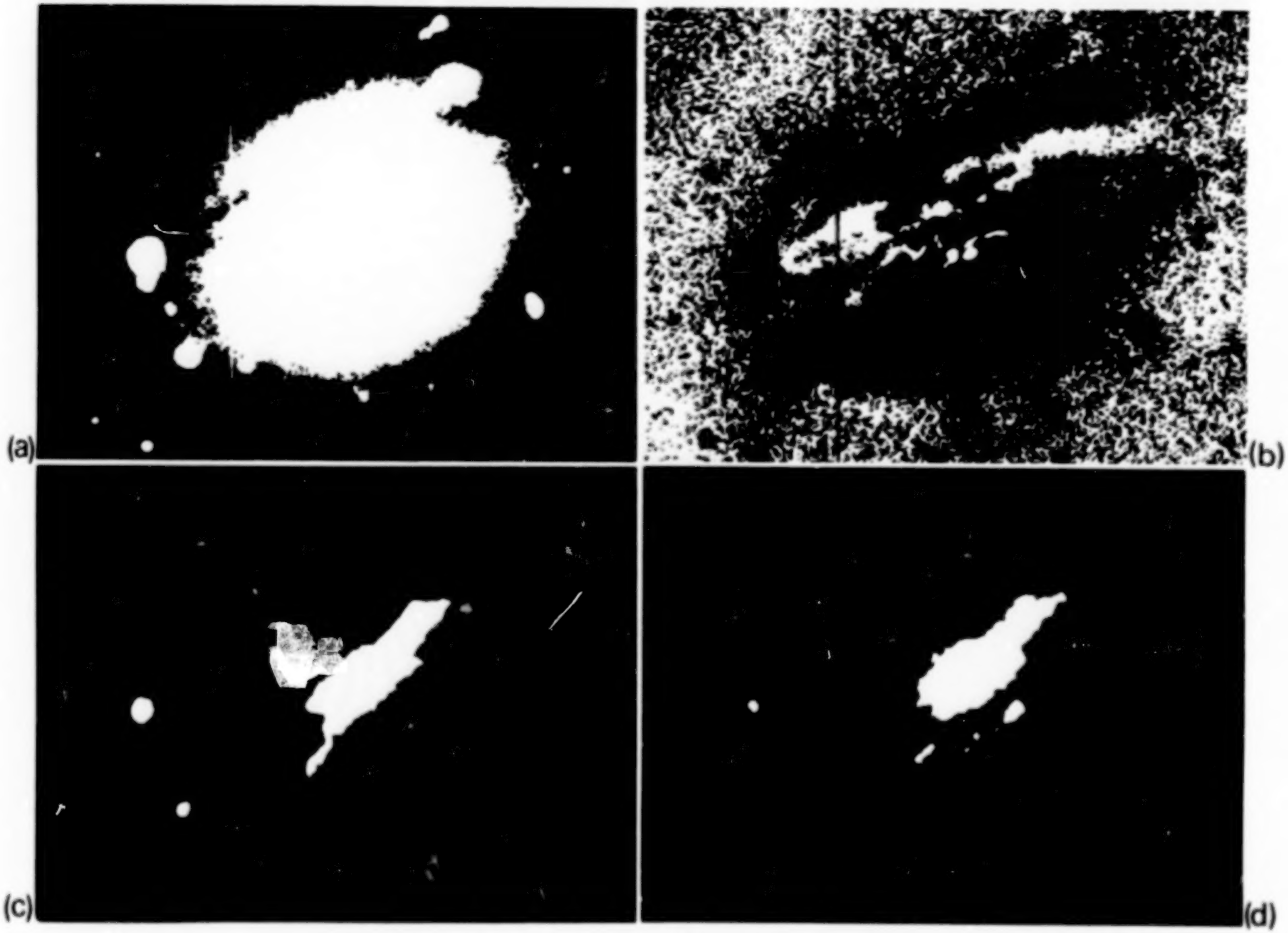

Figure 1: **(a)** Image of IC5063 in the *B* broad-band filter. **(b)** $B - R$ image of IC5063 obtained as explained in the text. The system of zig-zagging dust lanes in the northern half of the galaxy is clearly visible. **(c)** Image of IC5063 showing the extended emission line regions in the [OIII]λ5007 line. **(d)** Image of IC5063 showing the extended emission line regions in the Hα line. In all the figures north is at the top and east to the left and the field of view is 169″ x 155″.

BLANK PAGE

VI. REDSHIFT RELATED PROBLEMS

BLANK PAGE

PANEL DISCUSSION ON REDSHIFT PROBLEMS

The "redshift controversy" can be said to have originated from studies of pairs and compact groups. There are two potential problems involving the measured redshifts of galaxies in interacting systems: 1) the question of the physical association of galaxies in pairs and groups with discordant ($\Delta V_0 \geq 10^3$ kms^{-1} redshift and 2) the possible quantization of redshifts in samples of pairs regarded (on the basis of redshift difference) as physical. The emphasis in the panel discussion was on the latter problem.

Each panel member gave an opening statement followed by discussion. In lieu of a direct transcript of the panel the contributors have summarized their presentations and impressions in the following contributions. - Eds.

W. G. Tifft

At the very heart of this IAU meeting on the dynamics of pairs and systems of galaxies there is an underlying assumption that the redshift is a simple Doppler shift which we may use to measure motions and build dynamical models. For 20 years now I have been working to test this underlying assumption using studies of 1) correlations of redshift with intrinsic properties of galaxies, 2) tests of continuity, commonly referred to as 'redshift quantization', and most recently 3) tests for rapid variability. A remarkably consistent overall picture has emerged which is *not* critically tied to any single aspect of the work. The result, simply put, is that the redshift has properties which *are not consistent with a standard velocity interpretation*. This result is based upon a multitude of samples including a considerable amount of high quality 21 cm data.

Studies in the 1970-1975 period led to discovery of various redshift-magnitude and redshift-morphology correlations. These correlations are as unexplained today as they were then. In 1973 the first hints of quantization were presented at IAU Symposium 58. By 1975 the quantization concept was central in my thinking since it provided a very critical and clear test of conventional wisdom. Formal predictions were published in a series of three papers in the Astrophysical Journal in 1976. This original prediction of a basic redshift periodicity of 72.5 km s^{-1}was based primarily upon data in the Coma cluster and a review of internal dynamics of galaxies.

The 1976 predictions were not based significantly on any data on pairs of galaxies, but studies of pairs provided the first critical test of quantization. There now exist three independent accurate samples of pairs: 1) 21 cm pairs, beginning with the sample by S Peterson and evolving through several iterations into what we now refer to as the revised radio sample, 2) Optical studies of close Karachentsev pairs observed at Steward Observatory, and 3) A subsample of pairs observed optically by L Schweizer in the southern hemisphere. The most recent summary of work on pairs appeared in the Jan 1989 ApJ.

The picture for pairs is now quite sophisticated. The ΔV distribution has at least three peaks (24,72,145 km s^{-1}) and four minima (0,48,108,180 km s^{-1}). My one illustration for this brief review shows the composite of the three available samples to illustrate the current situation. Each sample alone provides a significant test of the 1976 predictions. Among the newest results, discussed in the January 1989 ApJ, is the conclusion that identical redshifts do not occur in close proximity. This 'zero deviation' concept is at distinct variance with conventional dynamics, and stands alone as a fundamental redshift test. Several new tests based upon this 'exclusion' concept have been developed and are discussed in the January ApJ paper.

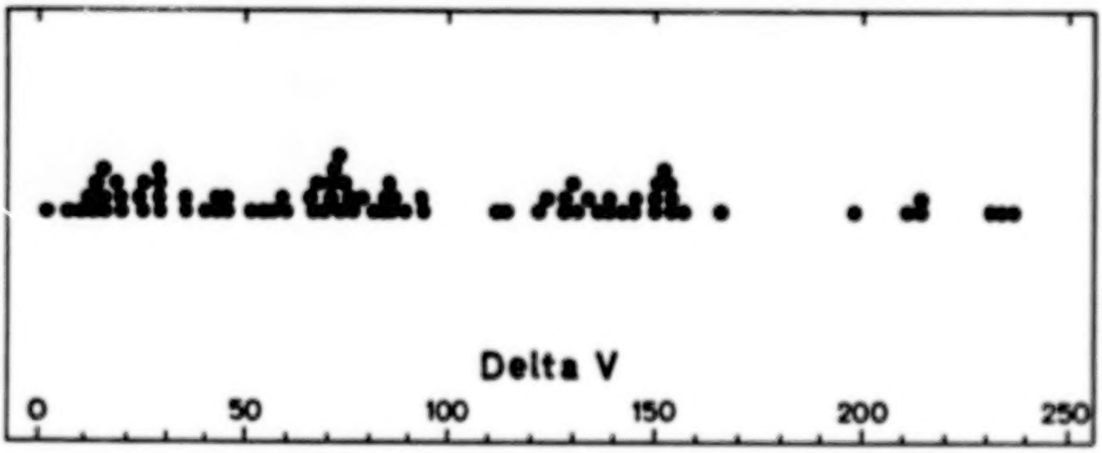

Figure 1. Cumulative differential redshift distribution of 84 points from the three best data sets, the revised radio sample (18), the Schweizer sample (25) and the high-weight Karachentsev pairs (41).

Recently Newman, Haynes and Terzian (ApJ 1989) have questioned the statistical framework used to test for quantization. They point out that clumping is commonly seen in small samples and is rarely significant. They do not account, however, for the fact that the particular pattern involved was specifically predicted in advance and not determined from the samples tested. Furthermore, multiple independent samples are involved. An interesting debate is also developing over the statistical approach used (Schneider and Sharp in this panel discussion, Sharp (1990), Cocke and Tifft (1990 ApJ in process) and Newman, Haynes and Terzian). No one has yet explained away the simple fact that predicted patterns have reoccured.

The quantization test was extended to the studies of groups of galaxies in 1983, again successfully. Important work showing quantization in groups has also been done by Arp and Sulentic. Bill Napier gave a paper at the Venice Symposium in 1987 which independently confirmed many of these studies. Steve Schneider of this panel was involved in work at Cornell which also found the 72 km s^{-1}peak in redshift differentials. They hope to explain this peak by selection (a study I strongly encourage). There are *multiple* peaks and valleys, however, including the very important hole at zero which they must also address. Groups are perhaps the most complex place to look for quantization effects. They are much more complex than simple isolated pairs. An attempt to predict what one might expect to find for triplets is contained in the January ApJ paper.

Clusters of galaxies also have an important role in redshift studies. The original quantization period came primarily from the Coma cluster analysis in 1976. Recent work using 21 cm data has confirmed the periodicity and was summarized in the Venice Symposium review in 1987. Guthrie and Napier have recently studied the Virgo cluster and find evidence for redshift periodicity.

A completely independent approach to redshift quantization has considered the redshift globally. In 1984 John Cocke and I demonstrated that redshifts of Fisher-Tully dwarf galaxies were globally quantized at 24.15 = 72.45/3 km s^{-1}after removal of the solar motion within the Galaxy. A second demonstration utilized the galaxies with wide 21 cm profiles which were periodic at 72.45/2 km s^{-1}. In a very important paper (ApJ **345**, 1989) Martin Croasdale has taken a new sample of galaxies from work by Giovanelli and associates and confirmed the global effect.

Quite recently John Cocke and I have extended the global quantization test to Lyman alpha forest lines in quasars. By combining simple theory, which suggests that the quantization interval should vary as $H^{1/2}$, with conventional Friedman cosmology, it is possible to relate the quantization interval, z, and q_o. We find the expected quantization if q_o is close to 1/2. This suggests to us that important aspects of conventional cosmology are intimately related to the quantization phenomenon. It is unlikely we will fully understand either without the other.

The newest, and perhaps the most stringent, test of the redshift concerns rapid time variability. Recent precision 21 cm data appears to indicate that redshifts are variable at the level of 1 km s^{-1} y^{-1}. The effect is intimately related to redshift quantization with the rate of change being a function of 'phase' within the periodicity. This phenomenon, along with an unexpected dependence of redshift on radius within galaxies, is the subject of Poster 49 at this colloquium. The first evidence for rapid variability was presented at the Venice Symposium in 1987. The first follow-up confirmation tests have now been made. By the time the new 300 foot radio telescope comes on line in the 1990s the predicted changes will have grown well outside of any reasonable uncertainty.

The main message of this brief introductory review is simply to point out that the failure of the redshift to pass muster as a simple Doppler shift is a broad one. The question does not hang on simply pairs or clusters or global periodicities, it cuts across many interlinked aspects which must be approached comprehensively. The redshift can very likely be 'cosmological'. It very likely can be a velocity, albeit constrained in some quantum framework. It seems very unlikely to me, however, that any approach to galaxies or cosmology which ignores the redshift question and proceeds on purely conventional dynamical grounds can be correct.

S. E. Schneider

This discussion involves the two most dangerous topics known to mankind: religion and statistics. For some reason, we have camps of 'believers' and 'non-believers' in discordant redshifts, and curiously the non-believers represent the 'orthodoxy.' With the black art of statistics being used as ammunition by both sides, we have a most explosive mixture! I have seen three attitudes at this meeting, covering the gamut of opinion about the significance of the whole topic of peculiar and discordant redshifts in groups of galaxies:

(1) There is no problem. The non-believers feel that if the statistics were properly handled, all of the discrepancies would fade away. It is indeed true that most of the claimed discrepancies depend on statistical arguments, and these arguments are rarely of a sufficiently clearcut character to allow a simple interpretation. Frequently, 'levels of confidence' of 95% or 99% are quoted for apparently discrepant data, but this amounts to only two or three statistical sigmas. I was taught not to believe anything less than five sigma, which if you think about it is an absurdly stringent requirement – something like a 99.9999% confidence level. But of course such a high limit is used because the actual size of sigma is almost never known. There are just too many free variables in astronomy that we can't control or don't know about. None of the discrepancies I am aware of have reached the five sigma level yet, although not all are readily amenable to statistical analysis.

I would like to see the non-believers work more at finding those overlooked variables that would reduce the statistical significance of some of the claimed redshift discrepancies. And publish them! All too often quick explanations are offered up like bad excuses, without careful consideration. We have heard claims and counter-claims at this meeting about the significance of the large number of compact groups with a discordant-redshift member. It is now being suggested that the high number seen can be explained by simple foreground or background contamination, although it is by no means obvious to most of us why this should be so common. Careful interloper studies, accounting for large- scale structure along the line of sight to these compact groups are reportedly underway (Paul Hickson, this meeting), and I hope we'll see the results soon.

(2) There is a problem that cannot be explained within the framework of standard astronomy. At the opposite extreme, the believers find there are some phenomena so contradictory to expectation that no statistical argument is needed. Redshifts that only take on values at discrete intervals, nearby galaxies with luminous connections to quasars, groups of galaxies in which the faint members all have higher redshifts than the brightest member – these phenomena are all plainly at odds with the standard model, and defy explanation.

Here, though, I fear we delve into a murky area of statistics. Patterns found in old data are not amenable to standard statistical analyses. Newman, Haynes, and Terzian (1989) have shown, for example, that periodicities can be found in random data, and they may incorrectly appear to be statistically significant. They demonstrate that too much freedom in the possible parameterization of the periodicity invalidates the standard statistical tests. Thus, statistical significance cannot be established unless there are prior constraints on the total dimensions of the possible 'hypothesis space.' Unfortunately, most of the discordant redshift data falls in the category of being found in current data sets. I would like to see the believers define the limits of their hypothesis space. For example, in an alignment between a quasar jet and an unusual galaxy at entirely different redshifts, what degree of alignment is adequate? with the inner or outer jet? at what separation? should there be one on each side? should all jets point at similar type galaxies? Until these and other possibilities are clearly laid out in advance of the observations, the significance of putative connections between objects with widely different redshift cannot be established. Most important of all, testable predictions must be made for future observations.

(3) There is a problem, but it can be explained within the framework of standard astronomy. The agnostics just don't know whether they don't believe. Probably most of us fall in this category. We would never claim that the standard model is infallible, and we are

intrigued by the strange discrepancies being reported.

Bill Tifft's 'redshift quantization' is one of the most intriguing claims. I think his binary galaxy data passes most of the statistical objections raised above (at least as well as most papers I read in the Ap.J.), and it is even getting beyond the three sigma level by some measures. I am worried by the evolution I see in the hypotheses being made about the important redshifts to consider, but his findings provide the the possibility of making testable predictions about binary galaxy orbits. My own analysis suggests that the phenomenon he discovered in binaries is probably caused by selection effects, but I suspect it may still provide a key to understanding the nature and cosmological origins of binary galaxy orbits (see my contribution elsewhere in this volume). Other phenomena like group members with discordant redshifts and redshift asymmetries in groups may also have explanations in the realm of 'interesting' physics rather than 'new' physics, like the suggestions by Valtonen and Byrd that dynamical ejections may be occurring. I hope we will see more effort put into these areas. The rewards are potentially large since the most exciting discoveries in science often come from resolving the discrepant observations with the standard model.

G. Burbidge

Over more than 20 years the observational evidence has grown that QSOs with large redshifts are to be found close to galaxies with small redshifts more frequently than expected by chance. The earlier evidence has been summarized by Burbidge (1979) and by Arp in his book (Arp 1987).

The most recent and most extensive study is that by Burbidge, Hewitt, Narlikar and das Gupta (in press in ApJ Supplements). They have shown that among the QSOs now known there are nearly 600 lying within 10′ of about 500 galaxies. This includes the small number of small redshift QSOs (about 40) known to be close to galaxies at the same redshift. The bulk of the remainder lie close to bright galaxies with very different (smaller) redshifts. Statistical analysis of this large sample shows that QSOs are preferentially found near galaxies, regardless of their redshifts. When looked at quantitatively, gravitational microlensing cannot explain these results. The conclusion is that a significant part of the redshifts of QSOs cannot be attributed to the expansion of the universe.

Most recently there has been further analysis of the distribution of redshifts of QSOs, and periodicity in the redshift distribution has been reconfirmed. This periodicity may be related to the periodicity found in analyzing the redshifts of faint galaxies.

N. A. Sharp

It is true that there are puzzling aspects to the distribution of redshifts, both in the issue of discordant redshift companions (which I have also studied), and in the area of debate here, which is the claim of a strong periodicity. I can only address this claim as it relates to double or binary galaxies, but, as it happens, this is one area where the conventionally quite inexplicable period seems to appear most convincingly.

Note that we have no physical theory for periodicity (just some attempts at a mathematical representation, which is not the same thing at all). Although one may yet appear, this lack accounts for at least some of the opposition to the very idea of non-cosmological, non-Doppler redshifts. In addition, remember that even if there is a compelling periodicity in the data, we are still not forced to conclude that it is present in the underlying physical systems. One might also puzzle over a quantization which appears in a *radial* measurement of redshift, which might seem to require that our Galaxy be somehow specially placed.

However, my main focus here is that the data are not as compelling as is suggested.

In the face of the highly periodic figures commonly shown for double galaxy systems, I am sometimes tempted to shout 'Foul !', due to the number of caveats and 'yes, but ...' remarks one wants to make.

Among the early work, claims were made that a strong period shows up in only the radio data collected by Peterson in his thesis work (Peterson, 1979), and that since radio-derived redshifts are more accurate than optical values, it must be more convincing. However, the data actually entering into that claim were not purely radio data, and some radio data were excluded. Although the reasons for exclusion were stated in the original paper, they are not repeated in other forums, and any and all *a posteriori* selection is suspect when we consider such a radical claim. The *purely* radio data make a much less compelling picture (Sharp, 1990).

A very accurate set of optical data was recently collected by Schweizer (1987), and held to reveal a strong periodicity. The original Schweizer data do not show a period at all (Sharp, 1990), and especially not at anything even remotely approaching the significance that a sample of this size and accuracy should reveal. But again the argument goes that we must exclude part of the data set in order to bring out the real physical effect. However, in the Schweizer sample, it is only the closest pairs which really begin to reveal the effect, whereas the previous 'best bet' samples were radio data, which are well-known to have much wider separations than optically-selected pairs (Sharp, 1990).

So, perhaps we should first ask, why is it that contradictory selections must be applied to different samples, if the effect is physical ?

On a different tack, comparisons between different authors' data for the same physical pairs suggest that the internal error estimates are rather low (not uncommon in astronomy), and that some samples should not show the period they seem to show, because the redshifts just aren't accurate enough (Sharp, 1990). Croasdale (1989) shows the other side of this same coin, in work on the 'global' quantization rather than on binaries, suggesting that the data errors had to be much larger than estimated in order to *degrade* the period to the level found. Although error analysis is complex and disputatious, again we find reasons to be cautious.

Another point was introduced by Newman *et al.* (1989), and followed up in a number of private conversations and correspondences which I hope will one day be restated for publication. The (very controversial) claim is that the 'I/O' statistic used to show that the period is highly significant is not, in fact, a properly designed statistic with a known and rigorously derived error distribution. Technically, the I/O value does not have 'statistical power', and is not discriminatory. This point has been, and no doubt will continue to be, strenuously argued. However, it is significant that the non-parametric Kolmogorov-Smirnov statistic (Sharp, 1984) showed no significant deviation from a classical model of double galaxy orbital motions, *until it was reduced to a form equivalent to that of the I/O statistic*. In retrospect, having looked again at the derivation of the error distribution for the KS test, I believe that the folding I used did considerable violence to the calculation, and probably vitiates the statistical conclusion. In passing, I would also like to emphasise that my 1984 paper is *in no way* an independent proof of periodicity: quite to the contrary, I found *no* discrepancy with the complex dynamical simulation method until *after* I used *both* the same data sets *and* an equivalent test of significance.

I take a skeptical stance: an effect of this importance should not be ignored, but I have serious doubts about the selection, presentation, and accuracy of the data. I return a Scottish verdict of 'Not proven'.

RADIO STRUCTURES IN QSO–GALAXY PAIRS

Chidi E. Akujor

Astrophysics Group, Department of Physics and Astronomy, University of Nigeria, Nsukka, Nigeria

Abstract

It is now generally agreed that if quasars and nearby low redshift galaxies are associated, then there should be luminous connections between them. However, most of the observational evidence being presented is in the optical domain, whereas such evidence should also exist at radio frequencies. We are, therefore, investigating some QSO–Galaxy pairs at radio frequencies to search for luminous connections and other structural peculiarities. Radio maps of some of these sources are presented.

A focus of current debate in modern astronomy is the apparent lack of consensus in the understanding of the relationship (or lack of it) between quasars and 'host' galaxies, and the controversy surrounding the conventional interpretation of redshifts (e.g Burbidge, 1981; Arp, 1986). Central to this puzzle is whether quasars are active nuclei of distant galaxies– that is whether quasar redshifts are cosmological. The conventional view is that quasars are relatively distant objects as indicated by their redshifts. On the other hand some astronomers believe quite strongly that quasars are comparatively local objects genetically related to galaxies, perhaps compact galaxies ejected from the nearby parent galaxy, the redshift excess being due to local Doppler effects (see Burbidge, *et al.* 1971).

It is therefore believed by the latter group that many quasars and nearby low redshift galaxies are physically related despite having discordant redshifts. Most of these evidence of physical association are presented in the form of optical images. But if such pairs of objects are physicaly related, then there might also be luminous radio connections between them, particularly if both objects are radio–loud. Morever, evidence of association cannot be placed on a firm foundation without supporting results at other wavebands. Such luminous radio connections may be in the form of either diffuse emission or bridges, or higher resolution features like connecting jets or knots. The type of radio connection found may also help to explain the type of relationship between the associated objects and the time–scale of any possible interaction compared with radio source life–times.

But a technical limitation exists since the separation of objects in these pairs is sometimes a few minutes of arc, making it difficult to obtain at high angular resolution a single image containing a pair of objects. Another approach, therefore, to this problem is to investigate the structures of the individual members of the pairs, in order to search for systematic effects or structural peculiarities than can distinguish them from non-pair objects.

In this paper we report the progress in our investigation of radio structures of some suggested quasar-galaxy pairs. Our sample consists of 16 sources chosen from the 3C and 4C catalogues (Table I, see Burbidge 1985 for a more comprehensive list). Each member of the pair is radio-loud. Radio images of the pairs or the dominant rado emitting object is being obtained with the VLA or MERLIN at different wavelegths. The aim is to, without prejudice, search for possible peculiarities of character and luminous connections between these pairs of objects. Radio maps of some of these objects are presented with brief comments on the individual soucres.

0114+074 (4C 07.04): The radio images of the objects have been obtained with the VLA and MERLIN at different wavelengths (Akujor, 1989; Akujor *et al.* 1989). The quasar 0114+074N is a point source (unresolved) at all wavelengths. The radio galaxy (0114+074) is a very asymmetric source with one component having a spectral index of 1.13 ($S \sim \nu^{-\alpha}$) while the other is flat, α=0.45.

0900+127 (4C 12.33): The VLA radio image is presented. The radio quasar has a steep spectrum source and is unresolved with the VLA at 5 GHz but there are indications of a surrounding fuzzy structure. The companion is a symmetric double radio galaxy.

0955+327 (3C232): The first ever radio images of this quasar are presented. Both Perley (1982) and Rogora et al (1986) had failed to detect extended emission with the VLA. The 408 MHz map shows a -two sided emission, while at 1.6 GHz there is a jet that points soutwards in the direction of the companion galaxy. It is interesting that the position angle of this jet corresponds to that seen in the recent HI observations of Carilli *et al* (1989).

1038+064 (4C 06.04): The maps of this radio quasar have been obtained with the VLA, MERLIN and VLBI (Akujor & McGruder, In preparation). The quasar has a flat radio spectrum with a core-jet structure. Akujor & McGruder do show that the changes in the position angle of the jet with increasing resolution imply that the jet, and hence the core may be rotating. The dominant companion radio galaxy (1037+067) has a possible tailed structure, but there are at least 5 other radio objects with $S_{327MHz} \geq$50 mJy within 2 arcmin of the radio quasar. Some of these objects probably belong to a cluster as suggested by Burns et al (1981).

1206+439 (3C268.4): This is a powerful quasar with a triple structure and a characteristic double hotspot in the southerly lobe (Lonsdale & Barthel, 1986). There is another weak radio source ~4 mJy SE of this source.

1218+339 (3C270.1): The MERLIN image of this source confirms the non-collinear structure usually refered to as 'dog-leg structure' (Stocke *et al*, 1985). Hintzen & Scott (1978) suggest that such quasars are members of galaxy clusters, while Stocke *et al* (1985) propose that the non-collinearity could arise from collisions of the radio lobes with nearby galaxy halo or an intergalactic cloud.

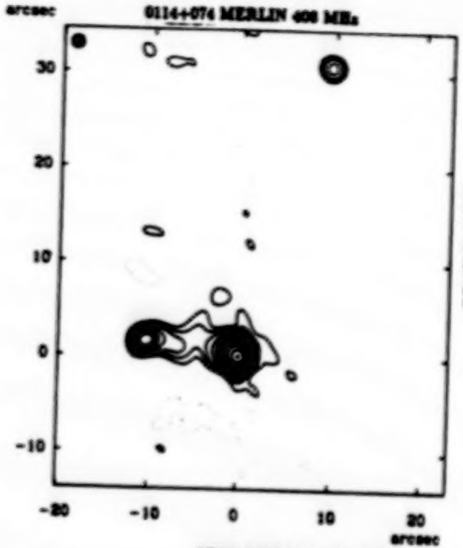
0114+074 MERLIN 408 MHz

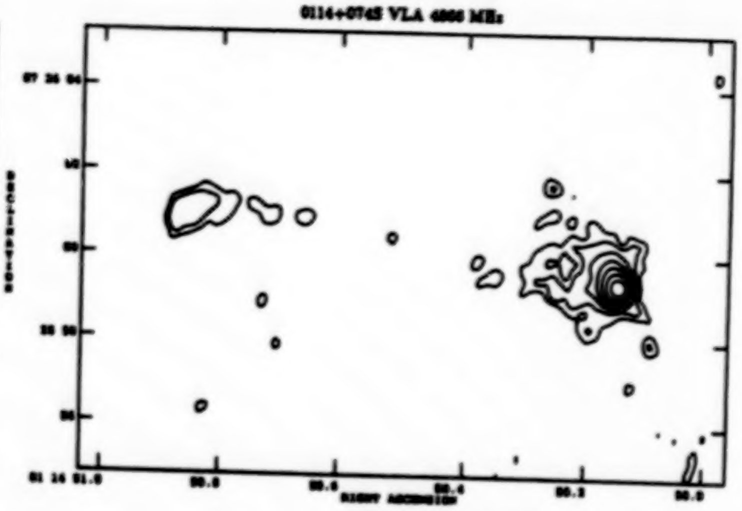
0114+074S VLA 4885 MHz

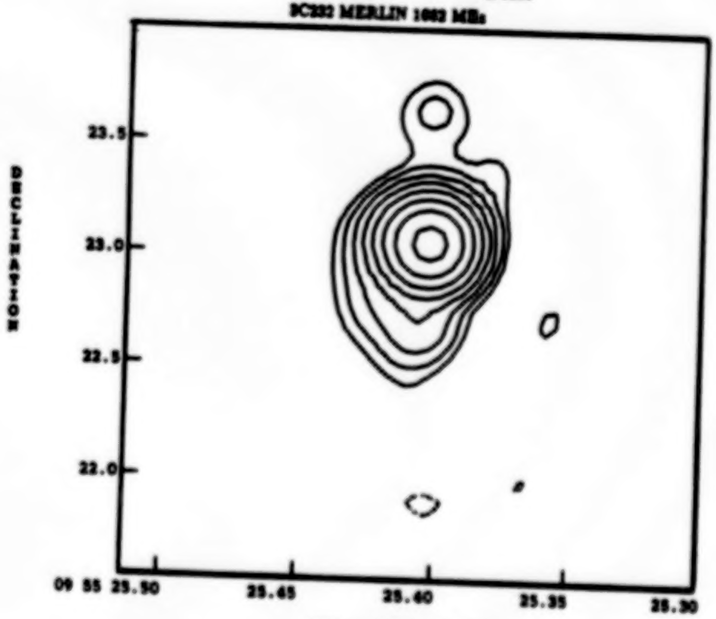
3C232 MERLIN 1662 MHz

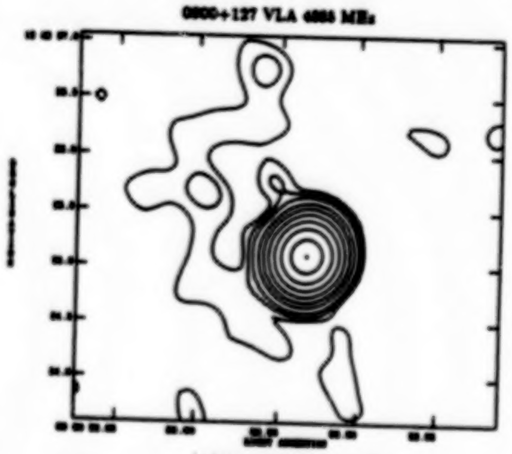
0800+127 VLA 4885 MHz

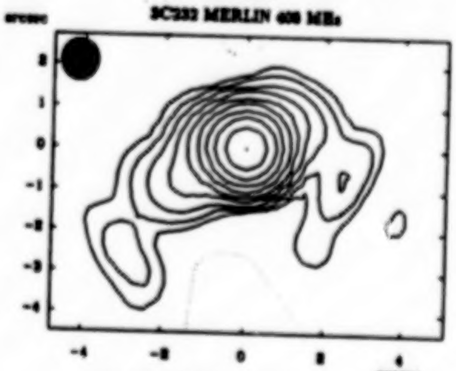
3C232 MERLIN 408 MHz

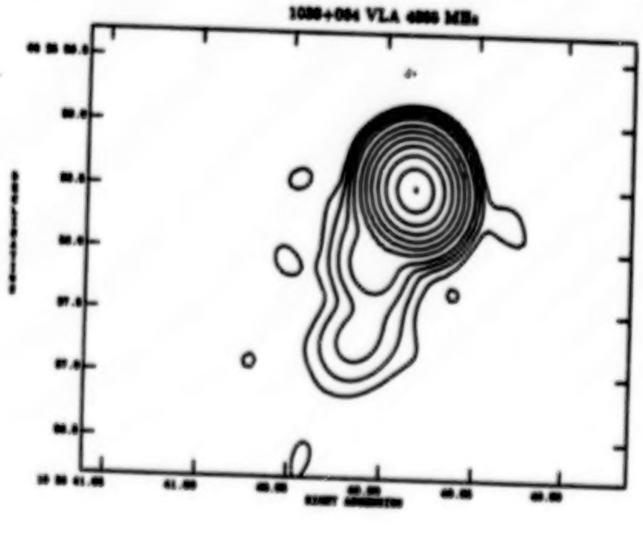
1038+064 VLA 4885 MHz

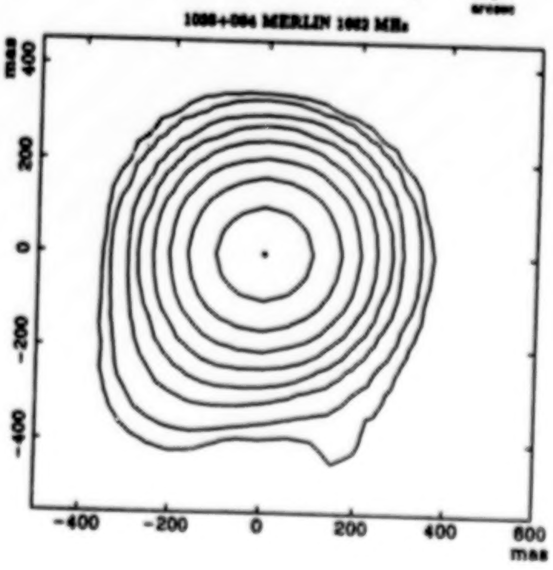
1038+064 MERLIN 1662 MHz

1241+166 (3C275.1): This is another 'dog-leg' (Stocke *et al* 1985) radio quasar. Our VLA map is broadly consistent with the higher resolution map of Stocke *et al.* Hintzen & Romanishin (1986) have detected a large cloud of line-emitting gas surrounding this quasar (see also Hintzen & Stocke 1986)

1441+522 (3C303): Our high resolution map shows clearly the compact features of this source– a bright core identified with a galaxy and a knotty jet that points to the western hotspot complex. The nearby quasar (Z=1.570) is south (~7 arcsec) of this hotspot complex, but is enclosed by an extended halo detected in low resolution maps (Kronberg *et al.* 1977). A recent VLA map by Perley (1988) reveals the extent of this halo and the presence of a compact hotspot East of the core.

1458+718 (3C309.1): This is compact source with a steep radio spectrum. Our MERLIN map shows an asymmetric structure, while high resolution maps by Wilkinson *et al* (1984) reveals a highly distorted structure on parsec scales. It has been suggested that such distorted structures in steep spectrum compact cores could arise from interaction of radio beams with ambient gas.

It is probably premature to look for systematic effects since we have not reduced all the data. But we note that a majority of the radio quasars have distorted structure. However, it is not yet clear whether this can be ascribed to any factors that are common to them.

Acknowledgement I am grateful to Drs P. Wilkinson & S. Garrington for permission to use their unpublished data, and Dr Ian Browne for encouragements.

References

Akujor, C.E. *et al.* 1989 *Astr. Astrophys. Suppl* **80**, 215.

Akujor, C.E., 1989. *Astron. J.* In Press.

Arp, H. 1986 *in* A. Hewitt *et al* (eds) *Observational Cosmology*, p. 479.

Burbidge, E.M. *et al.* 1971. *Astrophys. J.*, **170**, 233.

Burbidge, G., 1981. *Proc. N.Y.Acad. Sci.*, p.123.

Burbidge, G.R. 1985. *in* V.K. Kapahi (*ed*) *Extragalactic Energetic Sources*, p. 87.

Burns, J.O. *et al.* 1981 *Astron. J.* **86**, 1120.

Carilli, C. *et al.*, Nature, *338*, 132.

Hintzen, P. & Scott, J. 1978 *Astrophys. J. Letts* **224** L47.

Hintzen, P. & Romanishin, W. 1986. *Astrophys. J. Letts* **311**, L1.

3C268.4 VLA 4885 MHz 1206+439

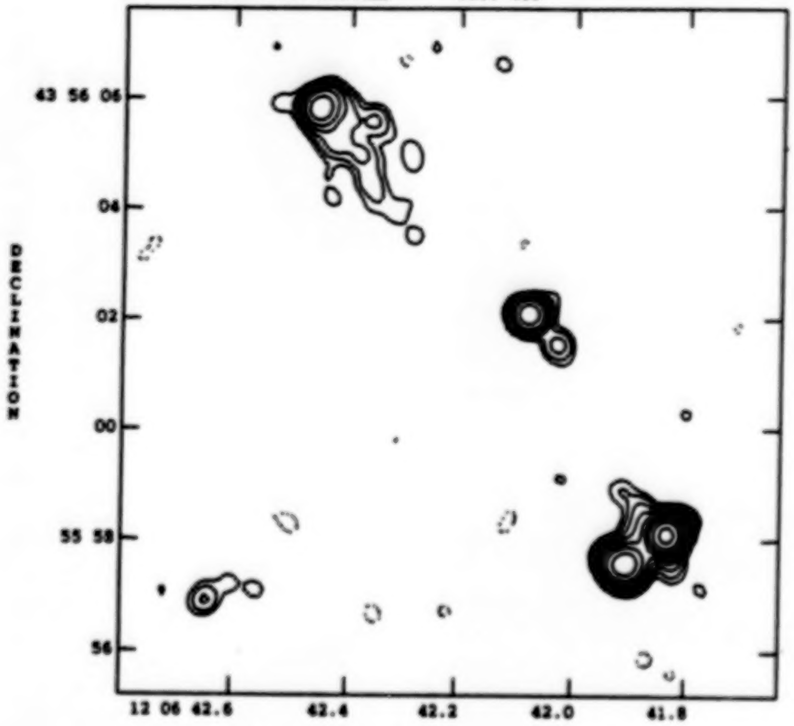

3C270.1 MERLIN 1.666 MHz

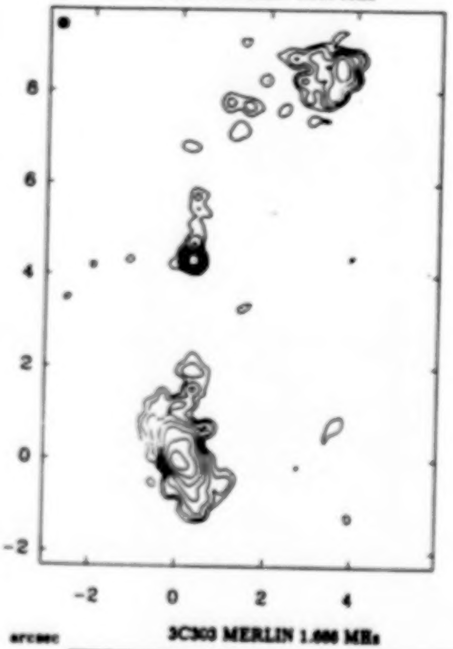

3C303 MERLIN 1.666 MHz

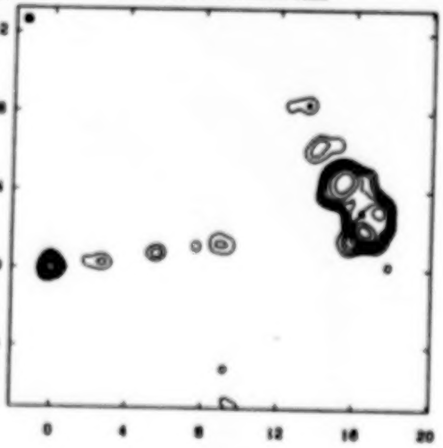

1241+16 3C275.1 VLA 1465 MHz

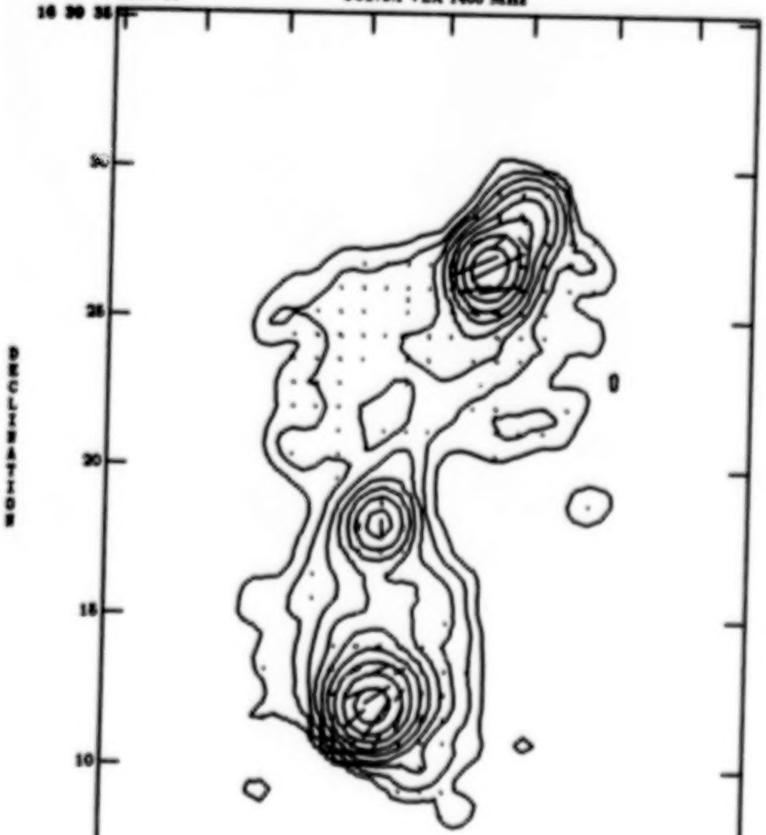

3C309.1 MERLIN 1.666 MHz

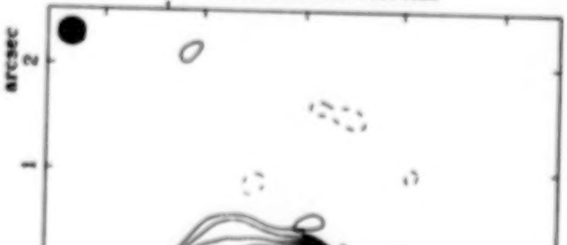

Hintzen, P. & Stocke, J. 1986. *Astrophy. J.* **308**, 540.

Kronberg, P., Burbidge, E.M., Smith, H.E. & Strom, R.G. 1977 *Astrophys. J.* **218**, 8.

Lonsdale, C & Barthel, P.D. 1986. *Astron. J.*, **92**, 12.

Perley, R. 1982. *Astron. J.* **87**, 859.

Perley, R. 1988. *Hotspots in EGRSs*, p.1.

Rogora, *et al* 1986. *Astron. Astrophys. Suppl* **64**, 557.

Stocke, J.T., Burns, J.O. & Christiansen, W.A. 1985. *Astrophys. J.* **299**, 799.

Table 1

QSO – GALAXY PAIRS

S/No	Name	3C/4C	Z(QSO)
1.	0114+074	4C 07.04	0.861
2.	0219+428	3C66	0.444
3.	0317-023	4C-02.15	2.092
4.	0900+127	4C12.33	-
5.	0955+327	3C232	0.533
6.	1038+064	4C06.04	1.270
7.	1049+616	4C61.20	0.422
8.	1107+036	4C03.21	0.960
9.	1206+439	3C268.4	1.400
10.	1218+339	3C270.1	1.519
11.	1241+166	3C275.1	0.557
12.	1441+522	3C303	1.570
13.	1458+718	3C309.1	0.905
14.	1545+210	3C323.1	0.264
15.	2252+129	3C455	0.543
16.	2305+187	4C18.68	0.313

RADIO LINE AND CONTINUUM OBSERVATIONS OF QUASAR-GALAXY PAIRS AND THE ORIGIN OF LOW REDSHIFT QUASAR ABSORPTION LINE SYSTEMS

C.L. Carilli (CfA), J.H. van Gorkom, E.M. Hauxthausen (Columbia Univ. and NRAO),
J.T. Stocke (Univ. of Colorado), and J. Salzer (Univ. of Michigan)

Abstract

There are a number of known quasars for which our line of sight to the high redshift quasar passes within a few Holmberg radii of a low redshift galaxy. In a few of these cases, spectra of the quasar reveal absorption by gas associated with the low redshift galaxy. A number of these pairs imply absorption by gas which lies well outside the optical disk of the associated galaxy, leading to models of galaxies with 'halos' or 'disks' of gas extending to large radii. We present observations of 4 such pairs. In three of the four cases, we find that the associated galaxy is highly disturbed, typically due to a gravitational interaction with a companion galaxy, while in the fourth case the absorption can be explained by clouds in the optical disk of the associated galaxy. We are led to an alternative hypothesis concerning the origin of the low redshift absorption line systems: *the absorption is by gas clouds which have been gravitationally stripped from the associated galaxy.* These galaxies are rapidly evolving, and should not be used as examples of absorption by clouds in halos of field spirals. We conclude by considering the role extended gas in interacting systems plays in the origin of higher redshift quasar absorption line systems.

A. 1327-206

This systems is one in which a radio loud quasar, PKS 1327-206 ($z_Q = 1.17$), sits 37" from the galaxy ESO 1327-2041 ($v_G = 5370$ km s^{-1})[1]. Deep optical plates show that ESO 1327-2041 is a polar ring galaxy[2]. The quasar projects behind the outer part of the ring to the east. High resolution spectra show narrow NaI absorption at velocities of 5246 and 5484. Lower resolution spectra show broad CaII absorption at a velocity of 5346 km s^{-1}.

In figure 1 we present our new radio observations of this galaxy. We find that the quasar continuum is extended, and that the galaxy ESO 1327-2041 is also radio loud, with an integrated flux of 12 mJy. We detect HI in absorption against the quasar core coincident in velocity with the low velocity optical absorption system ($v_{abs} = 5257$ km s^{-1}, FWHM $\leq$ 11 km s^{-1}). The column density in HI is $3.1 \times 10^{17} \times T_s$ cm^{-2}. We detect no absorption associated with the high velocity optical system to a 3σ column density of $1.7 \times 10^{17} \times T_s$ cm^{-2}.

The HI emission from ESO 1327-2041 confirms the idea that this is a polar ring galaxy. We find that the HI in ESO 1327-2041 rotates about an axis which is parallel to the minor axis of the ring, and hence perpendicular to the minor axis of the dominant optical galaxy. The total HI mass observed by the VLA is 7×10^9 $M_\odot$. A Nancay spectrum of this galaxy found a factor of three times more HI, which suggests an extended component in HI[6]. The optical and HI morphology suggest that ESO 1327-2041 is a system far from dynamical equilibrium,

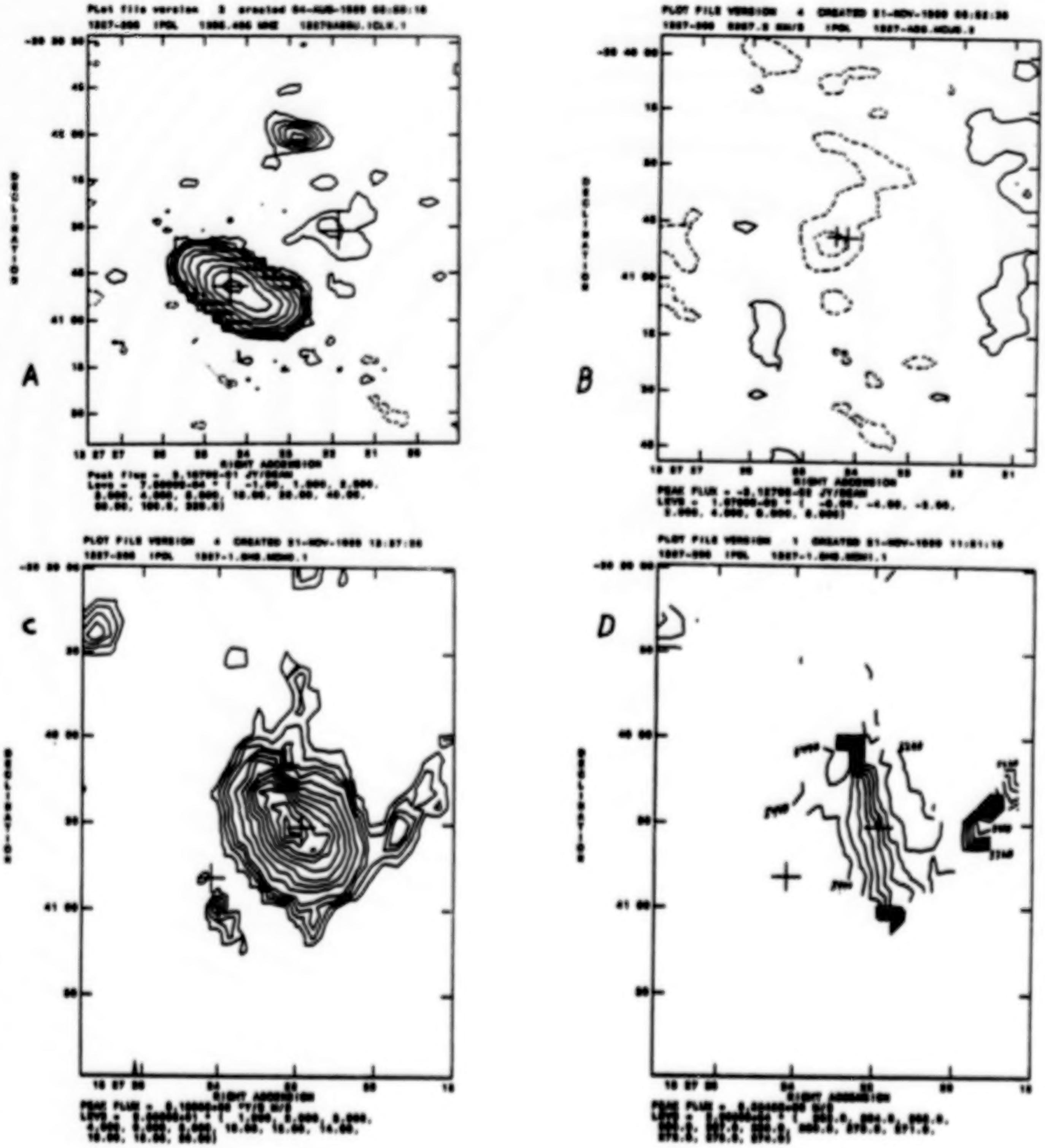

Fig. 1: Images of pair 1327-206. Crosses mark the position of the optical galaxy and the radio continuum peak of the quasar. Spatial resolution is 17". A. Continuum emission at 1396 MHz. B. Absorption channel (5257 km s^{-1}) at 10.5 km s^{-1} resolution. The smaller cross indicates the position of the optical quasar. C. HI column density. Units are 10^{20} cm^{-2}. D. Velocity field of HI.

which is evolving on dynamical timescales ($\leq 10^9$ years), much like the ring galaxy M -5-7-1 studied by van Gorkom *et al.* (1987).

The high velocity optical absorption line system fits in well with the observed rotation curve in HI, and implies flat rotation out to at least 20 kpc. The dynamical mass within this radius is 1.2x10^{11} $M_{\odot}$(using $i = 45°$). Of course, if the system is far from dynamical equilibrium then the rotational velocity may not be a good indicator of total dynamical mass. The low velocity absorption system has an anomolous velocity of 200 km $s^{-1}$with respect to the rotating HI. The most likely origin for this anomalous system is a cloud which has been accelerated during the merger, and has not had time to reach dynamical equilibrium.

B. 3C 232

The quasar 3C 232 ($z_Q = 0.513$) sits 2' north of the galaxy NGC 3067 ($v_G = 1456$ km s^{-1}). NGC 3067 displays a highly disturbed optical morphology, with prominent dust lanes and bright knots of Hα emission distributed throughout the disk[7]. The galaxy also has a large IRAS flux and radio continuum flux[8], which put it in the class of starburst galaxies such as M82. A starburst could be triggered by a recent merger. Note that this galaxy is an isolated spiral.

Optical spectra of the quasar[7] reveal narrow CaII and NaI absorption at 1371, 1417, and 1545 km s^{-1}. Radio spectra of the quasar[9] have shown narrow HI absorption at 1420 km s^{-1}. Emission studies of the HI associated with NGC 3067 reveal an extremely disturbed distribution, with a truncated disk in the western half of the galaxy, and a tail of HI extending towards and over the quasar[8].

Our continuum observations of NGC 3067 are shown in figure 2a. The radio continuum is knotty (much like the Hα emission), and the majority of the knots are resolved, with spectral indicies of -0.9± 0.2, as expected for synchrotron radiation from the disk of the galaxy. We also find an unresolved core, which may be evidence for a compact active nucleus. Notice the radio continuum emission extending above and below the disk of the galaxy. The projected distance off the plane is 1.6 kpc, although the emission could be from the spiral arms seen in projection.

C. 2020-370

In this pair, the quasar ($z_Q = 1.05$) sits behind a linear group of galaxies, the closest of which is a barred spiral 20" to the northwest of the quasar[10] ($v_G = 8634$), one arm of which comes to within 6 kpc of the quasar. The next closest galaxy is an elliptical which sits 45" to the east of the quasar. The relative morphology of the two galaxies suggests that they are interacting gravitationally (fig. 3). Optical spectra of the quasar[10] show CaII absorption at a velocity of 8590 km s^{-1}. Radio spectra of the quasar[11] reveal narrow HI absorption at a velocity of 8611 km s^{-1}.

Our recent search for HI emission detected signal from an edge-on spiral 3' northwest of the quasar at a velocity of 8460 km s^{-1}. There is also the suggestion of extended emission in the velocity range 8580 to 8640 km s^{-1}associated with the spiral close to the quasar. Nancay

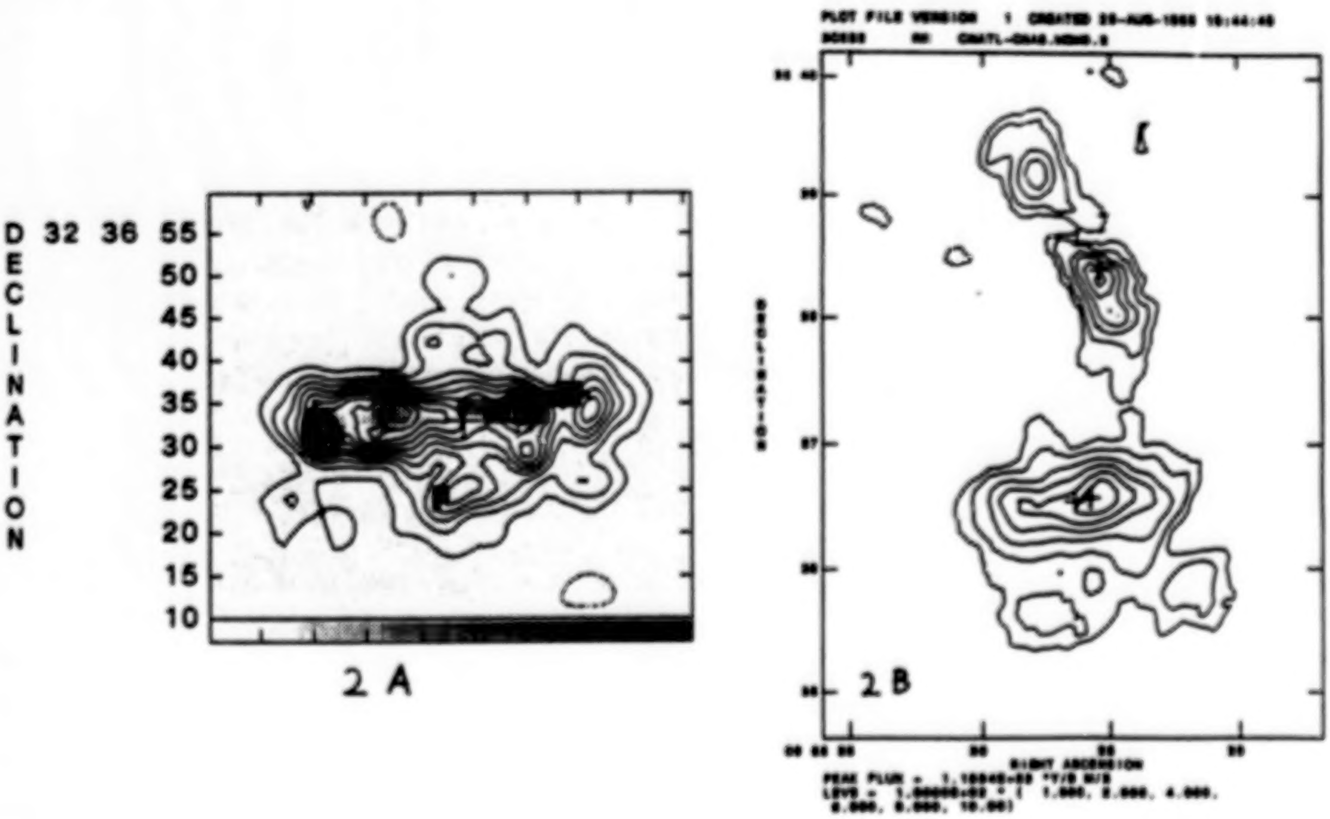

Fig. 2: A. A radio continuum image at 1450 MHz, 3" resolution of NGC 3067, with a greyscale of spectral index between 6 and 20 cm. Crosses mark the position of the optical (east) and dynamical (west) centers of the galaxy. B. HI column density. Units are $3x10^{20}$ cm^{-2}. The position of the quasar 3C 232 is marked by a cross to the north.

Fig. 3: A. Optical field of the quasar 2020-370.

Fig. 4: An overlay of radio continuum contours at 1330 MHz, 10" resolution, and optical contours[12] of the pair 0446-208.

3

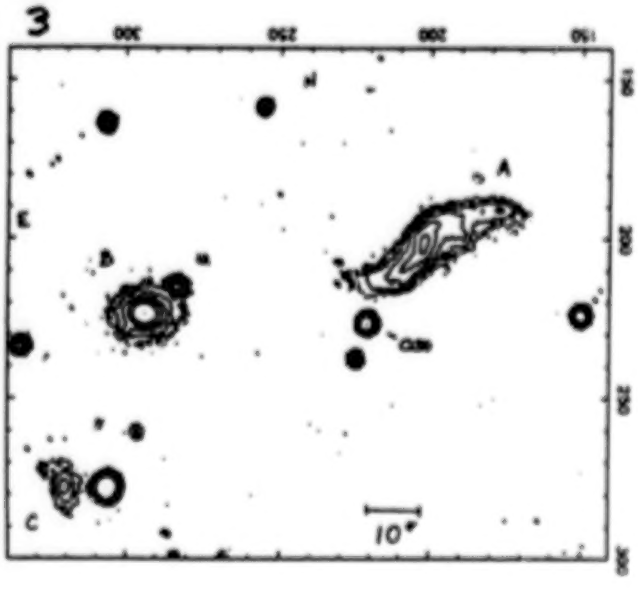

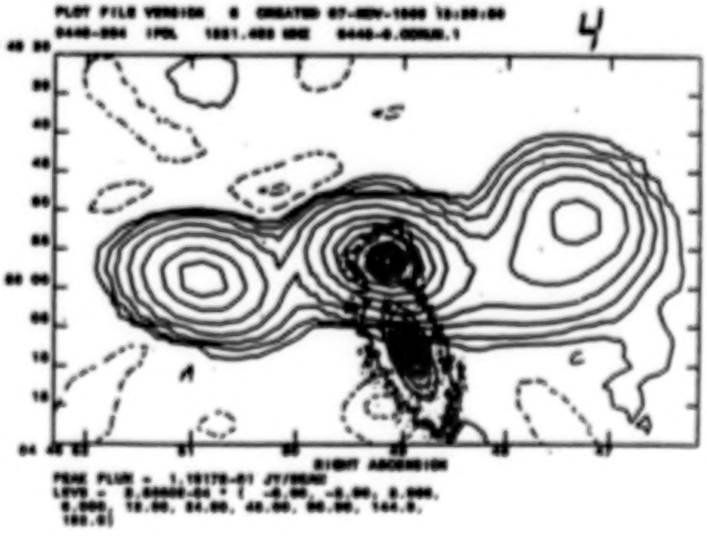

observations of this system detected an HI mass of 5.4×10^9 $M_\odot$ in this velocity range[6].

D. 0446-208

In this system, the quasar ($z_Q = 1.90$) sits 13" from the center of an inclined SO galaxy[12] ($v_G = 20070$ km s^{-1}). The galaxy is 26' from the center of the cluster A514, and the quasar lies at the edge of the optical disk of the galaxy. Optical spectra of the quasar reveal two NaI absorbing clouds at velocities of 19950 and 20040 km s^{-1}. CaII absorption is also seen, although in spectra of lower spectral resolution. From the ratio of NaI to CaII column densities, Baldwin *et al.* (1985) argue for absorption by a gas cloud in the disk of the associated galaxy.

Our radio continuum image of this source shows an extended background radio source (fig. 4). We do not detect absorption against any of the radio continuum structures at our highest spectral resolution of 5.8 km s^{-1}. We set a 3σ upper limit to the HI column densities towards the core of $2.9 \times 10^{17} \times T_s$ cm^{-2}. We detect no emission in the field to a 3σ level of 1.2 mJy/beam at a resolution 23 km s^{-1}. We set a limit of 1.1×10^9 $M_\odot$/channel for any HI within about 6' of the galaxy, in the velocity range of 19850 to 20120 km s^{-1}.

Discussion

From our limit sample, we draw the tentative conclusion that detecting absorbing gas well outside the optical disk of a galaxy signals a disturbed/interacting system which is evolving on short timescales (*i.e.* $0.1 \times H_o^{-1}$). If this conclusion holds for systems at higher redshift[14], then we have a number of interesting implications. First, it becomes uninteresting to discuss the statistics of quasar absorption lines in terms of extended halos of normal spiral galaxies. Second, the frequency of observed absorption systems requires that there be many systems still evolving on dynamical timescales down to a redshift of at least 0.5. In fact, the space density of these systems must have been about 1/10 that of field spirals. We should point out that observations of a number of higher redshift absorption line systems indicate that the galaxies associated with the absorbing clouds are not normal spiral galaxies[15]. In almost every case, the associated galaxy shows very bright [OII] emission, indicative of a starburst. Often, the [OII] emitting regions are distributed over a fairly large region (a few hundred kpc).

REFERENCES: 1. Kunth, D. and Bergeron, J. 1984, M.N.R.A.S., 210, 873; 2. Giraud, E. 1986, A. and A., 161, 206; 3. Bergeron, J. *et al.* 1987, A. and A., 180, 1; 4. Ho, P. *et al.* 1989, Ap.J., in press; 5. van Gorkom, J. *et al.* 1987, Ap.J., 314, 457; 6. Boisse, P., *etal.* 1988, A. and A., 191, 193; 7. Stocke, J. *et al* 1989, in Conference on the I.S.M. of External Galaxies, ed. H. Thronsen; 8. Carilli, C. *et al.* 1989, Nature, 338, 134; 9. Rubin, V. *et al.* 1982, A.J., 87, 477; 10. Boksenberg, A. *et al.* 1980, Ap.J., 242, L145; 11. Carilli, C., and van Gorkom J. 1987, Ap.J., 319, 683; 12. Blades, J., *et al.* 1981, M.N.R.A.S., 194, 669; 13. Baldwin, J. *et al.* 1985, M.N.R.A.S., 216, 41p; 14. Cottrell, G. and Icke, V. 1976, Nature, 264, 733; 15. Yanni, B. *et al* 1989, Ap.J., in press.

PROPERTIES OF THE REDSHIFT

W. G. Tifft, W. J. Cocke
Steward Observatory, Univ. of Arizona

Introduction

Central to any analysis of dynamical systems, or large scale motion, is the interpretation of redshifts of galaxies as classical Doppler velocity shifts. This is a testable assumption and for many years evidence has accumulated that is inconsistent with the assumption. Here we review recent evidence suggesting systematic radial dependence and temporal variation of redshifts.

Background

Early 1970s Redshift-Morphology and Redshift-Magnitude, ApJ **188**,221 (1974)
1973-4 Quantized redshift concept introduced, IAU Symp 58 (1973)
1976-7 Formal predictions, general discussion, ApJ **206**,38 (1976),**211**,31 and 377 (1977)
Mid 70s to mid 80s Double galaxy programs - ApJ **336**,128 (1989)
Early 80s Global quantization, ApJ **287**, 492 (1984), Croasdale ApJ **345**,72 (1989)
Mid 80s New precision 21-cm programs begun, ApJ Suppl **67**,1 (1988)
Mid 80s Early theoretical concepts, Astroph Lett **23**,239 (1983), ApJ **288**,22 (1985)
1987 Time variation concept introduced, Venice Symposium (1987)
Lyman Alpha forest quantization, q_o, ApJ **346**,613 (1989)
1987-88 21-cm multiple radio telescope investigations A&A Suppl (1990), ApJ Suppl (1990)

For summary up to 1988 see AAS Poster paper June 1988. Copies are available on request.

21 cm PROFILE PARAMETERS

V = Mean of redshift at 20% of average height of central 80% of profile area. Determined by polynomial fits to profile wings.

W = Profile Width, redshift difference across profile, 20% level.

F = Flux, Profile integral, converted to Jansky km/s units, with no corrections for beam size.

A = Profile shape or asymmetry index, ratio of velocity intervals from the mean redshift by AREA to the 20% profile crossing points. Taken as larger/smaller. + if larger interval on high redshift side, left leaning, − if larger interval on low redshift side, right leaning.

S/N = Signal-to-noise level, Ratio of average height of central 80% of profile area to rms baseline noise.

UNCERTAINTY IN 21 cm DATA

The *consistency* of a parameter measures the ability to reproduce a quantity. By changing specific factors the effects of the factors on consistency can be evaluated. Two critical factors we will consider later are radial scale (beam size), and the epoch of observation.

The *accuracy* with which a measurement represents some specific physical quantity, is much more difficult to obtain. Whether a physical quantity is stable or changes in some parameter dependent way can, however, be determined within the limits of consistent measurements.

Using a set of 100 system standards, observations were obtained at the Effelsberg 100-meter and the NRAO 140- and 300-foot telescopes within a one year span, 1987-88. At S/N of 10 or above comparisons show a redshift scatter, σ_V, with a simple bandwidth dependence.

$$\sigma_V = 0.85(BW/BW_5)^{1/2}\ km/s,$$

BW is the bandwidth in MHz and is 10, 5, 2.5, or 1.25 at NRAO. The rms reproducibility of a single measurement at S/N 10 or above is therefore 1.2, 0.85, 0.6, or 0.4 km/s at the respective bandwidths. See Tifft and Huchtmeier A&A Suppl (1990), Tifft ApJ Suppl (1990).

Uncertainty in widths is twice that in redshift. Aside from some obvious telescope system or software errors no systematic errors were detectable. Comparisons at the level of a fraction of a km/s are possible.

Absolute flux calibrations and comparisons between different telescopes permit flux growth curves to be measured as a function of beam size. This allows one to compare derived parameters as a function of radius. Comparisons of flux measures since 1984 at the 300-foot show an overall stability within about 2%, but show a systematic difference of a few percent in the long term behavior of fluxes for wide and narrow profiles. The behavior changes quite sharply at a width of 100 km/s.

RADIAL DEPENDENCE OF PROFILE PARAMETERS

The flux ratio between two telescopes provides a direct measurement of the degree to which the larger beam samples outlying hydrogen not seen by the smaller beam. Systematic deviations in any of the parameters of the 21 cm line as a function of radius should be apparent when plotted against flux ratio. The effect is readily seen for profile width when the 9 arc minute beam of the 100-m telescope is compared with the 21 arc minute beam of the 140-ft. When comparing galaxies at different distances, as in the Fisher-Tully method, slight systematic errors will occur unless beam size corrections are applied.

More surprisingly the comparison of redshift change with flux ratio appears to show that the redshift of the central parts of galaxies with disks (W > 100 km/s) are systematically blueshifted. The effect is opposite or absent for narrow profile galaxies. The effect changes at the same width that the long term flux behavior of the 300-ft data changes. At this width the standard double horned profiles associated with rotating disks have replaced the single peaked profiles characteristic of dwarf irregulars.

The effect implies that the central regions of a galaxy should have a systematically positive shape index relative to the outer parts. The comparison of the 100-m and 140-ft shape index A shows the expected trend with flux ratio. If the neutral hydrogen content of galaxies is optically thin, as is normally assumed, radial expansion cannot explain the shift. The redshift change can amount to several km/s when only 20-30% of the hydrogen lies outside the smaller beam.

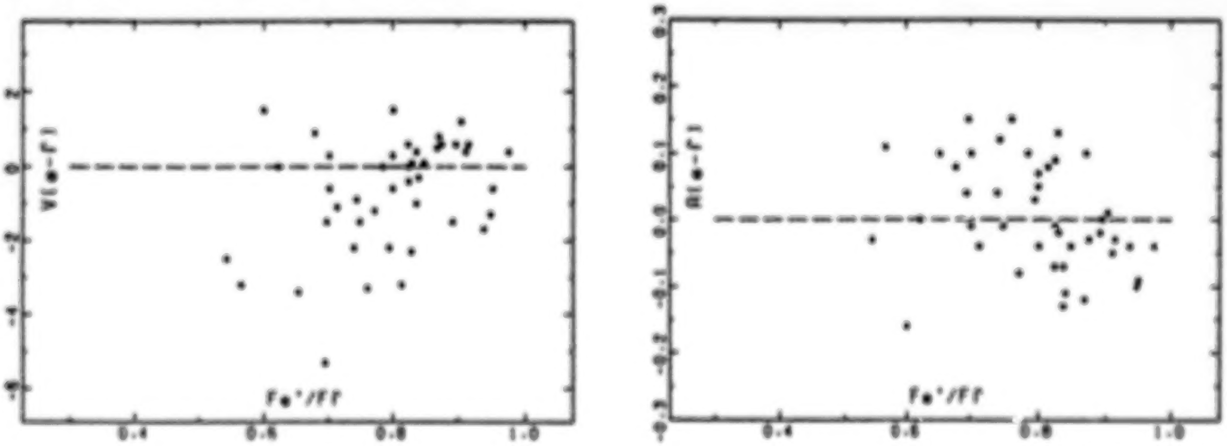

Radial variation in redshift (left) and profile shape (right) within galaxies. The redshift or asymmetry difference (100-m − 140-ft)=(9′− 21′ beam) is shown as a function of the flux ratio for individual galaxies with profile widths W > 100 km/s. Redshift becomes more negative toward the nucleus and profiles show an enhancement on the negative side at small radii.

REVIEW OF GLOBAL QUANTIZATION

Although quantization of redshifts on a global scale was implied by very early redshift work in the 70s, it was not until the early 80s that the Fisher-Tully study of dwarf galaxies permitted a clear solution for the solar motion. Correction for a velocity (circular, radial, z) = (231, −35, 1) produced strong global quantization at 24.15 km/s among dwarf galaxies with the narrowest profiles (W < 75 km/s). A separate test for the widest profile galaxies yielded a global periodicity of 36.2 km/s for the same solar motion. Recently M. Croasdale (ApJ **345** (1989)) has independently demonstrated the wide profile periodicity in independent data. Both periods are simple fractions of the 72.45 km/s interval associated with quantization in dynamical systems. Recently (ApJ **346** (1989)) the concept of global quantization has been applied to Lyman alpha forest data in quasars which carries with it a potential for determining q_0.

Redshift phase, ϕ_V, is defined as the fractional part of the galactocentric redshift, V_c, after divison by the quantum interval or period, P.

$$V_c/P = N + \phi_V.$$

Quantization is generally evaluated by comparing the number of galaxies which are in phase with a period with those out of phase. The resultant In/Out or Head/Tail ratio is evaluated statistically according to simple coin toss probability theory or more sophisticated Monte Carlo simulations depending upon the degree to which the phase intervals can be predicted in advance. A study of redshift phase dependence is crucial to the discussion of redshift time variability. Systematic errors will shift all phases in a nonselective manner. What is observed is that shifts appear to occur over time in specific phase intervals.

TIME VARIABILITY OF REDSHIFT

Comparisons of the accurate redshifts derived by Tifft and Cocke (TC) in the mid 80s with older redshifts generally show a scewed distribution toward negative values of V(new − old). When residuals are plotted against redshift phase deviant residuals cluster in phase. This effect was first seen in narrow profile data.

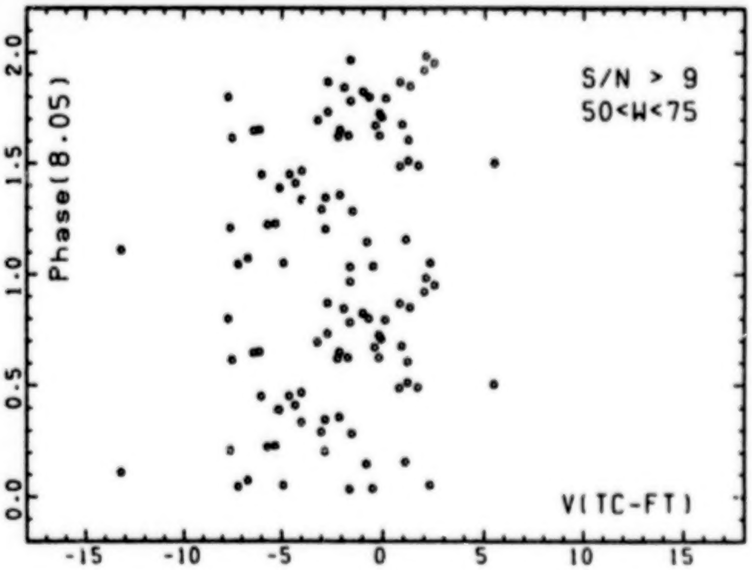

Original 1987 demonstration that Fisher-Tully redshifts from the 70s differ from new redshifts in the 80s in a phase dependent way. The implication is that redshifts near phase 0.25 are decreasing with time while those near phase 0.75 are stable. Phase is calculated on a global period of 8.05 km/s for narrow profile dwarf galaxies.

The characteristic 24.15 km/s periodicity associated with W < 75 km/s is apparently a modulation of a more fundamental period of 8.05 km/s. On an 8.05 period the narrow profile points near phase 0.75 show no shift when Fisher-Tully (FT) redshifts are compared with TC data. At phase 0.25 a shift of 4-5 km/s is observed. This effect was formally announced at the Venice Symposium on New Ideas in Astronomy held in 1987. In 1988 a set of the narrow line galaxies was reobserved and compared against the principal run of January 1986 from the TC study. The 0.75 phase group is at zero while the 0.25 phase group is again shifted. Uncertainty in the new data is well understood, and consistent with the observed scatter. A formal t test comparison of the means of the two phase groups gives t=4.9, p<0.001, that the 13 high S/N points have the same mean. Including three very bright resolved systems and lower S/N data lowers the probability of coincidence to about 0.01. The magnitudes of the shifts are, within their uncertainties, proportional to the time intervals between data sets. The shifts require rates of change of several tenths of a km/s per year.

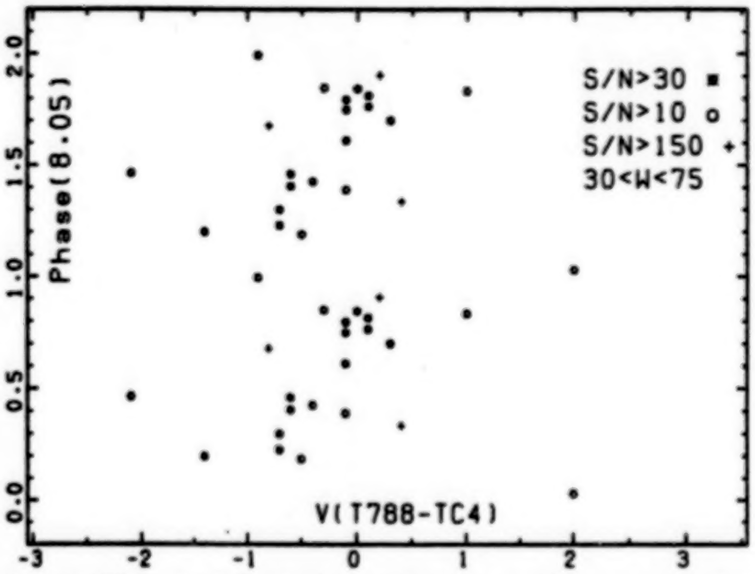

Current test of the variation of redshift for dwarf galaxies with narrow line profiles. Precison redshifts obtained in 1988 and 1986 show that galaxies near phase 0.25, for the basic 8.05 km/s period, continued to shift by an amount proportional to the time interval between observations.

To provide further tests for time change, and to establish a basis for further predictions, overlap was extended to compare redshifts with several other 300-ft investigations done in the mid 70s. This included work by Dickel and Rood (DR) and Shostak (SH). These studies tend toward more luminous wider profile galaxies than the Fisher-Tully program. However, both studies indicate the presence of an underlying 8.05 km/s periodicity, especially for W < 150 km/s and the larger residuals for wide profile data (W > 150 km/s). Without the distinction provided by the time differentials the periodicity would be essentially undetectable. Flux level and profile shape also appear to provide or sharpen sample discrimination in certain cases.

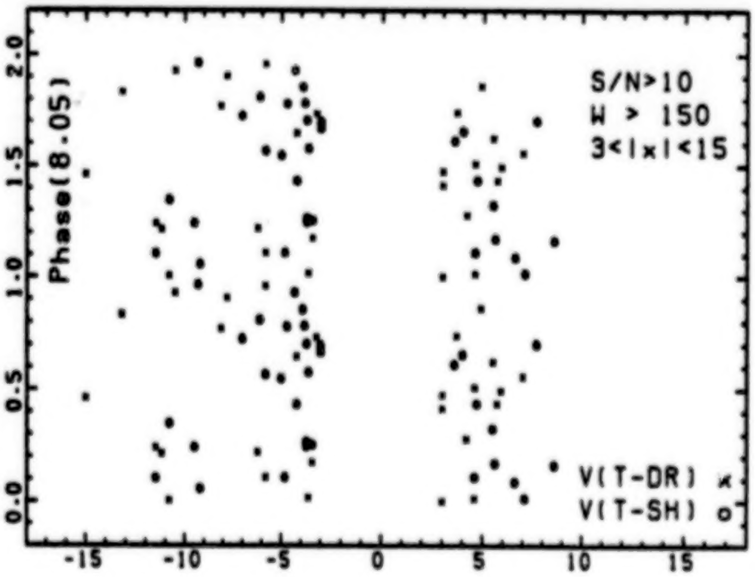

Demonstration that the basic 8.05 km/s periodicity extends to wide profile data and shows phase dependent shifts. Redshifts from the 70s by Dickel and Rood (DR) and Shostak (SH) are compared with new precision redshifts from the 80s.

HIGHER ORDER PERIODICITIES

With the advent of time differential comparisons it has become increasingly likely that most of the periodicities seen are modulations of an underlying 8.05 km/s interval. This appears especially to be the case for the narrow profile 24.15 km/s periodicity. The 24.15 km/s period in turn shows a population modulation over a triple 72.45 km/s period. It is now apparent that the fourth multiple of 8.05 = 32.2 km/s modulates major portions of wide profile data when time differentials are invoked.

The DR and SH time base comparisons are modulated at 32.2 km/s for differentials near zero on profile wider than 150 km/s. Deviations near phase 0.5, based upon P=32.2, show negative V(new − old) residuals. Near phase 0.2 residuals are positive. Still larger positive residuals fit the periodicity at phase 0.8-0.9. Portions of the residual range, especially the larger negative residuals, fit a 24.15 km/s modulation. Preliminary internal comparisons within the newest redshift data are consistent; however, the time baseline is still too short to provide significant separations. The basis now exists, however, to make specific predictions.

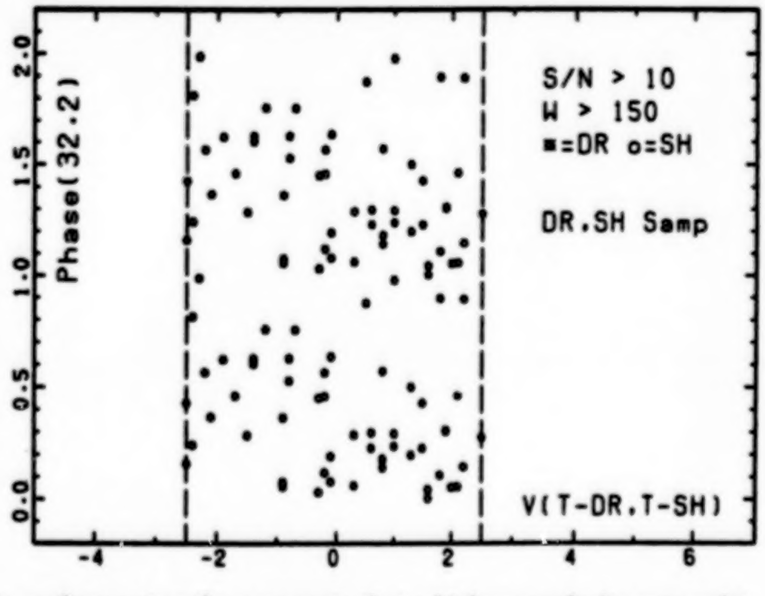

Illustration that the underlying 8.05 km/s periodicity for wide profile galaxies is modulated at 4 times 8.05 or 32.2 km/s for galaxies showing only small redshift differences over time. Future testing of the time variation of redshifts will be based upon confirming and mapping such changes.

The presence of certain multiples of 8.05 in preference to others suggests that a higher regularity may exist. There is some suggestion that higher multiples of the 8.05 km/s period relate to increasing width in a regular pattern. It will require longer time baselines and extended samples to seriously investigate such questions.

THEORETICAL DEVELOPMENTS

A self-consistent nonrelativistic theory of redshift quantization has been published (Astroph Lett **23**, ApJ **288**). These references established a quantum theory which represented the nonrelativistic redshift as a differential operator. The eigenvalues of this operator are quantized in an appropriate way if galaxies are fermions. The theory showed that, if the basic quantization interval $c\Delta z$ is 12 km/s, the Planck's constant for this sort of quantum mechanics is $\hbar \approx 2.4 \times 10^{73}$ erg s. A more basic quantity, however, is the analog of the Compton wavelength, $\mu = (\Delta z)^2/2H_0$. If $H_0 \approx 90$ km/s, then $\mu \approx 8 \times 10^{18}$ cm ≈ 3 pc.

An interesting feature of this theory is that the gravitational analogue of the Bohr radius, $\hbar^2/me^2 \rightarrow \mu^2c^2/GM$, turns out to be ≈ 3 kpc, for $M \approx 5 \times 10^{10} M_\odot$. Thus a galaxy might consist of two or more gravitationally bound fermions.

We propose a relativistic extension of this theory in which the fermions are governed by the Dirac equation in a Riemannian space-time. The background metric would be the usual Robertson-Walker metric. Nonrelativistic quantum mechanics would not predict observable changes in galaxy redshifts in anyone's lifetime. In relativistic QM, however, there is the phenomenon of 'jitter' (Ger. *Zitterbewegung*) with a time scale of $\hbar/m_e c^2 \approx 10^{-21}$ sec. This is the time that it takes light to cross the Compton wavelength. In our theory, this becomes $\mu/c \approx 3 \times 10^8$ sec ≈ 10 years. This time scale is roughly consistent with changes that have already been observed.

SELECTION EFFECTS AND BINARY GALAXY VELOCITY DIFFERENCES

Stephen E. Schneider, *University of Massachusetts*
Edwin E. Salpeter, *Cornell University*

I. Introduction

Measurements of the velocity differences (Δv's) in pairs of galaxies from large statistical samples have often been used to estimate the average masses of binary galaxies. A basic prediction of these models is that the Δv distribution ought to decline monotonically. However, some peculiar aspects of the kinematics have been uncovered, with an anomalous preference for $\Delta v \approx 72$ km s^{-1} appearing to be present in the data.

We examine a large sample of binary galaxies with accurate redshift measurements and confirm that the distribution of Δv's appears to be non-monotonic with peaks at 0 and $\sim$72 km s^{-1}. We suggest that the non-zero peak results from the isolation criteria employed in defining samples of binaries and that it indicates there are two populations of binary orbits contributing to the observed Δv distribution.

II. The Observed Form of the Δv Distribution

For a complete sample of binary galaxies with velocity vectors oriented at random to the line of sight, the distribution of their observed Δv's should be a monotonically declining function of Δv. Even if there was a range of orbital velocities that actually *were* absent, the resultant distribution would only be flat over this range. Tifft (1980), however, found non-monotonic behavior in the Δv distribution. Testing a hypothesis about possible non-monotonic behavior against observational data is difficult if the hypothesis is made after the data is collected (Newman, Haynes, and Terzian 1989), but fortunately, both the quality and quantity of data on binary galaxies has improved greatly since Tifft (1980) developed his paradigm of the peculiar non-monotonic behavior.

Neutral hydrogen velocity-difference measurements of normal spiral galaxies made at 21 cm are now generally accurate enough to clearly distinguish between the posited 72 km s^{-1} peak and the expected zero-velocity peak. Excluding the pairs from Tifft (1980), we have collected data on 102 isolated binaries that have accurate 21 cm velocities for both members in the literature (Schneider and Salpeter 1990). The distribution of Δv's is shown in Fig. 1 in the form of a frequency distribution f(Δv) (i.e., the value in the first bin is doubled to reflect its narrower range), using the same binning as suggested by Tifft (1980).

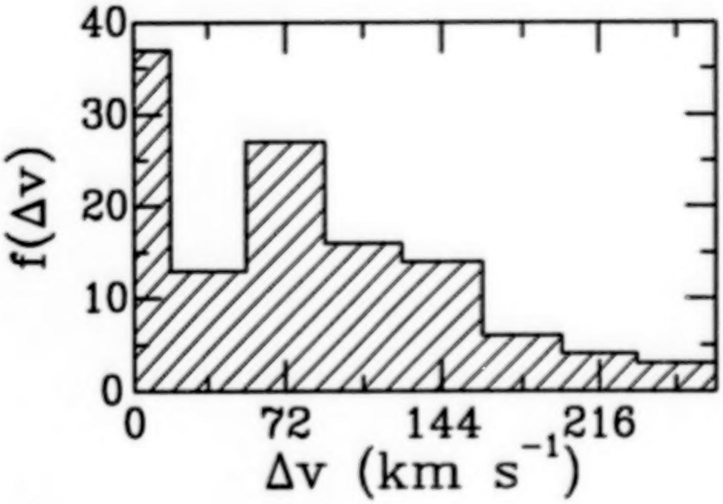

Fig. 1—Distribution of velocity differences among 102 binary galaxies measured at 21 cm.

The distribution has fairly significant peaks in both the 0 km s^{-1} and 72 km s^{-1} bins; beyond 72 km s^{-1} the numbers decline smoothly. Other largely independent samples and measurements of binaries and groups also show a peak in the 72 km s^{-1} bin. Tifft (1980) also found peaks at higher multiples of 72 km s^{-1}, but the evidence for any individual higher-velocity peaks has never been very strong. Newman, Haynes, and Terzian (1989) have shown that any freedom in the choice of the zero point or bin size can produce apparently significant but spurious periodic peaks. Similar problems with the statistics seem likely to arise if special selection criteria are applied to the data after it is collected; any resultant enhancements produced in the appearance of periodicity become uninterpretable. We do not comment further on the analysis papers claiming to find this periodicity (Tifft and Cocke 1989 and references therein) except to note that the statistical significance of these works is difficult to evaluate because of sample overlap, differing selection criteria, and differing binning intervals.

III. Effects of Incompleteness

The binaries in our sample were selected on the basis of there being no likely massive companions within a few times the separation of the pair. This selection criterion should eliminate most groups with three or more comparably massive members, but the result is a bias in the final sample: pairs with large angular separations (and large projected linear separations) tend to be excluded. The binary samples are therefore incomplete. Of the pairs in our sample, 90% have projected separations $< 136\ h^{-1}$ kpc. This cutoff has some interesting implications for the form of the Δv distribution.

The projected-separation cutoff will eliminate preferentially those pairs lying most nearly perpendicular to the line of sight. A selection procedure will influence f(Δv) when the apparent separation and velocity of pairs are interdependent. For circular orbits, the largest projected Δv' occur when the projected separations are largest, while for eccentric orbits, the smaller Δv's occur near apocenter, so a projected-separation cutoff may influence f(Δv).

When a projected-separation cutoff is applied to orbits of even small eccentricity a non-monotonic distribution can result. In Fig. 2, the effect of different projected separation cutoffs is shown for circular orbits and for orbits with an eccentricity of 0.33. These are analytic models, numerically integrated, in which we follow a Keplerian orbit, consider all possible orientations, and find the resultant projected separation and the line-of-sight velocity at equal time intervals around the entire orbit. For both eccentricities we show the complete sample, and then we apply more restrictive projected separation cutoffs of $\frac{1}{4}$, $\frac{1}{8}$, and $\frac{1}{16}$ of the apocenter separation; the velocities are scaled relative to the pericenter velocity of the orbit.

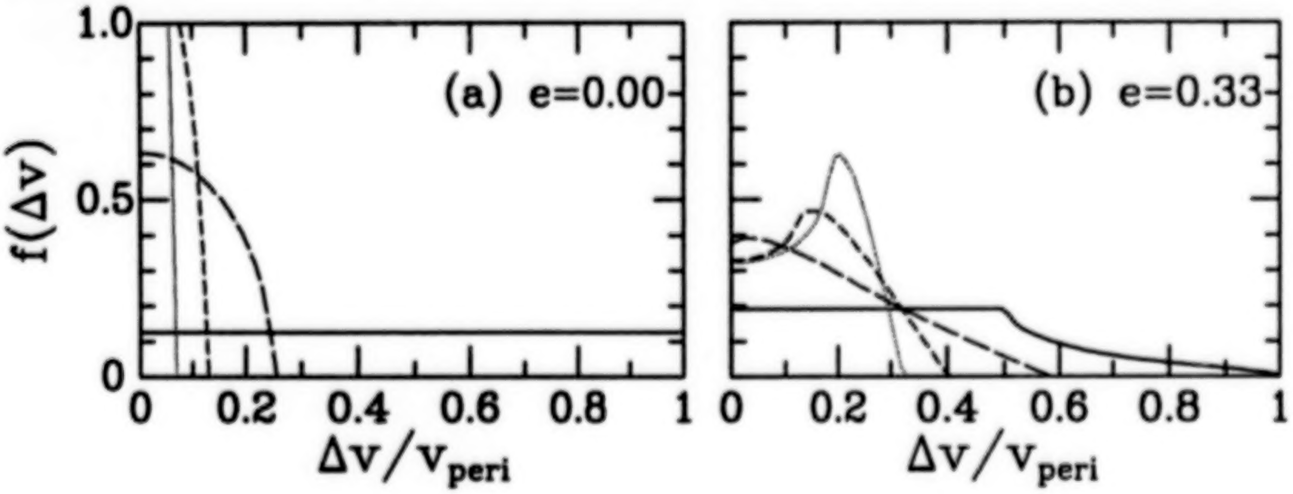

Fig. 2—Distribution of expected velocity differences for (a) circular and (b) eccentric orbits, using a complete sample (solid line) and then applying successively narrower projected-separation cutoffs at $\frac{1}{4}$ (long dash), $\frac{1}{8}$ (short dash), and $\frac{1}{16}$ (dotted) of the apocenter separation.

For non-circular orbits in general, f(Δv) peaks toward Δv=0 in a complete sample because the binaries spend more time at larger separations orbiting more slowly. The application of smaller cutoff radii makes f(Δv) more and more distinctly non-monotonic as the lower velocities are removed, and this could quite reasonably contribute to a peak near 72 km s^{-1} since the peak occurs at some fraction of the typical orbital velocity.

Of course, in a realistic model, a wide range of orbital parameters would be likely, which might "wash out" the effects seen for this simple Keplerian analysis. We therefore constructed a more detailed model in which we traced orbital parameters for a full population of pairs from the time of their formation, when they would have been expanding with the Hubble flow. We allowed a Gaussian distribution of angular momenta and then applied projected separation cutoffs to the sample at the present day. Interestingly, the only natural velocity scale in the model is the escape velocity of the pair on a zero-energy trajectory. Solving the energy-balance equation, this velocity is $v_{esc} = (\frac{4}{3}GM/t_H)^{1/3} \approx 72$ km s^{-1} for $M \approx 10^{12} M_\odot$.

The pairs still expanding at present are the most widely separated and when a projected separation cutoff is introduced, they contribute only slightly to f(Δv). On the other hand, the pairs that had initially small separations will presently be merging, and the major axes of their orbits will be made smaller still by dynamical friction. The intermediate "converging" pairs, which are falling back together, but which have not yet collided, prove to have the most interesting properties with respect to the projected-separation criterion. In Fig. 3, we show the effect of selection criteria on the population of converging pairs, with projected separation cutoffs relative to the escape separation as in Fig. 2. The non-zero peak in f(Δv) occurs at a velocity similar to 72 km s^{-1} for the known projected separation cutoff when the average pair mass is $\sim 3 \times 10^{11}$ M$_\odot$.

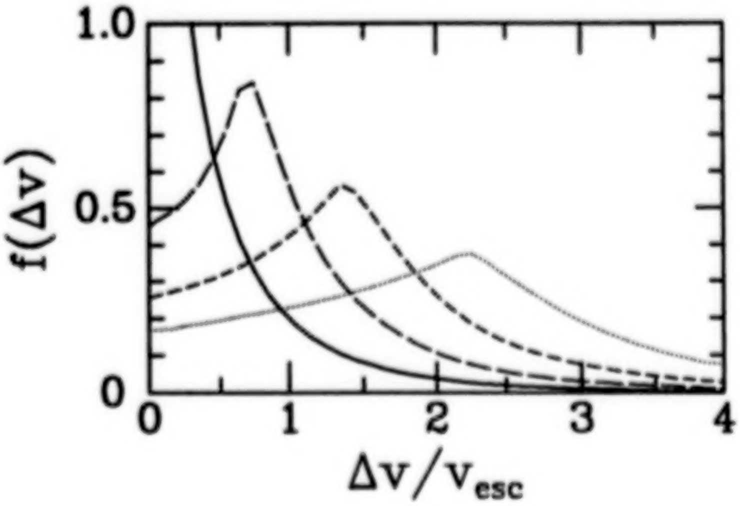

Fig. 3—Distribution of expected velocity differences for a modelled range of orbital parameters, using various projected separation cutoffs (relative to the escape-velocity separation) as in Fig. 2.

The peak around $\Delta v = 0$ in the observed distribution (Fig. 1) could be produced by the population of merging pairs, which would be more completely sampled because of their smaller major axes. A reasonable facsimile of this peak could be produced, for example, by completely sampled $e = 0.7$–0.8 orbits with typical 200 km s^{-1}rotation speeds at pericenter.

IV. Discussion

In summary, we see evidence of non-monotonic behavior in f(Δv) for $\Delta v < 100$ km s^{-1}. We have constructed a fairly realistic model of binary orbits, and we find that a peak occurs in the population of "converging" pairs at a velocity of the order of magnitude of $(GMH_o)^{1/3} \approx$ 72 km s^{-1}. We further speculate that the peak at 0 km s^{-1} is produced merging pairs.

We can make some predictions based on our two population model. For uniform samples of isolated pairs, we expect that the non-zero peak will move to larger values of Δv as the cutoff radius is decreased or the pair mass (based on absolute magnitudes, for example) increases. For current samples this point is difficult to test because of another bias present in the data—the isolation criteria also tend to select more massive pairs at larger projected separations. This bias may actually help keep the non-zero peak in f(Δv) from being smoothed out despite a range of contributing binary galaxy masses.

We suspect, therefore, that previous dynamical estimates of binary galaxy masses are likely to be in error. Even if our two-population model does not prove correct, it seems clear that selection effects must significantly limit the range of selected orbital orientations in binary samples, and these effects need to be better understood. If our model is correct, only the merging pair population has been (approximately) completely sampled, and the characteristic width of its f(Δv) distribution is substantially narrower than has been previously suspected; as a result these pairs' masses have probably been overestimated. We conclude, though, with a more positive message: if there is a non-zero peak in f(Δv), it may ultimately provide a much better tool for estimating not only the masses of converging binaries but for deciphering the origin and evolution of binary orbits as well.

References

Newman, W. I., Haynes, M. P., and Terzian, Y. 1989, *Ap. J.*, **344**, 111.

Schneider, S. E., and Salpeter, E. E. (1990) in preparation.

Tifft, W. G. 1980, *Ap. J.*, **236**, 70.

Tifft, W. G., and Cocke, W. J. 1989, *Ap. J.*, **336**, 128.

DISCUSSION

Miller: How bad will virial mass estimates be? Is it a 10% effect, a factor of two, or what?

Schneider: The mean velocity differences will tend to be overestimated, but the separations underestimated. The net effect will tend to be overestimated masses, but based on my simple models, probably only by factors like two for typical cut-off separations.

A TENTATIVE EXPLANATION OF COSMOLOGICAL RED SHIFT

T. Chang , D. G. Torr

Department of Physics
University of Alabama in Huntsville
Huntsville, Alabama 35899

ABSTRACT

In this paper we suggest a possible alternative explanation of cosmological red shift . We consider that there exists a background field in the universe, and that light (the photon) has an extremely weak interaction with this background, and as result, experiences an energy loss. By analogy with damped oscillations, we introduce a dumping term with the first derivative with respect to time in the wave equation. The solution yields a linearly reduced frequency of the light with travel distance. The purpose of this exercise is to demonstrate how a simple alternative interpretation of the Hubble relation can be generated.

1. Introduction

In 1929 E.Hubble discovered a roughly linear relation between red shift and distance for extragalaxies.[1] This relation was comfirmed by later observations. Hubble relation can be written as

$$z = (\lambda_0 - \lambda_1)/ \lambda_0 = (H_0/c)\ d \qquad (1)$$

where z is the red shift , λ_0 is the observed wavelength , λ_1 is the emitted wavelength, c is the constant of the speed of light,d is the distance between the observed galaxy and the earth. H_0 is known as the Hubble constant, which is given by[2]

$$50\ \mathrm{km/sec/Mpc} < H_0 < 130\ \mathrm{km/sec/Mpc} \qquad (2)$$

The interpretation of the red shift as a cosmological Doppler effect has been accepted through the decades since its conception stands. With this interpretation, the universe is in a continuous expansion. Below we explore a non-Doppler interpretation of this effect in this paper.

2. Some Physical Thinking

From modern physics, we know that space is not empty, which is permeated with fields such as the gravitational field, microwave radiation background, neutrino field and so on. These fields could in general constitute a background field . It is easily imagined that there would be some unknown extremely weak interaction between light (the photon) and the background field. We assume that propogation of photons through this field results in an energy loss. The interaction is presumed to be too weak to be detected on the scale of our galaxy , but it could become evident on cosmological scale (10^9 light years). Therefore, we assume mathematically that such an interaction will provide a damping term into the wave equation. We recall the case of damped oscillations, where an additional term $2b\,dx/dt$ is included in the the equation for simply harmonic oscillation: $d^2x/dt^2 + \omega^2 x = 0$. By analogy, we propose the following one dimensional wave equation here for light propagation:

$$\frac{\partial^2\psi}{\partial x^2} - f(\mu\ ct)\frac{2\mu}{c}\frac{\partial\psi}{\partial t} - \frac{1}{c^2}\frac{\partial^2\psi}{\partial t^2} = 0 \qquad (3)$$

The second term in Eq.(3) is the assumed interaction term, where the coefficient $\mu = H_0/c$. The function $f(\mu\,ct)$ could be a polynomial: $1 + \Sigma\ a_n(\mu\ ct)^n$; t is the travel time.

3. Solution and Discussion

We expect that the solution of eq.(3) has the following properties: (1) the speed of light should be constant, independent of the frequency; (2) the frequency should be linearly reduced with the travel time. Thus we suggest a trial solution as follows:

$$\psi = \psi_0 \sin[\omega(1 - \mu\ ct)(t - x/c + \delta)] \qquad (4)$$

where ψ_0 and δ are two integration constants; ω is the proper frequency. It is found that if we choose $f(\mu\,ct) = (1 - \mu\,ct)^{-1}$, then

Eq.(4) is a solution of the following equation:

$$\frac{\partial^2 \psi}{\partial x^2} - \frac{2\mu}{c(1 - \mu ct)} \frac{\partial \psi}{\partial t} - \frac{1}{c^2} \frac{\partial^2 \psi}{\partial t^2} = 0 \qquad (5)$$

From the solution, Eq.(4), the physical meaning is clearly as follows

$$x = ct \qquad (6)$$

for the propogation of the light, and

$$\omega' = \omega (1 - \mu ct) \qquad (7)$$

Eq.(7) could lead to the Hubble's relation: $(\omega - \omega')/\omega = \mu x = (H_0/c)d$.

According the above approach, the universe is not in a state of expansion although galaxies have random motion. If a photon travels a distance $R = 1/\mu$, it would lose all of its energy. From this sense, R is not the radius of the universe, but is an important constant which indicates the intensity (or weakness) of the interaction. Naturally, we need to identify the nature of the interaction, however, it may be premature to speculate on possible physical models which could give rise to this kind of interaction at the present stage.

Our primary objective in this brief communication is to introduce the concept as a posibility and to see if any arguments are forthcoming which eliminate the idea as a plausible alterative to current thinking.

References

[1] E.P.Hubble, Proc.Nat.Acad.Sci., 15, 168 (1929).

[2] A. Sandage, Physics Today, Feb. p.34 (1970).

MERGING GALAXIES AND BLACK HOLE EJECTIONS

M.J. Valtonen
Turku University Observatory, Finland

In mergers of galaxies their central black holes are accumulated together. We show that few-black hole systems arise which decay through black hole collisions and black hole ejections. The ejection statistics are calculated and compared with two observed systems where ejections have been previously suggested: double radio sources and high redshift quasars near low redshift galaxies. In both cases certain aspects of the associations are explained by the merger hypothesis.

The first stage in making of a few-black hole system is the formation of a supermassive black hole binary (Begelman, Blandford and Rees 1980). The binary forms when two galaxies merge and each contains a supermassive black hole in its center (Roos 1981, Gaskell 1985, Valtaoja, Valtonen and Byrd 1989). Such binaries are long lived, and if left undisturbed by other galaxy mergers, probably survive through the Hubble time.

But in many galaxies multiple mergers take place (Aarseth and Fall 1980, Mamon 1987) and thus three and possibly also four black hole systems come together. The instability of the few-body systems makes it difficult to collect large numbers of black holes in the same galactic nucleus. Only in some hierarchical systems can many black holes survive. Thus generally we have to consider what happens when three or four black holes, of comparable mass, come together.

As a representative example, let us take a few black hole system of the following parameters: diameter about 1 parsec, mass about $10^9 M_\odot$ and typical orbital speed of about 1000 km s^{-1}. There is nothing unique about these parameters, and in particular the mass could be different by several orders of magnitude.

According to the usual orbital evolution of the few-body problem (see e.g. Szebehely and Peters 1967), close encounters between the black holes take place. Gravitational radiation predicted by General Relativity becomes important at these encounters, and sooner or later an encounter takes place where large amount of orbital energy is lost. Then either a tight, short lived binary forms or two black holes coalesce.

The formation of a tight binary can be disruptive to the system. Another black hole passing by the binary can pick up enough speed to leave the system or even the whole galaxy. This is most likely to happen when the average orbital speed of the binary is about 10 000 km s^{-1}.

For an escape from the galaxy, a four-body system is much more effective than a three-body system. After a tight binary has formed, a third black hole must find it rather soon. Otherwise the binary is destroyed by gravitational radiation before much else happens. In a four-body system the chaotic nature of orbits of the binary center of mass and the two other black holes more or less quarantees a strong interaction. In a three-body system a hierarchical situation often developes which leads to a stable binary and no escapes.

In a few-body system the closest encounters tend to take place between the heaviest bodies (e.g. Szebehely and Peters 1967). Therefore the three black holes involved in the ejection event are likely to be among the most massive ones in the system and the lightest one is left aside. When a supermassive black hole is ejected and escapes from a galaxy, the binary is also of comparable mass and recoils in the opposite direction. The binary soon coalesces and thus in essence the few black hole systems decay through ejecting pairs of black holes. The light fourth black hole remains at the center of the galaxy.

The ejected pairs are not exactly symmetric since the masses of the escaping black holes are generally unequal. However, there is a tendency, enforced by several factors in the dynamical process, to look for maximal symmetry in the ejected masses. When the distribution of mass ratios of the escaping bodies in many ejections is formed, it peaks strongly towards equal masses (Valtonen and Mikkola 1990).

Another kind of asymmetry may appear with respect to the directions of escape. There is some scattering of the escaping black holes from the fourth black hole which causes a small bending angle between the two lines of escape. In case of strong scattering also the escape speed is significantly affected, and thus unusually strong escape speed asymmetry should be associated with strongly bent lines of ejection.

Double radio sources form an obvious application of the symmetric pair ejection of supermassive black holes. In double radio sources filaments frequently connect two strong regions of radio emission with the nucleus of the central galaxy. They seem to show that whatever produces the radio emission in the outer radio lobes has come from the nucleus of the galaxy. The outer lobes themselves often contain a sharp very high surface brightness spot (Carilli, Perley and Dreher 1988, Laing 1989), apparently the primary source of energy. It could well be a supermassive black hole. The black hole may interact with the interstellar medium via a twin-exhaust beam of relativistic plasma (Blandford and Rees 1974), the outward side of which terminates at a shock front, a secondary hot spot (Valtaoja 1984).

In this view there would generally be three supermassive black holes in a given double radio galaxy, each associated with its own twin-exhaust beam (Figure 1). Unlike in the so called "unified schemes" (Orr and Browne 1982), the central beam would not generally point toward the outer components. This appears to be also the current observational situation (Pearson and Readhead 1988). Nor would there be any strong reason why the beams in the outer lobes should be aligned with each other or with the central beam. Of course, the various manifestations of the black hole trails would still line up with the outer lobes as long as there are no strong non-radial winds in the tenuous interstellar medium surrounding the galaxy.

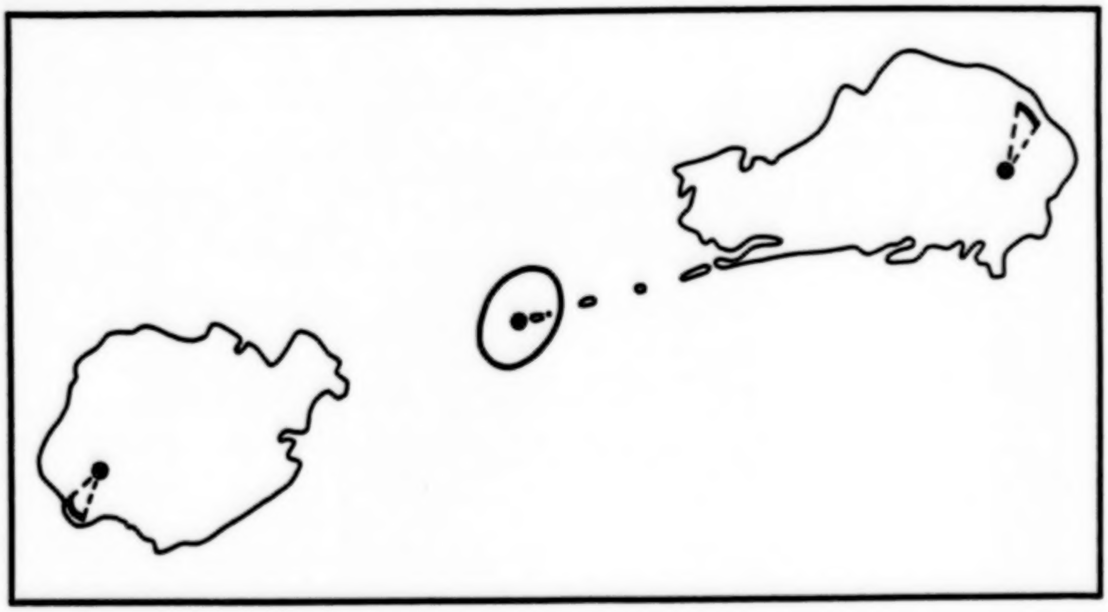

Fig. 1. Cygnus A and the three supermassive black holes (dots) according to the black hole ejection model. An ellipse describes the optical outline of the central galaxy, and the contour lines mark the regions of primary radio emission. They include a faint trail which connects the center of the galaxy with one of the radio lobes. A slightly fainter trail is observed on the opposite side. Two of the jets in the model are indicated by dashed lines. The illustration is adapted from the work of Perley, Dreher and Cowan (1984).

This theory can be tested quantitatively by studying the relation of the central component in radio galaxies to the symmetry properties of the lobes. A bright and presumably massive central component should induce asymmetry via scattering the escaping black holes. This asymmetry should appear both as bending and as component distance asymmetry. Indeed, a strong correlation exists between the two kinds of asymmetry (Macklin 1981) and between the strength of the central component and asymmetry (Valtonen 1977).

In conclusion, the double radio sources are well explained by the black hole ejection model. Quantitative comparisons between the calculated models and observed double radio sources show excellent agreement, especially the connection between the central component and the outer lobes (Mikkola and Valtonen 1990). The alignment properties which have caused many problems in the so called unified schemes obtain a natural explanation in this theory.

Even though the few black hole process produces naturally ejections of rather symmetric pairs, there is also another decay mode where a relatively light black hole escapes from the galaxy without any significant opposite recoil. Single black hole ejections could be much faster than the pair ejections: ejection speeds exceeding 100 000 km s^{-1} are possible.

For example, we could consider the following process. Let the central supermassive black hole be surrounded by several smaller satellite black holes. Let the primary black hole mass be 10^9 $M_\odot$ and let it have satellites of mass 10^4 $M_\odot$ The system is stable against collapse caused by gravitational radiation for about one Galactic year ($\sim 2 \cdot 10^8$ yr) if the satellite orbits are circular and the typical satellite speed is about 25 000 km s^{-1}. In that period of time a merger of galaxies may take place and bring a pair of massive black holes to the system. During the process of merger between the primary black hole and one of the newcomers, very high orbital speeds are obtained. Some fraction of the satellites will interact strongly with the high speed binary and will be ejected. This fraction is close to 100 % when the binary speed is 50 000 km s^{-1}, and about 1 % when the binary speed is 100 000 km s^{-1}.

Escape speeds are typically between one quarter and one third of the mean binary orbital speed, with the tail end of the distribution extending up to and even beyond the orbital speed. Thus we expect that satellites will be ejected with a speed distribution which extends all the way from 10 000 km s^{-1} to 100 000 km s^{-1}, such that most of the ejections take place at the lower end of the distribution. An ejection of Markarian 205 from NGC 4319, as proposed by Sulentic and Arp (1987a,b) could be well accommodated within this scenario.

Even if the supermassive black holes are not surrounded by satellite black holes, they should have a cluster of stars around them. The arrival of a pair of supermassive black holes would be equally disruptive to this system: stars and gas clouds (if stars are tidal disrupted, Rees 1988) would be ejected at speeds which extend up to the relativistic regime.

References

Aarseth, S.J. and Fall, S.M. 1980, Ap. J. **236**, 43

Begelman, M.C., Blandford, R.D. and Rees, M.J. 1980, Nature **287**, 307

Blandford, R.D. and Rees, M.J. 1974, M.N.R.A.S. **169**, 395

Carilli, C.L., Perley, R.A. and Dreher, J.H. 1988, Ap. J. (Lett.) **334**, L73

Gaskell, C.M. 1985, Nature **315**, 386

Laing, R.A. 1989, in Hot Spots in Extragalactic Radio Sources – Lecture Notes in Physics 327, ed. K. Meisenheimer and H.-J. Röser (Berlin: Springer), p. 27

Macklin, J.T. 1981, M.N.R.A.S. **196**, 967

Mamon, G.A. 1987, Ap. J. **321**, 622

Mikkola, S. and Valtonen, M.J. 1990, Ap. J. **348**, in press

Orr, M.J.L. and Browne, I.W.A. 1982, M.N.R.A.S. **200**, 1067

Pearson, T.J. and Readhead, A.C.S. 1988, Ap. J. **328**, 114

Perley, R.A., Dreher, J.W. and Cowan, J.J. 1984, Ap. J. (Lett.) **285**, L35

Rees, M.J. 1988, Nature **333**, 523

Roos, N. 1981, Astr. Ap. **104**, 218

Sulentic, J.W. and Arp, H. 1987a, Ap. J. **319**, 687

Sulentic, J.W. and Arp, H. 1987b, Ap. J. **319**, 693

Szebehely, V. and Peters, C.F. 1967, A. J. **72**, 876

Valtaoja, E. 1984, Astr. Ap. **140**, 148

Valtaoja, L., Valtonen, M.J. and Byrd, G.G. 1989, Ap. J. **343**, 47

Valtonen, M.J. 1977, Ap. J. **213**, 356

Valtonen M.J. and Mikkola, S. 1990, in preparation

DISCUSSION

Zasov: Can we expect any preferrable direction of black-hole ejection? Is it possible that the direction of the axis of rotation of a galaxy may be somehow distinguished?

Valtonen: There should not be any strong correlation between rotation and ejection axes.

Shlosman: I want to suggest the ultimate test for your ejection model. A SBH in the ISM or IGM would accrete at low $\dot{M}$, produce an ion-supported torus and may create radio jets. Look for these jets centered on empty space.

Valtonen: Actually this may be happening inside the lobes of double radio sources, which one could interpret as the jet-IGM interaction regions. It appears that the jet originates from "empty" space outside the galaxy, from the point where the black hole has proceeded after the ejection. In some cases this point may be identified as a so-called B hot spot.

Roos: I agree that many galaxies might harbour massive black holes. However, I think that a subsequent merger may trigger the flow of stars (and perhaps gas) through the orbit of the central binary. The central binary may then lose orbital energy as the third hole spirals inward and merge before the third hole reaches it. In that case ejections would not occur.

Valtonen: This process may be relevant to low-mass black-hole binaries, in which case it would set a lower limit (around 10^7 $M_\odot$) to the black hole masses which are involved in ejection. But it is not certain that the process you mentioned operates in many galaxies since it requires a slow approach by the incoming body and practically circular approach orbit. We did not obtain such orbits in our simulations.

VII. CLASSICAL THEORY OF PAIRS

DYNAMICAL INTERACTIONS OF GALAXY PAIRS

E. Athanassoula
Observatoire de Marseille - 2, Place Le Verrier
13248 Marseille Cedex 04 - France

I. INTRODUCTION

As the dynamics of galaxy interactions is too broad a subject to be discussed in any depth in a single review, I will concentrate only on a few topics proposed to me by the organisers. Since a pair should be "two things of a kind", I will not discuss merging and merger remnants. I will also leave out discussions on M/L and hence halo mass determinations. Good reviews covering these subjects, and some of the subjects treated here, have been given by Toomre (1977), Tremaine (1981), White (1982, 1983a), van Albada (1988), Barnes (1990) and others. Here I will briefly review the dynamics of sinking satellites and the effect of companions on elliptical galaxies, then discuss recent work on interacting disk systems, and finally focus on my favourite interacting pair NGC 5194/5195.

II. SINKING OF SATELLITES

a) Non rotating spheroids (Ellipticals or halo dominated galaxies)

A satellite orbiting around a galaxy experiences a drag force which leads to a gradual orbital decay and eventually a merging in a time scale no longer than a Hubble time. This loss of the satellite's orbital energy due to dynamical friction will excite internal motions in the main galaxy. Chandrasekhar's formula (1943), appealing for its simplicity, has often been used for estimating this deceleration. Yet it is in principle valid only for the motion of a point mass through an infinite homogeneous medium, and thus should not apply to satellite galaxies. Nevertheless several authors (e.g. Lin and Tremaine 1983, Bontekoe and van Albada 1987 etc.) have reported a fairly good agreement between their numerical results and the estimates obtained from Chandrasekhar's formula. This should indeed be the case if the distance of the satellite from the center of the parent galaxy is very large compared to the radius of the satellite or if the matter distribution in the main galaxy is self-similar (Weinberg 1989). However one should not conclude from this that dynamical friction is a local effect and in general one should not expect Chandrasekhar's formula to be an adequate approximation to the orbital decay of an extended satellite. A proper and elegant analytical treatment, including self-consistency, has been given recently by Weinberg (1989).

An ideal numerical treatment would include a fully self-consistent description of both the galaxy and the satellite, and a sufficiently large number of particles to eliminate spurious effects like enhanced two body relaxation. This is however not easy to achieve and many alternatives have been used so far including the semirestricted N body method, harmonic expansions for the calculation of the galaxy potential, the direct N body code and the tree code (Lin and Tremaine 1983, White 1983b, Bontekoe and van Albada 1987, Zaritsky and White 1988, Hernquist and Weinberg 1989). To cut a long story short one can say that the subtleties of the various codes, and in particular the treatment of the motion of the center of mass, can influence substantially the results. So it was not until the various approximations in the different numerical treatments were analyzed and understood that a good agreement between the various methods could be reached. Thus the latest attempt by Hernquist and Weinberg (1989) reports an agreement better than 2% between their results and those of Bontekoe and van Albada (1987) and Zaritsky and White (1988).

Weinberg (1989) and Hernquist and Weinberg (1989) argue that the inclusion of self-gravity necessarily requires also the correct treatment of the center of mass shift, since this determines the $m = 1$ Fourier component of the density and potential. They find then an increase of the decay time by a factor of 2 - 2.5 with respect to non-self-gravitating calculations. At first thought one could have expected the self-gravity to enhance the wake of the satellite, thus increasing the drag force and decreasing the decay time. However, the response of the main galaxy to the satellite is not local but global and thus the effect will depend on the phase difference between the satellite and the response of the main galaxy to it. Ideally of course the satellite should also be treated self-consistently since stripping will remove its more loosely bound stars. Compared to numerical calculations, analytical results give estimates of decay rates larger by factors of the order of 50%, due to the neglect of nonlinear effects. This discrepancy appears to vanish for sufficiently small satellite masses (Hernquist and Weinberg 1989).

Scaling the results of the various numerical simulations to the dimensions of real galaxies, one finds decay rates of the order of a few times 10^9 yr. The precise number will depend on various properties like the mass profile and the distribution of velocities in the main galaxy. In this respect we note that most of the simulations run so far have used Plummer profiles, which are less centrally concentrated than the light distribution in elliptical galaxies. Furthermore the inclusion of some rotation could increase the time scale of the orbital decay.

b) Disks

The situation for disks is much more complicated than for spheroids since there are now at least three different mechanisms active (e.g. Tremaine 1981, Quinn and Goodman 1986):

i) Standard dynamical friction as in the case of spheroids

ii) Exchange of energy and angular momentum between the satellite and stars around the Lindblad resonance of the parent disk

iii) Non perturbative "horseshoe" orbits.

The effect of the two first mechanisms is in the opposite sense, i.e. the first pulls the satellite inwards while the second one moves it to larger radii. This can explain the difference between the results of the analytical work of Palmer and Papaloizou (1982), focusing on the second effect, and those of the N-body simulations of Byrd *et al.* (1986). Quinn and Goodman (1986) stress the importance of self-consistency and of a correct treatment of the center of mass. It is a great pity that self-consistent treatments in which the center of mass of all components is allowed to move freely are not available. Yet existing numerical simulations (Quinn and Goodman 1986, Byrd *et al.* 1986, Valtonen *et al.* 1990, Valtaoja 1990) give us a lot of useful information. Satellites in retrograde or out of the plane orbits have much larger decay time than direct in plane ones, and heavier satellites decay faster than lighter ones.

III. THE EFFECT OF COMPANIONS ON ELLIPTICAL GALAXIES

As shown by the simulations of van Albada and van Gorkom (1977), White (1978), Miller and Smith (1980) and others, colliding spherical galaxies undergo a temporary contraction to about half of their original size, due to the extra inwards force each star feels during the overlap. After the separation the galaxies are larger, more loosely bound and often nonspherical.

Aguilar and White (1985) discussed the exchange of mass during the encounter. For slow collisions, where the relative velocity is smaller than the velocity dispersion in the galaxies, about one third of the mass lost by one galaxy is gained by the other. This fraction increases with decreasing galaxy separation. For distant encounters the exchange is larger for models with more stars on tangential motions, while for nearly head-on encounters it is larger for models with more stars on radial orbits. Thus one can say that the stars captured are those whose velocity vectors do not form a big angle with that of the perturber's.

Miller (1986) and Mc Glynn (1990) studied the effect which an encounter with a big galaxy can have on a small one. Miller argued that a spherical galaxy either suffers very little mass loss (less than one percent) or is totally disrupted. On the other hand the galaxies in Mc Glynn's simulations could loose up to half their mass and still survive. The explanation of this apparent contradiction lies in the density profiles used in the two cases. Miller, using a code with a cartesian grid, modelled galaxies with little central concentration, namely $n = 3$ polytropes. On the other hand McGlynn, using a tree code, modelled more centrally concentrated King profiles. He showed that the central core is little affected even in cases where 30% of the particles in the outer parts were lost. However this number could well depend on the properties of the distribution function used. Thus Miller's results describe the behaviour of less concentrated systems, like halos, and Mc Glynn's of more concentrated systems, like elliptical galaxies.

IV. THE EFFECT OF COMPANIONS ON GALAXIES WITH DISKS

a) Outer parts. Formation of bridges and tails

The now classical work by Toomre and Toomre (1972, hereafter TT) established that gravitational interactions alone can account for the formation of bridges and narrow tails. Using a simple model of test particle simulations they made a comprehensive survey of bridges and tails and of the effect of different encounter parameters on them. They showed that bridges are best seen in interactions with small companions, while tails manifest themselves better in interactions with equally or more massive companions. The amount of matter accreted by the companion is substantial for small angles between the plane of the galaxy and the orbital plane, but decreases rapidly as this angle increases. The effects of retrograde encounters are much less spectacular than the results of direct ones. TT also gave models for four very interesting interacting systems, Arp 295, NGC 4676 (the mice), NGC 4038/4039 (the antennae) and NGC 5194/5195 (M51).

That same year appeared another study on bridges and tails (Clutton-Brock 1972), remarkable not for the comprehensiveness of the survey but for the fact that the simulations reported were actually self-consistent, including both gas and stars. It showed that the gaseous tails could be indeed very thin and long.

Gerhard (1981) studied interactions of pairs with the help of two 250 - particle self-gravitating systems, where roughly half of these particles constitute a live halo. He showed that, due to the escaping particles, which carry away a substantial fraction of the internal angular momentum, and to the capture of new particles, which may even be counterrotating, the final internal spin of each disk is smaller than the initial one. Haloes receive angular momentum from the orbital motion. However, unless the orbital plane happens to coincide with the spin planes, the acquired halo angular momentum vector is not aligned with the one of the disk, a factor which could significantly affect galactic evolution. In general one can say that the strength of the interaction depends heavily on the three spins involved, those of the two galaxies and the orbital spin. Mass exchange was found to be more important than mass loss in these experiments. Thus if the perturber is modelled as a point mass, the mass loss calculated is artificially higher then when the perturber is treated as a collection of points. This is in agreement with the results on elliptical galaxies (Aguilar and White 1985) mentioned above.

Barnes (1988) used a tree code to repeat the TT simulation which gave the best fit to the antennae (NGC 4038/4039), in order to see the effects of self-consistency. He observed a strong coupling between orbital and internal energies, so that, at the time when the TT simulation showed the best fit to the observations, the two galaxies had already merged in the self-consistent simulation. At the time when the fit to the observations was at its best the main bodies for the two galaxies were very near each other and the two tails quite thin. The overall fit is good, particularly when one takes into account the fact that no scan of the parameter space for a best fitting model was attempted. Barnes discusses two drawbacks of his model. The first is the failure to match the velocities of the two main bodies. The second is the fact that the assumed orbit was elliptic with $e = 0.5$, while the effects of a previous encounter were neglected. Barnes also simulated the formation of tails during parabolic encounters. Haloes increase the relative velocity of the encounter and change substantially the morphology of the tails, without, however, inhibiting their appearance.

b) The response of the gas

Noguchi and Ishibashi (1986) returned to test particles and to two dimensional simulations including both stars and gas. The rate of gas cloud collisions in their simulations allowed them to estimate the variation of the star formation rate during the encounter and the corresponding change of colours of the galaxy. They concluded that the star formation rate will reach a maximum, of the order of several times the pre-encounter rate, some few times 10^8 years after perigalacticon.

This result was confirmed by Olson and Kwan (1990), who used three-dimensional models in which the change of potential of the two galaxies during the encounter is taken into account. They used more elaborate collision rules, inspired from Latanzio and Henriksen (1988), including coalescence and disruption of gas clouds. For these rules, the interaction increases the rate of disruptions more than the rate of coalescence, the effect being more important for stronger interactions. This should lead to a more disturbed and fragmented interstellar medium in more violently interacting systems. The region of high cloud collision rates is also more centrally concentrated for the stronger interactions.

c) Inner parts. The driving of spirals

Both analytical work and N-body simulations have shown that direct passages may drive two armed trailing grand design spirals (Toomre 1969, 1981; Goldreich and Tremaine 1979, Sundelius *et al.* 1987, Athanassoula 1990, etc). This is in good agreement with observations, which show a substantially larger percentage of grand design spirals amongst binaries and galaxies in groups, than amongst isolated galaxies (Kormendy and Norman 1979, Elmegreen and Elmegreen 1982).

Retrograde encounters may force both two armed trailing spirals and one armed leading ones. The latter comes from the interplay between the companion and an $m = 1$ resonance of the inner Lindblad type, which is the only one possible in the case of retrograde pattern speeds, and the result is an $m = 1$ (one armed) leading spiral (Athanassoula 1978). This is the case even if self-gravity is neglected (Kalnajs 1975, Noguchi and Ishibashi 1986), although its inclusion and the parameters describing the stellar and gaseous component influence the overall form of the spiral. Thomasson *et al.* (1989) modeled the effect of a retrograde companion with the help of N-body simulations and verified the formation of the one armed leading spiral. This was particularly obvious in the case of galaxies with high halo-to-disk mass ratio, where the swing amplification is inhibited and the $m = 2$ (two armed) trailing component is of low amplitude.

Some properties of the driven spirals have been discussed by Athanassoula (1990). She showed that the driven spiral patterns are neither permanent nor stationary and that their structure depends heavily on the properties of the perturbed disk. The initial velocity dispersion evolves drastically with time and is raised by the heating due to the spiral perturbations. In the case of unstable disks, the spiral structure which develops unaided interacts nonlinearly with the forcing and, depending on the relative differences of their pattern speeds and phases, this leads to a temporal increase or decrease of its amplitude.

d) Inner parts. The driving of bars

Noguchi (1987) and Gerin *et al.* (1990) showed that the main effect of an interaction on a bar unstable disk is to accelerate noticeably the bar formation. Thus, all other things being equal, the frequency of bars amongst pairs should be enhanced. This is in fact born out by the observations which show that there are 63% of SBs and SABs amongst isolated galaxies, compared to 81% for binaries (Elmegreen and Elmegreen 1982).

The bar instability sets in differently in interacting compared to noninteracting cases. In noninteracting cases the $m = 2$ component is sizeable only within the corotation radius, while in interacting cases there is an important $m = 2$ component outside corotation which travels inwards to enhance the $m = 2$ growing there.

Strong interactions may temporarily enhance (or decrease) the bar amplitude. This depends on whether the bar leads or lags behind the companion at perigalacticum. If the bar leads it slows down while its amplitude increases, and the opposite occurs when the bar lags behind. This can be easily understood if one considers the exchange of angular momentum between the bar and the companion. Finally 3D simulations show that the interaction will cause a thickening of the galactic disk, particularly in its outer parts.

V. NGC 5194/5195

NGC 5194 (M51) has one of the most spectacular spiral structures observed. Deep exposures (e.g. Burkhead 1978) show a faint outer disk, ending abruptly on the western side and giving the galaxy a comma-like structure, as well as feathers or streamers, which, as simulations have shown, are characteristic of gravitational interactions (e.g. Toomre 1978). Tully (1974) obtained a detailed Hα velocity field with Fabry-Perot interferometry, and established that the photometric and kinematical major axes do not agree. Indeed it is very difficult to decide on values for the position and inclination angles of this galaxy (Garcia-Gomez *et al.* 1990). Kinematical studies (Tully 1974; Shane 1975; Goad *et al.* 1979; Rots *et al.* 1990a and b) give position angles around 170°. On the other hand photometric studies (Boroson 1981; Grosbol 1985) as well as spiral structure analyses (Considre and Athanassoula 1982 and 1988) give values around 30°. For the inclination Tully (1974) gives 20°, and all other studies between 30° and 40°. It is not straightforward to assess these values. The motions in the inner parts might be affected by an oval (Pierce 1986; Wright and McLean 1988) while those in the outer parts by the interaction, resulting in nonnegligible departures from circular motions which could influence the kinematical methods. On the other hand the outermost isophotes may well be non circular, as can indeed be argued from the outermost isophotes of some simulations (e.g. Fig. 1; see Athanassoula 1990 for a description of the simulations). As for the spiral structure analysis, it has been so far applied to too few galaxies (16 so far) for all its shortcomings to be clear. So to sum up, the orientation in space of this galaxy is not clear.

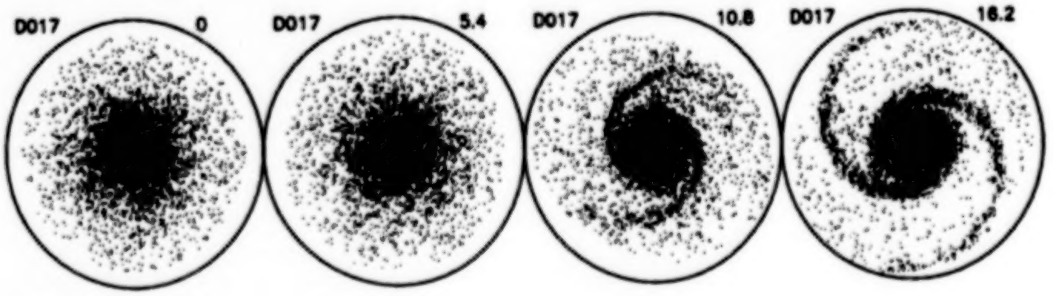

Fig. 1. Response of a disk to a strong external forcing

Rots *et al.* (1990a and b) observed this galaxy in HI using the B and D arrays of the VLA. Their channel maps show isocontours of the shape of the letter S or H, instead of the standard U shape due to differential rotation. They found a long extension in the form of a tail, starting at the SW of NGC 5194 and extending towards the south and then the east. Its total projected length is of the order of 90 kpc and its HI mass roughly $5 \times 10^8 M_\odot$. It does not connect onto one of the two bright arms but rather surrounds the bright disk. Such structures often develop in N-body simulations, and an example from a simulation by S. Engstrom, is given in Fig. 2. This is of course not a model of M51, only an example of a formation of such very long, semi-detached tail. It shows how the continuity of the very long tail to the inner spiral structure is lost with time because of the different motions of the inner and outer parts. The presence of such a tail argues that a longer time has elapsed since the pericenter of the NGC 5194/5195 pair than that proposed by TT and Toomre (1978).

The velocity field of M51 is shown in Fig. 3 (see also Fig. 7 in Rots *et al.* 1990b).

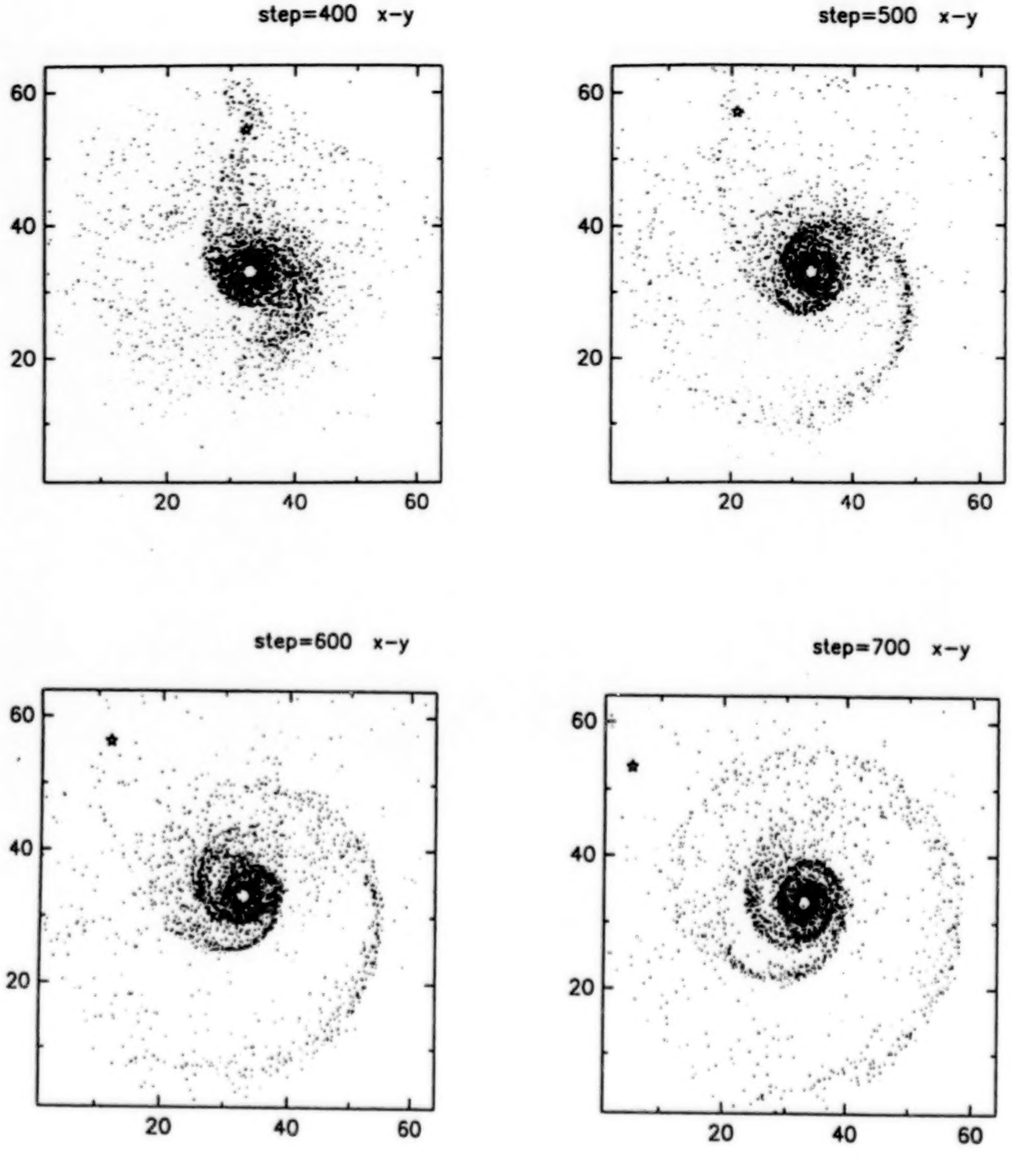

Figure 2. Formation and evolution of a long thin tail, reminiscent of the one observed in M51

In the southern part of the tail we observe velocities between 460 and 360 km/sec, i.e. values similar to those observed in the northern, not the southern part of the disk. A very simple, kinematical, explanation for this can be seen in Fig. 4. The upper left panel shows a greyscale plot of the velocity field of a Toomre disk to which is appended a tail partaking to the same motion. The disk and tail are on the same plane, with 0° position angle (PA) and 20° inclination. However numerical simulations show that the tail of interacting systems is often on a different plane from that of the disk (see e.g. Fig. 14 of TT). If we assume that the plane of the tail has an inclination of $-20°$, then the velocity field changes, as is shown in the upper right panel, and we get in the southern part of the tail similar velocities to the northern part of the disk, as in M51. Still in this simple example the PA of the maximum velocity in the tail is the same in the tail as in the disc, while in M51 the PA of the maximum velocity is roughly at $-20°$ in the disk and $-50°$ in the tail. A shift of the position angle can be found either by a twist of the line of nodes, or, as shown in the lower two panels of Fig. 3, by adding an inwards or outwards radial velocity component.

As could be expected the modelling of such an interesting object has proven to be both appealing and popular (e.g. TT, Appleton *et al.* 1986, Hernquist 1990, Howard and Byrd this volume). Hernquist made a self-consistent replay of the model favoured by TT. He showed that, in good agreement with what has been discussed above, a nice two arm spiral structure develops in the inner parts of the self-consistent disk. The outer structures bear some resemblance to those of the test particle simulation, but at an early time, when the companion is still not on the right projected position. Even when the companion reaches the right position the long HI tail has not developed yet.

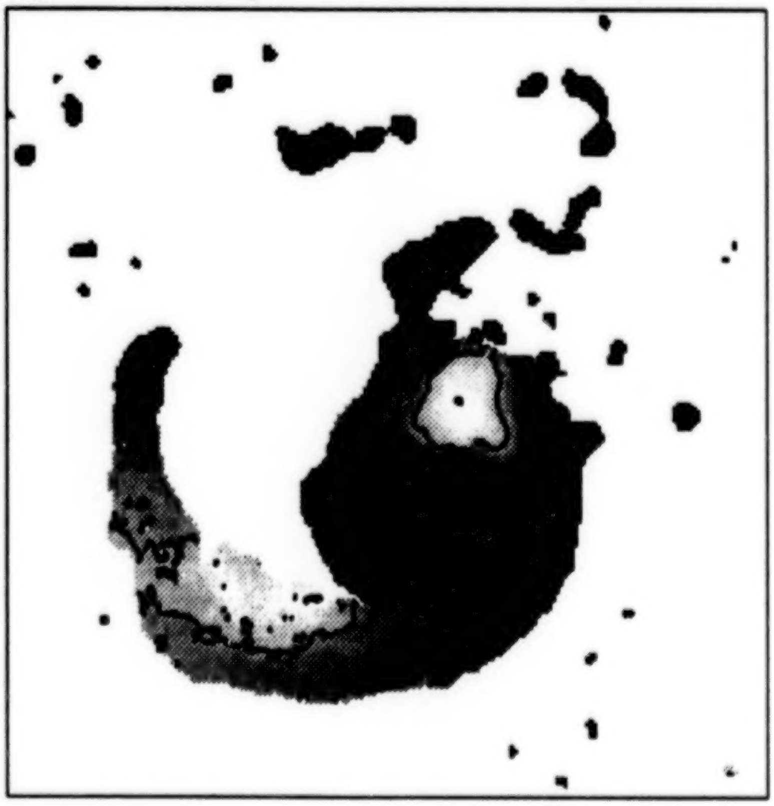

Figure 3. Velocity field of M51

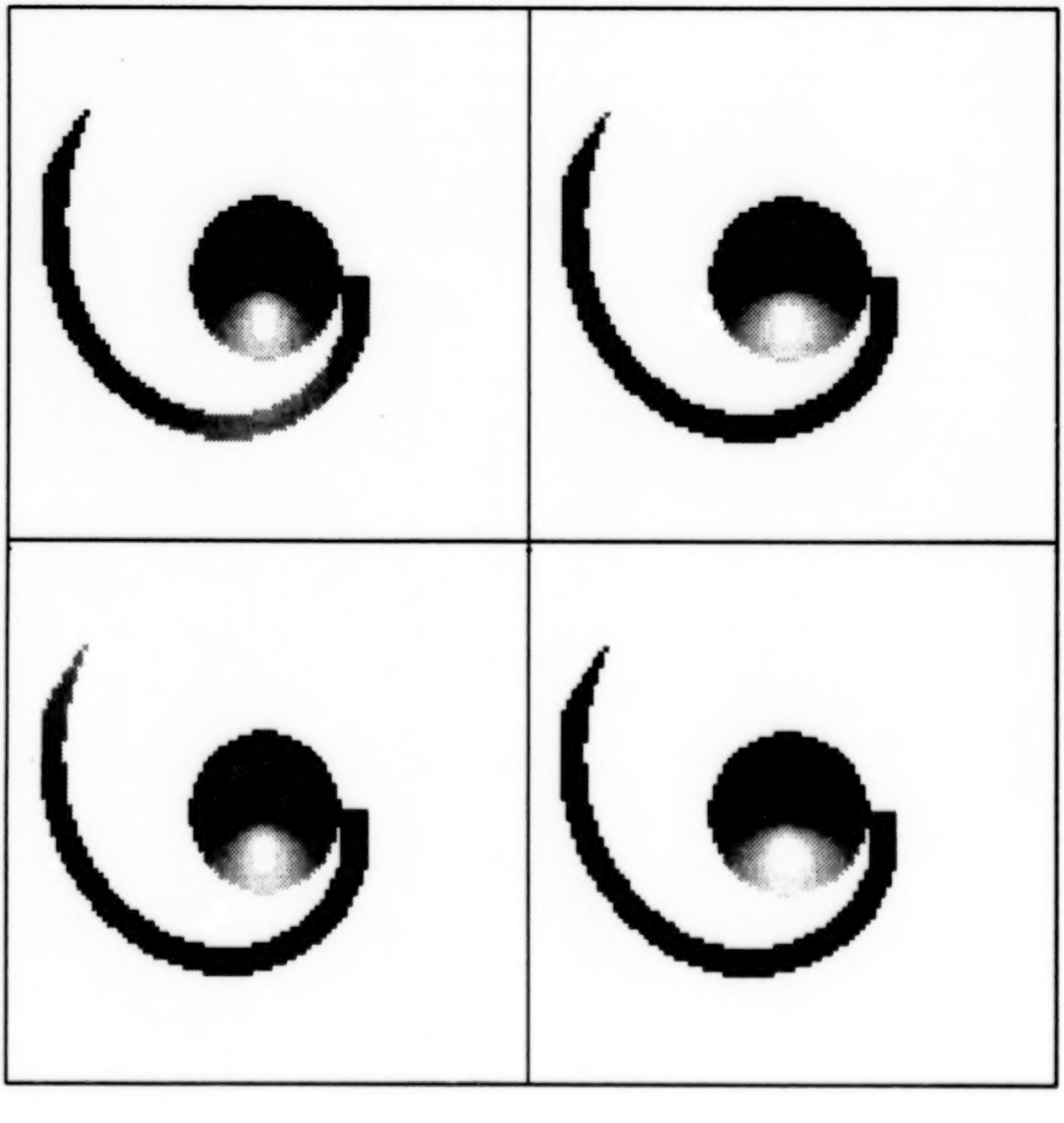

Figure 4. Simple kinematical model of the velocity field of a galaxy with a tail

Given the CPU time necessary for each simulation, it is not easy to make a full parameter survey, as done by TT. Yet Hernquist made, for parabolic encounters, a parameter search including several values of the orbital inclination, argument of the pericenter and impulse strength, thus giving precious insight to their effect. To get a better representation of the inner spiral and of the outer northern arm, one may need to try different models of the unperturbed M51 disk. If this had already a spiral before the encounter, a possibility that should not be neglected, then the problem becomes more complicated. Indeed the preexisting spiral would then interact with the forcing and the result would depend on their relative pattern speeds and phases (Athanassoula 1990). One could then expect secondary spiral features, breaks in the arms and/or evidence of more than one pattern speed. Whether this eventuality is the case or not, the interaction of M51 and NGC 5195 promises the modeler still many exciting moments.

ACKNOWLEDGEMENTS

I would like to thank J. Sellwood whose N-body program I used for the simulations shown in Fig. 1, S. Engstrom for producing the simulation shown in Fig. 2 and A. Bosma for Fig. 3 and for many useful discussions.

REFERENCES

Aguilar, L.A. and White, S.D.M.: 1985, Ap. J. 295, 374.
Albada, T.S., van : 1988, in *Large Scale Structures of the Universe*, ed. J. Audouze, M.C. Pelletan and A. Szalay (Reidel), p. 401.
Albada, T.S. van and van Gorkom, J.H.: 1977, Astr. Ap. 54, 121.
Appleton, P.N., Foster, P.A. and Davies, R.D.: 1986, M.N.R.A.S. 221, 393.
Athanassoula, E.: 1978, Astr. Ap. 69, 395.
Athanassoula, E.: 1990, in *Chemical and Dynamical Evolution of Galaxies*, eds.J. Franco and F. Matteuci (World Scientific Publ.), in press.
Barnes, J.: 1988, Ap. J. 331, 699.
Barnes, J.: 1990, in *Dynamics and Interactions of Galaxies*, ed. R. Wielen (Springer), in press.
Bontekoe, T. R. and van Albada, T.S.: 1987, M.N.R.A.S. 224, 349.
Boroson, T.: 1981, Ap. J. Suppl. 46, 177.
Burkhead, M.S.: 1978, Ap. J. Suppl. 38, 147.
Byrd, G.G., Saarinen, S. and Valtonen, M.J.: 1986, M.N.R.A.S. 220, 619.
Chandrasekhar, S.: 1943, Ap. J. 97, 251.
Clutton-Brock, M.: 1972, Astr. Sp. Sc. 17, 292.
Considre, S. and Athanassoula, E.: 1982, Astr. Ap. 111, 28.
Considre, S. and Athanassoula, E.: 1988, Astr. Ap. Suppl. 76, 36.5
Elmegreen, D.M. and Elmegreen, B.G.: 1982, M.N.R.A.S. 201, 1021.
Garcia-Gomez, C., Athanassoula, E. and Bosma, A.: 1990, in preparation.
Gerhard, O.E.: 1981, M.N.R.A.S. 197, 179.
Gerin, M.Y., Combes, F. and Athanassoula, E.: 1990, Astr. Ap. in press.
Goad, J.W., de Veny, J.B. and Goad, L.E.: 1979, Ap. J. Suppl. 39, 439.
Goldreich, P. and Tremaine, S.: 1979, Ap. J. 233, 857.

Grosbol, P.J.: 1985, Astron. Ap. Suppl. 60, 261.

Hernquist, L.: 1990, in *Dynamics and Interactions of Galaxies*, ed. R. Wielen, (Springer) in press.

Hernquist, L. and Weinberg, M.D.: 1989, M.N.R.A.S. 238, 407.

Kalnajs, A.J.: 1975, in *La Dynamique des Galaxies Spirales*, ed. L. Weliachew, (CNRS pub.) p. 103.

Kormendy, J. and Norman, C.A.: 1979, Ap. J. 233, 539.

Latanzio, J.C. and Henriksen, R.N.: 1988, M.N.R.A.S. 232, 565.

Lin, D.N.C. and Tremaine, S.: 1983, Ap. J. 264, 364.

Mc Glynn, T.A.: 1990, Ap. J. 348, 515.

Miller, R.H.: 1986, Astr. Ap. 167, 41.

Miller, R.H. and Smith, B.F.: 1980, Ap. J. 235, 421.

Noguchi, M.: 1987, M.N.R.A.S. 228, 635.

Noguchi, M. and Ishibashi, S.: 1986, M.N.R.A.S. 219, 305.

Olson, K.M. and Kwan, J.: 1990, Ap. J. 349, 480.

Palmer, P.L. and Papaloizou, J.: 1982, M.N.R.A.S. 199, 869.

Pierce, M.J.: 1986, A. J. 92, 285.

Quinn, P.J. and Goodman, J.: 1986, Ap. J. 309, 472.

Rots, A.H., Bosma, A., van der Hulst, J.M., Athanassoula, E. and Crane, P.C.: 1990a, in *Dynamics and Interactions of Galaxies*, ed. R. Wielen, (Springer) in press.

Rots, A.H., Bosma, A., van der Hulst, J.M., Athanassoula, E. and Crane, P.C.: 1990b, submitted to A.J.

Shane, W.W.: 1975, in *La Dynamique des Galaxies Spirales*, ed. L. Weliachew (CNRS publ.) p. 217.

Sundelius, B., Thomasson, M., Valtonen, M.J. and Byrd, G.G.: 1987, Astr. Ap. 174, 67.

Thomasson, M., Donner, K.J., Sundelius, B., Byrd, G.G., Huang, T.-Y. and Valtonen, M.J.: 1989, Astr. Ap. 211, 25.

Toomre, A.: 1969, Ap. J. 158, 899.

Toomre, A.: 1977, in *The Evolution of Galaxies and Stellar Populations*, eds. B.M. Tinsley and E.B. Larsen (Yale Univ. Obs.) p. 401.

Toomre, A.: 1978, in *The Large Scale Structure of the Universe*, eds. M.S. Longair and J. Einasto (Reidel) p. 109.

Toomre, A.: 1981 in *The Structure and Evolution of Normal Galaxies*, eds. S.M. Fall and D. Lynden-Bell (Cambridge University Press), p. 111.

Toomre, A. and Toomre, J.: 1972, Ap. J. 178, 623 (TT).

Tremaine, S.: 1981, in *The Structure and Evolution of Normal Galaxies*, eds. S.M. Fall and D. Lynden-Bell (Cambridge University Press), p. 67.

Tremaine, S.D., Ostriker, J.P. and Spitzer, L.: 1975, Ap. J. 196, 407.

Tully, B.: 1974, Ap. J. Suppl. 27, 415; 27, 437; 27, 449.

Valtaoja, L.: 1990, Astr. Ap. 228, 37.

Valtonen, M.J., Valtaoja, L., Sundelius, B., Donner, K.J., Byrd, G.: 1990, Cel. Mech. Dyn. Astr. in press.

Weinberg, M.D.: 1989, M.N.R.A.S., 239, 549.

White, S.D.D.: 1982, in *Morphology and Dynamics of Galaxies*, eds. L. Martinet and M.

Mayor, (Geneva Observatory), p. 289.

White, S.D.M.: 1978, M.N.R.A.S. 184, 185.

White, S.D.M.: 1983a, in *Internal Kinematics and Dynamics of Galaxies*, ed. E. Athanassoula, (Reidel), p. 337.

White, S.D.M.: 1983b, Ap. J. 274, 53.

Wright, G.S. and McLean, I.S.: 1988, Sky and Telescope 76, 346.

Zaritsky, D. and White, S.D.M.: 1988, M.N.R.A.S. 235, 289.

DISCUSSION

Simkin: M51 looks very similar to MKN 348 which J. Van Gorkom published in 1986. Will you coordinate a compilation of M51-type systems so we can get an observed time sequence of one type of encounter?

Athanassoula: It would indeed be interesting to have a compilation of M51-type systems (see Vorontsov-Velyaminov, 1977, Astron. Astrophys. Suppl. **28**, 1). However I do not think it easy to establish a time sequence.

Buta: An interesting example of an interacting barrel spiral is NGC 5850, which has a ring around the bar and corotation probably halfway out in the disk. Asymmetries in the HI disk outer spiral structure suggest an interaction with a nearby elliptical. The bar position angle in projection points toward the companion very closely. Could an interaction like this shift the Lagrangian points away from the bar minor axis line towards the companion?

Anthanassoula: I am not very familiar with this galaxy. In general a companion (by changing the pattern speed of the bar) may change not only the position of the Lagrangian points, but also their number.

Fridman: Can you formulate necessary and sufficient condition of leading spiral arms generation?

Athanassoula: All I can tell you is what has been found so far to generate leading arms in the framework of gravitational theory: a retrograde forcing can give rise to a one armed leading spiral. Leading modes have also been found in some cold disks. I believe you have formulated such a "necessary and sufficient" condition in the framework of your shallow water theory.

Galletta: It is possible to extend to the cases of gas counterrotation the result that retrograde collisions do not change much the galaxy structure?

Athanassoula: I talked about retrograde encounters, i.e. cases where the orbit of the companion around the target galaxy is in the sense opposite to that of the stars in this galaxy. In this case the results of the interaction are indeed less spectacular. On the other hand counterrotating gas may be the result of a merger of two galaxies with rotations (spins) in the opposite sense.

A STATISTICAL STUDY OF MERGING GALAXIES-THEORY AND OBSERVATIONS

Tapan K. Chatterjee
Facultad de Ciencias, Fisico-Matematicas
Universidad A. Puebla (A.P. 1152), Puebla, Mexico

ABSTRACT. A study of the expected frequency of merging galaxies is conducted, using the impulsive approximation. Results indicate that if we consider mergers involving galaxy pairs without halos in a single crossing time or orbital period, the expected frequency of mergers is two orders of magnitude below the observed value for the present epoch. If we consider mergers invovling several orbital periods or crossing times, the expected frequency goes up by an order of magnitude. Preliminary calculation indicate that if we consider galaxy mergers between pairs with massive halos, the merger is very much hastened.

INTRODUCTION

Observations indicate that the frequency of galaxy mergers (order of magnitude accuracy only) in the present epoch is ~0.3% (Toomre, 1977; Tremaine, 1980). An extrapolation to the past yields a frequency ~5%. Loosely bound pairs of galaxies, that had separated to great distancs in the general cosmic expansion, and have lately fallen together again (for the first or feweth time) in comet-like plunging ellipses, seem to be the most lucrative candidates for mergers. To tackle this problem it is necessary to determine the frequency of merging galaxies on the basis of the collision theory and compare the values so obtained with the observational ones.

In this work we have studied sphere-sphere and disk-sphere collisions. We have assumed that a galaxy and its nearest neighbor are likely to form a bound pair, for frequency determinations. We have not embedded the galaxies in massive halos, except for one case. A detailed paper on merger of galaxies with massive halos will be published soon. The determination of general results and the expected frequency of merging galaxies is greatly facilitated by using the impulsive approximation, as it is a suitable way of studying many collisions with varying parameters. As far as the order-of-magnitude results are concerned, those obtained by this method tally quite well with the results of N-body simulations (Toomre, 1977; Dekel et al., 1980; Alladin and Narasimhan, 1982; and Aguilar and White, 1985). Hence the order of magnitude of the frequency that we obtain by this method will be correct. At any rate, the crucial questions pertain to the order of magnitude of the frequency of merging galaxies.

THEORY

We model the spherical galaxy as a polytrope of index $n = 4$, and the disk galaxy as an exponential model disk with density distribution, $\sigma(r) = \sigma_c e^{-4r/R_D}$, where $\sigma_c = M_D/(2\pi R_D^2 b)$ is the central density, M_D and R_D being the mass and radius of the disk and b is a constant pertaining to its density distribution. This disk is thickened by a method indicated by Rohlfs and Kreitschmann (1981). A polytropic bulge of index $n = 4$ is superposed on this disk. The model is discussed in detail in Chatterjee, 1989.

The theory for studying sphere-sphere and disk sphere collisions for mergers taking place in a single orbital period is basically the same as in Chatterjee, 1987 (hereafter referred to as Paper I), except that in the case of disk-sphere collisions the appropriate function $\chi = \chi_{DS}$ is used, which defines the mutual potential energy function for the disk-sphere system (cf. Ballabh, 1975). M_1 and M_2 are the masses and $R_1 = R_2 = R$ their common radii. Mergers of disk-sphere systems are dealt with in detail in Chatterjee 1990a.

To study mergers taking place in several orbital periods we use the same method as outlined in Chatterjee, 1990b. The method is basically a modification of the method used by Alladin, 1965. In the case of disk-sphere collisions the appropriate function $\chi = \chi_{DS}$ is used. If r and θ denote the polar coordinates of the perturber galaxy (Galaxy 1) with respect to the test galaxy (Galaxy 2), in the orbital plane characterizing the relative motion, and μ, ℓ and E, the reduced mass, the angular momentum and the energy of orbital motion, respectively, then the Lagrangian equations for the problem give,

$$dt = dr/[2\mu^{-1}\{E - W(r) - r^2/(2\mu r^2)\}]^{1/2}$$

and $$d\theta = (\ell dr)/[2\mu^{-1}\{E - W(r) - \ell^2/(2\mu r^2)\}]^{1/2} \; (\mu r^2)$$

These equations can be used to determine the orbit and the variation of time along the orbit. The relative orbit is studied numerically by using these equations. At small intervals of r and θ the tidal effects, and the corresponding change in velocity of the stars , is studied by the same method as in Paper I. The change in internal energies of the two galaxies ΔU_1 and ΔU_2 at any time t can be obtained from,

$$V(t) = (dr/dt) = [2\mu^{-1}\{E_i - W(t) - \Delta U_1(t) - \Delta U_2(t)\}]^{1/2}$$

where $E_i = (1/2)\mu V_i{}^2 - (GM_1M_2/R_2)\,\chi_{si}$

and

$$W(t) = W(r) = W(s) = -(GM_1M_2/R_2)\,\chi_s$$

V_i and E_i are the initial relative velocity and orbital energy of the two galaxies, $W(t) = W(s)$ is the mutual potential energy of the two galaxies at the instantaneous separation $s = r/R$, χ_{s_i} and χ_s are the values of $\chi = \chi_{SS}$ or χ_{DS} (depending on whether it is a sphere-sphere or disk-sphere collision that is under study) (Alladin uses $\psi = s\chi$) at the initial separation $s_i = r_i/R$ and $s = r/R$, respectively.

We study many collisions between galaxies of equal dimensions. In the case of disk-sphere collisions as almost all of the mass of the spherical galaxy is concentrated within 1/3 of its radius, the effective radius of the spherical galaxy is 1/3 that of the disk. In the case of mergers taking place in a single crossing period, each collision is characterized by a value of the distance of closest approach, p, and initial velocity V_i, as discussed in Paper I. In the case of mergers taking place in several orbital periods, the initial separation is taken to play the part of p in frequency determination. In each case the change in velocity due to dynamical friction is calculated for small intervals as the galaxies advance in their relative orbit, and the instantaneous relative velocity so determined is used to continue the integrations of the equations of motion of the two galaxies. Merger takes place when the instantaneous relative velocity, V_i, of the two galaxies equals the velocity of escape between the pair characterized at the instantaneous separation, V_E, as discussed in Paper I. In the case of mergers taking place in a single crossing time the relative velocity at closest approach, V_p is used for frequency determinations, while V_i is taken to play the part of V_p for mergers in several orbital periods.

NUMERICAL RESULTS AND DISCUSSION

General Resuults

The computations of many collisions have been carried out, each collision being characterized by a value of V_p and p (measured in units of the radius of either galaxy) and scaled for different mass ratios of the two galaxies.

For sphere-sphere systems in collision, we find that for central impacts, merger takes place in a single crossing time provided $p \lesssim R_{1/4}$, the radius containing 1/4 of the mass of the victim galaxy, and $V_p \lesssim 1.2\ V_E$. The merger is affected in a single crossing time up to $p \lesssim R_{3/4}$, the radius containing 3/4 of the mass of the victim galaxy; while the merger is effected in more than one orbital period up to $p \sim R$. The merger is effected in $\lesssim 2$ orbital periods if $R_{3/4} \lesssim p \lesssim 4R_h$ ($4R_h = 1/2$ of the radius for polytropic $n = 4$ model), R_h being the galactic half-mass radius; and in several orbital periods (~5) for $4R_h \lesssim p \lesssim R$. In general beyond $p \sim 4R_h$ the dynamical friction process becomes quite ineffective and the merger is effected extremely slowly. The relative mass of the perturber with respect to the victim galaxy does not seem to affect the merger times markedly, unless the former has less than about 1/5 the mass of the latter. For $p \lesssim 4R_h$, the parabolic perturber orbit is circularized in the first orbital period, and the subsequent orbit effects the merger; while if p lies between $4R_h$ and R, the circularization is achieved in few orbital periods. Beyond $p \sim R$, mergers do not seem to take place as the dynamical friction lacks the ability of circularizing the parabolic perturber orbit and the same recede to an enormous distance from which it does not return in significant orbital timescales.

In the case of disk-sphere collisions, dynamical friction plays a very insignificant role, compared to sphere-sphere collisions, due to the small thickness of the victim disk and mergers do not seem to be possible for hyperbolic velocities, which implies $V \lesssim V_E$. The merger is effected in a single crossing time only if the impact is central or very nearly so, and the range of values of p depends strongly on the relative mass of the bulge with respect to the disk. For these reasons, for the purpose of frequency determinations, it seems to be more convenient to determine the range of values of p for which merger is possible in single and several orbital periods together (for a more detailed treatment see Chatterjee, 1990b). We find that in this case mergers are possible up to $p \sim R$. Only if $p \gtrsim R_h$ (for the victim disk), the merger takes place in a much longer time than otherwise. Beyond $p \sim R$ the perturber does not seem to return in significant orbital timescales.

We have studied only one collision with galaxies having massive halos. So we cannot comment on the frequency of merging galaxies with massive halos, but only mention the results of this simulation, as the parameters for this collision have been carefully chosen. The model used for the halo has the asymptotic dependence $M(r) \sim r$, where r is the distance measured from the center of the galaxy, and is discussed in detail by Allen and Martos (1986). This model is excellent for the study of many collisions as an analytical treatment of the halo is elucidated. The bulge component is modeled as a polytrope of index $n = 4$. A merger of two identical spherical galaxies is studied. The halo contains about 10 times the mass of the bulge component and 10 its radius, R_b. The initial separation of the two galaxies is taken to be $p = 2R_b$ and the initial relative velocity is taken to be $v_i = 2V_E$. Merger takes place in few orbital periods ($\lesssim 3$). The exact number of orbital periods depends upon the value of the separation of the centers of the two galaxies for which merger is defined to be complete. For frequency determinations, whether or not the merger takes place in a significant orbital timescale is the crucial fact.

Brief Comparison with Previous Work

The results of van Albada and van Gorkom (1977), White (1978), Roos and Norman (1979), are summed up in Figure 1 of Aarseth and Fall (1980). Translated in terms of our parameters, this figure is indicative of a high frequency of mergers in the region corresonding to $p \lesssim 0.8 \times 2R_h = 0.216R$, for polytrope $n = 4$ model, and $V_E \lesssim V_p \lesssim 1.2V_E$. Villumsen (1982) finds that for the distance of closest approach $p = R_i \lesssim 10$ units, corresponding to 0.22 R (as the tidal radius for his model is 45 units), merger is quite frequent; while for $p = R_i \approx 10$ units, merger occurs only for low relative velocities. Alladin and Parthasaraty (1978) indicate that stellar systems, modeled as polytropes of index $n = 4$, in mutual circular orbit, merge in about 15% of an orbital period for $p \lesssim 0.2R$; while for $p \gtrsim 0.2R$, merger takes considerably more time. All these results compare well with our results that merger in a single crossing time ceases, for sphere-sphere pairs, for $p \lesssim R_{3/4} \lesssim 0.2R$ (for polytrope $n = 4$). The results are not very much model dependent.

In the region $R_{3/4} \lesssim p \lesssim R_h$, merger is achieved in a time ~ 2 orbital periods, while it is achieved in several orbital periods in the region $4R_h \lesssim p \lesssim R$. These results compare quite well with the results of Borne (1984). (For more details see Chatterjee, 1990b.) It is interesting to note that Borne includes a relaxation time in his scheme, which we do not, but the resonating stars which hasten the orbital decay of the galaxies in his simulations play a comparatively insignificant part in our scheme.

Frequency Determinations

In dense regions a galaxy and its nearest neighbor can be visualized to form a loosely bound pair (Toomre, 1977; Tremaine, 1980). As mentioned before, the general opinion is that collisions between initially loosely bound pairs lead to the majority of mergers. In dense regions the average distance between galaxies is ~ $10R_a$, where R_a is the average radius of a galaxy (Mitton, 1977; Ogorodnikov, 1965). So though theoretically the parameter p can vary from 0 to ∞, its mean value in regions where mergers are frequency, can be taken as $p_\infty \lesssim 10$ (in units of the radius of a galaxy). We take the total range of variation of V_p to be from 0 to $4V_E$, as collisions with velocity $V_p \gtrsim 4V_E$ seldom occur

(i) Mergers of Spherical Systems in a Single Crossing Time. Central Impacts: $p \lesssim R_{1/4}$, $V_p \lesssim 1.2\ V_E$. The probability in terms of the energy of the collision is given by $P_E = (1.2\ V_E)^3/(4V_E)^3 = 0.027$; and the probability in terms of the impact parameter is given by $P_p = (R_{1/4}p_\infty)^2 = 4.56 \times 10^{-5}$; which gives the probability of mergers in this case as $P_C = P_E \times P_p = 1.2 \times 10^{-6}$. Which gives the expected frequency of such mergers as 1.2×10^{-4} %.

Off Center Impacts: $R_{1/4} \lesssim p \lesssim R_{3/4}$, leading to mergers only if $V_p \lesssim V_E$. The corresponding probabilities in this case are given by $P_E = [V_E/(4V_E)]^3 = 0.015625$, $P_p = (R^2{}_{3/4} - (R^2{}_{1/4})/p^2 = 3.645 \times 10^{-4}$, giving $P_{oc} = P_E \times P_p = 5.7 \times 10^{-6}$. This gives an expected frequency of 5.7×10^{-4} %. Since these are mutually exclusive events, the probability of mergers of spherical systems in an orbital period is, $P = P_c + P_{oc} = 6.9 \times 10^{-6}$, which leads to an expected frequency of such mergers as 6.9×10^{-4} %.

(ii) Mergers of Spherical Systems in Several Orbital Periods. $R_{3/4} \lesssim p \lesssim R$, $V \lesssim V_E$. In this case the respective probabilities are given by $P_E = [V_E/(4V_E]^3 = 0.015625$, $P_p =$

$(R^2{}_{3/4} - R^2{}_{1/4})/p^2 = 9.6 \times 10^{-3}$, which gives $P = P_E \times P_p = 1.5 \times 10^{-4}$; which gives the expected frequency of such mergers as 1.5×10^{-2} %.

Hence the expected frequency of mergers of spherical systems is given by 1.57×10^{-2} %.

(iii) Mergers of Disk-Sphere Systems.

$p \lesssim R$, $V_p \lesssim V_E$. In this case the respective probabilities are given by $P_E\ [V_E/(4V_E)]^3 = 0.015625$, $P_p = (R/p_\infty)^2 = 0.01$, which gives the merger probability as $P = P_E \times P_p = 1.56 \times 10^{-4}$, which gives the expected frequency of such mergers as 1.56×10^{-2} % ~ 10^{-2} %.

CONCLUSIONS

In general we conclude that the expected frequency of merging galaxies (not considering the effect of massive halos) is ~ 0.01%, which is an order of magnitude below the observational value ~0.1 %. The expected frequency of merging galaxies increases by an order of magnitude when we take into account mergers occurring in several orbital periods, as compared to those occurring in a single crossing time. More than 90% of the mergers take place in several orbital periods, and there is an indication that the majority of them take place in a time ~2 to 3 orbital periods. For mergers in a single crossing time, more than 80% of them are due to off-center impacts.

Spherical and disk-sphere systems in merger seem to be equally frequent.

If our single simulation with galaxies embedded in massive halos is at all typical (which in our view it is), then the frequency of galaxy mergers with massive halos will be at least an order of magnitude higher than in the absence of halos (approaching the observational value for the present epoch). We are studying more collisions of type to throw light on this aspect.

ACKNOWLEDGMENTS

It is a matter of great pleasure to thank all those with whom I had helpful discussions, especially Prof. A. Poveda, whose suggestions about the halo helped a lot in improving the presentation. I would also particularly like to thank Cristina Allen for discussions and numerical data regarding the halo model and all those who very kindly helped me with computations.

REFERENCES

Aarseth, S. J., and Fall, S. M. 1980, Astrophys. J., **236**, 43.

Aguilar, L. A., and White, S.D.M. 1985, Astrophys. J., **295**, 374.

Alladin, S. M. 1965, Astrophys. J., **141**, 768.

Alladin, S. M., and Narashimhan, K.S.V.S. 1980, Phys. Reports, **92**, 339.

Alladin, S. M., and Parthasarathy, M. 1978, Monthly Notices Roy. Astron. Soc., **184**, 871. (Corrigendum 1979, Monthly Notices Roy. Astron. Soc., **188**, 303.)

Allen, C., and Martos, M. A. 1986, Rev. Mex. Astron. Astrof., **13**, 137.

Ballabh, G. M. 1975, Astrophys. Space Science, **38**, 407.

Borne, K. D. 1984, Astrophys. J., **287**, 503.

Chatterjee, T. K. 1987, Astrophys. Space Science **137**, 267.

Chatterjee, T. K. 1989, Astrophys. Space Science (in press, 1990?).

Chatterjee, T. K. 1990a, *Astrophys. Space Science*, in press.

Chatterjee, T. K. 1990b, *Astrophys. Space Science*, submitted.

Dekel, A., Lecar, M., and Shaham, J. 1980, *Astrophys. J*, 241, 946.

Mitton, S. (ed.) 1977, "The Cambridge Encyclopedia of Astronomy," Jonathan Cape Ltd., London, p. 345.

Ogorodnikov, K. F. 1965, "Dynamics of Stellar Systems," Per., London, p. 100.

Rohlfs, K., and Kreitschmann, J. 1981, *Astrophys. Space Science*, 79, 289.

Roos, N., and Norman, C. A. 1979, *Astron. Astrophys.*, 76, 75.

Toomre, A. 1977, in B. M. Tinsley and R. B. Larson (eds.), "The Evolution of Galaxies and Stellar Populations," Yale Univ. Obs., p. 401.

Tremaine, S. D. 1980, in S. M. Fall and D. Lynden Bell (eds.), "The Structure and Evolution of Normal Galaxies," Univ. of Cambridge, p. 67.

Van Albada, T. S., and van Gorkom, J. H. 1977, Astron. Astrophys., **54**, 121.

Villumsen, J. V., 1982, Monthly Notices Roy. Astron. Soc., **199**, 493.

White, S.D.M. 1978, Monthly Notices Roy. Astron. Soc., **184**, 185.

DISCUSSION

Mamon: (answer to Burbidge's question to Chatterjee) The halo mass-to-light ratio is the one parameter entering our model. The optimal value for fitting the computed morphology-density relation to Postman and Geller's (1984) observed one is $\left(\frac{M}{L}\right) = 40\text{-}45\ h$. This value is large in comparison with the visible parts of galaxies, but small relative to the values found in large groups. Now, our results are very sensitive to this parameter. Varying (M/L) by a factor of two produces either two few ellipticals or too many.

Roos: (comment) I think that if you take into account the clustering of galaxies as described by the two-point correlation function and combine it with the mean relative velocity of pairs you find a present merger rate consistent with observations. Regarding the question posed by G. Burgidge about dark halos: The 2-point correlation function has been evaluated up to separations as small as ~10 kpc. You can make an estimate of the merger rate based on the number of neighbours and their separation and assuming that halo sizes are, let us say, 20 kpc. This already yields an appreciable merger rate.

Charlton: (comment on Chatterjee's talk) Roos has remarked that collision calculations by Bahcall and Tremaine predict a merger rate that is in accordance with the number of systems that observationally appear to have undergone mergers if the correlations between pairs are taken into account. He further stated that this meant that there was no need for halos larger than ~20 kpc to explain the observed merger rate.

One thing is being overlooked in this discussion so I will reiterate something I described in my contribution. The observed distribution of projected separations of pairs of galaxies in low density regions is flat down to separations below 20 kpc, and we already know that in many cases the rotation curves of galaxies are flat to beyond 50 kpc. At separations of <50 kpc the overlap between two 50 kpc halos is extreme and the orbital period short, thus mergers would take place extremely rapidly compared to a Hubble time. The number of pairs at small projected separations would thus be very small compared to larger projected separations (not about as observed) unless halos were much larger. With larger halos, pairs at larger separations would also approach one another due to the overlapping halos of the members and could fill in the "gap" left at small r_p (due to rapid mergers of smaller r_p systems).

PROBING THE TIDES IN INTERACTING GALAXY PAIRS

Kirk D. Borne
Space Telescope Science Institute
Baltimore, Maryland

ABSTRACT

Detailed spectroscopic and imaging observations of colliding elliptical galaxies have revealed unmistakable diagnostic signatures of the tidal interactions. It is possible to compare both the distorted luminosity distributions and the disturbed internal rotation profiles with numerical simulations in order to model the strength of the tidal gravitational field acting within a given pair of galaxies. Using the best-fit numerical model, one can then measure directly the mass of a specific interacting binary system. This technique applies to individual pairs and therefore complements the classical methods of measuring the masses of galaxy pairs in well-defined statistical samples. The "personalized" modeling of galaxy pairs also permits the derivation of each binary's orbit, spatial orientation, and interaction timescale. Similarly, one can probe the tides in less-detailed observations of disturbed galaxies in order to estimate some of the physical parameters for larger samples of interacting galaxy pairs. These parameters are useful inputs to the more universal problems of (1) the galaxy merger rate, (2) the strength and duration of the driving forces behind tidally-stimulated phenomena (e.g., starbursts and maybe QSOs), and (3) the identification of long-lived signatures of interaction/merger events.

1. INTRODUCTION

We have used the observed tidal disturbances in interacting galaxies to deduce various properties of the galaxies and of their relative orbits. The probes that we use to study these properties are the morphological and kinematic disturbances seen in the colliding galaxies. From these analyses, which employ a simple numerical simulation algorithm (Borne 1988*a*), we have been able to derive, for several interacting pairs, the galaxy masses, the internal properties of the galaxies (e.g., structure and rotation), the relative collision trajectory, the strength of the tidal encounter, and an age (or timescale) for the interaction (see Borne and Hoessel 1988; Borne 1988*b*; Borne, Balcells, and Hoessel 1988; and Balcells, Borne, and Hoessel 1989*a*,*b*). The most detailed analyses have been carried out for several pairs of interacting ellipticals identified in the Karachentsev (1972) catalog of isolated pairs; some of the results derived from "probing the tides" in these systems are described below (§4). In addition, we describe the results of some simple studies of other interacting galaxies (§§2-3), as well some preliminary results from a detailed study of the putative merger remnant NGC 7252 (§5; Borne and Richstone 1990). In every case but one we assume that gravity alone produces the observed tidal phenomena; the exception is in our simulations of the 3C 278 radio jets seen in NGC 4782 (§4[*c*]).

2. THE DOUBLE-NUCLEUS cD GALAXY IN ABELL 2052

The brightest galaxy in the rich cluster Abell 2052 is a double-nucleus cD. The nuclei are separated by 7″, having a relative velocity of 50 km s^{-1} (see Figs. 4 and 8 in Hoessel, Borne, and Schneider 1985). Kriss, Malumuth, and Borne (1990) have measured the radial variations of mean stellar velocity and velocity dispersion along the major axis of the primary galaxy, specifically excluding the small secondary nucleus. Their velocity profiles show that the velocity dispersion in the cD initially increases with radius in both directions, and then falls: ranging from 230 km s^{-1} at $R = 0''$, up to 380 km s^{-1} at $|R| \approx 6''$, and down to <200 km s^{-1} at $|R| \geq 12''$. The rotation profile also shows non-systematic variations at $|R| \approx 4 - 10''$.

We have run numerical simulations of this apparent cannibalism event, wherein a large galaxy accretes a small companion. We expected the size and shape of the velocity dispersion peaks at $|R| \approx 6''$ to vary with the assumed mass of the companion, but the actual results were surprising. We found that, as a result of the expected *dynamic* heating effect (i.e., the stirring of the cD by the companion), a large-mass companion produces a nearly *flat* projected velocity dispersion profile in the cD. On the other hand, a low-mass companion does not have a significant *dynamic* effect on the dispersion profile, but it does have a pronounced *kinematic* effect in that the lower mass companion suffers more extensive stripping around its orbit, leading to significant superposition of its stripped starlight onto the starlight of the cD. This produces the desired stellar velocity dispersion peaks at the location of the stripped stars (roughly at the orbital radius of the companion). Obviously, the mass of the companion cannot be so low as to produce statistically insignificant superposition. Hence, we were able to put rough constraints on the mass and orbit of the companion. These results are supported by the detection of increased surface brightness on one side of the cD (T. Lauer, private communication) and by a stream of gas, detected in Hα, which wraps around the cD in such a way that one end of the stream coincides with the secondary nucleus (S. Baum, private communication).

Therefore, from the tidal effects seen in this cD galaxy, we conclude that the small secondary galaxy probably had intermediate to low mass (mass ratio ≈ 0.1), and that stripping has already removed much of its mass (as evidenced by the Hα stream, the rotation anomalies and velocity dispersion peaks in the cD, and the asymmetries in the cD surface brightness distribution).

3. A MULTIPLE-RING GALAXY IN ABELL 2199

Pence and Oegerle (1989) have discovered a peculiar double ring galaxy in the rich cluster Abell 2199. The galaxy shows two complete *non-concentric* rings, with radii of 4.5 and 7.8 kpc (H_0 = 100 km s^{-1}Mpc^{-1}), and possibly a third incomplete ring (i.e., an arc) with a radius of 15 kpc. This galaxy is in a dense cluster environment, having several nearby companions (in projection). Pence, Oegerle, and Borne (1990) describe models for the formation of these multiple rings through deeply-penetrating collisions of massive companions into target disk galaxies. We found that the number of rings and the relative ring diameters vary with the mass of the impinging satellite: a high-mass satellite (mass ratio ≈ 0.4) produces many complete rings, with a large spacing between the two outermost rings, while a lower mass satellite (mass ratio ≈ 0.1) produces fewer rings, most of which are incomplete (i.e., arcs), with a smaller relative spacing between the two outermost rings. Given the near completeness of the rings observed in the Abell 2199 multiple-ring galaxy and given their relatively close spacing, we conclude that if the rings are in fact collisionally-induced, then the mass of the ring-producing companion is somewhere between the two extremes mentioned (i.e., mass ratio $\approx 0.2 - 0.3$).

4. DISTORTED E-E PAIRS

We have been involved for several years in analyzing the physical properties of strongly interacting pairs of elliptical galaxies (Borne 1988*a*,*b*; Borne and Hoessel 1988; Borne, Balcells, and Hoessel 1988; and Balcells, Borne, and Hoessel 1989*a*,*b*). We have been able to use the tidal disturbances observed both in morphological data and in positional velocity data to constrain collision models for the interacting pairs. From these models we have derived masses, orbits, spatial orientations, and interaction timescales. Among the tidal features that we have matched with our simulations are: the asymmetric light distributions, the U-shaped rotation profiles (Borne and Hoessel 1988; Borne 1990), and the heated velocity dispersion profiles. Though it is not possible to completely disentangle the two effects, it is found that the morphological distortions help to constrain the relative orbit of the galaxies, while the kinematic disturbances constrain the age and strength of the collision. Taken together, all of the observed distortions correlate with the strength and the active lifetime of the tidal potential field.

It should be possible to apply the results of our simulations of specific pairs to determinations of the age and duration of interactions in a much larger sample of tidally-disturbed galaxies. For example, the smallest radius at which the symmetry of the galaxy is broken due to tides corresponds roughly to the radius at which the time for orbital mixing (i.e., a few orbital periods) equals the time since maximum tidal impulse. Such age-dating can be calibrated using the several pairs for which we have already derived specific collision parameters.

We describe very briefly below a few of the physical results that were derived from our best-fit simulations of the tidal distortions seen in three particular pairs of interacting ellipticals.

(a) NGC 1587/1588 = Karachentsev 99

The tidal distortions observed in the surface brightness distribution of the primary galaxy constrain [illegible] mass of the smaller secondary galaxy: [illegible] M/L were smaller for the secondary galaxy th[illegible] the primary galaxy (as suggested by the small velocity dispersion of the secondary; [illegible] and Hoessel 1988), then there would be almost no tidal distortion in the larger galaxy; if [illegible] were larger for the secondary, then the predicted tidal distortions in the primary would be [illegible] than those actually observed; but if M/L were the same for the two galaxies, then the [illegible]ted tidal distortions in the primary galaxy can be made to agree with those observed. [illegible] result, we found that the mass ratio = luminosity ratio = 1/3 (Borne 1988*b*).

In K99, [illegible] well as in general collisions between other hot stellar systems, the position angles of the tidally compressed and tidally-distended isophotes correlate with the direction of the galaxies' motions: particles that are tidally stripped from hot stellar systems tend to trail the galaxy (Borne and Hoessel 1988; Borne 1990). In addition, we find that the narrowness of the tidal distention is directly related to the coldness of the internal stellar velocity distribution. We see this in the thin tidal tails emanating from strongly-rotating galaxies. In those cases, however, the direction of the tail does not correlate as well with the galaxy's orbital motion.

(b) NGC 2672/2673 = Karachentsev 175

We found that the tidal tails associated with the small galaxy were very difficult to reproduce (Balcells, Borne, and Hoessel 1989*a*,*b*), until we realized that the observed directions of the tails (extending to the north and to the east) required that the smaller galaxy be strongly rotating, even though we had no data either to support or to refute this claim. It was also found that the two orthogonal tails required the small galaxy to have passed partially through the core of the primary galaxy, in a reverse-tide regime, where $M(r)$ grows faster than r^2 (i.e., density falls more slowly than $1/r$). Tidal distortions can therefore probe the internal kinematics and structure of colliding galaxies, leading to testable predictions about these physical parameters.

(c) NGC 4782/4783 = 3C 278

The large central stellar velocity dispersions observed in these galaxies (i.e., $\sigma_{4782} \approx 390$ km s^{-1}; $\sigma_{4783} \approx 300$ km s^{-1}) appear to be evidence for strong nuclear tidal shocks that were induced by a deeply-penetrating collision between the two galaxies (Borne, Balcells, and Hoessel 1988; Balcells, Borne, and Hoessel 1989*b*). The strong nuclear tidal shock dumps a lot of matter into the cores of the galaxies, which could trigger some nuclear activity (i.e., "feed the monster"). This may be the cause of the radio jets (3C 278) seen emanating from NGC 4782, the galaxy with the largest velocity dispersion (i.e., the strongest tidal shock). Ballistic models of the radio jets (including both gravitational and ram pressure deflection; Borne and Colina 1990) indicate that the strong bends in the jets (particularly in the east jet) are *not* consistent with the galaxy motions required by our best-fit collision simulation (which was derived from the tidal distortions observed in optical light). In particular, it is not clear why the jet on the trailing (east) side of NGC 4782 should be bent so strongly and so much closer to the nucleus than the jet on the leading (west) edge, but it may relate to strong inhomogeneities in the spatial and velocity distributions of the ISM into which the jets are ejected. In this case, therefore, the observed tidal distortions have allowed us to test and make predictions about conditions related to the generation, propagation, and environments of extragalactic radio jets.

5. THE MERGER REMNANT NGC 7252

Borne and Richstone (1990) have examined the properties of the merger remnants from a large number of disk+disk collision simulations in an attempt to find a model for the claimed merger candidate NGC 7252 (Schweizer 1982). A set of orbit and disk galaxy parameters were found that indeed led to the desired final product (i.e., we were able to reproduce most of the peculiar morphological and kinematic features seen in this "train wreck"). Among the many useful results of this exercise (besides demonstrating that it is possible, in at least one instance, to make an elliptical-looking galaxy from the merger of two spirals) was the determination of a dynamical age for the system. In essence, the lengths and speeds of the tidal tails can be used to measure the time since the beginning of the interaction ($8 - 10 \times 10^8$ years). Our derived age agrees with that estimated by Schweizer (1982) both from the tail lengths ($9 - 10 \times 10^8$ years) and from the blue colors and starburst spectrum ($4 - 15 \times 10^8$ years).

6. SUMMARY

We have presented results from several studies in which the tidal distortions observed in specific interacting and merging galaxies have been used to probe the dynamical properties of the galaxies (e.g., masses, rotation, relative orbits, interaction ages). This type of analysis can be extended to a much wider variety of colliding, interacting, merging, and merged galaxies, each with its own set of peculiar tidal features. The character of the observed tidal disturbances helps to identify real cases of interaction, as opposed to cases of simple projection. Examples of tidally-induced features include: (1) asymmetric morphology (e.g., loops, tails, bridges, rings), (2) peculiar velocity fields (e.g., enhanced velocity dispersions, U-shaped rotation in ellipticals, tidal shocks, one-sided 21 cm HI profiles in spirals; see Borne 1990), (3) unusual spectral features (e.g., signatures of a starburst stellar population, blue elliptical colors), and (4) bent radio jets.

While case studies of specific interacting pairs can be very rewarding and informative, analyses of *large* samples of such pairs are needed to answer the global questions about the frequency and significance of interactions and mergers among galaxies in the universe. These remain among the most fundamental unresolved questions related to paired and interacting galaxies.

REFERENCES

Balcells, M., Borne, K. D., and Hoessel, J. G. 1989*a*, *Ap. J.*, **336**, 655.

______. 1989*b*, *Ap. Space Sci.*, **156**, 215.

Borne, K. D. 1988*a*, *Ap. J.*, **330**, 38.

______. 1988*b*, *Ap. J.*, **330**, 61.

______. 1990, in *Dynamics and Interactions of Galaxies*, ed. R. Wielen (Berlin: Springer), in press.

Borne, K. D., Balcells, M., and Hoessel, J. G. 1988, *Ap. J.*, **333**, 567.

Borne, K. D., and Colina, L. 1990, *Ap. J.*, submitted.

Borne, K. D., and Hoessel, J. G. 1988, *Ap. J.*, **330**, 51.

Borne, K. D., and Richstone, D. O. 1990, *Ap. J.*, submitted.

Hoessel, J. G., Borne, K. D., and Schneider, D. P. 1985, *Ap. J.*, **293**, 94.

Karachentsev, I. D. 1972, *Comm. Spec. Astrophys. Obs. USSR*, **7**, 3.

Kriss, G. A., Malumuth, E. M., and Borne, K. D. 1990, in preparation.

Pence, W., and Oegerle, W. 1989, *Bull. AAS*, **21**, 1170.

Pence, W., Oegerle, W., and Borne, K. D. 1990, in preparation.

Schweizer, F. 1982, *Ap. J.*, **252**, 455.

DISCUSSION

Mamon: You mention that you can follow galaxy orbits back in time, even in groups. Would it then be possible for you to investigate the galaxy orbits in compact groups, and therefore elucidate the space density and binding energy of compact groups?

Borne: Come back next year to ask us this question. Hal Jenson and I are currently studying this issue.

Osterbrock: What do you assume for the initial velocity of the jet in the NGC4782/3 simulation, and what other initial parameter do you assume besides the epoch at which it is introduced into the calculation?

Borne: The initial velocity is a function of the depth of our model potential at the center of the galaxy, and is therefore not a physical number, but it is probably close to the escape velocity. We also vary the density of the interstellar medium in each galaxy and the strength of the ram pressure term in our equation of motion.

Balsara: How would such modelling of extragalactic jets ever explain the Fanaroff-Riley classification of jets? The hydrodynamic model at least has a physical reason for classifying FR I & II jets.

Borne: We are simply investigating the response of an existing jet to the time-varying gravitational field and to the moving ISM in this pair of galaxies. Our inability to match the jet morphology perfectly indicates that we do need extra physics, perhaps no more than that which is represented in the hydrodynamic models.

Burbidge: I don't remember how many of the radio sources are identified with galaxies similar to NGC 4782-83. Are you proposing that in all of the cases of this kind a jet is produced?

Borne: Jets are seen in many pairs of interacting ellipticals. We are not proposing a physical mechanism for the generation of such jets, but we are investigating the behavior of the jets independent of their origin. It appears that something in the interaction favors the existence of jets, but we are not addressing this issue.

DYNAMICAL FRICTION IN PAIRS OF ELLIPTICAL GALAXIES

Philippe Prugniel
European Southern Observatory
Karl-Schwarzschild-Str. 2
D-8046 Garching, F.R.G.

Françoise Combes
Observatoire de Paris, DEMIRM
2, Pl. J. Janssen
F-92195 Meudon, France

Abstract: We present numerical experiments on dynamical friction in pairs of elliptical galaxies of unequal mass. We confirm that the self-gravity of the response is not important and show the drastic effect of the deformability of the companion which reduces the decay time by more than a factor 2. Almost the same amount of orbital energy is dissipated within the satellite than within the large galaxy. Finally, we discuss the importance of distant encounters for the dynamical evolution of systems of galaxies.

1. Introduction

This communication presents the first results from a N-body study of pairs of elliptical galaxies, they concern the investigation of the effect of various parameters on the dynamical friction in unequal mass pairs.

The important problem of the orbital decay of a "small" satellite onto a massive galaxy has been the object of a very open controversy over the last decade. The debate include the question of the *globality* of the response of the large galaxy and that of the importance of its *self-gravity* (Lin and Tremaine, 1983; White, 1983; Bontekoe and van Albada, 1987 (=BvA); Zaritsky and White, 1988 (=ZW); Hernquist and Weinberg, 1989). Although the most recent publications agree on the merging time and, to a very satisfying accuracy, on the shape of the decay curve (separation versus time), the actual interpretation of the physical phenomena is still discussed. According to BvA, the dynamical friction *can be characterized as a local process* and the global response is *not dynamically important.* ZW agree about this last point, but claim for the globality of the nature of the dynamical friction although it can be described by a local formula. This discussion obviously suffers from the lack of clear and well accepted definitions of the terms. In this respect, the recent claim by Weinberg (1989) of the strong importance of the self-gravity, in the sense it increases the decay time by a factor 2, is very confusing. Indeed, Weinberg includes in the self-gravity the motion of the center of gravity of the large galaxy while the other only consider the effect of the deformations on the internal potential.

In the present work we concentrate on the case of the friction at distance (when the two galaxies are well separated) which seems important for describing the earliest stages of the decay since the loose random encounters are strongly more usual in a cluster environment than the close ones. In addition, unlike previous work except Borne (1984), our companion is represented by a system of particles, and thus has the capability to absorb orbital energy as the large galaxy does.

The next part presents the experimental setup. The incidence of two physical ingredients is studied in 3 and 4: The effects of self-gravity and freedom degrees in the satellite. Then the importance of the friction at distance is investigated.

2. Experimental setup

We started from a self-gravitating system of two spherical galaxies since the *a priori* allowed approximations were not obvious. Since the internal potential of the galaxies is computed on a cubic grid of finite resolution, we added a rigid core in order to simulate the high central density peak characteristic of elliptical galaxies without using a too large number of particles. The equations of motion are:

$$\ddot{x}_{c1} = m_1 \sum_{k1} (x_{k1} - x_{c1}) p_{kc}^{-3} + m_2 \sum_{l2} (x_{l2} - x_{c1}) p_{lc}^{-3} + m_{c2}(x_{c2} - x_{c1}) p_{cc}^{-3} \tag{1a}$$

$$\begin{aligned} \ddot{x}_{j1} = m_1 \sum_{k1} (x_{k1} - x_{j1}) p_{kj}^{-3} + m_2 \sum_{l2} (x_{l2} - x_{j1}) p_{lj}^{-3} + \cdots \\ + m_{c1}(x_{c1} - x_{j1}) p_{c1j}^{-3} + m_{c2}(x_{c2} - x_{j1}) p_{c2j}^{-3} \end{aligned} \tag{1b}$$

Where we adopted the notations from White (1983), the indices 1 and 2 refers to each galaxy and should be inverted to obtain the accelerations of the second galaxy, m_1 and m_2 are the masses of the particles and m_{c1} and m_{c2} those of the cores.

For technical reasons the interaction between the particles of the two galaxies (second term of 1b) is approximated by a multipolar expansion (White, 1983). This approximation is a crucial point, but since for the experiments presented here we have made further simplifications which avoid the difficulty, we will not address the point.

Two cases are considered: (1) a rigid satellite. (2) a satellite represented by N-particles, without self-gravity.

In case (1) the second terms of Eq. 1a and b are ignored, and all the mass of the satellite is concentrated in the rigid potential. This makes the code formally equivalent to the classical problem of the decay of a satellite. The energy, angular and linear momentum are conserved.

In case (2) the two first terms of Eq. 1b are replaced by the interaction with fixed potential:

$$\sum_{k1} m_1 \quad \nabla\Phi_1(x_{j1}) + \sum_{l2} m_2 \quad \nabla\Phi_2(x_{j1})$$

The problem is then that considered by Borne (1984), and it does not formally conserve energy.

In our code, running on the CCVR CRAY 2, each galaxy is made by 20000 particles, and the self-gravitating potential is computed on a cubic 60x60x60 points grid. Forces are derived and interpolated from this grid. In the case (2) only the symmetric spherical part of the initial (relaxed) potential is taken into account.

The initial model has a central rigid Plummer containing 1/3 of the total mass and the particles are distributed according to a truncated $1/r^2$ density profile. The velocities follow an isotropic maxwellian distribution truncated at the escape velocity. Then, each galaxy is virialized separately, and the final density profile appears reasonably realistic. An important step, as stressed by Borne (1984), is the initial relaxation in the tidal field of the second galaxy before starting the interaction. We chose to not relax the initial galaxies in the actual initial tidal field, since such procedure is likely to exaggerate the phase coupling and the amplitude of the tidal bulges. Instead, we relax the galaxies in a spherically averaged tidal field. This has the advantage to avoid the energy shock responsible for strong transient effects (affecting the decay time by a factor two in Borne's experiments).

The mass ratio between the two galaxies lies in the range 3 to 10, typical of the distorted pairs of ellipticals presented by Prugniel and Davoust (this meeting). The mass of the primary galaxy is $10^{12} M_{\odot}$ and its radius 30 kpc, the radius of the companion is 10 kpc.

In all the experiments presented here the companion was launched on a circular orbit of radius in the range 30 - 60 kpc.

As a check of our procedure we run an experiment comparable to the standard experiment defined by White (1983). The decay curves are compared in Fig. 1. The agreement on the merging time is very good, but there are some difference in the shape of the decay curves. Although we did not check it, we believe the differences are due to the different mass profiles between these experiments.

Figure 1: Comparison with White (1983) experiment: decay of a point-mass satellite onto a large galaxy from a circular grazing orbit. The mass ratio is 10 and the mass of the large galaxy is $10^{12} M_{\odot}$. The broken line is White's data and the full line is our experiment.

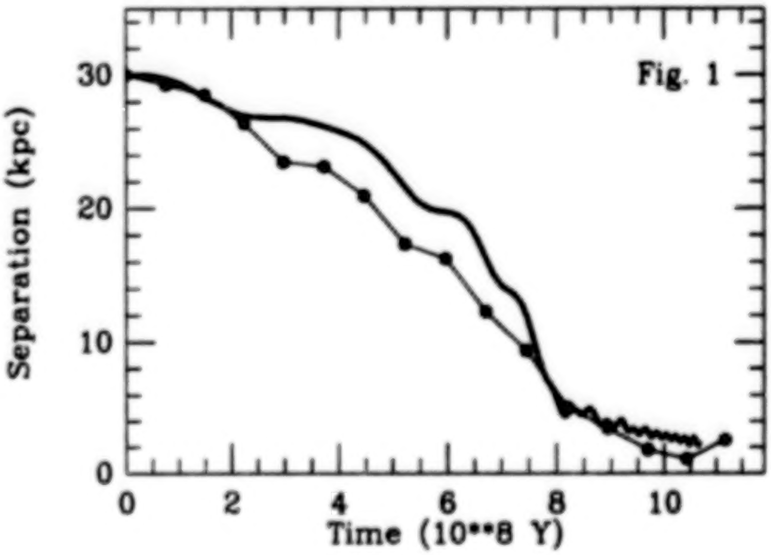

3. Effect of the self-gravity of the response

The first point investigated is the role of the self-gravity of the response. This is done by comparing experiments with the version (1) of the code with other done with version (2) but with a rigid satellite. Fig. 2 presents the decay curves for these experiments. The differences are not larger than the dispersion between experiments started from various initial conditions. This confirms the results of BvA and ZW and shows the consistency of the two versions of the code.

Figure 2: Effect of the self-gravity of the response of the large galaxy. Decay of a point mass satellite: same experimental setup as for Fig. 1. The full line includes the self-gravity of the deformation (case 1) while the dashed line does not (case 2). The difference is not significant.

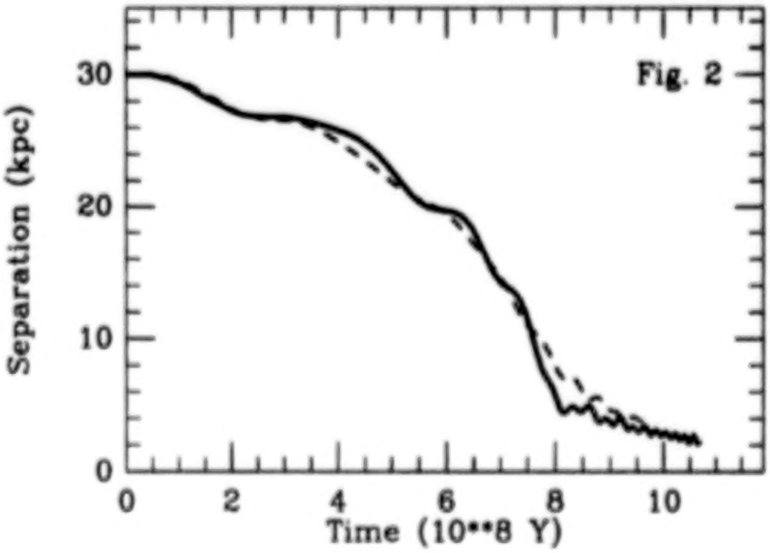

4. Effect of the deformability of the companion

The second point is the analysis of the effect of the ability of the satellite to absorb energy. Fig. 3 shows the results. The effect is considerable: the merging time is reduced by a factor 2.5 and scanning the range of realistic values for the size of the satellite it is always decreased by a factor 2 to 3.

Figure 3: Effect of the deformability of the satellite. Decay of an extended satellite (radius 10 kpc) starting on a circular orbit. The masses are $10^{12} M_\odot$ and $10^{11} M_\odot$, the radius of the large galaxy is 30 kpc. The full line is for a rigid satellite and in the experiment represented by a dashed line both galaxies are made with 20000 particles.

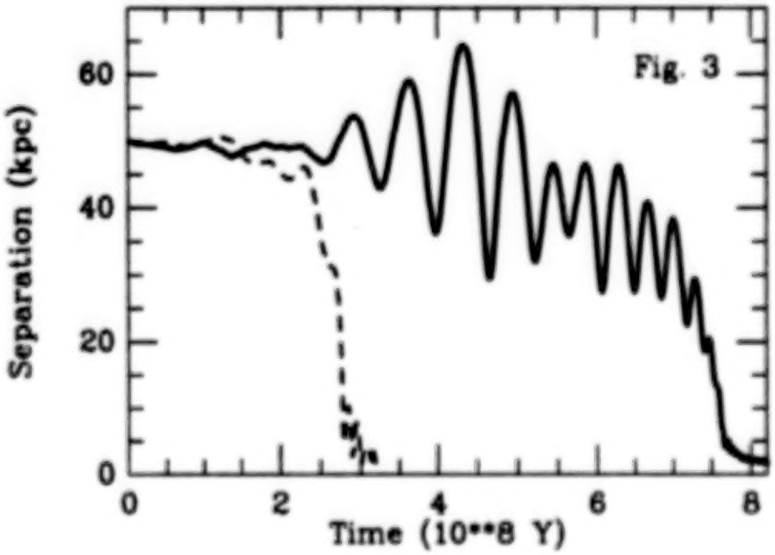

5. Importance of the friction at distance

Clearly, the classical formula for the dynamical friction does not apply when the galaxies are well separated (since in this model the drag is proportional to the local density). However, it is important to know the relative importance of loose encounter over close encounter for what concern the evolution of groups of galaxies. The alternative approach is the impulsive approximation (Spitzer, 1958), but it is not suitable to our problem where the relative velocity is of the same order or even smaller than the typical internal velocities. However, Dekel et al. (1980) have shown that the impulsive approximation still gives results compatible with numerical experiments for slow hyperbolic encounters.

We have conducted experiments starting from distant circular orbits. The difficulty of these experiments with low friction is the high sensitivity to the noise due to the limited number of particles. With 20000 particles, we were able to run experiments up to an initial orbital radius of 60 kpc (with a rigid satellite). The initial decay rates (dR/dt) are compared with the prediction of the impulsive approximation on Fig. 4. The dashed line corresponds to the classical impulsive approximation (Spitzer, 1958; $dR/dt \propto R^{-3}$) while the full line is the restriction to the drag due to the particles with a velocity smaller than the encounter velocity ($dR/dt \propto R^{-9/2}$).

Figure 4: Dependence of the initial decay rate (dR/dt) on the radius of the orbit. The masses are $10^{12} M_\odot$ and $10^{11} M_\odot$ and the satellite is rigid. The dashed line corresponds to the classical formula for impulsive approximation (Spitzer, 1958), in principle not suitable to this case, and the full line is the friction computed under the impulsive approximation restricted to the low velocity particles.

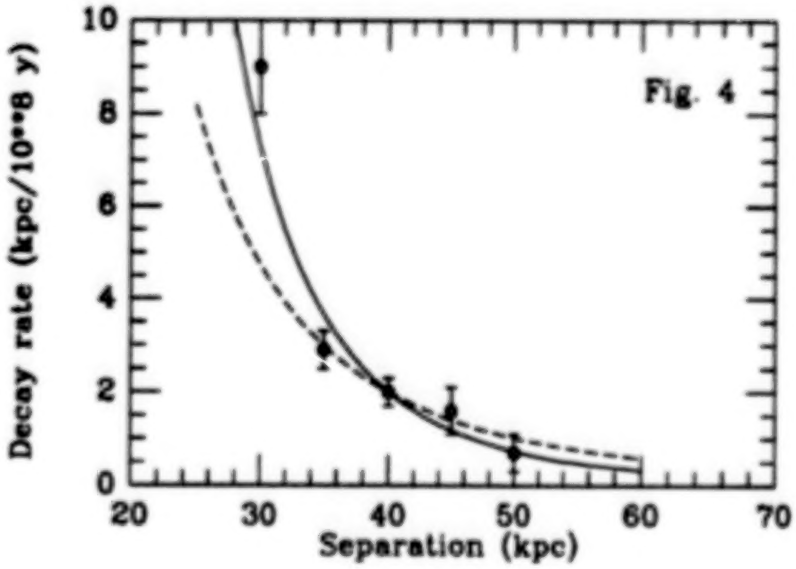

6. Conclusions

We have confirmed that the self-gravity of the response is not important and revealed the drastic effect of the ability of the small companion to absorb orbital energy. The amount of energy absorbed by the satellite is comparable to that dissipated within the large galaxy. This effect is associated to the very strong deformation of the satellite illustrated in Fig. 5. The distortion pattern of the simulated pairs looks very much like the one observed in real pairs (e.g. Davoust and Prugniel, 1988 or Prugniel and Davoust, this meeting). As for the global-local character of the friction phenomenon, we investigate this question in a subsequent publication (Prugniel and Combes, 1990).

Figure 5: Tidal distortion of the galaxies. This plot shows the density of particles in a logarithmic scale at an advanced stage of one of our experiments. The initial separation was 40 kpc and the mass ratio is 10. The field represented is 120 kpc wide and the actual separation is 10 kpc. The merging will occur in 5×10^7 years. Note the extended diffuse tail behind the satellite and the characteristic pattern of distortion symmetric with respect to the pair center.

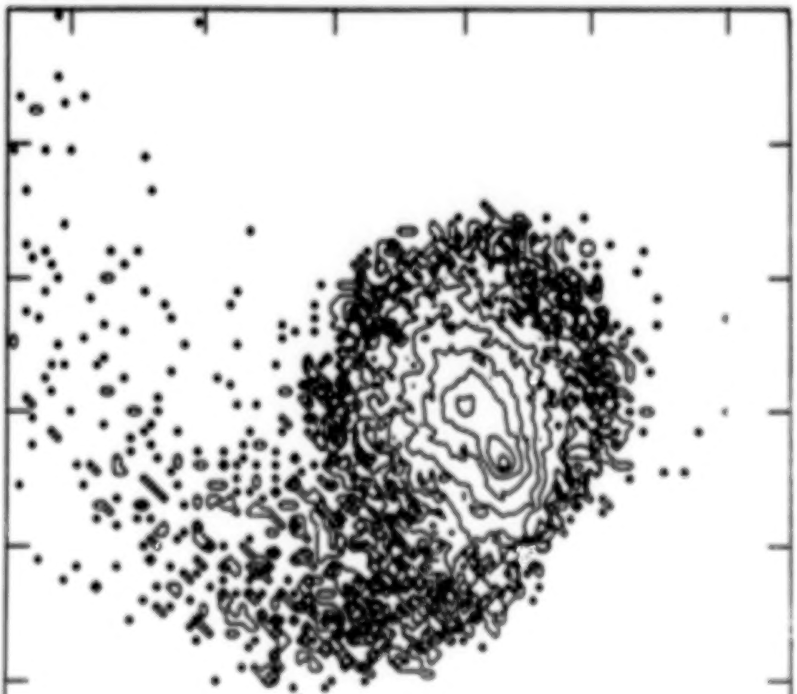

References

Bontekoe, Tj.R., van Albada, T.S.: 1987 (BvA), *Mon. Not. Roy. Ast. Soc.* **224**, 349

Borne, K.D.: 1984, *Astrophys. J.* **287**, 503

Davoust, E., Prugniel, Ph.: 1988, *Astron. Astrophys. Letters* **201**, L30

Dekel, A., Lecar, M., Saham, J.: 1980, *Astrophys. J.* **241**, 946

Hernquist, L., Weinberg, M.D.: 1989, *Mon. Not. Roy. Ast. Soc.* **238**, 407

Lin, D.N.C., Tremaine, S.: 1983, *Astrophys. J.* **264**, 364

Spitzer L.: 1958, *Astrophys. J.* **127**, 17

Weinberg, M.D.: 1989, *Mon. Not. Roy. Ast. Soc.* **239**, 549

White, S.D.M.: 1983, *Astrophys. J.* **274**, 53

Zaritsky, D., White, S.D.M.: 1987 (ZW), *Mon. Not. Roy. Ast. Soc.* **235**, 289

AN EXPERIMENTAL STUDY OF COUNTER-ROTATING CORES IN ELLIPTICAL GALAXIES

R. H. Miller, G. R. Roelofs, and B. F. Smith

University of Chicago
and
Theoretical Studies Branch, NASA-Ames Research Center

Introduction

Recent observational studies (Franx and Illingworth 1987; Jedrzejewski and Schechter 1988; Bender 1988; Illingworth and Franx 1989) have shown that some elliptical galaxies have a small region near the center that rotates in the opposite direction from the outer parts of the galaxy. Often the rotation in the central part is much faster than that in the outer part. A few other galaxies show a small region near the center that rotates in the same direction as the rest of the galaxy, but much faster. Either way, the part near the center that shows a strange pattern of rotation (the "core") has been interpreted as a distinct dynamical subsystem. Very briefly, the observational data seem to be that (1) anomalies show up in rotation curves near the centers of some elliptical galaxies and that (2) galaxies with these strange rotational properties do not show a photometric signature: there are no noticeable bumps in the brightness profile and no unusual shapes of isophotal contours that would suggest an excess of matter concentrated near the center. No strong color variations have been reported. The puzzle is to learn what we can about elliptical galaxies in general, and about galaxies with strange central regions in particular, from these observational facts.

Our approach is experimental. We make a guess about the form of the dynamically distinct subsystem, and then build a galaxy model to test experimental consequences such as the amount of matter required to produce observable effects and the length of time over which these effects would remain observable. We sidestep questions how the galaxy might have gotten to be that way in the first place. That gives us more freedom to explore a variety of suggestions about what kind of dynamical system might give rise to the observed rotational patterns.

Experiments with a Core

The first experiment was to put a core inside an otherwise unexceptional elliptical galaxy model. The galaxy was oblate and axisymmetrical, consisting of 100,000 particles, and a core consisting of 1024 particles was placed at rest near its center. Some rotation encouraged the main galaxy to remain oblate and axisymmetric. The core initially occupied a spherical region more or less the size of the galaxy's core radius, and velocity dispersions of core particles were low enough that the core did not disperse. In addition, the core could be made to rotate in some arbitrary direction defined by an angle, θ, measured from the galaxy's symmetry axis = the axis of angular momentum = the z-axis. Core particles are identical to galaxy particles from a dynamical point of view; they are marked to facilitate making movies and for later analysis.

Several experiments were run with this configuration, with differing amounts and directions of initial core rotation. The first control experiment with core angular momentum antiparallel to the galaxy's symmetry axis ($\theta = 180°$) showed nothing unusual. The angular momentum remained in that direction and did not change.

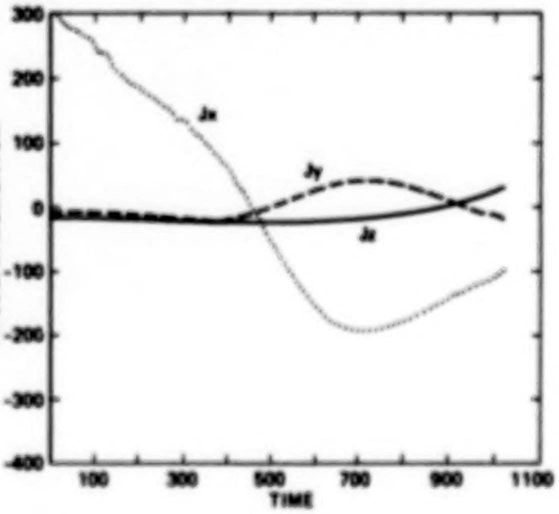

Figure 1. Components of total core angular momentum in an experiment with initial core angular momentum in the $x-$direction ($\theta = 90°$). J_x goes through zero and becomes negative. It damps out at long times, and it tends toward a state of no core rotation.

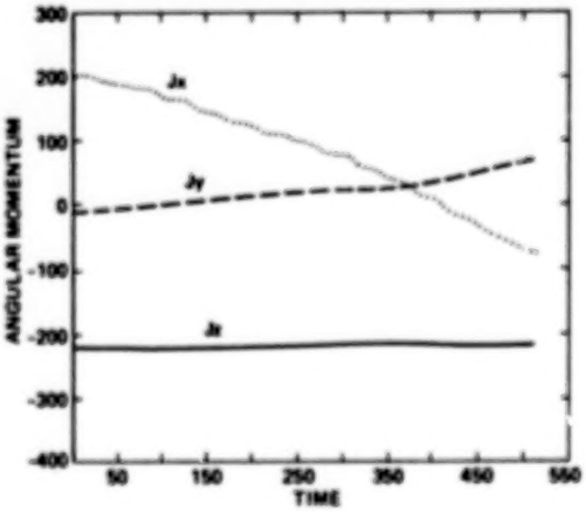

Figure 2. Components of total core angular momentum in an experiment with initial core angular momentum at $\theta = 135°$. J_x diminishes as before, while J_z remains nearly constant, ultimately leading to a counter-rotating core. The time scale differs from that of Figure 1.

Experiments in which the core angular momentum lay in other directions were more interesting. Results are most easily summarized by means of plots of the core angular momentum as functions of the time. Results from an experiment with core rotation perpendicular to the galaxy's rotation ($\theta = 90°$) are shown in Figure 1. All three components of core angular momentum are shown. The x-component decreases through zero, swings negative, and starts again toward zero, in the manner of a slow damped oscillation. The slow damping of perpendicular components of angular momentum appears to be a phase-mixing effect caused by anharmonicity of the galaxy's gravitational potential down near the center. The y- and z-components drift a bit at late times. We return to that shortly. Results from an experiment with $\theta = 135°$ are shown in Figure 2. Again, the component perpendicular to the galaxy's symmetry axis oscillates slowly and shows signs of damping.

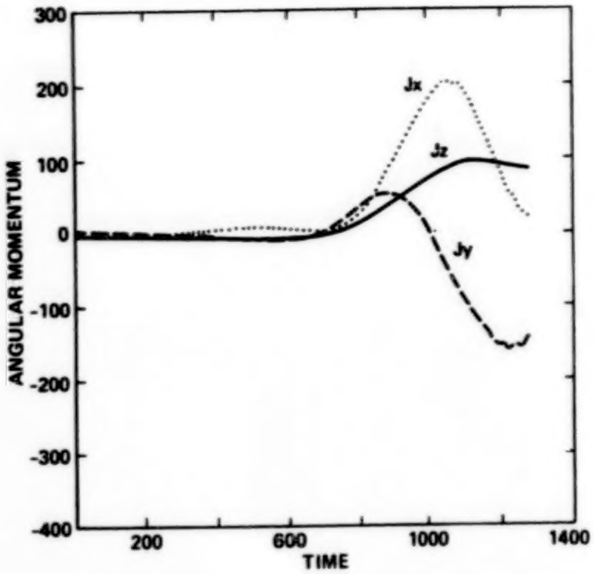

Figure 3. Components of total core angular momentum in an experiment with no initial core angular momentum. Growth of angular momentum at late times was found to result from slow disintegration of the core as it developed an orbiting motion around the center of the galaxy.

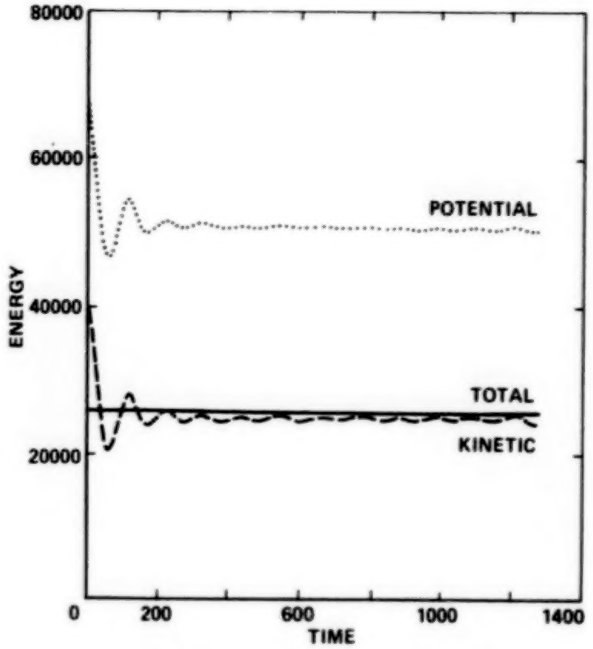

Figure 4. Total potential energy (dotted curve), total kinetic energy (dashed), and total energy as a function of the time. An initial lack of balance damps out quickly so most of the experiment runs in a very quiet galaxy ("virialized").

The drifts in angular momentum components that started out to be zero, as seen in Figures 1 and 2, invite further checks. We had to understand what causes them. They are allowed by the physics, since the core can exchange angular momentum with the parent galaxy. If they are real, they might suggest a way to generate rotation within a core. We checked this with an experiment in which the core angular momentum was initially zero (Figure 3). This experiment ran quite a bit longer than the others, and core angular momentum built up appreciably. Again the perpendicular components oscillate slowly while the z-component appears to drift. Plots of the total potential and total kinetic energy as a function of time in Figure 4 show that the galaxy is very quiet long before the angular momentum drifts appreciably.

A check to find out why the core angular momentum was drifting led back to a phenomenon we've reported before—the core starts to orbit around the galaxy center (Miller and Smith 1990a). The buildup of orbital motion is shown in Figure 5. Orbital motion is much faster than the slow oscillation period associated with core angular momentum drifts. The core takes a beating as a result of this orbiting—it builds a tail and it takes on a shape something like a comet. At this stage, corrections to take out core velocity and position in angular momentum estimates become tricky. The core is no longer a nice compact object.

Various parts are going in various directions. When angular momentum is computed relative to the center of mass for such an object, the result need not make a lot of sense. The drifts in Figures 1-3 are caused by this effect.

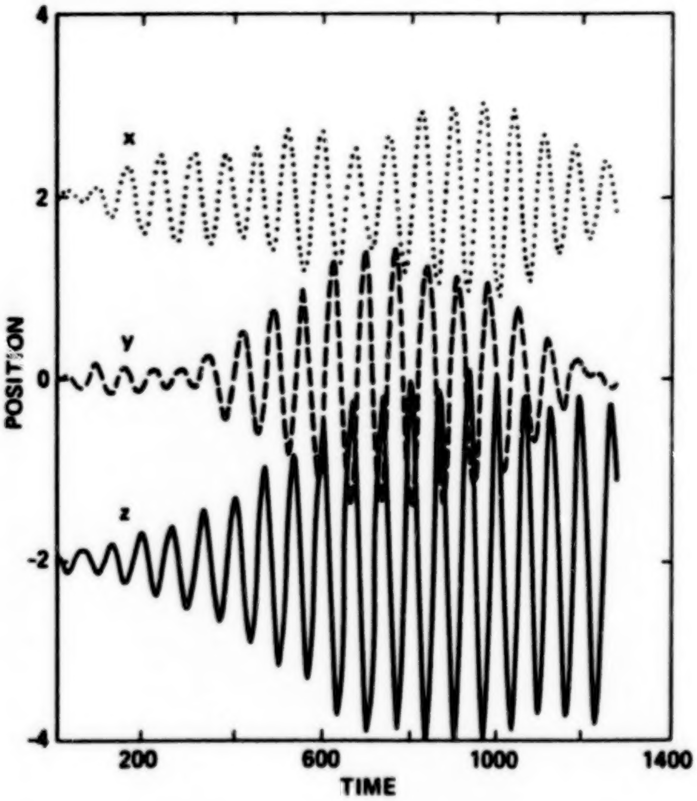

Figure 5. Position of the core's center of mass as a function of time in an experiment with no initial core angular momentum. The $x-$ and $z-$components have been displaced vertically for clarity; all three had zero mean displacements. The entire core starts to orbit.

One unit of time is about 3 million years in all these plots. A crossing time is about 100 million years or 35 units of time in the plots. The period of the slow oscillation in J_z is given by the difference of oscillation frequencies for a particle near the center to oscillat parallel to the equatorial plane or along the symmetry axis. A quarter cycle is about 500 time units or 1.5 billion years for the relatively round galaxies used here, and the damping due to phase mixing takes about 5 or 6 billion years. J_z oscillates faster for flatter configurations, but the phase-mixing damping rate appears to be about the same.

Density profiles were not affected noticeably in these experiments because the core has so little mass. We can get by with such a small core mass because we can study core rotation without the observer's signal-to-noise problem, but it is clear that quite a bit of mass would have to be included for the core to dominate the spectroscopic signature from the central region of a real galaxy. Further, speeds in the core's orbital motion are comparable to rotational speeds within the core. The observations seldom show translational motion of the core nearly as large as rotational velocities, so this doesn't seem to be a very good way to build counter-rotating cores. Slow disintegration of the core, associated with its orbital motions, also makes a distinct core seem an unlikely candidate to produce the observed counter-rotation effect.

A Sheet

A second possible configuration that might give rise to something that would look like a counter-rotating core is an apparent counter-streaming flow in a warped disk as seen from certain view directions. Imagine a sheet with a hat-brim warp and with a streaming flow in the same sense everywhere on the sheet. Imagine that you view this sheet from a direction nearly "face-on," but in which the inner portion of the sheet is inclined in one direction and the outer portions in the other direction relative to your view. You will then see one sense of rotation indicated by radial velocities in the inner portion, the opposite sense in the outer portions. Apparent changes of radial velocity become much more pronounced if the central portion of the disk is viewed nearly edge on, although this requires a fairly strong warp to yield reasonably large velocities in apparent counter-rotations. This effect is apparent in the warped disk of one of our recent studies (Miller and Smith 1990b). The long life of such a disk makes this an attractive picture, but strong counter-rotation is observable only from a fairly narrow range of viewing directions. Another problem with this picture is that most of the signal comes from the central portions—there is very poor signal-to-noise in the outer portions. Nonetheless, one can easily imagine that a small disk of material near the center of the galaxy, precessing within the main potential field, will show apparent rotation in unexpected directions, and might very well provide a reasonable model for counter-rotating cores.

Remarks

Many other configurations can be imagined that might look like counter-rotating cores from certain view directions. The two reported here are only those that we have tried so far. Any of these pictures has several problems. But any suggestion must be checked dynamically for surprises like the core oscillations shown in Figure 5.

One problem in any of these pictures is to get enough stuff to make anomalous velocities show up observationally without having a photometric signature.

References

Bender, R. 1988, *Astr.Ap.*, **202**, L5.

Franx, M., and Illingworth, G. 1988, *Ap.J.(Letters)* **327**, L55, *Fiche* 61-C2.

Illingworth, G. D., and Franx, M. 1989, In *Dynamics of Dense Stellar Systems*, Proceedings of a Workshop held at the University of Toronto, May 27–28 1988, Ed. D. Merritt (Cambridge: Cambridge University Press), pp. 13–23.

Jedrzejewski, R., and Schechter, P. L. 1988, *Ap.J.(Letters)* **330**, L87, *Fiche* 104-F1.

Miller, R. H., and Smith, B. F. 1990a, "Off-Center Nuclei in Galaxies" (submitted).

Miller, R. H., and Smith, B. F. 1990b, "An Experimental Study of Disks in Axisymmetric Galaxies" (submitted).

DISCUSSION

Galletta: About the possibility that box orbits are present in the galaxy: significant rotation in galaxies with counterrotating cores is an indication that box orbits are not dominant, since they contribute only to the velocity dispersion and not to the mean rotation.

Miller: That's the conventional picture. Numerical experiments show oscillations within a galaxy at a level of 2-5% of local density. Both the potential field and orbits of individual stars partake of this oscillation as well. Orbits that would be near the boundary that separates box and tube orbits in a static mean potential will diffuse across the boundary in a real galaxy. These are recently discovered effects whose importance is not yet known, but it seems likely that the distinction between box and tube orbits may become blurred. These oscillations may be thought of as the analog of solar oscillations in a galaxy.

Roos: Did you check whether the amplitude of the oscillations depends on parameters like the number of particles?

Miller: We checked many such things, as described in a paper that is in the reviewing process. Amplitudes vary inversely as the square root of particle number, but the growth rate is independent of particle number. That is more important. $\sqrt{N}$ dependence many sound artificial, but the real artificiality in n-body work is that we start the nucleus atop the mass centroid, something that could never happen in a real galaxy.

Bland: (Here's an opportunity for theoreticians to exonerate themselves.) Van Albada showed in the 50's that violent relaxation in collapsing systems gives rise to an $r^{1/4}$ law in the light profile. Given Gillian Wright's beautiful photometry on Arp 220, do numerical simulation still show the $r^{1/4}$ law as an eventual consequence.

Norman: T. van Albada (1982) showed that you only get an $r^{1/4}$ law from cold collapse systems.

Miller: Most n-body systems that have been shaken vigorously enough, whether by merger, fairly close collisions, or tidal stretching as the galaxy orbits near the center of a galaxy cluster, reshuffle their mass into a distribution that projects to a de Vaucouleurs profile. But the observed profile is a light profile, so association of this n-body result with the observed result requires that the light trace the mass faithfully, that the system be mixed to have constant M/L everywhere. Since pre-encounter galaxies are thought to have different M/L in different places, mixing is required. That is likely, and we all hope it's true, but mixing has not been demonstrated as the mass gets redistributed.

ON LEADING SPIRAL ARMS IN CLOSE PAIRS OF GALAXIES

A. M. Fridman
Astronomical Council of the USSR Academy of Sciences
48, Pyatnitskaya Stree, 109017
Moscow, USSR

ABSTRACT. It is explained why one can observe a leading spiral pattern in close pairs of galaxies where the direction of the orbital momentum of the satellite is opposite to the direction of the spin of the spiral galaxy.

INTRODUCTION

One can hardly find any other problem in galaxy physics which has been discussed so long and experienced so frequently changing opinions, than the problem of the direction of winding of galactic spiral arms. According to the initial point of view followed from Lindblad theory (1), all spiral galaxies must have leading spiral arms. The observations however have not confirmed this conclusion (2). Though the interpretation was critisized in (3), following (4) scientists give preference to trailing spirals almost unanimously. But the currently prevailing point of view that all spirals are trailing seems too categorical. There are exceptions to this rule (5), and the analysis of their reasons is the aim of the present note.

WHERE MAY THE LEADING GALACTIC SPIRAL ARMS BE OBSERVED?

Examining 190 spiral galaxies, Pasha has found that only three of them show leading arms (5). All the three have a close massive companion. One of them, NGC 5426, was studied more carefully; its spin is opposite to the orbital momentum. According to Werner (6), 69% of the paired galaxies show the same property.

BASIC HYPOTHESIS

Let us designate as leading those spirals which are rotating with their "tip" forward. Since the question is about the rotation of the spiral "tips," a peripheral region of the galactic disk is meant here. To identify a spiral as leading, it is enough for the largest part of the disk (including periphery) to be rotating in the same direction to which the spiral arms' tips are oriented. Let us now take a spiral to be trailing in the whole of the galactic disk except its periphery. Under the influence of the tidal wave from the galaxy's satellite, the main part of the disk (including periphery) is rotating opposite with respect to the rotation of the center part of the disk (Figure 1). Then determining the type of spiral with respect to the direction of rotation of the main part of the disk, we can make a conclusion about the leading form of the spiral pattern.

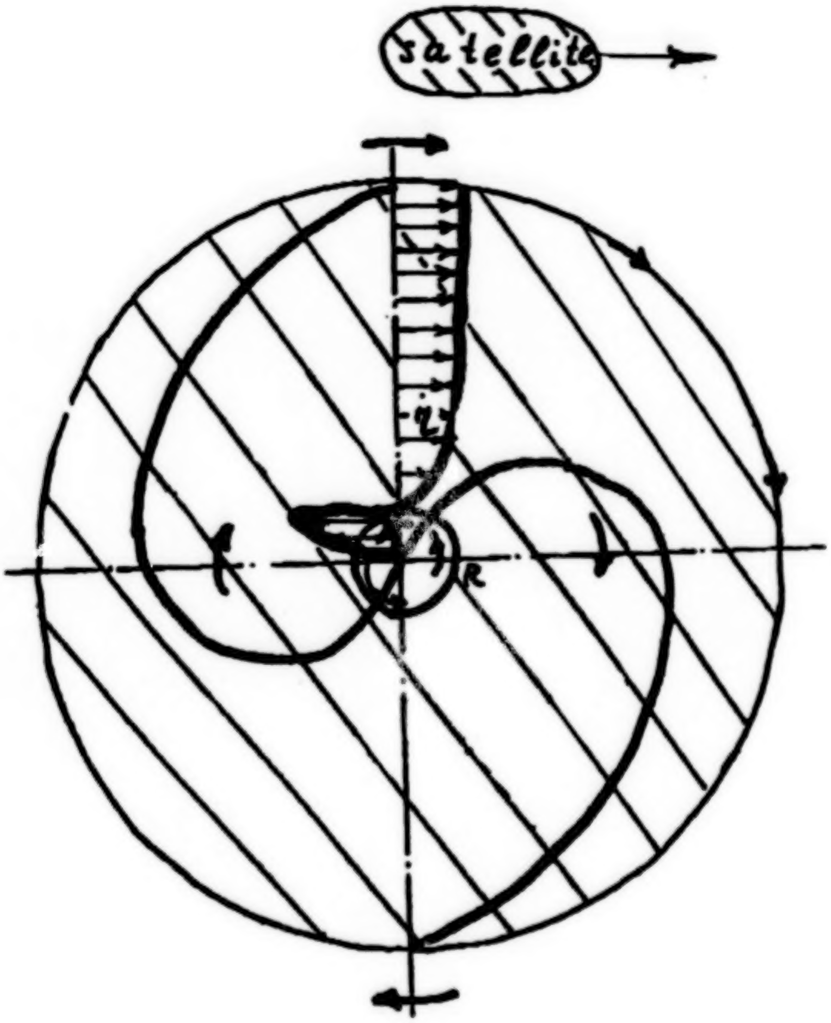

Figure 1. The center part of the spiral galaxy seen face-on rotating counter-clockwise; the main part of the disk (including the peripheral region) is rotating clockwise (as the satellite). Arrows show a vector field of linear velocities $\vec{V}_{o\phi}$ of the galactic disk and the satellite. On the radius r - R hodograph of motion has a "kink" which is typical of VK-galaxies (9, 10). It can be seen in Figure 1 that the same galactic spiral is trailing in the center part of the disk's region, but in the main part of the disk (dotted) the spiral is leading.

CONCLUSIONS OF THE THEORY

Last years' 6-meter telescope observations (7, 8) to determine the profiles of rotation velocities of the gas disk in spiral galaxies have shown that so-called VK-galaxies (with velocity kinks on their rotational velocity profiles (9, 10)) "to be a rule rather than an exception" (8). So let us assume all the three spiral galaxies identified as leading in (5) to belong to VK-type. Then according to (10), the density waves are generated in the gas disk in the form of spiral arms characterized by the perturbed surface density σ as the following function τ and ϕ:

$$\sigma(\tau\phi) \sim \tau^{-1/2} \exp\{- \frac{\Omega^2{}_1 R\tau}{Cg_1 Cg_2} \cdot \frac{(1-Q_q 2)}{1+Q\mu} + \text{im}\ [\phi + \frac{\Omega_1 \tau}{Cg_2} \cdot \frac{(1-q)}{(1+Q\mu)}]\}. \qquad (1)$$

Here we have introduced the following designations:

$$C^2_{gi} \equiv C^2_{si} - \frac{2\pi G\sigma_{oi}}{|K| R_g}, \quad R_g \approx \frac{1}{1+\frac{1}{2}\ |K|\ h_g}, \quad C^2_{si} \equiv \frac{dP_{oi}}{d\sigma_{oi}},$$

$$q \equiv \frac{\Omega_2}{\Omega_1}, \quad Q \equiv \frac{\sigma_1}{\sigma_2}, \quad \mu \equiv \frac{Cg_2}{Cg_1}, \quad i = 1,2 .$$

R is the radius of kink velocity of the gas disk (Figure 1), h is its typical thickness; parameters q, Q^{-I} and μ characterize the relations of values of angular velocities, surface densities, and dispersions of gas velocities in exterior region (r>R) to their values in interior regions (r<R).

The augend in curly brackets (I) describes the decrease of the perturbed amplitude with radius, the addend ~i determines the form of the spiral pattern. If the latter is rewritten in the form of $K_r \tau + m\phi = \text{const}$, then

$$K_\tau = m \frac{\Omega_1}{Cg_2} \cdot \frac{(1 - q)}{(\rho + Q\Gamma)} . \tag{2}$$

will correspond to the perturbation (1).

Let the interior region (r<R) be rotating counter clockwise, i.e., $\Omega_1 > Q$. Then as follows from (2), if $q<1$ no matter in which direction the external region (r>R) is rotating: $K_r/m>Q$, i.e., the spiral in the "wave meaning" (5) is trailing - it is rotating with its convex side forward. If the main part of the disk (including the periphery) is rotating in the opposite direction, the spiral will be rotating with its tips forward in this region, i.e., it will appear to be leading.

CONCLUSION OF THE LABORATORY EXPERIMENT

In (10) it is proved that with the help of a simple redesignation the main dynamic equations of the self-gravitating gas disk transform in shallow water equations. It makes possible to use a model "Spiral" with rotating shallow water for modeling the generation process of the galaxies' spiral structure (11-15). When the periphery was immovable ($\Omega_2 = 0$, i.e., $q = 0$) density waves were trailing spirals (11-15). It is obvious from physics of generation process that if we rotate the periphery slowly (no matter in which direction), i.e., if we keep to the condition $|q| \ll 1$, the form of the spirals will change very little.

At the same time, with respect to the counter-rotating periphery (i.e., when $q < 0$, but as before $|q| \ll 1$), the spiral waves will be oriented with their tips forward. The spiral in the "wave meaning" (5) will already be leading. Therefore, in all the region of the galactic disk, except for a small central part, the spiral will be oriented with its concave side in the direction of the rotation velocity vector. Without going into details, one can say that such a picture is observed in the laboratory experiment (13-15) (in detail see (15)). Thus, the region of the leading spiral (Figure 1) is wholly determined by the "trapped" region of the galactic disk by the tidal wave.

Let us note in conclusion that it is simple to determine from (3) the angle of the spiral winding $\alpha \equiv \arctan(m/\bar{\bar{k}}\,\tau)$.

$$\alpha(\tau) = \arctan \frac{Cg_2(1 + Q\mu)}{\Omega_1 \tau (1 - q)} \ . \qquad (3)$$

This formula can be experimentally checked substituting the parameters of the gas galactic disk by the parameters of the rotating shallow water and using (10). In particular, one can determine the relation tan α for leading and trailing spirals. If, for example, one manages all the parameters (except q sign) in both cases to make constant, then the leading spiral in its relation to the trailing one must look more winding, because $(\tan \alpha)$ lead/$(\tan \alpha)_{tr} = (1 - |q|)/(1 + |q|)$ and if $|a| << 1$, this relation $\approx 1-2|q|$.

ACKNOWLEDGMENTS

I express my gratitude to F. A. Tsytsyn, D. A. Werner, and A. V. Zasov for useful discussions.

REFERENCES

Afanasiev, V. L., et al. in *The Tenth European Regional Astronomy Meeting of the IAU*, Prague, Czechoslovakia, August 24-29, 1987.

Afanasiev, V. L., Burenkov, A. N., Zasov, A. V., Sil'chenko, O. K. 1988, *Astrophys. J.*, **28**, 243; **29**, 155.

Baev, P. V., Makov, Yu.N., Fridman, A. M. 1987, *Pis'ma v Astron. Zh.*, **13**, 964.

de Vaucouleurs, G. 1958, *Astrophys. J.*, **127**, 487.

Fridman, A. M. 1989, in *Dynamics of Astrohysical Disks*, edited by J. Sellwood, Cambridge University Press, Cambridge, p. 185.

Fridman, A. M., Morozov, A. G., Nezlin, M. V., Snezhkin, E. N. 1985, *Physics Letters*, **109A**, 228.

Fridman, A. M., Morozov, A. G., Nezlin, M. V., Pasha I. I., Polyachenko, V. L., Pylov, A.Yu, Snexhkin, E. N., Torkashin, Yu.N., Trubnikov, A. S. 1987, In *Observational Evidence of Activity of Galaxies*, eds. Khachikian et al., by IAU, pp. 147-157.

Hubble, E. 1943, *Astrophys. J.*, **97**, 112.

Lindblad, B. 1940, Astrophys. J., **92**, 1.

Lindblad, D., and Brahde R. 1945, Astrophys. J., **104**, 211.

Morozov, A. G., Nezlin, M. V., Snezhkin, E. N., Fridman, A. M. 1984, Pis'ma ZHETF, **39**, 504; Uspekhy Fiz. Nauk, 1985, **145**, 161.

Nezlin, M. V., Rylov, A.Yu., Snezhkin, E. N., Trubnikov, A. S. 1987, ZHETF, **92**, 8.

Pasha, I. I. 1985, Pisma v Astron. Zh., **11**, 3.

Werner, D. A. 1956, Astron. Tsirk., **1466**, 5.

Zasov, A. V., Sil'chenko, O. K. 1987, Pis'ma v Astron. Zh., **13**, 455.

A SIMULATION SURVEY OF GALAXY INTERACTIONS

G. Byrd, W. Keel(U. of Alabama) and S. Howard(Los Alamos)

Introduction

Many carefully selected samples of interacting galaxies have been observed extensively in attempts to clarify whether interaction produces activity in galaxies. Because the sample members represent a wide range of encounter parameters and times, one can then study whether there are correlations between observable encounter features and, for example, Seyfert activity. On the other hand, in theoretical studies, simulations typically deal with either time-consuming detailed modelling of single galaxy pairs or tracing a few model encounters over time. We are extending the observational survey approach by combining it with a simulation survey.

Simulations

We are conducting a **survey of model encounters**, covering the most important encounter parameters over a wide range. Some parameters, such as companion structure and initial velocity, are demonstratably less important and can be ignored in a first pass. The parameter range must be richly enough sampled so that we can evaluate the uniqueness of the observable morphology and velocity structure of the resulting simulated pairs to diagnose unobservable companion orbit parameters. We are using use a self-gravitating polar n-body code run on the Cray X-MP at the Alabama Supercomputer Network.

Comparison with Observational Samples

For each simulation, we will have stellar and gas distributions predicted over, typically, a billion years, along with information on gas motions within the disk and any material captured by the companion or lost to the system. Features of disturbed spiral galaxies are sensitive enough to time and encounter parameters so that a match of the simulation survey results to observations can be applied as starting points to infer unobservable orbital or system parameters in actual sample members. **This should enable us to examine whether interesting observed properties (Seyfert activity, nuclear star-formation rate) are functions of unobservable dynamical properties which characterize each encounter**. Any correlations (or lack of some expected ones!) will provide strong clues as to how or whether these phenomena are related to interactions. Aside from its use with such observed samples, this survey should greatly speed determination of initial orbital parameters for more detailed subsequent simulations of individual systems.

Display and Publication

The images are in **IRAF** format with 256x256 cells. Publication of a portion of the images via normal hardcopy is planned. However,the entire survey will be available on tape in FITS format so comparison with observations can be made on computer image processing systems.

Disk Parameters and Model Approximations

The **self-gravitating disk** has a finite radius with initially constant rotation curve (Mestel disk). In the disk, 30 percent of the particles are "**gas**" with no velocity dispersion and the rest "**stars**" with the appropriate stabilizing dispersion. The simulation code is a FFT particle-mesh code with a **polar grid** with bin size proportional to radius (small near center, large near edge as needed for disk simulations). Experience shows a **24 radial by 36 azimuthal grid with 180,000 particles** provides reasonable spatial resolution and sufficient numbers of particles per bin. The disk initially fills about one-third of the grid.

To maximize disk particle number, we make the following approximations: a 2 D self-gravitating disk, inert halo, and softened inert companion. These are reasonable for most encounters, but more elaborate simulations will be made where necessary. Because of uncertainty, we use **halo-to-disk ratios of 1.0 and 10.0.**

Encounter Parameters (Kicking the Disk in Different Ways)

We survey a variety of encounter parameter values. **Companion orbit inclination** values are 0, 30, 60, and 89 degrees. **Orbit sense** direct and retrograde relative to the disk "spin" will be tried. **Initial encounter distances** of one(grazing) and two times the disk radius will be simulated. **Companion masses** of 0.1, 0.5, and 1.0 times the target galaxy will be assumed. **Initial encounter orbits** will be assumed to be parabolic.

Examples of Results

Fig. 1 shows a set of 0 degree inclination, grazing encounters. The target galaxy turns counter clockwise. Direct companions orbit counter clockwise, retrograde clockwise. About 750 out of 1000 steps are shown with 50 steps between frames. A disk orbital period is about 300 steps. The left box is a direct encounter; the right, retrograde. Both have a 0.1 galaxy mass companion.

Example of Comparison with Observation

Fig. 2 shows photographs of systems and inset frames from our initial survey results. The left photo (NGC 2535/6) matches one of the direct Fig. 1 small-mass encounter shapes. The right photo (Arp 107) matches a direct 0.5 galaxy-mass companion encounter.(La Palma photos) We emphasize that the simulation frames were simply picked from the survey, showing how good fits to disk morphology can be easily obtained.

Some Encounter Morphology Generalizations

Direct encounters seem to preferentially generate the usual two-armed patterns with some interesting bends and kinks in the arms. See Fig. 1 left. **Retrograde encounters** are generally less violent in their effects but they can create interesting "scallop" patterns, off-center rings, and leading arms in the inner portions for strongly perturbed disks. The second from top right frame in the Fig. 1 retro encounter shows a scallop pattern. Such details are much clearer on an image processing system. **Inclined encounters** tend to generate one-sided patterns opposite to those seen in disk-plane encounters.

ACKNOWLEDGEMENTS

This work was supported in part by NSF/EPSCoR grant RII 8610669 and by Cray Research Inc. grant UA6. Computer time is provided by the Alabama Supercomputer Network. Our much-modified and extensively rewritten code is based on one kindly provided by R. Miller, who pioneered polar n-body code development. Photgraphs are from the Jacobus Kapteyn Telescope (operated by the Royal Greenwich Observatory at the Observatorio del Rogue de los Muchachos on La Palma).

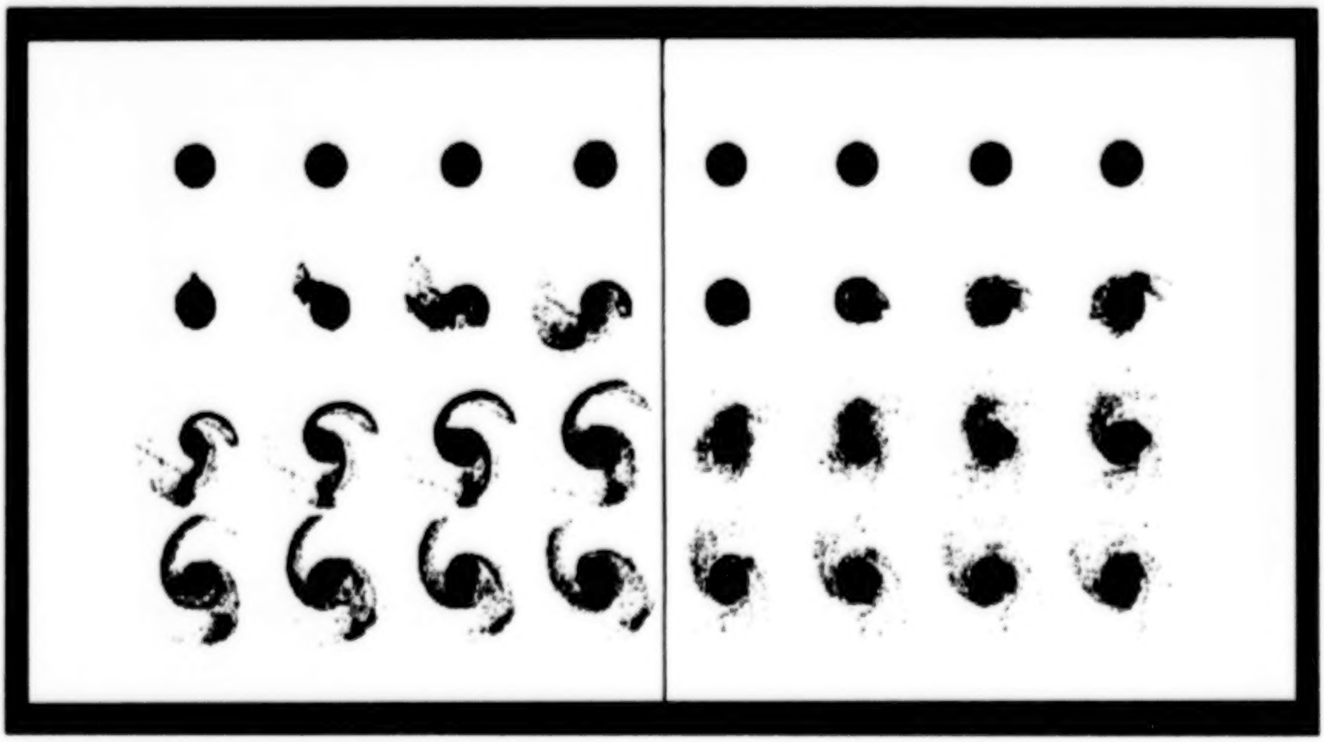

Fig. 1. Direct(l), Retrograde(r), "Gas," Companion/Galaxy 0.1

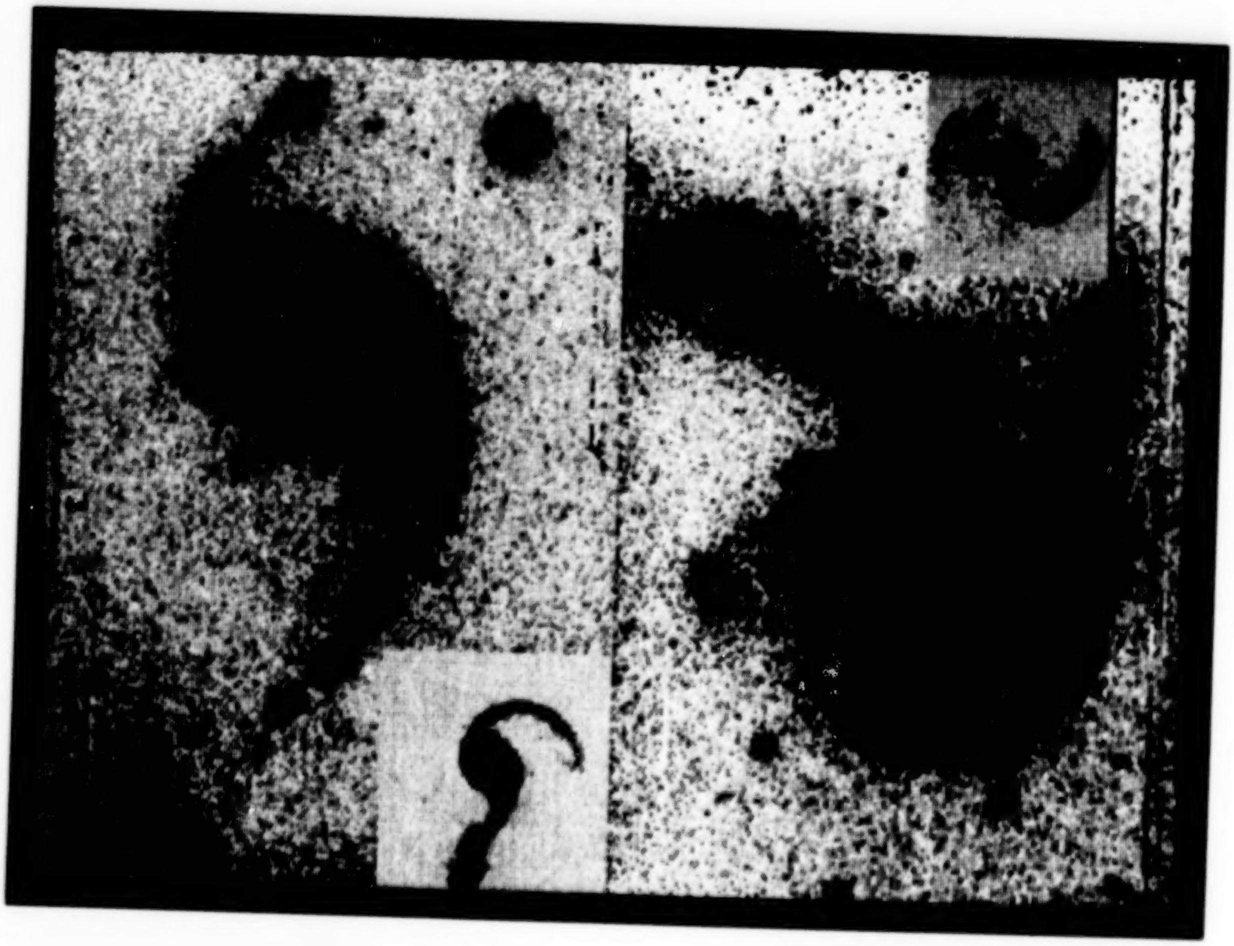

Fig. 2. Examples of matching survey frames to observations.

A DYNAMICAL PROXIMITY ANALYSIS OF INTERACTING GALAXY PAIRS

Tapan K. Chatterjee
Facultad de Ciencias, Fisico-Matematicas,
Universidad A. Puebla, (A.P. 1152), Puebla, Mexico

ABSTRACT. Using the impulsive approximation to study the velocity changes of stars during disk-sphere collisions and a method due to Bottlinger to study the post collision orbits of stars, the formation of various types of interacting galaxies is studied as a function of the distance of closest approach between the two galaxies.

INTRODUCTION

The interpretation of multiple interacting systems as the relics of gravitational interaction between galaxies is now strongly favored (see Toomre, 1974, for a review). Observations indicate that the proximity of the constituent galaxies in different types of interacting galaxies (eg., mildly perturbed galaxies, galaxies with bridges and tails, ring galaxies) is different. There seems to be a relation between the proximity of the constituent galaxies and the intensity of interaction between them. To study this relation it is necessary to study the formation of peculiar interacting systems, on the basis of the collision theory, as a function of the distance of closest approach between the constituent colliding galaxies.

An inspection of photographs of interacting galaxies from catalogues (eg. Voronotsov-Velyaminov, 1959; Arp, 1966) show that the majority of these systems consist of a disk and a spherical galaxy lying close to each other. Moreover the basic criteria determining the type of the interacting galaxy bears a strong relationship to the degree of perturbation encountered by the disk galaxy. Sphere-sphere collisions are important in a study of merging galaxies and do not lead to a variety of interacting galaxies, but rather to a particular variety. Hence, in subsequent work, we have studied the formation of peculiar interacting galaxies on the basis of collisions involving a disk and spherical galaxy, as our aim is a functional analysis of the type of peculiar interacting galaxy and the proximity of the constituent galaxies.

THEORY

In a previous paper (Chatterjee 1984; hereafter referred to as Paper I) the conditions of the formation of ring galaxies, during head-on collisions between disk and spherical galaxies, was studied. Using the same method we study in this paper both head-on as well as off-center and non-vertical collisions between disk and spherical galaxies and determine approximately the range of impact parameters favorable for the formation of different types of interacting systems.

The spherical galaxy is modeled as a polytrope of index $n=4$. The spiral galaxy is modeled as an exponential model disk, thickened by a method indicated by Rohlfs and Kreitschmann (1981), with a polytropic $n=4$ bulge superposed on this disk. The model is discussed in detail in Chatterjee 1989.

The theory is essentially the same as in Paper I. Using the impulsive approximation, the change in velocity ($\overline{\Delta\vec{v}}'$) of the representative star in the disk galaxy, due to the collision is given by, (case $R_S=R_D=R$),

$$\overline{\Delta\vec{v}}' = -[GM_S/(VR)]\vec{I} \tag{1}$$

$$I_x = -x_D \int_{-\infty}^{\infty}(1/s'')(d\phi_s/ds'')[s'/(s'^2-p^2)^{1/2}]ds' \tag{2}$$

$$I_y = (p-y_D) \int_{-\infty}^{\infty}(1/s'')(d\phi_s/ds'')[s'/(s'^2-p^2)^{1/2}]ds' -$$

$$p \int_{-\infty}^{\infty}(1/s'')(d\chi_{DS}/ds'')[s'/(s'^2 - p^2)^{1/2}]ds' \tag{3}$$

$$I_z = 0 \tag{4}$$

where the symbols have the same meaning as in Paper I, except for p, which is the distance of closest approach between the colliding galaxies, measured in units of the radius of either galaxy; and χ_{DS}, which a measure of the mutual potential due to the gravitational interaction between the disk and the spherical galaxy and is defined as the mutual potential function for the disk-sphere pair (Ballabh, 1975).

$\vec{I}$ and $\overline{\Delta\vec{v}}'$ are functions of both the distance of closest approach between the two galaxies, p, and the angle of inclination, i, of the disk to the direction of relative motion between the two galaxies (see Paper I). Using equations (1) to (4), we calculate the velocity perturbations of the representative stars for different collisions, each collision being characterized by a value of p and i. We then apply a method due to Bottlinger (Bottlinger, 1932, 1933) as discussed in Paper I, to study the post-collision orbits of the stars, the orbits of the innermost and outermost stars being studied by numerical integrtion due to the validity of the Bottlinger force law within a limited range of distance only. For convenience we define the angle $\alpha = 90° - i$, so that for $\alpha=0$ we have a collision whose trajectory is normal to the plane of the disk.

We increase p and α in small steps (of 0.05 and 5°), and find $\Delta v'$ for the representative stars for each collision and scale its value for different values of the collision parameters (M_S, M_D, R, V). Then we determine the final density distribution of disk galaxy for each collision, approximately, and test whether the rearrangement of stars leads to the formation of a peculiar galaxy (and if so, its shape and form, which determine its type).

NUMERICAL RESULTS AND DISCUSSION

We find that, for central or near central impacts, ring galaxies are formed provided the angle of inclination does not exceed about 45°. If $\alpha \lesssim 30°$ and the impact is central, or nearly so, we get very symmetrical and bright rings whose intensity distribution is almost uniform. If α is increased beyond 45°, we get messy, ill-defined structures. If p is increased the rings become asymmetrical and acquire non-uniform intensity distributions. Beyond $p \sim 1/3$, fairly well defined and prominent rings do not form. Messy ill-defined rings form up to $p \sim 2/3$.

Beyond $p \sim 2/3$, we get one-armed structures which do not close on themselves, but end abruptly. Beyond $p \sim 1$ we get very faint bridges and tails and extremely faint ring-like structures which do not close on themselves, resembling embryonic spiral arms, and are embedded in the background of the victim disk (see Chatterjee, 1986, for details).

Prominent bridges and tails start forming only when $p \sim 1\ 3/4$. Bridges and tails form for all orientations of the colliding galaxies to the trajectory of the collision, only they are better formed when the trajectory of the collision does not make a large angle with the plane of the disk, being most prominent when this angle is quite small but not zero (i.e., $i >$ 0° but $< 15^0$).

As the impact parameter is increased, we find that bridges and tails cease to form when p is slightly greater than 2 (about 2.1). However the shapes of the galaxies are affected due to tidal forces up to $p \sim 2\ 1/2$. Beyond this value of p the colliding galaxies do not affect each other enough to produce observable distortions.

CONCLUSIONS

As expected a dynamical study of the formation of peculiar interacting galaxies, on the basis of the collision theory, indicates that, as the distance of closest approach between the colliding galaxies increases, the interaction fades off rapidly but what is interesting is the existence of an almost continuous series of subtypes of different types of peculiar interacting galaxies as a function of the proximity of the constituent galaxies. Each subtype seems to have a characteristic range of values of the distance of closest approach, which leads to the conclusion that different subtypes should have different ranges of values for the proximity of the constituent galaxies. This may play an important role in the subjective classification of interacting galaxies. More observational surveys should be conducted in the light of these facts, to enable comparisons with the theoretical conclusions.

Finally we would like to mention that the various parameters which determine the degree of interaction between galaxies can be expressed in terms of the fractional change in internal energy incurred by either galaxy, $\Delta U/|U|$, where U is the initial internal energy and ΔU is its change due to the collision. If we define $\Delta U=(\Delta U/|U|)/(\Delta U/|U|)_M$, where $(\Delta U/|U|)_M$ is the fractional internal energy change for which merger is affected for the same value of p, then the ratio δU has characteristic values which determine the degree of interaction between the colliding galaxies and hence the peculiarity imparted to the system. It is interesting to note that these characteristic values of δU define the interaction in terms of a two parameter family, e.g., p and V, for a given pair of galaxies (for details see Chatterjee, 1989b).

REFERENCES

Arp, H. C. 1966, Astrophys. J. Suppl., **14**, 1.

Ballabh, G. M. 1975, Astrophys. Space Science, **38**, 307.

Bottlinger, K. F. 1932, Ergebn. Exacten Naturwissenschaften, **11**. 31.

Bottlinger, K. F. 1933, Veröff. Univ. Sternw. Berlin-Babelsberg, **10**, 2.

Chatterjee, T. K. 1984, Astrophys. Space Science, **106**, 309.

Chatterjee, T. K. 1986, Astrophys. Space Science, **121**, 212.

Chatterjee, T. K. 1989a, Astrophys. Space Science,**163**, 127.

Chatterjee, T. K. 1989b, Proceedings of the "VIth Latin-American Regional Meeting in Astronomy" in press in Rev. Mexicana Astron. Astrof.

Rohlfs, K. and Kreitschmann, J. 1981, Astrophys. Space Science, **79**, 289.

Toomre, A. 1974, in J. R. Shakeshaft (ed.), "The Formation and Dynamics of Galaxies," IAU Symp. **58**, 365.

Vorontsov-Velyaminov, B. A. 1959, "Atlas and Catalogue of Interacting Galaxies," Sternberg State Astronomical Institute, Moscow.

M51's SPIRAL STRUCTURE

S. Howard, Los Alamos National Laboratory
G. G. Byrd, University of Alabama, Tuscaloosa

The M51 system (NGC 5194/5195) provides an excellent problem both in spiral structure and in galaxy interactions. We present an analytic study of a computer experiment on the excitation mechanisms for M51's spiral arms and whether or not a halo is important for these mechanisms. This work extends previous numerical studies of the M51 system by including self-gravitation in a two component disk: 'gas' and 'stars', and a dark halo. The analytic study provides two new observational constraints: the time ($\approx 70 - 84$ million years ago) and position angle of perigalacticon (300°). By using these constraints and a simple conic approximation, the search for the companion's possible orbit is greatly simplified. This requires fewer N-body simulations than a fully self-gravitating orbit search. Fig. 1 shows the dust lane spiral pattern of M51 overlaid on an optical photograph. The analytically determined direction of perigalacticon is indicated with a line.

We assume a mass distribution in M51 that reproduces the observed flat rotation curve (Tully, 1974). The density distribution of a finite Mestel (1963) disk produces a flat rotation curve without the addition of any other components. The Mestel disk can be embedded in an appropriate inert halo to provide stability against small perturbations. We use a finite Mestel disk with adjustable halo mass to disk mass ratio, $\mathcal{H}/\mathcal{D}$. We fit the photometry of Burkhead (1978) to the Mestel mass distribution to estimate a radius, R_{Mestel}, for the Mestel disk. We find $R_{Mestel} = 15.5$ kpc (distance = 9.6 Mpc). Schweizer (1977) observed NGC 5195 to have a $\Delta V_r = 110$ km/sec for the radial velocity difference between M51 and its companion. By assuming a luminosity mass for NGC 5195 he also found that the mass ratio of $\frac{NGC\,5195}{NGC\,5914}$ is 1/3 to 1/2 . We use this value as a starting point for our simulations. Observations give an inclination between 10° and 20° for M51's disk. This tilt is too small to make any rectification necessary.

The original version of the code was written by Miller (1976, 1978) who used it to study the stabilty of disk galaxies. Sundelius, Thomasson, Valtonen and Byrd (1987) introduced two disk components which evolve simultaneously. One component begins 'cold', *i.e.*, with no velocity dispersion. This will represent disk gas clouds seen in the optical and radio. The other component begins 'warm', *i.e.*, with a velocity dispersion just equal to the critical value for stability against axisymmetric disturbances. This will represent old disk stars seen in the IR.

Each simulation time step = 1 $\Delta T \approx \frac{2\pi R_{Mestel}(\text{kpc})}{314 \cdot V(\text{km/s})}$ 10^9 yrs where V is the rotation curve velocity. For an $R_{Mestel} = 15.5$ kpc each time step is $\Delta T \approx 1.5 \cdot 10^6$ yrs.

We used a simple conic routine to obtain a family of orbits consistant with the analytic and observational constraints. We conducted an exhaustive set of simulations and compared the simulated galaxy with the M51 observations. We eliminated those orbits that did not produce the proper match. Orbits with eccentricities greater than 0.6 do not develop the inner structure in a timely fashion. Our best choice orbit has the current x,y position on the sky of the companion correct, the ΔV_r correct, the time since perigalacticon correct, and the azimuth of perigalacticon correct. The morphology matches M51's spiral pattern. We then varied $\frac{\mathcal{M}_{companion}}{\mathcal{M}_{M51}}$ from 0.1 to 0.5. $\frac{\mathcal{M}_{companion}}{\mathcal{M}_{M51}} = 0.1$ seems to work the best. This indicates that the companion may have an abnormal mass to luminosity ratio. By varying $\mathcal{H}/\mathcal{D}$ from 0.0 to 11.0 we determine that these simulations constrain $\mathcal{H}/\mathcal{D}$ to be between 1.0 and 3.0.

Our final set of orbit parameters is:

$e = 0.1$ $\quad$ $i = 50°$ $\quad$ $a = 1.07 \cdot R_{Mestel}$

$\Omega = 280°$ $\quad$ $\omega = 165°$ $\quad$ $\nu = 280°$

$R_{en} = 0.97 \cdot R_{Mestel}$ $\quad$ $\mathcal{M}_{companion} = \frac{1}{10}\mathcal{M}_{M51}$ $\quad$ $\mathcal{H}/\mathcal{D} = 1.0$ to 1.5

time step 119 $\Longrightarrow$ 70 million years since perigalacticon.

Fig. 2 shows the result from a run with $N_{total} = 180,000$, 30% gas. Both stars and gas are shown. Fig. 2a shows star particles. Fig. 2b shows gas particles. The time step is 125. The great number of particles strengthens all the features and also permits more particles to participate in the outermost features. The scales are not the same. The general agreement with Fig. 1 is good.

These simulations have no collisions among the gas clouds. As an extreme test of the effect of collisions, we ran a simulation with gas collisions using the same parameter set out to time step 119. Fig. 3 shows the results. This is a run with N = 15,000 (100% gas). The general results are the same. The direction towards perigalacticon is indicated with an arrow. Overlaid on this Figure are the dust lanes arms from Figure 1. The match is excellent.

The orbit is rather small, yet the success of the tidal arm match argues that this passage strongly disturbed a quiet disk. The latest radio observations (Rots, *et al.* 1990) of M51 are especially interesting. They may resove this problem. Fig. 4 is a tracing of the observations from a figure in Rots, *et al.* (1990). The companion is marked with a large 'X'. Their HI observations show a long, curving arm that extends well away from the optical regions of the system. The dust lanes in Fig. 1 fit within the disk contours of Fig. 4. In Fig. 4 the far-side arm appears separate from the extended arm. Shown beneath Fig. 4 is a scaled to match copy of Fig. 3.

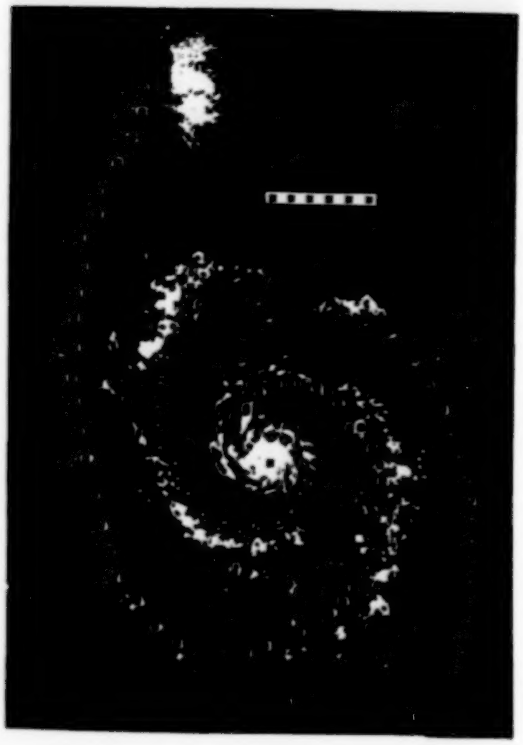

FIG. 1

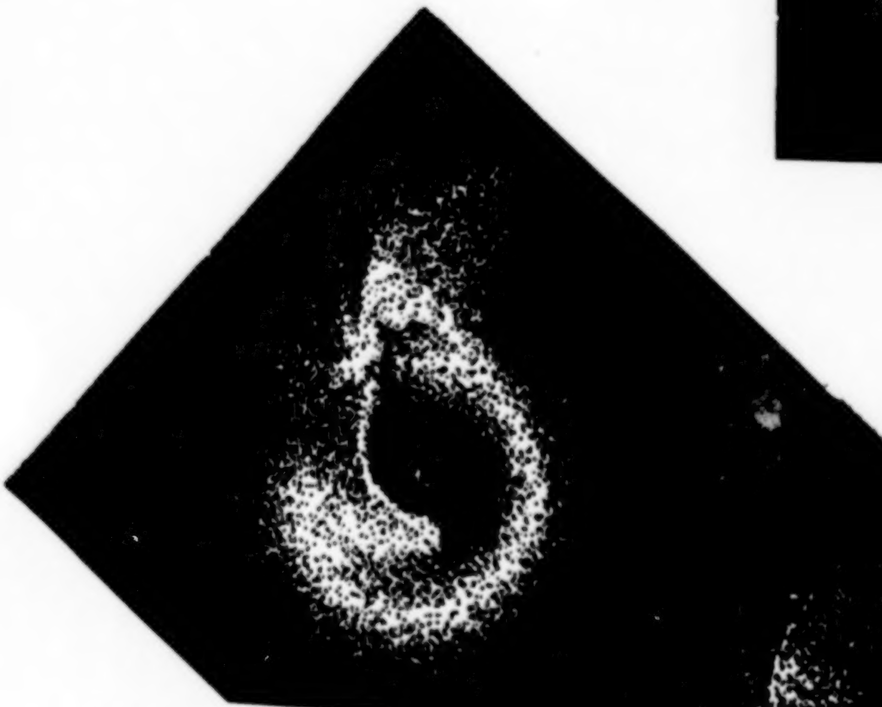

FIG. 2a - STARS

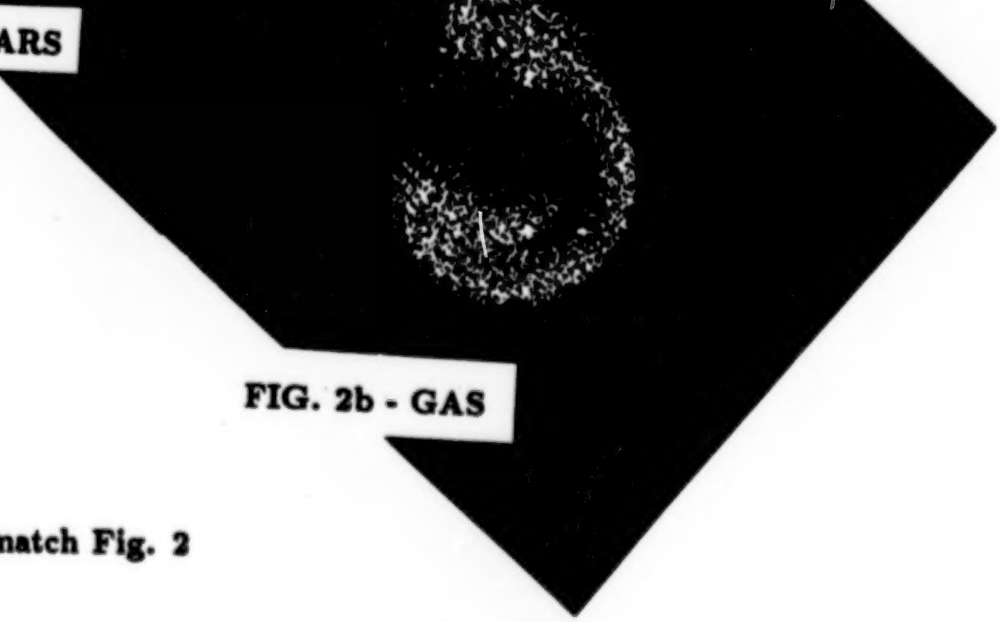

FIG. 2b - GAS

Fig. 1 scaled to match Fig. 2

The clump north of the companion seen in Figure 4 appears in our 180,000 and 15,000 particle simulations (Figs. 2b, 3). We interpret the orbit we found as the osculating conic orbit to NGC 5195's path as it decays towards a final merger with M51. This decay will result from the gravitational interaction of the companion with the halo and disk of M51 and the tidal breakup of the companion itself by M51. Decay time estimates imply less than three orbits before the final merger. We speculate that the extended HI tail is a remnant of the previous disk crossing.

The grand design spiral structure in M51 appears to result from the recent (70 million years ago) passage of NGC 5195. The outer spiral arms behave like material arms, *i.e.*, the gas clouds stay in the arms as the arm winds up. The inner spiral pattern behaves like a density wave triggered by the tidal arms, not directly by the companion. Collisions in the disk gas clouds are not *required* to produce the tidal arms. Instead, the tidal effect of the companion is the dominant driver of the gas. The simulations set limits to $\mathcal{H}/\mathcal{D}$ from at least 1.0 and perhaps a bit larger.

We propose three regions/types of spiral 'structure' in M51: (1) the Rots *et al.* extended HI tidal arm; (2) the tidal arms from the most recent passage; (3) the inner excited density wave.

Acknowledgments. This work was supported in part by Cray Research Grant U-6 and by NSF/EPSCoR grant RII 8610669.

Bibliography

Tully, R. B. (1974) *Astrophysical Journal Supplement*, **27**, 415.

Rots, A. H., van der Hulst, J. M., Athanassoula, E., Crane, P. (1989) *Proceedings of the Heidelberg Conference on the Dynamics and Interactions of Galaxies*, Springer-Verlag, Berlin, Editor: R. Wielen, A. Toomre, in press.

Miller, R. H. (1976). *J. Comput. Physics*, **21**, 400.

Miller, R. H. (1978a) *Astrophysical Journal*, **223**, 811.

Mestel, L. (1963) *Astrophysical Journal*, **126**, 553.

Schweizer, F. (1977) *Astrophysical Journal*, **211**, 324.

Sundelius, B., Thomasson, M., Valtonen, M., Byrd, G. G. (1987) *Astronomy and Astrophysics*, **174**, 67.

Burkhead, M. S. (1978) *Astrophysical Journal Supplement*, **38**, 147.

BLANK

PAGE

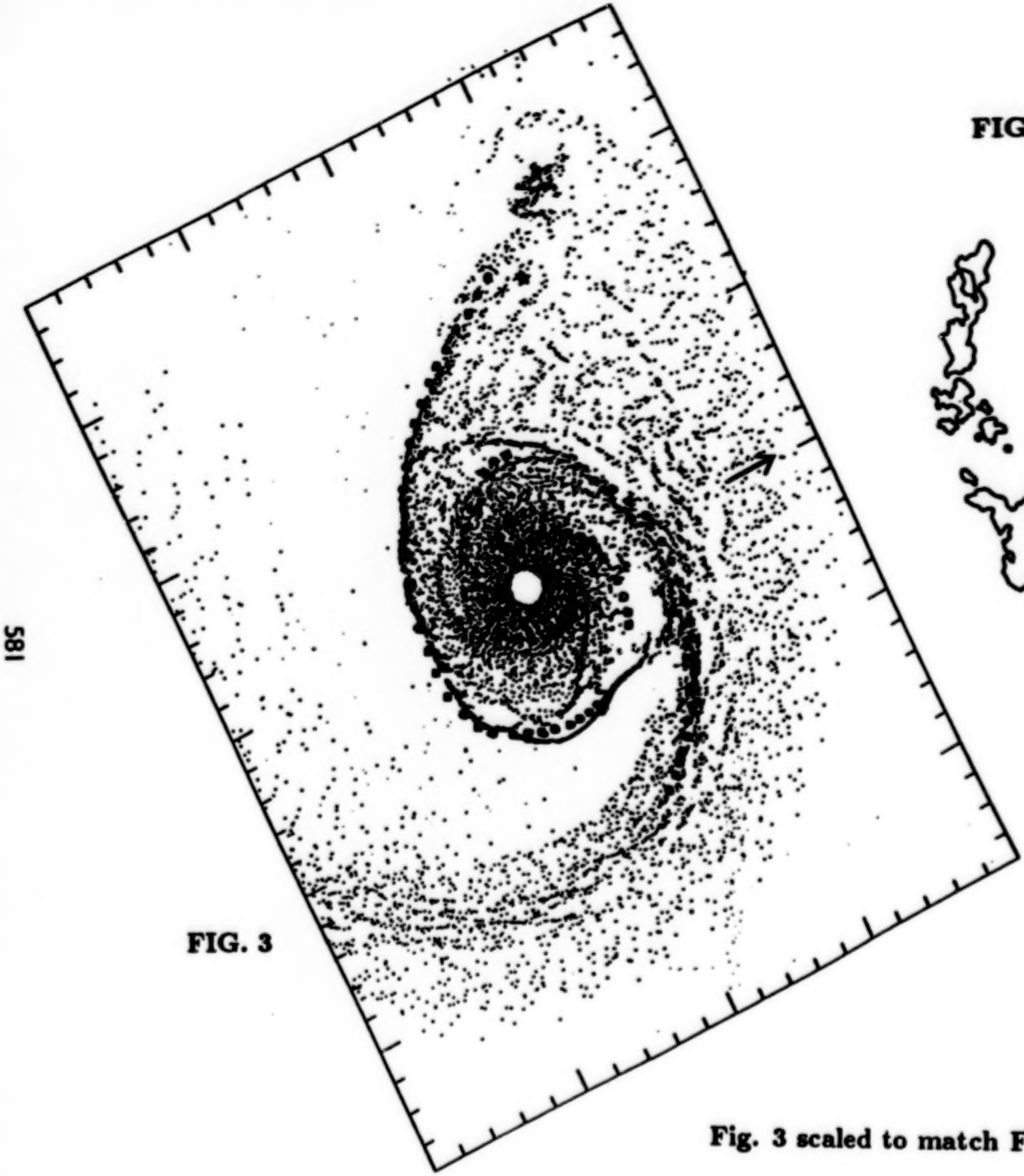

FIG. 3

FIG. 4

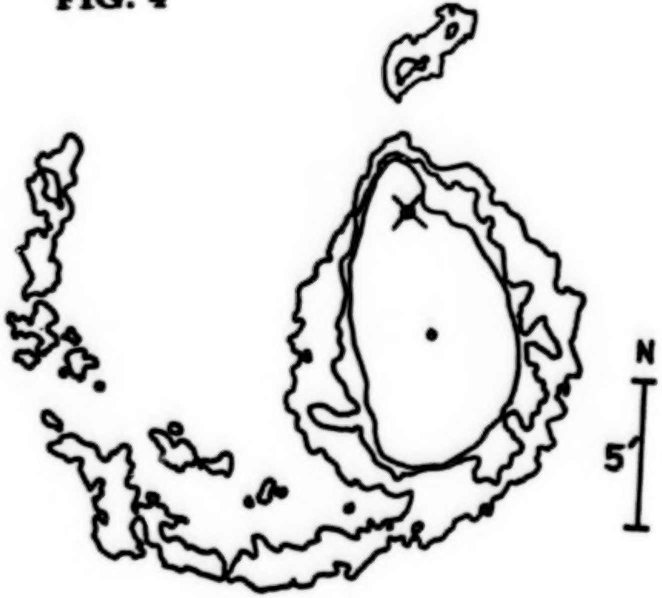

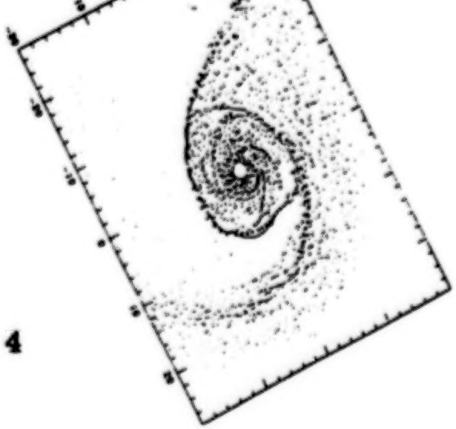

Fig. 3 scaled to match Fig. 4

THE SPIRAL-COMPACT GALAXY PAIR AM2208-251: COMPUTER SIMULATIONS VERSUS OBSERVATIONS

Mario Klarić
Department of Physics and Astronomy
University of Alabama
Tuscaloosa, Alabama 35487

Gene G. Byrd
Department of Physics and Astronomy
University of Alabama
Tuscaloosa, Alabama 35487

1. INTRODUCTION

The system AM2208-251 is a roughly edge-on spiral extending east-west with a smaller round compact E system about 60 arcsec east of the spiral nucleus along the major axis of the spiral (Fig. 1a). Further details are in A Catalog of Southern Peculiar Galaxies and Associations (Arp and Madore 1987).

Bertola, Huchtmeier, and Zeilinger (1990) have presented optical spectroscopic as well as single dish 21cm observations of this system. Their spectroscopic data show, via emission lines $\lambda\lambda 3727-29\AA$, a rising rotation curve near the nucleus (A in Fig. 1b). On the west half of the spiral's disk, the detectable curve does not extend farther than about 10 arcsec from the nucleus. Toward the east, the detectable curve extends all the way to the companion (B, C) and past it (D). This is in accord with the visual photo, which shows the spiral more extended toward the companion. The rotation curve flattens to about 150 km/s at about 7 arcsec from the nucleus (B). Then, at ≈ 28 arcsec, it dips and then slowly rises as it approaches the companion (C). Near the companion, the curve abruptly reverses slope (D), ending at ≈ 67 arcsec. The break in the curve (B) is possibly due to absorption in the spiral's disk. These spectroscopic observations may indicate a tidal interaction in the system. In order to learn more about such pairs, we simulate the interaction using the computer model

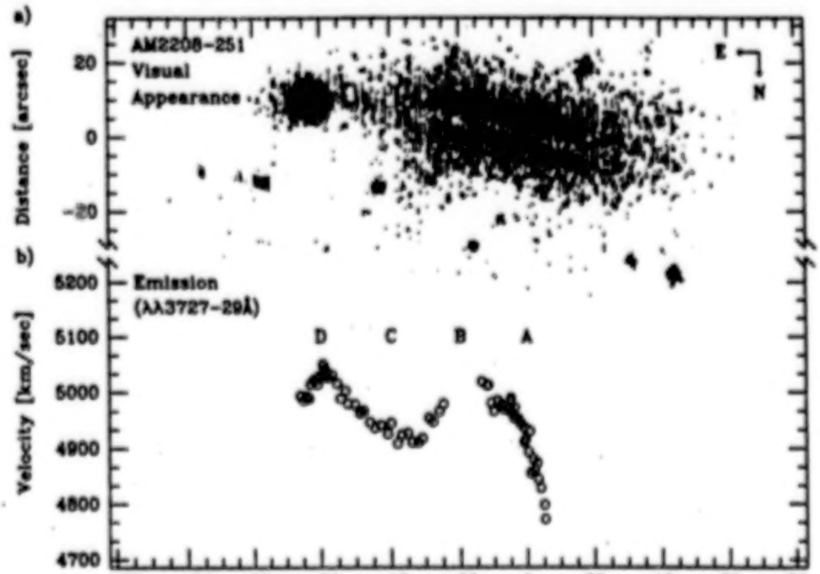

Fig. 1. a) Visual appearance of the system AM2208-251;
b) Velocities along the companion-spiral line.

developed by Miller (1976 a,b, 1978) and modified by us (Byrd 1986, 1987, 1988). To do the simulation we need an idea of the mutual orbits of the two galaxies.

2. ORBITS OF PAIR MEMBERS

Since the E galaxy is compact, we can use the work in Byrd and Valtonen (1987) to infer that the E is a close companion in an orbit within roughly 30^0 tilt with respect to the spiral's disk. The spectroscopic features indicate that the E galaxy has pulled gas from the spiral with the reversal in slope at D in Fig. 1b, interpreted as due to the E's gravitational field as the gas swings past the E galaxy. If the companion is in a small inclination orbit with respect to the spiral's disk, the spectroscopic data indicate it is moving in the same sense (direct) as the spiral's disk turns. The radial velocity is positive with respect to the spiral's nucleus at the E galaxy's location, as is that of the part of the disk between the companion and the spiral's nucleus, so the two senses match.

A small orbit tilt is also consistent with the accretion of gas from the spiral by the companion. The edge of the disk turns to follow the companion as it swings past its perigalactic point. The velocity difference between the companion and disk edge of the spiral is reduced, increasing the ease of accretion (see Fig. 2 for computer simulation). Retrograde encounters have much higher velocities relative to the disk and do not affect the perturbed spiral as much (Byrd et al. 1986, 1987).

3. THE COMPUTER MODEL

Our computer model is a two-dimensional polar N-body program. It consists of a self-gravitating disk of particles, within an inert axially symetric stabilizing halo potential. The particles are distributed in a 24(radial) by 36(azimuthal) polar grid. Self consistent calculations can be done only within the grid area. The disk is modeled with a finite Mestel disk, where all the particles initially move in circular orbits with constant tangential velocities (Mestel 1963), resulting in a flat rotation curve. For more complete description of the program see Byrd et al (1987, 1988).

The gas particles in the spiral's disk, which make up 30% of its mass, collide in the following manner. The number of particles in each bin of the polar grid is counted every time step. If it is greater than a given critical density, all the particles in the bin "collide", obtaining in the result the same velocities – equal to the average for the bin. This process produces clumps of gas particles – the star formation sites. We suppress the collision in the inner part of our disk (within the circle $r = 6$) to represent the "hole" seen in the gas in the nuclear bulge of spirals. We thus avoid spurious effects due to collisions in that region. We have also varied the size of the collisional bins, which did not affect our conclusions.

Under the guidance of the preceding reasoning and many different trials, we chose a direct encounter of a softened companion in a planar orbit. Using previous simulation experience, the degree of E-W asymmetry in the spiral, and the relative brightness of the companion and the spiral, we chose a companion 0.2 of the spiral galaxy mass which would approach to within 1.5 disk radii of the spiral on a zero energy direct orbit (roughly a parabola or elongated ellipse). With tidal energy loss the disturber actually gets to 1.36 disk radii. One disk radius corresponds to 36.44 arcsec, or 17.5 kpc ($H = 50\,\mathrm{km/s/Mpc}$). Taking the disk orbital speed to be 150 km/s, one time step equals 1.17×10^6 years.

The disturber is initially on the x-axis in a "three-o-clock" position in Fig. 2*a*. This direction corresponds to the 0° viewing angle by an observer, with viewing angle increasing counterclockwise in the Figures 2*a*, 2*b* and 2*c*. The disturber's initial tidal effects on the disk are minimal. It passes by the disk in a close approach, initially zero energy orbit affected by the halo field and the disk particles.

4. RESULTS OF COMPUTER SIMULATIONS

Which step in our "best choice" encounter orbit (Fig. 2a) best represents AM2208-251?

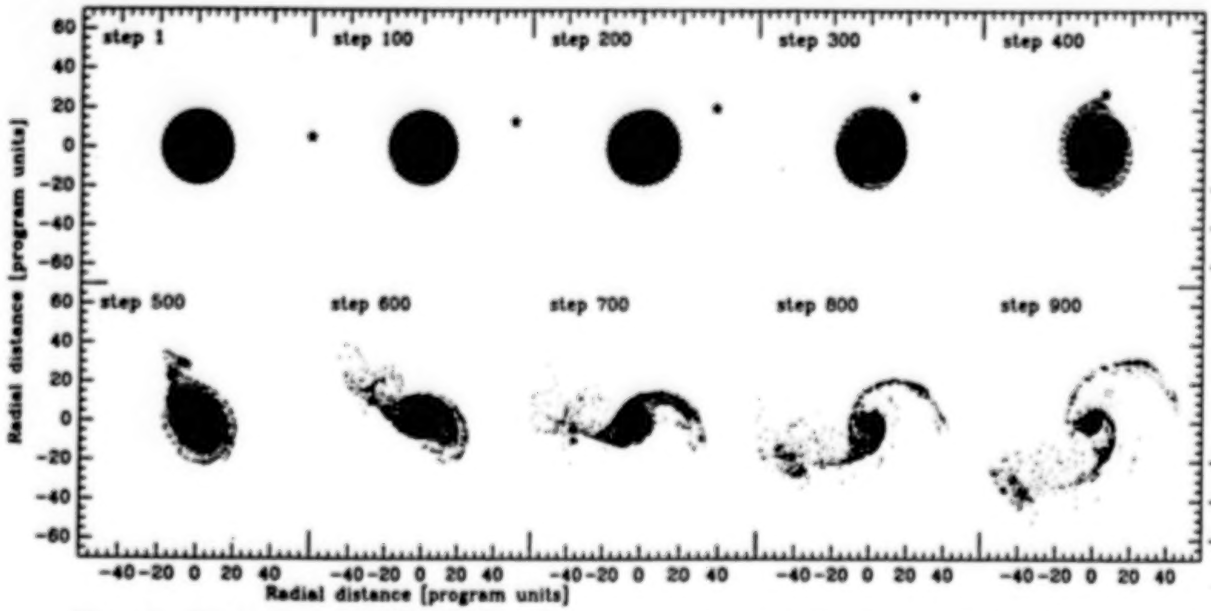

Fig. 2. Computer simulation results:
a) time steps 1 - 900;
b) time step 600.
(1 program unit ≈ 1.8 arcsec)

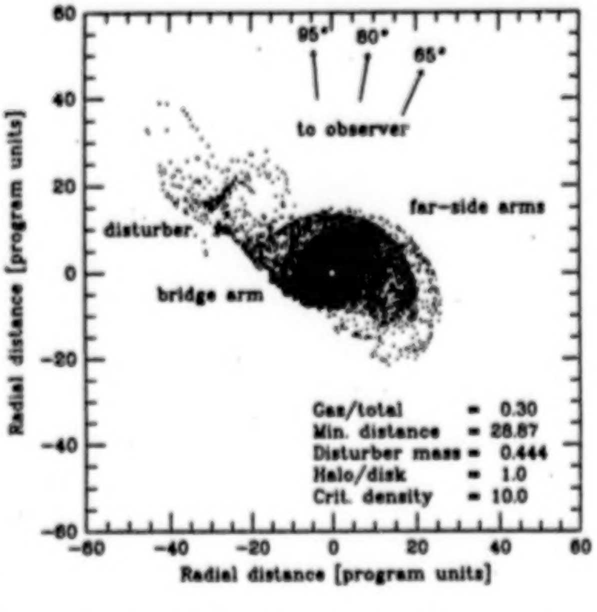

We see time steps 1 through 900. A "bridge arm" starts to develop toward the companion around the step 400, and is well developed at the step 500. The clumps start forming in the bridge arm. Around the step 700 the bridge starts to break, and the "far-side" arms on the other side of the disk are now more prominent. At the step 900 the bridge is broken, and the disturber is moving away from the disk. In light of this sequence above, the well-defined bridge in Fig. 1a implies that the companion has recently passed the perigalactic point. We display the result after perigalactic passage looking down from the galactic north pole on the disk in Fig. 2b. Examination of Fig. 1a indicates that, since the dust lane crosses the spiral nucleus slightly off-center (to the north), we are seeing the system in Fig. 2b from the upper right side, slightly below the plane of the paper.

In our galaxy, and in other spirals, emission nebulae are most abundant in the densest parts of the spiral arms. Examining Fig. 2a, we see that our simulation produces a well-defined bridge arm with a narrow front edge extending out to the companion, and some arms on the opposite "far side". Step 600 (Fig. 2b) produces the best bridge arm with material swinging out past the companion. We assume the gas clouds have collided in the manner explained above, producing young stars and emission nebulae along the arms in the spiral. This is evident in Fig. 3, which shows a close-up of the Step 600 bridge arm, with velocity vectors of the gas particles shown. Since collisions of gas clouds are probably the mechanism for a massive star formation in arms, we compute vector average velocities for particles near one another in the arms. The collision products (merged clouds, young stars, and emission nebulae) will have this net, inelastic collision velocity. The vectors cross along the arms, where collisions would occur. Note the big clumps of collided gas cloud particles along the arms in Fig. 3. The particles in these clumps move parallel to one another as a result of collisions. Assuming that emission nebulae are concentrated along the arms in these clumps, we plot the radial velocities along those arms that would be seen by the observer.

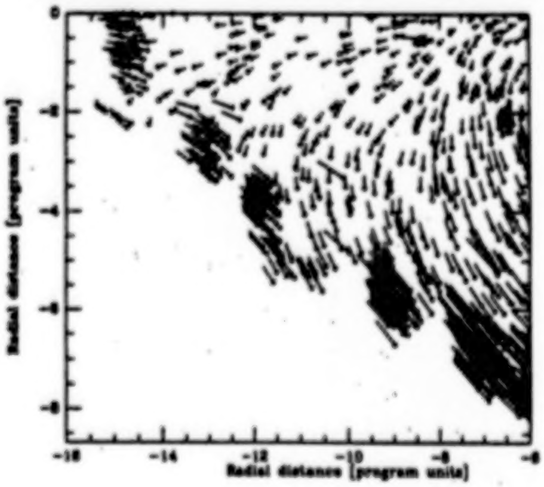

Fig. 3. The bridge-arm section of the time step 600.

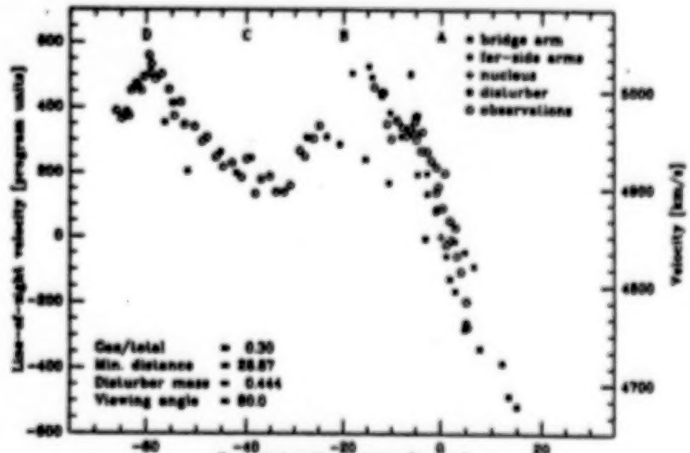

Fig. 4. The best-fit rotation curve with the observations.

Fig. 4 shows our model radial velocities versus position along the companion-spiral axis for step 600 (Fig. 2b) for the viewing angle of 80° (the best fit), with the observations superposed. One can see the remarkable agreement between the two curves, and from that deduce what parts of the spiral are actually visible. We think that the part A of the curve around the nucleus originates in the far-side arms, which are closer to the observer, and are blocking the bridge arm. The break in the observational curve (part B), from ≈ 14 arcsec to ≈ 20 east from the nucleus, is due to the absorption by the material in the spiral's disk. The bridge arm is visible from ≈ 20 arcsec to ≈ 67 arcsec east from the nucleus, with the dip, the rising slope (part C), agreeing very well

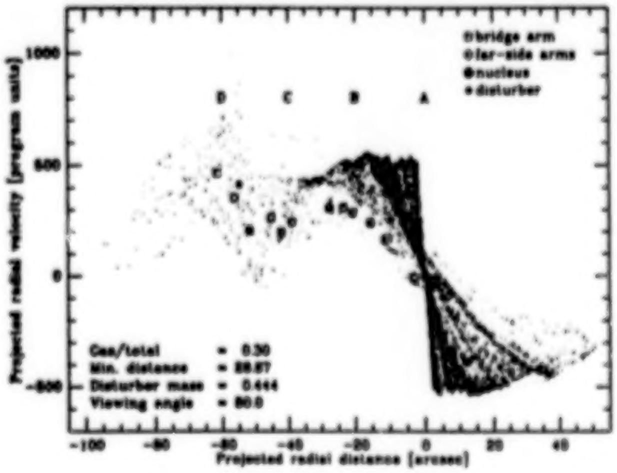

Fig. 5. HI velocity curve, with the best-fit rotation curve (80° viewing angle).

with the observations.

Fig. 5 shows the radial velocities of the computer simulation emission nebulae (found along the arms) on top of all the gas particles in the disk. These clouds best represent atomic H or alternatively stars with strong absorption lines scattered over the whole disk. Here we have enough particles to see the reverse slope of the gas particles beyond the disturber (part D).

We have varied azimuthal viewing angle ±20° before the correspondence with observations breaks down. We have reasonable confidence in the planar orbit chosen, and in the mass of our companion based on its being a compact galaxy, and the relative brightness of the compact and the spiral (see the AM catalog). The halo/disk ratio is quite uncertain, but 1/1 seems reasonable. The simulation results are not particularly sensitive to initial orbital energy. But the distance of closest approach (related to orbital angular momentum for a given energy) is crucial in forming the right sort of bridge. Beyond $\approx 1.5\times$ that chosen (1.36 disk radii) no bridge forms; if the approach is ≈ 0.5 that chosen, the disk is too greatly disturbed for the bridge arm to be stable.

Our results have implications in regard to possible measurement errors for rotation curves of nearly edge-on spirals. Recall Fig. 5 shows the optical HII regions rotation curve (squares) as well as the HI rotation curve (dots) in our computer simulation. In Fig. 5 note the great difference between the "real" HI tangent point rotation curve of our model galaxy ($\approx$ flat going from the nucleus outward) (left and right) and the rotation curves one would erroneously infer from the emission line measures of our edge-on model. Although one would certainly be cautious because of the spiral's edge-on orientation, our model results indicate that the gently rising parts of the emission line radial velocities near the nucleus in Fig. 1b are by no means a rotation curve. The actual curve is still flat close to the nucleus as the dots in Fig. 5 show. Also note that the curves for the far-side and bridge arms do not go through the nucleus' radial velocity. Again, the model points out how the observations may be misleading in disturbed spirals. Depending on the direction from which one observed this galaxy in HII, one could obtain almost exactly the nuclear velocity (the present side), or $\approx$ 100 km/s off if we were looking from the opposite side.

REFERENCES

Arp, H.C. and Madore, B.F. (1987). A Catalogue of Southern Galaxies and Associations, Cambridge University Press

Bertola, F., Huchtmeier, W.K., and Zeilinger, W.W. (1990). in *Proceedings of the Heidelberg Conference on the Dynamics and Interactions of Galaxies edited by R. Wielen. and A. Toomre (in press) (Springer Verlag).*

Byrd, G.G., Saarinen, S. and Valtonen, M.J. (1986). Mon.Not.Astron.Soc. **220**, 619

Byrd, G.G., Sundelius, B. and Valtonen, M.J. (1987). Astron. Astrophys. **171**, 16

Byrd, G.G., Valtonen, M.J., Sundelius, B. and Valtoaja, L. (1988). Astron. Astrophys. **166**, 75

Mestel, L. (1963). M.N.R.A.S. **126**, 553

Miller, R.H. (1976a). Journ. Comp. Phys. **21**, 400

Miller, R.H. (1976b). Astrophys. J. **207**, 408

Miller, R.H. (1978). Astrophys. J. **224**, 32

ENERGY AND ANGULAR MOMENTUM TRANSFER IN BINARY GALAXIES

P.M.S.Namboodiri and R.K.Kochhar

Indian Institute of Astrophysics

Koramangala Bangalore 560034 India

Abstract

We have numerically studied tidal effects of a massive perturber on a satellite galaxy. The model consists of a spherical satellite galaxy and a point mass perturber and the encounter is non-penetrating. A wide range of density ratios and eccentricities of the relative orbits have been considered. The disruption of the satellite galaxy has been observed when the numerical value of the fractional change in the energy is greater than two. The changes in the energy and angular momentum show smooth variation in the case of unbound orbits and irregular variation in the bound orbit cases. It is shown that for a constant pericentric distance, increasing the density ratio decreases the tidal effects; and for a given density ratio an increase in the eccentricity decreases the tidal effects.

1. Introduction

Tidal disruption and merger are two important processes in the dynamical evolution of a binary stellar system. Many earlier simulations concentrated either on the merger of two galaxies or on the tidal effects on slow hyperbolic collisions. We have performed numerical simulations using Aarseth's N-body 2 code of non-penetrating stellar systems to study the tidal effects on a satellite galaxy due to the passage of a heavy perturber.

2. Numerical simulations

We consider two model galaxies of which the more massive one is a point mass called the primary (or the perturber) and the less massive, the satellite (or the test galaxy). The mass of the test galaxy is denoted by M and that of the primary by M_1. The test galaxy is a spherical cluster of 250 particles having an initial radius R = 20 units. The gravitational constant G is set equal to unity. Aarseth's N-body 2 code is used to integrate the orbits of the particles. The details of the simulations are given in Namboodiri & Kochhar (1990). We consider three models in which the relative orbit of the perturber is parabolic (model P) elliptic (model E) and circular (model C). The initial eccentricity in elliptic case is e = 0.5. In all models the distance of closest approach p = 100. The mean density ρ_h of M within a sphere of radius R_h is

$$\rho_h = \frac{M/2}{4/3\ \pi\ R_h^3} \quad , \qquad (1)$$

where R_h is the half-mass radius of the satellite. The Roche density ρ_R is defined as

$$\rho_R = 2\rho_1 = 2\left[\frac{3\ M_1}{4\ \pi\ p^3}\right] \quad . \qquad (2)$$

The collision parameters are given in Table 1.

3. Results and discussion

The fractional change in the energy $\Delta U/|U|$ is plotted as a function of time by solid lines in figures 1 a, b and c. Here $\Delta U = U_f - U$ where U_f is the energy of the satellite after the encounter and U its unperturbed initial energy. The variation of the fractional angular momentum $\Lambda = J_T/J_{orb}$ is also shown by dashed lines in figures 1 a, b and c. Here J_T is the spin of the test galaxy after the encounter and J_{orb} is the initial orbital angular momentum of the pair. It can be seen that the changes in energy and angular momentum are smooth in unbound orbit encounters. Due to the partial reversal of the tidal acceleration, the changes in energy and

Table 1. Collision parameters and similation results

Model	ρ_h/ρ_R	M_1/M	$\Delta U/\|U\|$	$\Delta U/\|U\|_{IA}$	Λ	Λ_B	$\Delta M/M$
P4	5.34	166.7	2.297	1.021	0.142	9.43E-4	0.272
P5	10.68	83.3	0.970	0.507	0.115	1.09E-3	0.124
P6	21.36	41.7	0.449	0.251	0.058	2.64E-3	0.068
P7	42.71	20.8	0.066	0.122	0.014	1.05E-3	0.024
P8	85.41	10.4	0.051	0.059	0.024	2.32E-3	0.008
P10	341.63	2.6	0.003	0.012	0.002	2.86E-3	0.000
E4	5.34	166.7	8.711	2.420	0.582	7.84E-4	0.396
E5	10.68	83.3	3.774	1.202	0.381	1.08E-3	0.236
E6a	21.36	41.7	1.035	0.595	0.205	1.13E-3	0.140
E6b			1.754		0.419	1.30E-3	0.196
E7a	42.71	20.8	0.396	0.290	0.122	1.66E-3	0.076
E7b			0.838		0.363	8.68E-4	0.156
E8	85.41	10.4	0.167	0.139	0.060	5.02E-3	0.044
E10	341.63	2.6	0.026	0.028	0.070	9.53E-3	0.016
C6	21.36	41.7	11.470	2.008			1.000
C7	42.71	20.8	1.610	0.978	0.297	2.36E-3	0.172
C8a	85.41	10.4	0.553	0.467	0.163	5.44E-3	0.084
C8b			0.539		0.199	1.91E-3	0.128
C10a	341.63	2.6	0.032	0.093	0.029	7.41E-3	0.016
C10b			0.062		0.087	0.011	0.036

angular momentum show irregular variation in bound orbit cases. Disruption of the satellite occurs when $\Delta U/|U| > 2$, which approximately corresponds to a mass loss of 30 - 40 % . Miller (1986) has shown that the condition for a satellite not to be disrupted is $F_T/F_I < 1/4$ where F_T is the maximum tidal force and F_I is the internal force at median radius. The ratio F_I/F_T is nearly equivalent to the density ratio ρ_h/ρ_R and we note that disruption occurs when $\rho_h/\rho_R < 4$. The values of $\Delta U/|U|$, Λ and fractional mass loss $\Delta M/M$ are given in Table 1.

The fractional change in the energy of a galaxy undergoing collision can be obtained under impulse approximation using the following formula (Alladin & Narasimhan, 1982).

$$\left[\frac{U}{|U|}\right]_{IA} = \frac{2\,\Pi^2}{(1+e)^2}\quad\frac{G^2\,M_1^{\,2}}{p^4\,V_p^{\,2}}\left[\frac{R_{rms}}{V_{rms}}\right]^2 . \qquad (3)$$

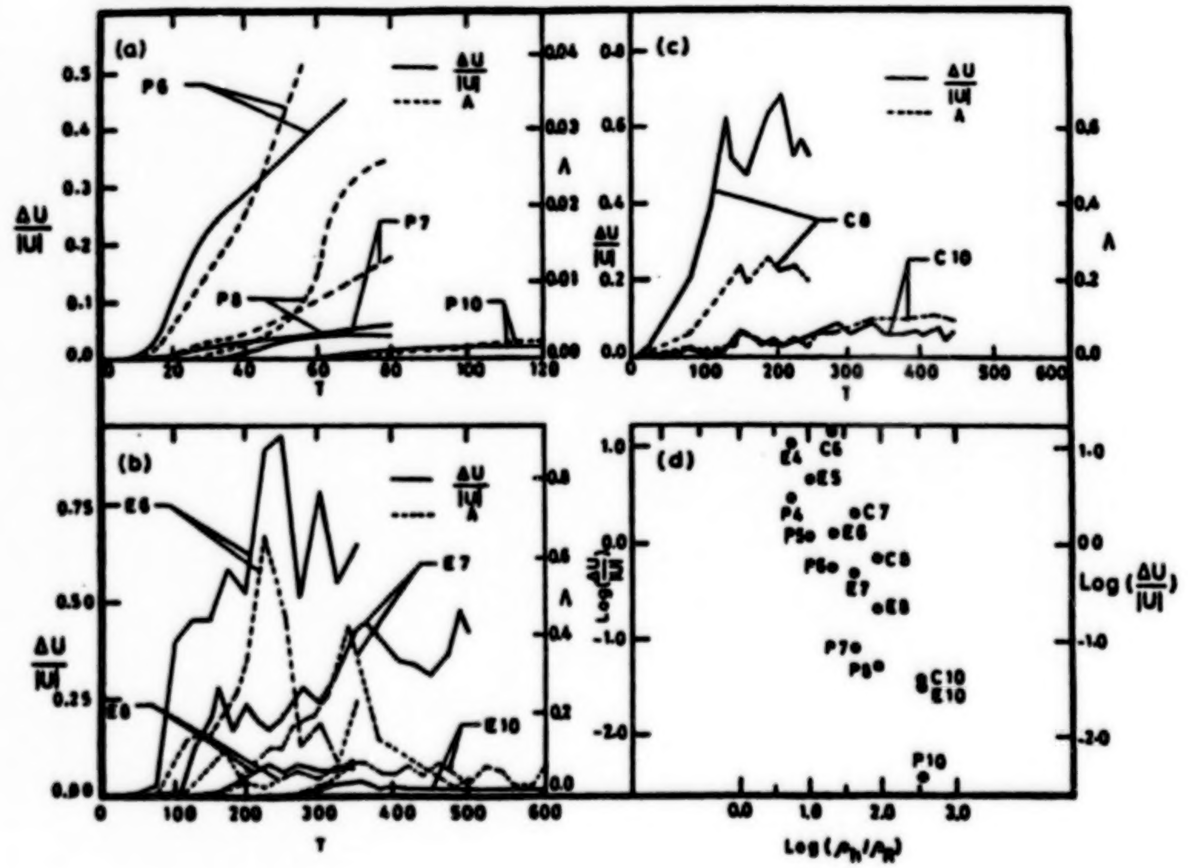

Figure 1. Time variation of $\Delta U/|U|$ and Λ for (a) P models, (b) for E models and (c) for C models. (d) variation of $\log(\Delta U/|U|)$ with $\log(\rho_h/\rho_R)$ for all models.

Here e is the eccentricity of the relative orbit; V_p is the velocity at closest approach; R_{rms} and v_{rms} are the root mean square radius and velocity of the satellite. The values of $\Delta U/|U|_{IA}$ are given in Table 1. The IA estimates agree with numerical results in the range $0.1 < \Delta U/|U| < 2$. The IA underestimates the tidal effects when $\Delta U/|U| > 2$ whereas it overestimates them when $\Delta U/|U| < 0.1$.

In figure 1d, we plot the variation of $\log(\Delta U/|U|)$ vs. $\log(\rho_h/\rho_R)$. It can be seen that for a constant pericentric distance the tidal effect decreases as the density ratio increases. We also note that for a given density ratio an increase in the eccentricity decreases the tidal effect. Our results show that the tidal effect in the parabolic case to be larger than that of the circular case.

4. Conclusions

The main conclusions of our numerical simulations are as follows.

i) Disruption of a satellite galaxy occurs if $\Delta U/|U| > 2$ and in this case the mass loss is greater than 30 - 40 % and $\rho_h/\rho_R < 4$. ii) Impulse approximation estimates of $\Delta U/|U|$ agree with numerical results in the range $0.1 < \Delta U/|U| < 2$. iii) Energy and angular momentum changes of the satellite galaxy show smooth variation in the case of unbound orbit encounters and irregular variation in bound orbit cases. iv) The tidal effect decreases as the density ratio increases and for constant density ratio the tidal effect decreases as the eccentricity of the relative orbit increases.

We thank Drs. S.J.Aarseth for kindly making his N-body code available to us and S.M.Alladin for many useful discussions.

References

Alladin,S.M. & Narasimhan,K.S.V.S. 1982. Phys. Rep. 92, 339.
Miller,R.H. 1986. Astr. Ap. 167, 41.
Namboodiri,P.M.S. & Kochhar,R.K. 1990. M.N.R.A.S.(in press).

SIMULATION OF DISK-DISK ENCOUNTERS WITH CO-MOVING POLAR GRIDS

Heikki Salo
Observatory, University of Helsinki, Finland

Abstract Two-grid simulation method combining advantages of both polar and cartesian mesh-codes is described. In addition to stellar component reacting solely to gravitational forces, gas component is included with dissipatively colliding particles. This allows fairly realistic simulation of planar encounters where both systems contain star+gas disks.

Introduction

Nowadays there exists a wealth of data suggesting connection between galaxy-galaxy interactions and the different kinds of star formation and nuclear activity manifested by them. However, this connection is all but simple: for example there seems to be no correlation between the mutual separation of the systems and the level of activity, implying that there must be a large number of factors governing the response to tidal perturbations. These probably include, in addition to the strength and geometry of the external perturbation, for example the internal dynamical state of the systems as well as the amount of gas and its distribution before the encounter. Also, mass transfers between the components might in some cases have significance. Most importantly, even individual galaxy encounter might turn out to be an evolutionary process with a whole time sequence of qualitatively different types of behaviour.

In order to address the connection between encounters and different types of activity, a new N-body code has been constructed, including both stellar and gaseous components of the galaxies. Therefore in addition to previously well-studied tidal phenomena induced in the mass-distributions of the systems, we can also get a handle to the behaviour of gas, and thus to the probable distribution of recent star formation regions, more closely related to the apparent luminosity distributions. The choice of the simulation model is based on the desire to be able to perform fast systematic surveys of as many as possible different model parameters of the systems. Therefore, 2-dimensional polar-mesh approach was chosen, extended to model two disks simultaneously. Here this method is briefly described together with few preliminary examples of disk-disk simulations.

Simulation method

Two dimensional particle-mesh codes, where total CPU time-consumption scales proportional to particle number, offer a fast method for surveys of the dynamical evolution of essentially flat systems. Self-gravity of the disk is typically calculated in rectangular or polar coordinate grids, by employing FFT-methods. Halos are treated as an inert component, based on the fact that due to their large velocity dispersion they react very weakly on perturbations, at least as long as penetrating encounters are excluded. The advantage of using cartesian grids lies in the fact that simple explicit leapfrog method can be used for orbital integrations. Also the application of FFT is very straight forward, as well as extension to 3-dimensional systems. On the other hand, logarithmic polar grids can offer a much better resolution in the central parts of the system, and are thus very efficient when simulating centrally condensated disks. Therefore, much smaller number of mesh boxes is needed to cover the area of interest with necessary resolution. However, there are disadvantages in using polar coordinates: implicit leapfrog schemas are needed as well as special treatment at the center of the grid. Also, if both systems are to possess a full disk, simple polar methods are not suitable, and cartesian grids covering both systems are usually applied. Since a large area must then be covered with equally sized bins, resolution is inevitably rather poor.

Present simulations try to combine the advantages of both cartesian and polar grids. The gravitational potential is evaluated simultaneously in two moving, mutually overlapping polar grids whose centers are attached to centers of the two halos (Fig. 1). For each particle coordinates are calculated with respect to both grids, while its mass is assigned only to the disk it originally belonged. At each step the logarithmic polar grid method of Miller (1976) is used for both grids separately after which forces from both grids are added together. Thus the good resolution is retained near the centers of both systems. On the other hand, orbital calculations, both for the particles and the halo centers, are performed in cartesian coordinate system, thus allowing the use of fast explicit leapfrog. This fact more than outweigths the extra time consumption in transformations between coordinate systems. Notice, that allowing the halos to move freely in the inertial frame is totally equivalent to the usual method of fixing the coordinate system to the main galaxy and letting the point-mass perturber to exert both direct and indirect forces. Since logaritmic grids can cover large areas with very limited number of mesh points there is practically no

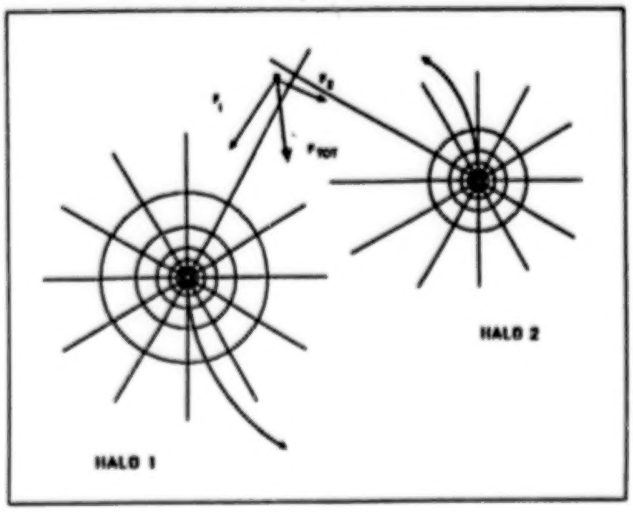

Figure 1. Schematic representation of the 2-grid coordinate system. Actual runs employ 36 azimuthal and 48 radial bins covering the area from 0.005 to about 20 initial disk radii.

restrictions on the distance between the systems: large initial separations can be used, thus assuring that systems have time to settle into steady state before tidal forces start to influence their dynamics.

Gas component

A certain fraction of the particles represents gas clouds, which are allowed to experience dissipative impacts. In contrast to typical treatment in N-body simulations where collisions are assumed to take place whenever two clouds fall into same 'collisional bin', here the orbits are followed to the exact location of impact, as is commonly done in collisional simulations of planetary rings (e.g. Salo, 1987, 1990a; Wisdom and Tremaine, 1988). Due to the simplicity of the leapfrog algorithm, even multiple collisions/time-step/cloud can be correctly calculated with iterative methods. Compared to bin methods, exact collisional calculations make it possible to follow to greater accuracy the formation of shock fronts in gas due to tidal perturbation. This is especially important in the case the gas disks penetrate each other, since then due to large streaming motions many impacts would be lost in collision bin methods (see legend for Fig. 3) and the results of the experiment might be even qualitatively different.

Applications and future refinements

So far the code has been applied to study tidal triggering of bars (Salo, 1990b), which has previously been shown (Noguchi, 1987, 1988) to be potentially able to cause large-scale infall of gas to central regions of galaxies, thus offering a possible source of fresh material for active nuclei. These experiments confirmed Noguchi's results, but also illustrated the dependence of bar formation on several factors like rotation curve, disk/halo mass-ratio, stressing the point that gas infall not necessarily occur in interaction, especially not for systems with high degree of central condensation. Here a few illustrative examples are shown for disk-disk encounters: Fig. 2 displays the different evolutionary phases during an encounter (including formation of shock fronts in various locations, as well as the final bar driven infall) while Fig. 3 gives an example how internal kinematics (sense of rotation) can affect induced activity. In future the code will be used for systematic surveys of activity in disk-disk encounters, and more realistic treatments for the cloud ensemble will be explored, including models where accretional and fragmentational evolution of clouds is taken into account. Possibility to extend multiple polar-grids to 3 dimensions is also investigated.

References

Miller, R.: 1976, *J. Comp. Phys.* **21**, 400.

Noguchi, M.: 1987, *M.N.R.a.S.* **228**, 635.

Noguchi, M.: 1988, *Astron. Astrophys.* **203**, 259.

Salo, H.: 1987, *Icarus* **70**, 37.

Salo, H.: 1990a, *submitted to Icarus.*

Salo, H.: 1990b, *submitted to Astron. Astrophys.*

Wisdom, J. and Tremaine, S.: 1988, *A.J.* **95**, 925

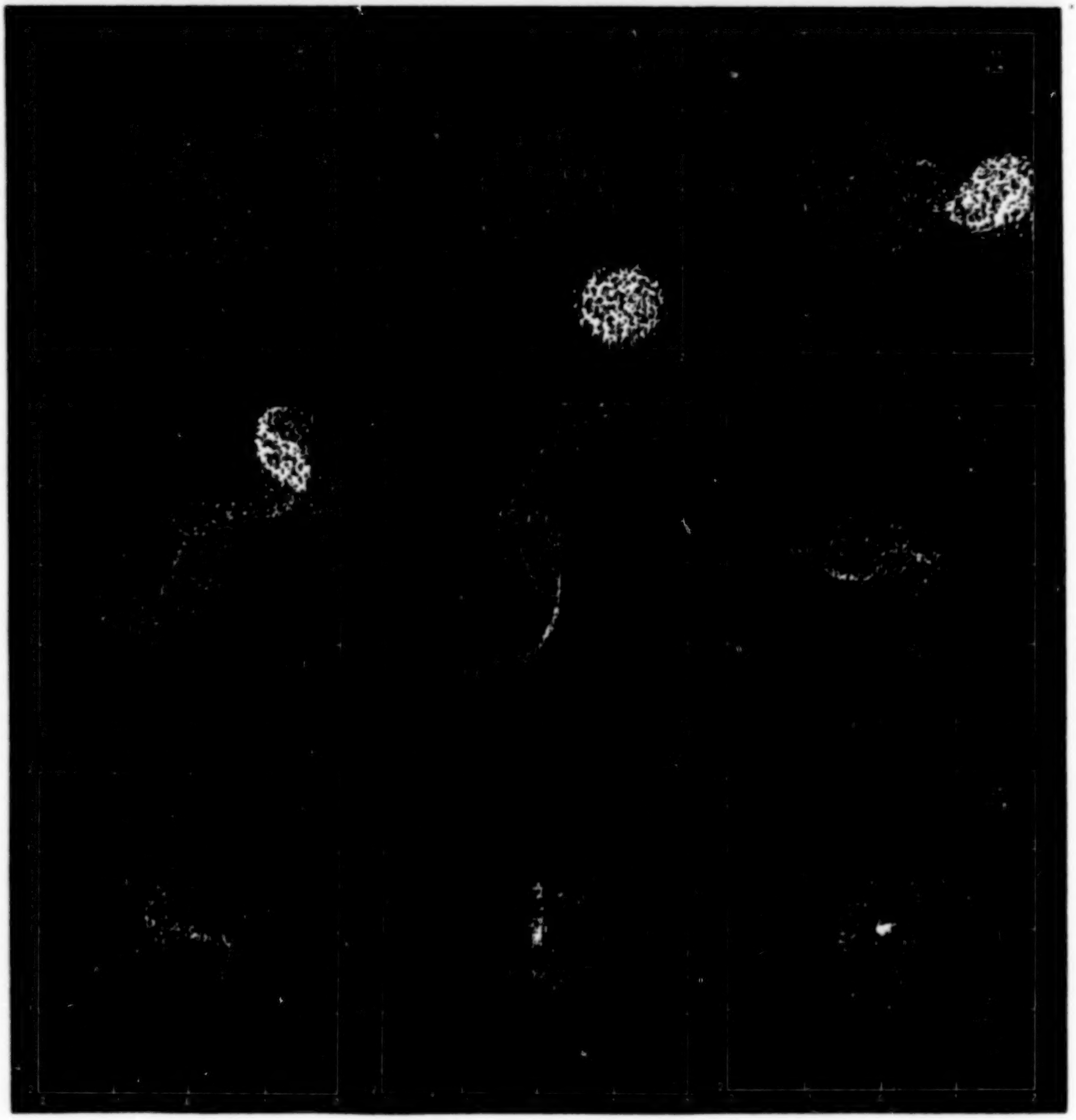

Figure 2. Example of disk-disk encounter in the frame centered at the main galaxy. Stellar components were represented with 20000 + 10000 particles (Toomre disks) containing 1/3 of the total mass, the rest being in inert halos (Plummer spheres). Companion galaxy ($m_2 = 0.5m_1, r_2 = 0.5r_1$) was in direct parabolic orbit with minimum separation of $r_1 + r_2$. Scale-radii for both the disk and the halo distributions were 0.5 and 0.2 times the initial disk radii for the main galaxy and the companion, respectively. Gas components (shown) were represented by 4000 + 1000 uniformly distributed clouds. One can see the formation of weak spiral structures before the encounter, as well as the shocks caused by direct tidal perturbations. In post-encounter phase stellar bar is formed (isolated model is stable against bar formation), forcing gas alignment as well as flow into nuclear regions due to angular momentum exchange in non-axisymmetric bar-potential. In the more compact secondary galaxy no infall occurred but a gas ring was formed. Notice that frames are not evenly spaced in time. This simulation with 3000 steps required about 2000 secs in Cray X-MP (only about 300 secs without gas cloud collisions). Frames are extracted from a MacIntosh Hypercard-animation sequence, able to display about 10 frames/sec in MacII cx (stack developed by T. Tokkonen at the Dept. of Astronomy, Univ. of Oulu, Finland).

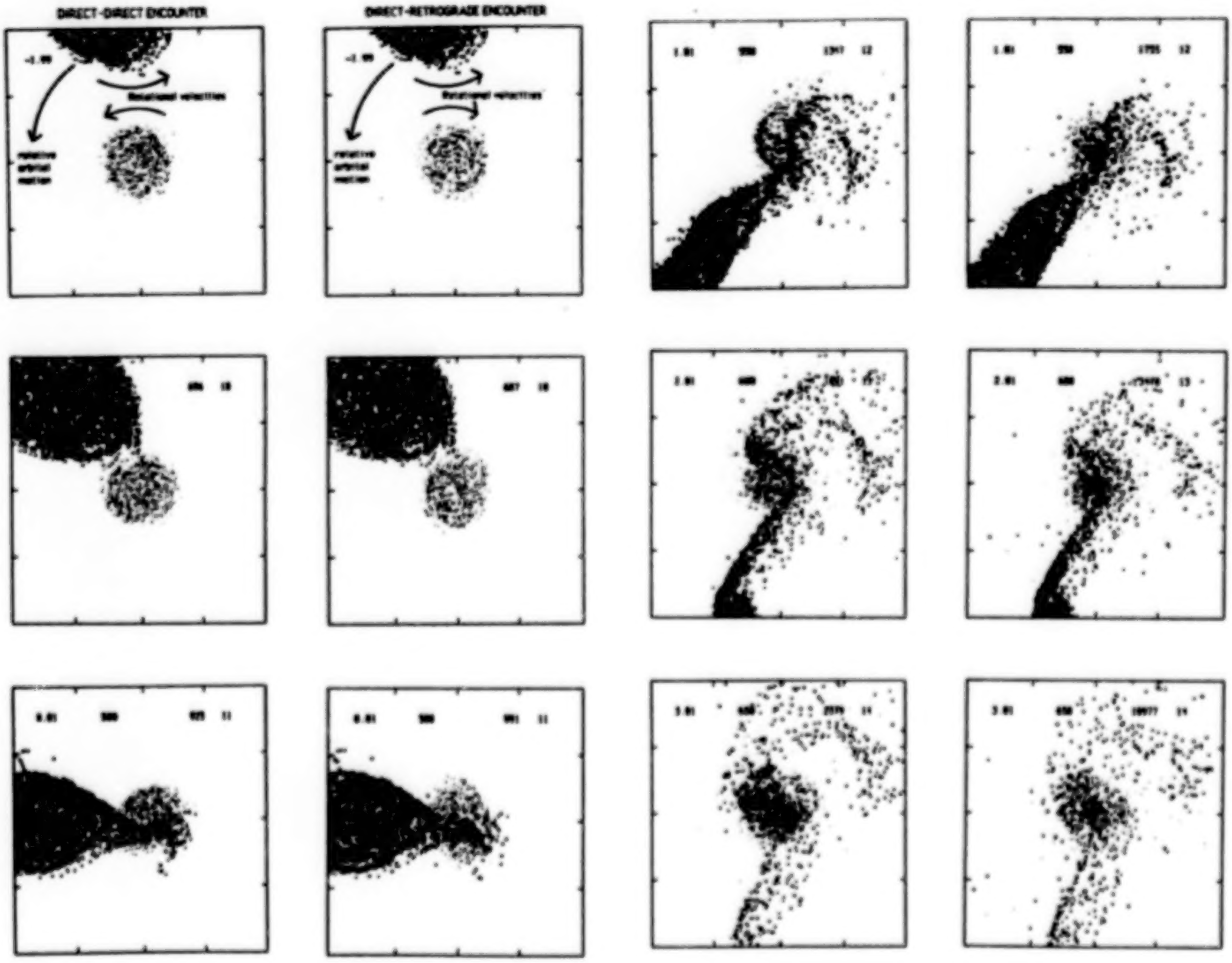

Figure 3. Details of the behaviour of the companion galaxy in the simulation of Fig.2. (direct-direct) and in another run with same parameters except that the direction of the rotation of the companion was reversed (direct-retrograde). In the direct-direct case the response of stellar components is strongest (both develop bridges etc.) but due to superposition of orbital and rotational velocities gas reacts strongest in the retrograde case where large net streaming motions occur between clouds originating from different systems. This leads to strong shocks and rapid loss of rotational angular momentum, and fast infall of gas just past the closest encounter, when the tidal bridge from the main galaxy hits the secondary. On the direct-direct case no infall occurred in the secondary. In an additional direct-retrograde experiment using collision bin method, the infall was considerably delayd, by almost 5 galaxy rotations. Notice, however, that the role of mass transfer is here considerably exaggareted due to planar geometry.

WHAT DETERMINES THE BULGE TO DISK RATIO OF GALAXIES

Nico Roos
Sterrewacht Leiden
Leiden, the Netherlands

Abstract

Galaxies having the same luminosity may have very different bulge to disk ratios, while the mean bulge to disk ratio slowly increases with total luminosity (Schechter and Dressler, 1987, Sandage et al., 1985). Such a behaviour is expected if ellipticals and the spheroidal components of disk galaxies are produced by secondary accretion of galaxies by larger galaxies. This is illustrated using a simple toy model of the evolution of the mass function of galaxies due to galaxy mergers.

Introduction

The form of the galaxy luminosity function (all types included) is not sensitive to the environment. However, the fraction of early type galaxies increases slowly with local galaxy density (Dressler, 1980, Postman and Geller, 1984). The increase in the fraction of early-type galaxies occurs predominantly at the high luminosity end of the luminosity function (Schechter and Dressler, 1987, Sandage et al., 1985). These are important clues to our understanding of the origin of Hubble sequence of galaxies. Another, perhaps equally important clue is that galaxies having similar luminosities and similar environments can have very different bulge to disk ratios (Schechter and Dressler, 1987; see figure 1). These facts taken together suggest that some stochastic process acting preferentially in regions of higher galaxy density, and affecting predominantly the more massive galaxies, has transformed some fraction of (originally late-type) galaxies into early-type galaxies. Galaxy interactions and mergers are of course prime candidates for this process.

Galaxy mergers are a natural part of the hierarchical clustering process in bottom-up scenarios for the formation of galaxies and clusters such as the Cold Dark Matter cosmology (Blumenthal et al. 1984). Luminous galaxies are supposed to form dissipatively in the potential wells of the dark matter. They may then survive as rapidly rotating and flattened subunits during the subsequent formation of groups and clusters (White and Rees,1978, Carlberg and Couchman, 1989). In such a scenario it is plausible that the formation and evolution of galaxies has evolved from a relatively rapid, dissipational collapse of mainly gaseous matter, towards slow accretion of more clumpy, mainly stellar systems. It seems plausible that galaxies were formed as gaseous disk-like systems at a redshift of 2 to 3 (Wolfe, 1989). Star formation in these sytems may have taken a much longer time and may have occurred in bursts (Lilly and Longair, 1984, Djorgovski, 1987), perhaps triggered by accretion events. One of the important questions is then: did bright elliptical galaxies and the spheroidal components of disk galaxies form early, when galaxies were still mainly gaseous (Silk and Norman, 1981), or did they form later? One way of obtaining an answer is to study the effects of galaxy interactions and mergers at the present epoch and try to make an extrapolation into the past.

This approach lead Toomre and Toomre (1972, see also Toomre 1977) to suggest that (bright) elliptical galaxies were the remnants of past mergers between spiral galaxies. This suggestion gained support from numerical studies of mergers in collapsing groups and clusters (Roos and Norman, 1979, Roos and Aarseth, 1982) and from cosmological simulations of galaxy clustering (Aarseth and Fall, 1979, Jones and Efstathiou, 1979, Roos, 1981). Several objections were raised against this hypothesis (Ostriker, 1980, Tremaine 1981, van den Bergh, 1984, Carlberg, 1986). The most important ones are probably: (i) can the high phase space density in the central regions of elliptical galaxies be explained without invoking extra dissipation (see Lake, 1989), and (ii) why do ellipticals have more globular clusters per unit luminosity than disk galaxies. In the last few years the evidence in favour of the merger hypothesis has grown considarably by both observational and theoretical studies of merger remnants (Schweizer, 1986, Lake and Dressler, 1986, Barnes, 1988), by the discovery of shells and ripples around 20% of ellipticals (Malin and Carter, 1983) and by studies of the kinematics of ellipticals (Franx and Illingworth, 1988).

Most mergers have occurred between galaxies of unequal mass. In a previous paper (Roos, 1981, hereafter Paper I) it was therefore hypothesized that infall of smaller galaxies would contribute to the formation of a galactic bulges along with thickening (and ultimately destruction) of a stellar disk and depletion of gas, leading to evolution of galaxies along the sequence (Sc→Sb→Sa)→SO→E. The most recent estimate of the present merging rate among galaxies indicates that a typical galaxy with luminosity L^*, at the break of the galaxy luminosity function has accreted about $0.3L^*$ since a redshift $z = 0.75$ (Bahcall and Tremaine, 1988), enough to account for a typical bulge mass. Some aspects of this hypothesis such as the morphology - density relation were investigated in Paper I. It was also found that the luminosity function should depend on galaxy type, the fraction of early type galaxies increasing with luminosity. This prediction is confirmed by the work of Sandage et al. (1985). The large scatter in bulge to disk ratios of galaxies having similar total luminosity provides a new argument in favour of the merger hypothesis for the origin of the spheroidal components of galaxies. This is illustrated in the next section using the simple Monte Carlo model of Paper I. A more extensive discussion of the distribution of bulge to disk ratios of galaxies and the dependence of the luminosity function on galaxy type will be published elsewhere.

A toy model for spheroid growth

As in paper I we assume that initially all the galactic mass is in disks. with a mass function given by the Schechter form:

$$n(M)dM \propto M^{\alpha} exp(M/M^*),$$

where $\alpha = -1.25$. We further assume that the mass to light ratio does not depend on mass. The evolution of this distribution due to merging is then simulated numerically by choosing pairs (M_1, M_2) with a probability proportional to $(M_1 + M_2)^{\lambda}$. The bulge to

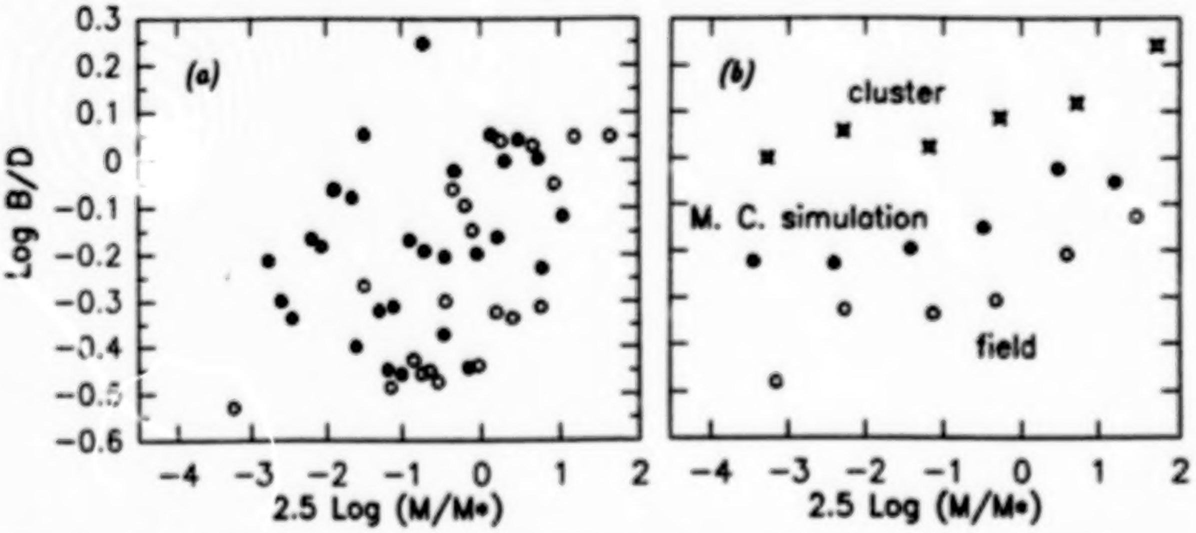

Figure 1 *(a) Average bulge to disk ratios as a function of mass (assuming constant M/L) for Schechter and Dressler's sample of field galaxies (open dots) having apparent visual magnitude brighter than 16.5. Each point represents an average for 10 galaxies having similar luminosities. The filled symbols are results from the toy model discussed below* ($\lambda = 0$). *(b) Idem, but here the average is determined over all galaxies in a particular magnitude interval. The open stars are mean bulge to disk ratios for Dressler's sample of cluster galaxies (see Schechter and Dressler, 1987)*

disk ratio of a galaxy is thought to be represented by Δ, the ratio of total accreted mass over the original mass of the galaxy. The dynamical friction time of a satellite orbiting in a larger (spherical) galaxy is roughly comparable with the orbital time divided by the mass ratio (satellite mass over the mass of the galaxy inside the orbital radius of the satellite) of the two systems. The satellite is tidally stripped as it moves inward. The mass ratio may increase or decrease with separation depending whether the density distribution in the parent galaxy is steeper or shallower than the density distribution of the satellite. So, satellites must be sufficiently massive and sufficiently centrally concentrated in order to have contributed to the mass of the central spheroid in the last 10 Gyr. Note that the dominant contribution to Δ comes from the more massive galaxies for $\lambda > -0.75$. The total number of mergers determines the mean Δ, which may be used as a scaling parameter to be compared with the mean B/D of galaxies. This parameter is a slowly increasing function of local galaxy density (see Paper I, and Roos and Aarseth, 1982). The results for $\lambda = 0$ are shown in Figure 1. Figure 1a illustrates the large (intrinsic) scatter in the observed values of B/D. The distribution of Δ in the model is similar to the observed distribution of bulge to disk ratios. The mean Δ increases slowly as a function of mass (figure 1b). The vertical position of this relation is determined by the total number of mergers, while its slope is determined by the value of λ.

In the Press and Schechter theory for hierarchical clustering (Press and Schechter, 1974) the slope of the low mass end of the mass function is determined by the index n of the initial density fluctuation spectrum: $\alpha_{PS} = (n-9)/6$. The Monte Carlo integration of the coagulation equation presented here also leads to a self-similar power law mass function with an exponential cut-off. In our case $\alpha_{coag} \approx -3\lambda/2$ for $0 < \lambda \leq 1$ (Nakano, 1966, see also Silk and White, 1978). In the cosmological simulations of paper I it was indeed found that the merging probability (and the amplitude of the two-point correlation function) were proportional to mass for an initially random distribution ($n = 0$) of particles. It may thus be possible to give a self-consistent description of the evolution of the mass function of galaxies and clusters which is based on the coagulation formalism.

Discussion

There is now considerable evidence that ellipticals are the remnants of past mergers. Ellipticals and bulges have similar properties (Davies, 1987, Kormendy and Djorgovski, 1989). It is therefore likely that they have a similar origin. Photometric and kinematic studies of galaxies with peanut-, X- or box-shaped bulges (Whitmore and Bell, 1988, Binney and Petrou, 1985, Statler, 1988) and of ripples in disk galaxies (Schweizer and Seitzer, 1988, Wallin and Struck-Marcell, 1988) lend support to the merger hypothesis for the origin of spheroidal components of galaxies. Quinn and Goodman (1986, see also Hernquist and Quinn, 1988) have performed numerical simulations of satellite accretion by stellar disks showing that stellar disks are puffed up considerably by a satellite only one tenth the mass of the parent galaxy. This seems to require that stellar disks are (re)formed after such an accretion event. Freeman (1987) has drawn attention to connection between thick disks and bulges. He also proposes that matter stripped from sinking satellites has contributed to the halo population and the thick disk of the Milky Way. Observational evidence for such accretion events during the lifetime of the Milky Way is presented by Searle and Zinn (1978) and Rodgers and Paltaglou (1984).

The main purpose of this contribution is to draw attention to the observational fact that galaxies having similar luminosities and similar environments may have very different bulge to disk ratios. this property is not easily explained in theories in which galaxy formation is regarded as a monolithic collapse of a single gas cloud (Eggen et al., 1962), while it is readily explained as a result of secondary accretion of smaller galaxies. The observed increase of the fraction of early-type galaxies with luminosity and with local galaxy density are also expected in this model. Further investigations of the evolution of galaxies due to accretion of smaller galaxies may prove to be very fruitful.

References

Aarseth, S. J., and Fall, S. M. 1980, *Ap. J.* **236**, 43.
Bahcall, S. R. and Tremaine, S. 1988, *Ap. J. Letters* **326**, L1
Barnes, J. E. 1988, *Ap. J.* **331**, 699.
Binney, J, and Petrou, M. 1985,*M.N.R.A.S.* **214**, 449.
Blumenthal, G. R., Faber, S. M., Primack, J. R., and Rees, M. J. 1984, *Nature* **311**, 517.
Carlberg, R. G. 1986, *Ap. J.* **310**, 593.
Carlberg, R. G. and Couchman, H. M. P. 1989, *Ap. J.* **340**, 47.
Davies, 1987, in IAU Symposium bf 127 *Structure and Dynamics of Elliptical Galaxies*, ed. T. de Zeeuw (Dordrecht: Reidel), p 63.

Djorgovski, S. 1987, in *Starbursts and Galaxy Evolution*, ed. T. X. Thuan et al. (Moriond, Edition Frontières) p 401.

Dressler, A. 1980, *Ap. J.* **236**, 351.

Eggen, O., Lynden-Bell, D., Sandage, A. 1962, *Ap.J.* **136**, 748.

Franx, M. and Illingworth, G. D. 1988, *Ap. J. Letters* **327**, L55.

Freeman, K. 1987, *Ann. Rev. Astr. Ap.* **25**, 603.

Hernquist, L., and Quinn, P. J. 1989, in *The epoch of Galaxy Formation*, eds. C. S. Frenk et al. (Dordrecht: Kluwer Academic Publishers), p 427.

Jones, B. J. T., and Efstathiou, G. 1979 *M. N. R. A. S.* **189**, 27.

Kormendy, J., and Djorgovski, S. 1989, *Ann. Rev. Astr. Ap.* **27**, .

Lake, G., and Dressler, A. 1986, *Ap. J.* **310**, 605.

Lake, G. 1989, *Astron. J.* **95**, 1312.

Lilly, S. J., and Longair, M. S. 1984, *M. N. R. A. S.* **211**, 833.

Malin, D. F., and Carter, D. 1983, *Ap. J.* **274**, 534.

Nakano, T. 1966, *Progr. Theor. Phys.* **36**, 515.

Ostriker, J. P. 1980, *Comments on Astrophysics* Vol. **8**, 177.

Postman, M. and Geller, M. J. 1984, *Ap. J.* **281**, 95.

Press, W. H., and Schechter, P. 1974, *Ap. J.* **187**, 425.

Quinn, P. J., and Goodman, J. 1986, it Ap. J. **309**, 372.

Rodgers, A., and Paltaglou, G. 1984, *Ap. J. (Letters)* **283**, L5.

Roos, N., and Norman, C. A. 1979, *Astr. Ap.* **76**, 75.

Roos, N. 1981, (Paper I), *Astr. Ap.* **95**, 349.

Roos, N., and Aarseth, S. J. 1982, *Astr. Ap.* **114**, 42.

Sandage, A. Binggeli, B., and Tammann, G. A. 1985, *Astron. J.* **90**, 1759.

Schechter, P. L., and Dressler, A. 1987, *Astron. J.* **94**, 563.

Schweizer, F. 1986, *Science* **231**, 227.

Schweizer, F., and Seitzer, P. 1988, *Ap. J.* **328**, 88.

Searle, L., and Zinn, R. J. 1978, *Ap. J* **225**, 357.

Silk, J., and Norman, C.A. 1981, *Ap. J.* **247**, 59.

Silk, J., and White, S. D. M. 1978, *Ap. J. Letters* **223**, L59.

Statler, T. S. 1988, *Ap. J.* **331** 71.

Toomre, J., and Toomre, A. 1972, *Ap. J.* **178**, 623.

Toomre, J. 1977, in *The Evolution of Galaxies and Stellar Populations*, eds. B. Tinsley and R. Larson (Yale University Press), p 420.

Tremaine, S. 1981, in *The Structure of Normal Galaxies*, ed. S. M. Fall and D. Lynden-Bell (Cambridge: Cambridge University Press), p 67.

van den Bergh, S. 1984, in *Clusters and Groups of Galaxies*, eds. F. Mardirossian et al. (Dordrecht: Reidel), p 139.

Wallin, J. F., and Struck-Marcell, C. 1988, *Astron. J.* **96**, 1850.

White, S. D. M., and Rees, M. J. 1978, *M. N. R. A. S.* **183**, 341.

Whitmore, B. C. and Bell, M. 1988, *Ap. J.* **324**, 74.

Wolfe, A. M. 1989, in *The Epoch of Galaxy Formation*, eds. C.S. Frenk et al. (Dordrecht: Kluwer Academic Publishers), p 101.

DISCUSSION

Whitmore: If bulges are produced by merging with smaller mass galaxies we would expect that roughly 50% are counter rotating with respect to the disk. I am not aware of any such cases. Are you?

Roos: No, I am not, but I am not sure we should expect that. I expect that big bulges indeed are very similar to elliptical galaxies. They might also show peculiar kinematics as found in many ellipiticals. Small bulges or spheroids, however, may be formed by small nearby satellite galaxies. I could imagine that in the tidal torque model for the origin of angular momentum of disk galaxies the orbital angular momentum of nearby small companions is correlated with the angular momentum of the big galaxy.

Navarro: How do thin disks survive the continuous merging process in your model? Also, I did not understand how you assign B/D ratios to your merger.

Roos: As a crude estimate I have assumed that disks are destroyed if the accreted mass is comparable to the disk mass. For smaller accreted masses I expect that accretion of smaller masses will produce thick disks. It seems likely that after such an accretion event the remaining gas in the disk will settle again in a thin disk. Regarding your second question, I just assumed that accretion of a smaller galaxy by a big disk galaxy will lead to the growth of the central bulge or spheroid.

Noreau: I have a big worry with your merging scheme from chemistry arguments. Smaller systems are usually metal poor. How can they contribute in building metal-rich bulges?

Roos: Small galaxies are more numerous, but the galaxies which contribute most to the mass of the central spheroid will have a mass which is comparable to the bulge mass. Such galaxies may not be so metal-poor. Nevertheless I do expect that many big bulges contain a population of metal-poor stars. Let me also make it clear that I did not consider the fate of the gas, not because I think it is not important, but because it is much more difficult to model. I merely want to point out that it may be possible to explain many aspects of the morphological evolution of galaxies in the simple-minded model I discussed.

Zasov: My question is related to the B/D ratio and the luminosity modelling. The luminosity of a galaxy, especially a disk, is a very complex function which depends on the rate of evolution (which, in turn, may depend on B/D), internal absorption, etc. Isn't it more convenient to consider the velocity of rotation or, say, the halfwidth of the HI line? I suppose that if we take those instead of the luminosity, the difference between cluster and field galaxies may disappear.

Roos: I have assumed that the mass-to-light ratio is constant. It would indeed be interesting to know how M/L varies with morphological type and/or with galaxy luminosity.

VIII. CLASSICAL THEORY

OF

MULTIPLETS

DYNAMICAL THEORY OF DENSE GROUPS OF GALAXIES

Gary A. Mamon
DAEC, Observatoire de Meudon
Meudon, France

It is well known that galaxies associate in groups and clusters. Perhaps 40% of all galaxies are found in groups of 4 to 20 galaxies (e.g., Tully 1987). Although most groups appear to be so loose that the galaxy interactions within them ought to be insignificant, the apparently densest groups, known as *compact groups* appear so dense when seen in projection onto the plane of the sky that their members often overlap. These groups thus appear as dense as the cores of rich clusters. The most popular catalog of compact groups, compiled by Hickson (1982), includes isolation among its selection critera. Therefore, in comparison with the cores of rich clusters, Hickson's compact groups (hereafter, HCGs) appear to be the densest isolated regions in the Universe (in galaxies per unit volume), and thus provide in principle a clean laboratory for studying the competition of very strong gravitational interactions. The $64,000 question here is then: *Are compact groups really bound systems as dense as they appear?* If dense groups indeed exist, then one expects that each of the dynamical processes leading to the interaction of their member galaxies should be greatly enhanced. This leads us to the questions: *How stable are dense groups? How do they form?* And the related question, fascinating to any theorist: *What dynamical processes predominate in dense groups of galaxies?*. If HCGs are not bound dense systems, but instead 1D chance alignments (Mamon 1986, 1987; Walke & Mamon 1989) or 3D transient cores (Rose 1979) within larger looser systems of galaxies, then the relevant question is: *How frequent are chance configurations within loose groups?* In this review, I will answer these last four questions after comparing in some detail the methods used and the results obtained in the different studies of dense groups, while in the accompanying contribution, I will attempt to reconcile the recent observations of galaxy interactions in HCGs with a negative answer to the first question.

Constructing dense groups

At first approximation, a group of galaxies is a collection of galaxies, each of which is a collection of point masses. In fact, one must add to this model a component for the dark matter that occupies perhaps 90% of the total mass, and here lies perhaps the greatest uncertainty in the modelling, whether on paper or numerical. In practice, either one assumes that the dark matter lies mainly in individual halos around galaxies, or else one has it stretch over an intergalactic background (hereafter, IGB). As for the galaxies, they can be spiral, with disk, bulge and dark halo, or elliptical (with in principle a dark halo too).

Studies of dense groups have always been numerical in nature (see the following section). The simulations published in the litterature can be subdivided into two main categories. In "self-consistent" simulations, authors have attempted to reproduce the galaxies in the groups with as many particles as computationally feasible to run at least one simulation. On the other hand, some authors have sacrificed accuracy by representing each galaxy as a single particle (Mamon 1987 models the IGB in the same way) in order to achieve computational speed. In this second scheme the dynamical processes must be explicitly included in the computational code, hence I coin the name "explicit-physics" method. Alternatively one could call the two the "slow and clean" and the "quick and dirty" methods. In Table 1 below, I list the pros and cons of each of these two methods.

Table 1: Two opposite philosophies with their advantages

SELF-CONSISTENT (many particles per galaxy)	EXPLICIT-PHYSICS (one particle per galaxy)
Confidence in results	Explore parameter space
Not only virialised initial conditions	Obtain statistical sets
Accurate description of close encounters	Compare dynamical processes
Simpler to code	
Project pretty movies	

Neither of the two methods is intrinsically superior to the other, but rather complementary. For example, if one is to understand the evolution of dense groups, one needs to study groups with different initial densities, membership, dark matter location, etc. The parameter space thus turns out to be quite large. Moreover, to build statistical sets of simulated evolving groups, one needs a quick method. What is the need for so many simulations? First, one would like to know if a small fraction (say 5%) of dense groups can survive as such for long periods of time. Second, one would like to perform a variety of statistical tests to both the simulated groups and the observed HCGs. For these reasons, a set of roughly 1000 simulations of dense groups seems required if one is to understand the evolution of dense groups, and at this point these are done by the less-accurate explicit-physics method. An interesting feature of the explicit-physics method lies in the fact that the importance of each dynamical process can be gauged by simulating groups with the dynamical process artificially turned off and comparing the results with those using the standard physics. However one should also stress that, simulations of the self-consistent type are required to give confidence to the builders of the explicit-physics simulations of the meaningfulness of their results. In Table 2 are listed the self-consistent studies of dense groups.

Table 2: Self-consistent studies

Author(s)	N	[illegible]	Galaxies	IGM	Init. Conds.	IMF	$\mathcal{N}$
Carnevali *et al.* (81)	10–20	20	Sph	0	Vir	δ	3
Ishisawa *et al.* (83)	10	100	Sph	0	Coll	δ	1
Cavaliere *et al.* (83)	10–20	20?	Sph	0.5–0.9	Vir, Exp	δ, Schechter	5?
Barnes (85)	5–10	75–300	Sph	0–0.75	Vir, Exp, Coll	δ	27
Ishisawa (86)	10–50	100	Sph	0	Coll, ~ Vir	δ	7
Barnes (89)	6	8k–16k	D+B+H	0	Vir	1,1,1,1,2,2	1

NOTES: N is the number of galaxies per group, n the number of particles per galaxy, "Galaxies" refers to the galaxy model (Sph → spherical, and D+B+H → disk+bulge+halo), "IGM" is the fraction of intergalactic mass, "Init. Conds." refers to the initial conditions (Vir → viri-

alized, Coll → collapsing, and Exp → expanding), "IMF" refers to the initial mass function (δ → equal masses), $\mathcal{N}$ is the number of simulations run.

Dynamical processes

The one physical mechanism at work in dense groups is classical gravitation, i.e., the direct gravitational attraction between galaxies and between galaxies and the IGB, dynamical friction of galaxies against the IGB and against the stars of other galaxies, tidal processes, and mergers. I analyze each in turn.

Galaxy motions are set by their gravitational attraction to one another, as well as to the IGB. Whatever the type of simulation method used, one has to modify the potential carried by a particle at close range. For the self-consistent simulations, this modification is required to avoid a spurrious rapid relaxation caused by close encounters. On the other hand, for the explicit-physics simulations, this *potential softening* is done to mimic the extended sizes of galaxies. In my thesis (Mamon 1985), I've shown that, for realistic spherical galaxies of different masses and density profiles, the standard softening $\phi(r) = -Gm_1m_2/(r^2 + \epsilon^2)^{1/2}$ produces more accurate *gradients* than any $\gamma \neq 2$ in the more general formula $\phi(r) = -Gm_1m_2/(r^\gamma + \epsilon^\gamma)^{1/\gamma}$. I also showed that the softening length ϵ is given to typically 25% accuracy by the rms of the half-mass radii of the two objects.

If the IGB is treated as a smooth medium (as in the explicit-physics methods), one needs to add the collective of effect of the encounters of galaxies with the much less massive particles that make up the IGB (e.g., black holes, brown dwarfs, or cold dark matter particles), known as *dynamical friction*. The analogous dynamical friction of the galaxies by the stars of the galaxies it encounters is implicit in any N-body explicit-physics or self-consistent method; and the latter method of course also includes implicitly the dynamical friction against the IGB, modelled as a collection of particles.

In dense environments, tidal effects are strong enough to significantly alter the member galaxies. Tidal processes come in two sorts: *collisional tides* caused by the passage of another galaxy, and the global *IGB tide* due to the non-uniform potential gradient of the IGB. By definition, tides cause various parts of a test galaxy to be subject to different accelerations. The galaxy is thus stretched and it's morphology can become quite disturbed, and can lose mass as some of its stars are accelerated beyond their escape velocity. Moreover, the stretching of the galaxy implies that energy is being imparted from the orbital motion of a colliding pair into their internal motions. With self-consistent simulations, collisional tides are implicit. As tidal processes cause the galaxies to shed stars, the IGB grows, and IGB tides are thus also implicit in this type of simulation. In explicit-physics simulations, one must include these tidal processes by hand, which is not always easy given the little that is understood about tides. More precisely, one must include a mass-loss, an internal energy-gain, a loss of orbital energy (often called *tidal friction*), hence a reduced galaxy velocity, and if the modeller has put some structure into his galaxies, he must know how to alter it. This is usually done by analysing the results of self-consistent two-body encounters usually done by others. The situation is all the more complicated that these parameter changes are a function of the internal orbits in the galaxies (Dekel *et al.* 1980) and of the galaxy orbits around the IGB (Mamon 1987).

An extreme case of the combination of dynamical friction of a galaxy against stars from another nearby galaxy, and collisional tides due to this encounter causes such a great loss of orbital energy that an unbound pair can become bound, and even worse, a bound pair can merge. Once again, this event occurs naturally in self-consistent simulations, but has to be mimicked explicitly in the explicit-physics type of calculation. And similarly to the case of non-merging encounters, one must specify for the larger ("cannibal") galaxy its new mass (some of the merging mass escapes to the IGB), internal and orbital energies, and structure.

In Table 3 below, I list the main ingredients of all the group and cluster simulations known to me that included at least tides or mergers. Note that the physics is the same for groups and clusters, which explains why cluster simulations are present in this table.

Table 3: Explicit-physics studies

Author(s)	Meth	N	Soft	IGB	ICs	IMF	DF	Merg	Tides	$\mathcal{N}$
Richstone (76)	QA	NR	NR	No	V	δ,O	NR	No	C	5
Jones & Efstathiou (79)	N	500	Fix	No	E	δ	NR	Yes	No	4
Roos & Norman (79)	N	10–60	Fix	No	V	δ	NR	Yes	C	4
Aarseth & Fall (80)	N	1000	$r_{1/2}$	No	E	δ,O	NR	Yes	No	6
Cooper & Miller (81)	N	100	Fix	No	V	δ	NR	Yes	No	3
Roos (81)	N	400	r	No	E	δ	NR	Yes	C	14
Roos & Aarseth (82)	N	350–700	r	No	E	S	NR	Yes	C	5
Schneider & Gunn (82)	N	1	NR	Yes	Circ	NR	Yes	NR	IGB	3
Miller (83)	3	100?	NR	Yes	E,V	δ,S	No	Yes	C	18
Merritt (83)	QA	NR	NR	Yes	V	S	No	No	C	3
Richstone & Malumuth (83)	3	100–1k	NR	Yes	V	δ,S	Yes	Yes	C	41
Malumuth & Richstone (84)	3	100–500	NR	Yes	V	S	Yes	Yes	C	30
Saarinen & Valtonen (85)	N	100	Fix	No	C,V	O	NR	Yes	No	48
Mamon (87)	N	5–20	$r_{1/2}$	Yes	V	δ,S	Yes	Yes	C+IGB	>1k
Navarro *et al.* (87)	N	50–100	$r_{1/2}$	Yes	V,C	δ	No	Yes	No	18

NOTES: "Meth" is the method used (QA → quasi-analytical, 3 → 3-body, N → N-body), N is the number of galaxies per group, "Soft" refers to the softening of the potential of the galaxy-galaxy interaction (Fix → fixed, r → scales as the galaxy radius, $r_{1/2}$ → scales as the galaxy half-mass radius), "IGB" indicates the presence of an intergalactic background of dark matter, "ICs" refers to the initial conditions (V → Virialized, C → Collapsing, E → Expanding, and Circ → Circular orbits), "IMF" refers to the initial mass function (δ → equal masses, S → a Schechter (1976) function, and O → something else), "DF" refers to dynamical friction of galaxies against the dark matter background, "Merg" to the presence of a merger criterion, while "Tides" indicates the type of tidal interactions included (C → collisional tides, IGB → IGB tides, and finally $\mathcal{N}$ is the number of simulations run. Moreover, the symbol "NR" indicates that the entry is not required for the type of simulations in consideration.

Results

I now concentrate on the self-consistent studies of groups listed in Table 2, and the two explicit-physics studies of Table 3 that correspond to groups (Roos & Norman 1979; Mamon 1987). *Qualitatively, the main result is rapid merging of galaxies leading to group coalescence*. This is agreed upon by all 7 studies. How fast does this merging take on average? In Table 4 below, I compare the different studies, by evaluating for each the mean time for one merger, averaging over the time for 4 mergers to occur, or the full simulation time if shorter. These merger times are expressed in terms of the half-mass free-fall time defined as $t_{ff} = (\pi/2)(R_h^3/GM)^{1/2}$, where R_h is the half-mass radius of the group *at maximum expansion*. I assume that R_h is twice the half-mass radius of virialized groups. This estimator has the advantage of being independent of the state of evolution of the group and is more robust than the standard free-fall time often used.

Table 4: Merging times compared

Author(s)	Run	N	n	IGB	ICs	r_h/R_h	t_{ff}	t_m	t_m/t_{ff}
Roos & Norman (79)	1	10	1	0.	Vir	0.034	11.3	6.6	0.59
Carnevali *et al.* (81)	26	10	20	0.	Vir	0.1	3.3	1.6	0.49
	28	20	20	0.	Vir	0.05	2.5	1.25	0.49
	29	20	20	0.	Vir	0.1	2.7	1.1	0.41
Cavaliere *et al.* (83)	12B	10	20	0.5	Vir	0.1?	1.7	1.0	0.59
Barnes (85)	A	5	300	0.	Vir	0.1?	0.52	0.7	1.4
	B	5	300	0.	Vir	0.1?	0.28	0.6	2.1
	C	5	300	0.	Coll	0.1?	0.52	0.6	1.2
	D	5	300	0.	Exp	0.1?	0.52	1.0	1.9
	E	5	150	0.5	Vir	0.1?	0.79	1.5	1.9
	F	5	150	0.5	Vir	0.1?	0.52	2.0	3.9
	G	10	100	0.5	Vir	0.1?	1.04	1.5	1.4
	H	5	150	0.5	Coll	0.1?	0.79	1.0	1.3
	I	5	150	0.5	Exp	0.1?	0.79	1.0	1.3
	J	5	75	0.75	Vir	0.1?	1.04	1.6	1.5
	K	5	75	0.75	Coll	0.1?	1.04	1.8	1.7
	L	5	75	0.75	Exp	0.1?	1.04	1.5	1.4
Ishizawa (86)	A	10	100	0.	Coll	0.055	10.6	2.0	0.19
	B	10	100	0.	Coll	0.026	31.6	7.5	0.24
	C	10	100	0.	Coll	0.058	6.8	1.75	0.26
	D	10	100	0.	Coll	0.052	11.5	2.75	0.24
	E	10	100	0.	Coll	0.052	14.2	4.25	0.30
	F	10	100	0.	Coll	0.052	14.6	4.25	0.29
Mamon (87)	Dense	8	1	0.1	Vir	0.39	0.35	0.125	0.32
	Dense	20	1	0.1	Vir	0.35	0.39	0.125	0.32
	Dense	8	1	0.75	Vir	0.1	0.28	0.75	2.7
	Dense	20	1	0.75	Vir	0.1	0.28	0.5	1.8
	Loose	8	1	0.1	Vir	0.04	8.6	6.67	0.77
	Loose	20	1	0.1	Vir	0.04	8.6	3.33	0.39
	Loose	8	1	0.75	Vir	0.015	3.9	10.	2.5
	Loose	20	1	0.75	Vir	0.015	3.9	6.67	1.7
Barnes (89)		6	8k–16k	0.	Vir	0.19	1.61	3.5	2.2

NOTES: N is the number of galaxies per group, n is the number of particles per galaxy, "IGB" indicates the fraction of the group mass in an intergalactic background of dark matter, "ICs" refers to the initial conditions (Vir → Virialized, Coll → Collapsing, Exp → Expanding), r_h and R_h are the initial galaxy and group half-mass radii, respectively, t_{ff} is the half-mass free-fall time, and t_m is the mean time between mergers (both are given in the units used in the study in consideraton). Note that Ishizawa's run A was presented in Ishizawa *et al.* (1983) and refers to an initial shell-like distribution of galaxies, his run C starting in a disk-like distribution, while his runs D to F are quite similar. The merging times of Barnes (1985) are based upon one to four runs, while Mamon's are based upon 50 and 10 runs for his groups of 8 and 20 galaxies, respectively.

From Table 4 on sees that collapsing groups merge at roughly the same rate as virialized groups. As an example, run F of Ishizawa, has a virial ratio of $2T_{\rm rand}/(-W) = 0.5$ compared to his runs B, D, and E for which this ratio is zero, and it's merging time is comparable with that of the other three runs. This is also well illustrated in the results of Barnes (1985). Ditto for expanding groups. Carnevali *et al.*'s results indicate little dependence of t_m on group membership. But Barnes' run G shows a longer merging time, while Mamon's results show a contrary trend. One would expect that the normalized merging time should be much shorter in dense groups compared to loose ones. This is evident in Mamon's simulations of groups of 8 galaxies with individual halos, but not so in groups where the dark matter is mainly in the IGB. Perhaps this means that in the former case, where merging is "direct", the merger cross-sections are important, but that in the second case this is less so because dynamical friction against the IGB really sets the merging rates. This hypothesis is confirmed in Mamon (1987), where the merging rates in the groups with significant IGB are insensitive to the adopted merger cross-sections. The importance of the IGB has little direct effect according to Barnes (1985), but has a strong effect in Mamon (1987), who found that high M/L groups with the same merger cross-sections have much longer merging times.

Are the normalized values of the merging time obtained in the different studies comparable? Consider first the runs with negligible mass in the IGB and starting from virialized initial conditions. Here, Mamon's merging times agree quite well with those of Roos & Norman and Carnevali *et al.*, while those of Barnes (1985, 1989) are roughly three to four times longer. Considering now virialized groups with half or more of their mass in an IGB, Cavaliere *et al.*'s merging time is roughly four times shorter than those of Barnes (1985) and Mamon. Now considering collapsing groups with no IGB, Ishizawa's merging times are typically five times shorter than those of Barnes (1985). These discrepancies are best explained as follows. Among self-consistent studies, those with the largest number of particles per galaxy are most reliable, so I prefer to emphasize the results of Ishizawa, Barnes (1985) and especially Barnes (1989). The departures of these studies from the other ones indicate that, for a negligible IGB, the merging times are longer than expected from two-body collisions, because the other galaxies in a group often come in and pump energy into the merging pair. This is well illustrated in the movie of Barnes (1989). Hence explicit-physics computations ought to use smaller merger cross-sections compared to those given in the litterature of two-galaxy collisions. For groups with a dominant IGB, this effect is not seen since the merging rates are less sensitive to the merging process itself (see above). The discrepancy between Barnes 1985 and Ishizawa may perhaps be explained by the combination of two factors: first in a collapsing group the merger rate ought to be proportional to the number of galaxies in the group, as they all collapse together. Second, Barnes uses three times as many particles and can probably thus distinguish the merging cores longer than Ishizawa.

One should note here that any discrepancy of a factor two is not significant as Mamon finds a standard deviation of 0.3 in the log of his evolution times. But how long can a lucky dense group survive merging? Mamon's simulations show that one can remain with 4 galaxies (starting with 8 to 20) after a Hubble time (only roughly 5% of the time and only for certain parameters). However, the surviving groups are always very "evolved" in the sense that their range of luminosities is greater than allowed by Hickson's HCG selection criteria. Therefore, if HCGs are dense and bound systems they cannot be the remnants of early very dense density pertubations, but must have formed instead more recently, presumably by two-body interactions within looser systems. This issue is addressed by Mamon (1987) who looked for examples of rapid succession of mergers in his simulated loose groups and found one possible case out of 50 simulations of loose groups of 8 galaxies and a dominant IGB, and argues that such events are insignificant in the loose groups of 8 galaxies with individual halos. On the other hand, Mamon found a probability of 5 to 25% of observing a a simulated loose group and finding a projected configuration that satisfied Hickson's HCG criteria. Recently, Walke & Mamon (1989) have argued that these numbers would be reduced to roughly one percent had Mamon adopted more realistic larger sizes for his loose groups. Finally, of these compact projected configurations seen by Mamon, roughly 15 and 45% of these are in fact caused by 3D chance configurations (transient cores).

What physical mechanisms are dominant? This question is well addressed by the explicit-physics simulations of Mamon. Merging turns out to be the dominant mechanism that causes a dense group to lose its HCG appearence, but while merging is "direct" when the galaxies have large merging cross-sections due to their individual halos of dark matter, the evolution of dense groups of galaxies orbiting within a dominant IGB is different. Here, dynamical friction of the galaxies against the IGB forces the galaxies to meet at the group center where they cannot avoid merging, but this takes much more time (see Table 4). When Mamon turned off dynamical friction, the first type of groups still merged at the same rate, while the second type barely did so. Contrary to the situation in globular clusters, evaporation is insignificant in groups of galaxies, simply because the potential wells of galaxies are not deep enough. In dense groups, tides turn out to be important in limiting the sizes of the dominant cannibal galaxies, and the IGB tides are much more effective than the collisional tides. Beyond a luminosity of roughly $4\,L_*$, a cannibal galaxy cannot hold on to its victims and returns them (in digested form!) to the IGB. Tides and the paucity of galaxies thus prevent any real merging instability as described by Ostriker & Hausman (1977): This is checked from the plots of mergers versus time of Mamon (1987), from which the merger rates start out constant in dense groups with individual halos, but vary as $1/t$ in dense groups with the dark matter in the IGB.

In the end one gets one giant cannibal, which appears very much like a giant elliptical, as well illustrated by the $r^{1/4}$ surface brightness distribution found by Barnes (1989), who can also just barely distinguish shells. Thus the outcome of multiple mergers in dense groups is naturally quite similar to that of simple mergers of colliding pairs (e.g., Barnes 1988).

After short periods of time, dense groups show strong signs of dynamical interaction, as well illustrated by the statistical averages over Mamon's explicit-physics simulations. For example, if the dark matter is mainly in the IGB, then luminosity segregation sets in quite rapidly (due to more rapid orbital decay by dynamical friction for high-mass galaxies). Moreover, wherever the dark matter was placed, the statistics of the bright-end of the galaxy luminosity functions, showed signatures of significant merging also develop very rapidly.

Conclusion

In summary, dense groups of galaxies have been simulated in seven different studies, with reasonably consistent results. These groups show rapid merging, although this is mainly due to their short dynamical times. It is very unlikely that more than a few percent of dense groups can survive for over a Hubble time, and the few that do bare little resemblence to Hickson's compact groups. Whether abundant in nature or not, dense groups provide a fascinating laboratory to study galaxy interactions pushed to the extreme, and one learns that tidal processes manage to slow down the merging process, and that orbital decay by dynamical friction of galaxies against an intergalactic background of dark matter is significant in speeding it up. With the advent of increasingly powerful computing facilities, time will come when the statistical studies done with explicit-physics studies will be achievable with self-consistent studies. Along these lines is the work by Borne and Levison (in preparation) who are using a restricted 3-body code to perform large numbers of dense group simulations that ought to be more reliable than Mamon's explicit-physics study.

I gratefully acknowledge Josh Barnes for providing on very short notice a movie for my talk.

References

Aarseth, S.J., and Fall, S.M. 1980, *Ap. J.*, **236**, 43.
Barnes, J. 1985, *M.N.R.A.S.*, **215**, 517.
Barnes, J. 1988, *Ap. J.*, **331**, 699.
Barnes, J. 1989, *Nature*, **338**, 123.
Carnevali, P., Cavaliere, A., and Santangelo, P. 1981, *Ap. J.*, **249**, 449.
Cavaliere, A., Santangelo, P., Tarquini, G., and Vittorio, N. 1982, in *Clustering in the Universe*, ed. D. Gerbal and A. Mazure (Gif-sur-Yvette: Editions Frontières), p. 25.
Cooper, R.G., and Miller, R.H. 1981, *Ap. J.*, **254**, [illegible]
Dekel, A., Lecar, M., and Shaham, J. 1980, *Ap. J.*, **241**, 946.
Hickson, P. 1982, *Ap. J.*, **255**, 382.
Ishizawa, T., Matsumoto, R., Tajima, T., Kageyama, H., and Sakai, H. 1983, *P.A.S.J.*, **35**, 61.
Ishizawa, T. 1986, *Ap. Sp. Sci.*, **119**, 221.
Jones, B.J.T., and Efstathiou, G. 1979, *M.N.R.A.S.*, **189**, 27.
Malumuth, E.M., and Richstone, D.O. 1984, *Ap. J.*, **276**, 413.
Mamon, G.A. 1985, Ph.D. thesis, Princeton University.
Mamon, G.A. 1986, *Ap. J.*, **307**, 426.
Mamon, G.A. 1987, *Ap. J.*, **321**, 622.
Merritt, D. 1983, *Ap. J.*, **264**, 24.
Miller, G.E. 1983, *Ap. J.*, **268**, 495.
Navarro, J.F., Mosconi, M.B., and Lambas, D.G. 1987, *M.N.R.A.S.*, **228**, 501.
Ostriker, J.P., and Hausman, M. 1977, *Ap. J. (Letters)*, **176**, L51.
Richstone, D.O. 1976, *Ap. J.*, **204**, 642.
Richstone, D.O., and Malumuth, E.M. 1983, *Ap. J.*, **268**, 30.
Roos, N. 1981, *Astr. Ap.*, **95**, 349.
Roos, N., and Aarseth, S.J. 1982, *Astr. Ap.*, **114**, 41.
Roos, N., and Norman, C.A. 1979, *Astr. Ap.*, **76**, 75.
Rose, J.A. 1979, *Ap. J.*, **231**, 10.
Saarinen, S., and Valtonen, M.J. 1985, *Astr. Ap.*, **153**, 130.
Schneider, D., and Gunn, J.E. 1982, *Ap. J.*, **263**, 14.
Tully, R.B. 1987, *Ap. J.*, **321**, 280.
Walke, D.G., and Mamon, G.A. 1989, *Astr. Ap.*, **295**, 291.

DISCUSSION

Kennicutt: 1. In a typical group merger what fraction of the stars are ejected from the system? 2. The end product of Barnes' simulation looked very much like a field CD galaxy. Are the observed space densities and luminosity functions of isolated CD and E galaxies consistent with the compact group densities and merger timescales?

Mamon: 1. I can't say for dense groups, but presumably, the fraction of ejected stars should be the same as in isolated mergers, i.e., 5-10% depending on who you ask. 2. Assuming a constant rate of compact group coalescence, I found that between 5 and 40% of all giant ellipticals outside of clusters ought to be the result of not one merger, but at least three consecutive mergers. However, it seems that dense groups must form within loose groups (and on fact I just showed that all nearby compact groups are situated within looser systems) - Hence the end product in this case could resemble more CD poor (MKW) clusters.

Hickson: I understand that in Barnes' simulation only about half the mass was in dark halos and that none of this was in a common envelope. This seems inconsistent with the high mass-to-light ratios that are observed in compact groups. What would be the effect of increasing the mass in dark halos and in a common envelope?

Mamon: I agree with you that Barnes has not put enough dark matter in his simulations. If you put significant additional dark matter in individual halos, then these will have larger cross-sections and the merging times will be decreased. If instead you put this additional dark matter in a diffuse intergalactic background there will be competition between two effects. On one hand, the galaxies will experience stronger dynamical friction, their orbits will decay faster and thus merge faster. On the other hand, the background will exert stronger tides on the galaxies, thus reducing the merger cross-sections and thus the merger rates. The level to which one should increase the dark matter background (assuming that is where you put it), I think, is such that the first effect should at least be comparable to the second.

M. Roos: (comment on Hickson's question) I think that increasing the M/L ratio of groups by increasing the amount of dark matter in the background will also decrease the merging time due to dynamical friction, although maybe not so strong as in the case where you increase the halo mass of the galaxies.

DISCUSSION

Appleton: Could you say something about the evolution of the dwarf galaxy population during the "merging instability" stage in compact group simulations? Do you think that the lower end of the group luminosity function might be a useful indicator of what is going on in such groups (i.e., how dynamically evolved the system is).

Mamon: The low mass galaxies, being smaller, merge less efficiently, and when they do, they presumably bump into massive galaxies. But whereas I've studied the evolution of the bright end of the luminosity functions of the simulated dense groups, I've not really paid any attention to what goes on at the faint end.

Zasov: Could you tell us a little more about the merger itself? Is it consistent with the Faber-Jackson or Tully-Fisher relations? What's the fraction of dark matter inside of the "optical" boundaries? What galaxy does it look like?

Mamon: The detailed simulations by Barnes show that the merger remnents look like the merger remnents of isolated pairs of colliding galaxies which themselves resemble elliptical galaxies. Presumably the outer regions of the halos heat up during the encounters and settle mainly beyond the "optical" boundary. In my own simulations the original Faber-Jackson relation was not too affected by mergers.

Fridman: Do you think that the process of an artificial satellite falling on the Earth because of an atmospheric friction can be considered "merging instability"?

Mamon: It all depends on the range of masses involved in the merging. Merging usually involves a massive galaxy being swallowed by an even more massive one - the typical ratio of merging masses is about 3. So a typical merger increases the main galaxy's mass by roughly one-third and its cross-section by roughly two-thirds. Granted, its not a drastic instability. Your example is in principle an instability too, although a very inefficient one!

EXPLAINING COMPACT GROUPS AS CHANCE ALIGNMENTS

Gary A. Mamon
DAEC, Observatoire de Meudon
Meudon, France

The physical nature of the apparently densest groups of galaxies, known as *compact groups* is a topic of some recent controversy, despite the detailed observations (Hickson, in these proceedings, and references therein) of a well-defined catalog of 100 isolated compact groups compiled by Hickson (1982). Whereas many authors have espoused the view that compact groups are bound systems, typically as dense as they appear in projection on the sky (e.g., Williams & Rood 1987; Sulentic 1987; Hickson & Rood 1988), others see them as the result of chance configurations within larger systems, either in 1D (*chance alignments*: Mamon 1986; Walke & Mamon 1989), or in 3D (*transient cores*: Rose 1979). As outlined in the companion review to this contribution (Mamon, in these proceedings), the implication of Hickson's compact groups (hereafter, HCGs) being dense bound systems is that they would then constitute the densest *isolated* systems of galaxies in the Universe and the privileged site for galaxy interactions.

In a previous paper (Mamon 1986), I reviewed the arguments given for the different theories of compact groups. Since then, a dozen papers have been published on the subject, including a thorough and perceptive review by White (1990), thus more than doubling the amount written on the subject. In this contribution, I first enumerate the arguments that I brought up in 1986 substantiating the chance alignment hypothesis, then review the current status of the numerous recent arguments arguing against chance alignments and/or for the bound dense group hypothesis (both for *the majority of HCGs but not all of them*), and finally reconsider each one of these "anti-chance alignment" arguments and show that, rather than being discredited, the chance alignment hypothesis remains a fully consistent explanation for the nature of compact groups.

Old Arguments for HCGs as Chance Alignments

I start by listing the arguments I gave in Mamon (1986) to suggest that most HCGs are caused by chance alignments of galaxies along the line of sight within looser systems.

1. *Frequency of chance alignments*

From my dynamical simulations of loose groups (hereafter, LGs), I estimated the frequency at which a projected configuration showed a subgroup that was compact using Hickson's (1982) criteria and found values ranging from 3% to 33%, depending on the number of galaxies in the LGs, and on where the dark matter was placed in them (Mamon 1987). I had also estimated the frequency at which compact configurations would have to have appeared in order to explain half of the HCGs as chance alignments, and found it to be 2.5% (Mamon 1986). The majority of these compact configurations were 1D chance alignments rather than

3D transient cores (Mamon 1987). Chance alignments were thus numerous enough to explain HCGs and perhaps even too frequent!

2. *Demographics*

As mentioned in my companion review, dense groups formed in less than 5% of the LGs simulated for a Hubble time, while I argued that a frequency of 6 to 45% of dense group occurrence within LGs was necessary (Mamon 1986). Thus, dense groups form too rarely to explain most HCGs.

Moreover, if HCGs are bound dense groups then they must rapidly coalesce into giant ellipticals or cDs, and I estimated that 5 to 40% of all such galaxies would then be the products of multiple mergers in dense groups (Mamon 1986, see also Barnes 1989). Williams & Rood (1987) argue that there ought to be more coalesced dense groups than observed giant ellipticals, and are thus led to worry about Newtonian theory as a whole.

3. *Dynamical evolution*

The large number of simulations performed by Mamon (1987) provided a useful statistical ensemble on which to study dynamical evolution. I found that dense groups rapidly show strong signs of luminosity segregation and evolution at the bright-end of the galaxy luminosity function. These are not seen in HCGs (Mamon 1986) thus questioning the bound dense group hypothesis.

4. *HCG galaxy morphological types*

The morphology-density relation linking the mix of galaxy morphologies to the local galaxy density, found for groups and clusters (e.g., Postman & Geller 1984) is not obeyed for HCGs (assuming that they are as dense in 3D as they appear), which follow their own relation, offset from the "universal" one by a factor of 200 in local galaxy number density. This is precisely what one predicts if HCGs are caused by chance alignments in looser groups, thus having the same mix of morphologies as their parent groups but appearing very much denser.

5. *HCG mass-to-light ratios*

Buckley & Mamon (1987, unpublished) and Hickson (quoted in White 1990) find the median HCG virial or projected mass-to-light ratio to be around 40 h, which is much smaller than the typical LG values (Tully 1987 and Ramella *et al.* 1989 find the median LG M/L to be 125 h and 180 h, respectively). Now if HCGs are chance alignments within LGs they should have the same velocity dispersion as their parent groups, and one should then expect that the ratio of HCG to LG median M/L is roughly equal to the corresponding ratio of sizes divided by that of total luminosities. Now, the ratio of total luminosities is $\simeq 2$. If Tully's groups are typical of HCG parents, then the ratio of sizes is 17, but if HCGs arise from typically denser LGs (Walke & Mamon 1989) then from the morphology-density relation offset, the ratio is 6. For the latter case one then obtains precisely the median HCG M/L expected. Alternatively, a low median M/L may be expected if HCGs are bound dense systems, extending much less than the dark matter, for example if they are part of looser groups.

Arguments for HCGs as Dense Bound Groups

There are many arguments pointing to the idea that *what you see is what you get*, i.e., that HCGs are as dense in 3D as they appear in 2D. I list these below.

1. *Frequency of chance alignments*

Hickson & Rood (1988) have performed static Monte-Carlo simulations of galaxy positions in a group, by placing points at random in a circle or a sphere, and computing the probability of an isolated compact subgroup occuring by chance (in projection when they start in the sphere). For typical LG parameters they find a chance alignment probability of 10^{-5} or 5×10^{-4}, depending on whether the typical parent LG has a binary within it or not. Their results seem inconsistent with the probabilities of 2 to 25% that I had found in my dynamical simulations (Mamon 1987), and moreover discredit the whole chance alignment phenomenon as much too rare to explain a significant fraction of HCGs.

2. *HCG environments*

By definition, HCGs are isolated: Denoting the angular radius of the smallest circumscribed circle containing the centers of the galaxies in an HCG by $\theta_{\rm HCG}$ and the magnitude of the brightest galaxy by m_1, there must be no galaxies brighter than $m_1 + 3$ in a concentric annulus of angular radii $\theta_{\rm HCG}$ and $3\,\theta_{\rm HCG}$. Various authors have attempted to measure the isolation of an HCG in a wider environment. If an HCG is isolated, then it is unlikely the result of chance alignments within looser systems. For Williams & Rood (1987), an HCG is isolated if there are fewer than four outside galaxies in the magnitude range (m_1, m_f) of the HCG members, within a distance of $3\,\theta_{\rm HCG}$ from *any* of the HCG galaxies, and thus find 89 isolated HCGs. Sulentic (1987) considers the surface number density of galaxies outside of the HCG out to $\theta = 0.5°$ and 1°, and brighter than $m_f + 1$. He concludes that HCGs have a surface number density 100 times greater than their immediate environment, and calls isolated the 38 HCGs whose immediate environment is less dense than the average field. Rood & Williams (1989) count the galaxies out to $10\,\theta_{\rm HCG}$ with mags in the range m_1 to m_f, and compare to the estimated field surface number density based on a model of galaxy counts (why not use the observed field counts instead?). They find 67 HCGs whose environments have a density that is less than 2σ above the expected field surface number density.

3. *HCG galaxy morphological types*

Sulentic (1987) found that the mix of morphological types of the galaxies in HCGs was roughly the same as in their environments (out to both 0.5° and 1°). However, Rood & Williams (1989) find that the environments of HCGs (out to $10\,\theta_{\rm HCG}$) are more spiral rich than the HCGs (whose morphological types were determined by Williams & Rood 1987), hence the HCGs are more evolved.

For Hickson & Rood (1988), the offset of the HCG morphology-density relation is caused by a stronger correlation of galaxy morphologies with the velocity dispersion of the group or cluster to which they belong. Their reasoning is based upon trends found in HCGs by Hickson, Kindl, & Huchra (1988), but with only global mean values for LGs and clusters. Such a morphology-velocity dispersion relation, if true, would be a fundamental clue to galaxy formation and evolution, but this has to be studied in more detail for LGs and clusters.

Finally there is a significant tendancy for the morphological types of individual galaxies within an HCG to agree among one another (Hickson, Kindl, & Huchra 1988; see also Sulentic 1987), which seems to indicate that HCGs are specific isolated systems.

4. *HCG elongations*

Sargent & Turner (1972, unpublished) and Rose (1977) studied the distribution of the elongations of compact groups, and both argued that the shapes of compact groups were consistent with random configurations viewed in projection, i.e., chance alignments perpendicular to the line of sight. This issue was addressed again by Hickson *et al.* (1984), who showed that the distribution of HCG elongations was inconsistent with random sampling from a sphere or a disk, in that there were too many observed highly elongated groups.

5. *Demographics*

Assuming that bound dense groups are created and destroyed at the same rate, Barnes (1989) has argued that the ratio of the number of dense groups to the number of LGs in the same volume of the Universe should be equal to the ratio of their lifetimes, which is close to the ratio of their crossing times, i.e., about 1%. Hence, he explains HCGs as bound dense groups forming within LGs by two-body interactions and being destroyed by mergers.

6. *Galaxy interaction in HCGs*

This is perhaps the most studied point, and I thus save the best for the end. Numerous studies have observed signs of galaxy interaction in HCGs, thus seemingly arguing for HCGs as bound dense groups. Menon & Hickson (1985, 1990) have shown that continuum radio sources in HCGs are always attached to individual galaxies, but whereas a spiral of any luminosity rank in its group can be a radio-source, an elliptical or lenticular must almost always be a first-ranked group member. Williams & Rood (1987) have argued that HCGs are deficient in HI. Hickson *et al.* (1989) found significant IR emission in HCG galaxies. Rubin, Hunter, & Ford (1990) found peculiar rotation curves in 14 of the 21 spiral galaxies they observed. Zepf & Whitmore (1990) argued that many HCG ellipticals (usually faint ones) are bluer than expected.

Discussion

I now reconsider each one of the arguments given in the preceding section.

1. *Frequency of chance alignments*

The frequency (instead of probability since one can have more than one compact subgroup within a large enough group) of chance alignments was reevaluated by Walke & Mamon (1989), who solve analytically the problem of forming isolated compact subgroups from a parent homogeneous distribution in a circle (the same problem as numerically simulated by Hickson & Rood). They find that the frequency of chance alignments is very sensitive to the size of the parent LG, typically varying as $R_{\rm LG}^{-4.5}$, and also increases rapidly with the membership of the parent LG. Their computed frequencies are consistent with both Mamon's (1987) dynamically simulated results as well as Hickson & Rood's very low values! The difference is caused by the relatively small initial sizes of my dynamically simulated LGs, and the fact that I searched for configurations that met the HCG selection criteria, while Hickson & Rood attempted to match the median HCG properties (the HCG sample turns out to be very incomplete at the faintest two mags arcsec^{-2} in surface magnitude). Moreover, Walke & Mamon argue that while the *median* loose group has a negligible frequency of chance alignments, the *mean* group does not, so that summing over an LG catalog (Tully 1987), they find a mean frequency of chance alignments of 7%, which remains as high as 1% if they exclude the Virgo cluster from the LG catalog. And such a one-percent frequency is what is required to account for roughly half of HCGs being caused by such chance alignments (within a factor of four). Finally, they suggest that clusters ought to contain compact groups embedded within them, and Mamon (1989) discovered such a compact group in the Virgo cluster by performing an automated search of isolated subgroups strictly satisfying the HCG selection criteria.

2. *HCG environments*

Do the closest and brightest HCGs belong to known loose groups or clusters? I've searched for membership in larger systems of all HCGs with at least two member galaxies with similar redshifts ($\Delta v < 1000\,\mathrm{km\,s^{-1}}$) included in a galaxy redshift survey (the remaining HCG galaxies being out of the boundaries of the galaxy survey, or too faint to be included in it). There were five such HCGs. *All of them* were found to belong to loose groups, as shown in Table 1.

Table 1: Nearby HCGs

HCG #	N	Embedding group	Isolation		
			WR87	S87	RW89
44	4	GH 58 (10), NBG 21–6 (12)	Isolated	Isolated	Non-isolated
58	5	GH 89 (7), MKW 10 (21)	Isolated	Non-isolated	Non-isolated
61	3	GH 101 (11), RGH 33 (6)	Isolated	Isolated	Isolated
68	5	GH 123 (17), NBG 42–1 (15)	Isolated	Isolated	Non-isolated
90	4	NBG 63–1 (6)	Isolated	(Isolated)	Non-isolated
101	5	GH 106 (248), NBG 11–1 (130)	Isolated	Isolated	Non-isolated

NOTES: N is the number of galaxies with accordant redshifts, WR87, S87, and RW89, are the studies of Williams & Rood (1987), Sulentic (1987), and Rood & Williams (1989), and GH, NBG, MKW, and RGH stand for the galaxy systems of Geller & Huchra (1983), Tully (1987), Morgan, Kayser & White (1975), and Ramella, Geller, & Huchra (1989), respectively. The number in parentheses is the number of galaxies in the embedding system. I also list as HCG 101 the compact group that I discovered in the Virgo cluster (Mamon 1989).

In addition to these, Tikhonov (in these proceedings) found six more HCGs within LGs. Sulentic (1987) would classify all of the HCGs listed in Table 1 as isolated, as the parent groups or cluster span far beyond his angular limits. But more surprising is the fact that Williams & Rood (1987) would have classified 5 out of 6 of these compact groups as isolated. On the other hand Rood & Williams (1989) would classify only one of the 6 compact groups as isolated, which tends to suggest that their isolation criterion is much better although not perfect. It would not be surprising that once deeper redshift surveys are established, the majority of HCGs would belong to greater 3D structures. Note however that while this saves the chance alignment hypothesis, it does not prove it since, if HCGs are bound dense systems, they would have to form within greater structures (see my review on dense groups in these proceedings).

3. *HCG galaxy morphological types*

Tikhonov (these proceedings) finds a significantly smaller fraction of spirals in more distant HCGs, thus suggesting that ellipticals are oversampled. I checked this using the very accurate morphologies based upon CCD frames given in Hickson, Kindl, & Auman (1989): HCG galaxies are $24 \pm 5\%$ spiral at $z \geq 0.04$, compared to $56 \pm 4\%$ for $z < 0.04$, a $\simeq 6\sigma$ result. It thus seems preferable to exclude the 24 HCGs with $z > 0.04$ when analysing morphologies.

Once Rood & Williams divide their HCG sample into the isolated and non-isolated HCGs (see previous section), they find that the morphologies are not significantly different between the 67 isolated HCGs and their sparse environments. A significant difference is present for the 33 remaining HCGs and their neighborhoods, but only for this minority.

White (1990) has argued that morphological concordance is the result of similar conditions at galaxy formation, and linked to a correlation of galaxy morphological types with some yet unknown physical quantity. I find that the quartets in the CfA LG catalog (Geller & Huchra 1983) present no such significant morphological concordance: perhaps because the correlation of quantities is less strong in LGs.

4. *HCG elongations*

Hickson *et al.* (1984) also studied the distribution of HCG elongations using simple dynamical models of both groups and subgroups within groups, and found the two distributions statistically consistent. Thus, the issue of dense bound groups versus chance alignments was thus not resolved here, in contrast to what is stated by Hickson & Rood (1988).

5. *Demographics*

The logic of Barnes is based upon the assumption that on average each loose group sees one (and only one) bound dense group form within it in its lifetime. Now, my simulations of LGs (Mamon 1987) were stopped at a Hubble time, while the LG lifetimes, based upon their crossing times and the merger rates summarized in my review in these proceedings, was about double. Hence, Barnes would expect me to have found bound dense groups within half of my simulated LGs, whereas I had only found roughly 5%, or, in other words, the formation rate of dense groups within LGs is ten times too low to explain HCGs.

6. *Galaxy interaction in HCGs*

Now to the fundamental point. If HCGs are caused by chance alignments, then these are not simply well separated individual galaxies lying along the line of sight. A compact quartet, could be such a "1+1+1+1" system, but could also be an alignment of binaries, or a triplet aligned with a single galaxy. The galaxies that are physically associated can moreover be bound to one another or not, for example one could have a transient unbound triplet. The mix of these populations is of fundamental importance in assessing the nature of HCGs, and unfortunately has not been yet looked for in the explicit-physics simulations (where statistical results can be obtained). I thus allowed myself to guess the expected mix for quartets appearing as chance alignments, and these appear in Table 2, where I also used the results of my simulations (Mamon 1987).

Table 2: Approximate distribution of HCGs

Individual Halos			Common Intergalactic Background
85%	Chance Alignments		55%
	$1+1+1+1$	(35%)	
	$\underline{\mathbf{2}}+1+1$	(35%)	
	$\underline{\mathbf{2}}+\underline{\mathbf{2}}$	(10%)	
	$3+1$	(10%)	
	$\underline{\mathbf{3}}+1$	(10%)	
13%	Transient Cores		40%
	4	100%	
2%	Bound Dense Groups		5%
	$\underline{\mathbf{4}}$	100%	

NOTES: The underlined numbers in bold correspond to bound systems of galaxies.

From the numbers in Table 2, I expect 32% or 24% of strongly interacting galaxies, if the dark matter resides in individual halos or a common intergalactic background, respectively. The weak interactors account for an additional 19% or 44% of the galaxies for the two dark matter situations, respectively. So a chance alignment model of HCGs turns out to be fully consistent with galaxy interactions. As a cautionary note, in the one dense group simulation of Barnes (1989), mergers occur mainly at the beginning and the end of the simulation, and little interaction is seen during most of the life of the group.

Now the predicted existence of galaxy interactions in chance aligned HCGs should affect somewhat the mix of morphologies in these systems relative to their environments, and might thus explain the differences discovered by Rood & Williams (1989).

Future Prospects

In summary, while a minority of HCGs display strong signs of interaction, these are consistent with chance alignments, which moreover are well justified from *statistical* arguments. While the controversy surrounding the nature of compact groups will certainly not end soon, there are quite a few tests that ought to be tried out, which I list below.

The explicit-physics simulations that I've carried out (Mamon 1987), although inaccurate in reproducing the details of the galaxy interactions, are probably the best way to assess the amount of binaries and triplets in chance aligned quartets and quintets. The distribution of group elongations can also be properly assessed in this way. One can also test the distribution of mass-to-light ratios of the compact configurations occurring in projected simulated loose groups, and compare with the HCG sample.

More detailed simulations like the restricted 3-body simulations being undertaken by Borne & Levison (in preparation) are then needed to obtain statistical estimates of the strength and the duration of galaxy interactions in dense groups, and in loose groups as well. In the long run, one will of course strive for a statistical set of self-consistent dense group simulations, perhaps with 1000 particles per galaxy.

Observationally, the day will come when POSS plates will be automatically scanned and standard group as well as HCG algorithms can be applied to these. We will thus find out if compact groups are always situated in looser groups or in clusters, and the importance of the latter environment. We would also have better statistics to assess the difference in morphologies.

References

Barnes, J. 1989, *Nature*, **338**, 123.
Geller, M.J., and Huchra, J.P. 1983, *Ap. J. Suppl.*, **52**, 61.
Hickson, P. 1982, *Ap. J.*, **255**, 382.
Hickson, P., Kindl, E., and Auman, J.R. 1989, *Ap. J. Suppl.*, **70**, 687.
Hickson, P., Kindl, E., and Huchra, J.P. 1988, *Ap. J.*, **331**, 64.
Hickson, P., Menon, T.K., Palumbo, G.G.C., and Persic, M. 1989, *Ap. J.*, **341**, 679.
Hickson, P., Ninkov, Z., Huchra, J.P., and Mamon, G.A. 1984, in *Clusters and Groups of Galaxies*, ed. F. Mardirossian, G. Giuricin, and M. Mezzetti (Dordrecht: Reidel), p. 367.
Hickson, P. and Rood, H.J. 1988, *Ap. J. (Letters)*, **331**, L69.
Mamon, G.A. 1986, *Ap. J.*, **307**, 426.
Mamon, G.A. 1987, *Ap. J.*, **321**, 622.
Mamon, G.A. 1989, *Astr. Ap.*, **219**, 98.

Menon, T.K., and Hickson, P. 1985, *Ap. J.*, **296**, 60.
Menon, T.K., and Hickson, P. 1990, in preparation.
Morgan, W.W., Kayser, S., and White, R.A. 1975, *Ap. J.*, **199**, 545.
Postman, M., and Geller, M.J. 1984, *Ap. J.*, **281**, 95.
Ramella, M., Geller, M.J., and Huchra, J.P. 1989, *Ap. J.*, **344**, 57.
Rood, H.J., and Williams, B.A. 1989, *Ap. J.*, **339**, 772.
Rose, J.A. 1977, *Ap. J.*, **211**, 311.
Rose, J.A. 1979, *Ap. J.*, **231**, 10.
Rubin, V.C., Hunter, D., and Ford, W.K. 1990, in preparation.
Sulentic, J.W. 1987, *Ap. J.*, **322**, 605.
Tully, R.B. 1987, *Ap. J.*, **321**, 280.
Walke, D.G., and Mamon, G.A. 1989, *Astr. Ap.*, **295**, 291.
White, S.D.M. 1990, in *Dynamics and Interactions of Galaxies*, ed. R. Wielen, in press.
Williams, B.A., and Rood, H.J. 1987, *Ap. J. Suppl.*, **63**, 265.
Zepf, S.E., and Whitmore, B.C., 1990, in preparation.

DISCUSSION

Sulentic: Three comments: 1) The failure of simulations to produce dense groups is not a basis for rejecting that they are physical systems. 2) I am surprised by the lack of infrared emission from the dense groups - it supports your view. I believe that Hickson et al. overestimate the FIR luminosities of group members (due to resolution of IRAS). 3) At least some dense groups do have luminous haloes. At least 3 are discordant groups--your model would increase the significance of these associations because these 3 groups would populate the reduced sample of physical groups.

Mamon: If F. Hammer were here, I guess he would respond to your last comment by arguing that the discordant member, if it is a background object, would be gravitationally lensed by the remaining group. This would amplify it enough to make it almost as bright as the other group members. Perhaps gravitational lensing of the background object could also be responsible for the diffuse light that you find in some of Hickson's compact groups.

Whitmore: 1. Vera Rubin has also looked at about a dozen ellipticals in compact groups, and finds that most of them have emission in Hα, and one case is a counterrotating system. 2. I recently reexamined the morphology-density relation using Dressler's data for 55 clusters. I found that the fundamental correlation is probably with the distance from the center of the cluster rather than local density (i.e., - high fractions of ellipticals are only found near the centers of clusters). This would explain why the morphology-density relation is offset for compact groups (i.e., not all ellipticals as would be predicted by high local density) without implying they are not physically related. The small number of galaxies in compact groups cannot produce the deep potential well found in clusters with hundreds of galaxies.

Mamon: I believe that loose groups cannot produce deep potential wells like those found in clusters. However, there is a morphology-density relation on loose groups (e.g., Postman & Geller) which follows that of clusters. So one must explain the offset of Hickson's compact groups relative to loose groups in the morphology-density relation.

Hickson: I think that you and I both agree that the probability of a sufficiently compact chance alignment of galaxies occuring in a typical loose group is extremely small. When you include the Virgo cluster you find a mean probability which is about an order of magnitude higher than when Virgo is excluded. This means that if compact groups are mostly chance alignments, they should almost all be in clusters as least as rich as Virgo. Yet very few of the compact groups in my catalog are anywhere near such clusters.

Mamon: One should therefore perform automated searches inside clusters (with N>50 accordant redshifts) such as the one I performed on Virgo, and one should perhaps expect to find a large number of new HCG's in such clusters.

TYPICAL MOTIONS IN MULTIPLE SYSTEMS

Joanna Anosova
Astronomical Observatory
Leningrad University
USSR

In very old times, people counted - one, two, many. I want to show you now that they were right.

Let's consider the motions of isolated bodies:

1. N = 1 - simple motion;

2. N = 2 - Keplerian orbits;

3. N = 3 - this is the difficult problem. In general, this problem can be studied only by computer simulations.

We studied this problem over many years (see, e.g., Agekian and Anosova, 1967; Anosova, 1986, 1989a,b). Our principal result is: two basic types of dynamics take place in triple systems. The first special type - the stable hierarchical systems with two almost Keplerian orbits. The second general type - the unstable triple systems with complicated motions of the bodies. By random choice of the initial conditions, by the Monte-Carlo method, the stable systems comprised about ~10% of the examined cases, the unstable systems comprised the other ~90% of cases under consideration.

4. N > 3 - the studies of dynamics of such systems by computer simulations show that we have in general also the motions roughly as at the cases 1 - 3 with the relative negative or positive energies of the bodies.

Our moving picture shows the typical trajectories of the bodies in unstable triple systems of the general type of dynamics. Such systems are disrupted always after close triple approaches of the bodies. These approaches play a like role the gravitational slingshot. Often, the velocities of escapers are very large. On the other hand, our move shows also the dynamical processes of a formation, dynamical evolution and distruption of the temporary wide binaries in triples and a formation of final hard massive binaries in the final evolution of triples.

The move "Dynamical evolution of triple systems" was shown.

At end, I want to say that the various intensive studies in the field of extragalactic astronomy carried out at the Leningrad University of Astronomical Observatory during many years. Now, we thanks very much the Scientific Organizing Committee of the Colloquim No. 124 of the IAU and in special Dr. J. Sulentic on this beautiful possibility to participate at this very interesting meeting.

REFERENCES

Agekian, T. A., and Anosova, J. P. 1967, Sov. Astron. Journ., 44, 6, p. 1261-1273.

Anosova, J. P. 1986, Astrophysics and Space Science, I24, 2, p. 217-241.

Anosova, J. P. 1989a, Comments on Astrophysics, 1414, 1, p. 17-36.

Anosova, J. P. 1989b, Comments on Astrophysics, 14, 1, p. 37-60.

DISCUSSION

Mamon: Are all your particles point masses or have you tried extended masses? Do you find that in the case of extended objects you have fewer particles escaping?

Anosova: We have in some instances used extended mass distributions such as $m \bullet r$. The answer to your second question is yes. The qualitative evolution of such systems is conserved, but the velocities of the escaping particles are less (decreases) as the very close triple approaches of the bodies take hot place.

DYNAMICS AND CONFIGURATIONS OF GALAXY TRIPLETS

Joanna P. Anosova
Victor V. Orlov
Astronomical Observatory
Leningrad State University
USSR

Arthur D. Chernin
Alexei V. Ivanov
Leningard Herzen Pedagogical Institute
USSR

Ljudmila G. Kiseleva
Leningrad Electro-Technical Institute
USSR

ABSTRACT. Two methods are proposed for describing the distributions of the triplet configuration parameters characterizing a tendency to alignment and hierarchy: (1) obtaining a representative sample of configurations and determining its statistical parameters (moments and percentages); and (2) dividing the region of possible configurations of triple systems (Agekian and Anosova, 1967) into a set of segments and finding the probabilities for the configurations to find themselves in each of them.

Both these methods allow representation of the data by numerical simulations as well as observations. The effect of projection has been studied. It rather overestimates the alignment and hierarchy of the triple systems. Among the parameters of interest there are found some parameters that are least sensitive to projection effects.

The samples consist of simulated galaxy triplets (with hidden mass) as well as of 46 probably physical triple galaxies (Karachentseva et al., 1979). The observed triplets as well as numerical models show a tendency to alignment. The triple galaxies do not show any tendency to hierarchy (formation of the temporary binaries), but this tendency may be present for simulated triplets without significant dark matter. The significant hidden mass (of order ten times the total mass of a triplet) decreases the probability of forming a binary and so weakens the hierarchy.

Small galaxy groups consisting of 3-7 members are probably the most prevalent types of galaxy aggregate (Gorbatsky, 1987). Galaxy triplets are the simplest groups, but dynamically non-trivial ones.

Gravitationally connected triplets with negative total energy may be in the following dynamical states (see, e.g., Anosova, 1985): (1) close triple approach; (2) simple interplay; (3) ejection with return; (4) escape; and (5) stable revolution. Every dynamical state correspondeds to its most probable type of the configuration, i.e., some correlation exists between the type of dynamics and the config[illegible]ons of triplets. The presence of large hidden mas[illegible]luences the dynamics strongly, and therefore the configu[illegible]ons of galaxy triplets.

A purpose of this work is to infer the p[illegible]able dynamical states of galaxy triplets by the observed data on their configurations.

The first attempt at a systematic selection of galaxy triplets was undertaken by Karachentseva et al. (1979). This list includes 84 isolated triple galaxies of the northern sky, the components having apparent magnitudes $m_p < 15.7$. Some detailed information on the triplets is included in a recent paper by Karachentseva et al. (1988).

In particular, the list includes the projected angular separations r_{ij} between the components.

Two methods of statistical study of the configurations of triplets are proposed:

1. a method of configuration parameters;
2. a method of configuration zones.

In the first method (Kiseleva and Orlov 1989), some chosen quantities are considered in order to characterize a degree of flatness or alignment as well as the hierarchy of the triplets.

The following parameters may characterize the alignment:

1. a sum of squares of the sines of angles in the configuration triangle

$$C = \sin^2 \alpha + \sin^2 \beta + \sin^2 \gamma \; ; \tag{1}$$

2. a ratio

$$Z = h/r_{max}, \tag{2}$$

where r_{max} is the length of the maximum side in a triangle, h is the distance from the third component to this side;

3. a ratio of area of a triangle to the area of the equilateral triangle with the same perimeter

$$Ke = S_\Delta/S^* ; \tag{3}$$

4. a difference

$$\beta = \pi - \phi_{max} \text{ (in radians)}, \tag{4}$$

where ϕ_{max} is the maximum angle in a triangle.

The following characteristics of the hierarchy of triplets are considered:

1. a variation of the squares of the mutual distances between components in a triplet

$$B = [(a^2 - A)^2 \pm (b^2 - A)^2 + (c^2 - A)^2]/(3A^2) \tag{5}$$

where a, b, and c are the lengths of the sides of a triangle, $A = (a^2 + b^2 + c^2)/3$;

2. a ratio

$$\rho = r_{min}/rd, \tag{6}$$

where r_{min} is the minimum mutual distance, r_d is the distance from the most distant component to the geometric center of a close pair;

3. a ratio

$$q = r_{min}/r_{max}; \qquad (7)$$

4. a ratio

$$\lambda = qr_{min}/(r_{max} + r_{int}), \qquad (8)$$

where r_{int} is the intermediate mutual distance between the components.

Because of projection effects, the distributions of the actual and apparent configuration parameters may be different. In this work we have selected the least sensitive of the above quantities to projection effects. The selection was carried out by some computer simulations: for 1000 random configurations within a circle of unit radius, we calculated the actual values of the parameters (1) - (8) as well as their apparent values obtained on a projection of the triangle plane to some "pictorial" plane. For every parameter X the following quantity S has been determined

$$S = \sum_{i=1}^{1000} (X_i - X_i')^2 / \bar{X}^2, \qquad (9)$$

where X_i and X_i' are the actual and projection values of the parameter, $\bar{X}$ is an average actual quantity. The least sensitive parameter to the projection effect is that having the minimum S. The quantity S characterizes the average individual deviation of the projected quantities from the actual ones. The means and medians of the actual versus apparent parameters are also compared. The effect of projection is shown to overestimate the degree of the alignment of a system as well as its hierarchy. The parameters β and λ are the least sensitive ones to projection effects. By these parameters we have studied some trends in alignment and hierarchy for the galaxy triplets from the list by Karachentseva et al. (1979, 1988), that have been classified as probably physical systems in accordance with a criterion by Anosova (1987). The average projected quantities $\bar{\beta}'$ and $\bar{\lambda}'$ have been calculated for a sample of 46 probably physical triplets. The quantity $\bar{\beta}$ obtained has been compared with the mathematical expectation M_β for the uniform distribution of three points within a circle. We have estimated the probability P_β that a deviation $\bar{\beta}'$ from M'_β is chance.

A trend in the alignment of galaxies has been shown to be statistically insignificant - the quantities $\bar{\beta}' = 1.14$ and $M'_\beta = 1.17$. In order to estimate the hierarchy of a structure one has compared an average quantity $\bar{\lambda}'$ for the galaxy triplets, with the mathematical expectation M_λ, for uniform distribution of points within the ellipse with the flattening ε such that $\bar{\beta} = M_\beta$, for the uniform distribution within this ellipse. We have found $\varepsilon \approx 1$ (this is a circle). In this case, $M'_\lambda = 0.51$, the observed $\lambda' = 0.49$.

Therefore no significant tendency to hierarchy has not been observed in the triplets by Karachentseva et al. (1979).

An analogous algorithm estimating a tendency to alignment and hierarchy has been used for the galaxy triplets simulated in the numerical experiemnts (see, e.g., Anosova et al. 1989). The dynamical evolution of triple galaxies with equal-mass components has been simulated; in a number of experiments we have included in a system hidden mass $M_o = 10$ M (M is the mass of a triplet), distributed according to the isothermal law within a sphere with radius R = 1d (d is the initial mean size of a triplet - Anosova et al., 1989). A tendency to alignment is observed in the numerical models as strongly with dark matter as without it. The hidden mass rather decreases the tendency to alignment. No significant tendency to the hierarchy is observed.

The second method of configuration zones consists of analysis of the distribution of points in the region D of all possible configurations (Figure 1 - see e.g., Agekian and Anosova, 1967). This region has been divided into four zones by degree of alignment and hierarchy of the structure. The bounds of these zones are circles with the radii 0.25, 0.50, and 0.75 with the centers at the point (0.5, 0.0). The procedure is complemented by determination of the density σ_i of the points in every zone: $\sigma_i = (n_i/S_i)/(\Sigma n_i/\Sigma S_i)$, where n_i is a number of hits in the zone i, S_i is the area of this zone.

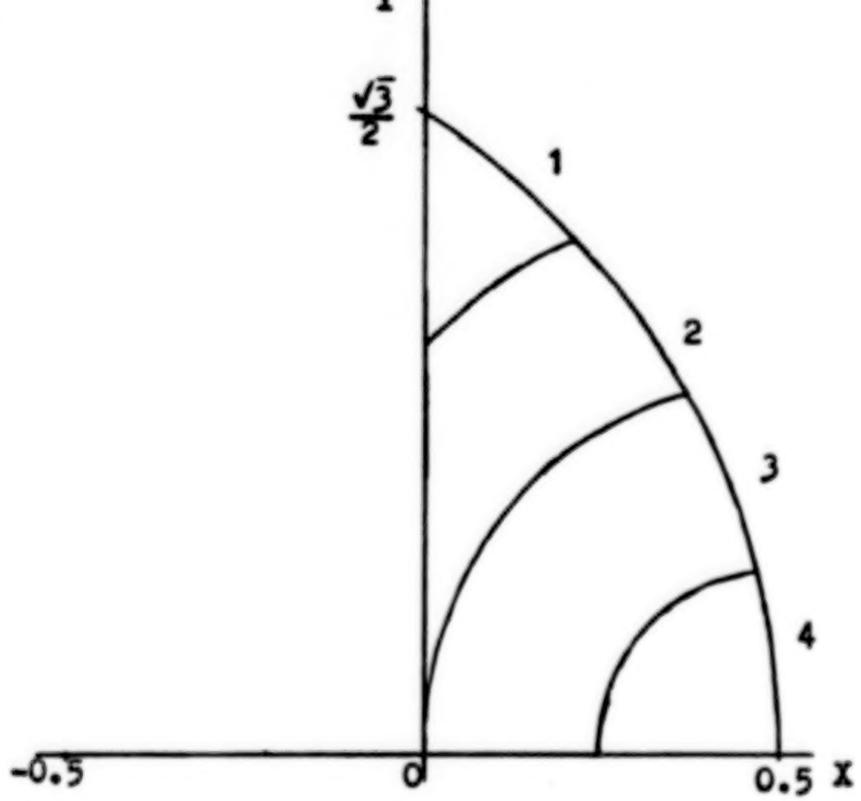

Fig. 1: The configuration diagram.

The points corresponding to the triplets from the list by Karachentseva et al. (1979, 1988) have been drawn within the region D. The distribution σ_i is shown in Figure 2a. The observed distribution by the Monte-Carlo method for random distribution of 46 points within the region D is shown in Fig. 2b.

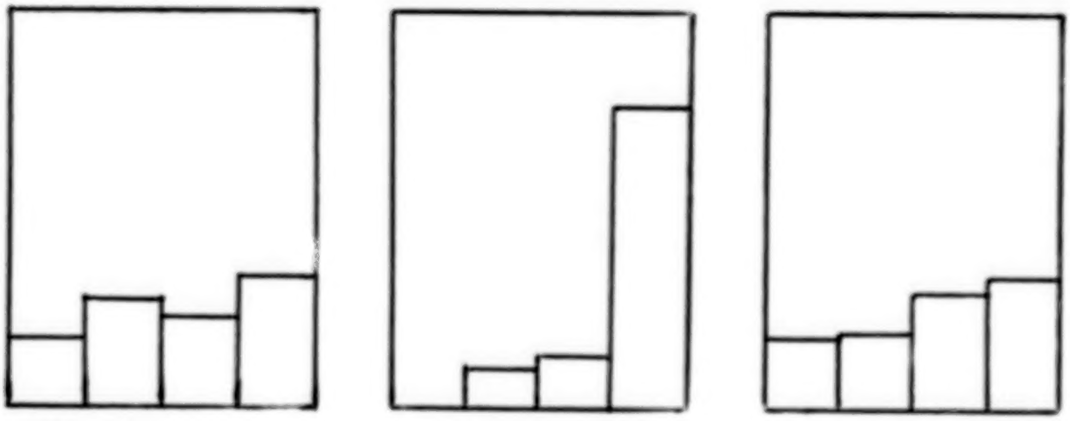

Fig.2a Fig.2b Fig.2c

Fig. 2: Density of points in zones 1-4 for observed triplets (a), simulated triplets without dark matter (b), and with significant ($M_o = 7M$) hidden mass (c).

We have also studied the configurations of simulated equal-mass systems during evolution; in a number of the simulations some hidden mass $M_o = 3, 7, 10$ M has been included in the models. The dark matter was distributed in accordance with the isothermal law within sphere with R = 1 (in scale of Figure 1). We have considered 50 trajectories for the equipartition distribution of the initial configurations within the region D and zero initial velocities.

The results of computer simulations strongly favor models with large hidden mass ($M_o = 10$ M) versus the ones with its absence.

In the absence of the hidden mass in the ensemble of 50 triple systems during a rather short time (about 0.5 ± 1 τ, where τ is the mean crossing time - see Anosova et al.

(1988)), a distribution is established which is characterized by strong excess in zone 4 (Figure 2b), that corresponds to the trends in alignment and hierarchy. This settled distribution weakly fluctuates during the time in spite of a rather small number of trajectories.

In the presence of a large hidden mass distributed within the volume of a triplet (the motion take place within a sphere R = 0.8), the apparent configurations have a significant diversity. Some excess of the configurations may take place within zone 1 as well as within zone 4 during the evolution. The most typical distribution is shown in Figure 2c.

Thus the statistics of configurations, forming during the dynamical evolution of the ensemble of the triple systems having some large dark mass, is in a better agreement with the statistics obtained by the analysis of galaxy triplets observed.

One can conclude that the two above methods of the study of distributions of configurations of the observed and simulated triplets of the galaxies have given similar results: no statistically significant tendency to alignment is observed.

No marked tendency to hierarchy is shown by the method of configuration parameters. The method of configuration zones does not allow division between the effects of alignment and hierarchy with certainty. The trend to alignment increases during evolution of the simulated triplets.

REFERENCES

Agekian, T. A., and Anosova, J. P. 1967, Sov. Astron. Zh., **44**, 1261.

Anosova, J. P. 1985, Totals of Science and Technology, Ser. Astron., **26**, 57.

Anosova, J. P. 1987, Astrofizika, **27**, 535.

Anosova, J. P., Orlov, V. V., Chernin, A. D., and Kiseleva, L. G. 1989, Astrophys. and Space Sci., **158**, 19.

Gorbatsky, V. G. 1986, Introduction to the Physics of Galaxies and Clusters of Galaxies, Moskow, Nauka.

Karachentseva, V. E., Karachentsev, I. D., and Lebedev, V. S. 1988, Izv. Special Astrophys. Observ., **26**, 42.

Karachentseva, V. E., Karachentsev, I. D., and Sherbanovsky, A. L. 1979, Izv. Special Astrophys. Observ., **11**, 3.

Kiseleva, L. G., and Orlov, V. V. 1989, Soobsch. Special Astrophys. Observ., **60**, 22.

DRAGGING FORCE ON GALAXIES DUE TO STREAMING DARK MATTER

Tetsuya HARA and Shigeru MIYOSHI*
Dept. of Physics, Kyoto Sangyo University, Kyoto 603,
* Institute of Astronomy, Cambridge, UK

It has been reported that galaxies in large regions ($\sim 10^2$Mpc), including some clusters of galaxies, may be streaming coherently with velocities up to 600km/sec or more with respect to the rest frame determined by the microwave background radiation.1) On the other hand, it is suggested that the dominant mass component of the universe is dark matter. Because we can only speculate the motion of dark matter from the galaxy motions, much attention should be paid to the correlation of velocities between the observed galaxies and cold dark matter. So we investigate whether such coherent large-scale streaming velocities are due to dark matter or only to baryonic objects which may be formed by piling up of gases due to some explosive events.

In fact, the observations of the large-scale structure of the universe 2) have changed the view of the formation of galaxies from the conservative one which mainly treates the increase of initial fluctuations in the expanding universe to some extreme ones as explosion scenarios or cosmic strings etc.3,4) In these cases, galaxies or other astronomical objects, named sometimes as population III, are formed by accumulation of baryonic gases due to some explosions. In such situations, the relative velocities between the objects and dark matter are expected.

In the following, we calculate the decrease of velocity difference between dark matter and the baryonic object in a simplified model, considering only the gravitational interaction between a condensed object and dust-like cold dark matter within the expandiNg universe. The equation for the relative velocity v between the dark matter and object is

$$dv/dt=-2v/(3t)-2\pi nmG^2M\ ln\,\Lambda/v^2 \qquad , \qquad (1)$$

where the first term represents the decay due to the expansion of the universe and the second term represents the dragging force due to the dynamical friction by the dust-like paticles of dark matter. Λ is a numerical factor given by

$$\Lambda=[1+(b_{max}v^2/GM)^2]/[1+(b_{min}v^2/GM)^2] \qquad ,$$

where b_{min} and b_{max} are taken as an order of the object size and mean distance between such objects.

The numerical calculations for equation (1) is given in Fig. 1 for $M=10^{12}M_\odot$. Then, if the observed peculiar velocity of $v_{ob}\simeq600$km/sec[1)] are due to the relic of some explosions at $(1+z_{ex})$, the initial velocity must be larger than $v_{ob}(1+z_{ex})$. As the galaxy formation era is speculated as $(1+z_{ex})\geq6$, such events must be very explosive.

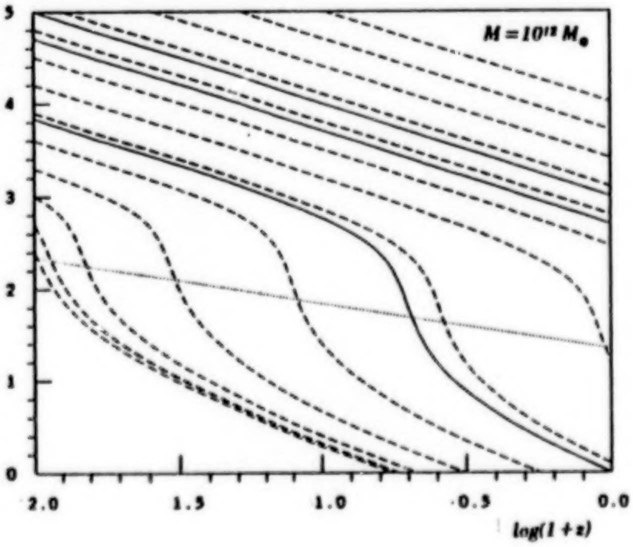

Fig. 1 The decrease of velocity difference for $M=10^{12}M_\odot$

The cases of boundary conditions for 1,500 and 10^3km/sec at 1+z=1 are given with solid lines. The cases of boundary conditions for 250×2^nkm/sec at $1+z=10^3$ where n=0,1,2,····12 are also shown by dashed lines. The values of $b_{min}=20$kpc and $b_{max}=4$Mpc/(1+z) are adopted. The criterion $GM/v^2\geqq vt$ is depicted by a dotted line.

The first term of equation (1) is greater than the second term when v is greater than v_c where v_c is given as

$$v_c = (3\pi nm G^2 M\ t \ln \Lambda)^{1/3}$$

$$= 9 \cdot 10\ h_{50}{}^{1/3} (M/10^{12} M_{\odot})^{1/3} (ln(\Lambda/10^2))^{1/3} (1+z)^{1/2}\ \mathrm{km/sec} \quad ,$$

taking $nm = 1/(6\pi G t^2)$. When v is much greater than v_c, the effect of dragging due to dark matter could be neglected. The velocity v_c at present ($v_c \simeq 10^2$km/sec) seems to be rather small compared to the observed dispersion velocity of galaxies ($\simeq$200km/sec), including the galaxies in pairs and groups. So, it seems rather difficult to imagine that each galaxy has followed the cold dark matter velocity field. There is the possibility that the field galaxies have followed the motion of dark matter as far as their dispersion velocities are smaller than v_c. 5)

If the velocity difference has much decreased due to such dragging force, dark matter may fall into the object. Hence it is interesting to investigate whether M/L ratio depends on the degree of the velocity dispersion. It seems natural to infer that M/L ratios are different between field galaxies and galaxies in cluster.

For clusters of galaxies where mass is order of $M \simeq 10^{15} M_{\odot}$, v_c is expected as large as $\simeq 10^3$ km/sec. M/L ratio is also very large for clusters of galaxies. Then it is probable that the motion of cluster of galaxies has followed that of dark matter. The numerical calculations for $M = 10^{15} M_{\odot}$ are given in Fig. 2. The cases for the dwarf galaxies of $M = 10^9 M_{\odot}$ are also shown in Fig. 3. If velocities of dwarf galaxies are smaller than $v_c \simeq 10(M/10^9 M_{\odot})^{1/3}$km/sec, they represent the velocity field of dark matter. It should be reminded here that, if the dispersion of cold dark matter is larger than v_c, there is no any such dragging effects, so the decrease of velocity difference could not be expected for the case of hot dark matter.

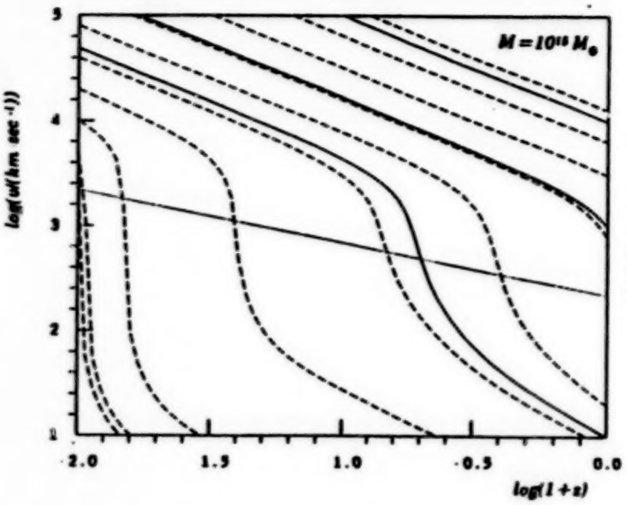

Fig. 2

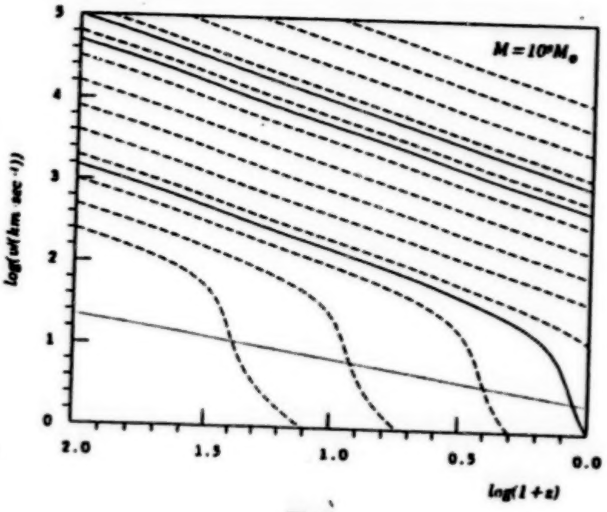

Fig. 3

In Eq. (1), it should be noted that $ln\,\Lambda$ term behaves as $(b_{max}v^2/GM)^2$ when v approaches to zero ($b_{max}v^2/GM \ll 1$), then the first term becomes dominant again and the velocity decreases as $v \propto (1+z)$. But the approximation of Rutherford scattering for the dragging term is inappropriate in the case that the accretion radius ($b \simeq GM/v^2$) is greater than the length that dark matter moves ($b \simeq GM/v^2 \geqq vt$).

Our scenario is as follows that the large-scale peculiar velocities ($\geq 10^2$ Mpc) are due to the motion of dark matter and clusters of galaxies follow such large-scale peculiar velocities. Such large scale peculiar velocities of dark matter may be due to density fluctuations of initial adiabatic perturbations which could be constrained by the observed isotropic background radiation. The velocity field of dark matter of such adiabatic perturbations is estimated from the continuity equation as

$$v \simeq \lambda\delta/t = 10^3(\lambda/10^2\,\mathrm{Mpc})(\delta/10^{-1})/(t/4\cdot10^{17}\mathrm{sec})\,\mathrm{km/sec}\ ,$$

where λ and δ are the characteristic wave length and density amplitude of the pertubations.

If we take Zeldovich spectrum for the initial adiabatic perturbations, the constraint for the density amplitude of scale $\lambda \leqq \lambda_c$ ($\lambda_c \simeq 10^2$ Mpc) is given [6]

$$\delta \leqq 3\times(1.4\times10^{-5})\times(1+z_{eq}) \quad ,$$

and for $\lambda \geqq \lambda_c$

$$\delta \leqq 3\times(1.4\times10^{-5})\times(1+z_{eq})\times(\lambda/\lambda_c)^{-2} \quad ,$$

where $1+z_{eq}$ and λ_c are the era of the equal density of radiation and matter and the present size of the horizen at $1+z_{eq}$. We take the observed upper limits of the background temperature fluctuations as $\Delta T/T \leq 1.4\times10^{-5}$ at 7.15 minutes. The upper limits for the velocity field of dark matter are depicted in Fig. 4. It could be said that the peculiar velocity field of dark matter in the large region ($\lambda \gg \lambda_c$) must be smaller than the value at λ_c.

The nonlinear density enhancements for the formation of galaxies and clusters of galaxies may not depend on the initial adiabatic perturbations. We would like to consider cosmic strings as the trigger for the formation of the objects, so the structure and velocity field around the cluster of galaxies would be determined by cosmic strings.

It seems that, although each galaxy will not follow the motion of dark matter, clusters of galaxies may represent the velocity field of dark matter. The origin of the velocity field of dark matter would be due to the initial adiabatic perturbations and, in fact, the observed peculiar velocities of clusters are within the allowed region constrained from the istropy of the microwave background radiation.

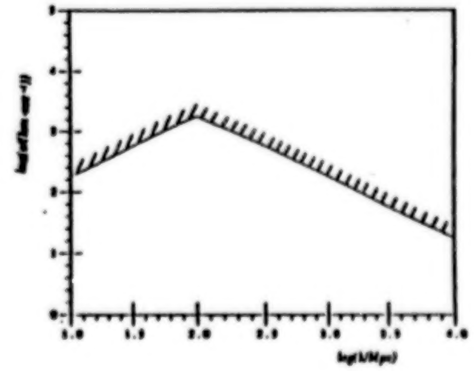

Fig. 4

REFERENCES

1) A. Dressler et al. Astrophys. J. 313(1987), L37.

2) V. de Lapparentet al, Astrophys. J. 302(1986), L1.

3) S. Ikeuchi, Publ. Astron. Soc. Jpn. 33 (1981)211.

4) A. Vilenkin, Phys. Rep. 121 (1985),263..

5) A. Sandage, Astrophys. J. 307(1986),1.

6) T, Hara, Prog. Theor. Phys. 70(1983), 1556.

TRIPLETS OF GALAXIES: THEIR DYNAMICS, EVOLUTION AND THE ORIGIN OF CHAOS IN THEM

Arthur D. Chernin
A. I. Herzen Pedagogical Institute
Leningrad, USSR

Alexei V. Ivanov
Institute of Astrophysics
Tadjik Academy of Science
Dushanbe, USSR

1. Recently Karachentsev's group at SAO (6-meter Telescope Observatory) published a list of 84 triple systems of galaxies with their distances, radial (line of sight) velocities, and angular sizes (Karachentseva et al., 1988). This gives a new ground for studies of the dark matter problem which fills the gap between the large cosmic scales (White, 1987; Dekel and Rees, 1987, and Einasto et al., 1977) and the scale of individual galaxies (Erickson et al., 1987). The data on the typical velocity dispersions and linear dimension of the triplets indicate that they contain considerable amounts of dark matter (see also earlier work of Karachentseva et al. (1979). Numerical simulations show that the statistical characteristics of the Karachentsev triplets can be imitated by model ensembles of triple systems with dark matter masses $M_d = (1 - 3) \times 10^{12} M_o$, which is almost ten times greater than the typical mass of stellar galaxies estimated by the standard mass-to-luminosity ratio (Kiseleva and Chernin, 1988).

Here we report that important information can be drawn from the data on the visible configurations of these systems. The statistics of configurations provide an independent evidence for dark matter in the triplets; moreover, it enables one to argue that dark matter seems to be distributed over the whole volume of the typical triplet forming its commom corona rather than concentrated within individual coronae (or haloes) of the member galaxies.

Let us consider a configuration diagram for triplets (Figure 1) where AB is the largest side of each of the visible configurational triangles; CBD is a part of circle of radius AB with the center in A; AB = AD, AC = DC, and CD is normal to AB. Any triangle finds its top (opposite to the largest side) in the area CBD, and therefore any triple system can be plotted as a point in this area (Agekian and Anosova, 1967).

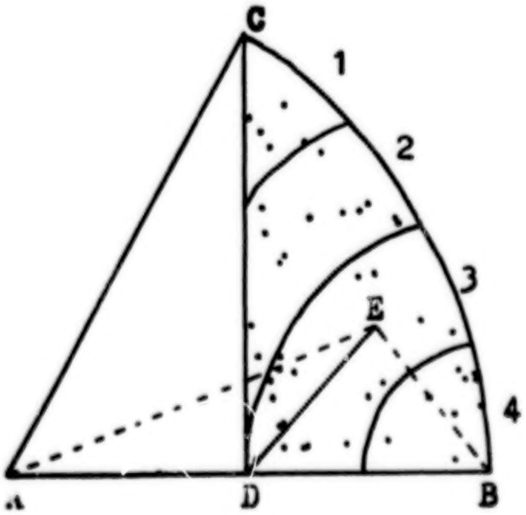

Figure 1 presents such a diagram for 46 "physical" triplets of the Karachentsev list. Their distribution over the diagram proves to be fairly homogeneous. The mean number density of the points in each of the four zones (as shown in Figure 1) is the same within the limits $\left|\frac{\delta n}{\langle n \rangle}\right| < 1.36\ \sigma$, where $\sigma = 0.28$, is the r.m.s. deviation in the Monte-Carlo experiment carried out especially for a random scattering of 46 points over the diagram area.

In our computer simulations, two types of numerical models imitating the observed triplets were studied: isolated three body system with components of equal masses (Model I), and three mass system with distributed dark matter spread spherically over the main volume of the system with density $\rho \sim 1/r^2$ ($r_1 < r < r_2$; $r_1 = 10$ Kpc, $r_2 = 1$ Mps) (Model II). The "softened" potential $\phi(r) = -Gm/(r^2 + \varepsilon^2)^{1/2}$ for body-body interactions was used, where $\varepsilon = 10^{-2}$ in the unit system with $G = m = 1$. The time was measured in the units of the crossing time $\tau = G(\sum_i m_i)^{1/2} \sum_{i,j} m_i m_j/(2|E|)^{3/2}$, where E is the total energy of the triplet. A set of ensembles of 46 triplets for each type of model has been compiled and analyzed. The results (Table 1) appear to be in favor of Model II.

TABLE 1

Relative Number Density, $\frac{n-\langle n\rangle}{\langle n\rangle}$, for Configuration Zones 1 - 4 of Figure 1

Zones	1	2	3	4
Observations	-0.32	0.10	-0.12	0.34
Model I	-0.70	-0.80	-0.30	1.80
Model II	-0.26	-0.24	0.16	0.34

Any ensemble of Model I reveals a considerable excess of configurations in zone 4: in a typical example shown in Table

1 $\left|\frac{\delta n}{\langle n\rangle}\right|_4 = 7.3\ \sigma$. Zone 4 contains hierarchial structures in which one side of the configurational triangle is much less than the other two. This excess of configurations in the physical space cannot be smoothed out by projection effects; on the contrary, projection would lead to an even greater excess of this kind in the statistics of visible configurations, as a special analysis shows. Only ensembles of Model II can provide homogeneous distributions of configurations over zones 1 - 4 similar to the observed statistics; in a typical example $\left|\frac{\delta n}{\langle n\rangle}\right| < 1.3\ \sigma$. Dynamical explanation of such a difference is related to the fact that the probability of formation and existance of a close binary within a system of three gravitating bodies is rather high (Kiseleva and Chernin, 1988). Systems with close binaries look in projection mostly like hierarchical configurations. However, distributed dark matter makes body-body interactions less effective and decreases essentially the probability of binary formation in Model II in comparison to Model I. Table 1 presents an example of ensembles in which this dynamical effect reveals itself most clearly. Generallly, ensembles of Models II demonstrate a wide variety of configuration statistics which merits a special study in the whole context of the statistical properties and stochatic behavior of triple galaxies.

2. Numerical experiments have demonstrated that chaotic dynamics can develop in the triple systems with a characteristic time scale which is sufficiently less than the age of the observed triple galaxies. We studied stochasticity of the

systems using the method by Casartelli et al. (1976) and computed the maximum Liapunov exponent $\Lambda(t) = \lim_{d(o) \to 0} (\frac{1}{t}) \ln \frac{d(t)}{d(0)}$ that gives one the mean exponential rate of divergence of two initially close trajectories. Here d(t) is distance between two trajectories in the phase space. More than 50 individual trajectories are analyzed. The Liapunov exponent proves to be positive for each of them, and reaches the values ~20 $1/\tau$. Figure 2 shows a typical curve for the time dependent Liapunov exponent. It provides a clear indication for dynamical instability in the system.

The numerical experiments enable one to trace also the divergence of trajectories directly. Figure 3 shows a typical evolution of d(t). It demonstrates the high sensitivity of the system to the small difference in the initial conditions which leads inevitably to stochastic behavior of the system in time.

Figure 4 demonstrates the autocorrelation function for the "configuration radius" $R(t) = \frac{|DE|}{|AB|}$. The rapid decrease (close to the exponential one) of the autocorrelation function is the characteristic feature of a system with stochastic motions.

The stochastic process described by Figures 2 - 4 develops in an extremely non-monotonic manner. The magnitude of d(t) increases (and then decreases) rapidly within the time period $\lesssim 10\ \tau$. Each of its jumps, by 200 - 400 times in value, is due to close approaches of the gravitating bodies. Distributed dark matter forming a common massive corona of the system stimulates transition to chaos because it decreases probability of regular structures like close binaries in these systems.

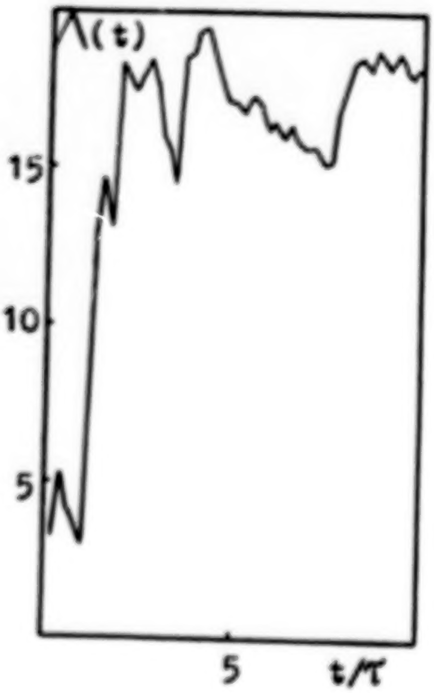

Figure 2

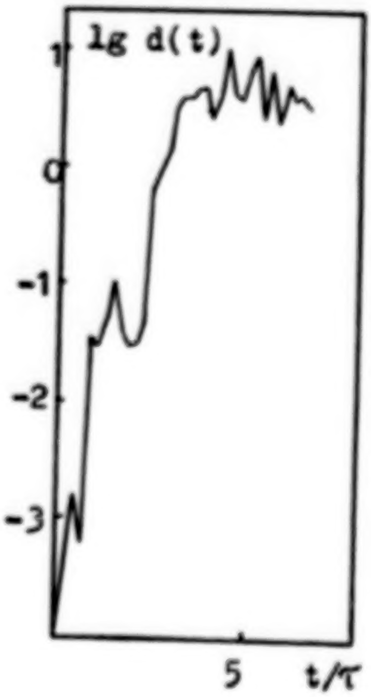

Figure 3

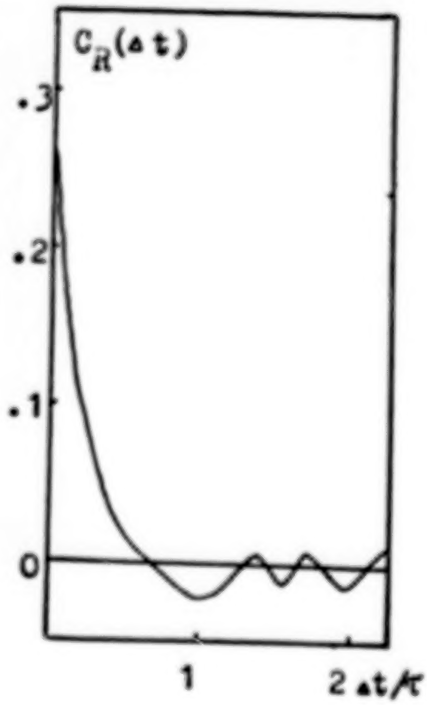

Figure 4

REFERENCES

Agekian, T. A., and Anosova, J. P., *Sov. Astron.*, **44**, 1261.

Casartelli, M., Diana, E., Galgani, L., and Scotti, A. 1976, *Phys. Rev. A*, **13**, 1921.

Chernin, A., Einasto, J., and Saar, E. 1976, *Astrophys. and Space Sci.*, **39**, 53.

Dekel, A., and Rees, M. J. 1987, *Nature*, **326**, 455.

Einasto, J., Kaasik, A., and Saar, E. 1977, *Nature*, **250**, 309.

Einasto, J., Saar, E., Kaasik, A., nd Chernin, A. D. 1974, *Nature*, **252**, 111.

Erickson, L. K., Gottesman, S. L., and Hunter J. H., Jr. 1987, *Nature*, **325**, 779.

Karachentsev, V. E., Karachentsev, I. D., and Lebedev, V. S. 1988, *Isvestia Spetsial'noi Astrofizicheskoi Observ.*, 26, 42.

Karachentsev, V. E., Karachentsev, I. D., and Sherbanovsky, A. J. 1979, *Isvestia Spetsial'noi Astrofizicheskoi Observ.*, 11, 3.

Kiseleva, L. G., and Chernin, A. D. 1988, Pis'ma v Astron. Zh., 14, 970.

Ostriker, J. P., Peebles, P.J.E., and Yahil, A. 1974, Astrophys. J. Lett., 193, 11.

White, S.D.M. 1987, Nature, 330, 451.

A CLASSIFICATION OF THE GALAXY GROUPS

Joanna P. Anosova
Astronomical Observatory
Leningrad State University
Bibliotechnaya pl.1
198904 Leningrad Petrodvorets USSR

ABSTRACT. A statistical criterion has been proposed to reveal the random and physical clusterings among stars, galaxies and other objects. This criterion has been applied to the galaxy triples of the list by Karachentseva, Karaschentsev and Scherbanovsky, and the double galaxies of the list by Dahari where the primary components are the Seyfert galaxies. The confident physical, probable physical, probable optical and confident optical groups have been identified. The limit difference of radial velocities of components for the confident physical multiple galaxies has also been estimated.

CLASSIFICATION OF GROUPS

The study of the structure of some class of gravitating bodies - the field of the stars or galaxies, as well as the simulated field of the N-body systems at some time of their evolution - is a search for the subsystems of different nature - the groups and the clusters with different numbers of members and the various forms, the chains, the voids, etc. It is possible to propose (Anosova 1986, 1988) the following classification of groups of gravitating objects (stars, galaxies or their groups, clusters, etc.) in order to detect these groups objectively:

(I) The groups in which all or a few compoents are by chance in the group region of the phase space; for these groups the criterion of isolation from the background object in the phase space is not fulfilled; one may qualify such groups as chance groups of objects or optical systems;

(II) The groups which are not such chance groups; their components have some common features; however, the gravitational forces between components are small or approximately equal to the regular forces of the environment; for these groups the criterion of isolation from the background objects in the coordinate space is not fulfilled; one may qualify such groups as non-chance groups of objects. One might divide these groups into two clsses:

(IIa) groups which are completely isolated in velocity space (e.g., moving star clusters);

(IIb) groups which are partially isolated in velocity space (e.g., in one or two of the velocity components, like some of the well-known Eggen's kinematical groups);

(III) the groups for which the criteria of isolation from the background objects are fulfulled in the coordinate space; in these groups the irregular gravitational forces between components (which are n in total number) essentially exceed the regular forces of the environment; one may qualify such groups as multiples with a physical connection between components.

(III-1) the multiple systems in which there is not a dynamical connection among all the components or a part of them; their total energy is non-negative $E > 0$. One might also divide such systems into two subclasses:

(III-1a) multiple systems in which there is no genetic connection among all the components or a part of them; all those n objects in a system, which are single, rapidly pass by each other or a number s ($s < n$) of single components and subsystems inside this system rapidly pass by each other;

(III-1b) multiple systems in which there is a genetic community of components but also there is a 'recession' of components ($E > 0$); e.g., according to the well-known concept of Ambartsumian;

(III-2) the multiples in which there is a dynamical connection between components, their total energy is negative $E < 0$; one might also divide such systems into two subclasses:

(III-2a) multiple systems in which there is no genetic community inside any part of components: s($s < n$) of single components and subsystems with a smaller multiplicity inside a system slowly ($E < 0$) pass by each other;

(III-2b) multiples in which there is a genetic community amongst all components (a co-formation), such systems may belong to one of the two dynamical types:

(III-I)* dynamically stable multiples;

(III-II)* dynamically unstable ones.

CRITERIA OF CLASSIFICATION

In order to recognize the systems of type I - the optical systems, or chance groups of objects, among the observed multiple stars or galaxies one can use a statistical criterion (see Anosova 1987) which consists in obtaining a probability P of this system being such one, and in estimating an expectation EX of the number of such chance groups in some phase volume Σ. One assumes for a calculation of P and EX that the objects under study are randomly distributed inside the Σ. Generally speaking, this criterion may be generalized for every distribution of the phase density of objects. If the values P and EX obtained are too big ($P \sim 1$, $EX \sim N/n$, where N/n is the maximum number of groups with multiplicity n in the volume Σ), then this group is a probable chance group. Otherwise ($P \sim 0$, $EX \lesssim I$), such a group is a probable non-chance group of objects and it belongs to the multiples of types II or III.

In order to recognize the groups of types II and III impartially one might use an analogous statistical criterion of isolation of the groups in the coordinate space. If such a criterion is not fulfilled, a group belongs to type II; otherwise, this multiple system is one with components connected physically.

The values P_n and EX_n can be expressed as follows:

$$P_n = C_{N-I}^{n-I}\, B^{n-I}(I - B)^{N-n}, \quad EX_n = C_N^n\, B^{n-I}\, (I-B)^{N-n};$$

$B = V(\sigma)/V(\Sigma)$, where $V(\sigma)$ and $V(\Sigma)$ are the volumes of σ and Σ, σ

is the phase space, of the group of multiplicity n, Σ is the phase space, of the whole sample of N objects, $N = (4\pi/3)R^3\nu$, r- the radius of the spherical volume Σ, ν-the mean number density of N objects in Σ.

When applied to galaxies, B has the following form

$$B = 0.25 \tan(\rho_n/2)^2 (r_I/R)^3 [I - (r_n/r_I)^3], \text{ by } r_n < r_I,$$

where ρ_n is the angular separation between the galaxies n and I; r_n and r_I are their line-of-sight distances (throughout this paper the Hubble constant H=75 km/s/Mpc is assumed). For obtaining the maximum estimate for P_n, we have taken $R = r_I$. If $r_n > r_I$, the indexes I and n change their positions by r in the formula for B.

We shall use the above statistical criterion for analyzing membership in the list of triples by Karachentseva, Karachentsev and Scherbanovsky (1979) and in the double galaxies of the list by Dahari (1985). Table I presents the distributions of multiples N(EX). Table I shows the numbers of the confident physical (EX < 1) and probably physical (EX < 300) systems as well as the numbers of the probably chance (300 < EX < 1000) and confident chance (EX > 1000) groups of galaxies. An increase of the cutoff value EX_{cr} = 300 may be caused by the internal dispersion of velocities of galaxies as well as by the uncertainties of the values.

One might also calculate by using the above statistical criterion the cutoff differences Δv_{cr} of the radial velocities of galaxies inside the confident physical multiples of EX < 1, the

Table 1. The distributions of the values EX for the triples (I) and the double galaxies (II).

EX	<1	1-10	10-100	100-300	300-500	500-1000	>1000
I	10	5	16	13	3	3	33
II	17	11	7	6	3	3	2

Table 2. The tolerant differences of the radial velocities of galaxies in the confident physical systems by EX < 1.

z^D kpc	IO	30	50	70
IO^{-2}	1000*	150	60	30
$2\ IO^{-2}$	200	20	10	5
$3\ IO^{-2}$	50	5	2	1
$4\ IO^{-2}$	25	2	1	0.5

*Δv_{cr}(km/s)

different separations D between the components and the Hubble distances cz/H_o. Table 2 shows such results for the Dahari's double galaxies: by the smaller D and Z the value $\Delta v_{cr} = 1000$ is possible, by an increasing D and Z the values Δv_{cr} are strong decreasing.

CONCLUSION

After constructing the hierarchical structure of some field (e.g., Materne 1978), one might use the above statistical criterion in order to recognize objectively the subsystems of various nature with different numbers of members and the various forms.

REFERENCES

Anosova, J.P. 1986, *Astrofizika*, **25**, 2,297.

Anosova, J. P. 1987, *Astrofizika*, **27**, 3,535.

Anosova, J. P. 1988, *Astrophys. Space Sci.*, **142**, 1-2,103.

Dahari, O. 1985, *Astron. J.*, **90**, 1772.

Karachentseva, V. E., Karachentsev, I. D., Sherbanovsky, A. L. 1979, *Izv. Spec. Astrofiz. Obs.*, **11**, 3.

Meterne, J. 1978, *Astron. Astrophys.*, **63**, 401.

VIRIAL COEFFICIENT AND HIDDEN MASS IN THE GALAXY GROUPS

J. P. Anosova and V. V. Orlov
Astronomical Observatory, Leningrad State University

L. G. Kiseleva
Leningrad Electro-Technical Institute, Leningrad USSR

ABSTRACT. The purpose of this work is a verification of the virial mass estimations for small galaxy groups. The dynamical evolution of triple and quintuple galaxies has been studied by the numerical simulations. The dependence of the virial coefficient k(t) versus time was derived. Initially k(0) = 0. The function k(t) has some strong oscillations from 0.02 to 0.99. Generally, these oscillations are quasiperiodical ones. Such a behavior of k(t) is caused by formation in a system of close isolated temporary double subsystems. A strong correlation between the virial coefficient and the least mutual distance in the system is observed.

Such wide oscillations may add into the estimation of virial mass of the galaxy groups an uncertainty of more than one order. An additional uncertainty is introduced by the projection effect. This uncertainty for the individual estimations of the masses approach three orders. Thus any individual estimation of the virial mass is impossible for small galaxy groups.

Some possibility of statistical estimation (median or average) of the total mass, including a hidden mass, is shown for the homogeneous samples. We propose a method for these

estimations based on a comparison of the medians of dynamical parameters (a mean size in projection and a dispersion of relative radial velocities) for the simulated and observed ensembles of the galaxy groups. This method has been applied to a sample of 46 probably physical triplets of galaxies. The probable median of the hidden mass in a volume of the triplet is about 4 M, where M is the total mass of visible matter.

On the study of galaxy groups, the problem of determination of the mass of a system on the basis of the data observed (the sizes and configurations of the systems on the sky and radial velocities of the components) arises. Usually, one uses the virial theorem in any form (Heisler et al. 1985) in order to estimate the dynamical mass of a galaxy system. The aim of this work is some verification of the virial estimates of masses for the small galaxy groups. A method of computer simulations has been used (e.g., Anosova et al. 1989).

One of the most important parameters of the dynamical state of the N-body system is the ratio of its kinetic energy T to the potential energy U: a virial coefficient $k = T/|U|$. The time averaged value for k is equal to 0.5 for an isolated stationary system of gravitating bodies, here one bears in mind a ratio of the mean kinetic energy $\overline{T}$ to the mean potential one $|\overline{U}|$.

The computer simulations (Anosova et al. 1989) have shown that the dynamical states of the multiple galaxies may strongly change during the evolution. Often the temporary isolated binaries are formed in systems which have as a rule elongated orbits. Such binaries result in some important variations of the energies T and U.

At first, let us consider a variation of the virial coefficient k versus time t, for isolated binaries in terms of the orbital eccentricity e. The functions k(t) are shown in Figure 1 for e = 0, 0.2, 0.6, 1.0. The time t is in units of the period P of the binary. The average over the period is

$$\bar{k} = \frac{1}{P} \int_0^P k(t)\, dt = 0.5 - e^2/4. \quad (1)$$

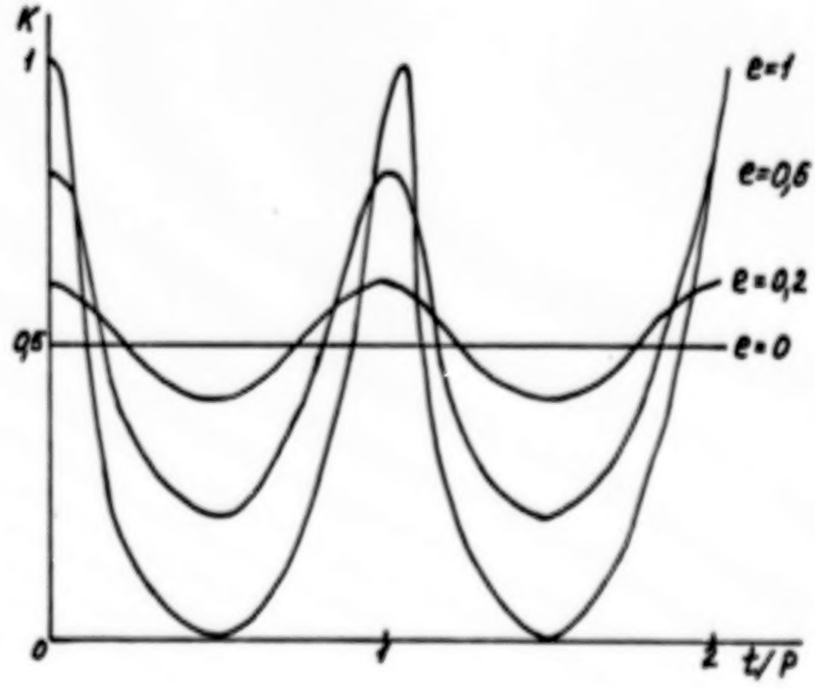

Figure 1. The dependence of the virial coefficient k(t) on time for binary systems with different eccentricities.

The average K over the eccentricity e within the interval (0,1) is equal to

$$\langle\bar{k}\rangle = \int_0^1 \bar{k}(e)\, de = 5/12 = 0.42 \quad (2)$$

in the case of a homogeneous distribution of e. Let us note that a ratio of the average of time quantities $\overline{T}$ and $|\overline{U}|$ does not depend on e, it is equal to 0.5.

Now, let us consider the behavior of the virial coefficient k versus the time t in 3- and 5-body systems. Some typical examples of k(t) are shown in Figures 2 and 3. The time t is in the units τ - the mean crossing time for the triple system (e.g., Anosova et al. 1989). One has adopted k(0) = 0 for the triple

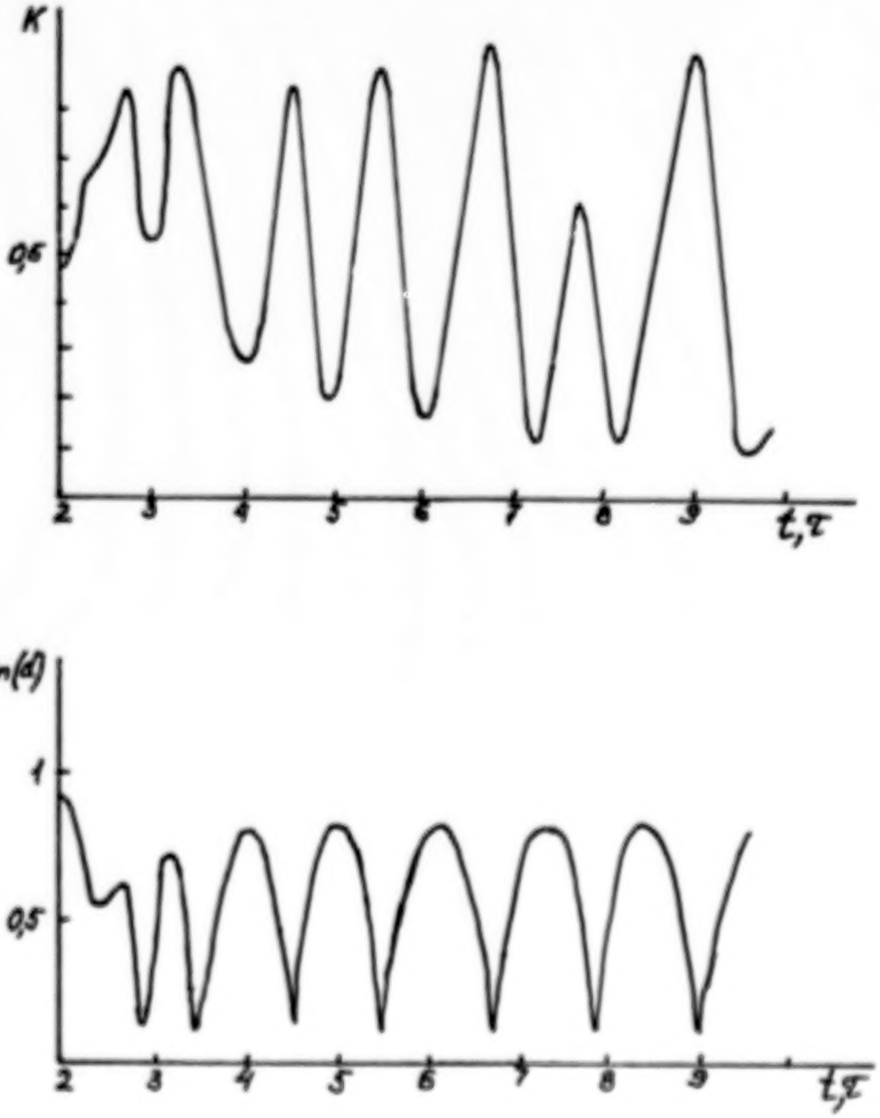

Figure 2. The dependence of the virial coefficient k(t) and the minimum separation $r_{min}(t)$ for the triple system. A strong correlation is observed.

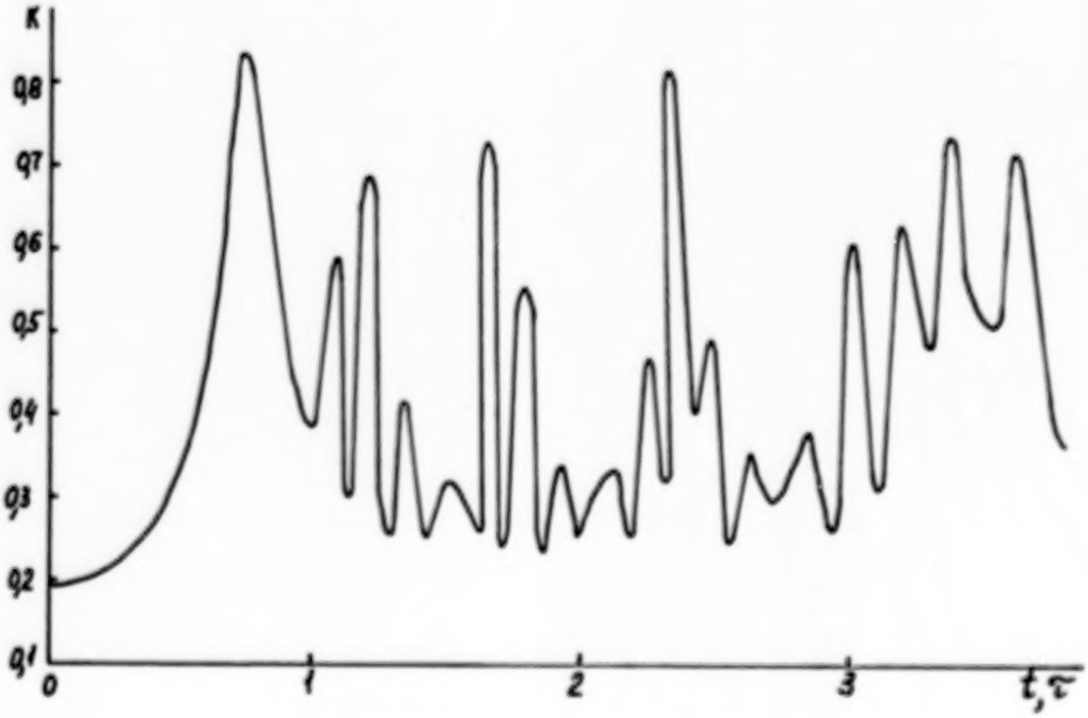

Figure 3. The dependence k(t) for the quintruple system.

systems; the dependences k(t) have been obtained, beginning from $t = 2\tau$ as the triple system "forgets" its intial state after this time. The functions k(t) have strong oscillations within the interval (0.02, 0.099). Often these oscillations for the triple systems have a quasiperiodical character; such a behavior is caused by the formation of temporary double subsystems. This conclusion is supported by the strong correlation between k and the minimum mutual separation r_{min} in a triplet (see Figure 2). The coefficients of correlation between k and r_{min} are shown in Table 1 for the models with equal-mass as well as different mass compoents. Here N is the number of realizations considered, and Δt is the time interval between two neighoring realizations. This Table shows strong correlation between k and r_{min} for all ratios of the masses considered. The coefficient of correlation weakly depends on the ratio of the masses.

Table 1

Mass ratio	1:1:1	1:1:3	1:3:3	1:2:6	1:3:9	1:4:12	1:5:15
Correlat. Coefficient	-0.88	-0.90	-0.83	-0.89	-0.81	-0.72	-0.79
N	525	525	525	2626	525	2625	2625
Δt	0.5	0.5	0.5	0.1	0.5	0.1	0.1

The distribution of f(k) is shown in Figure 4. It has been constructed from 4400 realizations fixed in $\Delta t = 0.2\tau$ within the interval $(2, 10)\tau$. The moments of this distribution are equal to $k = 0.41$, $\sigma_k = 0.21$.

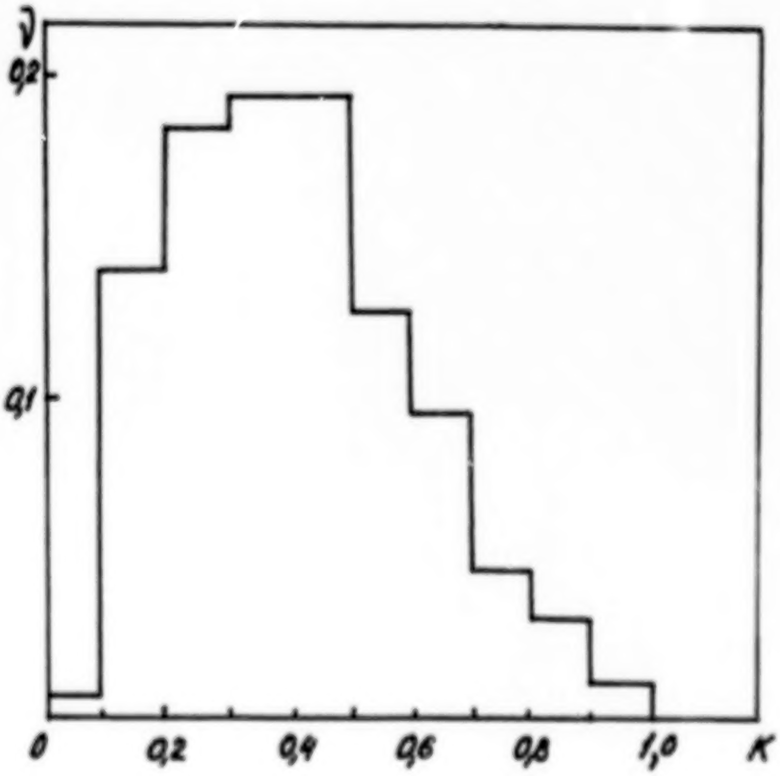

Figure 4. Distribution f(k) for the 4400 realizations of the simulated triplets.

Such strong oscillations of k(t) may make an uncertainty in the estimation of the virial mass of the galaxy groups of more than one order for an individual group. Some additional uncertainty will be made by the effect of projection - using projected distances and radial velocities instead of the three-dimensional sizes and velocities. The projection uncertainty of the individual virial mass of the galaxy group may be as large as three orders. In order to estimate the characteristic maximum uncertainty in the virial mass by both above effects, we have considered a sample from the simulated catalogues of triples with equal-mass components during the evolution. We have determined the medians of the minimum and maximum virial mass of the triplets $(M_{min})_{1/2} = 10^{-2.63}$ and $(M_{max})_{1/2} = 10^{0.25}$ in units of the actual mass of the triplet. Thus the characteristic scattering between the maximum and minimum virial estimations of the mass reaches to 3 orders. Therefore one may make a conclusion that any reliable individual estimation of the virial mass is impossible for galaxy triplets.

By the numerical simulations, we have shown some possibility for reliable statistical estimates (median or average) of the total mass of the galaxy triplets taking into account dark matter. This estimation is certain for homogenous samples of the objects. A statistical method has been proposed in order to make such estimates. This method is based on a comparison of the medians of the dynamical parameters (an average projected size r of the system and a dispersion s of the relative radial velocities of the galaxies) for the simulated and observed samples of galaxy groups. It has been applied to a sample of 46 probably physical systems from a list by Karachentseva et al. (1988), the selection of the probably physical triplets has been carried out using the criterion of Anosova (1987).

The simulated catalogues are compiled for equal-mass components and the different hidden mass M_0, as well as for different-mass components. The medians $r_{1/2}$ and $s_{1/2}$ are compared for the simulated catalogues and the physical galaxy triplets after a corresponding renormalization. It has been assumed that the simulated and observed ensembles are in agreement if the medians $r_{1/2}$ and $s_{1/2}$ do not differ more than 10% simultaneously. The results are shown in Table 2 and Table 3.

Table 2

Hidden mass	0	50	75	100	125
Number of the "coincidences" within 10%	0	4	7	5	4
Ave. dark mass within a volume of triplet	0	10.6	13.9	14.5	16.4

Table 3

Ratio of masses	1:1:1	1:1:3	1:3:3	1:2:6	1:3:9	1:4:12	1:5:15
Number of the "coincidences" within 10%	0	0	0	2	2	4	8

In the first line of Table 2, the hidden mass, distributed isothermally inside a sphere with radius equal to 10 d (d is the mean size of the triplets), is indicated in units of the mass of one component of the triplet. At the second line, a number of the compatible (within 10%) ensembles (26 out of 100) triplets are represented. At the last line, the mean hidden mass inside the volume of a triplet is shown (a dark mass inside a sphere with radius equal to a distance from a centre of its distribution to the most distant body from this centre). The probable median of the dark mass in the volume of the triplet is equal to about 4 M, where M is a total mass of the triplet. A noticeable number of "coincidences" are observed in a coase of the significant dispersion of the masses as 1:5:15 in the models without any hidden mass. However, the masses of the components of the galaxy triplets are similar (Karachentsev 1987), therefore a preference may be given to the dark matter hypothesis. May be, some superposition of two effects takes place that demands a further verification.

Authors thank Professor A. D. Chernin very much for the valuable discussion of the results and a number of the interesting propositions.

REFERENCES

Anosova, J. P. 1987 Astrofizika, **27**, 535.

Anosova, J. P., Orlov, V. V., Chernin, A. D., and Kiseleva, L. G. 1989, Astrophys. and Space Sci., **158**, 19.

Heisler, J. Tremaine, S., and Bahcall, J. N. 1985, Astrophys. J., **298**, 8.

Karachentsev, I. D. 1987, Private Communication.

Karachentseva, V. E., Karachentsev, I. D., and Lebedev, V. S. 1988, Izv. Special Astrophys. Observ., **26**, 42.

ON THE LARGE-SCALE STRUCTURES FORMED BY WAKES OF OPEN COSMIC STRINGS

Tetsuya HARA, Shoji Morioka and Shigeru Miyoshi*

Department of physics, Kyoto Sangyo University, Kyoto 603
* Institute of Astronomy, Cambridge, UK

Large-scale structures of the universe have been variously described as sheetlike, filamentary, cellular, bubbles or spongelike.1~2) Recently cosmic strings become one of viable candidates for galaxy formation scenario3~10), and some of the large-scale structures seem to be simply explained by the open cosmic strings6).

Due to this scenario, sheets are wakes which are traces of moving open cosmic strings where dark matter and baryonic matter have accumulated.7,10) Filaments are intersections of such wakes and high density regions are places where three wakes intersect almost orthogonally6). The wakes formed at t_{eq} become the largest surface density among all wakes, where t_{eq} is the epoch when matter density equals to radiation density7,9). Then it can be expected that the characteristic size of the sheets are $\sim 10^2$Mpc×10^2Mpc and length of filaments are $\sim 10^2$Mpc. It is explained that the typical surface density of sheets, line density of filaments and mass of clusters are $\sim 10^{12}(G\mu\beta\gamma/2\cdot 10^{-6})M_\odot/\mathrm{Mpc}^2$, $\sim 10^{13}(G\mu\beta\gamma/2\cdot 10^{-6})^2 M_\odot/\mathrm{Mpc}$ and $\sim 10^{15}(G\mu\beta\gamma/2\cdot 10^{-6})^3 M_\odot$6) where μ and β are the line density and the velocity of the string, and $\gamma=(1-\beta^2)^{-1/2}$.

If we assume that there is one open cosmic string per each horizon, then it can be explained that the typical distances among wakes, filaments and clusters are also $\sim 10^2$ Mpc11,6). This model does not exclude a much more large scale structure. Open cosmic string may move even now and accumulate cold dark matter after its traces, however, the surface density is much smaller than the ones formed at t_{eq}[8,9].

From this model, it is expected that the typical high density region will have extended features such as six filaments and three sheets and be surrounded by eight empty regions (voids)[6]. In this paper, we mainly concern with such structures and have made numerical simulations for the formation of such large scale structure.

We consider the Einstein-de Sitter universe with $\Omega=1$, consisting of dominant dark matter($\Omega_d \simeq 0.9$) and baryon matter($\Omega_b \simeq 0.1$), and h=0.5 is used ($h=H_0/(100\mathrm{km \cdot sec \cdot Mpc^{-1}})$ and H_0 is the Hubble constant at present). Near the sheet, the accumulated dark matter and baryon matter may be fragmented due to the plane instability and objects of mass of order $\sim 10^7 M_\odot$ are formed around $z=10^2$ when H_2 cooling becomes effective[7]. For the evolution of the massive star within such objects, the universe becomes again lumonous (flare up)[8]. Due to the explosion of such massive stars will form the plane shock waves and later the shock wave will accumulate the baryon matter like snow plough. Through fragmentations of such plane, more massive secondary objects will be formed and so on[8].

Through such mechanism, galaxies will be formed after $1+z \simeq 7$ when the cooling time of inverse Compton by background radiation becomes longer than the expansion time of the universe. The detailed physical process through which galaxies are formed including heating and cooling process of interwake and near wake medium are now in preparation. The decrease of velocity difference between baryon objects and dark matter are discussed and due to the calculations, the velocity difference decrese rapidly if the velocity difference is smaller than the critical value[12]. For simplicity, we just assumed that galaxies are formed at $1+z \simeq 7$ near wakes and follow the motion of dark matter.

Calculations are performed with 32^3 particles and 32^3 cells in a cube with comoving length $L=40h^{-1}$Mpc. Dark matter and galaxies are follwed by N-body code using the PM method with the CIC mass assignment scheme[13].

The constant density surface of dark matter where the wake is in the x-y plane is shown in Fig. 1a. The characteristic thickness of the dark matter is given as $h \sim 2.((1+z_1)/6.10^3)^{1/2}(1+z)^{-2}(G\mu\beta\gamma/10^{-6})\mathrm{Mpc}$ 8) and such wake could be extend $10^2 \times 10^2 \mathrm{Mpc}^2$ or so. The intersection of two wakes are shown for its distribution of dark matter in Fig. 2a . The cone diagram (velocity versus right ascension maps) for the galaxies are also shown in Fig. 2b. The case for orthogonal intersections of three wake is calculated and the distribution of the dark matter around the high density regions and cone diagrams are displayed in Figs. 3. The observation by Geller et al 1) is also shown in Fig. 3d.

The patterns in the cone diagram of Figs. 3 could be almost due to the combination of wall nature distributions of galaxies and slice observation. The filamentary or sheetlike distribution of galaxies around rich cluster could be checked by many slice observation.

It is difficult to estimate to what extent this model is fit to observations further than the impression of the similarity between the two graphs of Figs. 3c and 3d. Due to the impression, however details are different, it is not so bad correpondence between calculations and observations.

From the inspection of Figs. 2 and 3, the filamentary structure is the slice of the wall(wake). As galaxies in the wall move into the center, one wall structure, in the redshift plane, becomes discontinuous line at the center.

It seems a little bit difficult to find out 6 filaments from the slice of CfA redshift survey by Gellar et al 1). Then, Coma cluster must be explained by one sheet and some instability. It could also be considerd that the wakes may not pass through orthogonally or loop of cosmic string might contribute for the formation of Coma cluster.

In general, the wall structure is rather characteristic for our calculation. To make comparison with calculations to observations in detail, we must understand much more the mechanism of galaxiy formation.

It could be concluded that the scenario of open cosmic string with cold dark matter seems a one of good candidate for understanding the observed large scale structure of galaxies and this scenario could be enough falsifiable by observation.

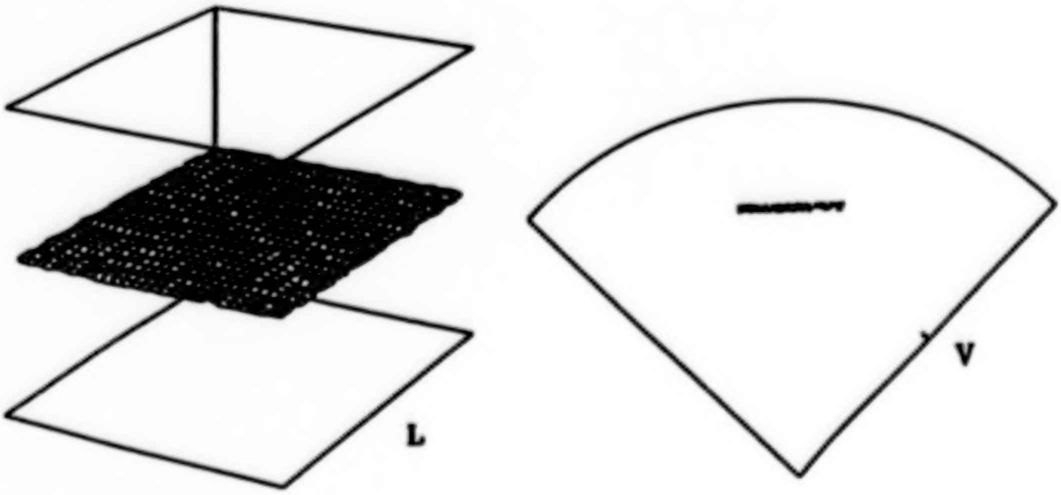

a) b)

Fig. 1

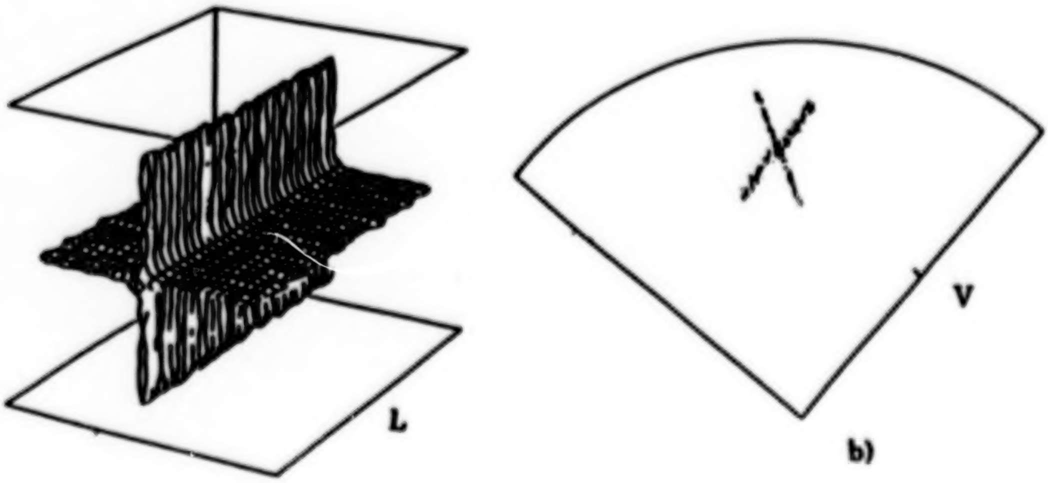

b)

a)

Fig. 2

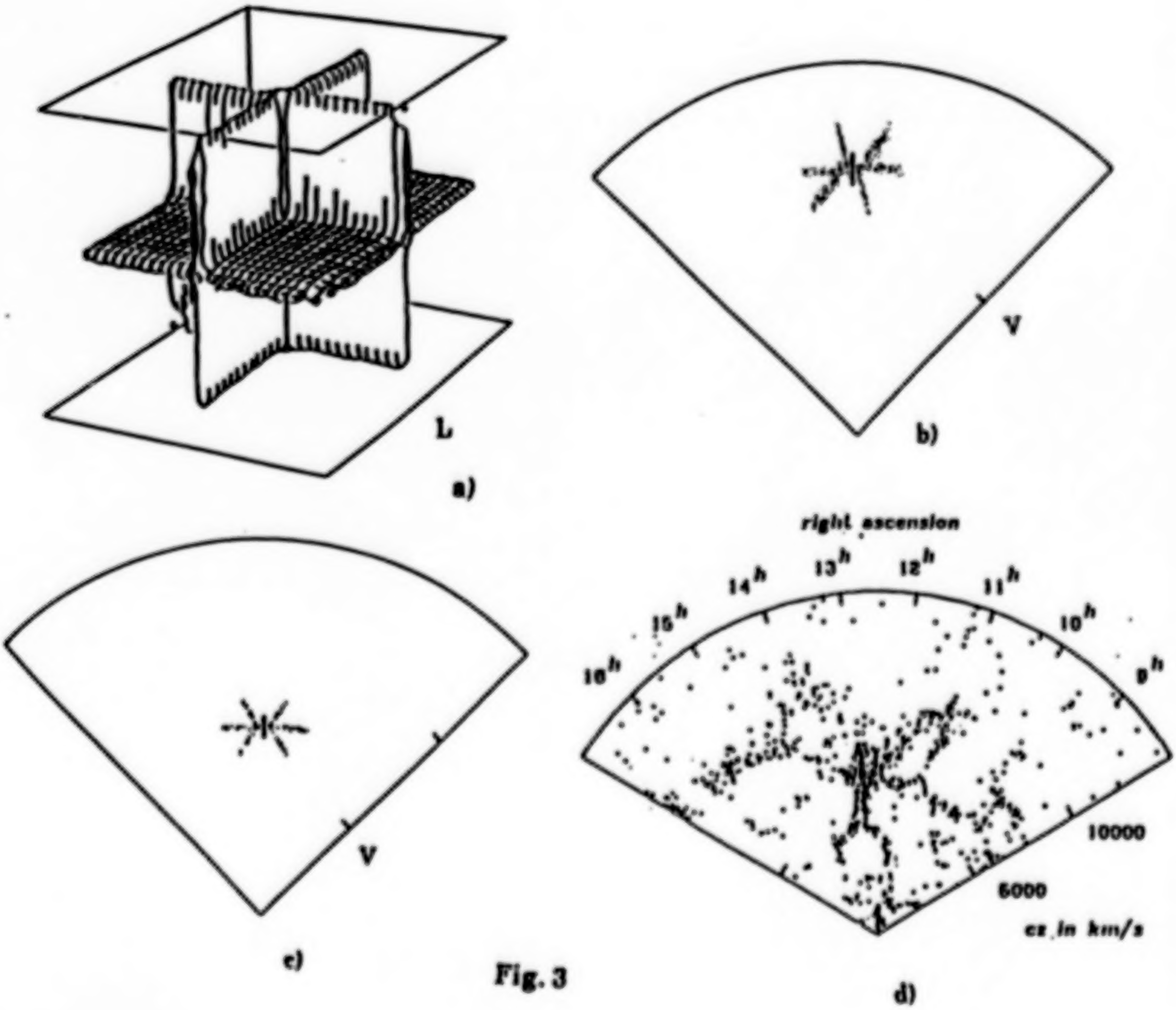

Fig. 3

REFERENCES

1) V. de Lapparent, M. J. Geller and J. P. Huchra, Astrophys. J. 302(1986), L1.
2) M. P. Haynes and R. Giovanelli, Astrophys. J. 306 (1986), L55.
3) A. Vilenkin, Phys. Rep. 121 (1985),263.
4) J. Silk and A. Vilenkin, Phys. Rev. Lett.53(1984),1700.
5) T. Vachaspati, Phys. Rev. Lett. 57(1986), 1655.
6) T. Hara and S. Miyoshi, Prog. Theor. Phys. 81(1989),1187.
7) T. Hara and S. Miyoshi, Prog. Theor. Phys. 77(1987),1152.
8) T. Hara and S. Miyoshi, Prog. Theor. Phys. 78(1987),1081.
9) A. Stebbins et. al. Astrophys. J. 322(1987), 1.
10) M. J. Rees, Mon. Not. R. Astron. Soc. 222(1986), 27p.
11) A. Albrecht and N. Turok, Phys. Rev. Lett. 54(1985), 1868.
12) T. Hara and S. Miyoshi, preprint
13) R.W.Hockney and J.W.Eastwood, "Computer Simulation Using Particles"(1981;MacGraw Hill,New York).

COLLISIONAL REMOVAL OF HI FROM THE INNER DISKS OF VIRGO CLUSTER GALAXIES

MONICA VALLURI and CHANDA J. JOG
Department of Physics, Indian Institute of Science,
Bangalore, INDIA

ABSTRACT

In addition to the well established global HI–deficiency seen in Virgo cluster spirals, many of them are found to be HI–deficient in their inner disks. We show that collisions between galaxies in a cluster can lead to the preferential removal of HI from these galaxies. This follows directly from the application of the Spitzer–Baade collisional gas removal mechanism to galaxies consisting of stars and a two-component ISM of HI and H_2, with HI having the largest filling factor. This can account for both the observed HI–deficiency in the inner disks of these galaxies as well as their normal H_2 contents. The frequency of galaxy collisions in the Virgo cluster is shown to be large enough to make collisional gas removal a viable mechanism.

INTRODUCTION

The global HI–deficiency in spiral galaxies in clusters is largely due to the loss of HI gas from their outer disks (for a review see Haynes, Giovanelli, and Chincarini 1984). It is believed that gas is removed from galaxies by ram–pressure stripping by the intracluster medium (ICM), (Gunn and Gott 1972), or during collisions between galaxies (Spitzer and Baade 1951) or by other mechanisms involving galaxy–ICM interactions. Using the HI data from Warmels (1986), for spiral galaxies in the Virgo cluster, we show that a large fraction of galaxies are not only deficient globally but also in their inner disk regions.

CO observation of HI–deficient galaxies in Virgo, (e.g. Kenney and Young 1989), have shown that the H_2 component in these galaxies has been unaffected by the removal of HI.

Ram–pressure stripping, the most popular gas removal mechanism, is expected to be less effective in removing HI from the inner disks, ($r < R_0/2$, with R_0 being the Holmberg radius), where the gravitational binding force is higher than it is at larger radii and where, in addition, the H_2 gas is concentrated. *We propose that collisions between galaxies is an important mechanism by which HI can be removed from their inner disks while leaving the H_2 component undisturbed.*

HI DEFICIENCY IN THE INNER DISKS

From high resolution mapping of spiral galaxies both in the Virgo cluster and in the field, Warmels (1986) has obtained estimates for the degree of HI–deficiency in the inner disks of cluster galaxies. The degree of deficiency of a cluster galaxy is estimated by the parameter

$$\mathrm{DEF_{IN}} = \log\left[\frac{< \sigma_{\rm HI} >_{\rm T,\ field}}{(\sigma_{\rm HI})_{\rm T,\ cluster}}\right] \tag{1}$$

where $(\sigma_{\rm HI})_{\rm T, cluster}$ is the HI surface density averaged over half the Holmberg radius ($R_0/2$) for a cluster galaxy, and $< \sigma_{\rm HI} >_{\rm T, field}$ is the mean value of $\sigma_{\rm HI}$ for a sample of field galaxies of the same morphological type T. A galaxy is usually considered HI–deficient if it has a factor of two less HI than an average field galaxy (i.e., $\mathrm{DEF_{IN}} \geq 0.3$). We show that, of the 26 galaxies in Warmels' sample lying within the Abell radius (5° from M87), 22% are HI–deficient in their inner disks, this is much greater than the 7% expected to have such a low value of $\sigma_{\rm HI}$ purely from the gaussian spread in this quantity. Kenney and Young (1989) have shown from the same data that galaxies that are globally deficient in HI by a factor of 10, are HI–deficient in their inner disks by a factor of 2-3.

PHYSICAL MECHANISM FOR COLLISIONAL GAS REMOVAL

Spitzer and Baade (1951) showed that when cluster galaxies collide with a high relative velocity ($V_{rel} \sim 2000$ km s^{-1}, their stellar components are unperturbed, but their ISM components with their large filling factors, undergo inelastic collisions. If $V_{rel} > V_{esc}$, the escape velocity from the galaxy, (with $V_{esc} \sim 300$ km s^{-1}), the colliding gas components would be lost from the galaxies since the kinetic energy of the collision would be thermalised and would heat the gas to a temperature of $\sim 5\times10^7$ K, giving it sufficient energy to escape from the disk. Even if the gas cooled rapidly, it would condense as a cold cloud and would be left behind at the center of mass of the receding galaxies.

The Importance Of Filling Factor

Gas clouds of a particular ISM component will collide if their mean free path, (λ), is less than the dimensions of the region of overlap of the two galaxies. Spherical clouds of radii, R_c, of an ISM component of filling factor, f, will have a mean free path (λ) given by

$$\lambda = \frac{2R_c}{3f} \tag{2}$$

Gas clouds from the two galaxies will collide if λ is less than the maximum dimension, d, of the overlapping region. The HI component consists of at least three sub-components, with the cold neutral medium of Kulkarni and Heiles (1987) having the smallest filling factor. If we consider the standard Spitzer clouds with R_c = 5pc, and f = 0.1, then the mean free path, λ = 35pc. In the extreme case of a face–on collision, d is a minimum $\approx 2Z_{1/2}$, or twice the scale height of the gas distribution. Since $Z_{1/2}$ = 100pc for the clouds of the cold neutral medium, $\lambda \ll$ d, and hence even in this case the HI clouds in the overlapping volume would collide. The other HI components are believed to be in sheet–like or filamentary clouds and to have a larger filling factor. Hence all the HI gas in the overlapping volume will be lost from the colliding galaxies.

For the H_2 clouds, on the other hand, R_c = 25pc, f = 0.02, and $Z_{1/2}$ = 65pc, hence from eq.(1), $\lambda = 1$ kpc which is much greater than d = 0.13 kpc. Hence the H_2 clouds will rarely collide and are unaffected by the encounter.

Therefore, the filling factor of a particular gas component is critical in determining whether or not it will be stripped from the colliding galaxies. Collisions between galaxies is therefore a mechanism by which HI can be preferentially removed from the inner disk of a galaxy leaving the H_2 unaffected (Valluri and Jog 1990a).

Collision Frequency

To obtain an estimate of the collision frequency we assume that spiral galaxies within the 5° -region have isotropic orbits and an isotropic velocity disribution. The one-dimensional velocity dispersion of spiral galaxies in this region is ~ 800 km s^{-1} and their number density, n ~ 15 galaxies Mpc^{-3}. The galaxies in Warmels' sample, (believed to represent the entire spectrum of galaxies in the cluster), are distributed into three bins of logarithmically increasing galaxy size (R_0). The number of galaxies in each bin (N_i) is almost the same and hence the bin number density $n_i = n/3$. The total collision frequency for a galaxy in the i^{th} bin with mean radius $< R_0 >_i$ is

$$\omega_{ci} = 2\pi \, \frac{n}{3} \, V_{rel} \sum_{j=1}^{3} \left[\frac{\langle R_0 \rangle_i + \langle R_0 \rangle_j}{2} \right]^2 \qquad (3)$$

If galaxies have been undergoing collisions for 1/2 the Hubble time (t ~ 6×10^9 yr), the collision probability $P_{ci} = \omega_{ci} \cdot 6\times10^9$. In Table 1 we compare the fraction (F_D) of deficient galaxies in each bin with the corresponding collision probability P_{ci}.

TABLE 1.

COMPARISON OF COLLISION PROBABILITY WITH DEFICIENT FRACTION

i	SIZE* RANGE $< R_0 >$	MEAN SIZE $< R_0 >_i$	NUMBER OF GALAXIES N_i	COLLISION PROBABILITY P_c	DEFICIENT FRACTION F_D
1	<7.0 kpc	5±1	8	0.06±0.02	0.13 (1/8)
2	7.0 – 11.0	9±1	9	0.09±0.03	0.22± (2/9)
3	> 11.0 kpc	15± 2	9	0.15±0.05	0.33 (3/9)

* Holmberg radius

We note that both P_c and F_D increase with galaxy size and in each case $P_c \sim 1/2 \cdot F_D$. The value of P_c may be uncertain by a factor of few due to the assumption of isotropic orbits and the uncertainty in the number density of galaxies. However the trend of an increase in the fraction of deficient galaxies with increasing size points to collisional gas removal as a likely mechanism rather than ram-pressure stripping.

In a related work currently in progress, we find that in the three rich clusters A262, A1367, and A1656, the fraction of globally HI–deficient spiral galaxies increases with size, dropping only for the largest size bin. We also find that the most highly deficient galaxies are always of the largest sizes. A much larger sample of 81 galaxies in the Virgo cluster also exhibits a similar trend. *This clearly indicates that the dominant gas removal mechanism is more effective on larger galaxies than on smaller galaxies.* We find that the collisional gas removal mechanism is the only one that is capable of qualitatively accounting for all the features of the size-dependence of HI–deficiency, (Valluri and Jog 1990b). We conclude, therefore, that collisions between galaxies in a cluster is a mechanism which can result in the preferential removal of the HI component of the ISM from galaxies both globally and from their inner disks.

REFERENCES

Gunn, J. E., and Gott, J. R. 1972, *Ap. J.*, **176**, 1.

Haynes, M. P., Giovanelli, R., and Chincarini, G. 1984, *Ann. Rev. Astron. Astrophys.*, **22**, 445.

Kenney, J. D., and Young, J. S. 1989, *Ap. J.*, **344**, 71.

Kulkarni, S. R., and Heiles, C. 1987, in *Galactic and Extragalactic Astronomy*, (2nd ed.), eds. G. Verschuur and K. Kellermann, (New York: Springer Verlag).

Spitzer, L., and Baade, W. 1951, *Ap. J.*, **113**, 413.

Valluri, M. and Jog, C. J. 1990a, *Ap. J.*, in press.

Valluri, M. and Jog, C. J. 1990b, *in preparation*.

Warmels R. 1986, *Ph. D. Thesis*, Univ. of Gronongen.

IX. THEORY OF INTERACTION

STIMULATED EFFECTS

INDUCED STARBURST AND NUCLEAR ACTIVITY: FAITH, FACTS AND THEORY

Isaac Shlosman

Theoretical Astrophysics 130-33
California Institute of Technology
Pasadena, CA 91125

ABSTRACT. The problem of the origin of starburst and nuclear (nonstellar) activity in galaxies is reviewed. A physical understanding of mechanism(s) that induce both types of activity requires one to address the following issues: 1) what is the source of fuel that powers starbursts and active galactic nuclei? and 2) how it is channeled towards the central regions of host galaxies? As a possible clue, we examine the role of non-axisymmetric perturbations of galactic disks and analyze their potential triggers. Global gravitational instabilities in the gas on scales ~ 100 pc appear to be crucial for fueling the active galactic nuclei.

1. Introduction

The nuclear and circumnuclear regions of some galaxies exhibit profound activity. First, a high rate of massive star formation (hereafter SFR) has been detected in the inner kpc of "starburst" galaxies (SBGs), which appear to be disk galaxies, at least at low redshifts. We define an SBG according to Weedman *et al.* (1981) and avoid discussing Clumpy Irregulars and Extragalactic HII Regions. Second, the highest level of a nonstellar activity is found in the innermost pc of an active galactic nucleus (AGN). It is associated with the accretion process onto a supermassive black hole (SBH) presumably taking place in AGNs (Begelman, Blandford and Rees 1984; Rees 1984).

The AGN phenomenon is usually discussed within the context of the radiative and dynamical effects it exerts on the surrounding interstellar medium (ISM). Here we shall address the issue of how the stellar and gas dynamics in the host galaxy can trigger this activity in the first place. To the extent that internal dynamics of the host itself is likely to depend on tidal interactions with its neighbors, the AGN and SBG phenomena spread over more than seven decades in radius. This explains the enormous difficulties one encounters when trying to model them.

For the discussion of the latest observational results see papers by Heckman and Kennicutt (these proceedings).

2. Fueling AGNs

Assuming a mass-to-energy conversion efficiency $\epsilon \sim 0.1$ for a typical AGN, the mass consumption rate can be estimated as

$$\dot{M}_{AGN} \sim 2\left(\frac{\epsilon}{0.1}\right)^{-1}\left(\frac{L}{10^{46}\mathrm{erg\ s^{-1}}}\right)\ \mathrm{M_{\odot}\ yr^{-1}}. \tag{1}$$

If τ_{AGN} is the duty-cycle of a typical AGN (*i.e.* the total activity time), then approximately

$$M_{cycle} \sim 2\times10^{9}\left(\frac{\epsilon}{0.1}\right)^{-1}\left(\frac{L}{10^{46}\mathrm{erg\ s^{-1}}}\right)\left(\frac{\tau_{AGN}}{10^{9}\mathrm{yr}}\right)\ \mathrm{M_{\odot}} \tag{2}$$

of gas must be at hand and confined to within

$$r_{cycle} \lesssim 4\alpha\left(\frac{T}{100\ \mathrm{K}}\right)\left(\frac{v_{\phi}}{200\ \mathrm{km\ s^{-1}}}\right)^{-1}\left(\frac{\tau_{AGN}}{10^{9}\ \mathrm{yr}}\right)\ \mathrm{pc} \tag{3}$$

of the SBH, if the extraction of angular momentum is done by a viscous torque in a geometrically thin accretion disk. Here α is defined by *viscous stress* $\sim \alpha \times$ *internal pressure* and is limited to $\alpha \lesssim 1$ for local viscosities, *e.g.*, subsonic turbulence; v_{ϕ} is the local Keplerian velocity; and T is the equatorial temperature of the disk. The equilibrium temperature in a dusty AGN disk beyond few pc will not exceed $T \sim 100$ K even if $\sim 10\%$ of the central radiation flux is backscattered from high lattitude (Shlosman and Begelman 1987, 1989; Phinney 1989). The formula (3) demonstrates the inefficiency of viscous torques in coupling the region beyond r_{cycle} to the vicinity of the SBH. The fuel must be stored locally, within r_{cycle}, or some other mechanism should be considered for redistributing the angular momentum. As we intend to show below, the locally stored fuel cannot be in the form of stars and there is a real problem to keep it in a gaseous form for many dynamical times.

Compact Star Clusters

"Local" sources, usually a dense stellar cluster with a core radius of $R_{cl} \sim$ few pc and a mass M_{cl}, have been considered repeatedly in the 1970s. Several mechanisms have been proposed in order to convert the stars in the cluster into a 'digestible' form of fuel. They been reviewed recently by Shlosman, Begelman and Frank (1990). Here we only give the main points. First, a normal stellar evolution produces only $\sim 10^{-11}\ \mathrm{M_{\odot}\ yr^{-1}\ M_{\odot}^{-1}}$ by means of the stellar mass loss. Second, stars can be tidally disrupted by the SBH, if the latter is less massive than $\sim 10^{8}\ \mathrm{M_{\odot}}$ (Hills 1975; Frank and Rees 1976; Lightman and Shapiro 1977). The resulting conversion rate of stars into gas is given by

$$\dot{M}_{TD} \sim 2\times10^{-5}\left(\frac{m_{*}}{1\ \mathrm{M_{\odot}}}\right)\left(\frac{M_{cl}}{10^{9}\ \mathrm{M_{\odot}}}\right)^{1/2}\left(\frac{R_{cl}}{10\ \mathrm{pc}}\right)^{-3/2}\mathrm{M_{\odot}\ yr^{-1}}, \tag{4}$$

where m_* is the mass of a typical star in the cluster. Clearly such a low rate cannot support even moderate AGN luminosities unless the average cluster density is pushed into collisional regime. Third, the collisions among the cluster stars with dispersion velocities σ_* will release

$$\dot{M}_{coll} \sim \dot{M}_{TD}\left(\frac{\sigma_*}{v_*}\right)^4, \tag{5}$$

where v_* is the escape velocity from a star. Apart from implicitly assuming that all tidally and collisionally produced stellar debris are accreted by the SBH, extremely compact star clusters are needed to support such high velocity dispersion. Fourth, hydrodynamical ablation of the cluster stars becomes relevant only when the cluster is close to a collisional regime and when the direct gas dynamical processes in the ISM are dominant. The ablation rate is limited to

$$\dot{M} \sim \left(\frac{\rho}{\rho_{cl}}\right)\dot{M}_{coll}, \tag{6}$$

where ρ is the density of the cluster ISM and ρ_{cl} is the distributed stellar density in the cluster. Fifth, radiative ablation of stars by the nonthermal AGN continuum was considered in a number of works (Edwards 1980; Shull 1983; Voit and Shull 1988; Norman and Scoville 1988; Scoville and Norman 1988). Irradiating main sequence stars will have a negligible effect on their mass loss. Moreover the main sequence lifetime is prolonged. Thus, although red giants will suffer increased mass loss rates, this evolution phase will be delayed. Unless τ_{AGN} exceeds 10^9 yrs, which seems to be highly unlikely (Padovani, Burg and Edelson 1990), the total mass loss will be reduced (Tout *et al* 1989).

The angular momentum problem is minimized in this class of "local" models, but it cannot be neglected. A combination of angular momentum and other constraints makes it difficult to obtain mass supplies adequate to fuel luminous AGNs. Star clusters of the requisite density and compactness have never been observed, and no compelling theoretical arguments demand their existence. As an alternative, we consider the ISM which is distributed throughout the main body of the host galaxy and is largely supported by its orbital motion.

Geometrically Thin Accretion Disks, Thick Accretion Flows, and all that

If the extraction of angular momentum is done by a viscous torque in a geometrically thin accretion disk, then M_{cycle} must be confined to within the nucleus (in the form of gas), because of inefficiency of viscous drag. Such an accumulation of a gas will probably dominate the background gravitational potential and will violate the condition of a continuous disk. The latter will happen because accretion rates in excess of

$$\dot{M}_{crit} \sim \frac{3\alpha c_s^3}{G} \sim 5\times 10^{-4}\alpha\left(\frac{T}{100\ \mathrm{K}}\right)^{3/2} \mathrm{M}_\odot\ \mathrm{yr}^{-1} \tag{7}$$

lead to a *locally* gravitationally unstable disk and to a fragmentation. Here c_s is the sound speed in the disk. The outcome to this instability in the gaseous disks depends upon the preferred equation of state: (i) the Jeans instability will saturate and the individual fragments will preserve finite cross sections and will interact by direct cloud-cloud collisions (Lin and Pringle 1987). An efficient cooling mechanism, *e.g.* high rate of collisions, will drive the disk deeper into domain of instability. This will allow for a whole range of unstable wavelengths, for an efficient transport of angular momentum outwards and for an inflow. (ii) Alternatively, the Jeans instability will proceed into nonlinear regime and as far as the resulting fragments are optically thin, they will contract to a point where they hardly interact at all and the disk will resemble more a stellar one than a turbulent gaseous disk (Shlosman and Begelman 1987). No substantial inflow is expected in this case.

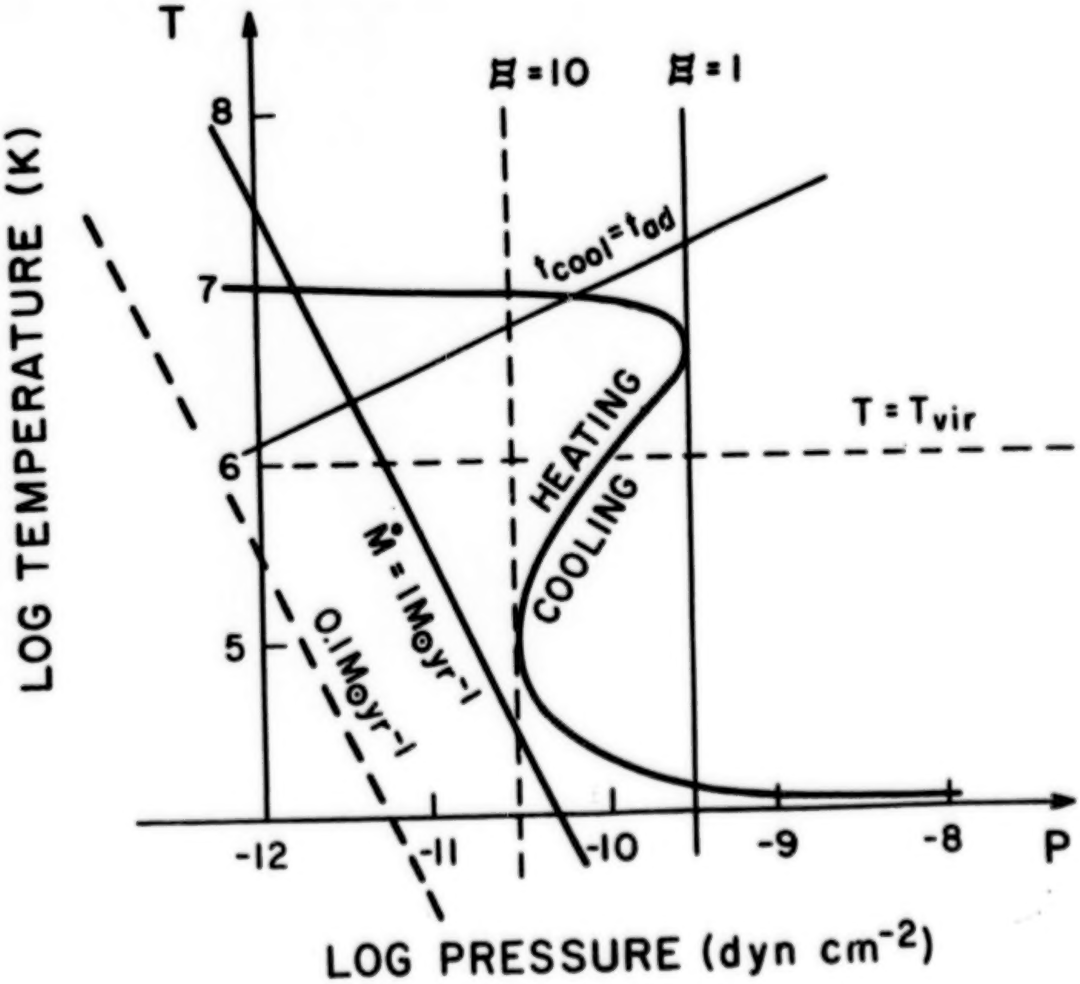

Fig. 1. Curves of a constant $\dot{M} = 1$ and 0.1 $M_\odot$ yr^{-1} on the $p-T$ plane for $\alpha = v_\phi/100$ km s^{-1} = $r/1$ kpc = 1. The horizontal line labeled "$T = T_{vir}$" indicates the virial temperature above which the gas will tend to escape from the gravitational well, rather than accrete. Also plotted is the curve "$t_{cool} = t_{ad}$", below which radiative cooling dominates over the compressional heating associated with the accretion flow. The threshold for runaway heating is shown schematically, assuming an ionizing luminosity of 10^{45} erg s^{-1} and an AGN spectrum with an inverse Compton temperature of 10^7 K (from Begelman, Frank and Shlosman [1989]).

To avoid fragmentation in a continuous disk a stable solution with $\alpha >> 1$ and/or $T >> 100$ K must be found. Shlosman and Begelman (1989) and Begelman, Frank and Shlosman (1989) concluded that both are unacceptable and different ways of heating up the disk, including winds from T Tauri and OB stars and supernovae (SN), are inefficient. An alternative way to preserve the continuous disk is to assume that the flow is being hot, $T >> 10^4$ K, from the beginning. However, under a wide range of parameters, some external source of heating is required to prevent such a flow from catastrophic cooling and collapsing to a galactic plane. This is a consequence of high thermal pressure, 2-3 magnitudes above typical ISM pressure, required in order to obtain the fueling rates for luminous AGNs without exceeding the virial temperature (Begelman, Frank and Shlosman 1989 and Figure 1). Both the heating by SN blast waves and the X-ray continuum from the central source are more likely to cause outflow (galactic wind) than promote steady accretion. The possibility that cooling flows fuel at least some AGNs, however, cannot be ruled out at present.

We conclude that a thin homogeneous accretion disk is not a viable means of delivering fuel to luminous AGNs on scales much larger than a pc because of a long inflow time scale and effects of self-gravity, which lead to fragmentation and possibly star formation. There are also serious obstacles to maintaining and regulating the energetics of geometrically thick, hot accretion flows. However, if the disk is not required to be quasi-continuous, one can draw a straightforward analogy between a standard accretion disk and the disk of discrete particles, which has been described in connection with Saturn's rings (Begelman, Frank and Shlosman 1989 and refs. therein). An alternative approach, using dynamically important magnetic fields to drive accretion in the inner few tens of pc from the SBH, has been recently reviewed by Blandford (1989).

3. Fueling Starbursts

Luminous starburst galaxies show SFRs that exceed the Galactic rate by two orders of magnitude or more. Most of it is confined to the inner kpc. High SFRs correlate with the amount of molecular gas (estimated from CO observations) concentrated in the same volume. The latter may correspond to about 50% of the total molecular gas in the galaxy (Sanders *et al.* 1988) and more than $\sim 10-20\%$ of the dynamical mass within few hundred pc (*e.g.*, Ishizuki *et al.* 1990). However, even $M_{gas} \sim 10^9 - few \times 10^{10}$ $M_\odot$ of gas will be exhausted in $\tau_{burst} \sim 10^7$ yrs and locked in the low-mass stars (using Salpeter's IMF). Maintaining this SFR over a cosmological time would contradict rotation curves of disk galaxies. Even with a truncated IMF (at ~ 3 $M_\odot$), τ_{burst} cannot be prolonged above $\sim 10^7 - 10^8$ yrs, because the gas would be heated up by SN and flow out in a wind (Chevalier and Clegg 1985).

The lifetime of a molecular cloud can hardly exceed $\sim 10^8$ yrs. It would be difficult, therefore, to explain a slow accumulation of a molecular gas to high densities and to dynamically important masses unless they are injected into the inner kpc on the comparable time scale. Injection rates $\sim 100\ \mathrm{M_\odot\ yr^{-1}}$ would satisfy the above requirement. The cloud-cloud collision time scale is given by

$$\tau_{coll} \sim \frac{t_{orb}}{C}, \tag{8}$$

where C is the cloud covering factor and t_{orb} is the cloud orbital time at radius r. If the gaseous disk is supported vertically by the cloud random motion,

$$C \sim 40\left(\frac{a_{cl}}{30\ \mathrm{pc}}\right)^2\left(\frac{r}{500\ \mathrm{pc}}\right)^{-2}\left(\frac{M_{gas}}{10^9\ \mathrm{M_\odot}}\right)\left(\frac{M_{cl}}{10^5\ \mathrm{M_\odot}}\right)^{-1}, \tag{9}$$

where a_{cl} and M_{cl} are the cloud size and mass, chosen to be similar to the Milky Way clouds. It would be difficult to decrease C substantially below unity. If massive star formation is *simply* related to molecular cloud collisions (Scoville, Sanders and Clemens 1986), eq.(9) results in $\tau_{burst} \sim \tau_{coll} \lesssim t_{orb}$. However, massive star formation in the disk may be initially suppressed and exhibit a *threshhold* behavior. Such a threshold may be the consequence of a velocity-dependent efficiency of massive star formation (*e.g.*, Smith 1982). Suppose the clouds are injected with velocities which are of the order of their orbital velocities and *not* necessarily confined to the galactic plane. These velocities will be "thermalized" in cloud-cloud collisions and the gas will continue to accumulate until the collisions will reduce the dispersion velocities, flatten the gas distribution towards the plane and the runaway star formation will follow. Another possibility is that clouds injected into inner kpc are made of atomic and not molecular hydrogen. Collisions between HI clouds do not result in gravitationally unstable configurations, do not lead to star formation but instead may induce the formation of H_2 clouds (Stone 1970; Tubbs 1982). Only when the latter become abundant, the massive star formation will be triggered.

We conjecture that both luminous AGNs and SBGs depend upon an external reservoir of fuel and its efficient channeling to the inner pc and kpc respectfully. Hence the problem which must be addressed at this point is one of redistribution of the angular momentum in the gaseous component of the disk galaxy. Clearly it will impose much more stringent conditions on AGNs than on SBGs.

4. Disk Galaxies: Angular Momentum Transfer

The origin of starburst and nuclear activity in galaxies appears to be intimately related to the problem of global stability of these galaxies. Understanding how disks respond to different perturbations will clarify what triggers are most efficient in exciting particular modes. The goal is to find a mechanism that efficiently transfers gas between different parts of the stellar disk, *i.e.* from large radii to small radii, and is doing this on a time scale comparable with the dynamical time in the disk.

Radial flows are not expected to occur in an axially symmetric galaxy under normal circumstances. Fortunately, galaxies are not completely axisymmetric and possess spiral arms, oval distortions, bars, lenses, warps, etc. We shall assume, for simplicity, that a bi-symmetrical disturbance of amplitude $\delta\Sigma$ is present within radius r in the otherwise homogeneous disk of density Σ. The $m = 2$ mode, where m is the azimuthal number, is preferred by Nature in building disk galaxies, which most frequently have bars and two spiral arms. Such a disturbance will impose a gravitational torque $T \sim G(\delta\Sigma)^2 r^3$ on the test particle outside r. Let the disk with the mass $M_d(r)$ be embedded in a massive halo, $M_h(r)$, and let $M_h(r)/M_d(r) > 1$, to ensure global stability at all relevant radii. The angular momentum within r is $J(< r) \sim r^3 \Sigma v_\phi$ and the time scale for extraction of this momentum is of the order of

$$\tau_J \sim \frac{J}{T} \sim \left(\frac{M_h}{M_d}\right)\left(\frac{\Sigma}{\delta\Sigma}\right)^2 t_{dyn}. \tag{10}$$

The above estimate was made more rigorously by Lynden-Bell and Kalnajs (1972) and Larson (1984). The eq.(10) underlines the dramatically short timescale of angular momentum transfer in self-gravitating disks when a mechanism for excitation and subsequent driving of non-axisymmetric perturbation exists. Because of the nature of a stellar "fluid", the growth rate of gravitational instability will probably saturate in the mildly nonlinear regime, *i.e.* $\delta\Sigma/\Sigma \lesssim 1$, but even $\sim 10\%$ addition of cold gas may result in shocks and dissipation. The gas can be easily driven into a strongly nonlinear regime.

Contrary to the common belief, axisymmetric disturbances can redistribute angular momentum on the large scale as well. In order to understand this let us define the threshold for the onset of these instabilities in a mildly self-gravitating disk (Toomre 1964; Goldreich and Lynden-Bell 1965a):

$$Q = \frac{c_s \kappa}{\pi G \Sigma}\ , \tag{11}$$

where c_s is the sound speed in a homogeneous disk or a dispersion velocity in a disk of clouds or stars; κ is the epicyclic frequency; and π should be replaced by 3.36 for a stellar disk. A geometrically thin disk will be unstable for values of $Q < 1$ and will fragment into clumps of the size of the disk thickness. This is the *local* Jeans instability discussed earlier in section 2. The smallest wavelength which is still unstable is given by $\lambda_{min} \sim c_s^2/G\Sigma$ and the largest unstable one is $\lambda_{max} \sim G\Sigma/\Omega^2$, where $\kappa \sim \Omega$, the local angular velocity is assumed. The instability manifests itself in the local compression (*i.e.* heating) and mass transfer. The latter is always accompanied by an angular momentum transfer. One can define an effective kinematic viscosity ν_{eff} which is responsible for such a transfer. Lin and Pringle (1987) gave a prescription to build ν_{eff}, assuming that the longest unstable wavelengths are the most efficient ones for J-transfer and the characteristic time scale is the dynamical time in the disk:

$$\nu_{eff} \sim \lambda^2_{max}/t_{orb}. \tag{12}$$

The resulting 'viscous' (inflow) timescale in the disk is:

$$t_{visc} \sim \frac{r^2}{\nu_{eff}} \sim \frac{1}{1-Q^2}\left(\frac{M_h}{M_d}\right)^2 t_{orb}. \tag{13}$$

In the α-disk notation this is equivalent to $\alpha \sim Q^{-2} \sim \lambda_{max}/h$, where h is the disk thickness and $Q < 1$. Hence this means $\alpha > 1$. However, because the longest wavelengths have the slowest growth rates, eq.(12) probably overestimates the effective viscosity while eq.(13) underestimates the inflow time. For the sake of completeness, we note that the growth of axisymmetric modes is always accompanied by the growth of non-axisymmetric modes of comparable λ.

5. Extrinsic vs Intrinsic Driving: Triggers

Mechanisms that excite large-scale non-axisymmetric modes in galactic disks can be divided into two groups: extrinsic and intrinsic. The former include tidal encounters between galaxies (flybys), orbital torques by their satellites and mergers. The latter include instabilities brought about by the evolution of the disk, *e.g.*, infall, distortions built in by initial conditions (bars, general triaxiality). In the absence of a comprehensive theory of self-gravitating disks, a variety of empirical methods have been used to map out domains of stability and to study the onset and nonlinear evolution of non-axisymmetric dynamical instabilites. Numerical modeling has shown that tidal interactions between galaxies, both flybys and mergers, usually lead to transient bars. Furthermore, a tidal interaction reinforces an already existing bar, provided the collision is not head-on (Combes 1987) and triggers the bar instability in otherwise stable stellar disk (Gerin, Combes and Athanassoula 1990). This is achieved by inducing or moving the inner Lindblad resonance (ILR). But a bar, in fact, may be a long-lived and self-sustained configuration resulting from a global self-gravitational instability, or even be relic from galaxy formation epoch. *N*-body simulations of collisionless stellar disks have revealed a strong tendency for low-order modes, and particularly for a bar-like mode, to grow in the absence of ILRs and a hot massive halo component. That disk experiences period(s) of dynamical instability may explain why such a high fraction, ~ 50%, of disk galaxies is barred.

Spiral Waves, Bars and Ovals

In order to understand the specifics of interaction of the unstable mode with the rest of the stellar disk and especially with the gaseous component, we shall discuss it in some detail. As a first step, we shall address the stellar dynamical instabilities, which occur on scales $\lesssim 1$ kpc, and their triggers. Gasdynamical instabilities within the central kpc are reviewed in section 6.

Spiral waves may have a two-fold effect on the galactic disk: (i) they cause slow angular momentum transport and radial inflow; and (ii) they strongly amplify the SFR when sufficient amount of gas is present, *i.e.* if one accepts that star formation is related to spiral waves through formation of molecular gas. The formation rate of the latter is enhanced by large quantities of gas going into nonlinear self-gravitating regime.

The nonlinear response of the gas to the background gravitational potential of a spiral arm was studied by Lubow, Balbus and Cowie (1986). For 15% gas contribution to the surface density in equilibrium disk, it dominates the region of the spiral density wave by a factor of a few. The global stellar mode is centrally condensed as the instability has more time to amplify itself at smaller radii as a result of short dynamical times there. This means that the amplitude of a stellar wave increases towards the center, *e.g.*, $\Sigma_{*1} \propto r^{-3/2}$ (Lubow 1988), and so does the gas response. With such a centrally concentrated response, the subsequent star formation will be centrally peaked either. This model will naturally prefer starbursts to occur in the late-type spirals, where gas is more abundant and its density is raising towards the center.

However, some important details have been omitted in the above estimates: (i) the effect of the starburst on cloud velocity dispersions (input of energy by SN); and (ii) the damping of stellar waves by cloud-cloud collisions. Because the gas response to stellar wave will be phase-shifted, the gas will produce torque on the stellar wave. As a result the stellar wave growth rate will be saturated and ultimately both waves will be damped. Lubow (1986) estimates the damping time scale for our Galaxy to be $\lesssim 10^9$ yrs, comparable or even shorter than growth rate for corresponding spiral modes (Haass 1983). Therefore cloud-cloud collisions are capable of limiting spiral density wave amplitudes; (iii) the effect of ILRs has been neglected; and (iv) the WKBJ approximation used breakes down at small radii because $kr \sim 1$ there.

As we have mentioned above, spiral waves have some effect on inducing radial flow of gas and may drastically increase the SFR. Unfortunately, spiral structure cannot extend across ILR and OLR (outer Lindblad resonance). It may of course reappear inside the ILR. If a bar exists, the actual living space for spirals may be even smaller. It is also important to remember that the inflow is limited to within the corotation radius (CR) because the torque will change the sign there: inflow at $r < r_{CR}$ towards the ILR and outflow at $r > r_{CR}$ towards the OLR. If no ILR is present, the spiral structure may be terminated at the Q-barrier (*i.e.* where Q exceeds unity). This typically occurs in the inner parts of stellar disks (Freeman 1987), at $\sim 1 - 2$ kpc and hence the outer spiral structure has no effect inside ~ 1 kpc.

Bars form spontaneously in a system with an excess of bulk motion (*e.g.*, rotation) over random motion and "where it is not prohibited by the law" (*e.g.*, Binney and Tremaine 1987). For a collisionless (stellar) disk a reliable measure of stability is the value of $t_{OP} \equiv T/|W|$, and $t_{OP} > 0.14$ is sufficient condition for a global dynamical instability (Ostriker and Peebles 1973) and bar formation. Here T is the total rotational energy and W is the integral gravitational energy of the system. More generally speaking, the physical reason for bar instability is a strong amplification of any leading disturbance in a sheared disk into a trailing disturbance (swing amplifier), which then propagates through the disk center (feedback) and appears as a leading one (Goldreich and Lynden-Bell 1965b; Toomre 1981). The best way to stabilize the disk is to cut the feedback by introducing ILR, by heating-up the inner disk ($Q > 3$), or by surrounding it with a hot and massive halo.

Bars can extend to corotation, but are not obliged to be so long. They are efficient drives of spiral structure which originates at the opposite ends of a bar (Schwarz 1984; Combes and Gerin 1985). What makes the stellar bar-like mode so attractive as a mechanism for inducing the radial flows is the strong response of the gas within the bar radius r_{bar}. It triggers a pair of *large-scale* shocks, *i.e.* regions of enhanced cloud-cloud collisions. A bar-like mode typically has a radial wavelength comparable to the size of the system; it is a *global* mode. It couples efficiently between very different radii and by doing so provides $\alpha >> 1$ (in the α-notation of the viscosity). Within the bar radius, the gas shocks on the leading edge of the bar and, in the absence of ILR, flows inwards on the dynamical time scale. But even in the absence of ILR, the radial flow will not extend all the way to the galactic nucleus ($\sim 1 - 10$ pc), as one can expect naively. The condition for the existense of leading shocks is violated at smaller radii and an order of magnitude estimate shows that the gas will probably accumulate at $\sim 0.1 r_{bar}$ (Shlosman, Frank and Begelman 1989).

The overwhelming majority of disk galaxies are explicitly non-axisymmetric, because they show spiral structure and oval distortions. It is clear both on kinematic (Bosma 1981) and photometric (Kormendy 1982) grounds that many unbarred galaxies contain oval disks with intrinsic equatorial axial ratios of ~ 0.8. Such ovals are entirely sufficient to produce the same inward gas flow as do bars. In fact, since all of the disk is oval while $\lesssim 20\%$ of a disk is in the bar, the potential of an oval disk is easily as non-axisymmetric as that of a barred galaxy. There are several important points regarding oval distortions in disk galaxies. First, oval galaxies do not look barred in visible light. Omitting such galaxies biases conclusions that Seyferts are not preferentially non-axisymmetric. For example, the classic Seyferts NGC 1068 and NGC 4151 are prototypical ovals. Second, oval disks are easy to recognize photometrically. Third, infrared images sometimes reveal bars underlying oval disks, as in NGC 1068 (Scoville *et al.* 1988). Once we recognize that oval disks exist and rearrange gas like the bars do, the correlation between galaxies that are non-axisymmetric and ones that show nuclear activity gets much cleaner.

Flybys and Mergers

We shall be interested here only in the effects of flybys and mergers on the galactic disk, ignoring the fate of the companion where it is possible. For our purposes, the most important result of a tidal interaction is the excitation of transient non-axisymmetric modes in otherwise stable stellar disk. Tidal forcing was first proposed by Holmberg (1941) and then by Toomre (1969). Relatively slow and direct passage results in a nice trailing spiral structure which lasts of the order of the passage time $\sim$ *few* $\times 10^8$ yrs, as was shown in a numerical simulation by Toomre and Toomre (1972). If only $\sim 1\%$ forcing (ratio of tangential-to-radial force) is needed to drive the spiral wave (Toomre 1981), a mass ratio between the flyby and the main galaxy of $\sim 10^{-2}$ or larger is required, if no interpenetration is allowed. The earliest numerical simulations showed that the largest effect (in terms of disturbing individual orbits) the flyby has on the outer disk. However, it was realized subsequently, that this was an artifact of an insufficient dynamic range used in simulations. Only very slow flybys will have no net effect on the inner stellar disk, because the perturbation will be adiabatic there.

Because of a strongly nonlinear response of a perturbed galaxy only numerical simulations of interaction are capable of treating the problem in a self-consistent manner. The large dynamic range makes it very difficult to actually follow the gaseous and stellar response (Noguchi 1988a,b). Generally, a transient bar $\sim$ few kpc develops in a few rotation periods after the closest approach. It disappears after some time and then reappears again, but weaker. In the intermediate phase, the galaxy looks very much similar to amorphous galaxies described by MacKenty (1990).

The perturber affects the gaseous component of a primary galaxy by (i) a direct tidal torque, forcing the gas to deviate from original motion; and (ii) by perturbing the gravitational potential of the stellar component which in turn provides additional and long-lived torque on the gas (Noguchi 1988b). When the stellar background potential is frozen, only the outer parts of the galaxy are affected (gas gravity is neglected here). The tidal force of the perturber alone fails to induce the infall. When the self-gravity of the stellar disk is taken into account the spiral structure also develops in the inner parts of the disk (still on kpc-scale, as the resolution of the numerical model is $\sim$ kpc). Initially, the massive star formation closely follows the large-scale spiral pattern and later peaks within the bar radius. At later stages the gas (cloud) dynamics is influenced only by the potential of the stellar disk, whereas effect of the perturber is negligible. The inflow rate is not a monotonic function of time (same as the bar strength). Therefore the galaxy still can show recurrent starburst activity, even when perturber has already receeded. These "latency periods" and episodic nature of the inflow have been also suggested to explain the absense of Seyfert nuclei in strongly interacting galaxies and the fact that not all galaxies in the multiple systems are Seyferts (Byrd, Sundelius and Valtonen 1987). Note, however, that the inflow on a kpc-scale may be completely unrelated to the inflow on a much smaller $\sim 10-100$ pc-scale, as we shall argue in section 6. It is worth mentioning that cloud-cloud collisions provide the necessary dissipation and when they are artificially switched off the behavior of gas is identical to that of a stellar "fluid".

Thus, transient stellar bars are typical products of tidal interactions. Even when initial conditions are unfavorable to bar formation, *e.g.*, $v_\phi = const$, they still show up in the simulations, but are not as dominant (Byrd *et al.* 1986; Thomasson 1987).

Mergers produce substantial dynamical effects on stellar disks which result in burst of star formation and radial flows. When a rotating disk experiences tidal forcing, the satellite galaxy will define the positions of major resonances in the disk. The pattern speed of the disturbance is fixed by the satellite angular velocity of revolution. The timescale to accrete a small satellite with the mass M_{pert} is given by Quinn and Goodman (1986):

$$t_{in} \sim 4 \times 10^9 \left(\frac{v_\phi}{220 \text{ km s}^{-1}}\right)\left(\frac{M_{pert}}{10^9 \text{ M}_\odot}\right)^{-1}\left(\frac{d_{pert}}{10 \text{ kpc}}\right)^2 \text{yr}, \qquad (14)$$

where d_{pert} is the galactocentric distance to the perturber. About 10% of the disk mass, *i.e.* $\sim M_{LMC}$, can come from accretion of small satellites. This accretion process heats up the stellar disk. The ratio of the kinetic energy of the random motion in the plane to that along the z-axis tends towards 3:1. A further increase in this ratio is limited by buckling of the disk plane, which acts to reduce the velocity anisotropy — the hose-pipe instability (Toomre 1987). The heating of the disk is quite substantial, as can be seen from simulations by Hernquist and Quinn (1989). There is a serious doubt that such a disk will respond with a strong spiral in case the event will repeat itself, as stellar velocity dispersions never decrease.

Numerical simulations of merging galaxies (*e.g.* Hernquist and Quinn 1989) have shown that $m = 2$ mode is the dominant mode of angular momentum transfer when the satellite is orbiting in a *direct* sense. In the case of a *retrograde* merger (Hernquist 1989), only $m = 1$ resonance is possible and a single leading spiral arm results, as expected (Athanassoula 1978). The gas is channeled towards the inner kpc (400 pc is the resolution limit), where its dynamical importance is amplified by the ability to dissipate its random motion. The energy input into the gas by SN and stellar winds and other sources is neglected in the above simulations as well as the star formation processes. These are expected to alter dramatically the last stages of evolution of the gas distribution.

The sinking satellite will be subject to the tidal torque which eventually will disrupt it, if its average density becomes less than that of the cannibal galaxy. The distributed density of a small galaxy, *i.e.* a dwarf spheroidal (except M32-type elliptical, but these are rare), which dominate the faint end of the Schechter luminosity function is too low for the appreciable part of the satellite to penetrate the inner kpc (Saito 1979). The latter may be crucial for populating the lose-cone orbits by stars that will be ultimately captured by the SBH (Roos 1981). But, as in the case of other triggers, the main effect of a merger will be on the gas.

6. Gas: Dynamical Effects

As we have already discussed, large-scale departures from axial symmetry are quite efficient in triggering radial flows in the galactic ISM, which then start to accumulate within the central kpc in the form of a gaseous ring. While this process can ultimately lead to a starburst, angular momentum residing in the gas will still prevent it from crossing another two to three decades in radius, which is necessary for the standard viscous processes and/or magnetic torques to take over and feed the SBH.

The dynamical importance of gas at large r is limited to within the spiral arms. In the circumnuclear regions, however, the gas may affect the global dynamics. A collisional disk of clouds is capable of dissipating its energy of random motions — a process that makes it relatively cold when compared with the stellar disk. As a result, the self-gravity of the gas and its dynamic response are greatly enhanced, and the disk becomes prone to global non-axisymmetric instabilities (Norman 1988; Shlosman, Frank and Begelman 1988; 1989). Future evolution of the gaseous distribution implies that it is the gravitational disturbance and not the cloud-cloud collisions that drives the inflow on scales ~ 100 pc. Recent data suggest that molecular bars are common in Seyferts (Heckman, these proceedings).

Alternatively, Lin, Pringle and Rees (1988) have assumed that clouds remain on circular orbits in the inner 2 kpc and this gaseous disk is only marginally stable, with $Q \sim 1-2$. A perturbation introduced by a tidal interaction penetrates down to ~ 0.5 kpc. Once perturbed the clouds rapidly increase their collision rate and drive the gaseous disk away from marginal stability, causing an inflow. To get required $\dot{M}$, however, the inflow time must be short, and hence the gas amount must exceed 10% of dynamical mass (*i.e.* of M_h in eq.[13]) in the inner 2 kpc. We note that global non-axisymmetric instabilities will develop under the same circumstances, but they will grow even for $Q > 1$, when the former instability is suppressed.

7. Conclusions

We have outlined theoretical models for induced starburst and nuclear activity in disk galaxies. The dynamic range of the phenomena exceeds seven orders of magnitude in radius. The fueling of AGNs and to a lesser degree that of SBGs require sources in the main body of the host galaxy. Gravitational torques applied to the stellar disks on scales of $\sim 1-10$ kpc are capable of inducing radial flows in the ISM of disk galaxies. Thus, both intrinsic as well as extrinsic triggers may be responsible for the SBG activity. We find that a two-step approach is necessary to explain the AGN phenomenon. The crucial second step consists of self-gravitational instabilities in the gas on scales of ~ 100 pc.

ACKNOWLEDGMENTS. It is a pleasure to thank the organizers of this stimulating meeting. I am indebted to my long-time collaborators Mitch Begelman and Juhan Frank. This work was supported by NSF grant AST84-51725.

References

Athanassoula, E. *Astron. Astrophys.* **69**, 395 (1978).

Begelman, M.C., Blandford, R.D. & Rees, M.J. *Rev. Mod. Phys.* **56**, 255 (1984).

Begelman, M.C., Frank, J. & Shlosman, I. (1989) in *Theory of Accretion Disks*, ed. F. Meyer *et al.* (Dordrecht: Kluwer Acad. Publ.), p. 373.

Binney, J. & Tremaine, S. (1987) *Galactic Dynamics* (Princeton: Princeton Univ. Press).

Blandford, R.D. (1989) in *Theory of Accretion Disks*, ed. F. Meyer *et al.* (Dordrecht: Kluwer Acad. Publ.), p. 35.

Bosma, *Astron. J.* **80**, 1825 (1981).

Byrd, G.G., Sundelius, B. & Valtonen, M. *Astron. Astrophys.* **171**, 16 (1987).

Byrd, G.G., Valtonen, M.J., Sundelius, B. & Valtaoja, L. *Astron. Astrophys.* **166**, 75 (1986).

Chevalier, R.A. & Clegg, A.W. *Nature* **317**, 44 (1985).

Combes, F. (1987) in *Starbursts and Galaxy Evolution*, eds. T.X. Thuan *et al.* (Editions Frontieres: Gif Sur Yvette), p. 313.

Combes, F. & Gerin, M. *Astron. Astrophys.* **150**, 327 (1985).

Edwards, A.C. *Mon. Not. R. astr. Soc.* **190**, 757 (1980).

Frank, J. & Rees, M.J. *Mon. Not. R. astr. Soc.* **176**, 633 (1976).

Freeman, K.C. *Ann. Rev. Astr. Ap.* **25**, 603 (1987).

Gerin, M., Combes, F. & Athanassoula, E. *Astron. Astrophys.* , in press.

Goldreich, P. & Lynden-Bell, D. *Mon. Not. R. astr. Soc.* **130**, 97 (1965a).

Goldreich, P. & Lynden-Bell, D. *Mon. Not. R. astr. Soc.* **130**, 125 (1965b).

Haass, J. (1983) in *Kinematics, Dynamics and Structure of the Milky Way*, ed. W.L.H. Schuter (Dordrecht: Reidel), p. 283.

Hernquist, L. *Nature* **340**, 687 (1989).

Hernquist, L. & Quinn, P.J. (1989) in *The Epoch of Galaxy Formation*, eds. C.S.Frenk *et al.* (Dordrecht: Kluwer Acad. Publ.), p. 427.

Hills, J.G. *Nature* **254**, 295 (1975).

Holmberg, E. *Astrophys. J.* **94**, 385 (1941).

Ishizuki, S. *et al.* *Astrophys. J.* , in press.

Kormendy, J. (1982) in *Morphology and Dynamics of Galaxies, 12th Saas-Fee Course*, eds. L. Martinet & M. Mayor (Geneva Observatory), p. 115.

Larson, R.B. *Mon. Not. R. astr. Soc.* **206**, 197 (1984).

Lin, D.N.C. & Pringle, J.E. *Mon. Not. R. astr. Soc.* **225**, 607 (1987).

Lin, D.N.C., Pringle, J.E. & Rees, M.J. *Astrophys. J.* **328**, 103 (1988).

Lightman, A.P. & Shapiro, S.L. *Astrophys. J.* **211**, 244 (1977).

Lubow, S.H. *Astrophys. J. (Letters)* **307**, L39 (1986).

Lubow, S.H. *Astrophys. J. (Letters)* **328**, L3 (1988).

Lubow, S.H., Balbus, S.A. & Cowie, L.L. *Astrophys. J.* **309**, 496 (1986).

Lynden-Bell, D. & Kalnajs, A.J. *Mon. Not. R. astr. Soc.* **157**, 1 (1972).

MacKenty, J.W. *Astrophys. J. Supp. Ser.* , in press.

Noguchi, M. *Astron. Astrophys.* **201**, 37 (1988a).

Noguchi, M. *Astron. Astrophys.* **203**, 259 (1988b).

Norman, C. (1988) in *Galactic & Extragalactic Star Formation*, eds. R.E. Pudritz & M. Fich (Dordrecht: Kluwer Acad. Publ.), p. 495.

Norman, C. & Scoville, N. *Astrophys. J.* **332**, 124 (1988).

Ostriker, J.P. & Peebles, P.J.E. *Astrophys. J.* **186**, 467 (1973).

Padovani, Burg, R. & Edelson, R.A. (1990) preprint.

Phinney, E.S. (1989) in *Theory of Accretion Disks*, ed. F. Meyer *et al.* (Dordrecht: Kluwer Acad. Publ.), p. 457.

Quinn, P.J. & Goodman, J. *Astrophys. J.* **309**, 472 (1986).

Rees, M.J. *Ann. Rev. Astr. Ap.* **22**, 471 (1984).

Roos, N. *Astron. Astrophys.* **104**, 218 (1981).

Saito, M. *Pub. Astr. Soc. Japan* **31**, 181 (1979).

Sanders, D.B. *et al.* *Astrophys. J.* **325**, 74 (1988).

Schwarz, M.P. *Mon. Not. R. astr. Soc.* **209**, 93 (1984).

Scoville, N., Matthews, K., Carico, D.P. & Sanders, D.B. *Astrophys. J. (Letters)* **327**, L61 (1988).

Scoville, N. & Norman, C. *Astrophys. J.* **332**, 163 (1988).

Scoville, N., Sanders, D.B. & Clemens, D.P. *Astrophys. J. (Letters)* **310**, L77 (1986).

Shlosman, I. & Begelman, M.C. *Nature* **329**, 810 (1987).

Shlosman, I. & Begelman, M.C. *Astrophys. J.* **341**, 685 (1989).

Shlosman, I., Begelman, M.C. & Frank, J. *Nature* , in press.

Shlosman, I., Frank, J. & Begelman, M.C. (1988) in *Active Galactic Nuclei*, eds. D. Osterbrock & J. Miller (Kluwer Acad. Publ.), p. 462.

Shlosman, I., Frank, J. & Begelman, M.C. *Nature* **338**, 45 (1989).

Shull, J.M. *Astrophys. J.* **264**, 446 (1983).

Smith, J. *Astrophys. J.* **238**, 842 (1982).

Stone, M.E. *Astrophys. J.* **159**, 293 (1970).

Thomasson, M. (1987) in *The Few Body Problem, IAU Colloq. 96*, ed. M. Valtonen (Dordrecht: Reidel).

Toomre, A. *Astrophys. J.* **139**, 1217 (1964).

Toomre, A. *Astrophys. J.* **158**, 899 (1969).

Toomre, A. (1981) in *Normal Galaxies*, eds. S.M. Fall & D. Lynden-Bell (Cambridge Univ. Press), p. 111.

Toomre, A. (1987) private communication.

Toomre, A. & Toomre, J. *Astrophys. J.* **178**, 623 (1972).

Tout, C.A., Eggleton, P.P., Fabian, A.C. & Pringle, J.E. *Mon. Not. R. astr. Soc.* **238**, 427 (1989).

Tubbs, A.D. *Astrophys. J.* **255**, 458 (1982).

Voit, G.M. & Shull, J.M. *Astrophys. J.* **331**, 197 (1988).

Weedman, D.W. it et al. *Astrophys. J.* **248**, 105 (1981).

Roos: I agree that dwarfs possibly do not survive in the central regions of bright galaxies. Also, their mass is so low that it probably takes more than a Hubble time for dynamical friction to drag them into the central region. The nuclei of small galaxies of ~ $0.1L_*$ however may be significantly dense to survive and to penetrate into the nucleus of a larger galaxy, especially if they contain a massive black hole.

Shlosman: I agree, but the effect on the stellar disk of the 'cannibal' will be amplified as well. This merger will probably lead to an elliptical galaxy. I find it difficult to reconcile with the fact that Seyferts are disk galaxies.

Balsara: I have a comment about your comment on testing the continuum limits of SPH. Myself along with Norman, Bickness and Gingold have done a lot of work to show that it can be done in a multidimensional context. More recently I have carried out the full Von Neumann stability analysis of SPH and shown that Γ_0, Γ^+ and Γ^- characteristics are very well propagated by SPH and also that the advection is in fact substantially superior to finite difference. You do have to incorporate all the results of my analysis to get this good behavior though!

STATIONARY ORBITS OF SATELLITES OF DISK GALAXIES

Valerij L. Polyachenko
Astronomical Council of the Academy of Sciences of the USSR

ABSTRACT. The satellite of an S-galaxy will experience opposing dynamical-friction forces from the stars of the disk and the halo. If these forces are in balance, the satellite may travel in a stable, near-circular orbit whose radius, for a wide range of physical parameters, should be limited to a zone 1.2 to 1.4 times the disk radius, much as is observed.

The idea of the paper (1) is very simple. The dynamical friction acting on a small satellite, moving through a stellar galactic halo, makes this satellite slow down. On the other hand, a stellar disk, rotating faster than a satellite, makes it speed up. But the density distributions in radius for disk's and halo's stars in real flat galaxies are quite different (respectively, exponential and power-law). Moreover, the observational data show that the exponential profile for disk's surface density drops abruptly at some radius (r_d). So it is natural to expect that a stationary orbit could place near the edge of a disk (where two effects are mutually compensated).

1. Dynamical friction for a satellite near a disk with a sharp edge. We begin with the well-known formula by Lynden-Bell and Kainajs (2) for the rate of change of the satellite's angular momentum due to interaction with the rotating stellar disk. It is a particular sum over resonances. If then we shall be interested in only the case when orbits of both a satellite and a disk are nearly circular, it will be sufficient to take into account only contributions from inner Lindblad resonances:

$$\mathcal{L}_d = \sum_{m}^{M_{max}} \mathcal{L}_d(m), \; m_{max} = \sqrt{2R/(R - 1)}, \tag{1}$$

where $R = r_s/r_d$, r_s is the satellite's orbit radius, $\mathcal{L}_d(m)$ can be calculated (these quantities correspond to contributions of separate resonances).

2. Dynamical friction of the satellite due to a halo. Collision effects in spherical stellar systems were considered in our old paper (3). One of the effects--dynamical friction--was then studied in more detail by Tremaine and Weinberg (4). The rate of change of the satellite's angular momentum due to resonance interaction with stars of the isothermal halo may be written as (5)

$$\mathcal{L}_h = - \Lambda_g I(R), \; (\Lambda_g = (2\pi)^{5/2} G M_s / e r_s V_o^{\,2}), \tag{2}$$

where M_s is the satellite's mass, $V_0 = \Omega(r_d)r_d$ is the circular velocity (and we consider the rotation curve to be flat),

$$I(R) = 0.0759 \ln(R/P) - 0.0228 \tag{3}$$

$P/R = (r_b/r_d)/(r_s/r_d)$, r_b is the effective radius of the satellite nucleus (the parameter arising due to the necessity to consider a satellite with finite size), and the potential of the satellite is

$$\Phi_b(r) = -GM_s/\sqrt{r^2 + r_b^2}. \tag{4}$$

(G is the gravitational constant.) Such an approximation allows us to remove some uncertainties of the point-mass approximation.

3. Location of the stationary orbit of a satellite. The condition for the satellite orbit to be stationary, $\mathcal{L}_d = \mathcal{L}_h$, reduces to the form, depending on three parameters: (1) $D = r_d/r_e$, where r_e is the scale of exponential decay of disk's surface density, $\sigma_0(r) = \sigma_0(0)\exp(-r/r_e)$, (2) $P = Rr_b/r_s$ - the dimensionless parameter of the satellite's features,

(3) $\gamma = eGM_d/4\pi r_e V_0^2$, where M_d is the total disk's mass, $\Gamma = 1$ for $M_d = 10^{11}\ M_o$, V_0 = 200 km/s, r_e = 4 Kpc.

Left and right sides of the stationary condition are represented in Figure 1 as the functions of dimensionless radius $R = r_s/r_d$, for $\gamma = 1$ and a few values of D and P parameters. These values cover the whole range of parameters for real galaxies as one could expect, the stair-like disk's curve is very sharp, while the halo's curve is rather smooth and its dependence on values of the parameter P is rather weak. It is evident from the figure that possible values for radii of the satellite orbit are strongly restricted to a rather narrow range: $1.2 < R < 1.4$, near the disk edge (where R = 1).

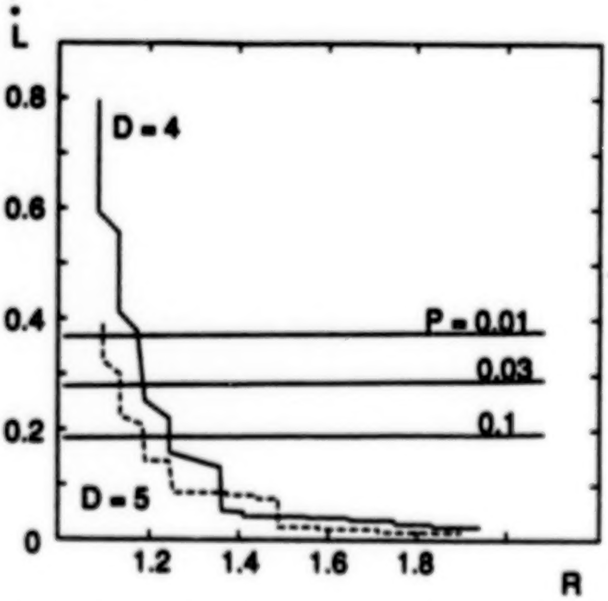

Figure 1. Radial dependence of the dynamical friction exerted on a satellite by (smooth lines) the halo stars and (stepped curves) the disk population. For a satellite at the disk edge, R = 1. Parameter P measures the effective size of the satellite's core; D measures the steepness of the exponential decline in the disk surface density. The two countervailing friction forces will be

in balance at the intersection points, which are limited to the zone R = 1.1 to 1.4.

The study of satellites' distribution over ratio $R = r_s/r_d$ (fulfilled recently by I.I.Pasha on the basis of the well-known Arp's Atlas of interacting galaxies) shows that this distribution has a distinct maximum, just corresponding to the region near R = 1.3. As to inclinations of orbits (and percentage of plane orbits among them) this problem needs to be studied.

Of course, all above is valid only for satellites with sufficiently small masses: the gravitational potential of the satellite should not destroy strongly the effective potential well of particles at the disk edge (so that these particles cannot reach the satellite orbit). Otherwise, we shall have the direct tidal interaction between the satellite and the tail of particles pulled out from the disk edge by the satellite (such an interaction leads inevitably to slowing down).

REFERENCES

Pasha, I. I., and Polyachenko, V. L. 1987, *Pis'ma Astron. Zh..*, **13**, 275. (Pasha, I. I. 1987, *Sov. Astron. Lett.*, **13**, 111.

Polyachenko, V. L., and Strel'nikov, A. V. 1988, *Pis'ma Astron. Zh.*, **14**, 195. (*Sov. Astron. Lett.*, **14**, 81 (1988)).

Lynden-Bell, D., and Kalnajs, A. J. 1972, *Mon. Not. R. Astron. Soc.*, **157**, 1.

Polyachenko, V. L., and Shukhman, I. G. 1982, *Atron. Zh.*, **59**, 228. (*Sov. Astron.*, **26**, 1410 (1982)).

Tremaine, S. D., and Weinberg, M. D. 1984, *Mon. Not. R. Astron. Soc.*, **209**, 729.

Weinberg, M. D. 1986, *Astrophys. J.*, **300**, 93.

NUMERICAL SIMULATIONS OF INTERACTING DISK GALAXIES

Masafumi Noguchi
University of Wales, College of Cardiff
Cardiff, United Kingdom

Galaxy-galaxy interactions have long attracted many extragalactic astronomers in various aspects. A number of computer simulations performed in the 1970s have successfully reproduced the peculiar morphologies observed in interacting disk galaxies and clarified that tidal deformation explains most of the observed global peculiarities. However, most of these simulations have used test particles in modelling the disk component. Tidal response of a self-gravitating disk remains to be further clarified.

Another topic which is intensely discussed at present is the relation between galaxy-galaxy interactoins and activity. Many observations suggest that interactions trigger strong starbursts and possibly active galactic nuclei (AGN). However, the detailed mechanism of triggering is not yet clear. It is vital here to understand the dynamics of interstellar gas.

In order to understand various phenomena related to galaxy-galaxy interactions (mainly for disk galaxies), we have performed a series of numerical simulations on close galaxy encounters which includes both interstellar gas and self-gravitating disk components (see Noguchi 1988 for details).

1. MODELS

In our simulations, the galaxy model to be perturbed (target galaxy) consists of a halo and a disk. The halo was treated as a rigid spherical gravitational field which is assumed to remain fixed during the interaction. The disk is composed of stars and gas. The stellar disk was constructed by 20000 collisionless particles of the same mass. Those particles move in the halo gravitational field, interacting with each other and with the perturber. Therefore, the self-gravity of the disk is properly taken into account. Stellar particles were initially given circular velocities with small random motions required to stabilize the disk against local axisymmetric disturbances. The gravitational field of the stellar disk was calculated by the particle-mesh scheme (e.g. Hockney and Eastwood 1981).

The gaseous component was modelled by the cloud-particle scheme (e.g. Roberts and Hausman 1984), namely we represented the gas as an ensemble of small spheres (i.e. clouds) and included the creation of an 'OB star' in a cloud-cloud collision and subsequent velocity push on nearby clouds due to a 'supernova explosion'. Also the cloud-cloud collisions were assumed to be highly inelastic and thus dissipate kinetic energy. The cloud particles are assumed to be massless. Their motion was calculated by using the combined gravitational field of the stellar disk, hale, and perturber. Therefore, the influence of the deformation of the stellar disk in which the gas is embedded was taken into account in addition to the direct effect of the tidal force.

The stability of this galaxy model was confirmed by running the model for a few rotation periods in the absence of a perturbing galaxy. The stellar disk maintains a nearly axisymmetric shape with exponential density distribution, because it is stabilized by a heavy halo component. Only weak, filamentary spiral structures are seen. Also the gas clouds keep moving on nearly circular orbits around the disk center. The velocity dispersion of gas clouds stays constant since the energy input by supernova explosions is balanced by dissipation in cloud-cloud collisions.

In the next stage, a point-mass perturber was introduced to disturb this galaxy model (target galaxy). Here we describe only the standard model from the several runs we have carried out. In the standard model, the disk has 20% of the total target mass (i.e. 80% is in the halo). The rotation-curve is nearly solid-body from the disk center to about 60% of the disk radius, outside of which it is nearly flat. The cloud-cloud collision timescale was set to be 1.62, comparable to the dynamical timescale. One rotation period at the outer disk edge is 6.28 in these units. The perturber has the same mass as the parent galaxy, and moves in a prograde parabolic orbit with perigalactic distance twice the target disk radius.

2. BAR FORMATION IN THE INNER REGION

Fig. 1 shows the morphological evolution of the standard model. In the early phase ($T = 2.50$), both stars and gas form a two-armed spiral structure which extends into a tail and bridge, consistent with the results of test-particle simulations (e.g. Toomre and Toomre 1972). The tidal force of the perturber is dominant in this phase.

About one rotation period (6×10^8 yr for a typical disk galaxy) after the perigalactic passage, a bar structure begins to develop in the inner region of the stellar disk. This point is quite different from the behavior of test-particle disks. In the case of the test-particle disks, only the outer part of the disk is deformed while the inner part remains almost unchanged (e.g. Toomre and Toomre 1972), consistent with the nature of the tidal force. It is evident that the self-gravity of the stellar disk is playing an important role in this bar formation. The initial amplitude of the tidal perturbation given by the perturber is smaller in the inner region than in the outer one. However, disk self-gravity is more dominant in the inner region. The gravitational field in the inner disk region is virtually governed by the disk component itself. The growth of the tidal perturbation is thus greatly accelerated in the inner region. The bar lasts for a few rotational periods but gradually weakens into a slightly oval structure.

Tidally-induced bar formation found here is closely related to the origin of barred galaxies. It is well known that a disk with a mass exceeding that given by the Ostriker-Peebles (1973) criterion develops a bar spontaneously. This bar instability may be the generating mechanism of barred galaxies. Comparison of the disk-to-halo mass ratio of barred versus unbarred galaxies would provide a direct check of this hypothesis; the former should be systematically larger than the latter. Unfortunately, the existence of large-scale noncircular motions makes reliable mass estimates difficult for barred galaxies.

The result presented here suggests that close galaxy pairs cam also generate barred galaxies from originally unbarred ones in which the disk mass fraction is small enough that the bar instability did not operate. If this is the case, we should observe barred galaxies more frequently in interacting galaxies than in isolated ones. One possible piece of observational support may come from simple statistics (Noguchi 1987), that spirals in the *Atlas of Peculiar Galaxies* (Arp 1966) show a slight hint of higher incidence of bars than field spiral galaxies. In the field spirals, 37% are barred, whereas 55% of Arp *interacting* spirals are barred. Unfortunately the statistical significance is very low in this case. More extensive study is urgently needed.

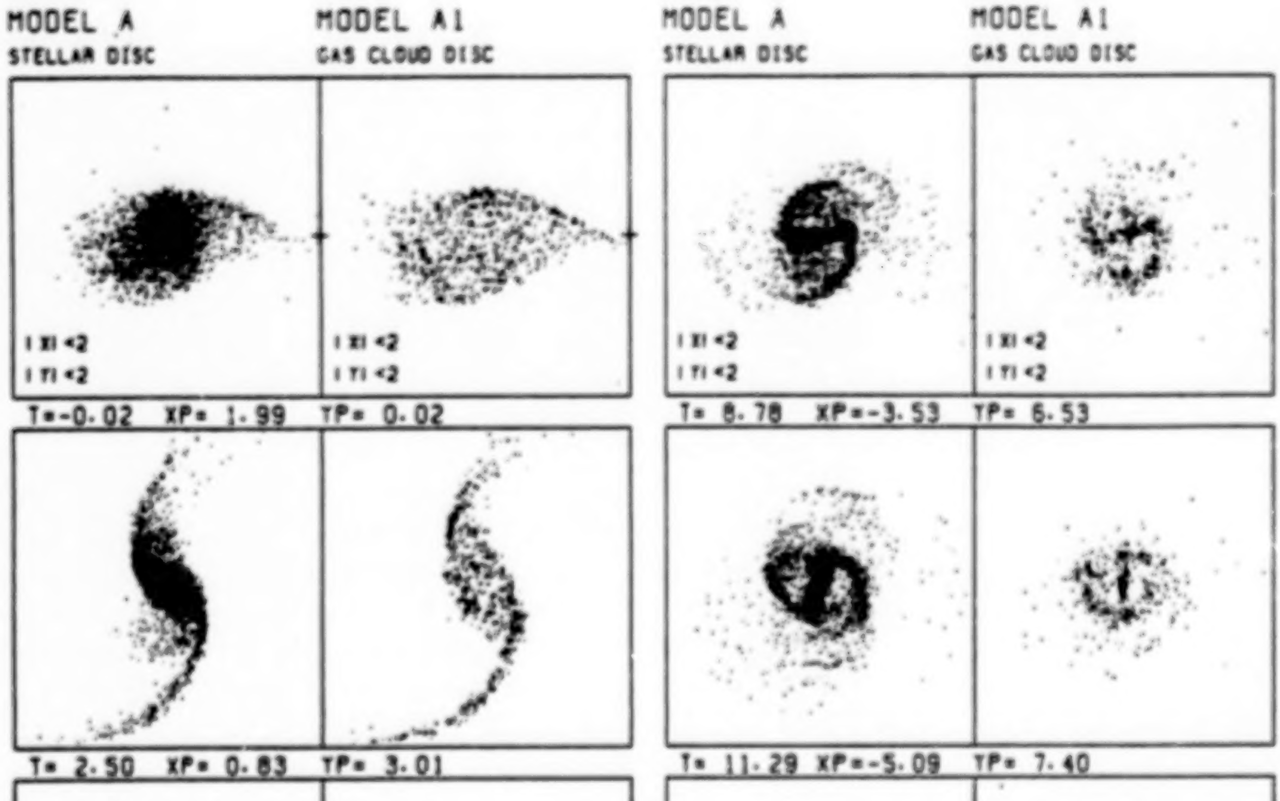

Fig. 1 - A close encounter model of a disk galaxy containing both stars and gas with an equally massive point-mass perturber (from Noguchi 1988). The left and right panels show the stars and gas clouds, respectively. The time T reckoned from perigalactic passage is given in dimensionless units. One unit corresponds to roughly 10^8 yr for a disk galaxy of typical size and mass. XP and YP are X and Y coordinates of the perturber, where X and Y axes are to the right and upward, respectively. The disk rotates counterclockwise.

3. NUCLEAR STARBURSTS FUELLED BY BARS

The most remarkable observational feature of the starbursts in interacting galaxies is that they take place in the nuclear regions (1-2 kpc) of host galaxies (e.g. Keel *et al.* 1985). Our numerical models explain the occurrence of nuclear starbursts quite satisfactorily. The right panels in Fig. 1 show the evolution of the gas-cloud disk in the standard model. It is seen that after the stellar bar has developed sufficiently, the gas clouds begin to fall to the disk center. This is because the stellar bar removes the angular momenta and kinetic energy from the gas clouds. About 20% of the total gas is swallowed within the 10% radius (1-2 kpc for a typical disk galaxy) from the nucleus up to $T = 13$. The maximum infall rate occurs $8 - 12 \times 10^8$ yr after the perigalactic passage and has a value of about 1 $M_\odot$ yr^{-1}. Therefore active star formation is expected to take place in the nuclear region about 10^9 yr after the perigalactic passage.

4. THE CASE OF NGC 1068

The higher incidence of nuclear starbursts in interacting galaxies seems to be established observationally fairly well. The situation for Seyfert galaxies and other AGN is much more controversial (see the review by Heckman in this volume). However, the well-known Seyfert galaxy NGC 1068 may provide an interesting example. There are several reasons for which we can consider that Seyfert activity in this galaxy has been triggered by a close encounter.

First, NGC 1068 has a possible companion galaxy. Although NGC 1068 is usually treated as an isolated galaxy, it has nearby galaxies such as NGC 1055 and NGC 1073. It is possible that NGC 1068 has interacted with one of these galaxies. Second, NGC 1068 has a stellar bar in the inner region as shown by near-infrared observations (Scoville *et al.* 1988, Thronson *et al.* 1989). Myers and Scoville (1987) have found a ring of molecular gas which lies on the ends of the bar, and a sharp peak at the nucleus. The molecular gas distribution they have observed is surprisingly similar to the one shown in Fig. 1 ($T = 11.29, 13.80$). Telesco and Decher (1988) have suggested that the bar is located within two inner Lindblad resonances (ILRs). Quite interestingly, a detailed study of individual stellar orbits indicates that the model bar in Fig. 1 is also located within two ILRs. On the other hand, numerical simulations for bar-unstable disks (Miller and Smith 1979, Sellwood 1981) show that the spontaneous bar usually ends near the corotation point. In view of the model results presented here, these observations make NGC 1068 a highly possible case of tidally-triggered Seyfert activity. Detection of a faint H I tidal feature connecting NGC and a companion would further strengthen this picture.

REFERENCES

Arp, H. 1966, *Atlas of Peculiar Galaxies* (Pasadena:Caltech).

Hockney, R.W. and Eastwood, J.W. 1981, *Computer Simulations Using Particles* (New York: McGraw-Hill).

Keel, W.C., Kennicutt, R.C., Jr., van der Hulst, J.M., and Hummel, E. 1985, Astron. J. 90,708.

Miller, R.H. and Smith, B.F. 1979, Astrophys. J. 227, 785.

Myers, S.T. and Scoville, N.Z. 1987, Astrophys. J. Lett. 312, L39.

Noguchi, M. 1987, Mon. Not. R. Astr. Soc. 228, 635.
Noguchi, M. 1988, Astron. Astrophys. 203, 259.
Ostriker, J.P. and Peebles, P.J.E. 1973, Astrophys. J. 186, 467.
Roberts, W.W. and Hausman, M.A. 1984, Astrophys. J. 277, 744.
Scoville, N.Z., Matthews, K., Carico, D.P. and Sanders, D.B. 1988, Astrophys. J. Lett. 327, L61.
Sellwood, J.A. 1981, Astron. Astrophys. 99, 362.
Telesco, C.M. and Decher, R. 1988, Astrophys. J. 334, 573.
Thronson, H.A. *et al.* 1989, Astrophys. J. 343, 158.
Toomre, A. and Toomre, J. 1972, Astrophys. J. 178, 623.

DISCUSSION

Balsara: I am somewhat uncomfortable with your having a set of simple algebraic rules for making OB stars with the net result of these OB stars being to blow up and heat the disk. So, all you have is an algebraic set of rules for heating the disk. Also, this heating is expected to blow out in the vertical direction (superbubbles and all that) and the old star population is expected to remain unaffected by that.

Noguchi: In the model presented here, the energy input from the explosion of OB stars is negligible compared with the total kinetic energy of stars and gas. In particular, the heating of stellar disk is a purely stellar-dynamical one, and OB stars do not contribute to it. So, the global phenomena discussed here (i.e., the formation of a stellar bar and the inflow of the gas) will not be sensitive to the detailed specification of the star formation process. Heating and blow out due to intensive star formation will be important in the case of small galactic mass.

Sotnikova: Did you consider the interaction between clouds escaping from the parent galaxy with a hot intergalactic medium, which also can lead to the disappearance of clouds.

M. Noguchi: No

M. Klaric: What happens with the clouds after they collide?

Noguchi: The clouds create an "OB star" at their center of mass. At the end of its lifetime (~10^7 yr), the "OB star" explodes as a "supernova" and gives a velocity boost to the clouds which reside within a certain radius (which corresponds to the size of super nova remnant) from the "OB star".

Zasov: Let's compare two types of galaxies. The first one is that of the early-type spiral, say, Sa - Sbc. The second one is, say, Sc. For the first type of galaxy we have a large non-disk component, large angular velocity, and probably non-self gravitating disk. For the second one, it is the other way around: a self-gravitating (at least in the inner parts) disk and a lower angular rotation. Judging from the results of your numerical modeling, we should expect more violent activity for the late-type galaxies. Nevertheless Seyfert nuclei and nuclear hot spots usually occur in early type systems. How can that be made to agree with your results?

Noguchi: It is not clear how the disk mass fraction changes with respect to the spheroidal component (not just the bulge, but the bulge + halo) and hence how the importance of self-gravity changes with the Hubble type. So we should be careful in comparing the results with the observations. Although Seyfert galaxies are more common in early type galaxies, nuclear starbursts are more often observed in late type galaxies.

Navarro: When does star formation occur in your simulations, and how sensitive are your results to this?

Noguchi: I assumed that one star formation event takes place per each cloud-cloud collision. I didn't investigate other cases.

Simkin: In the later epochs you see an alternating surge of star formation - first on one side, then on the other side of the bar. Is this sensitive to initial conditions?

Noguchi: I think that this is caused because the tidal interaction deviates from exact bi-symmetry.

Chatterjee: The formation of structures in your simulations seem to be extremely dependent on the rotation velocity of the victim disk?

Noguchi: Yes. For example, the length of the induced bar is well correlated with the radius of the solid-body part of the rotation curve.

GAS FLOWS IN S-E BINARY SYSTEMS OF GALAXIES

N. Ya. Sotnikova
Astronomical Observatory
Leningrad State University
Leningrad, USSR

OBSERVATIONAL EVIDENCE OF GAS FLOWS IN BINARY SYSTEMS

Tidal interaction between the galaxies in binary systems leads to important consequences. Some peculiarities in galactic morphology as well as the transfer of matter from one galaxy to another may be due to this factor. In particular, gas flows in intergalactic space may be formed. Such flows enriching one component with gas from the other may play a substantial role in the evolution of mixed (S-E) pairs. One can mention several facts corroborating the possibility of the gas transfer from the spiral to the elliptical galaxy.

1. High HI content (10^7 - 10^9 $M_\odot$) is detected in nearly 40 E galaxies (Bottinelli and Gougenheim, 1979; Knapp et al., 1985). Such galaxies are often members of pairs or of multiple systems including an S galaxy, which may be the source of gas (Smirnov and Komberg, 1980). Moreover, the gas kinematics and its distribution also indicate an external origin for this gas (Knapp et al., 1985). In many cases there is an outer gaseous disk. The directions of the disk and of stellar rotation don't always coincide (van Gorkom et al., 1985; Varnas et al., 1987).

2. The galaxy colors in S-E pairs are correlated (the Holmberg effect): bluer ellipticals have spiral components that are usually bluer (Demin et al., 1984).

3. The fraction of E galaxies with emission lines (N_{em}) in S-E pairs showing traces of tidal interaction is twice as large ($N_{em} \approx 0.24$) as in pairs without interaction ($N_{em} \approx 0.12$) (Sotnikova, 1988b). Since the presence of emission lines in a galaxy spectrum strongly depends on gas content this fact also leads to the conclusion that ellipticals in interacting S-E pairs are enriched with gas.

These facts may be considered as a serious indication of the existence of gas transfer. Hence, investigation of this process is of interest.

FORM OF THE GASEOUS STREAM

Taking into account the cloud structure of interstellar gas in spiral galaxies, one may assume that the gaseous stream in S-E pairs consists of discrete condensations. Hence, it is possible to consider the motion in the flow within the framework of the restricted three-body problem of celestial mechanics. To confirm such a possibility let us show that the clouds will not evaporate although they are heated by soft X-ray emission from the intergalactic gas. On the other hand, the clouds will not collapse under the action of the external pressure (P_{ext}) and form stars during their flight to the E galaxy. The fulfillment of these statements substantially depends on the parameters of the cloud and of the intergalactic medium. Time scales of the processes in question are smaller than the time of the cloud flight to E galaxy (Sotnikova 1988a).

Taking the cloud to be initially homogeneous both in temperature ($T_{c\ell} = T_{c\ell}(t)$) and in density ($\rho_{c\ell} = \rho_{c\ell}(t)$), one may write down the equations determining the changes of cloud radius R(t) and its temperature (Sotnikova 1986).

$$\frac{3}{5} MR \frac{d^2R}{dt^2} = \frac{3MkT_{c\ell}}{\mu m_H} - 4\pi R^3 P_{ext} - \frac{3}{5} \frac{GM^2}{R},$$

$$\frac{1}{2R^2} \frac{d}{dt} \left(\frac{3MkT_{c\ell}}{\mu m_H} R^2\right) = \int_{v(t)} (\Gamma-\Lambda)dV, \quad V(t) = \frac{4\pi}{3} R^3(t), \qquad (1)$$

$$T_{c\ell} = T_o, \; R = R_o \;\; t = 0.$$

Energy gain due to heating by X-rays has the following form: $\Gamma = 3\delta\rho_x c/2R$ (Sotnikova 1986), where ρ_x is the energy density and δ is the rate of transformation of the energy of X-rays to thermal energy. In calculating the cooling function Λ several different abundances of heavy elements were considered.

Numerical solution of simultaneous equations (1) has shown that the cloud neither evaporates nor collapses if its mass is: $30\ M_\odot < M < 200\ M_\odot$, if the gas is deficient in heavy elements, and the ratio $P_{ext}/n_{c\ell}kT_{c\ell}$ is not too large. Therefore, one can consider the gas flow as a stream consisting of discrete particles.

The changes of the radius and temperature of the cloud having $M = 50\ M_\odot$ are shown in Figure 1.

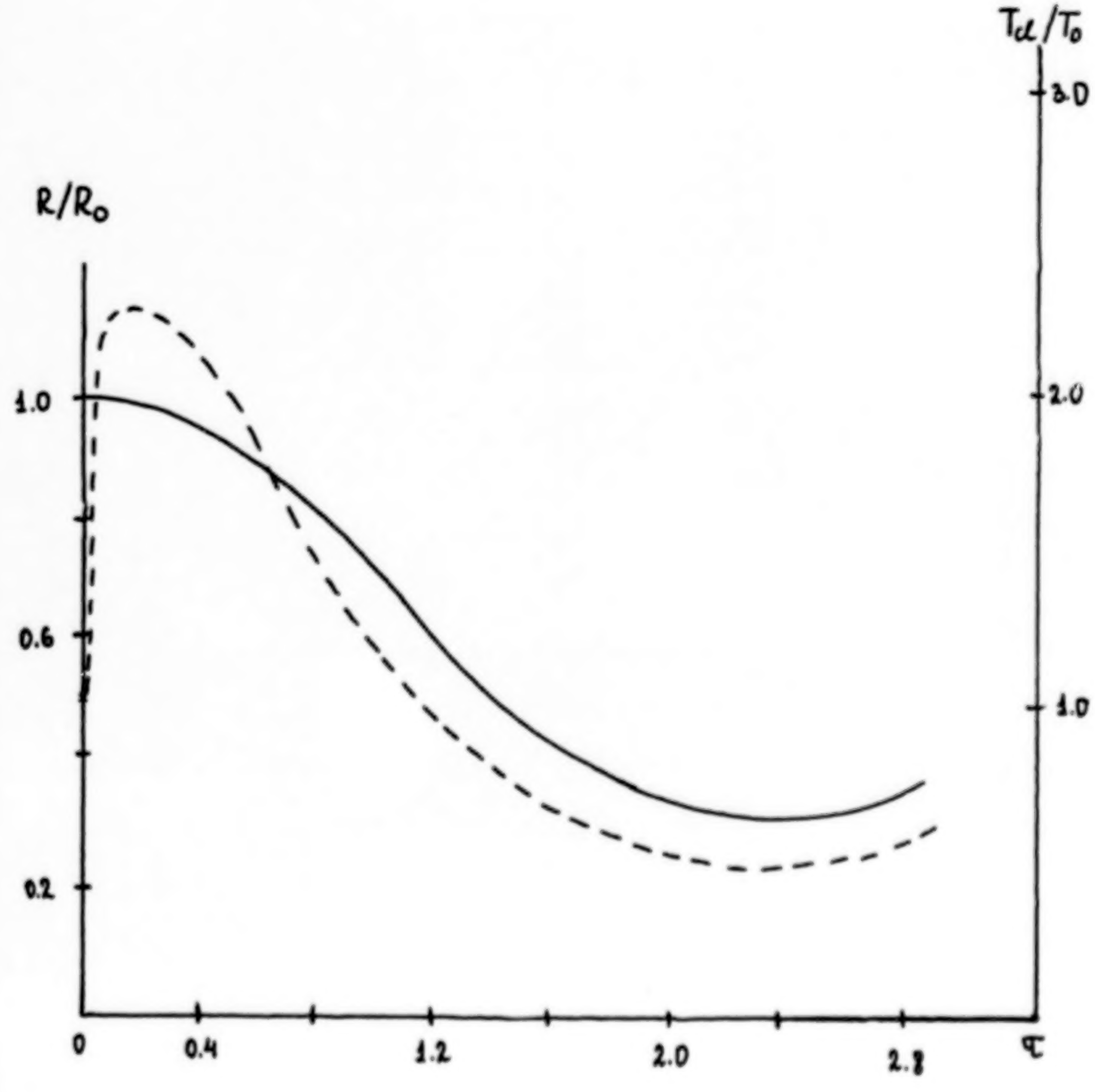

Figure 1. Changes of radius and temperature of a cloud by action of external pressure. $P_{ext}/n_{cl}kT_{cl} = 3$, $T_o = 50$ K, $R_o = 2.5$ kpc, $\delta = 0.7$, $n_{C+}/n_H = 0.1(n_c/n_H)_o$, $n_o/n_H = 0.5(n_o/n_H)_o$, $\tau = t/1.7 \times 10^6$ years.

TRANSFER OF GAS TO AN E GALAXY IN A BINARY SYSTEM: NUMERICAL SIMULATION

As is known, orbits of galaxies in pairs are almost circular (Karachentsev 1987). Therefore one has to solve the circular restricted three-body problem for clouds ("particles") to simulate the gaseous stream. Because the gravitational potential of galaxies differs from that of a point mass, a modification of this problem must be made (Sotnikova 1988a). The stellar mass distribution in the disk containing clouds was taken to obtain a flat rotation curve. The disk plane coincides with the orbital one. The halo potential is supposed to be spherically symmetric.

The efficiency of gas transfer depends on the following main factors (for given $q = M_E/M_S$):

a) the ratio of the radius of the spiral galaxy R_S to the distance between components r_{SE};

b) spiral galaxy orientation relative to orbital momentum;

c) gas content in the spiral.

The value of q may be estimated using the ratio of the luminosities L_E/L_S. Usually $0.1 < q < 10$ and the average value of q is 1 - 2 (Karachentsev 1987).

A reasonable value of R_S/r_{SE} may be estimated as follows. The outflow of gas from S galaxy cannot occur if the initial rotation velocity V_o of a cloud at the distance from the center of spiral galaxy equal to its radius R_S is not large enough to reach the Lagrangian point L_1. Let R_{Smin} be the minimal value of R_S for which V_o satisfies this requirement. The value of R_{smin}/μ_{SE} and the sizes of critical Roche surfaces $R_{cr,\ min}$ for point masses are given in Table 1.

Table 1.

q	R_{Smin}/r_{SE}	$R_{cr\ min}/r_{SE}$	q	R_{Smin}/r_{SE}	$R_{cr\ min}/r_{SE}$
0.1	0.421	0.594	2.0	0.198	0.313
0.5	0.287	0.439	5.0	0.153	0.242
1.0	0.240	0.373	10.0	0.125	0.197

For outflow of gas from the S galaxy to be possible the following inequality must be satisfied:

$$R_S/r_{SE} > R_{Smin}/r_{SE}. \tag{2}$$

Taking into account the mean value of $\langle q \rangle = 2$ calculated from the data of (Karachentsev 1987, Faber and Gallagher 1979), one can see from Table 1 that $R_{Smin}/r_{SE} = 0.20$.

Further, one can find the mean values of the parameters of S galaxies in pairs with and without observational traces of interaction and compare them with the value of R_{Smin}/r_{SE}.

In a sample of 41 pairs without any visible interaction $\langle R_S \rangle/\langle r_{SE} \rangle = 0.17$; i.e., $< R_{Smin}/r_{SE}$. Thus the "mean" galaxy of the sample does not satisfy the requirement for gas flow (2).

The S galaxies from a sample of 38 pairs with observational traces of tidal interaction given in Karachentsev (1987) have $\langle R_S \rangle/\langle r_{SE} \rangle = 0.40$ and therefore in these systems transfer of gas to E galaxy is possible.

To get the characteristics of the gaseous stream from S galaxy numerical solution of equations of test particle motion were carried out (Sotnikova 1988a). Many sets of initial conditions were used and two different cases were considered.

(i) The direction of spiral galaxy spin and that of orbital momentum are the same.

(ii) These directions are opposite.

The main results of the computations are:

1. In the case (i) the time scale of stream formation is much smaller than in case (ii). For example, in the last case the test particle has stayed on its circular orbit in S galaxy during the period of revolution of the whole system ($\sim 3.10^8$ years).

2. In case (i) during one revolution of the binary system the stream evolves to **quasi steady state** (Figure 2).

The S galaxy loses about 0.5% of the total amount of gas per period of the disk revolution ($\sim 10^8$ years). Mean values of the parameters for systems with interacting S-E galaxies from Karachentsev's list (1987) are: $r_{SE} = 34$ kpc, $M_S = (2 - 3) \cdot 10^{11} M_\odot$. The corresponding cloud transfer rate is $\dot{M}_{gas} \approx (0.1 - 0.3) M_\odot$ year^{-1} provided the total mass of gas in the galaxy is about 0.1 M_{stars}.

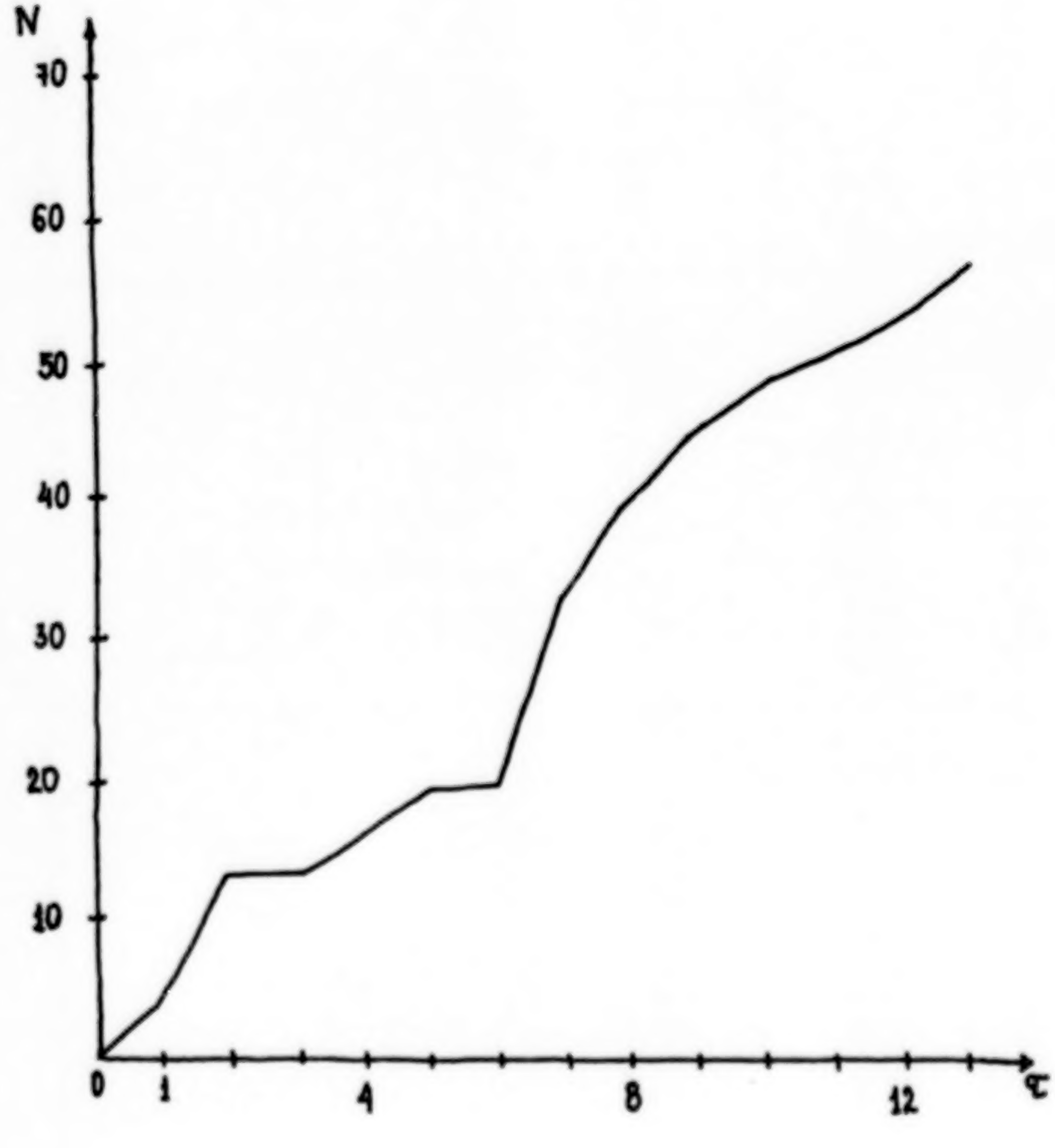

Figure 2. The number of test particles N (the units are arbitrary) lost by spiral galaxy at the time $\tau = t/2.1 \cdot 10^8$ years ($r_{SE} = 34$ kpc, $M_S = 2 \cdot 10^{11} M_\odot$), $q = I$, $R_S/r_{SE} = 0.35$, $R_E/r_{SE} = 0.35$.

CONCLUSIONS

In the course of S-E pair evolution ($t_{ev} \sim 10^9$ years) a significant amount of gas may be transferred to E galaxy ($\dot{M}_{gas} \cdot t_{ev} = 10^8\ M_o$). This value is of the order of observed HI content in E galaxies which are the members of multiple systems.

One may mention also that the presence of emission lines in spectra of many E components of close S-E pairs (25%) may be caused by gas gained by E galaxies due to the tidal interaction with S galaxies.

REFERENCES

Bottinelli, L., and Gougenheim, L. 1978, Astron. Astrophys., 76, 176.

Demin, V. V., Zasov, A. V., Dibaj, Eh. A., and Tomov, A. N. 1984, Astron. Zh., 61, 625.

Faber, S. M., Gallagher, J. S. 1979, Annu. Rev. Astron. Astrophys., 17, 135.

van Gorkom, J. H., Knapp, G. R., Raimond, E., Faber, S. M., Gallagher, J. S. 1986, Astron. J., 91, 791.

Karachentsev, I. D. 1987, Dvojnye Galaktiki, Nauka, Moscow, USSR, 248 pp.

Smirnov, M. A., and Komberg, B. V. 1980, Astrofizika, 16, 431.

Sotnikova, N. Ya. 1986, Astrifizika, 25, 139.

Sotnikova, N. Ya. 1988a, Astrofizika, 28, 495.

Sotnikova, N. Ya. 1988b, Ph.D. Thesis, Leningrad University, Leningrad.

Varnas, S. R., Bertola, F., Galleta, G. 1987, *Astrophys. J.*,. 313, 69.

OBSERVATIONS AND MODELS OF STAR FORMATION IN THE TIDAL FEATURES OF INTERACTING GALAXIES

John F. Wallin
Space Science Division, Naval Research Laboratory

James M. Schombert
Dept. of Astronomy, Univ. of Michigan

Curtis Struck-Marcell
Astronomy Program, Dept. of Physics, Iowa State University

ABSTRACT

Multi-color surface photometry (BVri) is presented for the tidal features in a sample of interacting galaxies. Large color variations are found between the morphological components and within the individual components. The blue colors in the primary and the tidal features are most dramatic in B-V, and not in V- i indicating that star formation instead of metallicity or age dominates the colors. Color variations between components is larger in systems shortly after interaction begins and diminishes to a very low level in systems which are merged. Photometric models for interacting systems are presented which suggest that a weak burst of star formation in the tidal features could cause the observed color distributions. Dynamical models indicate that compression occurs during the development of tidal features causing an increase in the local density by a factor of between 1.5 and 5. Assuming this density increase can be related to the star formation rate by a Schmidt law, the density increases observed in the dynamical models may be responsible for the variations in color seen in some of the interacting systems. Limitations of the dynamical models are also discussed.

INTRODUCTION

The IRAS mission has provided evidence that interaction can in some cases lead to enhanced rates of star formation in the disks of interacting galaxies (Larson and Tinsley 1978, Soifer et. al. 1987) Interaction has also been linked to nuclear activity in some studies (Hummel 1981, Bushouse 1986, Keel et al. 1985). In this paper, I wish to focus on the tidal features of interacting galaxies Because the surface brightness is fairly low (mag/arcsec^2) in these features, the rate of star formation cannot be considered large when compared to the huge bursts at the centers of some galaxies (i.e. Arp 220). However recent photometric results by Schombert, Wallin, and Struck-Marcell (1990) suggest that the rate of star formation in some tidal features must have increased during the interaction which formed them.

OBSERVATIONS

In order to gain additional information about the formation and development of tidal features, a multicolor CCD photometric study was conducted (Schombert et al. 1990) for a sample of galaxies from the Arp Atlas (1966). The surface brightness of the galaxies and their tidal features was measured in the B, V, Gunn r, and Gunn i photometric bands. The colors of the tidal features were then calculated and the distribution of colors across the systems was analysed. From these data, we concluded the following:

1. On average, about 25% of the light in these systems comes from the tidal features. Although the surface brightness is generally low, the area of these features is generally large.

2. The colors of the tidal features are generally bluer than the colors of the main galaxies. Since the colors of most of the tidal features are consistent with the colors of the outer regions of the disks they originate from, we have concluded that most of the differences in colors are due to the lower amounts of dust and younger population of star in the outer disk compared to the inner disk and bulge of the systems.

3. A few of the systems in the sample have tidal features which are very blue ($B-V<0.4$). The blue colors and knotty structure seen in these tidal features indicates that on-going star formation must be occurring in some of these systems. The result that star formation occurs in tidal features is not new. Schweizer (1978) has observed blue knots in the tails of interacting galaxies and Arp (1966) noted the "knotty" appearance of some of the tails in his atlas.

DYNAMICAL MODELS

Motivated by these observational results, simulations were conducted to understand the physical mechanisms for star formation in the outer regions of interacting galaxies. Details of the dynamical and photometric models can be found in Wallin (1989) and Wallin (1990). A restricted three body code (Toomre and Toomre 1972) is used to follow the density in co-moving regions which become part of the tidal tail. It is important to note that no hydrodynamical and self-gravitational forces are considered in these simulations. Because of this limitation, the simulations can only show where compression begins to occur due to the crossing of orbital paths in the particles. Despite this limitation, the low computational cost of the restricted three body method can allow a large number of particles to be used to increase the resolution of for the detection of density changes in small areas.

In the models, approximately 10,000 particles are initially placed in circular orbits around a softened point mass. A second softened point mass then interacts with the first as it passes in a parabolic orbit. A fixed time- step Runge-Kutta method is used as the integrator for the orbits. In order to follow the local star formation rate, regions holding approximately 0.1% of the test particles are placed in comoving orbits around the primary galaxy. As the interaction progresses, the positions of these regions are moved in the same way as the test particles. By following the number of test particles in each region as a function of time, it is possible to obtain a density history for comoving regions in the disk and tidal features. It is then assumed that the star formation rate is related to the density by a Schmidt law (Schmidt 1959).

At the beginning of the simulation, the particles are in placed circular orbits around the main galaxy. As the companion approaches and passes, a distinctive tidal tail is formed. As the companion galaxy recedes, the tidal tail grows in length and narrows at the base. A twist then develops in the tidal tail, resulting from the crossing of particle orbits in the tail. Until about 50 Myr after apoapse, the density in this region remains approximately constant. At about 80 Myr, the density increases to 350% of the original value. The timing of this density increase coincides with the passing of the twist in the tidal tail.

The density increase discussed above is a common feature of models that were run. The strength of the density increase, however, is found to depend on position of the region within the tidal tail, the inclination of the perturbing galaxy, and the mass ratio of the companion galaxy. In regions which are further from the main galaxy, the twist occurs later and in a lower density region. The compressions in the outer regions are found to be less strong than the compressions in the inner regions of the tail. As the inclination of the companion galaxy's orbit is increased, the density increase from the twist decreases. At about 30 degrees inclination, the density enhancements only occur in the inner third of the tidal tail. Although the 30 degree limit is set by the size of the region investigated in these simulations, in general, high inclination encounters increase the thickness of and decrease the compression in the tidal tails. Since the tidal tails are three dimensional features, the compression occurs only when the thickness of the tail is less then the size of the comoving regions. For non-zero inclination orbits, the thickness is greater in the outer parts of the tail than in the regions close to the disk.

PHOTOMETRIC MODELS

A broadband photometric evolutionary code was developed in order to test the effects a changing star formation rate have on the broad band colors of these regions (Wallin, 1989) . The method used is similar to that used by Larson and Tinsley (1978). In the models tested, star formation rate was initially held constant for 10 Gyr. At 10 Gyr, the star formation rate was increased. From this study, it is concluded that observationally detectable changes in the color can be seen if the star formation rate is increased by more than a factor of between two and five from the initial constant star formation rate. In terms of a Schmidt law, this change in the star formation rate indicates that a change in the local density by 200%-500% can account for the bluest colors seen in the tidal tails. This density change is consistent with the results from the dynamical models. It should be noted that the method used to understand star formation in the tidal features of interacting galaxies is similar to that of Noguchi and Ishibashi (1986). In our work, however, the local rather than global star formation was examined.

CONCLUSIONS

Although there is strong evidence that the majority of star formation during interactions takes place in the inner disks, multi-color photometry of some systems indicates that star formation occurs in the tidal features of interacting systems. In the particular case of tidal tails, this star formation may result from orbital crossings in the twist regions of tidal tails which propagate as a wave through the tail.

REFERENCES

Arp, H. C. (1966), *Atlas of Peculiar Galaxies*, (Pasadena : California Institute of Technology).

Bushouse, H. A. (1986), *A. J.*, **91**, 255.

Hummel, E. (1981), *Astron. Astrophys.*, **96**, 111.

Keel, W. C., Kennicutt, R. C. Jr., Hummel, E., and van der Hulst, J. M. (1985), *A. J.*, **90**, 708.

Larson, R. B. and Tinsley, B. M. (1978), *Ap. J.*, **219**, 46.

Noguchi, M. and Ishibashi, S. (1986), *M. N. R. A. S.*, **219**, 305.

Schmidt, M. (1959), *Ap. J.*, **129**, 243.

Schombert, J. M., Wallin, J. F., and Struck-Marcell, C. (1990), *to be appear in A. J.*

Schweizer, F. (1978), *in Structure and Properties of Nearby Galaxies*, eds. Berkhuijsen, E. M. and Wielebinski, R. (Dordrecht : D. Reidel) p. 279.

Soifer, B.T., Houck, J. R., and Neugebauer, G. 1987, *Annual Reviews of Astronomy and* Astrophysics 25, ed. G. Burbridge, D. Layzer, J. G. Phillips, p. 187.

Toomre, A. and Toomre, J. (1972), *Ap. J.*, **178**, 623.

Wallin, J. F. (1989), *Dynamical and Photometric Evolutionary Models of Tidal Tails and* Shells, Ph.D. Thesis, Iowa State University.

Wallin, J. F. (1990), *Dynamical and Photometric Evolutionary Models of Tidal Tails*, to be submitted to A. J.

DISCUSSION

Kennicutt: What is the typical dynamical age of your blue tidal features?

Wallin: Since we don't have velocity information or detailed models for all the galaxies we observed, it is difficult to give an exact answer. The blue tails seem to be in systems which are in the early stages of interaction. In most cases, these are tidal bridges between the galaxies.

Bushouse: Have you compared the colors of the tidal tails with the outer disk regions, as opposed to the integrated colors of the whole galaxy? If the colors of the tails and the outer disk are similar, then it should indicate that the tails are made up of stars that have been stripped from the outer disk.

Wallin: In most cases, the colors of the tails are very similar to the colors of the outer disk. In some cases, however, the colors of the tidal features are bluer than the colors of the outer regions indicating local star formation.

Zasov: Did you compare the colors of galaxies and their tidal features on a color-magnitude diagram? Are there any differences between their color excesses? A difference may take place if there is a redistribution of the interstellar medium due to the interaction.

Wallin: We did examine color-magnitude diagrams of regions in the tail and across systems. It is impossible to examine the changes in reddening since the surface brightness varies between regions.

STARBURSTS IN INTERACTING GALAXIES: OBSERVATIONS AND MODELS

Konrad Bernlöhr
Max-Planck-Institut für Astronomie
Königstuhl 17
D-6900 Heidelberg, F.R.Germany

1 Introduction

Starbursts have been a puzzling field of research for more than a decade. It is evident that they played a significant rôle in the evolution of many galaxies but still quite little is known about the starburst mechanisms. A way towards a better interpretation of the available data is the comparison with evolution models of starbursts. The modelling of starbursts and the fitting of such model starbursts to observed data will be discussed in this paper. The models have been applied to a subset of starburst and post-starburst galaxies in a sample of 30 interacting systems. These galaxies are not ultraluminous FIR galaxies but rather ordinary starburst galaxies with FIR luminosities of a few 10^{10} to a few 10^{11} $L_\odot$.

2 Starburst models

The method basically follows the evolution method of Barbara Tinsley (1968) and others. Only the differences from older models will be described here. Instead of using a grid of fixed masses and ages, stars of all masses and ages are generated by using the Monte Carlo technique. Therefore one has to interpolate stellar evolutionary tracks somehow. This can be done very efficiently if they are available at equivalent evolutionary phases. It is of crucial importance that most of the post-main sequence evolution is included in these tracks. Several sets of tracks have been used or put together from various sources (Maeder 1976, 1981a,b, Matraka et al. 1982, Bertelli 1986, Maeder and Meynet 1988, 1989). The only homogenous set covering the whole mass range of interest so far is that of Maeder and Meynet. Another improvement is the generation of model spectra consisting of an old component and a starburst component with H II region emission lines. A library of dereddened stellar spectra (Jacoby 1984 [illegible] ed to assemble the stellar components. The model spectra can be fitted to observed opt [illegible] ectra, with independant extinction coefficients of the old and the new component. When [illegible] ectra can be used in addition to photometric and bolometric data they give much bette [illegible] raints on model parameters than can be achieved without spectra.

3 Observations

The data includes long slit spectra covering the range from 3700 to 7000 Å at a resolution of 12 Å (FWHM) which are used for the model fits, and higher resolution spectra in the red to obtain dynamical masses. The sizes of starburst regions are taken from images in Hα or from published VLA maps. Photometric data of the starburst regions is obtained from calibrated CCD images in B, V, R, and I. Published data like IRAS and near-infrared data have been included if available.

4 The duration of starbursts and the deficiency of low mass stars

The first question is that of the duration of starbursts and the suspected deficiency of low mass stars in the starburst IMF. Constraints on both of them can be obtained from the ratio of mass to luminosity (here: bolometric luminosity), M/L. The extremely low M/L of many starbursts cannot be maintained for very long times. Since the pioneering work of Rieke et al. (1980) several groups came to the conclusion that the M/L of some starbursts is too small to be explained by even a very short starburst unless the starburst IMF has some kind of deficiency of low mass stars, which is usually described by a lower mass cutoff.

An example of that is NGC 520 with an M/L_{bol} of the starburst region of about 0.016 (±50%, assuming $H_0 = 75\ \mathrm{km\,s^{-1}\,Mpc^{-1}}$). Even if the mass of stars and remnants formed during the starburst were 20% of the dynamical mass, the starburst population itself would have an M/L of only 0.003.

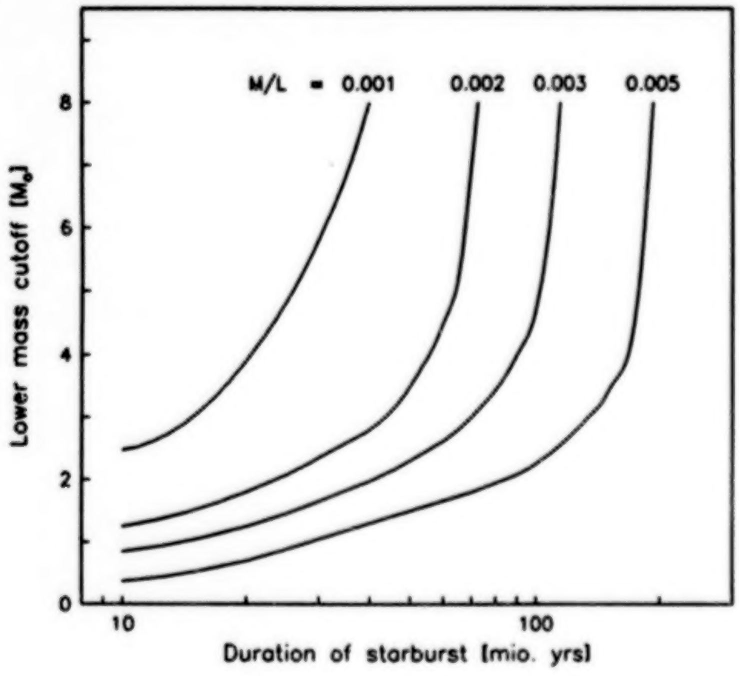

Fig. 1: Relation between the duration of a starburst and the required lower mass cutoff m_l for several values of the mass-to-bolometric-luminosity ratio M/L of the starburst population only. The IMF was assumed as a solar neighbourhood IMF (Scalo 1986) restricted to the mass range $m_l \leq m \leq 60\,M_\odot$.

Fig. 1 shows the relation between the duration of a starburst and the required lower mass cutoff of a solar neighbourhood IMF (Scalo 1986) for several values of M/L. It is evident that some low mass star deficiency is required even if the starburst is very short, corresponding to a lower mass cutoff of about 1–2 $M_\odot$. The diagram also shows that the starburst cannot be active for more than 100 mio. years even if only high mass stars were produced.

The starburst in NGC 520 is very obscured and the model spectra are of little help in this case. In the case of the starburst in NGC 7714 (see fig. 2) they are an excellent tool to examine the starburst parameters. The nulear starburst has a diameter of 9$''$ and a FWHM of 4$''$.5 in Hα. The dynamical mass inside the full diameter is about $6 \cdot 10^8\ M_\odot$. The spectrum of the

Tab. 1: Properties of the optimum starburst model for NGC 7714.

Duration: 20 mio. years, mass range: $1.2\,M_{\odot} \leq m \leq 50\,M_{\odot}$, distance: 39 Mpc.

	Observed	Model		Observed	Model
B	14.2±0.15 mag	14.1 mag	J	12.0 mag	12.4 mag
V	13.8	13.8	H	11.2	12.0
R	13.5	13.3	K	10.9	11.7
I	12.7	12.8	L	10.3	11.5
mass	$6 \cdot 10^8\,M_{\odot}$	$6 \cdot 10^8\,M_{\odot}$			
L_{bol}	$> 1.5 \cdot 10^{10}\,L_{\odot}$	$2.5 \cdot 10^{10}\,L_{\odot}$			

Tab. 2: Recalculation of M 82 model A.

	Rieke et al. (1980)	New models
L_{bol}	$4.6 \cdot 10^{10}\,L_{\odot}$	$4.6 \cdot 10^{10}\,L_{\odot}$
mass	$3.0 \cdot 10^8\,M_{\odot}$	$2.6 \cdot 10^8\,M_{\odot}$
M_K	−21.5 mag	−22.3 mag

(say less than 30 million years long) fit better than longer starbursts (say 100 million years long). About 15% of the dynamical mass are stars formed during the starburst, if no lower mass cutoff is applied. The dominating stars are in the mass range 6–8 $M_{\odot}$. Stars in the range 4–6 $M_{\odot}$, however, contribute sufficiently to test their presence or absence. It turns out that the spectra agree best when the 4–6 $M_{\odot}$ stars are included at approximately the expected amount. In older post-starbursts than this one, we should be able to test even lower masses. The problem with such tests is that in most post-starbursts, unlike in NGC 7715, the star formation has not ceased completely.

5 The time delay between starbursts

With the estimated starburst durations and post-starburst ages the time delay between starbursts in two interacting disk galaxies of very unequal (a factor of 5–10 different) masses can be determined. In the present sample there is a total of 8 such starburst systems:

- 5 pairs with a starburst in the minor component and little enhancement in the major component,
- 1 with starbursts in both components, and
- 2 with a starburst in the major component and post-starburst in the minor component.

Although this is statistically not very significant it gives some evidence that starbursts in the less massive component start earlier than in the more massive component. This could have several reasons: the stronger disturbance of the minor component by the major component than vice versa, smaller time scales for orbits and mass infall in the minor component, or even a larger fraction of gas mass to total mass in the smaller galaxy. The time delays determined so far are in the range 0–200 mio. years.

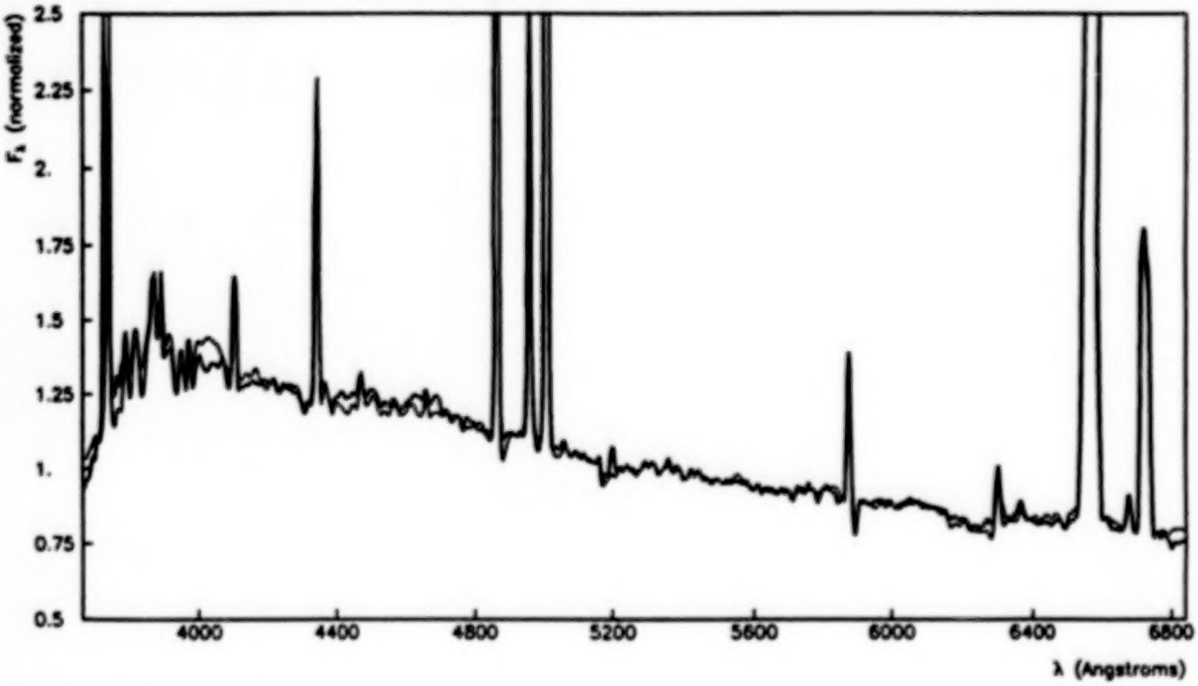

Fig. 2: Observed spectrum (thick line) and model spectrum (thin line) of the central starburst region of NGC 7714. Strong emission lines were clipped to emphasize the stellar continuum.

starburst region can be fitted very well with a starburst which has been active for about 15-50 mio years. Including uncertainties of the stellar evolutionary tracks and the heavy element abundances – which were assumed to be solar – the limits increase to about 10–100 million years. With spectra extending to shorter wavelengths and with better calibration quality at the blue end of the spectrum more precise limits could be obtained. Without a deficiency of low mass stars about half of the dynamical mass would be stars formed during the starburst. With a lower mass cutoff of about 1 $M_\odot$ this mass ratio would be in an acceptable range. In the 4."5 diameter the situation is certainly even more severe but the resolution of the radial velocity maps is insufficient to derive a dynamical mass. Results for the best model with a starburst duration of 20 mio. years are shown in table 1. The B, V, R, and, I magnitudes agree very well but in the near infrared there is a significant excess of the observed brightnesses. This excess is probably due to late stages of stellar evolution either not properly included in the stellar evolutionary tracks or in the colour calibration. With the more incomplete stellar tracks used by Rieke et al. (1980) for M 82 this effect was even more severe. A recalculation of their model A with the same IMF and star formation rate history gives twice their K band luminosity (see table 2) which reduces the need for a lower mass cutoff in M 82.

Direct observational evidence for a lower mass cutoff should be easier with post-starburst which are in a low state of star formation. There the very bright massive stars are no longer present. Such a post-starburst can be seen in NGC 7715, the companion of NGC 7714.

The spectrum of the central 1.5 kpc (see fig. 3) is dominated by late B stars and the galaxy shows no emission lines as signs of current star formation. The time when star formation ceased can be determined very well by fitting with model spectra: about 40–50 million years ago. The fits are not as sensitive to the duration of the starburst as to its end but very short starbursts

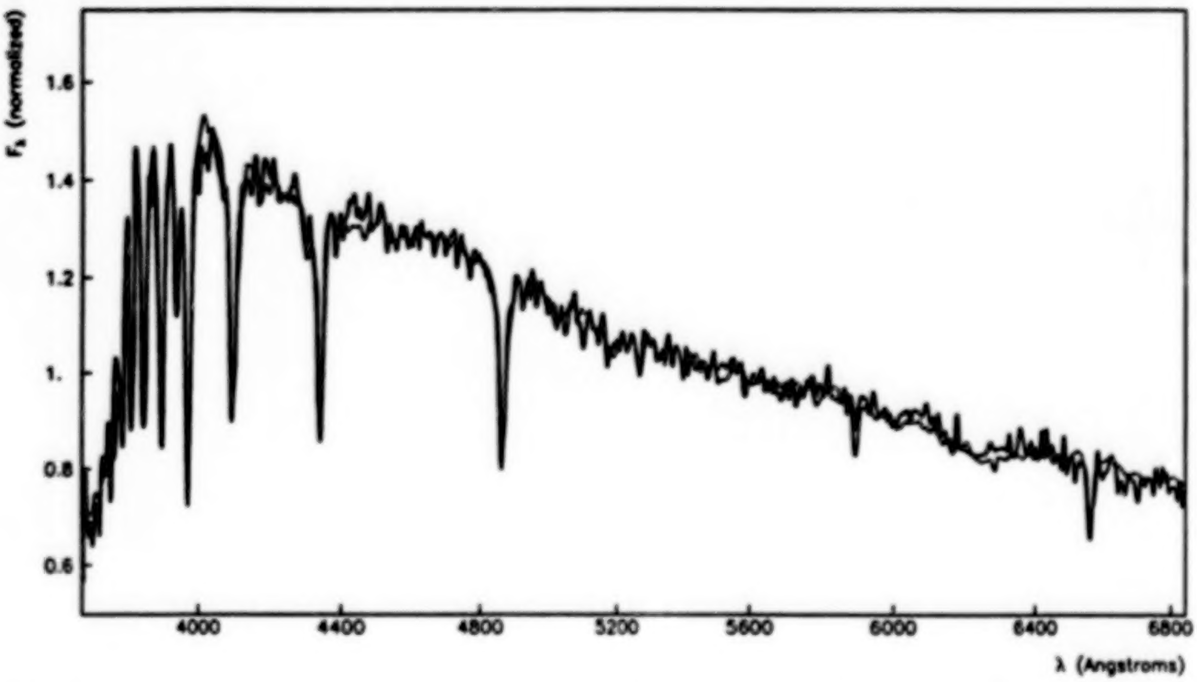

Fig. 3: Observed spectrum (thick line) and model spectrum (thin line) of NGC 7715.

6 Conclusions

There are signatures of a low mass star deficiency in several starburst galaxies. These can be explained with lower mass cutoffs of 1–2 $M_\odot$. No evidence was found for a cutoff of 6 $M_\odot$ or even more which was claimed by other investigators (Wright et al. 1988, Olofsson 1989). The lower mass cutoff found in post-starburst galaxies is less than about 4 $M_\odot$. There is little evidence for a low mass deficiency except from the mass-to-luminosity ratio. Starbursts in the less massive component of interacting pairs are triggered more quickly. The duration of a starburst is only a few 10^7 years but the delay between starbursts in two interacting galaxies may be a few 10^8 years. This can easily explain why so few pairs of interacting galaxies show starbursts in both components.

References

Bertelli, G., Bressan, A., Chiosi, C., and Angerer, K. 1986, *Astron. Astroph. Sup. Ser.*, **66**, 191.
Jacoby, G. H., Hunter, D. A., and Christian, C. E. 1984, *Astroph. J. Suppl.*, **56**, 257.
Maeder, A. 1976, *Astron. Astroph.*, **47**, 389.
Maeder, A. 1981a, *Astron. Astroph.*, **99**, 97.
Maeder, A. 1981b, *Astron. Astroph.*, **102**, 401.
Maeder, A. and Meynet, G. 1988, *Astron. Astroph. Sup. Ser.*, **76**, 411.
Maeder, A. and Meynet, G. 1989, *Astron. Astroph.*, **210**, 155.
Matraka, B., Wasserman, C., and Weigert, A. 1982, *Astron. Astroph.*, **107**, 283.
Olofsson, K. 1989, *Astron. Astroph. Sup. Ser.*, **80**, 317.
Rieke, G. H., Lebofsky, M. J., Thompson, R. I., Low, F. J., and Tokunaga, A. T. 1980, *Astroph. J.*, **238**, 24.
Scalo, J. M. 1986, *Fund. Cosm. Phys.*, **11**, 1.
Tinsley, B. M. 1968, *Astroph. J.*, **151**, 547.
Wright, G. S. et al. 1988, *Mon. Not. Roy. Astr. Soc.*, **233**, 1.

DISCUSSION

Khachikian: You mentioned NGC 520. What kind of galaxy is this one?

Bernlohr: It is a close interacting pair. The main component is a disk galaxy seen edge-on. The center of the rotation curve of this component coincides with the radio continuum source, the peak in K-band images, and the peak of the CO emission. The active starburst in the nuclear region is highly obscured. The visually brighter northwestern knot is a less massive companion where a starburst happened about 200 million years ago.

Kochhar: If you form very big stars in the nuclear regions, their supernova explosions should also be important.

Bernlohr: Maybe, but I did not include supernovae. In the average spectrum they are not very important.

Xu: The observational data exceeds your model prediction most seriously in the L band. My question is: have you included the contribution from small grains in your model?

Bernlohr: No additional dust has been included in the models. The dust grains may be responsible for most of the excess in the L band. In the J, H, and K bands, late stages of stellar evolution probably account for the discrepancy.

Gerber: You said that the smaller galaxy undergoes a starburst before the larger galaxy in unequal-mass pairs. What are the mass differences between the two galaxies in these systems?

Bernlohr: They are in the range from 1:5 to 1:20.

DYNAMICAL EXPERIMENTS ON MODELS OF COLLIDING DISK GALAXIES

Richard A. Gerber, Dinshaw S. Balsara,† and Susan A. Lamb*†*

I. Introduction.

Collisions between galaxies can induce large morphological changes in the participants and, in the case of colliding disk galaxies, bridges and tails are often formed. Observations of such systems indicate a wide variation in color (see Larson and Tinsley, 1978) and that some of the participants are experiencing enhanced rates of star formation, especially in their central regions (Bushouse 1986, 1987; Kennicutt et al., 1987, Bushouse, Lamb, and Werner, 1988). In this paper we describe progress we have made in understanding some of the dynamics of interacting galaxies using N-body stellar dynamical computer experiments, with the goal of extending these models to include a hydrodynamical treatment of the gas so that a better understanding of globally enhanced star formation will eventually be forthcoming.

Historically, N-body experiments have been used by a number of authors to study galactic collisions (eg. Toomre and Toomre, 1972; Miller and Smith, 1980; Noguchi, 1987). Our results, which were obtained using a three-dimensional grid-based Fast Fourier Transform N-body program, confirm the earlier results and lay the foundation for an explicit investigation of the gas dynamics in such systems. We are especially interested in eventually building models that will address the phenomenon of enhanced star formation rates and we plan to incorporate a representation of galactic gas into the computer models. We plan to follow the galactic gas continuum, looking for regions of enhanced gas density and locations of shocks. We will be using Balsara's Smoothed Particle Hydrodynamics code (Balsara and Norman, 1990), which includes the N-body code, to model both the stellar and gaseous components of disk galaxies during a collision.

We concentrate our present N-body study on the first stages of the interaction, that is the first flyby. We anticipate the both stars and any gas present in the galaxies will respond similarly to changes in the gravitational potential in the early stages of a collision. Only when the dissipative nature of the gas becomes important, as when shock fronts appear, will gas and star motions possibly decouple to a great extent. Thus we can obtain a first approximation to the locations of possible star formation by studying the first stages of the collision.

II. Model Parameters and Results

We model collisions between a spiral galaxy and an elliptical galaxy. The spiral galaxy is represented by a rotationally supported exponential disk of stars, stabilized by both internal velocity dispersions (Toomre Q=1.5) and a surrounding massive halo. The halo, with a mass three times that of the disk, is a spherical King Model (King, 1966) that was evolved as the disk potential was slowly grown within it, producing our starting disk galaxy model. The second galaxy, which represents a spherical galaxy, is a King Model with a mass equal to the halo mass in the spiral galaxy. There were approximately 55,000 particles used in each of the experiments, which were run on the Cray-2 supercomputer at the National Center for Supercomputing Applications at the University of Illinois at Urbana-Champaign.

We considered four disk/orbital orientations, all with an initial value of orbital energy at which two point masses would be on parabolic orbits (ie. zero total orbital energy). The four experiments are:

1) Prograde (orbital and disk rotational angular momentum vectors parallel), grazing (minimum center of mass separation of approximately two disk radii).

2) Retrograde (orbital and disk rotational angular momentum vectors antiparallel), grazing

3) Head on (zero orbital angular momentum), disk lying in orbital plane.

4) Head on, disk normal to orbital plane.

We choose to scale our experiments such that the spiral galaxy has parameters similar to those of our Galaxy. In these units, the disk has an exponential scale length of 4 kpc and both the disk and halo have similar outer radii of approximately 20 kpc. The disk's mass is $6 \times 10^{10} M_{\odot}$ and the halo has a mass of $1.8 \times 10^{11} M_{\odot}$. The disk has a thickness of about 500 pc and its rotational velocity at 8 kpc is 230 km/sec.

1. Prograde, in disk plane

The disk is violently affected in this first experiment. It has been known since the experiments of Toomre and Toomre (1972) that prograde collisions produce a great deal of damage, and indeed particles are sprayed in both the forward and backward directions; some stars appear to be captured by the elliptical galaxy, hinting at the possibility that gas as well as stars may be exchanged via this process. We note the formation of a bar-like structure in the central region of the disk galaxy. We also measure a global outward average radial streaming of disk particles at a maximum of 60 km/sec. As these velocities are greater than the sound speed and the structure is very non-axisymmetric (indicating a nonhomologous response), we expect that shocking will occur. An example of the resulting morphology is given in figure 1, which contains a sampling of the positions of the 'stellar' particles at time 120 million years after closest approach.

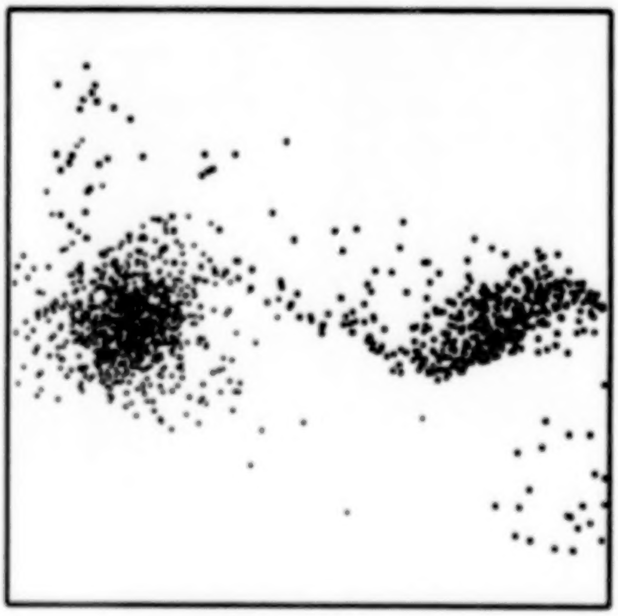

Figure 1

The morphology of the disk and elliptical galaxies for experiment 1 (prograde, grazing collision) is shown. The larger dots represent disk particles and the smaller dots represent the elliptical galaxy. The disk galaxy's halo particles are not shown. The time is 120 million years after closest approach. The disk system is moving to the right and upward while the elliptical is moving left and downward. The view is looking down onto the disk plane.

2. Retrograde, in disk plane

The retrograde collision exhibits drastically different behavior than that shown by the prograde experiment. The disk is only slightly affected in the retrograde encounter, generally maintaining its axisymmetric shape while expanding slightly. We find only very small average radial streaming velocities in this case. That such a close encounter produces such small effects may be at least part of the explanation of Bushouse's (1986) finding that a substantial proportion (~30 percent) of closely interacting pairs of disk galaxies show no evidence for enhanced star formation rates.

3. Head on, in disk plane.

A striking effect of this deeply interpenetrating collision is the sharp contraction of both disk and halo components soon after closest approach. In contrast to the grazing collisions, large inward velocity flows are triggered, reaching an average maximum value of 100 km/sec in the disk. All galactic components contract to nearly one-half their previous size and then later re-expand as material flows outward at a peak average velocity of 90 km/sec. The disk is quite disrupted with a definite, although transient, thin bar-like feature forming in the center. In real interactions of this type there may be a sizeable buildup of gas in the center of the disk galaxy due to dissipative interactions (such as shocking and high rates of cooling in dense regions) in the gas that flows into the center. That is, dissipation may halt the subsequent outward bounce of the gas that would otherwise follow the contraction of the gas and stars.

4. Head on, normal to disk plane

This collision produces a striking ring of disk particle soon after close passage. The disk and halo both contract and expand as in the previous experiment; with radial velocities in the disk having maximum inflow and outflow values on the order of 100 km/sec. These are illustrated in figure 2. A ring forms during the re-expansion phase and this strong density enhancement propagates outward through the disk attaining a peak amplitude approximately 4 times greater than the unperturbed disk stellar surface density. A time sequence showing the evolution of the density profile of the disk is shown in figure 3 and we see there that the enhancement damps significantly by the time it reaches the edge of the disk.

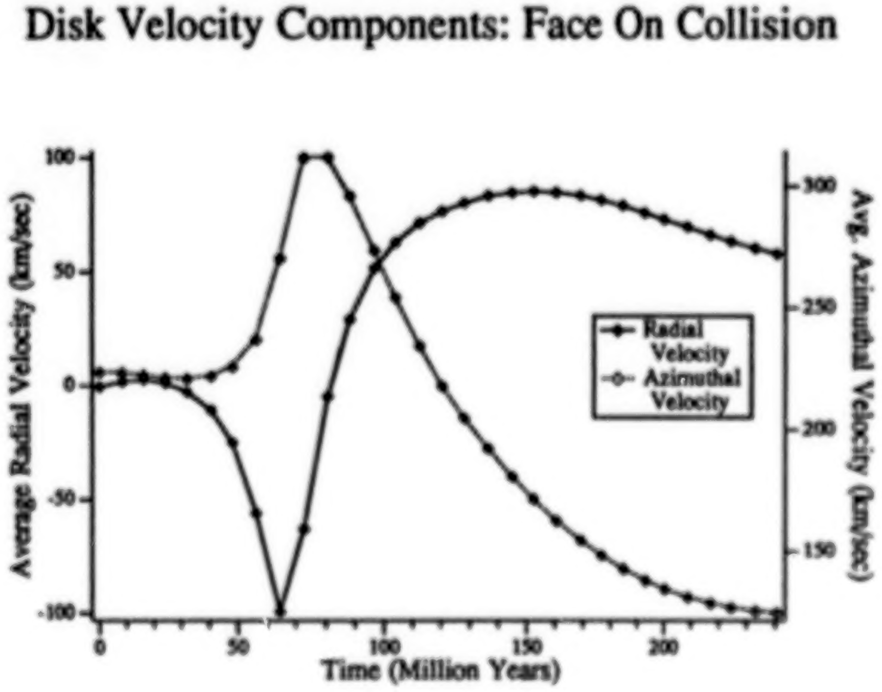
Disk Velocity Components: Face On Collision

Figure 2

Globally averaged radial and azimuthal velocities as a function of time for the disk particles in experiment 4.

Particles per Radial Bin: Normal to Disk Plane Collision

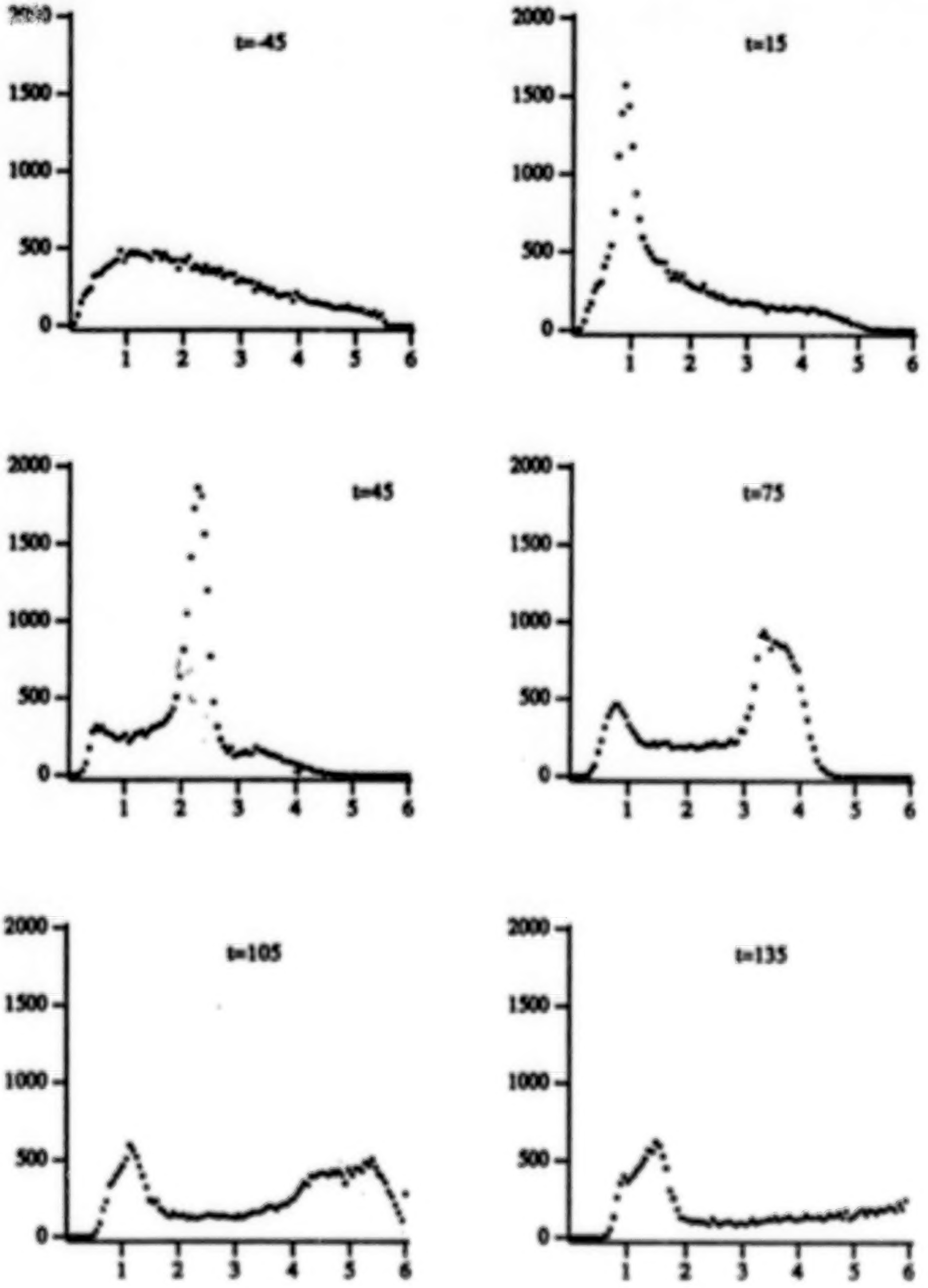

Figure 3

The number of particles per spherical bin at six different times in experiment 4 (the collision normal to the disk plane). The bins are spaced at constant radial intervals; each is centered on the system's center of mass. Time, t (given in million years) is measured relative to closest approach.

III. Conclusion

Close interactions between galaxies can produce large perturbations in both density and velocity fields. We have measured, via computational experiments that represent a galaxy's stars, average radial velocity flows as large as 100 km/sec and 400 percent density increases. These can occur in rings that move outwards through the disk of a galaxy, in roughly homologous inflows toward the nucleus, and in off center, non-axisymmetric regions. Here we have illustrated where the gas is likely to flow during the early stages of interaction and in future work we plan to investigate the fate of the gas more realistically by using an N-body/Smoothed Particle Hydrodynamics code to model both the stellar and gaseous components of a disk galaxy during a collision. Specifically, we will determine the locations of enhanced gas density and the strength and location of shock fronts that form during the interaction.

References

Balsara, D.S. and Norman, M.L. 1990, Submitted to Ap. J.

Bushouse, H.A. 1986, Astron. J., 91, 255.

Bushouse, H.A. 1987, Ap. J., 320, 49.

Bushouse, H.A., Lamb, S.A., and Werner, M.W., 1988, Ap. J., 325, 74.

Kennicutt, R.C., Keel, W.C., van der Hulst, J.M., Hummell, E. and Roettiger, K. 1987, Astron. J., 93, 1011.

King, I.E. 1966, Astron. J., 71, 64.

Larson, R.B. and Tinsley, B.M. 1978, Ap. J., 219, 46.

Miller, R.H. and Smith, B.F. 1980, Ap. J., 223, 122.

Noguchi, M. 1987, Mon. Not. R. astr. Soc., 228, 635.

* *Department of Physics, University of Illinois , Urbana, Illinois 61801.*

† *Department of Astronomy, University of Illinois , Urbana, Illinois 61801.*

CAUSTIC WAVES IN GALAXY DISKS PRODUCED IN COLLISIONS WITH LOW MASS COMPANIONS

Curtis Struck-Marcell
Astronomy Program, Physics Dept.
Iowa State University

At this meeting much attention has been focussed on interactions and mergers between roughly equal mass galaxies. On the contrary, I will begin by mentioning a few justifications for studying collisions with relatively low mass companions, specifically, less than about one third of the mass of the target galaxy. The first is simply that such collisions are likely to be common, given that the galaxy luminosity function is broad. The second reason is that such collisions have evidently been less well studied than collisions between nearly equal partners. However, there are a few important exceptions to this generalization, including the sinking satellite problem (e.g. Quinn and Goodman 1986), and the collisional model for the formation of shell galaxies in which a companion of negligible mass is completely disrupted(e.g. Dupraz and Combes 1986, Hernquist and Quinn 1988). The third, and potentially most important reason, is that the effects of a collision with a low-mass companion are less extreme (at least from the big galaxy's point of view!). Thus, these effects are closer to the theorist's ideal of a "small perturbation". This is important for both conceptually understanding the effects of the collision, and for justifying the use of approximate numerical techniques (e.g. restricted three-body) to study them.

The primary effect of such collisions on a target galaxy with a "cold", disk component is the generation of waves in the disk. Here I will focus on the purely stellar waves in such disks. Even within these limitations a large variety of transient wave morphologies, besides the well-known spirals and rings, are possible. Such nonlinear stellar waves are caustic surfaces, and I believe that singularity or catastrophe theory can be helpful in understanding their properties. (For an excellant introduction see Arnold (1986)). In persuing this understanding we can follow the lead of Arnold, Shandarin, and Zeldovich (1982) who haye applied singularity theory to the study of two and three dimensional "pancaking" in galaxy formation theory.

The word "caustic" has a variety of specific definitions. For present purposes it suffices to define a caustic as a (compact) zone of stellar orbit crossings, or a zone where two or more collisionless star streams intersect. This idea of orbit crossings immediately harkens back to the kinematic models of Lynds and Toomre (1976) for stellar rings, and Kalnajs' (1973) rotating ellipses model for spiral waves. Because of its cylindrical symmetry, the ring galaxy case provides a particularly simple example that is worth reviewing.

Figure 1 shows a phase plane cut illustrating ring structure and outward propagation. (The details of the specific kinematic calculation are not important here.) Before the collision we assume that all the stars were in circular orbits, with a negligible thermal velocity component, and zero systematic radial velocity. At times shortly after the central impact all the stars fall inward (negative radial velocity) in response. After the companion moves away from the disk the stars no longer feel the pull of the extra mass towards the center, so centrifugal force reverses the infall, and the stars will move back out, ultimately overshooting their equilibrium radius. For most reasonable disk potentials the epicyclic oscillation period will be shorter in the center, so rings will form there and propagate outward. Some time after ring formation, the innermost stars begin a second cycle of infall. Figure 1 shows a later time when the first ring has propagated well out into the disk and a second ring has formed.

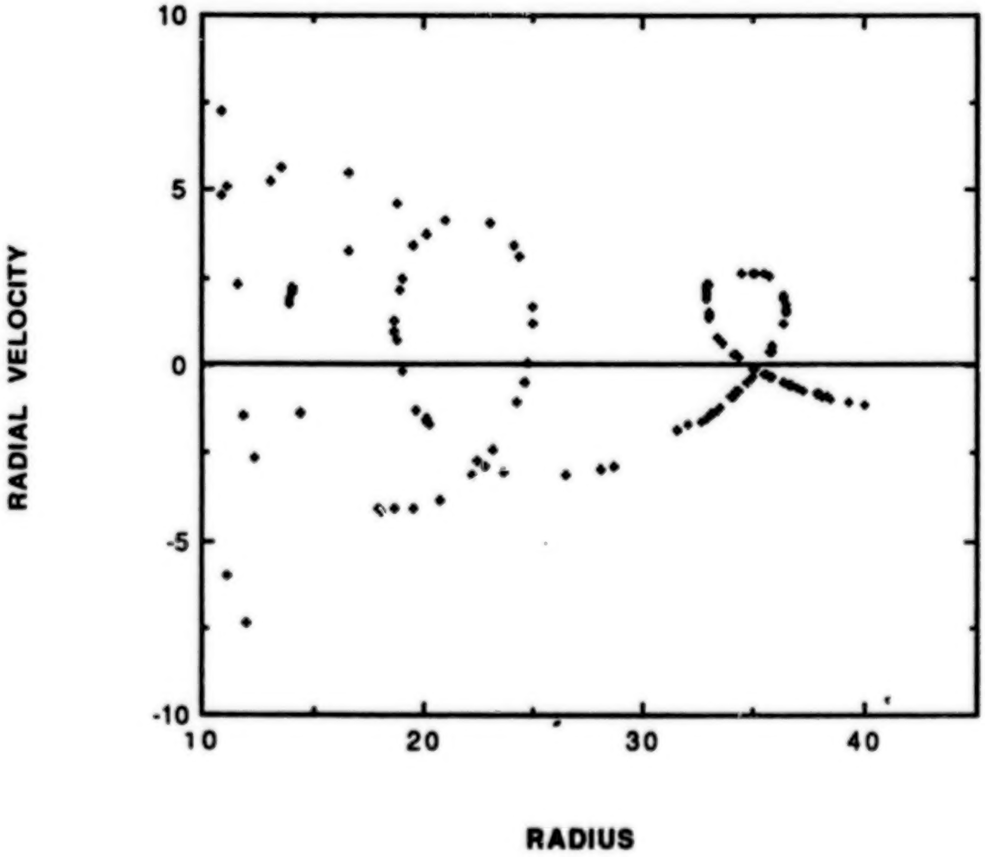

Fig. 1. Phase plane surface of section with dimensionless radial velocity vs. dimensionless radius plotted for particles within a narrow azimuthal range along a radius vector. The results are from a simple kinematical calculation of a ring-making collision. The two loops in the plot correspond to the two stellar rings that have formed by the time shown.

The rings appear as loops in these r-v_r phase space cuts. (N.B. crossings in the phase cut do not represent crossings in the four dimensional phase space, so there is no violation of Louisville's theorem.) A vertical line in the last frame shows that within the loop (ring) there are three interpenetrating star streams, satisfying our definition of caustic. Other verticals show that the ring edges are fold caustics, i.e. projections of a phase space fold onto the disk plane. In fact, such diagrams show that circular stellar rings are born as phase space cusps, and degenerate into paired fold caustics (loops) immediately thereafter. This is a standard sequence of caustic metamorphosis, and is locally the same as Zeldovich pancake formation.

Many ring properties can be calculated with the kinematic model illustrated in Figure 1, including: ring center positions, and the widths and mean densities of rings as a function of time. The idea of these calculations is as follows. If we adopt the idealization that the kinematic equations describe a continuous, collisionless stellar fluid, then these equations predict the occurance of an infinite stellar density at a caustic edge. The density singularity condition can be solved to determine which stars (identified by their initial unperturbed positions) lie within the caustic at any time. The kinematic orbit equation then specifies the location of the caustic edge. At least qualitatively the results seem to agree well with the few high-resolution N-body results available to date, for details see Struck-Marcell and Luban-Lotan (1990).

When we extend our consideration to off-center impacts new, and more complex caustics emerge, including the so-called swallowtail, and Arnold's pocket or purse (hyperbolic umbilic). As before, we can demonstrate the development of these caustics with a simple kinematic model, although in asymmetric cases it is very difficult to derive analytic results (see Struck-Marcell 1990). Figure 2, which is based on a numerical kinematic calculation, shows an example of a swallowtail caustic produced in a slightly off-center collision. At the top is a gray-scale representation of the stellar density in the disk (the range of densities is about an order of magnitude), which shows the high-density central region of the caustic and the several arms radiating out from it. It is still possible to see the familial relationship between this form and rings, or ring plus spirals. This is also true in the phase space cut at the bottom of Figure 2, where loops are again very evident. The swallowtail must appear as something like a bow-tie in the phase cut, since it is characterized by five intersecting star streams. Similarly, family resemblances aside, the swallowtail should be recognizable on the sky. Just on the basis of appearance, NGC 3145, a Hubble Atlas galaxy (Sandage 1961), is a possible candidate. It has not to my knowledge been cited as a possible collision remnant before, but it does have a companion (NGC 3143) with a similar redshift within about 5-6 diameters. Other possible examples of higher order caustics are given in Struck-Marcell (1990). Higher order caustics are also evident in most published high resolution restricted three-body or N-body simulations of interactions.

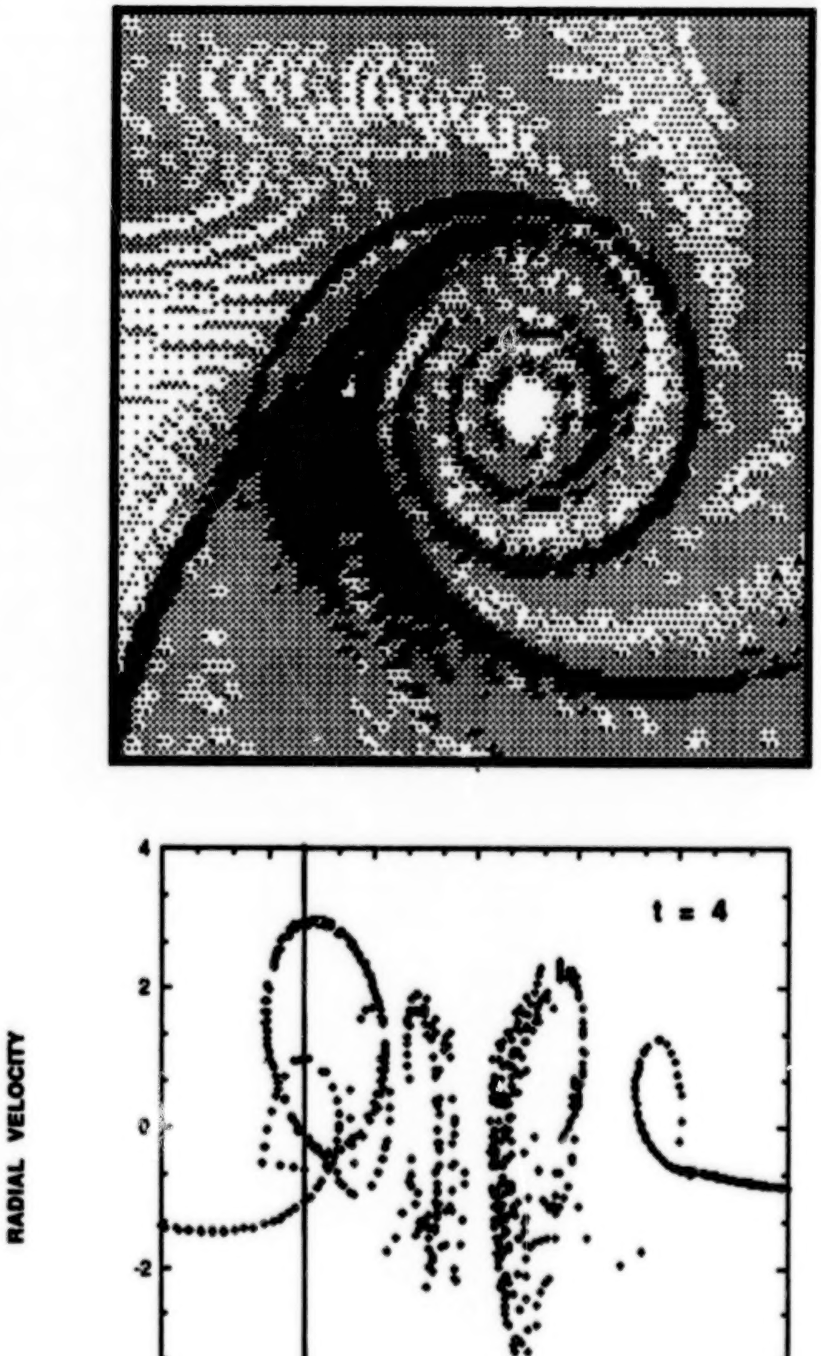

Fig. 2. *Top* : Gray-scale representation of the surface density of a swallowtail caustic. The gray-scale levels vary over a range of about an order of magnitude in surface density. *Bottom* : Phase plane section as in Figure 1, but for a slightly off-center collision, and with particles from a strip in both the positive and negative directions along the x-axis. The vertical line cuts the five star-streams that make-up a swallowtail caustic.

The stellar rings and the swallowtail examples suggest several specific ways in which the mathematical theory of caustics and singularities can be helpful in the study of colliding galaxies. These are not unique cases, and so I will conclude with a brief list of tentative answers to the question - why caustics? Possibly the most important reason, but also the least well-defined, is that caustics are a valuable conceptual tool. For example, it is easy to visualize morphological features like a flat surface density profile across a wave in terms of the superposition of several roughly uniform star streams. It is also easy to understand sharp boundaries of over-dense regions as folds in phase space.

A related point is that since there are only a relatively small number of generic caustic forms in two and three dimensions, these forms can provide the basis of a classification scheme for collisional disturbances. The caustic forms are sufficiently distinct that it should be possible to search for them automatically. However, caustics do not always appear in isolation, they can overlap each other, which would complicate such a search. At the same time, the structure of multiple caustics in a galaxy might provide enough information to allow the determination of the interaction parameters fairly uniquely. Moreover, the evolutionary disintegration of caustics by shear and phase mixing may facilitate dating by morphology in collisional systems.

Singularity theory suggests some specific observational checks. High-resolution spectra of a swallowtail morphology should reveal either the multiple star streams, or at least very broad spectral lines relative to surrounding regions.

Finally, at least in symmetric cases, singularity theory provides a method for (semi-)analytic calculation of nonlinear wave structure.

NASA grant NAGW 1009 is gratefully acknowledged for partial support of this work.

REFERENCES

Arnold, V.I.(1986), Catastrophe Theory, 2nd English edition (New York: Springer-Verlag).

Arnold, V.I., Shandarin, S.F. and Zeldovich, Ya. B.(1982), Geophys. Astrophys. Fluid Dynamics **20**, 111.

Dupraz, C., and Combes, F. (1986), Astron. Astrophys. **166**, 53.

Hernquist, L., and Quinn, P. J. (1988), Astrophys. J. **331**, 682.

Kalnajs, A. J. (1973), Proc. Astron. Soc. Aust. **2**, 174.

Lynds, R., and Toomre, A. (1976), Astrophys. J. **209**, 382.

Quinn, P. J., and Goodman, J. (1986), Astrophys. J. **309**, 472.

Sandage, A. (1961), The Hubble Atlas of Galaxies (Carnegie Inst.: Washington DC).

Struck-Marcell, C. (1990), Astron. J. **99**, 71.

Struck-Marcell, C., and Luban-Lotan, P. (1990), Astrophys. J., in press.

SIMULATIONS OF GAS CLOUDS IN INTERACTING GALAXIES

Magnus Thomasson
Onsala Space Observatory
S-439 00 Onsala
Sweden

1. Introduction

A companion can induce a varitey of morphological changes in a galaxy. I use N-body simulations to study the effects of different kinds of perturbations on the dynamics of a disk galaxy. The model is two-dimensional, with a disk consisting of about 60,000 particles. Most of the particles (80 %) represent the old stellar population with a high velocity dispersion, while the rest (20 %) represent gas clouds with a low velocity dispersion. Initially, the velocity dispersion corresponds to $Q = 1$ for the "star" particles, and $Q = 0$ for the "gas" particles, where Q is Toomre's (1964) stability parameter. The gas clouds can collide inelastically. The disk is stabilized by a rigid halo potential, and by the random motions of the old "star" particles. To simulate the effect of an encounter on the disk, a companion galaxy, modelled as a point mass, can move in a co-planar orbit around the disk. A complete description of the N-body code is found in Thomasson (1989).

In this contribution, I first present the spiral structures caused by a companion in first a direct and then a retrograde (with respect to the rotation of the disk) parabolic orbit. The associated velocity fields suggest a way to observationally distinguish between leading and trailing spiral arms. I then study the stability of the gas component in a disk in which tidally triggered infall of gas to the center occurs. Finally, I show how a ring of gas can form in a disk as a result of a co-planar encounter with another galaxy.

2. Leading and trailing spiral patterns

The galaxy model used in this section is that of a Mestel disk stabilized by a fixed halo potential of the same form as that of the axisymmetric disk. This model has a flat rotation curve and a finite radius.

Surrounded by a halo with the same mass as the disk, the unperturbed disk after a while looks like in Fig. 1. A spiral pattern with many arms, or rather fragments of arms, has developed in the gas population, while no structure is seen in the stellar disk.

A perturber in a direct parabolic orbit induces a *grand design two-armed trailing spiral pattern* in the disk (Sundelius *et. al.* 1987). In the example shown in Fig. 2, the perturber has a mass of 20 % of the disk + the halo, and a closest approach of about two disk radii. Two long arms dominate the picture, although there are also some other structures caused by the inelastic collisions between the clouds, and not found in runs without collisions. If the perturbation is strong enough, the global pattern can be seen both in the gas and the star component, contrary to the more fragmentary pattern in the unperturbed case. This is in general agreement with observations of flocculent and grand design galaxies (Elmegreen & Elmegreen 1984). The

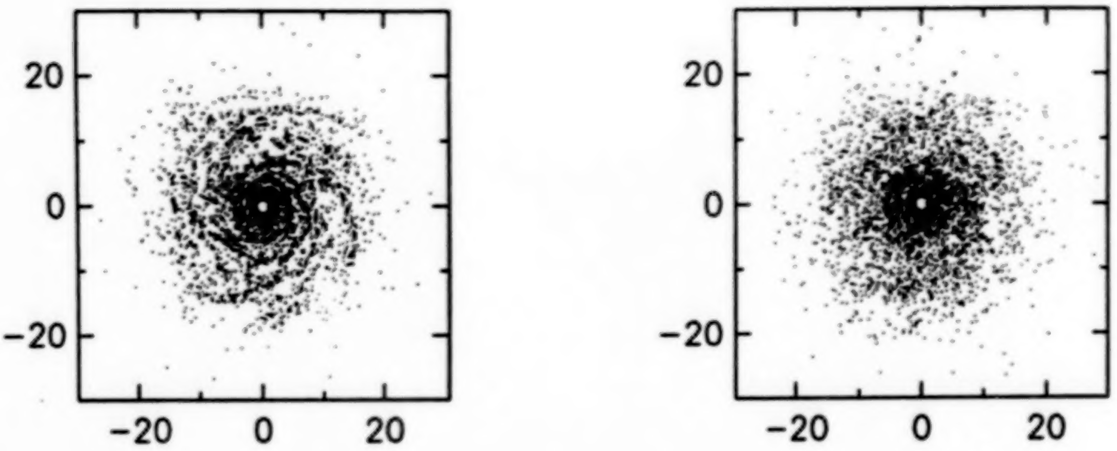

Fig. 1. Fragments of spiral arms in the gas (*left*), but no structure among the stars (*right*) after 2.5 revolutions of a particle at the edge of the disk, at $r = 20$.

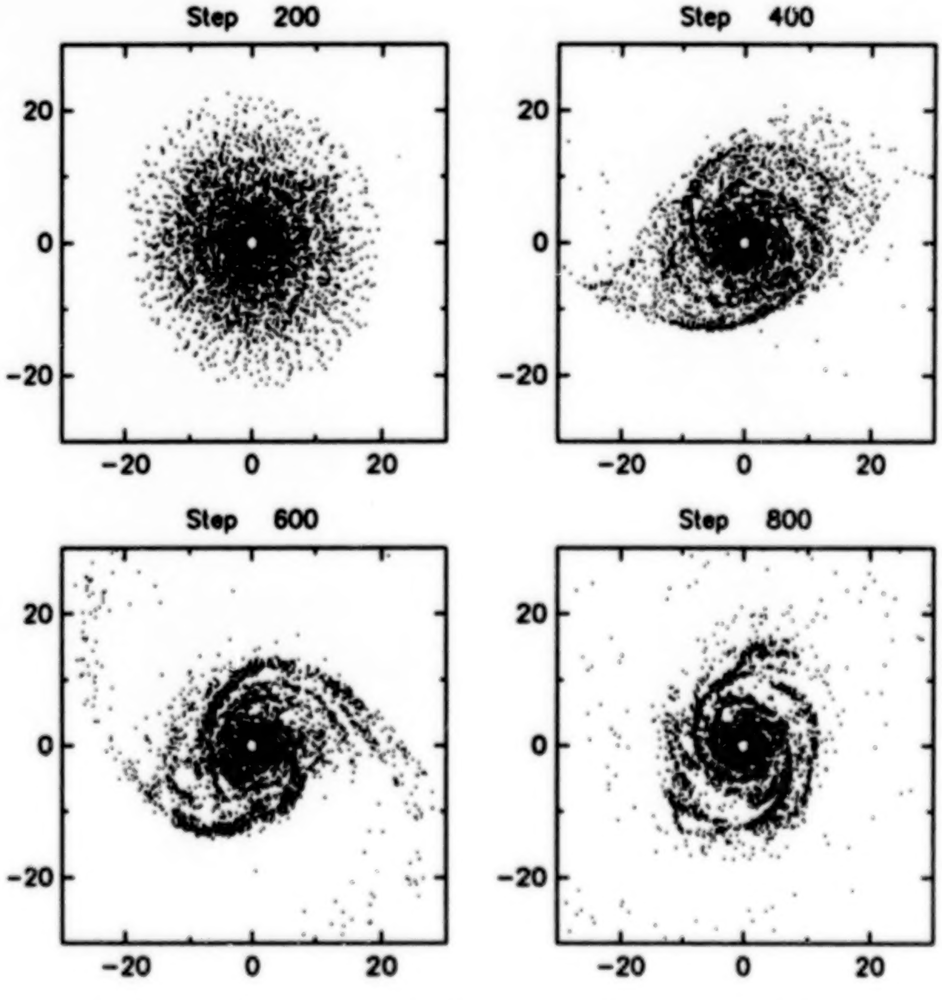

Fig. 2. The evolution of the gas population in a disk perturbed by a companion in a direct parabolic orbit. One revolution at the edge of the disk corresponds to 314 time steps.

rotation curve shows the usual "bumps", i.e. it has positive velocity gradients at the locations of the arms. The radial velocity is negative for objects in the arms.

A large retrograde perturber causes a ***one-armed leading spiral pattern*** to form in the disk (Thomasson *et. al.* 1989). A leading spiral arm is an arm who's tip points in the direction of rotation. Since leading arms are more clearly seen in galaxies with a large halo, I have increased the halo mass from 0.5 to 0.6 of the total mass of the primary galaxy in the example shown in Fig. 3. The perturber has here the same mass as the primary galaxy, and a closest approach just outside the disk. The rotation curve has the familiar "bumps" also in this case, but the radial velocities are now negative in the arms.

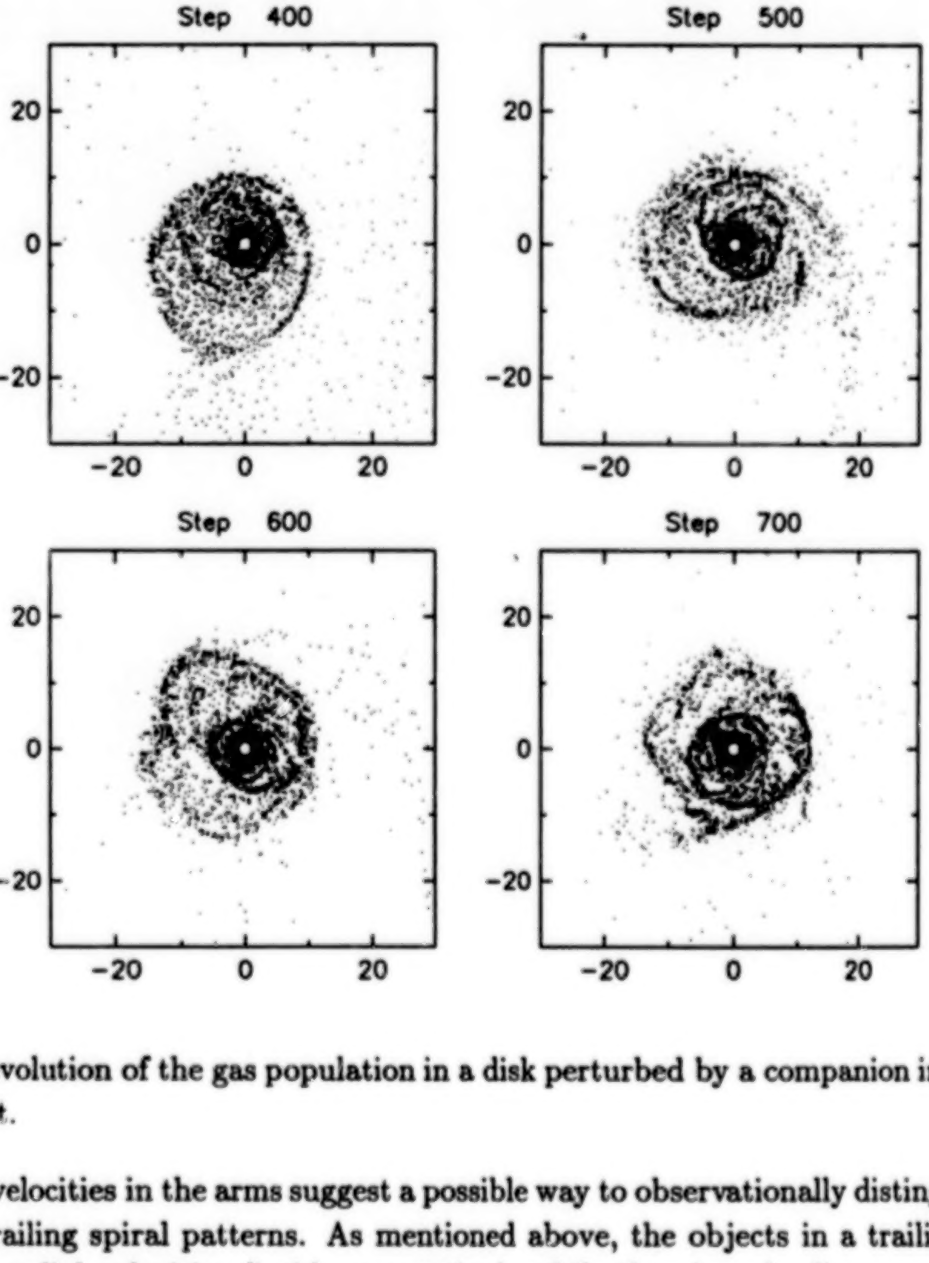

Fig. 3. The evolution of the gas population in a disk perturbed by a companion in a retrograde parabolic orbit.

The radial velocities in the arms suggest a possible way to observationally distinguish between leading and trailing spiral patterns. As mentioned above, the objects in a trailing spiral arm have *negative* radial velocities (inside co-rotation), while they in a leading arm have *positive* radial velocities. Also, since gas enters a trailing arm from the inner side, and a leading arm from the outer side, shocks and dust lanes should be found on different sides of the arms in trailing and leading patterns.

3. Infall of gas and activity in the center

(The work presented in this section was done in collaboration with Dr. B. G. Elmegreen.)

A tidal perturbation can also trigger infall of gas to the center of the disk. How this process can be responsible for the activity in the center of e.g. Seyfert galaxies has been studied by Byrd *et. al.* 1986, 1987. They used a Mestel disk in their simulations. Just to try something different, I used a Kuzmin disk ("Toomre's model 1") stabilized by a halo (of the same kind as the disk) with a mass of 0.7 of the total mass of the galaxy, and I found the same effect. The Kuzmin disk has a rotation curve that rises steeply to a maximum and then falls off slowly at larger radii. The "gas" particles were initially given a small velocity dispersion. A perturber with a mass of 0.2 moved past the galaxy in a parabolic orbit with a pericentre at somewhat more than twice the half mass radius of the galaxy.

Because of the tidal perturbation, gas starts to fall towards the center of the disk. If the gas disk is very unstable at medium and large radii, there is a risk that much of the gas will be used up in star formation before it reaches the center. In Fig. 4, Toomre's stability parameter Q is shown with a grey scale at a time step when the companion has moved far away from the disk. Q gives a rough measure of the stability of the gas. During the infall process, Q is large (white or light grey in the figure) except for in the central parts. A small region with very low Q (black) is found close to the nuclues of the galaxy. This means that the gas disk is unstable only in the most central parts, and we can expect a large amount of star formation there. The central region is just were most of the star formation activity in interacting galaxies take place (Bushouse 1987, Laurikainen *et. al.* 1989, Wright *et. al.* 1988).

4. Formation of a ring of gas clouds

If the Kuzmin model galaxy above is perturbed by a massive object in a retrograde orbit, a ring can form in the component of the disk consisting of colliding gas clouds. The ring shown in Fig. 5 was formed after the passage of a perturber as massive as the primary galaxy. A large number of cloud-cloud collisions occur in the ring. The stellar disk shows no ring structure at all.

References

Bushouse, H.A.: 1987, ***Astrophys. J.*** **320**, 49

Byrd, G.G., Sundelius, B., Valtonen, M.: 1987, ***Astron. Astrophys.*** **171**, 16

Byrd, G.G., Valtonen, M.J., Sundelius, B., Valtaoja, L.: 1986, ***Astron. Astrophys.*** **166**, 75

Elmegreen, D.M., Elmegreen, B.G.: 1984, ***Astrophys. J. Suppl. Ser.*** **54**, 127

Laurikainen, E., Moles, M.: 1989, ***Astrophys. J.*** **345**, 176

Sundelius, B., Thomasson, M., Valtonen, M.J., Byrd, G.G.: 1987, ***Astron. Astrophys.*** **174**, 67

Thomasson, M.: 1989, ***Research Report No. 162***, Department of Radio and Space Science with Onsala Space Observatory, Chalmers University of Technology, Göteborg

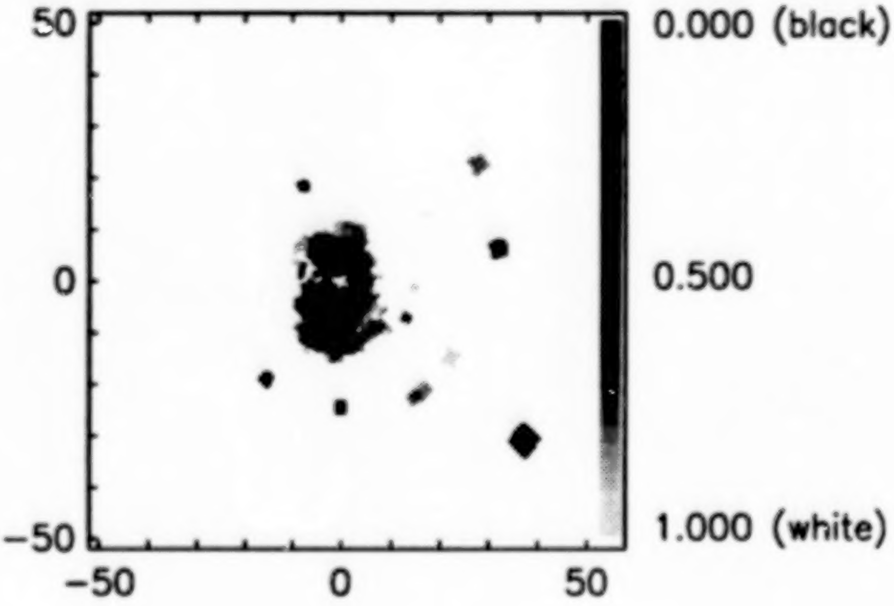

Fig. 4. A grey scale plot showing Toomre's Q for the gas (calculated using only the gas surface density) during the infall process. The half mass radius was initially 16, but particles filled the whole coordinate system. The black parts show where the gas is very unstable (Q is close to zero). White means either $Q > 1$ or zero surface density. In the very center of the disk, inside $r < 1$, there are no particles in the simulation.

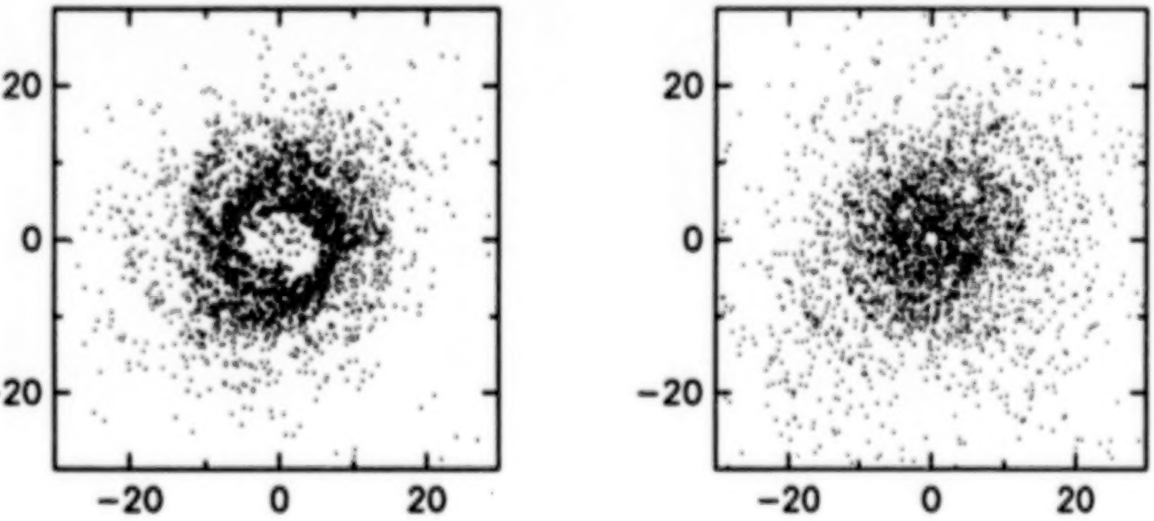

Fig. 5. The ring of gas clouds that formed after pericentre passage, at a radius of 28, of a massive perturber (*left*). No ring among the stars (*right*).

Thomasson, M., Donner, K.J., Sundelius, B., Byrd, G.G., Huang, T.-Y., Valtonen, M.J.: 1989, *Astron. Astrophys.* **211**, 25

Toomre, A.: 1964, *Astrophys. J.* **139**, 1217

Wright, G.S., Joseph, R.D., Robertson, N.A., James, P.A., Meikle, W.P.S.: 1988, *Monthly Notices Roy. Astron. Soc.* **233**, 1

Do elliptical galaxies have thick disks?

R C Thomson
Institute of Astronomy, Madingley Road,
Cambridge CB3 0HA, UK

A E Wright
Australia Telescope National Facility *,
PO Box 276, Parkes, N.S.W. 2870, Australia

February 18, 1990

Abstract. We discuss new evidence which supports the existence of thick disks in elliptical/S0 galaxies. Numerical simulations of weak interactions with thick disk systems produce shell structures very similar in appearance to those observed in many shell galaxies. We think this model presents a more plausible explanation for the formation of shell structures in elliptical/S0 galaxies than does the merger model and, if correct, supports the existence of thick disks in elliptical/S0 galaxies.

1 Introduction

The discovery of shell structures in elliptical galaxies (Malin and Carter 1980) was unexpected, and showed that these systems were not completely featureless. Malin and Carter (1983) estimated that about 17% of all elliptical galaxies had shell systems. More recently, Seitzer and Schweizer (1989) found that over half of the objects in a sample of 74 ellipticals/S0s exhibited shells. Shell structures are therefore not rare - they are a common phenomena in elliptical galaxies.

The currently accepted model for shell formation is by merger with another galaxy (Quinn 1984, Dupraz and Combes 1986, Hernquist and Quinn 1988). Several problems are noted by Thomson and Wright (1990). Briefly, in order to explain asymmetric shell structures, the merger model requires a head-on collision along the major axis of the primary galaxy, viewed nearly perpendicular to the line of impact, with another galaxy which has a similar stellar population to the that of the primary galaxy and which somehow produces shell structures with a radial brightness distribution similar to that of the underlying galaxy. We think the combination of all these factors makes this explanation of what is now known to be a relatively common phenomenon, highly improbable.

---

*The Australia Telescope National Facility is operated in association with the Division of Radiophysics by CSIRO.

2 A weak interaction model for shell galaxies

Numerical simulations of interacting thick disk systems (Thomson and Wright 1990) have shown that shell structures can be readily formed by this process. In these simulations, the thick disk is represented by a quasi-spherical distribution of massless test particles, with both the primary and secondary galaxies modelled by spherical Plummer potentials, and the interaction characterized by a parabolic orbit of the secondary. The test particles are set in motion at a tangent to their radius vector with a speed equal to their appropriate circular velocity, and the position of each particle is calculated under the influence of the combined time varying potential.

When such an interacting system is viewed along the effective axis of rotation, the induced stellar density wave is seen to have a spiral morphology (Fig.1; top row). When such a system is viewed nearly edge on, asymmetric shell structures are clearly visible (Fig.1; middle row). The asymmetry is more pronounced when the orbit of the secondary galaxy cuts through the simulated thick disk.

In the classification scheme described by Prieur (1989), type 1 shell systems are interleaved and well aligned along the major axis of the elliptical. According to our model, type 1 shell systems arise in elliptical galaxies which have a thick disk and a conspicuous spiral density wave viewed approximately edge on. When such a thick disk system is viewed more face-on, the density wave is seen to form fuller, but not complete arcs, and the shells also exhibit some spirality (Fig.1; bottom row). We associate this projection with type 2 ('all-round') shell systems. Furthermore, the observations that elongated shell galaxies are preferentially surrounded by type 1 shell systems, and that round-like shell galaxies are preferentially surrounded by type 2 systems (Prieur 1989) imply that these ellipticals are oblate spheroids when interpreted in terms of our model.

Shell galaxies that cannot be classified as type 1 or 2, are classified as type 3, which includes those galaxies with too few shells or which have complex structure (eg, Fornax A). In our model, galaxies with only a small number of shells may occur soon after the encounter (before the density wave has wound up by differential rotation). At the present stage of our modelling, we are unable to reproduce complex shell structures, probably because of the oversimplified assumptions of our model. However, we think that these complex shell systems are also caused by (possibly strong) interactions since these are observed in galaxies which are otherwise known to be interacting (eg, NGC1549/1553, NGC1316(Fornax A)/NGC1317).

3 Thick disks in elliptical/S0 galaxies

Featureless thick disks (ie, with no conspicuous spiral density wave) could exist in all elliptical galaxies without being observed. As such, most of the angular momentum in these systems could remain hidden. It is interesting to note that most of the elliptical galaxies in Malin and Carter's catalog of shell galaxies (Malin and Carter 1983) have been classified as S0 by Thronson et al. 1989. If this reclassification is correct, considerable angular momentum must be present in these (possibly thick disk) systems.

Detailed surface photometry of elliptical galaxies has revealed significant deviations from perfect ellipses (Jedrzedjewsi 1987, Franx 1988). In this respect, pointed isophotes (positive $\cos 4\theta$ term) are thought to indicate the presence of a thin disk. We think that 'boxy' isophotes (negative $\cos 4\theta$ term) may be the signature of thick disks in oblate spheroids viewed edge on. The extremely box-shaped elliptical IC3370 has been observed by Jarvis (1987). The maximum rotation velocity on the major axis is in good agreement with theoretical models of an oblate spheroid supported by rotation alone. For this reason, Jarvis proposed classifying this galaxy as S0pec. We think this galaxy is not peculiar, but just an extreme case of an elliptical galaxy with a featureless, but easily detectable, thick disk.

4 Discussion

The existence of thick disks in elliptical galaxies is postulated on the evidence of regular shell structures seen in a large number of these systems. By analogy with thin disk systems, if the thick disks extends much further than the visible bulge, elliptical galaxies may have much more angular momentum than previously thought. The stellar orbits in the outer regions of these galaxies could then be dominated by rotation. (NB. The shell system in NGC3923 extends more than 80kpc from the galaxy centre!) Due to the extremely low surface brightness in these regions, only thick disk systems with identifiable features (shells) could have reliable velocities measured, and even then only with great difficulty.

It is interesting to note that our thick disk model can explain the observed connection between shell morphology (type 1 vs type 2) and roundness in terms of a simple projection effect. The merger model cannot explain this connection in a unified way - the differences must be modelled by different initial conditions, and cannot be explained by projection effects alone (Dupraz and Combes 1986).

All galaxies interact to some extent, and our model only requires the existence of a dynamically cool population of stars in nearly circular orbits to produce shells similar to those seen in many elliptical/S0 galaxies. Our simulations show that only weak interactions with galaxies 1/10th the mass of the primary and at distances ~40kpc are needed to produce visible shell structures. Taking into account the small impact parameter and small relative velocity required by the merger model, the cross section

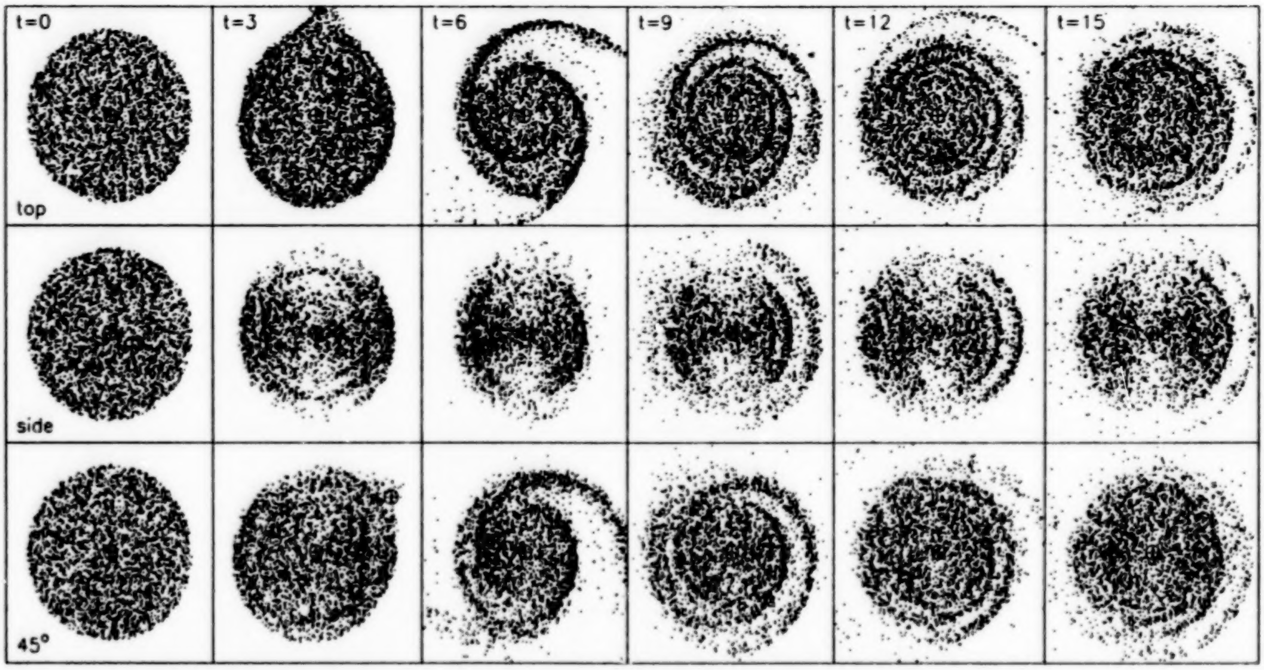

Figure 1: Weak interaction model simulation with 10000 particles and a secondary galaxy 1/10th mass of primary. Time unit $\sim 10^9$ years; initial radius of galaxy 80kpc. Top row — view from above; middle row — view from front; bottom row — view from 45^0. For clarity, only the band of particles from the projected equatorial region ($|z'| < 0.2$) is shown.

for producing shell structures by weak interactions in thick disks is many orders of magnitude greater than the cross section for shell production by merger.

In conclusion, we think that at least some elliptical galaxies have thick disks and that shell systems are formed in these thick disks by weak interaction with another galaxy.

5 References

Dupraz,C., & Combes,F., 1986. *Astr. Astrophys*, **166**, 53.
Franx,M., 1988. *Ph.D. Thesis*, Leiden.
Hernquist,L., & Quinn,P.J., 1988. *Astrophys. J.*, **331**, 682.
Jarvis,B.J., 1987. *IAU Symp. No. 127*, ed. De Zeeuw,T., Reidel, Dordrecht.
Jedrzejewski,R.I., 1987. *IAU Symp. No. 127*, ed. De Zeeuw,T., Reidel, Dordrecht.
Malin,D.F., & Carter,D., 1980. *Nature*, **285**, 643.
Malin,D.F., & Carter,D., 1983. *Astrophys. J.*, **274**, 534.
Prieur,J.-L., 1989. *European Southern Observatory Scientific Preprint.*
Quinn,P.J., 1984. *Astrophys. J.*, **279**, 596.
Seitzer,P., & Schweizer.F., 1989. *Preprint.*
Thomson,R.C., & Wright,A.E., 1990. *Cambridge University Astronomy Preprint.*
Thronson,H.A., Bally,J. & Hacking,P., 1989. *Astron. J.*, **97**, 363.

WING GALAXIES: A FORMATION MECHANISM OF THE CLUMPY IRREGULAR GALAXY MARKARIAN 297

YOSHIAKI TANIGUCHI
Kiso Observatory, Institute of Astronomy, The University of Tokyo

MASAFUMI NOGUCHI
Department of Physics, University of Wales

In order to contribute to an understanding of collision-induced starburst activities, we present a detailed case study on the starburst galaxy Markarian 297 (= NGC 6052 = Arp 209; hereafter Mrk 297). This galaxy is classified as a clumpy irregular galaxy (hereafter CIGs) according to its morphological properties (cf. Heidmann, 1987). Two major clumps and many small clumps are observed in the entire region of Mrk 297 (Hecquet, Coupinot, and Maucherat 1987). A typical major clump of CIGs has a diameter of a few hundred pc and its dynamical mass is estimated as an order of 10^8 $M_\odot$ (Taniguchi and Tamura 1987).

Since Mrk 297 looks like an isolated system, Schweizer (1983) included it as a candidate of mergers. On the other hand, Alloin and Duflot (1979) proposed another idea that Mrk 297 is just a colliding system between two late-type spiral galaxies because this galaxy has two kinematically distinct components (*the two major clumps*). Following their suggestion, we try to consider a possible geometry and orbit of the interaction in Mrk 297.

The overall morphology of Mrk 297 is highly chaotic and thus it seems difficult to determine possible orbits of galaxy-galaxy collision. However, we have serendipitously found a possible orbit during a course of numerical simulations for a radial-penetration collision between galaxies. The radial-penetration collision means that an intruder penetrates a target galaxy radially passing by its nucleus. This kind of collision is known to explain a formation mechanism of ripples around disk galaxies (Wallin and Struck-Marcell 1988). Here we show that the radial-penetration collision between galaxies successfully explains both overall morphological and kinematical properties of Mrk 297.

We made two kinds of numerical simulations for Mrk 297. One is N-body (1×10^4 particles) simulations in which effects of self gravity of the stellar disk is taken into account. These simulations are used to study detailed morphological feature of Mrk 297. The response of gas clouds are also investigated in order to estimate star formation rates in such collisions. The other is test-particle simulations, which are utilized to obtain a rough picture of Mrk 297 and to analyze the velocity field of Mrk 297. The techniques of the numerical simulations are the same as those in Noguchi (1988) and Noguchi and Ishibashi (1986). In the present model, an intruding galaxy with the same mass of a target galaxy moves on a rectilinear orbit which passes the center of the target.

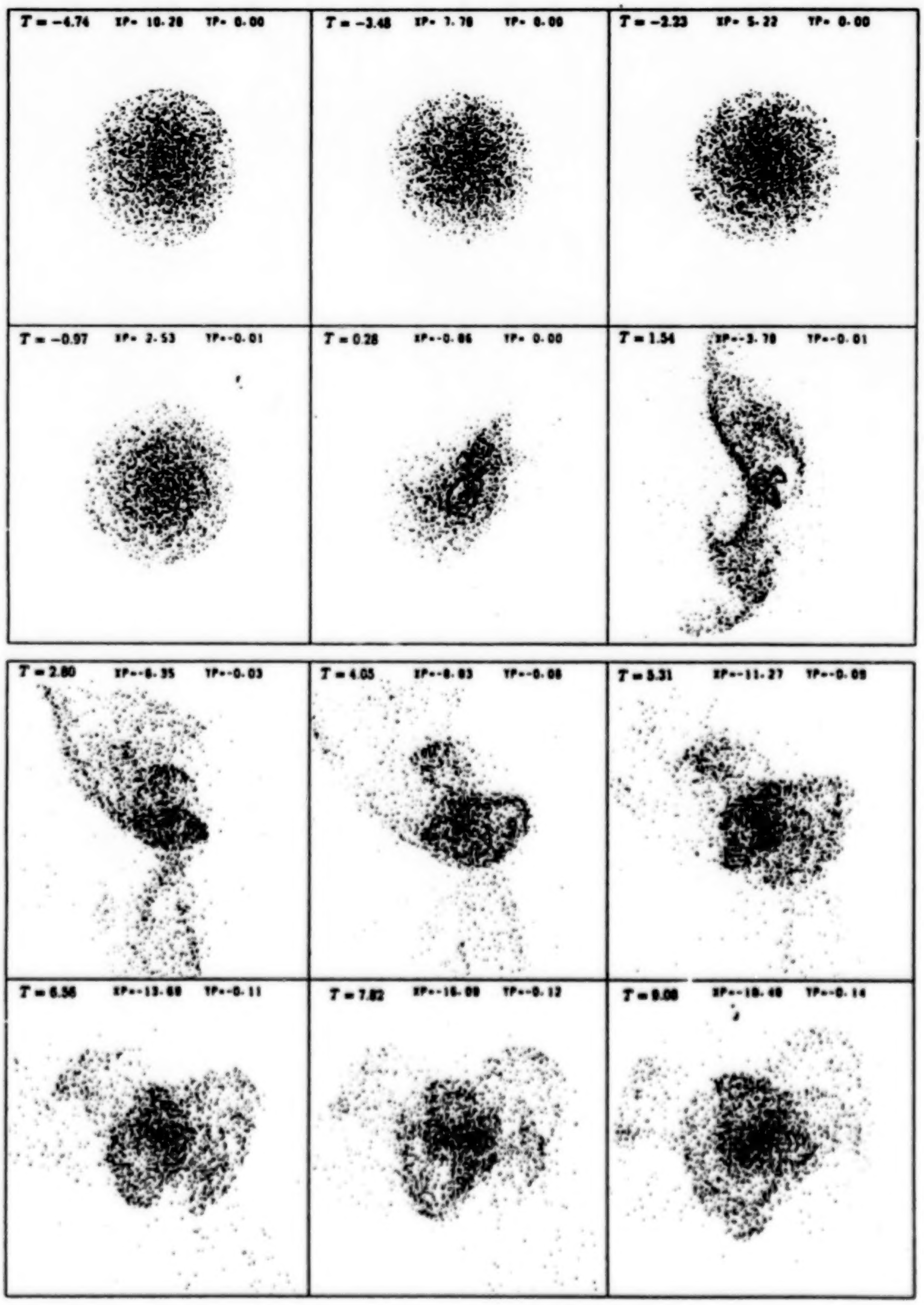

Fig. 1. The radial-penetration collision between galaxies. The morphological evolution of the target galaxy during the period of about two disk rotation time is shown. The wing phase discussed in this paper corresponds to the sixth panel ($T = 1.54$). This galaxy evolves into a barred galaxy, finally.

In Fig. 1, we show a morphological evolution of the radial-penetration collision based on the N-body simulation taking account of self gravity of the stellar disk. Nearly just after the impact (a few 10^7 years later), the target galaxy is deformed into a "*wing*"-like structure shown in the sixth panel of Fig. 1. This wing structure resembles with the eastern part of Mrk 297 in morphology. To demonstrate this, we compare the model result with the observation in Fig. 2. Our interpretation implies that the western part of Mrk 297 is an intruding galaxy. Although the morphological feature of this part is very complex, the basic structure appears to be a nearly round one with many clumps. Therefore, we may consider that the intruder is nearly observed from a face-on view. In the case that the colliding partner is deformed to a ring galaxy, the projected image of the two galaxies is quite similar to the observed shape of Mrk 297 (a rough sketch of given in Fig. 3, which is obtained with a test-particle simulation). Our analysis shows that a possible orbital plane of the collision is nearly parallel to the line of sight. Note that the intruder locates at a distance of twice of the galaxy diameter from the target when the wing structure is formed. Therefore, it is suggested that Mrk 297 is not a merger although it looks like a single object.

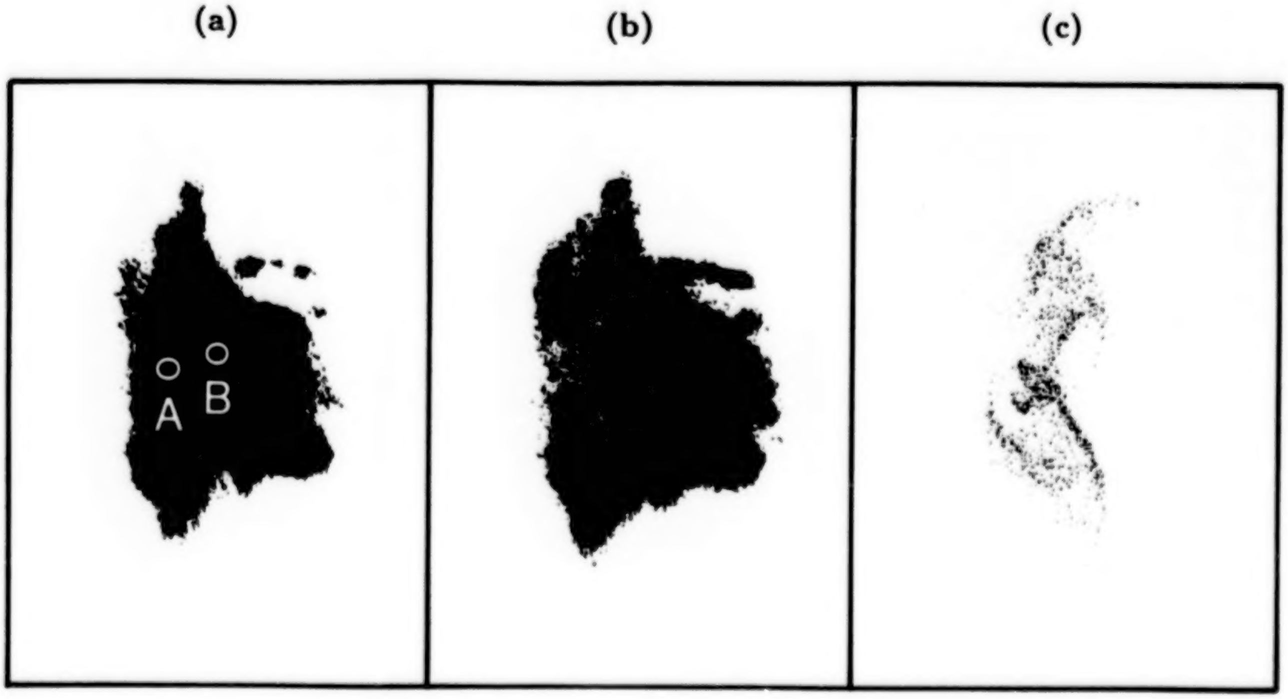

Fig. 2. A comparison of the morphology of Markarian 297 between (a) the observation (Arp 1966) and (c) our model (the sixth panel of Fig. 1). In the middle panel (b), the overlapped image of (a) and (c) is shown. Note that the wing structure corresponds to the eastern part of Mrk 297. The clumps A and B corresponds to the nuclei of the intruder and the target galaxies, respectively.

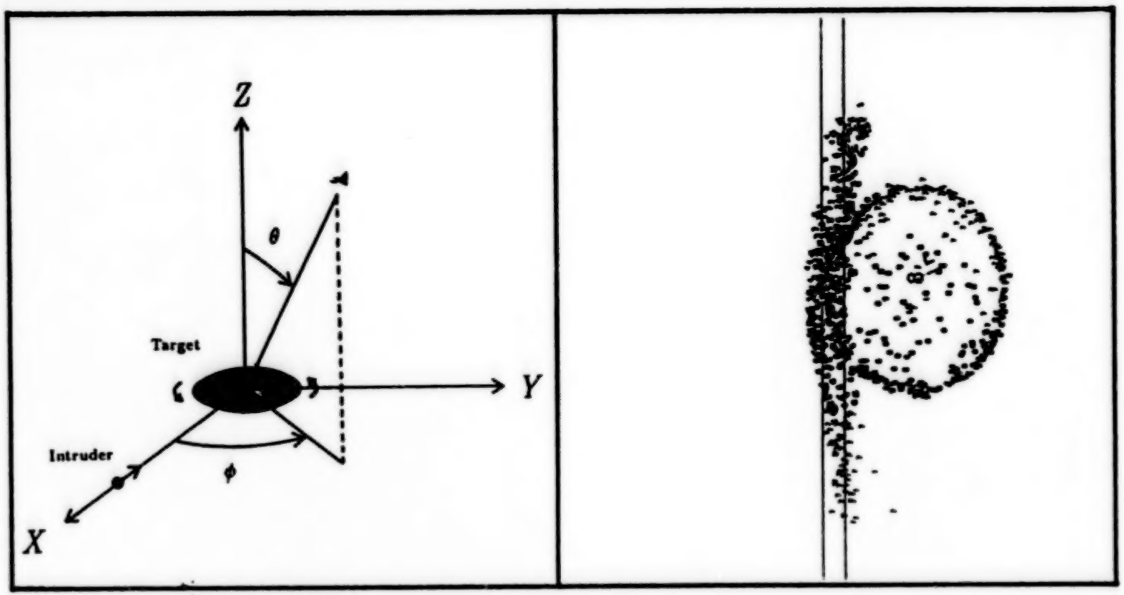

Fig. 3. Definition of observing angles of the collision (*left*) and the rough sketch of the overlapped image of the two galaxies at $\theta = 70°$ and $\phi = 180°$ (*right*). The stripe shown in the right panel corresponds to a slit position of the spectroscopy by Duflot, Lombard, and Perrin (1976).

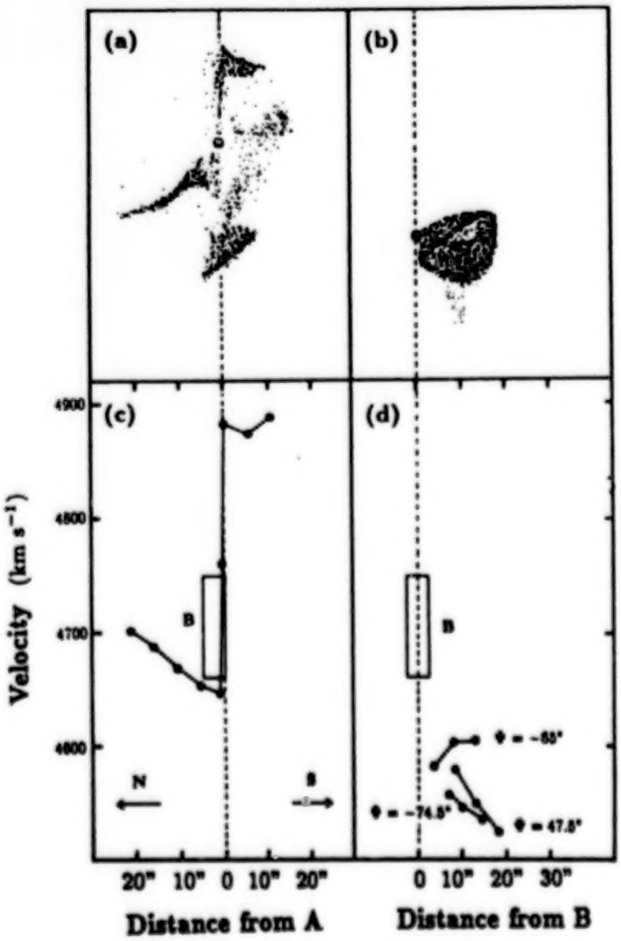

Fig. 4. A comparison of the velocity fields of Mrk 297 between the observation (*lower panels*) and our model (*upper panels*).

Next, we compare the velocity fields of Mrk 297 between the observation (Duflot, Lombard, and Perrin 1976) and our model (Fig. 4). In the left panels, the comparison is made for the data at PA = 0° through the clump B. The component trapped by the intruder is also seen in the model result. However, this component is not discriminated from the intrude in the observation. In the right panels, we show the velocity field of the intruder. The distance is measured from the clump B (i. e., the nucleus of the intruder). It is shown that the observed velocity field of Mrk 297 is well reproduced on the basis of our model.

As noted above, in our scheme, Mrk 297 is not a merger but an only interacting galaxy. Very recently, Sofue *et al.* (1990) detected ^{12}CO ($J = 1 - 0$) emission in Mrk 297 using the 45-m radio telescope of the Nobeyama Radio Observatory. Their CO mapping showed that the CO emission comes from outer regions as well as from the nuclear one. It is, however, known that molecular gas clouds are highly concentrated in the circumnuclear regions in merger galaxies (*e. g.,* Sanders *et al.* 1988). This difference in molecular gas distributions between Mrk 297 and the mergers also support our modeling.

REFERENCES

Alloin, D., and Duflot, R. 1979, *A. Ap.*78, L5.

Arp, H. C. 1966, *Atlas of Peculiar Galaxies* (Pasadena, California Institute of Astronomy).

Duflot, R., Lombard, J., and Perrin, Y. 1976, *A. Ap.*, 48, 437.

Hecquet, J., Coupinot, G., and Maucherat, A. J. 1987, *A. Ap.*, 183, 13.

Heidmann, J. 1987, in *Star Forming Regions, IAU Symp.* 115, eds. M. Peimbert, J. Jugaku, p. 599.

Noguchi, M. 1988, *A. Ap.*203, 259.

Noguchi, M., and Ishibashi, S. 1986, *M. N. R. A. S.*, 219, 305.

Sanders, D. B., Scoville, N. Z., Sargent, A. I., and Soifer, B. T. 1988, *Ap. J. (Letters)*, 324, L55.

Schweizer, F. 1983, In *Internal Kinematics and Dynamics of Galaxies, I. A. U. Symp.* 100, p. 319.

Sofue *et al.* 1990, in preparation.

Taniguchi, Y., and Tamura, S. 1987, *A. Ap.*, 181, 265.

Wallin, J. F., and Struck-Marcell, C. 1988, *A. J.*, 96, 1850.

PAIRED AND INTERACTING GALAXIES:
CONFERENCE SUMMARY

Colin A. Norman
Department of Physics and Astronomy,
Johns Hopkins University
and
Space Telescope Science Institute

1. INTRODUCTION

This has been an excellent conference with a very international component and a rich and wide ranging diversity of views on the topical subject of paired and interacting galaxies. The southern hospitality shown to us by our hosts Jack Sulentic and Bill Keel has been most gracious and the general growth of the astronomy group at the University of Alabama is most impressive.

The conference began with the presentation of the basic data sets on pairs, groups, and interacting galaxies with the latter being further discussed with respect to both global properties and properties of the galactic nuclei. Then followed the theory, modelling and interpretation using analytic techniques, simulations and general modelling for spirals and ellipticals, starbursts and active galactic nuclei. Before the conference I had written down the three questions concerning pairs, groups and interacting galaxies that I hoped would be answered at the meeting: (1) How do they form? including the role of initial conditions, the importance of subclustering, the evolution of groups to compact groups, and the fate of compact groups; (2) How do they evolve? including issues such as relevant timescales, the role of halos and the problem of overmerging, the triggering and enhancement of star formation and activity in the galactic nuclei, and the relative importance of dwarf versus giant encounters; and (3) Are they important? including the frequency of pairs and interactions, whether merging and interactions are very important aspects of the life of a normal galaxy at formation, during its evolution, in forming bars, shells, rings, bulges etc., and in the formation and evolution of active galaxies. In what follows I shall summarize the meeting and where possible focus on these three central issues. Since this is a conference summary my references are all to papers presented at this meeting.

2. PAIRS AND GROUPS

Karachentsev presented his beautiful work on paired galaxies consisting of a homogeneous sample of these galaxies with a strict set of selection criteria. Of the 585 selected pairs, 98 were excluded on the grounds that their M/L values exceeded 100. The mean spatial separation of the final sample is 83 kpc and the velocity separation is $120 kms^{-1}$. The M/L values ranged from 0-30. Pairs tend to have a similar Hubble type which seems to be due to formation processes and they also have similar colours. This effect was also found in the CfA redshift catalogue by Yamagata who coined the phrase twin galaxies for those with identical type and internal properties. Of course subtle consequences of the morphology density relation which would give similar effects need to be carefully taken into account here. Pairs are found in less dense regions of groups and clusters and 60% show evidence for tidal interactions and generally have an by Yamagata who coined the phrase twin galaxies for those with identical type and internal properties. Of course subtle consequences of the morphology density relation which would give similar effects need to be carefully taken into account here. Pairs are found in less dense regions of groups and clusters and 60% show evidence for tidal interactions and generally have an enhancement of emission lines, radio power, infrared luminosity, and probability of being active. In general pairs are correlated with respect to their physical properties such as luminosity, size, type, M/L, and angular momentum, although their is no spin vector correlation. Pairs seem to follow the general hierarchical clustering law and dynamical estimates indicate that close pairs merge in 2-3 revolutions with a lifetime of approximately 1/5 of a Hubble time. Obvious questions that arise here are whether simple evolutionary tracks for single galaxies may be subtly different from evolutionary tracks of double galaxies? Do the paired ellipticals lie on exactly the same fundamental plane defined by the surface brightness-core radius-velocity dispersion relation as the unpaired ellipticals and do they evolve along the plane?

A detailed study of a differently selected sample presented by Charlton showed that the distributions of paired galaxies is flat with equal numbers per unit separation. If galaxy halos were the canonical size of 50-100 kpc, then one would expect there to be a drop in the number distribution at this separation scale. This is not the case and she conjectures that the resolution may lie in galaxies possessing very large halos. Large M/L values for groups themselves were cited by a number of authors including Quintana, who presented evidence from dynamical studies of groups around Dumbell galaxies that M/L values for these groups were of order 10^3.

Hickson discussed his fundamental work on compact groups indicating that 30% of the galaxies appear interacting or disturbed, the morphological types are correlated, the morphology density relation was not strongly evident but there is a clear morphology-velocity dispersion relation. The overall luminosity function in compact groups is the same as that in the field although there is a deficit of faint galaxies and 1% of the light of the Universe is in compact groups. Sixty percent of the spiral galaxies studied in compact groups have peculiar rotation curves, 40% have compact nuclear continuum sources, the infrared luminosity is boosted by a factor of approximately two, and radio ellipticals are almost always first ranked. One question that arises is a consequence of the estimates discussed later that the merger timescale for these Hickson compact groups is 1/5 of a Hubble time. This implies that even with some fading that the post Hickson compact group phase should contain $3-5\%$ of the total luminosity of the Universe. Is this significant component identifiable and what is it? Relatively isolated ellipticals and possibly cDs come to mind as possible relics.

The neutral hydrogen properties described by Williams indicate that for the smaller, more compact groups the HI distribution envelopes the group. For the larger groups the HI is still mainly in the galaxies (although they are HI deficient) and extended tail structure is clearly evident. A search for merger products in compact groups was described by Zepf who inferred that a frequency of $10-15\%$ of the elliptical galaxies in compact groups should be blue and exhibit Balmer absorption lines as the signature of post merger products.

A lively panel discussion with substantial audience participation considered the question of an operational definition of tidal interactions and mergers. One possibility advocated by Simkin and Hutchings is that the mean separation should be $\leq 10R_{gal}$ but how big R_{gal} actually is including dark halo mass was not resolved within an order of magnitude. It was emphasized by Heckman that to really identify a merger product one should look at the old stars since much of the disurbed looking component could come from hydrodynamic effects such as outflows and ionization effects from young stars. Even multiple looking cores could be a superposition effect. Burbidge strongly advocated that most if not all so-called mergers and interactions could be associated with outflows as opposed to inflows and infalls and considerable and lively discussion ensued. One argument given by the merger and interaction proponents was that they could model the data quite well and a detailed atlas of models including stellar and gaseous dynamics, stellar populations, ages etc. as discussed by Byrd seems a most useful tool for future observational analysis.

3. GALAXY INTERACTIONS

The global effects of interactions as discussed by Kennicutt are typically to enhance the $H\alpha$, the far infrared, and the radio power by factors of 1.5-2.0 over the values they would have, for a given type, for non-interacting systems. The evidence for enhanced star formation has been clear since the work of Larson and Tinsley but it was strongly emphasized that the tidal features contained 1/4 of the light of the system and that they are blue, consistent with the presence of massive stars in them. Concerning the question of supernovae rates in these systems it is not yet clear whether the observed rate is enhanced or not. The typical derived constraints for the burst times were 10-100Myr with star formation masses of order $10^8 - 10^{10} M_\odot$. Studies of the IMF are not yet complete with quite unresolved issues such as the deconvolution of the relative contribution of the disk, spheroid and nuclear components. Detailed spectral synthesis and modelling by both Lamb and Bernlohr gave limits to the burst age, and their best estimates of the lower mass cut off was ($\sim 4M_\odot$). Wolf-Rayet spectra both in the optical and infrared can be particularly useful here in establishing constraints on the behaviour of the upper mass region of the IMF.

As shown by Wright the optical images of the IR powerful galaxies are distorted by young stars and dust. However, the IR continuum images are smooth with a reasonably smooth $r^{1/4}$ law behaviour. As noted in a number of contributions physically meaningful separation of the red continuum component into the giant and supergiant populations is most important. In Arp 220 there are two tiny nuclei observed in the infrared with very high resolution that have also been identified in the radio using VLBI techniques by Norris.

The cosmological evolution of paired and interacting systems has been estimated by Koo and Zepf to increase as $(1+z)^4$ with an uncertainty in the exponent of about 2. Even with this uncertainty by a redshift of order 2-3 the merging and interaction level approaches 100%. This indicates that one might take the view that the merging and interactions that we see now are merely the tail end of the normal process of galaxy formation. Observations of galaxy morphology and interactions with the Hubble Space Telescope should settle this question.

Turning now to the study of the nuclear regions (as opposed to the global properties discussed by Kennicutt) of merging and interacting systems as discussed by Heckman, we note that for pairs the $H\alpha$, infrared and radio power increases by about a factor of 2 in the nucleus, and that for strongly interacting systems there is another factor of 2 enhancement. For a sample of FIR selected galaxies there appears to be a definite enhancement of interactions but there is no excess of close neighbours. For Seyferts there is some excess of close neighbours with about 15% of Seyferts showing strong interactions and 6% weak interactions as compared to typically 5% in the field. The effect seems much stronger for Seyfert IIs than Seyfert Is. Radio galaxies are in regions where the local density is enhanced by a factor of 2-3 and bridges and tails are clearly evident for the most powerful radio galaxies. For QSOs with observed fuzz, 30 – 100% seem to be interacting. In terms of importance of the interaction process to the activity in the central region it is only the starburst galaxies and possibly the powerful radio galaxies and QSOs that seem to have a reasonably strong correlation with the effect on Seyferts and radio quiet QSOs being significantly more subtle.

The panel discussion on the reality of the cosmological redshift hypothesis was energetic, enthusiastic, and stimulating with many ideas put forward to support a diverse set of views. The end result is a set of predictions that this reviewer solicited from the most vocal participants that may be useful as a priori tests.

Steve Schneider: Secondary peaks in the δV distribution will move to higher velocity for narrower predicted physical separation (for homogeneously selected galaxy pairs). This will be a weak effect if the cutoff radii are within the halo radius.

William Tifft: We have been asked to make some predictions which might serve as benchmarks for future evaluations of redshift quantization. I will interpret this slightly more broadly to concern the nature of the redshift in general.

1) I will predict that continued work on close pairs of galaxies (product of redshift in km s^{-1} times separation in degrees < 300) will verify the exclusion of $\Delta V = 0$, and searches at larger separation will not find any excess, lost due to selection, which will fill in the hole. Normal dynamics and simple projection predicts a peak at zero.

2) I think the verification of the minimum between the 72 km s^{-1} peak and the 145 km s^{-1} peak for differential redshifts in close isolated pairs constitutes a second good bet. Perhaps this can be more simply put as the *multiple* nature of the peaks and valleys will continue to be verified.

3) Already mentioned in my introductory statement, and reinforced here, I believe that variability in redshift will be quite convincingly demonstrated within the next 5 to 7 years if not sooner.

Paul Hickson: About 35% of all my compact groups will be found to contain exactly one discordant redshift, as expected by chance superposition. These galaxies will generally be smaller and fainter than other group members, but not always as small or faint as typical galaxies at their redshift. They will be found near the centre of the group more often than expected. It will be possible to explain these effects by gravitational lensing from smoothly distributed dark matter in the groups.

Jack Sulentic: Dense group predictions:

(1) The majority of dense groups ($\sim 80\%$) will turn out to be physically dense systems rather than chance alignments of some kind. This realization will lead to a fundamental change in the dynamical theory of galaxy groups. This will involve something that inhibits merging in a few crossing times (or something related to 2).

(2) The discordant redshift groups will turn out to be:

(a) optical configurations (10 groups) and a lot of,

(b) lensed configurations *or* something new (young systems; $t \leq 10^9 yr$).

Geoffrey Burbidge: It will slowly be accepted that some significant part of the redshifts of extragalactic objects are not associated with the expansion of the universe. This will lead to a revolution in this field. Eventually on or two leaders will change their minds and then the bandwagon will change course. (In the interim the dirty tricks will continue. Papers will be interminably refereed, observing time on the Hubble Telescope and elsewhere will be denied, grant applications will be turned down, and "safe" people only will give summary talks.)

I hope that this happens in time for the radicals (those in Alabama plus Chip Arp and Fred Hoyle) to be acknowledged. However the odds are not good. Two previous cases come to mind. Wegener (continental drift) died before his ideas were accepted, as did Zwicky, who was hated by many at Caltech as Arp is, or at least as are his ideas today.

DYNAMICAL THEORY OF PAIRS AND INTERACTIONS

Significant progress has been made in the modelling of the dynamics of pairs and interactions. This work was elegantly summarised by Athanassoula. She noted that for one of the best merger cases, namely the Antennae, Barnes and Hernquist can now model the thin tails and the close separation of the cores. Some uncertainty remains about the relative velocity and the initial orbit eccentricity.

Spiral structure can be driven by prograde companions and a one- armed leading spiral is possible for retrograde companions if the main spiral galaxy has a low halo to disk ratio. She showed that the Q-parameter is not important for controlling the amplitude of the driven spiral due to non-linear disk heating effects and also that increased forcing does not imply a better spiral pattern. Clearly bars are enhanced by companions since the frequency of SAB, and SBB is 63% in the field and 80% in binary galaxies. An initially unbarred galaxy will have the bar instability growth significantly enhanced by a companion. If the galaxy is already barred the bar will be strongly increased in strength and will then decrease after the encounter. For out of the plane encounters they will have a shorter time to act and disk thickening may occur.

The dynamics of E-E pairs have asymmetric light distributions, U-shaped profiles and rising velocity dispersion profiles as discussed by Kirk Borne. His simulations show the stubby tails and indicate interesting orbits. Detailed simulations of large samples are necessary to determine the frequency and significance of interactions in these and other systems. Using the impulsive approximation, Chatterjee proved that without halos the merging frequency would be two orders below the present observed value of 1%. He concluded that halos are needed and indicated that with massive halos the correct value is achievable.

Double and multiple nuclei were discussed by Khachikian who reminded us of some of the theories of their origin including mass creation, double vortices and splitting of nuclei to give the twin nuclei that have nearly identical properties. Bulge formation from mergers was discussed by Roos using Monte Carlo simulations and the issue was raised about absence of evidence for counter rotating bulges. A beautiful dynamical friction calculation done analytically by Polyachenko was presented for both disks and halos which agreed exactly with the detailed numerical calculations.

Including both gas and stars in his numerical simulations, Noguchi gave a prescription for star formation due to cloud-cloud collisions and further prescribed the energy input fed back by supernovae into the interstellar medium. In models where a companion flies by a galaxy going bar unstable the bar instability is strongly enhanced, shocks form, significant stellar disk heating occurs and a large mass accumulates in the central regions. The duration of this phase is a few rotation periods. This set of calculations has real likeness to the observations of starbursts. Similar detailed calculations have been carried out by Hernquist.

The physics of compact groups can be modelled in two ways as discussed by Mamon. Self-consistent N-body codes such as the detailed group simulation of Barnes are extremely accurate and we have confidence in the results. The film resulting from their work shows how important are the three dimensional nature of the orbits. Many obvious two-dimensional mergers and interactions in fact turn out to be quite distant flybys in three dimensions. The thin tidal tails were apparently reproduced and give a significant contribution to the light, the merging process was relatively long with the resulting merged system having low angular momentum and exhibiting shell structures. The tidal tails are then blue and appear to have a dynamical age of 50-150 Myr.

The more explicit Fokker-Planck style calculations of Mamon have an advantage in their speed of execution and their inclusion of much more physics that is however put in by hand. For M/L of ~ 40, the merger timescale was found to be $\sim 3Gyr$ consistent with the more detailed dynamical calculations. With more dark matter in the halos the timescale is significantly altered and there was considerable debate whether it lengthened or shortened. If more mass is put in the halos, the merger cross section is increased but there is then less mass in the smooth background potentially decreasing the drag due to dynamical friction. More mass in a smooth background will increase the dynamical friction but the halos will be smaller. This important issue should be unambiguously resolvable in the near future. The question of the frequency of chance alignments within the compact groups was much debated here and ranged from $50\% - 10^{-6}\%$, clearly a narrower range is preferable. what is needed here is a series of cosmological simulations with a high dynamic range where individual galaxies and halos can be resolved.

5. GENERAL THEORY

The general problem of fuelling active galactic nuclei utilizing interactions as outlined by Shlosman is how to get $10^8 M_\odot$ from the galactic regions of dimensions of order say kpc into a region of order the size of the solar system at the rate of $1M_\odot yr^{-1}$. It seems possible to do the job down to scales of say 100pc as shown in the simulations of Noguchi and Hernquist but from then on the problem is harder to crack both observationally, and theoretically, although here again the resolving power of the HST will prove most useful. The questions still remains how the extrinsic forcing due to interactions, mergers, and sinking satellites influences the central regions via non-axisymmetric disturbances such as bars, triaxiality, spiral waves, or direct deposition in sinking satellites or mergers with sufficiently dense cores. One clue from starbursts is that the self gravity of the gas may be important.

Most of the posters showed beautifully detailed multiwavelength observations of individual objects and also many impressive models with both gas and stars incorporated. Realistic models of the interstellar medium that can be included in the simulations are still someway off. All this work will still be rather uncertain until more is understood about the star formation process. The general impression is that large quantities of complete samples with many detailed multiwavelength and complete modelling will unravel some of the problems we have come to at this meeting. Very significant progress was reported at this excellent meeting and the pace shows no signs of slowing, quite the contrary the mood here is to go away, work hard and solve the newly posed problems as soon as possible. Once again we thank the organizers, Jack Sulentic and Bill Keel for making this such an enjoyable and stimulating meeting.

It is a pleasure to thank Steve Zepf for a careful reading of the manuscript and Paul Hickson for enlightening correspondence on the evolution timescale for compact groups with evolving halos.

SUBJECT INDEX

Angular Momentum 3
Bars 711
Black Holes 497, 689
Bulget to Disk Ratio 601
Caustic Waves 743
cD Galaxies 195, 255, 537
Clusters of Galaxies 315, 327, 645, 683
Color Indices 55, 99, 215, 269, 331
Compact Groups (Definitions) 77, 143, 149, 609, 619
Compact Groups (Distribution) 77
Compact Groups (Dynamics) 77, 93, 133, 609, 619
Compact Groups (Morphology) 77, 99, 105, 617
Compact Groups (Statistics) 77, 105, 609, 619
Control Samples 3, 291, 297, 359
Correlation Functions 149, 353
Cosmic Strings 677
Counter-Rotation 159, 549
Dark Matter 645, 667
Discordant Redshifts 77, 459, 477, 479, 485, 491, 497
Dumb-Bell Galaxies 37, 261
Dust Absorption 431
Dynamics (Effects of Companions) 505, 565, 577, 583, 689, 705, 743
Dynamics (Pairs) 209, 505, 519, 555, 565, 569, 577, 583, 589, 595, 659, 711, 717, 737, 749, 759
Dynamics (Triples) 629, 633, 651, 659
Dynamics (Multiplets) 609, 659, 667
Dynamical Friction 505, 519, 543, 705
EE Pairs 33, 37, 65, 291, 537, 543
ES Pairs 47, 53, 291, 717, 737
Ejection 497
Emission Lines 3, 43, 169, 225, 251, 269, 327, 331, 393, 409, 441
Galaxy Formation 255
HI Measures 59, 69, 93, 129, 175, 183, 209, 245, 383, 479, 683
Holmberg Effect 269
ISM 403, 683, 717, 749
Infalling Gas 403
Infrared Emission 269, 285, 297, 309, 383, 415
Interaction (Definition) 159
Ionization Mechanisms 215, 221
IRAS Galaxies 25, 309, 353, 359, 387, 393, 409, 441, 445
IR Images 59, 285, 321, 347
M/L Ratios 3, 115, 129, 133
Markarian Galaxies 165
Masses 3, 19, 37, 183, 215
Mergers 3, 159, 215, 265, 321, 347, 359, 387, 451, 497, 519, 601, 609, 689, 755
Merger Rates 19, 269
Molecular Gas 285
Morphology 3, 25, 47, 55, 59, 159, 189, 245, 291, 297, 359, 393, 399
Multiple Nuclei 221, 269
Optical Luminosity Functions 297
Optical Spectrum 43, 169, 225, 251, 309, 331, 441, 451, 731
Pairs (Definition) 3, 19, 25, 143, 149, 265, 485

Pairs (Distribution) 3
Polar Rings 231
QSO's 359, 383, 387, 467
Radio Galaxies 309, 315, 359, 431, 467
Radio Observations 69, 245, 269, 309, 331, 343, 467
Redshift Quantization 459, 479, 485
Ringed Galaxies 189, 269, 537, 569
Seyfert Galaxies 165, 169, 201, 221, 331, 359, 399, 421, 437, 451, 689
Shells 755
Spiral Arms (Leading) 555
Star Formation 175, 269, 285, 303, 327, 331, 359, 415, 727
Starburst Galaxies 165, 359, 445, 689, 711, 731
Stellar Populations 309, 731
Supernovae 315
Surface Photometry 47, 65, 69, 189, 195, 201, 231, 321, 421, 727
Tidal Disturbances 505, 543, 569, 589, 727, 737
Triplets (Definitions) 115
Triplets (Dynamics) 115
Triplets (Masses) 115
Ultraviolet Data 303
Velocity Curves 33, 43, 169, 221, 225, 231, 347, 583
Velocity Dispersion 347
Velocity Fields 445
Wing Galaxies 759

AUTHOR INDEX

Z. Abraham 343
C. E. Akujor 467
A. S. Amirkhanian 133
J. P. Anosova 629, 633, 659, 667
P. Appleton 59
L. Armus 409
A. S. Asatrian 201
E. Athanassoula 505
D. J. Axon 245
M. Balcells 347
D. S. Balsara 737
S. F. Beaulieu 183
R. Bender 33
K. Bernlohr 731
D. Bettoni 159
B. Bhattacharya 195
J. Bland 445
K. D. Borne 537
F. Börngen 201
W. van Breugel 309
G. Burbidge 464
H. Bushouse 285, 302
R. Buta 189
G. Byrd 565, 577, 583
C. Carignan 129, 183
C. Carilli 473
T. Chang 491
J. C. Charlton 19
T. K. Chatterjee 519, 569
A. D. Chernin 633, 651
J. Cocke 479
L. Colina 451
F. Combes 543
R. M. Cutri 415
E. Davoust 65
A. Dey 309
M. Dietrich 43
R. Doyon 321
V. N. Dudinov 421
G. Fasano 159
D. Forbes 431
K. J. Fricke 437
A. M. Fridman 555
J. A. Frogel 393
G. Galletta 159
J. Gallimore 353
R. A. Gerber 737
J. H. van Gorkom 93, 473
S. T. Gottesman 209
P. GoudFrouij 215
S. A. Grandi 251
L. Gregorini 261
L. Hansen 215
T. Hara 645, 677
E. M. Hauxthausen 473
J. J. E. Hayes 195
T. Heckman 359, 409
C. A. Heisler 393
P. Hickson 77
P. Hintzen 55
S. Howard 565, 577
J. B. Hutchings 383
A. V. Ivanov 633, 651
P. A. James 321
C. J. Jog 683
T. de Jong 215
H. E. Jørgensen 215
R. D. Joseph 321
M. Kalinkov 143, 149
E. van Kampen 255
I. D. Karachentsev 3, 115
V. E. Karachentseva 115
W. C. Keel 265, 353, 441, 565
R. C. Kennicutt 269
E. Y. Khachikian 133
L. G. Kiseleva
M. Klaric 583
R. K. Kochhar 315, 589
W. Kollatschny 221, 437
P. P. Kronberg 69
I. Kuneva 143, 149
S. A. Lamb 285, 302, 737
V. S. Lebedev 115
K.-Y. Lo 285
S. Lord 285
C. R. Lynds 133
F. Macchetto 403, 431, 451
J. MacKenty 165
R. Madejsky 33
M. E. Mahon 209
G. Mamon 609, 617
P. Marziani 169, 225
B. McLean 165
I. S. McLean 321
P. M. McMahon 93
L. Metik 331

G. K. Miley 409
R. H. Miller 549
S. Miyoshi 645, 677
S. Morioka 677
C. Moss 327
P. M. S. Namboodiri 589
S. G. Neff 383
M. Noguchi 711, 759
L. Noreau 69
H. U. Nørgaard-Nielsen 215
C. Norman 765
R. Norris 387
S. B. Novikov 421
T. Oosterloo 159
V. V. Orlov 633, 667
P. Parma 261
A. Pedlar 245
A. Petrosian 201
V. Polyachenko 705
I. Pronik 331, 421
P. Prugniel 65, 543
D. Puche 129
H. Quintana 37
F. M. Rabaca 343
P. Rafanelli 169, 225
R. Rampazzo 47
V. P. Reshetnikov 231
G. Rhee 255
E. I. Robson 59
G. R. Roelofs 549
N. Roos 601
H. R. de Ruiter 261
D. J. Saikia 245
H. Salo 595
E. E. Salpeter 19, 485
J. Salzer 473
S. E. Schneider 462, 485
J. M. Schombert 59, 727
N. A. Sharp 53, 465
J. C. Shields 309
I. Shlosman 689
S. Simkin 399
C. E. Simpson 165
B. F. Smith 549
E. P. Smith 55
N. Ya Sotnikova 717
W. B. Sparks 403, 431, 451
A. Stanford 347
J. T. Stocke 473
C. Struck-Marcell 727, 743
J. W. Sulentic 47, 291, 297
Y. Taniguchi 759
M. Thomasson 749
R. C. Thomson 755
N. A. Tikhonov 105
W. G. Tifft 459, 479
D. G. Torr 491
J. W. Towns 302
V. S. Tsvetkova 421
R. B. Tully 445
S. W. Unger 245
J. P. Vader 393
M. Valluri 683
M. Valtonen 497
G. Vettolani 261
J. F. Wallin 727
M. Werner 285
B. Whitmore 99
B. A. Williams 93
A. S. Wilson 445
A. E. Wright 755
G. S. Wright 321
C. Xu 297
V. A. Yakovleva 231
T. Yamagata 25
G. J. Yates 245
A. V. Zasov 175
S. E. Zepf 99
W. Zheng 251

OBJECT INDEX

3C232 467, 473
3C390.3 251
Abell 1775 195
AM 0642-801 55
AM 1255-430 55
AM 2208-251 583
Arp 107 565
Arp 220 321, 387
Arp 238 409
Arp 248 303
CPG (=K) 144 53
CPG 148 53
CPG 149 53
CPG 153 53
CPG 155 53
CPG 158 53
GR 8 183
HCG 31 93
HCG 44 93
HCG 68 115
HCG 79 (Seyfert's Sextet) 93
HCG 99 115
IC 883 321
IC 1459 215, 431
IC 5049 (ESO341-IG15) 37
IC 5063 451
IC 5283 331
IRAS 0502-103 309
IRAS 05447-2114 409
Mark 266 221
Mark 273 201, 221
Mark 305/6 43
Mark 423 225
Mark 739 221. 225
Mark 788 221
Mark 1435 65
NGC 520 347
NGC 660 209
NGC 750/1 (Arp166) 33
NGC 1052 403, 431
NGC 1068 711
NGC 1275 421
NGC 1587/88 (CPG 99) 537
NGC 1614 409
NGC 2535/36 (Arp 82) 565
NGC 2623 321
NGC 2672/3 537
NGC 2685 231
NGC 3067 467, 473
NGC 3432 (Arp 206) 69
NGC 3808B (VV 300) 231
NGC 4486 (M87) 403
NGC 4782/3 (3C278) 33, 37, 537
NGC 5194/5 (VV1, M51) 505, 577
NGC 6052 (Mark 297) 321, 759
NGC 6240 441, 445
NGC 6958 431
NGC 7020 189
NGC 7148 65
NGC 7252 537
NGC 7469 331
NGC 7592 (VV731) 169
NGC 7714/15 731
NGC 7774 65
PKS 1327-206 473
Sculptor Group 129
Sersic 40-6 37
Shahbazian 4 133
UGC 367 65
UGC 8315N 303
UGC 1195 209

*U.S. GOVERNMENT PRINTING OFFICE: 1990 527-064/20007

Report Documentation Page

1. Report No. NASA CP-3098	2. Government Accession No.	3. Recipient's Catalog No.

4. Title and Subtitle

Paired and Interacting Galaxies -
International Astronomical Union Colloquium No. 124

5. Report Date

November 1990

6. Performing Organization Code

ES63

7. Author(s)

J. W. Sulentic, W. C. Keel, and C. M. Telesco, Editors

8. Performing Organization Report No.

10. Work Unit No.

M-652

9. Performing Organization Name and Address

George C. Marshall Space Flight Center
Marshall Space Flight Center, Alabama 35812

11. Contract or Grant No.

13. Type of Report and Period Covered

Conference Publication

12. Sponsoring Agency Name and Address

National Aeronautics and Space Administration
Washington, D.C. 20546

14. Sponsoring Agency Code

15. Supplementary Notes

J. W. Sulentic and W. C. Keel: University of Alabama at Tuscaloosa, Tuscaloosa, Alabama.
C. M. Telesco: George C. Marshall Space Flight Center, Marshall Space Flight Center, Alabama.
Prepared by Space Science Laboratory, Science and Engineering Directorate, MSFC.

16. Abstract

This document contains the proceedings of the International Astronomical Union Colloquium No. 124 held at the University of Alabama at Tuscaloosa, December 4-7, 1989. The purpose of the conference was to describe the current state of our observational and theoretical knowledge of interacting galaxies, with a particular emphasis on galaxies in pairs. The presentations and discussions embraced most of the topics of extragalactic astronomy, from star formation to the origin of active galactic nuclei.

17. Key Words (Suggested by Author(s)) Galaxies, Interactions, Dynamics	18. Distribution Statement Unclassified---Unlimited Subject Category: 90

19. Security Classif. (of this report) Unclassified	20. Security Classif. (of this page) Unclassified	21. No. of pages 793	22. Price A99

NASA FORM 1626 OCT 86

For sale by the National Technical Information Service, Springfield, VA 22161-2171

776